# UC Davis

## UC Davis Electronic Theses and Dissertations

### Title

Repeated lithospheric-scale reactivation of an inherited plate boundary in the eastern Alaska Range, Alaska, USA

### Permalink

https://escholarship.org/uc/item/2926d9qr

### Author

Waldien, Trevor

### Publication Date

2021

Peer reviewed|Thesis/dissertation

eScholarship.org Powered by the California Digital Library
University of California

Repeated lithospheric-scale reactivation of an inherited plate boundary in the eastern Alaska Range, Alaska, USA

By

TREVOR SCOTT WALDIEN
DISSERTATION

Submitted in partial satisfaction of the requirements for the degree of

DOCTORATE OF PHILOSOPHY

in

Geology

in the

OFFICE OF GRADUATE STUDIES

of the

UNIVERSITY OF CALIFORNIA

DAVIS

Approved:

_____
Sarah M. Roeske, Chair

_____
Eric S. Cowgill

_____
Richard O. Lease

Committee in Charge

2021

**ABSTRACT**

Accretionary orogens, such as the North American Cordillera, form by repeated collisions of allochthonous oceanic and continental fragments (terranes). Due to the closure of ocean basins that is required for far-traveled terranes to become part of the orogen, fault systems at the boundaries of allochthonous terranes commonly form as plate boundaries and experience multiple phases of reactivation after collision. The repeated phases of reactivation along the terrane-boundary fault systems often mask the earlier deformation events and lead to uncertainty regarding the location of the main lithospheric-scale geologic boundary between terranes. In this dissertation, I present the geologic evolution of the master reactivated plate boundary structure in the Alaska Range suture zone of southern Alaska.

In the first chapter, I use detailed geologic mapping, structural analysis, U-Pb and $^{40}Ar/^{39}Ar$ geochronology, geochemistry of spinel-group minerals, and receiver function seismology to parse metamorphic rocks in the suture zone. With these methods, I show that the main suturing structure is located along the boundary between amphibolite grade schists and gneisses associated with North America in the north and greenschist grade metagreywacke and slate associated with allochthonous oceanic terranes in the south. The main suturing structure was reactivated after ca. 32 Ma and nucleated an imbricate thrust system that progressed southward. I argue that reactivation along the boundary between the metasedimentary belts is the third phase of activity on this structure, owing to the penetration of that boundary through the lithosphere.

In the second chapter, I use regional geologic mapping, U-Pb and $^{40}Ar/^{39}Ar$ geochronology, Hf isotope analysis, and statistical tests to confirm the correlation between Alaska Range suture zone metamorphic rocks in the Alaska Range and hypothesized correlative metasedimentary and plutonic belts in southwestern Yukon Territory. After confirming the correlation, I use the

correlative rock packages to create a sequential restoration of slip on the Denali fault system. The outcome of this work shows that terrane accretion that metamorphosed the Alaska Range suture zone rocks took place at ca. 90 Ma along east-dipping shear zones, and subsequently those suture zone rocks have been dissected by ~480 km of dextral slip on the Denali fault since ca. 50 Ma.

In the third chapter, I use modern river detrital apatite fission-track thermochronology and $^{40}Ar/^{39}Ar$ geochronology to highlight southern Alaska as a type-example of long-lived oblique flat slab subduction. With the datasets, I show that the most recent and rapid bedrock exhumation in southern Alaska is spatially associated with strike-slip fault systems that were active at the time of slab flattening. Moreover, I argue that transpressional deformation and flat slab-associated magmatism were localized on the strike-slip structures due to their role as active lithospheric-scale shear zones. This analysis challenges models of diffuse upper-plate deformation in flat slab subduction environments and instead argues that strike-slip fault systems that penetrate the upper plate are essential for localizing deformation associated with obliquely convergent plate motion.

In my view, the overall impact of this dissertation is to show that by coupling detailed field and analytical work, each phase of reactivation for major orogenic structures can be resolved and coupled to regional tectonic/geodynamic scenarios at the time of formation and reactivation. Similarly, an overarching theme of the conclusions drawn herein is that the active strain distribution in strike-slip dominated orogens is strongly influenced by the locations of inherited structures that penetrate the lithosphere.

**ACKNOWEDGEMENTS**

I am indebted to several people and organizations who contributed to the completion of this dissertation.

On a logistical note, I am thankful for funding from the American Associated of Petroleum Geologists, Alaska Geological Society, EarthScope, Geological Society of America, UC Davis Durrell fund, USGS EdMap award #G16AC00206, and NSF Tectonics award #EAR-1828737. I am grateful to Wing Air, Alaska Land Exploration, 40-Mile Air, and Aurora Aviation for safe transportation to and from the field areas. I appreciate assistance and fun times in the field from Daniel Baldassare, Cait Livsey, Tyler Schlieder, Jordan Carey, Jack Foran, Michael Chen, and Sonny Hutchinson, and in the lab from Cait Livsey and staff at the Arizona Laserchron center. Greg Baxter cannot be thanked enough for the dozens of incredible thin sections and grain mounts, without which I could not do any of my analytical work.

On a more personal note, I am grateful for the support that I received from my family, friends, and mentors during my tenure as a graduate student at UC Davis. To my friends and family: particularly my parents, Cait Livsey, and Tyler Schlieder, I want to say thank you for the fun times and steadfast support; it made a huge impact even if that wasn't always clear at the time. I appreciate my committee members: Eric Cowgill, Mike Oskin, Richard Lease, and Magali Billen for the knowledge and wisdom that they've shared with me over the years. Lastly, to all of my mentors throughout my education: Frank Hladky, Andrew Meigs, and Sarah Roeske, I'd like to say that I appreciate your (gentle) prodding, hard work, and collaboration, which have allowed me to grow freely into the scientist and person that I am today. I feel that your mentorship has given me the tools to become an excellent mentor myself, and I look forward to our future endeavors.

# Ch. 1: Oligocene-Neogene lithospheric-scale reactivation of Mesozoic terrane accretionary structures in the Alaska Range suture zone, southern Alaska, USA

**Trevor S. Waldien[1], Sarah M. Roeske[1], Jeffrey A. Benowitz[2], Evan Twelker[3], Meghan S. Miller[4]**

*[1]Department of Earth and Planetary Sciences, University of California, Davis, 1 Shields Ave. Davis, California 95616, USA*

*[2]Geophysical Institute, University of Alaska, Fairbanks, 900 Yukon Drive Fairbanks, Alaska 99775, USA*

*[3]Alaska Division of Geological & Geophysical Surveys, 3354 College Road, Fairbanks, Alaska 99709, USA*

*[4]Research School of Earth Sciences, Australian National University, Building 142, Mills Road, Canberra, ACT 2601 Australia*

**ABSTRACT**

Terrane accretion forms lithospheric-scale fault systems that commonly experience long and complex slip histories. Unraveling the evolution of these suture zone fault systems yields valuable information regarding the relative importance of various upper crustal structures and their linkage through the lithosphere. We present new bedrock geologic mapping and geochronology documenting the geologic evolution of reactivated shortening structures and adjacent metamorphic rocks in the Alaska Range suture zone at the inboard margin of the Wrangellia composite terrane in the eastern Alaska Range, Alaska, USA. Detrital zircon Uranium-Lead (U-Pb) age spectra from metamorphic rocks in our study area reveal two distinct metasedimentary belts. The Maclaren schist occupies the inboard (northern) belt, which was derived from terranes along the western margin of North America during the mid-to-late Cretaceous. In contrast, the Clearwater metasediments occupy the outboard (southern) belt, which was derived from arcs built on the Wrangellia composite terrane during the late Jurassic-to-early Cretaceous. A newly discovered locality of Alaska-type zoned ultramafic bodies within the Clearwater metasediments provides an additional link to the Wrangellia composite terrane. The Maclaren and Clearwater metasedimentary belts are presently juxtaposed by the newly identified Valdez Creek fault, which is an upper crustal reactivation of the Valdez Creek shear zone, the late Cretaceous plate boundary fault zone that initially brought them together. $^{40}Ar/^{39}Ar$ mica ages reveal independent post-collisional thermal histories of hanging wall and footwall rocks until reactivation localized on the Valdez Creek fault after ca. 32 Ma. Slip on the Valdez Creek fault expanded into a thrust system that progressed southward to the Broxson Gulch fault at the southern margin of the suture zone, and eventually into the Wrangellia terrane. Detrital zircon U-Pb age spectra and clast assemblages from fault-bounded Cenozoic gravel deposits indicate that the thrust system was active during the

Oligocene and into the Pliocene, likely as a far-field result of ongoing flat-slab subduction and accretion of the Yakutat microplate. The Valdez Creek fault was the primary reactivated structure in the suture zone, likely due to its linkage with the reactivated boundary zone between the Wrangellia composite terrane and North America in the lithospheric mantle.

## INTRODUCTION

It has long been known that ancient intracontinental sutures are prone to structural reactivation (Dewey and Burke, 1973; Dewey, 1977). Within the crust, the orientation of inherited faults, presence of pre-existing rock fabrics, and mineral rheology are generally considered to be important factors controlling reactivation (e.g., Sibson, 1985; Ranalli, 2000; Beacom et al., 2001). However, a growing body of literature emphasizes the importance of mechanical properties of the lithospheric mantle as key factors controlling the structural evolution of polyphase accretionary orogens (Tikoff et al., 2001; Tommasi et al., 2009; Heron et al., 2016; Kelly et al., 2019; Goussin et al., 2020). If the mechanical properties of the lithospheric mantle do indeed control crustal fault reactivation, then post-collisional deformation would be more likely to focus onto pre-existing crustal structures that root into inherited mantle shear zones.

Southern Alaska contains a suite of reactivated suture zone structures that likely record such linkage to an inherited lithospheric scale boundary. Rocks within the Alaska Range suture zone represent a series of marine basins that closed during the Mesozoic collision of the Wrangellia composite island arc terrane with previously accreted terranes in western North America (Ridgway et al., 2002). Decades of regional mapping, geochronology, and geophysics have identified crustal scale faults at the northern and southern boundaries of the suture zone and inferred them to be the primary collisional structures (Coney et al., 1980; Csejtey et al., 1982; Brennan et al., 2011).

Recent detailed petrography and Uranium-Lead (U-Pb) detrital zircon analyses have shown that the marine strata and metamorphic equivalents within the suture zone may be split into a northern continental-derived succession and a southern Wrangellia composite terrane-derived succession (Hults et al., 2013; Yokelson et al., 2015; Box et al., 2019). A potentially deeply rooted accretionary structure has been inferred to juxtapose the two sedimentary successions and their basement in the western Alaska Range (Wallace et al., 1989; Decker et al., 1994), yet the structure has remained cryptic due to the similar rock types, prevalence of cover strata, and distributed deformation throughout the region. (e.g., Box et al., 2019). Although faults at the boundaries of the suture zone appear to have no significant displacement since the Cretaceous (Wahrhaftig, 1975; O'Neill et al., 2001), regional seismicity (Ruppert, 2008) indicates that the interior of the suture zone is actively deforming. Thus, post-suturing deformation may have focused onto a cryptic boundary juxtaposing the distinct sedimentary successions within the suture zone. Whereas the location of these intra-suture zone structures has remained enigmatic since the early studies in the western Alaska Range (e.g., Wallace et al., 1989; Box et al., 2019), the eastern Alaska Range contains correlative rock packages that have been highly shortened during and after the collision and thus offers an opportunity to evaluate the reactivation of suture zone structures in a well-exposed focus area.

In this paper we present new bedrock geologic mapping, U-Pb geochronology, and $^{40}Ar/^{39}Ar$ thermochronology from the eastern Alaska Range. We use our data to determine the burial and exhumation history of Alaska Range suture zone metamorphic rocks in the study area and then resolve the polyphase slip history of faults responsible for the burial and exhumation. Our data bear on the relative importance of Alaska Range suture zone boundary structures and intra-suture zone structures during Cenozoic reactivation.

## GEOLOGIC BACKGROUND

### Geology of the Alaska Range suture zone

The geology of the northern North American Cordillera is largely composed of allochthonous terranes that collided with the North American continent during the Mesozoic (Jones et al., 1977; Ridgway et al., 2002; Colpron et al., 2007) (Figure 1). Major allochthonous terranes in southern Alaska and adjacent Canada include the Wrangellia, Alexander, and Peninsular terranes, which were amalgamated prior to collision with the North American Cordillera (Gardner et al., 1988; Beranek et al., 2014; Israel et al., 2014) and have thus been termed the 'Wrangellia composite terrane' (Plafker and Berg, 1994), 'Insular Belt' (Monger et al., 1982), 'Insular Superterrane' (Rusmore, 1987) or Talkeetna Superterrane (Cjestey et al., 1982). We herein refer to the amalgamated terranes as the 'Wrangellia composite terrane' and distinguish the individual terranes only when necessary. A suite of Late Jurassic and Cretaceous marine basinal assemblages (Kahiltna-Nutzotin-Dezadeash-Gravina-Methow-Tyaughton basins) is discontinuously exposed along ~3000 km of the inboard (north and east) margin of the Wrangellia composite terrane throughout the northern Cordillera. These basin strata and their metamorphic equivalents are interpreted to represent south-to-north closure of a series of fringing ocean basins between previously accreted terranes and the Wrangellia composite terrane (Rubin and Saleeby, 1991; McClelland et al., 1992; Kapp and Gehrels, 1998; Hampton et al., 2007; Manuszak et al., 2007; Surpless et al., 2014; Yokelson et al., 2015; Lowey, 2018; Trop et al., 2020). Strata in these basins were structurally imbricated, buried by thrust sheets, variably metamorphosed, and intruded by plutons during accretion of the Wrangellia composite terrane (Csejtey et al., 1982; Nokleberg et al., 1985; Rubin et al., 1990; Haeussler, 1992; Davidson and McPhillips, 2007; Trop et al., 2020). Syn- and post- collisional dextral strike-slip faulting has dismembered the basinal

assemblages and contributed to northward transport of the outboard terranes (Nokleberg et al., 1985; Ridgway et al., 2002; Wyld et al., 2006).

The region between the Wrangellia composite terrane and previously accreted inboard terranes in southern Alaska presently exposes a large region of imbricated Kahiltna assemblage underlain by fragments of oceanic crust and disparate terranes (Amato et al., 2007a; Hampton et al., 2007; Nokleberg and Richter, 2007; Gilman et al., 2009). The geology in this region is interpreted to record closure of the Kahiltna basin, possibly involving a component of subduction, and has thus been named the Alaska Range suture zone (Ridgway et al., 2002).

Jurassic–Cretaceous Kahiltna strata and metamorphic equivalents within the suture zone have been split into northern and southern successions. The northern succession comprises compositionally mature sedimentary rocks with detrital zircon U-Pb age signatures that record sediment source areas in parauthochonous North America, the Yukon Tanana terrane, and Mesozoic igneous belts built on those terranes (Kalbas et al., 2007; Hampton et al., 2010; Huff, 2012; Hults et al., 2013; Box et al., 2019; Romero et al., 2020). The southern succession consists of compositionally immature sedimentary/volcano-sedimentary strata with detrital zircon U-Pb age signatures that match to Mesozoic arcs built on the Wrangellia composite terrane (Mooney, 2010; Hults et al., 2013; Box et al., 2019). In a regional mapping study of the western Alaska Range, Wallace et al. (1989) first separated the northern continental-derived strata of the Kahiltna assemblage from the southern ocean arc-derived Kahiltna assemblage, which they called the Koksetna River sequence, and depicted the two successions as juxtaposed by the NE-SW striking Mulchatna fault (Mulchatna Lineament-Figure 1). Although the Mulchatna fault is poorly exposed, the inferred surface trace aligns with a regional aeromagnetic lineament, which may record contrasting characteristics in basement rocks across the structure (Saltus et al., 2007). From the

western Alaska Range the northern and southern Kahiltna assemblages continue northeast where correlative structures may be covered by younger strata in the northern Talkeetna Mountains (Trop and Ridgway, 2007; Hampton et al., 2010) and are truncated by the Denali fault in the eastern Alaska Range (e.g., Hults et al., 2013) (Figure 1).

In the eastern Alaska Range the Maclaren metamorphic belt is a highly metamorphosed portion of the Kahiltna assemblage, which has undergone major syn-collisional shortening along the Valdez Creek shear zone. The Clearwater Mountains (Figure 1) contain the type locality of the Maclaren metamorphic belt, where it has been defined as a Barrovian inverted metamorphic belt that grades from lower greenschist facies metasedimentary strata in the south to amphibolite facies pelitic and quartzofeldspathic schist and gneiss in the north (Smith, 1981). The Valdez Creek shear zone, a ca. 75 Ma amphibolite facies S-vergent mylonitic thrust zone (Davidson et al., 1992; Ridgway et al., 2002), intersects the Maclaren metamorphic belt and marks an abrupt change in metamorphic grade between hanging wall and footwall rocks. The inverted metamorphic field gradient is restricted to the footwall of the Valdez Creek shear zone and is thus inferred to have developed during S-vergent motion on the shear zone (Smith, 1981; Davidson et al., 1992; Hollister, 1993; Beam and Fisher, 1999) (Figure 1 cross section). Hanging wall rocks, in contrast, experienced kyanite grade metamorphism prior to development of the shear zone (Davidson et al., 1992). Recent U-Pb detrital zircon studies in the Clearwater Mountains have shown that the hanging wall rocks (Maclaren schist and gneiss) are metamorphic equivalents of the northern succession of the Kahiltna assemblage and the footwall rocks (Clearwater metasediments) are equivalent to the southern succession (Mooney, 2010; Link, 2017).

**Cenozoic deformation in the Alaska Range suture zone**

The Alaska Range suture zone is cut by a number of major faults, several of which likely formed during Mesozoic terrane accretion and have been reactivated in the Cenozoic. The most prominent active fault in the region is the Denali fault, which transects the suture zone west of 145.7ºW and juxtaposes the Wrangellia composite terrane against inboard peri-Laurentian terranes east of 145.7ºW (Figure 1). Dextral slip in the Denali fault system has been ongoing since at least 57 Ma (Nokleberg et al., 1985; Murphy, 2018; Regan et al., 2020) and continues through the Holocene (St. Amand, 1957; Richter and Matson, 1971; Stout et al., 1973; Matmon et al., 2006; Meriaux et al., 2009; Haeussler et al., 2017a). Surface rupture during the 2002 $M_w$ 7.9 Denali earthquake illustrates that the fault is active today (Eberhart-Phillips et al., 2003).

The Hines Creek and Talkeetna-Broxson Gulch faults are generally considered to coincide with the northern and southern boundaries of the suture zone, respectively (Figure 1). Although geophysical observations suggest that the Hines Creek and Talkeetna faults are major crustal structures (Veenstra et al., 2006; Brennan et al., 2011; Allam et al., 2017), post-collisional deformation along these structures appears to be highly localized (cf., Wahrhaftig et al., 1975; Csejtey et al., 1982; O'Neill et al., 2001; Mooney, 2010; Bemis et al., 2012; Nokleberg et al., 2013; Koehler, 2013). The Broxson Gulch fault, in contrast, displays clear evidence for post-collisional reactivation where it marks the southern margin of the suture zone in the eastern Alaska Range (Stout and Chase, 1980; Nokleberg et al., 1985; this study).

Despite evidence for only local Cenozoic reactivation of faults at the margins of the Alaska Range suture zone, several lines of evidence indicate that post-collisional deformation has been focused within the suture zone: 1) Low-temperature thermochronology studies show widespread fault slip-related exhumation and topographic development throughout the suture zone (Fitzgerald

et al., 1993, 1995; Haeussler et al., 2008; Benowitz et al., 2011, 2012, 2014; Riccio et al., 2014; Lease et al., 2016; Lease, 2018), which has expanded Alaska Range topography (Bemis and Wallace, 2007; Ridgway et al., 2007; Bemis et al., 2015; Waldien et al., 2018; Bill et al., 2019); 2) Structural, stratigraphic, and geophysical studies show Neogene and Quaternary activity on faults at the margins on the *Denali* massif in the central Alaska Range (Burkett et al., 2016; Saltus et al., 2016; Haeussler et al., 2017b; Trop et al., 2019); 3) Geodetic data from southern Alaska support a model wherein upper plate deformation related to Alaska-Aleutian subduction zone convergence is concentrated in the suture zone (Freymueller et al., 2008; Kreemer et al., 2014); and 4) Multiple receiver-function studies show that the suture zone crust is ~5-to-15 km thicker than crust in adjacent terranes and suggest that a portion of this thickening developed during the Cenozoic (Veenstra et al., 2006; Brennan et al., 2011; Miller et al., 2018).

**Motivation for re-analysis of Broxson Gulch and Ann Creek**

Our map areas (Figure 2–Broxson Gulch and Ann Creek) are the locations of the first detailed studies of the Alaska Range suture zone rocks and structures in the eastern Alaska Range (e.g., Rose 1965, 1966; Stout, 1965). As a result, these areas contain the type locales of the Broxson Gulch fault and associated structures. Interpretations of the local geology in Broxson Gulch and the Ann Creek area fueled early analyses of strain partitioning in the Denali fault system (Stout and Chase, 1980), total slip on the Denali fault (Forbes et al., 1974), accretion of the Wrangellia composite terrane (Nokleberg et al., 1985), and ore deposit genesis associated with the Maclaren metamorphic belt (Rose, 1965, 1966; Smith, 1981). The inference of Quaternary slip on the Broxson Gulch fault (Nokleberg et al., 1985) and relocation of historic seismicity (Doser, 2004) suggest that the fault may be active.

The early geologic maps of Broxson Gulch and the Ann Creek area were foundational contributions and should continue to be viewed as useful maps. Yet, an updated examination of the map areas through the lens of modern structural analysis, geochronology, and regional tectonics is warranted. For example, Rose (1965) and Stout (1965) both recognized that metasedimentary rocks north of the Broxson Gulch fault displayed a variety of textures and mineral assemblages, and thus were likely metamorphosed from multiple protolith compositions. However, the protolith age was inferred to be Devonian or older on the basis of nearby strata containing Carboniferous fossils (Stout, 1965; Rose, 1966). Despite recognition that the metamorphic rocks had been metamorphosed from various protolith compositions, the original map units appear to have been defined on the basis of textural features. Such unit definitions led to inconsistent inclusion of foliated greenschist grade metaigneous rocks in the hanging wall of the Broxson Gulch fault, which in turn changed the location and shape of the fault on the various maps (cf., Rose, 1966; Stout, 1976; Nokleberg et al., 1992a). A common feature of all the existing maps is the apparent offset of the Broxson Gulch fault by a buried NW-striking sinistral tear fault in the center of Broxson Gulch.

Here, we aim to resolve some of the inconsistencies in the original maps by 1) developing regionally consistent unit definitions on the basis of protolith age and composition; 2) refining the location of major structures using the new unit definitions; and 3) reinterpreting the structural evolution and resulting fault geometries of major structures using modern structural analysis and geochronology. Our analysis reveals the existence of an additional structure, which we call the Valdez Creek fault and appears to be the key Cenozoic fault in the area.

## METHODS

### Mapping and structural analysis

We conducted 1:10,000-scale bedrock and surficial mapping during the summers of 2015, 2016, and 2018 over an area of 170 $km^2$. Our detailed mapping campaign worked in collaboration with a regional (1:100,000 scale) mapping and compilation project by the Alaska Division of Geological and Geophysical surveys (DGGS) (Twelker et al., in revision). Due to lack of road access, we accessed the field areas by helicopter and fixed-wing aircraft. Once in the field, we mapped the areas by foot using hillshade and contour paper basemaps constructed from the 5-meter-resolution Interferometric Satellite Aperture Radar (IfSAR) Alaska Digital Terrain Model (DTM). While mapping, we recorded sample locations using a handheld global positioning system.

Between the summer field mapping campaigns, we scanned our paper field maps and digitized them using ESRI ArcMap. To aid our map compilation we used high-resolution (25-meter pixel size) potential-field geophysical data published by the DGGS (Burns et al., 2003) and ≥1-meter resolution satellite imagery (available in ArcMap) to refine our bedrock mapping in areas of poor exposure or interpolate through areas of Quaternary cover. Here we present our bedrock mapping compiled at 1:55,000–Broxson Gulch (Figure 2A) and 1:50,000–Ann Creek (Figure 2B).

### Zircon U-Pb geochronology

#### *Sample preparation and data collection*

We performed single-grain zircon U-Pb geochronology by Laser Ablation Inductively Couple Mass Spectrometry (LA-ICP-MS) with three primary goals: 1) fingerprint metasedimentary rocks by determining the sediment source areas of the protolith; 2) estimate the maximum depositional age of the protolith; and 3) date igneous intrusions in the map areas. At UC

Davis, the lead author used standard crushing techniques, a miner's gold pan, Frantz isodynamic separator, and Lithium Polytungstate heavy liquid to concentrate zircon grains. Our mineral separation protocol for detrital zircon analysis involves concentrating zircon grains sufficiently to mount all of the grains by pouring, whereas for analysis of igneous grains we pick relatively large, inclusion-sparse grains. Prior to U-Pb analysis, all zircon grains and reference materials are mounted into 1" epoxy rounds, polished to expose the grain interiors, and imaged using the Cameca SX-100 Electron Microprobe housed in the Earth and Planetary Sciences department at UC Davis. The resulting high-contrast back-scattered electron images allow us to identify zoning and/or inherited cores in individual zircon grains, which inform our laser spot placement on each grain. We collected U-Pb data in two LA-ICP-MS laboratories: the Arizona Laserchron Center (ALC) in 2016 and 2017, and UC Davis in 2018. Supplemental file S1 contains detailed mineral extraction, analytical, data reduction, and data filtering methods used in the LA-ICP-MS analysis.

***Data representation***

Our fingerprinting of metasedimentary protoliths is based on analyzing distinctive populations of detrital zircon single grain U-Pb dates. To ensure that our comparisons between samples are statistically robust, each detrital zircon age dataset contains analyses on at least 117 grains (Vermeesch, 2004). We represent the data as Kernel Density Estimates (KDEs) using the Density Plotter program (Vermeesch, 2012). Because many of the rocks analyzed in our study experienced amphibolite and upper greenschist metamorphic temperatures and thus may have experienced metamorphic recrystallization and/or lead loss (e.g., Hoskin and Schaltegger, 2003), we take a conservative approach to calculating maximum depositional ages by calculating the weighted mean of the youngest statistical population of detrital grains (Herriott et al., 2019). The

ages of igneous zircon populations are determined by a weighted mean of single grain dates with propagated 2 sigma errors. Weighted mean ages are calculated and plotted using Isoplot (Ludwig, 2008). Reported uncertainties of weighted mean ages represent 95% confidence interval internal uncertainties and the quadratic addition of external uncertainties (e.g., Horstwood et al., 2016) (Supplemental files S1 and S2).

**$^{40}$Ar/$^{39}$Ar Thermochronology:**

$^{40}$Ar/$^{39}$Ar analysis was performed at the Geochronology laboratory at the University of Alaska, Fairbanks where samples were crushed, sieved, washed and hand-picked for a pure mineral phase of biotite, muscovite, or amphibole. The analyzed size fractions are given in Table 1. The mineral fractions and monitor mineral MMhb-1 (Samson and Alexander, 1987), which has an age of 523.5 Ma (Renne et al., 1994), were irradiated at McMaster University in Hamilton, Ontario, Canada. Upon their return from the reactor, the samples and monitors were loaded into 2 mm diameter holes in a copper tray and then loaded in an ultra-high vacuum extraction line. The monitors were fused, and samples heated, using a 6-watt argon-ion laser following the technique described in York et al. (1981), Layer et al. (1987), and Benowitz et al. (2014). Ar isotope measurements in this system were made using a VG-3600 mass spectrometer.

Supplemental file S3 contains detailed $^{40}$Ar/$^{39}$Ar analytical methods and summarizes the $^{40}$Ar/$^{39}$Ar results, wherein all ages are quoted at the 1 sigma level and calculated using the constants of Renne et al. (2010). The integrated age is the age given by the total gas measured and is equivalent to a potassium-argon (K-Ar) age. The spectrum provides a plateau age if three or more consecutive gas fractions represent at least 50% of the total gas release and are within two standard deviations of each other (mean square weighted deviation < 2.5).

### Spinel Geochemistry

Spinel geochemistry was determined using the Cameca SX-100 electron microprobe at UC Davis. The analysis used a beam intensity of 20 nA and voltage of 15 kV focused into a 1 um spot size. Analyses were calibrated to natural spinel reference materials. $Fe_2O_3$ and FeO were calculated from $Fe_{Total}$ using a Microsoft Excel-based calculation tool available from www.serc.carleton.edu/research_education/equilibria/mineralformulaerecalculation.

## RESULTS

### Map unit definitions, protolith ages, and primary structural features

We present new bedrock mapping from two locations along the southern margin of the Alaska Range suture zone in the eastern Alaska Range: Broxson Gulch (Figure 2A) and Ann Creek (Figure 2B). Our mapping and definition of rock units differs from previous workers in the area because we defined map units on the basis of protolith composition and age. This distinction is particularly important for metasedimentary rocks in the northern portion of the map areas. There are three primary bedrock lithologic packages in the map areas: Maclaren schist and associated felsic plutons, Clearwater metasedimentary rocks and associated intermediate-ultramafic intrusions, and Wrangellia meta-igneous rocks. A suite of N-dipping brittle faults juxtaposes these rock packages in both map areas. Here we describe the rock units and major structures from north to south.

#### *Geology between the Wrangellia terrane and Denali fault*

The Maclaren schist (map unit Ks) is a dark grey, quartzofeldspathic schist that occupies the highest structural level in our map areas (Figure 3A). Albite and, less commonly, garnet

porphyroclasts contain curved or spiral inclusion trails ($S_1$), which comprise rutile and graphite (Figure 4A). The inclusion trails cause the albite to appear nearly black in hand sample. Phyllosilicate minerals and graphite define a strong foliation ($S_2$), which is deflected by the porphyroclasts (Figure 4A). Quartz-rich pressure shadows around the porphyroclasts create a linear fabric element contained within $S_2$ that generally plunges down-dip to the north. Biotite parallel to the $S_2$ foliation is typically partly replaced by chlorite, except at the highest structural level (e.g., sample 16ATW-73–Figure 2A) where biotite overgrows the $S_2$ foliation (Figure 4B). Meso-scale asymmetric quartz vein boudinage parallels $S_2$ and shows top-to-the-south thrust kinematics (Figure 3B). Discontinuous cm-to-m-thick carbonate-rich lozenges also parallel $S_2$. Rare pelitic intervals contain relict kyanite, staurolite, and garnet, which are partially replaced by retrograde metamorphic assemblages. We use the peak assemblage to infer that the entire package of Maclaren schist reached amphibolite facies conditions (see also Davidson et al., 1992; Davidson and McPhillips, 2007).

A quartz monzonite body (Map unit Pgqm) intruded across the foliation in the Maclaren schist north of the Valdez Creek fault (Figures 2B and 3C). The quartz monzonite is not foliated and contains xenoliths of Maclaren schist (Stout, 1965; our observations). Zircon separated from one sample of the quartz monzonite (15ATW-47) yielded a U-Pb date of 51.9 ± 0.6 Ma (Figures 2B and 5) (Table 2). Farther west, a suite of ca. 75-70 Ma tonalitic rocks intrudes the Maclaren schist and along the Valdez Creek shear zone (Aleinikoff et al., 1981; Ridgway et al., 2002).

The Clearwater metasedimentary package (map units Jms, Jmg, Js) is a lithologically heterogeneous unit structurally below the Maclaren schist (Figure 3A). Rock types in the Clearwater metasediments include metagreywacke, graphite-muscovite-chlorite phyllitic schist, porphyroblastic pyrite-graphite phyllite, argillaceous slate, and albite-actinolite-epidote-chlorite

schist. We distinguish map units based on the prevalence of rock types (Jms-mafic schist, Jmg-metagreywacke, Js-slate). Our naming convention is based on that of Mooney (2010), who documented a nearly identical belt of low grade metasedimentary strata and inter-bedded lava flows in the Clearwater mountains ~60 km to the west of our study area. The Clearwater metasediments in our map areas generally display an increase in flattening strain, mica content, and feldspar recrystallization from south (lowest structural level) to north (highest structural level) (Figures 4C-E). The nearly ubiquitous presence of chlorite, epidote, and actinolite suggests that the belt experienced greenschist facies peak metamorphic conditions. The package displays a strong transposition fabric, wherein the $S_1$ foliation is isoclinally folded thereby creating $S_2$ axial surfaces parallel to $S_1$. Folding of the $S_1$ foliation manifests as tight crenulation folds (Figures 3D and 4C) and as folded quartz veins (Figure 3E). Crenulation axes in the metasediments generally plunge modestly to the west-southwest and are interrupted by sub-vertical opening fractures (Figures 3D and 6A).

The Clearwater metasediments are locally interfoliated with metamorphosed ultramafic rocks. Ultramafic rock types include serpentinite, amphibolite, and lesser talc-chlorite schist. The ultramafic rocks generally display a strong foliation defined by serpentine, Cr-chlorite, actinolite, and lesser fuchsite and talc (Figure 4F). Relict chromite in the serpentinite shows reaction textures involving brucite, Cr-chlorite, Cr-magnetite, and millerite (Supplemental file S4). Broxson Gulch also contains an outcrop (~24,000 $m^2$ map area) of unfoliated amphibolite (locale 16ATW-43), which contains amphibole up to 3 cm in diameter (Figure 3F). The coarse amphibole displays zoning consisting of hornblende cores that have reacted to patchy actinolite zones and rims (Supplemental file S4). Matrix minerals in the coarse amphibolite include titanite, epidote, chloritized biotite, and apatite (Supplemental file S4). The serpentinite and talc-chlorite schists are

interfoliated and folded with the Clearwater phyllitic schist (Figure 6A), whereas amphibolite pods are generally associated with Clearwater mafic schist (map unit Jmg).

A suite of small volume igneous bodies intruded the Clearwater metasedimentary rocks. In Broxson Gulch, these intrusive bodies are typically amphibole-bearing intermediate dikes up to one meter thick. The dikes intrude along, and locally display stretching parallel to, the $S_1$ foliation. Chlorite and/or actinolite form pseudomorphs of primary amphibole in the dikes. One dike sample from Broxson Gulch (15ATW-05) yielded an $^{40}Ar/^{39}Ar$ whole rock plateau age of 100.7 ± 1.6 Ma (Table 1; Supplemental file S5). Phyllite in the contact aureole of another amphibole dike yielded a population of high U/Th (up to ~6300) zircon grains that gave a weighted mean U-Pb age of 103.4 ± 1.6 Ma (Supplemental file S5). In the Ann Creek map area (Figure 2B) a tabular-shaped granodiorite body intruded the metagreywacke subunit of the Clearwater metasediments (Jmg) immediately north of the Broxson Gulch fault. The granodiorite contains a weak foliation defined by the alignment of amphibole and plagioclase along a plane sub-parallel to the margins of the body. The northern contact of the granodiorite displays co-magmatic textures with a pegmatitic hornblende-biotite pyroxenite (Stout, 1965; our observations). Amphibole from the pyroxenite body yielded K-Ar dates of 91.9 ± 2.8 Ma and 97.7 ± 2.9 Ma (Nokleberg et al., 1992b). One sample of the granodiorite (15ATW-51) yielded a U-Pb date of 102.4 ± 1.1 Ma (Figures 2B, 5; Table 2).

***Faulting between the Wrangellia terrane and Denali fault***

Two major north-dipping brittle faults, the Valdez Creek and Broxson Gulch faults, intersect metasedimentary rock units in the map areas (Figure 3A). Previous maps of the region emphasize the importance of the Broxson Gulch fault due to the juxtaposition of distinct rock types across it. Our mapping highlights the importance of the Valdez Creek fault as an important

reactivated structure juxtaposing distinct metasedimentary rock packages north of the Broxson Gulch fault.

The herein-named Valdez Creek fault places the Maclaren schist over the Clearwater metasediments and associated ultramafic rocks. In outcrop, the Valdez Creek fault is an ~10-15-meter-wide zone of clay-rich damaged rock. Hanging wall Maclaren schist adjacent to the Valdez Creek fault is intensely retrograded to lower greenschist facies assemblages and locally contains meso-scale asymmetric folds that indicate top-to-the south shear (Figure 3G). Antithetic brittle faults and quartz veins in opening fractures near the fault zone cross the metamorphic folia in adjacent rocks at a high angle (Figures 3H and 6B-D). Dispersed brittle faults over a ~1 km wide zone parallel the metamorphic foliation in the structurally lowest portion of the Maclaren schist and presumably record distributed hanging wall deformation related to slip on the Valdez Creek fault. Slickenlines on the foliation-parallel brittle slip surfaces within the Maclaren schist indicate reverse motion with a minor dextral component (Figure 6E).

The Broxson Gulch fault places the Clearwater metasediments and associated intrusions over Wrangellia rocks and is typically marked by a 30-to-50-meter-thick zone of brittle deformation. The core of the Broxson Gulch fault damage zone is not well exposed in the map areas. However, one exposed cross section of the fault in northeastern Broxson Gulch contains a ~1-meter-thick clay-rich principle shear plane oriented at approximately 265/50ºN in the core of a distributed brittle deformation zone. Brittle fault striae from the clay-rich zone at this locale plunge down dip and record reverse motion (Figure 6F). Damage associated with slip on the Broxson Gulch fault is distributed into the hanging wall where it is localized along foliation planes within the Clearwater metasediments.

***Geology of the Wrangellia terrane***

Wrangellia metavolcanic strata and associated intrusions occupy the footwall of the Broxson Gulch fault (Figures 2 and 3A). Wrangellia stratigraphy in this region of the Alaska Range consists of Carboniferous volcanic and volcaniclastic strata overlain by lesser Permian carbonate strata and regionally extensive Triassic flood basalts. Both the Carboniferous and Triassic volcanic strata have intrusive igneous rocks associated with them.

Carboniferous volcanic rocks (map unit CPvs) in southern Alaska have been called the Tetelna volcanics (Mendenhall, 1905; Bond, 1973, 1976; Stout et al., 1976), Skolai group (Smith and MacKevett, 1970), and Slana Spur–Eagle Creek formation (Nokleberg et al., 1985; 1992a). Nomenclature aside, the strata provide a record of a Carboniferous island arc, which has been named the Skolai arc (Bond, 1973; Beard and Barker, 1989), thus we herein refer to them as the Skolai arc strata. The stratigraphy of the Skolai arc in Broxson Gulch and Ann Creek is similar to that documented by Bond (1973) for a region approximately 20 km to the east: massive mafic volcanic rocks lower in the section, intermediate volcanic rocks and pyroclastic flow deposits in the middle of the section, and volcaniclastic and carbonate strata near the top of the >3000-meter-thick section. Some of the carbonate strata contain early Permian fossils (Bond, 1973; Nokleberg et al., 1992b, Richter and Dutro, 1975). We combined these strata with the Carboniferous strata for the purpose of our mapping. Igneous bodies of diorite-to-tonalite composition intruded the lower and middle portion of the Skolai arc strata (map unit Ci). Primary biotite and hornblende in the intrusions show reaction textures involving chlorite and actinolite. Skolai strata in the contact aureoles of the intrusions display a strong foliation defined primarily by chlorite, which parallels the margins of the intrusion (Figure 2A). Primary volcanic features are preserved farther from the intrusive rocks (Figure 3I). Three samples of representative intrusive igneous rock types from

Broxson Gulch yielded zircon suitable for analysis by LA-ICP-MS: 16ATW-49–diorite–314.3 ± 3.4 Ma; 16ATW-82–tonalite–310.9 ± 3.4 Ma; 16ATW-83–tonalite–306.9 ± 2.6 Ma (Figures 2A and 5) (Table 2). Zircon from one quartz diorite body exposed at the mouth of Ann Creek (18ATW-22) yielded a U-Pb date of 301.8 ± 5.5 Ma (Figures 2B and 5) (Table 2).

Massive aphanitic basalt flows and lesser interbedded carbonate unconformably overlie the Skolai arc rocks. The basalt flows belong to the Upper Triassic Nikolai flood basalt province (map unit Trn), which has been described in detail to the southwest and southeast of our study area (e.g., Greene et al., 2008, 2010). Large (>1 km across) bodies of gabbro and dunite (map unit Trum) related to the flood basalts are present within the Skolai and Nikolai strata. Twelker et al. (in revision) documented at least one location where Nikolai lava flows were deposited unconformably onto the gabbro-dunite complex. Secondary chlorite, actinolite, and serpentine indicate that both intrusive and extrusive Nikolai rocks experienced greenschist facies metamorphic conditions. Biostratigraphic and radiometric (U-Pb and $^{40}Ar/^{39}Ar$) age determinations yield dates of ca. 225-230 Ma for Nikolai strata (see Greene et al., 2010). Gabbro bodies in the region yielded $^{40}Ar/^{39}Ar$ biotite and hornblende dates of ca. 225-228 Ma (Bittenbender et al., 2007; Benowitz et al., 2017). We discovered an outcrop of pegmatitic hornblende-biotite-gabbro within the Nikolai gabbro-dunite complex in the Ann Creek map area (18ATW-13; Figure 2B). Zircon from this sample yielded a U-Pb date of 229.2 ± 2.0 Ma (Figure 5) (Table 2).

***Cenozoic cover strata***

Isolated exposures of fluvial and alluvial gravels (map unit Czg) unconformably overlie Skolai and Nikolai rocks in the central and southern portions of the map areas. Most exposures are

clast supported, poorly bedded, and poorly-to-moderately sorted (Supplemental file S6). Exposures in the Ann Creek map area (Figure 2B) generally contain subangular to subrounded clasts, whereas exposures in Broxson Gulch (Figure 2A) contain subrounded to rounded clasts. The clasts are composed of various proportions of volcanic, intrusive igneous, carbonate, and low-grade metamorphic rocks (Figure 7). Clasts of volcanic and metavolcanic rock are common among all exposures. Dunite and gabbro clasts are abundant in gravel exposures in the Ann Creek map area. Gravel exposures in the Broxson Gulch map area lack ultramafic clasts and instead contain a significant proportion of felsic intrusive igneous rocks. Low-grade metasedimentary rocks, carbonate, and quartz constitute subordinate clast populations in all of the exposures. Although the clast rounding, clast composition, detrital zircon age spectra, and structural position differ for each gravel exposure, we classify all of the gravel deposits into a single map unit for the purpose of this study.

***Faulting within the Wrangellia terrane***

Three major structures offset the Wrangellia bedrock and cover strata. From north to south, these structures are the Muddy Creek, Airstrip, and Rainy Creek faults.

The herein named Muddy Creek fault cuts through Wrangellia strata and associated intrusive rocks. Good exposures of the fault are found in the cliffs above Muddy Creek (Ann Creek map area: Figure 2B) and on a ridge in the central part of Broxson Gulch (Figure 2A). The fault can be accessed easily in Broxson Gulch, where it is a narrow (<10 meter) zone of serpentinized and cataclasized Nikolai flood basalt that dips to the northeast. A hanging wall imbricate carrying the gabbro-dunite complex steps up from the Muddy Creek fault ~500 m north of this locale, suggestive of duplexing within the Nikolai ultramafic rocks. The Alaska DGGS mapped a structure

in the Amphitheater Mountains ~10 km to the south of our map areas that we interpret to be an equivalent structure because it juxtaposes the same suites of rocks and also displays evidence of duplexing. They call this the fault the Fish Lake fault (Twelker et al., in revision). Evidence for duplexing and stratigraphic duplication associated with the Fish Lake-Muddy Creek fault suggest top-to-the southwest thrust kinematics (Twelker et al., in revision). The Broxson Gulch and Airstrip faults both appear to cut at a low angle or merge with the Muddy Creek fault (Figure 2). We favor a cross-cutting relationship because the Muddy Creek fault strikes more northwesterly than other faults in the map areas and has no demonstrable Cenozoic slip.

The Airstrip fault, first named by Rose (1965), places Skolai rocks and intrusive Nikolai rocks over Nikolai flood basalts and overlying Cenozoic gavel deposits in the center of the map areas. Our mapping of the Airstrip fault in Broxson Gulch is similar to that of Rose (1965), yet we were able to track the fault to both the east and west. Parallel to the strike of the fault, we mapped a synform in the footwall of the Airstrip fault, which contains Wrangellia meta-igneous rocks, Clearwater slate, and possibly the Muddy Creek fault (Figure 2). Despite an ~50-meter-thick zone of damaged rock associated with the fault trace, the core of the Airstrip fault damage zone is not well enough exposed to yield reliable kinematic indicators. However, we infer top-to-the-south reverse kinematics based on the associated synform and preservation of Cenozoic gravels in the footwall of the fault (Figure 2).

The Rainy Creek fault, first named by Nokleberg et al. (1985) is the range-bounding fault in the region. It is not exposed in Broxson Gulch and is poorly exposed in Ann Creek, but it shows up in both regions as a significant aeromagnetic and resistivity boundary because it places Triassic ultramafic rocks over Cenozoic gravels (Nokleberg et al., 1992a) (Figure 2; Supplemental file 7). Our mapping of the Rainy Creek fault is most similar to that of Nokleberg et al. (2015). We do not

have kinematic information for the Rainy Creek fault due to the lack of exposure. However, we infer primarily top-to-the-south thrust slip due to the location of the fault at the topographic range front, the shallow dip of the fault, and the juxtaposition of Wrangellia rocks in the hanging wall against Cenozoic gravels in the footwall.

## Detrital zircon U-Pb geochronology

### *Age spectra from metasedimentary rocks*

Detrital zircon U-Pb age spectra from two samples of Maclaren schist primarily display grains of Jurassic and Cretaceous age (Figure 8; Supplemental file S2). Grains with dates of ca. 85-95 Ma constitute the largest age population in each sample (45-85%). Other Phanerozoic age populations include ca. 160, 185, and 330-350 Ma. A distribution of Precambrian grains ranging from ca. 620-2800 Ma accounts for less than 10% of either Maclaren schist sample (Figure 9).

Detrital zircon U-Pb age spectra from all four samples of the Clearwater metasediments display nearly identical bimodal detrital age populations centered at ca. 155-160 Ma and 185-190 Ma (Figure 8; Supplemental file S2). The late Jurassic age population comprises the majority (55-75%) of the grains in all samples. Pre-Mesozoic grains are uncommon in the Clearwater metasediments, yet each sample yielded five or fewer grains at ca. 425 Ma and ca. 1100-1700 Ma (Figure 9). Sample 15ATW-52 yielded one grain with an age of 2785 Ma. Zircon grains extracted from Clearwater phyllite in the contact aureoles of the ca. 100 Ma amphibole-bearing dikes (samples 15ATW-07 and 16ATW-44b) display a sieve texture around the rims of the crystals and typical sector zoning patterns in the interiors of the crystals (Supplemental file S5). Laser spots placed on the concentric- or sector-zoned interiors of the zircon crystals yielded Jurassic dates commensurate with the other Clearwater samples. Laser spots placed near regions of sieve texture

generally yielded dates of ca. 80-120 Ma, but cluster at ca. 100 Ma. These dates are associated with elevated and variable U/Th ratios (Supplemental files S2 and S5). The population of Cretaceous high U/Th grains yielded a weighted mean U-Pb date of 103.4 ± 1.6 Ma (Figure 8; Supplement S5).

### *Age spectra from Cenozoic gravel deposits*

Cenozoic and Mesozoic grains dominate the detrital zircon U-Pb age spectra from three samples of Cenozoic gravel deposits in Broxson Gulch (Figure 10; Supplemental file S2). The structurally highest sample (16ATW-77) displays a nearly bimodal distribution of grain dates split between ca. 60 Ma (63%) and ca. 100 Ma (20%) populations. Jurassic-aged grains compose a minor age population at ca. 160 Ma (4%). In the intermediate structural position, sample 15ATW-06 displays a nearly unimodal age distribution wherein 83% of the analyzed grains constitute a single age population at ca. 30 Ma. Grains with ages of ca. 145 Ma (5%), 230 Ma (7%), and 305 Ma (3%) constitute subordinate age populations in this sample. Sample 16ATW-86 occupies the lowest structural position and displays the most heterogeneity in detrital ages from the dated Cenozoic gravel deposits. A bimodal distribution of Jurassic grains comprises the majority (79%) of the analyzed grains. The Jurassic population is contains modes at ca. 155 Ma and 185 Ma. The remaining grains compose smaller populations at ca. 310 Ma (13%), 60 Ma (2%), and 6 Ma (3%; n = 7). Grains with dates older than 400 Ma constitute less than 3% of analyzed zircon grains from all samples. Recurring >400 Ma age populations include: 430-470 Ma, 1500-1800 Ma, and 2300-2700 Ma.

## $^{40}Ar/^{39}Ar$ thermochronometry

We dated K-bearing mineral phases from samples in the hanging wall of the Broxson Gulch fault using the $^{40}Ar/^{39}Ar$ method, which resulted in one amphibole, three white mica, and three biotite dates (Table 1; Supplemental file S3).

### *Broxson Gulch map area*

Biotite and muscovite from the Maclaren schist in Broxson Gulch yield late Eocene-Oligocene dates (Figure 11). The $S_2$ foliation in the structurally highest sample (16ATW-73) is defined by intergrown muscovite, chlorite, and graphite. Biotite in this sample overgrows the $S_2$ foliation with a porphyroblastic texture (Figure 4B) and yielded a plateau age of 32.8 ± 0.3 Ma. Sample 15ATW-08 is located at a low structural level in the Maclaren schist near the Valdez Creek fault (Figure 2A). Biotite in this sample is oriented sub-parallel to the $S_2$ foliation, shows reaction textures involving chlorite, and yielded a weighted mean age of 45.9 ± 0.3 Ma.

Amphibole and mica from Clearwater metasediments and ultramafic rocks in Broxson Gulch yield mid-Cretaceous-earliest Paleogene dates (Figure 12). The zoned amphibole from the coarse amphibolite block (Supplement S4) in Broxson Gulch (16ATW-43c) yielded an $^{40}Ar/^{39}Ar$ release spectrum that displays a loss pattern, which is matched by the K/Ca spectrum over the same range of gas release steps (Figure 12). Our preferred date for the amphibole is the 93.8 ± 0.7 Ma weighted mean date because the duration of consistent gas release defining the date corresponds to a constant K/Ca ratio, which we infer to record Ar release from the K-bearing hornblende cores of the amphibole crystals. Sample 15ATW-35 is a serpentine-chlorite-brucite schist with minor kinked fuchsite sub-parallel to the foliation (Figure 4F). The fuchsite yielded a plateau age of 65.1 ± 0.4 Ma. One sample of muscovite graphite schist (16ATW-36) interfoliated with Clearwater

mafic schist yielded a similar plateau age of 64.3 ± 0.7 Ma. Muscovite in this sample is folded with the foliation and only locally is partially recrystallized into tabular grains near the crenulation axes (Figure 4D).

### *Ann Creek map area*

In the Ann Creek map area, the ca. 52 Ma quartz monzonite pluton carried in the hanging wall of the Valdez Creek fault contains a network of late cross-cutting pegmatite dikes. One sample of pegmatite (15ATW-45) yielded biotite and muscovite suitable for $^{40}Ar/^{39}Ar$ analysis. Biotite from this sample yielded a plateau age of 37.7 ± 0.6 Ma, whereas the muscovite gave a plateau age of 50.2 ± 0.5 Ma (Figure 11).

## Spinel Geochemistry

Ultramafic rocks hosted within the Clearwater metasediments contain minor (≤10%) proportions of opaque minerals including spinel group minerals, ilmenite, millerite, and chalcopyrite. The spinel group minerals display a variety of compositions ranging from chromite to magnetite with minor to moderate substitution of Ti, Mn, Mg, and Zn. Chromite-rich grains display reaction textures involving millerite, magnetite, and brucite (Supplement S4). Chromite cores and rims display Cr# ($Cr/[Cr + Ti + Al + Fe^{3+}]$) values ranging from 0.5-0.8 and $Fe^{2+}$# ($Fe^{2+}/[Mg + Mn + Fe^{2+}]$) ranging from 0.4-0.95 (Figure 13). Magnetite-rich grains display Cr# less than 0.3 and $Fe^{2+}$# values near 1 (Figure 13). Supplemental file S8 contains electron microprobe data of the spinel group phases.

## DISCUSSION

### Interpretation of geochronology and thermochronology

#### *Sediment source areas, unit ages, and terrane associations*

*Mesozoic metamorphic rocks*

Although the detrital zircon U-Pb age spectra for both the Maclaren schist and Clearwater metasedimentary rocks are dominated by Mesozoic ages, each unit records sediment input from distinct source areas inboard and outboard of the Denali fault. It is important to recognize that the eastern Denali fault has experienced more than 400 km of Cenozoic dextral displacement (Nokleberg et al., 1985). Moreover, stratigraphic studies of the Kahiltna assemblage demonstrate the predominance of margin parallel sediment transport as the strata were deposited (Ridgway et al., 2002; Kalbas et al., 2007). Therefore sediment provenance areas for metasedimentary rocks in our study area may be located several hundred kilometers along strike to the southeast.

Key detrital zircon U-Pb age populations in the Maclaren schist include: 85-100 Ma, 140-210 Ma, and 330-370 Ma (Figure 9). The distribution of Paleoproterozoic zircon grains and quartzofeldspathic-to-pelitic composition together suggest that the Maclaren schist protolith received detritus from a continental source area inboard of the Denali fault. Cretaceous and Jurassic igneous belts are abundant throughout British Columbia and Yukon (Gehrels et al., 2009; Allan et al., 2013) and represent a likely source area for Mesozoic age populations in the Maclaren schist. Devonian-to-early Mississippian igneous rocks are widespread in the Yukon-Tanana terrane in east-central Alaska and Yukon (Dusel-Bacon and Williams, 2009) and are a likely source for the mid-Paleozoic zircon population in the Maclaren schist. A Yukon-Tanana terrane source for the mid-Paleozoic grains is also supported by the presence of ca. 1.7-2.8 Ga detrital grains because the Yukon-Tanana terrane igneous rocks intruded into Paleozoic and Neoproterozoic

Laurentian continental margin rocks, which contain abundant Paleoproterozoic detrital zircon grains (Dusel-Bacon and Williams, 2009; Piercey and Colpron, 2009; Gehrels and Pecha, 2014; Pecha et al., 2016; Dusel-Bacon et al., 2017). In sum, detrital zircon age data suggest that the protolith of the Maclaren schist was principally sourced from Jurassic and Cretaceous igneous belts that were built on the western margin of North America. Considering the maximum depositional ages of ca. 94 and 86 Ma (Figure 8) places the Maclaren schist protolith in a basin system along the western margin of North America after 94 Ma. By ca. 75 Ma, the Maclaren schist was undergoing regional amphibolite facies metamorphism (Davidson et al., 1992; Ridgway et al., 2002).

The Clearwater metasedimentary rocks contain two major detrital zircon U-Pb age populations: 150-160 Ma and 175-200 Ma (Figure 9). Although sediment source areas of this age range are present inboard of the Denali fault (e.g., Gehrels et al., 2009; Allan et al., 2013), the dearth of Paleozoic and Precambrian zircon grains and generally mafic composition of the Clearwater metagreywacke suggest a sediment source within oceanic arc terranes outboard of the Denali fault. Jurassic source areas outboard of the Denali fault include Chitina arc rocks (ca. 160-140 Ma- Roeske et al., 2003; Day et al., 2016; Beranek et al., 2017) and Talkeetna arc rocks (ca. 205-150 Ma- Roeske et al., 1989; Amato et al., 2007b; Rioux et al., 2007). The scant Paleozoic (ca. 415 Ma) and Precambrian (ca. 1100, 1500, 2800 Ma) grains can be traced to Paleozoic sedimentary and igneous rocks within the Alexander terrane (e.g., Gehrels et al., 1996; Kapp and Gehrels, 1998; Beranek et al., 2013; White et al., 2016) or to the Tlikakila complex in the western Alaska Range (Amato et al., 2007a). On the basis of these data, we infer that the protolith of the Clearwater metasedimentary rocks was sourced primarily from Chitina and Talkeetna arc rocks and thus was likely deposited along the paleo-eastern margin of the Wrangellia composite terrane.

The protolith age is bracketed to 151-142 Ma by the maximum depositional ages of individual samples of the Clearwater metasediments (151-to-156 Ma-Figure 8) and intrusion of a ca.142 Ma alkali gabbro in the Clearwater Mountains (Mooney, 2010).

Association between the Clearwater metasediments and the Wrangellia composite terrane is also supported by the presence of ca. 100 Ma ultramafic to intermediate magmatism within the metasediments. Our data indicate that the Clearwater metasediments host a suite of ca. 100 Ma intermediate igneous intrusions and ultramafic cumulates (aforementioned hornblende-biotite-pyroxenite). Similar, albeit somewhat older (ca. 120 Ma), ultramafic and intermediate intrusive rocks have been mapped as intruding into Wrangellia rocks and Nutzotin basin strata ~30-50 km to the southeast of the Ann Creek map area (Bittenbender et al., 2007; Synder and Hart, 2007; Wilson et al., 2015). Farther to the southeast, ca. 100-115 Ma ultramafic and intermediate rocks have been described in southeast Alaska (Duke Island suite) and in the Yukon Territory (Pyroxenite Creek and Shorty Creek suites), where they form a series of compositionally zoned intrusions within the western Gravina belt, Alexander terrane, and Dezadeash formation (Eisbacher, 1976; Saleeby, 1992; Himmelberg and Loney, 1995). The zoned ultramafic intrusions in southeast Alaska and adjacent Yukon are geochemically distinct among ultramafic magmatic suites globally and have thus earned their own classification as “Alaska-type” ultramafic suites (Barnes and Roeder, 2001). Although the ca. 100 magmatic suite in the Clearwater metasediments does not clearly display the zoned structure common of other Alaska-type ultramafic localities, the spinel compositions from ultramafic rocks in our study areas plot among the Cr# and $Fe^{2+}$# values from other Alaska-type zoned ultramafic complexes (e.g., Barnes and Roeder, 2001) (Figure 13). The age, spinel geochemistry, petrography, and distribution of rock types together make a strong case that ultramafic cumulates and associated intermediate composition intrusive rocks within the

Clearwater metasediments represent a faulted and metamorphosed portion of an Alaska-type ultramafic intrusion rather than a structurally entrained fragment of lithospheric mantle or Nikolai intrusive rocks. Due to the clear connection between the Dezadeash formation and western Gravina belt with the Wrangellia composite terrane (e.g., Lowey, 1998, 2011, 2018; Yokelson et al., 2015) and the presence of early Cretaceous ultramafic bodies within Wrangellia in the Alaska Range (Bittenbender et al., 2007), it appears that the Alaska-type zoned magmatic suite formed across the paleo-eastern margin of the Wrangellia composite terrane.

The similarity in detrital zircon U-Pb age spectra between the Clearwater metasediments, Dezadeash formation, and western Gravina belt (cf., Mooney, 2010; Yokelson et al., 2015; Link, 2017; Lowey, 2018; this study) suggests that the Clearwater metasediments are part of the dismembered late Jurassic-early Cretaceous basin system at the inboard margin of the Wrangellia composite terrane. The proximity of the hornblende-biotite-pyroxenite in the Ann Creek map area to the Denali fault suggests that it may be an offset portion of the Pyroxenite Creek ultramafic body, which intrudes the Dezadeash formation and is cut by the Denali fault in southwestern Yukon Territory (Eisbacher, 1976). Such correlation is consistent with other estimates of >400 km of Cenozoic dextral separation on the Denali fault (Nokleberg et al., 1985).

*Cenozoic gravel deposits*

Exposures of Cenozoic gravels at the southern flank of the Alaska Range display a variety of clast compositions and detrital zircon U-Pb age spectra that suggest a range of proximal and distal source areas. Clast populations from exposures in the Ann Creek map area indicate that Paleozoic and Triassic rocks within Wrangellia were the primary sediment source areas (Figure 7). Alternatively, clast assemblages from exposures in Broxson Gulch suggest more heterogeneous

source areas that include felsic intrusive rocks and low-grade metasedimentary rocks. We infer that the heterogeneity in the characteristics of the Cenozoic gravel deposits in the map areas reflects variability in depositional setting for each of these deposits. For example, 18ATW-14 (Figure 2B) contains angular clasts of underlying Wrangellia rock (Figure 7) and therefore may represent a preserved portion of a local alluvial deposit. In contrast, 16ATW-77 (Figure 2A) contains rounded clasts of rock types that are not found near the sample location and thus were likely carried to their present location by a larger fluvial system. Aside from evidence for both local and distal sediment sources, the lack of Maclaren schist detritus in the gravel deposits suggests that the sediment source areas feeding the basins did not intersect the Maclaren schist.

The detrital zircon U-Pb age spectrum for 16ATW-77 displays a predominance of ca. 60 Ma and 100 Ma grains. Given the abundance of felsic igneous clasts in the deposit (Figure 7), we infer that these age populations record input from a source area rich in Paleogene and Cretaceous plutonic rocks. The population of ca. 100 Ma plutonic rocks may be locally sourced from the granodiorite body exposed in the Ann Creek map area (sample 15ATW-51–102.4 ± 1.1 Ma). The nearest potential source area for the Paleogene plutonic clasts is west of our study area in the northern Talkeenta Mountains (Csejtey et al., 1986; Davidson and McPhillips, 2007). In the northern Talkeetna Mountains, Paleogene plutons intruded into metasedimentary strata that contain Jurassic detrital zircon grains (cf., Davidson and McPhillips, 2007; Hults et al., 2013; Link, 2017; Hampton et al., 2010). These late Jurassic metasedimentary rocks provide a probable source for the low-grade metamorphic clasts and late Jurassic detrital zircon grains in sample 16ATW-77. Given that the youngest age population of detrital zircons (ca. 60 Ma) in sample 16ATW-77 is likely derived from plutonic rocks, it is tenable that the true depositional age is significantly

younger than the maximum depositional age determined from the detrital zircon U-Pb age distribution (ca. 54 Ma–Figure 10).

Sample 15ATW-06 also contains a suite of detrital zircon U-Pb dates that suggest derivation from a distal source area. The primary ca. 30 Ma age population in this sample cannot be traced to any local source in the Alaska Range or Talkeetna mountains, but does coincide with the onset of volcanism in the Wrangell Arc to the southeast of our study area and may reflect deposition of airfall ash deposits, although none were identified in the field (Berkelhammer et al., 2019; Brueseke et al., 2019). The minor ca. 145 Ma age population may be sourced from Chitina arc igneous rocks or early Cretaceous strata exposed in the Nutzotin Mountains (e.g., Manuszak et al., 2007; Trop et al., 2020). Both low-grade metasedimentary and plutonic clasts are present in 15ATW-06 (Figure 7), thus allowing for either source area. Triassic (ca. 230 Ma) and Carboniferous (ca. 300-310 Ma) zircon grains constitute the remaining minor age populations in the sample. These ages correlate well with the known ages of Nikolai and Skolai igneous provinces, which are widespread throughout the Wrangellia terrane (e.g., Beard and Barker, 1989; Greene et al., 2010; this study). As such, either proximal or distal source areas for Triassic and Carboniferous zircon grains are permissible. The maximum depositional age determined from the youngest population of zircon ages (ca. 30 Ma) is in agreement with Oligocene and Late Oligocene biostratigraphic ages (Metasequoia fossils) from an outcrop ~1 km to the south of 15ATW-06 (Stout et al., 1976; Locality #12 of Nokleberg et al., 1992b). We thus assign an Oligocene age to the deposit.

The southernmost sample (16ATW-86) represents the most heterogeneous zircon age distribution of the Cenozoic gravel deposits. However, the age populations can generally be traced to local source areas. Unlike the 16ATW-77 and 15ATW-06, the youngest age population (ca. 6

Ma) in sample 16ATW-86 is not the largest. Instead, the largest population comprises a ca. 155 Ma and 185 Ma bimodal distribution of Jurassic grains, which are identical to the ages and relative proportions of detrital zircon grains in the Clearwater metasediments (cf., Figures 9 and 10). The presence of low-grade metamorphic clasts in 16ATW-86 further supports the inference that the Jurassic grains were derived from the Clearwater metasedimentary rocks. A moderate-sized population of ca. 310 Ma zircon grains suggests that intrusive igneous clasts in the deposit were sourced from Skolai arc plutons. Intrusive igneous clasts may also have been recycled into the deposit from 16ATW-77, which would account for the small population of Paleogene zircon grains. An isolated cluster of seven grains give late Miocene ages and constitute the youngest age population at ca. 6 Ma. The late Miocene marks a time of major expansion of the Wrangell Arc (Preece and Hart, 2004) and several late Miocene-Pliocene tephras have been found throughout the eastern Alaska Range (Kunk, 1995; Allen, 2016). Because no tephra is exposed near the sample, we infer that the late Miocene zircon grains in sample 16ATW-86 were recycled into the deposit from a tephra sourced from the Wrangell Arc and thus brackets the age of the deposit to be late Miocene or younger.

The clast assemblages and detrital zircon U-Pb age spectra for the Cenozoic gravel deposits contain a record of sediment recycling and landscape evolution in response to Cenozoic faulting along the south flank of the eastern Alaska Range. We discuss the implications of these data below in the context of the reactivation and evolution of major structures in the map areas.

### *$^{40}Ar/^{39}Ar$ ages*

Mica and amphibole $^{40}Ar/^{39}Ar$ ages from metamorphic rocks in the hanging wall of the Broxson Gulch fault record over 60 Myr of metamorphism and cooling. The $^{40}Ar/^{39}Ar$ ages reveal

that each thrust panel of metamorphic rocks in the study area experienced unique thermal histories that may be used to reconstruct the structural evolution of faults bounding the thrust sheets.

Mica ages from the Maclaren schist record two phases of cooling. The older phase of cooling is recorded by sample 15ATW-08 in Broxson Gulch (45.9 ± 0.3 Ma biotite). Early-mid Eocene mica K-Ar and $^{40}Ar/^{39}Ar$ ages are widespread in the Maclaren schist to the west of Broxson Gulch (Turner and Smith, 1977; Riccio et al., 2014) and likely record cooling from early Eocene magmatism within the Maclaren schist. Because the quartz monzonite pluton in the Ann Creek map area appears to also be a part of the early Eocene magmatic suite, we infer that the Maclaren schist in our study area experienced the thermal effects of early Eocene magmatism and that the ca. 46 Ma $^{40}Ar/^{39}Ar$ biotite age on sample 15ATW-08 records cooling from that thermal event. A younger phase of cooling is recorded by sample 16ATW-73 in Broxson Gulch (32.8 ± 0.3 Ma biotite plateau age). Circa 32 Ma K-Ar and $^{40}Ar/^{39}Ar$ ages are widespread near the Denali fault in the eastern and northern regions of the Maclaren schist and are interpreted to record thermal resetting and subsequent cooling from intrusion of a suite of ca. 32-40 Ma plutons throughout the eastern and central Alaska Range (Benowitz et al., 2011, 2019; Trop et al., 2019). We infer that the biotite porphyroblasts in 16ATW-73 formed during heating associated with the 32-40 Ma magmatism. Sample 15ATW-45 in Ann Creek (37.7 ± 0.6 Ma biotite, 50.2 ± 0.5 Ma muscovite) contains evidence for both thermal resetting/cooling events. The similarity between the muscovite age and the U-Pb zircon age of the quartz monzonite pluton (51.9 ± 0.6 Ma) suggests that the muscovite records rapid post-emplacement cooling. The biotite age from 15ATW-45 may either record that the post-emplacement cooling rate slowed during the late Eocene or that the sample had cooled below argon closure in biotite prior to 40 Ma and the thermal effects of the 32-40 Ma magmatic event were significant enough to reset the biotite age. A third intermediate scenario

wherein the thermal effect of the late Eocene magmatism provided enough heat to slow the cooling rate of sample 15ATW-45 is also viable. The mica cooling ages collectively indicate that the Maclaren schist maintained temperatures in excess of ~350 ºC (Ar closure for coarse biotite during typical orogenic cooling rates–Harrison et al., 1985; Hodges, 2014) until the early Oligocene.

There is presently no evidence that any of the rocks south of the Valdez Creek fault experienced the thermal pulses of Eocene magmatism recorded by mica ages in the Maclaren schist. Instead, white mica ages from metamorphosed ultramafic rocks and the Clearwater muscovite-graphite schist record a single phase of prograde regional metamorphism and development of the inverted metamorphic gradient. The inference that white mica ages in the ultramafic rocks and Clearwater schist record the timing of peak metamorphism is supported by our observations of feldspar deformation textures, amphibole compositions, and mineral assemblages suggesting that peak regional metamorphic conditions in the inverted metamorphic belt did not exceed middle-to-upper greenschist facies conditions. White mica in the structurally highest position of the inverted metamorphic belt (i.e., the dated samples) is kinked parallel to the dominant foliation and displays undulose extinction due to the deformation (Figure 4D and F). The size fraction of the dated white mica grains (200-500 um) corresponds to an Ar closure temperature in excess of 425ºC for typical orogenic cooling rates (e.g., Harrison et al., 2009; Hodges, 2014). By considering the above petrographic observations and inferred Ar closure temperature together, we argue that the dated white mica samples have retained Ar since final recrystallization and deformation at middle-to-upper greenschist facies conditions. Thus, the mica ages from both 16ATW-36 (64.3 ± 0.7 Ma muscovite) and 15ATW-35 (65.1 ± 0.4 Ma fuchsite) record the peak of regional metamorphism and associated deformation in the earliest Paleogene. This timing compares well with age data from the Valdez Creek shear zone, where post-75 Ma ductile thrusting

of the Maclaren schist over the Clearwater metasedimentary rocks is inferred to have developed an inverted metamorphic gradient in the footwall rocks (Davidson et al., 1992; Hollister, 1993; Ridgway et al., 2002). Biotite $^{40}Ar/^{39}Ar$ cooling ages record uniform cooling across the Valdez Creek shear zone by ca. 64-61 Ma (Ridgway et al., 2002).

Amphibole from the amphibolite body (16ATW-43c) in Broxson Gulch provides a record of both mid-Cretaceous magmatism and late Cretaceous metamorphism within the Clearwater metasediments. The size of the amphibole in the sample (Figure 3F), lack of feldspar, and association with serpentinite suggest that the protolith of the amphibolite was a coarsely crystalline ultramafic rock. The amphibole $^{40}Ar/^{39}Ar$ weighted mean age of 93.8 ± 0.7 Ma on sample 16ATW-43c is similar to a ca. 92 Ma K-Ar amphibole age from the pegmatitic hornblende-biotite-pyroxenite (Alaska-type ultramafic cumulate) in the Ann Creek map area (Nokleberg et al., 1992b). Considering that the petrographic observations suggest a coarsely crystalline protolith and the similarity in amphibole age between 16ATW-43c and the pyroxenite body in the Ann Creek area, we infer that the amphibolite in Broxson Gulch was metamorphosed from a protolith composed of coarse ultramafic cumulate. The actinolite zones within the coarse amphibole and greenschist facies matrix minerals indicate that the rock experienced greenschist facies metamorphism following emplacement. This inference is consistent with the age and grade of metamorphism of the Clearwater metasediments recorded by the muscovite and fuchsite ages.

**Synthesis of mapping, cooling ages, and structural evolution**

The ability to definitively distinguish between the metasedimentary rocks in the study area and thus identify the major fault, the Valdez Creek fault, juxtaposing them is our most fundamental revision of the regional geologic framework. Similar to the early work by Rose (1965, 1966) and

Stout (1965), our mapping and petrography indicate that the Maclaren schist and Clearwater metasediments are distinguishable on the basis of protolith composition and rock fabrics. Moreover, detrital zircon age spectra (Figures 8 and 9) and ages of intrusive igneous rocks within the metasedimentary rocks (Figures 2 and 5) reveal that the protoliths of the Clearwater metasediments and Maclaren schist cannot be the same. Although the Clearwater metasediments display internal variation in protolith composition, the detrital zircon age spectra from zircon-bearing rock types throughout the package suggest that the various sedimentary protoliths were derived from the same sediment source area. Accordingly, the ages of the protoliths are likely similar across the various rock types in the Clearwater metasediments.

Our recognition of the Valdez Creek fault and the separate thermal histories of the rocks on either side further require that the Maclaren schist and Clearwater metasediments be split into distinct metasedimentary packages that evolved independently until structural juxtaposition. Our naming of the Valdez Creek fault is based on the Valdez Creek shear zone in the Clearwater mountains ~60 km to the southwest of our study area. $^{40}Ar/^{39}Ar$ biotite cooling ages across the Valdez Creek shear zone suggest there has been little or no slip across it since ca. 60 Ma (Ridgway et al., 2002). The same structural relationship is observed in the Ann Creek map area, Broxson Gulch map area, and the Clearwater mountains: the Maclaren schist is thrust southward over the Clearwater metasediments. However, the Maclaren schist in the Ann Creek and Broxson Gulch areas lacks the mylonitic fabric of the Valdez Creek shear zone and instead has a significant retrograde metamorphic fabric defined by a strong chlorite-muscovite penetrative foliation (e.g., Figure 3G), which intensifies down-section to the Valdez Creek fault. Thus, we interpret that the Cenozoic Valdez Creek fault developed within the hanging wall of the Late Cretaceous-Early Cenozoic Valdez Creek shear zone as a lower-dip, lower-grade shear zone, which evolved into a

brittle fault with continued slip and exhumation. In our naming of the Valdez Creek fault, we keep the location name 'Valdez Creek' because the structural relations are the same as those observed in the type locality. Our use of the word *fault* rather than *shear zone* is intended to convey that the boundary between the two units is a discrete zone of cataclastic deformation.

The timing of reactivation of the Valdez Creek shear zone as the Valdez Creek fault is recorded by the disparate thermal histories of rocks juxtaposed by the fault. Biotite and muscovite cooling ages from the hanging wall record multiple thermal pulses that held the Maclaren schist above ~350 ºC until ca. 32 Ma. Contrarily, rocks in the structurally highest section of the footwall cooled from peak metamorphic temperatures of ~350-450 ºC after ca. 65 Ma and had passed though the 350 ºC isotherm by 60 Ma (Ridgway et al., 2002). Map-based evidence highlighting the independent thermal histories comes from the Ann Creek map area where both the ca. 52 Ma quartz monzonite intrusion and sillimanite-bearing Maclaren gneiss in the contact aureole are cut by the Valdez Creek fault (Stout, 1965) (Figure 2B). Footwall rocks in this area display no textural evidence of static recrystallization and therefore apparently did not experience any significant heating by the quartz monzonite intrusion. The field, textural, and thermochronological evidence together indicate that the Maclaren schist and Clearwater metasediments experienced independent thermal paths until juxtaposition by the Valdez Creek fault after ca. 32 Ma.

The thermal evolution of the Clearwater metasediments is also distinct from Wrangellia rocks, which leads to refinement of the location of the Broxson Gulch fault. We define the Broxson Gulch fault as the boundary between low-grade metasedimentary rocks containing ca. 100 Ma ultramafic-intermediate intrusions (Clearwater) and pre-Jurassic metavolcanic rocks with associated intrusions (Skolai and Nikolai). Previous mappers had included intermediate intrusions and foliated Skolai rocks in the hanging wall of the Broxson Gulch fault due to similarities in

metamorphic grade and rock fabrics. However, the Carboniferous age of the intrusions (Figures 2 and 5; Table 2) and location of the fabric only in the contact aureole of the intrusions (Figure 2A) indicate that these rocks experienced a different metamorphic history than the Clearwater metasediments. Our reinterpretation of the map units near the Broxson Gulch fault is supported by the observation that the boundary between the Clearwater metasediments and Skolai rocks is always marked by a ~30-meter-thick zone of sheared rock, which we infer to mean that the rocks are juxtaposed by a large structure (i.e., the Broxson Gulch fault). Our re-mapping of the fault generally places it farther north in the northern portions of both map areas and refines the location of it near the range front in Broxson Gulch (cf., Figure 2 and Stout, 1976).

The structural evolution of Cenozoic faulting within Wrangellia yields additional insight to the geometry the Broxson Gulch fault. Because the Muddy Creek fault does not appear to have Cenozoic displacement, the Airstrip fault is the structurally highest fault within Wrangellia with clear evidence for Cenozoic slip. In both the Broxson Gulch and Ann Creek map areas, we map a shallowly west-plunging footwall synform associated with the Airstrip fault (Figures 2 and 14). The core of the synform in Broxson Gulch contains Clearwater slate and because the slate is always underlain by the Broxson Gulch fault in this area, the fold must also involve that fault (Figure 2A). Although previous mappers had recognized the Clearwater slate in southeastern Broxson Gulch, they attributed the apparent offset of the Broxson Gulch fault to a NW-striking sinistral tear fault that was inferred to exist beneath Quaternary surficial deposits (Rose, 1965; Stout, 1976; Nokleberg et al., 1992a). We contend that the presence of the synform in the footwall of the Airstrip fault implies the presence of a companion hanging wall antiform (e.g., Mitra, 1990), however the section of the Broxson Gulch fault that would display the inferred antiform is buried beneath glacial deposits (Figure 2A). We argue that because the synform is known from our

mapping, the sinuous map pattern of the Broxson Gulch fault is better explained by erosion of an antiform-synform pair rather than offset of the Broxson Gulch fault by a younger NW-SE-striking fault. Our new interpretation of the map pattern implies that the Airstrip fault became active before the overlying thrust sheets carried by the Broxson Gulch fault were completely eroded. As a result, accumulated slip on the Airstrip fault folded and eventually cut through the overlying Broxson Gulch fault (Figure 14).

The Rainy Creek fault is the southernmost and structurally lowest fault in the study area. Its position near the topographic range front and projected trace between Oligocene and late Miocene fluvial gravel deposits strongly suggest that the Rainy Creek fault is the most recently active fault in the map areas. Such an inference is supported by geophysical evidence in the Ann Creek area where the Rainy Creek fault appears to cross-cut the Airstrip fault (Figure 2B; Supplemental file S7).

The geologic evolution of both map areas suggests that structural reactivation initiated on the Valdez Creek fault and progressed into the Wrangellia terrane. $^{40}Ar/^{39}Ar$ cooling ages reveal that the Valdez Creek fault formed after ca. 32 Ma. The lack of Maclaren schist detritus in the Cenozoic gravel deposits further suggests that either the reactivation did not happen until after ca. 30 Ma and/or the Valdez Creek thrust sheet was topographically separated from the watersheds that fed the ca. 30 Ma and 6 Ma gravel deposits. Evidence for southward progression of thrusting is present in Broxson Gulch where slip on a subsidiary footwall structure within the Clearwater metasediments folded and cut an overlying klippe of Maclaren schist (Figures 2A, south of 15ATW-35, and 14). Slip on the Broxson Gulch fault is inferred to post-date the Valdez Creek fault because only cataclastic deformation is associated with slip on the Broxson Gulch fault and because all rocks in the hanging wall of the Broxson Gulch fault appear to share a Miocene cooling

history below ~200 ºC (Waldien et al., 2017). Folding of the Broxson Gulch fault over the Airstrip fault requires that slip on the Airstrip fault post dates slip on the Broxson Gulch fault and the burial of the northernmost Cenozoic gravel deposit (16ATW-77). Erosion related to slip on the Airstrip fault likely exhumed a portion of the <54 Ma gravel deposit (16ATW-77), which may have been recycled into the ca. 6 Ma gravel deposit (sample 16ATW-86) presently exposed at the range front (e.g., Figures 7 and 10). Such an inference requires that the Airstrip fault was active during the Miocene. The Rainy Creek fault cuts the gravel deposit at the range front (Figure 2B; Supplemental file S6), which suggests that the Rainy Creek fault has been active since ca. 6 Ma.

In summary, our mapping, petrography, geochronology, and thermochronology demonstrate that the Valdez Creek and Broxson Gulch faults are key structures that bound distinct packages of rocks with independent structural, metamorphic, and magmatic histories prior to juxtaposition. As such, each fault likely represents the Cenozoic reactivation of structures that formed individually during Mesozoic terrane accretion. Structural reactivation initiated on the Valdez Creek fault after ca. 32 Ma and has since shifted to the Broxson Gulch fault and then into Wrangellia (Figure 14). It is possible that the Broxson Gulch fault and imbricate Cenozoic structures within Wrangellia are restricted to the upper crust and root into the Valdez Creek fault at depth via some décollement system. Offset of the youngest fluvial gravel deposit by the Rainy Creek fault indicates that shortening in the system lasted until at least 6 Ma.

**Regional Significance**

A major shift in the tectonic configuration of southern Alaska took place between 30-20 Ma. The shift is recorded throughout southern Alaska by regional exhumation within the Alaska Range suture zone (Finzel et al., 2011; Lease et al., 2016; Terhune et al., 2019), onset of focused

exhumation along the Denali fault (Benowitz et al., 2011; 2014), cessation of magmatism along the Denali fault (Trop et al., 2019), topographic development and associated drainage reorganization (Ridgway et al., 2007; Finzel et al., 2015, 2016; Brennan and Ridgway, 2015; Benowitz et al., 2019), initiation of Wrangell Arc volcanism (Richter et al., 1990; Berkelhammer et al., 2019; Brueseke et al., 2019), and development of the St. Elias fold and thrust belt (Bruhn et al., 2004; Pavlis et al., 2012). These events are generally considered to be upper plate responses to increased plate coupling and eventual collision of the Yakutat block with the southern Alaska subduction zone (e.g., Enkelmann et al., 2008, 2010; Jadamec et al., 2013; Haynie and Jadamec, 2017). The post-32 Ma onset of slip on the Valdez Creek fault is contemporaneous with the above events and suggests that it too is related to Yakutat convergence. It is again important to convey that the rocks and structures in our study area were likely ~200-300 km along strike to the southeast at the time of reactivation and have since been moved into the curved section of the Denali fault. Therefore reactivation could not have initiated due to interaction with the curved section of the Denali fault and is inconsistent with models of thrust (re)activation in the core of the Alaska orocline (e.g., Glen, 2004). Instead, reactivation of the Valdez Creek fault and associated structures is better explained by translation along the Denali Fault system into increased alignment with the Queen Charlotte-Fairweather transform fault system (e.g. Riccio et al., 2014) in concert with strain transfer from the Yakutat collision zone to the mechanical contrast at the inboard margin of the Wrangellia terrane (e.g., Saltus and Hudson, 2007).

**Deep-seated structural reactivation of a cryptic suture**

Our data indicate that the Valdez Creek shear zone formed as a primary Mesozoic collisional structure between the North American continent and the allochthonous Wrangellia

composite terrane. The characteristics of rocks in the hanging wall of the Valdez Creek shear zone (Maclaren schist) place them along the western margin of North America at ca. 90 Ma. Contrarily, footwall rocks (Clearwater metasediments) accumulated along the paleo-eastern margin of the Wrangellia composite terrane at ca. 150 Ma. These distinctive assemblages were presumably brought together by a plate boundary fault system, possibly a subduction zone, that existed between them (Figure 15A). After tectonic burial of the Maclaren schist beneath the North American continental margin, the Valdez Creek shear zone formed along the former plate boundary and brought the Maclaren schist and Clearwater metasediments into contact by ca. 75 Ma, at which time they were deformed together during the peak of the collision (Figure 15B). Regional late Cretaceous exhumation of rocks northeast of the Denali fault in eastern Alaska and central Yukon (Dusel-Bacon et al., 2002, 2016) and Paleogene extension-related magmatism (Bacon et al., 1990; Moll-Stalcup et al., 1994) may be upper plate responses to underplating of the Maclaren schist and inferred slab detachment following collision.

The collision of the Wrangellia composite terrane marked a massive addition of juvenile lithosphere to the western margin of North America (Samson et al., 1990; Trop and Ridgway, 2007). The differences in crustal composition, age, thickness, and structure between the Wrangellia composite terrane and North American margin terranes correlate with unique geophysical characteristics in the crust and lithospheric mantle underlying each region (e.g., Glen et al., 2007; Saltus et al., 2007; O'Driscoll and Miller, 2015; Allam et al., 2017; Miller et al., 2018; Miller and Moresi, 2018; Feng and Ritzwoller, 2019; Berg et al., 2020). The P receiver function profile in figure 15C illustrates the correlation between terrane boundaries and distinct changes in crust and lithosphere thickness. The transition in lithospheric architecture across the eastern Alaska Range also coincides with a well-defined zone of fault parallel seismic anisotropy in the lower

crust and upper mantle that is inferred to record rock fabrics in the roots of the Denali fault system (Rasendra et al., 2014; Audet et al., 2016). These geophysical data sets together suggest that the eastern Denali fault formed along a lithospheric boundary between the Wrangellia composite terrane and previously accreted terranes to the north. Because structures south of the Denali fault along the profile in figure 15C have experienced limited activity since 32 Ma, we infer that the lithospheric structure of that region revealed by the P receiver functions approximates the geometry of the Denali fault, Valdez Creek shear zone, and Talkeetna fault prior to reactivation.

One key outcome of this study is that the Valdez Creek shear zone, rather than the Talkeetna fault, was the main reactivated structure. Both structures intersect the Moho (Figure 15C). Yet the Talkeetna fault in most places marks one of the most profound geophysical boundaries in southern Alaska due to differences in crustal thickness (Veenstra et al., 2006; Brennan et al., 2011; Miller et al., 2018) and strongly contrasting crustal gravity/magnetic properties across the fault (Glen et al., 2007; Saltus et al., 2007). These features of the Talkeetna fault may record differences in crustal strength across the fault (e.g., Saltus and Hudson, 2007), which would imply that it would localize reactivation. However, the data synthesized herein indicate that reactivation nucleated on the Valdez Creek shear zone. Our preferred reconciliation of these data sets is that the history of the Valdez Creek shear zone as a former convergent plate boundary implies that it penetrates the crust and links to the Denali fault in the upper mantle (Figure 15C). Such connectivity of major structures highlights the Valdez Creek shear zone as a lithospheric-scale zone of weakness that focused shortening when the Denali fault system transitioned from transcurrent to transpressional deformation. Post-32 Ma shortening on the Valdez Creek fault and imbricate structures resulted in underthrusting of the Wrangellia terrane, possibly as far north as the Denali fault (Allam et al., 2017) (Figure 15D).

Reactivation of suture zone structures is observed at all crustal levels in polyphase orogens worldwide (Sykes 1978; Bailey et al., 2000; Tikoff et al., 2001; Taylor et al., 2003, Jones et al., 2013; Cavazza et al., 2017, numerous others). Although the boundary between allochthonous terranes may manifest in the upper crust as a wide zone of distributed deformation between the disparate terranes, we have shown herein that rocks within a suture zone *sensu lato* may be parsed and assigned to terranes on either side of the collision zone. As a result, the main deformation zone marking the juxtaposition of rocks with independent histories may be relatively discrete. We further argue that the independent lithospheric evolution of each terrane prior to collision will result in a lithospheric scale boundary along the length of the collision zone. Post-collisional deformation is likely to focus onto the inherited lithospheric boundary in response to evolving plate boundary conditions. The reactivated fault system will grow initially by reactivation of major crustal structures that link through the lithosphere and eventually by incorporation of subordinate regional structures.

## CONCLUSIONS

We documented the polyphase structural and thermal evolution of metamorphic rocks within the Alaska Range suture zone in the eastern Alaska Range. Our analysis illuminates the Valdez Creek fault as the primary reactivated structure in the area, which formed by reactivation of the Valdez Creek shear zone after ca. 32 Ma. Subordinate Cenozoic faults include the Broxson Gulch fault at the northern boundary of the Wrangellia terrane, and the Airstrip and Rainy Creek faults within Wrangellia. The Maclaren schist in the hanging wall of the Valdez Creek fault likely formed along the western margin of North America during at ca. 90 Ma, whereas the protolith of the Clearwater metasediments in the footwall was deposited on the paleo-eastern margin of the

Wrangellia composite terrane at ca. 150 Ma. The Valdez Creek fault thus appears to have reactivated along the collisional boundary between North American lithosphere and allochthonous Wrangellia composite terrane lithosphere. Shortening subsequently progressed southward from the Valdez Creek fault to the Broxson Gulch fault and then into the Wrangellia terrane. The timing and style of deformation documented herein suggest that reactivation of structures in the Alaska Range suture zone is a far-field result of Yakutat flat slab subduction and accretion along the southern Alaska convergent margin in concert with the Denali fault tectonic conveyor belt system.

**FIGURES**

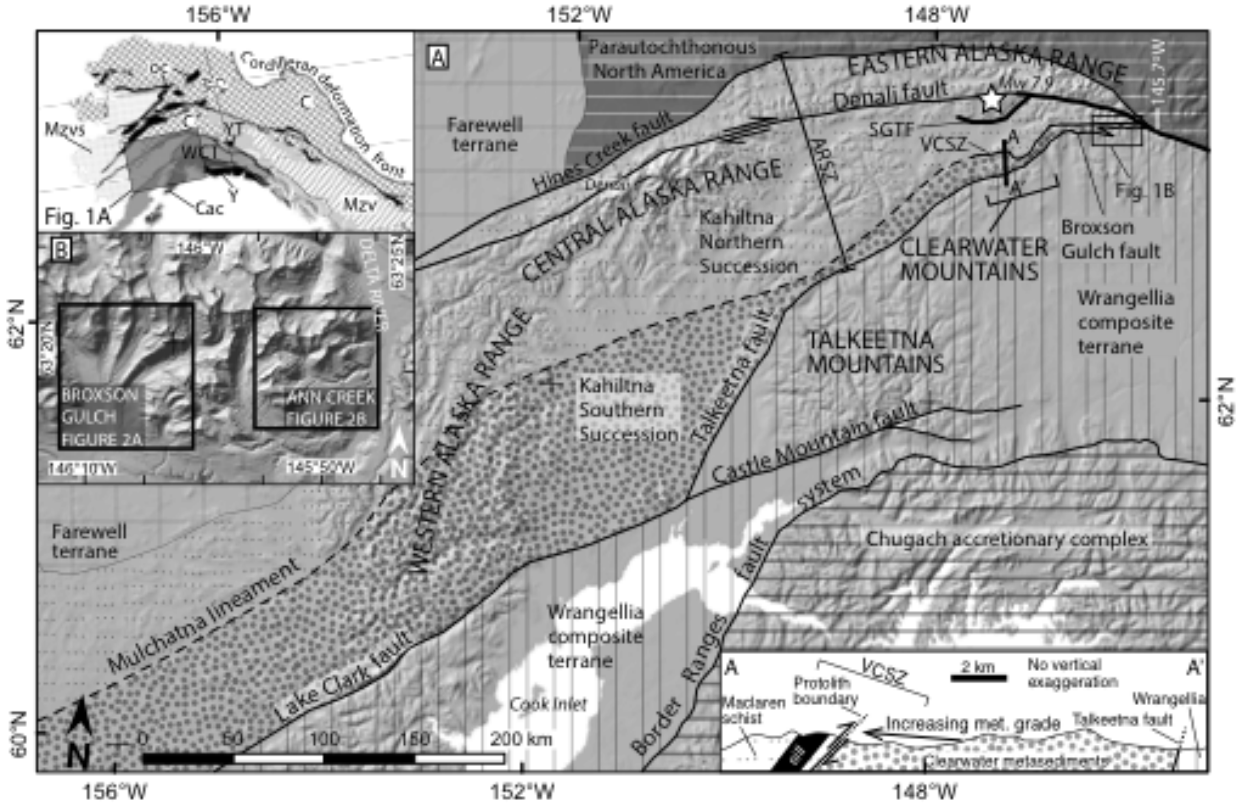
156°W
152°W
148°W
62°N
60°N
Fig. 1A
Mzvs
Cac
Mzv
WCT
YT
C
Cordilleran deformation front
A
B
Parautochthonous North America
Farewell terrane
Hines Creek fault
Denali fault
Mw 7.9
EASTERN ALASKA RANGE
SGTF
VCSZ
ARSZ
CENTRAL ALASKA RANGE
Kahiltna Northern Succession
CLEARWATER MOUNTAINS
Broxson Gulch fault
Fig. 1B
Wrangellia composite terrane
TALKEETNA MOUNTAINS
Talkeetna fault
Kahiltna Southern Succession
Castle Mountain fault system
WESTERN ALASKA RANGE
Chugach accretionary complex
Mulchatna lineament
Lake Clark fault
Border Ranges fault
Cook Inlet
BROXSON GULCH FIGURE 2A
ANN CREEK FIGURE 2B
63°25'N
63°20'N
146°10'W
145°50'W
0
50
100
150
200 km
N
2 km
No vertical exaggeration
Protolith boundary
Maclaren schist
Increasing met. grade
Clearwater metasediments

**Figure 1 (Previous page): A)** Hillshade and terrane map of southern Alaska showing the study area (Figure 1B) relative to major structures and terranes. The section of the Denali fault that had surface rupture during the 2002 $M_w$ 7.9 Denali earthquake is traced in bold. The star marks the epicenter of the main shock. ARSZ– Alaska Range suture zone; SGTF–Susitna Glacier thrust fault; VCSZ–Valdez Creek shear zone. Cross section A-A' shows the structural relationships across the Valdez Creek shear zone (Modified from Davidson et al., 1992). ***Inset–*** Terrane map of the northern North American Cordillera modified from Colpron and Nelson (2011) showing the area of figure 1A relative to other Cordilleran terranes. C–continental crystalline rocks and platform strata (not necessarily Laurentia); YT–Yukon-Tanana terrane; oc–ophiolites and fragments of oceanic crust; Mzv–accreted Mesozoic volcanic arcs (Stikinia, Cache Creek, Quesnellia); Mzvs–Mesozoic basinal assemblages (Kahiltna, Dezadeash, Nutzotin, Gravina, Kuskokwim) and underlying arc and sedimentary rocks; WCT– Wrangellia composite terrane (Wrangellia, Alexander, Peninsular); Cac–Chugach accretionary complex; Y–Yakutat terrane; AK–Alaska; CA–Canada. **B)** Shaded relief map showing the locations of the map areas (black boxes) relative to the Delta River. The confluence of the four glacial valleys in the area of figure 2A is referred to as Broxson Gulch. Ann Creek drains the center of the area of figure 2B from west to east.

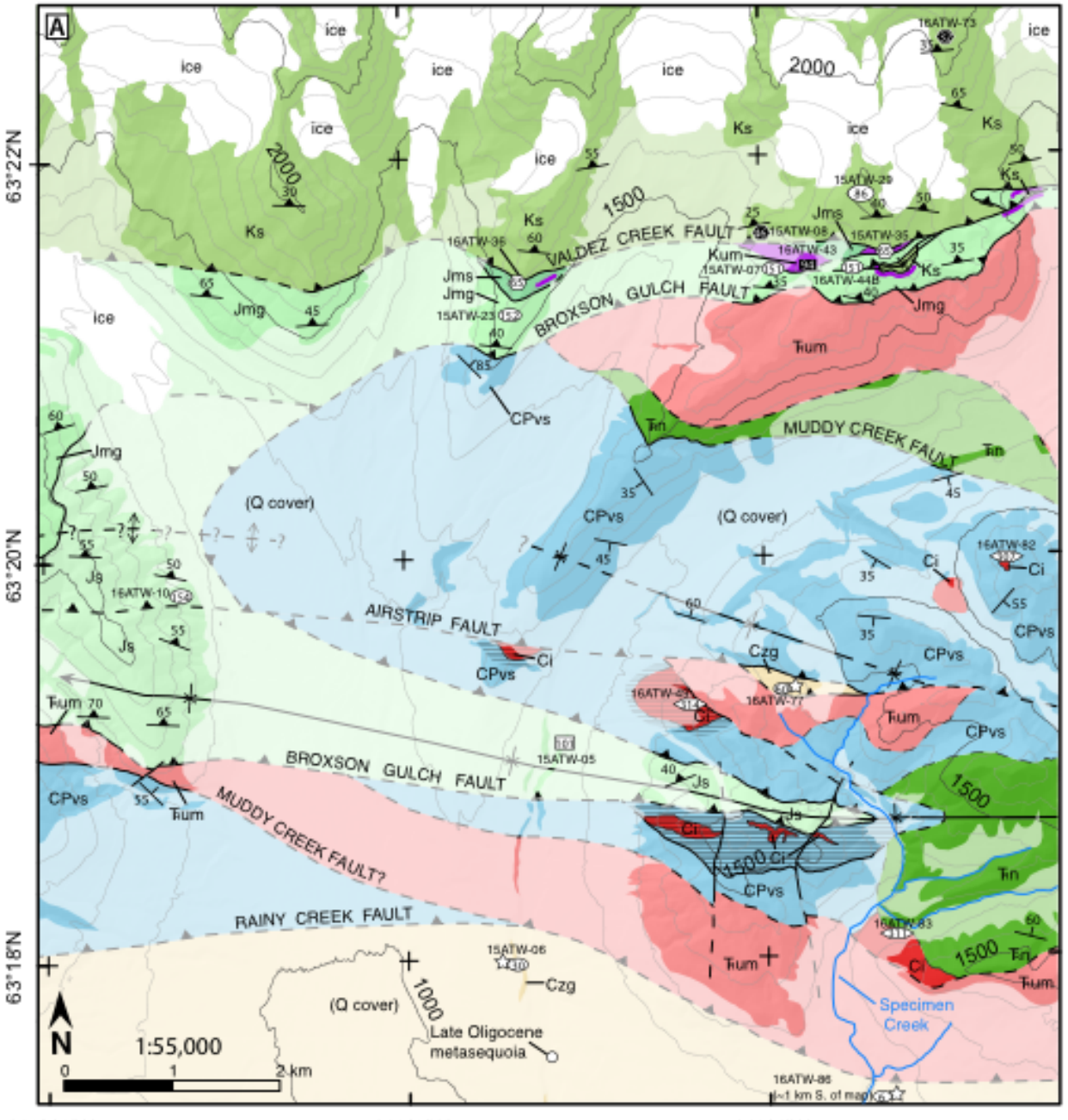


**LEGEND**

**Alaska Range Suture zone**

- Pgqm — Quartz Monzonite (ca. 52 Ma)
- Ks — Maclaren schist (ca. 86-94 Ma protolith age)
- Kgd / Kum — Granodiorite and ultramafic cumulate (ca. 102 Ma)
- Jmg — Clearwater metagreywacke (ca. 150 Ma protolith age)
- Js — Clearwater slate (ca. 150 Ma protolith age)
- Jms — Clearwater mafic schist (Late Jurassic? protolith age)
- Czg — Conglomerate and Breccia (Oligocene(?)-Miocene)

**Wrangellia**

- Tum — Nikolai gabbro and dunite (ca. 225-230 Ma)
- Trn — Nikolai flood basalt (225-230 Ma)
- CPvs — Skolai volcanics (Carboniferous-Permian)
- Ci — Skolai intrusions (ca. 300-315 Ma)
- Foliated Wrangellia rocks

Waldien et al. Figure 2A

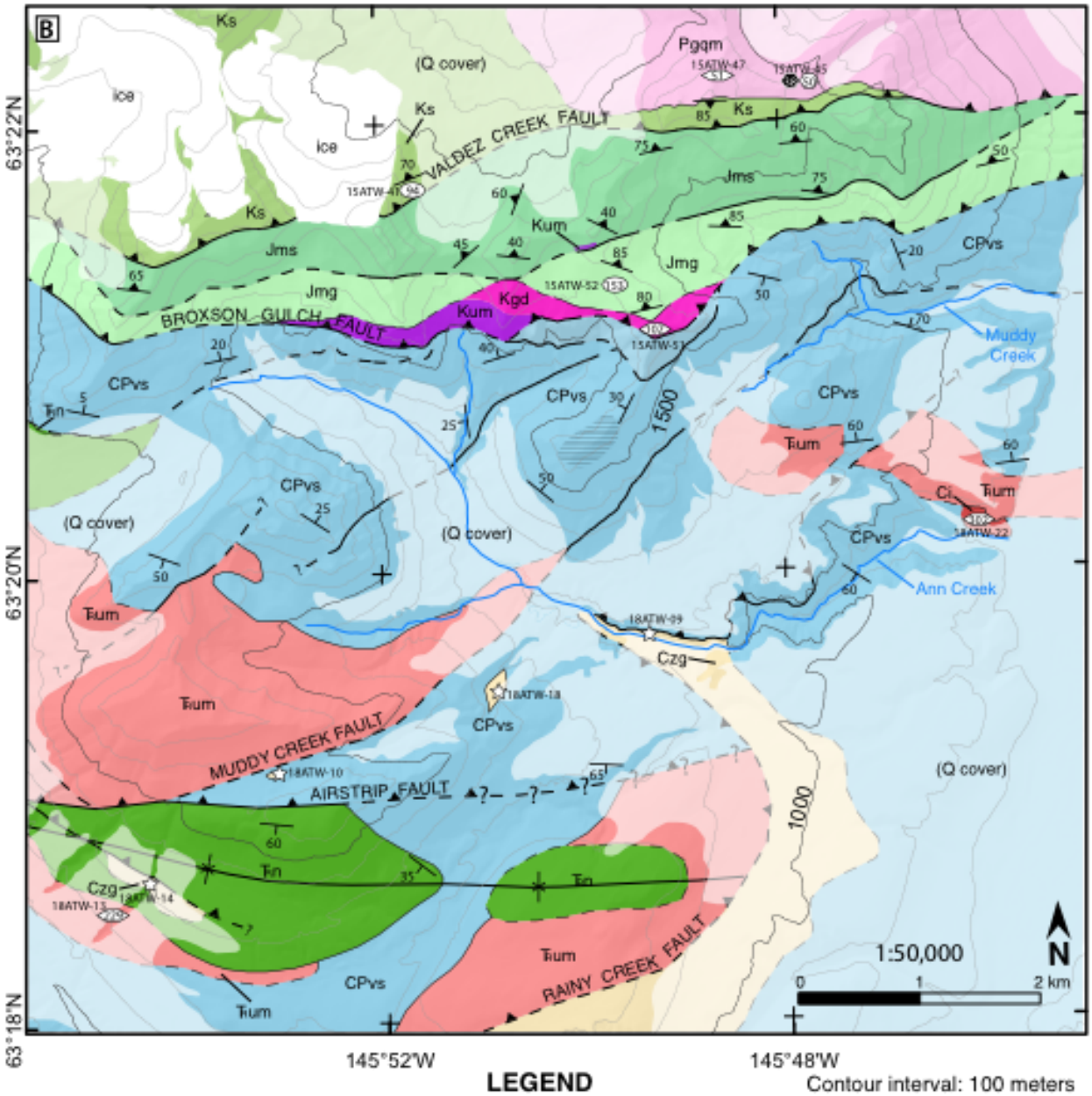


## LEGEND

Contour interval: 100 meters
Index contour: 500 meters

- Thrust fault contact- teeth on hanging wall (dashed where approximate or buried, question marks (?) where queried)
- Overturned thrust fault contact- teeth in dip direction (dashed where approximate or buried)
- Fault contact (kinematics unknown) (dashed where approximate or buried)
- Depositional or intrusive contact (dashed where approximate or buried)

Waldien et al. Figure 2B

- Bedding attitude
- Foliation attitude
- Anticline axis (Question marks (?) where queried)
- Syncline axis

Detrital zircon U-Pb locale | Igneous zircon U-Pb locale | $^{40}Ar/^{39}Ar$ locale | Clast count locale

*All location numbers indicated next to symbol

**Figure 2 (Previous pages):** Hillshade and bedrock geologic maps of the Broxson Gulch (A) and Ann Creek (B) map areas. The mapping presented herein is mostly original with the exception of some areas of the Ann Creek map that are based on mapping by Stout (1965) and Twelker et al. (in revision). Pastel regions (lighter than the legend) represent bedrock that is interpolated beneath Quaternary surficial deposits. Geochronology and clast assemblage sample locations are given. MDA– Maximum depositional age determined from detrital zircon U-Pb age spectra; bt– biotite; wm– white mica; hbl–hornblende; wr– whole rock. The legend applies to both maps.

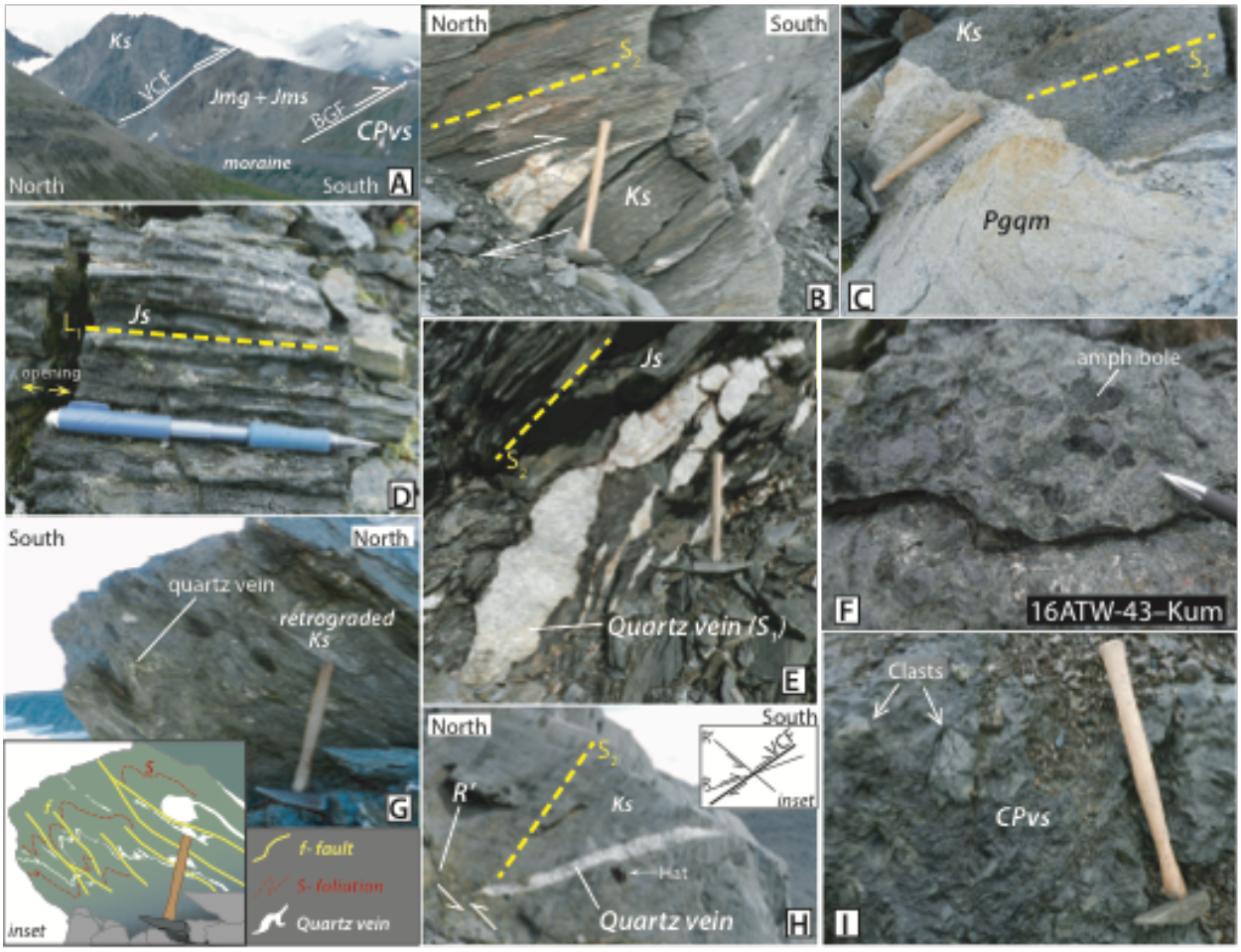
Ks
VCF
Jmg + Jms
BGF
CPvs
moraine
North
South
A
North
South
S2
Ks
B
Ks
S2
Pgqm
C
L1
Js
opening
D
Js
S2
Quartz vein (S1)
E
amphibole
F
16ATW-43–Kum
South
North
quartz vein
retrograded Ks
G
S
inset
f- fault
S- foliation
Quartz vein
North
South
S2
R'
Ks
VCF
inset
Flat
Quartz vein
H
Clasts
CPvs
I

**Figure 3 (Previous page):** Field photos of key relationships on the geologic maps. Hammer for scale is 38 cm long, pencil is 12 cm long, and hat is 30 cm long. All map unit labels are the same as figure 2. **(A)** The Valdez Creek fault (VCF) and Broxson Gulch fault (BGF) create an imbricate set of N-dipping faults that juxtapose the Maclaren schist (Ks) over the Clearwater metasedimentary rocks (Jmg and Jms) and Wrangellia terrane rocks (CPvs) in the map areas. View to the NNE from western Broxson Gulch. The highest point on the ridge is ~450 meters higher elevation than the moraine crest in the valley below. **(B)** Asymmetric boundinage of quartz veins records top-to-the-south (thrust) shear parallel to $S_2$ in the Maclaren schist (Ks). View to the east near location 15ATW-08 (Figure 2A). **(C)** The ca. 52 Ma quartz monzonite (Pgqm) exposed in the Ann Creek area intruded across the foliation in the Maclaren gneiss (Ks). Photo is from a location south of 15ATW-47 (Figure 2B). **(D)** Crenulation axes ($L_1$) are locally well expressed in fine-grained portions of the Clearwater metasedimentary rocks. Opening fractures orthogonal to $L_1$ are commonly associated with the crenulation fabric in the Clearwater slate (Js). The opening fractures are sometimes filled with quartz veins. Photo is from an outcrop near 16ATW-10 (Figure 2A). **(E)** Quartz veins in the Clearwater metasediments are stretched (boudinage) parallel to the $S_1$ foliation and isoclinally folded. Photo is from a fine-grained Clearwater metagreywacke (Jmg) outcrop on the ridge depicted in Figure 3A. **(F)** Amphibolite (Kum) in Broxson Gulch contains coarse amphibole surrounded by a granular aggregate of greenschist facies minerals. Amphibole from this sample (16ATW-43c–Figure 2A) yielded an $^{40}Ar/^{39}Ar$ weighted mean age of 93.8 ± 0.7 Ma (Table 1). **(G)** Maclaren schist (Ks) in the immediate hanging wall of the Valdez Creek fault is retrograded at lower greenschist facies conditions and contains abundant quartz veins. Both the quartz veins and retrograde fabric are folded and cut by faults. *Inset*– Traced photograph emphasizing the structures in the outcrop. View to west, ~30 meters south of location 15ATW-41 (Figure 2B). **(H)** Late quartz veins spatially associated with the Valdez Creek fault cross cut the $S_2$ foliation in the Maclaren schist (Ks). The quartz vein is cut by a S-dipping reverse fault. *Inset*– The reverse fault that cut the quartz vein is appropriately oriented to be an R' structure splaying from the master Valdez Creek fault. View to east from central Broxson Gulch (Figure 2A). **(I)** Primary features, such as coarse volcanic breccia, are commonly preserved in Wrangellia metavolcanic rocks (CPvs). Photo is from central Broxson Gulch (Figure 2A).

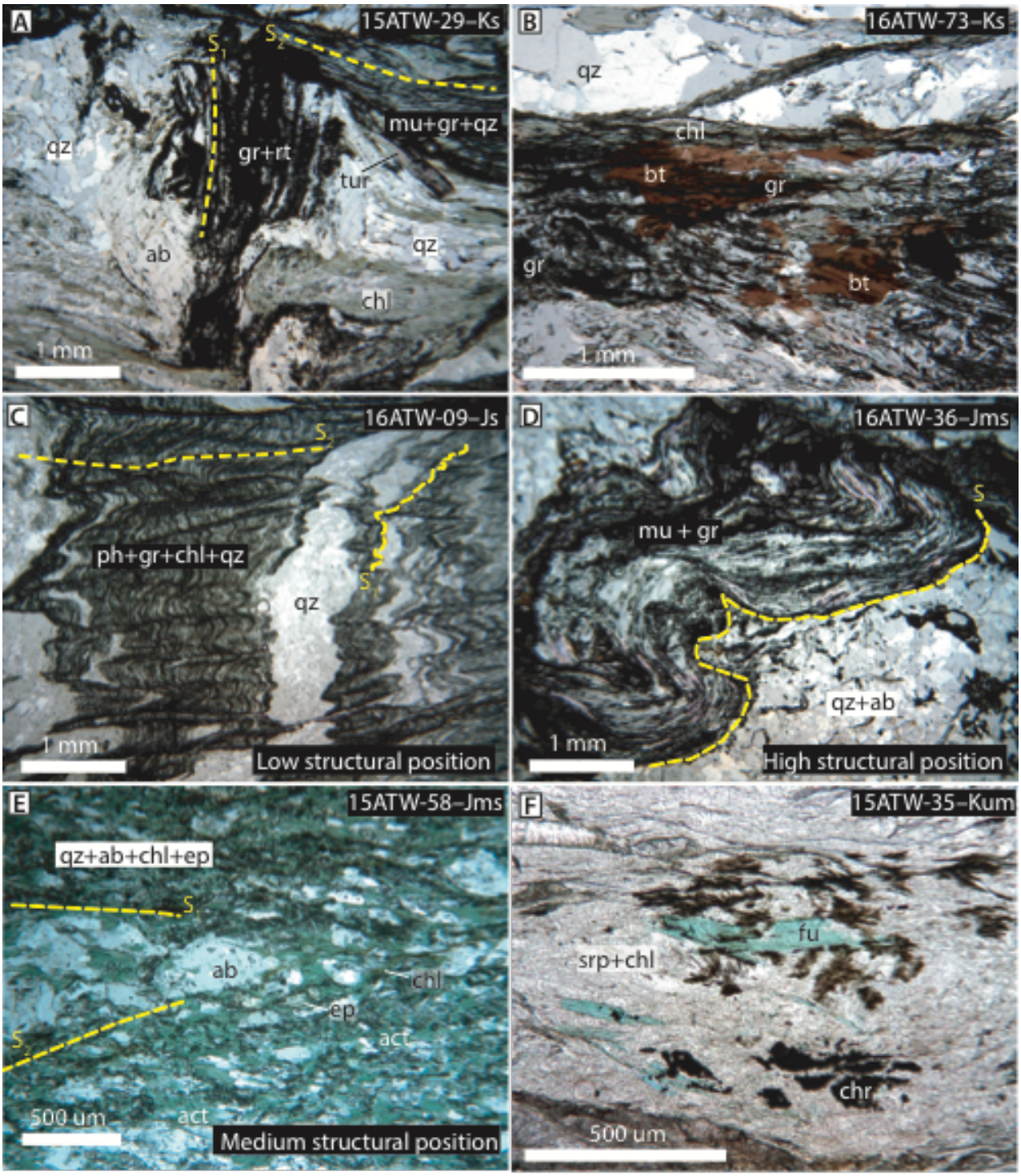
A
15ATW-29–Ks
S1
S2
mu+gr+qz
qz
gr+rt
tur
ab
qz
chl
1 mm
B
16ATW-73–Ks
qz
chl
bt
gr
gr
bt
1 mm
C
16ATW-09–Js
S2
ph+gr+chl+qz
S1
qz
1 mm
Low structural position
D
16ATW-36–Jms
S
mu + gr
qz+ab
1 mm
High structural position
E
15ATW-58–Jms
qz+ab+chl+ep
S1
ab
chl
ep
act
S2
500 um
act
Medium structural position
F
15ATW-35–Kum
fu
srp+chl
chr
500 um

**Figure 4 (Previous Page):** Photomicrographs of key mineralogical and textural features of metamorphic rocks in the hanging wall of the Broxson Gulch fault. Sample names and map units are given in the upper right of each photo. Abbreviations for mineral names follow the convention defined by Whitney and Evans (2010): ab-albite, act-actinolite, bt-biotite, chl-chlorite, chr-chromite, ep-epidote, fu-fuchsite, gr-graphite, mu-muscovite, ph-phengite, qz-quartz, rt-rutile, srp-serpentine, tur-tourmaline. **(A)** The quartzofeldspathic portion of the Maclaren schist contains diagnostic albite porphyroclasts up to ~5 mm in diameter. The porphyroclasts contain a curved internal foliation ($S_1$) defined by graphite and rutile, which is discordant with the exterior foliation ($S_2$). Phyllosilicate minerals defining the $S_2$ foliation wrap around the porphyroclasts. **(B)** The structurally higher portion of the Maclaren schist contains pophyroblastic biotite, which overgrew the $S_2$ foliation. Mineral cleavage in the biotite porphyroblasts is discordant with the $S_2$ foliation. Biotite from this sample yielded an $^{40}Ar/^{39}Ar$ plateau age of 32.8 ± 0.3 Ma (Table 1). **(C)** The Clearwater metasedimentary rocks display a strong transposition fabric wherein the $S_1$ foliation is isoclinally folded into parallelism with the $S_2$ foliation. **(D)** Graphite-muscovite schists interfoliated with mafic schists in the structurally highest section of the Clearwater metasediments display tight folding of mica in the foliation. Muscovite from this sample yielded an $^{40}Ar/^{39}Ar$ plateau age of 64.3 ± 0.7 Ma (Table 1). **(E)** Mafic schists in the Clearwater metasediments display a strong foliation defined by greenschist facies assemblages. In this sample, chlorite defining the $S_1$ foliation is kinked by the $S_2$ foliation. **(F)** Serpentinite interfoliated with the Clearwater metasediments contains fuchsite associated with relict chromite, serpentine, and Cr-rich chlorite. The fuchsite is kinked in the foliation and yielded an $^{40}Ar/^{39}Ar$ plateau age of 65.1 ± 0.4 Ma (Table 1).

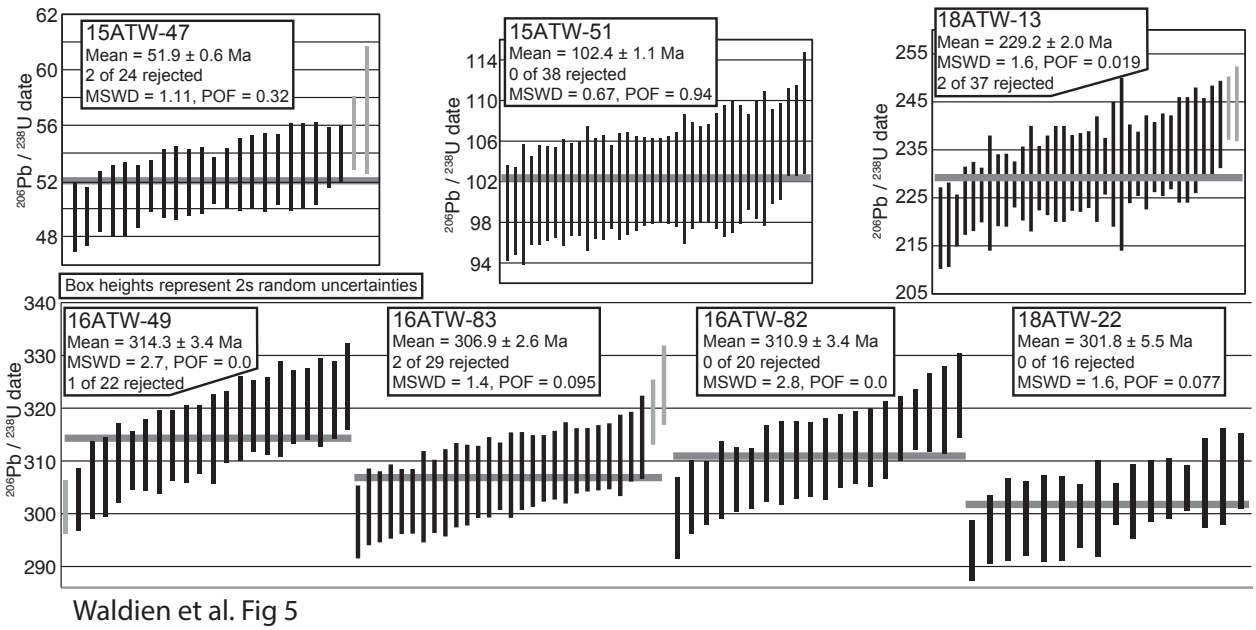


**Figure 5:** Weighted mean plots of U-Pb zircon dates from plutonic rocks in the map areas. Each vertical bar represents a single grain analysis, which is centered on the date and the length of the bar corresponds to the random 2s uncertainty associated with the date. Black bars are used in the age calculation, whereas gray bars passed our filtering criteria but were rejected from the age calculation by Isoplot. The weighted mean calculation uses only concordant analyses with <10% analytical uncertainty. Uncertainties quoted with the weighted mean ages of each sample include internal and external uncertainties at the 2 sigma level. POF- Probability of fit; MSWD- Mean Square of Weighted Deviation. See also table 2.

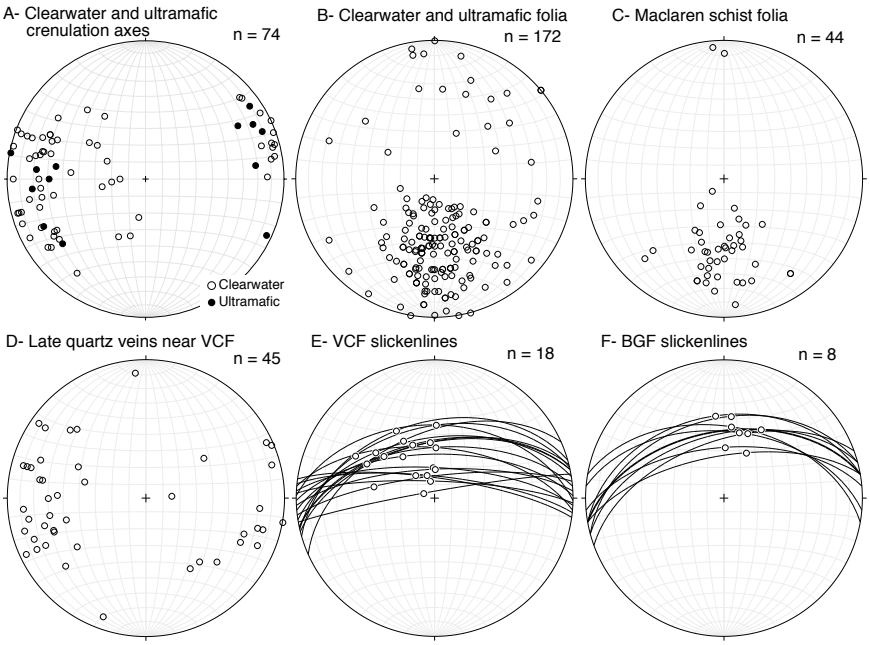


**Figure 6:** Lower hemisphere equal-area plots showing: **(A)** Crenulation axes from metamorphosed Alaska-type ultramafic rocks (filled circles) and the Clearwater metasedimentary rocks (open circles); **(B)** Poles to all foliation measurements in the Clearwater metasedimentary rocks and Alaska-type ultramafic rocks; **(C)** Poles to all foliation measurements in the Maclaren schist; **(D)** Poles to late quartz veins that cross-cut the $S_2$ foliation in the Maclaren schist (Figure 3H); **(E)** Brittle fault striae (open circles) from hanging wall imbricates of the Valdez Creek fault (VCF), which occupy foliation planes (great circles) in the Maclaren schist; and **(F)** Brittle fault striae (open circles) from fault surfaces (great circles) in a small exposure of the Broxson Gulch fault damage zone in northeastern Broxson Gulch. n– number of measurements shown in each plot. The plots were made using Rick Allmendinger's Stereonet program (version 9.2.1).

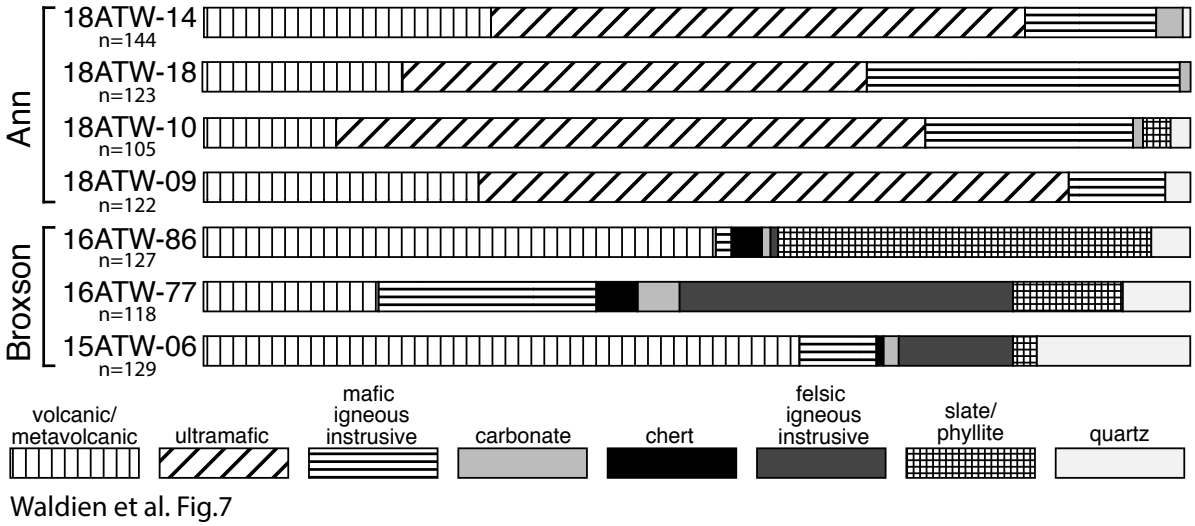


**Figure 7:** Normalized clast population histograms with number (n) of clasts from Cenozoic gravel deposits in the map areas. The samples are grouped by map area.

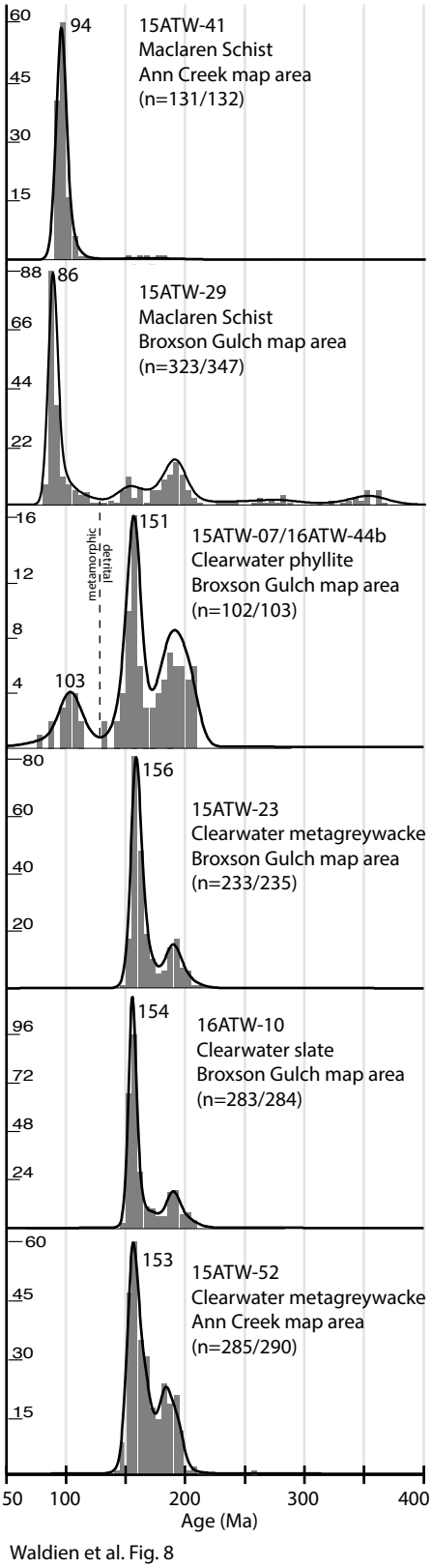


Waldien et al. Fig. 8

**Figure 8:** Kernel density estimate (KDE) and 5 Myr histogram plots of <400 Ma detrital zircon U-Pb dates from the Clearwater metasedimentary rocks and Maclaren schist. Sample numbers, map unit, map area, and the number of analyses constituting the plot out of total acceptable analyses (n) are indicated with each plot. The youngest statistical population of detrital dates, which is taken as the maximum depositional age, is labeled for each plot. Where applicable, the cutoff between detrital and post-depositional metamorphic grains is marked by a vertical broken line. Each vertical axis corresponds to the histogram in each plot. The plots were created using the DensityPlotter program (Vermeesch, 2012).

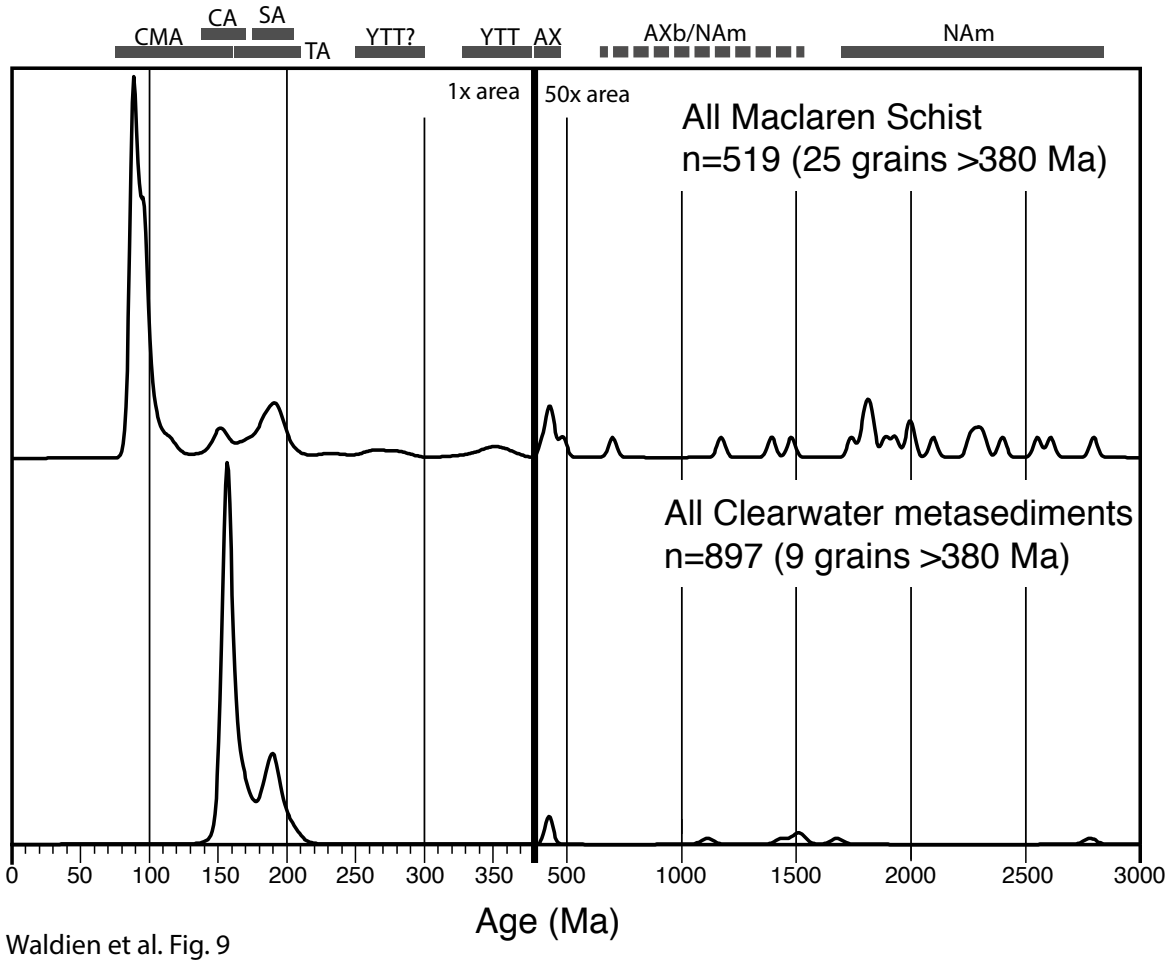


**Figure 9:** Combined kernel density estimate (KDE) plots of all acceptable detrital zircon U-Pb dates for the Clearwater metasedimentary rocks and Maclaren schist. Note the change in horizontal scale at 380 Ma. The area under the curve from 380-3000 Ma is increased by 50x. The KDE plots were created using the DensityPlotter program (Vermeesch, 2012). Sediment source areas: CMA–Coast Mountains Arc; CA–Chitina Arc; SA–Stikine Arc; TA–Talkeetna Arc; YTT–Yukon-Tanana Terrane; AX(b)–Alexander terrane (basement); NAm–North American strata and basement.

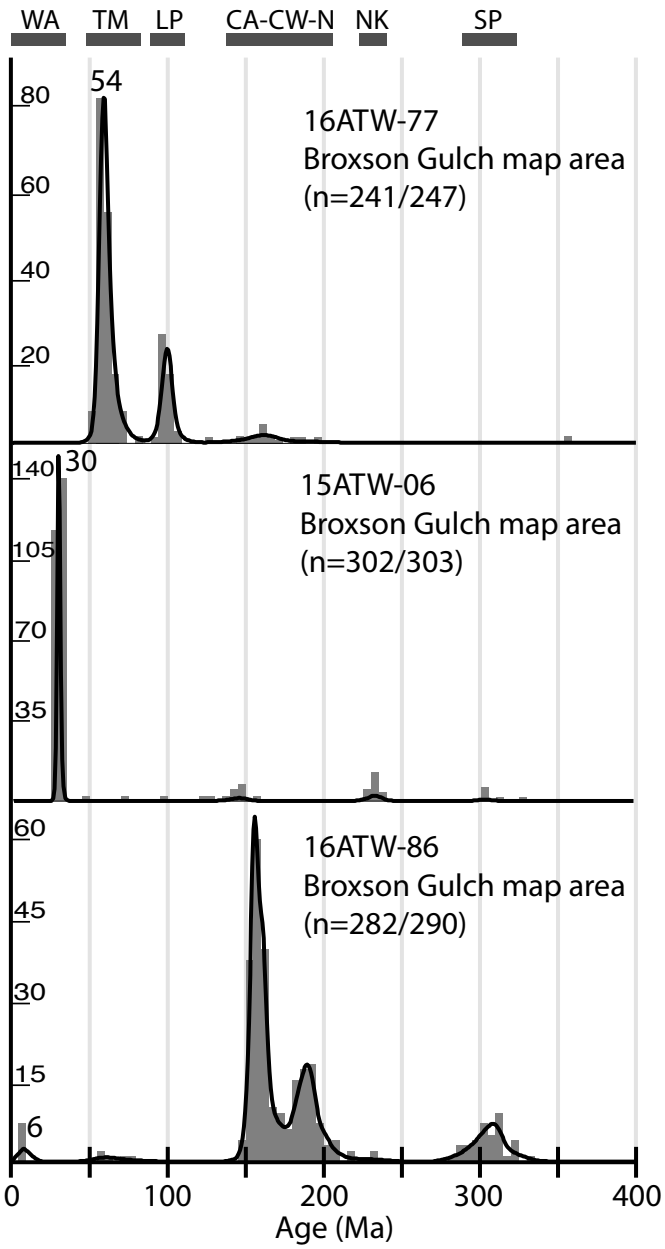


Waldien et al. Fig. 10

**Figure 10:** Kernel density estimate (KDE) and 5 Myr histogram plots of <400 Ma detrital zircon U-Pb dates from the Cenozoic gravel deposits in Broxson Gulch. Sample numbers and the number of analyses constituting the plot out of total acceptable analyses (n) are indicated with each plot. The youngest statistical population, which is taken as the maximum depositional age, is labeled for each plot. Each vertical axis corresponds to the histogram in each plot. The KDE plots were created using the DensityPlotter program (Vermeesch, 2012). Sediment source areas: WA–Wrangell Arc; TM–Talkeetna Mountains plutonic rocks; LP–local Mesozoic plutonic rocks; CA–Chitina Arc; CW–Clearwater Metasedimentary rocks; N–Nutzotin formation; NK–Nikolai igneous rocks; SP–Skolai arc plutonic rocks.

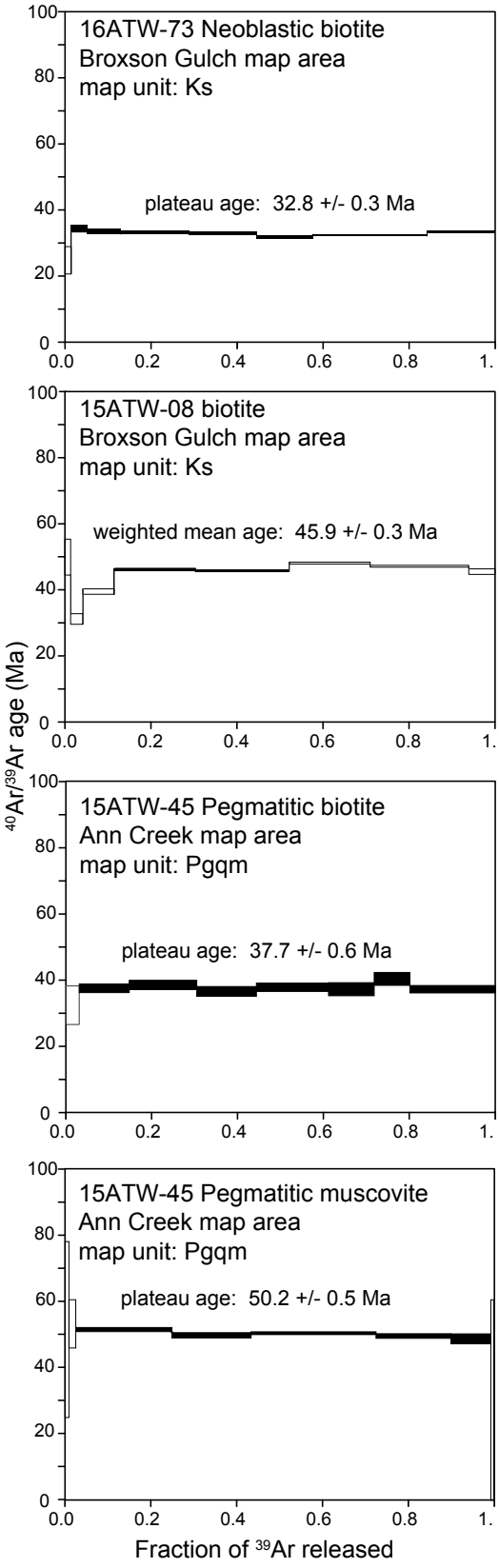


**Figure 11:** Mica $^{40}Ar/^{39}Ar$ age spectra for samples north of the Valdez Creek fault. The sample number, mineral phase dated, map unit, and plateau or weighted mean age determinations are given for each sample. Only filled Ar release steps are used to calculate plateau or weighted mean ages. See also table 1.

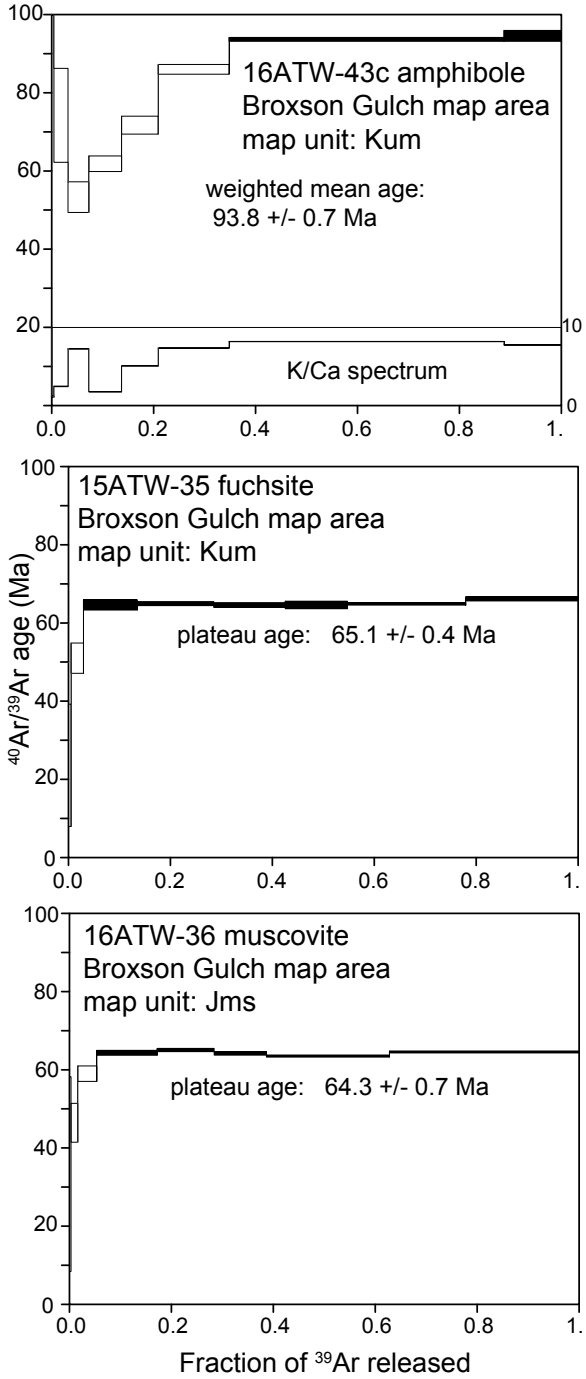


**Figure 12:** Mica and amphibole $^{40}Ar/^{39}Ar$ age spectra for samples south of the Valdez Creek fault. The sample number, mineral phase dated, map unit, and plateau or weighted mean age determinations are given for each sample. Only filled Ar release steps are used to calculate plateau or weighted mean ages. The K/Ca spectrum for sample 16ATW-43c is also given. See also table 1.

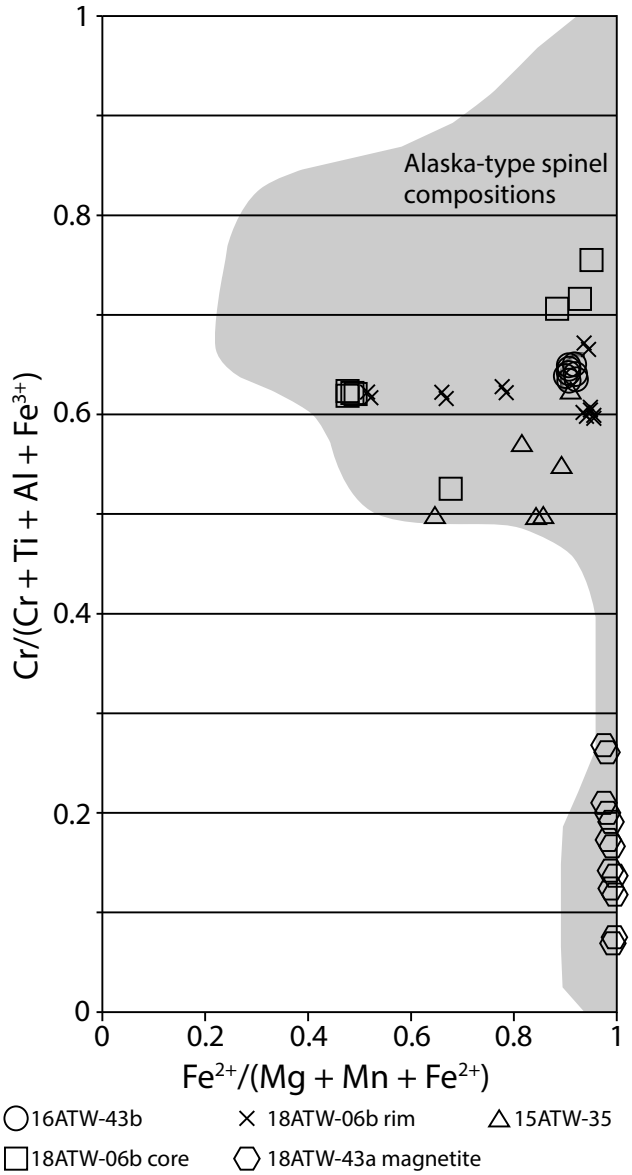


**Figure 13:** Plot of Cr# (Cr/[Cr + Ti + Al + $Fe^{3+}$]) versus $Fe^{2+}$# ($Fe^{2+}$/[Mg + Mn + $Fe^{2+}$]) for spinel group minerals (chromite unless otherwise noted) from ultramafic rocks within the Clearwater metasediments. Each sample is represented as a different symbol. The analytical uncertainty is smaller than the symbol. The shaded region represents the compositions of spinel group minerals from Alaska-type ultramafic complexes compiled by Barnes and Roeder (2001).

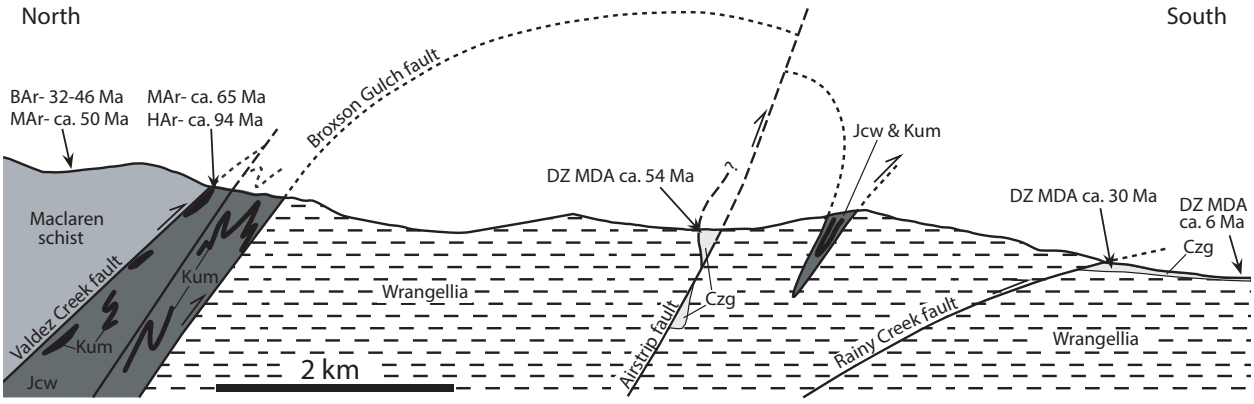


**Figure 14:** Schematic cross section showing key features compiled from both map areas. Broken lines represent faults projected above the surface. Each thrust panel is annotated with $^{40}Ar/^{39}Ar$ ages to show the diverse thermal histories of the individual thrust sheets. Kum–Alaska-type ultramafic rocks; Jcw–Clearwater metasedimentary rocks; Czg–Cenozoic gravel deposit; DZ MDA–Detrital zircon maximum depositional age; BAr–biotite $^{40}Ar/^{39}Ar$ age; MAr–muscovite $^{40}Ar/^{39}Ar$ age. HAr–hornblende $^{40}Ar/^{39}Ar$ age.

**(A) Ca. 90 Ma-**

Deposition and imbrication of Maclaren schist protolith

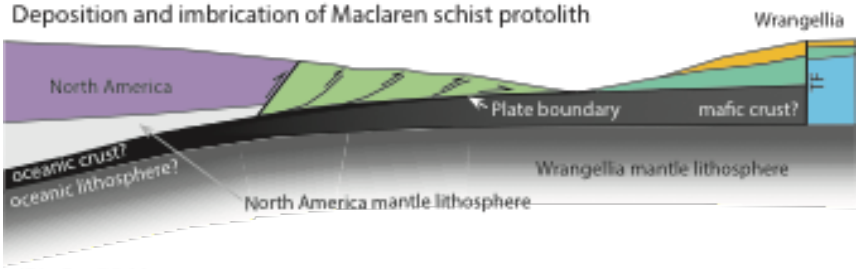


**(B) Ca. 75 Ma-**

Development of Valdez Creek shear zone along former plate boundary

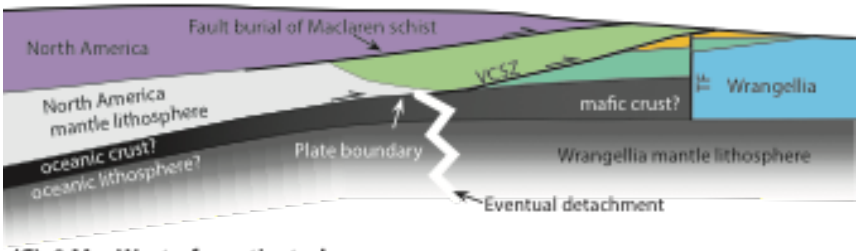


**(C) 0 Ma- West of reactivated zone**

-P receiver functions suggest Denali fault and Valdez Creek shear zone root into upper mantle shear zone

-Proxy for ca. 32 Ma crustal structure south of the Denali fault

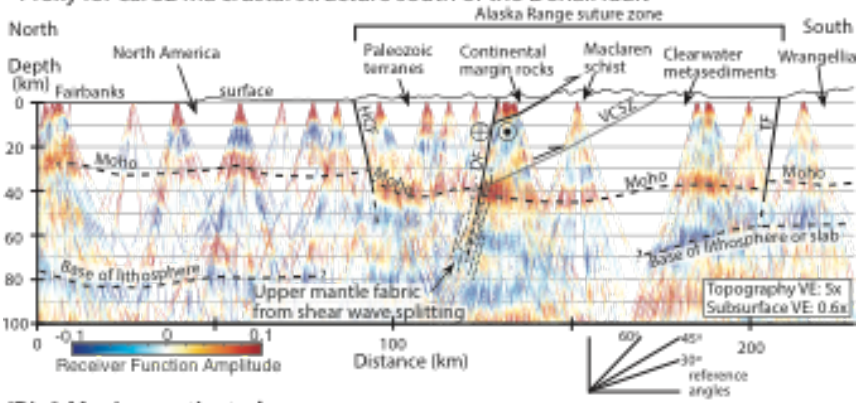


**(D) 0 Ma- In reactivated zone**

Imbricate Cenozoic structures shorten suture zone and northern Wrangellia

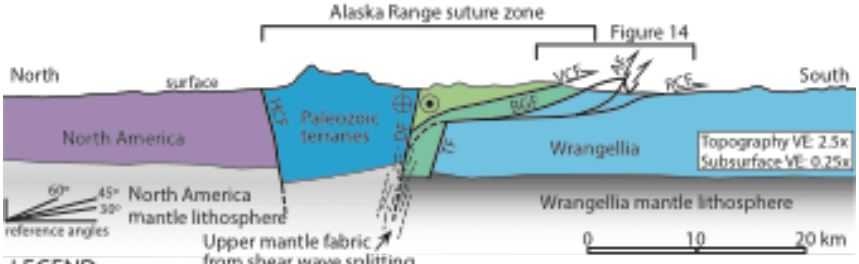


LEGEND

- Peri-continental terranes
- Pz terranes between HCF and DF
- Maclaren schist
- Early K Wrangellia strata
- Clearwater metasediments
- Wrangellia composite terrane

HCF- Hines Creek fault
TF- Talkeetna fault
BGF- Broxson Gulch fault
DF- Denali fault
VCSZ(F)- Valdez Creek shear zone (fault)

VE: Vertical Exaggeration

Thrust fault

Dextral fault

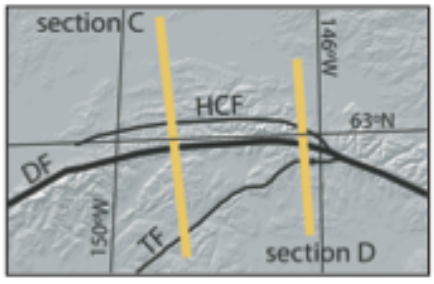

**Figure 15 (Previous page):** Proposed evolutionary model for the formation of the Valdez Creek shear zone and subsequent reactivation as the Valdez Creek fault. The vertical scale for all profiles is based on profile C. The horizontal distances in profiles A and B are schematic and not related to the vertical scale. Topography and subsurface geology in profiles C and D have been vertically exaggerated (VE); reference angles for each profile are given to help visualize the true dip of the structures. The locations of profiles C and D are shown as yellow lines on the accompanying map. **(A)** The Maclaren schist was deposited into a contractional basin on the western margin of North America at ca. 90 Ma. Shortening structures in the basin likely rooted into an E-dipping plate boundary fault zone, possibly a subduction zone, that consumed the marine basin between the Wrangellia composite terrane and North America. The Clearwater metasediments were previously deposited on the paleo-eastern margin of the Wrangellia composite terrane and were brought to North America with the terrane. **(B)** The Valdez Creek shear zone (VCSZ) developed along the pre-existing plate boundary after the Maclaren schist was buried and metamorphosed beneath the North American margin. Note that it remains unclear whether or not oceanic lithosphere was attached to the inboard margin of the Wrangellia composite terrane during the Cretaceous. If oceanic lithosphere were present, it would have likely detached in the latest Cretaceous. **(C)** Cross section showing depth-converted P receiver functions from seismic stations across interior Alaska, the Alaska Range suture zone, and the Wrangellia terrane annotated with crustal faults, interpreted Moho conversions (strong positive amplitude; red colors), interpreted asthenosphere-lithosphere conversions (negative amplitude; blue colors), and inferred anisotropic fabrics from shear wave splitting (Rasendra et al., 2014) along the Denali fault at depth. The receiver function data were processed using the methods of Miller et al. (2018) and updated for this study. The steep northward dip of the Denali fault is inferred from thermochronological data (Benowitz et al., 2011). **(D)** Schematic cross section along a profile from interior Alaska through our study area and into the Wrangellia terrane. The Denali fault juxtaposes crust and lithosphere of different thicknesses and geophysical properties belonging to the Wrangellia terrane and peri-continental terranes to the north. Alaska Range suture zone metamorphic rocks discussed herein occupy a highly shortened domain adjacent to the south side of the Denali fault. The location of the figure 14 cross section is given for reference.

TABLE 1: $^{40}Ar/^{39}Ar$ ANALYTICAL RESULTS

| Sample name | Latitude (ºN) | Longitude (ºW) | Rock type | Phase analyzed | Grain size analyzed (um) | Integrated age (Ma)* | Plateau age (Ma)* | Plateau information |
|---|---|---|---|---|---|---|---|---|
| 16ATW-73 | 63.3427 | 146.1547 | Quartz-mica schist | Biotite | 500-1000 | 32.7 ± 0.2 | **32.8 ± 0.3** | 7 of 8 frac. 98.5 % $^{39}Ar$ rel. MSWD = 2.01 |
| 15ATW-08 | 63.3605 | 146.0647 | Quartz-mica schist | Biotite | 212-500 | 45.8 ± 0.2 | **45.9 ± 0.3**** | 2 of 8 frac. 40.7 % $^{39}Ar$ rel. MSWD = 0.66 |
| 16ATW-36 | 63.3382 | 146.1754 | Quartz-mica schist | Muscovite | 212-590 | 63.8 ± 0.4 | **64.3 ± 0.7** | 5 of 8 frac. 94.6 % $^{39}Ar$ re. MSWD = 3.52 |
| 16ATW-35 | 63.3380 | 146.1759 | Serpentinite | Fuchsite | 125-212 | 64.5 ± 0.4 | **65.1 ± 0.4** | 6 of 8 frac. 97.0 % $^{39}Ar$ rel. MSWD =1.13 |
| 16ATW-43c | 63.3389 | 146.1718 | Amphibolite | Amphibole | 63-180 | 88.5 ± 0.7 | **93.8 ± 0.7**** | 2 of 8 frac. 65.2 % $^{39}Ar$ rel. MSWD = 0.38 |
| 15ATW-05 | 63.3172 | 146.1056 | Amphibole-porphyry dike | Whole rock | 500-1000 | 94.7 ± 0.9 | **100.7 ± 1.6** | 5 out of 8 frac. 54.5% $^{39}Ar$ rel. MSWD = 1.37 |
| 15ATW-45 | 63.3685 | 145.8110 | Quartz-Monzonite pegmatite | Biotite | 500-1000 | 37.5 ± 0.6 | **37.7 ± 0.6** | 7 of 8 frac. 96.9 % $^{39}Ar$ rel. MSWD = 0.5 |
| | | | | Muscovite | 500-1000 | 50.1 ± 0.4 | **50.2 ± 0.5** | 5 of 8 frac. 97.4 % $^{39}Ar$ rel. MSWD = 1.65 |

* Uncertainties are 1s.

**Did not meet all the criteria of a plateau age, hence a weighted average age is presented.

MSWD- Mean Square Weighted Deviation

TABLE 2: ZIRCON U-Pb ANALYTICAL RESULTS

| Map unit | Sample name | Latitude (°N) | Longitude (°W) | Rock type | Weighted mean $^{206}Pb/^{238}U$ Age (Ma)* | MSWD | Number of acceptable grains in age calculation[c] | Total number of zircons analyzed[d] |
|---|---|---|---|---|---|---|---|---|
| Kgd | 15ATW-51[a] | 63.3513 | 145.8205 | Grano-diorite | **102.4 ± 1.1** | 0.67 | 38 | 40 |
| Pgqm | 15ATW-47[a] | 63.3678 | 145.8160 | Quartz Monzonite | **51.9 ± 0.6** | 1.1 | 22 | 32 |
| Trum | 18ATW-13[b] | 63.3093 | 145.9100 | Gabbro pegmatite | **229.2 ± 2.0** | 1.6 | 35 | 40 |
| Ci | 18ATW-22[b] | 63.3363 | 145.7662 | Quartz diorite | **301.8 ± 5.5** | 1.6 | 16 | 26 |
| Ci | 16ATW-49[a] | 63.3397 | 146.1683 | Diorite | **314.3 ± 3.4** | 2.7 | 21 | 25 |
| Ci | 16ATW-82[a] | 63.3437 | 146.1502 | Tonalite | **310.9 ± 3.4** | 2.8 | 20 | 30 |
| Ci | 16ATW-83[a] | 63.3439 | 146.1497 | Tonalite | **306.9 ± 2.6** | 1.4 | 27 | 33 |

*Weighted mean uncertainties represent quadratic addition of internal and external uncertainties at 2s.

MSWD: Mean Square Weighted Deviation

a- Analyses performed at Arizona Laserchron Center

b- Analysis performed at UC Davis
c- The number of analyses that passed the filtering criteria
d- The total number of analyzed grains

## REFERENCES CITED


Aleinikoff, J. N., Nokleberg, W. J., and Herzon, P. L., 1981, Age of intrusion and metamorphism of the East Susitna batholith. Mount Hayes B-6 quadrangle, eastern Alaska Range, Alaska: U.S. Geological Survey Circular 844, p. 100-102.

Allam, A.A., Schulte-Pelkum, V., Ben-Zion, Y., Tape, C., Ruppert, N. and Ross, Z.E., 2017, Ten kilometer vertical Moho offset and shallow velocity contrast along the Denali fault zone from double-difference tomography, receiver functions, and fault zone head waves: Tectonophysics, v. 721, p. 56-69.

Allan, M.M., Mortensen, J.K., Hart, C.J.R., Bailey, L.A., Sánchez, M.G., Ciolkiewicz, W., McKenzie, G.G., and Creaser, R.A., 2013, Magmatic and metallogenic framework of west-central Yukon and eastern Alaska, *in* Colpron, M., Bissig, T., Rusk, B.G., and Thompson, J.F.H., eds., Tectonics, Metallogeny, and Discovery: The North American Cordillera and Similar Accretionary Settings: Society of Economic Geologists Special Publication 17, p. 111–168.

Allen, W.K., 2016, Miocene-Pliocene strike-slip basin development along the Denali fault system in the eastern Alaska Range: Chronostratigraphy and provenance of the McCallum formation and implications for displacement [M.S. Thesis]: Purdue University, 160 p.

Amato, J.M., Bogar, M.J., Gehrels, G.E., Farmer, G.L., McIntosh, W.C., 2007a, The Tlikakila complex in southern Alaska: A suprasubduction-zone ophiolite between the Wrangellia Composite terrane and North America, *in* Ridgway, K.D., Trop, J.M., Glen, J.M.G., O'Neill, M.O., eds., Tectonic Growth of a Collisional Continental Margin: Crustal Evolution of Southern Alaska: Geological Society of America Special Papers 431, p. 227–252, doi: 10.1130/2007.2431(20)

Amato, J.M., Rioux, M.E., Keleman, P.B., Gehrels, G.E., Clift, P.D., Pavlis, T.L., Draut, A.E., 2007b, U-Pb geochronology of volcanic rocks from the Jurassic Talkeetna Formation and detrital zircons from prearc and postarc sequences: Implications for the age of magmatism and inheritance in the Talkeetna Arc, *in* Ridgway, K.D., Trop, J.M., Glen, J.M.G., O'Neill, M.O., eds., Tectonic Growth of a Collisional Continental Margin: Crustal Evolution of Southern Alaska: Geological Society of America Special Papers 431, p. 253–271, doi: 10.1130/2007.2431(20)

Audet, P., Sole, C. and Schaeffer, A.J., 2016, Control of lithospheric inheritance on neotectonic activity in northwestern Canada?: Geology, v. 44(10), p. 807-810.

Bacon, C.R., Foster, H.L. and Smith, J.G., 1990, Rhyolitic calderas of the Yukon-Tanana Terrane, east central Alaska: Volcanic remnants of a Mid-Cretaceous magmatic arc: Journal of Geophysical Research: Solid Earth, v. 95(B13), p. 21451-21461.

Bailey, W. R., Holdsworth, R. E., & Swarbrick, R. E., 2000, Kinematic history of a reactivated oceanic suture: the Mamonia Complex Suture Zone, SW Cyprus: Journal of the Geological Society, v. 157(6), p. 1107-1126.

Barnes, S.J. and Roeder, P.L., 2001, The range of spinel compositions in terrestrial mafic and ultramafic rocks: Journal of petrology, v. *42*(12), p. 2279-2302.

Beacom, L.E., Holdsworth, R.E., McCaffrey, K.J.W. and Anderson, T.B., 2001, A quantitative study of the influence of pre-existing compositional and fabric heterogeneities upon fracture-zone development during basement reactivation: Geological Society, London, Special Publications, v. 186(1), p. 195-211.

Beam, E.C. and Fisher, D.M., 1999, An estimate of kinematic vorticity from rotated elongate porphyroblasts: Journal of Structural Geology, v. 21(11), p. 1553-1559.

Beard, J.S., and Barker, F., 1989, Petrology and tectonic significance of gabbros, tonalites, shoshonites, and anorthosites in a late Paleozoic arc-root complex in the Wrangellia terrane, southern Alaska: The Journal of Geology, v. 97, p. 667–683, doi:10.1086/629351.

Bemis, S.P., and Wallace, W.K., 2007, Neotectonic framework of the north-central Alaska Range foothills, *in* Ridgway, K.D., Trop, J.M., Glen, J.M.G., O'Neill, M.O., eds., Tectonic Growth of a Collisional Continental Margin: Crustal Evolution of Southern Alaska: Geological Society of America Special Paper 431, p. 549–572.

Bemis, S.P., Carver, G.A., and Koehler, R.D., 2012, The Quaternary thrust system of the northern Alaska Range: Geosphere, v. 8(1): p. 196-205.

Bemis, S.P., Weldon, R.J. and Carver, G.A., 2015, Slip partitioning along a continuously curved fault: Quaternary geologic controls on Denali fault system slip partitioning, growth of the Alaska Range, and the tectonics of south-central Alaska: Lithosphere, v. 7(3), p. 235-246.

Benowitz, J.A., Davis, K. and Roeske, S., 2019, A river runs through it both ways across time: $^{40}Ar/^{39}Ar$ detrital and bedrock muscovite geochronology constraints on the Neogene paleodrainage history of the Nenana River system, Alaska Range: Geosphere, v. 15(3), p. 682-701.

Benowitz, J.A., Haeussler, P.J., Layer, P.W., O'Sullivan, P.B., Wallace, W.K., and Gillis, R.J., 2012, Cenozoic tectono-thermal history of the Tordrillo Mountains, Alaska: Paleocene-Eocene ridge subduction, decreasing relief, and late Neogene faulting: Geochemistry, Geophysics, Geosystems, v. 13, p. 1–22, doi: 10.1029/2011GC003951.

Benowitz, J.A., Layer, P.W., and Vanlaningham S., 2014, Persistent long-term (c. 24Ma) exhumation In the Eastern Alaska Range constrained by stacked thermochronology: Geological Society, London, Special Publications, v. 378, p. 225-243. doi: 10.1144/SP378.12.

Benowitz, J.A., Layer, P.W., Armstrong, P., Perry, S.E., Haeussler, P.J., Fitzgerald, P.G., and Vanlaningham, S., 2011, Spatial variations in focused exhumation along a continental-scale strike-slip fault: The Denali fault of the eastern Alaska range: Geosphere, v. 7(2), p. 1-13. doi: 10.1130/GES00589.1.

Benowitz, J.A., Layer, P.W., Wypych, A., and Twelker, E., 2017, $^{40}Ar/^{39}Ar$ data from rocks collected in the 2015 Wrangellia mineral assessment project area, Mount Hayes A-5, Mount Hayes B-6, and Talkeetna Mountains D-2 quadrangles, Alaska: Alaska Division of Geological & Geophysical Surveys raw Data File 2017-1, p. 9, https:// doi .org /10 .14509 /29699.

Beranek, L.P., McClelland, W.C., van Staal, C.R., Israel, S. and Gordee, S.M., 2017, Late Jurassic flare-up of the Coast Mountains arc system, NW Canada, and dynamic linkages across the northern Cordilleran orogen: Tectonics, v. 36(5), p. 877-901.

Beranek, L.P., van Staal, C.R., McClelland, W.C., Israel, S. and Mihalynuk, M.G., 2013, Detrital zircon Hf isotopic compositions indicate a northern Caledonian connection for the Alexander terrane: Lithosphere, v. 5(2), p. 163-168.

Beranek, L.P., van Staal, C.R., McClelland, W.C., Joyce, N., and Israel, S., 2014, Late Paleozoic assembly of the AlexanderWrangellia-Peninsular composite terrane, Canadian and Alaskan Cordillera: Geological Society of America Bulletin, v. 126(11-12), p.1531-1550. doi:10.1130/B31066.1.

Berg, E.M., Lin, F.C., Allam, A., Schulte-Pelkum, V., Ward, K.M. and Shen, W., 2020, Shear Velocity Model of Alaska Via Joint Inversion of Rayleigh Wave Ellipticity, Phase Velocities, and Receiver Functions Across the Alaska Transportable Array: Journal of Geophysical Research: Solid Earth, v. 125(2), p.e2019JB018582.

Berkelhammer, S.E., Brueseke, M.E., Benowitz, J.A., Trop, J.M., Davis, K., Layer, P.W. and Weber, M., 2019, Geochemical and geochronological records of tectonic changes along a flat-slab arc-transform junction: Circa 30 Ma to ca. 19 Ma Sonya Creek volcanic field, Wrangell Arc, Alaska: Geosphere, v. 15(5), p. 1508-1538.

Bill, N.S., Mix, H.T., Clark, P.U., Reilly, S.P., Jensen, B.J., and Benowitz, J.A., 2018, A stable isotope record of late Cenozoic surface uplift of southern Alaska: Earth and Planetary Science Letters, v. 482, p. 300–311, https://doi.org /10.1016 /j.epsl.2017.11.029 .

Bittenbender, P.E., Bean, K.W., Kurtak, J.M., and Deininger, J., 2007, Mineral assessment of the Delta River mining district area, east-central Alaska: U.S. Bureau of Land Management Alaska Technical Report 57, 697 p

Black, L.P., Kamo, S.L., Allen, C.M., Davis, D.W., Aleinikoff, J.N., Valley, J.W., Mundil, R., Campbell, I.H., Korsch, R.J., Williams, I.S. and Foudoulis, C., 2004, Improved $^{206}Pb/^{238}U$ microprobe geochronology by the monitoring of a trace-element-related matrix effect; SHRIMP, ID–TIMS, ELA–ICP–MS and oxygen isotope documentation for a series of zircon standards: Chemical Geology, v. 205(1-2), p. 115-140.

Bond, G.C., 1973, A late Paleozoic volcanic arc in the eastern Alaska Range, Alaska: Journal of Geology, v. 81, p. 557-576.

Bond, G.C., 1976, Geology of the Rainbow Mountain-Gulkana Glacier Area, Eastern Alaska Range, with Emphasis on Upper Paleozoic Strata: State of Alaska Geologic Division of Geological & Geophysical Surveys Geologic Report 45, 47 p., scale 1:40:000, 3 sheets.

Box, S.E., Karl, S.M., Jones, J.V., Bradley, D.C., Haeussler, P.J. and O'Sullivan, P.B., 2019, Detrital zircon geochronology along a structural transect across the Kahiltna assemblage in the western Alaska Range: Implications for emplacement of the Alexander-Wrangellia-Peninsular terrane against North America: Geosphere, v. 15(6), p.1774-1808.

Brennan, P. R. K., Gilbert, H., and Ridgway, K. D. 2011, Crustal structure across the central Alaska Range: Anatomy of a Mesozoic collisional zone: Geochemistry, Geophysics, Geosystems, v. 12(4), Q04010, doi:10.1029/2011GC003519.

Brennan, P.R.K., and Ridgway, K.D., 2015, Detrital zircon record of Neogene exhumation of the central Alaska Range: A far-field upper plate response to flat-slab subduction: Geological Society of America Bulletin, v. 127(7-8), p. 1–17, doi: 10.1130/B31164.1.

Brueseke, M.E., Benowitz, J.A., Trop, J.M., Davis, K.N., Berkelhammer, S.E., Layer, P.W. and Morter, B.K., 2019, The Alaska Wrangell Arc:~ 30 Ma of subduction-related magmatism along a still active arc-transform junction. Terra Nova, v. 31(1), p. 59-66.

Bruhn, R.L., Pavlis, T.L., Plafker, G. and Serpa, L., 2004, Deformation during terrane accretion in the Saint Elias orogen, Alaska: Geological Society of America Bulletin, v. 116(7-8), p. 771-787.

Burkett, C.A., Bemis, S.P., and Benowitz, J.A., 2016, Along-fault migration of the Mount McKinley restraining bend of the Denali fault defined by late Quaternary fault patterns and seismicity, Denali National Park & Preserve, Alaska: Tectonophysics, v. 693, p. 489–506, doi: 10.1016/j.tecto.2016.05.009.

Burns, L.E., U.S. Bureau of Land Management, Fugro Airborne Surveys, and Stevens Exploration Management Corp., 2003, Total magnetic field and detailed electromagnetic

anomalies of the southern Delta River area, east-central Alaska, parts of Mt. Hayes A-3, A-4, B-3, and B-4 quadrangles, in Burns, L.E., U.S. Bureau of Land Management, Fugro Airborne Surveys, and Stevens Exploration Management Corp., Plot files of the airborne geophysical survey data of the southern Delta River area, east-central Alaska: Alaska Division of Geological & Geophysical Surveys Geophysical Report 2003-5-2C, 1 sheet, scale 1:31,680. http://doi.org/10.14509/3219

Cavazza, W., Albino, I., Zattin, M., Galoyan, G., Imamverdiyev, N. and Melkonyan, R., 2017, Thermochronometric evidence for Miocene tectonic reactivation of the Sevan–Akera suture zone (Lesser Caucasus): a far-field tectonic effect of the Arabia–Eurasia collision?: Geological Society, London, Special Publications, v. 428(1), p. 187-198.

Colpron, M. and Nelson, J.L., 2011, A Digital Atlas of Terranes for the Northern Cordillera: British Columbia Ministry of Energy and Mines, BCGS GeoFile 2011-11.

Colpron, M., Nelson, J.L., and Murphy, D.C., 2007, Northern Cordilleran terranes and their interactions through time: GSA Today, v. 17(4/5), p. 4, doi:10.1130/GSAT01704 -5A.1.

Coney, P.J., Jones, D.L. and Monger, J.W., 1980, Cordilleran suspect terranes: Nature, v. 288(5789), p. 329.

Csejtey, B., Cox, D. P., Evarts, R. C., Stricker, G. D., & Foster, H. L., 1982, The Cenozoic Denali fault system and the Cretaceous accretionary development of southern Alaska: Journal of Geophysical Research: Solid Earth, v. 87(B5), p. 3741-3754.

Csejtey, B., Mullen, M.W., Cox, D.P., Gilbert, W.G., Yeend, W.E., Smith, T.E., Wahrhaftig, Clyde, Craddock, Campbell, Brewer, W.M., Sherwood, K.W., Hickman, R.G., Stricker, G.D., St. Aubin, D.R., and Goerz, D.J., III, 1986, Geology and geochronology of the Healy Quadrangle, Alaska: U.S. Geological Survey Open-File Report 86-396, 92 p., 4 sheets, scale 1:250,000.

Danišík, M., McInnes, B.I., Kirkland, C.L., McDonald, B.J., Evans, N.J. and Becker, T., 2017, Seeing is believing: Visualization of He distribution in zircon and implications for thermal history reconstruction on single crystals: Science advances, v. 3(2), p. e1601121.

Davidson, C., & McPhillips, D., 2007, Along strike variations in metamorphism and deformation of the strata of the Kahiltna basin, south-central Alaska, *in* Ridgway, K.D., Trop, J.M., Glen, J.M.G., O'Neill, M.O., eds., Tectonic Growth of a Collisional Continental Margin: Crustal Evolution of Southern Alaska: Geological Society of America Special Papers 431, p. 439-453.

Davidson, C., Hollister, L. S., and Schmid, S. M., 1992, Role of Melt in the Formation of a Deep-crustal Compressive Shear zone: The Maclaren Glacier Metamorphic Belt, south central Alaska: Tectonics, v. 11(2), p. 348-359.

Day, E.M., Pavlis, T.L. and Amato, J.M., 2016, Detrital zircon ages indicate an Early Cretaceous episode of blueschist-facies metamorphism in southern Alaska: Implications for the Mesozoic paleogeography of the northern Cordillera: Lithosphere, v. *8*(5), p.451-462.

Decker, J., Bergman, S.C., Blodgett, R.B., Box, S.E., Bundtzen, T.K., Clough, J.G., Coonrad, W.L., Gilbert, W.G., Miller, M.L., Murphy, J.M., Robinson, M.S., and Wallace, W.K., 1994, Geology of southwestern Alaska, *in* Plafker, G., and Berg, H.C., eds., The Geology of Alaska: Boulder, Colorado, Geological Society of America, Geology of North America, v. G-1, p. 285–310.

Dewey, J. F., 1977, Suture zone complexities: a review: Tectonophysics, v. 40(1), p. 53-67.

Dewey, J.F. and Burke, K.C., 1973, Tibetan, Variscan, and Precambrian basement reactivation: products of continental collision: The Journal of Geology, v. 81(6), p. 683-692.

Doser, D.I., 2004, Seismicity of the denali-totschunda fault zone in central Alaska (1912-1988) and its relation to the 2002 Denali fault earthquake sequence: Bulletin of the Seismological Society of America, v. 94, p. 132–144, doi: 10.1785/0120040611.

Dusel-Bacon, C. and Williams, I.S., 2009, Evidence for prolonged mid-Paleozoic plutonism and ages of crustal sources in east-central Alaska from SHRIMP U–Pb dating of syn-magmatic, inherited, and detrital zircon: Canadian Journal of Earth Sciences, v. 46(1), p. 21-39.

Dusel-Bacon, C., Bacon, C.R., O'Sullivan, P.B. and Day, W.C., 2016, Apatite fission-track evidence for regional exhumation in the subtropical Eocene, block faulting, and localized fluid flow in east-central Alaska: Canadian Journal of Earth Sciences, v. *53*(3), p. 260-280.

Dusel-Bacon, C., Holm-Denoma, C.S., Jones, J.V., Aleinikoff, J.N. and Mortensen, J.K., 2017, Detrital zircon geochronology of quartzose metasedimentary rocks from parautochthonous North America, east-central Alaska: Lithosphere, v. 9(6), p. 927-952.

Dusel-Bacon, C., Lanphere, M.A., Sharp, W.D., Layer, P.W. and Hansen, V.L., 2002, Mesozoic thermal history and timing of structural events for the Yukon-Tanana Upland, east-central Alaska: $^{40}Ar/^{39}Ar$ data from metamorphic and plutonic rocks: Canadian Journal of Earth Sciences, v. 39(6), p.1013-1051.

Eberhart-Phillips, D., Haeussler, P.J., Freymueller, J.T., Frankel, A.D., Rubin, C.M., Craw, P., Ratchkovski, N. A, Anderson, G., Carver, G.A, Crone, A.J., Dawson, T.E., Fletcher, H., Hansen, R., Harp, E.L., et al., 2003, The 2002 Denali fault earthquake, Alaska: a large magnitude, slip-partitioned event: Science, v. 300, p. 1113–1118, doi: 10.1126/science.1082703.

Eisbacher, G.H., 1976, Sedimentology of the Dezadeash flysch and its implications for strike-slip faulting along the Denali fault, Yukon Territory and Alaska: Canadian Journal of Earth Sciences, v. 13(11), p. 1495-1513.

Enkelmann, E., Garver, J.I., and Pavlis, T.L., 2008, Rapid exhumation of ice-covered rocks of the Chugach - St. Elias orogen, Southeast Alaska: Geology, v. 36, p. 915–918, doi: 10.1130/G2252A.1.

Enkelmann, E., Zeitler, P. K., Garver, J. I., Pavlis, T. L., & Hooks, B. P., 2010, The thermochronological record of tectonic and surface process interaction at the Yakutat–North American collision zone in southeast Alaska: American Journal of Science, v. 310(4), p. 231-260.

Feng, L. and Ritzwoller, M.H., 2019, A 3-D shear velocity model of the crust and uppermost mantle beneath Alaska including apparent radial anisotropy: Journal of Geophysical Research: Solid Earth, v. 124(10), p.10468-10497.

Finzel, E.S., Enkelmann, E., Falkowski, S. and Hedeen, T., 2016, Long-term fore-arc basin evolution in response to changing subduction styles in southern Alaska: Tectonics, v. 35(7), p. 1735-1759.

Finzel, E.S., Ridgway, K.D., and Trop, J.M., 2015, Provenance signature of changing plate boundary conditions along a convergent margin: Detrital record of spreading-ridge and flat-slab subduction processes, Cenozoic forearc basins, Alaska: Geosphere, v. 11(3), p. 823-849.

Finzel, E.S., Trop, J.M., Ridgway, K.D., and Enkelmann, E., 2011, Upper plate proxies for flat-slab subduction processes in southern Alaska: Earth and Planetary Science Letters, v. 303, p. 348–360, doi: 10.1016/j.epsl.2011.01.014.

Fitzgerald, P.F., Sorkhabi, R.B., Redfield, T.F., & Stump, E., 1995, Uplift and denudation of the central Alaska Range: a case study in the use of apatite fission track thermochronology to determine absolute uplift parameters: Journal of Geophysical Research, v. (100), p. 20175-20191.

Fitzgerald, P.G., Roeske, S.M., Benowitz, J. A., Riccio, S.J., Perry, S.E., and Armstrong, P.A., 2014, Alternating asymmetric topography of the Alaska range along the strike-slip Denali fault: Strain partitioning and lithospheric control across a terrane suture zone: Tectonics, v. 33, doi: 10.1002/2013TC003432.

Fitzgerald, P.G., Stump, E., & Redfield, T.E., 1993, Late Cenozoic uplift of Denali and its relation to relative plate motion and fault morphology: Science, v. 259, p. 497-499.

Forbes, R. B., Smith, T. E., and Turner, D. L., 1974, Comparative petrology and structure of the Maclaren, Ruby Range, and Coast Range belts: Implications for offset along the Denali fault system: Geological Society of America Abstracts with Programs, v. 6, p. 177.

Freymueller, J.T., Cohen, S.C., Cross, R., Elliott, J., Fletcher, H., Larsen C., Hreinsdóttir, S., and Zweck, C., 2008, Active deformation processes in Alaska, based on 15 years of GPS measurements, in Freymueller, J.T., Haeussler, P.J., Wesson, R.L., & Ekström,G., ed., Active Tectonics and Seismic Potential of Alaska Washington, D. C., AGU, p. 1–42.

Gardner, M.C., Bergman, S.C., Cushing, G.W., MacKevett Jr, E.M., Plafker, G., Campbell, R.B., Dodds, C.J., McClelland, W.C. and Mueller, P.A., 1988, Pennsylvanian pluton stitching of Wrangellia and the Alexander terrane, Wrangell Mountains, Alaska: Geology, v. 16(11), p. 967-971.

Gardner, M.C., Bergman, S.C., Cushing, G.W., MacKevett Jr, E.M., Plafker, G., Campbell, R.B., Dodds, C.J., McClelland, W.C., and Mueller, P.A., 1988, Pennsylvanian pluton stitching of Wrangellia and the Alexander Terrane, Wrangell Mountains, Alaska: Geology, v. 16, no. 11, p. 967–971, doi: 10.1130/0091-7613(1988)016<0967:PPSOWA>2.3.CO;2.

Gehrels, G. and Pecha, M., 2014, Detrital zircon U-Pb geochronology and Hf isotope geochemistry of Paleozoic and Triassic passive margin strata of western North America: Geosphere, v. 10 (1), p. 49-65.

Gehrels, G., Rusmore, M., Woodsworth, G., Crawford, M., Andronicos, C., Hollister, L., Patchett, J., Ducea, M., Butler, R., Klepeis, K. and Davidson, C., 2009, U-Th-Pb geochronology of the Coast Mountains batholith in north-coastal British Columbia: Constraints on age and tectonic evolution: Geological Society of America Bulletin, v. 121(9-10), p.1341-1361.

Gehrels, G., Valencia, V. and Pullen, A., 2006, Detrital zircon geochronology by laser-ablation multicollector ICPMS at the Arizona LaserChron Center: The Paleontological Society Papers, v. 12, p. 67-76.

Gehrels, G.E., Butler, R.F. and Bazard, D.R., 1996, Detrital zircon geochronology of the Alexander terrane, southeastern Alaska: Geological Society of America Bulletin, v. 108(6), p. 722-734.

Gehrels, G.E., Valencia, V., Ruiz, J., 2008, Enhanced precision, accuracy, efficiency, and spatial resolution of U-Pb ages by laser ablation-multicollector-inductively coupled plasma-mass spectrometry: Geochemistry, Geophysics, Geosystems, v. 9, Q03017, doi:10.1029/2007GC001805.

Gilman, T., Feineman, M. and Fisher, D., 2009, The Chulitna terrane of south-central Alaska: A rifted volcanic arc caught between the Wrangellia composite terrane and the Mesozoic

margin of North America: Geological Society of America Bulletin, v. 121(7-8), p.979-991.
Glen, J.M.G., 2004, A kinematic model for the southern Alaska orocline based on regional fault patterns, *in* Sussman, A. and Weil, A.B., eds., Orogenic Curvature: Geological Society of America. Special Paper 383, p. 161-172.
Glen, J.M.G., Schmidt, J., Pellerin, L., McPhee, D.K., and O'Neill, J.M., 2007, Crustal structure of Wrangellia and adjacent terranes inferred from geophysical studies along the a transect through the northern Talkeetna Mountains, *in* Ridgway, K.D., Trop, J.M., Glen, J.M.G., O'Neill, M.O., eds., Tectonic Growth of a Collisional Continental Margin: Crustal Evolution of Southern Alaska: Geological Society of America Special Papers 431, p. 21–41, doi: 10.1130/2007.2431(20)
Goussin, F., Riel, N., Cordier, C., Guillot, S., Boulvais, P., Roperch, P., Replumaz, A., Schulmann, K., Dupont-Nivet, G., Rosas, F. and Guo, Z., 2020, Carbonated inheritance in the Eastern Tibetan lithospheric mantle: petrological evidences and geodynamic implications: Geochemistry, Geophysics, Geosystems, v. 21, e2019GC008495.
Greene, A.R., Scoates, J. S., & Weiss, D., 2008, Wrangellia flood basalts in Alaska: A record of plume-lithosphere interaction in a Late Triassic accreted oceanic plateau: Geochemistry, Geophysics, Geosystems, v. 9(12), 34 p.
Greene, A.R., Scoates, J.S., Weis, D., Katvala, E.C., Israel, S. and Nixon, G.T., 2010, The architecture of oceanic plateaus revealed by the volcanic stratigraphy of the accreted Wrangellia oceanic plateau: Geosphere, v. 6(1), p. 47-73.
Haeussler, P.J., 1992, Structural evolution of an arc-basin: The Gravina Belt in central southeastern Alaska: Tectonics, v. 11(6), p. 1245-1265.
Haeussler, P.J., Matmon, A., Schwartz, D.P., and Seitz, G.G., 2017b, Neotectonics of interior Alaska and the late Quaternary slip rate along the Denali fault system: Geosphere, v. 13, p. 1445–1463, doi: 10.1130/GES01447.1.
Haeussler, P.J., O'Sullivan, P., Berger, A.L., and Spotila, J.A, 2008, Neogene exhumation of the Tordrillo Mountains, Alaska, and correlations with Denali (Mount McKinley): in Freymueller, J. T, Haeussler, P. J., Wesson, R. L., and Ekström, G., ed., Active Tectonics and Seismic Potential of Alaska, AGU Monograph 179, p. 269–285, doi: http://dx.doi.org/10.1029/179GM15.
Haeussler, P.J., Saltus, R.W., Stanley, R.G., Ruppert, N., Lewis, K., Karl, S.M., and Bender, A., 2017a, The Peters Hills basin, a Neogene wedge-top basin on the Broad Pass thrust fault, south-central Alaska: Geosphere, v. 13, p. 1464–1488, doi: 10.1130/GES01487.1.
Hampton, B.A., Ridgway, K.D., & Gehrels, G.E., 2010, A detrital record of Mesozoic island arc accretion and exhumation in the North American Cordillera: U-Pb geochronology of the Kahiltna basin, southern Alaska: Tectonics, v. 29(TC4015), 21 p.
Hampton, B.A., Ridgway, K.D., O'Neill, J.M., Gehrels, G.E., Schmidt, J., & Blodgett, R.B., 2007, Pre-, syn-, and postcollisional stratigraphic framework and provenance of Upper Triassic–Upper Cretaceous strata in the northwestern Talkeetna Mountains, Alaska, *in* Ridgway, K.D., Trop, J.M., Glen, J.M.G., O'Neill, M.O., eds., Tectonic Growth of a Collisional Continental Margin: Crustal Evolution of Southern Alaska: Geological Society of America Special Papers 431, p. 401–438, doi: 10.1130/2007.2431(20)
Harrison, T. M., Duncan, I., & McDougall, I., 1985, Diffusion of $^{40}$Ar in biotite: temperature, pressure and compositional effects: Geochimica et Cosmochimica Acta, v. 49(11), p. 2461-2468.

Harrison, T.M., Célérier, J., Aikman, A.B., Hermann, J., and Heizler, M.T., 2009, Diffusion of $^{40}$Ar in muscovite: Geochimica et Cosmochimica Acta, v. 73, p. 1039–1051, doi: 10.1016/j.gca.2008.09.038.

Haynie, K.L. and Jadamec, M.A., 2017, Tectonic drivers of the Wrangell block: Insights on fore-arc sliver processes from 3-D geodynamic models of Alaska: Tectonics, v. 36(7), p. 1180-1206.

Heron, P.J., Pysklywec, R.N. and Stephenson, R., 2016, Lasting mantle scars lead to perennial plate tectonics: Nature communications, v. 7(1), p. 1-7.

Herriott, T.M., Crowley, J.L., Schmitz, M.D., Wartes, M.A. and Gillis, R.J., 2019, Exploring the law of detrital zircon: LA-ICP-MS and CA-TIMS geochronology of Jurassic forearc strata, Cook Inlet, Alaska, USA: Geology, v. 47(11), p. 1044-1048.

Himmelberg, G.R. and Loney, R.A., 1995, Characteristics and petrogenesis of Alaskan-type ultramafic-mafic intrusions, southeastern Alaska: U.S. Geological Survey Professional Paper 1564.

Hodges, K.V., 2014, Thermochronology in orogenic systems: Treatise on Geochemistry 2nd edition, p. 281-308.

Hollister, L.S., 1993, The role of melt in the uplift and exhumation of orogenic belts: Chemical Geology, v. 108(1-4), p. 31-48.

Horstwood, M.S., Košler, J., Gehrels, G., Jackson, S.E., McLean, N.M., Paton, C., Pearson, N.J., Sircombe, K., Sylvester, P., Vermeesch, P. and Bowring, J.F., 2016, Community-derived standards for LA-ICP-MS U-(Th-) Pb geochronology–Uncertainty propagation, age interpretation and data reporting: Geostandards and Geoanalytical Research, v. 40(3), p.311-332.

Hoskin, P.W. and Schaltegger, U., 2003, The composition of zircon and igneous and metamorphic petrogenesis: Reviews in mineralogy and geochemistry: Zircon: v. 53(1), p. 27-62.

Huff, C.J., 2012, Paleozoic to Neogene stratigraphic and structural history of the Alaska Range suture zone, north of the Denali fault, east central Alaska Range [M.S. Thesis]: Davis, University of California, 149 p.

Hults, C.P., Wilson, F.H., Donelick, R.A., and O'Sullivan, P.B., 2013, Two flysch belts having distinctly different provenance suggest no stratigraphic link between the Wrangellia composite terrane and the paleo-Alaskan margin: Lithosphere, v. 5(6), p. 575-594.

Israel, S., Beranek, L., Friedman, R.M., and Crowley, J.L., 2014, New ties between the Alexander terrane and Wrangellia and implication for North America Cordilleran evolution: Lithosphere v. 6(4), p. 270-276. doi:10.1130/L364.1

Jadamec, M.A., Billen, M.I., and Roeske, S.M., 2013, Three-dimensional numerical models of flat slab subduction and the Denali fault driving deformation in south-central Alaska: Earth and Planetary Science Letters, v. 376, p. 29–42, doi: 10.1016/j.epsl.2013.06.009.

Jones, D.L., Silberling, N.J., & Hillhouse, J., 1977, Wrangellia- a displaced terrane in northwestern North America: Canadian Journal of Earth Sciences, v. 14(11), p. 2565-2577.

Jones, D.S., Barnes, C.G., Premo, W.R. and Snoke, A.W., 2013, Reactivation of the Archean-Proterozoic suture along the southern margin of Laurentia during the Mazatzal orogeny: Petrogenesis and tectonic implications of ca. 1.63 Ga granite in southeastern Wyoming: Geological Society of America Bulletin, v. 125(1-2), p. 164-183.

Kalbas, J. L., K. D. Ridgway, and G. E. Gehrels, 2007, Stratigraphy, depositional systems, and

provenance of the Lower Cretaceous Kahiltna assemblage, western Alaska Range: Basin development in response to oblique collision, *in* Ridgway, K.D., Trop, J.M., Glen, J.M.G., O'Neill, M.O., eds., Tectonic Growth of a Collisional Continental Margin: Crustal Evolution of Southern Alaska: Geological Society of America Special Papers 431, 307–343, doi:10.1130/2007.2431(13).

Kapp, P.A. and Gehrels, G.E., 1998, Detrital zircon constraints on the tectonic evolution of the Gravina belt, southeastern Alaska: Canadian Journal of Earth Sciences, v. 35(3), p. 253-268.

Kelly, S., Beaumont, C. and Butler, J.P., 2019, Inherited terrane properties explain enigmatic post-collisional Himalayan-Tibetan evolution: Geology, v. 48(1), p.8-14

Koehler, R.D., 2013, Quaternary Faults and Folds (QFF), Alaska Division of Geological and Geophysical Surveys Digital Data Series 3. from http://maps.dggs.alaska.gov/qff/.

Kreemer, C., Blewitt, G. and Klein, E.C., 2014, A geodetic plate motion and Global Strain Rate Model: Geochemistry, Geophysics, Geosystems, v. 15(10), p. 3849-3889.

Kunk, M.J., 1995, $^{40}Ar/^{39}Ar$ Age-spectrum Data for Hornblende, Plagioclase and Biotite from Tephras Collected at Dan Creek and McCallum Creek, Alaska and in the Klondike Placer District Near Dawson, Yukon Territory, U.S. Geological Survey Open-File Report 95-217h, 52 p.

Layer, P.W., Hall, C.M., and York, D., 1987, The derivation of $^{40}Ar/^{39}Ar$ age spectra of single grains of hornblende and biotite by laser step heating: Geophysical Research Letters, v. 14, p. 757–760, https:// doi .org /10 .1029 /GL014i007p00757.

Lease, R.O., 2018, Pliocene erosional pulse and glacier-landscape feedbacks in the western Alaska Range, Earth and Planetary Science Letters, v. 497, p. 62-68, https://doi.org/10.1016/j.epsl.2018.06.009

Lease, R.O., Haeussler, P.J., & O'Sullivan, P.B., 2016, Changing exhumation patterns during Cenozoic growth and glaciation of the Alaska Range: Insights from detrital thermochronology and geochronology: Tectonics, v. 35, 22 p.

Link, B.J., 2017, From Deposition to Deformation Within an Accretionary Suture Zone: An Example from the Clearwater and Talkeetna Mountains, Alaska Range Suture Zone [M.S. Thesis]: West Lafayette, Indiana, Purdue University.

Lowey, G.W., 1998, A new estimate of the amount of displacement on the Denali fault system based on the occurrence of carbonate megaboulders in the Dezadeash Formation (Jura-Cretaceous), Yukon, and the Nutzotin Mountains sequence (Jura-Cretaceous), Alaska: Bulletin of Canadian Petroleum Geology, v. 46(3), p. 379-386.

Lowey, G.W., 2011, Volcaniclastic gravity flow deposits in the Dezadeash Formation (Jura-Cretaceous), Yukon, Canada: Implications regarding the tectonomagmatic evolution of the Chitina arc in the northern Cordillera of North America: Lithos, v. 125(1-2), p. 86-100.

Lowey, G.W., 2018, Provenance analysis of the Dezadeash Formation (Jurassic–Cretaceous), Yukon, Canada: implications regarding a linkage between the Wrangellia composite terrane and the western margin of Laurasia: Canadian Journal of Earth Sciences, v. 56(1), p. 77-100.

Ludwig, K., 2008, Isoplot 3.6: Berkeley Geochronology Center Special Publication 4, 77 p.

Manuszak, J.D., Ridgway, K.D., Trop, J.M. and Gehrels, G.E., 2007, Sedimentary record of the tectonic growth of a collisional continental margin: Upper Jurassic-Lower Cretaceous Nutzotin Mountains sequence, eastern Alaska Range, Alaska, *in* Ridgway, K.D., Trop,

J.M., Glen, J.M.G., O'Neill, M.O., eds., Tectonic Growth of a Collisional Continental Margin: Crustal Evolution of Southern Alaska: Geological Society of America Special Papers 431, p. 345-377.

Matmon, A., Schwartz, D.P., Haeussler, P.J., Finkel, R., Lienkaemper, J.J., Stenner, H.D., and Dawson, T.E., 2006, Denali fault slip rates and Holocene-late Pleistocene kinematics of central Alaska: Geology, v. 34, p. 645–648, doi: 10.1130/G22361.1.

Matthews, W.A. and Guest, B., 2017, A practical approach for collecting large-n detrital zircon U-Pb data sets by quadrupole LA-ICP-MS: Geostandards and Geoanalytical Research, v. 41(2), p. 161-180.

Mattinson, J.M., Graubard, C.M., Parkinson, D.L. and McClelland, W.C., 1996, U-Pb reverse discordance in zircons: the role of fine-scale oscillatory zoning and sub-micron transport of Pb: Geophysical Monograph-American Geophysical Union, v. 95, p. 355-370.

McClelland, W.C., Gehrels, G.E., Samson, S.D. and Patchett, P.J., 1992, Protolith relations of the Gravina belt and Yukon-Tanana terrane in central southeastern Alaska: The Journal of Geology, v. 100(1), p. 107-123.

Mendenhall, W.C., 1905, Geology of the central Copper River region, Alaska (No. 41). U.S. Geological Survey professional paper 41, 133 p.

Mériaux, A.-S., Sieh, K., Finkel, R.C., Rubin, C.M., Taylor, M.H., Meltzner, A.J., and Ryerson, F.J., 2009, Kinematic behavior of southern Alaska constrained by westward decreasing postglacial slip rates on the Denali Fault, Alaska: Journal of Geophysical Research, v. 114, p. 1–19, doi: 10.1029/2007JB005053.

Miller, M.S. and Moresi, L., 2018, Mapping the Alaskan Moho: Seismological Research Letters, v. 89(6), p. 2430-2436.

Miller, M.S., O'Driscoll, L.J., Porritt, R.W. and Roeske, S.M., 2018, Multiscale crustal architecture of Alaska inferred from P receiver functions: Lithosphere, v. 10(2), p. 267-278.

Mitra, S., 1990, Fault-propagation folds: Geometry, kinematic evolution, and hydrocarbon traps: American Association of Petroleum Geologists Bulletin, v. 74, p. 921-945.

Moll-Stalcup, E.J., Brew, D.A., and Vallier, T.L., 1994, Latest Cretaceous and Cenozoic magmatic rocks of Alaska, *in* Plafker, G., and Berg, H.C., eds., The Geology of Alaska: Boulder, Colorado, Geological Society of America, Geology of North America, v. G-1, 2 sheets, scale 1:2,500,000.

Monger, J.W.H., Price, R.A. and Tempelman-Kluit, D.J., 1982, Tectonic accretion and the origin of the two major metamorphic and plutonic welts in the Canadian Cordillera: Geology, v. 10(2), p. 70-75.

Mooney P.R., 2010, Geology of the Clearwater Mountains and Southern Boundary of the Alaska Range Suture Zone [M.S. Thesis]: Davis, University of California, 93 p.

Murphy, D.C., 2018, Latest Cretaceous–early Eocene Pacifi c-Arctic?-Atlantic connection: Co-evolution of strike-slip fault systems, oroclines, and transverse foldand-thrust belts in the northwestern North American Cordillera, in Piepjohn, K., Strauss, J.V., Reinhardt, L., and McClelland, W.C., eds., Circum-Arctic Structural Events: Tectonic Evolution of the Arctic Margins and Trans-Arctic Links with Adjacent Orogens: Geological Society of America Special Paper 541.

Nokleberg, W.J. Aleinikoff, J.N., Dutro, J.T., Jr. Lanphere, M.A. Silberling, N.J., Silva, S.R., Smith, T.E., and Turner, D.L., 1992b, Map, tables, and summary of fossil and isotopic age data, Mount Hayes quadrangle, eastern Alaska Range, Alaska: U.S. Geological

Survey Miscellaneous Field Studies map 1996-D, 43 p., 1 sheet, scale 1:250,000.
Nokleberg, W.J. and Richter, D.H., 2007, Origin of narrow terranes and adjacent major terranes occurring along the Denali fault in the Eastern and Central Alaska Range, Alaska: *in* Ridgway, K.D., Trop, J.M., Glen, J.M.G., O'Neill, M.O., eds., Tectonic Growth of a Collisional Continental Margin: Crustal Evolution of Southern Alaska: Geological Society of America Special Papers 431, p.129-154.
Nokleberg, W.J., Aleinikoff, J.N., Bond, G.C., Ferrians, O.J., Jr., Herzon, P.L., Lange, I.M., Miyaoka, R.T., Richter, D.H., Schwab, C.E., Silva, S.R., Smith, T.E., and Zehner, R.E., 2015, Geologic maps of the eastern Alaska Range, Alaska (44 quadrangles, 1:63,360 scale), with descriptions and interpretations of map units: Alaska Division of Geological & Geophysical Surveys Report of Investigation 2015-6, 64 p., 45 sheets, scale 1:63,360. doi:10.14509/29444
Nokleberg, W.J., Aleinikoff, J.N., Bundtzen, T.K., and Hanshaw, M.N., 2013, Geologic strip map along the Hines Creek Fault showing evidence for Cenozoic displacement in the western Mount Hayes and northeastern Healy quadrangles, eastern Alaska Range, Alaska: U.S. Geological Survey Scientific Investigations Map 3238, pamphlet 29 p., scale 1:63,360 [http://pubs.usgs.gov/sim/3238/].
Nokleberg, W.J., Aleinikoff, J.N., Lange, I.M., Silva, S.R., Miyaoka, R.T., Schwab, C.E., and Zehner, R.E., 1992a, Preliminary geologic map of the Mount Hayes quadrangle, eastern Alaska Range, Alaska. U.S. Geological Survey Open File Report 92-594, 39p., 1 sheet, scale 1:250,000.
Nokleberg, W.J., Jones, D.L., and Silberling, N.J., 1985, Origin and tectonic evolution of the Maclaren and Wrangellia terranes, eastern Alaska Range, Alaska: Geological Society of America Bulletin, v. 96(10), p. 1251-1270.
O'Driscoll, L.J. and Miller, M.S., 2015, Lithospheric discontinuity structure in Alaska, thickness variations determined by Sp receiver functions: Tectonics, v. 34(4), p. 694-714.
O'Neill, M., Ridgway, K.D., & Eastham, K.R., 2001, Mesozoic Sedimentation and Deformation Along the Talkeetna Thrust Fault, South-Central Alaska—New Insights and Their Regional Tectonic Significance: Studies by the U.S. Geological Survey in Alaska, U.S. Geological Survey Professional Paper 1678.
Paces, J.B. and Miller Jr, J.D., 1993, Precise U-Pb ages of Duluth complex and related mafic intrusions, northeastern Minnesota: Geochronological insights to physical, petrogenetic, paleomagnetic, and tectonomagmatic processes associated with the 1.1 Ga midcontinent rift system: Journal of Geophysical Research: Solid Earth, v. 98(B8), p. 13997-14013.
Paton, C., Woodhead, J.D., Hellstrom, J.C., Hergt, J.M., Greig, A. and Maas, R., 2010, Improved laser ablation U-Pb zircon geochronology through robust downhole fractionation correction: Geochemistry, Geophysics, Geosystems, v. 11(3).
Pavlis, T. L., Chapman, J. B., Bruhn, R. L., Ridgway, K., Worthington, L. L., Gulick, S. P., & Spotila, J., 2012, Structure of the actively deforming fold-thrust belt of the St. Elias orogen with implications for glacial exhumation and three-dimensional tectonic processes. Geosphere, v. 8(5), p. 991-1019.
Pecha, M.E., Gehrels, G.E., McClelland, W.C., Giesler, D., White, C. and Yokelson, I., 2016, Detrital zircon U-Pb geochronology and Hf isotope geochemistry of the Yukon-Tanana terrane, Coast Mountains, southeast Alaska: Geosphere, v. 12(5), p. 1556-1574.

Petrus, J.A. and Kamber, B.S., 2012, VizualAge: A novel approach to laser ablation ICP-MS U-Pb geochronology data reduction: Geostandards and Geoanalytical Research, v. 36(3), p. 247-270.

Piercey, S.J. and Colpron, M., 2009, Composition and provenance of the Snowcap assemblage, basement to the Yukon-Tanana terrane, northern Cordillera: Implications for Cordilleran crustal growth: Geosphere, v *5*(5), p. 439-464.

Plafker, G. and Berg, H.C., 1994. Overview of the geology and tectonic evolution of Alaska: Geological Society of America, Decade of North American Geology.

Preece, S.J. and Hart, W.K., 2004, Geochemical variations in the <5 Ma Wrangell Volcanic Field, Alaska: implications for the magmatic and tectonic development of a complex continental arc system: Tectonophysics, v. 392(1-4), p. 165-191.

Pullen, A., Ibanez-Mejia, M., Gehrels, G., Giesler, D., and Pecha, M., 2018, Optimization of a Laser Ablation-Single Collector-Inductively Coupled Plasma-Mass Spectrometer (Thermo Element 2) for Accurate, Precise, and Efficient Zircon U-Th-Pb Geochronology: Geochemistry, Geophysics, Geosystems, v. 19. https://doi. org/10.1029/2018GC007889

Ranalli, G., 2000, Rheology of the crust and its role in tectonic reactivation: Journal of geodynamics, v. 30(1), p. 3-15.

Rasendra, N., Bonnin, M., Mazzotti, S. and Tiberi, C., 2014, Crustal and upper-mantle anisotropy related to fossilized transpression fabric along the Denali Fault, northern Canadian Cordillera: Bulletin of the Seismological Society of America, v. 104(4), p. 1964-1975.

Regan, S.P., Benowitz, J.A. and Holland, M.E., 2020, A plutonic brother from another magma mother: disproving the Eocene Foraker-McGonagall pluton piercing point and implications for long-term slip on the Denali Fault: Terra Nova, v. 32, p. 66-74.

Renne, P.R., Deino, A.L., Walter, R.C., Turrin, B.D., Swisher, C.C., Becker, T.A., Curtis, G.H., Sharp, W.D., and Jaouni, A.R., 1994, Intercalibration of astronomical and radioisotopic time: Geology, v. 22, p. 783–786, https:// doi .org /10 .1130 /0091 -7613 (1994)022 <0783: IOAART>2 .3 .CO;2.

Renne, P.R., Mundil, R., Balco, G., Min, K., and Ludwig, K.R., 2010, Joint determination of $^{40}K$ decay constants and $^{40}Ar^*/^{40}K$ for the Fish Canyon sanidine standard, and improved accuracy for $^{40}Ar/^{39}Ar$ geochronology: Geochimica et Cosmochimica Acta, v. 74, p. 5349, https:// doi .org /10 .1016 /j .gca .2010 .06 .017.

Riccio, S.J., Fitzgerald, P.G., Benowitz, J.A., and Roeske, S.M., 2014, The role of thrust faulting in the formation of the eastern Alaska Range: Thermochronological constraints from the Susitna Glacier Thrust Fault region of the intracontinental strike-slip Denali Fault system: Tectonics, v. 33, p. 2195–2217, doi: 10.1002/2014TC003646.

Richter, D. H., Smith, J. G., Lanphere, M. A., Dalrymple, G. B., Reed, B. L., & Shew, N., 1990, Age and progression of volcanism, Wrangell volcanic field, Alaska: Bulletin of Volcanology, v. 53(1), p. 29-44.

Richter, D.H., and Dutro, J.T., Jr., 1975, Revision of the type Mankommen Formation (Pennsylvanian and Permian), Eagle Creek area, eastern Alaska Range, Alaska: U.S. Geological Survey Bulletin 1395–B, p. B1–B25.

Richter, D.H., and Matson, J.A., 1971, Quaternary faulting in the eastern Alaska Range: Bulletin of the Geological Society of America, v. 82, p. 1529–1540, doi: 10.1130/0016-7606(1971)82[1529:QFITEA]2.0.CO;2.

Ridgway, K.D., Thoms, E.E., Layer, P.W., Lesh, M.E., White, J.M., and Smith, S.V, 2007,

Neogene transpressionalforeland basin development on the north side of the central Alaska Range, Usibelli Group and Nenana Gravel, Tanana basin, *in* Ridgway, K.D., Trop, J.M., Glen, J.M.G., O'Neill, M.O., eds., Tectonic Growth of a Collisional Continental Margin: Crustal Evolution of Southern Alaska: Geological Society of America Special Papers 431, p. 507–547, doi: 10.1130/2007.2431(20)

Ridgway, K.D., Trop, J.M., Nokleberg, W.J., Davidson, C.M., and Eastham, K.R., 2002, Mesozoic and Cenozoic tectonics of the eastern and central Alaska Range: Progressive basin development and deformation in a suture zone: Bulletin of the Geological Society of America, v. 114, p. 1480–1504, doi: 10.1130/0016-7606(2002)114<1480:MACTOT>2.0.CO;2.

Rioux, M., Hacker, B., Mattinson, J., Kelemen, P., Blusztajn, J. and Gehrels, G., 2007, Magmatic development of an intra-oceanic arc: High-precision U-Pb zircon and whole-rock isotopic analyses from the accreted Talkeetna arc, south-central Alaska: Geological Society of America Bulletin, v. 119(9-10), p. 1168-1184.

Roeske, S.M., Mattinson, J.M. and Armstrong, R.L., 1989, Isotopic ages of glaucophane schists on the Kodiak Islands, southern Alaska, and their implications for the Mesozoic tectonic history of the Border Ranges fault system: Geological Society of America Bulletin, v. 101(8), p. 1021-1037.

Roeske, S.M., Snee, L.W., Pavlis, T.L., 2003, Dextral strike-slip reactivation of an arc-forearc boundary during Late Cretaceous-Early Eocene oblique convergence in the northern Cordillera, *in* Sisson, V.B., Roeske, S.M., Pavlis, T.L., eds., Geology of a Transpressional Orogen Developed during Ridge-Trench Interaction along the North Pacific Margin: Geological Society of America Special Paper 371, P. 141-170.

Romero, M.C., Ridgway, K.D. and Gehrels, G.E., 2020, Geology, U-Pb Geochronology, and Hf Isotope Geochemistry Across the Mesozoic Alaska Range Suture Zone (south-central Alaska): Implications for Cordilleran Collisional Processes and Tectonic Growth of North America: Tectonics, v. 39, e2019TC005946

Rose, A.W., 1965, Geology and mineral deposits of the Rainy Creek areas, Mt. Hayes Quadrangle, Alaska: Alaska Division of Mines and Minerals Geologic Report 14, 57 p., 1 sheet, scale 1:36,000. doi: 10.14509/343

Rose, A.W., 1966, Geological and geochemical investigations in the Eureka Creek and Rainy Creek areas, Mt. Hayes Quadrangle, Alaska: Alaska Division of Mines and Minerals Geologic Report 20, 41 p., 3 sheets, scale 1:40,000. doi: 10.14509/349.

Rubin, C.M., and Saleeby, J.B., 1991, The Gravina sequence: Remnants of a mid Mesozoic oceanic arc in southern southeast Alaska: Journal of Geophysical Research, v. 96, p. 14,551–14,568, https:// doi .org /10 .1029 /91JB00591.

Rubin, C.M., Saleeby, J.B., Cowan, D.S., Brandon, M.T. and McGroder, M.F., 1990, Regionally extensive mid-Cretaceous west-vergent thrust system in the northwestern Cordillera: Implications for continent-margin tectonism: Geology, v. 18(3), p. 276-280.

Ruppert, N.A., 2008, Stress map for Alaska from earthquake focal mechanisms, *in* Freymueller, J.T., Haeussler, P.J., Wesson, R., and Ekström, G., eds., Active Tectonics and Seismic Potential of Alaska: Washington, D.C., American Geophysical Union Geophysical Monograph Series 179, p. 351–367.

Rusmore, M.E., 1987, Geology of the Cadwallader Group and the Intermontane–Insular superterrane boundary, southwestern British Columbia: Canadian Journal of Earth Sciences, v. 24(11), p. 2279-2291.

Saleeby, J.B., 1992, Age and tectonic setting of the Duke Island ultramafic intrusion, southeast Alaska: Canadian Journal of Earth Sciences, v. 29(3), p. 506-522.
Saltus, R.W. and Hudson, T.L., 2007, Regional magnetic anomalies, crustal strength, and the location of the northern Cordilleran fold-and-thrust belt: Geology, v. 35(6), p. 567-570.
Saltus, R.W., Hudson, T.L., & Wilson, F.H., 2007, The geophysical character of southern Alaska—Implications for crustal evolution, *in* Ridgway, K.D., Trop, J.M., Glen, J.M.G., O'Neill, M.O., eds., Tectonic Growth of a Collisional Continental Margin: Crustal Evolution of Southern Alaska: Geological Society of America Special Papers 431, p. 1-20.
Saltus, R.W., Stanley, R.G., Haeussler, P.J., Jones III, J.V., Potter, C.J. and Lewis, K.A., 2016, Late Oligocene to present contractional structure in and around the Susitna basin, Alaska—Geophysical evidence and geological implications: Geosphere, v. 12(5), p. 1378-1390.
Samson, S.D., and Alexander, E.C., 1987, Calibration of the interlaboratory $^{40}Ar/^{39}Ar$ dating standard, MMhb1: Chemical Geology, v. 66, p. 27–34.
Samson, S.D., Patchett, P.J., Gehrels, G.E., and Anderson, R.G., 1990, Nd and Sr isotopic characterization of the Wrangellia terrane and implications for crustal growth of the Canadian Cordillera: The Journal of Geology, v. 98(5), p. 749-762.
Schmitz, M.D., Bowring, S.A. and Ireland, T.R., 2003, Evaluation of Duluth Complex anorthositic series (AS3) zircon as a U-Pb geochronological standard: New high-precision isotope dilution thermal ionization mass spectrometry results: Geochimica et Cosmochimica Acta, v. 67(19), p. 3665-3672.
Sibson, R.H., 1985, A note on fault reactivation: Journal of Structural Geology, v. 7(6), p. 751-754.
Smith, J.G., and MacKevett, E.M., Jr., 1970, The Skolai Group in the McCarthy B-4, C-4, C-5 Quadrangles, Wrangell Mountains, Alaska: U.S. Geological Survey Bulletin 1274-Q, p. Q1–Q26.
Smith, T.E., 1981, Geology of the Clearwater Mountains, south-central Alaska: Alaska Division of Geological & Geophysical Surveys Geologic Report 60, 72 p., 3 sheets, scale 1:63,360. doi:10.14509/406
Snyder, D.C. and Hart, W.K., 2007, The White Mountains Granitoid Suite: Isotopic constraints on source reservoirs for Cretaceous magmatsim within the Wrangellia terrane: *in* Ridgway, K.D., Trop, J.M., Glen, J.M.G., O'Neill, M.O., eds., Tectonic Growth of a Collisional Continental Margin: Crustal Evolution of Southern Alaska: Geological Society of America Special Papers 431, p. 379–399, doi: 10.1130/2007.2431(20)
St. Amand, P., 1957, Geological and geophysical synthesis of the tectonics of portions of British Columbia, the Yukon Territory, and Alaska: Geological Society of America Bulletin, v. 68(10), p. 1343-1370.
Stacey, J.S., and Kramers, J.D., 1975, Approximation of terrestrial lead isotope evolution by a two stage model: Earth and Planetary Science Letters, v. 26, p. 207-221.
Stout, J.H. and Chase, C.G., 1980, Plate kinematics of the Denali fault system: Canadian Journal of Earth Sciences, v. 17(11), p. 1527–1537, doi: 10.1139/e80-160.
Stout, J.H., 1965, Bedrock Geology between Rainy Creek and the Denali fault, Eastern Alaska Range, Alaska [M.S. Thesis]: Fairbanks, University of Alaska, 75 p.
Stout, J.H., 1976, Geology of the Eureka Creek area, east-central Alaska Range, State of Alaska, Department of Natural Resources, Division of Geological & Geophysical Surveys

Geologic Report 46, 32 p., 1 sheet, scale 1:63,360.
Stout, J.H., Brady, J.B., Weber, F. and Page, R.A., 1973, Evidence for Quaternary movement on the McKinley strand of the Denali fault in the Delta River area, Alaska: Geological Society of America Bulletin, v. 84(3), p. 939-948.
Surpless, K.D., Sickmann, Z.T. and Koplitz, T.A., 2014, East-derived strata in the Methow basin record rapid mid-Cretaceous uplift of the southern Coast Mountains batholith: Canadian Journal of Earth Sciences, v. 51(4), p. 339-357.
Sykes, L.R., 1978, Intraplate seismicity, reactivation of preexisting zones of weakness, alkaline magmatism, and other tectonism postdating continental fragmentation: Reviews of Geophysics, v. 16(4), p. 621-688.
Taylor, M., Yin, A., Ryerson, F. J., Kapp, P., and Ding, L., 2003, Conjugate strike-slip faulting along the Bangong-Nujiang suture zone accommodates coeval east-west extension and north-south shortening in the interior of the Tibetan Plateau: Tectonics, v. 22(4), 25 p.
Terhune, P.J., Benowitz, J.A., Trop, J.M., O'Sullivan, P.B., Gillis, R.J. and Freymueller, J.T., 2019, Cenozoic tectono-thermal history of the southern Talkeetna Mountains, Alaska: Insights into a potentially alternating convergent and transform plate margin: Geosphere, v. 15(5), p. 1539-1576.
Tikoff, B., Kelso, P., Manduca, C., Markley, M.J., and Gillaspy, J., 2001, Lithospheric and crustal reactivation of an ancient plate boundary: The assembly and disassembly of the Salmon River suture zone, Idaho, USA: Geological Society, London, Special Publications, v. 186(1), p. 213-231.
Tommasi, A., Knoll, M., Vauchez, A., Signorelli, J.W., Thoraval, C. and Logé, R., 2009, Structural reactivation in plate tectonics controlled by olivine crystal anisotropy: Nature Geoscience, v. 2(6), p. 423.
Trop, J.M. and Ridgway, K.D., 2007, Mesozoic and Cenozoic tectonic growth of southern Alaska: A sedimentary basin perspective: *in* Ridgway, K.D., Trop, J.M., Glen, J.M.G., O'Neill, M.O., eds., Tectonic Growth of a Collisional Continental Margin: Crustal Evolution of Southern Alaska: Geological Society of America Special Papers 431, p. 55-94.
Trop, J.M., Benowitz, J., Cole, R.B. and O'Sullivan, P., 2019, Cretaceous to Miocene magmatism, sedimentation, and exhumation within the Alaska Range suture zone: A polyphase reactivated terrane boundary: Geosphere, v. 15(4), p. 1066-1101.
Trop, J.M., Benowitz, J.A., Koepp, D.Q., Sunderlin, D., Brueseke, M.E., Layer, P.W. and Fitzgerald, P.G., 2020, Stitch in the ditch: Nutzotin Mountains (Alaska) fluvial strata and a dike record ca. 117–114 Ma accretion of Wrangellia with western North America and initiation of the Totschunda fault: Geosphere, v. 16(1), p.82-110.
Turner, D.L. and Smith, T.E., 1974, Geochronology and Generalized Geology of the Central Alaska Range, Clearwater Mountains, and Northern Talkeetna Mountains. Alaska, Alaska Division of Geological & Geophysical Surveys Open File Report 72, 13 p., 1 Sheet, Scale 1:250,000.
Twelker, E., Newberr, R.J., Freeman, L.K., Sicard, K.R., Waldien, T.S., Lande, L.L., Wypych, A., Reioux, D.A., Bachman, E.N., in revision, Bedrock geologic map of the eastern Denali highway area, Mount Hayes, Healy, and Talkeetna Mountains quadrangles, Alaska: Alaska Division of Geological and Geophysical Surveys, scale: 1:100,000, 1 sheet.
Veenstra, E., Christensen, D. H., Abers, G. A., & Ferris, A., 2006, Crustal thickness variation in

south-central Alaska: Geology, v. 34(9), p. 781-784.
Vermeesch, P., 2004, How many grains are needed for a provenance study?: Earth and Planetary Science Letters, v. 224(3-4), p.441-451.
Vermeesch, P., 2012, On the visualization of detrital age distributions: Chemical Geology, v. 312–313, p. 190–194, https://doi .org/10.1016/j.chemgeo.2012.04.021.
Wahrhaftig, C., Turner, D.L., Weber, F.R. and Smith, T.E., 1975, Nature and timing of movement on Hines Creek strand of Denali fault system, Alaska: Geology, v. 3(8), p. 463-466.
Waldien, T.S., Roeske, S.M., Benowitz, J.A., Allen, W.K., Ridgway, K.D. and O'Sullivan, P.B., 2018, Late Miocene to Quaternary evolution of the McCallum Creek thrust system, Alaska: Insights for range-boundary thrusts in transpressional orogens: Geosphere, v. 14(6), p. 2379-2406.
Waldien, T.S., Roeske, S.M., Benowitz., J.A., and Stockli, D.F., 2017, Cenozoivc reactivation of Cretaceous terrane accretionary structures in the eastern Alaska Range, Alaska. Geological Society of America Abstracts with Programs, v. 49, no. 6. doi: 10.1130/abs/2017AM-307791
Wallace, W.K., Hanks, C.L., and Rogers, J.F., 1989, The southern Kahiltna terrane: Implications for the tectonic evolution of southwestern Alaska: Geological Society of America Bulletin, v. 101, p. 1389–1407, https:// doi .org /10 .1130 /0016 -7606 (1989)101 <1389: TSKTIF>2 .3 .CO;2.
White, C., Gehrels, G.E., Pecha, M., Giesler, D., Yokelson, I., McClelland, W.C. and Butler, R.F., 2016, U-Pb and Hf isotope analysis of detrital zircons from Paleozoic strata of the southern Alexander terrane (southeast Alaska): Lithosphere, v. 8(1), p. 83-96.
Whitney, D.L. and Evans, B.W., 2010, Abbreviations for names of rock-forming minerals: American mineralogist, v. 95(1), p. 185-187.
Wilson, F.H., Hults, C.P., Mull, C.G., and Karl, S.M., comps., 2015, Geologic map of Alaska: U.S. Geological Survey Scientific Investigations Map 3340, pamphlet 196 p., 2 sheets, scale 1:1,584,000, http://dx.doi.org/10.3133/sim3340.
Wyld, S. J., P. J. Umhoefer, and J. E. Wright , 2006, Reconstructing northern Cordilleran terranes along known Cretaceous and Cenozoic strike-slip faults: Implications for the Baja British Columbia hypothesis and other models, *in* Haggert, J.W., Enkin, R.J., and Monger J.W.H., eds., Paleogeography of the North American Cordillera: Evidence For and Against Large-Scale displacements: Geological Association of Canada, Special Paper 46, p. 277–298.
Yokelson, I., Gehrels, G.E., Pecha, M., Giesler, D., White, C., and McClelland, W.C., 2015, U-Pb and Hf isotope analysis of detrital zircons from Mesozoic strata of the Gravina belt, southeast Alaska: Tectonics, v. 34, p. 2052–2066.

**SUPPLEMENTS:**

**Supplemental file S1:**

**Sample preparation and zircon extraction at UC Davis:**

Sample preparation for zircon extraction at UC Davis involves: 1) washing the sample with soap and warm water, 2) crushing the rock with a combination of a hydraulic press (if needed), mortar/pestle, and Bico Pulverizer, 3) sieving to the preferred size fraction (generally <250 um for detrital zircon samples, 63-125 um for igneous zircon samples), 4) heavy mineral concentration by decanting and panning, 5) magnetic separation using a Frantz isodynamic separater, 6) density separation with Lithium Polytungstate. These steps usually result in a sufficiently pure zircon separate. However, additional steps are sometimes required to further concentrate zircon. These steps include: 7) additional panning, 8) density separation with Methylene Iodide, 9) acid wash to dissolve pyrite. Once the mineral separate is sufficiently pure, zircon grains are mounted by pouring the detrital the zircon concentrate onto sticky tape or by picking for igneous zircon analysis.

**Mounting:**

Once the desired zircon separate is obtained, we mount the zircons in epoxy. This involves pressing double-sided sticky tape on a flat glass plate and placing (or pouring) the zircon grains and reference materials on the tape. Once grains are mounted, we submerge them en epoxy, which is contained by a 1” diameter plastic cylinder. After curing, the epoxy cylinder is removed from the sticky tape and ground/polished until the zircon interiors are exposed.

**Imaging:**

We image all zircon grains and standards prior to analysis by LA-ICP-MS. Our imaging protocol makes use of the Cameca SX-100 electron microprobe housed in the Earth and

Planetary Sciences department at UC Davis. We image the zircon grains using the 'high-gain' electron beam setting on the Cameca SX-100. By adjusting the brightness and contrast of the backscattered electron (BSE) image, the high gain beam reveals internal zoning structure of the zircon grains. Increasing the scan rate on these BSE images yields a high-resolution greyscale image of the zircon crystal and its internal zoning structure. For igneous or metamorphic zircon analyses, we image each individual crystal and use the high-resolution BSE images to choose our laser spots prior to analysis. We also use the Cameca SX-100 to measure the width of metamorphic growth rims, which helps us determine whether or not it will yield a reliable U-Pb date. For detrital analyses, we use the high-gain beam with a moderate scan rate. This approach still displays zoning features of the zircon grain interior, but at a decreased resolution, which allows imaging of an entire detrital mount in a reasonable timeframe (generally less than 1.5 hr). We image the detrital grain mounts using the 'Video map' feature of the Cameca SX-100. This feature images user-designated domains of the mount in series and then stiches the images together into a rasterized image of the entire grain mount. The end result is a moderate resolution, high contrast image of all grains on the 1" epoxy round. We print all zircon images for igneous, metamorphic, and detrital analyses prior to LA-ICP-MS analysis and mark the printed images during the laser session.

**U-Pb zircon data collection with the Element2 HR ICPMS at the ALC:**

U-Pb geochronology of zircons is conducted by laser ablation inductively coupled plasma mass spectrometry (LA-ICPMS) at the Arizona LaserChron Center (ALC) (Gehrels et al., 2006, 2008; Gehrels and Pecha, 2014). The analyses involve ablation of zircon with a Photon Machines Analyte G2 excimer laser equipped with HelEx ablation cell using a spot diameter of 20 microns. The ablated material is carried in helium into the plasma source of an Element2 HR ICPMS,

which sequences rapidly through masses corresponding to U, Th, and Pb isotopes. Signal intensities are measured with an SEM that operates in pulse counting mode for signals less than 50K cps, in both pulse-counting and analog mode for signals between 50K and 5M cps, and in analog mode above 5M cps. The calibration between pulse-counting and analog signals is determined line-by-line for signals between 50K and 5M cps, and is applied to >5M cps signals. Four intensities are determined and averaged for each isotope, with dwell times that are listed in Table S1.1.

With the laser set at an energy density of ~5 J/cm2, a repetition rate of 8 hz, and an ablation time of 10 seconds, ablation pits are ~12 microns in depth. Sensitivity with these settings is approximately ~5,000 cps/ppm. Each analysis consists of 5 sec on peaks with the laser off (for backgrounds), 10 sec with the laser firing (for peak intensities), and a 20 second delay to purge the previous sample and save files.

Table S1.1: Instrument settings and data processing at Arizona LaserChron Center

| **Analytical Settings for U-Pb Geochronology at the Arizona LaserChron Center (Element 2 Single Collector)** | |
|---|---|
| | |
| **Laboratory and Sample Preparation** | |
| Laboratory name | Arizona LaserChron Center |
| Sample type/mineral | Zircon |
| Sample preparation | Conventional mineral separation, 1 inch epoxy mount, polished to 1-micron finish |
| Imaging | Hitachi 3400N SEM with BSE and/or Cathodoluminesence |
| | |
| **Laser ablation system** | |
| Make, Model, and type | Photon Machines Analyte G2 Excimer laser |
| Ablation cell and volume | HelEx ablation cell |
| Laser wavelength | 193 nm |

| | |
|---|---|
| Pulse width | ~8 ns |
| Energy density | ~7 J/cm2 |
| Repetition rate | 8 Hz |
| Alation duration | 10 s |
| Ablation pit depth/ablation rate | ~12 microns & 0.8 microns/sec |
| Spot diameter nominal/actual | 20 microns |
| Sampling mode/pattern | Spot |
| Carrier gas | Helium |
| Cell carrier gas flow | 0.11 L/min He in inner cup, 0.29 L/min He in cell |
| | |
| **ICP-MS instrument** | |
| Make, Model, and type | Thermo Element2 HR ICPMS |
| Sample introduction | Ablation aerosol |
| RF power | 1200 W |
| Make-up gas flow | 0.8 L/min Ar |
| Detection system | Dual mode Secondary Electron Multiplier |
| Masses measured | 202Hg, 204(Hg+Pb), 206Pb, 207Pb, 208Pb, 232Th, 235U, 238U |
| Dwell times (ms) | 202=5.2, 204=7.8, 206=20.2, 207=28.4, 208=2.6, 232=2.6, 235=15.4, 238=10.4 |
| Total integration time per output data point (sec) | 202=1.5, 204=2.3, 206=5.9, 207=8.3, 208=7.6, 232=7.6, 235=4.5, 238=3.0 |
| Sensitivity as useful yield | ~5000 cps/ppm |
| IC dead time | 22 ns |
| | |
| **Data processing** | |
| Gas blank | 8 sec on-peak zero subtracted |
| Calibration strategy | SLM zircon used as primary standard |
| Reference material information | Gehrels et al. (2008) |
| Data processing package used/Correction for LIEF | E2agecalc |
| Mass discrimination | Normalized to primary standard |
| Common Pb correction, composition and uncertainty | Common Pb correction based on measured 206Pb/204 Pb and the assumed composition of common Pb based on Stacey and Kramers (1975) |
| Uncertainty level and propagation | Uncertainties for individual analyses propagated at 1-sigma. Uncertainty of pooled analyses propagated at 2-sigma. |

| | |
|---|---|
| Quality control/validation | FC-1 and R33 analyzed as secondary standards. |
| | |
| **Other information** | Primary and secondary standards mounted together with unknowns. |
| | Analytical methods described by Gehrels et al. (2008), Gehrels and Pecha (2014), and Pullen et al. (2018) |

**U-Pb data reduction methods at the ALC:**

Following analysis, data reduction is performed with an in-house Python decoding routine and an Excel spreadsheet (E2agecalc) that:

1. Decodes .dat files from the Thermo software such individual intensities for measurement are available (routine written by John Hartman, University of Arizona)

2. Imports intensities and a sample name for each analysis

3. Calculates average intensities for each isotope (based on the sum of all counts while the laser is firing)

4. Subtracts $^{204}$Hg from the 204 signal to yield $^{204}$Pb intensity (using natural $^{202}$Hg/$^{204}$Hg of 4.3). This Hg correction is not significant for most analyses because our Hg backgrounds are low (generally ~150 cps at mass 204).

5. Performs a common Pb correction based on the measured $^{206}$Pb/$^{204}$Pb and the assumed composition of common Pb based on Stacey and Kramers (1975)

6. Calculates measured 206/238, 206/207, and 208/232 ratios

7. Compares measured and known ratios for the three standards to determine fractionation factors for 206/238, 206/207, and 208/232. These correction factors are generally <5% for 206/238, <2% for 206/207, and <20% for 208/232.

8. Determines an overdispersion factor if the standard analyses show greater dispersion than expected from measurement uncertainties

9. Uses a sliding-window average to apply fractionation factors to unknowns (generally averaging 8 standard analyses)

10. Calculates fractionation-corrected 206/238, 206/207, and 208/232 ratios and ages for unknowns

11. Propagates measurement uncertainties for 206/238 and 208/232 that are based on the scatter about a regression of measured values. Uncertainties for 206/207 and 206/204 are based on the standard deviation of measured values since these ratios generally do not change during an analysis. The sum of this uncertainty and any overdispersion factor is reported as the internal (or measurement) uncertainty for each analysis. These uncertainties are reported at the 1-sigma level.

12. Calculates the down-hole slope of 206/238 to highlight analyses in which 206/238 is compromised due to heterogeneity in age (e.g., crossing an age boundary) or intersection of a fracture or inclusion.

13. Calculates concentrations of U and Th for unknowns based on the measured intensity and known concentrations of FC-1.

14. Calculates the external (systematic) uncertainties for 206/238, 206/207, and 208/232, which include contributions from (a) the scatter of standard analyses, (b) uncertainties in the ages of the standards, (c) uncertainties in the composition of common Pb, and (4) uncertainties in the decay constants for $^{235}U$ and $^{238}U$.

15. Determines a “Best Age” for each analysis, which is generally the 206/238 age for <900 Ma ages and the 206/207 age for >900 Ma ages.

16. Provides preliminary filters that highlight analyses with >20% discordance, >5% reverse discordance, or >10% internal (measurement) uncertainty.

17. Corrects 206/238U ages for U-Th disequilibrium. This has a significant impact only on very young (~<2 Ma) ages.

18. Calculates the radiation dosage that the analyzed portion of each zircon has experienced, assuming a value of 2.3 for the Th/U of the magma. This is plotted against 206/238 age to help identify Pb loss.

18. Creates a publication-ready datatable with concentrations, isotope ratios, and ages for unknowns.

**U-Pb zircon data collection with the LA-Q-ICP-MS at UC Davis:**

U-Pb geochronology of zircon is conducted by laser ablation quadrupole inductively coupled plasma mass spectrometry (LA-Q-ICP-MS) at UC Davis. The analyses involve ablation of zircon with a Photon Machines Analyte G2 excimer laser equipped with HelEx ablation cell using a spot diameter of 25 microns. The ablated material is carried in helium into the plasma source of an Agilent 7700 Series Q-ICP-MS, which sequences rapidly through masses corresponding to U, Th, Pb, and Hg isotopes. Dwell times for each of these masses are listed in Table S1.2.

Instrument settings on the LA-Q-ICP-MS system at UC Davis are based on a published calibration using nearly identical equipment (Matthews and Guest, 2017). Matthews and Guest (2017) used optical profilometry to measure a pit depth of ~12 um using the laser settings listed in Table S1.2. Since we used the instrument settings published by Matthews and Guest (2017), we infer that the analyses performed at UC Davis result in a laser pit depth of ~12 um. Uranium sensitivity with these settings is approximately ~230 cps/ppm, which we approximate using the

NIST 610 glass. Each analysis consists of 15 sec on peaks with the laser off (for backgrounds) and 15 sec with the laser firing (for peak intensities),

Table S1.2: Instrument settings and data processing at UC Davis

| **Laboratory & Sample Preparation** | |
|---|---|
| Laboratory name | Dept. of Earth and Planetary Sciences, UC Davis |
| Sample type/mineral | Zircon U-Pb detrital and igneous |
| Sample preparation | Conventional mineral separation, 1 inch resin mount, 1μm polish to finish |
| Imaging | BSE images Cameca SX-100 electron microprobe |
| **Laser ablation system** | |
| Make, Model & type | Photon Machines Analyte G2 Excimer Laser |
| Ablation cell & volume | HelEx ablation cell |
| Laser wavelength (nm) | 193 nm |
| Pulse width (ns) | ~8 ns |
| Fluence ($J.cm^{-2}$) | 1.88 $J.cm^{-2}$ |
| Repetition rate (Hz) | 10 Hz |
| Ablation duration (secs) | 15 s |
| Ablation pit depth / ablation rate | ~12μm pit depth, inferred from Mathews and Guest (2017). |
| Spot diameter (μm) nominal/actual | 25 μm / ~30 μm, square aperture |
| Sampling mode / pattern | Static spot ablation |
| Carrier gas | Helium |
| Cell carrier gas flow (l/min) | 0.75 |
| **ICP-MS Instrument** | |
| Make, Model & type | Agilent 7700 series Q-ICP-MS |
| Sample introduction | Ablation aerosol |
| RF power (W) | 1350W |
| Make-up gas flow (l/min) | 1.1 |
| Detection system | Electron Multiplier |
| Masses measured | 91, 201, 202, 204, 206 207, 235, 238 |

| | |
|---|---|
| Integration time per peak/dwell times (s); quadrupole settling time between mass jumps | 0.01, 0.01, 0.01, 0.03, 0.04, 0.07,<br>0.015, 0.015, 0.02 s. In order of masses listed above. |
| Total integration | 0.239 s |
| 'Sensitivity' as useful yield | ~230 cps/ppm U<br>Estimated on NIST 610 glass |
| IC Dead time (ns) | |
| **Data Processing** | |
| Gas blank | 15 second on-peak zero subtracted |
| Calibration strategy | FC-1 used as primary reference material, R-33 used as secondary/validation |
| Reference Material info | FC-1 (Paces and Miller, 1993; Schmitz et al., 2003)<br>R-33 (Black et al. 2004) |
| Data processing package used / Correction for LIEF | Iolite-Igor data reduction scheme based on methods of Patton et al, (2010) and Petrus and Kamber (2012). Laser-Induced Elemental Fractionation correction assumes reference material and samples behave identically. |
| Mass discrimination | $^{206}Pb/^{238}U$ additionally normalized to reference material |
| Common-Pb correction, composition and uncertainty | No common-Pb correction applied to the data. |
| Uncertainty level & propagation | Ages are quoted at 2*s* absolute, propagation is by quadratic addition. Reproducibility and age uncertainty of reference material are propagated where appropriate. |
| Quality control / Validation | FC-1 and R-33 natural zircon reference materials |
| **Other information** | |

**U-Pb data reduction methods at UC Davis:**

Data from the Q-ICP-MS are imported into Igor Pro-Iolite and displayed as a time series. Integration periods for gas blanks (backgrounds), standards, and unknowns are selected manually. FC-1 (Paces and Miller, 1993; Schmitz et al., 2003) is used as the primary reference material and R-33 (Black et al., 2004) is used as a secondary reference. Estimates of elemental

concentrations, and thus U/Th, are also determined using FC-1. Isotope ratios, dates, and associated uncertainties are calculated from the integrations using the *U_Pb_geochronology3* data reduction scheme (Paton et al., 2010). After initial dates are calculated, we use the *Live Concordia* feature of the *VizualAge* data reduction scheme (Petrus and Kamber, 2012) to screen each integration period for discordance related to inclusions and/or mixed age domains (e.g., a spurious date resulting from ablating through a younger rim into an older core). If an analysis is found to be discordant apparently related to the aforementioned causes, we conservatively adjust the integration interval to obtain the most reliable date at reasonable uncertainty. Once screened, we export the data, 2s internal and external uncertainties, and elemental concentrations. We report our data using the datatable template suggested by Horstwood et al. (2016), which may be found at www.Plasmage.org.

It is important to convey that the Agilent 7700 Q-ICP-MS at UC Davis is not currently equipped with a Hg trap in the carrier gas line. This results in generally high background $^{204}$Hg. Although we monitor mass 204 (Hg + Pb) during analysis sessions, the elevated background 204 signal precludes determination of meaningful $^{204}$Pb/$^{206}$Pb ratios. Thus, we do not apply any common Pb correction to the data. However, we do consider the 204 signal during integration periods. If the 204 signal is elevated above background levels during ablation of a zircon, it is likely indicating the presence of $^{204}$Pb. Due to the assumptions and high level of uncertainty that would be introduced by attempting to do a common Pb correction on such analyses, we reject analyses on grains that display elevated 204 relative to the background gas blank. Such rejections are uncommon.

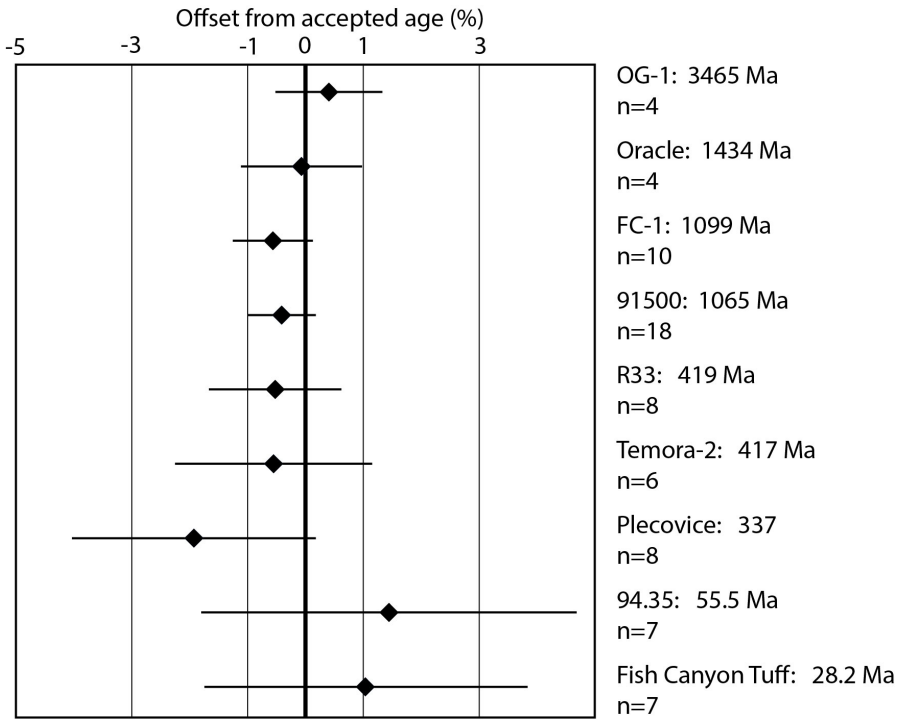


**Figure S1.1:** Calibration of zircon reference materials ranging from 28.2 to 3465 Ma using the LA-Q-ICP-MS at UC Davis. All analyses were performed using the ablation settings described above. Each diamond represents multiple analyses on multiple grains (n=number of analyses) during a single session.

**Data filtering methods:**

We parsed the single grain dates from both labs using Tera-Wasserburg concordia diagrams, U/Th ratios, and zoning patterns.

Reverse discordance- Single grain analyses from some of our samples suffered from reverse discordance. Because the causes of reverse discordance are not well understood, but may result either from heterogeneous distribution of U- and Pb-rich zones in a crystal (Danisik et al., 2017), or the partial dissolution of U-rich zones by fluids (Mattinson et al., 1996), we filtered our U-Pb dates to exclude those which are reverse discordant and do not overlap within uncertainty of the concordia curve. The $^{206}Pb/^{238}U$ dates from the reverse discordant grains generally overlap with

$^{206}Pb/^{238}U$ dates of concordant or normally discordant analyses. Yet, the $^{207}Pb/^{206}Pb$ ages are either very young, or in some cases, negative (i.e., future ages). Because the reverse discordant analyses come from samples that experienced upper greenschist to amphibolite facies conditions and several grains from these samples show textures indicating partial dissolution, we interpret the reverse discordant analyses as the result of interaction with corrosive fluids. Thus, we reject these analyses from the detrital population, despite the overlap in $^{206}Pb/^{238}U$ dates.

≤900 Ma detrital grain dates are used in KDE plots if the $^{206}Pb/^{238}U$ date has an uncertainty (2s internal) of <10% and <u>either</u> of the following criteria are met:

1. The 2s internal uncertainty ellipse intersects the concordia curve on a Tera-Wasserburg diagram, allowing the concordia curve to account for decay constant uncertainties.
2. The date is discordant, but the $^{207}Pb/^{206}Pb$ date is <3 times the $^{206}Pb/^{238}U$ date.

≥900 Ma detrital grain dates are used in KDE plots if <u>both</u> of the following criteria are met:

1. The date is <5% reverse discordant
2. The date is <20% normally discordant

Dates are interpreted to record post-depositional metamorphic recrystallization if the grain was recovered from a metamorphic rock that experienced appropriate temperatures to recrystallize zircon (estimated petrographically using mineral assemblages) and <u>one or more</u> of the following criteria are met:

1. The date overlaps with the known age of cross cutting intrusive rocks within the map unit.

2. The dated grain, or region of the grain, lacks internal zoning, which is suggestive of metamorphic recrystallization (Hoskin and Schaltegger, 2003).
3. The analysis targeted an overgrowth rim identified in BSE images.
4. The U/Th ratio of the analysis is elevated (>20) and/or variable within the population of dates.

Dates (as part of a population) are used to calculate metamorphic or igneous ages if all of the following criteria are met:

1. The 2s internal uncertainty ellipse intersects the concordia curve on a Tera-Wasserburg diagram, allowing the concordia curve to account for decay constant uncertainties.
2. The $^{206}Pb/^{238}U$ date has <10% uncertainty (2s internal) (For igneous analyses only).
3. Isoplot does not reject the date during the weighted mean calculation.

For populations of igneous or metamorphic grain dates, ages are calculated using the weighted mean function in Isoplot (Ludwig, 2008). Following the protocol of Horstwood et al. (2016), only 2s internal uncertainties are used in the weighted mean calculation and systematic uncertainties are added quadratically to the internal uncertainty after the weighted mean is calculated. Uncertainties on igneous or metamorphic ages reported in the main text include both internal (included in weighted mean calculation) and systematic (added on after weighted mean calculation) unless otherwise indicated.

Maximum depositional ages are estimated to be the mean age of the youngest statistical population of detrital dates (Herriott et al., 2019).

## Supplemental file S2

Table S2-1: Detrital zircon U-Pb sample locations

| Sample Number | Latitude (ºN) | Longitude (ºE) |
|---|---|---|
| 15ATW-06 | 63.3008 | -146.1135 |
| 15ATW-07 | 63.3566 | -146.0608 |
| 15ATW-29 | 63.3636 | -146.0478 |
| 15ATW-41b | 63.3611 | -145.8608 |
| 15ATW-52 | 63.3546 | -145.8297 |
| 15ATW-23 | 63.3555 | -146.1111 |
| 16ATW-10 | 63.3300 | -146.1733 |
| 16ATW-44b | 63.3392 | -146.1708 |
| 16ATW-77 | 63.3432 | -146.1527 |
| 16ATW-86 | 63.3443 | -146.1477 |

Table S2-2: Detrital zircon U-Pb data

| Sample 15ATW06 | | | | Isotope ratios | | | | | | | | | Apparent ages (Ma) | | | | | | |
|---|---|---|---|---|---|---|---|---|---|---|---|---|---|---|---|---|---|---|---|
| Analysis | U | 206Pb | U/Th | 206Pb * | ± | 207Pb * | ± | 206Pb * | ± | error | 206Pb * | ± | 207Pb * | ± | 206Pb * | ± | Best age | ± | Conc |
| | (ppm) | 204Pb | | 207Pb * | (%) | 235U * | (%) | 238U | (%) | corr. | 238U * | (Ma) | 235U | (Ma) | 207Pb * | (Ma) | (Ma) | (Ma) | (%) |
| -Spot 51 | 1541 | 36144 | 3.2 | 21.1 | 2.7 | 0.0 | 3.4 | 0.0 | 2.1 | 0.6 | 28.1 | 0.6 | 28.6 | 1.0 | 73.8 | 64.6 | 28.1 | 0.6 | NA |
| -Spot 200 | 1169 | 12004 | 3.3 | 22.3 | 2.5 | 0.0 | 3.5 | 0.0 | 2.4 | 0.7 | 28.3 | 0.7 | 27.3 | 0.9 | 61.3 | 61.3 | 28.3 | 0.7 | NA |
| -Spot 270 | 283 | 11593 | 3.9 | 21.4 | 6.1 | 0.0 | 6.6 | 0.0 | 2.7 | 0.4 | 28.3 | 0.7 | 28.5 | 1.9 | 37.6 | 145.7 | 28.3 | 0.7 | NA |
| -Spot 304 | 101 | 1751 | 5.1 | 24.1 | 7.3 | 0.0 | 8.0 | 0.0 | 3.2 | 0.4 | 28.4 | 0.9 | 25.3 | 2.0 | 254.9 | 185.6 | 28.4 | 0.9 | NA |
| -Spot 121 | 1398 | 28854 | 5.5 | 21.6 | 2.5 | 0.0 | 3.1 | 0.0 | 1.8 | 0.6 | 28.4 | 0.5 | 28.3 | 0.9 | 17.7 | 59.8 | 28.4 | 0.5 | NA |
| -Spot 153 | 1622 | 39216 | 2.0 | 21.5 | 2.6 | 0.0 | 3.5 | 0.0 | 2.3 | 0.7 | 28.5 | 0.6 | 28.4 | 1.0 | 23.8 | 63.1 | 28.5 | 0.6 | NA |
| -Spot 130 | 723 | 35424 | 6.3 | 20.8 | 3.2 | 0.0 | 3.7 | 0.0 | 1.8 | 0.5 | 28.5 | 0.5 | 29.4 | 1.1 | 102.5 | 75.2 | 28.5 | 0.5 | NA |
| -Spot 72 | 721 | 16574 | 2.9 | 21.3 | 4.2 | 0.0 | 4.6 | 0.0 | 2.0 | 0.4 | 28.6 | 0.6 | 28.7 | 1.3 | 41.2 | 99.5 | 28.6 | 0.6 | NA |
| -Spot 198 | 810 | 161507 | 2.1 | 21.3 | 2.3 | 0.0 | 2.8 | 0.0 | 1.7 | 0.6 | 28.7 | 0.5 | 28.9 | 0.8 | 48.3 | 54.5 | 28.7 | 0.5 | NA |
| -Spot 12 | 882 | 67192 | 5.4 | 21.2 | 2.3 | 0.0 | 3.0 | 0.0 | 2.0 | 0.7 | 28.8 | 0.6 | 29.1 | 0.9 | 58.4 | 53.7 | 28.8 | 0.6 | NA |
| -Spot 177 | 568 | 10428 | 3.1 | 21.2 | 5.2 | 0.0 | 5.6 | 0.0 | 2.0 | 0.4 | 28.8 | 0.6 | 29.2 | 1.6 | 58.4 | 124.7 | 28.8 | 0.6 | NA |
| -Spot 210 | 259 | 8921 | 4.3 | 20.7 | 5.5 | 0.0 | 5.9 | 0.0 | 2.1 | 0.4 | 28.8 | 0.6 | 29.9 | 1.7 | 115.7 | 129.7 | 28.8 | 0.6 | NA |
| -Spot 184 | 240 | 2371 | 4.7 | 17.0 | 7.7 | 0.0 | 8.1 | 0.0 | 2.3 | 0.3 | 28.9 | 0.7 | 36.4 | 2.9 | 565.5 | 168.7 | 28.9 | 0.7 | NA |
| -Spot 142 | 756 | 22771 | 2.9 | 20.9 | 3.6 | 0.0 | 4.7 | 0.0 | 3.0 | 0.6 | 28.9 | 0.9 | 29.7 | 1.4 | 93.0 | 85.2 | 28.9 | 0.9 | NA |
| -Spot 246 | 1202 | 40330 | 4.9 | 21.4 | 2.7 | 0.0 | 3.3 | 0.0 | 1.9 | 0.6 | 28.9 | 0.6 | 29.0 | 0.9 | 33.0 | 64.0 | 28.9 | 0.6 | NA |
| -Spot 160 | 895 | 17165 | 3.9 | 21.6 | 4.0 | 0.0 | 4.6 | 0.0 | 2.2 | 0.5 | 28.9 | 0.6 | 28.8 | 1.3 | 16.3 | 96.4 | 28.9 | 0.6 | NA |
| -Spot 14 | 1100 | 26984 | 2.0 | 21.6 | 3.0 | 0.0 | 3.8 | 0.0 | 2.3 | 0.6 | 29.0 | 0.7 | 28.7 | 1.1 | 8.2 | 72.1 | 29.0 | 0.7 | NA |
| -Spot 256 | 1274 | 19318 | 2.2 | 22.0 | 3.5 | 0.0 | 4.4 | 0.0 | 2.7 | 0.6 | 29.0 | 0.8 | 28.3 | 1.2 | 26.3 | 84.9 | 29.0 | 0.8 | NA |
| -Spot 48 | 423 | 46065 | 3.8 | 19.8 | 4.9 | 0.0 | 5.5 | 0.0 | 2.5 | 0.5 | 29.0 | 0.7 | 31.4 | 1.7 | 217.7 | 112.9 | 29.0 | 0.7 | NA |
| -Spot 306 | 67 | 3307 | 3.7 | 20.3 | 10.4 | 0.0 | 11.0 | 0.0 | 3.6 | 0.3 | 29.1 | 1.0 | 30.7 | 3.3 | 158.9 | 242.9 | 29.1 | 1.0 | NA |
| -Spot 166 | 406 | 5951 | 5.2 | 21.8 | 4.4 | 0.0 | 4.9 | 0.0 | 2.2 | 0.4 | 29.1 | 0.6 | 28.6 | 1.4 | 14.5 | 106.0 | 29.1 | 0.6 | NA |

| | | | | | | | | | | | | | | | | | | | |
|---|---|---|---|---|---|---|---|---|---|---|---|---|---|---|---|---|---|---|---|
| -Spot 107 | 450 | 35534 | 4.1 | 20.7 | 4.4 | 0.0 | 4.9 | 0.0 | 2.1 | 0.4 | 29.1 | 0.6 | 30.2 | 1.4 | 115.5 | 102.9 | 29.1 | 0.6 | NA |
| -Spot 214 | 1328 | 98363 | 2.2 | 21.2 | 2.9 | 0.0 | 3.5 | 0.0 | 2.0 | 0.6 | 29.2 | 0.6 | 29.5 | 1.0 | 56.3 | 68.6 | 29.2 | 0.6 | NA |
| -Spot 134 | 654 | 43205 | 3.1 | 21.8 | 3.8 | 0.0 | 4.4 | 0.0 | 2.3 | 0.5 | 29.2 | 0.7 | 28.7 | 1.3 | 9.5 | 91.1 | 29.2 | 0.7 | NA |
| -Spot 29 | 732 | 144513 | 5.7 | 20.7 | 3.2 | 0.0 | 3.8 | 0.0 | 2.1 | 0.6 | 29.2 | 0.6 | 30.3 | 1.1 | 118.6 | 75.2 | 29.2 | 0.6 | NA |
| -Spot 152 | 460 | 33342 | 3.8 | 21.5 | 4.9 | 0.0 | 5.3 | 0.0 | 2.0 | 0.4 | 29.2 | 0.6 | 29.2 | 1.5 | 29.0 | 116.4 | 29.2 | 0.6 | NA |
| -Spot 185 | 536 | 16044 | 5.9 | 20.8 | 3.8 | 0.0 | 4.3 | 0.0 | 2.0 | 0.5 | 29.2 | 0.6 | 30.2 | 1.3 | 106.5 | 89.8 | 29.2 | 0.6 | NA |
| -Spot 145 | 1416 | 30601 | 1.5 | 21.3 | 2.3 | 0.0 | 2.8 | 0.0 | 1.6 | 0.6 | 29.2 | 0.5 | 29.4 | 0.8 | 43.5 | 54.4 | 29.2 | 0.5 | NA |
| -Spot 187 | 526 | 47457 | 3.9 | 20.5 | 5.2 | 0.0 | 5.6 | 0.0 | 2.1 | 0.4 | 29.2 | 0.6 | 30.5 | 1.7 | 133.6 | 123.1 | 29.2 | 0.6 | NA |
| -Spot 141 | 1072 | 39728 | 4.6 | 21.2 | 2.6 | 0.0 | 3.2 | 0.0 | 1.9 | 0.6 | 29.2 | 0.5 | 29.5 | 0.9 | 55.1 | 62.5 | 29.2 | 0.5 | NA |
| -Spot 28 | 911 | 16888 | 4.5 | 21.5 | 2.5 | 0.0 | 3.1 | 0.0 | 1.8 | 0.6 | 29.2 | 0.5 | 29.1 | 0.9 | 21.1 | 60.2 | 29.2 | 0.5 | NA |
| -Spot 52 | 696 | 32467 | 7.8 | 21.4 | 3.0 | 0.0 | 3.6 | 0.0 | 2.0 | 0.5 | 29.2 | 0.6 | 29.3 | 1.0 | 32.5 | 72.0 | 29.2 | 0.6 | NA |
| -Spot 82 | 252 | 3437 | 6.1 | 20.8 | 5.6 | 0.0 | 6.4 | 0.0 | 2.9 | 0.5 | 29.2 | 0.9 | 30.2 | 1.9 | 107.0 | 133.2 | 29.2 | 0.9 | NA |
| -Spot 27 | 758 | 17071 | 3.6 | 21.4 | 4.1 | 0.0 | 5.0 | 0.0 | 2.7 | 0.5 | 29.3 | 0.8 | 29.4 | 1.4 | 39.6 | 99.2 | 29.3 | 0.8 | NA |
| -Spot 11 | 818 | 33279 | 2.5 | 21.8 | 3.9 | 0.0 | 4.6 | 0.0 | 2.6 | 0.6 | 29.3 | 0.8 | 28.8 | 1.3 | 13.0 | 93.3 | 29.3 | 0.8 | NA |
| -Spot 16 | 272 | 15882 | 3.4 | 21.0 | 6.5 | 0.0 | 6.9 | 0.0 | 2.3 | 0.3 | 29.3 | 0.7 | 29.9 | 2.0 | 80.7 | 154.4 | 29.3 | 0.7 | NA |
| -Spot 26 | 825 | 24344 | 3.7 | 21.4 | 3.0 | 0.0 | 3.8 | 0.0 | 2.3 | 0.6 | 29.3 | 0.7 | 29.3 | 1.1 | 30.6 | 73.1 | 29.3 | 0.7 | NA |
| -Spot 103 | 552 | 14347 | 4.3 | 21.5 | 4.4 | 0.0 | 4.8 | 0.0 | 1.8 | 0.4 | 29.3 | 0.5 | 29.3 | 1.4 | 24.7 | 106.6 | 29.3 | 0.5 | NA |
| -Spot 193 | 672 | 8734 | 2.5 | 22.7 | 3.6 | 0.0 | 4.0 | 0.0 | 1.8 | 0.4 | 29.3 | 0.5 | 27.7 | 1.1 | 107.4 | 89.2 | 29.3 | 0.5 | NA |
| -Spot 206 | 537 | 20981 | 3.5 | 21.5 | 3.9 | 0.0 | 4.5 | 0.0 | 2.2 | 0.5 | 29.3 | 0.7 | 29.3 | 1.3 | 25.4 | 94.0 | 29.3 | 0.7 | NA |
| -Spot 204 | 446 | 10444 | 5.7 | 20.6 | 3.1 | 0.0 | 3.8 | 0.0 | 2.2 | 0.6 | 29.4 | 0.6 | 30.5 | 1.1 | 124.3 | 73.3 | 29.4 | 0.6 | NA |
| -Spot 56 | 354 | 7823 | 3.2 | 21.4 | 5.8 | 0.0 | 6.5 | 0.0 | 3.0 | 0.5 | 29.4 | 0.9 | 29.5 | 1.9 | 38.9 | 137.7 | 29.4 | 0.9 | NA |
| -Spot 291 | 1083 | 39717 | 5.0 | 21.3 | 2.9 | 0.0 | 3.4 | 0.0 | 1.9 | 0.5 | 29.4 | 0.5 | 29.6 | 1.0 | 44.9 | 68.3 | 29.4 | 0.5 | NA |
| -Spot 8 | 1334 | 32318 | 4.2 | 21.4 | 2.6 | 0.0 | 3.5 | 0.0 | 2.3 | 0.7 | 29.4 | 0.7 | 29.5 | 1.0 | 40.4 | 62.6 | 29.4 | 0.7 | NA |
| -Spot 131 | 857 | 20923 | 3.1 | 21.3 | 2.5 | 0.0 | 3.4 | 0.0 | 2.4 | 0.7 | 29.4 | 0.7 | 29.6 | 1.0 | 43.6 | 58.8 | 29.4 | 0.7 | NA |
| -Spot 55 | 959 | 46814 | 7.4 | 21.2 | 3.1 | 0.0 | 3.6 | 0.0 | 1.8 | 0.5 | 29.4 | 0.5 | 29.7 | 1.1 | 55.6 | 74.4 | 29.4 | 0.5 | NA |
| -Spot 305 | 216 | 13191 | 5.4 | 20.9 | 5.8 | 0.0 | 6.4 | 0.0 | 2.7 | 0.4 | 29.4 | 0.8 | 30.2 | 1.9 | 92.5 | 137.5 | 29.4 | 0.8 | NA |
| -Spot 170 | 150 | 13663 | 6.5 | 19.6 | 6.9 | 0.0 | 7.5 | 0.0 | 3.0 | 0.4 | 29.5 | 0.9 | 32.2 | 2.4 | 242.5 | 158.9 | 29.5 | 0.9 | NA |
| -Spot 269 | 704 | 9511 | 4.7 | 22.1 | 3.7 | 0.0 | 4.5 | 0.0 | 2.6 | 0.6 | 29.5 | 0.8 | 28.6 | 1.3 | 43.3 | 89.7 | 29.5 | 0.8 | NA |
| -Spot 292 | 971 | 25053 | 2.3 | 21.8 | 2.8 | 0.0 | 3.6 | 0.0 | 2.2 | 0.6 | 29.5 | 0.6 | 29.1 | 1.0 | 6.6 | 67.4 | 29.5 | 0.6 | NA |
| -Spot 91 | 566 | 20895 | 6.5 | 21.6 | 3.7 | 0.0 | 4.4 | 0.0 | 2.3 | 0.5 | 29.5 | 0.7 | 29.4 | 1.3 | 17.3 | 89.9 | 29.5 | 0.7 | NA |
| -Spot 34 | 342 | 13952 | 5.7 | 21.3 | 5.5 | 0.0 | 6.2 | 0.0 | 2.7 | 0.4 | 29.5 | 0.8 | 29.7 | 1.8 | 48.8 | 132.2 | 29.5 | 0.8 | NA |
| -Spot 132 | 1577 | 72499 | 9.6 | 20.7 | 2.7 | 0.0 | 3.3 | 0.0 | 1.9 | 0.6 | 29.5 | 0.6 | 30.6 | 1.0 | 114.2 | 62.8 | 29.5 | 0.6 | NA |
| -Spot 167 | 348 | 3827 | 5.5 | 22.8 | 4.9 | 0.0 | 5.2 | 0.0 | 1.8 | 0.3 | 29.5 | 0.5 | 27.8 | 1.4 | 114.2 | 119.6 | 29.5 | 0.5 | NA |
| -Spot 126 | 366 | 6071 | 3.9 | 22.0 | 5.3 | 0.0 | 5.5 | 0.0 | 1.7 | 0.3 | 29.5 | 0.5 | 28.8 | 1.6 | 33.6 | 127.8 | 29.5 | 0.5 | NA |
| -Spot 146 | 580 | 17259 | 3.9 | 21.9 | 3.8 | 0.0 | 4.2 | 0.0 | 1.8 | 0.4 | 29.5 | 0.5 | 29.0 | 1.2 | 17.0 | 92.0 | 29.5 | 0.5 | NA |
| -Spot 46 | 755 | 79171 | 5.7 | 22.1 | 4.5 | 0.0 | 5.2 | 0.0 | 2.5 | 0.5 | 29.5 | 0.7 | 28.7 | 1.5 | 38.8 | 109.9 | 29.5 | 0.7 | NA |
| -Spot 100 | 506 | 7623 | 3.3 | 21.3 | 4.2 | 0.0 | 4.9 | 0.0 | 2.5 | 0.5 | 29.5 | 0.7 | 29.7 | 1.4 | 43.3 | 101.1 | 29.5 | 0.7 | NA |
| -Spot 223 | 301 | 7247 | 5.1 | 21.0 | 5.4 | 0.0 | 5.7 | 0.0 | 1.9 | 0.3 | 29.6 | 0.6 | 30.1 | 1.7 | 77.5 | 129.0 | 29.6 | 0.6 | NA |
| -Spot 42 | 501 | 15795 | 4.6 | 21.2 | 4.2 | 0.0 | 4.8 | 0.0 | 2.5 | 0.5 | 29.6 | 0.7 | 29.9 | 1.4 | 59.8 | 99.2 | 29.6 | 0.7 | NA |
| -Spot 191 | 479 | 22150 | 2.5 | 20.8 | 4.0 | 0.0 | 4.7 | 0.0 | 2.4 | 0.5 | 29.6 | 0.7 | 30.5 | 1.4 | 108.1 | 95.3 | 29.6 | 0.7 | NA |

| | | | | | | | | | | | | | | | | | | | |
|---|---|---|---|---|---|---|---|---|---|---|---|---|---|---|---|---|---|---|---|
| -Spot 138 | 398 | 24757 | 3.6 | 22.0 | 4.1 | 0.0 | 5.0 | 0.0 | 2.8 | 0.6 | 29.6 | 0.8 | 28.8 | 1.4 | 36.6 | 100.1 | 29.6 | 0.8 | NA |
| -Spot 9 | 392 | 18417 | 5.0 | 21.7 | 4.1 | 0.0 | 4.6 | 0.0 | 2.2 | 0.5 | 29.6 | 0.7 | 29.2 | 1.3 | 1.5 | 97.9 | 29.6 | 0.7 | NA |
| -Spot 290 | 411 | 18849 | 4.0 | 20.5 | 4.1 | 0.0 | 4.7 | 0.0 | 2.4 | 0.5 | 29.6 | 0.7 | 30.9 | 1.4 | 133.0 | 96.7 | 29.6 | 0.7 | NA |
| -Spot 307 | 669 | 60937 | 10.5 | 21.2 | 3.1 | 0.0 | 4.0 | 0.0 | 2.6 | 0.6 | 29.6 | 0.8 | 29.9 | 1.2 | 52.8 | 74.6 | 29.6 | 0.8 | NA |
| -Spot 20 | 1443 | 38618 | 7.6 | 21.2 | 2.9 | 0.0 | 3.6 | 0.0 | 2.2 | 0.6 | 29.6 | 0.7 | 30.0 | 1.1 | 62.7 | 67.9 | 29.6 | 0.7 | NA |
| -Spot 231 | 124 | 15481 | 5.0 | 20.7 | 7.6 | 0.0 | 8.1 | 0.0 | 2.8 | 0.3 | 29.6 | 0.8 | 30.6 | 2.5 | 109.9 | 180.8 | 29.6 | 0.8 | NA |
| -Spot 135 | 237 | 6605 | 4.0 | 21.3 | 6.3 | 0.0 | 6.9 | 0.0 | 2.9 | 0.4 | 29.6 | 0.9 | 29.8 | 2.0 | 47.4 | 150.4 | 29.6 | 0.9 | NA |
| -Spot 195 | 448 | 12559 | 2.7 | 22.5 | 4.2 | 0.0 | 5.0 | 0.0 | 2.6 | 0.5 | 29.6 | 0.8 | 28.3 | 1.4 | 84.9 | 104.0 | 29.6 | 0.8 | NA |
| -Spot 22 | 776 | 25769 | 7.0 | 20.7 | 2.6 | 0.0 | 3.2 | 0.0 | 1.7 | 0.5 | 29.6 | 0.5 | 30.7 | 1.0 | 115.0 | 62.1 | 29.6 | 0.5 | NA |
| -Spot 267 | 713 | 16751 | 2.6 | 21.3 | 4.0 | 0.0 | 5.0 | 0.0 | 3.1 | 0.6 | 29.6 | 0.9 | 29.9 | 1.5 | 48.1 | 95.1 | 29.6 | 0.9 | NA |
| -Spot 158 | 250 | 6943 | 3.6 | 22.3 | 5.0 | 0.0 | 5.8 | 0.0 | 3.0 | 0.5 | 29.6 | 0.9 | 28.5 | 1.6 | 67.8 | 121.3 | 29.6 | 0.9 | NA |
| -Spot 119 | 195 | 25297 | 4.4 | 22.9 | 5.5 | 0.0 | 5.9 | 0.0 | 2.1 | 0.4 | 29.6 | 0.6 | 27.8 | 1.6 | 128.6 | 136.8 | 29.6 | 0.6 | NA |
| -Spot 76 | 1342 | 28692 | 2.8 | 21.7 | 2.7 | 0.0 | 3.7 | 0.0 | 2.4 | 0.7 | 29.6 | 0.7 | 29.3 | 1.1 | 3.7 | 66.1 | 29.6 | 0.7 | NA |
| -Spot 83 | 745 | 103708 | 4.6 | 20.9 | 3.9 | 0.0 | 4.4 | 0.0 | 2.1 | 0.5 | 29.6 | 0.6 | 30.4 | 1.3 | 92.3 | 92.3 | 29.6 | 0.6 | NA |
| -Spot 168 | 647 | 11778 | 2.5 | 22.3 | 4.3 | 0.0 | 4.7 | 0.0 | 2.1 | 0.4 | 29.6 | 0.6 | 28.5 | 1.3 | 68.2 | 103.8 | 29.6 | 0.6 | NA |
| -Spot 211 | 393 | 27745 | 3.5 | 21.1 | 4.2 | 0.0 | 4.9 | 0.0 | 2.5 | 0.5 | 29.7 | 0.7 | 30.1 | 1.4 | 67.4 | 100.2 | 29.7 | 0.7 | NA |
| -Spot 118 | 397 | 9627 | 5.6 | 22.3 | 4.8 | 0.0 | 5.1 | 0.0 | 1.9 | 0.4 | 29.7 | 0.6 | 28.6 | 1.4 | 61.0 | 116.6 | 29.7 | 0.6 | NA |
| -Spot 171 | 1352 | 30354 | 13.1 | 21.4 | 3.2 | 0.0 | 3.8 | 0.0 | 2.0 | 0.5 | 29.7 | 0.6 | 29.7 | 1.1 | 31.9 | 76.4 | 29.7 | 0.6 | NA |
| -Spot 273 | 1047 | 29519 | 3.2 | 21.8 | 2.7 | 0.0 | 3.8 | 0.0 | 2.7 | 0.7 | 29.7 | 0.8 | 29.2 | 1.1 | 11.2 | 64.2 | 29.7 | 0.8 | NA |
| -Spot 106 | 486 | 18570 | 5.8 | 21.4 | 4.1 | 0.0 | 4.8 | 0.0 | 2.5 | 0.5 | 29.7 | 0.7 | 29.8 | 1.4 | 38.4 | 97.7 | 29.7 | 0.7 | NA |
| -Spot 278 | 422 | 4821 | 8.0 | 22.2 | 5.8 | 0.0 | 6.2 | 0.0 | 2.3 | 0.4 | 29.7 | 0.7 | 28.7 | 1.8 | 50.9 | 141.4 | 29.7 | 0.7 | NA |
| -Spot 216 | 448 | 11319 | 4.6 | 21.8 | 4.5 | 0.0 | 5.4 | 0.0 | 3.1 | 0.6 | 29.7 | 0.9 | 29.2 | 1.6 | 7.6 | 108.4 | 29.7 | 0.9 | NA |
| -Spot 102 | 513 | 23849 | 3.8 | 21.2 | 3.9 | 0.0 | 4.6 | 0.0 | 2.5 | 0.5 | 29.7 | 0.7 | 30.0 | 1.4 | 54.2 | 93.3 | 29.7 | 0.7 | NA |
| -Spot 241 | 925 | 27179 | 3.2 | 21.7 | 3.4 | 0.0 | 4.1 | 0.0 | 2.3 | 0.6 | 29.7 | 0.7 | 29.4 | 1.2 | 4.7 | 82.8 | 29.7 | 0.7 | NA |
| -Spot 225 | 422 | 3404 | 2.9 | 23.0 | 4.5 | 0.0 | 5.1 | 0.0 | 2.3 | 0.4 | 29.7 | 0.7 | 27.7 | 1.4 | 143.3 | 112.6 | 29.7 | 0.7 | NA |
| -Spot 186 | 364 | 4060 | 3.0 | 21.8 | 5.3 | 0.0 | 5.8 | 0.0 | 2.4 | 0.4 | 29.7 | 0.7 | 29.3 | 1.7 | 8.6 | 127.3 | 29.7 | 0.7 | NA |
| -Spot 144 | 859 | 24636 | 2.5 | 21.6 | 3.4 | 0.0 | 4.1 | 0.0 | 2.4 | 0.6 | 29.7 | 0.7 | 29.5 | 1.2 | 13.2 | 81.4 | 29.7 | 0.7 | NA |
| -Spot 92 | 479 | 33440 | 2.9 | 21.4 | 3.7 | 0.0 | 4.1 | 0.0 | 1.8 | 0.4 | 29.8 | 0.5 | 29.8 | 1.2 | 35.7 | 88.5 | 29.8 | 0.5 | NA |
| -Spot 300 | 320 | 11253 | 3.1 | 21.3 | 4.9 | 0.0 | 5.5 | 0.0 | 2.6 | 0.5 | 29.8 | 0.8 | 30.0 | 1.6 | 50.8 | 117.1 | 29.8 | 0.8 | NA |
| -Spot 71 | 945 | 27972 | 3.1 | 21.3 | 2.4 | 0.0 | 3.0 | 0.0 | 1.8 | 0.6 | 29.8 | 0.5 | 30.0 | 0.9 | 45.3 | 57.1 | 29.8 | 0.5 | NA |
| -Spot 111 | 1037 | 45876 | 3.5 | 21.2 | 2.2 | 0.0 | 3.0 | 0.0 | 2.1 | 0.7 | 29.8 | 0.6 | 30.1 | 0.9 | 59.0 | 51.9 | 29.8 | 0.6 | NA |
| -Spot 60 | 747 | 36403 | 4.2 | 22.3 | 3.8 | 0.0 | 4.2 | 0.0 | 1.8 | 0.4 | 29.8 | 0.5 | 28.7 | 1.2 | 61.9 | 92.7 | 29.8 | 0.5 | NA |
| -Spot 260 | 637 | 32800 | 3.0 | 22.0 | 3.8 | 0.0 | 4.4 | 0.0 | 2.2 | 0.5 | 29.8 | 0.7 | 29.0 | 1.3 | 32.2 | 93.0 | 29.8 | 0.7 | NA |
| -Spot 196 | 549 | 18329 | 2.1 | 21.7 | 4.3 | 0.0 | 4.9 | 0.0 | 2.2 | 0.5 | 29.8 | 0.7 | 29.5 | 1.4 | 7.1 | 104.6 | 29.8 | 0.7 | NA |
| -Spot 38 | 507 | 12218 | 5.7 | 22.1 | 5.2 | 0.0 | 5.6 | 0.0 | 2.1 | 0.4 | 29.8 | 0.6 | 29.0 | 1.6 | 39.9 | 127.6 | 29.8 | 0.6 | NA |
| -Spot 202 | 449 | 10122 | 5.6 | 21.4 | 4.1 | 0.0 | 4.8 | 0.0 | 2.5 | 0.5 | 29.8 | 0.8 | 29.8 | 1.4 | 30.1 | 98.4 | 29.8 | 0.8 | NA |
| -Spot 188 | 655 | 18715 | 5.2 | 21.6 | 4.2 | 0.0 | 4.6 | 0.0 | 1.9 | 0.4 | 29.8 | 0.6 | 29.7 | 1.4 | 17.5 | 101.4 | 29.8 | 0.6 | NA |
| -Spot 297 | 802 | 14033 | 2.7 | 21.5 | 4.3 | 0.0 | 4.8 | 0.0 | 2.2 | 0.5 | 29.8 | 0.7 | 29.7 | 1.4 | 20.3 | 103.3 | 29.8 | 0.7 | NA |
| -Spot 37 | 373 | 10238 | 4.6 | 22.8 | 4.8 | 0.0 | 5.3 | 0.0 | 2.2 | 0.4 | 29.8 | 0.7 | 28.0 | 1.5 | 122.9 | 118.7 | 29.8 | 0.7 | NA |
| -Spot 86 | 336 | 5415 | 4.6 | 22.6 | 4.5 | 0.0 | 5.0 | 0.0 | 2.0 | 0.4 | 29.8 | 0.6 | 28.3 | 1.4 | 99.1 | 111.3 | 29.8 | 0.6 | NA |

| | | | | | | | | | | | | | | | | | | | |
|---|---|---|---|---|---|---|---|---|---|---|---|---|---|---|---|---|---|---|---|
| -Spot 194 | 701 | 10131 | 3.3 | 21.8 | 3.1 | 0.0 | 3.7 | 0.0 | 2.0 | 0.5 | 29.8 | 0.6 | 29.4 | 1.1 | 9.8 | 75.5 | 29.8 | 0.6 | NA |
| -Spot 262 | 727 | 16188 | 5.2 | 20.9 | 3.5 | 0.0 | 4.5 | 0.0 | 2.9 | 0.6 | 29.8 | 0.9 | 30.6 | 1.4 | 88.6 | 82.4 | 29.8 | 0.9 | NA |
| -Spot 39 | 577 | 9563 | 3.4 | 21.8 | 4.2 | 0.0 | 4.6 | 0.0 | 1.9 | 0.4 | 29.8 | 0.6 | 29.3 | 1.3 | 13.5 | 101.4 | 29.8 | 0.6 | NA |
| -Spot 289 | 180 | 3687 | 5.1 | 23.1 | 6.4 | 0.0 | 6.9 | 0.0 | 2.4 | 0.3 | 29.9 | 0.7 | 27.8 | 1.9 | 149.0 | 160.0 | 29.9 | 0.7 | NA |
| -Spot 183 | 253 | 6757 | 6.3 | 22.4 | 5.8 | 0.0 | 6.5 | 0.0 | 2.9 | 0.4 | 29.9 | 0.9 | 28.6 | 1.8 | 79.9 | 142.1 | 29.9 | 0.9 | NA |
| -Spot 81 | 260 | 3240 | 5.1 | 22.9 | 4.7 | 0.0 | 5.3 | 0.0 | 2.3 | 0.4 | 29.9 | 0.7 | 28.0 | 1.5 | 132.3 | 117.0 | 29.9 | 0.7 | NA |
| -Spot 288 | 928 | 22564 | 5.4 | 21.1 | 3.5 | 0.0 | 4.0 | 0.0 | 2.1 | 0.5 | 29.9 | 0.6 | 30.4 | 1.2 | 68.5 | 82.4 | 29.9 | 0.6 | NA |
| -Spot 7 | 375 | 25361 | 3.8 | 21.7 | 4.0 | 0.0 | 4.6 | 0.0 | 2.3 | 0.5 | 29.9 | 0.7 | 29.5 | 1.3 | 1.3 | 96.3 | 29.9 | 0.7 | NA |
| -Spot 73 | 427 | 9769 | 6.1 | 22.1 | 3.9 | 0.0 | 4.3 | 0.0 | 1.9 | 0.4 | 29.9 | 0.6 | 29.0 | 1.2 | 42.8 | 93.9 | 29.9 | 0.6 | NA |
| -Spot 212 | 452 | 8150 | 4.5 | 21.1 | 5.2 | 0.0 | 6.1 | 0.0 | 3.2 | 0.5 | 29.9 | 1.0 | 30.4 | 1.8 | 66.6 | 124.0 | 29.9 | 1.0 | NA |
| -Spot 40 | 788 | 45310 | 3.1 | 21.5 | 3.6 | 0.0 | 4.1 | 0.0 | 2.0 | 0.5 | 29.9 | 0.6 | 29.8 | 1.2 | 22.8 | 86.5 | 29.9 | 0.6 | NA |
| -Spot 2 | 447 | 17790 | 5.4 | 20.8 | 4.5 | 0.0 | 5.0 | 0.0 | 2.1 | 0.4 | 29.9 | 0.6 | 30.9 | 1.5 | 105.2 | 106.7 | 29.9 | 0.6 | NA |
| -Spot 192 | 387 | 9446 | 2.7 | 21.1 | 4.9 | 0.0 | 5.3 | 0.0 | 2.1 | 0.4 | 29.9 | 0.6 | 30.4 | 1.6 | 69.6 | 117.2 | 29.9 | 0.6 | NA |
| -Spot 137 | 314 | 18424 | 7.4 | 20.1 | 4.1 | 0.0 | 5.0 | 0.0 | 2.7 | 0.6 | 29.9 | 0.8 | 31.8 | 1.6 | 178.9 | 96.3 | 29.9 | 0.8 | NA |
| -Spot 163 | 594 | 7644 | 4.2 | 22.9 | 4.5 | 0.0 | 5.2 | 0.0 | 2.5 | 0.5 | 30.0 | 0.7 | 28.1 | 1.4 | 124.5 | 111.5 | 30.0 | 0.7 | NA |
| -Spot 189 | 356 | 20987 | 4.0 | 21.9 | 5.3 | 0.0 | 6.0 | 0.0 | 2.8 | 0.5 | 30.0 | 0.8 | 29.3 | 1.7 | 21.7 | 128.2 | 30.0 | 0.8 | NA |
| -Spot 266 | 504 | 37066 | 3.3 | 20.0 | 5.2 | 0.0 | 5.8 | 0.0 | 2.6 | 0.4 | 30.0 | 0.8 | 32.0 | 1.8 | 190.9 | 120.3 | 30.0 | 0.8 | NA |
| -Spot 159 | 456 | 5539 | 5.4 | 22.0 | 5.6 | 0.0 | 6.0 | 0.0 | 2.2 | 0.4 | 30.0 | 0.7 | 29.2 | 1.7 | 29.6 | 135.3 | 30.0 | 0.7 | NA |
| -Spot 249 | 403 | 14310 | 4.0 | 21.3 | 4.6 | 0.0 | 5.3 | 0.0 | 2.6 | 0.5 | 30.0 | 0.8 | 30.2 | 1.6 | 49.0 | 109.8 | 30.0 | 0.8 | NA |
| -Spot 99 | 482 | 39703 | 5.4 | 21.4 | 4.7 | 0.0 | 5.1 | 0.0 | 2.0 | 0.4 | 30.0 | 0.6 | 30.0 | 1.5 | 33.8 | 112.2 | 30.0 | 0.6 | NA |
| -Spot 257 | 312 | 16185 | 3.7 | 22.4 | 5.2 | 0.0 | 5.9 | 0.0 | 2.8 | 0.5 | 30.0 | 0.8 | 28.7 | 1.7 | 76.4 | 127.4 | 30.0 | 0.8 | NA |
| -Spot 301 | 505 | 48007 | 3.3 | 20.8 | 4.3 | 0.0 | 4.9 | 0.0 | 2.2 | 0.5 | 30.0 | 0.7 | 30.9 | 1.5 | 99.0 | 102.1 | 30.0 | 0.7 | NA |
| -Spot 54 | 860 | 18371 | 6.2 | 21.2 | 3.9 | 0.0 | 4.5 | 0.0 | 2.2 | 0.5 | 30.0 | 0.7 | 30.3 | 1.3 | 55.9 | 92.9 | 30.0 | 0.7 | NA |
| -Spot 66 | 537 | 12063 | 7.5 | 22.0 | 3.5 | 0.0 | 4.0 | 0.0 | 1.9 | 0.5 | 30.0 | 0.6 | 29.2 | 1.1 | 34.5 | 84.0 | 30.0 | 0.6 | NA |
| -Spot 235 | 725 | 41211 | 3.7 | 21.4 | 3.9 | 0.0 | 4.9 | 0.0 | 3.0 | 0.6 | 30.0 | 0.9 | 30.0 | 1.5 | 31.2 | 93.8 | 30.0 | 0.9 | NA |
| -Spot 261 | 693 | 39065 | 4.1 | 21.1 | 4.0 | 0.0 | 4.4 | 0.0 | 1.9 | 0.4 | 30.0 | 0.6 | 30.5 | 1.3 | 73.2 | 94.7 | 30.0 | 0.6 | NA |
| -Spot 10 | 592 | 16361 | 4.5 | 21.0 | 3.2 | 0.0 | 4.2 | 0.0 | 2.7 | 0.6 | 30.0 | 0.8 | 30.6 | 1.3 | 80.2 | 76.2 | 30.0 | 0.8 | NA |
| -Spot 176 | 408 | 14340 | 3.1 | 21.3 | 4.5 | 0.0 | 5.0 | 0.0 | 2.1 | 0.4 | 30.0 | 0.6 | 30.3 | 1.5 | 49.7 | 108.4 | 30.0 | 0.6 | NA |
| -Spot 59 | 464 | 29471 | 3.4 | 20.7 | 4.3 | 0.0 | 5.0 | 0.0 | 2.4 | 0.5 | 30.0 | 0.7 | 31.1 | 1.5 | 111.4 | 102.5 | 30.0 | 0.7 | NA |
| -Spot 218 | 404 | 12552 | 5.0 | 21.2 | 4.3 | 0.0 | 4.9 | 0.0 | 2.2 | 0.5 | 30.0 | 0.7 | 30.4 | 1.5 | 62.7 | 102.7 | 30.0 | 0.7 | NA |
| -Spot 25 | 423 | 29846 | 2.4 | 20.3 | 4.6 | 0.0 | 5.5 | 0.0 | 3.1 | 0.6 | 30.0 | 0.9 | 31.7 | 1.7 | 162.5 | 107.7 | 30.0 | 0.9 | NA |
| -Spot 255 | 361 | 50442 | 4.3 | 20.3 | 5.0 | 0.0 | 5.4 | 0.0 | 2.2 | 0.4 | 30.0 | 0.7 | 31.7 | 1.7 | 158.2 | 116.4 | 30.0 | 0.7 | NA |
| -Spot 116 | 593 | 21466 | 5.9 | 20.6 | 3.0 | 0.0 | 3.9 | 0.0 | 2.4 | 0.6 | 30.0 | 0.7 | 31.3 | 1.2 | 131.3 | 70.7 | 30.0 | 0.7 | NA |
| -Spot 128 | 715 | 26763 | 4.2 | 21.4 | 3.9 | 0.0 | 4.5 | 0.0 | 2.2 | 0.5 | 30.0 | 0.6 | 30.1 | 1.3 | 35.9 | 94.1 | 30.0 | 0.6 | NA |
| -Spot 180 | 265 | 16398 | 2.4 | 21.5 | 5.7 | 0.0 | 6.3 | 0.0 | 2.7 | 0.4 | 30.0 | 0.8 | 30.0 | 1.9 | 27.0 | 137.2 | 30.0 | 0.8 | NA |
| -Spot 303 | 568 | 123511 | 4.4 | 21.0 | 3.9 | 0.0 | 4.4 | 0.0 | 2.1 | 0.5 | 30.0 | 0.6 | 30.7 | 1.3 | 81.1 | 92.9 | 30.0 | 0.6 | NA |
| -Spot 268 | 1101 | 24535 | 3.1 | 21.2 | 2.8 | 0.0 | 3.5 | 0.0 | 2.0 | 0.6 | 30.0 | 0.6 | 30.4 | 1.0 | 58.5 | 66.7 | 30.0 | 0.6 | NA |
| -Spot 150 | 465 | 7143 | 4.5 | 21.4 | 4.6 | 0.0 | 5.1 | 0.0 | 2.2 | 0.4 | 30.1 | 0.7 | 30.1 | 1.5 | 36.3 | 109.2 | 30.1 | 0.7 | NA |
| -Spot 203 | 624 | 38610 | 4.8 | 21.9 | 4.8 | 0.0 | 5.2 | 0.0 | 2.0 | 0.4 | 30.1 | 0.6 | 29.4 | 1.5 | 20.8 | 115.4 | 30.1 | 0.6 | NA |
| -Spot 182 | 734 | 29134 | 5.5 | 21.3 | 3.3 | 0.0 | 3.9 | 0.0 | 2.0 | 0.5 | 30.1 | 0.6 | 30.3 | 1.2 | 48.8 | 79.5 | 30.1 | 0.6 | NA |

| | | | | | | | | | | | | | | | | | | | |
|---|---|---|---|---|---|---|---|---|---|---|---|---|---|---|---|---|---|---|---|
| -Spot 68 | 483 | 9385 | 4.2 | 22.0 | 3.9 | 0.0 | 4.3 | 0.0 | 1.7 | 0.4 | 30.1 | 0.5 | 29.4 | 1.2 | 29.0 | 94.3 | 30.1 | 0.5 | NA |
| -Spot 313 | 251 | 22789 | 3.8 | 21.1 | 4.9 | 0.0 | 5.2 | 0.0 | 1.9 | 0.4 | 30.1 | 0.6 | 30.6 | 1.6 | 72.7 | 115.6 | 30.1 | 0.6 | NA |
| -Spot 284 | 484 | 21975 | 4.1 | 22.9 | 4.3 | 0.0 | 4.8 | 0.0 | 2.2 | 0.5 | 30.1 | 0.6 | 28.2 | 1.3 | 128.1 | 105.5 | 30.1 | 0.6 | NA |
| -Spot 285 | 584 | 18566 | 3.9 | 21.2 | 3.8 | 0.0 | 4.5 | 0.0 | 2.3 | 0.5 | 30.1 | 0.7 | 30.4 | 1.3 | 59.1 | 90.8 | 30.1 | 0.7 | NA |
| -Spot 94 | 217 | 9824 | 4.2 | 21.6 | 5.0 | 0.0 | 5.6 | 0.0 | 2.5 | 0.4 | 30.1 | 0.8 | 30.0 | 1.7 | 18.1 | 120.5 | 30.1 | 0.8 | NA |
| -Spot 287 | 552 | 31428 | 5.6 | 22.1 | 4.4 | 0.0 | 4.9 | 0.0 | 2.2 | 0.5 | 30.1 | 0.7 | 29.2 | 1.4 | 43.0 | 107.2 | 30.1 | 0.7 | NA |
| -Spot 240 | 640 | 8941 | 2.4 | 21.0 | 5.1 | 0.0 | 6.0 | 0.0 | 3.2 | 0.5 | 30.1 | 1.0 | 30.8 | 1.8 | 80.4 | 120.9 | 30.1 | 1.0 | NA |
| -Spot 65 | 909 | 69411 | 3.9 | 21.4 | 3.5 | 0.0 | 3.8 | 0.0 | 1.6 | 0.4 | 30.1 | 0.5 | 30.2 | 1.1 | 32.8 | 83.3 | 30.1 | 0.5 | NA |
| -Spot 23 | 334 | 14764 | 3.2 | 21.0 | 5.1 | 0.0 | 5.5 | 0.0 | 1.9 | 0.3 | 30.1 | 0.6 | 30.8 | 1.7 | 82.9 | 121.7 | 30.1 | 0.6 | NA |
| -Spot 314 | 679 | 23196 | 4.9 | 21.6 | 3.1 | 0.0 | 4.0 | 0.0 | 2.6 | 0.6 | 30.1 | 0.8 | 30.0 | 1.2 | 17.3 | 74.7 | 30.1 | 0.8 | NA |
| -Spot 197 | 591 | 11498 | 4.2 | 21.7 | 4.0 | 0.0 | 4.4 | 0.0 | 1.8 | 0.4 | 30.1 | 0.6 | 29.8 | 1.3 | 3.6 | 95.2 | 30.1 | 0.6 | NA |
| -Spot 47 | 458 | 4851 | 6.7 | 22.5 | 4.2 | 0.0 | 4.9 | 0.0 | 2.4 | 0.5 | 30.2 | 0.7 | 28.8 | 1.4 | 84.4 | 103.3 | 30.2 | 0.7 | NA |
| -Spot 125 | 689 | 94146 | 6.9 | 21.2 | 3.7 | 0.0 | 4.3 | 0.0 | 2.2 | 0.5 | 30.2 | 0.7 | 30.5 | 1.3 | 57.5 | 89.3 | 30.2 | 0.7 | NA |
| -Spot 224 | 481 | 7910 | 3.2 | 22.5 | 4.1 | 0.0 | 4.6 | 0.0 | 2.1 | 0.5 | 30.2 | 0.6 | 28.7 | 1.3 | 89.6 | 101.0 | 30.2 | 0.6 | NA |
| -Spot 178 | 326 | 5457 | 3.7 | 21.4 | 5.3 | 0.0 | 5.7 | 0.0 | 2.1 | 0.4 | 30.2 | 0.6 | 30.2 | 1.7 | 32.0 | 126.9 | 30.2 | 0.6 | NA |
| -Spot 248 | 717 | 8956 | 4.9 | 20.8 | 5.8 | 0.0 | 6.4 | 0.0 | 2.7 | 0.4 | 30.2 | 0.8 | 31.1 | 2.0 | 105.9 | 136.3 | 30.2 | 0.8 | NA |
| -Spot 149 | 492 | 19111 | 4.8 | 22.7 | 4.3 | 0.0 | 4.9 | 0.0 | 2.4 | 0.5 | 30.2 | 0.7 | 28.6 | 1.4 | 102.6 | 104.6 | 30.2 | 0.7 | NA |
| -Spot 140 | 851 | 22680 | 4.6 | 20.7 | 3.7 | 0.0 | 4.3 | 0.0 | 2.2 | 0.5 | 30.2 | 0.7 | 31.3 | 1.3 | 116.6 | 87.0 | 30.2 | 0.7 | NA |
| -Spot 143 | 415 | 10651 | 6.2 | 21.5 | 4.1 | 0.0 | 4.9 | 0.0 | 2.7 | 0.6 | 30.2 | 0.8 | 30.1 | 1.5 | 19.6 | 98.2 | 30.2 | 0.8 | NA |
| -Spot 97 | 303 | 5647 | 4.9 | 23.2 | 3.8 | 0.0 | 4.4 | 0.0 | 2.2 | 0.5 | 30.2 | 0.7 | 27.9 | 1.2 | 165.4 | 93.6 | 30.2 | 0.7 | NA |
| -Spot 120 | 759 | 11104 | 7.1 | 21.3 | 3.7 | 0.0 | 4.4 | 0.0 | 2.3 | 0.5 | 30.2 | 0.7 | 30.5 | 1.3 | 48.6 | 89.2 | 30.2 | 0.7 | NA |
| -Spot 13 | 316 | 10843 | 3.3 | 19.2 | 6.7 | 0.0 | 7.6 | 0.0 | 3.4 | 0.5 | 30.2 | 1.0 | 33.7 | 2.5 | 285.5 | 154.4 | 30.2 | 1.0 | NA |
| -Spot 201 | 495 | 15375 | 4.0 | 21.6 | 4.0 | 0.0 | 4.4 | 0.0 | 1.9 | 0.4 | 30.2 | 0.6 | 30.0 | 1.3 | 11.1 | 96.3 | 30.2 | 0.6 | NA |
| -Spot 222 | 551 | 14070 | 2.6 | 21.5 | 4.5 | 0.0 | 4.9 | 0.0 | 2.0 | 0.4 | 30.3 | 0.6 | 30.2 | 1.5 | 22.6 | 107.9 | 30.3 | 0.6 | NA |
| -Spot 64 | 358 | 13119 | 3.9 | 22.2 | 5.5 | 0.0 | 6.0 | 0.0 | 2.4 | 0.4 | 30.3 | 0.7 | 29.2 | 1.7 | 56.3 | 133.4 | 30.3 | 0.7 | NA |
| -Spot 254 | 454 | 9051 | 3.4 | 22.0 | 5.4 | 0.0 | 6.1 | 0.0 | 2.8 | 0.5 | 30.3 | 0.8 | 29.5 | 1.8 | 35.8 | 130.4 | 30.3 | 0.8 | NA |
| -Spot 239 | 736 | 16442 | 2.4 | 22.2 | 3.5 | 0.0 | 4.0 | 0.0 | 2.1 | 0.5 | 30.3 | 0.6 | 29.2 | 1.2 | 58.2 | 84.7 | 30.3 | 0.6 | NA |
| -Spot 53 | 582 | 67671 | 1.7 | 22.4 | 3.9 | 0.0 | 5.1 | 0.0 | 3.3 | 0.6 | 30.3 | 1.0 | 29.0 | 1.5 | 75.5 | 96.2 | 30.3 | 1.0 | NA |
| -Spot 294 | 782 | 63931 | 8.0 | 19.8 | 3.4 | 0.0 | 4.0 | 0.0 | 2.0 | 0.5 | 30.3 | 0.6 | 32.8 | 1.3 | 217.2 | 78.8 | 30.3 | 0.6 | NA |
| -Spot 190 | 329 | 8428 | 4.6 | 21.1 | 4.5 | 0.0 | 5.2 | 0.0 | 2.5 | 0.5 | 30.3 | 0.8 | 30.8 | 1.6 | 70.3 | 108.0 | 30.3 | 0.8 | NA |
| -Spot 161 | 483 | 9497 | 4.5 | 21.3 | 4.1 | 0.0 | 4.5 | 0.0 | 2.0 | 0.4 | 30.3 | 0.6 | 30.5 | 1.4 | 43.9 | 97.8 | 30.3 | 0.6 | NA |
| -Spot 62 | 471 | 9509 | 3.1 | 21.6 | 3.9 | 0.0 | 4.4 | 0.0 | 2.0 | 0.5 | 30.3 | 0.6 | 30.1 | 1.3 | 9.3 | 95.0 | 30.3 | 0.6 | NA |
| -Spot 77 | 414 | 14571 | 4.9 | 21.5 | 4.6 | 0.0 | 5.2 | 0.0 | 2.4 | 0.5 | 30.4 | 0.7 | 30.2 | 1.5 | 19.6 | 109.3 | 30.4 | 0.7 | NA |
| -Spot 70 | 446 | 13389 | 4.3 | 22.0 | 3.9 | 0.0 | 4.6 | 0.0 | 2.5 | 0.5 | 30.4 | 0.8 | 29.6 | 1.3 | 35.4 | 94.3 | 30.4 | 0.8 | NA |
| -Spot 115 | 457 | 9849 | 3.5 | 21.3 | 4.4 | 0.0 | 4.8 | 0.0 | 1.9 | 0.4 | 30.4 | 0.6 | 30.5 | 1.4 | 42.7 | 105.1 | 30.4 | 0.6 | NA |
| -Spot 105 | 1044 | 57658 | 2.2 | 20.8 | 2.6 | 0.0 | 3.1 | 0.0 | 1.6 | 0.5 | 30.4 | 0.5 | 31.3 | 0.9 | 103.8 | 61.5 | 30.4 | 0.5 | NA |
| -Spot 282 | 759 | 18865 | 1.9 | 21.3 | 3.1 | 0.0 | 4.1 | 0.0 | 2.7 | 0.7 | 30.4 | 0.8 | 30.5 | 1.2 | 42.0 | 74.2 | 30.4 | 0.8 | NA |
| -Spot 164 | 330 | 5705 | 2.3 | 20.7 | 5.6 | 0.0 | 5.9 | 0.0 | 2.0 | 0.3 | 30.4 | 0.6 | 31.5 | 1.8 | 119.3 | 131.9 | 30.4 | 0.6 | NA |
| -Spot 302 | 528 | 12442 | 4.9 | 22.5 | 4.1 | 0.0 | 4.6 | 0.0 | 2.2 | 0.5 | 30.4 | 0.7 | 29.0 | 1.3 | 89.0 | 100.0 | 30.4 | 0.7 | NA |
| -Spot 98 | 645 | 14903 | 4.6 | 21.2 | 4.3 | 0.0 | 4.8 | 0.0 | 2.2 | 0.5 | 30.4 | 0.7 | 30.7 | 1.5 | 54.9 | 101.9 | 30.4 | 0.7 | NA |

| | | | | | | | | | | | | | | | | | | | |
|---|---|---|---|---|---|---|---|---|---|---|---|---|---|---|---|---|---|---|---|
| -Spot 156 | 663 | 25052 | 4.5 | 22.1 | 3.9 | 0.0 | 4.2 | 0.0 | 1.5 | 0.4 | 30.4 | 0.5 | 29.5 | 1.2 | 47.1 | 94.5 | 30.4 | 0.5 | NA |
| -Spot 209 | 694 | 17266 | 2.8 | 22.0 | 4.2 | 0.0 | 5.2 | 0.0 | 3.0 | 0.6 | 30.4 | 0.9 | 29.7 | 1.5 | 30.9 | 102.9 | 30.4 | 0.9 | NA |
| -Spot 109 | 311 | 14131 | 5.7 | 20.9 | 5.8 | 0.0 | 6.1 | 0.0 | 1.9 | 0.3 | 30.4 | 0.6 | 31.2 | 1.9 | 88.1 | 137.6 | 30.4 | 0.6 | NA |
| -Spot 57 | 550 | 37423 | 3.6 | 21.7 | 4.5 | 0.0 | 5.0 | 0.0 | 2.1 | 0.4 | 30.4 | 0.6 | 30.0 | 1.5 | 1.6 | 109.2 | 30.4 | 0.6 | NA |
| -Spot 1 | 949 | 32297 | 6.8 | 21.3 | 3.3 | 0.0 | 4.0 | 0.0 | 2.3 | 0.6 | 30.4 | 0.7 | 30.6 | 1.2 | 44.5 | 79.3 | 30.4 | 0.7 | NA |
| -Spot 217 | 204 | 4645 | 5.7 | 23.1 | 5.8 | 0.0 | 6.3 | 0.0 | 2.5 | 0.4 | 30.4 | 0.7 | 28.3 | 1.8 | 149.3 | 144.0 | 30.4 | 0.7 | NA |
| -Spot 227 | 629 | 15813 | 2.4 | 21.4 | 4.0 | 0.0 | 4.4 | 0.0 | 1.7 | 0.4 | 30.5 | 0.5 | 30.5 | 1.3 | 34.7 | 96.3 | 30.5 | 0.5 | NA |
| -Spot 309 | 854 | 17025 | 8.2 | 20.9 | 3.7 | 0.0 | 4.4 | 0.0 | 2.4 | 0.5 | 30.5 | 0.7 | 31.3 | 1.3 | 96.0 | 87.4 | 30.5 | 0.7 | NA |
| -Spot 101 | 488 | 18639 | 4.9 | 21.0 | 3.8 | 0.0 | 4.4 | 0.0 | 2.3 | 0.5 | 30.5 | 0.7 | 31.1 | 1.3 | 81.8 | 89.7 | 30.5 | 0.7 | NA |
| -Spot 233 | 424 | 11975 | 3.2 | 21.9 | 3.5 | 0.0 | 4.0 | 0.0 | 1.9 | 0.5 | 30.5 | 0.6 | 29.8 | 1.2 | 25.6 | 85.8 | 30.5 | 0.6 | NA |
| -Spot 84 | 804 | 25986 | 3.1 | 21.4 | 3.5 | 0.0 | 4.5 | 0.0 | 2.9 | 0.6 | 30.5 | 0.9 | 30.5 | 1.4 | 34.2 | 83.6 | 30.5 | 0.9 | NA |
| -Spot 147 | 510 | 13774 | 5.9 | 21.4 | 3.8 | 0.0 | 4.1 | 0.0 | 1.7 | 0.4 | 30.5 | 0.5 | 30.5 | 1.2 | 33.1 | 90.6 | 30.5 | 0.5 | NA |
| -Spot 95 | 363 | 41477 | 4.0 | 21.0 | 3.7 | 0.0 | 4.4 | 0.0 | 2.3 | 0.5 | 30.5 | 0.7 | 31.1 | 1.3 | 78.7 | 88.3 | 30.5 | 0.7 | NA |
| -Spot 226 | 362 | 12190 | 3.6 | 21.2 | 5.1 | 0.0 | 5.5 | 0.0 | 2.1 | 0.4 | 30.6 | 0.6 | 30.9 | 1.7 | 52.5 | 122.4 | 30.6 | 0.6 | NA |
| -Spot 78 | 1038 | 47834 | 1.8 | 21.0 | 2.5 | 0.0 | 3.2 | 0.0 | 2.0 | 0.6 | 30.6 | 0.6 | 31.2 | 1.0 | 77.6 | 59.9 | 30.6 | 0.6 | NA |
| -Spot 49 | 318 | 11703 | 2.5 | 22.4 | 5.7 | 0.0 | 6.1 | 0.0 | 2.1 | 0.3 | 30.6 | 0.7 | 29.3 | 1.8 | 76.0 | 140.3 | 30.6 | 0.7 | NA |
| -Spot 265 | 356 | 15587 | 4.8 | 21.4 | 5.6 | 0.0 | 6.6 | 0.0 | 3.3 | 0.5 | 30.6 | 1.0 | 30.8 | 2.0 | 40.8 | 135.0 | 30.6 | 1.0 | NA |
| -Spot 174 | 118 | 25790 | 4.5 | 20.2 | 7.6 | 0.0 | 8.1 | 0.0 | 2.9 | 0.4 | 30.6 | 0.9 | 32.5 | 2.6 | 169.0 | 177.8 | 30.6 | 0.9 | NA |
| -Spot 298 | 708 | 20512 | 3.9 | 20.7 | 4.0 | 0.0 | 4.8 | 0.0 | 2.7 | 0.6 | 30.7 | 0.8 | 31.7 | 1.5 | 111.0 | 94.1 | 30.7 | 0.8 | NA |
| -Spot 33 | 356 | 8133 | 6.6 | 21.8 | 5.7 | 0.0 | 6.6 | 0.0 | 3.4 | 0.5 | 30.7 | 1.1 | 30.1 | 2.0 | 11.5 | 136.9 | 30.7 | 1.1 | NA |
| -Spot 310 | 389 | 7529 | 3.9 | 21.9 | 4.8 | 0.0 | 5.1 | 0.0 | 1.9 | 0.4 | 30.7 | 0.6 | 30.1 | 1.5 | 17.0 | 115.0 | 30.7 | 0.6 | NA |
| -Spot 63 | 328 | 6546 | 4.9 | 22.1 | 4.3 | 0.0 | 4.9 | 0.0 | 2.3 | 0.5 | 30.7 | 0.7 | 29.8 | 1.4 | 40.1 | 104.6 | 30.7 | 0.7 | NA |
| -Spot 61 | 198 | 8713 | 5.2 | 22.0 | 5.7 | 0.0 | 6.1 | 0.0 | 2.1 | 0.3 | 30.7 | 0.6 | 29.9 | 1.8 | 32.3 | 138.2 | 30.7 | 0.6 | NA |
| -Spot 274 | 326 | 18273 | 4.3 | 20.6 | 4.6 | 0.0 | 5.4 | 0.0 | 2.7 | 0.5 | 30.7 | 0.8 | 32.0 | 1.7 | 128.8 | 108.7 | 30.7 | 0.8 | NA |
| -Spot 229 | 296 | 29973 | 2.7 | 21.1 | 4.7 | 0.0 | 6.2 | 0.0 | 4.0 | 0.7 | 30.7 | 1.2 | 31.2 | 1.9 | 66.8 | 111.8 | 30.7 | 1.2 | NA |
| -Spot 272 | 281 | 21343 | 5.0 | 21.2 | 4.9 | 0.0 | 5.6 | 0.0 | 2.7 | 0.5 | 30.7 | 0.8 | 31.0 | 1.7 | 54.8 | 117.1 | 30.7 | 0.8 | NA |
| -Spot 169 | 139 | 2401 | 4.6 | 21.9 | 7.5 | 0.0 | 8.0 | 0.0 | 2.8 | 0.4 | 30.8 | 0.9 | 30.1 | 2.4 | 19.2 | 180.9 | 30.8 | 0.9 | NA |
| -Spot 230 | 893 | 25180 | 2.8 | 21.2 | 3.0 | 0.0 | 3.7 | 0.0 | 2.2 | 0.6 | 30.8 | 0.7 | 31.1 | 1.1 | 60.4 | 71.9 | 30.8 | 0.7 | NA |
| -Spot 133 | 400 | 11266 | 3.9 | 21.6 | 4.4 | 0.0 | 5.4 | 0.0 | 3.0 | 0.6 | 30.8 | 0.9 | 30.5 | 1.6 | 11.4 | 106.6 | 30.8 | 0.9 | NA |
| -Spot 232 | 237 | 24097 | 4.0 | 21.7 | 5.8 | 0.0 | 6.4 | 0.0 | 2.7 | 0.4 | 30.8 | 0.8 | 30.4 | 1.9 | 2.9 | 139.6 | 30.8 | 0.8 | NA |
| -Spot 90 | 397 | 6242 | 3.2 | 23.0 | 4.4 | 0.0 | 5.1 | 0.0 | 2.6 | 0.5 | 30.8 | 0.8 | 28.7 | 1.4 | 142.3 | 108.9 | 30.8 | 0.8 | NA |
| -Spot 250 | 127 | 8954 | 3.8 | 22.2 | 7.3 | 0.0 | 8.0 | 0.0 | 3.3 | 0.4 | 30.8 | 1.0 | 29.8 | 2.3 | 48.5 | 177.0 | 30.8 | 1.0 | NA |
| -Spot 15 | 391 | 7366 | 11.6 | 21.7 | 4.4 | 0.0 | 4.9 | 0.0 | 2.1 | 0.4 | 30.8 | 0.6 | 30.4 | 1.5 | 3.0 | 107.3 | 30.8 | 0.6 | NA |
| -Spot 199 | 425 | 13238 | 2.6 | 21.4 | 4.5 | 0.0 | 5.6 | 0.0 | 3.4 | 0.6 | 30.8 | 1.1 | 30.8 | 1.7 | 30.7 | 107.5 | 30.8 | 1.1 | NA |
| -Spot 117 | 320 | 8146 | 3.4 | 22.2 | 4.5 | 0.0 | 5.1 | 0.0 | 2.4 | 0.5 | 30.9 | 0.8 | 29.9 | 1.5 | 48.0 | 109.2 | 30.9 | 0.8 | NA |
| -Spot 245 | 361 | 6485 | 4.3 | 21.7 | 5.6 | 0.0 | 6.1 | 0.0 | 2.5 | 0.4 | 30.9 | 0.8 | 30.5 | 1.8 | 3.5 | 133.8 | 30.9 | 0.8 | NA |
| -Spot 124 | 355 | 41164 | 4.7 | 21.0 | 4.6 | 0.0 | 5.2 | 0.0 | 2.5 | 0.5 | 30.9 | 0.8 | 31.6 | 1.6 | 85.5 | 108.3 | 30.9 | 0.8 | NA |
| -Spot 154 | 401 | 7627 | 3.8 | 22.2 | 4.7 | 0.0 | 5.5 | 0.0 | 2.8 | 0.5 | 31.0 | 0.9 | 30.0 | 1.6 | 49.2 | 114.7 | 31.0 | 0.9 | NA |
| -Spot 295 | 234 | 4563 | 4.1 | 20.9 | 5.3 | 0.0 | 6.0 | 0.0 | 2.8 | 0.5 | 31.0 | 0.9 | 31.8 | 1.9 | 95.0 | 126.7 | 31.0 | 0.9 | NA |
| -Spot 87 | 297 | 11437 | 4.8 | 21.0 | 5.7 | 0.0 | 6.0 | 0.0 | 2.0 | 0.3 | 31.0 | 0.6 | 31.7 | 1.9 | 84.1 | 134.3 | 31.0 | 0.6 | NA |

| | | | | | | | | | | | | | | | | | | | |
|---|---|---|---|---|---|---|---|---|---|---|---|---|---|---|---|---|---|---|---|
| -Spot 155 | 335 | 23259 | 6.7 | 21.6 | 4.6 | 0.0 | 5.2 | 0.0 | 2.5 | 0.5 | 31.0 | 0.8 | 30.8 | 1.6 | 14.9 | 109.5 | 31.0 | 0.8 | NA |
| -Spot 276 | 230 | 35473 | 7.6 | 20.8 | 5.2 | 0.0 | 5.9 | 0.0 | 2.8 | 0.5 | 31.0 | 0.9 | 32.0 | 1.9 | 107.5 | 122.3 | 31.0 | 0.9 | NA |
| -Spot 162 | 599 | 23598 | 3.5 | 21.7 | 3.7 | 0.0 | 4.3 | 0.0 | 2.2 | 0.5 | 31.0 | 0.7 | 30.7 | 1.3 | 1.4 | 89.7 | 31.0 | 0.7 | NA |
| -Spot 30 | 377 | 4863 | 3.0 | 22.4 | 5.1 | 0.0 | 5.6 | 0.0 | 2.4 | 0.4 | 31.0 | 0.7 | 29.7 | 1.6 | 74.0 | 123.7 | 31.0 | 0.7 | NA |
| -Spot 127 | 170 | 46194 | 7.2 | 22.0 | 5.8 | 0.0 | 6.6 | 0.0 | 3.1 | 0.5 | 31.1 | 1.0 | 30.2 | 2.0 | 36.1 | 140.1 | 31.1 | 1.0 | NA |
| -Spot 113 | 782 | 8825 | 4.8 | 22.7 | 3.2 | 0.0 | 3.7 | 0.0 | 1.8 | 0.5 | 31.1 | 0.6 | 29.4 | 1.1 | 104.8 | 78.3 | 31.1 | 0.6 | NA |
| -Spot 228 | 620 | 43220 | 1.9 | 20.0 | 3.4 | 0.0 | 4.4 | 0.0 | 2.8 | 0.6 | 31.1 | 0.9 | 33.3 | 1.4 | 192.5 | 79.4 | 31.1 | 0.9 | NA |
| -Spot 17 | 575 | 16226 | 4.6 | 21.3 | 3.7 | 0.0 | 4.4 | 0.0 | 2.3 | 0.5 | 31.1 | 0.7 | 31.3 | 1.4 | 46.2 | 88.8 | 31.1 | 0.7 | NA |
| -Spot 129 | 465 | 7725 | 3.9 | 23.3 | 3.1 | 0.0 | 3.5 | 0.0 | 1.7 | 0.5 | 31.1 | 0.5 | 28.7 | 1.0 | 170.2 | 77.4 | 31.1 | 0.5 | NA |
| -Spot 74 | 229 | 16218 | 3.5 | 19.9 | 6.3 | 0.0 | 6.8 | 0.0 | 2.7 | 0.4 | 31.2 | 0.8 | 33.6 | 2.2 | 210.6 | 145.1 | 31.2 | 0.8 | NA |
| -Spot 312 | 268 | 21741 | 4.4 | 21.1 | 4.1 | 0.0 | 4.9 | 0.0 | 2.7 | 0.5 | 31.2 | 0.8 | 31.8 | 1.5 | 73.2 | 97.4 | 31.2 | 0.8 | NA |
| -Spot 213 | 252 | 3811 | 4.1 | 23.2 | 5.1 | 0.0 | 5.9 | 0.0 | 2.9 | 0.5 | 31.2 | 0.9 | 29.0 | 1.7 | 156.7 | 127.3 | 31.2 | 0.9 | NA |
| -Spot 311 | 425 | 10256 | 6.6 | 22.3 | 4.4 | 0.0 | 4.9 | 0.0 | 2.2 | 0.4 | 31.3 | 0.7 | 30.1 | 1.5 | 66.7 | 107.9 | 31.3 | 0.7 | NA |
| -Spot 79 | 402 | 6532 | 4.0 | 22.3 | 4.4 | 0.0 | 5.1 | 0.0 | 2.6 | 0.5 | 31.3 | 0.8 | 30.1 | 1.5 | 66.4 | 107.7 | 31.3 | 0.8 | NA |
| -Spot 286 | 687 | 32031 | 2.6 | 21.6 | 3.5 | 0.0 | 4.5 | 0.0 | 2.9 | 0.6 | 31.5 | 0.9 | 31.3 | 1.4 | 15.4 | 84.1 | 31.5 | 0.9 | NA |
| -Spot 58 | 561 | 31914 | 4.4 | 22.2 | 3.7 | 0.0 | 4.4 | 0.0 | 2.2 | 0.5 | 31.5 | 0.7 | 30.4 | 1.3 | 55.6 | 91.3 | 31.5 | 0.7 | NA |
| -Spot 279 | 646 | 87817 | 3.3 | 21.0 | 3.9 | 0.0 | 5.0 | 0.0 | 3.1 | 0.6 | 31.6 | 1.0 | 32.3 | 1.6 | 83.9 | 93.4 | 31.6 | 1.0 | NA |
| -Spot 4 | 160 | 34438 | 4.7 | 20.5 | 6.6 | 0.0 | 7.8 | 0.0 | 4.3 | 0.5 | 31.6 | 1.4 | 33.0 | 2.5 | 132.5 | 154.3 | 31.6 | 1.4 | NA |
| -Spot 251 | 234 | 4193 | 3.5 | 22.6 | 6.2 | 0.0 | 7.1 | 0.0 | 3.4 | 0.5 | 31.6 | 1.1 | 30.0 | 2.1 | 99.5 | 151.7 | 31.6 | 1.1 | NA |
| -Spot 299 | 433 | 13666 | 3.7 | 20.9 | 5.0 | 0.0 | 5.4 | 0.0 | 2.0 | 0.4 | 31.6 | 0.6 | 32.4 | 1.7 | 88.1 | 118.0 | 31.6 | 0.6 | NA |
| -Spot 85 | 318 | 6156 | 6.0 | 23.1 | 5.7 | 0.0 | 6.2 | 0.0 | 2.4 | 0.4 | 31.7 | 0.8 | 29.5 | 1.8 | 151.5 | 142.5 | 31.7 | 0.8 | NA |
| -Spot 88 | 397 | 23643 | 3.9 | 19.2 | 5.7 | 0.0 | 6.1 | 0.0 | 2.2 | 0.4 | 31.8 | 0.7 | 35.4 | 2.1 | 285.9 | 129.8 | 31.8 | 0.7 | NA |
| -Spot 175 | 464 | 21116 | 3.7 | 23.0 | 4.3 | 0.0 | 9.1 | 0.0 | 8.1 | 0.9 | 31.9 | 2.6 | 29.7 | 2.7 | 142.6 | 107.0 | 31.9 | 2.6 | NA |
| -Spot 172 | 340 | 5497 | 4.5 | 23.2 | 5.1 | 0.0 | 9.5 | 0.0 | 8.0 | 0.8 | 32.0 | 2.6 | 29.7 | 2.8 | 159.1 | 126.5 | 32.0 | 2.6 | NA |
| -Spot 280 | 98 | 2247 | 6.5 | 22.1 | 8.2 | 0.0 | 8.9 | 0.0 | 3.6 | 0.4 | 32.2 | 1.1 | 31.3 | 2.7 | 36.9 | 199.0 | 32.2 | 1.1 | NA |
| -Spot 3 | 312 | 12486 | 4.3 | 21.4 | 5.1 | 0.0 | 5.6 | 0.0 | 2.3 | 0.4 | 32.4 | 0.8 | 32.3 | 1.8 | 31.5 | 122.0 | 32.4 | 0.8 | NA |
| -Spot 264 | 809 | 109383 | 6.7 | 20.7 | 2.8 | 0.0 | 3.7 | 0.0 | 2.4 | 0.6 | 32.4 | 0.8 | 33.5 | 1.2 | 113.8 | 65.8 | 32.4 | 0.8 | NA |
| -Spot 271 | 493 | 11864 | 4.6 | 21.7 | 3.3 | 0.0 | 4.2 | 0.0 | 2.6 | 0.6 | 32.4 | 0.8 | 32.1 | 1.3 | 6.6 | 79.2 | 32.4 | 0.8 | NA |
| -Spot 263 | 155 | 11733 | 5.8 | 21.5 | 7.1 | 0.0 | 7.4 | 0.0 | 2.3 | 0.3 | 32.6 | 0.7 | 32.5 | 2.4 | 26.2 | 169.5 | 32.6 | 0.7 | NA |
| -Spot 236 | 201 | 6035 | 3.9 | 21.1 | 6.4 | 0.0 | 6.9 | 0.0 | 2.5 | 0.4 | 32.9 | 0.8 | 33.5 | 2.3 | 74.0 | 153.1 | 32.9 | 0.8 | NA |
| -Spot 157 | 343 | 19430 | 1.7 | 19.3 | 5.0 | 0.0 | 5.9 | 0.0 | 3.0 | 0.5 | 33.5 | 1.0 | 37.2 | 2.1 | 278.0 | 115.2 | 33.5 | 1.0 | NA |
| -Spot 252 | 320 | 39120 | 6.0 | 21.0 | 5.0 | 0.0 | 5.5 | 0.0 | 2.3 | 0.4 | 47.2 | 1.1 | 47.7 | 2.5 | 75.7 | 118.0 | 47.2 | 1.1 | NA |
| -Spot 293 | 194 | 6114 | 3.6 | 21.6 | 4.9 | 0.1 | 5.2 | 0.0 | 1.7 | 0.3 | 73.7 | 1.3 | 71.8 | 3.6 | 9.0 | 117.4 | 73.7 | 1.3 | NA |
| -Spot 93 | 797 | 27775 | 2.8 | 20.7 | 1.9 | 0.1 | 3.1 | 0.0 | 2.5 | 0.8 | 97.6 | 2.4 | 98.4 | 2.9 | 116.4 | 45.9 | 97.6 | 2.4 | NA |
| -Spot 112 | 175 | 36583 | 2.6 | 20.9 | 3.0 | 0.1 | 3.8 | 0.0 | 2.3 | 0.6 | 123.5 | 2.8 | 121.8 | 4.3 | 89.3 | 70.8 | 123.5 | 2.8 | NA |
| -Spot 41 | 95 | 17436 | 5.4 | 20.1 | 4.6 | 0.1 | 4.9 | 0.0 | 1.9 | 0.4 | 127.8 | 2.4 | 130.9 | 6.1 | 186.8 | 106.0 | 127.8 | 2.4 | NA |
| -Spot 50 | 186 | 29219 | 7.0 | 21.1 | 3.2 | 0.1 | 3.9 | 0.0 | 2.3 | 0.6 | 137.1 | 3.1 | 133.4 | 4.9 | 68.2 | 75.5 | 137.1 | 3.1 | NA |
| -Spot 165 | 1172 | 88192 | 2.0 | 20.4 | 1.5 | 0.1 | 2.6 | 0.0 | 2.1 | 0.8 | 140.6 | 2.9 | 140.9 | 3.4 | 146.4 | 34.5 | 140.6 | 2.9 | NA |
| -Spot 80 | 374 | 21383 | 6.2 | 20.5 | 1.9 | 0.1 | 3.1 | 0.0 | 2.4 | 0.8 | 141.4 | 3.4 | 141.0 | 4.0 | 133.9 | 44.8 | 141.4 | 3.4 | NA |
| -Spot 32 | 277 | 17854 | 10.9 | 21.2 | 2.7 | 0.1 | 3.2 | 0.0 | 1.6 | 0.5 | 142.3 | 2.3 | 137.5 | 4.1 | 55.5 | 64.7 | 142.3 | 2.3 | NA |

| | | | | | | | | | | | | | | | | | | | |
|---|---|---|---|---|---|---|---|---|---|---|---|---|---|---|---|---|---|---|---|
| -Spot 205 | 118 | 7242 | 12.8 | 21.1 | 4.0 | 0.1 | 4.5 | 0.0 | 2.2 | 0.5 | 142.6 | 3.1 | 138.7 | 5.9 | 72.7 | 93.9 | 142.6 | 3.1 | NA |
| -Spot 96 | 198 | 21062 | 20.1 | 20.6 | 3.9 | 0.2 | 4.3 | 0.0 | 1.9 | 0.4 | 144.4 | 2.7 | 143.2 | 5.7 | 121.8 | 91.0 | 144.4 | 2.7 | NA |
| -Spot 108 | 226 | 33944 | 9.7 | 20.3 | 3.3 | 0.2 | 4.0 | 0.0 | 2.2 | 0.6 | 145.7 | 3.2 | 146.7 | 5.4 | 163.6 | 76.6 | 145.7 | 3.2 | NA |
| -Spot 5 | 495 | 104218 | 2.4 | 20.5 | 2.1 | 0.2 | 2.8 | 0.0 | 1.9 | 0.7 | 146.3 | 2.7 | 145.7 | 3.8 | 135.8 | 48.7 | 146.3 | 2.7 | NA |
| -Spot 253 | 322 | 39402 | 2.4 | 20.3 | 2.0 | 0.2 | 3.1 | 0.0 | 2.4 | 0.8 | 146.5 | 3.4 | 147.3 | 4.3 | 160.2 | 47.3 | 146.5 | 3.4 | NA |
| -Spot 139 | 575 | 64826 | 2.5 | 20.0 | 2.1 | 0.2 | 2.8 | 0.0 | 1.8 | 0.7 | 147.2 | 2.7 | 149.8 | 3.9 | 191.3 | 49.1 | 147.2 | 2.7 | NA |
| -Spot 67 | 69 | 7250 | 10.9 | 19.6 | 5.1 | 0.2 | 5.6 | 0.0 | 2.5 | 0.4 | 147.3 | 3.6 | 153.1 | 8.0 | 243.7 | 117.2 | 147.3 | 3.6 | NA |
| -Spot 277 | 261 | 28864 | 8.5 | 19.8 | 2.5 | 0.2 | 3.6 | 0.0 | 2.6 | 0.7 | 148.1 | 3.7 | 152.0 | 5.1 | 214.3 | 58.6 | 148.1 | 3.7 | NA |
| -Spot 208 | 465 | 61577 | 12.1 | 20.3 | 2.2 | 0.2 | 3.0 | 0.0 | 2.0 | 0.7 | 148.5 | 2.9 | 149.0 | 4.1 | 156.4 | 51.8 | 148.5 | 2.9 | NA |
| -Spot 104 | 628 | 44432 | 5.0 | 19.4 | 1.8 | 0.2 | 2.5 | 0.0 | 1.7 | 0.7 | 155.4 | 2.7 | 162.7 | 3.8 | 270.8 | 42.3 | 155.4 | 2.7 | NA |
| -Spot 258 | 332 | 311803 | 7.4 | 18.9 | 2.5 | 0.2 | 4.0 | 0.0 | 3.1 | 0.8 | 157.4 | 4.8 | 168.2 | 6.1 | 322.8 | 55.9 | 157.4 | 4.8 | NA |
| -Spot 237 | 610 | 55514 | 1.1 | 19.9 | 1.5 | 0.2 | 2.4 | 0.0 | 1.9 | 0.8 | 225.1 | 4.2 | 223.7 | 4.9 | 208.9 | 34.6 | 225.1 | 4.2 | NA |
| -Spot 6 | 229 | 43405 | 2.7 | 19.5 | 2.8 | 0.3 | 3.4 | 0.0 | 2.0 | 0.6 | 227.4 | 4.4 | 229.8 | 7.0 | 254.6 | 64.6 | 227.4 | 4.4 | NA |
| -Spot 122 | 1738 | 186875 | 4.6 | 19.7 | 1.4 | 0.3 | 2.0 | 0.0 | 1.4 | 0.7 | 227.5 | 3.2 | 227.7 | 4.0 | 230.0 | 32.1 | 227.5 | 3.2 | NA |
| -Spot 35 | 569 | 32482 | 3.4 | 19.3 | 1.6 | 0.3 | 2.5 | 0.0 | 1.9 | 0.8 | 227.7 | 4.4 | 232.7 | 5.3 | 282.9 | 37.3 | 227.7 | 4.4 | NA |
| -Spot 296 | 2817 | 139934 | 2.6 | 19.5 | 1.5 | 0.3 | 2.3 | 0.0 | 1.8 | 0.8 | 227.7 | 4.0 | 230.0 | 4.8 | 252.8 | 34.6 | 227.7 | 4.0 | NA |
| -Spot 181 | 967 | 83981 | 1.2 | 19.6 | 1.5 | 0.3 | 2.3 | 0.0 | 1.8 | 0.8 | 230.0 | 4.0 | 230.6 | 4.8 | 237.2 | 34.5 | 230.0 | 4.0 | NA |
| -Spot 43 | 225 | 44767 | 1.9 | 19.8 | 2.4 | 0.3 | 3.0 | 0.0 | 1.8 | 0.6 | 231.8 | 4.0 | 230.4 | 6.1 | 216.3 | 54.9 | 231.8 | 4.0 | NA |
| -Spot 207 | 256 | 122486 | 0.8 | 19.6 | 2.3 | 0.3 | 3.2 | 0.0 | 2.2 | 0.7 | 232.0 | 5.0 | 233.1 | 6.6 | 245.1 | 53.2 | 232.0 | 5.0 | NA |
| -Spot 148 | 763 | 60558 | 1.7 | 19.4 | 1.6 | 0.3 | 2.4 | 0.0 | 1.8 | 0.8 | 232.1 | 4.2 | 234.8 | 5.1 | 261.2 | 36.2 | 232.1 | 4.2 | NA |
| -Spot 242 | 235 | 147237 | 1.4 | 19.3 | 2.3 | 0.3 | 2.6 | 0.0 | 1.2 | 0.5 | 232.5 | 2.8 | 236.6 | 5.6 | 278.2 | 53.4 | 232.5 | 2.8 | NA |
| -Spot 24 | 354 | 40035 | 1.1 | 19.5 | 2.0 | 0.3 | 2.9 | 0.0 | 2.0 | 0.7 | 233.0 | 4.6 | 235.4 | 6.0 | 258.7 | 46.9 | 233.0 | 4.6 | NA |
| -Spot 110 | 1488 | 113934 | 1.9 | 19.6 | 1.4 | 0.3 | 2.8 | 0.0 | 2.4 | 0.9 | 233.1 | 5.6 | 234.0 | 5.9 | 242.4 | 32.4 | 233.1 | 5.6 | NA |
| -Spot 220 | 1207 | 116599 | 1.1 | 19.7 | 1.4 | 0.3 | 2.4 | 0.0 | 2.0 | 0.8 | 233.2 | 4.5 | 232.8 | 5.0 | 227.9 | 32.2 | 233.2 | 4.5 | NA |
| -Spot 31 | 152 | 16733 | 1.7 | 21.1 | 3.0 | 0.2 | 3.9 | 0.0 | 2.5 | 0.6 | 233.6 | 5.8 | 218.9 | 7.8 | 63.9 | 72.5 | 233.6 | 5.8 | NA |
| -Spot 259 | 380 | 29355 | 1.5 | 19.9 | 1.9 | 0.3 | 2.7 | 0.0 | 1.9 | 0.7 | 233.7 | 4.3 | 231.5 | 5.5 | 209.7 | 43.9 | 233.7 | 4.3 | NA |
| -Spot 179 | 331 | 83659 | 0.8 | 19.7 | 2.4 | 0.3 | 3.2 | 0.0 | 2.2 | 0.7 | 233.8 | 5.0 | 233.6 | 6.7 | 231.9 | 54.5 | 233.8 | 5.0 | NA |
| -Spot 215 | 240 | 142931 | 2.6 | 20.0 | 2.3 | 0.3 | 3.0 | 0.0 | 2.0 | 0.7 | 234.7 | 4.5 | 231.4 | 6.2 | 198.0 | 52.6 | 234.7 | 4.5 | NA |
| -Spot 308 | 250 | 28619 | 1.9 | 19.5 | 2.5 | 0.3 | 3.2 | 0.0 | 2.0 | 0.6 | 236.5 | 4.6 | 238.4 | 6.8 | 257.5 | 58.4 | 236.5 | 4.6 | NA |
| -Spot 89 | 733 | 64772 | 2.4 | 19.5 | 1.7 | 0.3 | 2.3 | 0.0 | 1.4 | 0.6 | 236.5 | 3.4 | 237.8 | 4.8 | 250.9 | 40.0 | 236.5 | 3.4 | NA |
| -Spot 18 | 518 | 37408 | 2.3 | 19.8 | 1.6 | 0.3 | 2.5 | 0.0 | 1.9 | 0.8 | 238.5 | 4.5 | 237.2 | 5.3 | 223.4 | 37.5 | 238.5 | 4.5 | NA |
| -Spot 281 | 370 | 35709 | 1.7 | 20.0 | 1.7 | 0.3 | 3.0 | 0.0 | 2.5 | 0.8 | 239.1 | 5.8 | 235.3 | 6.3 | 197.5 | 39.0 | 239.1 | 5.8 | NA |
| -Spot 36 | 592 | 61501 | 4.4 | 19.7 | 1.8 | 0.3 | 2.7 | 0.0 | 2.0 | 0.7 | 269.4 | 5.2 | 265.8 | 6.3 | 234.8 | 41.4 | 269.4 | 5.2 | NA |
| -Spot 69 | 189 | 51802 | 6.7 | 18.8 | 1.9 | 0.4 | 3.0 | 0.0 | 2.3 | 0.8 | 301.3 | 6.8 | 305.2 | 7.9 | 334.6 | 43.2 | 301.3 | 6.8 | NA |
| -Spot 151 | 57 | 48961 | 3.7 | 19.6 | 3.6 | 0.3 | 4.2 | 0.0 | 2.2 | 0.5 | 302.0 | 6.4 | 295.5 | 10.9 | 244.0 | 84.1 | 302.0 | 6.4 | NA |
| -Spot 244 | 279 | 52336 | 9.1 | 19.2 | 1.9 | 0.3 | 2.6 | 0.0 | 1.7 | 0.7 | 302.4 | 5.1 | 301.5 | 6.8 | 294.7 | 44.0 | 302.4 | 5.1 | NA |
| -Spot 75 | 508 | 35580 | 3.6 | 19.3 | 1.5 | 0.3 | 2.3 | 0.0 | 1.7 | 0.8 | 303.3 | 5.1 | 300.4 | 5.9 | 277.4 | 34.1 | 303.3 | 5.1 | NA |
| -Spot 44 | 577 | 94727 | 5.6 | 18.9 | 1.3 | 0.4 | 2.0 | 0.0 | 1.5 | 0.8 | 303.8 | 4.5 | 306.3 | 5.2 | 325.3 | 28.5 | 303.8 | 4.5 | NA |
| -Spot 219 | 710 | 233325 | 4.4 | 19.1 | 1.7 | 0.4 | 2.8 | 0.0 | 2.3 | 0.8 | 304.9 | 6.8 | 304.7 | 7.4 | 303.6 | 38.1 | 304.9 | 6.8 | NA |
| -Spot 114 | 178 | 26904 | 4.7 | 19.2 | 2.2 | 0.4 | 3.0 | 0.0 | 2.0 | 0.7 | 312.9 | 6.2 | 309.6 | 7.9 | 284.7 | 49.4 | 312.9 | 6.2 | NA |

| | | | | | | | | | | | | | | | | | | |
|---|---|---|---|---|---|---|---|---|---|---|---|---|---|---|---|---|---|---|
| -Spot 315 | 294 | 26102 | 3.4 | 19.0 | 2.0 | 0.4 | 2.9 | 0.1 | 2.0 | 0.7 | 326.1 | 6.5 | 325.0 | 7.9 | 317.2 | 45.6 | 326.1 | 6.5 | NA |
| -Spot 275 | 220 | 158790 | 3.5 | 9.4 | 1.3 | 4.6 | 2.1 | 0.3 | 1.7 | 0.8 | 1741.2 | 25.6 | 1743.8 | 17.6 | 1746.8 | 23.6 | 1746.8 | 23.6 | 99.7 |
| -Spot 19 | 48 | 896 | 2.9 | 33.0 | 9.1 | 0.0 | 9.7 | 0.0 | 3.4 | 0.3 | 31.3 | 1.0 | 20.5 | 2.0 | 1126.4 | 276.8 | 31.3 | 1.0 | NA |
| -Spot 221 | 208 | 19191 | 6.0 | 14.9 | 8.0 | 0.1 | 8.5 | 0.0 | 2.6 | 0.3 | 49.1 | 1.3 | 69.4 | 5.7 | 841.9 | 167.6 | 49.1 | 1.3 | NA |
| -Spot 247 | 116 | 37427 | 17.5 | 14.0 | 7.0 | 0.2 | 7.4 | 0.0 | 2.6 | 0.3 | 153.1 | 3.9 | 215.7 | 14.5 | 969.8 | 142.4 | 153.1 | 3.9 | NA |
| -Spot 173 | 527 | 13721 | 4.8 | 16.1 | 6.5 | 0.0 | 7.0 | 0.0 | 2.7 | 0.4 | 31.2 | 0.9 | 41.3 | 2.8 | 675.9 | 138.2 | 31.2 | 0.9 | NA |
| -Spot 123 | 150 | 1410 | 4.0 | 25.9 | 5.6 | 0.0 | 6.4 | 0.0 | 3.2 | 0.5 | 29.2 | 0.9 | 24.3 | 1.5 | 443.9 | 146.6 | 29.2 | 0.9 | NA |

Sample 15ATW23

| Analysis | U | 206Pb | U/Th | 206Pb* | ± | 207Pb* | ± | 206Pb* | ± | error | 206Pb* | ± | 207Pb* | ± | 206Pb* | ± | Best age | ± | Conc |
|---|---|---|---|---|---|---|---|---|---|---|---|---|---|---|---|---|---|---|---|
| | (ppm) | 204Pb | | 207Pb* | (%) | 235U* | (%) | 238U | (%) | corr. | 238U* | (Ma) | 235U | (Ma) | 207Pb* | (Ma) | (Ma) | (Ma) | (%) |
| 15ATW23-Spot 156 | 1519 | 599735 | 2.6 | 20.5 | 1.1 | 0.2 | 3.2 | 0.0 | 3.0 | 0.9 | 149.8 | 4.5 | 149.2 | 4.5 | 140.5 | 26.2 | 149.8 | 4.5 | NA |
| 15ATW23-Spot 44 | 215 | 28746 | 2.3 | 20.9 | 1.4 | 0.2 | 2.9 | 0.0 | 2.5 | 0.9 | 150.4 | 3.8 | 147.2 | 4.0 | 96.6 | 33.6 | 150.4 | 3.8 | NA |
| 15ATW23-Spot 225 | 197 | 38872 | 2.5 | 20.4 | 1.3 | 0.2 | 3.1 | 0.0 | 2.8 | 0.9 | 152.2 | 4.2 | 152.0 | 4.4 | 150.4 | 31.6 | 152.2 | 4.2 | NA |
| 15ATW23-Spot 251 | 139 | 13519 | 2.0 | 20.8 | 1.5 | 0.2 | 3.3 | 0.0 | 2.9 | 0.9 | 152.3 | 4.3 | 149.4 | 4.5 | 105.5 | 36.5 | 152.3 | 4.3 | NA |
| 15ATW23-Spot 262 | 156 | 412711 | 2.2 | 19.6 | 1.9 | 0.2 | 2.9 | 0.0 | 2.2 | 0.8 | 152.6 | 3.4 | 158.4 | 4.3 | 247.2 | 43.9 | 152.6 | 3.4 | NA |
| 15ATW23-Spot 248 | 100 | 17602 | 1.6 | 19.4 | 1.9 | 0.2 | 3.2 | 0.0 | 2.6 | 0.8 | 152.9 | 3.9 | 159.6 | 4.7 | 262.1 | 42.5 | 152.9 | 3.9 | NA |
| 15ATW23-Spot 250 | 119 | 117529 | 3.1 | 19.7 | 1.7 | 0.2 | 3.1 | 0.0 | 2.6 | 0.8 | 152.9 | 4.0 | 157.4 | 4.6 | 225.8 | 40.0 | 152.9 | 4.0 | NA |
| 15ATW23-Spot 97 | 48 | 9075 | 2.9 | 19.8 | 3.1 | 0.2 | 4.1 | 0.0 | 2.7 | 0.7 | 152.9 | 4.0 | 157.1 | 5.9 | 221.1 | 71.2 | 152.9 | 4.0 | NA |
| 15ATW23-Spot 270 | 126 | 207779 | 2.2 | 19.6 | 2.4 | 0.2 | 3.5 | 0.0 | 2.6 | 0.7 | 153.1 | 3.9 | 158.8 | 5.1 | 245.2 | 54.8 | 153.1 | 3.9 | NA |
| 15ATW23-Spot 298 | 75 | 27284 | 2.4 | 20.3 | 2.6 | 0.2 | 3.6 | 0.0 | 2.5 | 0.7 | 153.2 | 3.8 | 153.8 | 5.1 | 164.0 | 59.7 | 153.2 | 3.8 | NA |
| 15ATW23-Spot 38 | 84 | 16163 | 3.0 | 20.4 | 3.0 | 0.2 | 4.0 | 0.0 | 2.7 | 0.7 | 153.6 | 4.0 | 152.9 | 5.7 | 143.9 | 70.5 | 153.6 | 4.0 | NA |
| 15ATW23-Spot 88 | 132 | 124590 | 2.6 | 19.4 | 2.0 | 0.2 | 3.4 | 0.0 | 2.8 | 0.8 | 153.9 | 4.2 | 160.9 | 5.1 | 265.8 | 46.8 | 153.9 | 4.2 | NA |
| 15ATW23-Spot 21 | 123 | 661063 | 2.4 | 20.3 | 1.6 | 0.2 | 3.0 | 0.0 | 2.5 | 0.8 | 153.9 | 3.8 | 154.1 | 4.3 | 157.5 | 38.2 | 153.9 | 3.8 | NA |
| 15ATW23-Spot 195 | 110 | 183767 | 2.5 | 20.1 | 1.8 | 0.2 | 2.9 | 0.0 | 2.3 | 0.8 | 154.0 | 3.4 | 155.5 | 4.2 | 180.2 | 42.7 | 154.0 | 3.4 | NA |
| 15ATW23-Spot 86 | 150 | 55084 | 3.6 | 20.3 | 1.6 | 0.2 | 3.2 | 0.0 | 2.8 | 0.9 | 154.0 | 4.2 | 154.1 | 4.6 | 155.3 | 38.3 | 154.0 | 4.2 | NA |
| 15ATW23-Spot 31 | 308 | 66800 | 1.3 | 20.1 | 1.5 | 0.2 | 2.9 | 0.0 | 2.5 | 0.9 | 154.7 | 3.8 | 156.2 | 4.3 | 180.7 | 35.9 | 154.7 | 3.8 | NA |
| 15ATW23-Spot 301 | 164 | 734554 | 1.6 | 19.6 | 1.6 | 0.2 | 3.1 | 0.0 | 2.6 | 0.9 | 154.7 | 4.0 | 159.7 | 4.5 | 236.3 | 36.2 | 154.7 | 4.0 | NA |
| 15ATW23-Spot 118 | 256 | 156839 | 1.2 | 20.4 | 1.7 | 0.2 | 2.9 | 0.0 | 2.4 | 0.8 | 154.7 | 3.6 | 154.5 | 4.2 | 153.5 | 39.5 | 154.7 | 3.6 | NA |
| 15ATW23-Spot 285 | 136 | 139175 | 1.7 | 20.2 | 1.7 | 0.2 | 3.3 | 0.0 | 2.9 | 0.9 | 155.0 | 4.4 | 156.3 | 4.8 | 176.8 | 39.1 | 155.0 | 4.4 | NA |
| 15ATW23-Spot 4 | 146 | 47149 | 2.8 | 20.0 | 2.0 | 0.2 | 2.9 | 0.0 | 2.1 | 0.7 | 155.0 | 3.3 | 157.4 | 4.3 | 194.7 | 46.2 | 155.0 | 3.3 | NA |
| 15ATW23-Spot 85 | 127 | 51442 | 2.7 | 19.6 | 2.0 | 0.2 | 3.4 | 0.0 | 2.8 | 0.8 | 155.0 | 4.2 | 160.8 | 5.1 | 247.2 | 46.5 | 155.0 | 4.2 | NA |
| 15ATW23-Spot 142 | 131 | 11877 | 3.5 | 20.4 | 2.2 | 0.2 | 3.4 | 0.0 | 2.5 | 0.8 | 155.1 | 3.9 | 154.8 | 4.8 | 150.2 | 51.9 | 155.1 | 3.9 | NA |
| 15ATW23-Spot 34 | 139 | 32602 | 1.8 | 20.0 | 1.9 | 0.2 | 3.5 | 0.0 | 3.0 | 0.8 | 155.4 | 4.6 | 157.9 | 5.2 | 196.7 | 44.8 | 155.4 | 4.6 | NA |
| 15ATW23-Spot 45 | 126 | 26646 | 1.6 | 20.4 | 1.5 | 0.2 | 3.5 | 0.0 | 3.2 | 0.9 | 155.4 | 4.9 | 154.7 | 5.1 | 145.3 | 35.1 | 155.4 | 4.9 | NA |

| | | | | | | | | | | | | | | | | | | | |
|---|---|---|---|---|---|---|---|---|---|---|---|---|---|---|---|---|---|---|---|
| 15ATW23-Spot 198 | 189 | 78470 | 1.8 | 20.2 | 1.6 | 0.2 | 3.1 | 0.0 | 2.6 | 0.9 | 155.5 | 4.1 | 156.4 | 4.5 | 170.3 | 37.6 | 155.5 | 4.1 | NA |
| 15ATW23-Spot 261 | 34 | 65510 | 2.1 | 19.6 | 3.2 | 0.2 | 4.4 | 0.0 | 3.1 | 0.7 | 155.6 | 4.7 | 160.7 | 6.6 | 238.5 | 73.7 | 155.6 | 4.7 | NA |
| 15ATW23-Spot 39 | 72 | 9999 | 2.6 | 20.1 | 2.4 | 0.2 | 3.8 | 0.0 | 3.0 | 0.8 | 155.6 | 4.6 | 157.6 | 5.6 | 188.1 | 55.9 | 155.6 | 4.6 | NA |
| 15ATW23-Spot 1 | 110 | 39329 | 3.5 | 19.4 | 2.3 | 0.2 | 3.3 | 0.0 | 2.4 | 0.7 | 155.7 | 3.7 | 162.8 | 5.0 | 269.3 | 52.7 | 155.7 | 3.7 | NA |
| 15ATW23-Spot 237 | 95 | 14986 | 1.8 | 20.8 | 2.1 | 0.2 | 3.5 | 0.0 | 2.9 | 0.8 | 155.8 | 4.4 | 152.7 | 5.0 | 106.4 | 48.6 | 155.8 | 4.4 | NA |
| 15ATW23-Spot 286 | 132 | 12997 | 2.5 | 19.6 | 1.9 | 0.2 | 3.0 | 0.0 | 2.4 | 0.8 | 155.9 | 3.7 | 161.1 | 4.5 | 240.2 | 42.9 | 155.9 | 3.7 | NA |
| 15ATW23-Spot 282 | 124 | 129624 | 3.7 | 20.1 | 1.8 | 0.2 | 3.1 | 0.0 | 2.6 | 0.8 | 155.9 | 4.0 | 157.8 | 4.6 | 186.5 | 41.0 | 155.9 | 4.0 | NA |
| 15ATW23-Spot 116 | 191 | 73313 | 1.4 | 20.2 | 2.0 | 0.2 | 3.3 | 0.0 | 2.7 | 0.8 | 156.2 | 4.2 | 157.1 | 4.8 | 172.5 | 45.5 | 156.2 | 4.2 | NA |
| 15ATW23-Spot 293 | 157 | 78316 | 2.3 | 20.1 | 1.4 | 0.2 | 2.5 | 0.0 | 2.1 | 0.8 | 156.2 | 3.2 | 158.1 | 3.7 | 187.7 | 32.9 | 156.2 | 3.2 | NA |
| 15ATW23-Spot 99 | 85 | 17283 | 1.9 | 20.6 | 1.9 | 0.2 | 3.5 | 0.0 | 2.9 | 0.8 | 156.3 | 4.5 | 154.6 | 5.0 | 130.1 | 45.1 | 156.3 | 4.5 | NA |
| 15ATW23-Spot 93 | 43 | 15674 | 2.1 | 20.3 | 2.8 | 0.2 | 4.0 | 0.0 | 2.9 | 0.7 | 156.3 | 4.5 | 156.7 | 5.9 | 163.7 | 66.4 | 156.3 | 4.5 | NA |
| 15ATW23-Spot 20 | 31 | 9482 | 3.6 | 20.1 | 3.1 | 0.2 | 4.9 | 0.0 | 3.8 | 0.8 | 156.4 | 5.9 | 158.3 | 7.2 | 188.4 | 71.6 | 156.4 | 5.9 | NA |
| 15ATW23-Spot 29 | 55 | 42443 | 4.1 | 19.3 | 2.5 | 0.2 | 4.6 | 0.0 | 3.9 | 0.8 | 156.4 | 6.0 | 164.3 | 7.0 | 279.7 | 56.2 | 156.4 | 6.0 | NA |
| 15ATW23-Spot 144 | 62 | 45892 | 3.6 | 20.1 | 2.2 | 0.2 | 3.5 | 0.0 | 2.6 | 0.8 | 156.5 | 4.1 | 157.9 | 5.1 | 179.3 | 51.8 | 156.5 | 4.1 | NA |
| 15ATW23-Spot 291 | 293 | 42083 | 1.7 | 20.1 | 1.6 | 0.2 | 3.9 | 0.0 | 3.6 | 0.9 | 156.5 | 5.5 | 157.9 | 5.7 | 179.6 | 36.7 | 156.5 | 5.5 | NA |
| 15ATW23-Spot 160 | 127 | 34751 | 2.7 | 19.7 | 1.8 | 0.2 | 3.2 | 0.0 | 2.7 | 0.8 | 156.5 | 4.2 | 161.4 | 4.8 | 233.8 | 41.5 | 156.5 | 4.2 | NA |
| 15ATW23-Spot 110 | 234 | 78863 | 2.4 | 20.5 | 1.8 | 0.2 | 3.4 | 0.0 | 2.9 | 0.9 | 156.7 | 4.5 | 155.1 | 4.9 | 132.2 | 41.8 | 156.7 | 4.5 | NA |
| 15ATW23-Spot 51 | 106 | 27851 | 2.2 | 19.9 | 2.1 | 0.2 | 3.6 | 0.0 | 3.0 | 0.8 | 156.8 | 4.6 | 159.5 | 5.4 | 201.6 | 48.8 | 156.8 | 4.6 | NA |
| 15ATW23-Spot 241 | 87 | 23471 | 3.3 | 20.9 | 2.0 | 0.2 | 3.4 | 0.0 | 2.7 | 0.8 | 156.8 | 4.2 | 152.8 | 4.8 | 93.2 | 47.6 | 156.8 | 4.2 | NA |
| 15ATW23-Spot 169 | 236 | 20612 | 2.5 | 20.4 | 1.6 | 0.2 | 3.6 | 0.0 | 3.2 | 0.9 | 157.0 | 4.9 | 156.4 | 5.2 | 147.8 | 38.6 | 157.0 | 4.9 | NA |
| 15ATW23-Spot 311 | 192 | 135163 | 4.3 | 19.6 | 1.6 | 0.2 | 3.8 | 0.0 | 3.4 | 0.9 | 157.0 | 5.3 | 162.6 | 5.6 | 245.2 | 36.3 | 157.0 | 5.3 | NA |
| 15ATW23-Spot 308 | 36 | 497458 | 2.1 | 19.3 | 3.2 | 0.2 | 4.6 | 0.0 | 3.4 | 0.7 | 157.1 | 5.3 | 164.6 | 7.1 | 274.9 | 72.9 | 157.1 | 5.3 | NA |
| 15ATW23-Spot 47 | 65 | 75619 | 3.7 | 18.5 | 3.2 | 0.2 | 4.3 | 0.0 | 2.9 | 0.7 | 157.2 | 4.6 | 171.5 | 6.8 | 373.7 | 71.6 | 157.2 | 4.6 | NA |
| 15ATW23-Spot 265 | 188 | 46519 | 2.8 | 20.5 | 1.6 | 0.2 | 3.4 | 0.0 | 3.0 | 0.9 | 157.3 | 4.7 | 155.9 | 4.9 | 135.7 | 37.8 | 157.3 | 4.7 | NA |
| 15ATW23-Spot 243 | 62 | 24309 | 3.6 | 20.8 | 2.3 | 0.2 | 3.8 | 0.0 | 3.1 | 0.8 | 157.3 | 4.8 | 153.8 | 5.5 | 101.8 | 54.2 | 157.3 | 4.8 | NA |
| 15ATW23-Spot 132 | 115 | 47685 | 2.6 | 20.2 | 2.2 | 0.2 | 3.4 | 0.0 | 2.6 | 0.8 | 157.3 | 4.1 | 158.4 | 5.0 | 176.9 | 50.8 | 157.3 | 4.1 | NA |
| 15ATW23-Spot 204 | 63 | 31581 | 2.9 | 20.7 | 2.4 | 0.2 | 4.5 | 0.0 | 3.8 | 0.8 | 157.4 | 5.9 | 155.0 | 6.5 | 118.8 | 56.1 | 157.4 | 5.9 | NA |
| 15ATW23-Spot 122 | 104 | 37260 | 2.9 | 20.7 | 2.4 | 0.2 | 3.5 | 0.0 | 2.5 | 0.7 | 157.5 | 3.8 | 154.7 | 5.0 | 112.9 | 57.8 | 157.5 | 3.8 | NA |
| 15ATW23-Spot 284 | 40 | 30519 | 2.7 | 20.6 | 4.0 | 0.2 | 5.3 | 0.0 | 3.5 | 0.7 | 157.5 | 5.4 | 155.4 | 7.6 | 124.8 | 94.7 | 157.5 | 5.4 | NA |
| 15ATW23-Spot 226 | 119 | 29144 | 2.0 | 20.5 | 1.9 | 0.2 | 3.3 | 0.0 | 2.7 | 0.8 | 157.5 | 4.2 | 156.5 | 4.8 | 142.7 | 45.4 | 157.5 | 4.2 | NA |
| 15ATW23-Spot 158 | 159 | 38281 | 2.0 | 20.2 | 1.8 | 0.2 | 3.9 | 0.0 | 3.5 | 0.9 | 157.5 | 5.4 | 158.7 | 5.7 | 176.8 | 42.3 | 157.5 | 5.4 | NA |
| 15ATW23-Spot 312 | 85 | 11688 | 3.7 | 20.7 | 2.5 | 0.2 | 4.4 | 0.0 | 3.6 | 0.8 | 157.5 | 5.6 | 155.1 | 6.3 | 118.3 | 59.1 | 157.5 | 5.6 | NA |
| 15ATW23-Spot 77 | 157 | 73568 | 1.8 | 18.2 | 2.6 | 0.2 | 3.6 | 0.0 | 2.6 | 0.7 | 157.7 | 4.0 | 174.9 | 5.9 | 414.8 | 58.0 | 157.7 | 4.0 | NA |
| 15ATW23-Spot 246 | 119 | 53967 | 3.3 | 20.4 | 2.2 | 0.2 | 4.2 | 0.0 | 3.6 | 0.9 | 157.7 | 5.6 | 157.2 | 6.1 | 151.2 | 50.6 | 157.7 | 5.6 | NA |

| | | | | | | | | | | | | | | | | | | | |
|---|---|---|---|---|---|---|---|---|---|---|---|---|---|---|---|---|---|---|---|
| 15ATW23-Spot 271 | 122 | 29311 | 1.5 | 20.1 | 2.1 | 0.2 | 3.3 | 0.0 | 2.6 | 0.8 | 157.8 | 4.0 | 159.5 | 4.9 | 184.9 | 48.2 | 157.8 | 4.0 | NA |
| 15ATW23-Spot 267 | 261 | 53665 | 3.0 | 19.9 | 1.5 | 0.2 | 2.9 | 0.0 | 2.5 | 0.9 | 158.0 | 4.0 | 160.9 | 4.4 | 204.7 | 33.7 | 158.0 | 4.0 | NA |
| 15ATW23-Spot 151 | 491 | 39917 | 0.9 | 20.4 | 1.2 | 0.2 | 2.4 | 0.0 | 2.1 | 0.9 | 158.0 | 3.3 | 157.4 | 3.5 | 149.3 | 27.7 | 158.0 | 3.3 | NA |
| 15ATW23-Spot 256 | 107 | 25739 | 3.2 | 20.6 | 2.0 | 0.2 | 3.6 | 0.0 | 3.0 | 0.8 | 158.0 | 4.7 | 155.9 | 5.2 | 125.0 | 45.9 | 158.0 | 4.7 | NA |
| 15ATW23-Spot 163 | 102 | 71529 | 1.9 | 19.9 | 2.2 | 0.2 | 3.2 | 0.0 | 2.4 | 0.7 | 158.1 | 3.7 | 161.1 | 4.8 | 207.2 | 50.5 | 158.1 | 3.7 | NA |
| 15ATW23-Spot 190 | 576 | 240843 | 1.5 | 20.3 | 1.3 | 0.2 | 3.0 | 0.0 | 2.7 | 0.9 | 158.1 | 4.2 | 158.2 | 4.4 | 160.9 | 30.3 | 158.1 | 4.2 | NA |
| 15ATW23-Spot 138 | 39 | 36375 | 2.6 | 21.4 | 3.4 | 0.2 | 4.2 | 0.0 | 2.5 | 0.6 | 158.1 | 4.0 | 150.8 | 5.9 | 38.1 | 81.4 | 158.1 | 4.0 | NA |
| 15ATW23-Spot 89 | 112 | 45662 | 2.2 | 20.4 | 2.1 | 0.2 | 3.7 | 0.0 | 3.0 | 0.8 | 158.1 | 4.7 | 157.8 | 5.4 | 154.3 | 49.7 | 158.1 | 4.7 | NA |
| 15ATW23-Spot 67 | 89 | 25432 | 3.8 | 20.4 | 2.0 | 0.2 | 3.5 | 0.0 | 2.8 | 0.8 | 158.4 | 4.4 | 157.8 | 5.1 | 149.6 | 47.2 | 158.4 | 4.4 | NA |
| 15ATW23-Spot 145 | 119 | 34195 | 2.5 | 20.6 | 2.1 | 0.2 | 3.4 | 0.0 | 2.7 | 0.8 | 158.4 | 4.2 | 156.3 | 4.9 | 125.1 | 48.4 | 158.4 | 4.2 | NA |
| 15ATW23-Spot 196 | 376 | 134377 | 1.6 | 20.0 | 1.4 | 0.2 | 2.8 | 0.0 | 2.4 | 0.9 | 158.4 | 3.7 | 161.0 | 4.1 | 200.6 | 32.0 | 158.4 | 3.7 | NA |
| 15ATW23-Spot 27 | 167 | 44928 | 1.9 | 20.7 | 1.7 | 0.2 | 2.6 | 0.0 | 2.0 | 0.8 | 158.5 | 3.1 | 155.8 | 3.8 | 115.4 | 41.2 | 158.5 | 3.1 | NA |
| 15ATW23-Spot 172 | 74 | 48924 | 3.6 | 19.0 | 2.5 | 0.2 | 3.8 | 0.0 | 2.9 | 0.8 | 158.5 | 4.6 | 168.8 | 6.0 | 316.1 | 56.5 | 158.5 | 4.6 | NA |
| 15ATW23-Spot 8 | 99 | 15382 | 2.5 | 20.7 | 2.0 | 0.2 | 3.6 | 0.0 | 3.0 | 0.8 | 158.6 | 4.7 | 155.6 | 5.2 | 112.2 | 47.4 | 158.6 | 4.7 | NA |
| 15ATW23-Spot 147 | 313 | 772706 | 2.2 | 19.8 | 1.4 | 0.2 | 3.2 | 0.0 | 2.9 | 0.9 | 158.6 | 4.5 | 162.3 | 4.7 | 217.5 | 31.7 | 158.6 | 4.5 | NA |
| 15ATW23-Spot 125 | 136 | 18806 | 1.6 | 20.3 | 1.7 | 0.2 | 3.1 | 0.0 | 2.6 | 0.8 | 158.7 | 4.1 | 159.0 | 4.6 | 164.9 | 40.8 | 158.7 | 4.1 | NA |
| 15ATW23-Spot 202 | 212 | 45600 | 2.2 | 20.4 | 1.6 | 0.2 | 3.2 | 0.0 | 2.8 | 0.9 | 158.8 | 4.4 | 158.1 | 4.7 | 149.9 | 37.1 | 158.8 | 4.4 | NA |
| 15ATW23-Spot 154 | 141 | 52719 | 1.9 | 20.3 | 1.6 | 0.2 | 2.9 | 0.0 | 2.5 | 0.8 | 158.8 | 3.9 | 158.5 | 4.3 | 155.0 | 37.5 | 158.8 | 3.9 | NA |
| 15ATW23-Spot 214 | 146 | 531241 | 2.6 | 19.4 | 1.9 | 0.2 | 3.5 | 0.0 | 3.0 | 0.9 | 158.8 | 4.7 | 165.7 | 5.4 | 265.4 | 42.5 | 158.8 | 4.7 | NA |
| 15ATW23-Spot 107 | 150 | 93355 | 1.9 | 20.6 | 1.7 | 0.2 | 3.0 | 0.0 | 2.5 | 0.8 | 158.9 | 3.9 | 156.6 | 4.4 | 124.1 | 40.0 | 158.9 | 3.9 | NA |
| 15ATW23-Spot 193 | 855 | 414396 | 1.9 | 19.7 | 1.1 | 0.2 | 2.9 | 0.0 | 2.7 | 0.9 | 158.9 | 4.2 | 163.5 | 4.4 | 232.4 | 24.7 | 158.9 | 4.2 | NA |
| 15ATW23-Spot 108 | 101 | 39841 | 3.3 | 20.5 | 2.2 | 0.2 | 3.3 | 0.0 | 2.4 | 0.7 | 158.9 | 3.8 | 157.7 | 4.8 | 141.4 | 52.3 | 158.9 | 3.8 | NA |
| 15ATW23-Spot 9 | 332 | 475688 | 2.3 | 20.7 | 1.3 | 0.2 | 3.1 | 0.0 | 2.9 | 0.9 | 158.9 | 4.5 | 155.9 | 4.5 | 111.9 | 29.7 | 158.9 | 4.5 | NA |
| 15ATW23-Spot 7 | 1209 | 338947 | 1.7 | 20.4 | 1.0 | 0.2 | 2.6 | 0.0 | 2.4 | 0.9 | 159.0 | 3.8 | 158.0 | 3.9 | 144.4 | 23.6 | 159.0 | 3.8 | NA |
| 15ATW23-Spot 115 | 24 | 7088 | 3.0 | 20.0 | 4.3 | 0.2 | 5.5 | 0.0 | 3.5 | 0.6 | 159.2 | 5.4 | 161.1 | 8.2 | 189.9 | 99.8 | 159.2 | 5.4 | NA |
| 15ATW23-Spot 18 | 195 | 40708 | 3.1 | 20.5 | 1.6 | 0.2 | 3.1 | 0.0 | 2.7 | 0.9 | 159.2 | 4.3 | 157.7 | 4.6 | 135.3 | 36.6 | 159.2 | 4.3 | NA |
| 15ATW23-Spot 32 | 217 | 19845 | 2.1 | 20.5 | 1.6 | 0.2 | 2.9 | 0.0 | 2.4 | 0.8 | 159.3 | 3.8 | 157.9 | 4.3 | 138.0 | 37.4 | 159.3 | 3.8 | NA |
| 15ATW23-Spot 14 | 193 | 54562 | 1.7 | 20.4 | 1.4 | 0.2 | 3.4 | 0.0 | 3.1 | 0.9 | 159.3 | 4.8 | 158.6 | 4.9 | 149.3 | 33.0 | 159.3 | 4.8 | NA |
| 15ATW23-Spot 96 | 81 | 49354 | 2.1 | 19.8 | 2.9 | 0.2 | 4.2 | 0.0 | 3.1 | 0.7 | 159.4 | 4.9 | 163.2 | 6.3 | 220.6 | 66.0 | 159.4 | 4.9 | NA |
| 15ATW23-Spot 199 | 36 | 30039 | 3.3 | 19.8 | 2.9 | 0.2 | 4.6 | 0.0 | 3.6 | 0.8 | 159.4 | 5.7 | 163.2 | 6.9 | 220.1 | 66.7 | 159.4 | 5.7 | NA |
| 15ATW23-Spot 309 | 136 | 137344 | 2.5 | 20.0 | 1.7 | 0.2 | 3.0 | 0.0 | 2.4 | 0.8 | 159.5 | 3.8 | 162.0 | 4.5 | 200.1 | 40.4 | 159.5 | 3.8 | NA |
| 15ATW23-Spot 82 | 254 | 122634 | 1.3 | 20.2 | 1.6 | 0.2 | 3.7 | 0.0 | 3.3 | 0.9 | 159.5 | 5.3 | 160.6 | 5.5 | 177.3 | 36.2 | 159.5 | 5.3 | NA |
| 15ATW23-Spot 233 | 88 | 38016 | 1.6 | 20.4 | 1.9 | 0.2 | 3.3 | 0.0 | 2.7 | 0.8 | 159.5 | 4.3 | 159.0 | 4.9 | 152.4 | 44.3 | 159.5 | 4.3 | NA |
| 15ATW23-Spot 76 | 94 | 17451 | 2.0 | 19.8 | 2.0 | 0.2 | 3.2 | 0.0 | 2.5 | 0.8 | 159.6 | 4.0 | 163.4 | 4.8 | 220.5 | 45.6 | 159.6 | 4.0 | NA |

| | | | | | | | | | | | | | | | | | | | |
|---|---|---|---|---|---|---|---|---|---|---|---|---|---|---|---|---|---|---|---|
| 15ATW23-Spot 175 | 240 | 184892 | 1.4 | 18.8 | 2.1 | 0.2 | 3.2 | 0.0 | 2.5 | 0.8 | 159.6 | 3.9 | 171.0 | 5.1 | 332.5 | 47.6 | 159.6 | 3.9 | NA |
| 15ATW23-Spot 16 | 557 | 63228 | 1.5 | 20.7 | 1.5 | 0.2 | 3.3 | 0.0 | 2.9 | 0.9 | 159.7 | 4.6 | 156.8 | 4.8 | 115.6 | 34.9 | 159.7 | 4.6 | NA |
| 15ATW23-Spot 257 | 2930 | 408526 | 1.5 | 19.8 | 0.9 | 0.2 | 2.8 | 0.0 | 2.7 | 1.0 | 159.7 | 4.2 | 163.0 | 4.2 | 213.5 | 20.2 | 159.7 | 4.2 | NA |
| 15ATW23-Spot 244 | 554 | 481342 | 1.4 | 20.0 | 1.4 | 0.2 | 2.5 | 0.0 | 2.1 | 0.8 | 159.7 | 3.3 | 161.7 | 3.8 | 191.9 | 32.9 | 159.7 | 3.3 | NA |
| 15ATW23-Spot 37 | 99 | 27688 | 2.2 | 20.7 | 2.1 | 0.2 | 3.1 | 0.0 | 2.3 | 0.7 | 159.7 | 3.6 | 157.1 | 4.6 | 118.4 | 50.3 | 159.7 | 3.6 | NA |
| 15ATW23-Spot 81 | 468 | 350757 | 7.2 | 20.4 | 1.4 | 0.2 | 3.5 | 0.0 | 3.2 | 0.9 | 159.8 | 5.1 | 159.1 | 5.1 | 148.5 | 31.8 | 159.8 | 5.1 | NA |
| 15ATW23-Spot 123 | 201 | 27011 | 1.8 | 20.7 | 1.5 | 0.2 | 3.0 | 0.0 | 2.6 | 0.9 | 159.9 | 4.0 | 156.7 | 4.3 | 110.4 | 36.2 | 159.9 | 4.0 | NA |
| 15ATW23-Spot 306 | 156 | 117846 | 1.8 | 20.5 | 2.0 | 0.2 | 3.5 | 0.0 | 2.9 | 0.8 | 160.2 | 4.5 | 158.4 | 5.1 | 132.5 | 47.5 | 160.2 | 4.5 | NA |
| 15ATW23-Spot 216 | 165 | 16761 | 2.0 | 20.3 | 1.6 | 0.2 | 3.1 | 0.0 | 2.6 | 0.8 | 160.3 | 4.1 | 160.1 | 4.6 | 158.2 | 38.0 | 160.3 | 4.1 | NA |
| 15ATW23-Spot 137 | 46 | 7689 | 2.5 | 20.5 | 2.6 | 0.2 | 3.9 | 0.0 | 2.9 | 0.7 | 160.6 | 4.6 | 158.9 | 5.8 | 135.4 | 62.1 | 160.6 | 4.6 | NA |
| 15ATW23-Spot 281 | 36 | 14451 | 2.1 | 20.7 | 3.0 | 0.2 | 4.6 | 0.0 | 3.4 | 0.8 | 160.6 | 5.5 | 157.7 | 6.7 | 114.7 | 70.9 | 160.6 | 5.5 | NA |
| 15ATW23-Spot 117 | 146 | 43252 | 1.5 | 20.1 | 2.2 | 0.2 | 3.6 | 0.0 | 2.8 | 0.8 | 160.7 | 4.5 | 161.9 | 5.4 | 180.7 | 51.5 | 160.7 | 4.5 | NA |
| 15ATW23-Spot 128 | 144 | 32627 | 2.4 | 20.4 | 1.8 | 0.2 | 3.6 | 0.0 | 3.1 | 0.9 | 160.9 | 4.9 | 160.2 | 5.3 | 151.1 | 42.7 | 160.9 | 4.9 | NA |
| 15ATW23-Spot 94 | 216 | 52226 | 1.6 | 19.7 | 1.5 | 0.2 | 3.2 | 0.0 | 2.8 | 0.9 | 160.9 | 4.5 | 165.4 | 4.9 | 231.2 | 35.3 | 160.9 | 4.5 | NA |
| 15ATW23-Spot 252 | 170 | 141838 | 2.6 | 19.9 | 2.0 | 0.2 | 4.1 | 0.0 | 3.6 | 0.9 | 160.9 | 5.8 | 163.7 | 6.3 | 204.9 | 45.7 | 160.9 | 5.8 | NA |
| 15ATW23-Spot 260 | 209 | 17194 | 3.1 | 18.6 | 1.5 | 0.2 | 3.6 | 0.0 | 3.3 | 0.9 | 161.0 | 5.3 | 174.3 | 5.8 | 360.2 | 32.9 | 161.0 | 5.3 | NA |
| 15ATW23-Spot 40 | 159 | 92951 | 2.7 | 19.9 | 2.0 | 0.2 | 3.6 | 0.0 | 2.9 | 0.8 | 161.1 | 4.6 | 163.9 | 5.4 | 204.6 | 47.1 | 161.1 | 4.6 | NA |
| 15ATW23-Spot 162 | 110 | 56255 | 2.4 | 19.5 | 2.0 | 0.2 | 3.8 | 0.0 | 3.3 | 0.9 | 161.2 | 5.2 | 167.4 | 5.9 | 257.3 | 46.0 | 161.2 | 5.2 | NA |
| 15ATW23-Spot 136 | 261 | 9381666 | 1.4 | 19.9 | 1.5 | 0.2 | 2.8 | 0.0 | 2.4 | 0.8 | 161.2 | 3.8 | 164.4 | 4.3 | 211.2 | 35.0 | 161.2 | 3.8 | NA |
| 15ATW23-Spot 64 | 237 | 56920 | 2.8 | 20.2 | 1.3 | 0.2 | 2.5 | 0.0 | 2.2 | 0.9 | 161.5 | 3.5 | 161.9 | 3.8 | 169.2 | 29.6 | 161.5 | 3.5 | NA |
| 15ATW23-Spot 28 | 87 | 23192 | 2.4 | 20.1 | 1.7 | 0.2 | 3.3 | 0.0 | 2.8 | 0.8 | 161.7 | 4.4 | 163.2 | 4.9 | 187.1 | 40.5 | 161.7 | 4.4 | NA |
| 15ATW23-Spot 245 | 172 | 76289 | 2.4 | 20.5 | 1.9 | 0.2 | 3.3 | 0.0 | 2.7 | 0.8 | 161.7 | 4.4 | 160.3 | 4.9 | 141.0 | 44.3 | 161.7 | 4.4 | NA |
| 15ATW23-Spot 84 | 270 | 43022 | 2.1 | 20.0 | 1.8 | 0.2 | 3.2 | 0.0 | 2.7 | 0.8 | 161.8 | 4.2 | 164.1 | 4.8 | 197.3 | 41.6 | 161.8 | 4.2 | NA |
| 15ATW23-Spot 187 | 211 | 105761 | 2.3 | 19.6 | 1.7 | 0.2 | 3.1 | 0.0 | 2.6 | 0.8 | 161.8 | 4.2 | 166.7 | 4.7 | 237.8 | 38.2 | 161.8 | 4.2 | NA |
| 15ATW23-Spot 177 | 63 | 27926 | 3.2 | 20.4 | 2.7 | 0.2 | 3.7 | 0.0 | 2.5 | 0.7 | 161.9 | 4.0 | 160.7 | 5.5 | 144.6 | 63.1 | 161.9 | 4.0 | NA |
| 15ATW23-Spot 272 | 288 | 67073 | 1.9 | 20.1 | 1.2 | 0.2 | 3.3 | 0.0 | 3.1 | 0.9 | 161.9 | 4.9 | 163.1 | 5.0 | 181.9 | 28.6 | 161.9 | 4.9 | NA |
| 15ATW23-Spot 221 | 107 | 133067 | 2.1 | 19.6 | 1.9 | 0.2 | 3.4 | 0.0 | 2.8 | 0.8 | 162.1 | 4.5 | 167.2 | 5.2 | 241.7 | 43.4 | 162.1 | 4.5 | NA |
| 15ATW23-Spot 203 | 389 | 54611 | 2.1 | 20.1 | 1.1 | 0.2 | 2.9 | 0.0 | 2.7 | 0.9 | 162.3 | 4.3 | 163.8 | 4.4 | 187.2 | 25.6 | 162.3 | 4.3 | NA |
| 15ATW23-Spot 310 | 90 | 603794 | 1.8 | 20.5 | 2.8 | 0.2 | 3.7 | 0.0 | 2.5 | 0.7 | 162.3 | 3.9 | 160.8 | 5.6 | 139.6 | 66.2 | 162.3 | 3.9 | NA |
| 15ATW23-Spot 157 | 666 | 192346 | 2.0 | 20.0 | 1.4 | 0.2 | 2.6 | 0.0 | 2.2 | 0.8 | 162.3 | 3.5 | 164.3 | 3.9 | 194.1 | 31.6 | 162.3 | 3.5 | NA |
| 15ATW23-Spot 5 | 218 | 262248 | 1.5 | 20.3 | 1.4 | 0.2 | 2.8 | 0.0 | 2.4 | 0.9 | 162.4 | 3.8 | 162.1 | 4.2 | 159.2 | 32.7 | 162.4 | 3.8 | NA |
| 15ATW23-Spot 155 | 533 | 181098 | 1.8 | 20.2 | 1.2 | 0.2 | 2.7 | 0.0 | 2.5 | 0.9 | 162.4 | 4.0 | 162.9 | 4.1 | 170.9 | 27.0 | 162.4 | 4.0 | NA |
| 15ATW23-Spot 103 | 162 | 786063 | 2.5 | 19.7 | 1.7 | 0.2 | 3.4 | 0.0 | 3.0 | 0.9 | 162.5 | 4.8 | 166.7 | 5.3 | 227.2 | 39.7 | 162.5 | 4.8 | NA |
| 15ATW23-Spot 83 | 105 | 137454 | 3.6 | 20.0 | 2.0 | 0.2 | 3.8 | 0.0 | 3.2 | 0.8 | 162.5 | 5.1 | 164.5 | 5.7 | 193.8 | 46.5 | 162.5 | 5.1 | NA |

| | | | | | | | | | | | | | | | | | | | |
|---|---|---|---|---|---|---|---|---|---|---|---|---|---|---|---|---|---|---|---|
| 15ATW23-Spot 215 | 229 | 152510 | 1.5 | 20.3 | 1.9 | 0.2 | 3.6 | 0.0 | 3.1 | 0.9 | 162.6 | 5.0 | 162.6 | 5.5 | 162.9 | 44.9 | 162.6 | 5.0 | NA |
| 15ATW23-Spot 92 | 89 | 70510 | 1.7 | 20.8 | 2.2 | 0.2 | 3.2 | 0.0 | 2.3 | 0.7 | 162.7 | 3.7 | 158.5 | 4.6 | 97.7 | 52.0 | 162.7 | 3.7 | NA |
| 15ATW23-Spot 164 | 337 | 621792 | 3.0 | 20.1 | 1.6 | 0.2 | 3.2 | 0.0 | 2.8 | 0.9 | 162.7 | 4.5 | 164.1 | 4.9 | 185.2 | 37.7 | 162.7 | 4.5 | NA |
| 15ATW23-Spot 30 | 238 | 125539 | 2.3 | 20.4 | 1.2 | 0.2 | 2.7 | 0.0 | 2.4 | 0.9 | 162.8 | 3.9 | 162.2 | 4.1 | 153.5 | 27.4 | 162.8 | 3.9 | NA |
| 15ATW23-Spot 300 | 101 | 28195 | 2.1 | 19.4 | 2.4 | 0.2 | 3.6 | 0.0 | 2.7 | 0.7 | 163.0 | 4.3 | 169.5 | 5.6 | 262.0 | 56.0 | 163.0 | 4.3 | NA |
| 15ATW23-Spot 127 | 897 | 152689 | 1.1 | 20.3 | 1.0 | 0.2 | 3.0 | 0.0 | 2.8 | 0.9 | 163.1 | 4.6 | 162.6 | 4.5 | 156.1 | 23.9 | 163.1 | 4.6 | NA |
| 15ATW23-Spot 258 | 229 | 50438 | 2.0 | 19.5 | 1.5 | 0.2 | 3.1 | 0.0 | 2.8 | 0.9 | 163.1 | 4.5 | 168.9 | 4.9 | 251.4 | 34.2 | 163.1 | 4.5 | NA |
| 15ATW23-Spot 274 | 254 | 92367 | 1.6 | 19.3 | 1.8 | 0.2 | 2.6 | 0.0 | 1.9 | 0.7 | 163.2 | 3.1 | 170.6 | 4.1 | 275.4 | 40.6 | 163.2 | 3.1 | NA |
| 15ATW23-Spot 191 | 144 | 33147 | 2.2 | 20.3 | 1.9 | 0.2 | 3.8 | 0.0 | 3.3 | 0.9 | 163.9 | 5.3 | 163.9 | 5.7 | 165.0 | 43.9 | 163.9 | 5.3 | NA |
| 15ATW23-Spot 126 | 224 | 142820 | 2.6 | 20.1 | 1.4 | 0.2 | 2.5 | 0.0 | 2.0 | 0.8 | 163.9 | 3.3 | 165.2 | 3.8 | 184.0 | 32.6 | 163.9 | 3.3 | NA |
| 15ATW23-Spot 275 | 504 | 389294 | 1.5 | 19.6 | 0.9 | 0.2 | 3.5 | 0.0 | 3.3 | 1.0 | 164.0 | 5.4 | 169.0 | 5.4 | 240.9 | 20.4 | 164.0 | 5.4 | NA |
| 15ATW23-Spot 303 | 120 | 27732 | 3.8 | 20.2 | 1.9 | 0.2 | 4.1 | 0.0 | 3.6 | 0.9 | 164.0 | 5.8 | 164.6 | 6.2 | 173.8 | 45.5 | 164.0 | 5.8 | NA |
| 15ATW23-Spot 152 | 232 | 58475 | 1.5 | 20.5 | 1.5 | 0.2 | 2.9 | 0.0 | 2.5 | 0.8 | 164.1 | 4.0 | 162.0 | 4.4 | 131.9 | 36.2 | 164.1 | 4.0 | NA |
| 15ATW23-Spot 197 | 972 | 420189 | 1.6 | 20.1 | 1.2 | 0.2 | 2.5 | 0.0 | 2.2 | 0.9 | 164.1 | 3.5 | 165.1 | 3.8 | 180.1 | 27.6 | 164.1 | 3.5 | NA |
| 15ATW23-Spot 139 | 107 | 15359 | 2.0 | 20.7 | 2.3 | 0.2 | 3.4 | 0.0 | 2.4 | 0.7 | 164.2 | 4.0 | 161.1 | 5.0 | 116.7 | 54.7 | 164.2 | 4.0 | NA |
| 15ATW23-Spot 239 | 35 | 9200 | 4.9 | 19.6 | 4.0 | 0.2 | 5.1 | 0.0 | 3.1 | 0.6 | 164.2 | 5.0 | 169.6 | 7.9 | 246.1 | 93.1 | 164.2 | 5.0 | NA |
| 15ATW23-Spot 98 | 463 | 492684 | 8.0 | 20.5 | 1.1 | 0.2 | 2.8 | 0.0 | 2.6 | 0.9 | 164.3 | 4.2 | 162.8 | 4.3 | 142.0 | 26.8 | 164.3 | 4.2 | NA |
| 15ATW23-Spot 95 | 78 | 256429 | 3.1 | 19.1 | 2.2 | 0.2 | 3.4 | 0.0 | 2.6 | 0.8 | 164.4 | 4.2 | 173.1 | 5.4 | 295.6 | 49.6 | 164.4 | 4.2 | NA |
| 15ATW23-Spot 41 | 60 | 27759 | 2.7 | 20.9 | 2.2 | 0.2 | 3.8 | 0.0 | 3.0 | 0.8 | 164.4 | 4.9 | 159.8 | 5.6 | 93.6 | 52.6 | 164.4 | 4.9 | NA |
| 15ATW23-Spot 25 | 211 | 306892 | 1.6 | 20.2 | 1.6 | 0.2 | 3.3 | 0.0 | 2.9 | 0.9 | 164.6 | 4.7 | 164.9 | 5.0 | 170.8 | 36.7 | 164.6 | 4.7 | NA |
| 15ATW23-Spot 153 | 185 | 34131 | 2.0 | 20.1 | 1.8 | 0.2 | 3.2 | 0.0 | 2.7 | 0.8 | 164.7 | 4.3 | 166.2 | 4.9 | 188.6 | 41.2 | 164.7 | 4.3 | NA |
| 15ATW23-Spot 168 | 298 | 83449 | 2.4 | 20.8 | 1.7 | 0.2 | 2.8 | 0.0 | 2.2 | 0.8 | 165.1 | 3.6 | 161.2 | 4.2 | 104.4 | 41.3 | 165.1 | 3.6 | NA |
| 15ATW23-Spot 143 | 51 | 13599 | 3.0 | 20.9 | 2.9 | 0.2 | 3.9 | 0.0 | 2.6 | 0.7 | 165.2 | 4.3 | 160.8 | 5.8 | 96.7 | 67.8 | 165.2 | 4.3 | NA |
| 15ATW23-Spot 266 | 1100 | 1293057 | 4.8 | 20.2 | 0.9 | 0.2 | 2.5 | 0.0 | 2.3 | 0.9 | 165.6 | 3.8 | 165.7 | 3.8 | 168.6 | 21.2 | 165.6 | 3.8 | NA |
| 15ATW23-Spot 165 | 149 | 29129 | 2.5 | 19.4 | 1.8 | 0.2 | 2.9 | 0.0 | 2.3 | 0.8 | 165.6 | 3.8 | 172.4 | 4.6 | 267.2 | 40.8 | 165.6 | 3.8 | NA |
| 15ATW23-Spot 217 | 56 | 63743 | 3.7 | 19.9 | 2.7 | 0.2 | 3.9 | 0.0 | 2.8 | 0.7 | 165.6 | 4.7 | 168.6 | 6.0 | 211.8 | 61.5 | 165.6 | 4.7 | NA |
| 15ATW23-Spot 178 | 75 | 96940 | 2.9 | 20.5 | 2.0 | 0.2 | 3.1 | 0.0 | 2.3 | 0.8 | 166.2 | 3.9 | 164.5 | 4.7 | 140.9 | 46.8 | 166.2 | 3.9 | NA |
| 15ATW23-Spot 180 | 314 | 59947 | 2.0 | 20.1 | 1.5 | 0.2 | 2.9 | 0.0 | 2.5 | 0.9 | 166.8 | 4.1 | 168.0 | 4.5 | 185.8 | 33.8 | 166.8 | 4.1 | NA |
| 15ATW23-Spot 49 | 143 | 34041 | 2.4 | 20.6 | 1.6 | 0.2 | 2.7 | 0.0 | 2.1 | 0.8 | 166.9 | 3.5 | 164.1 | 4.1 | 124.6 | 38.7 | 166.9 | 3.5 | NA |
| 15ATW23-Spot 33 | 133 | 264833 | 1.8 | 19.4 | 2.0 | 0.2 | 3.4 | 0.0 | 2.8 | 0.8 | 167.1 | 4.5 | 173.7 | 5.4 | 265.6 | 46.1 | 167.1 | 4.5 | NA |
| 15ATW23-Spot 13 | 307 | 136498 | 1.8 | 19.9 | 1.5 | 0.2 | 2.9 | 0.0 | 2.5 | 0.9 | 167.5 | 4.1 | 169.8 | 4.5 | 203.1 | 34.0 | 167.5 | 4.1 | NA |
| 15ATW23-Spot 222 | 214 | 47906 | 2.4 | 20.1 | 1.6 | 0.2 | 3.2 | 0.0 | 2.7 | 0.9 | 167.8 | 4.5 | 168.7 | 4.9 | 181.8 | 37.7 | 167.8 | 4.5 | NA |
| 15ATW23-Spot 263 | 109 | 58290 | 2.1 | 18.6 | 2.4 | 0.2 | 3.6 | 0.0 | 2.7 | 0.8 | 168.2 | 4.6 | 181.6 | 6.0 | 362.0 | 53.2 | 168.2 | 4.6 | NA |
| 15ATW23-Spot 140 | 356 | 112936 | 1.8 | 20.5 | 1.4 | 0.2 | 3.2 | 0.0 | 2.9 | 0.9 | 168.3 | 4.8 | 166.3 | 4.9 | 138.8 | 32.0 | 168.3 | 4.8 | NA |

| | | | | | | | | | | | | | | | | | | | |
|---|---|---|---|---|---|---|---|---|---|---|---|---|---|---|---|---|---|---|---|
| 15ATW23-Spot 10 | 226 | 69019 | 1.4 | 20.2 | 1.3 | 0.2 | 2.5 | 0.0 | 2.1 | 0.8 | 168.5 | 3.4 | 168.8 | 3.8 | 173.5 | 31.4 | 168.5 | 3.4 | NA |
| 15ATW23-Spot 2 | 170 | 205219 | 3.2 | 19.7 | 2.2 | 0.2 | 3.9 | 0.0 | 3.2 | 0.8 | 168.8 | 5.4 | 172.8 | 6.2 | 229.7 | 49.9 | 168.8 | 5.4 | NA |
| 15ATW23-Spot 101 | 495 | 259035 | 1.5 | 19.6 | 1.3 | 0.2 | 3.2 | 0.0 | 2.9 | 0.9 | 168.9 | 4.8 | 173.4 | 5.0 | 236.4 | 28.9 | 168.9 | 4.8 | NA |
| 15ATW23-Spot 228 | 147 | 25060 | 2.3 | 20.0 | 1.8 | 0.2 | 3.0 | 0.0 | 2.5 | 0.8 | 169.2 | 4.2 | 171.1 | 4.8 | 199.7 | 40.9 | 169.2 | 4.2 | NA |
| 15ATW23-Spot 146 | 193 | 24761 | 1.6 | 20.5 | 1.3 | 0.2 | 3.0 | 0.0 | 2.7 | 0.9 | 169.4 | 4.5 | 167.2 | 4.7 | 136.7 | 31.5 | 169.4 | 4.5 | NA |
| 15ATW23-Spot 19 | 151 | 33646 | 3.9 | 19.8 | 2.0 | 0.2 | 3.1 | 0.0 | 2.4 | 0.8 | 169.5 | 4.0 | 172.6 | 4.9 | 216.1 | 45.3 | 169.5 | 4.0 | NA |
| 15ATW23-Spot 120 | 61 | 183637 | 2.7 | 20.8 | 2.3 | 0.2 | 3.3 | 0.0 | 2.4 | 0.7 | 170.0 | 4.0 | 165.2 | 5.0 | 98.7 | 54.0 | 170.0 | 4.0 | NA |
| 15ATW23-Spot 135 | 518 | 153848 | 1.6 | 20.4 | 1.2 | 0.2 | 3.3 | 0.0 | 3.1 | 0.9 | 170.2 | 5.1 | 168.6 | 5.1 | 147.2 | 28.2 | 170.2 | 5.1 | NA |
| 15ATW23-Spot 173 | 439 | 188797 | 2.0 | 20.0 | 1.4 | 0.2 | 2.9 | 0.0 | 2.6 | 0.9 | 170.4 | 4.3 | 172.3 | 4.7 | 199.3 | 33.2 | 170.4 | 4.3 | NA |
| 15ATW23-Spot 186 | 143 | 55732 | 2.2 | 19.9 | 1.8 | 0.2 | 2.8 | 0.0 | 2.1 | 0.8 | 170.8 | 3.6 | 173.5 | 4.4 | 210.4 | 41.4 | 170.8 | 3.6 | NA |
| 15ATW23-Spot 201 | 81 | 22583 | 2.4 | 20.4 | 1.9 | 0.2 | 3.2 | 0.0 | 2.6 | 0.8 | 171.4 | 4.4 | 169.5 | 5.0 | 143.4 | 43.8 | 171.4 | 4.4 | NA |
| 15ATW23-Spot 220 | 275 | 96019 | 1.3 | 20.0 | 1.5 | 0.2 | 3.3 | 0.0 | 3.0 | 0.9 | 171.7 | 5.0 | 173.2 | 5.3 | 194.6 | 34.5 | 171.7 | 5.0 | NA |
| 15ATW23-Spot 105 | 523 | 178597 | 1.2 | 20.0 | 1.2 | 0.2 | 3.6 | 0.0 | 3.4 | 0.9 | 172.1 | 5.7 | 173.5 | 5.7 | 193.1 | 28.4 | 172.1 | 5.7 | NA |
| 15ATW23-Spot 104 | 728 | 1208830 | 2.3 | 20.2 | 1.0 | 0.2 | 3.0 | 0.0 | 2.9 | 0.9 | 172.8 | 4.9 | 172.8 | 4.8 | 173.9 | 22.3 | 172.8 | 4.9 | NA |
| 15ATW23-Spot 106 | 172 | 239990 | 1.9 | 18.4 | 2.8 | 0.2 | 3.4 | 0.0 | 1.9 | 0.6 | 173.3 | 3.3 | 189.0 | 5.8 | 391.4 | 62.0 | 173.3 | 3.3 | NA |
| 15ATW23-Spot 148 | 238 | 1462636 | 1.3 | 20.2 | 1.2 | 0.2 | 3.6 | 0.0 | 3.4 | 0.9 | 174.1 | 5.9 | 174.2 | 5.8 | 176.0 | 28.2 | 174.1 | 5.9 | NA |
| 15ATW23-Spot 15 | 172 | 19520 | 3.2 | 19.3 | 3.1 | 0.2 | 3.9 | 0.0 | 2.3 | 0.6 | 175.0 | 4.0 | 182.0 | 6.5 | 274.9 | 71.5 | 175.0 | 4.0 | NA |
| 15ATW23-Spot 299 | 162 | 76541 | 3.3 | 20.4 | 1.8 | 0.2 | 3.6 | 0.0 | 3.1 | 0.9 | 175.7 | 5.4 | 174.2 | 5.8 | 154.2 | 42.6 | 175.7 | 5.4 | NA |
| 15ATW23-Spot 6 | 265 | 468413 | 4.7 | 20.2 | 1.6 | 0.2 | 3.3 | 0.0 | 2.9 | 0.9 | 176.2 | 5.0 | 175.5 | 5.3 | 167.3 | 37.4 | 176.2 | 5.0 | NA |
| 15ATW23-Spot 307 | 421 | 89527 | 2.7 | 20.5 | 1.3 | 0.2 | 2.6 | 0.0 | 2.3 | 0.9 | 177.2 | 4.0 | 174.7 | 4.2 | 142.5 | 29.9 | 177.2 | 4.0 | NA |
| 15ATW23-Spot 112 | 375 | 119527 | 2.4 | 20.3 | 1.3 | 0.2 | 2.6 | 0.0 | 2.2 | 0.9 | 178.8 | 3.9 | 177.6 | 4.2 | 162.5 | 31.2 | 178.8 | 3.9 | NA |
| 15ATW23-Spot 119 | 558 | 1342202 | 4.9 | 19.9 | 1.2 | 0.2 | 2.9 | 0.0 | 2.7 | 0.9 | 180.3 | 4.7 | 182.4 | 4.9 | 210.0 | 28.3 | 180.3 | 4.7 | NA |
| 15ATW23-Spot 171 | 183 | 67882 | 3.1 | 20.1 | 1.8 | 0.2 | 3.1 | 0.0 | 2.6 | 0.8 | 182.4 | 4.6 | 182.1 | 5.2 | 179.1 | 41.7 | 182.4 | 4.6 | NA |
| 15ATW23-Spot 111 | 1227 | 218088 | 2.6 | 20.2 | 1.0 | 0.2 | 2.9 | 0.0 | 2.7 | 0.9 | 182.5 | 4.8 | 181.7 | 4.8 | 171.8 | 24.2 | 182.5 | 4.8 | NA |
| 15ATW23-Spot 280 | 103 | 49837 | 3.3 | 20.3 | 1.8 | 0.2 | 4.1 | 0.0 | 3.7 | 0.9 | 184.0 | 6.6 | 181.9 | 6.8 | 156.3 | 41.6 | 184.0 | 6.6 | NA |
| 15ATW23-Spot 102 | 133 | 31711 | 2.0 | 20.0 | 1.5 | 0.2 | 3.5 | 0.0 | 3.1 | 0.9 | 184.4 | 5.7 | 184.9 | 5.9 | 192.8 | 35.0 | 184.4 | 5.7 | NA |
| 15ATW23-Spot 240 | 1021 | 1438231 | 2.1 | 19.7 | 1.1 | 0.2 | 2.9 | 0.0 | 2.6 | 0.9 | 184.6 | 4.8 | 187.8 | 4.9 | 228.6 | 26.4 | 184.6 | 4.8 | NA |
| 15ATW23-Spot 161 | 342 | 177585 | 1.6 | 19.6 | 1.5 | 0.2 | 2.8 | 0.0 | 2.4 | 0.9 | 185.8 | 4.4 | 190.0 | 4.9 | 243.5 | 33.5 | 185.8 | 4.4 | NA |
| 15ATW23-Spot 255 | 380 | 135961 | 1.7 | 19.9 | 1.3 | 0.2 | 2.8 | 0.0 | 2.5 | 0.9 | 185.9 | 4.5 | 186.9 | 4.7 | 201.2 | 29.1 | 185.9 | 4.5 | NA |
| 15ATW23-Spot 212 | 377 | 63681 | 1.8 | 19.1 | 2.0 | 0.2 | 3.3 | 0.0 | 2.6 | 0.8 | 186.7 | 4.9 | 195.4 | 5.8 | 303.1 | 44.5 | 186.7 | 4.9 | NA |
| 15ATW23-Spot 184 | 472 | 3141542 | 1.5 | 20.5 | 1.2 | 0.2 | 3.0 | 0.0 | 2.7 | 0.9 | 187.2 | 5.0 | 183.6 | 5.0 | 139.3 | 28.9 | 187.2 | 5.0 | NA |
| 15ATW23-Spot 295 | 257 | 47547 | 2.3 | 20.0 | 1.4 | 0.2 | 3.1 | 0.0 | 2.8 | 0.9 | 187.2 | 5.1 | 188.0 | 5.4 | 198.6 | 33.4 | 187.2 | 5.1 | NA |
| 15ATW23-Spot 210 | 245 | 254582 | 2.5 | 20.0 | 1.5 | 0.2 | 3.0 | 0.0 | 2.6 | 0.9 | 187.6 | 4.7 | 188.4 | 5.1 | 199.9 | 34.1 | 187.6 | 4.7 | NA |
| 15ATW23-Spot 100 | 318 | 98531 | 2.2 | 19.9 | 1.3 | 0.2 | 3.2 | 0.0 | 2.9 | 0.9 | 187.9 | 5.4 | 189.4 | 5.5 | 208.0 | 30.8 | 187.9 | 5.4 | NA |

| | | | | | | | | | | | | | | | | | | | |
|---|---|---|---|---|---|---|---|---|---|---|---|---|---|---|---|---|---|---|---|
| 15ATW23-Spot 253 | 211 | 34067 | 2.8 | 19.6 | 1.8 | 0.2 | 3.5 | 0.0 | 3.0 | 0.9 | 188.0 | 5.6 | 191.6 | 6.1 | 237.0 | 41.1 | 188.0 | 5.6 | NA |
| 15ATW23-Spot 109 | 154 | 56104 | 2.6 | 19.8 | 1.4 | 0.2 | 2.7 | 0.0 | 2.3 | 0.9 | 188.7 | 4.2 | 191.1 | 4.6 | 222.2 | 32.0 | 188.7 | 4.2 | NA |
| 15ATW23-Spot 24 | 376 | 447862 | 1.1 | 20.2 | 1.5 | 0.2 | 3.4 | 0.0 | 3.0 | 0.9 | 188.8 | 5.6 | 187.6 | 5.8 | 173.2 | 35.8 | 188.8 | 5.6 | NA |
| 15ATW23-Spot 174 | 227 | 174623 | 1.7 | 19.7 | 1.7 | 0.2 | 3.2 | 0.0 | 2.7 | 0.8 | 189.0 | 4.9 | 191.7 | 5.5 | 225.3 | 39.5 | 189.0 | 4.9 | NA |
| 15ATW23-Spot 289 | 171 | 61572 | 3.1 | 20.2 | 1.5 | 0.2 | 3.2 | 0.0 | 2.8 | 0.9 | 189.7 | 5.2 | 187.9 | 5.5 | 166.1 | 35.4 | 189.7 | 5.2 | NA |
| 15ATW23-Spot 46 | 163 | 31930 | 1.9 | 19.9 | 1.7 | 0.2 | 3.2 | 0.0 | 2.7 | 0.8 | 189.7 | 5.0 | 190.7 | 5.5 | 203.7 | 39.3 | 189.7 | 5.0 | NA |
| 15ATW23-Spot 176 | 196 | 47704 | 2.6 | 18.0 | 2.9 | 0.2 | 3.7 | 0.0 | 2.4 | 0.6 | 189.9 | 4.4 | 208.8 | 7.0 | 429.0 | 63.6 | 189.9 | 4.4 | NA |
| 15ATW23-Spot 11 | 342 | 84530 | 2.2 | 20.0 | 1.1 | 0.2 | 3.1 | 0.0 | 2.9 | 0.9 | 190.0 | 5.4 | 190.7 | 5.4 | 200.6 | 26.2 | 190.0 | 5.4 | NA |
| 15ATW23-Spot 182 | 253 | 109170 | 1.7 | 20.1 | 1.5 | 0.2 | 2.6 | 0.0 | 2.2 | 0.8 | 190.0 | 4.0 | 189.5 | 4.5 | 183.6 | 34.3 | 190.0 | 4.0 | NA |
| 15ATW23-Spot 183 | 835 | 141084 | 1.5 | 20.1 | 1.0 | 0.2 | 3.5 | 0.0 | 3.3 | 1.0 | 190.5 | 6.3 | 190.0 | 6.0 | 185.1 | 23.5 | 190.5 | 6.3 | NA |
| 15ATW23-Spot 114 | 636 | 519323 | 2.6 | 19.9 | 1.1 | 0.2 | 3.0 | 0.0 | 2.8 | 0.9 | 190.6 | 5.2 | 191.5 | 5.3 | 203.1 | 26.6 | 190.6 | 5.2 | NA |
| 15ATW23-Spot 3 | 366 | 62888 | 2.7 | 20.4 | 1.2 | 0.2 | 2.9 | 0.0 | 2.6 | 0.9 | 190.6 | 4.9 | 187.4 | 4.9 | 147.4 | 27.5 | 190.6 | 4.9 | NA |
| 15ATW23-Spot 170 | 2060 | 164685 | 2.4 | 20.1 | 1.0 | 0.2 | 2.7 | 0.0 | 2.5 | 0.9 | 190.7 | 4.6 | 190.3 | 4.7 | 186.6 | 24.0 | 190.7 | 4.6 | NA |
| 15ATW23-Spot 167 | 483 | 61536 | 1.8 | 19.8 | 1.4 | 0.2 | 2.9 | 0.0 | 2.5 | 0.9 | 191.0 | 4.8 | 192.7 | 5.1 | 214.8 | 31.5 | 191.0 | 4.8 | NA |
| 15ATW23-Spot 290 | 102 | 17553 | 2.4 | 19.8 | 1.6 | 0.2 | 3.0 | 0.0 | 2.5 | 0.8 | 191.1 | 4.7 | 192.9 | 5.2 | 216.0 | 37.7 | 191.1 | 4.7 | NA |
| 15ATW23-Spot 124 | 950 | 123418 | 1.8 | 19.6 | 1.0 | 0.2 | 3.0 | 0.0 | 2.8 | 0.9 | 191.2 | 5.3 | 194.9 | 5.3 | 241.1 | 22.3 | 191.2 | 5.3 | NA |
| 15ATW23-Spot 200 | 220 | 56379 | 1.9 | 19.0 | 1.5 | 0.2 | 3.4 | 0.0 | 3.1 | 0.9 | 191.4 | 5.8 | 200.5 | 6.2 | 309.6 | 34.9 | 191.4 | 5.8 | NA |
| 15ATW23-Spot 181 | 394 | 202071 | 1.6 | 19.5 | 1.2 | 0.2 | 2.8 | 0.0 | 2.5 | 0.9 | 191.5 | 4.8 | 196.2 | 5.0 | 254.7 | 28.6 | 191.5 | 4.8 | NA |
| 15ATW23-Spot 35 | 150 | 122785 | 2.4 | 20.2 | 1.4 | 0.2 | 3.2 | 0.0 | 2.8 | 0.9 | 191.7 | 5.3 | 189.9 | 5.5 | 168.9 | 33.5 | 191.7 | 5.3 | NA |
| 15ATW23-Spot 129 | 233 | 70332 | 2.3 | 19.8 | 1.6 | 0.2 | 3.0 | 0.0 | 2.5 | 0.8 | 193.3 | 4.8 | 195.4 | 5.4 | 221.2 | 37.6 | 193.3 | 4.8 | NA |
| 15ATW23-Spot 131 | 793 | 425544 | 2.7 | 19.8 | 0.9 | 0.2 | 2.6 | 0.0 | 2.5 | 0.9 | 193.4 | 4.7 | 195.4 | 4.6 | 221.0 | 20.1 | 193.4 | 4.7 | NA |
| 15ATW23-Spot 224 | 210 | 92460 | 2.4 | 20.1 | 1.4 | 0.2 | 2.6 | 0.0 | 2.3 | 0.9 | 193.6 | 4.3 | 192.8 | 4.6 | 183.7 | 32.3 | 193.6 | 4.3 | NA |
| 15ATW23-Spot 141 | 860 | 198415 | 1.8 | 19.8 | 1.4 | 0.2 | 2.9 | 0.0 | 2.6 | 0.9 | 194.0 | 4.9 | 196.1 | 5.2 | 222.1 | 31.7 | 194.0 | 4.9 | NA |
| 15ATW23-Spot 292 | 249 | 105815 | 1.6 | 20.2 | 1.2 | 0.2 | 3.2 | 0.0 | 2.9 | 0.9 | 194.9 | 5.6 | 192.7 | 5.6 | 167.0 | 28.0 | 194.9 | 5.6 | NA |
| 15ATW23-Spot 22 | 432 | 102365 | 2.3 | 20.2 | 1.1 | 0.2 | 2.9 | 0.0 | 2.7 | 0.9 | 196.7 | 5.3 | 194.7 | 5.2 | 172.1 | 25.5 | 196.7 | 5.3 | NA |
| 15ATW23-Spot 283 | 219 | 87460 | 2.5 | 20.1 | 1.4 | 0.2 | 2.8 | 0.0 | 2.4 | 0.9 | 196.7 | 4.6 | 195.6 | 4.9 | 183.5 | 33.2 | 196.7 | 4.6 | NA |
| 15ATW23-Spot 71 | 265 | 50837 | 3.0 | 20.1 | 1.3 | 0.2 | 2.6 | 0.0 | 2.2 | 0.9 | 197.0 | 4.4 | 196.3 | 4.6 | 188.2 | 30.3 | 197.0 | 4.4 | NA |
| 15ATW23-Spot 232 | 246 | 48917 | 3.0 | 19.9 | 1.5 | 0.2 | 2.8 | 0.0 | 2.4 | 0.9 | 197.1 | 4.6 | 197.9 | 5.0 | 208.5 | 34.2 | 197.1 | 4.6 | NA |
| 15ATW23-Spot 179 | 343 | 141230 | 3.5 | 19.5 | 1.0 | 0.2 | 2.9 | 0.0 | 2.7 | 0.9 | 198.1 | 5.3 | 202.0 | 5.3 | 248.6 | 23.7 | 198.1 | 5.3 | NA |
| 15ATW23-Spot 36 | 1104 | 736841 | 3.6 | 19.9 | 1.1 | 0.2 | 2.9 | 0.0 | 2.6 | 0.9 | 199.0 | 5.2 | 199.4 | 5.2 | 205.9 | 26.6 | 199.0 | 5.2 | NA |
| 15ATW23-Spot 188 | 173 | 1490106 | 2.3 | 19.9 | 1.5 | 0.2 | 2.6 | 0.0 | 2.2 | 0.8 | 199.5 | 4.2 | 200.2 | 4.7 | 209.8 | 33.8 | 199.5 | 4.2 | NA |
| 15ATW23-Spot 23 | 450 | 1097708 | 1.7 | 20.3 | 1.0 | 0.2 | 2.9 | 0.0 | 2.7 | 0.9 | 201.1 | 5.4 | 198.3 | 5.2 | 165.3 | 23.6 | 201.1 | 5.4 | NA |
| 15ATW23-Spot 159 | 214 | 378630 | 2.4 | 19.5 | 1.2 | 0.2 | 2.6 | 0.0 | 2.3 | 0.9 | 201.4 | 4.5 | 205.1 | 4.8 | 249.0 | 28.2 | 201.4 | 4.5 | NA |
| 15ATW23-Spot 264 | 202 | 59349 | 3.6 | 19.5 | 1.0 | 0.2 | 2.9 | 0.0 | 2.7 | 0.9 | 202.7 | 5.5 | 207.1 | 5.5 | 258.4 | 23.7 | 202.7 | 5.5 | NA |

| | | | | | | | | | | | | | | | | | | | |
|---|---|---|---|---|---|---|---|---|---|---|---|---|---|---|---|---|---|---|---|
| 15ATW23-Spot 236 | 273 | 49496 | 2.9 | 20.0 | 1.4 | 0.2 | 2.9 | 0.0 | 2.5 | 0.9 | 203.5 | 5.1 | 202.6 | 5.3 | 192.6 | 32.8 | 203.5 | 5.1 | NA |
| 15ATW23-Spot 130 | 123 | 35414 | 2.8 | 19.6 | 1.9 | 0.2 | 3.7 | 0.0 | 3.1 | 0.9 | 203.7 | 6.3 | 206.7 | 6.9 | 242.4 | 44.3 | 203.7 | 6.3 | NA |
| 15ATW23-Spot 192 | 241 | 68714 | 2.7 | 19.7 | 1.7 | 0.2 | 3.4 | 0.0 | 2.9 | 0.9 | 203.9 | 5.9 | 205.7 | 6.3 | 226.9 | 39.9 | 203.9 | 5.9 | NA |
| 15ATW23-Spot 134 | 242 | 22552143 | 2.0 | 19.7 | 1.6 | 0.2 | 3.6 | 0.0 | 3.3 | 0.9 | 205.0 | 6.6 | 206.6 | 6.8 | 225.7 | 36.5 | 205.0 | 6.6 | NA |
| 15ATW23-Spot 166 | 915 | 349292 | 2.3 | 19.9 | 0.8 | 0.2 | 2.4 | 0.0 | 2.2 | 0.9 | 210.1 | 4.6 | 209.4 | 4.5 | 202.5 | 19.1 | 210.1 | 4.6 | NA |
| 15ATW23-Spot 294 | 569 | 381864 | 2.9 | 18.2 | 1.0 | 0.5 | 2.5 | 0.1 | 2.3 | 0.9 | 425.3 | 9.6 | 423.4 | 8.8 | 413.9 | 22.3 | 425.3 | 9.6 | 102.7 |
| 15ATW23-Spot 269 | 451 | 1633801 | 1.7 | 13.0 | 0.9 | 2.0 | 2.1 | 0.2 | 1.9 | 0.9 | 1098.1 | 19.1 | 1103.2 | 14.2 | 1114.1 | 18.5 | 1114.1 | 18.5 | 98.6 |
| 15ATW23-Spot 296 | 120 | 22104 | 2.1 | 14.7 | 4.0 | 0.2 | 4.8 | 0.0 | 2.6 | 0.5 | 156.3 | 4.0 | 210.5 | 9.2 | 871.1 | 83.9 | 156.3 | 4.0 | NA |
| 15ATW23-Spot 314 | 389 | 37184 | 1.6 | 15.7 | 4.1 | 0.2 | 5.5 | 0.0 | 3.7 | 0.7 | 159.8 | 5.8 | 201.8 | 10.1 | 726.8 | 87.5 | 159.8 | 5.8 | NA |
| 15ATW23-Spot 259 | 112 | 32123 | 2.3 | 16.2 | 4.9 | 0.2 | 8.4 | 0.0 | 6.8 | 0.8 | 160.9 | 10.8 | 197.9 | 15.1 | 666.9 | 105.7 | 160.9 | 10.8 | NA |
| 15ATW23-Spot 297 | 183 | 14118 | 1.5 | 12.3 | 5.0 | 0.3 | 6.0 | 0.0 | 3.2 | 0.5 | 163.0 | 5.2 | 255.7 | 13.5 | 1224.8 | 98.8 | 163.0 | 5.2 | NA |
| 15ATW23-Spot 231 | 142 | 29974 | 2.3 | 15.7 | 3.7 | 0.2 | 4.6 | 0.0 | 2.8 | 0.6 | 163.5 | 4.5 | 206.8 | 8.7 | 735.0 | 78.3 | 163.5 | 4.5 | NA |
| 15ATW23-Spot 17 | 133 | 13559 | 2.2 | 12.7 | 6.7 | 0.3 | 7.7 | 0.0 | 3.8 | 0.5 | 165.8 | 6.2 | 252.3 | 17.2 | 1160.9 | 133.2 | 165.8 | 6.2 | NA |
| 15ATW23-Spot 278 | 86 | 10912 | 2.2 | 9.5 | 9.7 | 0.4 | 10.2 | 0.0 | 3.3 | 0.3 | 169.0 | 5.5 | 330.3 | 28.9 | 1715.2 | 178.5 | 169.0 | 5.5 | NA |
| 15ATW23-Spot 12 | 111 | 56605 | 2.6 | 14.0 | 7.0 | 0.3 | 8.0 | 0.0 | 3.9 | 0.5 | 174.0 | 6.7 | 241.7 | 17.2 | 965.1 | 142.5 | 174.0 | 6.7 | NA |
| 15ATW23-Spot 305 | 127 | 18895 | 3.5 | 13.8 | 8.0 | 0.3 | 12.7 | 0.0 | 9.8 | 0.8 | 174.6 | 16.9 | 245.4 | 27.7 | 993.6 | 163.3 | 174.6 | 16.9 | NA |
| 15ATW23-Spot 223 | 334 | 44815 | 1.6 | 16.1 | 3.2 | 0.2 | 4.0 | 0.0 | 2.4 | 0.6 | 185.0 | 4.4 | 226.2 | 8.1 | 680.7 | 68.7 | 185.0 | 4.4 | NA |
| 15ATW23-Spot 238 | 170 | 35895 | 2.9 | 16.5 | 3.8 | 0.2 | 4.7 | 0.0 | 2.8 | 0.6 | 187.6 | 5.1 | 223.2 | 9.3 | 618.8 | 81.0 | 187.6 | 5.1 | NA |
| 15ATW23-Spot 194 | 420 | 262703 | 1.2 | 16.1 | 2.5 | 0.3 | 3.8 | 0.0 | 2.8 | 0.7 | 202.1 | 5.6 | 245.4 | 8.2 | 683.9 | 54.1 | 202.1 | 5.6 | NA |
| 15ATW23-Spot 58 | 61 | 7023 | 2.9 | 16.7 | 3.2 | 0.2 | 4.0 | 0.0 | 2.4 | 0.6 | 156.9 | 3.7 | 187.8 | 6.9 | 596.5 | 69.7 | 156.9 | 3.7 | NA |
| 15ATW23-Spot 276 | 124 | 150274 | 2.3 | 15.9 | 5.6 | 0.2 | 6.1 | 0.0 | 2.5 | 0.4 | 161.5 | 4.0 | 201.6 | 11.1 | 701.1 | 118.5 | 161.5 | 4.0 | NA |
| 15ATW23-Spot 313 | 169 | 79878 | 2.7 | 20.7 | 1.6 | 0.2 | 3.4 | 0.0 | 3.0 | 0.9 | 191.0 | 5.6 | 185.3 | 5.8 | 114.1 | 38.0 | 191.0 | 5.6 | NA |
| 15ATW23-Spot 26 | 337 | 57825 | 1.6 | 20.7 | 1.4 | 0.2 | 2.6 | 0.0 | 2.2 | 0.8 | 173.7 | 3.8 | 169.9 | 4.1 | 118.2 | 32.3 | 173.7 | 3.8 | NA |
| 15ATW23-Spot 90 | 61 | 10782 | 3.2 | 21.4 | 2.4 | 0.2 | 3.8 | 0.0 | 3.0 | 0.8 | 153.4 | 4.5 | 146.4 | 5.2 | 36.7 | 57.8 | 153.4 | 4.5 | NA |
| 15ATW23-Spot 268 | 95 | 92873 | 3.9 | 21.1 | 2.1 | 0.2 | 3.4 | 0.0 | 2.7 | 0.8 | 155.3 | 4.1 | 150.3 | 4.7 | 72.7 | 49.5 | 155.3 | 4.1 | NA |
| 15ATW23-Spot 150 | 55 | 13136 | 3.0 | 21.3 | 2.6 | 0.2 | 3.7 | 0.0 | 2.7 | 0.7 | 158.4 | 4.3 | 151.8 | 5.3 | 50.8 | 61.0 | 158.4 | 4.3 | NA |
| 15ATW23-Spot 288 | 26 | 4457 | 2.6 | 23.3 | 4.9 | 0.1 | 5.8 | 0.0 | 3.1 | 0.5 | 159.0 | 4.9 | 139.6 | 7.6 | NA | NA | 159.0 | 4.9 | NA |
| 15ATW23-Spot 121 | 201 | 59930 | 1.5 | 20.9 | 1.5 | 0.2 | 2.9 | 0.0 | 2.5 | 0.9 | 159.9 | 4.0 | 155.4 | 4.2 | 89.1 | 36.4 | 159.9 | 4.0 | NA |
| 15ATW23-Spot 304 | 43 | 21099 | 3.0 | 22.0 | 3.1 | 0.2 | 4.5 | 0.0 | 3.3 | 0.7 | 160.0 | 5.1 | 148.7 | 6.2 | NA | NA | 160.0 | 5.1 | NA |
| 15ATW23-Spot 133 | 27 | 5764 | 2.9 | 22.8 | 4.0 | 0.2 | 4.8 | 0.0 | 2.7 | 0.6 | 161.3 | 4.3 | 144.9 | 6.5 | NA | NA | 161.3 | 4.3 | NA |
| 15ATW23-Spot 87 | 152 | 20633 | 2.6 | 21.3 | 1.8 | 0.2 | 2.9 | 0.0 | 2.3 | 0.8 | 162.4 | 3.8 | 155.3 | 4.2 | 50.4 | 42.6 | 162.4 | 3.8 | NA |
| 15ATW23-Spot 277 | 117 | 25597 | 3.6 | 21.3 | 2.6 | 0.2 | 3.8 | 0.0 | 2.8 | 0.7 | 164.0 | 4.5 | 156.8 | 5.5 | 50.8 | 61.9 | 164.0 | 4.5 | NA |
| 15ATW23-Spot 273 | 157 | 1956300 | 1.7 | 20.8 | 1.7 | 0.2 | 3.2 | 0.0 | 2.7 | 0.9 | 164.2 | 4.4 | 159.9 | 4.8 | 98.2 | 39.6 | 164.2 | 4.4 | NA |
| 15ATW23-Spot 242 | 164 | 20306 | 2.4 | 21.0 | 1.8 | 0.2 | 3.0 | 0.0 | 2.5 | 0.8 | 171.0 | 4.2 | 164.9 | 4.6 | 79.2 | 42.2 | 171.0 | 4.2 | NA |

| | | | | | | | | | | | | | | | | | | | |
|---|---|---|---|---|---|---|---|---|---|---|---|---|---|---|---|---|---|---|---|
| 15ATW23-Spot 113 | 191 | 78604 | 2.7 | 20.6 | 1.3 | 0.2 | 3.2 | 0.0 | 3.0 | 0.9 | 183.1 | 5.4 | 179.3 | 5.3 | 129.6 | 29.6 | 183.1 | 5.4 | NA |
| 15ATW23-Spot 279 | 168 | 80789 | 1.8 | 20.7 | 1.6 | 0.2 | 3.0 | 0.0 | 2.6 | 0.8 | 189.1 | 4.8 | 183.4 | 5.1 | 111.7 | 38.0 | 189.1 | 4.8 | NA |
| 15ATW23-Spot 189 | 258 | 315998 | 5.4 | 20.7 | 1.7 | 0.2 | 3.4 | 0.0 | 2.9 | 0.9 | 210.4 | 6.1 | 202.7 | 6.2 | 114.8 | 40.0 | 210.4 | 6.1 | NA |

Sample 15ATW29

| Analysis | U | 206Pb | U/Th | 206Pb * | ± | 207Pb * | ± | 206Pb * | ± | erro r | 206Pb * | ± | 207Pb * | ± | 206Pb * | ± | Best age | ± | Conc |
|---|---|---|---|---|---|---|---|---|---|---|---|---|---|---|---|---|---|---|---|
| | (ppm) | 204Pb | | 207Pb * | (%) | 235U * | (%) | 238U | (%) | corr . | 238U * | (Ma) | 235U | (Ma) | 207Pb * | (Ma) | (Ma) | (Ma) | (%) |
| Roeske 15ATW29A 8Mar16-Sample 1 Spot 42 | 119 | 2016 | 4.7 | 22.3 | 5.3 | 0.1 | 5.9 | 0.0 | 2.7 | 0.5 | 83.0 | 2.2 | 78.2 | 4.5 | 65.0 | 129.1 | 83.0 | 2.2 | NA |
| Roeske 15ATW29A 8Mar16-Sample 1 Spot 60 | 355 | 10123 | 2.0 | 20.5 | 1.8 | 0.1 | 2.6 | 0.0 | 1.9 | 0.7 | 84.2 | 1.6 | 85.9 | 2.2 | 133.0 | 41.8 | 84.2 | 1.6 | NA |
| Roeske 15ATW-29 3-7-2017-Spot 165 | 184 | 12332 | 1.5 | 19.6 | 2.9 | 0.1 | 3.6 | 0.0 | 2.2 | 0.6 | 84.4 | 1.8 | 89.8 | 3.1 | 237.3 | 66.8 | 84.4 | 1.8 | NA |
| Roeske 15ATW32 8Mar16-Spot 9 | 378 | 6051 | 1.9 | 21.3 | 2.1 | 0.1 | 3.3 | 0.0 | 2.5 | 0.8 | 84.6 | 2.1 | 83.3 | 2.6 | 46.9 | 50.3 | 84.6 | 2.1 | NA |
| Roeske 15ATW29A 8Mar16-Sample 1 Spot 5 | 312 | 17826 | 1.7 | 20.8 | 1.3 | 0.1 | 2.9 | 0.0 | 2.5 | 0.9 | 84.8 | 2.1 | 85.2 | 2.3 | 97.7 | 31.7 | 84.8 | 2.1 | NA |
| Roeske 15ATW32 8Mar16-Spot 51 | 429 | 284569 | 1.1 | 20.7 | 1.4 | 0.1 | 2.7 | 0.0 | 2.3 | 0.9 | 84.8 | 2.0 | 86.0 | 2.3 | 118.9 | 33.8 | 84.8 | 2.0 | NA |
| Roeske 15ATW29A 8Mar16-Sample 1 Spot 43 | 199 | 3937 | 2.3 | 20.4 | 1.3 | 0.1 | 3.1 | 0.0 | 2.8 | 0.9 | 84.8 | 2.3 | 87.1 | 2.6 | 150.5 | 31.2 | 84.8 | 2.3 | NA |
| Roeske 15ATW32 8Mar16-Spot 29 | 3031 | 62388 | 0.7 | 20.5 | 0.7 | 0.1 | 1.6 | 0.0 | 1.5 | 0.9 | 84.9 | 1.2 | 86.8 | 1.3 | 140.2 | 15.4 | 84.9 | 1.2 | NA |
| Roeske 15ATW-29 3-7-2017-Spot 179 | 160 | 112938 | 1.6 | 20.3 | 3.1 | 0.1 | 4.2 | 0.0 | 2.9 | 0.7 | 85.0 | 2.4 | 87.7 | 3.5 | 165.0 | 71.6 | 85.0 | 2.4 | NA |
| Roeske 15ATW-29 3-7-2017-Spot 216 | 330 | 94123 | 0.9 | 20.4 | 1.7 | 0.1 | 3.2 | 0.0 | 2.6 | 0.8 | 85.2 | 2.2 | 87.3 | 2.6 | 146.7 | 41.0 | 85.2 | 2.2 | NA |
| Roeske 15ATW32 8Mar16-Spot 23 | 793 | 83766 | 4.0 | 20.4 | 1.1 | 0.1 | 2.1 | 0.0 | 1.8 | 0.9 | 85.3 | 1.5 | 87.5 | 1.8 | 148.6 | 24.8 | 85.3 | 1.5 | NA |
| Roeske 15ATW29A 8Mar16-Sample 1 Spot 36 | 174 | 53387 | 3.4 | 19.8 | 2.0 | 0.1 | 3.5 | 0.0 | 2.9 | 0.8 | 85.7 | 2.5 | 90.4 | 3.1 | 216.1 | 45.5 | 85.7 | 2.5 | NA |
| Roeske 15ATW-29 3-7-2017-Spot 246 | 263 | 26828 | 1.2 | 21.1 | 2.8 | 0.1 | 5.0 | 0.0 | 4.1 | 0.8 | 85.8 | 3.5 | 85.3 | 4.1 | 72.7 | 66.3 | 85.8 | 3.5 | NA |
| Roeske 15ATW-29 3-7-2017-Spot 69 | 214 | 44940 | 2.1 | 20.2 | 2.1 | 0.1 | 3.6 | 0.0 | 2.9 | 0.8 | 85.9 | 2.5 | 88.7 | 3.0 | 166.4 | 50.0 | 85.9 | 2.5 | NA |
| Roeske 15ATW29A 8Mar16-Sample 1 Spot 50 | 222 | 9726 | 2.7 | 20.5 | 1.6 | 0.1 | 2.4 | 0.0 | 1.8 | 0.8 | 85.9 | 1.6 | 87.7 | 2.0 | 136.0 | 36.5 | 85.9 | 1.6 | NA |
| Roeske 15ATW29A 8Mar16-Sample 1 Spot 16 | 399 | 12788 | 0.9 | 20.7 | 1.3 | 0.1 | 2.2 | 0.0 | 1.8 | 0.8 | 86.0 | 1.6 | 86.9 | 1.8 | 113.3 | 29.9 | 86.0 | 1.6 | NA |
| Roeske 15ATW-29 3-7-2017-Spot 46 | 238 | 8789 | 1.5 | 21.3 | 2.4 | 0.1 | 3.3 | 0.0 | 2.2 | 0.7 | 86.0 | 1.9 | 84.4 | 2.7 | 41.1 | 58.2 | 86.0 | 1.9 | NA |
| Roeske 15ATW-29 3-7-2017-Spot 156 | 75 | 5328 | 1.8 | 20.1 | 3.3 | 0.1 | 4.8 | 0.0 | 3.5 | 0.7 | 86.3 | 3.0 | 89.7 | 4.1 | 181.0 | 75.8 | 86.3 | 3.0 | NA |
| Roeske 15ATW-29 3-7-2017-Spot 196 | 91 | 185575 | 2.8 | 20.1 | 3.9 | 0.1 | 4.9 | 0.0 | 3.0 | 0.6 | 86.4 | 2.6 | 89.9 | 4.2 | 186.8 | 90.4 | 86.4 | 2.6 | NA |
| Roeske 15ATW29A 8Mar16-Sample 1 Spot 45 | 253 | 9251 | 2.6 | 20.6 | 2.0 | 0.1 | 3.1 | 0.0 | 2.4 | 0.8 | 86.5 | 2.1 | 87.8 | 2.6 | 122.3 | 47.0 | 86.5 | 2.1 | NA |
| Roeske 15ATW-29 3-7-2017-Spot 302 | 240 | 76472 | 1.7 | 19.6 | 2.1 | 0.1 | 3.7 | 0.0 | 3.1 | 0.8 | 86.6 | 2.6 | 92.4 | 3.3 | 247.6 | 47.8 | 86.6 | 2.6 | NA |
| Roeske 15ATW-29 3-7-2017-Spot 177 | 1282 | 98980 | 1.1 | 20.7 | 1.1 | 0.1 | 2.1 | 0.0 | 1.8 | 0.9 | 86.8 | 1.6 | 87.7 | 1.8 | 113.7 | 26.4 | 86.8 | 1.6 | NA |
| Roeske 15ATW-29 3-7-2017-Spot 220 | 316 | 27890 | 2.2 | 20.6 | 2.2 | 0.1 | 3.4 | 0.0 | 2.6 | 0.8 | 86.8 | 2.3 | 88.2 | 2.9 | 127.4 | 51.6 | 86.8 | 2.3 | NA |
| Roeske 15ATW-29 3-7-2017-Spot 67 | 85 | 4842 | 2.3 | 20.8 | 4.0 | 0.1 | 4.8 | 0.0 | 2.7 | 0.6 | 86.8 | 2.3 | 87.4 | 4.0 | 105.6 | 93.6 | 86.8 | 2.3 | NA |
| Roeske 15ATW-29 3-7-2017-Spot 110 | 398 | 798544253 | 1.1 | 20.6 | 1.6 | 0.1 | 2.6 | 0.0 | 2.0 | 0.8 | 86.8 | 1.7 | 88.3 | 2.2 | 129.6 | 37.9 | 86.8 | 1.7 | NA |
| Roeske 15ATW-29 3-7-2017-Spot 211 | 180 | 171366 | 1.3 | 19.9 | 2.3 | 0.1 | 3.9 | 0.0 | 3.1 | 0.8 | 86.9 | 2.7 | 91.4 | 3.4 | 209.8 | 52.9 | 86.9 | 2.7 | NA |
| Roeske 15ATW-29 3-7-2017-Spot 137 | 637 | 177031 | 0.7 | 19.9 | 1.8 | 0.1 | 3.2 | 0.0 | 2.7 | 0.8 | 86.9 | 2.3 | 91.3 | 2.8 | 206.8 | 40.8 | 86.9 | 2.3 | NA |
| Roeske 15ATW-29 3-7-2017-Spot 138 | 264 | 30415 | 1.3 | 20.2 | 1.8 | 0.1 | 3.2 | 0.0 | 2.6 | 0.8 | 87.0 | 2.3 | 90.1 | 2.8 | 174.3 | 43.1 | 87.0 | 2.3 | NA |
| Roeske 15ATW-29 3-7-2017-Spot 223 | 154 | 26900 | 1.3 | 20.7 | 2.6 | 0.1 | 3.4 | 0.0 | 2.2 | 0.7 | 87.1 | 1.9 | 87.9 | 2.9 | 111.6 | 60.7 | 87.1 | 1.9 | NA |
| Roeske 15ATW-29 3-7-2017-Spot 219 | 742 | 56928 | 1.1 | 20.8 | 1.1 | 0.1 | 2.8 | 0.0 | 2.6 | 0.9 | 87.1 | 2.2 | 87.5 | 2.4 | 99.2 | 26.4 | 87.1 | 2.2 | NA |
| Roeske 15ATW29A 8Mar16-Sample 1 Spot 61 | 324 | 56676 | 1.9 | 19.8 | 1.6 | 0.1 | 2.5 | 0.0 | 1.9 | 0.8 | 87.2 | 1.7 | 91.9 | 2.2 | 215.4 | 37.0 | 87.2 | 1.7 | NA |
| Roeske 15ATW29A 8Mar16-Sample 1 Spot 55 | 129 | 30784 | 2.7 | 19.6 | 2.7 | 0.1 | 3.9 | 0.0 | 2.8 | 0.7 | 87.3 | 2.4 | 93.2 | 3.5 | 247.0 | 62.2 | 87.3 | 2.4 | NA |

| | | | | | | | | | | | | | | | | | | | |
|---|---|---|---|---|---|---|---|---|---|---|---|---|---|---|---|---|---|---|---|
| Roeske 15ATW-29 3-7-2017-Spot 28 | 157 | 16836 | 1.2 | 20.2 | 2.3 | 0.1 | 3.4 | 0.0 | 2.5 | 0.7 | 87.4 | 2.2 | 90.3 | 3.0 | 169.2 | 54.2 | 87.4 | 2.2 | NA |
| Roeske 15ATW-29 3-7-2017-Spot 71 | 119 | 11717 | 1.9 | 20.5 | 2.3 | 0.1 | 3.4 | 0.0 | 2.5 | 0.7 | 87.4 | 2.2 | 89.2 | 2.9 | 137.5 | 55.1 | 87.4 | 2.2 | NA |
| Roeske 15ATW32 8Mar16-Spot 10 | 976 | 51623 | 2.4 | 20.8 | 1.0 | 0.1 | 2.2 | 0.0 | 2.0 | 0.9 | 87.4 | 1.7 | 88.1 | 1.8 | 107.4 | 23.0 | 87.4 | 1.7 | NA |
| Roeske 15ATW-29 3-7-2017-Spot 253 | 151 | 6126 | 2.1 | 21.3 | 2.4 | 0.1 | 3.4 | 0.0 | 2.5 | 0.7 | 87.6 | 2.2 | 86.2 | 2.8 | 47.3 | 56.3 | 87.6 | 2.2 | NA |
| Roeske 15ATW-29 3-7-2017-Spot 263 | 83 | 13820 | 4.1 | 19.5 | 3.5 | 0.1 | 4.5 | 0.0 | 2.7 | 0.6 | 87.6 | 2.4 | 93.9 | 4.0 | 258.0 | 81.6 | 87.6 | 2.4 | NA |
| Roeske 15ATW29A 8Mar16-Sample 1 Spot 6 | 367 | 15781 | 1.1 | 19.7 | 1.1 | 0.1 | 2.4 | 0.0 | 2.1 | 0.9 | 87.7 | 1.8 | 92.9 | 2.1 | 230.8 | 26.2 | 87.7 | 1.8 | NA |
| Roeske 15ATW-29 3-7-2017-Spot 117 | 265 | 44143 | 1.2 | 20.6 | 2.1 | 0.1 | 3.6 | 0.0 | 2.9 | 0.8 | 87.7 | 2.6 | 89.1 | 3.1 | 129.4 | 49.7 | 87.7 | 2.6 | NA |
| Roeske 15ATW-29 3-7-2017-Spot 120 | 184 | 69389 | 1.8 | 20.9 | 2.3 | 0.1 | 3.2 | 0.0 | 2.3 | 0.7 | 87.7 | 2.0 | 88.0 | 2.7 | 96.2 | 54.3 | 87.7 | 2.0 | NA |
| Roeske 15ATW-29 3-7-2017-Spot 134 | 234 | 2461899 | 2.4 | 19.5 | 2.6 | 0.1 | 3.9 | 0.0 | 2.9 | 0.7 | 87.8 | 2.6 | 93.7 | 3.5 | 248.3 | 60.3 | 87.8 | 2.6 | NA |
| Roeske 15ATW-29 3-7-2017-Spot 55 | 115 | 5396 | 2.1 | 20.9 | 3.9 | 0.1 | 5.2 | 0.0 | 3.3 | 0.6 | 87.8 | 2.9 | 87.9 | 4.3 | 91.8 | 93.5 | 87.8 | 2.9 | NA |
| Roeske 15ATW-29 3-7-2017-Spot 127 | 61 | 11424 | 2.4 | 21.5 | 4.1 | 0.1 | 5.0 | 0.0 | 2.9 | 0.6 | 87.9 | 2.5 | 85.8 | 4.1 | 28.8 | 98.4 | 87.9 | 2.5 | NA |
| Roeske 15ATW-29 3-7-2017-Spot 148 | 179 | 16033 | 1.4 | 21.2 | 2.1 | 0.1 | 3.5 | 0.0 | 2.8 | 0.8 | 88.0 | 2.5 | 87.0 | 2.9 | 62.4 | 51.1 | 88.0 | 2.5 | NA |
| Roeske 15ATW29A 8Mar16-Sample 1 Spot 39 | 907 | 50295 | 3.0 | 20.4 | 1.0 | 0.1 | 1.9 | 0.0 | 1.6 | 0.8 | 88.0 | 1.4 | 90.0 | 1.7 | 143.7 | 24.0 | 88.0 | 1.4 | NA |
| Roeske 15ATW-29 3-7-2017-Spot 16 | 1221 | 76331 | 1.0 | 20.9 | 1.1 | 0.1 | 2.6 | 0.0 | 2.4 | 0.9 | 88.0 | 2.1 | 88.2 | 2.2 | 94.1 | 25.9 | 88.0 | 2.1 | NA |
| Roeske 15ATW-29 3-7-2017-Spot 159 | 406 | 72894 | 1.1 | 20.9 | 1.4 | 0.1 | 2.8 | 0.0 | 2.4 | 0.9 | 88.1 | 2.1 | 88.3 | 2.3 | 93.9 | 33.2 | 88.1 | 2.1 | NA |
| Roeske 15ATW-29 3-7-2017-Spot 130 | 80 | 56197 | 2.9 | 20.1 | 3.7 | 0.1 | 4.6 | 0.0 | 2.7 | 0.6 | 88.2 | 2.4 | 91.4 | 4.0 | 178.1 | 86.0 | 88.2 | 2.4 | NA |
| Roeske 15ATW-29 3-7-2017-Spot 193 | 70 | 20581 | 2.9 | 19.5 | 3.9 | 0.1 | 5.1 | 0.0 | 3.3 | 0.6 | 88.2 | 2.9 | 94.2 | 4.6 | 250.2 | 89.3 | 88.2 | 2.9 | NA |
| Roeske 15ATW-29 3-7-2017-Spot 210 | 1058 | 417795 | 1.1 | 20.7 | 1.1 | 0.1 | 2.7 | 0.0 | 2.5 | 0.9 | 88.2 | 2.2 | 89.2 | 2.3 | 116.8 | 25.6 | 88.2 | 2.2 | NA |
| Roeske 15ATW-29 3-7-2017-Spot 77 | 230 | 42351 | 2.1 | 21.0 | 1.8 | 0.1 | 3.1 | 0.0 | 2.6 | 0.8 | 88.2 | 2.2 | 88.1 | 2.7 | 86.0 | 43.4 | 88.2 | 2.2 | NA |
| Roeske 15ATW-29 3-7-2017-Spot 276 | 75 | 3780 | 1.9 | 21.6 | 4.0 | 0.1 | 5.2 | 0.0 | 3.3 | 0.6 | 88.2 | 2.9 | 85.7 | 4.3 | 18.7 | 96.4 | 88.2 | 2.9 | NA |
| Roeske 15ATW-29 3-7-2017-Spot 20 | 132 | 40210 | 1.2 | 20.8 | 2.6 | 0.1 | 3.9 | 0.0 | 2.9 | 0.7 | 88.3 | 2.5 | 89.0 | 3.3 | 108.7 | 62.3 | 88.3 | 2.5 | NA |
| Roeske 15ATW-29 3-7-2017-Spot 313 | 391 | 167124 | 0.7 | 20.7 | 1.9 | 0.1 | 3.0 | 0.0 | 2.4 | 0.8 | 88.3 | 2.1 | 89.3 | 2.6 | 116.6 | 45.1 | 88.3 | 2.1 | NA |
| Roeske 15ATW-29 3-7-2017-Spot 40 | 433 | 23502 | 1.5 | 20.1 | 1.7 | 0.1 | 3.2 | 0.0 | 2.7 | 0.8 | 88.3 | 2.3 | 91.9 | 2.8 | 186.7 | 40.3 | 88.3 | 2.3 | NA |
| Roeske 15ATW-29 3-7-2017-Spot 222 | 66 | 12758 | 1.6 | 19.9 | 3.2 | 0.1 | 4.2 | 0.0 | 2.8 | 0.7 | 88.3 | 2.5 | 92.6 | 3.8 | 205.7 | 73.6 | 88.3 | 2.5 | NA |
| Roeske 15ATW-29 3-7-2017-Spot 53 | 159 | 45631 | 2.2 | 19.9 | 2.6 | 0.1 | 4.0 | 0.0 | 3.1 | 0.8 | 88.4 | 2.7 | 92.7 | 3.6 | 205.3 | 59.3 | 88.4 | 2.7 | NA |
| Roeske 15ATW-29 3-7-2017-Spot 93 | 911 | 918992 | 2.4 | 20.4 | 1.3 | 0.1 | 2.7 | 0.0 | 2.4 | 0.9 | 88.4 | 2.1 | 90.6 | 2.4 | 148.4 | 31.1 | 88.4 | 2.1 | NA |
| Roeske 15ATW-29 3-7-2017-Spot 135 | 232 | 21507 | 1.4 | 20.7 | 2.1 | 0.1 | 3.3 | 0.0 | 2.6 | 0.8 | 88.4 | 2.3 | 89.1 | 2.8 | 109.5 | 48.5 | 88.4 | 2.3 | NA |
| Roeske 15ATW-29 3-7-2017-Spot 102 | 219 | 33050 | 2.0 | 20.1 | 2.2 | 0.1 | 3.4 | 0.0 | 2.6 | 0.8 | 88.4 | 2.3 | 91.8 | 3.0 | 179.9 | 50.4 | 88.4 | 2.3 | NA |
| Roeske 15ATW29A 8Mar16-Sample 1 Spot 31 | 94 | 2284 | 2.1 | 22.2 | 3.1 | 0.1 | 4.2 | 0.0 | 2.8 | 0.7 | 88.5 | 2.5 | 83.6 | 3.4 | 54.6 | 75.9 | 88.5 | 2.5 | NA |
| Roeske 15ATW-29 3-7-2017-Spot 160 | 930 | 1449806 | 1.3 | 20.8 | 1.4 | 0.1 | 3.0 | 0.0 | 2.7 | 0.9 | 88.5 | 2.3 | 89.0 | 2.6 | 102.5 | 34.1 | 88.5 | 2.3 | NA |
| Roeske 15ATW-29 3-7-2017-Spot 81 | 664 | 112424 | 1.2 | 21.4 | 1.4 | 0.1 | 3.1 | 0.0 | 2.7 | 0.9 | 88.6 | 2.4 | 86.8 | 2.5 | 40.3 | 32.8 | 88.6 | 2.4 | NA |
| Roeske 15ATW-29 3-7-2017-Spot 2 | 270 | 13860 | 1.7 | 21.2 | 1.4 | 0.1 | 3.4 | 0.0 | 3.1 | 0.9 | 88.6 | 2.7 | 87.5 | 2.9 | 57.4 | 34.3 | 88.6 | 2.7 | NA |
| Roeske 15ATW-29 3-7-2017-Spot 90 | 102 | 11642 | 1.3 | 20.3 | 2.9 | 0.1 | 3.7 | 0.0 | 2.4 | 0.6 | 88.6 | 2.1 | 91.1 | 3.3 | 157.9 | 66.9 | 88.6 | 2.1 | NA |
| Roeske 15ATW-29 3-7-2017-Spot 173 | 176 | 356242 | 3.0 | 20.4 | 2.6 | 0.1 | 3.7 | 0.0 | 2.6 | 0.7 | 88.7 | 2.3 | 90.6 | 3.2 | 143.2 | 61.1 | 88.7 | 2.3 | NA |
| Roeske 15ATW-29 3-7-2017-Spot 98 | 237 | 177696 | 1.8 | 20.8 | 2.0 | 0.1 | 3.0 | 0.0 | 2.2 | 0.7 | 88.7 | 2.0 | 89.0 | 2.5 | 99.7 | 46.6 | 88.7 | 2.0 | NA |
| Roeske 15ATW-29 3-7-2017-Spot 287 | 181 | 12292 | 2.4 | 21.0 | 2.9 | 0.1 | 4.5 | 0.0 | 3.4 | 0.8 | 88.8 | 3.0 | 88.5 | 3.8 | 83.1 | 70.0 | 88.8 | 3.0 | NA |
| Roeske 15ATW32 8Mar16-Spot 53 | 259 | 9997 | 1.7 | 20.0 | 2.2 | 0.1 | 3.4 | 0.0 | 2.6 | 0.8 | 88.9 | 2.3 | 92.8 | 3.0 | 193.7 | 51.9 | 88.9 | 2.3 | NA |
| Roeske 15ATW-29 3-7-2017-Spot 68 | 77 | 6670 | 2.3 | 21.6 | 4.0 | 0.1 | 5.2 | 0.0 | 3.3 | 0.6 | 88.9 | 2.9 | 86.1 | 4.3 | 10.0 | 96.6 | 88.9 | 2.9 | NA |
| Roeske 15ATW29A 8Mar16-Sample 1 Spot 1 | 60 | 7563 | 2.4 | 21.4 | 2.7 | 0.1 | 4.1 | 0.0 | 3.1 | 0.8 | 89.0 | 2.7 | 87.1 | 3.4 | 36.6 | 65.2 | 89.0 | 2.7 | NA |
| Roeske 15ATW-29 3-7-2017-Spot 293 | 134 | 17494 | 1.5 | 20.2 | 2.8 | 0.1 | 3.9 | 0.0 | 2.6 | 0.7 | 89.1 | 2.3 | 91.9 | 3.4 | 167.4 | 65.9 | 89.1 | 2.3 | NA |

| | | | | | | | | | | | | | | | | | | | |
|---|---|---|---|---|---|---|---|---|---|---|---|---|---|---|---|---|---|---|---|
| Roeske 15ATW-29 3-7-2017-Spot 241 | 123 | 18043 | 1.9 | 21.5 | 2.9 | 0.1 | 4.0 | 0.0 | 2.7 | 0.7 | 89.1 | 2.4 | 86.9 | 3.3 | 29.0 | 69.9 | 89.1 | 2.4 | NA |
| Roeske 15ATW-29 3-7-2017-Spot 97 | 278 | 23275 | 1.7 | 21.0 | 1.6 | 0.1 | 2.9 | 0.0 | 2.4 | 0.8 | 89.1 | 2.1 | 88.9 | 2.5 | 84.3 | 38.1 | 89.1 | 2.1 | NA |
| Roeske 15ATW-29 3-7-2017-Spot 257 | 77 | 3314 | 2.7 | 21.6 | 3.8 | 0.1 | 4.7 | 0.0 | 2.7 | 0.6 | 89.1 | 2.4 | 86.5 | 3.9 | 17.5 | 92.0 | 89.1 | 2.4 | NA |
| Roeske 15ATW-29 3-7-2017-Spot 285 | 174 | 36352 | 2.4 | 20.8 | 2.6 | 0.1 | 3.9 | 0.0 | 2.9 | 0.7 | 89.1 | 2.5 | 89.6 | 3.3 | 103.1 | 61.9 | 89.1 | 2.5 | NA |
| Roeske 15ATW-29 3-7-2017-Spot 153 | 69 | 6255 | 2.9 | 20.7 | 3.6 | 0.1 | 5.1 | 0.0 | 3.6 | 0.7 | 89.2 | 3.2 | 90.2 | 4.4 | 117.8 | 84.0 | 89.2 | 3.2 | NA |
| Roeske 15ATW-29 3-7-2017-Spot 194 | 779 | 327270 | 1.2 | 21.5 | 1.6 | 0.1 | 2.9 | 0.0 | 2.5 | 0.8 | 89.2 | 2.2 | 87.0 | 2.5 | 29.5 | 39.2 | 89.2 | 2.2 | NA |
| Roeske 15ATW-29 3-7-2017-Spot 181 | 151 | 13098 | 1.9 | 20.7 | 2.4 | 0.1 | 3.8 | 0.0 | 2.9 | 0.8 | 89.2 | 2.6 | 90.1 | 3.2 | 114.5 | 55.7 | 89.2 | 2.6 | NA |
| Roeske 15ATW-29 3-7-2017-Spot 301 | 86 | 8420 | 2.3 | 20.5 | 3.8 | 0.1 | 5.0 | 0.0 | 3.3 | 0.7 | 89.2 | 2.9 | 91.0 | 4.4 | 138.1 | 88.6 | 89.2 | 2.9 | NA |
| Roeske 15ATW-29 3-7-2017-Spot 312 | 290 | 10611 | 2.3 | 20.6 | 1.8 | 0.1 | 2.9 | 0.0 | 2.3 | 0.8 | 89.3 | 2.0 | 90.5 | 2.5 | 124.1 | 43.2 | 89.3 | 2.0 | NA |
| Roeske 15ATW-29 3-7-2017-Spot 91 | 254 | 233343 | 2.3 | 20.5 | 2.3 | 0.1 | 3.4 | 0.0 | 2.5 | 0.7 | 89.3 | 2.3 | 91.1 | 3.0 | 139.3 | 52.9 | 89.3 | 2.3 | NA |
| Roeske 15ATW-29 3-7-2017-Spot 58 | 146 | 35727 | 1.6 | 21.5 | 3.3 | 0.1 | 4.6 | 0.0 | 3.2 | 0.7 | 89.3 | 2.8 | 87.2 | 3.8 | 29.2 | 79.4 | 89.3 | 2.8 | NA |
| Roeske 15ATW-29 3-7-2017-Spot 94 | 154 | 10867 | 1.7 | 20.3 | 2.6 | 0.1 | 3.7 | 0.0 | 2.6 | 0.7 | 89.4 | 2.3 | 91.8 | 3.3 | 155.6 | 61.8 | 89.4 | 2.3 | NA |
| Roeske 15ATW-29 3-7-2017-Spot 126 | 407 | 25861 | 2.5 | 20.8 | 1.7 | 0.1 | 4.0 | 0.0 | 3.6 | 0.9 | 89.4 | 3.2 | 89.9 | 3.4 | 103.4 | 40.9 | 89.4 | 3.2 | NA |
| Roeske 15ATW-29 3-7-2017-Spot 26 | 993 | 587773 | 1.2 | 20.5 | 1.3 | 0.1 | 2.6 | 0.0 | 2.3 | 0.9 | 89.4 | 2.0 | 90.9 | 2.2 | 131.9 | 29.6 | 89.4 | 2.0 | NA |
| Roeske 15ATW-29 3-7-2017-Spot 163 | 489 | 63526 | 1.0 | 20.2 | 1.5 | 0.1 | 2.9 | 0.0 | 2.5 | 0.9 | 89.5 | 2.2 | 92.6 | 2.6 | 173.8 | 35.2 | 89.5 | 2.2 | NA |
| Roeske 15ATW-29 3-7-2017-Spot 57 | 221 | 3470203 | 1.6 | 19.5 | 1.9 | 0.1 | 3.3 | 0.0 | 2.7 | 0.8 | 89.6 | 2.4 | 96.0 | 3.0 | 258.7 | 44.2 | 89.6 | 2.4 | NA |
| Roeske 15ATW-29 3-7-2017-Spot 22 | 41 | 5592 | 4.4 | 20.6 | 4.2 | 0.1 | 5.6 | 0.0 | 3.7 | 0.7 | 89.7 | 3.3 | 90.9 | 4.9 | 123.7 | 99.1 | 89.7 | 3.3 | NA |
| Roeske 15ATW-29 3-7-2017-Spot 290 | 153 | 12045 | 1.7 | 21.8 | 2.4 | 0.1 | 3.8 | 0.0 | 3.0 | 0.8 | 89.8 | 2.6 | 86.2 | 3.1 | NA | NA | 89.8 | 2.6 | NA |
| Roeske 15ATW-29 3-7-2017-Spot 195 | 225 | 32270 | 1.3 | 21.9 | 2.0 | 0.1 | 3.2 | 0.0 | 2.5 | 0.8 | 89.8 | 2.2 | 86.0 | 2.6 | NA | NA | 89.8 | 2.2 | NA |
| Roeske 15ATW-29 3-7-2017-Spot 161 | 205 | 261004 | 1.9 | 19.8 | 3.0 | 0.1 | 4.3 | 0.0 | 3.1 | 0.7 | 89.8 | 2.7 | 94.5 | 3.9 | 216.8 | 69.4 | 89.8 | 2.7 | NA |
| Roeske 15ATW-29 3-7-2017-Spot 289 | 416 | 93372 | 1.9 | 20.6 | 1.5 | 0.1 | 2.9 | 0.0 | 2.5 | 0.9 | 89.8 | 2.3 | 91.0 | 2.6 | 123.3 | 35.8 | 89.8 | 2.3 | NA |
| Roeske 15ATW-29 3-7-2017-Spot 114 | 496 | 116551 | 1.9 | 21.1 | 1.4 | 0.1 | 3.0 | 0.0 | 2.6 | 0.9 | 89.8 | 2.3 | 88.9 | 2.5 | 65.6 | 32.6 | 89.8 | 2.3 | NA |
| Roeske 15ATW-29 3-7-2017-Spot 109 | 237 | 19800 | 1.9 | 20.6 | 1.8 | 0.1 | 3.5 | 0.0 | 3.0 | 0.9 | 89.8 | 2.6 | 91.1 | 3.0 | 123.8 | 42.3 | 89.8 | 2.6 | NA |
| Roeske 15ATW-29 3-7-2017-Spot 306 | 461 | 79362 | 1.6 | 21.1 | 1.6 | 0.1 | 3.0 | 0.0 | 2.5 | 0.8 | 89.9 | 2.2 | 89.2 | 2.5 | 71.9 | 37.7 | 89.9 | 2.2 | NA |
| Roeske 15ATW-29 3-7-2017-Spot 172 | 229 | 11829 | 1.1 | 21.0 | 2.5 | 0.1 | 3.7 | 0.0 | 2.7 | 0.7 | 89.9 | 2.4 | 89.4 | 3.1 | 75.7 | 59.6 | 89.9 | 2.4 | NA |
| Roeske 15ATW-29 3-7-2017-Spot 118 | 789 | 152305 | 2.8 | 21.1 | 1.3 | 0.1 | 2.7 | 0.0 | 2.3 | 0.9 | 89.9 | 2.0 | 89.2 | 2.3 | 70.3 | 31.8 | 89.9 | 2.0 | NA |
| Roeske 15ATW-29 3-7-2017-Spot 273 | 455 | 136375 | 2.6 | 20.4 | 1.7 | 0.1 | 3.1 | 0.0 | 2.6 | 0.8 | 89.9 | 2.3 | 91.9 | 2.7 | 144.2 | 40.7 | 89.9 | 2.3 | NA |
| Roeske 15ATW-29 3-7-2017-Spot 74 | 108 | 6051 | 1.4 | 20.1 | 2.9 | 0.1 | 3.5 | 0.0 | 2.1 | 0.6 | 90.0 | 1.9 | 93.6 | 3.2 | 188.1 | 66.6 | 90.0 | 1.9 | NA |
| Roeske 15ATW-29 3-7-2017-Spot 140 | 443 | 47224 | 2.7 | 20.5 | 1.5 | 0.1 | 2.5 | 0.0 | 2.1 | 0.8 | 90.2 | 1.8 | 92.0 | 2.2 | 140.0 | 34.9 | 90.2 | 1.8 | NA |
| Roeske 15ATW-29 3-7-2017-Spot 108 | 251 | 11510 | 2.0 | 20.8 | 2.2 | 0.1 | 3.4 | 0.0 | 2.7 | 0.8 | 90.3 | 2.4 | 90.6 | 3.0 | 99.5 | 51.4 | 90.3 | 2.4 | NA |
| Roeske 15ATW-29 3-7-2017-Spot 274 | 593 | 38282 | 1.1 | 20.8 | 1.9 | 0.1 | 3.8 | 0.0 | 3.2 | 0.9 | 90.3 | 2.9 | 90.9 | 3.3 | 108.0 | 45.3 | 90.3 | 2.9 | NA |
| Roeske 15ATW-29 3-7-2017-Spot 280 | 370 | 60644 | 1.3 | 20.9 | 2.0 | 0.1 | 3.6 | 0.0 | 2.9 | 0.8 | 90.4 | 2.6 | 90.6 | 3.1 | 97.0 | 47.8 | 90.4 | 2.6 | NA |
| Roeske 15ATW-29 3-7-2017-Spot 104 | 373 | 211816 | 2.0 | 20.8 | 1.7 | 0.1 | 3.5 | 0.0 | 3.1 | 0.9 | 90.4 | 2.7 | 90.7 | 3.0 | 98.3 | 40.1 | 90.4 | 2.7 | NA |
| Roeske 15ATW-29 3-7-2017-Spot 103 | 72 | 14495 | 1.6 | 21.5 | 3.7 | 0.1 | 5.0 | 0.0 | 3.4 | 0.7 | 90.5 | 3.0 | 87.9 | 4.2 | 21.0 | 88.5 | 90.5 | 3.0 | NA |
| Roeske 15ATW-29 3-7-2017-Spot 82 | 124 | 27945 | 2.0 | 20.3 | 2.6 | 0.1 | 4.5 | 0.0 | 3.7 | 0.8 | 90.6 | 3.3 | 93.2 | 4.0 | 163.6 | 60.3 | 90.6 | 3.3 | NA |
| Roeske 15ATW-29 3-7-2017-Spot 5 | 69 | 7125 | 2.0 | 22.0 | 3.7 | 0.1 | 5.1 | 0.0 | 3.4 | 0.7 | 90.6 | 3.1 | 86.3 | 4.2 | NA | NA | 90.6 | 3.1 | NA |
| Roeske 15ATW-29 3-7-2017-Spot 255 | 1824 | 117787 | 0.7 | 21.0 | 1.2 | 0.1 | 2.7 | 0.0 | 2.5 | 0.9 | 90.8 | 2.2 | 90.4 | 2.4 | 83.4 | 27.8 | 90.8 | 2.2 | NA |
| Roeske 15ATW-29 3-7-2017-Spot 23 | 159 | 21545 | 1.4 | 21.7 | 3.0 | 0.1 | 4.1 | 0.0 | 2.8 | 0.7 | 90.8 | 2.5 | 87.5 | 3.4 | NA | NA | 90.8 | 2.5 | NA |
| Roeske 15ATW-29 3-7-2017-Spot 235 | 122 | 7173 | 1.7 | 21.3 | 3.5 | 0.1 | 4.5 | 0.0 | 2.9 | 0.6 | 90.8 | 2.6 | 89.3 | 3.9 | 51.2 | 83.1 | 90.8 | 2.6 | NA |
| Roeske 15ATW-29 3-7-2017-Spot 295 | 100 | 18401 | 1.8 | 21.6 | 3.3 | 0.1 | 4.7 | 0.0 | 3.3 | 0.7 | 90.8 | 3.0 | 88.1 | 3.9 | 15.6 | 79.4 | 90.8 | 3.0 | NA |

| | | | | | | | | | | | | | | | | | | | |
|---|---|---|---|---|---|---|---|---|---|---|---|---|---|---|---|---|---|---|---|
| Roeske 15ATW-29 3-7-2017-Spot 34 | 153 | 28331 | 1.6 | 20.9 | 2.8 | 0.1 | 3.7 | 0.0 | 2.5 | 0.7 | 90.8 | 2.3 | 91.0 | 3.3 | 96.5 | 66.0 | 90.8 | 2.3 | NA |
| Roeske 15ATW-29 3-7-2017-Spot 21 | 131 | 11227 | 1.3 | 20.8 | 2.4 | 0.1 | 3.5 | 0.0 | 2.5 | 0.7 | 90.9 | 2.3 | 91.1 | 3.0 | 98.6 | 56.4 | 90.9 | 2.3 | NA |
| Roeske 15ATW-29 3-7-2017-Spot 307 | 178 | 63332 | 2.2 | 19.6 | 2.3 | 0.1 | 3.0 | 0.0 | 2.0 | 0.6 | 91.0 | 1.8 | 96.6 | 2.8 | 237.7 | 53.7 | 91.0 | 1.8 | NA |
| Roeske 15ATW32 8Mar16-Spot 52 | 138 | 4888 | 1.7 | 21.7 | 4.2 | 0.1 | 5.3 | 0.0 | 3.2 | 0.6 | 91.0 | 2.9 | 88.0 | 4.4 | 6.1 | 101.6 | 91.0 | 2.9 | NA |
| Roeske 15ATW-29 3-7-2017-Spot 215 | 150 | 19617 | 1.3 | 21.5 | 2.8 | 0.1 | 4.2 | 0.0 | 3.1 | 0.7 | 91.1 | 2.8 | 88.5 | 3.5 | 19.5 | 66.6 | 91.1 | 2.8 | NA |
| Roeske 15ATW-29 3-7-2017-Spot 251 | 275 | 366703 | 1.9 | 20.3 | 2.1 | 0.1 | 3.6 | 0.0 | 2.9 | 0.8 | 91.1 | 2.6 | 93.7 | 3.2 | 162.3 | 49.6 | 91.1 | 2.6 | NA |
| Roeske 15ATW-29 3-7-2017-Spot 95 | 31 | 2231 | 2.0 | 20.9 | 5.3 | 0.1 | 6.4 | 0.0 | 3.4 | 0.5 | 91.1 | 3.1 | 91.2 | 5.5 | 95.7 | 126.5 | 91.1 | 3.1 | NA |
| Roeske 15ATW-29 3-7-2017-Spot 299 | 123 | 15557 | 1.8 | 21.3 | 3.1 | 0.1 | 4.4 | 0.0 | 3.1 | 0.7 | 91.1 | 2.8 | 89.3 | 3.7 | 42.3 | 74.2 | 91.1 | 2.8 | NA |
| Roeske 15ATW-29 3-7-2017-Spot 12 | 72 | 19762 | 1.6 | 22.7 | 3.6 | 0.1 | 4.5 | 0.0 | 2.7 | 0.6 | 91.3 | 2.5 | 84.4 | 3.7 | NA | NA | 91.3 | 2.5 | NA |
| Roeske 15ATW-29 3-7-2017-Spot 221 | 87 | 32967 | 2.3 | 20.9 | 3.3 | 0.1 | 4.4 | 0.0 | 2.9 | 0.7 | 91.7 | 2.7 | 91.5 | 3.8 | 86.9 | 77.9 | 91.7 | 2.7 | NA |
| Roeske 15ATW-29 3-7-2017-Spot 277 | 116 | 30948 | 1.5 | 21.0 | 2.9 | 0.1 | 4.5 | 0.0 | 3.4 | 0.8 | 91.7 | 3.1 | 91.4 | 3.9 | 82.9 | 69.3 | 91.7 | 3.1 | NA |
| Roeske 15ATW-29 3-7-2017-Spot 265 | 433 | 130427 | 1.3 | 20.7 | 1.6 | 0.1 | 3.2 | 0.0 | 2.7 | 0.9 | 91.8 | 2.5 | 92.7 | 2.8 | 115.7 | 38.5 | 91.8 | 2.5 | NA |
| Roeske 15ATW-29 3-7-2017-Spot 180 | 759 | 813111 | 0.9 | 20.8 | 1.6 | 0.1 | 3.2 | 0.0 | 2.8 | 0.9 | 92.0 | 2.5 | 92.6 | 2.8 | 108.4 | 38.6 | 92.0 | 2.5 | NA |
| Roeske 15ATW-29 3-7-2017-Spot 189 | 242 | 906138 | 2.8 | 20.9 | 2.0 | 0.1 | 3.3 | 0.0 | 2.6 | 0.8 | 92.2 | 2.4 | 92.1 | 2.9 | 90.8 | 48.0 | 92.2 | 2.4 | NA |
| Roeske 15ATW-29 3-7-2017-Spot 48 | 257 | 26248 | 1.9 | 19.7 | 1.9 | 0.1 | 3.6 | 0.0 | 3.0 | 0.9 | 92.4 | 2.8 | 97.6 | 3.3 | 228.4 | 43.0 | 92.4 | 2.8 | NA |
| Roeske 15ATW-29 3-7-2017-Spot 62 | 642 | 357721 | 1.7 | 20.3 | 1.6 | 0.1 | 2.6 | 0.0 | 2.0 | 0.8 | 92.5 | 1.9 | 94.8 | 2.4 | 154.9 | 38.0 | 92.5 | 1.9 | NA |
| Roeske 15ATW29A 8Mar16-Sample 1 Spot 63 | 360 | 4937 | 2.2 | 21.2 | 1.4 | 0.1 | 2.5 | 0.0 | 2.0 | 0.8 | 92.6 | 1.9 | 91.5 | 2.1 | 61.7 | 32.4 | 92.6 | 1.9 | NA |
| Roeske 15ATW-29 3-7-2017-Spot 248 | 54 | 51760 | 2.1 | 21.4 | 3.8 | 0.1 | 4.9 | 0.0 | 3.0 | 0.6 | 92.8 | 2.8 | 90.6 | 4.2 | 33.5 | 91.5 | 92.8 | 2.8 | NA |
| Roeske 15ATW-29 3-7-2017-Spot 139 | 899 | 201318 | 1.9 | 20.6 | 1.1 | 0.1 | 3.1 | 0.0 | 2.9 | 0.9 | 92.9 | 2.7 | 94.3 | 2.8 | 130.2 | 25.2 | 92.9 | 2.7 | NA |
| Roeske 15ATW-29 3-7-2017-Spot 116 | 225 | 33190 | 1.8 | 20.5 | 1.9 | 0.1 | 3.3 | 0.0 | 2.7 | 0.8 | 93.0 | 2.5 | 94.8 | 3.0 | 143.0 | 44.0 | 93.0 | 2.5 | NA |
| Roeske 15ATW-29 3-7-2017-Spot 168 | 491 | 76764 | 2.1 | 20.3 | 1.4 | 0.1 | 2.8 | 0.0 | 2.4 | 0.9 | 93.2 | 2.3 | 95.9 | 2.6 | 165.8 | 33.2 | 93.2 | 2.3 | NA |
| Roeske 15ATW-29 3-7-2017-Spot 190 | 237 | 84506 | 2.9 | 20.4 | 1.9 | 0.1 | 3.1 | 0.0 | 2.5 | 0.8 | 93.3 | 2.3 | 95.2 | 2.9 | 145.0 | 44.8 | 93.3 | 2.3 | NA |
| Roeske 15ATW-29 3-7-2017-Spot 141 | 106 | 18212 | 2.0 | 20.3 | 3.6 | 0.1 | 4.6 | 0.0 | 2.9 | 0.6 | 93.3 | 2.7 | 95.8 | 4.2 | 158.0 | 85.3 | 93.3 | 2.7 | NA |
| Roeske 15ATW-29 3-7-2017-Spot 266 | 388 | 654393 | 1.6 | 21.1 | 1.8 | 0.1 | 2.8 | 0.0 | 2.1 | 0.8 | 93.4 | 1.9 | 92.5 | 2.4 | 70.8 | 43.2 | 93.4 | 1.9 | NA |
| Roeske 15ATW-29 3-7-2017-Spot 33 | 193 | 24223 | 1.7 | 21.2 | 2.8 | 0.1 | 4.1 | 0.0 | 2.9 | 0.7 | 93.7 | 2.7 | 92.5 | 3.6 | 62.3 | 67.7 | 93.7 | 2.7 | NA |
| Roeske 15ATW-29 3-7-2017-Spot 187 | 1929 | 3104850 | 7.8 | 20.5 | 0.9 | 0.1 | 2.3 | 0.0 | 2.1 | 0.9 | 94.9 | 2.0 | 96.4 | 2.1 | 136.1 | 21.4 | 94.9 | 2.0 | NA |
| Roeske 15ATW-29 3-7-2017-Spot 228 | 65 | 7578 | 1.9 | 20.1 | 3.2 | 0.1 | 4.4 | 0.0 | 3.1 | 0.7 | 95.2 | 2.9 | 98.7 | 4.2 | 183.2 | 74.2 | 95.2 | 2.9 | NA |
| Roeske 15ATW-29 3-7-2017-Spot 298 | 95 | 35351 | 2.5 | 21.9 | 2.9 | 0.1 | 4.0 | 0.0 | 2.7 | 0.7 | 95.9 | 2.6 | 91.7 | 3.5 | NA | NA | 95.9 | 2.6 | NA |
| Roeske 15ATW-29 3-7-2017-Spot 112 | 577 | 26304 | 2.0 | 20.1 | 1.5 | 0.1 | 2.7 | 0.0 | 2.3 | 0.8 | 96.0 | 2.2 | 99.6 | 2.6 | 187.3 | 34.8 | 96.0 | 2.2 | NA |
| Roeske 15ATW-29 3-7-2017-Spot 11 | 704 | 52441 | 1.8 | 20.9 | 1.6 | 0.1 | 3.6 | 0.0 | 3.2 | 0.9 | 96.6 | 3.1 | 96.5 | 3.3 | 94.9 | 37.0 | 96.6 | 3.1 | NA |
| Roeske 15ATW29A 8Mar16-Sample 1 Spot 40 | 243 | 6491 | 1.7 | 20.8 | 1.4 | 0.1 | 2.5 | 0.0 | 2.1 | 0.8 | 97.0 | 2.1 | 97.3 | 2.4 | 105.8 | 32.4 | 97.0 | 2.1 | NA |
| Roeske 15ATW32 8Mar16-Spot 34 | 970 | 82226 | 2.4 | 20.4 | 1.1 | 0.1 | 2.6 | 0.0 | 2.3 | 0.9 | 97.3 | 2.2 | 99.3 | 2.4 | 147.6 | 26.4 | 97.3 | 2.2 | NA |
| Roeske 15ATW29A 8Mar16-Sample 1 Spot 46 | 85 | 2430 | 3.5 | 21.7 | 3.5 | 0.1 | 4.3 | 0.0 | 2.6 | 0.6 | 97.8 | 2.5 | 94.1 | 3.9 | 2.8 | 83.9 | 97.8 | 2.5 | NA |
| Roeske 15ATW-29 3-7-2017-Spot 150 | 838 | 91613 | 2.6 | 20.6 | 1.3 | 0.1 | 2.6 | 0.0 | 2.3 | 0.9 | 98.1 | 2.2 | 99.3 | 2.5 | 129.5 | 30.4 | 98.1 | 2.2 | NA |
| Roeske 15ATW-29 3-7-2017-Spot 158 | 75 | 6805 | 2.6 | 21.6 | 3.9 | 0.1 | 5.3 | 0.0 | 3.6 | 0.7 | 98.7 | 3.5 | 95.6 | 4.9 | 18.3 | 94.2 | 98.7 | 3.5 | NA |
| Roeske 15ATW32 8Mar16-Spot 1 | 313 | 5482 | 3.3 | 20.9 | 1.9 | 0.1 | 3.2 | 0.0 | 2.5 | 0.8 | 98.8 | 2.5 | 98.5 | 3.0 | 91.1 | 46.1 | 98.8 | 2.5 | NA |
| Roeske 15ATW-29 3-7-2017-Spot 72 | 119 | 22369 | 2.0 | 19.1 | 2.8 | 0.1 | 3.9 | 0.0 | 2.7 | 0.7 | 99.8 | 2.7 | 108.1 | 4.0 | 295.1 | 63.7 | 99.8 | 2.7 | NA |
| Roeske 15ATW-29 3-7-2017-Spot 264 | 614 | 368931 | 1.9 | 20.6 | 1.2 | 0.1 | 3.5 | 0.0 | 3.2 | 0.9 | 100.5 | 3.2 | 101.5 | 3.3 | 124.8 | 28.6 | 100.5 | 3.2 | NA |
| Roeske 15ATW29A 8Mar16-Sample 1 Spot 11 | 52 | 4848 | 3.1 | 20.0 | 3.3 | 0.1 | 4.4 | 0.0 | 3.0 | 0.7 | 100.7 | 3.0 | 104.5 | 4.4 | 193.3 | 77.2 | 100.7 | 3.0 | NA |
| Roeske 15ATW-29 3-7-2017-Spot 144 | 228 | 156300 | 2.8 | 21.5 | 2.2 | 0.1 | 3.2 | 0.0 | 2.3 | 0.7 | 100.9 | 2.3 | 98.0 | 3.0 | 28.6 | 52.9 | 100.9 | 2.3 | NA |

| | | | | | | | | | | | | | | | | | | | |
|---|---|---|---|---|---|---|---|---|---|---|---|---|---|---|---|---|---|---|---|
| Roeske 15ATW-29 3-7-2017-Spot 41 | 351 | 110346 | 1.9 | 20.9 | 1.7 | 0.1 | 3.2 | 0.0 | 2.6 | 0.8 | 101.7 | 2.7 | 101.1 | 3.0 | 86.7 | 41.4 | 101.7 | 2.7 | NA |
| Roeske 15ATW-29 3-7-2017-Spot 37 | 796 | 128946 | 2.1 | 20.4 | 0.9 | 0.1 | 2.7 | 0.0 | 2.6 | 0.9 | 102.5 | 2.6 | 104.4 | 2.7 | 148.5 | 22.1 | 102.5 | 2.6 | NA |
| Roeske 15ATW-29 3-7-2017-Spot 52 | 136 | 18855 | 2.8 | 20.0 | 2.2 | 0.1 | 3.1 | 0.0 | 2.1 | 0.7 | 103.5 | 2.2 | 107.2 | 3.1 | 190.8 | 51.4 | 103.5 | 2.2 | NA |
| Roeske 15ATW-29 3-7-2017-Spot 308 | 663 | 69984 | 1.9 | 20.8 | 1.7 | 0.1 | 3.1 | 0.0 | 2.6 | 0.8 | 103.7 | 2.7 | 103.6 | 3.0 | 103.3 | 39.5 | 103.7 | 2.7 | NA |
| Roeske 15ATW-29 3-7-2017-Spot 311 | 78 | 11552 | 2.5 | 21.4 | 3.4 | 0.1 | 4.7 | 0.0 | 3.2 | 0.7 | 103.9 | 3.3 | 101.1 | 4.5 | 37.7 | 81.3 | 103.9 | 3.3 | NA |
| Roeske 15ATW-29 3-7-2017-Spot 192 | 551 | 335177 | 1.1 | 20.0 | 1.5 | 0.1 | 3.4 | 0.0 | 3.1 | 0.9 | 105.2 | 3.2 | 109.3 | 3.6 | 200.8 | 35.4 | 105.2 | 3.2 | NA |
| Roeske 15ATW-29 3-7-2017-Spot 96 | 672 | 179768 | 1.6 | 20.5 | 0.9 | 0.1 | 2.0 | 0.0 | 1.8 | 0.9 | 105.5 | 1.9 | 106.8 | 2.0 | 136.9 | 20.8 | 105.5 | 1.9 | NA |
| Roeske 15ATW-29 3-7-2017-Spot 27 | 614 | 92023 | 2.4 | 20.5 | 1.0 | 0.1 | 2.8 | 0.0 | 2.6 | 0.9 | 105.8 | 2.8 | 107.0 | 2.9 | 134.3 | 24.3 | 105.8 | 2.8 | NA |
| Roeske 15ATW-29 3-7-2017-Spot 282 | 394 | 63106 | 3.3 | 21.1 | 1.6 | 0.1 | 2.5 | 0.0 | 2.0 | 0.8 | 106.3 | 2.1 | 104.9 | 2.5 | 73.8 | 36.9 | 106.3 | 2.1 | NA |
| Roeske 15ATW-29 3-7-2017-Spot 182 | 2595 | 441020 | 1.8 | 20.5 | 1.3 | 0.1 | 2.5 | 0.0 | 2.1 | 0.8 | 109.3 | 2.3 | 110.3 | 2.6 | 132.2 | 31.1 | 109.3 | 2.3 | NA |
| Roeske 15ATW29A 8Mar16-Sample 1 Spot 35 | 1711 | 22895 | 1.7 | 20.9 | 0.8 | 0.1 | 1.9 | 0.0 | 1.8 | 0.9 | 109.4 | 1.9 | 108.8 | 2.0 | 95.3 | 19.5 | 109.4 | 1.9 | NA |
| Roeske 15ATW-29 3-7-2017-Spot 174 | 866 | 75933 | 0.8 | 20.4 | 1.2 | 0.1 | 2.4 | 0.0 | 2.1 | 0.9 | 111.3 | 2.3 | 112.7 | 2.6 | 144.4 | 27.4 | 111.3 | 2.3 | NA |
| Roeske 15ATW29A 8Mar16-Sample 1 Spot 54 | 534 | 72051 | 1.3 | 20.1 | 1.2 | 0.1 | 2.9 | 0.0 | 2.6 | 0.9 | 112.5 | 2.9 | 115.5 | 3.1 | 178.7 | 27.6 | 112.5 | 2.9 | NA |
| Roeske 15ATW-29 3-7-2017-Spot 73 | 432 | 137145 | 1.4 | 20.5 | 1.5 | 0.1 | 3.0 | 0.0 | 2.6 | 0.9 | 113.7 | 3.0 | 114.7 | 3.3 | 137.5 | 34.7 | 113.7 | 3.0 | NA |
| Roeske 15ATW29A 8Mar16-Sample 1 Spot 57 | 97 | 14514 | 4.4 | 19.8 | 2.5 | 0.1 | 4.1 | 0.0 | 3.3 | 0.8 | 114.1 | 3.8 | 118.8 | 4.6 | 213.4 | 57.3 | 114.1 | 3.8 | NA |
| Roeske 15ATW-29 3-7-2017-Spot 218 | 213 | 40535 | 2.4 | 20.8 | 1.7 | 0.1 | 3.1 | 0.0 | 2.5 | 0.8 | 115.1 | 2.9 | 114.5 | 3.3 | 103.5 | 41.1 | 115.1 | 2.9 | NA |
| Roeske 15ATW29A 8Mar16-Sample 1 Spot 37 | 106 | 10948 | 3.1 | 19.9 | 2.1 | 0.1 | 3.5 | 0.0 | 2.7 | 0.8 | 116.1 | 3.1 | 120.3 | 3.9 | 203.6 | 49.7 | 116.1 | 3.1 | NA |
| Roeske 15ATW29A 8Mar16-Sample 1 Spot 7 | 157 | 3336 | 7.1 | 19.5 | 3.6 | 0.1 | 4.9 | 0.0 | 3.3 | 0.7 | 117.1 | 3.8 | 123.7 | 5.7 | 254.3 | 82.1 | 117.1 | 3.8 | NA |
| Roeske 15ATW-29 3-7-2017-Spot 78 | 204 | 69847 | 3.0 | 20.5 | 2.5 | 0.1 | 3.9 | 0.0 | 3.1 | 0.8 | 117.3 | 3.6 | 118.3 | 4.4 | 140.0 | 58.0 | 117.3 | 3.6 | NA |
| Roeske 15ATW-29 3-7-2017-Spot 106 | 424 | 39064 | 2.8 | 20.3 | 1.6 | 0.1 | 2.6 | 0.0 | 2.1 | 0.8 | 117.6 | 2.4 | 119.6 | 2.9 | 159.4 | 37.0 | 117.6 | 2.4 | NA |
| Roeske 15ATW-29 3-7-2017-Spot 249 | 461 | 60475 | 286.7 | 20.8 | 1.3 | 0.1 | 2.9 | 0.0 | 2.6 | 0.9 | 124.2 | 3.2 | 123.0 | 3.4 | 101.2 | 31.8 | 124.2 | 3.2 | NA |
| Roeske 15ATW-29 3-7-2017-Spot 50 | 917 | 112426 | 2.4 | 20.3 | 1.1 | 0.1 | 2.4 | 0.0 | 2.2 | 0.9 | 127.0 | 2.7 | 128.8 | 2.9 | 164.4 | 25.1 | 127.0 | 2.7 | NA |
| Roeske 15ATW-29 3-7-2017-Spot 204 | 108 | 32274 | 1.6 | 19.9 | 3.0 | 0.1 | 4.1 | 0.0 | 2.8 | 0.7 | 132.9 | 3.6 | 136.7 | 5.2 | 204.7 | 69.9 | 132.9 | 3.6 | NA |
| Roeske 15ATW32 8Mar16-Spot 28 | 981 | 253588 | 1.1 | 20.4 | 1.1 | 0.1 | 2.6 | 0.0 | 2.3 | 0.9 | 136.2 | 3.2 | 137.2 | 3.3 | 154.5 | 25.3 | 136.2 | 3.2 | NA |
| Roeske 15ATW29A 8Mar16-Sample 1 Spot 21 | 211 | 23580 | 2.6 | 20.4 | 1.5 | 0.1 | 3.0 | 0.0 | 2.6 | 0.9 | 137.6 | 3.6 | 138.2 | 3.9 | 147.1 | 35.5 | 137.6 | 3.6 | NA |
| Roeske 15ATW-29 3-7-2017-Spot 202 | 1053 | 423361 | 1.1 | 20.3 | 1.1 | 0.2 | 2.4 | 0.0 | 2.2 | 0.9 | 141.0 | 3.0 | 142.1 | 3.2 | 161.8 | 25.5 | 141.0 | 3.0 | NA |
| Roeske 15ATW32 8Mar16-Spot 7 | 153 | 5527 | 3.8 | 20.2 | 1.6 | 0.2 | 3.0 | 0.0 | 2.5 | 0.8 | 146.2 | 3.6 | 147.7 | 4.1 | 171.6 | 38.1 | 146.2 | 3.6 | NA |
| Roeske 15ATW32 8Mar16-Spot 16 | 764 | 56289 | 2.6 | 20.2 | 0.9 | 0.2 | 2.0 | 0.0 | 1.8 | 0.9 | 146.7 | 2.6 | 148.3 | 2.8 | 174.5 | 21.0 | 146.7 | 2.6 | NA |
| Roeske 15ATW-29 3-7-2017-Spot 261 | 192 | 20124 | 1.7 | 20.2 | 1.6 | 0.2 | 3.5 | 0.0 | 3.1 | 0.9 | 147.3 | 4.5 | 148.4 | 4.8 | 167.3 | 38.5 | 147.3 | 4.5 | NA |
| Roeske 15ATW-29 3-7-2017-Spot 24 | 168 | 14654 | 1.9 | 20.1 | 2.0 | 0.2 | 3.0 | 0.0 | 2.3 | 0.8 | 148.6 | 3.4 | 150.9 | 4.3 | 188.1 | 45.5 | 148.6 | 3.4 | NA |
| Roeske 15ATW-29 3-7-2017-Spot 239 | 57 | 6101 | 4.0 | 19.6 | 3.0 | 0.2 | 4.0 | 0.0 | 2.7 | 0.7 | 148.8 | 3.9 | 154.7 | 5.8 | 247.3 | 69.1 | 148.8 | 3.9 | NA |
| Roeske 15ATW32 8Mar16-Spot 8 | 240 | 502118 | 2.5 | 19.5 | 1.5 | 0.2 | 2.6 | 0.0 | 2.2 | 0.8 | 149.0 | 3.2 | 155.5 | 3.8 | 255.1 | 34.0 | 149.0 | 3.2 | NA |
| Roeske 15ATW-29 3-7-2017-Spot 237 | 69 | 57310 | 1.8 | 20.3 | 2.6 | 0.2 | 3.7 | 0.0 | 2.7 | 0.7 | 150.1 | 4.0 | 150.3 | 5.2 | 154.7 | 60.7 | 150.1 | 4.0 | NA |
| Roeske 15ATW-29 3-7-2017-Spot 170 | 456 | 81737 | 1.7 | 19.7 | 1.8 | 0.2 | 3.2 | 0.0 | 2.6 | 0.8 | 150.5 | 3.9 | 155.1 | 4.6 | 228.2 | 40.6 | 150.5 | 3.9 | NA |
| Roeske 15ATW-29 3-7-2017-Spot 49 | 159 | 24960 | 4.1 | 20.4 | 2.1 | 0.2 | 3.4 | 0.0 | 2.7 | 0.8 | 151.1 | 4.0 | 151.2 | 4.8 | 152.6 | 49.6 | 151.1 | 4.0 | NA |
| Roeske 15ATW-29 3-7-2017-Spot 294 | 83 | 65291 | 2.7 | 20.4 | 2.5 | 0.2 | 3.7 | 0.0 | 2.7 | 0.7 | 152.1 | 4.1 | 151.9 | 5.2 | 150.3 | 57.8 | 152.1 | 4.1 | NA |
| Roeske 15ATW-29 3-7-2017-Spot 286 | 178 | 13603 | 4.7 | 20.5 | 1.9 | 0.2 | 3.0 | 0.0 | 2.4 | 0.8 | 152.4 | 3.6 | 151.3 | 4.2 | 135.6 | 44.0 | 152.4 | 3.6 | NA |
| Roeske 15ATW29A 8Mar16-Sample 1 Spot 32 | 63 | 7748 | 3.6 | 20.6 | 1.8 | 0.2 | 3.3 | 0.0 | 2.8 | 0.8 | 152.6 | 4.2 | 151.2 | 4.7 | 128.6 | 43.2 | 152.6 | 4.2 | NA |
| Roeske 15ATW-29 3-7-2017-Spot 3 | 267 | 272577 | 1.6 | 20.5 | 1.5 | 0.2 | 2.8 | 0.0 | 2.3 | 0.8 | 152.8 | 3.5 | 151.7 | 3.9 | 135.8 | 34.9 | 152.8 | 3.5 | NA |
| Roeske 15ATW-29 3-7-2017-Spot 14 | 491 | 144129 | 1.9 | 20.4 | 1.3 | 0.2 | 3.2 | 0.0 | 2.9 | 0.9 | 152.8 | 4.4 | 152.8 | 4.5 | 154.1 | 30.4 | 152.8 | 4.4 | NA |

| | | | | | | | | | | | | | | | | | | | |
|---|---|---|---|---|---|---|---|---|---|---|---|---|---|---|---|---|---|---|---|
| Roeske 15ATW-29 3-7-2017-Spot 89 | 214 | 39701 | 2.3 | 19.7 | 1.3 | 0.2 | 3.5 | 0.0 | 3.2 | 0.9 | 153.5 | 4.8 | 157.9 | 5.0 | 225.6 | 30.4 | 153.5 | 4.8 | NA |
| Roeske 15ATW29A 8Mar16-Sample 1 Spot 44 | 98 | 6595 | 3.1 | 21.1 | 3.0 | 0.2 | 3.7 | 0.0 | 2.1 | 0.6 | 153.6 | 3.2 | 148.7 | 5.1 | 71.7 | 72.0 | 153.6 | 3.2 | NA |
| Roeske 15ATW-29 3-7-2017-Spot 271 | 34 | 54161 | 3.4 | 18.7 | 3.4 | 0.2 | 4.7 | 0.0 | 3.2 | 0.7 | 154.0 | 4.9 | 166.7 | 7.2 | 351.0 | 76.7 | 154.0 | 4.9 | NA |
| Roeske 15ATW-29 3-7-2017-Spot 185 | 314 | 79948 | 2.0 | 20.2 | 1.7 | 0.2 | 3.1 | 0.0 | 2.6 | 0.8 | 155.0 | 3.9 | 155.9 | 4.4 | 169.3 | 38.7 | 155.0 | 3.9 | NA |
| Roeske 15ATW-29 3-7-2017-Spot 147 | 280 | 57323 | 6.0 | 20.6 | 1.7 | 0.2 | 3.3 | 0.0 | 2.8 | 0.9 | 157.7 | 4.4 | 155.9 | 4.8 | 129.9 | 41.1 | 157.7 | 4.4 | NA |
| Roeske 15ATW-29 3-7-2017-Spot 83 | 234 | 16702 | 2.8 | 20.8 | 1.8 | 0.2 | 3.2 | 0.0 | 2.7 | 0.8 | 159.7 | 4.2 | 156.2 | 4.7 | 104.3 | 42.6 | 159.7 | 4.2 | NA |
| Roeske 15ATW-29 3-7-2017-Spot 236 | 1077 | 74224 | 1.8 | 20.5 | 1.1 | 0.2 | 2.5 | 0.0 | 2.3 | 0.9 | 160.7 | 3.6 | 158.8 | 3.7 | 132.5 | 26.1 | 160.7 | 3.6 | NA |
| Roeske 15ATW-29 3-7-2017-Spot 13 | 121 | 204978 | 2.8 | 19.2 | 1.8 | 0.2 | 3.6 | 0.0 | 3.1 | 0.9 | 160.8 | 4.9 | 168.8 | 5.6 | 284.5 | 42.0 | 160.8 | 4.9 | NA |
| Roeske 15ATW-29 3-7-2017-Spot 288 | 292 | 336487 | 4.5 | 20.6 | 1.7 | 0.2 | 3.3 | 0.0 | 2.8 | 0.9 | 161.6 | 4.5 | 159.2 | 4.9 | 125.0 | 40.8 | 161.6 | 4.5 | NA |
| Roeske 15ATW-29 3-7-2017-Spot 278 | 435 | 70475 | 2.5 | 20.4 | 1.6 | 0.2 | 3.2 | 0.0 | 2.8 | 0.9 | 163.4 | 4.6 | 162.3 | 4.9 | 147.4 | 36.5 | 163.4 | 4.6 | NA |
| Roeske 15ATW-29 3-7-2017-Spot 36 | 113 | 12380 | 2.4 | 19.4 | 2.8 | 0.2 | 4.0 | 0.0 | 2.8 | 0.7 | 163.9 | 4.5 | 171.0 | 6.2 | 270.6 | 64.7 | 163.9 | 4.5 | NA |
| Roeske 15ATW-29 3-7-2017-Spot 304 | 317 | 27126 | 1.3 | 20.1 | 1.6 | 0.2 | 4.6 | 0.0 | 4.4 | 0.9 | 164.2 | 7.1 | 165.7 | 7.1 | 189.0 | 36.8 | 164.2 | 7.1 | NA |
| Roeske 15ATW-29 3-7-2017-Spot 9 | 98 | 35769 | 3.7 | 20.0 | 3.2 | 0.2 | 5.0 | 0.0 | 3.9 | 0.8 | 164.7 | 6.3 | 166.6 | 7.7 | 195.2 | 74.1 | 164.7 | 6.3 | NA |
| Roeske 15ATW32 8Mar16-Spot 5 | 208 | 10793 | 3.2 | 20.6 | 1.7 | 0.2 | 3.3 | 0.0 | 2.8 | 0.9 | 169.7 | 4.7 | 166.5 | 5.0 | 121.7 | 40.0 | 169.7 | 4.7 | NA |
| Roeske 15ATW29A 8Mar16-Sample 1 Spot 38 | 111 | 4897 | 2.4 | 20.5 | 2.6 | 0.2 | 3.6 | 0.0 | 2.5 | 0.7 | 170.4 | 4.2 | 168.4 | 5.6 | 140.3 | 60.7 | 170.4 | 4.2 | NA |
| Roeske 15ATW29A 8Mar16-Sample 1 Spot 59 | 207 | 15304 | 1.7 | 20.4 | 1.3 | 0.2 | 2.7 | 0.0 | 2.3 | 0.9 | 171.7 | 4.0 | 170.1 | 4.2 | 148.3 | 31.5 | 171.7 | 4.0 | NA |
| Roeske 15ATW-29 3-7-2017-Spot 136 | 229 | 26218 | 2.6 | 19.6 | 1.5 | 0.2 | 3.1 | 0.0 | 2.7 | 0.9 | 172.4 | 4.6 | 177.5 | 5.0 | 247.4 | 33.9 | 172.4 | 4.6 | NA |
| Roeske 15ATW-29 3-7-2017-Spot 45 | 447 | 119041 | 2.4 | 20.5 | 1.3 | 0.2 | 3.0 | 0.0 | 2.7 | 0.9 | 172.4 | 4.6 | 170.3 | 4.7 | 142.8 | 30.2 | 172.4 | 4.6 | NA |
| Roeske 15ATW-29 3-7-2017-Spot 154 | 89 | 34292 | 2.6 | 19.8 | 2.1 | 0.2 | 3.1 | 0.0 | 2.3 | 0.7 | 174.7 | 4.0 | 178.0 | 5.0 | 223.7 | 47.5 | 174.7 | 4.0 | NA |
| Roeske 15ATW-29 3-7-2017-Spot 162 | 171 | 324415 | 2.7 | 20.5 | 1.7 | 0.2 | 3.0 | 0.0 | 2.4 | 0.8 | 174.8 | 4.2 | 172.4 | 4.7 | 140.1 | 40.4 | 174.8 | 4.2 | NA |
| Roeske 15ATW32 8Mar16-Spot 45 | 521 | 834461 | 3.4 | 19.8 | 1.2 | 0.2 | 2.4 | 0.0 | 2.1 | 0.9 | 175.2 | 3.7 | 178.4 | 4.0 | 221.0 | 27.5 | 175.2 | 3.7 | NA |
| Roeske 15ATW-29 3-7-2017-Spot 184 | 181 | 39555 | 2.5 | 19.8 | 2.0 | 0.2 | 3.7 | 0.0 | 3.1 | 0.8 | 176.7 | 5.5 | 179.3 | 6.1 | 215.3 | 46.7 | 176.7 | 5.5 | NA |
| Roeske 15ATW32 8Mar16-Spot 33 | 674 | 85951 | 2.3 | 19.9 | 0.9 | 0.2 | 2.3 | 0.0 | 2.1 | 0.9 | 177.7 | 3.7 | 179.5 | 3.8 | 203.3 | 20.3 | 177.7 | 3.7 | NA |
| Roeske 15ATW29A 8Mar16-Sample 1 Spot 2 | 120 | 9781 | 1.5 | 19.6 | 1.4 | 0.2 | 3.1 | 0.0 | 2.8 | 0.9 | 178.1 | 4.9 | 182.2 | 5.2 | 236.4 | 33.2 | 178.1 | 4.9 | NA |
| Roeske 15ATW-29 3-7-2017-Spot 242 | 164 | 173900 | 4.4 | 20.1 | 1.8 | 0.2 | 3.9 | 0.0 | 3.5 | 0.9 | 179.3 | 6.2 | 179.4 | 6.5 | 182.5 | 41.8 | 179.3 | 6.2 | NA |
| Roeske 15ATW-29 3-7-2017-Spot 113 | 370 | 58104 | 1.0 | 19.7 | 1.3 | 0.2 | 2.9 | 0.0 | 2.6 | 0.9 | 179.8 | 4.7 | 183.5 | 4.9 | 231.8 | 29.0 | 179.8 | 4.7 | NA |
| Roeske 15ATW32 8Mar16-Spot 24 | 811 | 62741 | 2.4 | 20.2 | 0.9 | 0.2 | 1.8 | 0.0 | 1.6 | 0.9 | 180.7 | 2.9 | 179.7 | 3.0 | 167.3 | 20.7 | 180.7 | 2.9 | NA |
| Roeske 15ATW-29 3-7-2017-Spot 208 | 103 | 68355 | 2.0 | 19.8 | 2.7 | 0.2 | 5.1 | 0.0 | 4.3 | 0.9 | 182.0 | 7.8 | 184.2 | 8.6 | 212.8 | 62.4 | 182.0 | 7.8 | NA |
| Roeske 15ATW-29 3-7-2017-Spot 88 | 241 | 181965 | 1.8 | 19.7 | 1.1 | 0.2 | 2.7 | 0.0 | 2.5 | 0.9 | 182.4 | 4.5 | 185.7 | 4.6 | 228.8 | 25.5 | 182.4 | 4.5 | NA |
| Roeske 15ATW-29 3-7-2017-Spot 244 | 525 | 89250 | 1.4 | 20.0 | 1.0 | 0.2 | 2.7 | 0.0 | 2.5 | 0.9 | 182.4 | 4.5 | 183.0 | 4.5 | 191.5 | 23.5 | 182.4 | 4.5 | NA |
| Roeske 15ATW-29 3-7-2017-Spot 269 | 195 | 67378 | 1.6 | 20.0 | 1.3 | 0.2 | 2.8 | 0.0 | 2.5 | 0.9 | 182.6 | 4.4 | 183.8 | 4.7 | 200.1 | 31.1 | 182.6 | 4.4 | NA |
| Roeske 15ATW29A 8Mar16-Sample 1 Spot 64 | 308 | 45486 | 2.7 | 19.5 | 1.0 | 0.2 | 2.3 | 0.0 | 2.0 | 0.9 | 183.2 | 3.7 | 188.0 | 3.9 | 248.8 | 23.6 | 183.2 | 3.7 | NA |
| Roeske 15ATW-29 3-7-2017-Spot 234 | 379 | 75794 | 2.3 | 20.2 | 1.5 | 0.2 | 2.6 | 0.0 | 2.2 | 0.8 | 183.5 | 3.9 | 182.2 | 4.4 | 166.6 | 34.9 | 183.5 | 3.9 | NA |
| Roeske 15ATW-29 3-7-2017-Spot 205 | 726 | 109537 | 1.7 | 19.8 | 1.1 | 0.2 | 2.5 | 0.0 | 2.2 | 0.9 | 183.6 | 4.0 | 185.7 | 4.2 | 214.0 | 25.9 | 183.6 | 4.0 | NA |
| Roeske 15ATW29A 8Mar16-Sample 1 Spot 12 | 290 | 47946 | 2.2 | 19.7 | 0.9 | 0.2 | 2.4 | 0.0 | 2.2 | 0.9 | 184.7 | 4.0 | 188.1 | 4.1 | 231.5 | 21.2 | 184.7 | 4.0 | NA |
| Roeske 15ATW-29 3-7-2017-Spot 229 | 429 | 54093 | 1.8 | 20.3 | 1.2 | 0.2 | 2.4 | 0.0 | 2.0 | 0.9 | 184.8 | 3.7 | 182.8 | 4.0 | 158.1 | 29.1 | 184.8 | 3.7 | NA |
| Roeske 15ATW-29 3-7-2017-Spot 151 | 1024 | 186455 | 1.2 | 20.2 | 1.0 | 0.2 | 2.8 | 0.0 | 2.6 | 0.9 | 185.3 | 4.7 | 184.4 | 4.7 | 174.3 | 23.7 | 185.3 | 4.7 | NA |
| Roeske 15ATW-29 3-7-2017-Spot 275 | 404 | 143194 | 2.4 | 20.1 | 1.2 | 0.2 | 3.1 | 0.0 | 2.8 | 0.9 | 186.1 | 5.1 | 186.0 | 5.2 | 186.5 | 28.2 | 186.1 | 5.1 | NA |
| Roeske 15ATW-29 3-7-2017-Spot 155 | 239 | 68522 | 2.2 | 20.1 | 1.8 | 0.2 | 3.0 | 0.0 | 2.4 | 0.8 | 186.2 | 4.5 | 186.1 | 5.1 | 186.2 | 40.9 | 186.2 | 4.5 | NA |
| Roeske 15ATW-29 3-7-2017-Spot 43 | 445 | 141335 | 2.1 | 20.5 | 1.1 | 0.2 | 2.6 | 0.0 | 2.4 | 0.9 | 186.2 | 4.4 | 182.3 | 4.4 | 132.5 | 26.6 | 186.2 | 4.4 | NA |

| | | | | | | | | | | | | | | | | | | | |
|---|---|---|---|---|---|---|---|---|---|---|---|---|---|---|---|---|---|---|---|
| Roeske 15ATW-29 3-7-2017-Spot 258 | 937 | 312431 | 1.3 | 19.9 | 1.1 | 0.2 | 2.7 | 0.0 | 2.5 | 0.9 | 186.2 | 4.5 | 187.8 | 4.6 | 208.9 | 25.2 | 186.2 | 4.5 | NA |
| Roeske 15ATW-29 3-7-2017-Spot 133 | 449 | 114374 | 1.6 | 19.6 | 1.5 | 0.2 | 3.2 | 0.0 | 2.8 | 0.9 | 186.2 | 5.1 | 190.5 | 5.5 | 244.9 | 34.9 | 186.2 | 5.1 | NA |
| Roeske 15ATW-29 3-7-2017-Spot 256 | 329 | 67347 | 2.1 | 19.8 | 1.7 | 0.2 | 3.2 | 0.0 | 2.7 | 0.8 | 187.1 | 5.0 | 189.5 | 5.5 | 220.2 | 39.4 | 187.1 | 5.0 | NA |
| Roeske 15ATW-29 3-7-2017-Spot 209 | 877 | 133004 | 3.7 | 19.9 | 1.1 | 0.2 | 2.6 | 0.0 | 2.4 | 0.9 | 187.9 | 4.4 | 188.9 | 4.5 | 203.0 | 26.0 | 187.9 | 4.4 | NA |
| Roeske 15ATW-29 3-7-2017-Spot 119 | 926 | 119485 | 1.3 | 20.1 | 0.8 | 0.2 | 2.0 | 0.0 | 1.9 | 0.9 | 188.8 | 3.4 | 188.4 | 3.5 | 183.7 | 19.7 | 188.8 | 3.4 | NA |
| Roeske 15ATW-29 3-7-2017-Spot 186 | 525 | 361929 | 1.5 | 19.7 | 1.2 | 0.2 | 3.1 | 0.0 | 2.8 | 0.9 | 189.0 | 5.2 | 192.0 | 5.4 | 230.2 | 28.8 | 189.0 | 5.2 | NA |
| Roeske 15ATW29A 8Mar16-Sample 1 Spot 13 | 239 | 5371 | 2.1 | 20.7 | 2.1 | 0.2 | 3.0 | 0.0 | 2.2 | 0.7 | 189.4 | 4.1 | 183.9 | 5.1 | 114.9 | 49.6 | 189.4 | 4.1 | NA |
| Roeske 15ATW-29 3-7-2017-Spot 44 | 328 | 261125 | 2.0 | 19.9 | 1.5 | 0.2 | 3.1 | 0.0 | 2.7 | 0.9 | 189.4 | 5.1 | 190.6 | 5.5 | 206.3 | 35.5 | 189.4 | 5.1 | NA |
| Roeske 15ATW29A 8Mar16-Sample 1 Spot 41 | 212 | 5610 | 2.5 | 20.8 | 1.4 | 0.2 | 2.5 | 0.0 | 2.0 | 0.8 | 190.0 | 3.8 | 183.9 | 4.2 | 106.4 | 33.8 | 190.0 | 3.8 | NA |
| Roeske 15ATW-29 3-7-2017-Spot 19 | 339 | 129798 | 2.2 | 20.1 | 1.5 | 0.2 | 2.8 | 0.0 | 2.3 | 0.8 | 190.0 | 4.4 | 189.4 | 4.8 | 182.5 | 35.2 | 190.0 | 4.4 | NA |
| Roeske 15ATW-29 3-7-2017-Spot 176 | 281 | 1423726 | 3.6 | 19.3 | 1.6 | 0.2 | 2.9 | 0.0 | 2.4 | 0.8 | 190.3 | 4.4 | 196.8 | 5.1 | 275.7 | 36.8 | 190.3 | 4.4 | NA |
| Roeske 15ATW-29 3-7-2017-Spot 152 | 1143 | 611936 | 1.7 | 19.6 | 1.0 | 0.2 | 2.4 | 0.0 | 2.2 | 0.9 | 190.4 | 4.1 | 194.6 | 4.3 | 247.4 | 23.8 | 190.4 | 4.1 | NA |
| Roeske 15ATW-29 3-7-2017-Spot 100 | 136 | 33149 | 1.9 | 20.1 | 1.7 | 0.2 | 3.1 | 0.0 | 2.6 | 0.8 | 191.6 | 4.9 | 190.7 | 5.4 | 181.3 | 39.5 | 191.6 | 4.9 | NA |
| Roeske 15ATW-29 3-7-2017-Spot 250 | 190 | 44106 | 2.7 | 20.3 | 1.7 | 0.2 | 3.0 | 0.0 | 2.5 | 0.8 | 191.6 | 4.8 | 189.1 | 5.2 | 158.4 | 39.3 | 191.6 | 4.8 | NA |
| Roeske 15ATW-29 3-7-2017-Spot 270 | 175 | 103094 | 2.2 | 19.9 | 1.7 | 0.2 | 3.5 | 0.0 | 3.1 | 0.9 | 191.7 | 5.8 | 192.5 | 6.1 | 203.3 | 39.0 | 191.7 | 5.8 | NA |
| Roeske 15ATW29A 8Mar16-Sample 1 Spot 67 | 628 | 23316 | 3.3 | 20.0 | 0.8 | 0.2 | 2.2 | 0.0 | 2.1 | 0.9 | 192.1 | 4.0 | 192.0 | 3.9 | 191.1 | 18.8 | 192.1 | 4.0 | NA |
| Roeske 15ATW-29 3-7-2017-Spot 8 | 640 | 125123 | 1.5 | 20.2 | 1.1 | 0.2 | 2.9 | 0.0 | 2.7 | 0.9 | 192.2 | 5.0 | 190.9 | 5.0 | 176.8 | 26.7 | 192.2 | 5.0 | NA |
| Roeske 15ATW-29 3-7-2017-Spot 310 | 425 | 175774 | 2.2 | 19.4 | 1.4 | 0.2 | 3.0 | 0.0 | 2.7 | 0.9 | 192.6 | 5.1 | 198.0 | 5.4 | 264.6 | 31.8 | 192.6 | 5.1 | NA |
| Roeske 15ATW-29 3-7-2017-Spot 76 | 553 | 62373 | 3.6 | 19.6 | 1.2 | 0.2 | 2.9 | 0.0 | 2.7 | 0.9 | 192.7 | 5.1 | 196.4 | 5.2 | 242.2 | 27.7 | 192.7 | 5.1 | NA |
| Roeske 15ATW-29 3-7-2017-Spot 283 | 292 | 140283 | 1.3 | 20.8 | 1.7 | 0.2 | 3.0 | 0.0 | 2.5 | 0.8 | 193.1 | 4.8 | 186.7 | 5.2 | 106.9 | 39.4 | 193.1 | 4.8 | NA |
| Roeske 15ATW-29 3-7-2017-Spot 200 | 1091 | 472866 | 2.1 | 19.9 | 0.9 | 0.2 | 2.5 | 0.0 | 2.3 | 0.9 | 193.6 | 4.3 | 194.9 | 4.4 | 212.4 | 21.9 | 193.6 | 4.3 | NA |
| Roeske 15ATW29A 8Mar16-Sample 1 Spot 22 | 206 | 25460 | 3.9 | 19.4 | 1.3 | 0.2 | 2.2 | 0.0 | 1.8 | 0.8 | 193.8 | 3.4 | 199.1 | 4.0 | 262.5 | 30.4 | 193.8 | 3.4 | NA |
| Roeske 15ATW32 8Mar16-Spot 14 | 404 | 292472 | 4.3 | 19.8 | 1.1 | 0.2 | 2.7 | 0.0 | 2.4 | 0.9 | 194.1 | 4.7 | 196.2 | 4.8 | 222.1 | 24.9 | 194.1 | 4.7 | NA |
| Roeske 15ATW-29 3-7-2017-Spot 291 | 149 | 46808 | 2.1 | 19.7 | 2.0 | 0.2 | 2.8 | 0.0 | 1.9 | 0.7 | 194.2 | 3.7 | 197.3 | 4.9 | 235.4 | 45.4 | 194.2 | 3.7 | NA |
| Roeske 15ATW-29 3-7-2017-Spot 61 | 853 | 293349 | 1.0 | 20.0 | 1.3 | 0.2 | 3.6 | 0.0 | 3.4 | 0.9 | 194.6 | 6.5 | 194.2 | 6.4 | 190.3 | 29.9 | 194.6 | 6.5 | NA |
| Roeske 15ATW32 8Mar16-Spot 11 | 490 | 6843933 | 2.7 | 19.1 | 1.1 | 0.2 | 2.4 | 0.0 | 2.1 | 0.9 | 195.7 | 4.1 | 203.9 | 4.5 | 299.8 | 25.9 | 195.7 | 4.1 | NA |
| Roeske 15ATW-29 3-7-2017-Spot 101 | 311 | 731416 | 1.6 | 19.5 | 1.3 | 0.2 | 3.0 | 0.0 | 2.7 | 0.9 | 195.7 | 5.2 | 200.5 | 5.4 | 257.4 | 30.0 | 195.7 | 5.2 | NA |
| Roeske 15ATW-29 3-7-2017-Spot 206 | 303 | 129612 | 2.4 | 19.8 | 1.4 | 0.2 | 3.1 | 0.0 | 2.8 | 0.9 | 196.1 | 5.3 | 197.5 | 5.6 | 215.9 | 33.0 | 196.1 | 5.3 | NA |
| Roeske 15ATW-29 3-7-2017-Spot 227 | 807 | 522861 | 1.3 | 19.9 | 1.0 | 0.2 | 2.7 | 0.0 | 2.5 | 0.9 | 196.4 | 4.8 | 197.4 | 4.8 | 210.2 | 22.8 | 196.4 | 4.8 | NA |
| Roeske 15ATW-29 3-7-2017-Spot 66 | 73 | 476813 | 3.4 | 19.9 | 2.3 | 0.2 | 3.7 | 0.0 | 3.0 | 0.8 | 196.8 | 5.8 | 197.9 | 6.7 | 211.9 | 52.2 | 196.8 | 5.8 | NA |
| Roeske 15ATW-29 3-7-2017-Spot 247 | 315 | 182823 | 2.0 | 20.1 | 1.4 | 0.2 | 2.8 | 0.0 | 2.4 | 0.9 | 197.1 | 4.7 | 196.3 | 5.0 | 187.0 | 33.1 | 197.1 | 4.7 | NA |
| Roeske 15ATW-29 3-7-2017-Spot 51 | 148 | 27017 | 2.9 | 19.9 | 2.0 | 0.2 | 3.2 | 0.0 | 2.5 | 0.8 | 197.4 | 4.8 | 197.6 | 5.7 | 201.0 | 46.5 | 197.4 | 4.8 | NA |
| Roeske 15ATW-29 3-7-2017-Spot 214 | 928 | 3229001 | 1.3 | 20.0 | 1.0 | 0.2 | 3.0 | 0.0 | 2.8 | 0.9 | 197.8 | 5.5 | 197.6 | 5.4 | 196.2 | 23.0 | 197.8 | 5.5 | NA |
| Roeske 15ATW-29 3-7-2017-Spot 297 | 110 | 195011 | 3.9 | 19.4 | 2.3 | 0.2 | 3.3 | 0.0 | 2.4 | 0.7 | 198.1 | 4.6 | 203.6 | 6.1 | 269.3 | 53.7 | 198.1 | 4.6 | NA |
| Roeske 15ATW-29 3-7-2017-Spot 92 | 153 | 11685 | 5.2 | 20.4 | 2.0 | 0.2 | 3.5 | 0.0 | 2.8 | 0.8 | 198.4 | 5.5 | 194.7 | 6.1 | 152.3 | 47.2 | 198.4 | 5.5 | NA |
| Roeske 15ATW-29 3-7-2017-Spot 284 | 255 | 43922 | 2.3 | 20.2 | 1.6 | 0.2 | 2.7 | 0.0 | 2.2 | 0.8 | 199.1 | 4.3 | 197.3 | 4.9 | 176.8 | 37.4 | 199.1 | 4.3 | NA |
| Roeske 15ATW-29 3-7-2017-Spot 63 | 422 | 146062 | 6.0 | 19.4 | 1.1 | 0.2 | 2.9 | 0.0 | 2.7 | 0.9 | 199.9 | 5.2 | 205.5 | 5.4 | 270.4 | 25.4 | 199.9 | 5.2 | NA |
| Roeske 15ATW-29 3-7-2017-Spot 260 | 489 | 462440 | 2.0 | 19.7 | 1.5 | 0.2 | 2.9 | 0.0 | 2.5 | 0.9 | 201.1 | 5.0 | 202.9 | 5.4 | 225.8 | 34.5 | 201.1 | 5.0 | NA |
| Roeske 15ATW32 8Mar16-Spot 37 | 544 | 1854505 | 2.1 | 19.0 | 1.0 | 0.2 | 2.1 | 0.0 | 1.9 | 0.9 | 201.4 | 3.8 | 210.0 | 4.0 | 307.1 | 21.7 | 201.4 | 3.8 | NA |
| Roeske 15ATW-29 3-7-2017-Spot 292 | 348 | 93524 | 1.7 | 20.2 | 1.5 | 0.2 | 2.8 | 0.0 | 2.4 | 0.8 | 201.5 | 4.7 | 199.0 | 5.1 | 169.7 | 36.1 | 201.5 | 4.7 | NA |

| | | | | | | | | | | | | | | | | | | | |
|---|---|---|---|---|---|---|---|---|---|---|---|---|---|---|---|---|---|---|---|
| Roeske 15ATW-29 3-7-2017-Spot 32 | 162 | 63295 | 2.4 | 20.2 | 1.8 | 0.2 | 3.2 | 0.0 | 2.6 | 0.8 | 202.2 | 5.3 | 199.4 | 5.8 | 167.5 | 41.4 | 202.2 | 5.3 | NA |
| Roeske 15ATW-29 3-7-2017-Spot 230 | 136 | 22252 | 1.4 | 19.4 | 2.0 | 0.2 | 3.8 | 0.0 | 3.3 | 0.9 | 202.6 | 6.5 | 208.0 | 7.2 | 270.8 | 46.1 | 202.6 | 6.5 | NA |
| Roeske 15ATW-29 3-7-2017-Spot 164 | 198 | 40366 | 3.6 | 19.7 | 1.5 | 0.2 | 2.6 | 0.0 | 2.1 | 0.8 | 204.1 | 4.2 | 205.9 | 4.9 | 228.0 | 35.5 | 204.1 | 4.2 | NA |
| Roeske 15ATW29A 8Mar16-Sample 1 Spot 69 | 246 | 7261 | 3.1 | 20.5 | 1.4 | 0.2 | 3.0 | 0.0 | 2.7 | 0.9 | 206.4 | 5.5 | 200.6 | 5.5 | 132.9 | 31.8 | 206.4 | 5.5 | NA |
| Roeske 15ATW-29 3-7-2017-Spot 64 | 282 | 42469 | 2.5 | 19.6 | 1.9 | 0.2 | 2.8 | 0.0 | 2.1 | 0.8 | 206.5 | 4.4 | 209.1 | 5.4 | 239.9 | 42.8 | 206.5 | 4.4 | NA |
| Roeske 15ATW-29 3-7-2017-Spot 70 | 253 | 54906 | 3.7 | 20.0 | 1.4 | 0.2 | 2.4 | 0.0 | 2.0 | 0.8 | 207.5 | 4.0 | 206.7 | 4.6 | 199.0 | 33.3 | 207.5 | 4.0 | NA |
| Roeske 15ATW-29 3-7-2017-Spot 233 | 125 | 25219 | 3.3 | 20.1 | 1.9 | 0.2 | 3.5 | 0.0 | 3.0 | 0.8 | 212.7 | 6.2 | 210.6 | 6.7 | 188.4 | 43.5 | 212.7 | 6.2 | NA |
| Roeske 15ATW-29 3-7-2017-Spot 149 | 174 | 33480 | 1.7 | 16.8 | 1.8 | 0.3 | 3.2 | 0.0 | 2.6 | 0.8 | 226.5 | 5.9 | 261.3 | 7.4 | 587.9 | 39.5 | 226.5 | 5.9 | NA |
| Roeske 15ATW32 8Mar16-Spot 20 | 429 | 19579 | 3.6 | 16.6 | 1.4 | 0.3 | 3.1 | 0.0 | 2.8 | 0.9 | 229.1 | 6.2 | 266.7 | 7.3 | 611.7 | 29.6 | 229.1 | 6.2 | NA |
| Roeske 15ATW29A 8Mar16-Sample 1 Spot 9 | 399 | 100980 | 3.3 | 18.5 | 1.0 | 0.3 | 2.4 | 0.0 | 2.2 | 0.9 | 231.0 | 5.0 | 243.7 | 5.2 | 367.8 | 22.3 | 231.0 | 5.0 | NA |
| Roeske 15ATW-29 3-7-2017-Spot 29 | 653 | 4106239 | 4.1 | 18.9 | 0.7 | 0.3 | 3.4 | 0.0 | 3.3 | 1.0 | 232.8 | 7.6 | 241.2 | 7.3 | 324.9 | 16.6 | 232.8 | 7.6 | NA |
| Roeske 15ATW-29 3-7-2017-Spot 4 | 115 | 50739 | 3.5 | 20.2 | 2.4 | 0.3 | 4.0 | 0.0 | 3.2 | 0.8 | 238.2 | 7.4 | 232.4 | 8.3 | 174.8 | 55.7 | 238.2 | 7.4 | NA |
| Roeske 15ATW-29 3-7-2017-Spot 238 | 369 | 117334 | 1.7 | 19.1 | 1.1 | 0.3 | 3.0 | 0.0 | 2.8 | 0.9 | 242.4 | 6.7 | 247.6 | 6.6 | 298.1 | 24.2 | 242.4 | 6.7 | NA |
| Roeske 15ATW-29 3-7-2017-Spot 303 | 60 | 42899 | 4.3 | 19.6 | 2.3 | 0.3 | 3.6 | 0.0 | 2.8 | 0.8 | 243.0 | 6.8 | 242.9 | 7.9 | 243.2 | 52.9 | 243.0 | 6.8 | NA |
| Roeske 15ATW-29 3-7-2017-Spot 212 | 35 | 24200 | 2.0 | 19.3 | 4.0 | 0.3 | 5.5 | 0.0 | 3.8 | 0.7 | 255.3 | 9.4 | 257.3 | 12.5 | 276.9 | 91.1 | 255.3 | 9.4 | NA |
| Roeske 15ATW29A 8Mar16-Sample 1 Spot 53 | 13 | 2064 | 1.7 | 19.3 | 3.3 | 0.3 | 6.6 | 0.0 | 5.7 | 0.9 | 261.3 | 14.6 | 262.6 | 15.3 | 274.5 | 76.5 | 261.3 | 14.6 | NA |
| Roeske 15ATW29A 8Mar16-Sample 1 Spot 51 | 197 | 16260 | 3.2 | 18.6 | 1.0 | 0.3 | 6.1 | 0.0 | 6.0 | 1.0 | 261.9 | 15.4 | 272.4 | 14.5 | 363.7 | 21.7 | 261.9 | 15.4 | NA |
| Roeske 15ATW-29 3-7-2017-Spot 207 | 430 | 75323 | 3.0 | 18.8 | 1.5 | 0.3 | 2.5 | 0.0 | 2.0 | 0.8 | 264.4 | 5.1 | 272.3 | 5.9 | 342.4 | 33.1 | 264.4 | 5.1 | NA |
| Roeske 15ATW29A 8Mar16-Sample 1 Spot 33 | 28 | 2427 | 2.3 | 17.3 | 6.9 | 0.3 | 9.4 | 0.0 | 6.3 | 0.7 | 266.7 | 16.5 | 294.5 | 24.0 | 521.3 | 152.2 | 266.7 | 16.5 | NA |
| Roeske 15ATW29A 8Mar16-Sample 1 Spot 70 | 563 | 76054 | 2.5 | 18.7 | 0.9 | 0.3 | 1.9 | 0.0 | 1.7 | 0.9 | 271.0 | 4.5 | 279.4 | 4.7 | 350.0 | 19.7 | 271.0 | 4.5 | NA |
| Roeske 15ATW-29 3-7-2017-Spot 268 | 193 | 112328 | 0.7 | 18.7 | 1.5 | 0.3 | 2.7 | 0.0 | 2.3 | 0.8 | 274.8 | 6.2 | 283.1 | 6.7 | 353.1 | 33.2 | 274.8 | 6.2 | NA |
| Roeske 15ATW-29 3-7-2017-Spot 199 | 1359 | 26354292 | 3.3 | 19.3 | 0.9 | 0.3 | 2.7 | 0.0 | 2.5 | 0.9 | 279.1 | 6.8 | 279.0 | 6.5 | 279.0 | 20.8 | 279.1 | 6.8 | NA |
| Roeske 15ATW-29 3-7-2017-Spot 31 | 136 | 377481 | 1.8 | 18.9 | 1.7 | 0.3 | 2.7 | 0.0 | 2.1 | 0.8 | 280.5 | 5.7 | 285.2 | 6.6 | 325.1 | 38.2 | 280.5 | 5.7 | NA |
| Roeske 15ATW-29 3-7-2017-Spot 191 | 1901 | 398551 | 7.2 | 18.5 | 1.2 | 0.3 | 3.3 | 0.0 | 3.1 | 0.9 | 280.9 | 8.4 | 290.3 | 8.3 | 367.6 | 26.8 | 280.9 | 8.4 | NA |
| Roeske 15ATW-29 3-7-2017-Spot 42 | 66 | 22246 | 3.8 | 19.9 | 2.4 | 0.3 | 3.4 | 0.0 | 2.3 | 0.7 | 282.0 | 6.4 | 273.5 | 8.1 | 203.1 | 56.3 | 282.0 | 6.4 | NA |
| Roeske 15ATW-29 3-7-2017-Spot 86 | 777 | 102334 | 2.1 | 19.1 | 0.8 | 0.3 | 2.6 | 0.0 | 2.4 | 0.9 | 284.7 | 6.8 | 285.7 | 6.4 | 295.2 | 18.3 | 284.7 | 6.8 | NA |
| Roeske 15ATW29A 8Mar16-Sample 1 Spot 3 | 1116 | 248523 | 2.2 | 19.1 | 0.6 | 0.3 | 1.7 | 0.0 | 1.6 | 0.9 | 286.1 | 4.5 | 287.7 | 4.3 | 300.5 | 12.6 | 286.1 | 4.5 | NA |
| Roeske 15ATW32 8Mar16-Spot 3 | 626 | 61203 | 4.0 | 18.6 | 0.9 | 0.4 | 2.1 | 0.0 | 1.9 | 0.9 | 314.4 | 5.9 | 319.7 | 5.8 | 358.6 | 20.6 | 314.4 | 5.9 | NA |
| Roeske 15ATW-29 3-7-2017-Spot 296 | 169 | 28145 | 2.0 | 17.9 | 1.8 | 0.4 | 3.0 | 0.1 | 2.4 | 0.8 | 322.9 | 7.5 | 338.5 | 8.6 | 448.1 | 40.0 | 322.9 | 7.5 | NA |
| Roeske 15ATW32 8Mar16-Spot 56 | 577 | 1690001 | 1.8 | 18.4 | 0.9 | 0.4 | 2.4 | 0.1 | 2.2 | 0.9 | 323.2 | 6.9 | 330.3 | 6.6 | 380.7 | 19.3 | 323.2 | 6.9 | NA |
| Roeske 15ATW-29 3-7-2017-Spot 240 | 447 | 170678 | 3.0 | 18.2 | 1.2 | 0.4 | 3.0 | 0.1 | 2.7 | 0.9 | 331.2 | 8.7 | 340.4 | 8.5 | 404.9 | 27.2 | 331.2 | 8.7 | NA |
| Roeske 15ATW32 8Mar16-Spot 35 | 509 | 56167 | 2.2 | 18.2 | 0.9 | 0.4 | 2.4 | 0.1 | 2.2 | 0.9 | 335.6 | 7.1 | 344.6 | 6.9 | 405.5 | 21.1 | 335.6 | 7.1 | NA |
| Roeske 15ATW32 8Mar16-Spot 36 | 619 | 100394 | 3.1 | 16.4 | 0.9 | 0.5 | 3.1 | 0.1 | 3.0 | 1.0 | 338.2 | 9.7 | 379.6 | 9.8 | 640.8 | 18.9 | 338.2 | 9.7 | NA |
| Roeske 15ATW-29 3-7-2017-Spot 17 | 284 | 269216 | 1.3 | 18.8 | 0.9 | 0.4 | 3.1 | 0.1 | 3.0 | 1.0 | 342.0 | 10.0 | 341.3 | 9.0 | 337.3 | 19.6 | 342.0 | 10.0 | NA |
| Roeske 15ATW29A 8Mar16-Sample 1 Spot 62 | 96 | 14004 | 4.6 | 18.5 | 1.6 | 0.4 | 3.2 | 0.1 | 2.8 | 0.9 | 342.1 | 9.3 | 345.6 | 9.4 | 369.4 | 35.8 | 342.1 | 9.3 | NA |
| Roeske 15ATW-29 3-7-2017-Spot 18 | 634 | 194021 | 1.8 | 18.5 | 1.3 | 0.4 | 2.5 | 0.1 | 2.2 | 0.9 | 344.4 | 7.3 | 348.0 | 7.4 | 373.5 | 29.3 | 344.4 | 7.3 | NA |
| Roeske 15ATW-29 3-7-2017-Spot 157 | 518 | 149828 | 1.8 | 18.7 | 0.8 | 0.4 | 2.8 | 0.1 | 2.7 | 1.0 | 348.2 | 9.2 | 347.6 | 8.4 | 344.5 | 19.1 | 348.2 | 9.2 | NA |
| Roeske 15ATW32 8Mar16-Spot 27 | 1014 | 50722 | 2.0 | 18.7 | 0.7 | 0.4 | 2.0 | 0.1 | 1.9 | 0.9 | 348.7 | 6.3 | 348.1 | 5.9 | 343.8 | 16.7 | 348.7 | 6.3 | NA |
| Roeske 15ATW-29 3-7-2017-Spot 111 | 980 | 341147 | 1.1 | 18.8 | 0.9 | 0.4 | 2.3 | 0.1 | 2.1 | 0.9 | 350.9 | 7.1 | 348.4 | 6.8 | 332.3 | 21.2 | 350.9 | 7.1 | NA |
| Roeske 15ATW-29 3-7-2017-Spot 87 | 432 | 335898 | 1.5 | 18.6 | 0.8 | 0.4 | 2.8 | 0.1 | 2.7 | 1.0 | 351.2 | 9.3 | 352.6 | 8.4 | 362.8 | 18.6 | 351.2 | 9.3 | NA |

| | | | | | | | | | | | | | | | | | | |
|---|---|---|---|---|---|---|---|---|---|---|---|---|---|---|---|---|---|---|
| Roeske 15ATW-29 3-7-2017-Spot 75 | 548 | 116298 | 2.2 | 18.5 | 0.9 | 0.4 | 2.5 | 0.1 | 2.3 | 0.9 | 351.8 | 7.9 | 354.3 | 7.4 | 371.9 | 19.5 | 351.8 | 7.9 | NA |
| Roeske 15ATW-29 3-7-2017-Spot 167 | 540 | 183569 | 0.4 | 18.1 | 1.0 | 0.4 | 2.5 | 0.1 | 2.3 | 0.9 | 352.3 | 8.0 | 361.0 | 7.7 | 417.9 | 23.1 | 352.3 | 8.0 | NA |
| Roeske 15ATW-29 3-7-2017-Spot 142 | 216 | 147228 | 1.5 | 18.8 | 1.1 | 0.4 | 2.3 | 0.1 | 2.1 | 0.9 | 353.1 | 7.1 | 350.2 | 6.9 | 331.6 | 25.4 | 353.1 | 7.1 | NA |
| Roeske 15ATW-29 3-7-2017-Spot 145 | 273 | 75557 | 2.0 | 18.2 | 1.1 | 0.4 | 3.0 | 0.1 | 2.8 | 0.9 | 354.4 | 9.7 | 361.4 | 9.2 | 407.2 | 23.9 | 354.4 | 9.7 | NA |
| Roeske 15ATW-29 3-7-2017-Spot 105 | 877 | 431412 | 1.3 | 18.7 | 1.0 | 0.4 | 2.6 | 0.1 | 2.4 | 0.9 | 360.2 | 8.5 | 359.0 | 7.9 | 351.8 | 22.5 | 360.2 | 8.5 | NA |
| Roeske 15ATW-29 3-7-2017-Spot 305 | 324 | 62179 | 2.8 | 18.8 | 1.4 | 0.4 | 2.6 | 0.1 | 2.2 | 0.8 | 360.9 | 7.6 | 357.7 | 7.7 | 337.8 | 30.7 | 360.9 | 7.6 | NA |
| Roeske 15ATW-29 3-7-2017-Spot 272 | 660 | 131200 | 1.8 | 18.8 | 1.1 | 0.4 | 2.9 | 0.1 | 2.7 | 0.9 | 362.6 | 9.5 | 359.3 | 8.8 | 339.2 | 24.8 | 362.6 | 9.5 | NA |
| Roeske 15ATW-29 3-7-2017-Spot 267 | 744 | 173268 | 2.1 | 18.3 | 0.9 | 0.4 | 2.7 | 0.1 | 2.5 | 0.9 | 363.1 | 8.8 | 366.9 | 8.2 | 391.9 | 20.9 | 363.1 | 8.8 | NA |
| Roeske 15ATW-29 3-7-2017-Spot 59 | 199 | 393911 | 1.8 | 18.6 | 1.3 | 0.4 | 2.4 | 0.1 | 2.1 | 0.9 | 363.1 | 7.4 | 362.9 | 7.5 | 362.7 | 29.0 | 363.1 | 7.4 | NA |
| Roeske 15ATW-29 3-7-2017-Spot 129 | 534 | 148617 | 2.0 | 18.6 | 1.0 | 0.4 | 3.0 | 0.1 | 2.8 | 0.9 | 363.3 | 9.8 | 362.7 | 9.0 | 359.6 | 22.8 | 363.3 | 9.8 | NA |
| Roeske 15ATW-29 3-7-2017-Spot 84 | 672 | 581529 | 1.0 | 18.8 | 1.2 | 0.4 | 2.7 | 0.1 | 2.5 | 0.9 | 369.5 | 8.9 | 364.4 | 8.4 | 333.0 | 27.1 | 369.5 | 8.9 | NA |
| Roeske 15ATW32 8Mar16-Spot 17 | 180 | 19030 | 1.2 | 17.9 | 0.9 | 0.5 | 2.5 | 0.1 | 2.4 | 0.9 | 412.9 | 9.5 | 417.3 | 8.6 | 441.5 | 19.1 | 412.9 | 9.5 | 93.5 |
| Roeske 15ATW-29 3-7-2017-Spot 39 | 300 | 411974 | 1.5 | 18.0 | 1.2 | 0.5 | 3.0 | 0.1 | 2.8 | 0.9 | 437.2 | 11.8 | 437.6 | 10.8 | 440.3 | 26.4 | 437.2 | 11.8 | 99.3 |
| Roeske 15ATW-29 3-7-2017-Spot 107 | 557 | 361208 | 3.0 | 17.7 | 1.1 | 0.6 | 3.1 | 0.1 | 2.9 | 0.9 | 483.5 | 13.5 | 482.3 | 11.8 | 477.4 | 23.9 | 483.5 | 13.5 | 101.3 |
| Roeske 15ATW-29 3-7-2017-Spot 226 | 441 | 397179 | 12.7 | 16.0 | 1.0 | 1.0 | 2.3 | 0.1 | 2.1 | 0.9 | 701.1 | 13.9 | 697.9 | 11.7 | 688.3 | 20.7 | 701.1 | 13.9 | 101.9 |
| Roeske 15ATW-29 3-7-2017-Spot 254 | 51 | 57541 | 1.9 | 12.6 | 1.2 | 2.1 | 2.9 | 0.2 | 2.7 | 0.9 | 1119.1 | 27.4 | 1137.7 | 19.9 | 1174.2 | 23.1 | 1174.2 | 23.1 | 95.3 |
| Roeske 15ATW-29 3-7-2017-Spot 198 | 84 | 297906 | 1.0 | 11.3 | 1.0 | 2.8 | 2.8 | 0.2 | 2.7 | 0.9 | 1338.7 | 32.0 | 1360.0 | 21.1 | 1394.6 | 18.4 | 1394.6 | 18.4 | 96.0 |
| Roeske 15ATW-29 3-7-2017-Spot 300 | 620 | 1661688 | 1.7 | 10.8 | 0.9 | 3.0 | 2.5 | 0.2 | 2.3 | 0.9 | 1378.0 | 28.8 | 1418.3 | 19.0 | 1480.3 | 16.9 | 1480.3 | 16.9 | 93.1 |
| Roeske 15ATW32 8Mar16-Spot 15 | 158 | 406939 | 1.0 | 9.4 | 0.7 | 4.1 | 2.7 | 0.3 | 2.6 | 1.0 | 1569.7 | 36.5 | 1645.0 | 22.0 | 1742.5 | 12.5 | 1742.5 | 12.5 | 90.1 |
| Roeske 15ATW32 8Mar16-Spot 4 | 888 | 494582 | 3.0 | 9.1 | 0.7 | 4.3 | 2.0 | 0.3 | 1.9 | 0.9 | 1619.2 | 26.7 | 1696.8 | 16.3 | 1794.0 | 11.8 | 1794.0 | 11.8 | 90.3 |
| Roeske 15ATW-29 3-7-2017-Spot 35 | 76 | 224059 | 0.8 | 9.0 | 0.9 | 4.7 | 2.8 | 0.3 | 2.7 | 0.9 | 1744.2 | 40.8 | 1773.1 | 23.6 | 1808.2 | 16.2 | 1808.2 | 16.2 | 96.5 |
| Roeske 15ATW-29 3-7-2017-Spot 124 | 320 | 571485 | 1.4 | 9.0 | 0.9 | 5.1 | 2.4 | 0.3 | 2.2 | 0.9 | 1839.6 | 35.4 | 1831.1 | 20.1 | 1822.2 | 15.5 | 1822.2 | 15.5 | 101.0 |
| Roeske 15ATW-29 3-7-2017-Spot 85 | 132 | 330053 | 3.4 | 8.9 | 1.2 | 4.7 | 3.0 | 0.3 | 2.7 | 0.9 | 1717.0 | 41.1 | 1769.5 | 24.9 | 1832.9 | 21.4 | 1832.9 | 21.4 | 93.7 |
| Roeske 15ATW-29 3-7-2017-Spot 6 | 63 | 65063 | 0.8 | 8.6 | 1.2 | 5.3 | 2.4 | 0.3 | 2.1 | 0.9 | 1838.4 | 33.2 | 1862.8 | 20.4 | 1891.0 | 21.4 | 1891.0 | 21.4 | 97.2 |
| Roeske 15ATW32 8Mar16-Spot 59 | 121 | 694244 | 1.4 | 8.4 | 0.7 | 5.6 | 2.2 | 0.3 | 2.1 | 0.9 | 1892.2 | 34.3 | 1911.8 | 19.1 | 1933.3 | 13.4 | 1933.3 | 13.4 | 97.9 |
| Roeske 15ATW-29 3-7-2017-Spot 131 | 103 | 165046 | 1.0 | 8.2 | 1.0 | 6.1 | 2.6 | 0.4 | 2.4 | 0.9 | 1983.2 | 40.5 | 1987.2 | 22.3 | 1992.2 | 16.9 | 1992.2 | 16.9 | 99.5 |
| Roeske 15ATW-29 3-7-2017-Spot 213 | 207 | 227009 | 0.8 | 8.1 | 1.1 | 6.1 | 2.7 | 0.4 | 2.5 | 0.9 | 1976.1 | 42.5 | 1990.9 | 23.8 | 2007.1 | 19.6 | 2007.1 | 19.6 | 98.5 |
| Roeske 15ATW-29 3-7-2017-Spot 80 | 81 | 151248 | 0.9 | 7.7 | 0.9 | 7.0 | 2.5 | 0.4 | 2.4 | 0.9 | 2122.3 | 42.7 | 2110.5 | 22.4 | 2099.8 | 15.4 | 2099.8 | 15.4 | 101.1 |
| Roeske 15ATW-29 3-7-2017-Spot 15 | 68 | 160490 | 1.1 | 7.0 | 0.8 | 8.0 | 2.4 | 0.4 | 2.2 | 0.9 | 2203.7 | 41.5 | 2233.6 | 21.4 | 2261.9 | 14.4 | 2261.9 | 14.4 | 97.4 |
| Roeske 15ATW-29 3-7-2017-Spot 183 | 271 | 672601 | 1.0 | 6.9 | 0.7 | 7.1 | 3.4 | 0.4 | 3.3 | 1.0 | 1954.2 | 55.6 | 2122.9 | 30.1 | 2291.3 | 12.6 | 2291.3 | 12.6 | 85.3 |
| Roeske 15ATW-29 3-7-2017-Spot 1 | 323 | 1129250 | 1.4 | 6.8 | 0.9 | 8.5 | 4.0 | 0.4 | 3.9 | 1.0 | 2247.4 | 74.1 | 2284.6 | 36.4 | 2318.7 | 15.0 | 2318.7 | 15.0 | 96.9 |
| Roeske 15ATW-29 3-7-2017-Spot 10 | 389 | 4597435 | 2.1 | 6.5 | 1.0 | 8.4 | 2.2 | 0.4 | 1.9 | 0.9 | 2145.1 | 35.0 | 2278.6 | 19.6 | 2401.3 | 17.0 | 2401.3 | 17.0 | 89.3 |
| Roeske 15ATW-29 3-7-2017-Spot 217 | 195 | 540248 | 2.1 | 5.9 | 0.9 | 11.0 | 2.4 | 0.5 | 2.2 | 0.9 | 2487.9 | 44.8 | 2524.1 | 21.9 | 2554.0 | 15.2 | 2554.0 | 15.2 | 97.4 |
| Roeske 15ATW-29 3-7-2017-Spot 259 | 167 | 335123 | 1.2 | 5.7 | 0.8 | 12.0 | 1.9 | 0.5 | 1.8 | 0.9 | 2596.0 | 37.8 | 2604.7 | 18.3 | 2612.1 | 13.6 | 2612.1 | 13.6 | 99.4 |
| Roeske 15ATW-29 3-7-2017-Spot 243 | 84 | 1537785 | 1.5 | 5.1 | 0.7 | 14.3 | 2.3 | 0.5 | 2.2 | 1.0 | 2733.1 | 48.4 | 2770.9 | 21.7 | 2799.2 | 11.3 | 2799.2 | 11.3 | 97.6 |
| Roeske 15ATW-29 3-7-2017-Spot 197 | 253 | 27965 | 1.6 | 19.1 | 1.6 | 0.1 | 2.8 | 0.0 | 2.3 | 0.8 | 96.3 | 2.2 | 104.9 | 2.8 | 304.9 | 37.0 | 96.3 | 2.2 | NA |
| Roeske 15ATW-29 3-7-2017-Spot 122 | 61 | 4670 | 2.0 | 19.2 | 4.8 | 0.1 | 6.1 | 0.0 | 3.7 | 0.6 | 90.7 | 3.3 | 98.4 | 5.7 | 289.5 | 110.0 | 90.7 | 3.3 | NA |
| Roeske 15ATW-29 3-7-2017-Spot 65 | 87 | 7355 | 2.5 | 19.2 | 3.1 | 0.1 | 4.3 | 0.0 | 3.0 | 0.7 | 88.4 | 2.7 | 96.2 | 4.0 | 294.0 | 70.4 | 88.4 | 2.7 | NA |
| Roeske 15ATW-29 3-7-2017-Spot 171 | 85 | 16670 | 2.0 | 19.2 | 3.3 | 0.1 | 4.7 | 0.0 | 3.3 | 0.7 | 87.7 | 2.9 | 95.4 | 4.2 | 293.0 | 74.7 | 87.7 | 2.9 | NA |
| Roeske 15ATW-29 3-7-2017-Spot 60 | 144 | 158435 | 1.5 | 19.0 | 2.7 | 0.1 | 3.7 | 0.0 | 2.5 | 0.7 | 87.4 | 2.2 | 95.8 | 3.4 | 310.7 | 62.5 | 87.4 | 2.2 | NA |

| | | | | | | | | | | | | | | | | | | | |
|---|---|---|---|---|---|---|---|---|---|---|---|---|---|---|---|---|---|---|---|
| Roeske 15ATW-29 3-7-2017-Spot 203 | 1180 | 50988 | 9.3 | 19.0 | 2.3 | 0.1 | 3.4 | 0.0 | 2.6 | 0.7 | 89.1 | 2.3 | 97.9 | 3.2 | 318.1 | 51.8 | 89.1 | 2.3 | NA |
| Roeske 15ATW-29 3-7-2017-Spot 99 | 165 | 13922 | 1.9 | 19.0 | 2.7 | 0.1 | 3.7 | 0.0 | 2.5 | 0.7 | 87.7 | 2.1 | 96.3 | 3.4 | 317.0 | 61.6 | 87.7 | 2.1 | NA |
| Roeske 15ATW-29 3-7-2017-Spot 128 | 192 | 34157 | 2.3 | 15.5 | 2.5 | 0.3 | 3.7 | 0.0 | 2.7 | 0.7 | 203.6 | 5.3 | 254.9 | 8.3 | 758.2 | 53.3 | 203.6 | 5.3 | NA |
| Roeske 15ATW-29 3-7-2017-Spot 79 | 50 | 6192 | 2.7 | 18.8 | 3.8 | 0.1 | 5.1 | 0.0 | 3.4 | 0.7 | 88.5 | 2.9 | 97.8 | 4.7 | 331.4 | 86.7 | 88.5 | 2.9 | NA |
| Roeske 15ATW-29 3-7-2017-Spot 279 | 135 | 9986 | 2.1 | 18.3 | 4.9 | 0.1 | 6.2 | 0.0 | 3.8 | 0.6 | 101.8 | 3.8 | 115.1 | 6.8 | 400.6 | 110.5 | 101.8 | 3.8 | NA |
| Roeske 15ATW-29 3-7-2017-Spot 54 | 92 | 69907 | 1.6 | 18.5 | 3.4 | 0.1 | 4.2 | 0.0 | 2.5 | 0.6 | 91.1 | 2.2 | 102.2 | 4.0 | 370.7 | 75.6 | 91.1 | 2.2 | NA |
| Roeske 15ATW-29 3-7-2017-Spot 262 | 140 | 6503 | 2.4 | 18.5 | 2.2 | 0.1 | 3.3 | 0.0 | 2.5 | 0.7 | 89.0 | 2.2 | 99.9 | 3.2 | 370.0 | 50.6 | 89.0 | 2.2 | NA |
| Roeske 15ATW-29 3-7-2017-Spot 47 | 286 | 28130 | 1.1 | 18.1 | 3.3 | 0.1 | 3.9 | 0.0 | 2.1 | 0.5 | 95.3 | 2.0 | 109.3 | 4.0 | 426.8 | 72.6 | 95.3 | 2.0 | NA |
| Roeske 15ATW-29 3-7-2017-Spot 146 | 153 | 61764 | 1.3 | 18.0 | 2.9 | 0.1 | 4.0 | 0.0 | 2.8 | 0.7 | 92.1 | 2.6 | 105.8 | 4.1 | 428.7 | 64.5 | 92.1 | 2.6 | NA |
| Roeske 15ATW-29 3-7-2017-Spot 231 | 46 | 2146 | 2.6 | 17.6 | 7.4 | 0.1 | 8.0 | 0.0 | 2.9 | 0.4 | 92.6 | 2.6 | 109.2 | 8.3 | 489.5 | 164.4 | 92.6 | 2.6 | NA |
| Roeske 15ATW-29 3-7-2017-Spot 315 | 493 | 29460 | 1.4 | 16.7 | 3.4 | 0.1 | 4.9 | 0.0 | 3.5 | 0.7 | 110.7 | 3.8 | 135.3 | 6.2 | 592.8 | 74.6 | 110.7 | 3.8 | NA |
| Roeske 15ATW-29 3-7-2017-Spot 56 | 127 | 38831 | 1.2 | 17.3 | 3.5 | 0.1 | 4.5 | 0.0 | 2.9 | 0.6 | 90.5 | 2.6 | 108.4 | 4.6 | 522.5 | 76.6 | 90.5 | 2.6 | NA |
| Roeske 15ATW-29 3-7-2017-Spot 121 | 119 | 7689 | 2.0 | 17.1 | 2.7 | 0.1 | 4.4 | 0.0 | 3.5 | 0.8 | 91.2 | 3.2 | 110.1 | 4.6 | 542.1 | 58.2 | 91.2 | 3.2 | NA |
| Roeske 15ATW-29 3-7-2017-Spot 178 | 82 | 61926 | 1.8 | 16.9 | 4.0 | 0.1 | 5.2 | 0.0 | 3.3 | 0.6 | 91.7 | 3.0 | 112.0 | 5.5 | 569.9 | 87.9 | 91.7 | 3.0 | NA |
| Roeske 15ATW-29 3-7-2017-Spot 232 | 845 | 349027 | 11.2 | 14.7 | 1.6 | 0.2 | 3.0 | 0.0 | 2.5 | 0.8 | 135.3 | 3.4 | 183.7 | 5.0 | 863.7 | 33.1 | 135.3 | 3.4 | NA |
| Roeske 15ATW-29 3-7-2017-Spot 132 | 572 | 29358 | 1.1 | 15.7 | 3.4 | 0.1 | 4.3 | 0.0 | 2.6 | 0.6 | 89.9 | 2.3 | 118.0 | 4.7 | 731.8 | 71.8 | 89.9 | 2.3 | NA |
| Roeske 15ATW-29 3-7-2017-Spot 309 | 52 | 11133 | 2.5 | 15.2 | 4.0 | 0.1 | 4.8 | 0.0 | 2.8 | 0.6 | 93.4 | 2.6 | 126.5 | 5.8 | 805.6 | 83.0 | 93.4 | 2.6 | NA |
| Roeske 15ATW-29 3-7-2017-Spot 224 | 78 | 9049 | 2.8 | 13.8 | 8.7 | 0.1 | 9.3 | 0.0 | 3.3 | 0.4 | 93.6 | 3.1 | 138.5 | 12.0 | 1000.2 | 176.8 | 93.6 | 3.1 | NA |
| Roeske 15ATW-29 3-7-2017-Spot 245 | 69 | 3373 | 2.1 | 13.4 | 3.6 | 0.2 | 4.9 | 0.0 | 3.4 | 0.7 | 94.5 | 3.1 | 144.0 | 6.6 | 1065.0 | 71.6 | 94.5 | 3.1 | NA |
| Roeske 15ATW-29 3-7-2017-Spot 252 | 222 | 7236 | 3.5 | 9.1 | 3.4 | 0.3 | 4.0 | 0.0 | 2.1 | 0.5 | 111.7 | 2.3 | 237.7 | 8.4 | 1791.6 | 61.9 | 111.7 | 2.3 | NA |
| Roeske 15ATW-29 3-7-2017-Spot 188 | 179 | 3569 | 1.5 | 5.3 | 8.0 | 0.4 | 10.1 | 0.0 | 6.2 | 0.6 | 109.7 | 6.7 | 374.2 | 31.7 | 2728.1 | 132.3 | 109.7 | 6.7 | NA |
| Roeske 15ATW32 8Mar16-Spot 18 | 118 | 10958 | 1.6 | 10.1 | 2.4 | 2.9 | 3.7 | 0.2 | 2.9 | 0.8 | 1248.4 | 32.4 | 1389.9 | 28.2 | 1614.2 | 44.5 | 1614.2 | 44.5 | 77.3 |
| Roeske 15ATW32 8Mar16-Spot 2 | 181 | 2701668 | 2.1 | 9.4 | 0.8 | 3.3 | 4.2 | 0.2 | 4.1 | 1.0 | 1306.3 | 48.8 | 1482.1 | 32.8 | 1743.7 | 14.8 | 1743.7 | 14.8 | 74.9 |
| Roeske 15ATW32 8Mar16-Spot 30 | 1296 | 345390 | 3.5 | 9.0 | 0.8 | 1.9 | 5.8 | 0.1 | 5.8 | 1.0 | 758.3 | 41.3 | 1082.7 | 38.8 | 1810.1 | 14.8 | 1810.1 | 14.8 | 41.9 |
| Roeske 15ATW32 8Mar16-Spot 12 | 550 | 61432 | 3.1 | 6.7 | 0.9 | 6.8 | 2.3 | 0.3 | 2.1 | 0.9 | 1846.1 | 33.8 | 2083.3 | 20.4 | 2326.8 | 16.2 | 2326.8 | 16.2 | 79.3 |
| Roeske 15ATW32 8Mar16-Spot 31 | 588 | 30272 | 4.9 | 7.8 | 0.6 | 2.2 | 5.2 | 0.1 | 5.2 | 1.0 | 770.9 | 37.9 | 1192.5 | 36.8 | 2066.3 | 10.8 | 2066.3 | 10.8 | 37.3 |
| Roeske 15ATW32 8Mar16-Spot 32 | 1007 | 12114 | 8.4 | 8.8 | 2.5 | 1.5 | 15.1 | 0.1 | 14.9 | 1.0 | 576.1 | 81.9 | 917.6 | 91.3 | 1863.2 | 45.0 | 1863.2 | 45.0 | 30.9 |
| Roeske 15ATW32 8Mar16-Spot 47 | 290 | 22430 | 2.2 | 16.1 | 1.2 | 0.3 | 2.4 | 0.0 | 2.1 | 0.9 | 200.3 | 4.1 | 242.9 | 5.2 | 678.5 | 26.2 | 200.3 | 4.1 | NA |
| Roeske 15ATW32 8Mar16-Spot 39 | 808 | 18076 | 13.6 | 19.0 | 1.4 | 0.1 | 2.5 | 0.0 | 2.0 | 0.8 | 90.9 | 1.8 | 99.5 | 2.3 | 310.0 | 32.9 | 90.9 | 1.8 | NA |
| Roeske 15ATW32 8Mar16-Spot 13 | 237 | 8717 | 7.0 | 18.6 | 2.9 | 0.1 | 4.3 | 0.0 | 3.1 | 0.7 | 90.4 | 2.8 | 101.2 | 4.1 | 362.6 | 64.9 | 90.4 | 2.8 | NA |
| Roeske 15ATW32 8Mar16-Spot 21 | 1210 | 16211 | 7.6 | 14.3 | 5.6 | 0.3 | 6.9 | 0.0 | 4.0 | 0.6 | 201.3 | 7.9 | 271.0 | 16.3 | 927.0 | 114.9 | 201.3 | 7.9 | NA |
| Roeske 15ATW32 8Mar16-Spot 54 | 766 | 1370261 | 17.6 | 18.3 | 2.5 | 0.1 | 4.2 | 0.0 | 3.4 | 0.8 | 79.5 | 2.7 | 90.5 | 3.7 | 392.3 | 55.0 | 79.5 | 2.7 | NA |
| Roeske 15ATW32 8Mar16-Spot 19 | 2476 | 5487 | 2.7 | 13.2 | 5.4 | 0.4 | 7.0 | 0.0 | 4.4 | 0.6 | 213.4 | 9.3 | 304.9 | 18.4 | 1081.1 | 108.9 | 213.4 | 9.3 | NA |
| Roeske 15ATW32 8Mar16-Spot 50 | 2723 | 14341 | 147.0 | 17.5 | 2.7 | 0.1 | 3.1 | 0.0 | 1.6 | 0.5 | 88.8 | 1.4 | 105.5 | 3.2 | 499.6 | 59.3 | 88.8 | 1.4 | NA |
| Roeske 15ATW32 8Mar16-Spot 44 | 271 | 74676 | 44.1 | 16.6 | 4.6 | 0.1 | 14.3 | 0.0 | 13.5 | 0.9 | 104.3 | 14.0 | 129.0 | 17.3 | 613.0 | 100.1 | 104.3 | 14.0 | NA |
| Roeske 15ATW32 8Mar16-Spot 25 | 1209 | 7236 | 7.2 | 13.8 | 5.4 | 0.2 | 6.9 | 0.0 | 4.3 | 0.6 | 127.2 | 5.4 | 184.8 | 11.6 | 1005.0 | 109.6 | 127.2 | 5.4 | NA |
| Roeske 15ATW32 8Mar16-Spot 40 | 274 | 7707 | 13.9 | 13.5 | 4.3 | 0.2 | 8.0 | 0.0 | 6.8 | 0.8 | 100.6 | 6.8 | 151.1 | 11.3 | 1041.8 | 85.9 | 100.6 | 6.8 | NA |
| Roeske 15ATW32 8Mar16-Spot 48 | 492 | 2059 | 13.4 | 6.4 | 18.2 | 0.5 | 38.5 | 0.0 | 33.9 | 0.9 | 149.5 | 50.2 | 414.6 | 131.8 | 2411.7 | 312.1 | 149.5 | 50.2 | NA |
| Roeske 15ATW32 8Mar16-Spot 26 | 1124 | 708 | 7.0 | 8.3 | 7.1 | 0.2 | 9.8 | 0.0 | 6.7 | 0.7 | 94.9 | 6.4 | 223.8 | 19.7 | 1965.5 | 127.5 | 94.9 | 6.4 | NA |
| Roeske 15ATW32 8Mar16-Spot 6 | 144 | 950 | 4.3 | 5.9 | 3.5 | 0.4 | 5.3 | 0.0 | 3.9 | 0.7 | 115.4 | 4.5 | 358.0 | 15.9 | 2555.5 | 59.0 | 115.4 | 4.5 | NA |

| | | | | | | | | | | | | | | | | | | |
|---|---|---|---|---|---|---|---|---|---|---|---|---|---|---|---|---|---|---|
| Roeske 15ATW32 8Mar16-Spot 60 | 592 | 913 | 29.4 | 4.2 | 5.9 | 0.6 | 28.6 | 0.0 | 27.9 | 1.0 | 112.4 | 31.1 | 465.3 | 107.0 | 3118.3 | 94.6 | 112.4 | 31.1 | NA |
| Roeske 15ATW29A 8Mar16-Sample 1 Spot 14 | 250 | 7360 | 1.9 | 19.4 | 1.5 | 0.1 | 2.3 | 0.0 | 1.7 | 0.7 | 88.3 | 1.5 | 95.2 | 2.1 | 269.6 | 35.2 | 88.3 | 1.5 | NA |
| Roeske 15ATW29A 8Mar16-Sample 1 Spot 58 | 76 | 20840 | 2.0 | 19.4 | 2.6 | 0.1 | 3.7 | 0.0 | 2.6 | 0.7 | 86.1 | 2.2 | 92.6 | 3.3 | 265.2 | 59.3 | 86.1 | 2.2 | NA |
| Roeske 15ATW29A 8Mar16-Sample 1 Spot 56 | 97 | 5744 | 2.9 | 17.1 | 4.1 | 0.2 | 7.4 | 0.0 | 6.2 | 0.8 | 160.0 | 9.7 | 187.0 | 12.6 | 542.7 | 89.7 | 160.0 | 9.7 | NA |
| Roeske 15ATW29A 8Mar16-Sample 1 Spot 34 | 553 | 9847 | 5.9 | 18.7 | 2.5 | 0.1 | 3.7 | 0.0 | 2.7 | 0.7 | 84.2 | 2.3 | 94.1 | 3.3 | 354.5 | 56.3 | 84.2 | 2.3 | NA |
| Roeske 15ATW29A 8Mar16-Sample 1 Spot 47 | 348 | 8398 | 3.1 | 15.2 | 2.3 | 0.2 | 3.1 | 0.0 | 2.0 | 0.7 | 114.4 | 2.3 | 152.4 | 4.4 | 793.8 | 49.2 | 114.4 | 2.3 | NA |
| Roeske 15ATW29A 8Mar16-Sample 1 Spot 15 | 305 | 6062 | 2.9 | 19.4 | 2.3 | 0.2 | 10.4 | 0.0 | 10.1 | 1.0 | 181.8 | 18.1 | 187.7 | 17.8 | 261.9 | 52.4 | 181.8 | 18.1 | NA |
| Roeske 15ATW29A 8Mar16-Sample 1 Spot 52 | 354 | 8312 | 3.4 | 20.6 | 1.1 | 0.2 | 2.4 | 0.0 | 2.2 | 0.9 | 191.6 | 4.1 | 186.8 | 4.1 | 126.4 | 24.7 | 191.6 | 4.1 | NA |
| Roeske 15ATW-29 3-7-2017-Spot 25 | 157 | 15094 | 2.8 | 21.0 | 2.1 | 0.2 | 2.9 | 0.0 | 2.1 | 0.7 | 198.9 | 4.1 | 189.8 | 5.1 | 78.4 | 49.0 | 198.9 | 4.1 | NA |
| Roeske 15ATW-29 3-7-2017-Spot 281 | 154 | 6833 | 2.3 | 22.3 | 2.3 | 0.1 | 3.3 | 0.0 | 2.3 | 0.7 | 88.5 | 2.0 | 83.0 | 2.6 | NA | NA | 88.5 | 2.0 | NA |
| Roeske 15ATW-29 3-7-2017-Spot 125 | 138 | 10387 | 1.5 | 22.3 | 2.3 | 0.1 | 3.8 | 0.0 | 3.0 | 0.8 | 86.9 | 2.6 | 82.0 | 3.0 | NA | NA | 86.9 | 2.6 | NA |
| Roeske 15ATW29A 8Mar16-Sample 1 Spot 66 | 255 | 3200 | 1.3 | 22.7 | 1.9 | 0.1 | 2.7 | 0.0 | 2.0 | 0.7 | 83.9 | 1.6 | 77.7 | 2.0 | 108.9 | 45.6 | 83.9 | 1.6 | NA |
| Roeske 15ATW29A 8Mar16-Sample 1 Spot 65 | 35 | 415 | 2.8 | 58.7 | 7.2 | 0.0 | 7.8 | 0.0 | 3.0 | 0.4 | 86.0 | 2.6 | 31.6 | 2.4 | 0.0 | 1513.5 | 86.0 | 2.6 | NA |
| Roeske 15ATW29A 8Mar16-Sample 1 Spot 68 | 61 | 3925 | 3.4 | 21.7 | 2.3 | 0.2 | 3.9 | 0.0 | 3.1 | 0.8 | 154.1 | 4.7 | 145.4 | 5.3 | 5.3 | 56.3 | 154.1 | 4.7 | NA |

Sasmple 16ATW10

| Analysis | U | 206Pb | U/Th | 206Pb * | ± | 207Pb * | ± 1s | 206Pb * | ± 1s | error | 206Pb * | ± | 207Pb * | ± | 206Pb * | ± | Best age | ± (1s random) | Conc |
|---|---|---|---|---|---|---|---|---|---|---|---|---|---|---|---|---|---|---|---|
| | (ppm) | 204Pb | | 207Pb * | (%) | 235U * | (%) | 238U | (%) | corr. | 238U * | (Ma) | 235U | (Ma) | 207Pb * | (Ma) | (Ma) | (Ma) | (%) |
| 16ATW-10-Spot 40 | 68 | 34375 | 3.1 | 20.1 | 1.9 | 0.2 | 3.0 | 0.0 | 2.3 | 0.8 | 148.5 | 3.4 | 150.8 | 4.2 | 188.9 | 45.1 | 148.5 | 3.4 | NA |
| 16ATW-10-Spot 179 | 736 | 226841 | 19.9 | 20.3 | 1.1 | 0.2 | 2.4 | 0.0 | 2.1 | 0.9 | 149.1 | 3.2 | 149.8 | 3.3 | 161.5 | 25.1 | 149.1 | 3.2 | NA |
| 16ATW-10-Spot 295 | 56 | 23483 | 4.0 | 19.6 | 2.7 | 0.2 | 3.6 | 0.0 | 2.4 | 0.7 | 149.8 | 3.5 | 155.3 | 5.2 | 240.8 | 62.3 | 149.8 | 3.5 | NA |
| 16ATW-10-Spot 268 | 74 | 37272 | 2.5 | 20.9 | 1.8 | 0.2 | 3.0 | 0.0 | 2.4 | 0.8 | 150.5 | 3.6 | 146.7 | 4.1 | 88.0 | 42.3 | 150.5 | 3.6 | NA |
| 16ATW-10-Spot 132 | 32 | 8286 | 3.6 | 20.0 | 2.6 | 0.2 | 3.5 | 0.0 | 2.4 | 0.7 | 150.6 | 3.5 | 153.3 | 5.0 | 197.3 | 59.6 | 150.6 | 3.5 | NA |
| 16ATW-10-Spot 22 | 94 | 25892 | 1.5 | 20.5 | 1.8 | 0.2 | 3.1 | 0.0 | 2.6 | 0.8 | 150.8 | 3.8 | 150.3 | 4.3 | 143.0 | 41.5 | 150.8 | 3.8 | NA |
| 16ATW-10-Spot 237 | 22 | 10862 | 3.3 | 19.4 | 3.7 | 0.2 | 4.4 | 0.0 | 2.5 | 0.6 | 151.0 | 3.7 | 158.4 | 6.5 | 270.6 | 84.2 | 151.0 | 3.7 | NA |
| 16ATW-10-Spot 6 | 56 | 61561 | 4.3 | 19.8 | 2.1 | 0.2 | 3.3 | 0.0 | 2.6 | 0.8 | 151.5 | 3.9 | 155.8 | 4.8 | 223.0 | 49.5 | 151.5 | 3.9 | NA |
| 16ATW-10-Spot 284 | 75 | 20267 | 2.3 | 21.5 | 2.1 | 0.2 | 4.0 | 0.0 | 3.4 | 0.8 | 151.5 | 5.0 | 144.4 | 5.3 | 29.2 | 50.1 | 151.5 | 5.0 | NA |
| 16ATW-10-Spot 290 | 19 | 5517 | 3.0 | 20.5 | 4.2 | 0.2 | 5.1 | 0.0 | 2.9 | 0.6 | 151.6 | 4.3 | 150.7 | 7.2 | 136.3 | 99.2 | 151.6 | 4.3 | NA |
| 16ATW-10-Spot 173 | 177 | 41981 | 1.5 | 20.2 | 1.3 | 0.2 | 2.4 | 0.0 | 2.0 | 0.8 | 151.8 | 3.0 | 152.8 | 3.4 | 168.9 | 31.4 | 151.8 | 3.0 | NA |
| 16ATW-10-Spot 129 | 35 | 132485 | 2.3 | 20.3 | 2.8 | 0.2 | 4.2 | 0.0 | 3.2 | 0.8 | 151.8 | 4.8 | 152.2 | 6.0 | 158.1 | 64.5 | 151.8 | 4.8 | NA |
| 16ATW-10-Spot 299 | 64 | 21656 | 3.0 | 20.1 | 2.2 | 0.2 | 3.3 | 0.0 | 2.4 | 0.7 | 151.9 | 3.7 | 154.1 | 4.7 | 188.8 | 51.3 | 151.9 | 3.7 | NA |

| | | | | | | | | | | | | | | | | | | | |
|---|---|---|---|---|---|---|---|---|---|---|---|---|---|---|---|---|---|---|---|
| 16ATW-10-Spot 309 | 28 | 13160 | 2.8 | 20.8 | 2.9 | 0.2 | 3.8 | 0.0 | 2.5 | 0.7 | 152.0 | 3.8 | 148.9 | 5.3 | 100.2 | 68.1 | 152.0 | 3.8 | NA |
| 16ATW-10-Spot 4 | 81 | 50716 | 3.4 | 20.6 | 2.3 | 0.2 | 3.1 | 0.0 | 2.1 | 0.7 | 152.0 | 3.2 | 150.0 | 4.3 | 120.3 | 53.2 | 152.0 | 3.2 | NA |
| 16ATW-10-Spot 149 | 21 | 4991 | 3.6 | 19.7 | 4.5 | 0.2 | 5.3 | 0.0 | 2.8 | 0.5 | 152.0 | 4.3 | 157.0 | 7.7 | 234.3 | 103.1 | 152.0 | 4.3 | NA |
| 16ATW-10-Spot 69 | 36 | 7315 | 4.7 | 20.6 | 3.6 | 0.2 | 4.4 | 0.0 | 2.5 | 0.6 | 152.2 | 3.7 | 150.5 | 6.1 | 124.1 | 84.5 | 152.2 | 3.7 | NA |
| 16ATW-10-Spot 155 | 78 | 73491 | 2.5 | 20.3 | 1.8 | 0.2 | 2.8 | 0.0 | 2.2 | 0.8 | 152.2 | 3.3 | 152.3 | 4.0 | 155.0 | 41.5 | 152.2 | 3.3 | NA |
| 16ATW-10-Spot 277 | 29 | 114135 | 2.1 | 19.3 | 3.2 | 0.2 | 4.4 | 0.0 | 2.9 | 0.7 | 152.3 | 4.4 | 160.3 | 6.5 | 281.7 | 73.6 | 152.3 | 4.4 | NA |
| 16ATW-10-Spot 197 | 81 | 319940 | 2.0 | 19.7 | 1.6 | 0.2 | 2.7 | 0.0 | 2.2 | 0.8 | 152.4 | 3.3 | 156.9 | 4.0 | 226.8 | 37.8 | 152.4 | 3.3 | NA |
| 16ATW-10-Spot 275 | 39 | 60500 | 3.3 | 19.4 | 2.3 | 0.2 | 3.5 | 0.0 | 2.6 | 0.7 | 152.6 | 3.9 | 159.4 | 5.2 | 263.3 | 53.3 | 152.6 | 3.9 | NA |
| 16ATW-10-Spot 261 | 33 | 9082 | 3.3 | 20.7 | 2.5 | 0.2 | 3.9 | 0.0 | 3.0 | 0.8 | 152.7 | 4.6 | 150.4 | 5.5 | 114.7 | 59.3 | 152.7 | 4.6 | NA |
| 16ATW-10-Spot 158 | 38 | 24228 | 3.2 | 20.7 | 2.8 | 0.2 | 4.1 | 0.0 | 2.9 | 0.7 | 152.7 | 4.4 | 150.6 | 5.7 | 118.4 | 67.1 | 152.7 | 4.4 | NA |
| 16ATW-10-Spot 171 | 15 | 10738 | 6.4 | 20.9 | 4.0 | 0.2 | 5.6 | 0.0 | 3.9 | 0.7 | 152.7 | 5.9 | 149.1 | 7.7 | 92.8 | 93.8 | 152.7 | 5.9 | NA |
| 16ATW-10-Spot 126 | 30 | 8736 | 1.9 | 20.7 | 3.1 | 0.2 | 4.2 | 0.0 | 2.8 | 0.7 | 152.8 | 4.3 | 150.1 | 5.9 | 109.4 | 72.9 | 152.8 | 4.3 | NA |
| 16ATW-10-Spot 216 | 25 | 8787 | 3.0 | 19.7 | 3.2 | 0.2 | 4.5 | 0.0 | 3.2 | 0.7 | 152.8 | 4.8 | 157.7 | 6.6 | 233.7 | 75.0 | 152.8 | 4.8 | NA |
| 16ATW-10-Spot 206 | 36 | 36353 | 3.1 | 20.3 | 2.5 | 0.2 | 4.1 | 0.0 | 3.3 | 0.8 | 152.8 | 4.9 | 153.2 | 5.9 | 160.3 | 59.4 | 152.8 | 4.9 | NA |
| 16ATW-10-Spot 163 | 25 | 8200 | 2.4 | 20.2 | 3.1 | 0.2 | 3.6 | 0.0 | 1.8 | 0.5 | 153.0 | 2.8 | 154.3 | 5.2 | 174.9 | 72.8 | 153.0 | 2.8 | NA |
| 16ATW-10-Spot 1 | 66 | 23262 | 2.6 | 20.1 | 1.8 | 0.2 | 3.2 | 0.0 | 2.6 | 0.8 | 153.0 | 3.9 | 154.9 | 4.5 | 184.5 | 42.9 | 153.0 | 3.9 | NA |
| 16ATW-10-Spot 182 | 38 | 16145 | 2.4 | 19.8 | 2.7 | 0.2 | 3.7 | 0.0 | 2.5 | 0.7 | 153.1 | 3.8 | 157.2 | 5.4 | 221.1 | 63.2 | 153.1 | 3.8 | NA |
| 16ATW-10-Spot 267 | 72 | 573006 | 3.5 | 19.2 | 2.4 | 0.2 | 4.1 | 0.0 | 3.4 | 0.8 | 153.1 | 5.1 | 161.8 | 6.2 | 292.1 | 54.0 | 153.1 | 5.1 | NA |
| 16ATW-10-Spot 214 | 37 | 14389 | 2.4 | 20.1 | 2.4 | 0.2 | 3.4 | 0.0 | 2.5 | 0.7 | 153.1 | 3.7 | 154.6 | 4.9 | 177.8 | 55.0 | 153.1 | 3.7 | NA |
| 16ATW-10-Spot 211 | 23 | 402669 | 3.4 | 19.2 | 3.6 | 0.2 | 4.4 | 0.0 | 2.4 | 0.5 | 153.3 | 3.6 | 161.5 | 6.5 | 284.0 | 83.4 | 153.3 | 3.6 | NA |
| 16ATW-10-Spot 297 | 35 | 12292 | 2.2 | 20.6 | 3.0 | 0.2 | 3.7 | 0.0 | 2.2 | 0.6 | 153.4 | 3.3 | 151.4 | 5.3 | 121.1 | 71.7 | 153.4 | 3.3 | NA |
| 16ATW-10-Spot 234 | 76 | 20878 | 2.9 | 20.2 | 1.8 | 0.2 | 3.2 | 0.0 | 2.7 | 0.8 | 153.4 | 4.1 | 154.6 | 4.6 | 174.1 | 41.1 | 153.4 | 4.1 | NA |
| 16ATW-10-Spot 99 | 46 | 12498 | 4.2 | 20.3 | 2.9 | 0.2 | 3.6 | 0.0 | 2.2 | 0.6 | 153.4 | 3.4 | 153.6 | 5.2 | 156.5 | 66.7 | 153.4 | 3.4 | NA |
| 16ATW-10-Spot 229 | 31 | 10066 | 3.1 | 19.6 | 2.7 | 0.2 | 3.8 | 0.0 | 2.6 | 0.7 | 153.5 | 4.0 | 159.0 | 5.5 | 243.1 | 62.0 | 153.5 | 4.0 | NA |

| | | | | | | | | | | | | | | | | | | | |
|---|---|---|---|---|---|---|---|---|---|---|---|---|---|---|---|---|---|---|---|
| 16ATW-10-Spot 147 | 34 | 26788 | 6.8 | 20.0 | 2.7 | 0.2 | 3.6 | 0.0 | 2.4 | 0.7 | 153.5 | 3.6 | 156.0 | 5.2 | 195.9 | 63.4 | 153.5 | 3.6 | NA |
| 16ATW-10-Spot 187 | 45 | 9598 | 3.8 | 21.5 | 2.4 | 0.2 | 3.7 | 0.0 | 2.8 | 0.8 | 153.5 | 4.3 | 145.8 | 5.0 | 23.8 | 56.6 | 153.5 | 4.3 | NA |
| 16ATW-10-Spot 296 | 40 | 15231 | 3.6 | 19.4 | 2.5 | 0.2 | 3.3 | 0.0 | 2.2 | 0.7 | 153.5 | 3.4 | 160.8 | 5.0 | 270.4 | 57.2 | 153.5 | 3.4 | NA |
| 16ATW-10-Spot 256 | 42 | 13816 | 2.8 | 20.7 | 2.5 | 0.2 | 3.8 | 0.0 | 2.8 | 0.7 | 153.7 | 4.2 | 151.1 | 5.3 | 112.2 | 59.4 | 153.7 | 4.2 | NA |
| 16ATW-10-Spot 196 | 62 | 15115 | 3.6 | 21.4 | 2.5 | 0.2 | 3.7 | 0.0 | 2.8 | 0.8 | 153.7 | 4.3 | 146.6 | 5.1 | 34.3 | 59.2 | 153.7 | 4.3 | NA |
| 16ATW-10-Spot 307 | 53 | 56102 | 4.0 | 19.8 | 2.2 | 0.2 | 3.4 | 0.0 | 2.6 | 0.8 | 153.7 | 4.0 | 157.8 | 5.0 | 219.4 | 50.9 | 153.7 | 4.0 | NA |
| 16ATW-10-Spot 46 | 21 | 11107 | 2.7 | 20.5 | 3.7 | 0.2 | 4.8 | 0.0 | 3.0 | 0.6 | 154.0 | 4.6 | 152.7 | 6.8 | 134.5 | 86.8 | 154.0 | 4.6 | NA |
| 16ATW-10-Spot 145 | 54 | 14145 | 1.8 | 19.9 | 2.6 | 0.2 | 3.5 | 0.0 | 2.5 | 0.7 | 154.1 | 3.8 | 157.5 | 5.2 | 209.9 | 59.2 | 154.1 | 3.8 | NA |
| 16ATW-10-Spot 222 | 13 | 55988 | 3.9 | 19.7 | 3.6 | 0.2 | 5.0 | 0.0 | 3.4 | 0.7 | 154.1 | 5.2 | 159.0 | 7.3 | 233.9 | 82.2 | 154.1 | 5.2 | NA |
| 16ATW-10-Spot 314 | 43 | 23059 | 4.5 | 20.0 | 1.8 | 0.2 | 3.1 | 0.0 | 2.5 | 0.8 | 154.1 | 3.8 | 156.5 | 4.5 | 193.4 | 42.6 | 154.1 | 3.8 | NA |
| 16ATW-10-Spot 199 | 111 | 36342 | 2.1 | 20.6 | 1.9 | 0.2 | 3.2 | 0.0 | 2.6 | 0.8 | 154.2 | 3.9 | 152.2 | 4.5 | 121.7 | 45.1 | 154.2 | 3.9 | NA |
| 16ATW-10-Spot 103 | 188 | 41012 | 2.3 | 20.1 | 1.3 | 0.2 | 2.4 | 0.0 | 2.0 | 0.8 | 154.2 | 3.0 | 156.1 | 3.4 | 185.8 | 30.3 | 154.2 | 3.0 | NA |
| 16ATW-10-Spot 94 | 118 | 426178 | 7.2 | 20.3 | 1.8 | 0.2 | 3.2 | 0.0 | 2.7 | 0.8 | 154.3 | 4.1 | 154.3 | 4.6 | 154.9 | 41.3 | 154.3 | 4.1 | NA |
| 16ATW-10-Spot 86 | 33 | 48024 | 3.8 | 20.0 | 2.6 | 0.2 | 3.9 | 0.0 | 3.0 | 0.8 | 154.3 | 4.5 | 156.8 | 5.7 | 196.3 | 60.0 | 154.3 | 4.5 | NA |
| 16ATW-10-Spot 150 | 97 | 19993 | 1.4 | 21.2 | 1.6 | 0.2 | 2.6 | 0.0 | 2.0 | 0.8 | 154.4 | 3.1 | 148.7 | 3.5 | 60.2 | 37.9 | 154.4 | 3.1 | NA |
| 16ATW-10-Spot 122 | 27 | 5076 | 3.6 | 21.7 | 3.0 | 0.2 | 3.8 | 0.0 | 2.3 | 0.6 | 154.4 | 3.5 | 145.5 | 5.1 | 3.9 | 72.7 | 154.4 | 3.5 | NA |
| 16ATW-10-Spot 37 | 44 | 12389 | 4.8 | 21.0 | 1.9 | 0.2 | 3.3 | 0.0 | 2.6 | 0.8 | 154.4 | 4.0 | 149.9 | 4.6 | 79.5 | 46.1 | 154.4 | 4.0 | NA |
| 16ATW-10-Spot 300 | 55 | 109556 | 5.3 | 19.8 | 2.2 | 0.2 | 3.2 | 0.0 | 2.3 | 0.7 | 154.4 | 3.4 | 158.3 | 4.6 | 217.0 | 51.4 | 154.4 | 3.4 | NA |
| 16ATW-10-Spot 305 | 69 | 45492 | 2.4 | 19.8 | 2.9 | 0.2 | 4.1 | 0.0 | 2.9 | 0.7 | 154.5 | 4.5 | 158.4 | 6.1 | 218.6 | 67.6 | 154.5 | 4.5 | NA |
| 16ATW-10-Spot 34 | 68 | 83836 | 3.1 | 20.5 | 2.0 | 0.2 | 3.3 | 0.0 | 2.5 | 0.8 | 154.5 | 3.9 | 153.2 | 4.6 | 135.2 | 48.1 | 154.5 | 3.9 | NA |
| 16ATW-10-Spot 279 | 41 | 12889 | 5.0 | 20.0 | 2.1 | 0.2 | 3.5 | 0.0 | 2.7 | 0.8 | 154.5 | 4.2 | 157.1 | 5.0 | 197.2 | 49.6 | 154.5 | 4.2 | NA |
| 16ATW-10-Spot 114 | 51 | 65746 | 2.1 | 19.0 | 2.9 | 0.2 | 4.0 | 0.0 | 2.8 | 0.7 | 154.5 | 4.3 | 164.8 | 6.1 | 316.9 | 65.3 | 154.5 | 4.3 | NA |
| 16ATW-10-Spot 184 | 158 | 567502 | 3.2 | 20.2 | 1.3 | 0.2 | 3.0 | 0.0 | 2.6 | 0.9 | 154.5 | 4.0 | 155.7 | 4.3 | 174.9 | 31.5 | 154.5 | 4.0 | NA |
| 16ATW-10-Spot 119 | 50 | 36001 | 4.2 | 20.4 | 2.1 | 0.2 | 3.1 | 0.0 | 2.2 | 0.7 | 154.5 | 3.4 | 154.3 | 4.4 | 152.7 | 49.4 | 154.5 | 3.4 | NA |

| | | | | | | | | | | | | | | | | | | | |
|---|---|---|---|---|---|---|---|---|---|---|---|---|---|---|---|---|---|---|---|
| 16ATW-10-Spot 274 | 35 | 13118 | 2.4 | 20.5 | 3.3 | 0.2 | 4.2 | 0.0 | 2.6 | 0.6 | 154.6 | 3.9 | 153.7 | 5.9 | 140.4 | 76.6 | 154.6 | 3.9 | NA |
| 16ATW-10-Spot 298 | 29 | 4913 | 3.3 | 20.9 | 4.5 | 0.2 | 5.2 | 0.0 | 2.6 | 0.5 | 154.6 | 3.9 | 150.6 | 7.3 | 89.1 | 107.3 | 154.6 | 3.9 | NA |
| 16ATW-10-Spot 301 | 65 | 10636 | 3.9 | 20.8 | 2.4 | 0.2 | 3.6 | 0.0 | 2.7 | 0.7 | 154.7 | 4.1 | 151.3 | 5.1 | 99.8 | 57.7 | 154.7 | 4.1 | NA |
| 16ATW-10-Spot 269 | 97 | 116016 | 3.7 | 19.6 | 1.8 | 0.2 | 3.3 | 0.0 | 2.7 | 0.8 | 154.7 | 4.1 | 160.4 | 4.8 | 246.9 | 41.8 | 154.7 | 4.1 | NA |
| 16ATW-10-Spot 111 | 28 | 23370 | 2.8 | 19.7 | 2.2 | 0.2 | 3.5 | 0.0 | 2.6 | 0.8 | 154.7 | 4.0 | 159.1 | 5.1 | 227.1 | 51.5 | 154.7 | 4.0 | NA |
| 16ATW-10-Spot 98 | 18 | 54618 | 3.7 | 19.4 | 3.5 | 0.2 | 5.2 | 0.0 | 3.8 | 0.7 | 154.7 | 5.8 | 161.6 | 7.7 | 264.3 | 79.5 | 154.7 | 5.8 | NA |
| 16ATW-10-Spot 80 | 59 | 99319 | 1.9 | 19.8 | 2.1 | 0.2 | 3.2 | 0.0 | 2.5 | 0.8 | 154.8 | 3.8 | 158.6 | 4.8 | 215.9 | 48.7 | 154.8 | 3.8 | NA |
| 16ATW-10-Spot 16 | 117 | 80516 | 1.5 | 20.1 | 1.4 | 0.2 | 3.0 | 0.0 | 2.6 | 0.9 | 154.9 | 4.0 | 156.8 | 4.3 | 185.7 | 33.0 | 154.9 | 4.0 | NA |
| 16ATW-10-Spot 226 | 57 | 19456 | 2.0 | 19.6 | 2.5 | 0.2 | 4.1 | 0.0 | 3.2 | 0.8 | 154.9 | 4.9 | 160.3 | 6.0 | 241.1 | 57.7 | 154.9 | 4.9 | NA |
| 16ATW-10-Spot 96 | 19 | 4309 | 3.5 | 20.9 | 2.6 | 0.2 | 3.9 | 0.0 | 2.8 | 0.7 | 155.1 | 4.4 | 151.1 | 5.4 | 89.1 | 62.5 | 155.1 | 4.4 | NA |
| 16ATW-10-Spot 13 | 67 | 21664 | 2.7 | 21.0 | 2.4 | 0.2 | 3.4 | 0.0 | 2.4 | 0.7 | 155.1 | 3.7 | 150.5 | 4.7 | 79.4 | 56.5 | 155.1 | 3.7 | NA |
| 16ATW-10-Spot 168 | 21 | 7681 | 2.6 | 21.0 | 2.7 | 0.2 | 3.6 | 0.0 | 2.5 | 0.7 | 155.2 | 3.8 | 150.6 | 5.1 | 79.9 | 63.1 | 155.2 | 3.8 | NA |
| 16ATW-10-Spot 72 | 23 | 5497 | 3.5 | 20.3 | 3.5 | 0.2 | 4.3 | 0.0 | 2.5 | 0.6 | 155.2 | 3.9 | 155.6 | 6.2 | 162.9 | 81.5 | 155.2 | 3.9 | NA |
| 16ATW-10-Spot 258 | 41 | 337324 | 5.0 | 19.4 | 2.4 | 0.2 | 3.6 | 0.0 | 2.7 | 0.7 | 155.2 | 4.1 | 162.0 | 5.4 | 263.0 | 55.8 | 155.2 | 4.1 | NA |
| 16ATW-10-Spot 239 | 47 | 14322 | 4.2 | 20.1 | 2.7 | 0.2 | 4.0 | 0.0 | 2.9 | 0.7 | 155.2 | 4.4 | 157.2 | 5.8 | 188.4 | 63.2 | 155.2 | 4.4 | NA |
| 16ATW-10-Spot 278 | 29 | 145738 | 3.7 | 19.6 | 2.8 | 0.2 | 3.7 | 0.0 | 2.4 | 0.7 | 155.2 | 3.7 | 160.5 | 5.5 | 239.8 | 63.6 | 155.2 | 3.7 | NA |
| 16ATW-10-Spot 130 | 33 | 62011 | 4.0 | 19.9 | 2.9 | 0.2 | 4.1 | 0.0 | 2.9 | 0.7 | 155.3 | 4.4 | 158.5 | 6.0 | 207.8 | 66.9 | 155.3 | 4.4 | NA |
| 16ATW-10-Spot 113 | 24 | 45057 | 3.8 | 19.9 | 3.4 | 0.2 | 4.5 | 0.0 | 2.9 | 0.7 | 155.3 | 4.5 | 158.5 | 6.5 | 207.1 | 78.1 | 155.3 | 4.5 | NA |
| 16ATW-10-Spot 90 | 31 | 38009 | 2.3 | 21.3 | 2.6 | 0.2 | 3.6 | 0.0 | 2.4 | 0.7 | 155.3 | 3.8 | 149.1 | 5.0 | 51.7 | 62.2 | 155.3 | 3.8 | NA |
| 16ATW-10-Spot 84 | 52 | 671905 | 4.4 | 18.6 | 3.2 | 0.2 | 4.0 | 0.0 | 2.5 | 0.6 | 155.3 | 3.8 | 168.4 | 6.2 | 357.6 | 71.3 | 155.3 | 3.8 | NA |
| 16ATW-10-Spot 205 | 104 | 190764 | 3.0 | 20.4 | 1.5 | 0.2 | 2.3 | 0.0 | 1.8 | 0.8 | 155.3 | 2.8 | 154.8 | 3.4 | 147.7 | 34.5 | 155.3 | 2.8 | NA |
| 16ATW-10-Spot 200 | 29 | 6693 | 3.2 | 20.8 | 3.0 | 0.2 | 4.0 | 0.0 | 2.6 | 0.7 | 155.4 | 4.0 | 152.1 | 5.6 | 102.5 | 71.0 | 155.4 | 4.0 | NA |
| 16ATW-10-Spot 254 | 74 | 45904 | 3.8 | 20.5 | 2.0 | 0.2 | 3.5 | 0.0 | 2.8 | 0.8 | 155.4 | 4.3 | 154.1 | 5.0 | 134.7 | 47.5 | 155.4 | 4.3 | NA |
| 16ATW-10-Spot 68 | 57 | 69855 | 3.4 | 19.6 | 2.3 | 0.2 | 3.3 | 0.0 | 2.4 | 0.7 | 155.4 | 3.7 | 161.1 | 5.0 | 246.1 | 52.5 | 155.4 | 3.7 | NA |
| 16ATW-10-Spot 51 | 67 | 18741 | 3.2 | 20.3 | 2.1 | 0.2 | 3.2 | 0.0 | 2.4 | 0.8 | 155.5 | 3.7 | 156.0 | 4.6 | 164.9 | 48.2 | 155.5 | 3.7 | NA |
| 16ATW-10-Spot 100 | 24 | 66590 | 3.5 | 18.2 | 3.0 | 0.2 | 4.5 | 0.0 | 3.3 | 0.7 | 155.5 | 5.1 | 172.2 | 7.2 | 408.5 | 68.1 | 155.5 | 5.1 | NA |

| | | | | | | | | | | | | | | | | | | | |
|---|---|---|---|---|---|---|---|---|---|---|---|---|---|---|---|---|---|---|---|
| 16ATW-10-Spot 8 | 55 | 45072 | 2.6 | 20.7 | 1.8 | 0.2 | 3.2 | 0.0 | 2.7 | 0.8 | 155.5 | 4.1 | 152.7 | 4.6 | 110.4 | 41.9 | 155.5 | 4.1 | NA |
| 16ATW-10-Spot 195 | 25 | 4992 | 2.0 | 19.9 | 4.3 | 0.2 | 5.2 | 0.0 | 2.9 | 0.6 | 155.6 | 4.5 | 158.5 | 7.6 | 201.7 | 99.4 | 155.6 | 4.5 | NA |
| 16ATW-10-Spot 202 | 92 | 390963 | 2.4 | 20.2 | 1.8 | 0.2 | 3.4 | 0.0 | 2.9 | 0.9 | 155.7 | 4.5 | 156.6 | 5.0 | 172.8 | 41.5 | 155.7 | 4.5 | NA |
| 16ATW-10-Spot 54 | 96 | 36858 | 2.4 | 20.1 | 1.7 | 0.2 | 3.2 | 0.0 | 2.8 | 0.8 | 155.7 | 4.2 | 157.3 | 4.7 | 181.5 | 40.1 | 155.7 | 4.2 | NA |
| 16ATW-10-Spot 242 | 21 | 15977 | 4.1 | 20.2 | 3.5 | 0.2 | 4.4 | 0.0 | 2.7 | 0.6 | 155.8 | 4.1 | 156.4 | 6.4 | 167.8 | 81.8 | 155.8 | 4.1 | NA |
| 16ATW-10-Spot 207 | 31 | 22004 | 2.2 | 19.5 | 2.9 | 0.2 | 3.5 | 0.0 | 2.1 | 0.6 | 155.8 | 3.2 | 161.5 | 5.3 | 248.1 | 65.6 | 155.8 | 3.2 | NA |
| 16ATW-10-Spot 112 | 20 | 8135 | 3.8 | 21.9 | 3.6 | 0.2 | 4.7 | 0.0 | 2.9 | 0.6 | 155.8 | 4.5 | 145.6 | 6.3 | NA | NA | 155.8 | 4.5 | NA |
| 16ATW-10-Spot 14 | 46 | 12704 | 3.1 | 21.3 | 2.8 | 0.2 | 3.5 | 0.0 | 2.0 | 0.6 | 155.8 | 3.2 | 149.1 | 4.8 | 43.8 | 67.1 | 155.8 | 3.2 | NA |
| 16ATW-10-Spot 140 | 32 | 16887 | 3.1 | 20.2 | 3.1 | 0.2 | 4.5 | 0.0 | 3.2 | 0.7 | 155.9 | 5.0 | 156.8 | 6.5 | 172.1 | 72.9 | 155.9 | 5.0 | NA |
| 16ATW-10-Spot 148 | 59 | 26674 | 2.4 | 21.0 | 2.4 | 0.2 | 3.4 | 0.0 | 2.4 | 0.7 | 155.9 | 3.7 | 151.0 | 4.7 | 76.1 | 56.5 | 155.9 | 3.7 | NA |
| 16ATW-10-Spot 273 | 18 | 30167 | 3.8 | 19.3 | 3.8 | 0.2 | 4.8 | 0.0 | 2.9 | 0.6 | 156.0 | 4.5 | 163.4 | 7.2 | 273.1 | 86.6 | 156.0 | 4.5 | NA |
| 16ATW-10-Spot 236 | 29 | 9099 | 3.4 | 21.4 | 3.6 | 0.2 | 4.3 | 0.0 | 2.3 | 0.5 | 156.0 | 3.6 | 148.8 | 5.9 | 36.0 | 86.5 | 156.0 | 3.6 | NA |
| 16ATW-10-Spot 201 | 223 | 122664 | 3.1 | 20.3 | 1.4 | 0.2 | 2.3 | 0.0 | 1.9 | 0.8 | 156.0 | 2.9 | 156.5 | 3.4 | 164.7 | 31.9 | 156.0 | 2.9 | NA |
| 16ATW-10-Spot 50 | 28 | 46343 | 3.5 | 20.3 | 1.8 | 0.2 | 3.1 | 0.0 | 2.5 | 0.8 | 156.2 | 3.9 | 156.3 | 4.5 | 158.4 | 41.1 | 156.2 | 3.9 | NA |
| 16ATW-10-Spot 32 | 115 | 129761 | 1.8 | 19.8 | 1.8 | 0.2 | 2.8 | 0.0 | 2.1 | 0.8 | 156.2 | 3.3 | 159.9 | 4.1 | 215.5 | 41.3 | 156.2 | 3.3 | NA |
| 16ATW-10-Spot 151 | 49 | 10643 | 2.0 | 20.9 | 1.9 | 0.2 | 3.1 | 0.0 | 2.5 | 0.8 | 156.3 | 3.8 | 152.2 | 4.4 | 89.8 | 44.4 | 156.3 | 3.8 | NA |
| 16ATW-10-Spot 227 | 66 | 13145 | 4.1 | 21.3 | 2.3 | 0.2 | 3.5 | 0.0 | 2.6 | 0.8 | 156.3 | 4.1 | 149.7 | 4.9 | 46.8 | 55.2 | 156.3 | 4.1 | NA |
| 16ATW-10-Spot 56 | 38 | 36949 | 4.3 | 19.5 | 2.8 | 0.2 | 3.7 | 0.0 | 2.3 | 0.6 | 156.4 | 3.6 | 162.8 | 5.5 | 259.2 | 64.6 | 156.4 | 3.6 | NA |
| 16ATW-10-Spot 85 | 133 | 66390 | 2.0 | 20.1 | 1.6 | 0.2 | 2.8 | 0.0 | 2.3 | 0.8 | 156.4 | 3.5 | 157.8 | 4.1 | 180.1 | 38.0 | 156.4 | 3.5 | NA |
| 16ATW-10-Spot 293 | 25 | 41663 | 3.2 | 21.1 | 3.2 | 0.2 | 4.5 | 0.0 | 3.2 | 0.7 | 156.4 | 4.9 | 151.1 | 6.3 | 70.3 | 75.4 | 156.4 | 4.9 | NA |
| 16ATW-10-Spot 190 | 31 | 12270 | 3.7 | 19.6 | 3.0 | 0.2 | 4.3 | 0.0 | 3.0 | 0.7 | 156.4 | 4.7 | 161.8 | 6.4 | 242.2 | 68.9 | 156.4 | 4.7 | NA |
| 16ATW-10-Spot 265 | 22 | 24789 | 3.8 | 19.9 | 4.0 | 0.2 | 4.8 | 0.0 | 2.7 | 0.6 | 156.4 | 4.2 | 159.6 | 7.1 | 207.2 | 92.6 | 156.4 | 4.2 | NA |
| 16ATW-10-Spot 192 | 33 | 6172 | 3.3 | 20.4 | 2.3 | 0.2 | 3.4 | 0.0 | 2.4 | 0.7 | 156.6 | 3.7 | 156.3 | 4.9 | 153.3 | 54.9 | 156.6 | 3.7 | NA |
| 16ATW-10-Spot 292 | 35 | 83581 | 5.1 | 19.9 | 2.5 | 0.2 | 3.9 | 0.0 | 3.0 | 0.8 | 156.6 | 4.6 | 159.7 | 5.7 | 207.3 | 57.4 | 156.6 | 4.6 | NA |
| 16ATW-10-Spot 146 | 20 | 20681 | 2.7 | 20.3 | 4.0 | 0.2 | 5.0 | 0.0 | 2.9 | 0.6 | 156.6 | 4.5 | 157.0 | 7.2 | 164.7 | 94.0 | 156.6 | 4.5 | NA |

| | | | | | | | | | | | | | | | | | | | |
|---|---|---|---|---|---|---|---|---|---|---|---|---|---|---|---|---|---|---|---|
| 16ATW-10-Spot 60 | 61 | 39545 | 2.2 | 20.3 | 2.5 | 0.2 | 3.9 | 0.0 | 3.0 | 0.8 | 156.7 | 4.7 | 156.8 | 5.7 | 160.4 | 57.8 | 156.7 | 4.7 | NA |
| 16ATW-10-Spot 231 | 21 | 5761 | 4.3 | 19.9 | 3.7 | 0.2 | 4.5 | 0.0 | 2.6 | 0.6 | 156.7 | 4.0 | 160.0 | 6.7 | 210.1 | 86.6 | 156.7 | 4.0 | NA |
| 16ATW-10-Spot 101 | 40 | 12319 | 3.8 | 20.5 | 2.4 | 0.2 | 3.4 | 0.0 | 2.3 | 0.7 | 156.7 | 3.6 | 155.2 | 4.8 | 133.3 | 57.4 | 156.7 | 3.6 | NA |
| 16ATW-10-Spot 55 | 25 | 12109 | 3.3 | 21.6 | 3.3 | 0.2 | 4.1 | 0.0 | 2.4 | 0.6 | 156.7 | 3.7 | 148.3 | 5.7 | 17.0 | 80.2 | 156.7 | 3.7 | NA |
| 16ATW-10-Spot 29 | 82 | 70069 | 2.7 | 20.4 | 1.3 | 0.2 | 3.3 | 0.0 | 3.0 | 0.9 | 156.8 | 4.6 | 155.9 | 4.7 | 144.1 | 31.0 | 156.8 | 4.6 | NA |
| 16ATW-10-Spot 286 | 39 | 8516 | 2.4 | 20.5 | 2.5 | 0.2 | 3.8 | 0.0 | 2.9 | 0.8 | 156.8 | 4.5 | 155.5 | 5.5 | 136.7 | 58.2 | 156.8 | 4.5 | NA |
| 16ATW-10-Spot 164 | 30 | 61481 | 2.9 | 20.2 | 3.2 | 0.2 | 4.2 | 0.0 | 2.6 | 0.6 | 156.8 | 4.1 | 157.9 | 6.1 | 175.1 | 75.1 | 156.8 | 4.1 | NA |
| 16ATW-10-Spot 74 | 57 | 40279 | 2.8 | 20.2 | 2.3 | 0.2 | 3.4 | 0.0 | 2.5 | 0.7 | 156.9 | 3.9 | 157.5 | 4.9 | 168.3 | 52.9 | 156.9 | 3.9 | NA |
| 16ATW-10-Spot 59 | 69 | 50550 | 3.7 | 20.1 | 2.3 | 0.2 | 3.1 | 0.0 | 2.1 | 0.7 | 156.9 | 3.3 | 158.3 | 4.6 | 179.2 | 53.6 | 156.9 | 3.3 | NA |
| 16ATW-10-Spot 315 | 88 | 60860 | 4.5 | 20.1 | 1.8 | 0.2 | 2.5 | 0.0 | 1.8 | 0.7 | 157.0 | 2.8 | 158.8 | 3.7 | 187.0 | 41.0 | 157.0 | 2.8 | NA |
| 16ATW-10-Spot 289 | 32 | 19101 | 3.0 | 20.7 | 2.4 | 0.2 | 3.7 | 0.0 | 2.8 | 0.8 | 157.0 | 4.4 | 154.5 | 5.3 | 117.5 | 56.5 | 157.0 | 4.4 | NA |
| 16ATW-10-Spot 5 | 56 | 400660 | 2.3 | 21.1 | 1.9 | 0.2 | 3.4 | 0.0 | 2.8 | 0.8 | 157.0 | 4.4 | 151.8 | 4.8 | 72.2 | 45.4 | 157.0 | 4.4 | NA |
| 16ATW-10-Spot 66 | 23 | 18338 | 2.5 | 20.2 | 2.3 | 0.2 | 3.4 | 0.0 | 2.5 | 0.7 | 157.1 | 3.9 | 157.9 | 4.9 | 170.6 | 52.8 | 157.1 | 3.9 | NA |
| 16ATW-10-Spot 33 | 33 | 15730 | 3.0 | 21.1 | 2.6 | 0.2 | 3.7 | 0.0 | 2.7 | 0.7 | 157.1 | 4.2 | 152.0 | 5.2 | 74.1 | 60.7 | 157.1 | 4.2 | NA |
| 16ATW-10-Spot 52 | 83 | 23794 | 4.7 | 21.1 | 1.7 | 0.2 | 3.0 | 0.0 | 2.5 | 0.8 | 157.1 | 3.8 | 151.5 | 4.2 | 65.6 | 40.9 | 157.1 | 3.8 | NA |
| 16ATW-10-Spot 175 | 51 | 20167 | 3.1 | 20.7 | 1.9 | 0.2 | 3.3 | 0.0 | 2.7 | 0.8 | 157.1 | 4.2 | 154.2 | 4.7 | 110.1 | 44.0 | 157.1 | 4.2 | NA |
| 16ATW-10-Spot 63 | 30 | 41991 | 2.7 | 19.8 | 3.0 | 0.2 | 3.8 | 0.0 | 2.4 | 0.6 | 157.2 | 3.8 | 160.8 | 5.7 | 214.3 | 68.4 | 157.2 | 3.8 | NA |
| 16ATW-10-Spot 23 | 30 | 8839 | 3.9 | 20.8 | 3.1 | 0.2 | 3.7 | 0.0 | 2.1 | 0.6 | 157.3 | 3.2 | 154.2 | 5.3 | 107.9 | 72.5 | 157.3 | 3.2 | NA |
| 16ATW-10-Spot 263 | 42 | 20112 | 4.0 | 20.1 | 2.7 | 0.2 | 4.0 | 0.0 | 3.0 | 0.7 | 157.3 | 4.7 | 158.7 | 5.9 | 179.9 | 61.9 | 157.3 | 4.7 | NA |
| 16ATW-10-Spot 75 | 32 | 39730 | 3.6 | 19.8 | 3.1 | 0.2 | 4.5 | 0.0 | 3.3 | 0.7 | 157.4 | 5.1 | 160.9 | 6.7 | 213.8 | 72.4 | 157.4 | 5.1 | NA |
| 16ATW-10-Spot 3 | 82 | 119699 | 3.6 | 20.2 | 1.6 | 0.2 | 3.0 | 0.0 | 2.6 | 0.9 | 157.4 | 4.0 | 158.1 | 4.4 | 169.1 | 36.8 | 157.4 | 4.0 | NA |
| 16ATW-10-Spot 82 | 87 | 32621 | 2.3 | 20.9 | 1.6 | 0.2 | 3.0 | 0.0 | 2.6 | 0.9 | 157.4 | 4.0 | 153.3 | 4.3 | 91.4 | 37.0 | 157.4 | 4.0 | NA |
| 16ATW-10-Spot 276 | 26 | 6555 | 3.4 | 21.4 | 2.5 | 0.2 | 3.5 | 0.0 | 2.3 | 0.7 | 157.5 | 3.6 | 149.8 | 4.8 | 31.1 | 61.0 | 157.5 | 3.6 | NA |
| 16ATW-10-Spot 176 | 23 | 10130 | 3.8 | 20.8 | 3.8 | 0.2 | 4.9 | 0.0 | 3.1 | 0.6 | 157.5 | 4.8 | 154.1 | 6.9 | 102.3 | 89.3 | 157.5 | 4.8 | NA |
| 16ATW-10-Spot 41 | 101 | 359100 | 4.7 | 20.4 | 1.4 | 0.2 | 2.4 | 0.0 | 2.0 | 0.8 | 157.6 | 3.1 | 157.0 | 3.5 | 147.9 | 31.8 | 157.6 | 3.1 | NA |
| 16ATW-10-Spot 65 | 24 | 20374 | 3.0 | 21.0 | 2.5 | 0.2 | 3.6 | 0.0 | 2.5 | 0.7 | 157.7 | 4.0 | 152.8 | 5.1 | 77.5 | 60.1 | 157.7 | 4.0 | NA |
| 16ATW-10-Spot 133 | 68 | 16823 | 2.9 | 20.6 | 2.2 | 0.2 | 3.3 | 0.0 | 2.5 | 0.8 | 157.7 | 3.8 | 155.9 | 4.7 | 129.1 | 50.9 | 157.7 | 3.8 | NA |
| 16ATW-10-Spot 170 | 28 | 43379 | 3.4 | 20.9 | 2.6 | 0.2 | 3.2 | 0.0 | 1.8 | 0.6 | 157.8 | 2.9 | 153.6 | 4.6 | 90.3 | 62.4 | 157.8 | 2.9 | NA |

| | | | | | | | | | | | | | | | | | | | |
|---|---|---|---|---|---|---|---|---|---|---|---|---|---|---|---|---|---|---|---|
| 16ATW-10-Spot 152 | 24 | 34377 | 3.8 | 20.6 | 3.2 | 0.2 | 4.0 | 0.0 | 2.4 | 0.6 | 157.8 | 3.8 | 155.5 | 5.8 | 121.5 | 76.0 | 157.8 | 3.8 | NA |
| 16ATW-10-Spot 154 | 39 | 24408 | 3.6 | 20.8 | 2.5 | 0.2 | 3.4 | 0.0 | 2.3 | 0.7 | 157.8 | 3.5 | 154.7 | 4.8 | 107.2 | 58.7 | 157.8 | 3.5 | NA |
| 16ATW-10-Spot 44 | 38 | 73935 | 2.6 | 20.2 | 2.5 | 0.2 | 3.7 | 0.0 | 2.8 | 0.7 | 157.9 | 4.3 | 158.8 | 5.4 | 173.8 | 57.3 | 157.9 | 4.3 | NA |
| 16ATW-10-Spot 304 | 54 | 71803 | 5.3 | 20.9 | 2.3 | 0.2 | 3.6 | 0.0 | 2.8 | 0.8 | 158.0 | 4.3 | 154.0 | 5.2 | 94.7 | 54.3 | 158.0 | 4.3 | NA |
| 16ATW-10-Spot 240 | 22 | 51364 | 3.6 | 19.8 | 2.5 | 0.2 | 3.6 | 0.0 | 2.5 | 0.7 | 158.0 | 4.0 | 161.6 | 5.3 | 215.2 | 58.0 | 158.0 | 4.0 | NA |
| 16ATW-10-Spot 257 | 36 | 53328 | 3.1 | 20.5 | 2.3 | 0.2 | 3.8 | 0.0 | 3.0 | 0.8 | 158.0 | 4.7 | 156.5 | 5.5 | 135.0 | 55.0 | 158.0 | 4.7 | NA |
| 16ATW-10-Spot 169 | 29 | 9250 | 3.7 | 21.2 | 3.1 | 0.2 | 4.0 | 0.0 | 2.5 | 0.6 | 158.0 | 3.9 | 151.9 | 5.6 | 58.7 | 73.9 | 158.0 | 3.9 | NA |
| 16ATW-10-Spot 287 | 161 | 71510 | 2.6 | 20.1 | 1.5 | 0.2 | 2.5 | 0.0 | 2.0 | 0.8 | 158.2 | 3.1 | 159.4 | 3.7 | 178.2 | 35.4 | 158.2 | 3.1 | NA |
| 16ATW-10-Spot 53 | 36 | 10597 | 2.6 | 21.3 | 3.4 | 0.2 | 4.3 | 0.0 | 2.7 | 0.6 | 158.3 | 4.2 | 151.3 | 6.1 | 44.3 | 81.1 | 158.3 | 4.2 | NA |
| 16ATW-10-Spot 71 | 69 | 205355 | 2.1 | 20.0 | 1.8 | 0.2 | 2.7 | 0.0 | 2.1 | 0.8 | 158.3 | 3.3 | 160.6 | 4.0 | 195.2 | 40.8 | 158.3 | 3.3 | NA |
| 16ATW-10-Spot 178 | 20 | 12315 | 2.8 | 21.1 | 3.6 | 0.2 | 4.8 | 0.0 | 3.1 | 0.7 | 158.4 | 4.9 | 152.9 | 6.8 | 70.2 | 85.8 | 158.4 | 4.9 | NA |
| 16ATW-10-Spot 89 | 29 | 5886 | 3.5 | 20.6 | 2.6 | 0.2 | 4.2 | 0.0 | 3.3 | 0.8 | 158.4 | 5.2 | 156.5 | 6.1 | 128.9 | 60.5 | 158.4 | 5.2 | NA |
| 16ATW-10-Spot 189 | 34 | 11100 | 2.9 | 20.8 | 2.7 | 0.2 | 3.5 | 0.0 | 2.1 | 0.6 | 158.4 | 3.3 | 154.6 | 5.0 | 97.8 | 64.2 | 158.4 | 3.3 | NA |
| 16ATW-10-Spot 57 | 21 | 41005 | 4.6 | 19.5 | 4.1 | 0.2 | 5.0 | 0.0 | 2.9 | 0.6 | 158.5 | 4.6 | 164.6 | 7.7 | 254.0 | 94.4 | 158.5 | 4.6 | NA |
| 16ATW-10-Spot 81 | 76 | 22239 | 3.8 | 20.8 | 1.9 | 0.2 | 3.4 | 0.0 | 2.8 | 0.8 | 158.5 | 4.3 | 155.1 | 4.8 | 103.6 | 44.6 | 158.5 | 4.3 | NA |
| 16ATW-10-Spot 17 | 306 | 205607 | 11.6 | 20.5 | 1.2 | 0.2 | 2.5 | 0.0 | 2.2 | 0.9 | 158.7 | 3.5 | 157.1 | 3.6 | 133.7 | 27.3 | 158.7 | 3.5 | NA |
| 16ATW-10-Spot 35 | 26 | 10160 | 2.3 | 20.5 | 3.7 | 0.2 | 4.6 | 0.0 | 2.7 | 0.6 | 158.7 | 4.2 | 157.5 | 6.7 | 141.0 | 87.0 | 158.7 | 4.2 | NA |
| 16ATW-10-Spot 251 | 36 | 9475 | 3.0 | 19.9 | 2.4 | 0.2 | 3.4 | 0.0 | 2.4 | 0.7 | 158.7 | 3.8 | 161.7 | 5.1 | 207.0 | 55.3 | 158.7 | 3.8 | NA |
| 16ATW-10-Spot 313 | 23 | 16729 | 4.3 | 19.1 | 3.6 | 0.2 | 4.6 | 0.0 | 2.8 | 0.6 | 158.9 | 4.4 | 168.3 | 7.1 | 303.8 | 83.0 | 158.9 | 4.4 | NA |
| 16ATW-10-Spot 204 | 50 | 35962 | 2.5 | 20.7 | 2.2 | 0.2 | 3.5 | 0.0 | 2.7 | 0.8 | 159.1 | 4.2 | 156.2 | 5.0 | 114.1 | 51.9 | 159.1 | 4.2 | NA |
| 16ATW-10-Spot 45 | 17 | 12455 | 3.4 | 21.3 | 3.9 | 0.2 | 4.9 | 0.0 | 2.9 | 0.6 | 159.3 | 4.6 | 152.2 | 6.9 | 44.3 | 93.7 | 159.3 | 4.6 | NA |
| 16ATW-10-Spot 143 | 28 | 21064 | 3.5 | 21.0 | 3.4 | 0.2 | 4.6 | 0.0 | 3.1 | 0.7 | 159.3 | 4.8 | 154.3 | 6.5 | 78.5 | 80.6 | 159.3 | 4.8 | NA |
| 16ATW-10-Spot 144 | 52 | 100674 | 4.2 | 21.2 | 1.9 | 0.2 | 3.0 | 0.0 | 2.3 | 0.8 | 159.3 | 3.7 | 153.2 | 4.3 | 61.2 | 46.2 | 159.3 | 3.7 | NA |
| 16ATW-10-Spot 203 | 69 | 80762 | 3.2 | 20.2 | 2.0 | 0.2 | 3.2 | 0.0 | 2.5 | 0.8 | 159.4 | 4.0 | 159.8 | 4.7 | 166.7 | 46.5 | 159.4 | 4.0 | NA |
| 16ATW-10-Spot 47 | 29 | 51677 | 2.4 | 19.6 | 2.8 | 0.2 | 4.3 | 0.0 | 3.3 | 0.8 | 159.6 | 5.2 | 164.7 | 6.6 | 240.6 | 64.5 | 159.6 | 5.2 | NA |
| 16ATW-10-Spot 128 | 26 | 21113 | 3.6 | 20.2 | 3.2 | 0.2 | 4.5 | 0.0 | 3.2 | 0.7 | 159.7 | 5.0 | 160.6 | 6.7 | 174.8 | 75.5 | 159.7 | 5.0 | NA |

| | | | | | | | | | | | | | | | | | | | |
|---|---|---|---|---|---|---|---|---|---|---|---|---|---|---|---|---|---|---|---|
| 16ATW-10-Spot 303 | 63 | 118611 | 4.0 | 20.1 | 1.9 | 0.2 | 3.4 | 0.0 | 2.7 | 0.8 | 160.0 | 4.3 | 161.5 | 5.0 | 185.3 | 45.2 | 160.0 | 4.3 | NA |
| 16ATW-10-Spot 125 | 330 | 360092 | 29.6 | 20.3 | 1.2 | 0.2 | 2.8 | 0.0 | 2.6 | 0.9 | 160.0 | 4.1 | 159.7 | 4.2 | 155.6 | 27.9 | 160.0 | 4.1 | NA |
| 16ATW-10-Spot 217 | 54 | 80335 | 3.2 | 20.3 | 2.1 | 0.2 | 3.3 | 0.0 | 2.6 | 0.8 | 160.6 | 4.2 | 160.3 | 4.9 | 156.7 | 48.2 | 160.6 | 4.2 | NA |
| 16ATW-10-Spot 95 | 91 | 97549 | 2.4 | 20.0 | 2.0 | 0.2 | 3.3 | 0.0 | 2.6 | 0.8 | 160.6 | 4.1 | 162.7 | 4.9 | 194.7 | 46.4 | 160.6 | 4.1 | NA |
| 16ATW-10-Spot 26 | 37 | 92713 | 3.0 | 21.3 | 2.2 | 0.2 | 3.4 | 0.0 | 2.6 | 0.8 | 160.7 | 4.2 | 153.6 | 4.9 | 46.5 | 52.3 | 160.7 | 4.2 | NA |
| 16ATW-10-Spot 43 | 29 | 394199 | 2.5 | 20.8 | 2.9 | 0.2 | 3.9 | 0.0 | 2.6 | 0.7 | 160.8 | 4.2 | 157.1 | 5.7 | 102.2 | 67.7 | 160.8 | 4.2 | NA |
| 16ATW-10-Spot 185 | 91 | 17360 | 2.1 | 19.9 | 2.0 | 0.2 | 3.4 | 0.0 | 2.7 | 0.8 | 160.8 | 4.3 | 163.4 | 5.1 | 202.5 | 45.4 | 160.8 | 4.3 | NA |
| 16ATW-10-Spot 73 | 77 | 21386 | 1.9 | 20.5 | 1.9 | 0.2 | 3.0 | 0.0 | 2.3 | 0.8 | 160.8 | 3.6 | 159.1 | 4.4 | 134.7 | 45.0 | 160.8 | 3.6 | NA |
| 16ATW-10-Spot 64 | 38 | 12820 | 3.1 | 19.9 | 2.2 | 0.2 | 3.5 | 0.0 | 2.7 | 0.8 | 160.9 | 4.3 | 164.0 | 5.2 | 210.7 | 50.7 | 160.9 | 4.3 | NA |
| 16ATW-10-Spot 162 | 110 | 87000 | 3.5 | 20.2 | 1.2 | 0.2 | 3.1 | 0.0 | 2.8 | 0.9 | 161.0 | 4.5 | 161.8 | 4.6 | 174.2 | 28.3 | 161.0 | 4.5 | NA |
| 16ATW-10-Spot 174 | 189 | 204864 | 2.5 | 20.0 | 1.4 | 0.2 | 3.1 | 0.0 | 2.8 | 0.9 | 161.0 | 4.4 | 163.2 | 4.7 | 196.1 | 32.8 | 161.0 | 4.4 | NA |
| 16ATW-10-Spot 247 | 171 | 169581 | 2.9 | 20.2 | 1.3 | 0.2 | 2.8 | 0.0 | 2.4 | 0.9 | 161.1 | 3.9 | 161.7 | 4.1 | 172.4 | 30.3 | 161.1 | 3.9 | NA |
| 16ATW-10-Spot 42 | 55 | 389327 | 2.1 | 20.8 | 2.2 | 0.2 | 4.0 | 0.0 | 3.4 | 0.8 | 161.1 | 5.4 | 157.4 | 5.9 | 103.0 | 51.6 | 161.1 | 5.4 | NA |
| 16ATW-10-Spot 102 | 66 | 224977 | 3.4 | 20.9 | 1.9 | 0.2 | 2.9 | 0.0 | 2.2 | 0.8 | 161.1 | 3.6 | 157.0 | 4.3 | 96.0 | 45.0 | 161.1 | 3.6 | NA |
| 16ATW-10-Spot 79 | 57 | 42068 | 3.0 | 20.0 | 2.7 | 0.2 | 3.7 | 0.0 | 2.6 | 0.7 | 161.2 | 4.1 | 163.3 | 5.6 | 195.7 | 62.3 | 161.2 | 4.1 | NA |
| 16ATW-10-Spot 283 | 57 | 131360 | 2.8 | 21.0 | 1.6 | 0.2 | 3.2 | 0.0 | 2.8 | 0.9 | 161.2 | 4.4 | 156.3 | 4.7 | 84.0 | 38.4 | 161.2 | 4.4 | NA |
| 16ATW-10-Spot 291 | 19 | 3837 | 3.6 | 21.9 | 4.5 | 0.2 | 5.2 | 0.0 | 2.5 | 0.5 | 161.2 | 3.9 | 150.1 | 7.2 | NA | NA | 161.2 | 3.9 | NA |
| 16ATW-10-Spot 105 | 71 | 28102 | 4.9 | 20.9 | 1.8 | 0.2 | 2.8 | 0.0 | 2.1 | 0.8 | 161.2 | 3.4 | 156.7 | 4.1 | 89.8 | 43.3 | 161.2 | 3.4 | NA |
| 16ATW-10-Spot 271 | 54 | 21790 | 3.5 | 20.5 | 2.0 | 0.2 | 3.3 | 0.0 | 2.6 | 0.8 | 161.3 | 4.1 | 160.1 | 4.9 | 142.7 | 48.1 | 161.3 | 4.1 | NA |
| 16ATW-10-Spot 48 | 282 | 100353 | 4.0 | 20.4 | 1.3 | 0.2 | 2.3 | 0.0 | 1.9 | 0.8 | 161.7 | 3.0 | 160.7 | 3.4 | 147.8 | 29.6 | 161.7 | 3.0 | NA |
| 16ATW-10-Spot 25 | 31 | 20075 | 4.7 | 20.9 | 3.0 | 0.2 | 4.3 | 0.0 | 3.1 | 0.7 | 161.9 | 4.9 | 157.5 | 6.3 | 92.5 | 70.6 | 161.9 | 4.9 | NA |
| 16ATW-10-Spot 262 | 34 | 9098 | 2.4 | 20.7 | 2.9 | 0.2 | 3.9 | 0.0 | 2.5 | 0.7 | 161.9 | 4.0 | 159.0 | 5.7 | 117.1 | 68.7 | 161.9 | 4.0 | NA |
| 16ATW-10-Spot 306 | 54 | 54793 | 1.9 | 20.3 | 2.1 | 0.2 | 3.1 | 0.0 | 2.2 | 0.7 | 162.1 | 3.5 | 161.9 | 4.6 | 160.3 | 49.7 | 162.1 | 3.5 | NA |
| 16ATW-10-Spot 238 | 33 | 42756 | 5.4 | 20.4 | 2.7 | 0.2 | 3.9 | 0.0 | 2.7 | 0.7 | 162.6 | 4.3 | 161.5 | 5.8 | 146.5 | 64.2 | 162.6 | 4.3 | NA |
| 16ATW-10-Spot 77 | 34 | 36610 | 5.6 | 19.9 | 2.4 | 0.2 | 3.5 | 0.0 | 2.6 | 0.7 | 162.7 | 4.2 | 165.8 | 5.4 | 211.7 | 54.5 | 162.7 | 4.2 | NA |
| 16ATW-10-Spot 259 | 32 | 23788 | 3.7 | 19.5 | 3.0 | 0.2 | 3.9 | 0.0 | 2.4 | 0.6 | 163.1 | 3.8 | 168.7 | 6.0 | 248.7 | 70.2 | 163.1 | 3.8 | NA |

| | | | | | | | | | | | | | | | | | | | |
|---|---|---|---|---|---|---|---|---|---|---|---|---|---|---|---|---|---|---|---|
| 16ATW-10-Spot 88 | 162 | 54415 | 4.0 | 20.6 | 1.1 | 0.2 | 2.4 | 0.0 | 2.2 | 0.9 | 164.7 | 3.5 | 162.0 | 3.6 | 123.5 | 25.0 | 164.7 | 3.5 | NA |
| 16ATW-10-Spot 11 | 52 | 17749 | 3.5 | 20.8 | 2.2 | 0.2 | 3.1 | 0.0 | 2.3 | 0.7 | 164.8 | 3.7 | 160.9 | 4.7 | 105.6 | 51.9 | 164.8 | 3.7 | NA |
| 16ATW-10-Spot 218 | 113 | 44874 | 3.4 | 20.6 | 1.6 | 0.2 | 3.0 | 0.0 | 2.6 | 0.8 | 165.3 | 4.2 | 162.9 | 4.5 | 128.6 | 37.7 | 165.3 | 4.2 | NA |
| 16ATW-10-Spot 223 | 287 | 187997 | 3.6 | 20.0 | 1.0 | 0.2 | 2.4 | 0.0 | 2.2 | 0.9 | 165.9 | 3.6 | 167.9 | 3.8 | 197.0 | 23.8 | 165.9 | 3.6 | NA |
| 16ATW-10-Spot 308 | 135 | 51157 | 3.9 | 20.4 | 1.6 | 0.2 | 2.7 | 0.0 | 2.1 | 0.8 | 167.4 | 3.5 | 166.3 | 4.1 | 151.7 | 38.2 | 167.4 | 3.5 | NA |
| 16ATW-10-Spot 31 | 83 | 86156 | 2.9 | 19.9 | 2.0 | 0.2 | 2.9 | 0.0 | 2.1 | 0.7 | 167.6 | 3.4 | 169.8 | 4.6 | 202.1 | 47.4 | 167.6 | 3.4 | NA |
| 16ATW-10-Spot 18 | 56 | 39035 | 5.1 | 19.9 | 2.3 | 0.2 | 3.4 | 0.0 | 2.5 | 0.7 | 167.6 | 4.2 | 170.2 | 5.4 | 206.7 | 53.2 | 167.6 | 4.2 | NA |
| 16ATW-10-Spot 135 | 275 | 124456 | 3.1 | 20.3 | 1.4 | 0.2 | 3.0 | 0.0 | 2.6 | 0.9 | 168.1 | 4.3 | 167.4 | 4.6 | 158.1 | 31.8 | 168.1 | 4.3 | NA |
| 16ATW-10-Spot 139 | 92 | 64027 | 3.9 | 19.9 | 1.6 | 0.2 | 2.9 | 0.0 | 2.5 | 0.8 | 168.4 | 4.1 | 170.8 | 4.6 | 205.9 | 36.5 | 168.4 | 4.1 | NA |
| 16ATW-10-Spot 221 | 59 | 16110 | 4.0 | 20.4 | 1.9 | 0.2 | 3.1 | 0.0 | 2.4 | 0.8 | 168.9 | 4.0 | 167.2 | 4.7 | 143.1 | 45.1 | 168.9 | 4.0 | NA |
| 16ATW-10-Spot 272 | 135 | 20745 | 3.5 | 20.3 | 1.7 | 0.2 | 3.2 | 0.0 | 2.7 | 0.8 | 169.3 | 4.5 | 168.7 | 4.9 | 161.6 | 40.5 | 169.3 | 4.5 | NA |
| 16ATW-10-Spot 39 | 75 | 220756 | 4.9 | 20.3 | 1.8 | 0.2 | 2.5 | 0.0 | 1.8 | 0.7 | 169.8 | 3.0 | 169.4 | 3.9 | 165.9 | 42.1 | 169.8 | 3.0 | NA |
| 16ATW-10-Spot 188 | 14 | 10414 | 4.4 | 20.5 | 3.2 | 0.2 | 4.3 | 0.0 | 2.8 | 0.7 | 169.9 | 4.8 | 168.0 | 6.6 | 142.8 | 75.5 | 169.9 | 4.8 | NA |
| 16ATW-10-Spot 159 | 226 | 358629 | 3.4 | 20.4 | 1.3 | 0.2 | 2.9 | 0.0 | 2.6 | 0.9 | 170.0 | 4.4 | 168.8 | 4.6 | 153.4 | 30.1 | 170.0 | 4.4 | NA |
| 16ATW-10-Spot 160 | 93 | 38935 | 5.0 | 20.7 | 1.6 | 0.2 | 3.2 | 0.0 | 2.8 | 0.9 | 170.3 | 4.7 | 166.5 | 5.0 | 113.5 | 37.9 | 170.3 | 4.7 | NA |
| 16ATW-10-Spot 58 | 53 | 64773 | 4.2 | 20.1 | 2.0 | 0.2 | 2.9 | 0.0 | 2.1 | 0.7 | 171.0 | 3.6 | 171.6 | 4.6 | 179.8 | 46.0 | 171.0 | 3.6 | NA |
| 16ATW-10-Spot 312 | 173 | 325514 | 3.4 | 20.1 | 1.3 | 0.2 | 2.3 | 0.0 | 1.9 | 0.8 | 171.7 | 3.2 | 172.8 | 3.7 | 189.0 | 30.4 | 171.7 | 3.2 | NA |
| 16ATW-10-Spot 233 | 145 | 62737 | 4.3 | 20.4 | 1.2 | 0.2 | 2.8 | 0.0 | 2.6 | 0.9 | 172.0 | 4.3 | 170.5 | 4.4 | 150.4 | 28.5 | 172.0 | 4.3 | NA |
| 16ATW-10-Spot 97 | 53 | 41900 | 3.2 | 19.7 | 1.7 | 0.2 | 2.8 | 0.0 | 2.2 | 0.8 | 172.6 | 3.8 | 176.6 | 4.5 | 231.7 | 38.9 | 172.6 | 3.8 | NA |
| 16ATW-10-Spot 142 | 43 | 24597 | 4.7 | 20.6 | 2.3 | 0.2 | 2.8 | 0.0 | 1.7 | 0.6 | 172.7 | 2.9 | 169.2 | 4.4 | 122.5 | 54.0 | 172.7 | 2.9 | NA |
| 16ATW-10-Spot 249 | 55 | 127398 | 3.0 | 20.2 | 2.3 | 0.2 | 3.4 | 0.0 | 2.6 | 0.7 | 174.4 | 4.4 | 174.4 | 5.5 | 174.9 | 53.0 | 174.4 | 4.4 | NA |
| 16ATW-10-Spot 136 | 58 | 24178 | 2.7 | 20.0 | 1.9 | 0.2 | 3.5 | 0.0 | 3.0 | 0.8 | 174.6 | 5.1 | 176.1 | 5.7 | 197.5 | 43.8 | 174.6 | 5.1 | NA |
| 16ATW-10-Spot 124 | 123 | 48997 | 2.7 | 19.5 | 1.9 | 0.2 | 2.9 | 0.0 | 2.1 | 0.7 | 174.7 | 3.7 | 179.9 | 4.7 | 250.0 | 43.7 | 174.7 | 3.7 | NA |
| 16ATW-10-Spot 121 | 286 | 47153 | 2.2 | 20.3 | 1.0 | 0.2 | 2.5 | 0.0 | 2.4 | 0.9 | 175.5 | 4.1 | 174.7 | 4.1 | 164.4 | 22.6 | 175.5 | 4.1 | NA |
| 16ATW-10-Spot 252 | 160 | 147886 | 4.0 | 20.5 | 1.3 | 0.2 | 3.1 | 0.0 | 2.8 | 0.9 | 176.6 | 4.9 | 173.7 | 4.9 | 136.2 | 29.7 | 176.6 | 4.9 | NA |

| | | | | | | | | | | | | | | | | | | | |
|---|---|---|---|---|---|---|---|---|---|---|---|---|---|---|---|---|---|---|---|
| 16ATW-10-Spot 93 | 2673 | 600610 | 1.6 | 19.8 | 0.9 | 0.2 | 2.4 | 0.0 | 2.2 | 0.9 | 177.6 | 3.9 | 180.3 | 4.0 | 216.4 | 21.1 | 177.6 | 3.9 | NA |
| 16ATW-10-Spot 260 | 94 | 61560 | 2.7 | 19.8 | 1.5 | 0.2 | 2.5 | 0.0 | 2.0 | 0.8 | 178.2 | 3.5 | 180.9 | 4.1 | 217.2 | 34.6 | 178.2 | 3.5 | NA |
| 16ATW-10-Spot 131 | 299 | 560445 | 1.8 | 20.2 | 1.2 | 0.2 | 2.7 | 0.0 | 2.4 | 0.9 | 178.5 | 4.3 | 178.3 | 4.4 | 176.6 | 27.8 | 178.5 | 4.3 | NA |
| 16ATW-10-Spot 67 | 124 | 2199340 | 2.4 | 20.0 | 1.6 | 0.2 | 2.8 | 0.0 | 2.3 | 0.8 | 179.4 | 4.1 | 180.3 | 4.6 | 193.0 | 36.3 | 179.4 | 4.1 | NA |
| 16ATW-10-Spot 61 | 99 | 90310 | 2.0 | 20.0 | 1.7 | 0.2 | 4.3 | 0.0 | 4.0 | 0.9 | 182.2 | 7.1 | 182.7 | 7.2 | 190.8 | 40.6 | 182.2 | 7.1 | NA |
| 16ATW-10-Spot 241 | 347 | 872976 | 4.6 | 19.9 | 1.3 | 0.2 | 2.6 | 0.0 | 2.3 | 0.9 | 183.0 | 4.1 | 184.4 | 4.4 | 203.3 | 29.9 | 183.0 | 4.1 | NA |
| 16ATW-10-Spot 310 | 90 | 13085 | 3.0 | 20.8 | 1.9 | 0.2 | 2.9 | 0.0 | 2.1 | 0.7 | 183.5 | 3.9 | 178.1 | 4.7 | 107.9 | 44.9 | 183.5 | 3.9 | NA |
| 16ATW-10-Spot 193 | 441 | 199561 | 2.3 | 20.3 | 1.1 | 0.2 | 2.4 | 0.0 | 2.1 | 0.9 | 183.9 | 3.8 | 182.0 | 3.9 | 158.7 | 25.8 | 183.9 | 3.8 | NA |
| 16ATW-10-Spot 311 | 120 | 753386 | 3.3 | 20.5 | 1.4 | 0.2 | 2.6 | 0.0 | 2.2 | 0.9 | 183.9 | 4.0 | 180.4 | 4.3 | 136.3 | 32.0 | 183.9 | 4.0 | NA |
| 16ATW-10-Spot 138 | 374 | 408281 | 2.9 | 20.3 | 1.2 | 0.2 | 2.5 | 0.0 | 2.1 | 0.9 | 184.4 | 3.9 | 182.9 | 4.1 | 164.2 | 28.8 | 184.4 | 3.9 | NA |
| 16ATW-10-Spot 76 | 19 | 19457 | 2.8 | 19.7 | 3.1 | 0.2 | 4.1 | 0.0 | 2.7 | 0.7 | 185.7 | 5.0 | 188.8 | 7.1 | 228.3 | 72.0 | 185.7 | 5.0 | NA |
| 16ATW-10-Spot 36 | 66 | 79839 | 1.7 | 20.1 | 1.9 | 0.2 | 2.9 | 0.0 | 2.1 | 0.7 | 186.4 | 3.9 | 186.0 | 4.9 | 182.1 | 44.4 | 186.4 | 3.9 | NA |
| 16ATW-10-Spot 9 | 71 | 20370 | 2.6 | 20.4 | 1.7 | 0.2 | 3.1 | 0.0 | 2.5 | 0.8 | 186.5 | 4.6 | 183.7 | 5.1 | 148.9 | 40.6 | 186.5 | 4.6 | NA |
| 16ATW-10-Spot 134 | 134 | 856567 | 3.2 | 20.0 | 1.6 | 0.2 | 3.3 | 0.0 | 2.9 | 0.9 | 187.0 | 5.3 | 187.4 | 5.6 | 193.9 | 36.2 | 187.0 | 5.3 | NA |
| 16ATW-10-Spot 180 | 336 | 139933 | 2.8 | 19.9 | 1.3 | 0.2 | 2.4 | 0.0 | 2.1 | 0.8 | 187.1 | 3.8 | 188.1 | 4.2 | 202.2 | 30.2 | 187.1 | 3.8 | NA |
| 16ATW-10-Spot 27 | 152 | 81480 | 2.7 | 20.4 | 1.3 | 0.2 | 2.6 | 0.0 | 2.3 | 0.9 | 187.3 | 4.2 | 184.3 | 4.5 | 147.0 | 30.7 | 187.3 | 4.2 | NA |
| 16ATW-10-Spot 244 | 193 | 149422 | 3.0 | 20.5 | 1.1 | 0.2 | 2.9 | 0.0 | 2.7 | 0.9 | 187.3 | 4.9 | 183.9 | 4.9 | 141.0 | 25.7 | 187.3 | 4.9 | NA |
| 16ATW-10-Spot 288 | 51 | 57947 | 1.3 | 20.5 | 2.6 | 0.2 | 3.7 | 0.0 | 2.7 | 0.7 | 187.7 | 4.9 | 183.7 | 6.2 | 134.0 | 60.6 | 187.7 | 4.9 | NA |
| 16ATW-10-Spot 209 | 463 | 111634 | 1.9 | 20.1 | 1.0 | 0.2 | 2.2 | 0.0 | 2.0 | 0.9 | 187.7 | 3.7 | 187.8 | 3.8 | 189.2 | 23.1 | 187.7 | 3.7 | NA |
| 16ATW-10-Spot 246 | 105 | 73571 | 4.2 | 20.1 | 1.5 | 0.2 | 2.7 | 0.0 | 2.3 | 0.8 | 187.8 | 4.2 | 187.4 | 4.6 | 183.8 | 34.3 | 187.8 | 4.2 | NA |
| 16ATW-10-Spot 166 | 1149 | 3287784 | 4.2 | 19.8 | 1.0 | 0.2 | 2.2 | 0.0 | 2.0 | 0.9 | 188.0 | 3.6 | 190.1 | 3.8 | 217.0 | 23.6 | 188.0 | 3.6 | NA |
| 16ATW-10-Spot 28 | 76 | 43426 | 3.9 | 20.3 | 1.4 | 0.2 | 3.0 | 0.0 | 2.6 | 0.9 | 188.5 | 4.8 | 186.0 | 5.0 | 154.6 | 33.9 | 188.5 | 4.8 | NA |
| 16ATW-10-Spot 253 | 313 | 202540 | 0.8 | 20.0 | 1.2 | 0.2 | 2.4 | 0.0 | 2.1 | 0.9 | 188.9 | 4.0 | 189.7 | 4.2 | 200.0 | 27.5 | 188.9 | 4.0 | NA |
| 16ATW-10-Spot 118 | 159 | 202664 | 2.3 | 20.4 | 1.1 | 0.2 | 2.9 | 0.0 | 2.6 | 0.9 | 189.0 | 4.9 | 185.9 | 4.9 | 147.8 | 26.8 | 189.0 | 4.9 | NA |
| 16ATW-10-Spot 224 | 859 | 357426 | 3.0 | 20.0 | 1.2 | 0.2 | 2.8 | 0.0 | 2.6 | 0.9 | 189.1 | 4.8 | 189.2 | 4.9 | 192.1 | 27.3 | 189.1 | 4.8 | NA |

| | | | | | | | | | | | | | | | | | | | |
|---|---|---|---|---|---|---|---|---|---|---|---|---|---|---|---|---|---|---|---|
| 16ATW-10-Spot 157 | 61 | 163508 | 2.4 | 19.9 | 1.7 | 0.2 | 3.4 | 0.0 | 3.0 | 0.9 | 189.1 | 5.6 | 190.3 | 6.0 | 206.5 | 38.8 | 189.1 | 5.6 | NA |
| 16ATW-10-Spot 215 | 1157 | 593424 | 4.7 | 20.2 | 0.7 | 0.2 | 2.3 | 0.0 | 2.2 | 1.0 | 189.4 | 4.2 | 188.4 | 4.0 | 176.3 | 16.9 | 189.4 | 4.2 | NA |
| 16ATW-10-Spot 167 | 67 | 322940 | 2.9 | 20.3 | 1.5 | 0.2 | 2.6 | 0.0 | 2.1 | 0.8 | 189.5 | 3.8 | 187.7 | 4.4 | 165.9 | 35.6 | 189.5 | 3.8 | NA |
| 16ATW-10-Spot 127 | 189 | 171505 | 3.2 | 20.3 | 1.3 | 0.2 | 2.6 | 0.0 | 2.2 | 0.9 | 190.1 | 4.2 | 187.5 | 4.4 | 156.3 | 30.1 | 190.1 | 4.2 | NA |
| 16ATW-10-Spot 225 | 271 | 162027 | 2.8 | 20.0 | 1.0 | 0.2 | 2.9 | 0.0 | 2.7 | 0.9 | 190.3 | 5.1 | 190.8 | 5.0 | 197.7 | 22.3 | 190.3 | 5.1 | NA |
| 16ATW-10-Spot 24 | 58 | 974153 | 3.1 | 20.3 | 2.1 | 0.2 | 3.1 | 0.0 | 2.3 | 0.7 | 190.7 | 4.3 | 188.0 | 5.3 | 155.3 | 48.5 | 190.7 | 4.3 | NA |
| 16ATW-10-Spot 78 | 78 | 25251 | 2.9 | 20.8 | 2.1 | 0.2 | 3.1 | 0.0 | 2.3 | 0.7 | 190.8 | 4.3 | 184.2 | 5.2 | 101.4 | 48.7 | 190.8 | 4.3 | NA |
| 16ATW-10-Spot 15 | 183 | 53853 | 3.3 | 20.3 | 1.3 | 0.2 | 2.5 | 0.0 | 2.1 | 0.9 | 191.4 | 4.0 | 189.1 | 4.3 | 162.1 | 30.1 | 191.4 | 4.0 | NA |
| 16ATW-10-Spot 115 | 272 | 1917632 | 4.1 | 19.9 | 1.0 | 0.2 | 2.7 | 0.0 | 2.5 | 0.9 | 191.6 | 4.7 | 192.9 | 4.7 | 209.8 | 23.9 | 191.6 | 4.7 | NA |
| 16ATW-10-Spot 302 | 286 | 535295 | 4.5 | 20.0 | 0.9 | 0.2 | 2.5 | 0.0 | 2.4 | 0.9 | 191.7 | 4.5 | 192.1 | 4.4 | 198.0 | 20.0 | 191.7 | 4.5 | NA |
| 16ATW-10-Spot 83 | 99 | 69438 | 1.7 | 20.2 | 1.6 | 0.2 | 2.9 | 0.0 | 2.4 | 0.8 | 191.9 | 4.5 | 190.7 | 5.0 | 177.1 | 37.4 | 191.9 | 4.5 | NA |
| 16ATW-10-Spot 161 | 139 | 55542 | 3.3 | 20.1 | 1.3 | 0.2 | 2.7 | 0.0 | 2.3 | 0.9 | 192.2 | 4.4 | 191.6 | 4.7 | 186.1 | 31.1 | 192.2 | 4.4 | NA |
| 16ATW-10-Spot 191 | 1096 | 1774590 | 3.7 | 19.9 | 1.0 | 0.2 | 2.2 | 0.0 | 2.0 | 0.9 | 192.2 | 3.8 | 193.0 | 3.9 | 204.0 | 22.6 | 192.2 | 3.8 | NA |
| 16ATW-10-Spot 186 | 72 | 194385 | 3.2 | 20.0 | 1.9 | 0.2 | 3.1 | 0.0 | 2.5 | 0.8 | 192.2 | 4.7 | 192.2 | 5.4 | 193.5 | 43.6 | 192.2 | 4.7 | NA |
| 16ATW-10-Spot 232 | 855 | 922097 | 2.1 | 20.1 | 0.8 | 0.2 | 2.5 | 0.0 | 2.4 | 0.9 | 192.3 | 4.5 | 191.5 | 4.3 | 183.6 | 18.9 | 192.3 | 4.5 | NA |
| 16ATW-10-Spot 230 | 48 | 14581 | 3.4 | 20.0 | 1.9 | 0.2 | 3.2 | 0.0 | 2.6 | 0.8 | 192.4 | 5.0 | 192.2 | 5.6 | 191.3 | 43.2 | 192.4 | 5.0 | NA |
| 16ATW-10-Spot 245 | 65 | 23581 | 2.2 | 20.1 | 1.5 | 0.2 | 2.5 | 0.0 | 2.0 | 0.8 | 192.7 | 3.8 | 191.5 | 4.3 | 178.5 | 35.2 | 192.7 | 3.8 | NA |
| 16ATW-10-Spot 165 | 603 | 511243 | 2.1 | 20.3 | 0.9 | 0.2 | 2.1 | 0.0 | 1.9 | 0.9 | 192.7 | 3.5 | 190.0 | 3.6 | 157.0 | 21.2 | 192.7 | 3.5 | NA |
| 16ATW-10-Spot 280 | 34 | 12345 | 2.3 | 21.4 | 3.0 | 0.2 | 4.4 | 0.0 | 3.2 | 0.7 | 193.1 | 6.0 | 181.3 | 7.3 | 30.3 | 72.1 | 193.1 | 6.0 | NA |
| 16ATW-10-Spot 181 | 133 | 312556 | 2.2 | 20.1 | 1.1 | 0.2 | 2.3 | 0.0 | 2.0 | 0.9 | 193.2 | 3.8 | 192.4 | 4.0 | 183.8 | 25.0 | 193.2 | 3.8 | NA |
| 16ATW-10-Spot 120 | 163 | 152176 | 2.8 | 18.9 | 1.2 | 0.2 | 2.9 | 0.0 | 2.6 | 0.9 | 194.2 | 5.0 | 204.1 | 5.3 | 320.9 | 28.4 | 194.2 | 5.0 | NA |
| 16ATW-10-Spot 172 | 469 | 679002 | 2.2 | 20.1 | 1.0 | 0.2 | 2.2 | 0.0 | 2.0 | 0.9 | 194.8 | 3.8 | 193.6 | 3.9 | 180.6 | 23.9 | 194.8 | 3.8 | NA |
| 16ATW-10-Spot 212 | 104 | 266319 | 2.9 | 19.9 | 1.4 | 0.2 | 3.0 | 0.0 | 2.7 | 0.9 | 195.6 | 5.2 | 196.2 | 5.4 | 204.2 | 33.3 | 195.6 | 5.2 | NA |
| 16ATW-10-Spot 177 | 99 | 79041 | 2.6 | 20.7 | 1.3 | 0.2 | 3.3 | 0.0 | 3.0 | 0.9 | 196.1 | 5.7 | 190.0 | 5.7 | 116.5 | 31.7 | 196.1 | 5.7 | NA |

| | | | | | | | | | | | | | | | | | | | |
|---|---|---|---|---|---|---|---|---|---|---|---|---|---|---|---|---|---|---|---|
| 16ATW-10-Spot 285 | 38 | 12419 | 6.1 | 20.6 | 2.2 | 0.2 | 3.3 | 0.0 | 2.4 | 0.7 | 196.3 | 4.6 | 190.6 | 5.7 | 122.6 | 51.7 | 196.3 | 4.6 | NA |
| 16ATW-10-Spot 38 | 361 | 373391 | 4.0 | 20.0 | 1.0 | 0.2 | 2.3 | 0.0 | 2.1 | 0.9 | 197.4 | 4.1 | 196.7 | 4.1 | 189.5 | 22.1 | 197.4 | 4.1 | NA |
| 16ATW-10-Spot 220 | 209 | 107642 | 2.3 | 19.4 | 1.2 | 0.2 | 2.6 | 0.0 | 2.3 | 0.9 | 197.6 | 4.5 | 202.5 | 4.8 | 261.6 | 26.7 | 197.6 | 4.5 | NA |
| 16ATW-10-Spot 156 | 484 | 182722 | 3.1 | 20.2 | 0.9 | 0.2 | 2.4 | 0.0 | 2.2 | 0.9 | 198.4 | 4.3 | 196.2 | 4.2 | 170.4 | 20.8 | 198.4 | 4.3 | NA |
| 16ATW-10-Spot 294 | 512 | 292337 | 3.1 | 19.8 | 1.0 | 0.2 | 2.8 | 0.0 | 2.6 | 0.9 | 199.4 | 5.0 | 200.9 | 5.0 | 219.1 | 23.6 | 199.4 | 5.0 | NA |
| 16ATW-10-Spot 10 | 124 | 238191 | 4.3 | 18.9 | 1.3 | 0.2 | 2.8 | 0.0 | 2.5 | 0.9 | 200.2 | 4.9 | 210.1 | 5.3 | 323.9 | 28.9 | 200.2 | 4.9 | NA |
| 16ATW-10-Spot 7 | 114 | 70837 | 2.8 | 20.0 | 1.4 | 0.2 | 2.6 | 0.0 | 2.2 | 0.8 | 201.1 | 4.4 | 200.4 | 4.8 | 194.2 | 32.7 | 201.1 | 4.4 | NA |
| 16ATW-10-Spot 183 | 194 | 529151 | 4.4 | 20.1 | 1.2 | 0.2 | 2.6 | 0.0 | 2.4 | 0.9 | 201.4 | 4.7 | 200.0 | 4.8 | 184.6 | 26.8 | 201.4 | 4.7 | NA |
| 16ATW-10-Spot 228 | 305 | 79342 | 3.7 | 19.5 | 1.4 | 0.2 | 2.6 | 0.0 | 2.2 | 0.9 | 202.9 | 4.5 | 206.8 | 4.9 | 252.4 | 31.5 | 202.9 | 4.5 | NA |
| 16ATW-10-Spot 235 | 181 | 2684697 | 3.8 | 19.7 | 1.3 | 0.2 | 2.3 | 0.0 | 1.9 | 0.8 | 202.9 | 3.8 | 204.6 | 4.3 | 225.6 | 30.3 | 202.9 | 3.8 | NA |
| 16ATW-10-Spot 282 | 314 | 212559 | 4.4 | 20.2 | 1.1 | 0.2 | 2.7 | 0.0 | 2.5 | 0.9 | 203.4 | 5.1 | 200.4 | 5.0 | 166.4 | 25.1 | 203.4 | 5.1 | NA |
| 16ATW-10-Spot 270 | 270 | 702348 | 3.8 | 19.7 | 1.3 | 0.2 | 2.7 | 0.0 | 2.4 | 0.9 | 203.5 | 4.8 | 205.8 | 5.0 | 233.2 | 29.0 | 203.5 | 4.8 | NA |
| 16ATW-10-Spot 12 | 131 | 206082 | 3.2 | 19.9 | 1.3 | 0.2 | 2.5 | 0.0 | 2.1 | 0.8 | 203.6 | 4.2 | 203.8 | 4.5 | 207.4 | 30.4 | 203.6 | 4.2 | NA |
| 16ATW-10-Spot 194 | 115 | 98621 | 4.3 | 19.9 | 1.4 | 0.2 | 2.8 | 0.0 | 2.4 | 0.9 | 205.1 | 4.9 | 204.7 | 5.2 | 201.6 | 32.4 | 205.1 | 4.9 | NA |
| 16ATW-10-Spot 198 | 106 | 128247 | 2.7 | 19.5 | 1.5 | 0.2 | 2.7 | 0.0 | 2.3 | 0.8 | 205.7 | 4.6 | 209.5 | 5.1 | 253.8 | 33.5 | 205.7 | 4.6 | NA |
| 16ATW-10-Spot 70 | 124 | 35271 | 3.3 | 20.3 | 1.5 | 0.2 | 2.6 | 0.0 | 2.2 | 0.8 | 207.2 | 4.5 | 203.7 | 4.8 | 164.8 | 34.1 | 207.2 | 4.5 | NA |
| 16ATW-10-Spot 92 | 195 | 108984 | 3.3 | 20.1 | 1.2 | 0.2 | 2.8 | 0.0 | 2.5 | 0.9 | 208.3 | 5.1 | 206.4 | 5.2 | 185.4 | 28.0 | 208.3 | 5.1 | NA |
| 16ATW-10-Spot 91 | 46 | 62780 | 3.0 | 11.0 | 1.5 | 2.7 | 2.8 | 0.2 | 2.4 | 0.9 | 1260.0 | 27.7 | 1327.3 | 21.0 | 1438.5 | 28.3 | 1438.5 | 28.3 | 87.6 |
| 16ATW-10-Spot 19 | 54 | 13490 | 3.6 | 16.7 | 4.4 | 0.2 | 5.4 | 0.0 | 3.2 | 0.6 | 156.6 | 4.9 | 187.8 | 9.3 | 601.9 | 94.6 | 156.6 | 4.9 | NA |
| 16ATW-10-Spot 219 | 20 | 21282 | 2.8 | 15.8 | 3.9 | 0.2 | 4.9 | 0.0 | 2.8 | 0.6 | 160.1 | 4.5 | 201.3 | 8.9 | 716.2 | 83.7 | 160.1 | 4.5 | NA |
| 16ATW-10-Spot 104 | 34 | 5116 | 3.8 | 15.7 | 4.2 | 0.2 | 5.5 | 0.0 | 3.6 | 0.7 | 154.0 | 5.5 | 195.5 | 9.8 | 732.9 | 88.5 | 154.0 | 5.5 | NA |
| 16ATW-10-Spot 281 | 13 | 5681 | 4.3 | 15.2 | 7.2 | 0.2 | 7.8 | 0.0 | 3.0 | 0.4 | 167.5 | 4.9 | 217.3 | 15.3 | 798.5 | 152.1 | 167.5 | 4.9 | NA |
| 16ATW-10-Spot 208 | 37 | 61626 | 2.0 | 14.1 | 3.8 | 0.3 | 4.4 | 0.0 | 2.2 | 0.5 | 196.7 | 4.3 | 269.3 | 10.4 | 961.4 | 77.3 | 196.7 | 4.3 | NA |
| 16ATW-10-Spot 62 | 24 | 19246 | 2.9 | 14.1 | 7.4 | 0.2 | 8.0 | 0.0 | 3.0 | 0.4 | 162.2 | 4.8 | 225.4 | 16.2 | 951.3 | 152.3 | 162.2 | 4.8 | NA |
| 16ATW-10-Spot 107 | 39 | 24601 | 4.3 | 2.0 | 50.0 | 1.8 | 51.6 | 0.0 | 12.6 | 0.2 | 166.3 | 20.6 | 1044.3 | 349.5 | NA | NA | 166.3 | 20.6 | NA |
| 16ATW-10-Spot 109 | 21 | 11956 | 2.9 | 31.2 | 3.4 | 0.1 | 33.3 | 0.0 | 33.2 | 1.0 | 168.8 | 55.3 | 112.6 | 35.5 | NA | NA | 168.8 | 55.3 | NA |

| | | | | | | | | | | | | | | | | | | | |
|---|---|---|---|---|---|---|---|---|---|---|---|---|---|---|---|---|---|---|---|
| 16ATW-10-Spot 110 | 28 | 15272 | 2.6 | 21.8 | 3.1 | 0.2 | 8.7 | 0.0 | 8.1 | 0.9 | 166.6 | 13.4 | 155.4 | 12.6 | NA | NA | 166.6 | 13.4 | NA |
| 16ATW-10-Spot 108 | 13 | 8505 | 3.0 | 31.7 | 4.4 | 0.1 | 41.6 | 0.0 | 41.3 | 1.0 | 161.9 | 66.1 | 106.3 | 42.0 | NA | NA | 161.9 | 66.1 | NA |
| 16ATW-10-Spot 137 | 36 | 22732 | 3.8 | 21.7 | 2.4 | 0.2 | 3.9 | 0.0 | 3.1 | 0.8 | 156.5 | 4.8 | 147.4 | 5.4 | 4.9 | 58.0 | 156.5 | 4.8 | NA |
| 16ATW-10-Spot 266 | 67 | 27001 | 3.4 | 21.3 | 1.7 | 0.2 | 3.0 | 0.0 | 2.5 | 0.8 | 151.9 | 3.8 | 145.5 | 4.1 | 44.4 | 41.3 | 151.9 | 3.8 | NA |
| 16ATW-10-Spot 20 | 96 | 333176 | 2.3 | 21.3 | 1.8 | 0.2 | 3.0 | 0.0 | 2.4 | 0.8 | 159.6 | 3.9 | 152.7 | 4.3 | 48.5 | 43.3 | 159.6 | 3.9 | NA |
| 16ATW-10-Spot 210 | 76 | 19748 | 2.9 | 21.2 | 1.7 | 0.2 | 3.0 | 0.0 | 2.4 | 0.8 | 160.9 | 3.9 | 154.4 | 4.3 | 56.5 | 41.5 | 160.9 | 3.9 | NA |
| 16ATW-10-Spot 141 | 129 | 27689 | 1.8 | 21.0 | 1.5 | 0.2 | 2.8 | 0.0 | 2.4 | 0.9 | 168.0 | 4.0 | 162.0 | 4.2 | 74.9 | 34.7 | 168.0 | 4.0 | NA |
| 16ATW-10-Spot 87 | 85 | 30566 | 3.4 | 20.9 | 1.5 | 0.2 | 2.9 | 0.0 | 2.5 | 0.9 | 184.3 | 4.5 | 177.6 | 4.7 | 90.6 | 35.6 | 184.3 | 4.5 | NA |
| 16ATW-10-Spot 255 | 295 | 131136 | 3.6 | 20.7 | 1.1 | 0.2 | 2.8 | 0.0 | 2.6 | 0.9 | 199.3 | 5.1 | 193.1 | 5.0 | 118.7 | 26.1 | 199.3 | 5.1 | NA |
| 16ATW-10-Spot 243 | 280 | 171177 | 2.4 | 20.5 | 1.1 | 0.2 | 3.1 | 0.0 | 2.9 | 0.9 | 214.9 | 6.1 | 208.9 | 5.8 | 142.1 | 25.4 | 214.9 | 6.1 | NA |
| 16ATW-10-Spot 30 | 16 | 25569 | 4.2 | 22.6 | 3.5 | 0.1 | 4.0 | 0.0 | 2.1 | 0.5 | 154.2 | 3.2 | 139.6 | 5.3 | NA | NA | 154.2 | 3.2 | NA |
| 16ATW-10-Spot 250 | 18 | 30466 | 3.4 | 23.2 | 3.7 | 0.1 | 4.5 | 0.0 | 2.6 | 0.6 | 154.6 | 4.0 | 136.6 | 5.8 | NA | NA | 154.6 | 4.0 | NA |
| 16ATW-10-Spot 153 | 19 | 6698 | 3.2 | 22.7 | 3.7 | 0.1 | 4.7 | 0.0 | 2.9 | 0.6 | 155.3 | 4.4 | 140.2 | 6.2 | NA | NA | 155.3 | 4.4 | NA |
| 16ATW-10-Spot 213 | 36 | 11804 | 3.4 | 22.0 | 2.7 | 0.2 | 3.8 | 0.0 | 2.7 | 0.7 | 155.3 | 4.2 | 144.5 | 5.2 | NA | NA | 155.3 | 4.2 | NA |
| 16ATW-10-Spot 2 | 23 | 21839 | 3.6 | 22.1 | 3.2 | 0.2 | 3.9 | 0.0 | 2.2 | 0.6 | 155.7 | 3.4 | 143.8 | 5.2 | NA | NA | 155.7 | 3.4 | NA |
| 16ATW-10-Spot 21 | 27 | 12193 | 3.3 | 22.0 | 2.7 | 0.2 | 4.3 | 0.0 | 3.3 | 0.8 | 156.5 | 5.1 | 145.4 | 5.8 | NA | NA | 156.5 | 5.1 | NA |
| 16ATW-10-Spot 248 | 24 | 4379 | 5.6 | 22.4 | 3.0 | 0.2 | 4.2 | 0.0 | 3.0 | 0.7 | 156.6 | 4.6 | 143.2 | 5.7 | NA | NA | 156.6 | 4.6 | NA |
| 16ATW-10-Spot 49 | 23 | 8647 | 4.5 | 23.7 | 3.4 | 0.1 | 4.1 | 0.0 | 2.3 | 0.6 | 159.1 | 3.6 | 137.9 | 5.3 | NA | NA | 159.1 | 3.6 | NA |
| 16ATW-10-Spot 123 | 18 | 7964 | 3.6 | 22.0 | 3.2 | 0.2 | 4.2 | 0.0 | 2.7 | 0.6 | 161.8 | 4.3 | 149.8 | 5.9 | NA | NA | 161.8 | 4.3 | NA |
| 16ATW-10-Spot 264 | 21 | 11548 | 3.4 | 24.5 | 2.8 | 0.1 | 4.1 | 0.0 | 3.0 | 0.7 | 159.2 | 4.6 | 133.8 | 5.1 | NA | NA | 159.2 | 4.6 | NA |

Sample 16ATW44b

| Analysis | U | 206Pb | U/Th | 206Pb * | ± | 207Pb * | ± | 206Pb * | ± | error | 206Pb * | ± | 207Pb * | ± | 206Pb * | ± | Best age | ± (1s random) | Conc |
|---|---|---|---|---|---|---|---|---|---|---|---|---|---|---|---|---|---|---|---|
| | (ppm) | 204Pb | | 207Pb * | (%) | 235U * | (%) | 238U | (%) | corr. | 238U * | (Ma) | 235U | (Ma) | 207Pb * | (Ma) | (Ma) | (Ma) | (%) |
| 16ATW-44B-Spot 76 | 1979 | 355688 | 489.6 | 20.6 | 1.0 | 0.1 | 2.4 | 0.0 | 2.1 | 0.9 | 78.8 | 1.7 | 80.3 | 1.8 | 124.8 | 23.9 | 78.8 | 1.7 | NA |
| 16ATW-44B-Spot 27 | 2374 | 198295 | 1847.1 | 19.9 | 0.8 | 0.1 | 2.6 | 0.0 | 2.4 | 1.0 | 99.6 | 2.4 | 104.0 | 2.5 | 207.5 | 18.0 | 99.6 | 2.4 | NA |

| | | | | | | | | | | | | | | | | | | | |
|---|---|---|---|---|---|---|---|---|---|---|---|---|---|---|---|---|---|---|---|
| 16ATW-44B-Spot 47 | 1269 | 395756 | 2684.2 | 20.4 | 1.0 | 0.1 | 2.0 | 0.0 | 1.8 | 0.9 | 99.7 | 1.7 | 101.8 | 2.0 | 151.9 | 23.4 | 99.7 | 1.7 | NA |
| 16ATW-44B-Spot 56 | 1079 | 222279 | 1311.1 | 19.3 | 3.7 | 0.1 | 7.7 | 0.0 | 6.8 | 0.9 | 100.4 | 6.7 | 108.0 | 7.9 | 280.0 | 83.8 | 100.4 | 6.7 | NA |
| 16ATW-44B-Spot 81 | 1326 | 94825 | 50.3 | 19.8 | 1.1 | 0.1 | 6.9 | 0.0 | 6.8 | 1.0 | 101.7 | 6.8 | 106.6 | 6.9 | 218.6 | 25.8 | 101.7 | 6.8 | NA |
| 16ATW-44B-Spot 70 | 3298 | 176604 | 88.0 | 19.5 | 1.1 | 0.1 | 1.9 | 0.0 | 1.6 | 0.8 | 103.4 | 1.6 | 109.9 | 2.0 | 255.4 | 25.9 | 103.4 | 1.6 | NA |
| 16ATW-44B-Spot 66 | 1693 | 222807 | 541.7 | 19.6 | 1.1 | 0.1 | 4.0 | 0.0 | 3.8 | 1.0 | 107.0 | 4.0 | 113.2 | 4.2 | 246.5 | 25.4 | 107.0 | 4.0 | NA |
| 16ATW-44B-Spot 4 | 888 | 400449 | 451.6 | 20.0 | 0.9 | 0.1 | 2.0 | 0.0 | 1.8 | 0.9 | 107.6 | 1.9 | 111.2 | 2.1 | 191.0 | 21.6 | 107.6 | 1.9 | NA |
| 16ATW-44B-Spot 67 | 488 | 57341 | 923.9 | 20.6 | 1.2 | 0.1 | 2.3 | 0.0 | 2.0 | 0.9 | 109.1 | 2.1 | 109.8 | 2.4 | 125.3 | 27.4 | 109.1 | 2.1 | NA |
| 16ATW-44B-Spot 41 | 547 | 163103 | 24.7 | 20.3 | 1.1 | 0.1 | 2.5 | 0.0 | 2.2 | 0.9 | 109.1 | 2.4 | 111.3 | 2.6 | 159.1 | 26.1 | 109.1 | 2.4 | NA |
| 16ATW-44B-Spot 78 | 658 | 97747 | 33.1 | 20.1 | 1.1 | 0.1 | 3.1 | 0.0 | 2.8 | 0.9 | 111.5 | 3.1 | 114.9 | 3.3 | 186.2 | 26.3 | 111.5 | 3.1 | NA |
| 16ATW-44B-Spot 28 | 182 | 76868 | 10.9 | 20.0 | 1.3 | 0.1 | 3.6 | 0.0 | 3.4 | 0.9 | 130.3 | 4.4 | 133.6 | 4.6 | 193.2 | 30.2 | 130.3 | 4.4 | NA |
| 16ATW-44B-Spot 3 | 719 | 1565031 | 7.9 | 20.2 | 0.9 | 0.1 | 2.1 | 0.0 | 1.9 | 0.9 | 131.3 | 2.5 | 133.1 | 2.6 | 166.8 | 21.4 | 131.3 | 2.5 | NA |
| 16ATW-44B-Spot 57 | 835 | 72086 | 12.7 | 18.2 | 1.2 | 0.2 | 3.8 | 0.0 | 3.6 | 1.0 | 142.2 | 5.1 | 158.2 | 5.6 | 406.6 | 26.3 | 142.2 | 5.1 | NA |
| 16ATW-44B-Spot 6 | 775 | 300560 | 3.5 | 20.2 | 0.9 | 0.2 | 2.5 | 0.0 | 2.3 | 0.9 | 152.2 | 3.5 | 153.5 | 3.5 | 173.9 | 19.9 | 152.2 | 3.5 | NA |
| 16ATW-44B-Spot 58 | 81 | 208321 | 6.8 | 20.1 | 1.6 | 0.2 | 3.3 | 0.0 | 2.8 | 0.9 | 152.6 | 4.3 | 154.3 | 4.7 | 181.7 | 37.6 | 152.6 | 4.3 | NA |
| 16ATW-44B-Spot 1 | 183 | 62000 | 4.7 | 19.7 | 1.4 | 0.2 | 2.5 | 0.0 | 2.1 | 0.8 | 153.4 | 3.2 | 158.0 | 3.7 | 227.2 | 32.1 | 153.4 | 3.2 | NA |
| 16ATW-44B-Spot 11 | 514 | 44215 | 1.3 | 20.3 | 1.1 | 0.2 | 2.0 | 0.0 | 1.6 | 0.8 | 157.1 | 2.5 | 157.1 | 2.8 | 158.4 | 24.8 | 157.1 | 2.5 | NA |
| 16ATW-44B-Spot 9 | 67 | 35770 | 3.9 | 20.3 | 2.5 | 0.2 | 3.9 | 0.0 | 2.9 | 0.8 | 158.3 | 4.6 | 158.2 | 5.7 | 158.4 | 59.5 | 158.3 | 4.6 | NA |
| 16ATW-44B-Spot 29 | 98 | 45094 | 3.5 | 20.0 | 1.4 | 0.2 | 2.5 | 0.0 | 2.1 | 0.8 | 159.8 | 3.3 | 161.8 | 3.8 | 192.8 | 32.9 | 159.8 | 3.3 | NA |
| 16ATW-44B-Spot 68 | 94 | 20694 | 2.6 | 20.7 | 1.7 | 0.2 | 2.7 | 0.0 | 2.0 | 0.8 | 160.5 | 3.2 | 157.2 | 3.9 | 109.5 | 41.0 | 160.5 | 3.2 | NA |
| 16ATW-44B-Spot 19 | 90 | 25637 | 2.4 | 19.0 | 1.9 | 0.2 | 3.1 | 0.0 | 2.5 | 0.8 | 165.0 | 4.1 | 174.6 | 5.0 | 307.2 | 42.5 | 165.0 | 4.1 | NA |
| 16ATW-44B-Spot 21 | 270 | 65696 | 15.2 | 20.8 | 1.6 | 0.2 | 3.2 | 0.0 | 2.8 | 0.9 | 172.5 | 4.8 | 167.8 | 5.0 | 103.8 | 37.0 | 172.5 | 4.8 | NA |
| 16ATW-44B-Spot 65 | 201 | 468910 | 1.7 | 19.0 | 2.5 | 0.2 | 3.7 | 0.0 | 2.7 | 0.7 | 172.5 | 4.6 | 182.6 | 6.2 | 315.3 | 57.5 | 172.5 | 4.6 | NA |
| 16ATW-44B-Spot 40 | 283 | 112714 | 3.7 | 18.8 | 1.3 | 0.2 | 2.2 | 0.0 | 1.8 | 0.8 | 180.9 | 3.2 | 192.6 | 3.9 | 339.9 | 30.4 | 180.9 | 3.2 | NA |

| | | | | | | | | | | | | | | | | | | | |
|---|---|---|---|---|---|---|---|---|---|---|---|---|---|---|---|---|---|---|---|
| 16ATW-44B-Spot 53 | 80 | 241824 | 1.8 | 19.5 | 1.8 | 0.2 | 3.0 | 0.0 | 2.4 | 0.8 | 182.9 | 4.3 | 188.2 | 5.2 | 256.0 | 41.3 | 182.9 | 4.3 | NA |
| 16ATW-44B-Spot 59 | 614 | 116748 | 3.3 | 20.6 | 1.3 | 0.2 | 2.6 | 0.0 | 2.2 | 0.9 | 183.3 | 4.1 | 179.2 | 4.3 | 126.5 | 31.0 | 183.3 | 4.1 | NA |
| 16ATW-44B-Spot 79 | 578 | 385509 | 1.4 | 20.0 | 0.9 | 0.2 | 2.1 | 0.0 | 2.0 | 0.9 | 183.8 | 3.5 | 184.4 | 3.6 | 193.7 | 20.7 | 183.8 | 3.5 | NA |
| 16ATW-44B-Spot 31 | 1374 | 265024 | 1.2 | 20.3 | 1.0 | 0.2 | 2.3 | 0.0 | 2.1 | 0.9 | 185.5 | 3.9 | 183.3 | 3.9 | 156.7 | 22.2 | 185.5 | 3.9 | NA |
| 16ATW-44B-Spot 62 | 90 | 31130 | 2.0 | 20.6 | 1.9 | 0.2 | 3.3 | 0.0 | 2.6 | 0.8 | 186.4 | 4.8 | 182.0 | 5.4 | 125.9 | 45.4 | 186.4 | 4.8 | NA |
| 16ATW-44B-Spot 39 | 211 | 65133 | 1.2 | 20.0 | 1.5 | 0.2 | 2.5 | 0.0 | 2.0 | 0.8 | 188.0 | 3.7 | 188.5 | 4.3 | 197.0 | 35.5 | 188.0 | 3.7 | NA |
| 16ATW-44B-Spot 16 | 328 | 324792 | 3.2 | 19.6 | 1.0 | 0.2 | 3.9 | 0.0 | 3.8 | 1.0 | 188.1 | 7.0 | 191.9 | 6.8 | 240.7 | 22.8 | 188.1 | 7.0 | NA |
| 16ATW-44B-Spot 75 | 916 | 1301966 | 0.9 | 20.1 | 0.8 | 0.2 | 2.2 | 0.0 | 2.0 | 0.9 | 188.4 | 3.8 | 187.7 | 3.7 | 180.6 | 18.9 | 188.4 | 3.8 | NA |
| 16ATW-44B-Spot 50 | 39 | 9542 | 2.5 | 20.5 | 2.1 | 0.2 | 3.2 | 0.0 | 2.5 | 0.8 | 191.3 | 4.7 | 186.9 | 5.5 | 131.7 | 48.9 | 191.3 | 4.7 | NA |
| 16ATW-44B-Spot 71 | 373 | 263567 | 1.3 | 20.2 | 0.8 | 0.2 | 2.4 | 0.0 | 2.3 | 0.9 | 191.4 | 4.3 | 190.1 | 4.2 | 176.0 | 18.8 | 191.4 | 4.3 | NA |
| 16ATW-44B-Spot 72 | 242 | 70683 | 0.8 | 19.3 | 1.9 | 0.2 | 3.3 | 0.0 | 2.6 | 0.8 | 193.6 | 5.0 | 199.8 | 5.9 | 275.0 | 43.9 | 193.6 | 5.0 | NA |
| 16ATW-44B-Spot 61 | 177 | 144410 | 1.6 | 20.4 | 1.2 | 0.2 | 2.3 | 0.0 | 1.9 | 0.8 | 193.8 | 3.6 | 190.3 | 3.9 | 148.1 | 29.2 | 193.8 | 3.6 | NA |
| 16ATW-44B-Spot 36 | 117 | 28109 | 2.0 | 20.6 | 1.7 | 0.2 | 3.6 | 0.0 | 3.2 | 0.9 | 195.0 | 6.1 | 189.8 | 6.2 | 127.1 | 40.1 | 195.0 | 6.1 | NA |
| 16ATW-44B-Spot 15 | 652 | 248100 | 2.8 | 20.1 | 1.1 | 0.2 | 2.4 | 0.0 | 2.1 | 0.9 | 197.9 | 4.1 | 196.5 | 4.2 | 180.1 | 26.1 | 197.9 | 4.1 | NA |
| 16ATW-44B-Spot 63 | 316 | 291330 | 3.2 | 19.9 | 1.0 | 0.2 | 3.0 | 0.0 | 2.8 | 0.9 | 198.9 | 5.5 | 199.4 | 5.5 | 205.9 | 23.9 | 198.9 | 5.5 | NA |
| 16ATW-44B-Spot 17 | 109 | 43100 | 3.0 | 20.5 | 1.5 | 0.2 | 2.8 | 0.0 | 2.4 | 0.8 | 199.6 | 4.7 | 194.4 | 5.0 | 132.2 | 35.1 | 199.6 | 4.7 | NA |
| 16ATW-44B-Spot 60 | 246 | 65752 | 3.3 | 20.0 | 1.6 | 0.2 | 3.2 | 0.0 | 2.8 | 0.9 | 200.7 | 5.5 | 199.9 | 5.8 | 191.4 | 36.2 | 200.7 | 5.5 | NA |
| 16ATW-44B-Spot 7 | 103 | 386477 | 4.7 | 20.1 | 1.7 | 0.2 | 2.8 | 0.0 | 2.2 | 0.8 | 202.9 | 4.5 | 201.6 | 5.1 | 187.7 | 38.8 | 202.9 | 4.5 | NA |
| 16ATW-44B-Spot 64 | 216 | 43834 | 2.1 | 20.0 | 1.4 | 0.2 | 2.8 | 0.0 | 2.5 | 0.9 | 203.2 | 5.0 | 202.2 | 5.2 | 191.2 | 32.3 | 203.2 | 5.0 | NA |
| 16ATW-44B-Spot 54 | 97 | 499610 | 3.6 | 19.7 | 1.7 | 0.2 | 3.2 | 0.0 | 2.7 | 0.9 | 204.8 | 5.5 | 206.9 | 6.0 | 232.7 | 38.2 | 204.8 | 5.5 | NA |
| 16ATW-44B-Spot 13 | 176 | 160901 | 2.8 | 19.8 | 1.2 | 0.2 | 2.3 | 0.0 | 2.0 | 0.9 | 204.8 | 3.9 | 206.2 | 4.3 | 222.7 | 27.5 | 204.8 | 3.9 | NA |
| 16ATW-44B-Spot 26 | 253 | 270570 | 3.2 | 19.9 | 1.3 | 0.2 | 2.7 | 0.0 | 2.4 | 0.9 | 205.1 | 4.8 | 205.6 | 5.0 | 211.8 | 29.3 | 205.1 | 4.8 | NA |
| 16ATW-44B-Spot 42 | 826 | 960517 | 2.4 | 20.0 | 0.9 | 0.2 | 2.3 | 0.0 | 2.1 | 0.9 | 205.4 | 4.2 | 204.4 | 4.2 | 193.6 | 21.7 | 205.4 | 4.2 | NA |

| | | | | | | | | | | | | | | | | | | | |
|---|---|---|---|---|---|---|---|---|---|---|---|---|---|---|---|---|---|---|---|
| 16ATW-44B-Spot 12 | 288 | 104110 | 2.1 | 19.9 | 1.4 | 0.2 | 2.8 | 0.0 | 2.4 | 0.9 | 207.0 | 4.9 | 206.8 | 5.2 | 205.6 | 32.0 | 207.0 | 4.9 | NA |
| 16ATW-44B-Spot 73 | 104 | 65750 | 2.8 | 19.8 | 1.4 | 0.2 | 2.9 | 0.0 | 2.5 | 0.9 | 207.3 | 5.1 | 208.1 | 5.4 | 217.7 | 33.2 | 207.3 | 5.1 | NA |
| 16ATW-44B-Spot 38 | 532 | 115663 | 2.2 | 20.2 | 1.1 | 0.2 | 2.2 | 0.0 | 1.9 | 0.9 | 208.9 | 3.9 | 206.3 | 4.1 | 176.9 | 25.3 | 208.9 | 3.9 | NA |
| 16ATW-44B-Spot 37 | 700 | 177711 | 1.3 | 19.9 | 1.0 | 0.2 | 2.5 | 0.0 | 2.3 | 0.9 | 209.7 | 4.7 | 209.2 | 4.7 | 204.7 | 23.5 | 209.7 | 4.7 | NA |
| 16ATW-44B-Spot 45 | 4515 | 107856 | 1688.9 | 18.9 | 2.3 | 0.1 | 3.0 | 0.0 | 2.0 | 0.7 | 101.4 | 2.0 | 110.9 | 3.2 | 322.2 | 51.8 | 101.4 | 2.0 | NA |
| 16ATW-44B-Spot 25 | 843 | 86904 | 9.8 | 18.0 | 1.2 | 0.2 | 2.8 | 0.0 | 2.5 | 0.9 | 127.6 | 3.2 | 145.0 | 3.8 | 440.5 | 27.5 | 127.6 | 3.2 | NA |
| 16ATW-44B-Spot 43 | 465 | 125510 | 1354.3 | 18.5 | 3.9 | 0.1 | 7.6 | 0.0 | 6.5 | 0.9 | 92.1 | 5.9 | 103.3 | 7.4 | 372.5 | 88.1 | 92.1 | 5.9 | NA |
| 16ATW-44B-Spot 18 | 185 | 62212 | 9.4 | 17.6 | 1.7 | 0.1 | 3.3 | 0.0 | 2.8 | 0.8 | 120.2 | 3.3 | 139.7 | 4.3 | 487.0 | 38.5 | 120.2 | 3.3 | NA |
| 16ATW-44B-Spot 32 | 187 | 552530 | 131.9 | 18.5 | 1.9 | 0.1 | 3.3 | 0.0 | 2.7 | 0.8 | 80.7 | 2.2 | 91.2 | 2.9 | 374.6 | 42.5 | 80.7 | 2.2 | NA |
| 16ATW-44B-Spot 34 | 784 | 117602 | 1451.1 | 17.4 | 1.7 | 0.1 | 2.7 | 0.0 | 2.0 | 0.8 | 101.2 | 2.0 | 120.0 | 3.0 | 511.1 | 37.3 | 101.2 | 2.0 | NA |
| 16ATW-44B-Spot 55 | 272 | 16176 | 4.7 | 9.9 | 10.7 | 0.7 | 11.1 | 0.1 | 2.8 | 0.2 | 316.7 | 8.5 | 540.0 | 46.5 | 1645.7 | 199.7 | 316.7 | 8.5 | NA |
| 16ATW-44B-Spot 14 | 3462 | 91491 | 170.5 | 17.2 | 1.9 | 0.1 | 3.4 | 0.0 | 2.9 | 0.8 | 102.3 | 2.9 | 122.6 | 4.0 | 537.2 | 41.7 | 102.3 | 2.9 | NA |
| 16ATW-44B-Spot 52 | 2662 | 60335 | 23.8 | 16.8 | 1.4 | 0.1 | 2.9 | 0.0 | 2.5 | 0.9 | 108.8 | 2.7 | 132.5 | 3.6 | 581.1 | 30.8 | 108.8 | 2.7 | NA |
| 16ATW-44B-Spot 48 | 394 | 254386 | 11.9 | 14.5 | 3.8 | 0.2 | 7.9 | 0.0 | 6.9 | 0.9 | 144.8 | 9.9 | 197.9 | 14.2 | 890.6 | 79.1 | 144.8 | 9.9 | NA |
| 16ATW-44B-Spot 5 | 580 | 18001 | 18.9 | 13.0 | 3.5 | 0.2 | 6.4 | 0.0 | 5.4 | 0.8 | 141.2 | 7.6 | 213.7 | 12.4 | 1114.6 | 69.3 | 141.2 | 7.6 | NA |
| 16ATW-44B-Spot 23 | 552 | 47494 | 311.5 | 14.5 | 4.5 | 0.1 | 5.7 | 0.0 | 3.5 | 0.6 | 95.5 | 3.3 | 134.5 | 7.2 | 894.2 | 93.0 | 95.5 | 3.3 | NA |
| 16ATW-44B-Spot 69 | 78 | 6894 | 199.9 | 12.2 | 5.7 | 0.2 | 9.1 | 0.0 | 7.1 | 0.8 | 116.0 | 8.1 | 190.0 | 15.7 | 1250.1 | 110.8 | 116.0 | 8.1 | NA |
| 16ATW-44B-Spot 33 | 1174 | 24457 | 246.3 | 13.1 | 6.6 | 0.2 | 6.8 | 0.0 | 1.6 | 0.2 | 95.5 | 1.5 | 147.6 | 9.3 | 1096.8 | 131.7 | 95.5 | 1.5 | NA |
| 16ATW-44B-Spot 8 | 1026 | 11345 | 8.2 | 10.3 | 3.4 | 0.3 | 6.3 | 0.0 | 5.3 | 0.8 | 123.8 | 6.5 | 234.6 | 13.1 | 1571.6 | 62.8 | 123.8 | 6.5 | NA |
| 16ATW-44B-Spot 49 | 242 | 8216 | 9.0 | 7.5 | 16.4 | 0.5 | 17.8 | 0.0 | 7.0 | 0.4 | 163.3 | 11.3 | 392.7 | 58.0 | 2144.9 | 287.9 | 163.3 | 11.3 | NA |
| 16ATW-44B-Spot 22 | 338 | 7762 | 24.5 | 8.2 | 5.0 | 0.3 | 6.3 | 0.0 | 3.8 | 0.6 | 118.2 | 4.5 | 274.1 | 15.2 | 1979.2 | 89.8 | 118.2 | 4.5 | NA |
| 16ATW-44B-Spot 44 | 87 | 1229 | 2.5 | 2.0 | 6.8 | 8.0 | 22.9 | 0.1 | 21.9 | 1.0 | 719.8 | 149.0 | 2230.8 | 209.7 | NA | NA | 5000.0 | 100.3 | NA |

Sample 16ATW77

| Analysis | U (ppm) | 206Pb 204Pb | U/Th | 206Pb* 207Pb* | ± (%) | 207Pb* 235U* | ± (%) | 206Pb* 238U | ± (%) | error corr. | 206Pb* 238U* | ± (Ma) | 207Pb* 235U | ± (Ma) | 206Pb* 207Pb* | ± (Ma) | Best age (Ma) | ± (Ma) | Conc (%) |
|---|---|---|---|---|---|---|---|---|---|---|---|---|---|---|---|---|---|---|---|
| 16ATW-77 -Spot 224 | 722 | 20818 | 3.5 | 20.4 | 1.4 | 0.1 | 3.1 | 0.0 | 2.8 | 0.9 | 51.8 | 1.4 | 53.7 | 1.6 | 143.6 | 32.6 | 51.8 | 1.4 | NA |
| 16ATW-77 -Spot 228 | 262 | 13479 | 3.4 | 20.0 | 2.7 | 0.1 | 3.6 | 0.0 | 2.4 | 0.7 | 51.8 | 1.2 | 54.8 | 1.9 | 189.4 | 62.3 | 51.8 | 1.2 | NA |
| 16ATW-77 -Spot 276 | 3275 | 141031 | 1.3 | 21.0 | 1.0 | 0.1 | 2.3 | 0.0 | 2.1 | 0.9 | 53.3 | 1.1 | 53.8 | 1.2 | 80.0 | 23.2 | 53.3 | 1.1 | NA |
| 16ATW-77 -Spot 124 | 3448 | 65273 | 3.9 | 20.6 | 1.1 | 0.1 | 2.2 | 0.0 | 1.9 | 0.9 | 53.4 | 1.0 | 55.0 | 1.2 | 123.6 | 24.9 | 53.4 | 1.0 | NA |
| 16ATW-77 -Spot 234 | 658 | 30387 | 2.8 | 20.6 | 1.6 | 0.1 | 3.1 | 0.0 | 2.6 | 0.9 | 54.2 | 1.4 | 55.6 | 1.7 | 120.3 | 37.4 | 54.2 | 1.4 | NA |
| 16ATW-77 -Spot 29 | 2292 | 3897990 | 4.3 | 20.5 | 1.1 | 0.1 | 2.7 | 0.0 | 2.4 | 0.9 | 54.5 | 1.3 | 56.3 | 1.5 | 136.1 | 25.9 | 54.5 | 1.3 | NA |
| 16ATW-77 -Spot 180 | 841 | 125898 | 2.6 | 20.3 | 1.3 | 0.1 | 2.8 | 0.0 | 2.4 | 0.9 | 54.6 | 1.3 | 57.1 | 1.5 | 163.5 | 31.1 | 54.6 | 1.3 | NA |
| 16ATW-77 -Spot 218 | 1687 | 176778 | 1.7 | 20.9 | 0.9 | 0.1 | 2.5 | 0.0 | 2.3 | 0.9 | 54.9 | 1.3 | 55.7 | 1.4 | 92.7 | 22.5 | 54.9 | 1.3 | NA |
| 16ATW-77 -Spot 216 | 452 | 21293 | 5.8 | 20.6 | 2.0 | 0.1 | 3.6 | 0.0 | 3.0 | 0.8 | 55.2 | 1.7 | 56.9 | 2.0 | 128.8 | 46.0 | 55.2 | 1.7 | NA |
| 16ATW-77 -Spot 175 | 845 | 61184 | 2.3 | 20.7 | 1.8 | 0.1 | 2.9 | 0.0 | 2.3 | 0.8 | 55.4 | 1.3 | 56.8 | 1.6 | 117.8 | 41.6 | 55.4 | 1.3 | NA |
| 16ATW-77 -Spot 203 | 2751 | 811057 | 1.6 | 20.7 | 0.7 | 0.1 | 2.0 | 0.0 | 1.9 | 0.9 | 55.8 | 1.0 | 57.0 | 1.1 | 111.1 | 16.5 | 55.8 | 1.0 | NA |
| 16ATW-77 -Spot 38 | 1792 | 75150 | 5.6 | 20.7 | 0.9 | 0.1 | 2.0 | 0.0 | 1.8 | 0.9 | 55.9 | 1.0 | 57.2 | 1.1 | 111.8 | 22.1 | 55.9 | 1.0 | NA |
| 16ATW-77 -Spot 282 | 2292 | 27925 | 3.7 | 21.1 | 1.2 | 0.1 | 2.4 | 0.0 | 2.1 | 0.9 | 56.0 | 1.1 | 56.4 | 1.3 | 74.0 | 28.0 | 56.0 | 1.1 | NA |
| 16ATW-77 -Spot 110 | 1190 | 19843 | 4.2 | 20.4 | 1.3 | 0.1 | 3.0 | 0.0 | 2.7 | 0.9 | 56.0 | 1.5 | 58.1 | 1.7 | 145.8 | 31.4 | 56.0 | 1.5 | NA |
| 16ATW-77 -Spot 68 | 1348 | 59667 | 2.9 | 20.4 | 1.3 | 0.1 | 2.7 | 0.0 | 2.4 | 0.9 | 56.1 | 1.3 | 58.4 | 1.5 | 153.6 | 31.2 | 56.1 | 1.3 | NA |
| 16ATW-77 -Spot 259 | 2980 | 58303 | 20.2 | 20.8 | 1.0 | 0.1 | 2.2 | 0.0 | 2.0 | 0.9 | 56.2 | 1.1 | 57.2 | 1.2 | 101.6 | 22.6 | 56.2 | 1.1 | NA |
| 16ATW-77 -Spot 313 | 1655 | 82158 | 2.5 | 21.3 | 1.0 | 0.1 | 2.3 | 0.0 | 2.1 | 0.9 | 56.3 | 1.2 | 56.1 | 1.3 | 47.5 | 24.7 | 56.3 | 1.2 | NA |
| 16ATW-77 -Spot 12 | 794 | 23354 | 1.8 | 21.0 | 1.8 | 0.1 | 3.1 | 0.0 | 2.5 | 0.8 | 56.3 | 1.4 | 56.9 | 1.7 | 83.9 | 42.5 | 56.3 | 1.4 | NA |
| 16ATW-77 -Spot 127 | 188 | 23741 | 4.3 | 20.8 | 2.8 | 0.1 | 3.4 | 0.0 | 1.9 | 0.6 | 56.3 | 1.1 | 57.4 | 1.9 | 105.8 | 65.9 | 56.3 | 1.1 | NA |
| 16ATW-77 -Spot 265 | 514 | 10508 | 3.7 | 20.6 | 1.5 | 0.1 | 2.6 | 0.0 | 2.1 | 0.8 | 56.3 | 1.2 | 58.0 | 1.5 | 129.5 | 36.4 | 56.3 | 1.2 | NA |
| 16ATW-77 -Spot 19 | 2032 | 170206 | 4.7 | 20.7 | 1.2 | 0.1 | 2.7 | 0.0 | 2.4 | 0.9 | 56.4 | 1.3 | 57.9 | 1.5 | 118.5 | 28.8 | 56.4 | 1.3 | NA |

| | | | | | | | | | | | | | | | | | | | |
|---|---|---|---|---|---|---|---|---|---|---|---|---|---|---|---|---|---|---|---|
| 16ATW-77 -Spot 246 | 1457 | 181861 | 2.4 | 20.4 | 1.0 | 0.1 | 2.6 | 0.0 | 2.3 | 0.9 | 56.4 | 1.3 | 58.5 | 1.5 | 146.0 | 24.5 | 56.4 | 1.3 | NA |
| 16ATW-77 -Spot 63 | 426 | 75611 | 2.7 | 20.2 | 2.0 | 0.1 | 2.8 | 0.0 | 2.0 | 0.7 | 56.4 | 1.1 | 59.2 | 1.6 | 175.9 | 45.8 | 56.4 | 1.1 | NA |
| 16ATW-77 -Spot 152 | 1740 | 76816 | 3.9 | 20.9 | 1.1 | 0.1 | 2.0 | 0.0 | 1.7 | 0.8 | 56.5 | 0.9 | 57.2 | 1.1 | 88.7 | 27.0 | 56.5 | 0.9 | NA |
| 16ATW-77 -Spot 93 | 2171 | 39641 | 2.5 | 20.8 | 0.9 | 0.1 | 2.2 | 0.0 | 2.0 | 0.9 | 56.5 | 1.1 | 57.5 | 1.2 | 101.4 | 20.5 | 56.5 | 1.1 | NA |
| 16ATW-77 -Spot 247 | 856 | 19415 | 4.1 | 20.9 | 2.3 | 0.1 | 3.9 | 0.0 | 3.1 | 0.8 | 56.6 | 1.7 | 57.4 | 2.2 | 90.8 | 55.3 | 56.6 | 1.7 | NA |
| 16ATW-77 -Spot 54 | 732 | 41984 | 2.7 | 20.6 | 1.6 | 0.1 | 2.7 | 0.0 | 2.2 | 0.8 | 56.6 | 1.3 | 58.3 | 1.5 | 128.9 | 36.7 | 56.6 | 1.3 | NA |
| 16ATW-77 -Spot 283 | 706 | 122093 | 3.0 | 20.4 | 1.7 | 0.1 | 2.5 | 0.0 | 1.9 | 0.8 | 56.6 | 1.1 | 58.8 | 1.4 | 153.9 | 39.5 | 56.6 | 1.1 | NA |
| 16ATW-77 -Spot 183 | 2727 | 85466 | 1.9 | 20.9 | 1.1 | 0.1 | 2.4 | 0.0 | 2.1 | 0.9 | 56.8 | 1.2 | 57.5 | 1.3 | 86.2 | 25.2 | 56.8 | 1.2 | NA |
| 16ATW-77 -Spot 184 | 1949 | 89623 | 4.6 | 20.8 | 1.1 | 0.1 | 2.2 | 0.0 | 2.0 | 0.9 | 56.8 | 1.1 | 57.7 | 1.3 | 99.3 | 25.4 | 56.8 | 1.1 | NA |
| 16ATW-77 -Spot 192 | 57 | 2212 | 6.5 | 21.9 | 8.1 | 0.1 | 8.6 | 0.0 | 2.9 | 0.3 | 56.8 | 1.6 | 55.0 | 4.6 | NA | NA | 56.8 | 1.6 | ##### |
| 16ATW-77 -Spot 115 | 364 | 7029 | 6.4 | 20.9 | 1.9 | 0.1 | 3.1 | 0.0 | 2.4 | 0.8 | 56.9 | 1.4 | 57.7 | 1.7 | 89.2 | 44.3 | 56.9 | 1.4 | NA |
| 16ATW-77 -Spot 202 | 1084 | 30418 | 7.2 | 20.7 | 1.1 | 0.1 | 2.4 | 0.0 | 2.2 | 0.9 | 56.9 | 1.2 | 58.1 | 1.4 | 112.6 | 26.3 | 56.9 | 1.2 | NA |
| 16ATW-77 -Spot 89 | 522 | 18082 | 5.5 | 20.3 | 2.0 | 0.1 | 3.8 | 0.0 | 3.2 | 0.8 | 56.9 | 1.8 | 59.2 | 2.2 | 154.9 | 47.9 | 56.9 | 1.8 | NA |
| 16ATW-77 -Spot 268 | 2234 | 763762 | 2.2 | 21.0 | 1.2 | 0.1 | 3.0 | 0.0 | 2.7 | 0.9 | 57.0 | 1.5 | 57.6 | 1.7 | 81.9 | 28.7 | 57.0 | 1.5 | NA |
| 16ATW-77 -Spot 50 | 1015 | 77302 | 4.1 | 20.5 | 1.3 | 0.1 | 2.9 | 0.0 | 2.6 | 0.9 | 57.0 | 1.5 | 58.8 | 1.6 | 134.5 | 30.8 | 57.0 | 1.5 | NA |
| 16ATW-77 -Spot 284 | 727 | 24907 | 3.1 | 20.5 | 1.3 | 0.1 | 2.8 | 0.0 | 2.5 | 0.9 | 57.0 | 1.4 | 58.8 | 1.6 | 135.0 | 31.3 | 57.0 | 1.4 | NA |
| 16ATW-77 -Spot 219 | 253 | 6841 | 4.0 | 20.9 | 2.7 | 0.1 | 3.5 | 0.0 | 2.3 | 0.6 | 57.1 | 1.3 | 57.9 | 2.0 | 90.4 | 64.4 | 57.1 | 1.3 | NA |
| 16ATW-77 -Spot 81 | 321 | 11266 | 4.2 | 20.9 | 2.2 | 0.1 | 2.9 | 0.0 | 1.9 | 0.7 | 57.1 | 1.1 | 57.9 | 1.6 | 92.5 | 51.7 | 57.1 | 1.1 | NA |
| 16ATW-77 -Spot 306 | 455 | 73057 | 4.3 | 21.0 | 1.8 | 0.1 | 2.9 | 0.0 | 2.2 | 0.8 | 57.2 | 1.2 | 57.8 | 1.6 | 82.9 | 43.7 | 57.2 | 1.2 | NA |
| 16ATW-77 -Spot 3 | 1129 | 62098 | 26.0 | 20.5 | 1.3 | 0.1 | 2.3 | 0.0 | 1.9 | 0.8 | 57.2 | 1.1 | 59.1 | 1.3 | 134.9 | 29.6 | 57.2 | 1.1 | NA |
| 16ATW-77 -Spot 103 | 495 | 9934 | 3.6 | 20.9 | 1.6 | 0.1 | 2.9 | 0.0 | 2.5 | 0.8 | 57.3 | 1.4 | 58.2 | 1.7 | 94.7 | 38.1 | 57.3 | 1.4 | NA |
| 16ATW-77 -Spot 262 | 641 | 59022 | 3.0 | 20.5 | 1.5 | 0.1 | 2.6 | 0.0 | 2.1 | 0.8 | 57.3 | 1.2 | 59.1 | 1.5 | 135.0 | 35.0 | 57.3 | 1.2 | NA |
| 16ATW-77 -Spot 189 | 586 | 45119 | 3.2 | 20.6 | 1.7 | 0.1 | 3.1 | 0.0 | 2.6 | 0.8 | 57.4 | 1.5 | 59.1 | 1.8 | 130.2 | 39.9 | 57.4 | 1.5 | NA |

| | | | | | | | | | | | | | | | | | | | |
|---|---|---|---|---|---|---|---|---|---|---|---|---|---|---|---|---|---|---|---|
| 16ATW-77 -Spot 85 | 757 | 47439 | 3.5 | 20.4 | 1.6 | 0.1 | 2.4 | 0.0 | 1.9 | 0.8 | 57.4 | 1.1 | 59.5 | 1.4 | 148.0 | 37.2 | 57.4 | 1.1 | NA |
| 16ATW-77 -Spot 28 | 1349 | 63047 | 2.8 | 20.7 | 1.1 | 0.1 | 2.3 | 0.0 | 2.1 | 0.9 | 57.6 | 1.2 | 59.0 | 1.3 | 118.7 | 25.7 | 57.6 | 1.2 | NA |
| 16ATW-77 -Spot 158 | 348 | 8891 | 3.6 | 20.5 | 1.8 | 0.1 | 3.1 | 0.0 | 2.5 | 0.8 | 57.6 | 1.4 | 59.4 | 1.8 | 134.0 | 42.8 | 57.6 | 1.4 | NA |
| 16ATW-77 -Spot 104 | 1825 | 110049 | 5.7 | 20.2 | 0.9 | 0.1 | 2.1 | 0.0 | 1.9 | 0.9 | 57.6 | 1.1 | 60.3 | 1.2 | 168.4 | 21.9 | 57.6 | 1.1 | NA |
| 16ATW-77 -Spot 87 | 341 | 23967 | 4.3 | 20.0 | 2.2 | 0.1 | 3.4 | 0.0 | 2.5 | 0.8 | 57.6 | 1.4 | 60.9 | 2.0 | 195.6 | 52.0 | 57.6 | 1.4 | NA |
| 16ATW-77 -Spot 162 | 425 | 18609 | 1.3 | 20.9 | 1.7 | 0.1 | 3.0 | 0.0 | 2.5 | 0.8 | 57.7 | 1.4 | 58.6 | 1.7 | 96.8 | 39.7 | 57.7 | 1.4 | NA |
| 16ATW-77 -Spot 240 | 273 | 6110 | 4.2 | 20.6 | 2.2 | 0.1 | 3.4 | 0.0 | 2.6 | 0.8 | 57.7 | 1.5 | 59.4 | 2.0 | 130.5 | 51.2 | 57.7 | 1.5 | NA |
| 16ATW-77 -Spot 301 | 560 | 20756 | 2.5 | 20.5 | 1.6 | 0.1 | 2.6 | 0.0 | 2.0 | 0.8 | 57.7 | 1.1 | 59.6 | 1.5 | 136.6 | 38.6 | 57.7 | 1.1 | NA |
| 16ATW-77 -Spot 274 | 636 | 104799 | 4.4 | 20.2 | 1.5 | 0.1 | 2.7 | 0.0 | 2.3 | 0.8 | 57.7 | 1.3 | 60.3 | 1.6 | 167.3 | 36.0 | 57.7 | 1.3 | NA |
| 16ATW-77 -Spot 174 | 468 | 28874 | 3.2 | 21.1 | 1.7 | 0.1 | 3.3 | 0.0 | 2.9 | 0.9 | 57.9 | 1.6 | 58.2 | 1.9 | 71.4 | 39.9 | 57.9 | 1.6 | NA |
| 16ATW-77 -Spot 307 | 706 | 28945 | 5.8 | 21.0 | 2.0 | 0.1 | 3.2 | 0.0 | 2.6 | 0.8 | 57.9 | 1.5 | 58.6 | 1.8 | 85.5 | 47.3 | 57.9 | 1.5 | NA |
| 16ATW-77 -Spot 60 | 1850 | 74299 | 9.5 | 20.3 | 0.9 | 0.1 | 2.6 | 0.0 | 2.5 | 1.0 | 57.9 | 1.4 | 60.3 | 1.5 | 156.8 | 19.9 | 57.9 | 1.4 | NA |
| 16ATW-77 -Spot 182 | 354 | 11077 | 3.7 | 21.2 | 1.9 | 0.1 | 3.3 | 0.0 | 2.7 | 0.8 | 58.0 | 1.5 | 58.1 | 1.9 | 61.2 | 45.5 | 58.0 | 1.5 | NA |
| 16ATW-77 -Spot 263 | 705 | 37377 | 2.3 | 21.3 | 1.5 | 0.1 | 2.3 | 0.0 | 1.8 | 0.8 | 58.1 | 1.0 | 57.7 | 1.3 | 45.5 | 35.8 | 58.1 | 1.0 | NA |
| 16ATW-77 -Spot 123 | 558 | 15096 | 6.6 | 21.1 | 2.4 | 0.1 | 3.7 | 0.0 | 2.9 | 0.8 | 58.1 | 1.6 | 58.3 | 2.1 | 66.5 | 57.9 | 58.1 | 1.6 | NA |
| 16ATW-77 -Spot 164 | 695 | 24959 | 3.4 | 21.2 | 1.6 | 0.1 | 2.8 | 0.0 | 2.3 | 0.8 | 58.2 | 1.3 | 58.3 | 1.6 | 62.7 | 37.3 | 58.2 | 1.3 | NA |
| 16ATW-77 -Spot 27 | 471 | 16310 | 3.1 | 20.3 | 1.7 | 0.1 | 3.0 | 0.0 | 2.4 | 0.8 | 58.3 | 1.4 | 60.7 | 1.8 | 155.4 | 40.3 | 58.3 | 1.4 | NA |
| 16ATW-77 -Spot 112 | 221 | 13241 | 5.9 | 21.0 | 2.5 | 0.1 | 4.1 | 0.0 | 3.3 | 0.8 | 58.4 | 1.9 | 58.8 | 2.4 | 76.8 | 59.8 | 58.4 | 1.9 | NA |
| 16ATW-77 -Spot 198 | 184 | 14349 | 4.5 | 19.6 | 3.1 | 0.1 | 3.8 | 0.0 | 2.1 | 0.6 | 58.4 | 1.2 | 62.9 | 2.3 | 236.7 | 72.4 | 58.4 | 1.2 | NA |
| 16ATW-77 -Spot 226 | 274 | 8083 | 3.0 | 21.0 | 2.1 | 0.1 | 3.3 | 0.0 | 2.5 | 0.8 | 58.5 | 1.5 | 58.8 | 1.9 | 76.0 | 50.6 | 58.5 | 1.5 | NA |
| 16ATW-77 -Spot 237 | 349 | 5851 | 4.4 | 21.5 | 2.0 | 0.1 | 3.0 | 0.0 | 2.3 | 0.8 | 58.8 | 1.4 | 58.1 | 1.7 | 29.0 | 47.7 | 58.8 | 1.4 | NA |
| 16ATW-77 -Spot 285 | 445 | 15130 | 4.1 | 20.8 | 1.7 | 0.1 | 2.7 | 0.0 | 2.1 | 0.8 | 58.8 | 1.2 | 59.7 | 1.6 | 97.6 | 40.9 | 58.8 | 1.2 | NA |
| 16ATW-77 -Spot 35 | 393 | 8123 | 3.0 | 20.9 | 2.6 | 0.1 | 3.5 | 0.0 | 2.3 | 0.7 | 58.9 | 1.4 | 59.7 | 2.0 | 91.1 | 61.1 | 58.9 | 1.4 | NA |

| | | | | | | | | | | | | | | | | | | | |
|---|---|---|---|---|---|---|---|---|---|---|---|---|---|---|---|---|---|---|---|
| 16ATW-77 -Spot 148 | 538 | 19184 | 2.4 | 20.4 | 2.1 | 0.1 | 3.0 | 0.0 | 2.2 | 0.7 | 58.9 | 1.3 | 61.1 | 1.8 | 150.8 | 48.5 | 58.9 | 1.3 | NA |
| 16ATW-77 -Spot 304 | 262 | 6951 | 3.1 | 21.6 | 2.8 | 0.1 | 3.8 | 0.0 | 2.5 | 0.7 | 59.0 | 1.5 | 57.8 | 2.1 | 10.0 | 67.1 | 59.0 | 1.5 | NA |
| 16ATW-77 -Spot 275 | 521 | 32335 | 1.9 | 21.3 | 1.8 | 0.1 | 3.1 | 0.0 | 2.6 | 0.8 | 59.0 | 1.5 | 58.6 | 1.8 | 41.7 | 42.5 | 59.0 | 1.5 | NA |
| 16ATW-77 -Spot 135 | 394 | 14361 | 2.7 | 20.2 | 1.8 | 0.1 | 3.2 | 0.0 | 2.6 | 0.8 | 59.0 | 1.5 | 61.7 | 1.9 | 167.9 | 42.4 | 59.0 | 1.5 | NA |
| 16ATW-77 -Spot 310 | 258 | 5462 | 4.2 | 22.5 | 2.4 | 0.1 | 3.2 | 0.0 | 2.1 | 0.7 | 59.1 | 1.3 | 55.8 | 1.7 | NA | NA | 59.1 | 1.3 | ##### |
| 16ATW-77 -Spot 51 | 960 | 203611 | 4.0 | 20.3 | 1.4 | 0.1 | 2.9 | 0.0 | 2.6 | 0.9 | 59.2 | 1.5 | 61.6 | 1.8 | 154.6 | 32.1 | 59.2 | 1.5 | NA |
| 16ATW-77 -Spot 293 | 142 | 10126 | 7.7 | 20.0 | 3.1 | 0.1 | 4.1 | 0.0 | 2.7 | 0.7 | 59.2 | 1.6 | 62.7 | 2.5 | 197.3 | 72.1 | 59.2 | 1.6 | NA |
| 16ATW-77 -Spot 195 | 327 | 7475 | 4.1 | 21.6 | 2.3 | 0.1 | 3.4 | 0.0 | 2.5 | 0.7 | 59.3 | 1.5 | 58.1 | 1.9 | 9.5 | 56.1 | 59.3 | 1.5 | NA |
| 16ATW-77 -Spot 260 | 227 | 14229 | 3.5 | 21.0 | 2.0 | 0.1 | 3.2 | 0.0 | 2.5 | 0.8 | 59.3 | 1.4 | 59.8 | 1.9 | 79.0 | 48.7 | 59.3 | 1.4 | NA |
| 16ATW-77 -Spot 305 | 481 | 17440 | 2.7 | 20.5 | 2.0 | 0.1 | 3.3 | 0.0 | 2.6 | 0.8 | 59.3 | 1.5 | 61.2 | 1.9 | 136.1 | 47.4 | 59.3 | 1.5 | NA |
| 16ATW-77 -Spot 238 | 265 | 72492 | 8.2 | 20.7 | 2.5 | 0.1 | 3.7 | 0.0 | 2.7 | 0.7 | 59.4 | 1.6 | 60.9 | 2.2 | 119.8 | 60.0 | 59.4 | 1.6 | NA |
| 16ATW-77 -Spot 156 | 516 | 30765 | 3.2 | 20.3 | 1.4 | 0.1 | 2.3 | 0.0 | 1.9 | 0.8 | 59.4 | 1.1 | 61.8 | 1.4 | 156.2 | 33.3 | 59.4 | 1.1 | NA |
| 16ATW-77 -Spot 140 | 557 | 23350 | 2.5 | 20.0 | 2.1 | 0.1 | 2.7 | 0.0 | 1.7 | 0.6 | 59.4 | 1.0 | 62.8 | 1.7 | 192.7 | 50.0 | 59.4 | 1.0 | NA |
| 16ATW-77 -Spot 25 | 263 | 5969 | 5.0 | 21.4 | 2.1 | 0.1 | 3.7 | 0.0 | 3.0 | 0.8 | 59.5 | 1.8 | 58.9 | 2.1 | 36.7 | 51.3 | 59.5 | 1.8 | NA |
| 16ATW-77 -Spot 215 | 500 | 7175 | 3.8 | 20.7 | 1.5 | 0.1 | 2.5 | 0.0 | 2.1 | 0.8 | 59.5 | 1.2 | 60.7 | 1.5 | 109.0 | 35.1 | 59.5 | 1.2 | NA |
| 16ATW-77 -Spot 157 | 499 | 37619 | 3.3 | 20.7 | 1.8 | 0.1 | 3.0 | 0.0 | 2.4 | 0.8 | 59.5 | 1.4 | 60.8 | 1.8 | 111.8 | 42.8 | 59.5 | 1.4 | NA |
| 16ATW-77 -Spot 105 | 1015 | 83037 | 20.7 | 20.6 | 1.4 | 0.1 | 2.4 | 0.0 | 2.0 | 0.8 | 59.5 | 1.2 | 61.1 | 1.4 | 124.1 | 32.7 | 59.5 | 1.2 | NA |
| 16ATW-77 -Spot 186 | 217 | 5840 | 4.4 | 22.0 | 2.4 | 0.1 | 3.2 | 0.0 | 2.1 | 0.7 | 59.5 | 1.3 | 57.2 | 1.8 | NA | NA | 59.5 | 1.3 | ##### |
| 16ATW-77 -Spot 299 | 655 | 108365 | 6.4 | 20.7 | 1.5 | 0.1 | 2.7 | 0.0 | 2.2 | 0.8 | 59.6 | 1.3 | 61.0 | 1.6 | 114.0 | 35.0 | 59.6 | 1.3 | NA |
| 16ATW-77 -Spot 77 | 326 | 22704 | 5.0 | 20.5 | 2.1 | 0.1 | 3.1 | 0.0 | 2.3 | 0.7 | 59.6 | 1.4 | 61.6 | 1.9 | 137.5 | 49.1 | 59.6 | 1.4 | NA |
| 16ATW-77 -Spot 10 | 466 | 18067 | 4.0 | 20.5 | 2.0 | 0.1 | 3.6 | 0.0 | 3.0 | 0.8 | 59.6 | 1.8 | 61.6 | 2.2 | 141.4 | 45.9 | 59.6 | 1.8 | NA |
| 16ATW-77 -Spot 272 | 760 | 51076 | 5.3 | 20.1 | 1.5 | 0.1 | 2.6 | 0.0 | 2.1 | 0.8 | 59.6 | 1.3 | 62.7 | 1.6 | 181.5 | 33.8 | 59.6 | 1.3 | NA |
| 16ATW-77 -Spot 309 | 1566 | 32444 | 3.6 | 21.1 | 1.1 | 0.1 | 2.7 | 0.0 | 2.5 | 0.9 | 59.7 | 1.5 | 60.0 | 1.6 | 72.4 | 26.0 | 59.7 | 1.5 | NA |

| | | | | | | | | | | | | | | | | | | | |
|---|---|---|---|---|---|---|---|---|---|---|---|---|---|---|---|---|---|---|---|
| 16ATW-77 -Spot 179 | 227 | 7597 | 4.4 | 20.9 | 1.9 | 0.1 | 3.0 | 0.0 | 2.3 | 0.8 | 59.8 | 1.3 | 60.6 | 1.8 | 94.0 | 45.8 | 59.8 | 1.3 | NA |
| 16ATW-77 -Spot 144 | 324 | 60242 | 3.4 | 20.7 | 1.8 | 0.1 | 3.0 | 0.0 | 2.4 | 0.8 | 59.9 | 1.4 | 61.2 | 1.8 | 114.0 | 42.0 | 59.9 | 1.4 | NA |
| 16ATW-77 -Spot 78 | 882 | 31641 | 2.4 | 20.2 | 1.3 | 0.1 | 2.3 | 0.0 | 1.9 | 0.8 | 59.9 | 1.1 | 62.7 | 1.4 | 172.5 | 29.7 | 59.9 | 1.1 | NA |
| 16ATW-77 -Spot 17 | 883 | 17322 | 4.0 | 21.1 | 1.5 | 0.1 | 2.9 | 0.0 | 2.4 | 0.9 | 60.0 | 1.5 | 60.1 | 1.7 | 66.0 | 36.5 | 60.0 | 1.5 | NA |
| 16ATW-77 -Spot 59 | 244 | 24285 | 4.3 | 20.2 | 2.5 | 0.1 | 3.5 | 0.0 | 2.4 | 0.7 | 60.0 | 1.4 | 62.7 | 2.1 | 168.3 | 58.6 | 60.0 | 1.4 | NA |
| 16ATW-77 -Spot 6 | 160 | 3356 | 7.5 | 22.5 | 3.8 | 0.1 | 5.0 | 0.0 | 3.4 | 0.7 | 60.0 | 2.0 | 56.5 | 2.8 | NA | NA | 60.0 | 2.0 | ##### |
| 16ATW-77 -Spot 138 | 319 | 7368 | 4.3 | 21.1 | 2.2 | 0.1 | 2.8 | 0.0 | 1.8 | 0.6 | 60.1 | 1.1 | 60.2 | 1.7 | 65.0 | 52.5 | 60.1 | 1.1 | NA |
| 16ATW-77 -Spot 133 | 142 | 4068 | 5.6 | 21.1 | 3.2 | 0.1 | 3.8 | 0.0 | 2.0 | 0.5 | 60.2 | 1.2 | 60.3 | 2.2 | 64.2 | 77.3 | 60.2 | 1.2 | NA |
| 16ATW-77 -Spot 209 | 2085 | 73530 | 17.2 | 20.7 | 1.1 | 0.1 | 2.2 | 0.0 | 1.9 | 0.9 | 60.2 | 1.1 | 61.4 | 1.3 | 111.8 | 25.1 | 60.2 | 1.1 | NA |
| 16ATW-77 -Spot 239 | 356 | 24156 | 3.4 | 20.2 | 2.0 | 0.1 | 3.2 | 0.0 | 2.4 | 0.8 | 60.2 | 1.4 | 62.9 | 1.9 | 166.3 | 47.7 | 60.2 | 1.4 | NA |
| 16ATW-77 -Spot 102 | 309 | 301670 | 6.8 | 19.7 | 2.9 | 0.1 | 4.0 | 0.0 | 2.8 | 0.7 | 60.2 | 1.7 | 64.5 | 2.5 | 228.4 | 67.7 | 60.2 | 1.7 | NA |
| 16ATW-77 -Spot 255 | 241 | 8540 | 4.4 | 20.6 | 2.8 | 0.1 | 3.3 | 0.0 | 1.7 | 0.5 | 60.5 | 1.0 | 62.2 | 2.0 | 127.2 | 66.6 | 60.5 | 1.0 | NA |
| 16ATW-77 -Spot 200 | 912 | 119421 | 38.3 | 20.2 | 1.2 | 0.1 | 2.7 | 0.0 | 2.4 | 0.9 | 60.5 | 1.4 | 63.2 | 1.6 | 167.8 | 27.7 | 60.5 | 1.4 | NA |
| 16ATW-77 -Spot 193 | 306 | 41709 | 2.8 | 20.2 | 2.0 | 0.1 | 2.9 | 0.0 | 2.1 | 0.7 | 60.5 | 1.3 | 63.4 | 1.8 | 173.8 | 47.2 | 60.5 | 1.3 | NA |
| 16ATW-77 -Spot 292 | 191 | 7048 | 4.4 | 21.2 | 2.2 | 0.1 | 3.5 | 0.0 | 2.8 | 0.8 | 60.6 | 1.7 | 60.4 | 2.1 | 55.4 | 52.1 | 60.6 | 1.7 | NA |
| 16ATW-77 -Spot 16 | 401 | 56168 | 8.0 | 20.6 | 2.1 | 0.1 | 3.8 | 0.0 | 3.2 | 0.8 | 60.6 | 1.9 | 62.3 | 2.3 | 128.5 | 48.9 | 60.6 | 1.9 | NA |
| 16ATW-77 -Spot 163 | 303 | 16863 | 4.0 | 20.5 | 2.0 | 0.1 | 3.2 | 0.0 | 2.5 | 0.8 | 60.6 | 1.5 | 62.4 | 1.9 | 133.7 | 47.6 | 60.6 | 1.5 | NA |
| 16ATW-77 -Spot 142 | 382 | 12876 | 2.9 | 20.9 | 2.2 | 0.1 | 3.4 | 0.0 | 2.6 | 0.8 | 60.7 | 1.6 | 61.5 | 2.0 | 95.3 | 51.3 | 60.7 | 1.6 | NA |
| 16ATW-77 -Spot 108 | 229 | 8910 | 3.7 | 20.7 | 2.0 | 0.1 | 2.9 | 0.0 | 2.1 | 0.7 | 60.7 | 1.3 | 62.0 | 1.7 | 116.4 | 47.4 | 60.7 | 1.3 | NA |
| 16ATW-77 -Spot 161 | 431 | 10532 | 6.8 | 20.7 | 1.5 | 0.1 | 2.3 | 0.0 | 1.7 | 0.8 | 60.7 | 1.0 | 62.1 | 1.4 | 116.5 | 35.7 | 60.7 | 1.0 | NA |
| 16ATW-77 -Spot 221 | 222 | 10609 | 3.6 | 21.4 | 2.4 | 0.1 | 3.3 | 0.0 | 2.3 | 0.7 | 60.9 | 1.4 | 60.2 | 1.9 | 33.5 | 57.5 | 60.9 | 1.4 | NA |
| 16ATW-77 -Spot 213 | 1254 | 41384 | 3.5 | 20.4 | 1.4 | 0.1 | 2.9 | 0.0 | 2.5 | 0.9 | 60.9 | 1.5 | 63.1 | 1.8 | 149.2 | 33.0 | 60.9 | 1.5 | NA |
| 16ATW-77 -Spot 8 | 155 | 8068 | 5.1 | 20.7 | 3.1 | 0.1 | 4.1 | 0.0 | 2.6 | 0.6 | 61.1 | 1.6 | 62.4 | 2.5 | 112.9 | 73.8 | 61.1 | 1.6 | NA |

| | | | | | | | | | | | | | | | | | | | |
|---|---|---|---|---|---|---|---|---|---|---|---|---|---|---|---|---|---|---|---|
| 16ATW-77 -Spot 18 | 357 | 18903 | 3.3 | 20.5 | 2.1 | 0.1 | 3.5 | 0.0 | 2.8 | 0.8 | 61.1 | 1.7 | 63.1 | 2.1 | 140.9 | 48.4 | 61.1 | 1.7 | NA |
| 16ATW-77 -Spot 315 | 275 | 52662 | 4.0 | 20.2 | 2.0 | 0.1 | 3.1 | 0.0 | 2.4 | 0.8 | 61.1 | 1.4 | 63.8 | 1.9 | 169.0 | 47.9 | 61.1 | 1.4 | NA |
| 16ATW-77 -Spot 269 | 627 | 171104 | 10.6 | 20.4 | 2.2 | 0.1 | 3.4 | 0.0 | 2.5 | 0.8 | 61.2 | 1.5 | 63.5 | 2.1 | 152.0 | 51.8 | 61.2 | 1.5 | NA |
| 16ATW-77 -Spot 271 | 616 | 47361 | 4.6 | 20.2 | 1.2 | 0.1 | 2.6 | 0.0 | 2.3 | 0.9 | 61.2 | 1.4 | 63.9 | 1.6 | 167.4 | 27.4 | 61.2 | 1.4 | NA |
| 16ATW-77 -Spot 278 | 922 | 55824 | 2.8 | 21.1 | 1.4 | 0.1 | 2.8 | 0.0 | 2.4 | 0.9 | 61.4 | 1.5 | 61.7 | 1.7 | 72.7 | 34.0 | 61.4 | 1.5 | NA |
| 16ATW-77 -Spot 72 | 2070 | 149298 | 6.5 | 20.5 | 1.0 | 0.1 | 2.9 | 0.0 | 2.7 | 0.9 | 61.4 | 1.7 | 63.4 | 1.8 | 140.1 | 23.6 | 61.4 | 1.7 | NA |
| 16ATW-77 -Spot 206 | 117 | 2777 | 5.9 | 22.7 | 3.4 | 0.1 | 3.9 | 0.0 | 2.0 | 0.5 | 61.4 | 1.2 | 57.3 | 2.2 | NA | NA | 61.4 | 1.2 | ##### |
| 16ATW-77 -Spot 69 | 855 | 59551 | 5.6 | 20.2 | 1.1 | 0.1 | 2.7 | 0.0 | 2.5 | 0.9 | 61.5 | 1.5 | 64.4 | 1.7 | 174.6 | 26.7 | 61.5 | 1.5 | NA |
| 16ATW-77 -Spot 15 | 202 | 4741 | 4.0 | 21.2 | 2.4 | 0.1 | 3.7 | 0.0 | 2.8 | 0.8 | 61.6 | 1.7 | 61.4 | 2.2 | 54.1 | 58.2 | 61.6 | 1.7 | NA |
| 16ATW-77 -Spot 241 | 331 | 34687 | 3.1 | 20.3 | 2.1 | 0.1 | 3.1 | 0.0 | 2.2 | 0.7 | 61.6 | 1.4 | 64.2 | 1.9 | 164.1 | 49.1 | 61.6 | 1.4 | NA |
| 16ATW-77 -Spot 11 | 278 | 35267 | 5.2 | 19.8 | 2.4 | 0.1 | 4.0 | 0.0 | 3.2 | 0.8 | 61.6 | 1.9 | 65.5 | 2.5 | 214.2 | 55.0 | 61.6 | 1.9 | NA |
| 16ATW-77 -Spot 154 | 462 | 15466 | 3.9 | 21.1 | 1.9 | 0.1 | 3.0 | 0.0 | 2.3 | 0.8 | 61.8 | 1.4 | 62.0 | 1.8 | 71.3 | 44.1 | 61.8 | 1.4 | NA |
| 16ATW-77 -Spot 57 | 181 | 4583 | 5.2 | 21.1 | 2.9 | 0.1 | 4.2 | 0.0 | 3.0 | 0.7 | 61.9 | 1.9 | 62.1 | 2.5 | 69.6 | 69.4 | 61.9 | 1.9 | NA |
| 16ATW-77 -Spot 264 | 528 | 61272 | 4.5 | 20.2 | 1.6 | 0.1 | 3.2 | 0.0 | 2.8 | 0.9 | 61.9 | 1.7 | 64.8 | 2.0 | 171.7 | 36.7 | 61.9 | 1.7 | NA |
| 16ATW-77 -Spot 106 | 621 | 271701 | 6.1 | 20.2 | 1.4 | 0.1 | 2.8 | 0.0 | 2.5 | 0.9 | 62.0 | 1.5 | 64.8 | 1.8 | 171.3 | 32.4 | 62.0 | 1.5 | NA |
| 16ATW-77 -Spot 173 | 1242 | 85785 | 28.0 | 20.6 | 1.4 | 0.1 | 2.7 | 0.0 | 2.3 | 0.9 | 62.2 | 1.4 | 63.7 | 1.6 | 120.2 | 33.4 | 62.2 | 1.4 | NA |
| 16ATW-77 -Spot 117 | 305 | 30141 | 6.1 | 20.0 | 2.2 | 0.1 | 2.8 | 0.0 | 1.8 | 0.6 | 62.2 | 1.1 | 65.7 | 1.8 | 196.0 | 50.2 | 62.2 | 1.1 | NA |
| 16ATW-77 -Spot 289 | 1718 | 196093 | 2.9 | 20.3 | 1.0 | 0.1 | 2.4 | 0.0 | 2.2 | 0.9 | 62.4 | 1.4 | 64.9 | 1.5 | 160.0 | 23.9 | 62.4 | 1.4 | NA |
| 16ATW-77 -Spot 287 | 698 | 23281 | 2.7 | 20.2 | 1.5 | 0.1 | 2.9 | 0.0 | 2.5 | 0.9 | 62.4 | 1.6 | 65.4 | 1.8 | 175.9 | 34.4 | 62.4 | 1.6 | NA |
| 16ATW-77 -Spot 113 | 206 | 15182 | 4.5 | 20.9 | 3.0 | 0.1 | 3.7 | 0.0 | 2.1 | 0.6 | 62.5 | 1.3 | 63.1 | 2.2 | 88.8 | 70.8 | 62.5 | 1.3 | NA |
| 16ATW-77 -Spot 270 | 198 | 11434 | 4.6 | 20.4 | 2.5 | 0.1 | 4.0 | 0.0 | 3.1 | 0.8 | 62.9 | 2.0 | 65.2 | 2.5 | 151.4 | 59.4 | 62.9 | 2.0 | NA |
| 16ATW-77 -Spot 139 | 554 | 95573 | 2.2 | 20.3 | 2.4 | 0.1 | 4.1 | 0.0 | 3.3 | 0.8 | 62.9 | 2.1 | 65.4 | 2.6 | 160.5 | 55.0 | 62.9 | 2.1 | NA |
| 16ATW-77 -Spot 137 | 497 | 9930 | 4.8 | 20.9 | 1.3 | 0.1 | 3.3 | 0.0 | 3.1 | 0.9 | 63.0 | 1.9 | 63.6 | 2.1 | 88.1 | 30.9 | 63.0 | 1.9 | NA |

| | | | | | | | | | | | | | | | | | | | |
|---|---|---|---|---|---|---|---|---|---|---|---|---|---|---|---|---|---|---|---|
| 16ATW-77 -Spot 24 | 1464 | 185918 | 5.6 | 20.1 | 1.3 | 0.1 | 3.1 | 0.0 | 2.8 | 0.9 | 63.1 | 1.8 | 66.2 | 2.0 | 178.0 | 30.1 | 63.1 | 1.8 | NA |
| 16ATW-77 -Spot 26 | 294 | 23465 | 5.1 | 20.4 | 2.0 | 0.1 | 3.3 | 0.0 | 2.6 | 0.8 | 63.2 | 1.6 | 65.4 | 2.1 | 148.2 | 47.6 | 63.2 | 1.6 | NA |
| 16ATW-77 -Spot 90 | 1108 | 60204 | 4.0 | 20.2 | 1.0 | 0.1 | 2.9 | 0.0 | 2.7 | 0.9 | 63.4 | 1.7 | 66.3 | 1.9 | 170.8 | 24.2 | 63.4 | 1.7 | NA |
| 16ATW-77 -Spot 33 | 323 | 16917 | 9.3 | 20.0 | 1.9 | 0.1 | 3.1 | 0.0 | 2.4 | 0.8 | 63.5 | 1.5 | 66.9 | 2.0 | 189.9 | 44.2 | 63.5 | 1.5 | NA |
| 16ATW-77 -Spot 244 | 1286 | 45653 | 5.3 | 21.0 | 1.2 | 0.1 | 3.0 | 0.0 | 2.7 | 0.9 | 63.7 | 1.7 | 64.1 | 1.8 | 83.5 | 28.6 | 63.7 | 1.7 | NA |
| 16ATW-77 -Spot 267 | 394 | 297350 | 3.6 | 20.5 | 1.8 | 0.1 | 3.0 | 0.0 | 2.4 | 0.8 | 63.7 | 1.5 | 65.7 | 1.9 | 139.3 | 42.8 | 63.7 | 1.5 | NA |
| 16ATW-77 -Spot 190 | 553 | 20998 | 7.0 | 20.7 | 1.9 | 0.1 | 2.9 | 0.0 | 2.2 | 0.8 | 63.9 | 1.4 | 65.4 | 1.8 | 119.9 | 44.7 | 63.9 | 1.4 | NA |
| 16ATW-77 -Spot 84 | 699 | 76233 | 4.7 | 20.4 | 1.4 | 0.1 | 2.7 | 0.0 | 2.3 | 0.9 | 63.9 | 1.5 | 66.1 | 1.7 | 149.7 | 33.8 | 63.9 | 1.5 | NA |
| 16ATW-77 -Spot 280 | 1453 | 111827 | 3.8 | 21.1 | 1.0 | 0.1 | 1.9 | 0.0 | 1.7 | 0.9 | 64.0 | 1.1 | 64.1 | 1.2 | 68.2 | 22.9 | 64.0 | 1.1 | NA |
| 16ATW-77 -Spot 314 | 639 | 41841 | 6.9 | 20.3 | 1.5 | 0.1 | 3.0 | 0.0 | 2.6 | 0.9 | 64.0 | 1.6 | 66.4 | 1.9 | 156.1 | 34.2 | 64.0 | 1.6 | NA |
| 16ATW-77 -Spot 251 | 644 | 39362 | 6.6 | 20.5 | 1.3 | 0.1 | 3.2 | 0.0 | 2.9 | 0.9 | 64.3 | 1.9 | 66.3 | 2.1 | 137.1 | 30.3 | 64.3 | 1.9 | NA |
| 16ATW-77 -Spot 199 | 661 | 26221 | 7.4 | 20.4 | 1.5 | 0.1 | 3.2 | 0.0 | 2.8 | 0.9 | 64.5 | 1.8 | 66.7 | 2.1 | 146.1 | 35.8 | 64.5 | 1.8 | NA |
| 16ATW-77 -Spot 1 | 1029 | 27412 | 4.1 | 20.3 | 1.6 | 0.1 | 3.0 | 0.0 | 2.6 | 0.9 | 64.5 | 1.7 | 67.0 | 2.0 | 158.9 | 36.6 | 64.5 | 1.7 | NA |
| 16ATW-77 -Spot 44 | 677 | 36528 | 9.2 | 20.3 | 1.5 | 0.1 | 2.5 | 0.0 | 2.0 | 0.8 | 64.6 | 1.3 | 67.1 | 1.7 | 157.1 | 35.6 | 64.6 | 1.3 | NA |
| 16ATW-77 -Spot 7 | 579 | 17718 | 7.7 | 21.0 | 1.9 | 0.1 | 2.9 | 0.0 | 2.2 | 0.8 | 65.0 | 1.4 | 65.3 | 1.8 | 77.2 | 44.2 | 65.0 | 1.4 | NA |
| 16ATW-77 -Spot 149 | 539 | 22128 | 5.9 | 20.4 | 2.0 | 0.1 | 3.2 | 0.0 | 2.5 | 0.8 | 65.1 | 1.6 | 67.4 | 2.1 | 148.5 | 46.4 | 65.1 | 1.6 | NA |
| 16ATW-77 -Spot 41 | 589 | 84668 | 8.8 | 20.2 | 1.9 | 0.1 | 3.7 | 0.0 | 3.2 | 0.9 | 65.4 | 2.1 | 68.4 | 2.4 | 177.0 | 43.6 | 65.4 | 2.1 | NA |
| 16ATW-77 -Spot 220 | 466 | 16606 | 2.9 | 20.2 | 1.7 | 0.1 | 2.8 | 0.0 | 2.2 | 0.8 | 65.7 | 1.4 | 68.5 | 1.8 | 167.6 | 39.3 | 65.7 | 1.4 | NA |
| 16ATW-77 -Spot 277 | 669 | 55214 | 4.7 | 20.8 | 1.5 | 0.1 | 2.6 | 0.0 | 2.2 | 0.8 | 65.8 | 1.4 | 66.8 | 1.7 | 103.2 | 34.9 | 65.8 | 1.4 | NA |
| 16ATW-77 -Spot 31 | 649 | 22833 | 7.2 | 20.5 | 1.4 | 0.1 | 2.6 | 0.0 | 2.3 | 0.9 | 66.0 | 1.5 | 68.0 | 1.7 | 141.4 | 31.9 | 66.0 | 1.5 | NA |
| 16ATW-77 -Spot 120 | 685 | 19885 | 7.0 | 20.6 | 1.3 | 0.1 | 2.6 | 0.0 | 2.3 | 0.9 | 66.1 | 1.5 | 67.7 | 1.7 | 125.4 | 30.3 | 66.1 | 1.5 | NA |
| 16ATW-77 -Spot 171 | 620 | 16043 | 6.8 | 21.1 | 1.6 | 0.1 | 2.9 | 0.0 | 2.4 | 0.8 | 66.3 | 1.6 | 66.3 | 1.9 | 65.8 | 38.9 | 66.3 | 1.6 | NA |
| 16ATW-77 -Spot 168 | 645 | 45182 | 3.3 | 21.1 | 1.4 | 0.1 | 2.8 | 0.0 | 2.4 | 0.9 | 66.6 | 1.6 | 66.5 | 1.8 | 65.7 | 33.9 | 66.6 | 1.6 | NA |

| | | | | | | | | | | | | | | | | | | | |
|---|---|---|---|---|---|---|---|---|---|---|---|---|---|---|---|---|---|---|---|
| 16ATW-77 -Spot 196 | 347 | 33880 | 4.1 | 20.7 | 1.8 | 0.1 | 3.3 | 0.0 | 2.7 | 0.8 | 67.1 | 1.8 | 68.5 | 2.2 | 118.0 | 43.4 | 67.1 | 1.8 | NA |
| 16ATW-77 -Spot 23 | 471 | 17780 | 8.0 | 20.4 | 1.5 | 0.1 | 3.1 | 0.0 | 2.8 | 0.9 | 67.8 | 1.9 | 70.2 | 2.1 | 154.1 | 34.6 | 67.8 | 1.9 | NA |
| 16ATW-77 -Spot 80 | 519 | 114794 | 5.5 | 20.5 | 1.6 | 0.1 | 2.6 | 0.0 | 2.1 | 0.8 | 67.9 | 1.4 | 69.7 | 1.8 | 131.6 | 37.5 | 67.9 | 1.4 | NA |
| 16ATW-77 -Spot 65 | 349 | 38228 | 5.3 | 20.0 | 1.3 | 0.1 | 2.5 | 0.0 | 2.1 | 0.9 | 68.0 | 1.4 | 71.6 | 1.7 | 194.5 | 30.9 | 68.0 | 1.4 | NA |
| 16ATW-77 -Spot 126 | 458 | 28029 | 9.1 | 20.0 | 2.0 | 0.1 | 3.3 | 0.0 | 2.7 | 0.8 | 68.1 | 1.8 | 71.7 | 2.3 | 196.5 | 45.5 | 68.1 | 1.8 | NA |
| 16ATW-77 -Spot 159 | 678 | 60816 | 6.3 | 20.6 | 1.5 | 0.1 | 2.6 | 0.0 | 2.1 | 0.8 | 68.2 | 1.4 | 69.8 | 1.7 | 123.8 | 36.1 | 68.2 | 1.4 | NA |
| 16ATW-77 -Spot 111 | 100 | 7963 | 3.6 | 21.0 | 3.9 | 0.1 | 5.1 | 0.0 | 3.3 | 0.6 | 68.8 | 2.2 | 69.2 | 3.4 | 82.0 | 93.3 | 68.8 | 2.2 | NA |
| 16ATW-77 -Spot 153 | 998 | 100130 | 4.8 | 20.7 | 1.0 | 0.1 | 2.4 | 0.0 | 2.2 | 0.9 | 69.5 | 1.5 | 71.0 | 1.7 | 119.9 | 23.5 | 69.5 | 1.5 | NA |
| 16ATW-77 -Spot 109 | 1313 | 172285 | 4.1 | 19.9 | 1.4 | 0.1 | 2.5 | 0.0 | 2.1 | 0.8 | 70.5 | 1.5 | 74.6 | 1.8 | 208.1 | 31.4 | 70.5 | 1.5 | NA |
| 16ATW-77 -Spot 256 | 135 | 9911 | 4.8 | 19.7 | 3.1 | 0.1 | 4.2 | 0.0 | 2.8 | 0.7 | 70.6 | 2.0 | 75.3 | 3.0 | 228.2 | 70.9 | 70.6 | 2.0 | NA |
| 16ATW-77 -Spot 181 | 129 | 22721 | 4.6 | 20.4 | 3.2 | 0.1 | 4.3 | 0.0 | 2.8 | 0.7 | 70.8 | 2.0 | 73.1 | 3.0 | 149.4 | 75.3 | 70.8 | 2.0 | NA |
| 16ATW-77 -Spot 230 | 160 | 5384 | 4.4 | 21.5 | 2.7 | 0.1 | 3.5 | 0.0 | 2.3 | 0.7 | 72.1 | 1.6 | 70.7 | 2.4 | 24.0 | 64.9 | 72.1 | 1.6 | NA |
| 16ATW-77 -Spot 170 | 148 | 5726 | 5.5 | 21.5 | 2.7 | 0.1 | 3.5 | 0.0 | 2.3 | 0.6 | 72.3 | 1.6 | 70.9 | 2.4 | 26.2 | 65.5 | 72.3 | 1.6 | NA |
| 16ATW-77 -Spot 146 | 384 | 12638 | 2.9 | 20.9 | 2.1 | 0.1 | 3.4 | 0.0 | 2.6 | 0.8 | 73.4 | 1.9 | 74.1 | 2.4 | 96.5 | 49.2 | 73.4 | 1.9 | NA |
| 16ATW-77 -Spot 169 | 656 | 43800 | 9.9 | 20.5 | 1.3 | 0.1 | 2.5 | 0.0 | 2.2 | 0.9 | 74.3 | 1.6 | 76.2 | 1.9 | 139.2 | 30.3 | 74.3 | 1.6 | NA |
| 16ATW-77 -Spot 96 | 146 | 8788 | 2.7 | 20.9 | 2.0 | 0.1 | 3.0 | 0.0 | 2.3 | 0.8 | 74.5 | 1.7 | 75.0 | 2.2 | 92.9 | 47.1 | 74.5 | 1.7 | NA |
| 16ATW-77 -Spot 258 | 442 | 85467 | 4.7 | 20.0 | 1.3 | 0.1 | 3.2 | 0.0 | 3.0 | 0.9 | 80.5 | 2.4 | 84.5 | 2.6 | 199.2 | 30.1 | 80.5 | 2.4 | NA |
| 16ATW-77 -Spot 185 | 47 | 5114 | 2.4 | 19.6 | 3.8 | 0.1 | 5.3 | 0.0 | 3.7 | 0.7 | 84.3 | 3.1 | 89.9 | 4.6 | 240.4 | 87.9 | 84.3 | 3.1 | NA |
| 16ATW-77 -Spot 178 | 1483 | 234247 | 2.6 | 20.5 | 1.0 | 0.1 | 3.0 | 0.0 | 2.8 | 1.0 | 93.7 | 2.6 | 95.5 | 2.7 | 142.0 | 22.6 | 93.7 | 2.6 | NA |
| 16ATW-77 -Spot 294 | 1547 | 833895 | 2.8 | 20.3 | 1.0 | 0.1 | 2.4 | 0.0 | 2.2 | 0.9 | 95.0 | 2.1 | 97.3 | 2.2 | 155.3 | 23.6 | 95.0 | 2.1 | NA |
| 16ATW-77 -Spot 232 | 1919 | 48457 | 3.8 | 20.4 | 1.1 | 0.1 | 2.5 | 0.0 | 2.2 | 0.9 | 95.5 | 2.1 | 97.5 | 2.3 | 147.2 | 26.5 | 95.5 | 2.1 | NA |
| 16ATW-77 -Spot 245 | 1255 | 880885 | 4.2 | 20.3 | 1.0 | 0.1 | 2.4 | 0.0 | 2.1 | 0.9 | 95.9 | 2.0 | 98.6 | 2.2 | 165.4 | 24.0 | 95.9 | 2.0 | NA |
| 16ATW-77 -Spot 4 | 1609 | 178100 | 4.0 | 20.5 | 1.3 | 0.1 | 2.4 | 0.0 | 2.1 | 0.9 | 96.3 | 2.0 | 98.1 | 2.3 | 142.5 | 29.5 | 96.3 | 2.0 | NA |

| | | | | | | | | | | | | | | | | | | | |
|---|---|---|---|---|---|---|---|---|---|---|---|---|---|---|---|---|---|---|---|
| 16ATW-77 -Spot 214 | 1929 | 125397 | 2.6 | 20.5 | 0.8 | 0.1 | 1.8 | 0.0 | 1.6 | 0.9 | 96.5 | 1.6 | 98.1 | 1.7 | 138.3 | 18.7 | 96.5 | 1.6 | NA |
| 16ATW-77 -Spot 34 | 1122 | 473093 | 2.6 | 20.2 | 1.3 | 0.1 | 2.9 | 0.0 | 2.5 | 0.9 | 96.5 | 2.4 | 99.5 | 2.7 | 173.8 | 31.5 | 96.5 | 2.4 | NA |
| 16ATW-77 -Spot 145 | 1371 | 171338 | 4.0 | 20.6 | 1.1 | 0.1 | 2.6 | 0.0 | 2.4 | 0.9 | 97.1 | 2.3 | 98.3 | 2.4 | 128.4 | 25.0 | 97.1 | 2.3 | NA |
| 16ATW-77 -Spot 99 | 964 | 36431 | 6.7 | 20.1 | 1.3 | 0.1 | 2.2 | 0.0 | 1.7 | 0.8 | 97.2 | 1.6 | 100.6 | 2.1 | 183.5 | 31.0 | 97.2 | 1.6 | NA |
| 16ATW-77 -Spot 147 | 1160 | 225830 | 4.8 | 19.2 | 1.7 | 0.1 | 2.7 | 0.0 | 2.0 | 0.8 | 97.6 | 1.9 | 105.5 | 2.7 | 287.6 | 39.7 | 97.6 | 1.9 | NA |
| 16ATW-77 -Spot 43 | 1239 | 101482 | 4.5 | 19.7 | 1.2 | 0.1 | 2.9 | 0.0 | 2.6 | 0.9 | 98.1 | 2.5 | 103.3 | 2.8 | 226.4 | 28.5 | 98.1 | 2.5 | NA |
| 16ATW-77 -Spot 236 | 1408 | 142633 | 4.0 | 20.6 | 1.2 | 0.1 | 3.0 | 0.0 | 2.7 | 0.9 | 98.3 | 2.7 | 99.1 | 2.8 | 121.0 | 29.2 | 98.3 | 2.7 | NA |
| 16ATW-77 -Spot 288 | 1222 | 111236 | 3.0 | 20.7 | 1.1 | 0.1 | 2.5 | 0.0 | 2.2 | 0.9 | 98.6 | 2.2 | 99.3 | 2.3 | 116.1 | 25.1 | 98.6 | 2.2 | NA |
| 16ATW-77 -Spot 311 | 600 | 41099 | 4.3 | 20.0 | 1.3 | 0.1 | 2.6 | 0.0 | 2.3 | 0.9 | 98.6 | 2.2 | 102.2 | 2.6 | 189.6 | 30.2 | 98.6 | 2.2 | NA |
| 16ATW-77 -Spot 22 | 1341 | 4783244 | 4.5 | 20.0 | 1.2 | 0.1 | 2.6 | 0.0 | 2.3 | 0.9 | 99.0 | 2.3 | 102.7 | 2.6 | 191.7 | 28.5 | 99.0 | 2.3 | NA |
| 16ATW-77 -Spot 79 | 1436 | 202458 | 2.3 | 20.0 | 1.0 | 0.1 | 2.6 | 0.0 | 2.4 | 0.9 | 99.2 | 2.3 | 103.1 | 2.5 | 197.0 | 24.3 | 99.2 | 2.3 | NA |
| 16ATW-77 -Spot 2 | 1030 | 65308 | 4.1 | 20.6 | 1.3 | 0.1 | 2.3 | 0.0 | 1.9 | 0.8 | 99.3 | 1.8 | 100.3 | 2.2 | 124.9 | 31.3 | 99.3 | 1.8 | NA |
| 16ATW-77 -Spot 187 | 914 | 105740 | 6.4 | 20.3 | 1.0 | 0.1 | 2.1 | 0.0 | 1.9 | 0.9 | 99.3 | 1.8 | 101.9 | 2.0 | 164.8 | 22.8 | 99.3 | 1.8 | NA |
| 16ATW-77 -Spot 9 | 1529 | 59116 | 3.0 | 20.9 | 1.0 | 0.1 | 2.5 | 0.0 | 2.2 | 0.9 | 99.4 | 2.2 | 99.0 | 2.3 | 88.8 | 24.0 | 99.4 | 2.2 | NA |
| 16ATW-77 -Spot 82 | 1913 | 162950 | 4.5 | 20.8 | 0.7 | 0.1 | 1.7 | 0.0 | 1.6 | 0.9 | 99.4 | 1.6 | 99.6 | 1.6 | 106.5 | 16.3 | 99.4 | 1.6 | NA |
| 16ATW-77 -Spot 212 | 882 | 210134 | 4.1 | 20.1 | 1.1 | 0.1 | 3.1 | 0.0 | 2.9 | 0.9 | 99.5 | 2.8 | 102.9 | 3.0 | 183.3 | 26.7 | 99.5 | 2.8 | NA |
| 16ATW-77 -Spot 211 | 455 | 37420 | 3.6 | 20.0 | 1.4 | 0.1 | 2.3 | 0.0 | 1.8 | 0.8 | 99.5 | 1.8 | 103.2 | 2.2 | 191.5 | 33.5 | 99.5 | 1.8 | NA |
| 16ATW-77 -Spot 160 | 1457 | 1256676 | 3.5 | 20.8 | 1.2 | 0.1 | 2.2 | 0.0 | 1.9 | 0.9 | 99.7 | 1.8 | 100.1 | 2.1 | 108.7 | 27.7 | 99.7 | 1.8 | NA |
| 16ATW-77 -Spot 73 | 1536 | 169959 | 3.0 | 20.5 | 1.0 | 0.1 | 2.0 | 0.0 | 1.7 | 0.9 | 99.7 | 1.7 | 101.2 | 2.0 | 138.4 | 24.5 | 99.7 | 1.7 | NA |
| 16ATW-77 -Spot 20 | 795 | 156886 | 2.7 | 20.2 | 1.0 | 0.1 | 1.9 | 0.0 | 1.6 | 0.9 | 99.7 | 1.6 | 102.7 | 1.8 | 172.7 | 22.8 | 99.7 | 1.6 | NA |
| 16ATW-77 -Spot 40 | 1309 | 119713 | 3.6 | 20.2 | 1.0 | 0.1 | 2.3 | 0.0 | 2.0 | 0.9 | 99.7 | 2.0 | 102.8 | 2.2 | 175.2 | 23.7 | 99.7 | 2.0 | NA |
| 16ATW-77 -Spot 176 | 603 | 46415 | 3.6 | 20.4 | 1.4 | 0.1 | 2.5 | 0.0 | 2.1 | 0.8 | 99.9 | 2.1 | 102.0 | 2.5 | 153.6 | 32.9 | 99.9 | 2.1 | NA |
| 16ATW-77 -Spot 141 | 1074 | 192565 | 3.7 | 20.0 | 1.1 | 0.1 | 2.6 | 0.0 | 2.3 | 0.9 | 99.9 | 2.3 | 103.8 | 2.5 | 194.8 | 25.5 | 99.9 | 2.3 | NA |

| | | | | | | | | | | | | | | | | | | | |
|---|---|---|---|---|---|---|---|---|---|---|---|---|---|---|---|---|---|---|---|
| 16ATW-77 -Spot 296 | 1103 | 71937 | 4.2 | 20.4 | 1.1 | 0.1 | 2.5 | 0.0 | 2.2 | 0.9 | 100.0 | 2.2 | 102.0 | 2.4 | 149.2 | 24.8 | 100.0 | 2.2 | NA |
| 16ATW-77 -Spot 194 | 1319 | 128504 | 3.0 | 20.4 | 1.1 | 0.1 | 2.7 | 0.0 | 2.5 | 0.9 | 100.0 | 2.5 | 102.1 | 2.7 | 152.3 | 25.3 | 100.0 | 2.5 | NA |
| 16ATW-77 -Spot 92 | 917 | 24362 | 3.8 | 20.5 | 1.0 | 0.1 | 2.2 | 0.0 | 2.0 | 0.9 | 100.5 | 2.0 | 101.9 | 2.2 | 136.0 | 23.5 | 100.5 | 2.0 | NA |
| 16ATW-77 -Spot 52 | 1440 | 95998 | 4.5 | 20.0 | 1.2 | 0.1 | 2.5 | 0.0 | 2.2 | 0.9 | 100.5 | 2.2 | 104.3 | 2.5 | 191.7 | 27.4 | 100.5 | 2.2 | NA |
| 16ATW-77 -Spot 257 | 536 | 45267 | 3.2 | 19.8 | 1.2 | 0.1 | 2.5 | 0.0 | 2.2 | 0.9 | 100.8 | 2.2 | 105.7 | 2.5 | 218.9 | 26.7 | 100.8 | 2.2 | NA |
| 16ATW-77 -Spot 222 | 1077 | 65457 | 4.9 | 19.6 | 1.1 | 0.1 | 2.4 | 0.0 | 2.1 | 0.9 | 101.0 | 2.1 | 107.0 | 2.4 | 242.3 | 25.6 | 101.0 | 2.1 | NA |
| 16ATW-77 -Spot 116 | 903 | 393396 | 3.5 | 20.2 | 1.2 | 0.1 | 2.8 | 0.0 | 2.6 | 0.9 | 101.1 | 2.6 | 103.7 | 2.8 | 166.3 | 27.5 | 101.1 | 2.6 | NA |
| 16ATW-77 -Spot 273 | 756 | 51018 | 3.2 | 20.6 | 1.2 | 0.1 | 2.2 | 0.0 | 1.9 | 0.8 | 101.2 | 1.9 | 102.2 | 2.2 | 126.9 | 29.4 | 101.2 | 1.9 | NA |
| 16ATW-77 -Spot 74 | 1386 | 244255 | 3.9 | 20.4 | 0.9 | 0.1 | 2.4 | 0.0 | 2.2 | 0.9 | 101.2 | 2.2 | 103.0 | 2.4 | 146.1 | 22.3 | 101.2 | 2.2 | NA |
| 16ATW-77 -Spot 201 | 838 | 103668 | 4.0 | 20.5 | 1.4 | 0.1 | 2.9 | 0.0 | 2.5 | 0.9 | 101.3 | 2.5 | 102.9 | 2.8 | 140.3 | 32.1 | 101.3 | 2.5 | NA |
| 16ATW-77 -Spot 205 | 1046 | 41662 | 4.0 | 20.3 | 1.1 | 0.1 | 2.4 | 0.0 | 2.1 | 0.9 | 101.3 | 2.1 | 103.6 | 2.3 | 158.8 | 25.7 | 101.3 | 2.1 | NA |
| 16ATW-77 -Spot 62 | 205 | 14203 | 3.1 | 20.3 | 2.0 | 0.1 | 3.4 | 0.0 | 2.7 | 0.8 | 101.5 | 2.7 | 103.8 | 3.3 | 156.5 | 46.5 | 101.5 | 2.7 | NA |
| 16ATW-77 -Spot 207 | 396 | 29521 | 4.2 | 19.8 | 1.6 | 0.1 | 3.4 | 0.0 | 3.0 | 0.9 | 101.6 | 3.0 | 106.5 | 3.4 | 217.9 | 36.9 | 101.6 | 3.0 | NA |
| 16ATW-77 -Spot 53 | 342 | 37654 | 5.7 | 20.0 | 1.5 | 0.1 | 2.7 | 0.0 | 2.3 | 0.8 | 102.3 | 2.3 | 106.4 | 2.7 | 199.7 | 34.8 | 102.3 | 2.3 | NA |
| 16ATW-77 -Spot 172 | 1851 | 248865 | 2.1 | 20.5 | 0.9 | 0.1 | 2.3 | 0.0 | 2.2 | 0.9 | 103.4 | 2.2 | 104.8 | 2.3 | 137.2 | 20.0 | 103.4 | 2.2 | NA |
| 16ATW-77 -Spot 100 | 119 | 7021 | 16.5 | 20.5 | 3.1 | 0.1 | 4.1 | 0.0 | 2.6 | 0.7 | 104.7 | 2.7 | 106.1 | 4.1 | 138.8 | 72.5 | 104.7 | 2.7 | NA |
| 16ATW-77 -Spot 114 | 617 | 38665 | 2.5 | 19.9 | 0.9 | 0.1 | 2.2 | 0.0 | 2.0 | 0.9 | 104.9 | 2.1 | 109.1 | 2.3 | 201.1 | 20.1 | 104.9 | 2.1 | NA |
| 16ATW-77 -Spot 76 | 870 | 156788 | 3.6 | 20.4 | 1.4 | 0.1 | 2.8 | 0.0 | 2.4 | 0.9 | 105.4 | 2.5 | 107.3 | 2.8 | 150.0 | 31.7 | 105.4 | 2.5 | NA |
| 16ATW-77 -Spot 58 | 559 | 178841 | 2.9 | 19.3 | 1.5 | 0.1 | 3.5 | 0.0 | 3.2 | 0.9 | 106.2 | 3.4 | 113.9 | 3.8 | 277.8 | 33.7 | 106.2 | 3.4 | NA |
| 16ATW-77 -Spot 37 | 217 | 8464 | 2.9 | 21.1 | 2.2 | 0.1 | 3.1 | 0.0 | 2.2 | 0.7 | 107.3 | 2.4 | 105.7 | 3.1 | 72.1 | 52.0 | 107.3 | 2.4 | NA |
| 16ATW-77 -Spot 308 | 275 | 28960 | 2.5 | 19.4 | 1.6 | 0.1 | 3.3 | 0.0 | 2.8 | 0.9 | 127.5 | 3.6 | 134.6 | 4.1 | 262.3 | 37.0 | 127.5 | 3.6 | NA |
| 16ATW-77 -Spot 48 | 230 | 32978 | 3.6 | 19.9 | 1.6 | 0.2 | 3.1 | 0.0 | 2.7 | 0.9 | 149.0 | 4.0 | 152.3 | 4.4 | 204.9 | 36.4 | 149.0 | 4.0 | NA |
| 16ATW-77 -Spot 235 | 181 | 12604 | 2.6 | 19.5 | 1.8 | 0.2 | 2.9 | 0.0 | 2.3 | 0.8 | 149.2 | 3.4 | 155.3 | 4.2 | 249.5 | 40.9 | 149.2 | 3.4 | NA |

| | | | | | | | | | | | | | | | | | | | |
|---|---|---|---|---|---|---|---|---|---|---|---|---|---|---|---|---|---|---|---|
| 16ATW-77 -Spot 233 | 131 | 12699 | 3.2 | 19.7 | 1.6 | 0.2 | 2.7 | 0.0 | 2.1 | 0.8 | 153.4 | 3.2 | 158.4 | 3.9 | 234.9 | 37.9 | 153.4 | 3.2 | NA |
| 16ATW-77 -Spot 70 | 77 | 8304 | 3.1 | 20.1 | 2.6 | 0.2 | 3.5 | 0.0 | 2.3 | 0.7 | 156.6 | 3.6 | 158.3 | 5.1 | 185.5 | 60.1 | 156.6 | 3.6 | NA |
| 16ATW-77 -Spot 250 | 191 | 26733 | 2.3 | 19.7 | 1.7 | 0.2 | 3.1 | 0.0 | 2.6 | 0.8 | 161.3 | 4.1 | 165.8 | 4.8 | 231.7 | 40.2 | 161.3 | 4.1 | NA |
| 16ATW-77 -Spot 107 | 227 | 31133 | 2.0 | 18.8 | 1.7 | 0.2 | 2.8 | 0.0 | 2.2 | 0.8 | 161.6 | 3.5 | 173.4 | 4.5 | 337.9 | 39.2 | 161.6 | 3.5 | NA |
| 16ATW-77 -Spot 166 | 40 | 3250 | 2.3 | 21.8 | 5.6 | 0.2 | 6.2 | 0.0 | 2.6 | 0.4 | 162.0 | 4.2 | 151.6 | 8.7 | NA | NA | 162.0 | 4.2 | ##### |
| 16ATW-77 -Spot 125 | 81 | 16403 | 3.2 | 18.9 | 2.2 | 0.2 | 3.2 | 0.0 | 2.4 | 0.7 | 162.8 | 3.8 | 173.4 | 5.1 | 321.6 | 49.3 | 162.8 | 3.8 | NA |
| 16ATW-77 -Spot 42 | 202 | 63937 | 1.0 | 19.3 | 1.6 | 0.2 | 4.3 | 0.0 | 4.0 | 0.9 | 164.6 | 6.4 | 172.0 | 6.8 | 277.0 | 37.5 | 164.6 | 6.4 | NA |
| 16ATW-77 -Spot 254 | 555 | 35025 | 1.9 | 19.9 | 1.2 | 0.2 | 2.8 | 0.0 | 2.6 | 0.9 | 165.6 | 4.2 | 168.4 | 4.4 | 210.1 | 27.5 | 165.6 | 4.2 | NA |
| 16ATW-77 -Spot 13 | 30 | 21175 | 4.9 | 18.8 | 4.5 | 0.2 | 5.6 | 0.0 | 3.3 | 0.6 | 172.8 | 5.7 | 184.3 | 9.4 | 336.3 | 102.3 | 172.8 | 5.7 | NA |
| 16ATW-77 -Spot 47 | 1015 | 205184 | 4.4 | 19.4 | 0.9 | 0.2 | 2.1 | 0.0 | 1.9 | 0.9 | 181.3 | 3.4 | 187.4 | 3.6 | 266.4 | 21.4 | 181.3 | 3.4 | NA |
| 16ATW-77 -Spot 231 | 701 | 276083 | 6.0 | 18.2 | 1.2 | 0.2 | 2.8 | 0.0 | 2.5 | 0.9 | 188.8 | 4.7 | 205.8 | 5.2 | 406.2 | 25.9 | 188.8 | 4.7 | NA |
| 16ATW-77 -Spot 297 | 246 | 139948 | 4.6 | 19.4 | 1.3 | 0.2 | 2.3 | 0.0 | 1.9 | 0.8 | 199.6 | 3.7 | 204.7 | 4.3 | 264.7 | 30.6 | 199.6 | 3.7 | NA |
| 16ATW-77 -Spot 45 | 283 | 85863 | 2.6 | 18.5 | 1.3 | 0.4 | 3.3 | 0.1 | 3.0 | 0.9 | 356.7 | 10.5 | 359.1 | 10.0 | 375.9 | 29.2 | 356.7 | 10.5 | NA |
| 16ATW-77 -Spot 21 | 571 | 475692 | 1.6 | 17.4 | 1.0 | 0.6 | 2.9 | 0.1 | 2.7 | 0.9 | 444.2 | 11.7 | 454.1 | 10.6 | 505.4 | 21.5 | 444.2 | 11.7 | 87.9 |
| 16ATW-77 -Spot 155 | 9 | 20263 | 1.4 | 10.7 | 2.0 | 3.3 | 3.2 | 0.3 | 2.5 | 0.8 | 1453.8 | 32.6 | 1471.2 | 24.8 | 1497.3 | 37.2 | 1497.3 | 37.2 | 97.1 |
| 16ATW-77 -Spot 64 | 664 | 16356374 | 3.8 | 10.4 | 1.0 | 3.0 | 2.6 | 0.2 | 2.4 | 0.9 | 1331.5 | 28.5 | 1415.1 | 19.5 | 1544.1 | 18.1 | 1544.1 | 18.1 | 86.2 |
| 16ATW-77 -Spot 56 | 167 | 79001 | 1.8 | 9.5 | 0.9 | 4.3 | 2.7 | 0.3 | 2.6 | 0.9 | 1674.7 | 38.0 | 1697.0 | 22.6 | 1725.4 | 17.2 | 1725.4 | 17.2 | 97.1 |
| 16ATW-77 -Spot 94 | 256 | 13280122 | 2.9 | 6.8 | 0.8 | 7.7 | 2.3 | 0.4 | 2.1 | 0.9 | 2079.3 | 37.8 | 2194.6 | 20.3 | 2304.9 | 13.4 | 2304.9 | 13.4 | 90.2 |
| 16ATW-77 -Spot 91 | 49 | 323891 | 2.7 | 5.5 | 0.8 | 12.3 | 2.3 | 0.5 | 2.1 | 0.9 | 2565.4 | 44.4 | 2628.3 | 21.2 | 2677.8 | 13.7 | 2677.8 | 13.7 | 95.8 |
| 16ATW-77 -Spot 118 | 247 | 4091 | 5.9 | 22.2 | 1.5 | 0.1 | 2.8 | 0.0 | 2.3 | 0.8 | 74.2 | 1.7 | 70.3 | 1.9 | NA | NA | 74.2 | 1.7 | ##### |
| 16ATW-77 -Spot 252 | 668 | 55644 | 3.6 | 20.2 | 1.7 | 0.1 | 3.5 | 0.0 | 3.0 | 0.9 | 55.0 | 1.7 | 57.6 | 1.9 | 168.0 | 38.8 | 55.0 | 1.7 | NA |
| 16ATW-77 -Spot 95 | 1116 | 42703 | 4.7 | 20.2 | 1.2 | 0.1 | 3.1 | 0.0 | 2.8 | 0.9 | 54.8 | 1.5 | 57.4 | 1.7 | 169.3 | 28.9 | 54.8 | 1.5 | NA |
| 16ATW-77 -Spot 83 | 1261 | 104337 | 4.5 | 20.1 | 1.3 | 0.1 | 2.2 | 0.0 | 1.7 | 0.8 | 58.6 | 1.0 | 61.6 | 1.3 | 184.6 | 31.3 | 58.6 | 1.0 | NA |

| | | | | | | | | | | | | | | | | | | | |
|---|---|---|---|---|---|---|---|---|---|---|---|---|---|---|---|---|---|---|---|
| 16ATW-77 -Spot 49 | 500 | 12828 | 2.0 | 20.1 | 1.9 | 0.1 | 3.9 | 0.0 | 3.4 | 0.9 | 57.4 | 1.9 | 60.4 | 2.3 | 182.6 | 44.3 | 57.4 | 1.9 | NA |
| 16ATW-77 -Spot 122 | 2472 | 95017 | 2.8 | 20.1 | 1.0 | 0.1 | 2.1 | 0.0 | 1.8 | 0.9 | 58.3 | 1.1 | 61.5 | 1.3 | 186.8 | 23.6 | 58.3 | 1.1 | NA |
| 16ATW-77 -Spot 150 | 926 | 95348 | 3.5 | 18.8 | 1.4 | 0.1 | 3.0 | 0.0 | 2.6 | 0.9 | 103.2 | 2.7 | 113.4 | 3.2 | 336.2 | 31.1 | 103.2 | 2.7 | NA |
| 16ATW-77 -Spot 242 | 257 | 33253 | 3.5 | 20.0 | 2.3 | 0.1 | 3.5 | 0.0 | 2.7 | 0.8 | 59.9 | 1.6 | 63.3 | 2.2 | 196.2 | 52.9 | 59.9 | 1.6 | NA |
| 16ATW-77 -Spot 131 | 906 | 42865 | 8.8 | 19.9 | 1.3 | 0.1 | 2.2 | 0.0 | 1.8 | 0.8 | 62.8 | 1.1 | 66.6 | 1.4 | 206.9 | 30.8 | 62.8 | 1.1 | NA |
| 16ATW-77 -Spot 88 | 932 | 32948 | 2.1 | 18.8 | 2.5 | 0.1 | 3.1 | 0.0 | 1.9 | 0.6 | 101.3 | 1.9 | 111.4 | 3.3 | 334.0 | 57.5 | 101.3 | 1.9 | NA |
| 16ATW-77 -Spot 61 | 530 | 190752 | 6.4 | 20.0 | 1.6 | 0.1 | 2.6 | 0.0 | 2.0 | 0.8 | 58.0 | 1.2 | 61.2 | 1.6 | 192.0 | 38.3 | 58.0 | 1.2 | NA |
| 16ATW-77 -Spot 165 | 522 | 41669 | 5.3 | 19.9 | 1.7 | 0.1 | 2.7 | 0.0 | 2.1 | 0.8 | 62.2 | 1.3 | 66.0 | 1.7 | 207.2 | 38.9 | 62.2 | 1.3 | NA |
| 16ATW-77 -Spot 229 | 489 | 187920 | 2.9 | 20.1 | 1.4 | 0.1 | 3.1 | 0.0 | 2.8 | 0.9 | 55.9 | 1.6 | 59.0 | 1.8 | 186.4 | 31.7 | 55.9 | 1.6 | NA |
| 16ATW-77 -Spot 97 | 666 | 40680 | 3.2 | 20.0 | 1.6 | 0.1 | 3.2 | 0.0 | 2.8 | 0.9 | 56.9 | 1.6 | 60.1 | 1.9 | 192.4 | 36.7 | 56.9 | 1.6 | NA |
| 16ATW-77 -Spot 217 | 709 | 751702 | 3.9 | 19.8 | 1.3 | 0.1 | 2.3 | 0.0 | 1.9 | 0.8 | 64.5 | 1.2 | 68.8 | 1.5 | 219.0 | 30.2 | 64.5 | 1.2 | NA |
| 16ATW-77 -Spot 303 | 853 | 332001 | 6.2 | 19.8 | 1.4 | 0.1 | 2.7 | 0.0 | 2.3 | 0.9 | 62.3 | 1.4 | 66.3 | 1.7 | 213.7 | 33.2 | 62.3 | 1.4 | NA |
| 16ATW-77 -Spot 227 | 690 | 153014 | 6.0 | 19.7 | 1.3 | 0.1 | 2.8 | 0.0 | 2.5 | 0.9 | 65.2 | 1.6 | 69.7 | 1.9 | 226.5 | 29.1 | 65.2 | 1.6 | NA |
| 16ATW-77 -Spot 121 | 266 | 8447 | 3.6 | 19.9 | 2.3 | 0.1 | 2.9 | 0.0 | 1.8 | 0.6 | 58.3 | 1.1 | 62.0 | 1.8 | 205.9 | 53.2 | 58.3 | 1.1 | NA |
| 16ATW-77 -Spot 225 | 530 | 27497 | 3.6 | 19.9 | 1.7 | 0.1 | 2.6 | 0.0 | 2.0 | 0.8 | 58.8 | 1.1 | 62.6 | 1.6 | 209.3 | 39.1 | 58.8 | 1.1 | NA |
| 16ATW-77 -Spot 128 | 278 | 105499 | 6.2 | 19.8 | 2.4 | 0.1 | 3.5 | 0.0 | 2.6 | 0.7 | 60.3 | 1.6 | 64.3 | 2.2 | 214.8 | 55.0 | 60.3 | 1.6 | NA |
| 16ATW-77 -Spot 177 | 390 | 17796 | 4.3 | 20.1 | 1.8 | 0.1 | 2.9 | 0.0 | 2.3 | 0.8 | 52.0 | 1.2 | 54.9 | 1.6 | 186.3 | 40.8 | 52.0 | 1.2 | NA |
| 16ATW-77 -Spot 55 | 1493 | 33080 | 5.1 | 19.8 | 1.2 | 0.1 | 2.5 | 0.0 | 2.2 | 0.9 | 59.0 | 1.3 | 63.0 | 1.5 | 216.3 | 28.1 | 59.0 | 1.3 | NA |
| 16ATW-77 -Spot 188 | 344 | 42411 | 3.2 | 18.4 | 1.7 | 0.1 | 2.4 | 0.0 | 1.7 | 0.7 | 105.6 | 1.8 | 118.6 | 2.7 | 389.1 | 38.1 | 105.6 | 1.8 | NA |
| 16ATW-77 -Spot 167 | 217 | 22234 | 10.0 | 19.5 | 2.6 | 0.1 | 3.9 | 0.0 | 2.9 | 0.8 | 67.9 | 2.0 | 73.4 | 2.7 | 257.9 | 59.0 | 67.9 | 2.0 | NA |
| 16ATW-77 -Spot 66 | 466 | 134933 | 3.7 | 19.8 | 1.7 | 0.1 | 2.8 | 0.0 | 2.3 | 0.8 | 56.6 | 1.3 | 60.5 | 1.7 | 215.2 | 38.2 | 56.6 | 1.3 | NA |
| 16ATW-77 -Spot 208 | 318 | 21740 | 3.2 | 19.7 | 1.8 | 0.1 | 2.7 | 0.0 | 2.0 | 0.7 | 59.6 | 1.2 | 63.8 | 1.7 | 227.4 | 41.8 | 59.6 | 1.2 | NA |
| 16ATW-77 -Spot 36 | 794 | 121133 | 5.1 | 19.8 | 1.5 | 0.1 | 2.5 | 0.0 | 2.0 | 0.8 | 57.4 | 1.2 | 61.4 | 1.5 | 220.4 | 35.4 | 57.4 | 1.2 | NA |

| | | | | | | | | | | | | | | | | | | | |
|---|---|---|---|---|---|---|---|---|---|---|---|---|---|---|---|---|---|---|---|
| 16ATW-77 -Spot 86 | 163 | 25577 | 4.3 | 19.6 | 2.3 | 0.1 | 3.1 | 0.0 | 2.1 | 0.7 | 63.1 | 1.3 | 67.9 | 2.0 | 244.2 | 52.6 | 63.1 | 1.3 | NA |
| 16ATW-77 -Spot 204 | 734 | 41241 | 2.3 | 19.8 | 1.5 | 0.1 | 2.6 | 0.0 | 2.2 | 0.8 | 55.6 | 1.2 | 59.4 | 1.5 | 217.3 | 34.1 | 55.6 | 1.2 | NA |
| 16ATW-77 -Spot 130 | 467 | 21953 | 8.0 | 19.6 | 1.8 | 0.1 | 3.3 | 0.0 | 2.7 | 0.8 | 62.2 | 1.7 | 67.1 | 2.1 | 244.6 | 41.9 | 62.2 | 1.7 | NA |
| 16ATW-77 -Spot 295 | 435 | 70238 | 2.4 | 19.6 | 1.6 | 0.1 | 2.9 | 0.0 | 2.4 | 0.8 | 61.0 | 1.5 | 65.7 | 1.9 | 241.3 | 37.4 | 61.0 | 1.5 | NA |
| 16ATW-77 -Spot 298 | 235 | 19837 | 4.8 | 19.6 | 2.1 | 0.1 | 3.2 | 0.0 | 2.4 | 0.8 | 59.1 | 1.4 | 63.5 | 2.0 | 236.2 | 49.5 | 59.1 | 1.4 | NA |
| 16ATW-77 -Spot 71 | 549 | 716200 | 8.5 | 19.5 | 1.2 | 0.1 | 2.3 | 0.0 | 2.0 | 0.9 | 62.6 | 1.2 | 67.7 | 1.5 | 253.3 | 27.1 | 62.6 | 1.2 | NA |
| 16ATW-77 -Spot 223 | 733 | 311876 | 2.5 | 18.1 | 1.7 | 0.1 | 2.9 | 0.0 | 2.4 | 0.8 | 99.7 | 2.4 | 113.7 | 3.2 | 419.2 | 38.2 | 99.7 | 2.4 | NA |
| 16ATW-77 -Spot 253 | 1012 | 34759 | 2.8 | 19.5 | 1.5 | 0.1 | 2.5 | 0.0 | 1.9 | 0.8 | 58.1 | 1.1 | 62.8 | 1.5 | 248.8 | 35.1 | 58.1 | 1.1 | NA |
| 16ATW-77 -Spot 197 | 1366 | 170664 | 2.7 | 19.6 | 1.2 | 0.1 | 2.3 | 0.0 | 2.0 | 0.9 | 57.0 | 1.1 | 61.6 | 1.4 | 246.3 | 26.7 | 57.0 | 1.1 | NA |
| 16ATW-77 -Spot 98 | 461 | 9544 | 2.9 | 19.7 | 2.0 | 0.1 | 2.9 | 0.0 | 2.1 | 0.7 | 51.5 | 1.1 | 55.4 | 1.5 | 229.0 | 45.3 | 51.5 | 1.1 | NA |
| 16ATW-77 -Spot 143 | 341 | 158212 | 2.6 | 19.5 | 2.3 | 0.1 | 3.6 | 0.0 | 2.8 | 0.8 | 58.1 | 1.6 | 63.1 | 2.2 | 258.4 | 52.9 | 58.1 | 1.6 | NA |
| 16ATW-77 -Spot 119 | 171 | 11077 | 3.1 | 19.3 | 2.6 | 0.1 | 3.7 | 0.0 | 2.7 | 0.7 | 61.2 | 1.6 | 66.9 | 2.4 | 277.8 | 58.7 | 61.2 | 1.6 | NA |
| 16ATW-77 -Spot 30 | 438 | 40059 | 2.3 | 19.4 | 2.1 | 0.1 | 3.4 | 0.0 | 2.7 | 0.8 | 58.4 | 1.6 | 63.7 | 2.1 | 267.7 | 47.9 | 58.4 | 1.6 | NA |
| 16ATW-77 -Spot 46 | 857 | 23841 | 4.2 | 17.7 | 2.0 | 0.1 | 3.1 | 0.0 | 2.4 | 0.8 | 102.6 | 2.5 | 119.5 | 3.5 | 471.6 | 43.7 | 102.6 | 2.5 | NA |
| 16ATW-77 -Spot 261 | 1424 | 34350 | 3.5 | 19.4 | 1.2 | 0.1 | 2.5 | 0.0 | 2.2 | 0.9 | 58.5 | 1.3 | 63.8 | 1.5 | 270.0 | 27.5 | 58.5 | 1.3 | NA |
| 16ATW-77 -Spot 210 | 545 | 24524 | 2.2 | 19.3 | 1.9 | 0.1 | 2.7 | 0.0 | 2.0 | 0.7 | 57.4 | 1.1 | 62.9 | 1.7 | 282.2 | 43.0 | 57.4 | 1.1 | NA |
| 16ATW-77 -Spot 312 | 567 | 44098 | 2.4 | 19.2 | 2.2 | 0.1 | 3.2 | 0.0 | 2.3 | 0.7 | 56.9 | 1.3 | 62.6 | 1.9 | 288.9 | 49.4 | 56.9 | 1.3 | NA |
| 16ATW-77 -Spot 286 | 620 | 21195 | 2.5 | 19.1 | 1.7 | 0.1 | 2.8 | 0.0 | 2.1 | 0.8 | 57.4 | 1.2 | 63.5 | 1.7 | 298.8 | 39.6 | 57.4 | 1.2 | NA |
| 16ATW-77 -Spot 136 | 405 | 12130 | 3.2 | 18.3 | 4.0 | 0.1 | 4.6 | 0.0 | 2.2 | 0.5 | 75.4 | 1.6 | 86.0 | 3.8 | 393.3 | 89.5 | 75.4 | 1.6 | NA |
| 16ATW-77 -Spot 101 | 312 | 18163 | 5.9 | 18.7 | 2.0 | 0.1 | 3.2 | 0.0 | 2.4 | 0.8 | 62.2 | 1.5 | 70.1 | 2.1 | 349.1 | 45.6 | 62.2 | 1.5 | NA |
| 16ATW-77 -Spot 129 | 1442 | 166459 | 2.0 | 18.5 | 1.0 | 0.1 | 2.0 | 0.0 | 1.7 | 0.9 | 59.5 | 1.0 | 67.7 | 1.3 | 371.9 | 22.1 | 59.5 | 1.0 | NA |
| 16ATW-77 -Spot 5 | 1103 | 21608 | 4.1 | 18.6 | 1.7 | 0.1 | 3.0 | 0.0 | 2.5 | 0.8 | 55.3 | 1.4 | 62.8 | 1.9 | 362.4 | 37.8 | 55.3 | 1.4 | NA |
| 16ATW-77 -Spot 300 | 1443 | 22120 | 5.9 | 18.2 | 1.9 | 0.1 | 2.6 | 0.0 | 1.7 | 0.7 | 60.6 | 1.1 | 69.9 | 1.8 | 404.6 | 43.1 | 60.6 | 1.1 | NA |

| | | | | | | | | | | | | | | | | | | | |
|---|---|---|---|---|---|---|---|---|---|---|---|---|---|---|---|---|---|---|---|
| 16ATW-77 -Spot 132 | 2149 | 101773 | 6.4 | 18.0 | 1.4 | 0.1 | 2.6 | 0.0 | 2.2 | 0.9 | 63.5 | 1.4 | 74.2 | 1.9 | 437.1 | 30.6 | 63.5 | 1.4 | NA |
| 16ATW-77 -Spot 191 | 292 | 10001 | 4.1 | 18.1 | 3.0 | 0.1 | 4.1 | 0.0 | 2.8 | 0.7 | 59.1 | 1.6 | 68.9 | 2.7 | 422.3 | 66.7 | 59.1 | 1.6 | NA |
| 16ATW-77 -Spot 32 | 531 | 11280 | 6.8 | 17.8 | 1.9 | 0.1 | 2.8 | 0.0 | 2.1 | 0.7 | 64.4 | 1.3 | 76.1 | 2.1 | 461.3 | 42.4 | 64.4 | 1.3 | NA |
| 16ATW-77 -Spot 249 | 524 | 16047 | 2.6 | 18.0 | 2.1 | 0.1 | 2.9 | 0.0 | 1.9 | 0.7 | 59.5 | 1.1 | 69.6 | 1.9 | 434.5 | 47.8 | 59.5 | 1.1 | NA |
| 16ATW-77 -Spot 67 | 709 | 105120 | 8.0 | 16.4 | 2.5 | 0.1 | 3.4 | 0.0 | 2.3 | 0.7 | 61.6 | 1.4 | 78.8 | 2.5 | 638.6 | 53.1 | 61.6 | 1.4 | NA |
| 16ATW-77 -Spot 134 | 710 | 14903 | 5.4 | 16.7 | 4.8 | 0.1 | 5.5 | 0.0 | 2.7 | 0.5 | 57.2 | 1.5 | 72.1 | 3.8 | 599.2 | 103.3 | 57.2 | 1.5 | NA |
| 16ATW-77 -Spot 266 | 178 | 78862 | 5.1 | 16.3 | 3.2 | 0.1 | 4.3 | 0.0 | 2.9 | 0.7 | 61.8 | 1.8 | 79.7 | 3.3 | 657.8 | 68.6 | 61.8 | 1.8 | NA |
| 16ATW-77 -Spot 302 | 449 | 44126 | 4.0 | 16.6 | 3.5 | 0.1 | 4.1 | 0.0 | 2.1 | 0.5 | 58.0 | 1.2 | 73.7 | 2.9 | 618.0 | 75.0 | 58.0 | 1.2 | NA |
| 16ATW-77 -Spot 151 | 94 | 4189 | 1.9 | 7.0 | 16.4 | 0.7 | 16.6 | 0.0 | 2.6 | 0.2 | 211.6 | 5.3 | 511.4 | 66.7 | 2256.2 | 284.9 | 211.6 | 5.3 | NA |
| 16ATW-77 -Spot 279 | 971 | 7655 | 4.5 | 14.5 | 1.8 | 0.1 | 2.6 | 0.0 | 1.9 | 0.7 | 61.1 | 1.2 | 87.8 | 2.2 | 894.0 | 37.5 | 61.1 | 1.2 | NA |
| 16ATW-77 -Spot 281 | 4600 | 12229 | 1.9 | 14.7 | 4.2 | 0.1 | 4.9 | 0.0 | 2.5 | 0.5 | 56.4 | 1.4 | 80.3 | 3.8 | 868.2 | 87.5 | 56.4 | 1.4 | NA |
| 16ATW-77 -Spot 243 | 746 | 7954 | 2.8 | 13.8 | 6.4 | 0.1 | 6.7 | 0.0 | 2.1 | 0.3 | 60.8 | 1.3 | 92.0 | 5.9 | 1002.5 | 129.4 | 60.8 | 1.3 | NA |
| 16ATW-77 -Spot 75 | 274 | 2337 | 3.3 | 6.9 | 12.1 | 0.2 | 13.3 | 0.0 | 5.5 | 0.4 | 63.5 | 3.5 | 184.4 | 22.4 | 2299.2 | 208.1 | 63.5 | 3.5 | NA |

Sample 16ATW86

| Analysis | U | 206Pb | U/Th | 206Pb* | ± | 207Pb* | ± | 206Pb* | ± | error | 206Pb* | ± | 207Pb* | ± | 206Pb* | ± | Best age | ± | Conc |
|---|---|---|---|---|---|---|---|---|---|---|---|---|---|---|---|---|---|---|---|
| | (ppm) | 204Pb | | 207Pb* | (%) | 235U* | (%) | 238U | (%) | corr. | 238U* | (Ma) | 235U | (Ma) | 207Pb* | (Ma) | (Ma) | (Ma) | (%) |
| 16ATW-86-Spot 207 | 62 | 150 | 1.8 | 22.2 | 10.5 | 0.0 | 13.2 | 0.0 | 8.0 | 0.6 | 5.8 | 0.5 | 5.7 | 0.7 | NA | NA | 5.8 | 0.5 | NA |
| 16ATW-86-Spot 195 | 401 | 6526 | 3.0 | 18.0 | 5.0 | 0.0 | 6.1 | 0.0 | 3.5 | 0.6 | 5.8 | 0.2 | 7.0 | 0.4 | 433.9 | 112.5 | 5.8 | 0.2 | NA |
| 16ATW-86-Spot 133 | 149 | 1180 | 1.8 | 34.3 | 9.8 | 0.0 | 10.8 | 0.0 | 4.6 | 0.4 | 5.9 | 0.3 | 3.7 | 0.4 | NA | NA | 5.9 | 0.3 | NA |
| 16ATW-86-Spot 217 | 557 | 19115 | 2.4 | 20.0 | 3.6 | 0.0 | 4.4 | 0.0 | 2.6 | 0.6 | 6.3 | 0.2 | 6.8 | 0.3 | 196.8 | 82.6 | 6.3 | 0.2 | NA |
| 16ATW-86-Spot 228 | 130 | 4222 | 1.9 | 12.2 | 9.5 | 0.0 | 10.8 | 0.0 | 5.2 | 0.5 | 6.8 | 0.4 | 11.9 | 1.3 | 1244.2 | 186.1 | 6.8 | 0.4 | NA |
| 16ATW-86-Spot 255 | 54 | 2484 | 1.2 | 14.9 | 13.0 | 0.0 | 14.6 | 0.0 | 6.7 | 0.5 | 6.8 | 0.5 | 9.9 | 1.4 | 843.1 | 270.8 | 6.8 | 0.5 | NA |
| 16ATW-86-Spot 114 | 336 | 1075 | 1.3 | 26.1 | 4.9 | 0.0 | 5.9 | 0.0 | 3.2 | 0.6 | 7.5 | 0.2 | 6.3 | 0.4 | NA | NA | 7.5 | 0.2 | NA |
| 16ATW-86-Spot 12 | 474 | 262067 | 5.2 | 20.7 | 1.5 | 0.1 | 2.9 | 0.0 | 2.5 | 0.9 | 59.0 | 1.5 | 60.4 | 1.7 | 117.7 | 35.0 | 59.0 | 1.5 | NA |

| | | | | | | | | | | | | | | | | | | | |
|---|---|---|---|---|---|---|---|---|---|---|---|---|---|---|---|---|---|---|---|
| 16ATW-86-Spot 52 | 125 | 5068 | 4.5 | 21.2 | 3.4 | 0.1 | 4.3 | 0.0 | 2.6 | 0.6 | 59.3 | 1.5 | 59.4 | 2.5 | 62.1 | 81.7 | 59.3 | 1.5 | NA |
| 16ATW-86-Spot 260 | 183 | 5213 | 4.9 | 20.4 | 3.1 | 0.1 | 4.0 | 0.0 | 2.6 | 0.6 | 60.6 | 1.5 | 62.9 | 2.4 | 153.8 | 72.2 | 60.6 | 1.5 | NA |
| 16ATW-86-Spot 242 | 548 | 58709 | 5.2 | 20.1 | 1.6 | 0.1 | 3.2 | 0.0 | 2.8 | 0.9 | 71.5 | 2.0 | 74.7 | 2.3 | 179.6 | 36.1 | 71.5 | 2.0 | NA |
| 16ATW-86-Spot 151 | 344 | 29977 | 3.5 | 20.8 | 2.3 | 0.1 | 3.3 | 0.0 | 2.3 | 0.7 | 79.0 | 1.8 | 79.5 | 2.5 | 97.4 | 54.9 | 79.0 | 1.8 | NA |
| 16ATW-86-Spot 264 | 55 | 10727 | 9.5 | 18.5 | 2.7 | 0.2 | 4.0 | 0.0 | 2.9 | 0.7 | 145.9 | 4.2 | 159.6 | 5.9 | 369.1 | 61.3 | 145.9 | 4.2 | NA |
| 16ATW-86-Spot 225 | 319 | 179116 | 1.2 | 19.5 | 1.4 | 0.2 | 3.9 | 0.0 | 3.6 | 0.9 | 147.6 | 5.2 | 154.3 | 5.5 | 258.9 | 32.9 | 147.6 | 5.2 | NA |
| 16ATW-86-Spot 169 | 139 | 11085 | 1.9 | 19.9 | 2.0 | 0.2 | 3.2 | 0.0 | 2.5 | 0.8 | 149.1 | 3.7 | 152.5 | 4.5 | 205.8 | 46.1 | 149.1 | 3.7 | NA |
| 16ATW-86-Spot 283 | 514 | 62886 | 2.9 | 19.4 | 1.1 | 0.2 | 2.2 | 0.0 | 1.9 | 0.9 | 149.7 | 2.8 | 156.4 | 3.2 | 260.5 | 25.7 | 149.7 | 2.8 | NA |
| 16ATW-86-Spot 170 | 159 | 23556 | 1.8 | 19.6 | 2.0 | 0.2 | 3.1 | 0.0 | 2.4 | 0.8 | 150.5 | 3.5 | 156.3 | 4.5 | 247.3 | 46.1 | 150.5 | 3.5 | NA |
| 16ATW-86-Spot 297 | 98 | 14309 | 1.8 | 19.7 | 2.5 | 0.2 | 3.5 | 0.0 | 2.5 | 0.7 | 150.5 | 3.7 | 155.2 | 5.1 | 228.7 | 57.6 | 150.5 | 3.7 | NA |
| 16ATW-86-Spot 216 | 33 | 1853 | 4.8 | 22.3 | 3.8 | 0.1 | 4.9 | 0.0 | 3.1 | 0.6 | 150.9 | 4.6 | 138.9 | 6.3 | NA | NA | 150.9 | 4.6 | NA |
| 16ATW-86-Spot 252 | 228 | 29173 | 2.7 | 19.2 | 1.2 | 0.2 | 2.6 | 0.0 | 2.3 | 0.9 | 151.4 | 3.4 | 160.0 | 3.8 | 290.5 | 28.5 | 151.4 | 3.4 | NA |
| 16ATW-86-Spot 83 | 64 | 28223 | 2.0 | 19.1 | 3.0 | 0.2 | 3.8 | 0.0 | 2.3 | 0.6 | 151.5 | 3.4 | 161.1 | 5.7 | 305.5 | 69.3 | 151.5 | 3.4 | NA |
| 16ATW-86-Spot 161 | 41 | 8350 | 3.0 | 18.8 | 3.1 | 0.2 | 3.9 | 0.0 | 2.2 | 0.6 | 151.5 | 3.4 | 163.3 | 5.8 | 338.6 | 71.1 | 151.5 | 3.4 | NA |
| 16ATW-86-Spot 5 | 131 | 13991 | 1.6 | 19.6 | 1.6 | 0.2 | 2.9 | 0.0 | 2.5 | 0.8 | 151.9 | 3.7 | 157.7 | 4.3 | 245.6 | 36.5 | 151.9 | 3.7 | NA |
| 16ATW-86-Spot 122 | 43 | 13013 | 1.8 | 19.2 | 2.9 | 0.2 | 3.8 | 0.0 | 2.6 | 0.7 | 152.0 | 3.8 | 160.8 | 5.7 | 292.9 | 65.3 | 152.0 | 3.8 | NA |
| 16ATW-86-Spot 88 | 43 | 8101 | 3.5 | 19.7 | 3.7 | 0.2 | 4.8 | 0.0 | 3.1 | 0.6 | 152.1 | 4.6 | 156.7 | 7.0 | 228.1 | 85.3 | 152.1 | 4.6 | NA |
| 16ATW-86-Spot 282 | 217 | 72416 | 3.1 | 19.5 | 1.1 | 0.2 | 2.4 | 0.0 | 2.2 | 0.9 | 152.1 | 3.3 | 158.3 | 3.6 | 253.2 | 24.8 | 152.1 | 3.3 | NA |
| 16ATW-86-Spot 100 | 80 | 10771 | 1.6 | 19.8 | 2.5 | 0.2 | 3.5 | 0.0 | 2.5 | 0.7 | 152.2 | 3.7 | 156.3 | 5.1 | 220.8 | 58.2 | 152.2 | 3.7 | NA |
| 16ATW-86-Spot 64 | 70 | 18417 | 3.1 | 20.0 | 3.1 | 0.2 | 3.9 | 0.0 | 2.3 | 0.6 | 152.3 | 3.5 | 154.8 | 5.6 | 195.3 | 72.6 | 152.3 | 3.5 | NA |
| 16ATW-86-Spot 51 | 82 | 32013 | 2.7 | 19.2 | 2.1 | 0.2 | 3.0 | 0.0 | 2.1 | 0.7 | 152.4 | 3.1 | 161.1 | 4.4 | 292.2 | 49.0 | 152.4 | 3.1 | NA |
| 16ATW-86-Spot 223 | 152 | 30974 | 1.7 | 19.4 | 1.6 | 0.2 | 2.5 | 0.0 | 2.0 | 0.8 | 152.8 | 3.0 | 160.1 | 3.7 | 270.4 | 36.7 | 152.8 | 3.0 | NA |
| 16ATW-86-Spot 98 | 79 | 34314 | 2.1 | 18.7 | 2.0 | 0.2 | 3.5 | 0.0 | 2.8 | 0.8 | 153.2 | 4.3 | 165.5 | 5.3 | 345.4 | 45.4 | 153.2 | 4.3 | NA |
| 16ATW-86-Spot 182 | 133 | 36659 | 2.6 | 19.3 | 1.7 | 0.2 | 2.9 | 0.0 | 2.3 | 0.8 | 153.3 | 3.5 | 160.7 | 4.3 | 272.5 | 39.9 | 153.3 | 3.5 | NA |
| 16ATW-86-Spot 69 | 583 | 244299 | 2.8 | 19.7 | 1.2 | 0.2 | 2.7 | 0.0 | 2.4 | 0.9 | 153.3 | 3.6 | 157.8 | 3.9 | 226.4 | 28.4 | 153.3 | 3.6 | NA |

| | | | | | | | | | | | | | | | | | | | |
|---|---|---|---|---|---|---|---|---|---|---|---|---|---|---|---|---|---|---|---|
| 16ATW-86-Spot 107 | 184 | 37036 | 3.6 | 19.1 | 1.6 | 0.2 | 3.1 | 0.0 | 2.7 | 0.9 | 153.4 | 4.1 | 162.5 | 4.7 | 298.1 | 36.3 | 153.4 | 4.1 | NA |
| 16ATW-86-Spot 73 | 118 | 42406 | 1.8 | 19.4 | 2.0 | 0.2 | 3.0 | 0.0 | 2.3 | 0.8 | 153.4 | 3.4 | 160.3 | 4.5 | 264.4 | 45.7 | 153.4 | 3.4 | NA |
| 16ATW-86-Spot 32 | 129 | 22094 | 2.7 | 20.4 | 2.1 | 0.2 | 2.9 | 0.0 | 1.9 | 0.7 | 153.7 | 3.0 | 153.6 | 4.1 | 153.0 | 49.2 | 153.7 | 3.0 | NA |
| 16ATW-86-Spot 84 | 129 | 13208 | 1.9 | 19.9 | 1.9 | 0.2 | 3.3 | 0.0 | 2.7 | 0.8 | 153.9 | 4.2 | 156.9 | 4.9 | 203.1 | 44.5 | 153.9 | 4.2 | NA |
| 16ATW-86-Spot 265 | 54 | 10461 | 3.0 | 18.8 | 3.4 | 0.2 | 4.8 | 0.0 | 3.5 | 0.7 | 153.9 | 5.3 | 165.3 | 7.4 | 331.7 | 76.7 | 153.9 | 5.3 | NA |
| 16ATW-86-Spot 198 | 78 | 132986 | 2.4 | 18.8 | 2.5 | 0.2 | 3.5 | 0.0 | 2.4 | 0.7 | 154.0 | 3.7 | 165.6 | 5.3 | 335.0 | 56.5 | 154.0 | 3.7 | NA |
| 16ATW-86-Spot 219 | 69 | 6621 | 2.4 | 20.5 | 3.1 | 0.2 | 4.1 | 0.0 | 2.6 | 0.6 | 154.1 | 4.0 | 153.2 | 5.8 | 141.2 | 73.2 | 154.1 | 4.0 | NA |
| 16ATW-86-Spot 72 | 120 | 19095 | 1.6 | 18.9 | 1.8 | 0.2 | 3.0 | 0.0 | 2.4 | 0.8 | 154.3 | 3.7 | 165.3 | 4.6 | 326.9 | 40.5 | 154.3 | 3.7 | NA |
| 16ATW-86-Spot 159 | 188 | 43491 | 2.3 | 19.4 | 1.6 | 0.2 | 2.7 | 0.0 | 2.3 | 0.8 | 154.3 | 3.5 | 161.4 | 4.1 | 268.2 | 35.6 | 154.3 | 3.5 | NA |
| 16ATW-86-Spot 299 | 137 | 16651 | 2.1 | 19.4 | 1.6 | 0.2 | 3.6 | 0.0 | 3.2 | 0.9 | 154.3 | 4.9 | 161.4 | 5.4 | 268.0 | 37.6 | 154.3 | 4.9 | NA |
| 16ATW-86-Spot 165 | 59 | 6130 | 1.8 | 20.0 | 3.5 | 0.2 | 4.3 | 0.0 | 2.5 | 0.6 | 154.3 | 3.8 | 156.6 | 6.3 | 191.9 | 81.9 | 154.3 | 3.8 | NA |
| 16ATW-86-Spot 315 | 118 | 14954 | 2.9 | 19.3 | 1.9 | 0.2 | 3.6 | 0.0 | 3.0 | 0.8 | 154.4 | 4.6 | 161.7 | 5.3 | 272.0 | 43.8 | 154.4 | 4.6 | NA |
| 16ATW-86-Spot 136 | 193 | 73417 | 1.4 | 19.2 | 1.6 | 0.2 | 3.0 | 0.0 | 2.5 | 0.8 | 154.4 | 3.8 | 162.7 | 4.4 | 285.9 | 36.5 | 154.4 | 3.8 | NA |
| 16ATW-86-Spot 130 | 109 | 10779 | 2.5 | 19.7 | 1.8 | 0.2 | 3.0 | 0.0 | 2.4 | 0.8 | 154.4 | 3.7 | 158.9 | 4.5 | 227.8 | 42.2 | 154.4 | 3.7 | NA |
| 16ATW-86-Spot 300 | 328 | 48585 | 1.7 | 19.4 | 1.3 | 0.2 | 3.2 | 0.0 | 2.9 | 0.9 | 154.5 | 4.5 | 161.2 | 4.8 | 263.1 | 29.4 | 154.5 | 4.5 | NA |
| 16ATW-86-Spot 38 | 75 | 10985 | 1.8 | 21.2 | 2.9 | 0.2 | 4.2 | 0.0 | 3.1 | 0.7 | 154.6 | 4.7 | 148.5 | 5.8 | 53.3 | 68.8 | 154.6 | 4.7 | NA |
| 16ATW-86-Spot 306 | 33 | 3288 | 3.3 | 19.0 | 4.1 | 0.2 | 4.9 | 0.0 | 2.6 | 0.5 | 154.6 | 4.0 | 164.7 | 7.4 | 313.6 | 94.2 | 154.6 | 4.0 | NA |
| 16ATW-86-Spot 30 | 74 | 7544 | 2.2 | 18.2 | 3.4 | 0.2 | 4.3 | 0.0 | 2.6 | 0.6 | 154.8 | 4.0 | 171.4 | 6.8 | 408.0 | 76.1 | 154.8 | 4.0 | NA |
| 16ATW-86-Spot 201 | 40 | 74124 | 3.7 | 18.5 | 2.9 | 0.2 | 3.9 | 0.0 | 2.6 | 0.7 | 154.8 | 3.9 | 168.8 | 6.1 | 370.8 | 66.4 | 154.8 | 3.9 | NA |
| 16ATW-86-Spot 303 | 136 | 41259 | 2.6 | 20.5 | 2.1 | 0.2 | 3.1 | 0.0 | 2.3 | 0.7 | 154.9 | 3.5 | 153.6 | 4.4 | 134.3 | 48.7 | 154.9 | 3.5 | NA |
| 16ATW-86-Spot 233 | 223 | 56382 | 1.8 | 19.6 | 1.4 | 0.2 | 2.7 | 0.0 | 2.3 | 0.8 | 155.0 | 3.5 | 160.5 | 4.0 | 243.3 | 33.0 | 155.0 | 3.5 | NA |
| 16ATW-86-Spot 248 | 79 | 16269 | 2.7 | 19.2 | 2.7 | 0.2 | 3.6 | 0.0 | 2.3 | 0.6 | 155.0 | 3.5 | 163.6 | 5.4 | 290.6 | 62.6 | 155.0 | 3.5 | NA |
| 16ATW-86-Spot 295 | 297 | 57301 | 5.1 | 19.2 | 1.4 | 0.2 | 3.1 | 0.0 | 2.7 | 0.9 | 155.0 | 4.2 | 163.4 | 4.6 | 287.5 | 32.1 | 155.0 | 4.2 | NA |
| 16ATW-86-Spot 36 | 48 | 18913 | 2.9 | 19.4 | 2.5 | 0.2 | 3.7 | 0.0 | 2.7 | 0.7 | 155.1 | 4.1 | 161.7 | 5.5 | 260.9 | 56.8 | 155.1 | 4.1 | NA |
| 16ATW-86-Spot 294 | 69 | 93476 | 1.8 | 19.2 | 2.6 | 0.2 | 3.8 | 0.0 | 2.7 | 0.7 | 155.2 | 4.1 | 163.4 | 5.7 | 285.2 | 60.2 | 155.2 | 4.1 | NA |

| | | | | | | | | | | | | | | | | | | | |
|---|---|---|---|---|---|---|---|---|---|---|---|---|---|---|---|---|---|---|---|
| 16ATW-86-Spot 183 | 130 | 15446 | 2.2 | 20.1 | 1.6 | 0.2 | 2.8 | 0.0 | 2.3 | 0.8 | 155.2 | 3.5 | 156.8 | 4.1 | 182.4 | 37.3 | 155.2 | 3.5 | NA |
| 16ATW-86-Spot 8 | 67 | 38986 | 2.8 | 19.2 | 2.4 | 0.2 | 3.2 | 0.0 | 2.2 | 0.7 | 155.2 | 3.4 | 163.6 | 4.9 | 286.9 | 54.4 | 155.2 | 3.4 | NA |
| 16ATW-86-Spot 239 | 41 | 3474 | 2.7 | 21.5 | 4.2 | 0.2 | 4.9 | 0.0 | 2.4 | 0.5 | 155.3 | 3.7 | 147.6 | 6.7 | 27.0 | 101.5 | 155.3 | 3.7 | NA |
| 16ATW-86-Spot 124 | 89 | 178676 | 2.6 | 19.3 | 2.5 | 0.2 | 3.5 | 0.0 | 2.5 | 0.7 | 155.3 | 3.8 | 163.2 | 5.3 | 279.4 | 57.2 | 155.3 | 3.8 | NA |
| 16ATW-86-Spot 57 | 129 | 35974 | 2.2 | 19.1 | 1.5 | 0.2 | 3.5 | 0.0 | 3.1 | 0.9 | 155.4 | 4.8 | 164.6 | 5.3 | 300.5 | 34.5 | 155.4 | 4.8 | NA |
| 16ATW-86-Spot 117 | 129 | 54711 | 2.1 | 19.8 | 2.2 | 0.2 | 3.1 | 0.0 | 2.2 | 0.7 | 155.5 | 3.3 | 159.6 | 4.5 | 220.9 | 50.5 | 155.5 | 3.3 | NA |
| 16ATW-86-Spot 3 | 230 | 29485 | 1.5 | 19.5 | 1.5 | 0.2 | 2.7 | 0.0 | 2.3 | 0.8 | 155.6 | 3.5 | 161.4 | 4.0 | 249.2 | 34.6 | 155.6 | 3.5 | NA |
| 16ATW-86-Spot 119 | 109 | 55439 | 4.3 | 19.0 | 1.7 | 0.2 | 3.0 | 0.0 | 2.5 | 0.8 | 155.6 | 3.8 | 165.4 | 4.6 | 309.5 | 38.5 | 155.6 | 3.8 | NA |
| 16ATW-86-Spot 56 | 247 | 109941 | 3.6 | 19.4 | 1.6 | 0.2 | 3.6 | 0.0 | 3.2 | 0.9 | 155.7 | 5.0 | 162.9 | 5.5 | 270.6 | 37.6 | 155.7 | 5.0 | NA |
| 16ATW-86-Spot 213 | 31 | 18784 | 3.3 | 19.2 | 3.6 | 0.2 | 4.3 | 0.0 | 2.2 | 0.5 | 155.7 | 3.4 | 164.6 | 6.5 | 294.9 | 82.9 | 155.7 | 3.4 | NA |
| 16ATW-86-Spot 47 | 49 | 7484 | 2.3 | 20.1 | 3.4 | 0.2 | 4.4 | 0.0 | 2.8 | 0.6 | 155.8 | 4.2 | 157.8 | 6.4 | 188.4 | 78.5 | 155.8 | 4.2 | NA |
| 16ATW-86-Spot 154 | 323 | 103260 | 2.5 | 17.9 | 2.4 | 0.2 | 3.2 | 0.0 | 2.1 | 0.7 | 156.0 | 3.3 | 175.3 | 5.1 | 445.7 | 52.6 | 156.0 | 3.3 | NA |
| 16ATW-86-Spot 48 | 122 | 13621 | 1.5 | 19.8 | 2.2 | 0.2 | 3.2 | 0.0 | 2.3 | 0.7 | 156.0 | 3.6 | 159.5 | 4.7 | 212.7 | 50.5 | 156.0 | 3.6 | NA |
| 16ATW-86-Spot 110 | 79 | 75341 | 3.9 | 19.7 | 2.1 | 0.2 | 3.0 | 0.0 | 2.1 | 0.7 | 156.0 | 3.2 | 160.9 | 4.4 | 234.0 | 48.9 | 156.0 | 3.2 | NA |
| 16ATW-86-Spot 277 | 71 | 12183 | 2.5 | 19.6 | 2.5 | 0.2 | 3.5 | 0.0 | 2.5 | 0.7 | 156.2 | 3.9 | 161.8 | 5.3 | 245.8 | 57.1 | 156.2 | 3.9 | NA |
| 16ATW-86-Spot 61 | 37 | 4993 | 3.0 | 20.3 | 4.1 | 0.2 | 5.1 | 0.0 | 3.1 | 0.6 | 156.3 | 4.8 | 156.7 | 7.5 | 164.1 | 95.3 | 156.3 | 4.8 | NA |
| 16ATW-86-Spot 138 | 120 | 15434 | 1.5 | 19.3 | 1.8 | 0.2 | 3.5 | 0.0 | 3.1 | 0.9 | 156.3 | 4.8 | 163.9 | 5.4 | 275.7 | 40.3 | 156.3 | 4.8 | NA |
| 16ATW-86-Spot 174 | 83 | 14986 | 2.1 | 19.7 | 2.9 | 0.2 | 3.6 | 0.0 | 2.2 | 0.6 | 156.4 | 3.4 | 160.8 | 5.4 | 226.8 | 67.0 | 156.4 | 3.4 | NA |
| 16ATW-86-Spot 132 | 91 | 141237 | 1.7 | 19.4 | 2.2 | 0.2 | 3.6 | 0.0 | 2.9 | 0.8 | 156.4 | 4.4 | 163.6 | 5.5 | 270.3 | 51.1 | 156.4 | 4.4 | NA |
| 16ATW-86-Spot 74 | 75 | 27403 | 2.1 | 19.0 | 2.3 | 0.2 | 3.4 | 0.0 | 2.5 | 0.7 | 156.5 | 3.9 | 166.9 | 5.2 | 318.6 | 52.4 | 156.5 | 3.9 | NA |
| 16ATW-86-Spot 309 | 72 | 11573 | 2.1 | 19.4 | 2.4 | 0.2 | 3.9 | 0.0 | 3.0 | 0.8 | 156.5 | 4.7 | 163.6 | 5.8 | 268.2 | 55.5 | 156.5 | 4.7 | NA |
| 16ATW-86-Spot 150 | 60 | 67358 | 2.0 | 18.9 | 2.5 | 0.2 | 3.6 | 0.0 | 2.6 | 0.7 | 156.8 | 4.0 | 167.4 | 5.6 | 321.5 | 57.5 | 156.8 | 4.0 | NA |
| 16ATW-86-Spot 37 | 58 | 209308 | 3.0 | 19.0 | 3.2 | 0.2 | 4.1 | 0.0 | 2.5 | 0.6 | 156.8 | 3.9 | 167.0 | 6.3 | 314.6 | 73.0 | 156.8 | 3.9 | NA |
| 16ATW-86-Spot 6 | 160 | 60173 | 4.8 | 18.8 | 1.9 | 0.2 | 3.0 | 0.0 | 2.4 | 0.8 | 156.9 | 3.7 | 168.3 | 4.7 | 332.9 | 43.9 | 156.9 | 3.7 | NA |
| 16ATW-86-Spot 118 | 190 | 47471 | 1.5 | 19.2 | 1.5 | 0.2 | 2.9 | 0.0 | 2.5 | 0.9 | 157.0 | 4.0 | 165.4 | 4.5 | 289.3 | 33.6 | 157.0 | 4.0 | NA |
| 16ATW-86-Spot 95 | 100 | 42445 | 1.8 | 19.8 | 2.1 | 0.2 | 3.3 | 0.0 | 2.6 | 0.8 | 157.1 | 4.1 | 161.2 | 5.0 | 223.3 | 48.1 | 157.1 | 4.1 | NA |

| | | | | | | | | | | | | | | | | | | | |
|---|---|---|---|---|---|---|---|---|---|---|---|---|---|---|---|---|---|---|---|
| 16ATW-86-Spot 112 | 84 | 52316 | 3.0 | 19.5 | 2.0 | 0.2 | 3.4 | 0.0 | 2.8 | 0.8 | 157.1 | 4.3 | 163.3 | 5.2 | 255.1 | 45.9 | 157.1 | 4.3 | NA |
| 16ATW-86-Spot 40 | 53 | 18354 | 2.0 | 19.4 | 2.3 | 0.2 | 3.4 | 0.0 | 2.5 | 0.7 | 157.1 | 3.9 | 163.8 | 5.1 | 261.5 | 52.1 | 157.1 | 3.9 | NA |
| 16ATW-86-Spot 97 | 75 | 11528 | 2.4 | 19.7 | 2.3 | 0.2 | 3.4 | 0.0 | 2.4 | 0.7 | 157.2 | 3.8 | 161.6 | 5.1 | 228.5 | 54.0 | 157.2 | 3.8 | NA |
| 16ATW-86-Spot 259 | 117 | 7270 | 2.2 | 19.4 | 2.2 | 0.2 | 3.7 | 0.0 | 3.0 | 0.8 | 157.2 | 4.6 | 164.0 | 5.7 | 263.4 | 51.6 | 157.2 | 4.6 | NA |
| 16ATW-86-Spot 58 | 86 | 65267 | 3.7 | 19.7 | 2.4 | 0.2 | 3.9 | 0.0 | 3.0 | 0.8 | 157.3 | 4.7 | 162.1 | 5.8 | 233.9 | 56.5 | 157.3 | 4.7 | NA |
| 16ATW-86-Spot 10 | 64 | 10667 | 2.2 | 20.0 | 2.2 | 0.2 | 3.2 | 0.0 | 2.3 | 0.7 | 157.5 | 3.5 | 159.5 | 4.7 | 191.5 | 50.7 | 157.5 | 3.5 | NA |
| 16ATW-86-Spot 148 | 115 | 8358 | 2.8 | 20.0 | 2.1 | 0.2 | 3.3 | 0.0 | 2.6 | 0.8 | 157.5 | 4.1 | 159.5 | 4.9 | 191.0 | 47.7 | 157.5 | 4.1 | NA |
| 16ATW-86-Spot 46 | 99 | 41661 | 4.5 | 19.5 | 1.9 | 0.2 | 2.8 | 0.0 | 2.1 | 0.7 | 157.6 | 3.3 | 163.6 | 4.2 | 251.4 | 42.9 | 157.6 | 3.3 | NA |
| 16ATW-86-Spot 215 | 69 | 55257 | 3.2 | 19.3 | 2.4 | 0.2 | 3.9 | 0.0 | 3.1 | 0.8 | 157.7 | 4.8 | 165.4 | 5.9 | 279.4 | 54.0 | 157.7 | 4.8 | NA |
| 16ATW-86-Spot 33 | 247 | 27868 | 2.9 | 20.1 | 1.6 | 0.2 | 2.3 | 0.0 | 1.6 | 0.7 | 157.8 | 2.5 | 159.7 | 3.4 | 188.4 | 37.7 | 157.8 | 2.5 | NA |
| 16ATW-86-Spot 54 | 280 | 38576 | 1.5 | 19.4 | 1.5 | 0.2 | 3.0 | 0.0 | 2.6 | 0.9 | 157.8 | 4.0 | 165.0 | 4.6 | 269.5 | 34.4 | 157.8 | 4.0 | NA |
| 16ATW-86-Spot 314 | 64 | 12596 | 2.2 | 19.4 | 2.6 | 0.2 | 4.1 | 0.0 | 3.1 | 0.8 | 158.0 | 4.9 | 165.0 | 6.2 | 266.7 | 60.3 | 158.0 | 4.9 | NA |
| 16ATW-86-Spot 111 | 31 | 82756 | 5.2 | 19.7 | 2.7 | 0.2 | 4.0 | 0.0 | 2.9 | 0.7 | 158.0 | 4.6 | 162.6 | 6.0 | 230.9 | 61.4 | 158.0 | 4.6 | NA |
| 16ATW-86-Spot 190 | 87 | 60451 | 2.5 | 18.7 | 2.4 | 0.2 | 3.1 | 0.0 | 2.0 | 0.6 | 158.2 | 3.1 | 170.9 | 4.9 | 351.8 | 55.0 | 158.2 | 3.1 | NA |
| 16ATW-86-Spot 152 | 164 | 44090 | 1.4 | 19.6 | 2.0 | 0.2 | 3.4 | 0.0 | 2.7 | 0.8 | 158.3 | 4.2 | 163.5 | 5.1 | 241.5 | 46.2 | 158.3 | 4.2 | NA |
| 16ATW-86-Spot 274 | 710 | 87264 | 1.9 | 19.7 | 1.2 | 0.2 | 2.8 | 0.0 | 2.5 | 0.9 | 158.4 | 4.0 | 162.6 | 4.2 | 225.1 | 27.2 | 158.4 | 4.0 | NA |
| 16ATW-86-Spot 280 | 43 | 4996 | 3.5 | 20.3 | 3.4 | 0.2 | 4.1 | 0.0 | 2.3 | 0.6 | 158.4 | 3.5 | 158.6 | 6.0 | 162.6 | 79.3 | 158.4 | 3.5 | NA |
| 16ATW-86-Spot 94 | 94 | 32336 | 3.5 | 18.8 | 2.0 | 0.2 | 3.2 | 0.0 | 2.5 | 0.8 | 158.5 | 3.8 | 170.1 | 5.0 | 335.3 | 45.5 | 158.5 | 3.8 | NA |
| 16ATW-86-Spot 102 | 128 | 11014 | 1.4 | 19.8 | 1.9 | 0.2 | 3.8 | 0.0 | 3.3 | 0.9 | 158.6 | 5.1 | 162.6 | 5.7 | 222.1 | 43.8 | 158.6 | 5.1 | NA |
| 16ATW-86-Spot 78 | 46 | 662259 | 3.0 | 18.7 | 3.2 | 0.2 | 4.3 | 0.0 | 2.9 | 0.7 | 159.2 | 4.5 | 171.6 | 6.8 | 347.9 | 73.5 | 159.2 | 4.5 | NA |
| 16ATW-86-Spot 226 | 108 | 24506 | 2.7 | 18.7 | 2.1 | 0.2 | 3.7 | 0.0 | 3.1 | 0.8 | 159.3 | 4.9 | 172.0 | 5.9 | 351.6 | 46.9 | 159.3 | 4.9 | NA |
| 16ATW-86-Spot 125 | 71 | 26383 | 2.2 | 19.1 | 2.2 | 0.2 | 3.2 | 0.0 | 2.3 | 0.7 | 159.4 | 3.6 | 168.3 | 5.0 | 296.0 | 51.3 | 159.4 | 3.6 | NA |
| 16ATW-86-Spot 71 | 66 | 35886 | 2.7 | 18.9 | 2.0 | 0.2 | 3.1 | 0.0 | 2.3 | 0.8 | 159.4 | 3.7 | 169.9 | 4.9 | 319.6 | 46.6 | 159.4 | 3.7 | NA |
| 16ATW-86-Spot 87 | 114 | 109856 | 2.2 | 18.8 | 1.6 | 0.2 | 2.9 | 0.0 | 2.4 | 0.8 | 159.4 | 3.8 | 170.9 | 4.6 | 332.9 | 37.3 | 159.4 | 3.8 | NA |
| 16ATW-86-Spot 142 | 182 | 28519 | 2.8 | 19.3 | 1.4 | 0.2 | 3.2 | 0.0 | 2.8 | 0.9 | 159.7 | 4.5 | 167.5 | 4.9 | 279.6 | 32.3 | 159.7 | 4.5 | NA |
| 16ATW-86-Spot 39 | 45 | 23391 | 3.1 | 19.8 | 3.2 | 0.2 | 4.1 | 0.0 | 2.6 | 0.6 | 159.8 | 4.1 | 163.3 | 6.2 | 215.0 | 73.7 | 159.8 | 4.1 | NA |
| 16ATW-86-Spot 25 | 75 | 8532 | 2.2 | 19.9 | 2.9 | 0.2 | 3.8 | 0.0 | 2.4 | 0.6 | 159.9 | 3.8 | 162.8 | 5.7 | 206.1 | 68.1 | 159.9 | 3.8 | NA |

| | | | | | | | | | | | | | | | | | | | |
|---|---|---|---|---|---|---|---|---|---|---|---|---|---|---|---|---|---|---|---|
| 16ATW-86-Spot 105 | 275 | 274852 | 2.9 | 19.1 | 1.4 | 0.2 | 3.1 | 0.0 | 2.7 | 0.9 | 159.9 | 4.3 | 169.2 | 4.8 | 302.3 | 31.1 | 159.9 | 4.3 | NA |
| 16ATW-86-Spot 92 | 32 | 5680 | 3.0 | 20.9 | 3.5 | 0.2 | 4.3 | 0.0 | 2.6 | 0.6 | 160.0 | 4.0 | 155.5 | 6.2 | 89.0 | 82.8 | 160.0 | 4.0 | NA |
| 16ATW-86-Spot 121 | 176 | 29342 | 2.7 | 19.6 | 1.6 | 0.2 | 2.6 | 0.0 | 2.1 | 0.8 | 160.0 | 3.3 | 165.0 | 4.0 | 238.7 | 36.0 | 160.0 | 3.3 | NA |
| 16ATW-86-Spot 175 | 232 | 27285 | 1.8 | 19.4 | 1.5 | 0.2 | 2.6 | 0.0 | 2.1 | 0.8 | 160.0 | 3.3 | 166.4 | 4.0 | 259.5 | 34.5 | 160.0 | 3.3 | NA |
| 16ATW-86-Spot 243 | 123 | 267672 | 3.0 | 19.7 | 1.8 | 0.2 | 3.2 | 0.0 | 2.6 | 0.8 | 160.1 | 4.2 | 164.4 | 4.8 | 228.7 | 41.0 | 160.1 | 4.2 | NA |
| 16ATW-86-Spot 31 | 265 | 19035 | 5.0 | 19.8 | 1.4 | 0.2 | 2.5 | 0.0 | 2.1 | 0.8 | 160.2 | 3.4 | 164.3 | 3.9 | 224.0 | 32.4 | 160.2 | 3.4 | NA |
| 16ATW-86-Spot 42 | 90 | 257633 | 2.6 | 19.1 | 2.3 | 0.2 | 3.6 | 0.0 | 2.8 | 0.8 | 160.3 | 4.4 | 169.8 | 5.7 | 304.9 | 53.0 | 160.3 | 4.4 | NA |
| 16ATW-86-Spot 164 | 85 | 40837 | 2.9 | 19.6 | 1.7 | 0.2 | 3.1 | 0.0 | 2.5 | 0.8 | 160.5 | 4.0 | 165.3 | 4.7 | 236.4 | 39.4 | 160.5 | 4.0 | NA |
| 16ATW-86-Spot 203 | 136 | 18701 | 3.0 | 19.7 | 2.2 | 0.2 | 3.5 | 0.0 | 2.7 | 0.8 | 160.7 | 4.2 | 165.2 | 5.3 | 231.0 | 51.3 | 160.7 | 4.2 | NA |
| 16ATW-86-Spot 9 | 42 | 4547 | 3.1 | 21.6 | 3.6 | 0.2 | 4.2 | 0.0 | 2.3 | 0.5 | 160.8 | 3.6 | 152.1 | 6.0 | 18.3 | 85.9 | 160.8 | 3.6 | NA |
| 16ATW-86-Spot 128 | 94 | 72995 | 3.0 | 19.2 | 2.0 | 0.2 | 3.1 | 0.0 | 2.3 | 0.8 | 160.9 | 3.7 | 168.9 | 4.8 | 283.8 | 45.5 | 160.9 | 3.7 | NA |
| 16ATW-86-Spot 218 | 331 | 175358 | 1.5 | 19.4 | 1.1 | 0.2 | 2.2 | 0.0 | 1.8 | 0.9 | 160.9 | 2.9 | 167.7 | 3.4 | 265.7 | 26.2 | 160.9 | 2.9 | NA |
| 16ATW-86-Spot 79 | 191 | 68700 | 1.5 | 19.7 | 1.4 | 0.2 | 2.4 | 0.0 | 1.9 | 0.8 | 161.0 | 3.1 | 165.1 | 3.6 | 225.3 | 32.5 | 161.0 | 3.1 | NA |
| 16ATW-86-Spot 253 | 112 | 80083 | 2.3 | 18.0 | 2.1 | 0.2 | 3.3 | 0.0 | 2.6 | 0.8 | 161.1 | 4.1 | 180.1 | 5.5 | 437.9 | 46.6 | 161.1 | 4.1 | NA |
| 16ATW-86-Spot 185 | 319 | 32689 | 7.2 | 19.6 | 1.2 | 0.2 | 2.9 | 0.0 | 2.6 | 0.9 | 161.2 | 4.1 | 166.1 | 4.4 | 237.8 | 28.0 | 161.2 | 4.1 | NA |
| 16ATW-86-Spot 19 | 704 | 130102 | 1.9 | 20.0 | 1.1 | 0.2 | 2.1 | 0.0 | 1.8 | 0.9 | 161.4 | 2.9 | 163.7 | 3.2 | 198.5 | 24.7 | 161.4 | 2.9 | NA |
| 16ATW-86-Spot 241 | 168 | 19447 | 2.8 | 19.9 | 1.5 | 0.2 | 3.2 | 0.0 | 2.8 | 0.9 | 161.6 | 4.5 | 164.8 | 4.8 | 211.5 | 34.6 | 161.6 | 4.5 | NA |
| 16ATW-86-Spot 14 | 68 | 15413 | 3.0 | 20.1 | 2.5 | 0.2 | 3.1 | 0.0 | 1.8 | 0.6 | 161.6 | 2.9 | 163.2 | 4.6 | 186.7 | 57.4 | 161.6 | 2.9 | NA |
| 16ATW-86-Spot 222 | 109 | 23755 | 3.0 | 19.2 | 1.9 | 0.2 | 3.1 | 0.0 | 2.5 | 0.8 | 161.6 | 4.0 | 169.6 | 4.9 | 283.7 | 44.0 | 161.6 | 4.0 | NA |
| 16ATW-86-Spot 249 | 133 | 195068 | 2.9 | 19.4 | 2.3 | 0.2 | 3.6 | 0.0 | 2.8 | 0.8 | 161.7 | 4.5 | 168.6 | 5.6 | 268.2 | 51.9 | 161.7 | 4.5 | NA |
| 16ATW-86-Spot 311 | 115 | 14232 | 6.1 | 19.9 | 2.3 | 0.2 | 3.5 | 0.0 | 2.6 | 0.7 | 161.7 | 4.1 | 164.3 | 5.3 | 203.2 | 54.3 | 161.7 | 4.1 | NA |
| 16ATW-86-Spot 34 | 93 | 32817 | 2.8 | 19.7 | 2.1 | 0.2 | 2.8 | 0.0 | 1.9 | 0.7 | 161.8 | 3.1 | 165.8 | 4.3 | 224.5 | 47.7 | 161.8 | 3.1 | NA |
| 16ATW-86-Spot 75 | 109 | 49248 | 2.7 | 19.5 | 2.3 | 0.2 | 3.4 | 0.0 | 2.5 | 0.7 | 162.0 | 4.0 | 168.2 | 5.3 | 257.4 | 51.9 | 162.0 | 4.0 | NA |
| 16ATW-86-Spot 2 | 26 | 2849 | 2.8 | 17.9 | 4.7 | 0.2 | 5.6 | 0.0 | 3.0 | 0.5 | 162.1 | 4.8 | 181.4 | 9.3 | 442.6 | 104.3 | 162.1 | 4.8 | NA |
| 16ATW-86-Spot 106 | 54 | 4540 | 2.2 | 20.1 | 2.8 | 0.2 | 4.3 | 0.0 | 3.3 | 0.8 | 162.1 | 5.3 | 163.5 | 6.5 | 185.2 | 65.2 | 162.1 | 5.3 | NA |
| 16ATW-86-Spot 160 | 334 | 228845 | 1.7 | 20.1 | 1.3 | 0.2 | 3.5 | 0.0 | 3.2 | 0.9 | 162.1 | 5.2 | 163.4 | 5.2 | 183.5 | 29.8 | 162.1 | 5.2 | NA |

| | | | | | | | | | | | | | | | | | | | |
|---|---|---|---|---|---|---|---|---|---|---|---|---|---|---|---|---|---|---|---|
| 16ATW-86-Spot 267 | 393 | 35971 | 1.3 | 19.7 | 1.2 | 0.2 | 2.4 | 0.0 | 2.1 | 0.9 | 162.1 | 3.3 | 166.5 | 3.7 | 230.3 | 28.6 | 162.1 | 3.3 | NA |
| 16ATW-86-Spot 15 | 815 | 129313 | 1.3 | 19.5 | 1.0 | 0.2 | 2.3 | 0.0 | 2.1 | 0.9 | 162.4 | 3.4 | 168.6 | 3.6 | 257.2 | 23.2 | 162.4 | 3.4 | NA |
| 16ATW-86-Spot 91 | 134 | 41010 | 2.4 | 20.1 | 1.6 | 0.2 | 2.6 | 0.0 | 2.0 | 0.8 | 162.6 | 3.3 | 164.0 | 3.9 | 185.3 | 37.8 | 162.6 | 3.3 | NA |
| 16ATW-86-Spot 210 | 69 | 8274 | 2.8 | 20.0 | 2.9 | 0.2 | 3.7 | 0.0 | 2.4 | 0.6 | 162.9 | 3.9 | 165.0 | 5.7 | 196.5 | 66.4 | 162.9 | 3.9 | NA |
| 16ATW-86-Spot 45 | 100 | 20981 | 1.5 | 20.1 | 2.5 | 0.2 | 3.5 | 0.0 | 2.4 | 0.7 | 163.0 | 3.9 | 164.5 | 5.3 | 186.9 | 57.7 | 163.0 | 3.9 | NA |
| 16ATW-86-Spot 65 | 354 | 57611 | 3.9 | 19.9 | 1.4 | 0.2 | 2.0 | 0.0 | 1.4 | 0.7 | 163.1 | 2.3 | 165.9 | 3.1 | 206.4 | 32.6 | 163.1 | 2.3 | NA |
| 16ATW-86-Spot 77 | 316 | 37931 | 2.2 | 19.5 | 1.2 | 0.2 | 2.4 | 0.0 | 2.1 | 0.9 | 163.2 | 3.4 | 169.2 | 3.8 | 255.5 | 28.6 | 163.2 | 3.4 | NA |
| 16ATW-86-Spot 200 | 768 | 63635 | 1.4 | 18.5 | 1.7 | 0.2 | 2.9 | 0.0 | 2.4 | 0.8 | 163.5 | 3.8 | 177.5 | 4.8 | 370.3 | 38.8 | 163.5 | 3.8 | NA |
| 16ATW-86-Spot 17 | 78 | 90643 | 2.4 | 19.4 | 1.4 | 0.2 | 2.8 | 0.0 | 2.4 | 0.9 | 163.8 | 3.9 | 170.2 | 4.4 | 260.7 | 32.9 | 163.8 | 3.9 | NA |
| 16ATW-86-Spot 11 | 82 | 11431 | 2.4 | 19.9 | 2.4 | 0.2 | 3.3 | 0.0 | 2.4 | 0.7 | 163.8 | 3.8 | 166.9 | 5.1 | 211.5 | 54.5 | 163.8 | 3.8 | NA |
| 16ATW-86-Spot 204 | 146 | 95903 | 1.5 | 19.5 | 1.7 | 0.2 | 3.4 | 0.0 | 2.9 | 0.9 | 163.9 | 4.6 | 170.0 | 5.3 | 257.4 | 40.1 | 163.9 | 4.6 | NA |
| 16ATW-86-Spot 144 | 180 | 17985 | 1.9 | 19.3 | 1.7 | 0.2 | 3.3 | 0.0 | 2.9 | 0.9 | 164.2 | 4.6 | 171.7 | 5.2 | 277.8 | 37.8 | 164.2 | 4.6 | NA |
| 16ATW-86-Spot 285 | 67 | 10926 | 2.4 | 19.0 | 2.3 | 0.2 | 3.5 | 0.0 | 2.7 | 0.8 | 164.6 | 4.4 | 175.0 | 5.7 | 318.2 | 51.4 | 164.6 | 4.4 | NA |
| 16ATW-86-Spot 60 | 133 | 107925 | 2.3 | 19.6 | 1.8 | 0.2 | 2.7 | 0.0 | 2.0 | 0.7 | 164.9 | 3.2 | 169.8 | 4.2 | 239.1 | 41.5 | 164.9 | 3.2 | NA |
| 16ATW-86-Spot 208 | 238 | 54253 | 2.6 | 19.2 | 1.3 | 0.2 | 2.6 | 0.0 | 2.2 | 0.9 | 165.2 | 3.7 | 173.3 | 4.1 | 286.7 | 29.5 | 165.2 | 3.7 | NA |
| 16ATW-86-Spot 27 | 89 | 1110710 | 1.9 | 18.9 | 2.1 | 0.2 | 3.1 | 0.0 | 2.3 | 0.7 | 165.7 | 3.7 | 176.5 | 5.0 | 325.2 | 46.7 | 165.7 | 3.7 | NA |
| 16ATW-86-Spot 153 | 92 | 410664 | 2.5 | 18.9 | 1.4 | 0.2 | 3.2 | 0.0 | 2.8 | 0.9 | 166.1 | 4.6 | 176.6 | 5.1 | 320.4 | 32.1 | 166.1 | 4.6 | NA |
| 16ATW-86-Spot 18 | 204 | 56010 | 1.6 | 20.0 | 1.6 | 0.2 | 3.2 | 0.0 | 2.8 | 0.9 | 166.4 | 4.6 | 168.2 | 5.0 | 194.6 | 37.5 | 166.4 | 4.6 | NA |
| 16ATW-86-Spot 50 | 225 | 101112 | 3.7 | 19.4 | 1.8 | 0.2 | 3.1 | 0.0 | 2.5 | 0.8 | 166.6 | 4.1 | 172.9 | 4.9 | 261.5 | 41.9 | 166.6 | 4.1 | NA |
| 16ATW-86-Spot 23 | 96 | 145083 | 3.0 | 18.4 | 1.6 | 0.2 | 2.8 | 0.0 | 2.3 | 0.8 | 167.7 | 3.9 | 182.9 | 4.7 | 385.6 | 35.4 | 167.7 | 3.9 | NA |
| 16ATW-86-Spot 191 | 285 | 31355 | 1.5 | 19.3 | 1.2 | 0.2 | 2.8 | 0.0 | 2.6 | 0.9 | 167.8 | 4.2 | 175.5 | 4.6 | 281.7 | 28.1 | 167.8 | 4.2 | NA |
| 16ATW-86-Spot 221 | 52 | 5998 | 3.7 | 19.3 | 3.2 | 0.2 | 4.4 | 0.0 | 2.9 | 0.7 | 168.1 | 4.9 | 175.8 | 7.0 | 282.0 | 74.1 | 168.1 | 4.9 | NA |
| 16ATW-86-Spot 271 | 220 | 28021 | 2.5 | 19.7 | 1.3 | 0.2 | 2.9 | 0.0 | 2.6 | 0.9 | 169.6 | 4.4 | 173.7 | 4.7 | 230.7 | 30.8 | 169.6 | 4.4 | NA |
| 16ATW-86-Spot 13 | 273 | 290215 | 2.0 | 19.3 | 1.5 | 0.2 | 3.4 | 0.0 | 3.1 | 0.9 | 169.6 | 5.1 | 176.8 | 5.5 | 274.5 | 33.9 | 169.6 | 5.1 | NA |
| 16ATW-86-Spot 53 | 125 | 12338 | 1.7 | 19.8 | 2.0 | 0.2 | 2.9 | 0.0 | 2.1 | 0.7 | 170.1 | 3.5 | 173.2 | 4.5 | 217.0 | 45.7 | 170.1 | 3.5 | NA |
| 16ATW-86-Spot 189 | 124 | 152889 | 3.3 | 19.6 | 2.1 | 0.2 | 3.1 | 0.0 | 2.2 | 0.7 | 170.6 | 3.8 | 175.0 | 4.9 | 236.8 | 48.5 | 170.6 | 3.8 | NA |
| 16ATW-86-Spot 141 | 101 | 87125 | 2.1 | 19.9 | 1.9 | 0.2 | 2.8 | 0.0 | 2.1 | 0.7 | 171.7 | 3.5 | 173.8 | 4.6 | 202.9 | 44.9 | 171.7 | 3.5 | NA |

| | | | | | | | | | | | | | | | | | | | |
|---|---|---|---|---|---|---|---|---|---|---|---|---|---|---|---|---|---|---|---|
| 16ATW-86-Spot 247 | 119 | 92216 | 2.0 | 18.8 | 1.8 | 0.2 | 2.5 | 0.0 | 1.7 | 0.7 | 171.8 | 2.9 | 183.8 | 4.2 | 341.7 | 40.6 | 171.8 | 2.9 | NA |
| 16ATW-86-Spot 238 | 283 | 107525 | 1.9 | 19.7 | 1.4 | 0.2 | 2.9 | 0.0 | 2.6 | 0.9 | 172.3 | 4.4 | 176.2 | 4.7 | 229.1 | 32.1 | 172.3 | 4.4 | NA |
| 16ATW-86-Spot 101 | 134 | 38821 | 2.9 | 19.5 | 1.8 | 0.2 | 3.0 | 0.0 | 2.4 | 0.8 | 172.7 | 4.1 | 178.3 | 5.0 | 253.6 | 41.6 | 172.7 | 4.1 | NA |
| 16ATW-86-Spot 231 | 88 | 11037 | 3.4 | 19.3 | 3.3 | 0.2 | 4.4 | 0.0 | 2.9 | 0.7 | 173.0 | 5.0 | 179.8 | 7.2 | 271.4 | 74.8 | 173.0 | 5.0 | NA |
| 16ATW-86-Spot 263 | 82 | 99442 | 3.0 | 18.8 | 2.3 | 0.2 | 3.8 | 0.0 | 3.0 | 0.8 | 173.2 | 5.1 | 185.2 | 6.4 | 341.7 | 53.1 | 173.2 | 5.1 | NA |
| 16ATW-86-Spot 250 | 140 | 145442 | 4.9 | 19.3 | 1.8 | 0.2 | 3.1 | 0.0 | 2.5 | 0.8 | 173.5 | 4.3 | 180.7 | 5.1 | 277.4 | 40.5 | 173.5 | 4.3 | NA |
| 16ATW-86-Spot 286 | 216 | 442423 | 2.2 | 19.3 | 1.3 | 0.2 | 3.1 | 0.0 | 2.8 | 0.9 | 176.8 | 4.9 | 184.2 | 5.2 | 280.8 | 30.7 | 176.8 | 4.9 | NA |
| 16ATW-86-Spot 49 | 58 | 71788 | 1.1 | 18.7 | 2.9 | 0.2 | 3.6 | 0.0 | 2.1 | 0.6 | 177.3 | 3.7 | 189.8 | 6.2 | 348.2 | 64.7 | 177.3 | 3.7 | NA |
| 16ATW-86-Spot 109 | 644 | 647685 | 1.4 | 19.8 | 1.2 | 0.2 | 2.7 | 0.0 | 2.4 | 0.9 | 178.1 | 4.2 | 180.8 | 4.4 | 218.2 | 27.1 | 178.1 | 4.2 | NA |
| 16ATW-86-Spot 140 | 724 | 121405 | 2.4 | 19.6 | 1.0 | 0.2 | 2.4 | 0.0 | 2.2 | 0.9 | 178.3 | 3.8 | 182.5 | 4.0 | 238.5 | 24.2 | 178.3 | 3.8 | NA |
| 16ATW-86-Spot 235 | 251 | 169170 | 2.4 | 19.1 | 1.3 | 0.2 | 3.2 | 0.0 | 2.9 | 0.9 | 178.5 | 5.1 | 187.1 | 5.4 | 297.0 | 30.8 | 178.5 | 5.1 | NA |
| 16ATW-86-Spot 273 | 1442 | 301347 | 2.6 | 19.9 | 1.1 | 0.2 | 2.5 | 0.0 | 2.2 | 0.9 | 179.5 | 4.0 | 181.0 | 4.1 | 202.2 | 24.6 | 179.5 | 4.0 | NA |
| 16ATW-86-Spot 234 | 161 | 47515 | 2.1 | 19.5 | 1.7 | 0.2 | 3.2 | 0.0 | 2.7 | 0.9 | 180.1 | 4.8 | 185.4 | 5.4 | 254.6 | 38.5 | 180.1 | 4.8 | NA |
| 16ATW-86-Spot 131 | 124 | 211053 | 2.2 | 18.9 | 2.0 | 0.2 | 2.8 | 0.0 | 2.0 | 0.7 | 180.2 | 3.6 | 191.0 | 5.0 | 327.7 | 45.7 | 180.2 | 3.6 | NA |
| 16ATW-86-Spot 24 | 200 | 139169 | 2.1 | 19.5 | 1.2 | 0.2 | 2.3 | 0.0 | 2.0 | 0.9 | 180.7 | 3.5 | 185.8 | 3.9 | 251.3 | 27.2 | 180.7 | 3.5 | NA |
| 16ATW-86-Spot 134 | 105 | 17724 | 3.3 | 19.2 | 2.4 | 0.2 | 4.2 | 0.0 | 3.5 | 0.8 | 180.8 | 6.2 | 188.3 | 7.2 | 285.0 | 55.1 | 180.8 | 6.2 | NA |
| 16ATW-86-Spot 261 | 174 | 184664 | 3.2 | 18.5 | 1.4 | 0.2 | 2.6 | 0.0 | 2.2 | 0.8 | 181.6 | 3.9 | 195.7 | 4.6 | 370.1 | 32.6 | 181.6 | 3.9 | NA |
| 16ATW-86-Spot 179 | 81 | 33006 | 3.0 | 19.0 | 2.0 | 0.2 | 3.5 | 0.0 | 2.9 | 0.8 | 183.0 | 5.2 | 192.7 | 6.1 | 313.6 | 45.8 | 183.0 | 5.2 | NA |
| 16ATW-86-Spot 177 | 380 | 91419 | 1.9 | 19.5 | 1.3 | 0.2 | 3.5 | 0.0 | 3.3 | 0.9 | 183.1 | 5.9 | 188.3 | 6.1 | 255.6 | 30.8 | 183.1 | 5.9 | NA |
| 16ATW-86-Spot 76 | 90 | 10404 | 2.0 | 19.9 | 2.2 | 0.2 | 3.3 | 0.0 | 2.4 | 0.7 | 183.2 | 4.4 | 184.7 | 5.5 | 205.1 | 50.4 | 183.2 | 4.4 | NA |
| 16ATW-86-Spot 227 | 491 | 37523 | 1.1 | 19.6 | 1.3 | 0.2 | 2.8 | 0.0 | 2.5 | 0.9 | 184.1 | 4.6 | 188.3 | 4.9 | 242.3 | 30.3 | 184.1 | 4.6 | NA |
| 16ATW-86-Spot 145 | 109 | 42439 | 2.0 | 19.8 | 1.6 | 0.2 | 2.4 | 0.0 | 1.9 | 0.8 | 184.2 | 3.4 | 186.8 | 4.2 | 221.8 | 36.5 | 184.2 | 3.4 | NA |
| 16ATW-86-Spot 167 | 400 | 242782 | 1.4 | 19.4 | 1.2 | 0.2 | 2.7 | 0.0 | 2.4 | 0.9 | 184.3 | 4.3 | 189.8 | 4.7 | 260.0 | 28.7 | 184.3 | 4.3 | NA |
| 16ATW-86-Spot 108 | 83 | 11671 | 2.9 | 19.1 | 2.6 | 0.2 | 3.6 | 0.0 | 2.5 | 0.7 | 184.3 | 4.5 | 192.8 | 6.3 | 299.0 | 58.9 | 184.3 | 4.5 | NA |

| | | | | | | | | | | | | | | | | | | | |
|---|---|---|---|---|---|---|---|---|---|---|---|---|---|---|---|---|---|---|---|
| 16ATW-86-Spot 194 | 92 | 33535 | 2.3 | 18.7 | 1.5 | 0.2 | 2.9 | 0.0 | 2.5 | 0.9 | 184.3 | 4.5 | 197.1 | 5.2 | 354.8 | 33.7 | 184.3 | 4.5 | NA |
| 16ATW-86-Spot 181 | 146 | 24477 | 2.0 | 19.5 | 1.7 | 0.2 | 3.0 | 0.0 | 2.4 | 0.8 | 184.5 | 4.4 | 189.4 | 5.1 | 252.4 | 39.6 | 184.5 | 4.4 | NA |
| 16ATW-86-Spot 93 | 274 | 24567 | 2.4 | 18.8 | 2.2 | 0.2 | 3.4 | 0.0 | 2.7 | 0.8 | 184.5 | 4.9 | 196.3 | 6.1 | 341.5 | 48.8 | 184.5 | 4.9 | NA |
| 16ATW-86-Spot 312 | 158 | 102426 | 1.6 | 19.5 | 1.8 | 0.2 | 3.4 | 0.0 | 2.8 | 0.8 | 185.4 | 5.2 | 190.7 | 5.9 | 257.5 | 41.6 | 185.4 | 5.2 | NA |
| 16ATW-86-Spot 266 | 1061 | 269601 | 2.1 | 19.9 | 0.8 | 0.2 | 2.2 | 0.0 | 2.1 | 0.9 | 185.7 | 3.8 | 187.4 | 3.8 | 209.7 | 18.8 | 185.7 | 3.8 | NA |
| 16ATW-86-Spot 135 | 113 | 253373 | 2.1 | 19.1 | 1.7 | 0.2 | 2.9 | 0.0 | 2.3 | 0.8 | 186.4 | 4.3 | 195.0 | 5.1 | 302.0 | 39.4 | 186.4 | 4.3 | NA |
| 16ATW-86-Spot 276 | 73 | 14297 | 1.3 | 18.9 | 2.1 | 0.2 | 3.1 | 0.0 | 2.2 | 0.7 | 186.5 | 4.1 | 197.3 | 5.6 | 328.8 | 48.6 | 186.5 | 4.1 | NA |
| 16ATW-86-Spot 4 | 107 | 19985 | 3.2 | 19.2 | 1.4 | 0.2 | 3.0 | 0.0 | 2.6 | 0.9 | 186.5 | 4.9 | 194.5 | 5.3 | 292.5 | 31.5 | 186.5 | 4.9 | NA |
| 16ATW-86-Spot 244 | 1800 | 739572 | 1.0 | 19.5 | 0.8 | 0.2 | 2.2 | 0.0 | 2.1 | 0.9 | 187.1 | 3.8 | 191.9 | 3.9 | 252.7 | 19.0 | 187.1 | 3.8 | NA |
| 16ATW-86-Spot 26 | 221 | 363582 | 2.6 | 19.1 | 1.4 | 0.2 | 2.8 | 0.0 | 2.5 | 0.9 | 187.8 | 4.5 | 195.9 | 5.0 | 296.7 | 31.8 | 187.8 | 4.5 | NA |
| 16ATW-86-Spot 137 | 3785 | 627060 | 1.6 | 19.7 | 1.2 | 0.2 | 2.8 | 0.0 | 2.5 | 0.9 | 187.9 | 4.6 | 191.1 | 4.8 | 232.0 | 28.3 | 187.9 | 4.6 | NA |
| 16ATW-86-Spot 126 | 77 | 13556 | 2.6 | 20.1 | 2.6 | 0.2 | 3.9 | 0.0 | 2.9 | 0.7 | 188.0 | 5.4 | 187.4 | 6.7 | 181.9 | 61.2 | 188.0 | 5.4 | NA |
| 16ATW-86-Spot 284 | 522 | 165413 | 1.9 | 19.4 | 1.0 | 0.2 | 2.5 | 0.0 | 2.3 | 0.9 | 188.4 | 4.3 | 194.3 | 4.5 | 268.0 | 22.6 | 188.4 | 4.3 | NA |
| 16ATW-86-Spot 90 | 81 | 152594 | 2.3 | 18.6 | 2.4 | 0.2 | 6.5 | 0.0 | 6.1 | 0.9 | 188.7 | 11.3 | 202.1 | 12.0 | 363.1 | 55.1 | 188.7 | 11.3 | NA |
| 16ATW-86-Spot 178 | 83 | 14029 | 1.2 | 19.7 | 2.1 | 0.2 | 3.1 | 0.0 | 2.2 | 0.7 | 188.7 | 4.1 | 191.9 | 5.4 | 233.3 | 49.0 | 188.7 | 4.1 | NA |
| 16ATW-86-Spot 270 | 73 | 20449 | 2.7 | 19.5 | 2.0 | 0.2 | 4.1 | 0.0 | 3.6 | 0.9 | 188.8 | 6.7 | 194.0 | 7.2 | 259.3 | 44.9 | 188.8 | 6.7 | NA |
| 16ATW-86-Spot 21 | 139 | 28727 | 2.0 | 19.3 | 2.1 | 0.2 | 3.7 | 0.0 | 3.1 | 0.8 | 188.8 | 5.7 | 195.3 | 6.6 | 274.8 | 47.6 | 188.8 | 5.7 | NA |
| 16ATW-86-Spot 293 | 146 | 41042 | 3.0 | 19.4 | 1.3 | 0.2 | 2.8 | 0.0 | 2.5 | 0.9 | 189.0 | 4.6 | 195.1 | 5.0 | 271.0 | 29.6 | 189.0 | 4.6 | NA |
| 16ATW-86-Spot 305 | 69 | 38117 | 2.7 | 18.7 | 2.3 | 0.2 | 3.4 | 0.0 | 2.6 | 0.7 | 189.3 | 4.8 | 201.9 | 6.2 | 352.7 | 51.0 | 189.3 | 4.8 | NA |
| 16ATW-86-Spot 99 | 299 | 852325 | 2.6 | 19.3 | 1.1 | 0.2 | 2.4 | 0.0 | 2.1 | 0.9 | 189.7 | 3.9 | 196.0 | 4.2 | 272.3 | 25.2 | 189.7 | 3.9 | NA |
| 16ATW-86-Spot 7 | 120 | 13158 | 3.2 | 19.2 | 1.7 | 0.2 | 2.9 | 0.0 | 2.3 | 0.8 | 190.5 | 4.3 | 198.1 | 5.1 | 290.9 | 39.5 | 190.5 | 4.3 | NA |
| 16ATW-86-Spot 298 | 126 | 31028 | 2.2 | 17.6 | 2.1 | 0.2 | 3.3 | 0.0 | 2.6 | 0.8 | 190.7 | 4.8 | 214.8 | 6.4 | 488.8 | 46.0 | 190.7 | 4.8 | NA |
| 16ATW-86-Spot 16 | 136 | 25916 | 2.0 | 19.2 | 1.4 | 0.2 | 2.8 | 0.0 | 2.4 | 0.9 | 191.0 | 4.6 | 198.4 | 5.1 | 287.6 | 32.5 | 191.0 | 4.6 | NA |
| 16ATW-86-Spot 202 | 170 | 199525 | 1.5 | 19.1 | 1.7 | 0.2 | 3.2 | 0.0 | 2.7 | 0.8 | 191.3 | 5.1 | 200.1 | 5.8 | 305.8 | 39.3 | 191.3 | 5.1 | NA |
| 16ATW-86-Spot 302 | 633 | 178119 | 1.7 | 19.4 | 0.9 | 0.2 | 2.4 | 0.0 | 2.2 | 0.9 | 191.7 | 4.2 | 197.5 | 4.3 | 268.5 | 20.8 | 191.7 | 4.2 | NA |

| | | | | | | | | | | | | | | | | | | | |
|---|---|---|---|---|---|---|---|---|---|---|---|---|---|---|---|---|---|---|---|
| 16ATW-86-Spot 103 | 442 | 242634 | 1.5 | 19.5 | 1.3 | 0.2 | 2.8 | 0.0 | 2.5 | 0.9 | 191.8 | 4.7 | 196.3 | 5.0 | 252.1 | 30.1 | 191.8 | 4.7 | NA |
| 16ATW-86-Spot 224 | 199 | 98626 | 1.4 | 19.3 | 1.3 | 0.2 | 2.6 | 0.0 | 2.3 | 0.9 | 191.9 | 4.3 | 198.6 | 4.7 | 279.9 | 28.7 | 191.9 | 4.3 | NA |
| 16ATW-86-Spot 139 | 185 | 309408 | 2.9 | 18.9 | 1.4 | 0.2 | 2.6 | 0.0 | 2.2 | 0.8 | 192.0 | 4.2 | 202.2 | 4.8 | 323.5 | 31.6 | 192.0 | 4.2 | NA |
| 16ATW-86-Spot 115 | 165 | 2938937 | 1.8 | 19.2 | 1.6 | 0.2 | 2.7 | 0.0 | 2.2 | 0.8 | 192.2 | 4.2 | 199.8 | 4.9 | 292.1 | 36.2 | 192.2 | 4.2 | NA |
| 16ATW-86-Spot 275 | 163 | 190952 | 2.1 | 19.0 | 1.6 | 0.2 | 3.0 | 0.0 | 2.6 | 0.8 | 192.3 | 4.9 | 201.5 | 5.5 | 310.7 | 36.4 | 192.3 | 4.9 | NA |
| 16ATW-86-Spot 171 | 537 | 221968 | 1.8 | 19.7 | 1.0 | 0.2 | 2.0 | 0.0 | 1.7 | 0.9 | 192.9 | 3.3 | 195.8 | 3.6 | 231.9 | 24.2 | 192.9 | 3.3 | NA |
| 16ATW-86-Spot 289 | 756 | 214496 | 1.6 | 19.7 | 1.1 | 0.2 | 2.3 | 0.0 | 2.0 | 0.9 | 193.0 | 3.8 | 196.0 | 4.0 | 234.2 | 25.1 | 193.0 | 3.8 | NA |
| 16ATW-86-Spot 180 | 192 | 98227 | 1.8 | 18.5 | 1.0 | 0.2 | 2.3 | 0.0 | 2.1 | 0.9 | 193.1 | 4.0 | 207.0 | 4.4 | 369.1 | 22.8 | 193.1 | 4.0 | NA |
| 16ATW-86-Spot 22 | 341 | 22313194 | 2.7 | 19.8 | 1.2 | 0.2 | 2.4 | 0.0 | 2.1 | 0.9 | 193.3 | 4.0 | 195.0 | 4.2 | 215.9 | 27.6 | 193.3 | 4.0 | NA |
| 16ATW-86-Spot 157 | 915 | 63741 | 2.7 | 17.7 | 1.2 | 0.2 | 2.8 | 0.0 | 2.6 | 0.9 | 193.4 | 4.9 | 215.6 | 5.5 | 466.9 | 26.0 | 193.4 | 4.9 | NA |
| 16ATW-86-Spot 168 | 665 | 101740 | 1.0 | 18.9 | 1.2 | 0.2 | 2.9 | 0.0 | 2.6 | 0.9 | 194.2 | 5.0 | 204.4 | 5.3 | 325.2 | 27.1 | 194.2 | 5.0 | NA |
| 16ATW-86-Spot 246 | 866 | 171001 | 1.5 | 19.4 | 1.2 | 0.2 | 2.4 | 0.0 | 2.1 | 0.9 | 194.4 | 4.0 | 200.2 | 4.3 | 269.5 | 26.4 | 194.4 | 4.0 | NA |
| 16ATW-86-Spot 63 | 363 | 162387 | 2.1 | 19.1 | 1.3 | 0.2 | 2.8 | 0.0 | 2.5 | 0.9 | 194.5 | 4.8 | 202.5 | 5.2 | 297.5 | 30.3 | 194.5 | 4.8 | NA |
| 16ATW-86-Spot 55 | 670 | 58437 | 2.5 | 19.8 | 1.1 | 0.2 | 2.7 | 0.0 | 2.5 | 0.9 | 196.5 | 4.8 | 198.2 | 4.8 | 219.2 | 24.3 | 196.5 | 4.8 | NA |
| 16ATW-86-Spot 28 | 569 | 214208 | 1.5 | 19.6 | 1.4 | 0.2 | 4.7 | 0.0 | 4.5 | 1.0 | 198.0 | 8.7 | 201.5 | 8.6 | 243.5 | 31.8 | 198.0 | 8.7 | NA |
| 16ATW-86-Spot 62 | 512 | 59723 | 3.0 | 19.5 | 0.9 | 0.2 | 2.3 | 0.0 | 2.1 | 0.9 | 198.4 | 4.2 | 202.3 | 4.3 | 249.6 | 21.6 | 198.4 | 4.2 | NA |
| 16ATW-86-Spot 186 | 211 | 34584 | 1.9 | 19.2 | 1.5 | 0.2 | 2.8 | 0.0 | 2.4 | 0.9 | 198.7 | 4.8 | 206.2 | 5.3 | 293.8 | 33.4 | 198.7 | 4.8 | NA |
| 16ATW-86-Spot 220 | 311 | 308793 | 3.1 | 19.5 | 1.7 | 0.2 | 3.3 | 0.0 | 2.9 | 0.9 | 199.2 | 5.7 | 203.0 | 6.1 | 249.2 | 38.4 | 199.2 | 5.7 | NA |
| 16ATW-86-Spot 209 | 435 | 1960070 | 2.3 | 19.3 | 1.2 | 0.2 | 2.6 | 0.0 | 2.3 | 0.9 | 199.3 | 4.6 | 205.7 | 4.8 | 281.8 | 26.5 | 199.3 | 4.6 | NA |
| 16ATW-86-Spot 41 | 518 | 4999463 | 2.9 | 19.5 | 0.8 | 0.2 | 2.6 | 0.0 | 2.5 | 1.0 | 199.3 | 4.9 | 204.0 | 4.9 | 259.1 | 18.0 | 199.3 | 4.9 | NA |
| 16ATW-86-Spot 287 | 384 | 122690 | 2.5 | 19.1 | 1.1 | 0.2 | 2.8 | 0.0 | 2.6 | 0.9 | 200.1 | 5.1 | 207.8 | 5.3 | 297.1 | 25.5 | 200.1 | 5.1 | NA |
| 16ATW-86-Spot 206 | 339 | 85545 | 2.0 | 19.5 | 1.4 | 0.2 | 3.0 | 0.0 | 2.6 | 0.9 | 200.4 | 5.1 | 204.4 | 5.5 | 252.6 | 32.1 | 200.4 | 5.1 | NA |
| 16ATW-86-Spot 262 | 599 | 389610 | 2.9 | 19.4 | 1.1 | 0.2 | 2.5 | 0.0 | 2.2 | 0.9 | 201.9 | 4.3 | 207.3 | 4.6 | 270.6 | 26.1 | 201.9 | 4.3 | NA |
| 16ATW-86-Spot 187 | 676 | 211745 | 2.0 | 19.6 | 1.0 | 0.2 | 2.3 | 0.0 | 2.1 | 0.9 | 205.7 | 4.2 | 208.3 | 4.4 | 237.7 | 23.4 | 205.7 | 4.2 | NA |
| 16ATW-86-Spot 68 | 446 | 94686 | 3.3 | 19.4 | 1.1 | 0.2 | 2.6 | 0.0 | 2.3 | 0.9 | 205.8 | 4.7 | 210.4 | 4.9 | 262.6 | 24.6 | 205.8 | 4.7 | NA |

| | | | | | | | | | | | | | | | | | | | |
|---|---|---|---|---|---|---|---|---|---|---|---|---|---|---|---|---|---|---|---|
| 16ATW-86-Spot 304 | 148 | 16598 | 2.4 | 19.3 | 1.4 | 0.2 | 3.1 | 0.0 | 2.8 | 0.9 | 206.2 | 5.7 | 212.1 | 6.0 | 279.0 | 31.8 | 206.2 | 5.7 | NA |
| 16ATW-86-Spot 123 | 635 | 225914 | 2.3 | 19.2 | 1.1 | 0.2 | 2.8 | 0.0 | 2.6 | 0.9 | 206.6 | 5.2 | 213.7 | 5.4 | 293.0 | 25.2 | 206.6 | 5.2 | NA |
| 16ATW-86-Spot 127 | 466 | 70453 | 2.3 | 18.9 | 1.5 | 0.2 | 2.6 | 0.0 | 2.2 | 0.8 | 215.6 | 4.6 | 225.1 | 5.3 | 326.6 | 34.9 | 215.6 | 4.6 | NA |
| 16ATW-86-Spot 258 | 372 | 61131 | 2.4 | 18.7 | 1.3 | 0.3 | 2.5 | 0.0 | 2.1 | 0.9 | 217.2 | 4.5 | 228.9 | 5.1 | 351.3 | 28.8 | 217.2 | 4.5 | NA |
| 16ATW-86-Spot 199 | 541 | 370727 | 2.4 | 19.4 | 1.2 | 0.3 | 3.5 | 0.0 | 3.3 | 0.9 | 231.7 | 7.4 | 234.7 | 7.3 | 265.1 | 27.3 | 231.7 | 7.4 | NA |
| 16ATW-86-Spot 257 | 79 | 46306 | 1.5 | 19.1 | 2.1 | 0.3 | 3.4 | 0.0 | 2.7 | 0.8 | 234.1 | 6.2 | 240.0 | 7.4 | 298.9 | 49.0 | 234.1 | 6.2 | NA |
| 16ATW-86-Spot 308 | 1016 | 1497857 | 2.1 | 18.9 | 0.8 | 0.3 | 2.4 | 0.0 | 2.2 | 0.9 | 283.9 | 6.2 | 288.7 | 6.0 | 329.1 | 18.7 | 283.9 | 6.2 | NA |
| 16ATW-86-Spot 1 | 55 | 120880 | 3.9 | 17.7 | 2.0 | 0.4 | 6.2 | 0.0 | 5.8 | 0.9 | 285.3 | 16.2 | 307.2 | 16.3 | 477.7 | 44.2 | 285.3 | 16.2 | NA |
| 16ATW-86-Spot 188 | 927 | 143850 | 1.9 | 19.2 | 1.0 | 0.3 | 2.5 | 0.0 | 2.3 | 0.9 | 287.8 | 6.6 | 287.9 | 6.4 | 289.2 | 22.9 | 287.8 | 6.6 | NA |
| 16ATW-86-Spot 268 | 139 | 1220203 | 1.9 | 16.0 | 1.6 | 0.4 | 3.0 | 0.0 | 2.6 | 0.8 | 287.9 | 7.3 | 337.5 | 8.7 | 695.8 | 34.3 | 287.9 | 7.3 | NA |
| 16ATW-86-Spot 86 | 1432 | 242771 | 2.2 | 18.7 | 0.9 | 0.3 | 2.1 | 0.0 | 1.9 | 0.9 | 293.4 | 5.4 | 299.1 | 5.4 | 344.8 | 20.6 | 293.4 | 5.4 | NA |
| 16ATW-86-Spot 278 | 201 | 39727 | 4.0 | 18.3 | 1.0 | 0.4 | 3.4 | 0.0 | 3.3 | 1.0 | 294.5 | 9.5 | 305.9 | 9.1 | 394.8 | 21.8 | 294.5 | 9.5 | NA |
| 16ATW-86-Spot 155 | 660 | 279865 | 4.3 | 18.9 | 0.9 | 0.3 | 2.3 | 0.0 | 2.1 | 0.9 | 294.9 | 6.0 | 298.7 | 5.9 | 329.5 | 21.4 | 294.9 | 6.0 | NA |
| 16ATW-86-Spot 272 | 930 | 293324 | 1.9 | 18.7 | 1.0 | 0.3 | 2.4 | 0.0 | 2.1 | 0.9 | 296.2 | 6.2 | 302.0 | 6.2 | 347.8 | 23.4 | 296.2 | 6.2 | NA |
| 16ATW-86-Spot 158 | 691 | 262794 | 4.8 | 18.4 | 0.9 | 0.4 | 2.2 | 0.0 | 2.0 | 0.9 | 298.0 | 5.7 | 308.0 | 5.8 | 385.8 | 21.1 | 298.0 | 5.7 | NA |
| 16ATW-86-Spot 147 | 620 | 176164 | 3.6 | 19.0 | 0.9 | 0.3 | 3.2 | 0.0 | 3.1 | 1.0 | 298.3 | 8.9 | 300.3 | 8.3 | 316.6 | 19.8 | 298.3 | 8.9 | NA |
| 16ATW-86-Spot 288 | 154 | 364800 | 1.8 | 18.2 | 1.3 | 0.4 | 3.1 | 0.0 | 2.8 | 0.9 | 299.7 | 8.2 | 312.1 | 8.3 | 407.1 | 28.9 | 299.7 | 8.2 | NA |
| 16ATW-86-Spot 96 | 385 | 251723 | 3.2 | 18.7 | 1.0 | 0.4 | 2.4 | 0.0 | 2.2 | 0.9 | 300.1 | 6.5 | 306.0 | 6.5 | 352.4 | 22.3 | 300.1 | 6.5 | NA |
| 16ATW-86-Spot 196 | 411 | 1858031 | 1.9 | 18.8 | 1.1 | 0.4 | 3.0 | 0.0 | 2.7 | 0.9 | 302.6 | 8.1 | 306.9 | 7.9 | 340.3 | 25.6 | 302.6 | 8.1 | NA |
| 16ATW-86-Spot 85 | 508 | 165537 | 3.0 | 18.8 | 1.0 | 0.4 | 3.2 | 0.0 | 3.0 | 1.0 | 302.9 | 9.0 | 307.3 | 8.5 | 341.7 | 22.3 | 302.9 | 9.0 | NA |
| 16ATW-86-Spot 291 | 934 | 798179 | 6.5 | 18.9 | 1.0 | 0.4 | 2.4 | 0.0 | 2.2 | 0.9 | 303.0 | 6.4 | 304.9 | 6.3 | 320.0 | 23.0 | 303.0 | 6.4 | NA |
| 16ATW-86-Spot 232 | 454 | 203019 | 5.8 | 18.5 | 0.9 | 0.4 | 2.9 | 0.0 | 2.8 | 0.9 | 304.3 | 8.3 | 312.7 | 7.9 | 376.5 | 21.0 | 304.3 | 8.3 | NA |
| 16ATW-86-Spot 162 | 411 | 95146 | 1.9 | 18.9 | 0.9 | 0.4 | 1.9 | 0.0 | 1.7 | 0.9 | 304.5 | 5.1 | 306.6 | 5.1 | 323.7 | 19.5 | 304.5 | 5.1 | NA |
| 16ATW-86-Spot 116 | 1258 | 159377 | 6.6 | 19.1 | 1.0 | 0.3 | 2.1 | 0.0 | 1.9 | 0.9 | 304.7 | 5.7 | 304.4 | 5.6 | 302.4 | 22.0 | 304.7 | 5.7 | NA |

| | | | | | | | | | | | | | | | | | | | |
|---|---|---|---|---|---|---|---|---|---|---|---|---|---|---|---|---|---|---|---|
| 16ATW-86-Spot 29 | 547 | 209909 | 4.3 | 19.1 | 0.9 | 0.4 | 2.5 | 0.0 | 2.3 | 0.9 | 305.3 | 6.8 | 305.2 | 6.5 | 305.4 | 21.3 | 305.3 | 6.8 | NA |
| 16ATW-86-Spot 129 | 153 | 262715 | 4.2 | 18.1 | 1.6 | 0.4 | 3.5 | 0.0 | 3.1 | 0.9 | 306.8 | 9.1 | 320.2 | 9.5 | 419.9 | 36.0 | 306.8 | 9.1 | NA |
| 16ATW-86-Spot 146 | 1264 | 235164 | 4.7 | 18.9 | 1.0 | 0.4 | 2.5 | 0.0 | 2.3 | 0.9 | 308.4 | 6.8 | 310.1 | 6.5 | 324.4 | 21.7 | 308.4 | 6.8 | NA |
| 16ATW-86-Spot 212 | 294 | 123934 | 2.7 | 18.4 | 1.0 | 0.4 | 2.6 | 0.0 | 2.4 | 0.9 | 308.8 | 7.2 | 318.4 | 7.1 | 390.7 | 23.2 | 308.8 | 7.2 | NA |
| 16ATW-86-Spot 44 | 377 | 131267 | 4.1 | 18.7 | 0.9 | 0.4 | 2.1 | 0.0 | 1.9 | 0.9 | 309.2 | 5.7 | 313.8 | 5.7 | 348.4 | 21.0 | 309.2 | 5.7 | NA |
| 16ATW-86-Spot 120 | 73 | 30097 | 4.5 | 17.9 | 1.9 | 0.4 | 3.2 | 0.0 | 2.6 | 0.8 | 310.1 | 7.9 | 326.1 | 9.0 | 442.7 | 42.7 | 310.1 | 7.9 | NA |
| 16ATW-86-Spot 236 | 510 | 461841 | 5.1 | 18.7 | 1.0 | 0.4 | 2.6 | 0.0 | 2.4 | 0.9 | 310.2 | 7.3 | 314.7 | 7.0 | 349.3 | 22.5 | 310.2 | 7.3 | NA |
| 16ATW-86-Spot 184 | 341 | 256160 | 3.8 | 19.2 | 1.0 | 0.4 | 2.5 | 0.0 | 2.3 | 0.9 | 310.5 | 6.9 | 307.9 | 6.6 | 289.0 | 21.8 | 310.5 | 6.9 | NA |
| 16ATW-86-Spot 245 | 230 | 78435 | 2.2 | 18.0 | 1.1 | 0.4 | 2.6 | 0.0 | 2.4 | 0.9 | 310.8 | 7.3 | 325.0 | 7.3 | 429.0 | 23.6 | 310.8 | 7.3 | NA |
| 16ATW-86-Spot 70 | 270 | 392040 | 4.3 | 18.7 | 1.2 | 0.4 | 2.1 | 0.0 | 1.7 | 0.8 | 312.2 | 5.3 | 316.0 | 5.8 | 344.4 | 28.2 | 312.2 | 5.3 | NA |
| 16ATW-86-Spot 176 | 1480 | 6471981 | 1.6 | 19.2 | 0.8 | 0.4 | 2.5 | 0.0 | 2.4 | 0.9 | 312.5 | 7.2 | 309.9 | 6.6 | 291.4 | 18.8 | 312.5 | 7.2 | NA |
| 16ATW-86-Spot 67 | 313 | 201305 | 3.2 | 18.5 | 1.0 | 0.4 | 2.0 | 0.0 | 1.8 | 0.9 | 313.0 | 5.5 | 320.3 | 5.6 | 374.6 | 22.3 | 313.0 | 5.5 | NA |
| 16ATW-86-Spot 296 | 148 | 44329 | 1.2 | 17.7 | 1.5 | 0.4 | 2.7 | 0.0 | 2.2 | 0.8 | 313.0 | 6.8 | 333.0 | 7.7 | 476.1 | 34.1 | 313.0 | 6.8 | NA |
| 16ATW-86-Spot 59 | 373 | 592322 | 1.3 | 18.6 | 1.1 | 0.4 | 2.4 | 0.0 | 2.1 | 0.9 | 313.4 | 6.5 | 319.4 | 6.6 | 364.6 | 24.4 | 313.4 | 6.5 | NA |
| 16ATW-86-Spot 240 | 181 | 23740 | 3.7 | 18.4 | 1.1 | 0.4 | 2.6 | 0.1 | 2.3 | 0.9 | 319.8 | 7.3 | 328.1 | 7.2 | 388.4 | 24.1 | 319.8 | 7.3 | NA |
| 16ATW-86-Spot 104 | 458 | 788566 | 3.4 | 18.1 | 0.9 | 0.4 | 2.6 | 0.1 | 2.4 | 0.9 | 321.0 | 7.5 | 333.1 | 7.3 | 420.0 | 19.7 | 321.0 | 7.5 | NA |
| 16ATW-86-Spot 290 | 318 | 61109 | 2.1 | 16.0 | 1.4 | 0.4 | 3.1 | 0.1 | 2.8 | 0.9 | 321.5 | 8.7 | 371.0 | 9.7 | 694.0 | 30.7 | 321.5 | 8.7 | NA |
| 16ATW-86-Spot 156 | 91 | 17939 | 3.9 | 16.7 | 1.6 | 0.4 | 3.1 | 0.1 | 2.6 | 0.9 | 323.0 | 8.3 | 358.9 | 9.4 | 598.7 | 34.9 | 323.0 | 8.3 | NA |
| 16ATW-86-Spot 89 | 382 | 124589 | 1.6 | 17.9 | 1.7 | 0.4 | 2.9 | 0.1 | 2.3 | 0.8 | 324.6 | 7.3 | 339.8 | 8.2 | 445.8 | 37.5 | 324.6 | 7.3 | NA |
| 16ATW-86-Spot 229 | 466 | 197616 | 2.6 | 18.6 | 0.9 | 0.4 | 2.5 | 0.1 | 2.3 | 0.9 | 333.0 | 7.5 | 336.8 | 7.0 | 364.0 | 19.6 | 333.0 | 7.5 | NA |
| 16ATW-86-Spot 143 | 336 | 204163 | 1.1 | 18.0 | 1.0 | 0.5 | 2.8 | 0.1 | 2.6 | 0.9 | 431.5 | 10.7 | 431.6 | 9.7 | 433.0 | 22.0 | 431.5 | 10.7 | 99.6 |
| 16ATW-86-Spot 20 | 295 | 322005 | 2.7 | 17.6 | 1.3 | 0.6 | 2.4 | 0.1 | 2.0 | 0.8 | 446.5 | 8.6 | 452.8 | 8.6 | 486.1 | 27.6 | 446.5 | 8.6 | 91.8 |
| 16ATW-86-Spot 279 | 300 | 78622 | 5.1 | 17.6 | 0.9 | 0.6 | 2.9 | 0.1 | 2.8 | 1.0 | 467.3 | 12.6 | 470.2 | 11.0 | 485.4 | 19.1 | 467.3 | 12.6 | 96.3 |
| 16ATW-86-Spot 172 | 50 | 82550 | 2.6 | 16.1 | 1.4 | 0.8 | 2.5 | 0.1 | 2.1 | 0.8 | 558.2 | 11.3 | 583.2 | 11.2 | 683.0 | 29.9 | 558.2 | 11.3 | 81.7 |
| 16ATW-86-Spot 43 | 43 | 66962 | 2.0 | 16.5 | 1.7 | 0.8 | 3.0 | 0.1 | 2.5 | 0.8 | 562.7 | 13.5 | 574.8 | 13.3 | 623.8 | 36.6 | 562.7 | 13.5 | 90.2 |

| | | | | | | | | | | | | | | | | | | |
|---|---|---|---|---|---|---|---|---|---|---|---|---|---|---|---|---|---|---|
| 16ATW-86-Spot 281 | 76 | 58203 | 2.9 | 11.8 | 1.1 | 2.5 | 3.0 | 0.2 | 2.8 | 0.9 | 1265.5 | 32.6 | 1280.5 | 22.1 | 1306.5 | 20.8 | 1306.5 | 20.8 | 96.9 |
| 16ATW-86-Spot 313 | 107 | 627307 | 1.3 | 9.9 | 1.1 | 4.1 | 2.8 | 0.3 | 2.6 | 0.9 | 1675.3 | 37.8 | 1663.8 | 22.9 | 1650.1 | 20.9 | 1650.1 | 20.9 | 101.5 |
| 16ATW-86-Spot 81 | 143 | 244740 | 1.8 | 5.6 | 0.9 | 11.8 | 2.5 | 0.5 | 2.3 | 0.9 | 2510.0 | 48.2 | 2588.7 | 23.3 | 2651.5 | 14.9 | 2651.5 | 14.9 | 94.7 |
| 16ATW-86-Spot 301 | 217 | 195163 | 1.4 | 16.8 | 2.3 | 0.2 | 3.3 | 0.0 | 2.4 | 0.7 | 172.9 | 4.1 | 204.1 | 6.1 | 582.6 | 49.9 | 172.9 | 4.1 | 3.4 |
| 16ATW-86-Spot 192 | 543 | 196904 | 4.0 | 19.7 | 1.6 | 0.1 | 2.8 | 0.0 | 2.3 | 0.8 | 67.3 | 1.6 | 72.1 | 1.9 | 234.8 | 35.8 | 67.3 | 1.6 | 3.5 |
| 16ATW-86-Spot 211 | 100 | 99629 | 1.7 | 17.1 | 3.2 | 0.2 | 4.0 | 0.0 | 2.4 | 0.6 | 154.2 | 3.7 | 180.7 | 6.7 | 545.3 | 70.8 | 154.2 | 3.7 | 3.5 |
| 16ATW-86-Spot 35 | 170 | 60577 | 2.9 | 16.8 | 2.1 | 0.2 | 3.0 | 0.0 | 2.1 | 0.7 | 159.0 | 3.3 | 188.9 | 5.1 | 581.6 | 45.8 | 159.0 | 3.3 | 3.7 |
| 16ATW-86-Spot 113 | 159 | 691081 | 1.0 | 15.1 | 3.9 | 0.2 | 4.8 | 0.0 | 2.7 | 0.6 | 169.7 | 4.6 | 221.0 | 9.5 | 812.0 | 81.5 | 169.7 | 4.6 | 4.8 |
| 16ATW-86-Spot 205 | 59 | 334416 | 2.2 | 14.3 | 2.1 | 0.2 | 3.3 | 0.0 | 2.5 | 0.8 | 158.3 | 3.9 | 217.8 | 6.4 | 923.3 | 43.4 | 158.3 | 3.9 | 5.8 |
| 16ATW-86-Spot 163 | 151 | 34696 | 2.0 | 13.9 | 5.2 | 0.2 | 5.8 | 0.0 | 2.5 | 0.4 | 156.4 | 3.9 | 220.7 | 11.4 | 977.8 | 105.1 | 156.4 | 3.9 | 6.3 |
| 16ATW-86-Spot 214 | 221 | 13810 | 1.6 | 13.4 | 5.1 | 0.3 | 5.6 | 0.0 | 2.3 | 0.4 | 169.8 | 3.9 | 246.9 | 12.3 | 1064.4 | 102.3 | 169.8 | 3.9 | 6.3 |
| 16ATW-86-Spot 82 | 194 | 14221 | 3.0 | 11.6 | 6.9 | 0.4 | 7.3 | 0.0 | 2.2 | 0.3 | 198.8 | 4.3 | 321.5 | 20.1 | 1344.4 | 134.3 | 198.8 | 4.3 | 6.8 |
| 16ATW-86-Spot 269 | 115 | 6452 | 3.1 | 11.8 | 8.6 | 0.4 | 9.5 | 0.0 | 4.0 | 0.4 | 190.2 | 7.5 | 304.9 | 24.9 | 1312.6 | 166.7 | 190.2 | 7.5 | 6.9 |
| 16ATW-86-Spot 173 | 168 | 6829 | 3.1 | 10.5 | 7.2 | 0.3 | 7.7 | 0.0 | 2.8 | 0.4 | 163.7 | 4.5 | 294.2 | 19.7 | 1525.1 | 135.3 | 163.7 | 4.5 | 9.3 |
| 16ATW-86-Spot 307 | 107 | 12943 | 2.0 | 10.4 | 3.8 | 0.3 | 4.4 | 0.0 | 2.3 | 0.5 | 165.2 | 3.8 | 299.1 | 11.4 | 1543.1 | 70.8 | 165.2 | 3.8 | 9.3 |
| 16ATW-86-Spot 166 | 42 | 9764 | 2.2 | 10.0 | 8.5 | 0.3 | 8.9 | 0.0 | 2.7 | 0.3 | 158.7 | 4.2 | 301.1 | 23.2 | 1633.1 | 157.9 | 158.7 | 4.2 | 10.3 |
| 16ATW-86-Spot 80 | 45 | 8885 | 2.1 | 7.9 | 10.1 | 0.5 | 10.6 | 0.0 | 3.3 | 0.3 | 172.3 | 5.6 | 393.3 | 34.5 | 2052.2 | 178.1 | 172.3 | 5.6 | 11.9 |
| 16ATW-86-Spot 197 | 263 | 6835 | 3.3 | 14.2 | 5.2 | 0.1 | 5.6 | 0.0 | 2.2 | 0.4 | 75.4 | 1.7 | 109.5 | 5.8 | 935.8 | 106.3 | 75.4 | 1.7 | 12.4 |
| 16ATW-86-Spot 237 | 114 | 4794 | 1.7 | 7.1 | 7.9 | 0.5 | 8.5 | 0.0 | 3.1 | 0.4 | 169.3 | 5.2 | 424.6 | 29.4 | 2246.1 | 136.4 | 169.3 | 5.2 | 13.3 |
| 16ATW-86-Spot 254 | 111 | 7564 | 3.3 | 8.3 | 10.1 | 0.2 | 11.9 | 0.0 | 6.3 | 0.5 | 79.4 | 4.9 | 189.5 | 20.6 | 1958.6 | 180.9 | 79.4 | 4.9 | 24.7 |
| 16ATW-86-Spot 149 | 399 | 178519 | 2.4 | 22.7 | 1.6 | 0.2 | 15.5 | 0.0 | 15.5 | 1.0 | 194.3 | 29.6 | 173.2 | 24.8 | NA | NA | 194.3 | 29.6 | ##### |

Sample 15ATW47

| Analysis | U | 206Pb | U/Th | 206Pb* | ± | 207Pb* | ± (1s random) | 206Pb* | ± (1s random) | error | 206Pb* | ± | 207Pb* | ± | 206Pb* | ± | Best age | ± (1s random) | Conc |
|---|---|---|---|---|---|---|---|---|---|---|---|---|---|---|---|---|---|---|---|
| | (ppm) | 204Pb | | 207Pb* | (%) | 235U* | (%) | 238U | (%) | corr. | 238U* | (Ma) | 235U | (Ma) | 207Pb* | (Ma) | (Ma) | (Ma) | (%) |
| -15ATW-47 Spot 33 | 5063 | 42932 | 15.2 | 21.2 | 1.0 | 0.1 | 2.7 | 0.0 | 2.5 | 0.9 | 49.5 | 1.2 | 49.6 | 1.3 | 58.2 | 23.2 | 49.5 | 1.2 | NA |

| | | | | | | | | | | | | | | | | | | | |
|---|---|---|---|---|---|---|---|---|---|---|---|---|---|---|---|---|---|---|---|
| -15ATW-47 Spot 2 | 5072 | 219755 | 8.0 | 21.4 | 0.9 | 0.0 | 2.3 | 0.0 | 2.1 | 0.9 | 49.5 | 1.0 | 49.3 | 1.1 | 40.4 | 21.1 | 49.5 | 1.0 | NA |
| -15ATW-47 Spot 1 | 3000 | 49780 | 5.6 | 20.8 | 1.3 | 0.1 | 2.5 | 0.0 | 2.2 | 0.9 | 50.6 | 1.1 | 51.7 | 1.3 | 105.1 | 30.7 | 50.6 | 1.1 | NA |
| -15ATW-47 Spot 3 | 3973 | 83021 | 4.7 | 20.8 | 1.0 | 0.1 | 2.7 | 0.0 | 2.5 | 0.9 | 50.6 | 1.3 | 51.6 | 1.4 | 98.2 | 24.2 | 50.6 | 1.3 | NA |
| -15ATW-47 Spot 27 | 2788 | 21005 | 3.9 | 21.2 | 1.0 | 0.1 | 2.8 | 0.0 | 2.6 | 0.9 | 50.7 | 1.3 | 50.9 | 1.4 | 60.9 | 23.7 | 50.7 | 1.3 | NA |
| -15ATW-47 Spot 19 | 4755 | 105137 | 13.8 | 21.3 | 1.0 | 0.1 | 2.4 | 0.0 | 2.2 | 0.9 | 50.9 | 1.1 | 50.8 | 1.2 | 46.8 | 23.6 | 50.9 | 1.1 | NA |
| -15ATW-47 Spot 4 | 3206 | 32760 | 10.3 | 21.1 | 0.9 | 0.1 | 2.0 | 0.0 | 1.8 | 0.9 | 51.6 | 0.9 | 52.0 | 1.0 | 69.6 | 21.2 | 51.6 | 0.9 | NA |
| -15ATW-47 Spot 5 | 2312 | 119635 | 16.6 | 21.0 | 1.2 | 0.1 | 2.7 | 0.0 | 2.4 | 0.9 | 51.9 | 1.2 | 52.4 | 1.4 | 76.5 | 27.4 | 51.9 | 1.2 | NA |
| -15ATW-47 Spot 13 | 1226 | 43336 | 6.7 | 20.7 | 1.3 | 0.1 | 2.9 | 0.0 | 2.6 | 0.9 | 51.9 | 1.3 | 53.3 | 1.5 | 118.3 | 30.2 | 51.9 | 1.3 | NA |
| -15ATW-47 Spot 10 | 1311 | 15633 | 6.4 | 21.0 | 1.4 | 0.1 | 2.7 | 0.0 | 2.3 | 0.9 | 51.9 | 1.2 | 52.6 | 1.4 | 82.9 | 32.5 | 51.9 | 1.2 | NA |
| -15ATW-47 Spot 16 | 1019 | 16628 | 3.9 | 20.8 | 1.5 | 0.1 | 2.8 | 0.0 | 2.3 | 0.8 | 52.0 | 1.2 | 53.1 | 1.4 | 100.8 | 36.6 | 52.0 | 1.2 | NA |
| -15ATW-47 Spot 37 | 2577 | 33955 | 4.3 | 21.1 | 0.9 | 0.1 | 1.8 | 0.0 | 1.6 | 0.9 | 52.0 | 0.8 | 52.3 | 0.9 | 64.1 | 20.8 | 52.0 | 0.8 | NA |
| -15ATW-47 Spot 29 | 2761 | 93415 | 6.8 | 21.1 | 1.1 | 0.1 | 2.3 | 0.0 | 2.0 | 0.9 | 52.2 | 1.1 | 52.5 | 1.2 | 65.1 | 27.0 | 52.2 | 1.1 | NA |
| -15ATW-47 Spot 21 | 2095 | 6405 | 3.8 | 21.5 | 1.1 | 0.1 | 2.7 | 0.0 | 2.5 | 0.9 | 52.5 | 1.3 | 51.9 | 1.4 | 26.7 | 26.8 | 52.5 | 1.3 | NA |
| -15ATW-47 Spot 32 | 1303 | 11672 | 10.5 | 20.7 | 1.4 | 0.1 | 2.9 | 0.0 | 2.5 | 0.9 | 52.7 | 1.3 | 54.1 | 1.5 | 119.0 | 34.0 | 52.7 | 1.3 | NA |
| -15ATW-47 Spot 12 | 1496 | 13947 | 3.7 | 20.8 | 1.4 | 0.1 | 3.0 | 0.0 | 2.7 | 0.9 | 52.7 | 1.4 | 53.8 | 1.6 | 104.4 | 32.0 | 52.7 | 1.4 | NA |
| -15ATW-47 Spot 26 | 2113 | 18891 | 5.3 | 21.0 | 1.0 | 0.1 | 2.6 | 0.0 | 2.4 | 0.9 | 52.8 | 1.3 | 53.3 | 1.3 | 76.4 | 23.2 | 52.8 | 1.3 | NA |
| -15ATW-47 Spot 38 | 437 | 5712 | 6.4 | 20.8 | 1.7 | 0.1 | 3.4 | 0.0 | 3.0 | 0.9 | 53.0 | 1.6 | 54.0 | 1.8 | 99.5 | 40.2 | 53.0 | 1.6 | NA |
| -15ATW-47 Spot 17 | 916 | 5942 | 4.0 | 21.3 | 1.5 | 0.1 | 3.3 | 0.0 | 2.9 | 0.9 | 53.1 | 1.5 | 52.9 | 1.7 | 44.6 | 36.9 | 53.1 | 1.5 | NA |
| -15ATW-47 Spot 20 | 665 | 4667 | 3.6 | 21.6 | 1.6 | 0.1 | 3.2 | 0.0 | 2.8 | 0.9 | 53.2 | 1.5 | 52.4 | 1.7 | 16.7 | 39.0 | 53.2 | 1.5 | NA |
| -15ATW-47 Spot 15 | 655 | 26144 | 2.1 | 20.7 | 1.7 | 0.1 | 2.6 | 0.0 | 2.0 | 0.8 | 53.7 | 1.1 | 55.0 | 1.4 | 116.1 | 39.2 | 53.7 | 1.1 | NA |
| -15ATW-47 Spot 6 | 901 | 6661 | 4.5 | 21.7 | 2.7 | 0.1 | 3.3 | 0.0 | 1.9 | 0.6 | 53.9 | 1.0 | 52.7 | 1.7 | NA | NA | 53.9 | 1.0 | NA |
| -15ATW-47 Spot 36 | 1379 | 11004 | 4.5 | 21.1 | 1.3 | 0.1 | 2.7 | 0.0 | 2.4 | 0.9 | 55.5 | 1.3 | 55.6 | 1.5 | 65.1 | 31.9 | 55.5 | 1.3 | NA |
| -15ATW-47 Spot 22 | 222 | 4407 | 5.3 | 20.0 | 4.0 | 0.1 | 5.6 | 0.0 | 4.0 | 0.7 | 57.1 | 2.3 | 60.4 | 3.3 | 193.6 | 91.9 | 57.1 | 2.3 | NA |
| -15ATW-47 Spot 7 | 2884 | 1678632 | 5.5 | 20.7 | 1.0 | 0.1 | 3.1 | 0.0 | 2.9 | 0.9 | 52.2 | 1.5 | 53.5 | 1.6 | 115.7 | 23.6 | 52.2 | 1.5 | NA |
| -15ATW-47 Spot 8 | 1079 | 92339 | 7.8 | 20.5 | 1.3 | 0.1 | 3.3 | 0.0 | 3.0 | 0.9 | 54.1 | 1.6 | 56.0 | 1.8 | 138.5 | 30.4 | 54.1 | 1.6 | NA |
| -15ATW-47 Spot 9 | 1805 | 47380 | 8.6 | 20.2 | 1.0 | 0.1 | 2.7 | 0.0 | 2.5 | 0.9 | 52.7 | 1.3 | 55.3 | 1.4 | 170.8 | 23.9 | 52.7 | 1.3 | NA |
| -15ATW-47 Spot 18 | 2048 | 8429342 | 5.9 | 19.8 | 1.6 | 0.1 | 4.9 | 0.0 | 4.7 | 0.9 | 52.9 | 2.5 | 56.7 | 2.7 | 222.0 | 37.3 | 52.9 | 2.5 | NA |
| -15ATW-47 Spot 34 | 914 | 8030 | 2.8 | 19.3 | 2.2 | 0.1 | 5.0 | 0.0 | 4.4 | 0.9 | 56.8 | 2.5 | 62.3 | 3.0 | 279.5 | 50.3 | 56.8 | 2.5 | NA |
| -15ATW-47 Spot 11 | 612 | 13987 | 4.3 | 19.2 | 1.8 | 0.1 | 3.3 | 0.0 | 2.7 | 0.8 | 53.2 | 1.4 | 58.8 | 1.9 | 293.4 | 41.7 | 53.2 | 1.4 | NA |
| -15ATW-47 Spot 14 | 1612 | 7677 | 11.1 | 18.0 | 2.6 | 0.1 | 4.4 | 0.0 | 3.6 | 0.8 | 57.0 | 2.1 | 66.8 | 2.9 | 435.6 | 57.3 | 57.0 | 2.1 | NA |
| -15ATW-47 Spot 31 | 646 | 2829 | 5.2 | 9.5 | 8.0 | 0.1 | 8.6 | 0.0 | 3.2 | 0.4 | 58.1 | 1.8 | 125.2 | 10.1 | 1719.2 | 147.2 | 58.1 | 1.8 | NA |

Sample 15ATW51

| Analysis | U | 206Pb | U/Th | 206Pb* | ± | 207Pb* | ± | 206Pb* | ± | error | 206Pb* | ± | 207Pb* | ± | 206Pb* | ± | Best age | ± (1s random) | Conc |
|---|---|---|---|---|---|---|---|---|---|---|---|---|---|---|---|---|---|---|---|

| | (ppm) | 204Pb | | 207Pb* | (%) | 235U* | (%) | 238U | (%) | corr. | 238U* | (Ma) | 235U | (Ma) | 207Pb* | (Ma) | (Ma) | (Ma) | (%) |
|---|---|---|---|---|---|---|---|---|---|---|---|---|---|---|---|---|---|---|---|
| -15ATW-51 Spot 81 | 505 | 21080 | 6.5 | 20.7 | 1.6 | 0.1 | 2.9 | 0.0 | 2.4 | 0.8 | 98.9 | 2.4 | 99.3 | 2.7 | 109.7 | 37.0 | 98.9 | 2.4 | NA |
| -15ATW-51 Spot 79 | 1165 | 13547 | 2.9 | 20.8 | 1.0 | 0.1 | 2.4 | 0.0 | 2.2 | 0.9 | 99.2 | 2.1 | 99.1 | 2.2 | 98.1 | 22.9 | 99.2 | 2.1 | NA |
| -15ATW-51 Spot 65 | 544 | 6807 | 4.6 | 20.9 | 2.6 | 0.1 | 4.0 | 0.0 | 3.0 | 0.8 | 99.8 | 3.0 | 99.4 | 3.8 | 89.6 | 62.2 | 99.8 | 3.0 | NA |
| -15ATW-51 Spot 51 | 681 | 1811587 | 4.0 | 20.7 | 1.1 | 0.1 | 2.4 | 0.0 | 2.2 | 0.9 | 100.2 | 2.2 | 100.7 | 2.3 | 114.3 | 25.6 | 100.2 | 2.2 | NA |
| -15ATW-51 Spot 53 | 714 | 218985 | 4.2 | 20.2 | 1.4 | 0.1 | 2.8 | 0.0 | 2.5 | 0.9 | 100.8 | 2.5 | 103.8 | 2.8 | 174.0 | 33.6 | 100.8 | 2.5 | NA |
| -15ATW-51 Spot 58 | 773 | 88026 | 2.9 | 20.6 | 1.2 | 0.1 | 2.6 | 0.0 | 2.3 | 0.9 | 100.9 | 2.3 | 102.0 | 2.5 | 127.9 | 28.7 | 100.9 | 2.3 | NA |
| -15ATW-51 Spot 72 | 650 | 16274 | 4.0 | 20.8 | 1.0 | 0.1 | 2.4 | 0.0 | 2.2 | 0.9 | 101.0 | 2.2 | 101.1 | 2.4 | 106.4 | 24.1 | 101.0 | 2.2 | NA |
| -15ATW-51 Spot 74 | 648 | 25536 | 4.1 | 20.8 | 1.3 | 0.1 | 2.9 | 0.0 | 2.6 | 0.9 | 101.0 | 2.6 | 101.2 | 2.8 | 107.5 | 31.5 | 101.0 | 2.6 | NA |
| -15ATW-51 Spot 85 | 224 | 7543 | 4.4 | 21.3 | 1.7 | 0.1 | 2.8 | 0.0 | 2.3 | 0.8 | 101.3 | 2.3 | 99.1 | 2.7 | 47.3 | 39.9 | 101.3 | 2.3 | NA |
| -15ATW-51 Spot 84 | 405 | 38120 | 4.9 | 20.6 | 1.2 | 0.1 | 2.6 | 0.0 | 2.3 | 0.9 | 101.3 | 2.3 | 102.5 | 2.5 | 130.2 | 27.6 | 101.3 | 2.3 | NA |
| -15ATW-51 Spot 67 | 231 | 49840 | 11.4 | 20.4 | 1.6 | 0.1 | 3.4 | 0.0 | 3.0 | 0.9 | 101.4 | 3.1 | 103.4 | 3.4 | 151.2 | 38.0 | 101.4 | 3.1 | NA |
| -15ATW-51 Spot 62 | 743 | 32862 | 2.6 | 20.6 | 1.4 | 0.1 | 2.8 | 0.0 | 2.5 | 0.9 | 101.4 | 2.5 | 102.1 | 2.7 | 120.1 | 32.8 | 101.4 | 2.5 | NA |
| -15ATW-51 Spot 59 | 471 | 70335 | 4.7 | 20.7 | 1.4 | 0.1 | 2.9 | 0.0 | 2.6 | 0.9 | 101.4 | 2.6 | 101.9 | 2.8 | 113.0 | 33.8 | 101.4 | 2.6 | NA |
| -15ATW-51 Spot 76 | 550 | 14295 | 4.7 | 20.8 | 1.5 | 0.1 | 2.5 | 0.0 | 2.0 | 0.8 | 101.5 | 2.1 | 101.8 | 2.5 | 108.1 | 35.4 | 101.5 | 2.1 | NA |
| -15ATW-51 Spot 75 | 423 | 27838 | 6.6 | 20.6 | 1.4 | 0.1 | 2.9 | 0.0 | 2.6 | 0.9 | 101.5 | 2.6 | 102.3 | 2.9 | 121.1 | 32.2 | 101.5 | 2.6 | NA |
| -15ATW-51 Spot 54 | 504 | 12278 | 6.5 | 20.9 | 1.5 | 0.1 | 2.9 | 0.0 | 2.5 | 0.9 | 101.8 | 2.5 | 101.2 | 2.8 | 87.2 | 36.1 | 101.8 | 2.5 | NA |
| -15ATW-51 Spot 73 | 809 | 19719 | 3.2 | 20.9 | 1.3 | 0.1 | 2.6 | 0.0 | 2.3 | 0.9 | 101.9 | 2.3 | 101.4 | 2.6 | 92.1 | 31.3 | 101.9 | 2.3 | NA |
| -15ATW-51 Spot 88 | 783 | 99491 | 3.4 | 20.2 | 1.2 | 0.1 | 2.5 | 0.0 | 2.1 | 0.9 | 102.1 | 2.2 | 104.7 | 2.4 | 166.5 | 28.0 | 102.1 | 2.2 | NA |
| -15ATW-51 Spot 78 | 442 | 28951 | 4.6 | 20.8 | 1.3 | 0.1 | 2.4 | 0.0 | 2.1 | 0.9 | 102.1 | 2.1 | 102.2 | 2.4 | 104.7 | 29.8 | 102.1 | 2.1 | NA |
| -15ATW-51 Spot 66 | 633 | 83781 | 6.3 | 20.1 | 1.3 | 0.1 | 2.4 | 0.0 | 2.1 | 0.8 | 102.1 | 2.1 | 105.5 | 2.4 | 183.5 | 30.7 | 102.1 | 2.1 | NA |
| -15ATW-51 Spot 57 | 866 | 42364 | 2.4 | 20.9 | 1.3 | 0.1 | 2.5 | 0.0 | 2.1 | 0.9 | 102.2 | 2.2 | 101.5 | 2.4 | 86.2 | 29.8 | 102.2 | 2.2 | NA |
| -15ATW-51 Spot 87 | 363 | 12441 | 3.8 | 20.6 | 1.8 | 0.1 | 2.9 | 0.0 | 2.3 | 0.8 | 102.3 | 2.3 | 103.2 | 2.9 | 125.7 | 43.0 | 102.3 | 2.3 | NA |
| -15ATW-51 Spot 68 | 687 | 16981 | 3.9 | 20.6 | 1.5 | 0.1 | 3.5 | 0.0 | 3.1 | 0.9 | 102.3 | 3.2 | 103.3 | 3.4 | 127.2 | 35.0 | 102.3 | 3.2 | NA |
| -15ATW-51 Spot 90 | 417 | 24280 | 6.1 | 20.7 | 1.3 | 0.1 | 2.9 | 0.0 | 2.6 | 0.9 | 102.7 | 2.6 | 102.9 | 2.8 | 110.8 | 31.0 | 102.7 | 2.6 | NA |
| -15ATW-51 Spot 61 | 365 | 14648 | 7.0 | 21.1 | 1.5 | 0.1 | 2.7 | 0.0 | 2.3 | 0.8 | 102.8 | 2.4 | 101.6 | 2.7 | 74.3 | 35.2 | 102.8 | 2.4 | NA |
| -15ATW-51 Spot 89 | 439 | 26304 | 4.1 | 20.9 | 1.3 | 0.1 | 2.7 | 0.0 | 2.4 | 0.9 | 102.8 | 2.4 | 102.4 | 2.6 | 93.6 | 31.3 | 102.8 | 2.4 | NA |
| -15ATW-51 Spot 63 | 624 | 23049 | 2.5 | 20.5 | 1.3 | 0.1 | 3.1 | 0.0 | 2.8 | 0.9 | 103.0 | 2.8 | 104.4 | 3.0 | 136.4 | 30.8 | 103.0 | 2.8 | NA |
| -15ATW-51 Spot 70 | 374 | 8564 | 5.2 | 21.4 | 1.7 | 0.1 | 3.6 | 0.0 | 3.2 | 0.9 | 103.1 | 3.2 | 100.5 | 3.4 | 40.5 | 41.7 | 103.1 | 3.2 | NA |
| -15ATW-51 Spot 71 | 356 | 37085 | 3.0 | 20.5 | 1.3 | 0.1 | 3.4 | 0.0 | 3.2 | 0.9 | 103.5 | 3.2 | 104.8 | 3.4 | 135.6 | 30.5 | 103.5 | 3.2 | NA |
| -15ATW-51 Spot 82 | 524 | 40399 | 2.6 | 20.8 | 1.5 | 0.1 | 3.2 | 0.0 | 2.8 | 0.9 | 103.7 | 2.9 | 103.9 | 3.2 | 107.9 | 35.4 | 103.7 | 2.9 | NA |
| -15ATW-51 Spot 92 | 416 | 20629 | 5.5 | 20.7 | 1.6 | 0.1 | 2.8 | 0.0 | 2.3 | 0.8 | 104.0 | 2.3 | 104.4 | 2.8 | 116.3 | 37.9 | 104.0 | 2.3 | NA |
| -15ATW-51 Spot 69 | 630 | 47191 | 4.6 | 20.4 | 1.5 | 0.1 | 3.2 | 0.0 | 2.8 | 0.9 | 104.2 | 2.9 | 106.1 | 3.2 | 151.9 | 35.3 | 104.2 | 2.9 | NA |
| -15ATW-51 Spot 91 | 368 | 39620 | 3.0 | 20.2 | 1.6 | 0.1 | 3.6 | 0.0 | 3.2 | 0.9 | 104.4 | 3.3 | 107.0 | 3.6 | 166.7 | 38.3 | 104.4 | 3.3 | NA |

| | | | | | | | | | | | | | | | | | | | |
|---|---|---|---|---|---|---|---|---|---|---|---|---|---|---|---|---|---|---|---|
| -15ATW-51 Spot 52 | 943 | 34333 | 2.2 | 20.6 | 1.4 | 0.1 | 2.7 | 0.0 | 2.3 | 0.8 | 104.5 | 2.3 | 105.2 | 2.7 | 122.4 | 33.9 | 104.5 | 2.3 | NA |
| -15ATW-51 Spot 83 | 511 | 9346 | 3.5 | 21.2 | 1.2 | 0.1 | 2.6 | 0.0 | 2.3 | 0.9 | 105.0 | 2.4 | 103.1 | 2.5 | 60.5 | 28.5 | 105.0 | 2.4 | NA |
| -15ATW-51 Spot 86 | 603 | 72685 | 3.1 | 20.3 | 1.0 | 0.1 | 2.3 | 0.0 | 2.0 | 0.9 | 107.0 | 2.2 | 109.2 | 2.3 | 158.3 | 22.8 | 107.0 | 2.2 | NA |
| -15ATW-51 Spot 55 | 350 | 3886333 | 3.5 | 20.8 | 1.7 | 0.1 | 2.7 | 0.0 | 2.1 | 0.8 | 107.0 | 2.2 | 106.9 | 2.8 | 105.1 | 41.2 | 107.0 | 2.2 | NA |
| -15ATW-51 Spot 60 | 349 | 6518 | 4.3 | 20.9 | 1.4 | 0.1 | 3.1 | 0.0 | 2.8 | 0.9 | 107.8 | 3.0 | 106.9 | 3.2 | 87.3 | 32.9 | 107.8 | 3.0 | NA |
| -15ATW-51 Spot 64 | 1118 | 85731 | 1.8 | 19.9 | 1.4 | 0.1 | 2.6 | 0.0 | 2.2 | 0.8 | 100.9 | 2.2 | 105.1 | 2.6 | 203.9 | 32.7 | 100.9 | 2.2 | NA |
| -15ATW-51 Spot 56 | 420 | 25485 | 4.7 | 19.8 | 1.2 | 0.1 | 2.7 | 0.0 | 2.4 | 0.9 | 103.1 | 2.5 | 108.0 | 2.8 | 218.0 | 27.5 | 103.1 | 2.5 | NA |

Sample 16ATW49

| Analysis | U | 206Pb | U/Th | 206Pb * | ± | 207Pb * | ± | 206Pb * | ± | erro r | 206Pb * | ± | 207Pb * | ± | 206Pb * | ± | Best age | ± (1s rando m) | Conc |
|---|---|---|---|---|---|---|---|---|---|---|---|---|---|---|---|---|---|---|---|
| | (ppm) | 204Pb | | 207Pb * | (%) | 235U * | (%) | 238U | (%) | corr . | 238U * | (Ma) | 235U | (Ma) | 207Pb * | (Ma) | (Ma) | (Ma) | (%) |
| -16ATW-49 Spot 23 | 460 | 91058 | 4.3 | 18.9 | 0.6 | 0.3 | 1.1 | 0.0 | 0.9 | 0.8 | 301.4 | 2.6 | 303.8 | 2.8 | 322.4 | 13.9 | 301.4 | 2.6 | NA |
| -16ATW-49 Spot 9 | 227 | 289596 | 4.2 | 18.8 | 1.0 | 0.4 | 1.4 | 0.0 | 1.0 | 0.7 | 302.7 | 2.9 | 306.7 | 3.8 | 337.0 | 23.2 | 302.7 | 2.9 | NA |
| -16ATW-49 Spot 1 | 381 | 97056 | 4.0 | 19.1 | 0.6 | 0.4 | 1.4 | 0.0 | 1.2 | 0.9 | 306.5 | 3.7 | 306.2 | 3.7 | 303.8 | 14.8 | 306.5 | 3.7 | NA |
| -16ATW-49 Spot 4 | 395 | 701147 | 3.5 | 18.9 | 0.8 | 0.4 | 1.5 | 0.0 | 1.2 | 0.9 | 307.0 | 3.7 | 309.2 | 3.9 | 325.9 | 17.2 | 307.0 | 3.7 | NA |
| -16ATW-49 Spot 11 | 1017 | 720228 | 2.8 | 19.0 | 0.9 | 0.4 | 1.5 | 0.0 | 1.3 | 0.8 | 309.7 | 3.8 | 310.5 | 4.1 | 316.2 | 20.1 | 309.7 | 3.8 | NA |
| -16ATW-49 Spot 19 | 948 | 76186 | 2.8 | 19.1 | 0.6 | 0.4 | 1.1 | 0.0 | 0.9 | 0.8 | 310.1 | 2.8 | 309.4 | 2.9 | 304.4 | 14.0 | 310.1 | 2.8 | NA |
| -16ATW-49 Spot 12 | 233 | 126480 | 5.9 | 18.9 | 0.8 | 0.4 | 1.4 | 0.0 | 1.1 | 0.8 | 311.1 | 3.4 | 312.7 | 3.7 | 324.6 | 18.3 | 311.1 | 3.4 | NA |
| -16ATW-49 Spot 10 | 494 | 337175 | 4.9 | 19.1 | 0.7 | 0.4 | 1.5 | 0.0 | 1.3 | 0.9 | 311.7 | 4.0 | 309.7 | 3.9 | 294.9 | 15.1 | 311.7 | 4.0 | NA |
| -16ATW-49 Spot 13 | 429 | 158127 | 3.0 | 19.2 | 0.7 | 0.4 | 1.3 | 0.0 | 1.1 | 0.8 | 313.0 | 3.3 | 310.5 | 3.5 | 292.1 | 16.0 | 313.0 | 3.3 | NA |
| -16ATW-49 Spot 8 | 655 | 96378 | 3.5 | 18.8 | 0.7 | 0.4 | 1.4 | 0.0 | 1.2 | 0.9 | 313.3 | 3.7 | 315.5 | 3.7 | 331.8 | 14.8 | 313.3 | 3.7 | NA |
| -16ATW-49 Spot 2 | 736 | 92492 | 2.6 | 18.9 | 0.8 | 0.4 | 1.3 | 0.0 | 1.1 | 0.8 | 314.2 | 3.2 | 315.3 | 3.6 | 323.6 | 17.9 | 314.2 | 3.2 | NA |
| -16ATW-49 Spot 24 | 663 | 184111 | 2.9 | 19.0 | 0.7 | 0.4 | 1.6 | 0.0 | 1.4 | 0.9 | 314.2 | 4.2 | 313.4 | 4.2 | 307.3 | 16.9 | 314.2 | 4.2 | NA |
| -16ATW-49 Spot 14 | 427 | 104130 | 4.2 | 19.1 | 0.9 | 0.4 | 1.4 | 0.1 | 1.1 | 0.8 | 316.5 | 3.4 | 314.3 | 3.8 | 297.9 | 20.3 | 316.5 | 3.4 | NA |
| -16ATW-49 Spot 22 | 226 | 189160 | 5.4 | 19.4 | 0.9 | 0.4 | 1.6 | 0.1 | 1.3 | 0.8 | 318.1 | 4.0 | 312.1 | 4.2 | 267.8 | 20.3 | 318.1 | 4.0 | NA |
| -16ATW-49 Spot 7 | 451 | 498360 | 3.2 | 19.1 | 0.8 | 0.4 | 1.3 | 0.1 | 1.1 | 0.8 | 318.5 | 3.4 | 316.9 | 3.7 | 304.7 | 17.9 | 318.5 | 3.4 | NA |
| -16ATW-49 Spot 16 | 221 | 298468 | 4.4 | 18.8 | 0.8 | 0.4 | 1.4 | 0.1 | 1.2 | 0.8 | 318.6 | 3.7 | 320.3 | 3.9 | 332.5 | 17.5 | 318.6 | 3.7 | NA |
| -16ATW-49 Spot 21 | 226 | 51725 | 3.2 | 19.2 | 1.0 | 0.4 | 1.8 | 0.1 | 1.5 | 0.8 | 319.9 | 4.5 | 315.9 | 4.8 | 286.2 | 22.6 | 319.9 | 4.5 | NA |
| -16ATW-49 Spot 25 | 620 | 291760 | 3.4 | 19.2 | 0.5 | 0.4 | 1.2 | 0.1 | 1.1 | 0.9 | 320.3 | 3.5 | 317.0 | 3.3 | 293.1 | 11.8 | 320.3 | 3.5 | NA |
| -16ATW-49 Spot 20 | 716 | 107587 | 3.2 | 19.1 | 0.7 | 0.4 | 1.3 | 0.1 | 1.1 | 0.8 | 320.8 | 3.4 | 317.9 | 3.5 | 296.4 | 15.5 | 320.8 | 3.4 | NA |
| -16ATW-49 Spot 17 | 499 | 122887 | 3.6 | 19.0 | 0.8 | 0.4 | 1.6 | 0.1 | 1.3 | 0.8 | 321.2 | 4.2 | 319.4 | 4.3 | 306.1 | 19.0 | 321.2 | 4.2 | NA |
| -16ATW-49 Spot 5 | 235 | 101526 | 5.4 | 19.1 | 0.8 | 0.4 | 1.4 | 0.1 | 1.2 | 0.8 | 321.6 | 3.6 | 319.0 | 3.9 | 300.7 | 19.1 | 321.6 | 3.6 | NA |
| -16ATW-49 Spot 6 | 263 | 54876 | 4.6 | 19.0 | 0.9 | 0.4 | 1.6 | 0.1 | 1.3 | 0.8 | 324.1 | 4.1 | 322.2 | 4.4 | 308.5 | 20.5 | 324.1 | 4.1 | NA |
| -16ATW-49 Spot 15 | 216 | 20693 | 4.6 | 19.4 | 0.8 | 0.4 | 1.4 | 0.1 | 1.2 | 0.8 | 319.6 | 3.6 | 313.4 | 3.7 | 268.3 | 17.2 | 319.6 | 3.6 | NA |

| | | | | | | | | | | | | | | | | | | |
|---|---|---|---|---|---|---|---|---|---|---|---|---|---|---|---|---|---|---|
| -16ATW-49 Spot 18 | 475 | 90604 | 2.5 | 19.2 | 0.7 | 0.4 | 1.3 | 0.1 | 1.1 | 0.8 | 338.2 | 3.7 | 331.6 | 3.7 | 285.6 | 16.0 | 338.2 | 3.7 | NA |
| -16ATW-49 Spot 3 | 815 | 189114 | 2.6 | 19.2 | 0.7 | 0.4 | 1.4 | 0.1 | 1.2 | 0.9 | 329.7 | 3.9 | 324.2 | 3.9 | 284.7 | 16.2 | 329.7 | 3.9 | NA |

Sample 16ATW82

| Analysis | U | 206Pb | U/Th | 206Pb * | ± | 207Pb * | ± | 206Pb * | ± | error | 206Pb * | ± | 207Pb * | ± | 206Pb * | ± | Best age | ± (1s Random) | Conc |
|---|---|---|---|---|---|---|---|---|---|---|---|---|---|---|---|---|---|---|---|
| | (ppm) | 204Pb | | 207Pb * | (%) | 235U * | (%) | 238U | (%) | corr. | 238U * | (Ma) | 235U | (Ma) | 207Pb * | (Ma) | (Ma) | (Ma) | (%) |
| -16ATW-82 Spot 27 | 785 | 107579 | 3.8 | 19.1 | 0.7 | 0.3 | 1.5 | 0.0 | 1.3 | 0.9 | 299.2 | 3.9 | 299.1 | 3.9 | 298.2 | 15.5 | 299.2 | 3.9 | NA |
| -16ATW-82 Spot 28 | 378 | 41504 | 5.9 | 19.1 | 0.7 | 0.3 | 1.3 | 0.0 | 1.2 | 0.9 | 303.3 | 3.5 | 303.4 | 3.5 | 304.2 | 15.0 | 303.3 | 3.5 | NA |
| -16ATW-82 Spot 22 | 340 | 53705 | 5.6 | 19.1 | 0.6 | 0.3 | 1.2 | 0.0 | 1.0 | 0.8 | 303.9 | 3.0 | 303.2 | 3.1 | 298.1 | 14.6 | 303.9 | 3.0 | NA |
| -16ATW-82 Spot 21 | 569 | 291432 | 6.1 | 18.8 | 0.9 | 0.4 | 1.5 | 0.0 | 1.2 | 0.8 | 306.5 | 3.7 | 310.3 | 4.1 | 339.3 | 20.3 | 306.5 | 3.7 | NA |
| -16ATW-82 Spot 24 | 480 | 155997 | 4.8 | 18.6 | 1.2 | 0.4 | 1.5 | 0.0 | 1.0 | 0.7 | 306.6 | 3.0 | 313.6 | 4.1 | 366.1 | 26.1 | 306.6 | 3.0 | NA |
| -16ATW-82 Spot 20 | 478 | 472289 | 7.4 | 19.1 | 0.8 | 0.4 | 1.2 | 0.0 | 1.0 | 0.8 | 306.7 | 2.9 | 305.3 | 3.3 | 294.7 | 17.9 | 306.7 | 2.9 | NA |
| -16ATW-82 Spot 25 | 365 | 123793 | 5.8 | 19.1 | 0.7 | 0.4 | 1.4 | 0.0 | 1.2 | 0.9 | 309.6 | 3.6 | 308.9 | 3.7 | 303.2 | 15.4 | 309.6 | 3.6 | NA |
| -16ATW-82 Spot 2 | 370 | 70574 | 7.3 | 19.2 | 0.8 | 0.4 | 1.5 | 0.0 | 1.3 | 0.8 | 309.6 | 3.9 | 307.6 | 4.1 | 292.2 | 18.6 | 309.6 | 3.9 | NA |
| -16ATW-82 Spot 11 | 385 | 43611 | 4.9 | 19.2 | 1.2 | 0.4 | 1.7 | 0.0 | 1.2 | 0.7 | 310.3 | 3.6 | 307.3 | 4.5 | 285.0 | 27.2 | 310.3 | 3.6 | NA |
| -16ATW-82 Spot 16 | 398 | 27195 | 6.7 | 18.9 | 0.9 | 0.4 | 1.5 | 0.0 | 1.2 | 0.8 | 310.4 | 3.5 | 311.6 | 3.9 | 320.5 | 20.6 | 310.4 | 3.5 | NA |
| -16ATW-82 Spot 15 | 453 | 114090 | 6.2 | 19.2 | 0.7 | 0.4 | 1.5 | 0.0 | 1.3 | 0.9 | 310.5 | 3.9 | 307.8 | 3.9 | 287.3 | 16.2 | 310.5 | 3.9 | NA |
| -16ATW-82 Spot 18 | 364 | 114116 | 7.6 | 19.2 | 0.8 | 0.4 | 1.4 | 0.0 | 1.1 | 0.8 | 312.0 | 3.5 | 309.3 | 3.7 | 288.8 | 18.4 | 312.0 | 3.5 | NA |
| -16ATW-82 Spot 3 | 368 | 46702 | 6.9 | 19.1 | 0.8 | 0.4 | 1.4 | 0.0 | 1.1 | 0.8 | 312.6 | 3.4 | 311.5 | 3.7 | 303.7 | 17.7 | 312.6 | 3.4 | NA |
| -16ATW-82 Spot 12 | 589 | 213329 | 6.1 | 19.0 | 0.7 | 0.4 | 1.4 | 0.0 | 1.2 | 0.9 | 312.7 | 3.7 | 312.1 | 3.8 | 307.6 | 16.2 | 312.7 | 3.7 | NA |
| -16ATW-82 Spot 23 | 463 | 127687 | 4.8 | 19.0 | 0.7 | 0.4 | 1.4 | 0.0 | 1.2 | 0.9 | 314.0 | 3.7 | 314.4 | 3.8 | 317.3 | 16.3 | 314.0 | 3.7 | NA |
| -16ATW-82 Spot 13 | 618 | 1050994 | 4.9 | 19.1 | 0.8 | 0.4 | 1.3 | 0.1 | 1.0 | 0.8 | 316.2 | 3.0 | 314.2 | 3.5 | 299.3 | 18.6 | 316.2 | 3.0 | NA |
| -16ATW-82 Spot 10 | 350 | 119458 | 4.3 | 19.0 | 0.8 | 0.4 | 1.2 | 0.1 | 0.9 | 0.8 | 317.9 | 2.9 | 317.7 | 3.3 | 316.0 | 17.6 | 317.9 | 2.9 | NA |
| -16ATW-82 Spot 30 | 602 | 52345 | 4.9 | 19.1 | 0.9 | 0.4 | 1.5 | 0.1 | 1.2 | 0.8 | 319.2 | 3.7 | 316.4 | 4.1 | 295.9 | 21.3 | 319.2 | 3.7 | NA |
| -16ATW-82 Spot 8 | 804 | 5145215 | 3.9 | 19.0 | 0.9 | 0.4 | 1.6 | 0.1 | 1.3 | 0.8 | 319.7 | 4.2 | 318.2 | 4.4 | 307.0 | 20.9 | 319.7 | 4.2 | NA |
| -16ATW-82 Spot 17 | 293 | 179434 | 7.1 | 19.2 | 1.0 | 0.4 | 1.6 | 0.1 | 1.3 | 0.8 | 322.4 | 4.0 | 318.0 | 4.4 | 286.1 | 23.2 | 322.4 | 4.0 | NA |
| -16ATW-82 Spot 1 | 431 | 19593 | 6.0 | 16.5 | 1.1 | 0.4 | 1.5 | 0.0 | 1.0 | 0.6 | 297.6 | 2.8 | 337.6 | 4.3 | 623.5 | 24.7 | 297.6 | 2.8 | NA |
| -16ATW-82 Spot 26 | 648 | 3611 | 3.8 | 6.8 | 12.7 | 1.0 | 12.8 | 0.0 | 1.2 | 0.1 | 307.5 | 3.7 | 701.1 | 64.9 | 2318.7 | 219.4 | 307.5 | 3.7 | NA |
| -16ATW-82 Spot 4 | 660 | 17671 | 3.7 | 16.3 | 1.7 | 0.4 | 2.0 | 0.0 | 1.1 | 0.5 | 308.9 | 3.3 | 353.0 | 5.9 | 654.8 | 35.7 | 308.9 | 3.3 | NA |
| -16ATW-82 Spot 14 | 424 | 81323 | 5.8 | 17.8 | 0.8 | 0.4 | 1.4 | 0.0 | 1.1 | 0.8 | 309.5 | 3.3 | 327.0 | 3.8 | 453.8 | 18.5 | 309.5 | 3.3 | NA |
| -16ATW-82 Spot 9 | 397 | 21764 | 5.7 | 16.4 | 2.0 | 0.4 | 2.2 | 0.0 | 1.1 | 0.5 | 309.9 | 3.2 | 351.4 | 6.6 | 635.9 | 42.2 | 309.9 | 3.2 | NA |
| -16ATW-82 Spot 29 | 403 | 9846 | 5.3 | 15.3 | 1.9 | 0.4 | 2.2 | 0.0 | 1.2 | 0.5 | 313.7 | 3.6 | 375.8 | 6.9 | 779.1 | 39.0 | 313.7 | 3.6 | NA |
| -16ATW-82 Spot 6 | 557 | 48768 | 4.6 | 18.2 | 0.8 | 0.4 | 1.3 | 0.0 | 1.0 | 0.8 | 307.3 | 3.1 | 318.9 | 3.6 | 404.4 | 18.3 | 307.3 | 3.1 | NA |

| | | | | | | | | | | | | | | | | | | |
|---|---|---|---|---|---|---|---|---|---|---|---|---|---|---|---|---|---|---|
| -16ATW-82 Spot 19 | 779 | 79088 | 4.5 | 18.3 | 1.5 | 0.4 | 2.1 | 0.0 | 1.5 | 0.7 | 305.6 | 4.3 | 316.6 | 5.8 | 398.6 | 34.4 | 305.6 | 4.3 | NA |
| -16ATW-82 Spot 5 | 429 | 53562 | 6.0 | 19.6 | 0.8 | 0.3 | 1.5 | 0.0 | 1.3 | 0.8 | 305.2 | 3.8 | 298.2 | 3.9 | 244.0 | 18.8 | 305.2 | 3.8 | NA |
| -16ATW-82 Spot 7 | 585 | 106846 | 4.0 | 19.5 | 0.6 | 0.4 | 1.3 | 0.1 | 1.1 | 0.9 | 319.0 | 3.6 | 311.7 | 3.5 | 257.7 | 14.1 | 319.0 | 3.6 | NA |

Sample 16ATW83

| Analysis | U | 206Pb | U/Th | 206Pb* | ± | 207Pb* | ± | 206Pb* | ± | error | 206Pb* | ± | 207Pb* | ± | 206Pb* | ± | Best age | ± (1s random) | Conc |
|---|---|---|---|---|---|---|---|---|---|---|---|---|---|---|---|---|---|---|---|
| | (ppm) | 204Pb | | 207Pb* | (%) | 235U* | (%) | 238U | (%) | corr. | 238U* | (Ma) | 235U | (Ma) | 207Pb* | (Ma) | (Ma) | (Ma) | (%) |
| -16ATW-83 Spot 50 | 174 | 1303892 | 5.4 | 19.1 | 1.0 | 0.3 | 1.5 | 0.0 | 1.2 | 0.8 | 298.5 | 3.4 | 298.9 | 4.0 | 301.8 | 23.2 | 298.5 | 3.4 | 98.9 |
| -16ATW-83 Spot 62 | 1576 | 1870325 | 3.3 | 19.0 | 0.8 | 0.3 | 1.4 | 0.0 | 1.2 | 0.8 | 301.4 | 3.6 | 302.3 | 3.8 | 309.4 | 17.3 | 301.4 | 3.6 | 97.4 |
| -16ATW-83 Spot 53 | 389 | 110881 | 3.7 | 18.9 | 0.7 | 0.3 | 1.3 | 0.0 | 1.1 | 0.8 | 301.4 | 3.3 | 303.8 | 3.5 | 322.5 | 16.2 | 301.4 | 3.3 | 93.5 |
| -16ATW-83 Spot 51 | 345 | 34324 | 4.5 | 19.0 | 0.8 | 0.3 | 1.4 | 0.0 | 1.2 | 0.8 | 302.4 | 3.5 | 302.9 | 3.7 | 306.4 | 18.6 | 302.4 | 3.5 | 98.7 |
| -16ATW-83 Spot 57 | 1162 | 197511 | 2.5 | 19.2 | 0.7 | 0.3 | 1.2 | 0.0 | 1.0 | 0.8 | 302.4 | 3.0 | 300.6 | 3.2 | 286.6 | 15.9 | 302.4 | 3.0 | 105.5 |
| -16ATW-83 Spot 70 | 1758 | 242937 | 3.0 | 19.1 | 0.6 | 0.3 | 1.2 | 0.0 | 1.0 | 0.9 | 302.4 | 3.0 | 301.7 | 3.1 | 296.3 | 14.0 | 302.4 | 3.0 | 102.1 |
| -16ATW-83 Spot 48 | 1664 | 398014 | 2.7 | 18.8 | 0.8 | 0.4 | 1.6 | 0.0 | 1.4 | 0.9 | 303.3 | 4.3 | 306.5 | 4.3 | 330.6 | 17.4 | 303.3 | 4.3 | 91.7 |
| -16ATW-83 Spot 42 | 694 | 103978 | 4.1 | 19.2 | 0.8 | 0.3 | 1.4 | 0.0 | 1.2 | 0.8 | 303.4 | 3.4 | 301.3 | 3.6 | 284.9 | 17.6 | 303.4 | 3.4 | 106.5 |
| -16ATW-83 Spot 46 | 594 | 108160 | 2.6 | 18.9 | 0.9 | 0.4 | 1.6 | 0.0 | 1.4 | 0.8 | 304.1 | 4.1 | 305.9 | 4.3 | 320.0 | 20.1 | 304.1 | 4.1 | 95.0 |
| -16ATW-83 Spot 60 | 244 | 349625 | 6.1 | 18.8 | 0.9 | 0.4 | 1.6 | 0.0 | 1.3 | 0.8 | 305.5 | 3.9 | 309.2 | 4.2 | 336.9 | 19.3 | 305.5 | 3.9 | 90.7 |
| -16ATW-83 Spot 64 | 1004 | 209962 | 3.4 | 19.1 | 0.8 | 0.3 | 1.5 | 0.0 | 1.3 | 0.9 | 305.5 | 3.8 | 304.6 | 3.9 | 297.5 | 17.2 | 305.5 | 3.8 | 102.7 |
| -16ATW-83 Spot 40 | 450 | 66692 | 4.8 | 19.1 | 0.8 | 0.4 | 1.4 | 0.0 | 1.1 | 0.8 | 306.1 | 3.4 | 305.2 | 3.7 | 298.1 | 19.2 | 306.1 | 3.4 | 102.7 |
| -16ATW-83 Spot 61 | 985 | 112383 | 4.5 | 18.9 | 0.6 | 0.4 | 1.4 | 0.0 | 1.3 | 0.9 | 307.0 | 3.8 | 309.2 | 3.7 | 326.0 | 14.0 | 307.0 | 3.8 | 94.2 |
| -16ATW-83 Spot 39 | 803 | 1735690 | 4.5 | 19.0 | 0.7 | 0.4 | 1.2 | 0.0 | 1.0 | 0.8 | 307.2 | 3.1 | 307.3 | 3.3 | 307.5 | 15.1 | 307.2 | 3.1 | 99.9 |
| -16ATW-83 Spot 43 | 584 | 101965 | 7.2 | 19.1 | 0.7 | 0.4 | 1.5 | 0.0 | 1.3 | 0.9 | 307.4 | 4.0 | 306.0 | 4.0 | 295.2 | 16.0 | 307.4 | 4.0 | 104.1 |
| -16ATW-83 Spot 63 | 971 | 403884 | 2.9 | 19.2 | 0.7 | 0.4 | 1.4 | 0.0 | 1.2 | 0.9 | 308.2 | 3.6 | 306.5 | 3.8 | 293.3 | 16.9 | 308.2 | 3.6 | 105.1 |
| -16ATW-83 Spot 44 | 900 | 100699 | 4.3 | 19.1 | 0.6 | 0.4 | 1.3 | 0.0 | 1.1 | 0.9 | 308.2 | 3.3 | 307.3 | 3.4 | 300.1 | 13.8 | 308.2 | 3.3 | 102.7 |
| -16ATW-83 Spot 38 | 859 | 329862 | 5.1 | 19.1 | 0.6 | 0.4 | 1.2 | 0.0 | 1.0 | 0.9 | 308.7 | 3.1 | 307.6 | 3.2 | 299.3 | 14.0 | 308.7 | 3.1 | 103.2 |
| -16ATW-83 Spot 65 | 980 | 99983 | 3.6 | 18.8 | 0.7 | 0.4 | 1.3 | 0.0 | 1.1 | 0.8 | 309.3 | 3.2 | 311.8 | 3.4 | 330.3 | 15.1 | 309.3 | 3.2 | 93.7 |
| -16ATW-83 Spot 52 | 355 | 200152 | 5.0 | 18.8 | 0.9 | 0.4 | 1.5 | 0.0 | 1.3 | 0.8 | 309.7 | 3.8 | 313.0 | 4.1 | 337.0 | 19.3 | 309.7 | 3.8 | 91.9 |
| -16ATW-83 Spot 55 | 1733 | 359674 | 2.7 | 19.2 | 0.6 | 0.4 | 1.1 | 0.0 | 1.0 | 0.9 | 310.1 | 3.0 | 307.4 | 3.0 | 286.9 | 12.8 | 310.1 | 3.0 | 108.1 |
| -16ATW-83 Spot 68 | 1170 | 124982 | 3.5 | 18.8 | 0.6 | 0.4 | 1.1 | 0.0 | 1.0 | 0.9 | 310.3 | 3.0 | 313.5 | 3.1 | 336.7 | 13.2 | 310.3 | 3.0 | 92.2 |
| -16ATW-83 Spot 54 | 1050 | 199270 | 4.5 | 19.1 | 0.7 | 0.4 | 1.2 | 0.0 | 1.0 | 0.8 | 310.7 | 3.0 | 309.1 | 3.3 | 296.7 | 16.5 | 310.7 | 3.0 | 104.7 |
| -16ATW-83 Spot 37 | 155 | 112604 | 7.6 | 18.6 | 1.3 | 0.4 | 1.6 | 0.0 | 1.0 | 0.6 | 311.0 | 3.1 | 316.8 | 4.5 | 359.7 | 29.1 | 311.0 | 3.1 | 86.5 |
| -16ATW-83 Spot 59 | 437 | 103733 | 4.7 | 19.1 | 0.8 | 0.4 | 1.5 | 0.0 | 1.3 | 0.8 | 311.2 | 3.8 | 310.5 | 3.9 | 305.7 | 17.7 | 311.2 | 3.8 | 101.8 |
| -16ATW-83 Spot 67 | 1505 | 600967 | 3.5 | 19.1 | 0.7 | 0.4 | 1.3 | 0.0 | 1.1 | 0.8 | 312.8 | 3.3 | 310.9 | 3.4 | 296.2 | 15.9 | 312.8 | 3.3 | 105.6 |
| -16ATW-83 Spot 45 | 334 | 97374 | 3.3 | 19.0 | 0.8 | 0.4 | 1.5 | 0.1 | 1.3 | 0.9 | 314.6 | 3.9 | 314.6 | 4.0 | 314.4 | 17.8 | 314.6 | 3.9 | 100.1 |

| | | | | | | | | | | | | | | | | | | | |
|---|---|---|---|---|---|---|---|---|---|---|---|---|---|---|---|---|---|---|---|
| -16ATW-83 Spot 49 | 1437 | 2274564 | 4.4 | 18.9 | 0.7 | 0.4 | 1.2 | 0.1 | 1.0 | 0.8 | 319.4 | 3.0 | 319.3 | 3.3 | 318.8 | 16.3 | 319.4 | 3.0 | 100.2 |
| -16ATW-83 Spot 47 | 789 | 383071 | 5.6 | 18.9 | 0.6 | 0.4 | 1.3 | 0.1 | 1.2 | 0.9 | 324.5 | 3.7 | 324.0 | 3.7 | 320.8 | 14.6 | 324.5 | 3.7 | 101.1 |
| -16ATW-83 Spot 41 | 486 | 27482 | 3.8 | 17.7 | 1.9 | 0.4 | 2.2 | 0.0 | 1.1 | 0.5 | 310.7 | 3.2 | 329.9 | 6.1 | 467.2 | 42.0 | 310.7 | 3.2 | 66.5 |
| -16ATW-83 Spot 66 | 758 | 27555 | 4.6 | 17.3 | 1.1 | 0.4 | 1.7 | 0.1 | 1.3 | 0.8 | 318.0 | 4.0 | 344.2 | 4.9 | 525.5 | 23.5 | 318.0 | 4.0 | 60.5 |
| -16ATW-83 Spot 56 | 1424 | 422177 | 4.8 | 18.6 | 0.8 | 0.4 | 1.4 | 0.0 | 1.2 | 0.8 | 298.6 | 3.4 | 305.4 | 3.7 | 358.3 | 17.1 | 298.6 | 3.4 | 83.3 |
| -16ATW-83 Spot 58 | 1329 | 151341 | 3.4 | 18.7 | 0.6 | 0.4 | 1.4 | 0.0 | 1.2 | 0.9 | 306.1 | 3.6 | 310.9 | 3.7 | 347.2 | 14.2 | 306.1 | 3.6 | 88.2 |

# Supplemental file S3

Table S3-1: $^{40}Ar/^{39}Ar$ data

**16ATW-36**
**MU#L1**

Weighted average of J from standards = 5.073e-03 +/- 2.571e-05

| Laser Power | Cumulative 39Ar | 40Ar/39Ar meas. | +/- | 37Ar/39Ar meas. | +/- | 36Ar/39Ar meas. | +/- | % Atm. 40Ar | +/- | Ca/K | +/- | Cl/K | +/- | 40*/39K | +/- | Age (Ma) | +/- (Ma) |
|---|---|---|---|---|---|---|---|---|---|---|---|---|---|---|---|---|---|
| (mW) | | | | | | | | | | | | | | | | | |
| 500.00 | 0.00 | 46.44 | 0.92 | 0.06 | 0.02 | 0.14 | 0.01 | 92.07 | 5.98 | 0.10 | 0.04 | 0.02 | 0.00 | 3.68 | 2.78 | 33.32 | 24.92 |
| 1000.00 | 0.02 | 11.85 | 0.10 | 0.02 | 0.01 | 0.02 | 0.00 | 56.49 | 4.70 | 0.03 | 0.01 | 0.00 | 0.00 | 5.14 | 0.56 | 46.43 | 4.97 |
| 1500.00 | 0.05 | 8.17 | 0.04 | 0.01 | 0.00 | 0.01 | 0.00 | 19.43 | 2.72 | 0.01 | 0.00 | 0.00 | 0.00 | 6.56 | 0.22 | 59.01 | 1.99 |
| 2000.00 | 0.17 | 8.04 | 0.03 | 0.00 | 0.00 | 0.00 | 0.00 | 10.52 | 0.82 | 0.00 | 0.00 | 0.00 | 0.00 | 7.16 | 0.07 | 64.33 | 0.62 |
| 2500.00 | 0.28 | 7.80 | 0.03 | 0.00 | 0.00 | 0.00 | 0.00 | 6.77 | 0.48 | 0.00 | 0.00 | 0.00 | 0.00 | 7.25 | 0.05 | 65.07 | 0.40 |
| 3000.00 | 0.39 | 7.61 | 0.03 | 0.00 | 0.00 | 0.00 | 0.00 | 5.74 | 0.60 | 0.00 | 0.00 | 0.00 | 0.00 | 7.15 | 0.05 | 64.21 | 0.46 |
| 5000.00 | 0.63 | 7.57 | 0.02 | 0.00 | 0.00 | 0.00 | 0.00 | 6.25 | 0.29 | 0.00 | 0.00 | 0.00 | 0.00 | 7.07 | 0.03 | 63.50 | 0.26 |
| 9000.00 | 1.00 | 7.54 | 0.02 | 0.00 | 0.00 | 0.00 | 0.00 | 4.21 | 0.31 | 0.00 | 0.00 | 0.00 | 0.00 | 7.19 | 0.03 | 64.56 | 0.27 |
| Integrated | | 7.85 | 0.01 | 0.00 | 0.00 | 0.00 | 0.00 | 9.21 | 0.26 | 0.00 | 0.00 | 0.00 | 0.00 | 7.10 | 0.02 | 63.75 | 0.37 |

**16ATW08**
**BI#L1**

Weighted average of J from standards = 4.945e-03 +/- 1.594e-05

| Laser Power | Cumulative 39Ar | 40Ar/39Ar meas. | +/- | 37Ar/39Ar meas. | +/- | 36Ar/39Ar meas. | +/- | % Atm. 40Ar | +/- | Ca/K | +/- | Cl/K | +/- | 40*/39K | +/- | Age (Ma) | +/- (Ma) |
|---|---|---|---|---|---|---|---|---|---|---|---|---|---|---|---|---|---|
| (mW) | | | | | | | | | | | | | | | | | |
| 500.00 | 0.01 | 46.76 | 0.36 | 0.10 | 0.00 | 0.14 | 0.00 | 87.85 | 1.34 | 0.18 | 0.01 | 0.00 | 0.00 | 5.68 | 0.63 | 49.88 | 5.43 |
| 1000.00 | 0.04 | 5.57 | 0.03 | 0.09 | 0.00 | 0.01 | 0.00 | 36.28 | 3.27 | 0.17 | 0.00 | 0.00 | 0.00 | 3.53 | 0.18 | 31.16 | 1.60 |
| 1500.00 | 0.11 | 5.13 | 0.03 | 0.12 | 0.00 | 0.00 | 0.00 | 12.15 | 1.81 | 0.21 | 0.00 | 0.00 | 0.00 | 4.48 | 0.10 | 39.47 | 0.84 |
| 2000.00 | 0.30 | 5.47 | 0.02 | 0.01 | 0.00 | 0.00 | 0.00 | 3.64 | 0.63 | 0.01 | 0.00 | 0.00 | 0.00 | 5.25 | 0.04 | 46.15 | 0.36 |
| 2500.00 | 0.52 | 5.36 | 0.02 | 0.00 | 0.00 | 0.00 | 0.00 | 2.37 | 0.49 | 0.01 | 0.00 | 0.00 | 0.00 | 5.20 | 0.03 | 45.78 | 0.29 |
| 3000.00 | 0.71 | 5.68 | 0.02 | 0.00 | 0.00 | 0.00 | 0.00 | 3.17 | 0.47 | 0.01 | 0.00 | 0.00 | 0.00 | 5.47 | 0.03 | 48.10 | 0.29 |
| 5000.00 | 0.94 | 5.46 | 0.01 | 0.00 | 0.00 | 0.00 | 0.00 | 1.26 | 0.51 | 0.00 | 0.00 | 0.00 | 0.00 | 5.36 | 0.03 | 47.15 | 0.27 |
| 9000.00 | 1.00 | 5.51 | 0.02 | 0.01 | 0.00 | 0.00 | 0.00 | 5.71 | 1.73 | 0.01 | 0.00 | 0.00 | 0.00 | 5.17 | 0.10 | 45.50 | 0.85 |
| Integrated | | 6.02 | 0.01 | 0.02 | 0.00 | 0.00 | 0.00 | 13.12 | 0.30 | 0.03 | 0.00 | 0.00 | 0.00 | 5.20 | 0.02 | 45.76 | 0.22 |

**16ATW73**
**BI#L1**

Weighted average of J from standards = 4.945e-03 +/- 1.594e-05

| Laser Power | Cumulative | 40Ar/39Ar | +/- | 37Ar/39Ar | +/- | 36Ar/39Ar | +/- | % Atm. 40Ar | +/- | Ca/K | +/- | Cl/K | +/- | 40*/39K | +/- | Age | +/- |
|---|---|---|---|---|---|---|---|---|---|---|---|---|---|---|---|---|---|
| (mW) | 39Ar | meas. | | meas. | | meas. | | | | | | | | | | (Ma) | (Ma) |
| 500.00 | 0.01 | 12.35 | 0.07 | 0.04 | 0.00 | 0.03 | 0.00 | 77.29 | 3.82 | 0.07 | 0.01 | 0.00 | 0.00 | 2.80 | 0.47 | 24.77 | 4.15 |
| 1000.00 | 0.05 | 5.67 | 0.03 | 0.03 | 0.00 | 0.01 | 0.00 | 31.04 | 2.30 | 0.06 | 0.00 | 0.00 | 0.00 | 3.89 | 0.13 | 34.32 | 1.15 |
| 1500.00 | 0.13 | 5.23 | 0.01 | 0.36 | 0.00 | 0.00 | 0.00 | 27.19 | 1.70 | 0.66 | 0.00 | 0.00 | 0.00 | 3.79 | 0.09 | 33.44 | 0.78 |
| 2000.00 | 0.29 | 4.20 | 0.02 | 0.04 | 0.00 | 0.00 | 0.00 | 9.84 | 1.40 | 0.08 | 0.00 | 0.00 | 0.00 | 3.76 | 0.06 | 33.18 | 0.53 |
| 2500.00 | 0.45 | 4.10 | 0.01 | 0.07 | 0.00 | 0.00 | 0.00 | 8.64 | 1.30 | 0.12 | 0.00 | 0.00 | 0.00 | 3.72 | 0.05 | 32.82 | 0.48 |
| 3000.00 | 0.58 | 4.00 | 0.01 | 0.05 | 0.00 | 0.00 | 0.00 | 9.32 | 1.37 | 0.10 | 0.00 | 0.00 | 0.00 | 3.60 | 0.06 | 31.81 | 0.49 |
| 5000.00 | 0.84 | 3.87 | 0.01 | 0.07 | 0.00 | 0.00 | 0.00 | 4.66 | 0.72 | 0.12 | 0.00 | 0.00 | 0.00 | 3.67 | 0.03 | 32.37 | 0.27 |
| 9000.00 | 1.00 | 3.91 | 0.01 | 0.08 | 0.00 | 0.00 | 0.00 | 2.62 | 0.96 | 0.15 | 0.00 | 0.00 | 0.00 | 3.77 | 0.04 | 33.32 | 0.34 |
| Integrated | | 4.28 | 0.01 | 0.09 | 0.00 | 0.00 | 0.00 | 12.85 | 0.48 | 0.16 | 0.00 | 0.00 | 0.00 | 3.70 | 0.02 | 32.69 | 0.21 |

**15ATW-45**
**MU#L1**

Weighted average of J from standards = 5.645e-03 ± 2.188e-05 (1-sigma error)

Days since irradiation = 49

| Laser Power | Cumulative | 40Ar | ± | 39Ar | ± | 38Ar | ± | 37Ar | ± | 36Ar | ± | % Atm. 40Ar | ± | Ca/K | ± | Cl/K | ± | 40Ar*/39ArK | ± | Age | ± |
|---|---|---|---|---|---|---|---|---|---|---|---|---|---|---|---|---|---|---|---|---|---|
| (mW) | 39Ar | mV | mV | mV | mV | mV | mV | mV | mV | mV | mV | | | | | | | | | (Ma) | (Ma) |
| 700.00 | 0.00 | 83.04 | 5.14 | 5.13 | 0.10 | 0.34 | 0.05 | 0.00 | 0.17 | 0.19 | 0.04 | ## ## | 15.97 | 0.01 | 0.06 | 0.01 | 0.00 | 5.14 | 2.69 | 51.58 | ## ## |
| 1200.00 | 0.02 | 179.69 | 4.95 | 19.56 | 0.11 | 0.32 | 0.05 | 0.00 | 0.18 | 0.26 | 0.05 | ## ## | 7.67 | -0.01 | 0.02 | 0.00 | 0.00 | 5.31 | 0.74 | 53.18 | 7.30 |
| 1800.00 | 0.25 | 1442.14 | 4.01 | 242.82 | 0.48 | 3.14 | 0.06 | 0.00 | 0.17 | 0.64 | 0.05 | ## ## | 1.02 | 0.00 | 0.00 | 0.00 | 0.00 | 5.13 | 0.06 | 51.45 | 0.63 |
| 2600.00 | 0.43 | 1032.17 | 4.25 | 197.44 | 0.32 | 2.35 | 0.05 | 0.00 | 0.18 | 0.16 | 0.05 | 4.60 | 1.45 | 0.00 | 0.00 | 0.00 | 0.00 | 4.96 | 0.08 | 49.75 | 0.78 |
| 3800.00 | 0.72 | 1633.48 | 3.77 | 312.64 | 0.62 | 3.55 | 0.06 | 0.00 | 0.00 | 0.28 | 0.04 | 3.35 | 0.74 | 0.00 | 0.00 | 0.00 | 0.00 | 5.02 | 0.04 | 50.37 | 0.41 |
| 5200.00 | 0.90 | 1016.94 | 4.05 | 186.92 | 0.38 | 2.25 | 0.05 | 0.00 | 0.16 | 0.30 | 0.04 | 8.79 | 1.21 | 0.00 | 0.00 | 0.00 | 0.00 | 4.94 | 0.07 | 49.52 | 0.69 |
| 8000.00 | 1.00 | 567.82 | 4.71 | 105.38 | 0.35 | 1.37 | 0.06 | 0.00 | 0.18 | 0.18 | 0.05 | 9.53 | 2.70 | 0.00 | 0.00 | 0.00 | 0.00 | 4.85 | 0.15 | 48.66 | 1.51 |
| 11500.00 | 1.00 | 41.83 | 5.37 | 3.71 | 0.10 | 0.23 | 0.06 | 0.00 | 0.16 | 0.12 | 0.05 | ## ## | 33.99 | 0.16 | 0.08 | 0.01 | 0.00 | 2.10 | 3.91 | 21.19 | ## ## |
| Integrated | | 5997.11 | 12.91 | 1073.58 | 1.01 | 13.54 | 0.16 | 0.00 | 0.49 | 2.03 | 0.13 | ## ## | 0.65 | 0.00 | 0.00 | 0.00 | 0.00 | 5.00 | 0.04 | 50.14 | 0.42 |

**15ATW-45**
**BI#L1**

Weighted average of J from standards = 5.645e-03 ± 2.188e-05 (1-sigma error)

Days since irradiation =
50

| Laser Power | Cumulative | 40Ar | ± | 39Ar | ± | 38Ar | ± | 37Ar | ± | 36Ar | ± | % Atm. | ± | Ca/K | ± | Cl/K | ± | 40Ar*/39ArK | ± | Age | ± |
|---|---|---|---|---|---|---|---|---|---|---|---|---|---|---|---|---|---|---|---|---|---|
| (mW) | 39Ar | mV | mV | mV | mV | mV | mV | mV | mV | mV | mV | 40Ar | | | | | | | | (Ma) | (Ma) |
| 700.00 | 0.03 | 245.81 | 5.01 | 19.93 | 0.10 | 0.82 | 0.06 | 0.00 | 0.04 | 0.61 | 0.04 | ## | 4.62 | 0.02 | 0.01 | 0.01 | 0.00 | 3.21 | 0.59 | 32.36 | 5.93 |
| 1200.00 | 0.15 | 353.78 | 4.78 | 74.25 | 0.16 | 1.32 | 0.06 | 0.00 | 0.06 | 0.25 | 0.03 | ## | 2.41 | 0.00 | 0.00 | 0.00 | 0.00 | 3.72 | 0.13 | 37.47 | 1.30 |
| 1800.00 | 0.30 | 463.77 | 4.70 | 100.59 | 0.20 | 1.80 | 0.07 | 0.00 | 0.04 | 0.26 | 0.05 | ## | 2.89 | 0.00 | 0.00 | 0.00 | 0.00 | 3.82 | 0.14 | 38.49 | 1.40 |
| 2600.00 | 0.44 | 413.51 | 4.88 | 88.80 | 0.32 | 1.47 | 0.06 | 0.00 | 0.03 | 0.30 | 0.04 | ## | 3.01 | 0.00 | 0.00 | 0.00 | 0.00 | 3.63 | 0.15 | 36.53 | 1.49 |
| 3800.00 | 0.61 | 442.22 | 4.53 | 107.32 | 0.25 | 1.72 | 0.07 | 0.00 | 0.05 | 0.12 | 0.04 | 8.26 | 2.90 | 0.00 | 0.00 | 0.00 | 0.00 | 3.75 | 0.13 | 37.78 | 1.26 |
| 5200.00 | 0.72 | 275.59 | 4.69 | 67.88 | 0.17 | 1.06 | 0.05 | 0.00 | 0.06 | 0.68 | 0.04 | 8.33 | 4.61 | 0.00 | 0.00 | 0.00 | 0.00 | 3.69 | 0.20 | 37.20 | 1.98 |
| 8000.00 | 0.80 | 218.76 | 4.83 | 53.04 | 0.19 | 0.84 | 0.05 | 0.00 | 0.04 | 0.02 | 0.03 | 2.15 | 4.22 | 0.00 | 0.01 | 0.00 | 0.00 | 4.01 | 0.20 | 40.31 | 1.95 |
| 11500.00 | 1.00 | 493.39 | 4.98 | 127.18 | 0.34 | 1.80 | 0.07 | 0.00 | 0.05 | 0.17 | 0.05 | 3.98 | 2.72 | 0.01 | 0.00 | 0.00 | 0.00 | 3.70 | 0.11 | 37.22 | 1.12 |
| Integrated | | 2906.83 | 13.59 | 638.98 | 0.65 | 10.83 | 0.18 | 0.00 | 0.01 | 1.71 | 0.11 | ## | 1.15 | 0.00 | 0.00 | 0.00 | 0.00 | 3.73 | 0.06 | 37.55 | 0.58 |

**16-43C**
**HO#L1**

Weighted average of J from standards = 5.073e-03 +/-
2.571e-05

| Laser Power | Cumulative | 40Ar/39Ar | +/- | 37Ar/39Ar | +/- | 36Ar/39Ar | +/- | % Atm. 40Ar | +/- | Ca/K | +/- | Cl/K | +/- | 40*/39K | +/- | Age | +/- |
|---|---|---|---|---|---|---|---|---|---|---|---|---|---|---|---|---|---|
| (mW) | 39Ar | meas. | | meas. | | meas. | | | | | | | | | | (Ma) | (Ma) |
| 500.00 | 0.00 | 226.28 | 8.19 | 0.63 | 0.06 | 0.59 | 0.03 | 77.52 | 2.14 | 1.16 | 0.11 | 0.15 | 0.01 | 50.89 | 5.20 | ###### | 37.82 |
| 1000.00 | 0.03 | 20.37 | 0.32 | 1.34 | 0.02 | 0.04 | 0.00 | 59.28 | 6.64 | 2.45 | 0.03 | 0.01 | 0.00 | 8.29 | 1.37 | 74.23 | 12.00 |
| 1500.00 | 0.07 | 9.44 | 0.06 | 3.95 | 0.02 | 0.01 | 0.00 | 37.25 | 4.65 | 7.26 | 0.04 | 0.00 | 0.00 | 5.92 | 0.44 | 53.31 | 3.91 |
| 2000.00 | 0.14 | 9.11 | 0.04 | 0.96 | 0.01 | 0.01 | 0.00 | 24.23 | 2.44 | 1.76 | 0.01 | 0.00 | 0.00 | 6.88 | 0.22 | 61.86 | 1.98 |
| 2500.00 | 0.21 | 9.09 | 0.05 | 2.76 | 0.01 | 0.00 | 0.00 | 11.79 | 2.83 | 5.08 | 0.03 | 0.00 | 0.00 | 8.00 | 0.26 | 71.73 | 2.30 |
| 3000.00 | 0.35 | 10.28 | 0.04 | 4.00 | 0.01 | 0.00 | 0.00 | 6.31 | 1.33 | 7.37 | 0.02 | 0.00 | 0.00 | 9.63 | 0.14 | 85.98 | 1.25 |
| 5000.00 | 0.89 | 11.19 | 0.03 | 4.45 | 0.01 | 0.00 | 0.00 | 6.06 | 0.46 | 8.20 | 0.02 | 0.01 | 0.00 | 10.51 | 0.06 | 93.66 | 0.50 |
| 9000.00 | 1.00 | 11.78 | 0.04 | 4.22 | 0.01 | 0.01 | 0.00 | 9.94 | 1.33 | 7.76 | 0.03 | 0.01 | 0.00 | 10.62 | 0.16 | 94.56 | 1.40 |
| Integrated | | 12.00 | 0.02 | 3.89 | 0.01 | 0.01 | 0.00 | 17.34 | 0.54 | 7.17 | 0.01 | 0.01 | 0.00 | 9.92 | 0.07 | 88.52 | 0.73 |

**15ATW-35**
**FU#L1**

Weighted average of J from standards = 5.073e-03 +/- 2.571e-05

| Laser Power | Cumulative | 40Ar/39Ar | +/- | 37Ar/39Ar | +/- | 36Ar/39Ar | +/- | %Atm. 40Ar | +/- | Ca/K | +/- | Cl/K | +/- | 40*/39K | +/- | Age (Ma) | +/- (Ma) |
|---|---|---|---|---|---|---|---|---|---|---|---|---|---|---|---|---|---|
| (mW) | 39Ar | meas. | | meas. | | meas. | | | | | | | | | | | |
| 500.00 | 0.01 | 71.92 | 0.82 | 0.21 | 0.02 | 0.23 | 0.01 | 96.39 | 2.41 | 0.38 | 0.03 | 0.01 | 0.00 | 2.60 | 1.74 | 23.59 | 15.66 |
| 1000.00 | 0.03 | 18.58 | 0.13 | 0.14 | 0.01 | 0.04 | 0.00 | 69.50 | 2.34 | 0.25 | 0.01 | 0.00 | 0.00 | 5.66 | 0.44 | 51.01 | 3.88 |
| 1500.00 | 0.14 | 9.90 | 0.05 | 0.04 | 0.00 | 0.01 | 0.00 | 27.13 | 1.45 | 0.08 | 0.00 | 0.00 | 0.00 | 7.20 | 0.15 | 64.62 | 1.30 |
| 2000.00 | 0.28 | 8.91 | 0.03 | 0.02 | 0.00 | 0.01 | 0.00 | 18.53 | 0.55 | 0.03 | 0.00 | 0.00 | 0.00 | 7.23 | 0.06 | 64.94 | 0.51 |
| 2500.00 | 0.43 | 8.97 | 0.03 | 0.01 | 0.00 | 0.01 | 0.00 | 19.53 | 0.73 | 0.01 | 0.00 | 0.00 | 0.00 | 7.19 | 0.07 | 64.59 | 0.62 |
| 3000.00 | 0.55 | 8.90 | 0.03 | 0.02 | 0.00 | 0.01 | 0.00 | 18.87 | 1.20 | 0.04 | 0.00 | 0.00 | 0.00 | 7.19 | 0.11 | 64.59 | 0.97 |
| 5000.00 | 0.78 | 8.44 | 0.03 | 0.00 | 0.00 | 0.00 | 0.00 | 14.13 | 0.29 | 0.01 | 0.00 | 0.00 | 0.00 | 7.22 | 0.03 | 64.87 | 0.30 |
| 9000.00 | 1.00 | 8.73 | 0.03 | 0.00 | 0.00 | 0.00 | 0.00 | 15.28 | 0.64 | 0.01 | 0.00 | 0.00 | 0.00 | 7.37 | 0.06 | 66.17 | 0.54 |
| Integrated | | 9.45 | 0.01 | 0.02 | 0.00 | 0.01 | 0.00 | 23.73 | 0.32 | 0.03 | 0.00 | 0.00 | 0.00 | 7.18 | 0.03 | 64.51 | 0.43 |

**15ATW-05 WR#L1**

Weighted average of J from standards = 4.263e-03 +/- 1.092e-05

| Laser Power | Cumulative | 40Ar/39Ar | +/- | 37Ar/39Ar | +/- | 36Ar/39Ar | +/- | %Atm. 40Ar | +/- | Ca/K | +/- | Cl/K | +/- | 40*/39K | +/- | Age (Ma) | +/- (Ma) |
|---|---|---|---|---|---|---|---|---|---|---|---|---|---|---|---|---|---|
| (mW) | 39Ar | meas. | | meas. | | meas. | | | | | | | | | | | |
| 500.00 | 0.05 | 21.58 | 0.17 | 1.33 | 0.03 | 0.04 | 0.00 | 58.84 | 3.76 | 2.44 | 0.05 | 0.01 | 0.00 | 8.88 | 0.82 | 66.95 | 6.04 |
| 1000.00 | 0.25 | 12.99 | 0.06 | 3.17 | 0.02 | 0.01 | 0.00 | 13.24 | 1.22 | 5.84 | 0.05 | 0.00 | 0.00 | 11.27 | 0.17 | 84.58 | 1.23 |
| 1500.00 | 0.46 | 14.05 | 0.06 | 2.14 | 0.02 | 0.00 | 0.00 | 8.95 | 1.22 | 3.93 | 0.04 | 0.00 | 0.00 | 12.79 | 0.18 | 95.66 | 1.31 |
| 2000.00 | 0.60 | 14.96 | 0.06 | 5.19 | 0.04 | 0.01 | 0.00 | 9.55 | 2.07 | 9.55 | 0.08 | 0.00 | 0.00 | 13.55 | 0.32 | ### ## | 2.29 |
| 2500.00 | 0.70 | 14.85 | 0.07 | 3.42 | 0.03 | 0.01 | 0.00 | 14.43 | 2.41 | 6.28 | 0.06 | 0.00 | 0.00 | 12.71 | 0.36 | 95.13 | 2.65 |
| 3000.00 | 0.80 | 15.64 | 0.08 | 1.06 | 0.02 | 0.01 | 0.00 | 10.39 | 3.63 | 1.94 | 0.03 | 0.00 | 0.00 | 14.00 | 0.57 | ### ## | 4.14 |
| 5000.00 | 0.97 | 16.50 | 0.06 | 4.00 | 0.03 | 0.01 | 0.00 | 18.23 | 1.65 | 7.36 | 0.05 | 0.00 | 0.00 | 13.51 | 0.28 | ### ## | 2.01 |
| 8000.00 | 1.00 | 25.64 | 0.30 | 8.60 | 0.12 | 0.04 | 0.00 | 45.80 | 4.32 | 15.87 | 0.23 | 0.03 | 0.00 | 13.97 | 1.13 | ### ## | 8.16 |
| Integrated | | 15.33 | 0.03 | 3.28 | 0.01 | 0.01 | 0.00 | 17.45 | 0.75 | 6.03 | 0.02 | 0.00 | 0.00 | 12.66 | 0.12 | 94.71 | 0.89 |

## Supplemental file S4

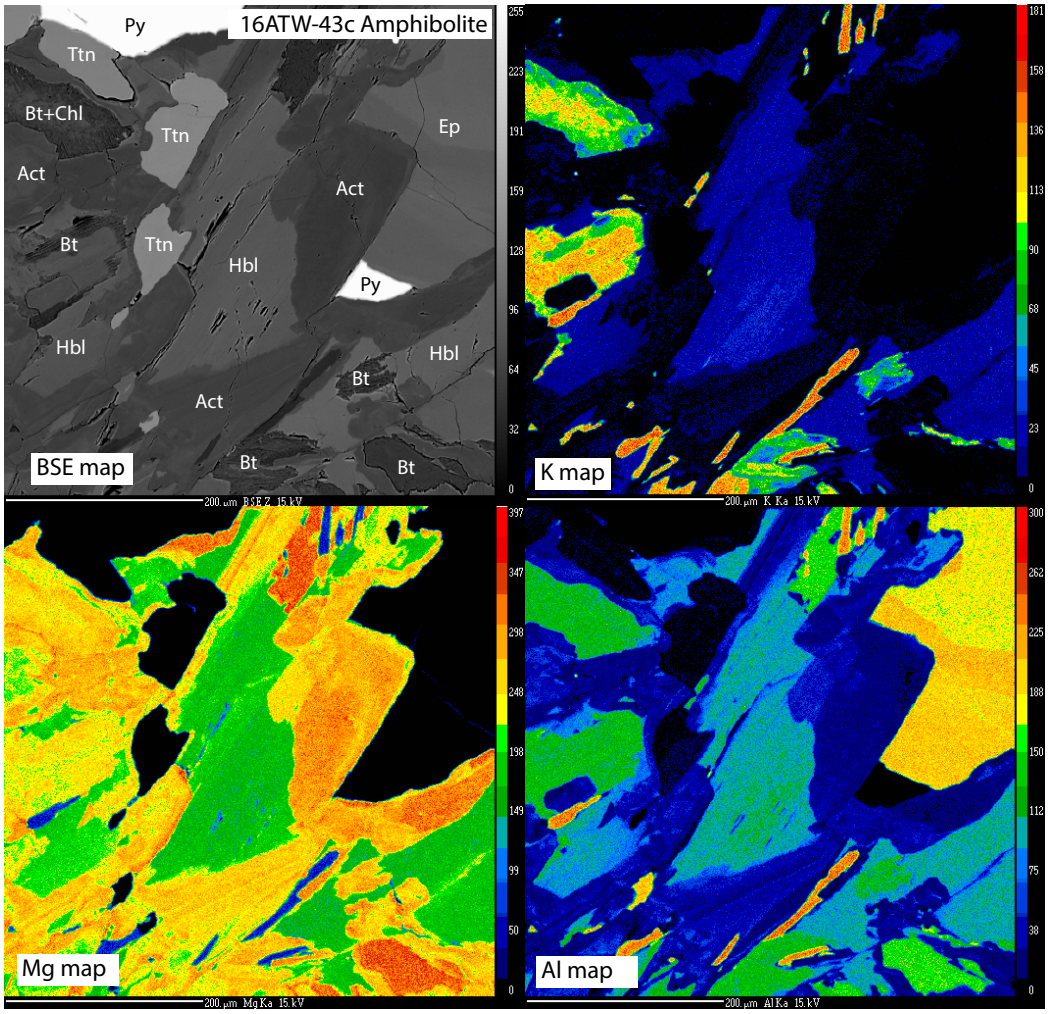


**Figure S4-1–** Amphibole x-ray maps for sample 16ATW-43c showing amphibole zoning textures. Mineral abbreviations are from Whitney and Evans (2010).

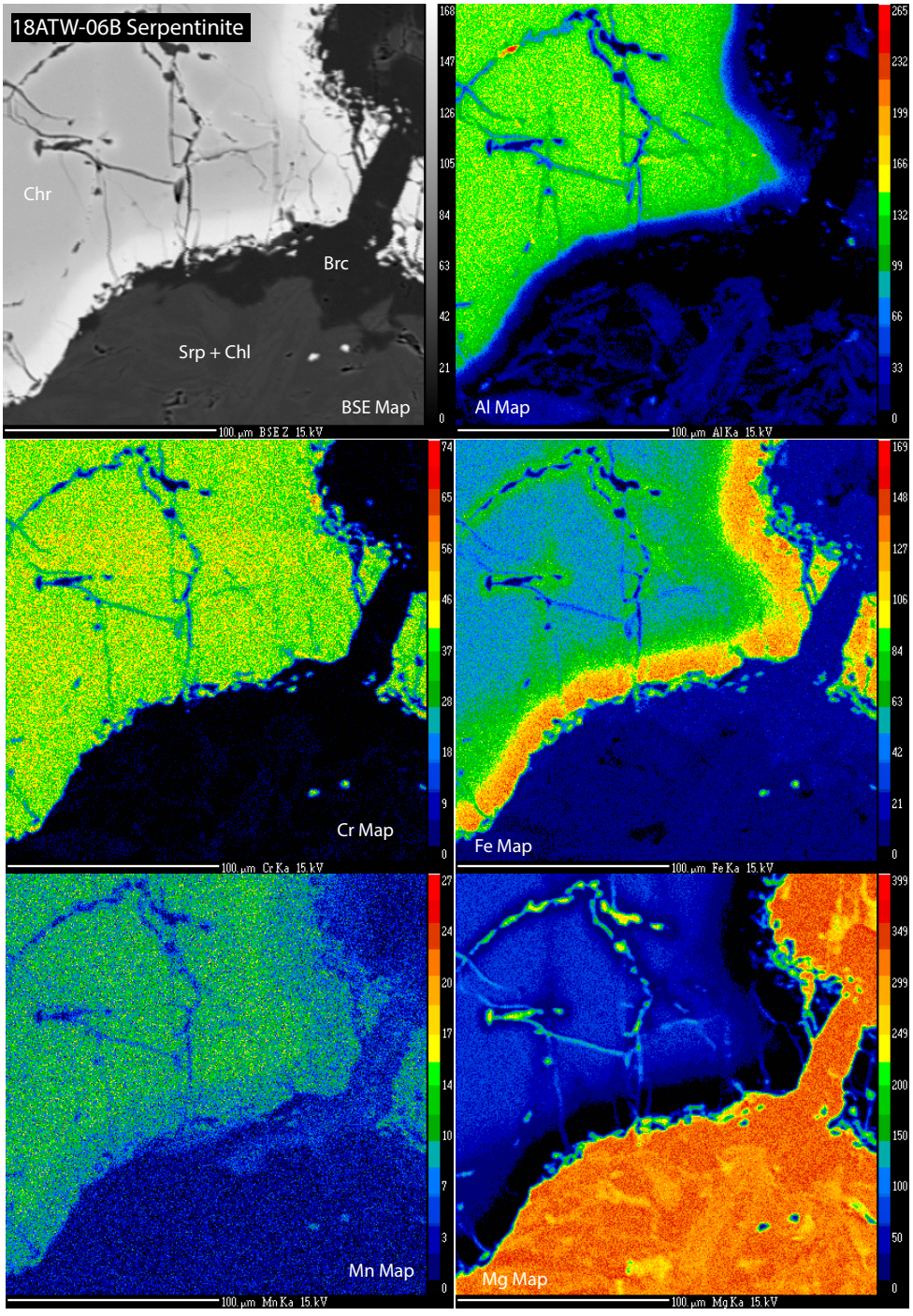


**Figure S4-3**– Zoomed-in chromite x-ray maps for sample 18ATW-06b showing zoning at the margins of the grains. Mineral abbreviations are from Whitney and Evans (2010).

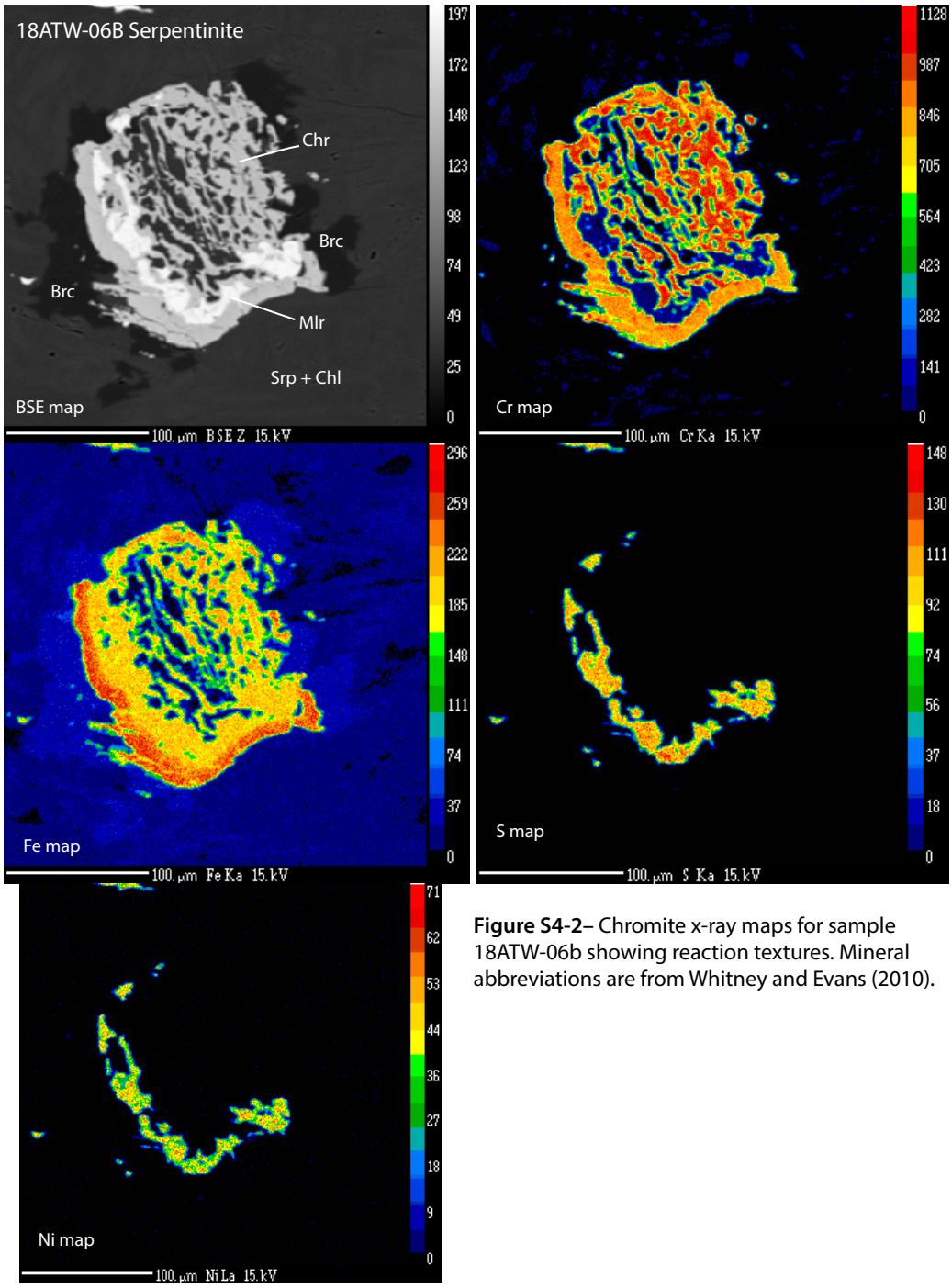


**Figure S4-2**– Chromite x-ray maps for sample 18ATW-06b showing reaction textures. Mineral abbreviations are from Whitney and Evans (2010).

## Supplemental file S5:

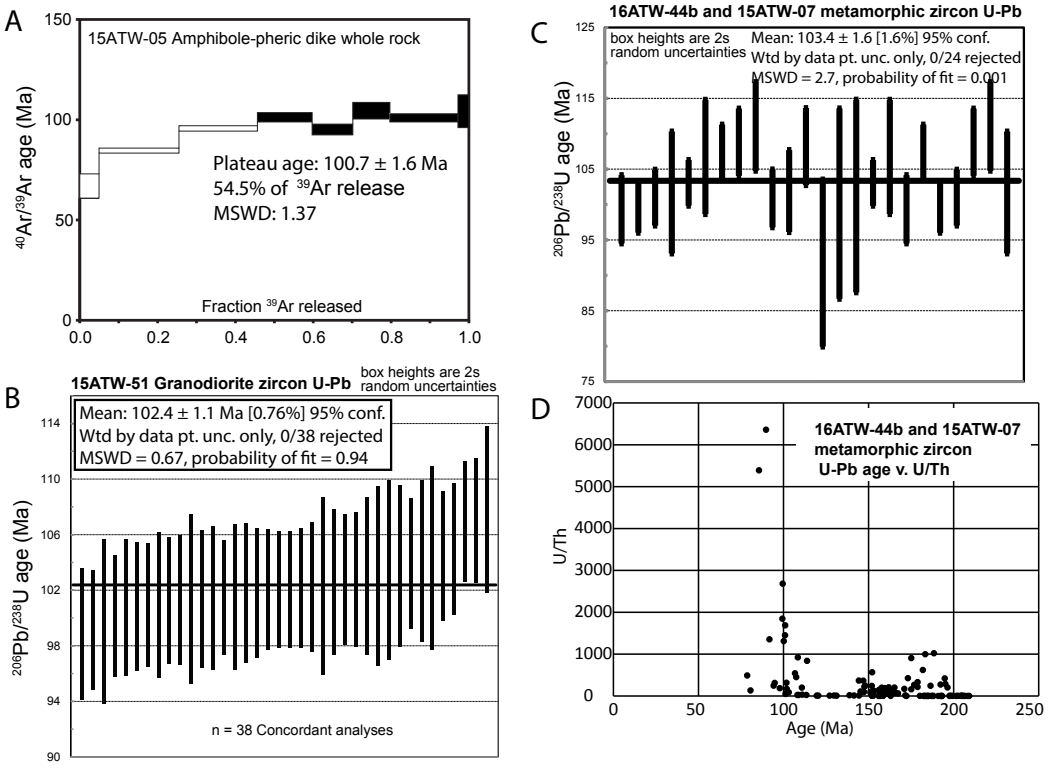


**Figure S5-1– A:** $^{40}Ar/^{39}Ar$ whole rock age spectrum for sample 15ATW-05 (amphibole dike in Broxson Gulch). Filled release steps define the plateau age. **B:** Weighted mean age of analyzed zircon grains from sample 15ATW-51 (granodiorite in Ann Creek). **C:** Weighted mean of ca. 100 Ma metamorphic zircon grains in samples 16ATW-44b and 15ATW-07. **D:** U/Th vs. age plot for Phanerozoic zircon grains in samples 16ATW-44b and 15ATW-07.

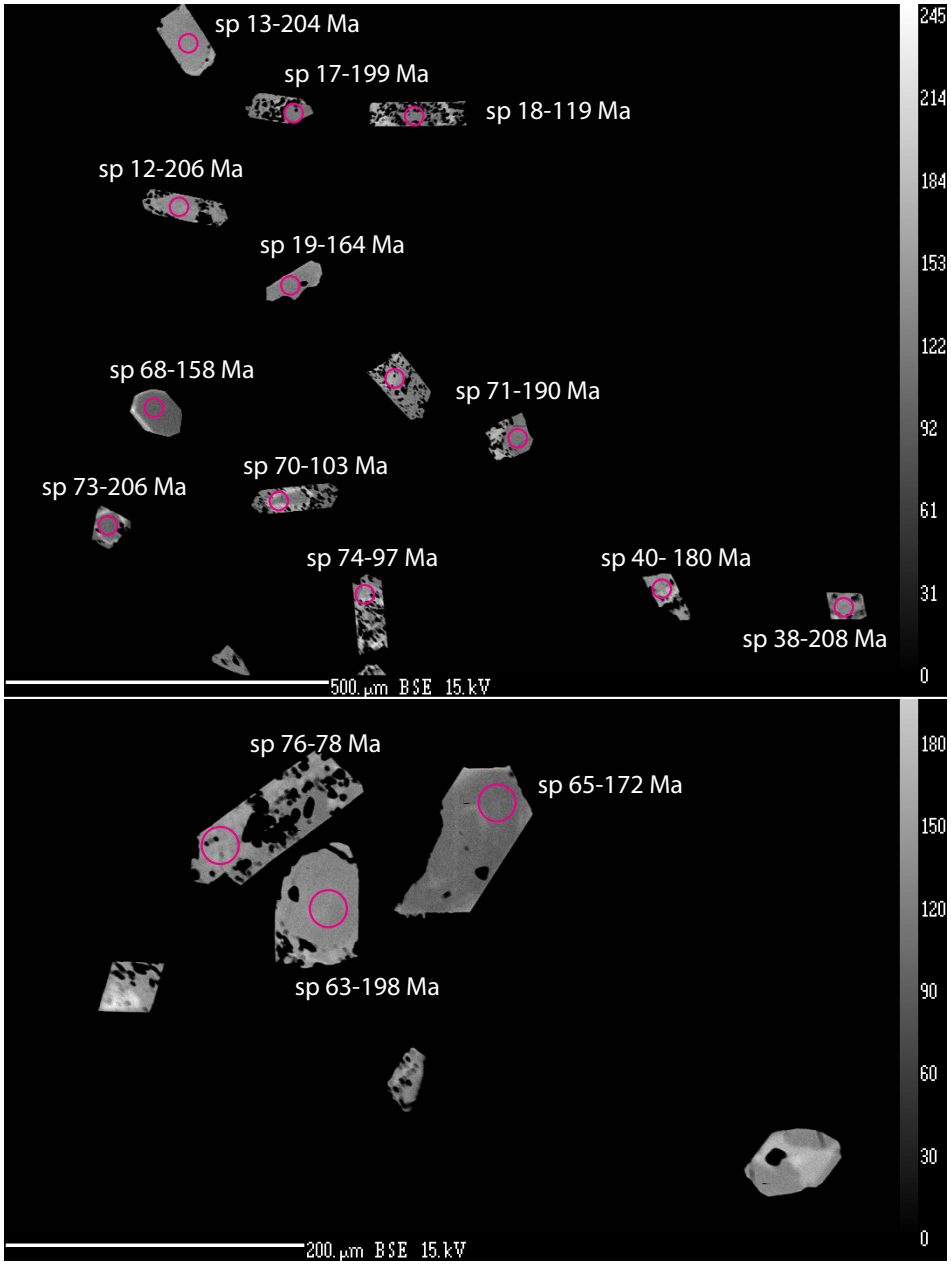


**Figure S5-2–** Backscatter electron maps of zircons in sample 16ATW-44b. Pink circles represent laser spot locations. The spot number (sp) and age of each spot are given next to each grain.

## Supplemental file S6

Supplemental file S6- Representative pictures of Cenozoic gravel deposits.

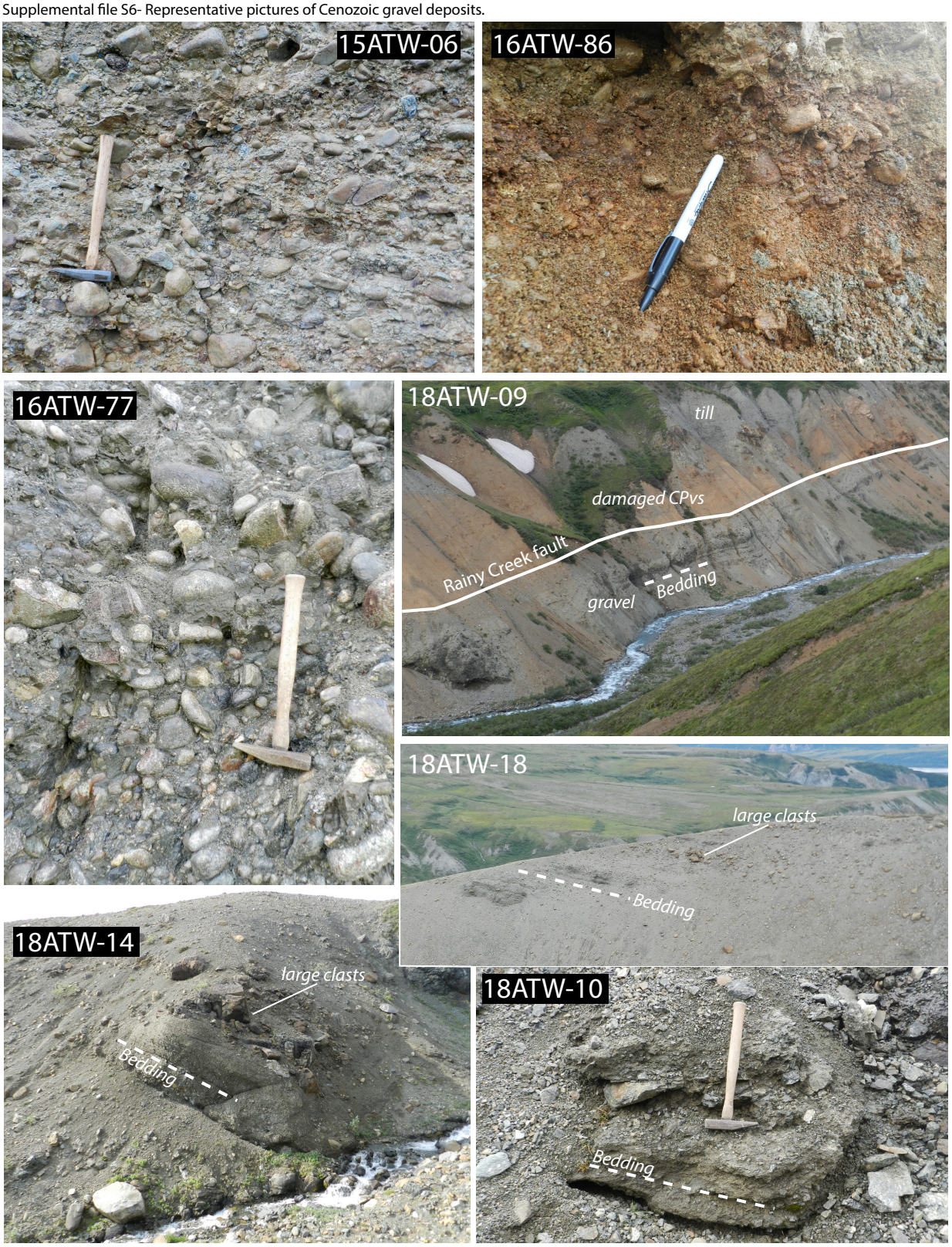

## Supplemental File S7

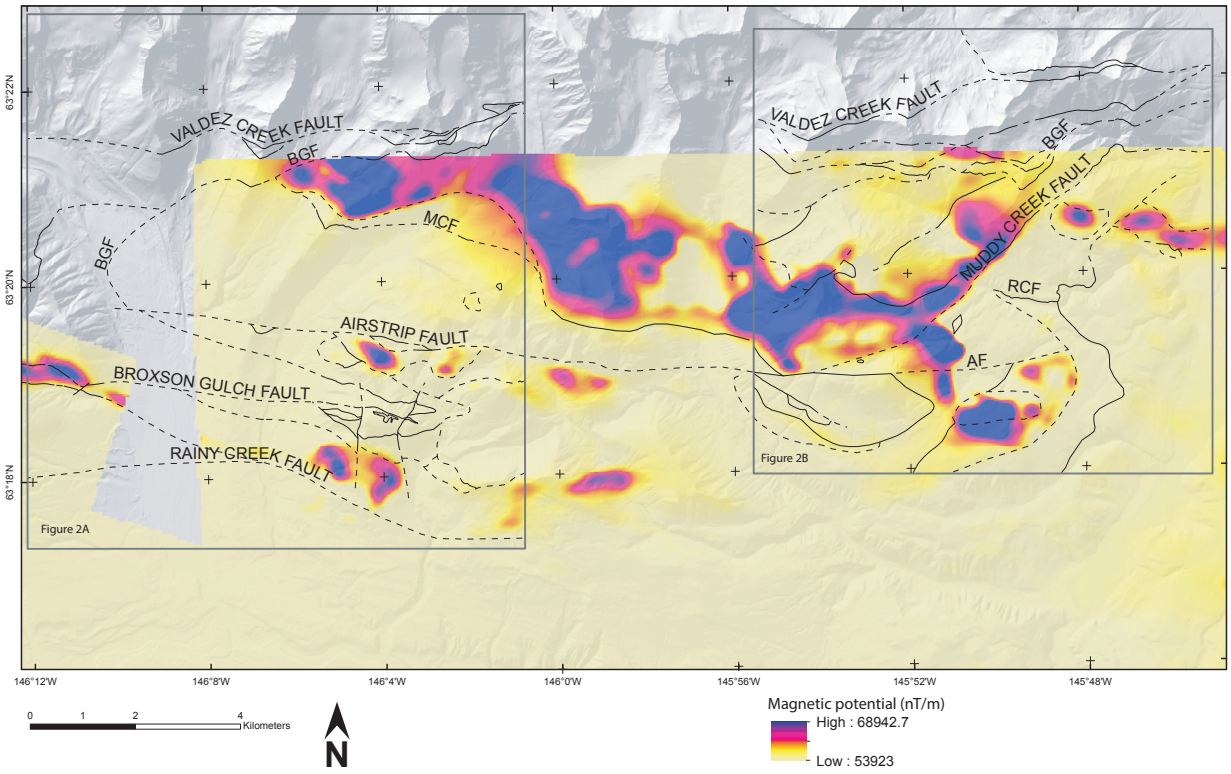


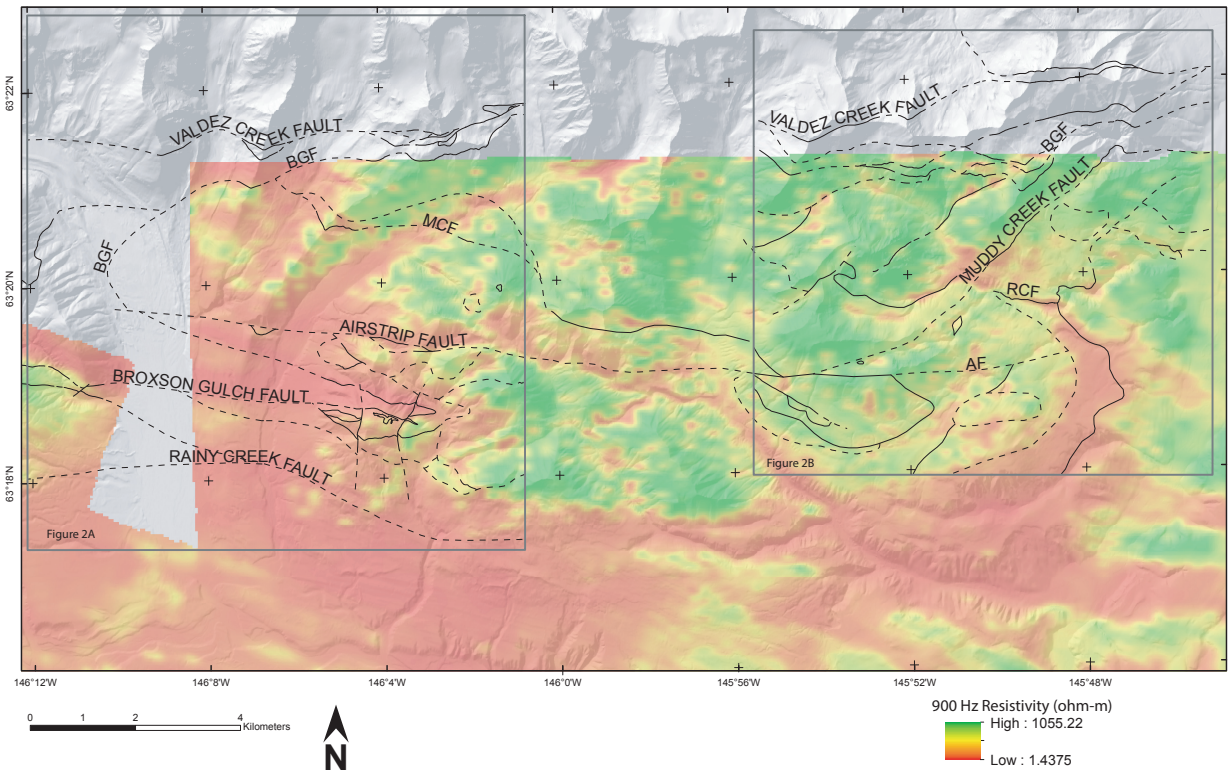

## Supplemental file S8:

Table S8.1: Electron Microprobe analyses of spinel group minerals

| Comment | MgO | MnO | Fe total (as FeO) | Fe2O3 (calc) | FeO (calc) | Al2O3 | Cr2O3 | TiO2 | Total | Adjusted Total* |
|---|---|---|---|---|---|---|---|---|---|---|
| 16ATW-43b chrm 1-1** | 0.77 | 1.28 | 33.25 | 2.47 | 30.78 | 15.35 | 45.50 | 0.08 | 96.29 | 96.52 |
| 16ATW-43b chrm 1-2** | 1.27 | 1.07 | 33.06 | 2.51 | 30.55 | 15.39 | 46.14 | 0.12 | 97.14 | 97.14 |
| 16ATW-43b chrm 1-3** | 1.21 | 1.04 | 32.85 | 2.21 | 30.64 | 15.33 | 46.27 | 0.11 | 96.90 | 96.90 |
| 16ATW-43b chrm 1-4** | 0.65 | 1.37 | 33.60 | 3.12 | 30.48 | 14.72 | 44.98 | 0.11 | 95.49 | 95.49 |
| 16ATW-43b chrm 2-1** | 0.89 | 1.30 | 32.94 | 2.22 | 30.72 | 15.50 | 45.71 | 0.09 | 96.52 | 96.52 |
| 16ATW-43b chrm 2-2** | 0.92 | 1.21 | 32.48 | 1.79 | 30.69 | 15.49 | 45.81 | 0.11 | 96.08 | 96.08 |
| 16ATW-43b chrm 2-3** | 0.77 | 1.29 | 32.66 | 1.79 | 30.87 | 15.42 | 45.74 | 0.12 | 96.09 | 96.09 |
| 18ATW-06b chrm 1-1 | 10.81 | 0.41 | 20.50 | 2.61 | 17.89 | 18.31 | 49.99 | 0.05 | 100.09 | 100.09 |
| 18ATW-06b chrm 1-2 | 10.59 | 0.42 | 20.89 | 2.76 | 18.13 | 18.18 | 49.92 | 0.05 | 100.06 | 100.06 |
| 18ATW-06b chrm 1-3 | 10.43 | 0.39 | 20.83 | 2.41 | 18.42 | 18.45 | 49.53 | 0.05 | 99.74 | 99.74 |
| 18ATW-06b chrm 1-4 | 10.39 | 0.43 | 20.91 | 2.51 | 18.40 | 18.31 | 49.68 | 0.05 | 99.86 | 99.86 |
| 18ATW-06b chrm 1-5 | 10.49 | 0.40 | 20.60 | 2.26 | 18.34 | 18.47 | 49.75 | 0.06 | 99.78 | 99.78 |
| 18ATW-06b chrm Fe rim 1-6 | 0.98 | 0.21 | 46.53 | 17.63 | 28.90 | 5.29 | 42.47 | 0.50 | 95.98 | 97.75 |
| 18ATW-06b chrm Fe rim 1-7 | 0.72 | 0.13 | 50.04 | 22.10 | 27.94 | 1.63 | 41.46 | 0.45 | 94.46 | 96.67 |
| 18ATW-06b chrm 2-1 | 1.13 | 0.19 | 38.51 | 8.83 | 29.68 | 6.54 | 50.54 | 0.14 | 97.08 | 97.97 |
| 18ATW-06b chrm 2-2 | 1.10 | 0.13 | 38.36 | 2.37 | 35.99 | 6.62 | 50.72 | 0.14 | 97.07 | 97.07 |
| 18ATW-06b chrm 2-3 | 0.77 | 0.19 | 41.59 | 12.65 | 28.94 | 1.51 | 51.50 | 0.31 | 95.92 | 97.19 |
| 18ATW-06b chrm rim 2-5 | 0.76 | 0.19 | 48.79 | 19.94 | 28.85 | 3.21 | 42.06 | 0.69 | 95.72 | 97.71 |
| 18ATW-06b chrm rim 2-6 | 0.95 | 0.20 | 41.66 | 12.35 | 29.32 | 5.81 | 46.87 | 0.30 | 95.83 | 97.06 |
| 18ATW-06b chrm rim 3-2 | 4.17 | 0.45 | 29.67 | 1.84 | 27.83 | 17.44 | 47.64 | 0.05 | 99.50 | 99.50 |
| 18ATW-06b chrm rim 3-3 | 6.66 | 0.43 | 26.35 | 2.15 | 24.20 | 17.98 | 48.42 | 0.07 | 99.93 | 99.93 |
| 18ATW-06b chrm rim 3-4 | 9.73 | 0.47 | 22.30 | 2.93 | 19.37 | 17.79 | 49.42 | 0.07 | 99.84 | 99.84 |
| 15ATW-35 chrm 1-1 | 0.34 | 2.16 | 34.89 | 1.66 | 33.23 | 7.77 | 48.00 | 0.31 | 93.97 | 94.51 |
| 15ATW-35 chrm 1-2 | 0.79 | 2.14 | 31.61 | 1.52 | 30.09 | 20.13 | 39.27 | 0.13 | 94.17 | 94.17 |
| 15ATW-35 chrm 1-3 | 0.27 | 2.44 | 36.27 | 2.36 | 33.90 | 7.74 | 45.05 | 0.55 | 92.51 | 92.51 |
| 15ATW-35 chrm 2-1 | 1.95 | 1.50 | 34.19 | 3.80 | 30.39 | 22.25 | 37.88 | 0.18 | 98.05 | 98.05 |
| 15ATW-35 chrm 2-2 | 2.35 | 1.35 | 34.17 | 4.02 | 30.15 | 22.48 | 38.19 | 0.17 | 98.75 | 98.75 |
| 15ATW-35 chrm 2-3 | 0.58 | 1.91 | 30.87 | 0.74 | 30.13 | 16.24 | 42.90 | 0.24 | 93.10 | 93.10 |
| 16ATW-43a mag 1-1 | 0.13 | 0.25 | 81.37 | 56.64 | 24.73 | 0.05 | 11.12 | 0.05 | 92.98 | 98.64 |
| 16ATW-43a mag 1-2 | 0.09 | 0.20 | 83.25 | 58.65 | 24.60 | 0.04 | 9.03 | 0.05 | 92.69 | 98.56 |
| 16ATW-43a mag 2-3 | 0.16 | 0.30 | 79.26 | 54.22 | 25.04 | 0.06 | 13.66 | 0.08 | 93.51 | 98.94 |
| 16ATW-43a mag 2-4 | 0.18 | 0.44 | 74.92 | 49.68 | 25.24 | 0.07 | 17.76 | 0.10 | 93.47 | 98.45 |
| 16ATW-43a mag 2-5 | 0.07 | 0.04 | 88.06 | 63.60 | 24.46 | 0.02 | 4.78 | 0.03 | 93.04 | 99.40 |
| 16ATW-43a mag 2-6 | 0.08 | 0.18 | 84.79 | 60.20 | 24.59 | 0.03 | 7.87 | 0.04 | 93.02 | 99.05 |
| 16ATW-43a mag 2-7 | 0.14 | 0.30 | 79.48 | 54.67 | 24.81 | 0.05 | 12.88 | 0.05 | 92.92 | 98.39 |

* Total adjusted to account for extra oxygen related to calculated Fe2O3

** Zn detected by EDS; lower totals may reflect lack of Zn in analysis

*** Variable totals may reflect small grain size (<10 micron)

# Ch. 2: Tectonic underplating and dismemberment of the Maclaren-Kluane schist records late Cretaceous terrane accretion polarity and ~480 km of post-52 Ma dextral displacement on the Denali fault

**T. S. Waldien[1], S. M. Roeske[1], J. A. Benowitz[2]**

*[1]Department of Earth and Planetary Sciences, University of California, Davis, 1 Shields Ave. Davis, California 95616, USA*

*[2]Geophysical Institute, University of Alaska, Fairbanks, 900 Yukon Drive Fairbanks, Alaska 99775, USA*

**ABSTRACT**

Terrane accretion introduces irregular geometry and allochthonous material to obliquely-convergent margins, which create opportunities to quantify strike-slip displacement along otherwise margin-parallel fault systems. Our new bedrock geologic mapping and U-Pb and $^{40}Ar/^{39}Ar$ geochronology from the Alaska Range suture zone in the eastern Alaska Range confirms a long-hypothesized correlation between the Maclaren Glacier metamorphic belt (Alaska, USA) and the Kluane metamorphic assemblage (Yukon Territory, Canada). Our palinspastic reconstruction uses the new data and updated geologic maps of eastern Alaska and southwestern Yukon to show that the metamorphic belts and associated rocks record ~480 km of right-lateral displacement along the Denali fault since ca. 52 Ma. Prior to strike-slip separation, the Maclaren-Kluane schist formed by west-vergent forearc underplating in the waning stage of the ca. 100-90 Ma arc built upon the Yukon-Tanana terrane. The prograde structural and metamorphic evolution of the Maclaren-Kluane schist records final collision of the Wrangellia composite terrane at ca. 75-65 Ma along a set of east-dipping thrust shear zones, which we infer to record the polarity of the late Cretaceous plate boundary between the composite terrane and North America. Paleogene extension partially exhumed the schists to the upper crust and may be a consequence of regionally distributed strike-slip faulting at that time. Localization of the modern Denali fault after ca. 52 Ma dismembered the schist and four neighboring belts of plutonic, metasedimentary, and volcanic rocks. The transition to Yakutat oblique flat slab subduction at ca. 30-25 Ma marks the onset of transpressional deformation in the Denali fault system, which reactivated late Cretaceous collisional structures bounding the Maclaren schist. Neogene reactivation of the Totschunda fault reduced strike-slip motion on the Denali fault east of the Denali-Totschunda intersection and continues to transfer residual plate boundary slip onto the Denali fault west of the intersection.

Key outcomes of our synthesis include: (1) Much of the ~480 km of displacement on the Denali fault accumulated after strike-slip on the neighboring Tintina and Border Ranges fault systems had largely shut down; (2) The modern Denali fault system should not be grouped with strike-slip faults credited with large-scale margin-parallel transport of Cordilleran terranes in the Cretaceous. Instead, a poorly understood proto-Denali fault system may be a candidate for large-scale Cretaceous translation; and (3) the longevity (≥33 Myr) of the highly localized Denali fault master strand (≤1 km wide) suggests that it occupies a major mechanical boundary that penetrates the lithosphere.

## INTRODUCTION

Quantitative restoration of strike-slip deformation along obliquely convergent margins is commonly hindered by strike-slip localization within the arc (e.g. Busby-Spera and Saleeby, 1990; Lange et al., 2008) or forearc (Jarrard, 1986; Avé Lallemant, 1997), which translates sub-parallel elements of the margin relative to each other but may not cross cut restorable features (Beck, 1986). Terrane accretion and associated geometric modification of the margin (e.g. Dominguez et al., 1998) form unique markers that may be used to track syn- and post-collisional margin-parallel translation. Recognition, correlation, and restoration of such features requires identifying the suite of diagnostic characteristics by which they can be identified and correlated, knowledge of where/when the feature accreted to the margin, and how each part of the displaced feature has evolved since dismemberment.

Assembly of the North American Cordillera involved multiple episodes of strike-slip faulting and terrane accretion. Although both terrane accretion and translation have long been recognized as fundamental processes shaping the geologic evolution of western North America

(e.g., Moores, 1970; Coney et al., 1980), they persist as controversial topics. Shortening structures formed during terrane accretion are essential for reconstructing strike-slip deformation in the Cordillera because they have been found in multiple places to be cut by strike-slip faults and thus create reliable geological markers for estimating strike-slip separation (Nokleberg et al., 1985; Gabrielse et al., 2006). New views of the Mesozoic Cordilleran orogeny (Johnston, 2008; Hildebrand, 2015; Sigloch and Mihalynuk, 2017), however, call into question the timing and polarity of various terrane accretionary events (e.g. Pavlis et al., 2019). A detailed reappraisal of terrane accretionary rocks and structures is necessary to vet the various models of Cordilleran assembly and associated margin-parallel translation.

Metamorphic belts and structures formed during closure of the ocean basin between the Wrangellia composite terrane and North America have been used to estimate total strike-slip displacement on the Denali fault between southern Alaska, USA and southwestern Yukon Territory, Canada. The purported correlative rock packages include schists, gneisses, and plutons in the Maclaren Glacier metamorphic belt[1] (Alaska) and Kluane metamorphic assemblage-Ruby Range batholith (Yukon) (Nokleberg et al., 1985; Figure 1). Since the correlation between these two metamorphic belts was first proposed by Forbes et al. (1974), the tectono-metamorphic evolution of the Kluane metamorphic assemblage has been the focus of a number of detailed studies (e.g., Mezger et al., 1999, 2001a, b, 2002; Israel et al., 2011; Stanley, 2012; Canil et al., 2015). In contrast, metamorphic and plutonic rocks near the Maclaren Glacier have mainly been studied as part of early regional mapping efforts (Smith, 1981; Nokleberg et al., 1985; 1992a), other than detailed studies on a small accessible portion (Davidson et al., 1992; Beam and Fisher, 1999; Davidson and McPhillips, 2007; Link, 2017). The difference in study resolution has led to doubt as to whether the rock units correlate (e.g., Mezger et al., 2001a). Moreover, tectonic models

describing the prograde metamorphic path of the Maclaren and Kluane belts have argued for opposing vergence directions for syn-collisional structures (cf. Csejtey et al., 1982; Nokleberg et al., 1985; Johnston and Canil, 2007). If the disparate tectonic models are correct, then the proposed correlation of the Maclaren and Kluane belts may be refutable and estimates of total displacement along the Denali fault system would require revision.

Here, we present a new regional synthesis map (Figure 2), zircon U-Pb age data from nine metasedimentary and thirteen plutonic samples, zircon Hf isotopic data from three metasedimentary samples, and $^{40}Ar/^{39}Ar$ geochronology on four volcanic samples located south of the Denali fault in the eastern Alaska Range. Our data bear on the timing of initial burial and tectono-metamorphic evolution of the Maclaren and Clearwater metasedimentary belts in Alaska leading up to and after strike-slip separation. We compare our data to equivalent datasets from the Kluane metamorphic assemblage and argue that the metasedimentary/plutonic belts represent a single body that was cut and displaced by the Denali fault. By integrating our data with other regional datasets, we are able to place the Maclaren-Kluane metamorphic belt into a regional tectonic framework during final accretion of the Wrangellia composite terrane and arrive at more precise measurements and timing of subsequent strike-slip separation.

[1]Recent studies by Link (2017) and Waldien et al. (2021) have shown that the Maclaren Glacier metamorphic belt is a composite metamorphic belt wherein rocks at various structural positions have different protoliths, which experienced different metamorphic, magmatic, and structural histories prior to final juxtaposition by the Valdez Creek shear zone during Wrangellia composite terrane accretion to North America. The term "Maclaren Glacier metamorphic belt" as originally defined does not convey the disparate polyphase tectonic evolution of the metamorphic rocks in the area. We propose that the recent advances in understanding have rendered the term "Maclaren Glacier metamorphic belt" obsolete. We argue that parsing the metamorphic rocks into the Maclaren schist/gneiss (structurally above the Valdez Creek shear zone) and Clearwater metasediments (structurally below the Valdez Creek shear zone) is more informative and thus will be more useful for future studies in the region.

## GEOLOGIC BACKGROUND

### Slip on the modern Denali fault

The Denali fault system is an arcuate set of structures that transect the Cordillera from northern British Columbia to western Alaska (St. Amand, 1957). Active dextral slip is likely routed to the Denali fault master strand from the plate boundary fault systems by way of the Connector fault (Doser, 2014; Brothers et al., 2018; Elliott and Freymueller, 2020; Choi et al., 2021; Figure 1). Published estimates of total offset on the Denali fault range from 370 to 400 km and are based on a variety of offset markers ranging from topography to terrane boundaries. Lowey (1998) provided a synopsis of strike-slip displacement estimates and Table 1 contains an updated list of separation estimates for the Denali fault, including those presented here for the first time. It is important to emphasize that the tabulated separation estimates consider only the active strand of the Denali fault. We recognize the likelihood of an older Denali fault system, which may have had multiple strands active during the Cretaceous (Wahrhaftig et al., 1975; Miller et al., 2002; McDermott et al., 2019). Herein, our use of the words *Denali fault* refer to the active strand of the fault, which appears to have been a single highly localized strand for much of the Cenozoic (Cole et al., 1999; Regan et al., 2021). When necessary for clarity, we distinguish the *modern-* or *proto-*Denali fault to refer to the Cenozoic and Cretaceous fault systems, respectively. Our use of the words *Denali fault system* includes the active Denali fault master strand, Totschunda fault, and thrust systems at the northern and southern flanks of the Alaska Range.

### Mesozoic terrane accretion and strike-slip faulting in the Cordillera

The Mesozoic geology of the North American Cordillera is characterized by the accretion and margin-parallel transport of allochthonous terranes (Coney et al., 1980; Nelson and Colpron,

2007; Colpron et al., 2015). The outboard belt of the Cordillera is largely composed of Paleozoic and Mesozoic arc rocks belonging to the Wrangellia, Peninsular, and Alexander terranes, which had accreted to each other prior to collision with the Cordilleran margin (Gardner et al., 1988; Beranek et al., 2014; Israel et al., 2014). Herein, we refer to the amalgamated terranes as the "Wrangellia composite terrane" and distinguish the individual terranes only when necessary. The structural polarity during accretion of the Wrangellia composite terrane to the Cordillera is disputed; some authors argue for W-dipping subduction (Hildebrand, 2015; Sigloch and Mihalynuk, 2017; Lowey, 2019), whereas others argue for E-dipping collisional structures and an unclear role of subduction during the collision (Trop and Ridgway, 2007; Pavlis et al., 2019). Regardless of structural polarity, the collision coincided with along-strike diachronous oblique closure of a marginal marine basin system from Late Jurassic to Late Cretaceous (McClelland et al., 1992; Ridgway et al., 2002; Manselle et al., 2020). Deformed and variably metamorphosed packages of clastic strata representing the closed marginal marine basins are exposed over 3000 km length of the Cordillera from southern British Columbia to western Alaska (Methow-Tyaughton-Gravina-Dezadeash-Nutzotin-Kahiltna basins-Figure 1B). In southern Alaska, the highly deformed region underlain by imbricated and metamorphosed Kahiltna basin strata, fragments of oceanic crust, and disparate continental terranes is referred to as the Alaska Range suture zone (Ridgway et al., 2002; Fitzgerald et al., 2014; Trop et al., 2019; ARSZ–Figure 1B).

Syn-and post-collisional strike-slip faulting contributed to margin-parallel transport of the Wrangellia composite terrane and dismemberment of the basinal assemblages along the inboard margin of the composite terrane. The strike-slip faulting is generally taken to accommodate the margin-parallel component of oblique relative plate motion between western North America and outboard oceanic plates (e.g. Monger and Gibson, 2019). Regional deformation patterns are

consistent with southward transport of outboard terranes along sinistral fault systems during the late Jurassic and early Cretaceous (Evenchick, 1991; Monger et al., 1994; Chardon et al., 1999; Israel et al., 2006; Mahoney et al., 2009; Cobbett et al., 2016). By the late Cretaceous, widespread dextral shear in the Cordillera contributed to northward transport of the terranes relative to the North American craton, which continued into the Cenozoic (Avé Lallemant and Oldow, 1988; Wyld et al., 2006). Many paleomagnetic-based studies call for large-scale (>1500 km) of Cretaceous-Cenozoic northward displacement of the Cordilleran terranes (e.g. Hillhouse and Coe, 1994; Johnston et al., 1996a; Stamatakos et al., 2001; Enkin, 2006). However, the sum of geology-based slip estimates does not reach the magnitude of translation inferred from the paleomagnetic estimates (e.g., Wyld et al., 2006), thus implying the potential for missing slip.

Much of the strike length of the Denali fault marks the boundary between rocks belonging to, or derived from, the Wrangellia composite terrane and rocks with peri-continental affinity. Thermochronological, structural, and stratigraphic datasets suggest that oblique closure of the Kahiltna basin, and associated development of the Alaska Range suture zone, involved slip on a potentially multi-stranded proto-Denali fault system along the paleo-eastern margin of the Wrangellia composite terrane, which may have translated the composite terrane relative to Mesozoic strata to the east (McDermott et al., 2019; Trop et al., 2020). In contrast, the modern Denali fault cuts obliquely through the Mesozoic basinal assemblages, continental margin rocks, and plutonic belts (Figure 1). The section of the Denali fault between the longitudes of the Delta River (~145.5ºW–Alaska) and Kluane Lake (~139ºW–Yukon) juxtaposes the Wrangellia terrane rocks directly against peri-Laurentian rocks, whereas Mesozoic basin strata and associated crystalline rocks are largely absent from that section of the fault system (Figure 1A). The similarities among Mesozoic-Paleogene rocks near the Delta River and Kluane Lake, and lack of

similar rocks between the two areas, has made them a target for estimating offset on the modern Denali fault (e.g., Eisbacher, 1976; Nokleberg et al., 1985).

**Geology south of the Denali fault near the Delta River in the eastern Alaska Range**

South of the Denali fault and west of the Delta River, a series of north-dipping thrust panels contain Triassic continental margin strata, Alaska Range suture zone metasedimentary and plutonic rocks, and Wrangellia terrane meta-igneous rocks. From north to south, important structures bounding the thrust panels are the Susitna Glacier thrust fault, Valdez Creek shear zone/fault, and the Talkeetna-Broxson Gulch fault (Figures 1A and 2).

The Triassic continental margin rocks in the northernmost and structurally highest panel south of the Denali fault comprise carbonate and clastic strata that are intruded by ca. 98-57 Ma plutons in the hanging wall of the Susitna Glacier thrust fault (Csejtey et al., 1992; Riccio et al., 2014). In the footwall south of the Susitna Glacier thrust fault, amphibolite facies pelitic-to-quartzofeldspathic schists and gneisses of the Maclaren schist are intruded by the East Susitna batholith (Davidson et al., 1992; Nokleberg et al., 1985; Waldien et al., 2021). Individual plutons within the East Susitna batholith have yielded crystallization ages ranging from ca. 74-33 Ma (Turner and Smith, 1974; Aleinikoff et al., 1981; Ridgway et al., 2002; Davidson and McPhillips, 2007; Regan et al., 2021). Across the Valdez Creek fault/shear zone to the south, the Clearwater metasediments comprise ca. 160-144 Ma generally arkosic-to-mafic metasedimentary strata with lesser argillaceous slate and phyllite, which are intruded by small volume intermediate-ultramafic intrusions with crystallization ages ranging from ca. 142 to 102 Ma (Mooney, 2010; Waldien et al. 2021). All of these metasedimentary and plutonic rocks are thrust southward over the Wrangellia terrane by the Broxson Gulch fault.

In the eastern Alaska Range, Wrangellia stratigraphy consists of Carboniferous volcanic and volcaniclastic strata overlain by lesser Permian carbonate strata and regionally extensive Triassic flood basalts. The Carboniferous strata in the area host generally intermediate composition intrusions that range in age from ca. 300-to-315 Ma (Waldien et al., 2021). Both the strata and the intrusions have been linked to the Skolai arc that forms the base of the Wrangellia terrane in south-central Alaska (Bond, 1973; Beard and Barker, 1989). Carbonate strata containing early Permian fossils unconformably overly the Skolai arc rocks (Bond, 1973, 1976; Nokleberg et al., 1992b, Richter and Dutro, 1975) and may record cessation of Skolai arc magmatism in the Late Pennsylvanian (e.g., Beranek et al., 2014; Israel et al., 2014). Triassic Nikolai flood basalt strata unconformably overly the Paleozoic rocks in the region (Greene et al., 2008, 2010; Twelker et al., 2020). Intrusions and strata within the Nikolai province yield dates of 225-230 Ma (Bittenbender et al., 2007; Greene et al., 2010; Twelker et al., 2020; Waldien et al., 2021).

South of the Denali fault and east of the Delta River, a belt of Eocene felsic volcanic rocks with lesser basalt unconformably overlies and is faulted against pre-Cenozoic Wrangellia rocks between the Delta River in the west and the Chistochina River in the east (Nokleberg et al., 1992a; Gillis et al., 2019; Figures 1 and 2). The Eocene volcanic strata and Wrangellia rocks are carried in the hanging wall of the south-vergent McCallum-Slate Creek thrust system. The footwall south of the McCallum-Slate Creek fault system contains the Oligocene-Pliocene fluvial-lacustrine McCallum basin strata (Allen et al., 2016; Waldien et al., 2018).

The tectono-metamorphic evolution of rocks south of the Denali fault near the Delta River records imbrication of North American-affinity and Wrangellia-affinity rocks during late Cretaceous terrane accretion and late Cenozoic reactivation of the terrane accretionary structures. Prior to juxtaposition during terrane accretion, the Maclaren schist protolith was derived from, and

deposited upon, the western margin of North America at ca. 94-86 Ma, whereas the Clearwater metasediments were deposited along the paleo-eastern margin of the Wrangellia terrane at ca. 150 Ma (Waldien et al., 2021). Initial juxtaposition of the Maclaren schist and Clearwater metasediments took place with formation of the Valdez Creek shear zone, which is a south-vergent thrust shear zone intruded by a ca. 74 Ma syn-kinematic tonalite sill (Ridgway et al., 2002). Motion on the shear zone produced a well-preserved inverted metamorphic gradient in the footwall Clearwater metasediments, which records the Cretaceous history of prograde metamorphism related to Wrangellia terrane accretion (Smith, 1981; Davidson et al., 1992; Hollister, 1993). In the Alaska Range east of the Maclaren River, the Maclaren schist experienced a pervasive greenschist facies retrograde metamorphic overprint that has been linked to post-32 Ma reactivation of the Valdez Creek shear zone as the Valdez Creek fault (Waldien et al., 2021). Reactivation of the shear zone nucleated a south-vergent imbricate thrust system that includes the Broxson Gulch fault at the northern margin of the Wrangellia terrane and reverse faults within the Wrangellia terrane to the south (Waldien et al., 2021). The Denali fault truncates the Maclaren schist and associated rocks and structures near the Delta River (Figures 1 and 2).

**Geology northeast of the Denali fault near Kluane Lake in southwestern Yukon**

Near Kluane Lake northeast of the Denali fault, a series of north-to-northeast-dipping thrust panels contain peri-Laurentian Yukon-Tanana terrane rocks, the Kluane Metamorphic assemblage, the Dezadeash formation, and the Bear Creek formation. Important structures in the region are the Kluhini River thrust and Tatshenshini shear zone/Shakwak fault.

Rocks belonging to the Yukon-Tanana terrane occupy the highest structural panel, which consist of pre-Carboniferous quartzose metasedimentary rocks with lesser carbonate and

amphibolite that host late Devonian and younger intrusions (Johnston et al., 1996b; Israel et al., 2011). South of the Yukon-Tanana terrane, the Ruby Range batholith is a ca. 77-57 Ma composite intrusive suite emplaced along the boundary between Yukon-Tanana terrane rocks to the north and the Kluane metamorphic assemblage to the south (Israel et al., 2011; Stanley, 2012). The Kluane metamorphic assemblage consists of late Cretaceous amphibolite facies pelitic and quartzofeldspathic schist and gneiss (Mezger et al., 2001a). For simplicity, we hereafter refer to these rocks as the Kluane schist. The batholith largely obscures the contact between the Kluane schist and Yukon Tanana terrane, yet vestiges of a late Cretaceous W-vergent thrust shear zone (Kluhini River thrust-Vice et al., 2020) are preserved locally. Smaller intrusions within the 54-48 Ma Hayden Lake suite intruded the low structural position of the Kluane schist (Colpron et al., 2016).

The southern margin of the Ruby Range batholith and Kluane schist are juxtaposed against Dezadeash and Bear Creek formations to the southwest along the Shakwak fault and Tatshenshini shear zone (Lowey, 2000; Colpron et al., 2016; Vice et al., 2020). The Bear Creek assemblage consists of Upper Triassic marine strata and lava flows (Israel et al., 2015). The Late Jurassic-early Cretaceous Dezadeash formation unconformably overlies the Bear Creek assemblage and consists of ≥1 km of marine turbidite strata (Eisbacher, 1976; Lowey, 1998). Both the Bear Creek and Dezadeash strata host the ca. 126-106 Ma (K-Ar dates) Shorty Creek and Pyroxenite Creek intermediate-ultramafic intrusive suite (Eisbacher, 1976). The NW-striking Denali fault truncates the western margin of the entire package of north-dipping structural panels in southwestern Yukon.

The geologic evolution of rocks near Kluane Lake records closure of an ocean basin during the late Cretaceous (Mezger et al., 2001). Detrital zircon U-Pb data indicate that both schistose and gneissic Kluane rocks have ca. 95-90 Ma protolith ages and received sediment from Yukon-

Tanana and other peri-Laurentian terranes (Israel et al., 2011; Stanley 2012) prior to imbrication and prograde metamorphism along east-northeast-dipping convergent structures (Erdmer and Mortensen, 1993). In contrast, the Dezadeash formation was likely sourced from the Mesozoic arcs built upon the Wrangellia composite terrane as indicated by paleo-current indicators and detrital zircon U-Pb age spectra (Lowey, 2018). Similarly, the Bear Creek formation may correlate with similar age and composition rocks within the Alexander terrane (Israel et al., 2015). During Wrangellia composite terrane accretion, the Kluane schist experienced regional metamorphism as early as 82 Ma and was intruded by the Ruby Range batholith from ca. 77 to 57 Ma (Israel et al., 2011; Stanley 2012). The ca. 57 Ma phase of the Ruby Range batholith displays regional plutonic-to-volcanic textural gradation that link it to the Rhyolite Creek volcanics to the north (Israel et al., 2011), which may record tilting of the crustal section following terrane accretion (Johnston and Canil, 2007).

## METHODS

### Geologic mapping

We performed 1:20,000-scale bedrock geologic mapping during the summers of 2018 and 2019 on base maps constructed from IfSAR Alaska and ArcticDEM digital terrain models. Mapping focused on along-strike correlation of major structures and bedrock units between the eastern Alaska Range and Clearwater mountains. Here we present a new bedrock geologic map (Figure 2), compiled from the new mapping and prior mapping by Turner and Smith (1974), Smith (1981), Mooney (2010), Waldien et al. (2018), Twelker et al. (2020), and Waldien et al. (2021).

## Separation measurements

We measured the strike-slip separation of correlative rock units along the Denali fault on a NAD83 Alaska Albers Conic equal area projection using the *ruler* tool in ESRI Arcmap. If the body of rock used for measurement is cut by the Denali fault, then measurements represent the distance between the midpoints of the cut faces of the correlative units. If the body is not mapped as cut by the Denali fault, then we measured from the location on the fault nearest to the body. Differences in deformation, rotation, and erosional exhumation of the correlative rocks on opposite sides of the fault introduces uncertainty into the separation measurements that is difficult to quantify. A simple trigonometric calculation accounting for the dip of reactivated structures near the Delta River (~40-70ºN), the inferred differential exhumation between the Maclaren and Kluane schist (~5-10 km), and the timing of the differential exhumation relative to slip on the Denali fault (post-32 Ma exhumation of Maclaren schist; Waldien et al., 2021) suggests that separation measurements have associated uncertainties as great as ~8.5 km. In lieu of measurement-specific uncertainties, we infer that the measurements of strike-slip separation presented and discussed herein have associated uncertainties of less than ±10 km.

## Zircon U-Pb dating

*Sample preparation and data collection*

We performed single-grain zircon U-Pb geochronology by Laser Ablation Quadrupole Inductively Couple Mass Spectrometry (LA-Q-ICP-MS) with three primary goals: 1) to fingerprint metasedimentary rocks by determining the sediment source areas of the protolith, 2) to estimate the maximum depositional age of the protolith, and 3) to date igneous intrusions in the map area. Mineral separation at UC Davis involved standard crushing techniques, a miner's gold pan, Frantz

isodynamic separator, and Lithium Polytungstate and/or Methylene Iodide heavy liquids to concentrate zircon grains. For detrital zircon samples, we concentrated zircon grains enough to mount them by pouring; for igneous samples we hand-picked relatively large, inclusion-sparse zircon grains. Prior to LA-Q-ICP-MS analysis, we mounted the zircon grains and reference materials into 1" epoxy rounds, polished the rounds to expose the grain surface, and imaged them using a Cameca SX-100 Electron Microprobe. High-contrast back-scattered electron images allowed us to identify zoning and/or inherited cores in individual zircon grains, which informed our laser spot placement on each grain. We collected isotopic data using an Agilent 7700 series Q-ICP-MS coupled to a Photon Machines 193 nm Excimer laser ablation system at UC Davis. By polishing the grain mounts until zircon surfaces are exposed, rather than grinding to the core of the crystal, we were in some cases able to ablate through metamorphic rims into detrital cores. Obtaining dates on both the rim and core was achieved using the *VizualAge* plug-in as implemented with the *U_Pb_geochronology3* data reduction scheme in the Iolite program (Paton et al., 2010; Petrus and Kamber, 2012). Supporting Information S1 contains detailed mineral extraction, analytical, data reduction, and data filtering methods used in the LA-Q-ICP-MS analyses. Supporting Information S2 contains the single-grain U-Pb data.

*Data presentation*

Our fingerprinting of metasedimentary protoliths is based on identifying distinctive populations of detrital zircon single grain U-Pb dates. Each multimodal detrital zircon age data set contains analyses on at least 117 grains (Vermeesch, 2004). One detrital sample displays a unimodal age spectrum that is defined by 50 single-grain analyses. We represent the detrital U-Pb data as Kernel Density Estimates using the DZStats and Density Plotter programs (Saylor and

Sundell, 2016 and Vermeesch, 2012, respectively). Because many of the rocks analyzed in our study experienced amphibolite and upper greenschist metamorphic temperatures and thus may have experienced metamorphic recrystallization and/or lead loss (e.g., Hoskin and Schaltegger, 2003), we screened each analysis from the youngest age population of each sample to parse detrital and post-depositional metamorphic grains on the basis of U content (ppm), U/Th ratio, imaged zoning patterns, age relative to the known ages of intrusions within the rock unit, and presence of age zoning reveled by laser depth profiling (Supporting Information S1). After parsing detrital and metamorphic grains, we calculated a maximum depositional age for each sample using the age of the youngest statistical population of the detrital grains (e.g., Herriott et al., 2019).

We used Isoplot (Ludwig, 2008) to determine the ages of igneous zircon populations by calculating the weighted mean of single grain dates with internal 2s errors. Reported uncertainties of weighted mean ages represent 95% confidence interval internal uncertainties and the quadratic addition of external uncertainties (e.g., Horstwood et al., 2016; Supporting Information S1).

*Statistical tests*

To assess the similarities between metasedimentary assemblages across the Denali fault, we performed statistical tests on the detrital zircon U-Pb age data using the multidimensional scaling program DZmds from Saylor et al (2017). We focused our multidimensional scaling approach on the cross-correlation of probability density distributions because that approach has been shown to work well with both simple and complex datasets that range in sample size (Saylor and Sundell, 2016).

## Hf isotopic data

In order to refine sediment source areas of metasedimentary protoliths, we performed Hf isotopic analysis on Mesozoic detrital zircon grains from two samples of Clearwater metasediment and one sample of Maclaren schist. Hf analyses were performed using a Photon Machines 193 nm Analyte G2 excimer laser (40 um spot size) coupled to a Nu High Resolution Multicollector ICP-MS at the Arizona Laserchron Center. The analytical approach used the sample bracketing technique, wherein we performed at least one analysis on each of the six reference materials (FC, Mud Tank, 91500, Temora, Plesovice, R-33, and Sri Lanka natural zircon) between every 15-20 unknowns. U-Pb age data for the analyzed grains are published in Waldien et al. (2021). Complete Hf analysis methods and data are available in Supporting Information S1.

## $^{40}Ar/^{39}Ar$ dating methods

In order to determine the age of faulted volcanic rocks, we conducted $^{40}Ar/^{39}Ar$ analyses at the Geochronology Laboratory at the University of Alaska, Fairbanks, where samples were crushed, sieved, washed, and hand-picked for a pure phase of phenocryst-free groundmass or biotite. The sample aliquots and monitor mineral MMhb-1 (Samson and Alexander, 1987), which has an age of 523.5 Ma (Renne et al., 1994), were irradiated at McMaster University in Hamilton, Ontario, Canada. Upon their return from the reactor, the samples and monitors were loaded into 2 mm diameter holes in a copper tray and then loaded in an ultra-high vacuum extraction line. The monitors were fused, and samples heated, using a 6-watt argon-ion laser following the technique described in York et al. (1981), Layer et al. (1987), and Benowitz et al. (2014). Ar isotope measurements in this system were made using a VG-3600 mass spectrometer.

Supporting information S3 contains detailed $^{40}Ar/^{39}Ar$ analytical methods and contains the $^{40}Ar/^{39}Ar$ data, wherein all ages are reported at the 1σ level and calculated using the constants of Renne et al. (2010). The integrated age is the age given by the total gas measured and is equivalent to a potassium-argon (K-Ar) age. The spectrum provides a plateau age if three or more consecutive gas fractions represent at least 50% of the total gas release and are within two standard deviations of each other (mean square weighted deviation <2.5).

## RESULTS

### New mapping and synthesis with existing maps

Our new mapping and U-Pb geochronology (discussed below) link two regions of previous detailed mapping to the west (Smith, 1981) and east (Waldien et al. 2021). Accordingly, the mapping presented herein addresses the correlation between Mesozoic structures in the Clearwater Mountains (bold faults on Figure 2) and reactivated versions of those structures to the east (thin faults on Figure 2). The transition between reactivated and non-reactivated structures broadly coincides with the Maclaren River, which is also the location of a 1:250,000-scale quadrangle boundary (147° W) (cf., Csejtey et al., 1992; Nokleberg et al., 1992a; Wilson et al., 1998, 2015). To our knowledge, our study is the first to attempt to correlate the geology across the region. Our along-strike correlation of structures from the Clearwater Mountains to the eastern Alaska Range relies on the continuity of distinct rock packages between the two regions (Figure 2).

#### *Geology of the Maclaren River corridor*

The 10-km-wide region between the Maclaren Glacier in the east and west fork of the Maclaren River in the west exposes the Maclaren schist, Clearwater metasediments, and the

Wrangellia terrane (Figure 2). The structurally highest panel contains the Maclaren schist and a cross-cutting granodiorite body carried in the hanging wall of the Valdez Creek fault. South of the Valdez Creek fault, the Clearwater metasediments in this region are dominated by fine-grained metagreywacke and slate. East of the middle fork of the Maclaren River, the metasediments host a volumetrically-small zoned gabbro-diorite intrusion. Diorite dikes near the intrusion are folded with the foliation in the Clearwater slate (Figure 3A). Due to the composition of the intrusion, the zonal structure, and the deformation shared with the host rocks, we infer that the intrusion is early Cretaceous in age, which has been documented within the Clearwater metasediments to both the east and southwest (Mooney, 2010; Waldien et al., 2021). The Clearwater metasediments and associated intrusions were thrust southward over Wrangellia terrane rocks, which in this region are predominantly composed of Nikolai rocks and lesser Permian carbonate strata in the north near the Broxson Gulch fault. The Wrangellia strata host zoned intermediate-mafic composition granitoids.

Along the west and middle forks of the Maclaren River, two approximately north-striking faults cut the dominant east-west structural fabric in the region. Although the faults are not exposed due to their location in the river valleys, their existence is implied by the misalignment of east-west-trending structures across the river valleys and the steep topographic gradient between the eastern Alaska Range and Susitna River valley.

A northeast-southwest–trending belt of topography separates the Maclaren River from the Susitna River valley (headwaters of Boulder Creek- Figure 2). Structures in the area include the Talkeetna fault and the herein-named Boulder Creek fault (BCF-Figure 2). The Talkeetna fault in the area is a steeply northwest-dipping structure exposed near the southeastern margin of the topography, which likely has limited Cenozoic slip, based on modest offset of late Cretaceous

sedimentary rocks (O'Neill et al., 2001; Mooney, 2010). The map pattern suggests that the Boulder Creek fault dips steeply to the southeast and the topographic gradient across the fault trace marks the eastern boundary of the Susitna River valley. The Boulder Creek fault juxtaposes low-grade metagreywacke and slate of the Clearwater metasediments to the east against tonalite intrusions to the west (Figure 2). Thus, the southeast-side-up sense of slip on the Boulder Creek fault has cut out the higher-grade portion of the inverted metamorphic field gradient that is elsewhere present in the footwall of the Valdez Creek shear zone. Cataclastic deformation associated with the Boulder Creek fault overprints late Cretaceous (e.g., Ridgway et al., 2002) ductile fabrics in the tonalite body, thus implying Cenozoic slip on the Boulder Creek fault. Although post-collisional brittle faults are present in the Clearwater Mountains to the southwest of the Boulder Creek fault (e.g., Smith, 1981; Mooney, 2010), the Valdez Creek shear zone does not appear to have experienced reactivation (e.g., Davidson et al., 1992) and is crosscut by the Boulder Creek fault (Figure 2).

*Along-strike correlation of structures*

Published synthesis maps of the eastern Alaska Range have correlated the Valdez Creek shear zone in the west with a structure east of the Maclaren Glacier named the Meteor Peak fault (Wilson et al., 1998, 2015). The correlation appears to have stemmed from the location of the two structures at the southern margin of plutons within the Maclaren schist and the inference that all of the plutons in the area intruded at ca. 70 Ma (e.g., Aleinikoff et al., 1981; Nokleberg et al., 1992a, b).

Multiple lines of evidence indicate that the Valdez Creek shear zone and Meteor Peak fault are not correlative structures. Mainly, the Cenozoic evolution of structures east of the Maclaren

River reveals that the Valdez Creek fault formed as a reactivation of the Valdez Creek shear zone during the Oligocene (Waldien et al., 2021). Moreover, our observations of the Meteor Peak fault between the Black Rapids and Augustana Glaciers (BRG and AG-Figure 2) show it to be an anastomosing brittle fault system that follows the southern margin of the 42-33 Ma phase of the East Susitna batholith. Dikes along the margin of the 42-33 Ma composite pluton are generally offset by fewer than 10 m and cataclasis associated with slip on strands of the Meteor Peak fault is poorly developed and restricted to discrete zones less than 5 m wide (Figure 3B). These observations together indicate that the Meteor Peak fault is a minor brittle fault that formed after ca. 33 Ma and thus is not related to the late Cretaceous Valdez Creek shear zone.

After reconciling the structural complications near the headwaters of the Maclaren River described above, the along-strike continuity in metasedimentary belts reveals the transition between Cretaceous structures in the Clearwater Mountains and reactivated versions of those structures nearer to the Denali fault in the eastern Alaska Range (Figure 2). The Talkeetna-Broxson Gulch fault marks the boundary between the Wrangellia terrane and the Wrangellia-affiliated Clearwater metasediments. The Talkeetna fault in the Clearwater Mountains is a steeply dipping to sub-vertical crustal-scale fault with limited evidence for Cenozoic slip (O'Neill et al., 2001; Brennan et al., 2011). The Broxson Gulch fault in the Alaska Range is a moderately north-dipping reverse fault that is part of the post-32 Ma thrust system along the south flank of the Alaska Range (Waldien et al., 2021). The boundary between the Maclaren schist and Clearwater metasediments is the Valdez Creek shear zone in the west and Valdez Creek fault to the east. Late Cretaceous syn-collisional ductile thrusting is preserved on the Valdez Creek shear zone in the Clearwater Mountains (Davidson et al., 1992), whereas the shear zone has been reactivated as a brittle fault in

the eastern Alaska Range (Waldien et al., 2021). The Meteor Peak fault appears to have no correlative structure in the Clearwater Mountains.

## Zircon U-Pb dating

*Metasedimentary rocks*

Detrital zircon U-Pb age spectra from four samples of Clearwater metagreywacke (621 grains, Figure 4) are dominated by Jurassic grains. Three of the samples (18ATW20, 18ATW23, 19ATW46) display bimodal distributions with modes at ca. 155 and 185 Ma. Pre-Jurassic grains in two of the samples define subordinate populations at ca. 550 Ma, 1100-1800 Ma, and 2500-2800 Ma. Sample 17ATW09 yielded a unimodal age peak centered at ca. 150 Ma (Figure 4). Maximum depositional ages of the samples range from ca. 155-144 Ma (Figure 4). Near the middle fork of the Maclaren River, sample 19ATW39 is a quartz-muscovite phyllite interfoliated with the Clearwater slate, which we interpret as a metamorphosed felsic tuff based on the composition and unimodal distribution of zircon dates, yielded a weighted mean age of 160.4 ± 1.5 Ma (Table 2).

Detrital zircon U-Pb age spectra from five samples of Maclaren schist (1,094 grains, Figure 5) display: (1) dominant Mesozoic age populations at ca. 110-85 Ma, 160-145 Ma, and 200-180 Ma, although the relative proportions vary; (2) a subordinate population of ca. 370-330 Ma grains; (3) Proterozoic and Archean grains in all samples, although abundances are low; (4) post-depositional metamorphic rims or recrystallized domains with dates of ca. 84-55 Ma (Supplemental Information S1); and (5) mid-Cretaceous maximum depositional ages of ca. 91-88 Ma (Figure 5).

*Plutonic rocks*

Multiple intrusive phases are present in the study area, each of which has a distinctive age-composition relationship that is unique to the thrust panels that host them. Here we present the ages of the plutonic suites from structurally highest (youngest) to structurally lowest (oldest) level. The new ages are reported in Table 2 and Supporting Information S4 contains additional details.

Maclaren schist: The Maclaren schist hosts three intrusive suites that are distinguishable on the basis of age and petrographic features. The youngest phase intruded the structurally highest portion of the Maclaren schist adjacent to the Denali fault. Compositions in this plutonic suite are varied and include biotite tonalite, hornblende-biotite granodiorite, and biotite-muscovite granite. The margins of the bodies are zones of mutually crosscutting dikes that crosscut the metamorphic foliation in the Maclaren schist (Figure 3C). Many samples from the suite display a high temperature fabric defined by the alignment of amphibole and plagioclase grains. Some samples display sub-solidus mylonitic fabrics. Samples from this suite yielded U-Pb zircon dates ranging from ca. 42 Ma to 33 Ma (Benowitz et al., 2011; Regan et al., 2021).

An intermediate-age plutonic suite intruded the structurally lowest portion of the retrograded Maclaren schist in the Alaska Range and is cut by the Valdez Creek fault (Waldien et al., 2021). Plutons in this suite consist of non-foliated biotite or hornblende granodiorite with late biotite-muscovite-K-feldspar pegmatite veins. The margins of the plutons crosscut the Maclaren schist foliation (Waldien et al., 2021). One sample from this suite near the middle fork of the Maclaren River (19ATW79) yielded a U-Pb zircon weighted mean date of 51.9 ± 0.6 Ma.

The oldest intrusions in the Maclaren schist are tonalitic, found in the western portion of the study area near Boulder and Valdez Creeks (Figure 2), and generally contains a well-developed,

high-temperature foliation defined by strained mafic enclaves and aligned biotite, plagioclase, and amphibole (Davidson et al., 1992; Figure 3D). The tonalite bodies display reaction textures wherein primary clinopyroxene has reacted to amphibole and then to biotite. Three samples from the tonalite suite yielded U-Pb zircon weighted mean dates of 70.5 ± 1.0 Ma (17ATW03), 68.3 ± 1.3 (18ATW21), and 64.6 ± 0.7, (19ATW40). In the headwaters of the west fork of the Maclaren River, the tonalite suite is associated with a garnet-and-biotite-bearing leucocratic body. The leucocratic body generally lacks internal structure and forms a series of disseminated veins and dikelets into the Maclaren schist along the margins. Zircon crystals separated from the leucocratic body (sample 19ATW66) display core-rim textures wherein the cores yield ages common of detrital zircons within the Maclaren schist and the rims yielded a weighted mean date of 75.8 ± 1.9 Ma.

Clearwater metasediments: Sample 19ATW55 came from a small (<50 meters across) body of non-foliated hornblende diorite, which intrudes the Clearwater metasediments east of Boulder Creek and yielded a weighted mean date of 53.1 ± 0.6 Ma. The new date on sample 19ATW55 expands the known age range of small volume intrusions within the Clearwater metasediments, which elsewhere have been dated at ca. 142 Ma, 102 Ma, and 63-68 Ma (Davidson and McPhillips, 2007; Mooney, 2010; Waldien et al., 2021).

Wrangellia terrane: Our zircon U-Pb dating of plutonic rocks bears on two phases of magmatism within the Wrangellia terrane (Figure 2). The oldest dates come from a tabular granodiorite body east of the Delta River, which yielded weighted mean dates of 309.8 ± 3.9 Ma (14ATW50) and 307.2 ± 6.1 Ma (17ATW11). Similarly, a composite granodiorite-granite body near the Eureka

Glacier (16CSR17) yielded a weighted mean date of 306.3 ± 4.0 Ma. Younger dates come from the Maclaren River corridor, where concentric diorite-granodiorite bodies with marginal diorite-gabbro dike systems intrude Skolai and Nikolai rocks. Samples from these bodies yielded weighted mean dates of 144.1 ± 2.3 Ma (15DR140–hornblende diorite body), 129.8 ± 2.4 Ma (13ET270–biotite granodiorite body) and 112.9 ± 1.3 Ma (19ATW81–hornblende diorite dike).

**Hf isotopic signatures of Mesozoic detrital zircon grains**

Detrital zircon grains from both age populations in the Clearwater metasediments (ca. 155 and 185 Ma) display juvenile εHf isotopic signatures (Figure 6). Zircon grains belonging to the early Jurassic age population in sample 16ATW10 display εHf values ranging from +4 to +11, whereas early Jurassic grains in sample 15ATW23 have values of +5 to +16. Late Jurassic zircon grains in sample 16ATW10 yielded εHf values ranging from +6 to +10 and sample 15ATW23 contains grains with values of +8 to +15.

Hf isotopic signatures from detrital zircon grains in the Maclaren schist (sample 15ATW29) show a range of juvenile and evolved εHf compositions (Figure 6). Early Jurassic zircon grains display εHf values ranging from -10 to +12. Late Jurassic grains are more juvenile and display εHf values ranging from +2 to +15. The small population (3 grains) of ca. 100 Ma zircon grains displays a spread of εHf values ranging from -18 to +13. Circa 90 Ma detrital zircon grains have more juvenile εHf compositions ranging from +8 to +13.

**$^{40}Ar/^{39}Ar$ dates on volcanic strata**

Volcanic strata overlap and are faulted against Paleozoic Wrangellia rocks along the southern margin of the Alaska Range east of the Delta River. The volcanic strata are generally

felsic in composition, yet mafic flows, mafic dikes, and conglomeratic strata are found locally (Bond, 1976; Hults and Athey, 2011; Waldien et al., 2018; Gillis et al., 2019). Four felsic extrusive samples southeast of the Gulkana Glacier in our study area (Figure 2) yielded $^{40}Ar/^{39}Ar$ dates of 50.9 ± 0.5 Ma (12HODO–rhyodacite tuff, biotite plateau age), 45.5 ± 0.2 Ma (46GUNN–dacite flow, whole rock plateau age), 49.3 ± 0.7 Ma (15BG216–dacite flow, whole rock weighted mean age), and 49.8 ± 0.3 Ma (15BG209–rhyodacite tuff, whole rock weighted mean age) (Table 3; Supporting Information S3).

## DISCUSSION

### Protolith provenance and paleogeographic setting for metasedimentary assemblages

*Clearwater metasediments*

Detrital zircon U-Pb age spectra and Hf isotopic signatures suggest that the Clearwater metasedimentary rocks formed along the paleo-eastern margin of the Wrangellia composite terrane during the Late Jurassic-Early Cretaceous. Although terranes along the Laurentian margin contain Jurassic rocks that could have supplied Jurassic zircon grains to the Clearwater metasediment protolith (e.g., Gehrels et al., 2009; Allan et al., 2013; Sack et al., 2020), the general lack of pre-Mesozoic grains and juvenile εHf values of the Jurassic grains together suggest that the protolith sediment was derived from juvenile arc crust within the Wrangellia composite terrane (Figures 4 and 7). Jurassic source areas within the Wrangellia composite terrane include Chitina arc rocks (ca. 160-140 Ma: Roeske et al., 2003; Day et al., 2016; Beranek et al., 2017) and Talkeetna arc rocks (ca. 205-150 Ma: Roeske et al., 1989; Amato et al., 2007b; Rioux et al., 2007). The maximum depositional ages of the Clearwater metasediments and the ages of inter-bedded volcanics indicate that the strata were deposited between ca. 160 and 144 Ma (Mooney, 2010; Table 2). Intrusion of

a ca. 142 Ma alkali gabbro in the Clearwater Mountains post-dates deposition of the Clearwater protolith strata (Mooney, 2010; Figure 2).

Depositional ages, interpreted sediment source areas, detrital zircon Hf signatures, and stratigraphic features place the Clearwater metasediments among a suite of late Jurassic-Early Cretaceous basinal assemblages that span the inboard (north and east in present coordinates) margin of the Wrangellia composite terrane from western Alaska to British Columbia. From west to southeast, these basinal assemblages include the Koksetna River sequence (Wallace et al., 1989; Hults et al., 2013; Box et al., 2019), Clearwater metasediments (Mooney, 2010; Waldien et al., 2021; this study), Nutzotin Mountains sequence (Manuszak et al., 2007; Trop et al, 2020; Fasulo et al., 2020), Dezadeash formation (Lowey, 2019), Vand Creek assemblage (Vice, 2017), and western Gravina belt (Yokelson et al., 2015). It is not necessary that these basinal assemblages were linked as a single basin system at the time of deposition (e.g. Hults et al., 2013); however the similarities in depositional setting and interpreted provenance within the Wrangellia composite terrane do suggest that they together represent a regionally extensive clastic marine sequence linked to the paleo-eastern margin of the Wrangellia composite terrane. An Early-mid Cretaceous phase of strike-slip faulting may have translated the marine sequence relative to the Wrangellia composite terrane (e.g., Gehrels et al., 2009; Mooney, 2010; Yokelson et al., 2015; McDermott et al., 2019), yet the displacement history for those structures remains unclear.

*Maclaren schist*

Detrital zircon U-Pb age spectra indicate that the protolith of the Maclaren schist was deposited into a basin between previously accreted Cordilleran terranes to the east and the Wrangellia composite terrane to the west at ca. 94-86 Ma. As with other detrital zircon U-Pb

studies of the Maclaren schist (Link, 2017; Waldien et al., 2021), the samples presented herein comprise dominant detrital age populations at ca. 100-85 Ma, 200-145 Ma, and 370-330 Ma (Figures 5 and 7). The ubiquitous presence of pre-Mesozoic grains suggests that the protolith strata received sediment from regions within the Yukon-Tanana terrane and parautochthonous North America (e.g. Dusel-Bacon and Williams, 2009; Piercey and Colpron, 2009; Gehrels and Pecha, 2014; Pecha et al., 2016; Dusel-Bacon et al., 2017). The overlap between periods of high magmatic flux in the Coast Mountains arc and the populations of detrital zircon grains in the Maclaren schist further suggests that the protolith sediment was sourced from rocks along the western margin of North America (Figure 8). Hf isotopic compositions from Mesozoic zircon grains in the Maclaren schist display a range of juvenile and evolved εHf values that may record either isotopic heterogeneity in the peri-continental source area (e.g., Piercy et al., 2003; Cecil et al., 2011; Sack et al., 2020), sediment sourced from igneous belts built upon both the Wrangellia composite terrane and the North American margin, and/or sediment recycling from the Clearwater metasediments. All samples presented in this study display a population of metamorphic growth rims dated at ca. 84-55 Ma, which we interpret to post-date deposition (Figures 5 and 7; Supplemental information S1).

The Maclaren schist displays both similarities and differences compared to other Mesozoic basinal assemblages in the suture zone between the Wrangellia composite terrane and North America. Ca. 110-90 Ma strata are exposed in the northern domain of the Kahiltna assemblage throughout the central and western Alaska Range (Hampton et al., 2007, 2010; Kalbas et al., 2007; Hults et al., 2013; Box et al., 2019; Romero et a., 2020). The eastern Gravina belt of southeastern Alaska contains similar continental-derived strata, yet detrital zircon age spectra and available biostratigraphic information suggest the strata were deposited at ca. 120-110 Ma (Berg et al., 1972;

Kapp and Gehrels, 1998; Yokelson et al., 2015). The Maclaren schist, northern Kahiltna, and eastern Gravina assemblages all share a ca. 100-120 Ma detrital zircon age population that, in addition to Precambrian grains, likely records a sediment source from igneous belts corresponding to the Teslin, Whitehorse, and Coffee Creek plutonic suites built upon the western margin of North America (Tempelman-Kluit and Wanless, 1975; Allan et al., 2013). The additional presence of Jurassic age populations with juvenile εHf signatures in these basin assemblages permits sediment input from approaching outboard terranes as the marine basin closed. The Maclaren schist, however, differs from much of the northern Kahiltna and eastern Gravina strata in that it is 10-30 Myr younger and experienced amphibolite facies metamorphism during collision of the Wrangellia composite terrane. The sum of information suggests that the protolith of the Maclaren schist formed in one of the youngest, if not the youngest, known syn-collisional marine basins between the Wrangellia composite terrane and North American margin.

**Correlative rock packages and strike-slip separation**

Our restoration of the Denali fault system relies on the correlation of metasedimentary, plutonic, and volcanic belts across the fault. The correlative rock packages are listed in Table 1, located as boxed numbers on Figure 1, and described below.

*Dezadeash-Nutzotin-Clearwater (meta)sedimentary strata*

Our new data from the Clearwater metasediments suggest that they correlate with the Nutzotin Mountains sequence and Dezadeash formation. Presently, the Clearwater metasediments are exposed south of the Denali fault in the eastern Alaska Range, the Nutzotin Mountains sequence is exposed south of the Denali fault and east of the Totschunda fault in eastern Alaska,

and the Dezadeash formation is exposed the northeast of the Denali fault in southwestern Yukon (Figure 1). A correlation between the Dezadeash and Nutzotin strata was initially proposed on the basis of age and sedimentological features that are shared between the two successions (Eisbacher, 1976). Later work by Lowey (1998) documented the existence of a paleochannel carrying distinctive limestone boulders incised into the Dezadeash and Nutzotin strata, which has been offset ~370 km by the Denali fault. More recent studies involving detrital zircon U-Pb dating show similar age populations and distribution of Jurassic and early Cretaceous zircon grains within the Dezadeash formation, Nutzotin Mountains sequence, and Clearwater metasediments, which are interpreted to be sourced from Jurassic arcs built upon the Wrangellia composite terrane (Manuszak et al., 2007; Mooney, 2010; Link, 2017; Lowey, 2019; Fasulo et al 2020; Trop et al., 2020; Waldien et al., 2021). Among the dated samples, the Dezadeash formation and Clearwater metasediments of the Alaska Range show the greatest similarity because they both include a ca. 185 Ma age population that is absent from the Nutzotin strata and Clearwater metasediments of the Clearwater mountains (cf. Mooney, 2010; Lowey, 2019; Trop et al., 2020; Fasulo et al., 2020; Figure 7 and 9). Hf isotopic signatures from detrital zircon grains in the Clearwater metasediments show juvenile εHf values (Figure 6), which compare well with juvenile whole rock εNd values from the Dezadeash formation (Lowey, 2011) and juvenile zircon εHf values from detrital zircon grains in the Nutzotin Mountains sequence (Fasulo et al., 2020). Biostratigraphic and U-Pb radioisotopic ages indicate that Clearwater-Nutzotin-Dezadeash rocks were deposited from ca. 160 to 135 Ma (Lowey, 2011; Mooney, 2010; Fasulo et al., 2020; Trop et al., 2020; Figure 4).

Because the Clearwater, Nutzotin, and Dezadeash rocks are presently separated from each other along the Denali fault system, their restoration requires slip on both the Denali fault and Totschunda fault. The incised paleochannel records ~370 km of dextral separation between the

Dezadeash formation and Nutzotin Mountains sequence (Lowey, 1998). The measured 80-90 km of separation between the Clearwater and Nutzotin strata likely resulted from right-lateral slip transfer from the Totschunda fault to the Denali fault (e.g., Waldien et al., 2018; Brueseke et al., 2019; Berkelhammer et al., 2019). Cumulative translation and dissection of the Clearwater, Nutzotin, and Dezadeash assemblages records at least 465 km of separation on the Denali fault.

*Ann Creek-Pyroxenite Creek intrusions*

Ultramafic-to-intermediate intrusive bodies within the Clearwater metasediments (AK) and Dezadeash formation (YT) correlate on the basis of petrography and possibly age. Early workers in both the Clearwater metasediments and Dezadeash formation had described pegmatitic biotite-hornblende clinopyroxenite bodies associated with granodiorite (Stout, 1965; Eisbacher, 1976). In Yukon, the Pyroxenite Creek ultramafic body and associated Shorty Creek granodiorite within the Dezadeash formation yielded amphibole and biotite K-Ar dates ranging from ca. 126-106 Ma (Eisbacher, 1976). In the Alaska Range, similar biotite-hornblende clinopyroxenite cumulates and associated granodiorite bodies intrude the Clearwater metasediments north of Ann Creek and have been dated at ca. 102 Ma (Stout, 1965; Waldien et al., 2021). Due to similarities in petrography, structural position, proximity to the Denali fault, and general age information, the Pyroxenite Creek and Ann Creek ultramafic cumulate bodies may be dismembered portions of the same body. This correlation results in up to 505 km of dextral separation across the Denali fault.

*Maclaren-Kluane schist*

The Maclaren schist (AK) and Kluane schist (YT) correlate on the basis of petrography, metamorphic history, and detrital zircon U-Pb age spectra (Figures 7 and 9). Both schist bodies

display a dominant foliation that dips toward the continent (north or northeast). The foliation in both bodies contains porphyroclasts of garnet and distinctive 'black' plagioclase, both of which contain curved inclusion trails defined by rutile and graphite (Mezger et al., 2001; Stanley, 2012; Waldien et al., 2021). The shared metamorphic history involves an early Barrovian series path that peaked at Temperature (T) ~ 500 ºC and Pressure (P) ≥ 7 kbar, followed by a phase of isothermal decompression, and subsequent Buchan series conditions of T ~ 550-750 ºC and P ≤ 5 kbar (Mezger et al., 2001; Davidson and McPhillips, 2007). In the Alaska Range, the eastern portion of the Maclaren schist experienced a post-32 Ma retrograde metamorphic event that has been linked to reactivation of adjacent structures (Waldien et al., 2021). The absence of the retrograde event in the Kluane schist does not preclude the correlation because the retrogression took place after the bodies were separated by the Denali fault (see section 5.3). Detrital zircon age spectra from the Maclaren and Kluane schists both contain a predominance of Mesozoic grains accompanied by smaller Paleozoic and Precambrian populations and metamorphic overgrowth rims ranging in age from ca. 84 to 55 Ma (Figures 7 and 9). All published detrital zircon U-Pb datasets yield maximum depositional ages between 95 and 86 Ma (Figure 5; Supporting information S2). Because each schist body is cut obliquely by the Denali fault and no discrete diagnostic feature within the schists has been found for correlation, the measurement of strike-slip separation between the bodies is approximate. However, measuring from center-to-center of the cut face of each body yields ~445 km of dextral separation.

*East Susitna-Ruby Range Batholith (74-57 Ma phase)*

Late Cretaceous and Paleocene plutonic belts within the Maclaren and Kluane schists have similar ages and compositions. Both comprise predominantly late Cretaceous tonalite and

Paleocene granodiorite, although their proportions differ. In the East Susitna batholith (AK), syn-collisional tonalite bodies dated at ca. 74-65 Ma represent the oldest phase of magmatism within the Maclaren schist (Aleinikoff et al., 1981; Ridgway et al., 2002; this study). The oldest dated rocks within the Ruby Range batholith (YT) come from intermediate and mafic intrusions dated at 72-68 Ma (Israel et al., 2011), and possibly as old as 77 Ma (Stanley, 2012). Voluminous ca. 64-57 Ma granodiorite-to-granite plutons compose the main phase of the Ruby Range batholith (Israel et al., 2011). Granodiorite bodies dated at ca. 57 Ma represent a volumetrically minor portion of the East Susitna batholith (Riccio et al., 2014; Figure 2), but are present throughout the Talkeetna Mountains to the west (Csejtey et al., 1992). Although the proportions of each magmatic phase do not appear to be equal within the East Susitna and Ruby Range batholiths, the range of ages and composition of the intrusions are nearly identical. It remains unclear if there are individual bodies in the dissected 74-57 Ma batholith that can be matched across the Denali fault, yet correlating the easternmost 57 Ma pluton south of the Denali fault in Alaska to the Ruby Range batholith in Yukon results in a minimum dextral separation of 425 km.

*Shakwak-Ann Creek pluton (52-48 Ma)*

Early Eocene plutonic rocks hosted within the Maclaren and Kluane schists correlate on the basis of structural position, composition, and age. In Yukon, the Hayden Lake plutonic suite comprises ca. 55-48 Ma felsic plutons intruded into the structurally lowest portion of the Kluane schist (Stanley, 2012; Colpron et al., 2016). Similar plutons in Alaska include the ca. 52 Ma biotite granodiorite-monzonite plutons north of Ann Creek and in the west fork of the Maclaren River (Figure 2). The westernmost pluton within the Hayden Lake suite (Shakwak pluton) is a >54-to-46 Ma (K-Ar biotite cooling and U-Pb zircon crystallization dates, respectively) composite body

consisting of unfoliated biotite tonalite, biotite granodiorite, and quartz diorite (Yukon Geological Survey, 2020). Due to the overlap in age, identical structural position, similar rock types, and proximity to the Denali fault, we propose a correlation between the Shakwak pluton and the ca. 52 Ma biotite quartz monzonite body north of Ann Creek. Matching these two igneous bodies results in ~465 km of dextral separation along the Denali fault. We regard this correlation as our highest quality match across the Denali fault and most accurate measurement of strike-slip separation.

*Paleogene volcanic rocks-*

Post-collisional volcanic strata may correlate on the basis of composition, structural setting, and general age. South of the Denali fault, ca. 51-46 Ma volcanic strata between the Delta and Chistochina Rivers (Figure 1) in Alaska consist predominantly of syn-extensional felsic tuffs with lesser basalt-to-andesite flows and dikes (Bond, 1976; Waldien et al., 2018; Gillis et al., 2019; Figure 2; Table 3). The volcanic rocks near the Chistochina River appear to be the eastern-most isolated extent of the Paleogene volcanic belt that covers much of the Talkeetna Mountains (Csejtey et al., 1978, 1992; Nokleberg et al., 1992a). Potentially correlative rocks northeast of the Denali fault in southwestern Yukon include graben-bounded rhyolite tuffs with lesser andesite and basalt (Miskovic and Francis, 2004; Colpron et al., 2016). Field relationships and radiometric ages link the volcanic rocks to the ca. 57-55 Ma plutonic suite throughout southwestern Yukon (Morris and Creaser, 2003; Miskovic and Francis, 2004; Israel et al., 2011). The Bennett Lake igneous complex near the Yukon-British Columbia border, however, contains lava flows as young as ca. 50 Ma (Morrison et al., 1979; Morris and Creaser, 2003). Although no unique correlation between Eocene volcanic complexes across the Denali fault has yet been identified, we propose that the ca. 50 Ma volcanic strata and intrusions in the eastern Alaska Range may be a displaced portion of

the Bennett Lake igneous complex or a suite of distal channelized flows. Moreover, the northern Talkeetna Mountains west of our study area contain a suite of ca. 63-50 Ma bimodal volcanic strata and associated intrusions (Csejtey et al., 1992; Cole et al., 2007), which may correlate with the Rhyolite Creek volcanics and associated intrusions north of the Ruby Range batholith in Yukon. Each of these potential correlations would result in more than 480 km of dextral separation across the Denali fault, which we view as an upper bound for Cenozoic displacement (see section 5.4.1). The potential correlation raises the possibility that mineralization associated with the Eocene volcanic strata in Canada may also be present in the Alaskan volcanic rocks (e.g. Light et al., 1990), but more field-based geochemical and geochronological studies of Paleogene volcanic rocks in the Alaska Range and Talkeetna Mountains will be necessary to vet these hypotheses.

**Palinspastic reconstruction**

The Maclaren-Kluane schist and associated rocks record nearly 100 Myr of tectonic evolution in the North American Cordillera. Our palinspastic reconstruction of the Denali fault begins with deposition of the Maclaren-Kluane protolith in the middle Cretaceous and culminates with historic dextral slip in the Denali fault system. In addition to our data highlighting the total offset history on the modern Denali fault, we use markers presented by Regan et al. (2021) to restore post-33 Ma slip (Table 1).

Ca. 95-82 Ma (Figure 10): The protolith of the Maclaren-Kluane schist was deposited into a marine basin west of the Coast Mountains arc. Sediment was delivered to the basin from uplifted regions to the east, south, and west. Due to stratigraphic, structural, and thermochronological evidence for Early-mid Cretaceous oblique shortening in the region (e.g. Johnston, 1999; Ridgway et al., 2002;

Mair et al., 2006; McDermott et al., 2019), it is likely that the Maclaren-Kluane protolith was deposited in a contractional setting. We infer that syn-depositional imbrication of the Maclaren-Kluane protolith took place along E-dipping structures because the prograde structures within the Maclaren-Kluane schist dip north and east toward the North American continent (Davidson et al., 1992; Lowey, 2000; Johnston and Canil, 2007) and the timing of deposition corresponds to an eastward migration of arc magmatism across present-day southwestern Yukon (cf. Tempelman-Kluit and Wanless, 1975; Hart et al., 2004, Allan et al., 2013). Taken together, these data suggest that the Maclaren-Kluane protolith sediment formed in a contractional forearc position during the waning stage of the west-facing mid-Cretaceous arc built upon the Yukon-Tanana terrane. Maximum depositional ages from the Maclaren schist require that final closure of the forearc basin and associated tectonic underplating of the Maclaren-Kluane schist took place after ca. 86 Ma.

In remains unclear whether late Cretaceous syn-collisional underplating of the Maclaren-Kluane schist requires a subduction zone between the Wrangellia composite terrane and the North American margin at that time. Hypotheses regarding the nature of the crust along the inboard margin of the Wrangellia terrane in the mid-to-late Cretaceous include oceanic crust, a thickened oceanic(?) plateau, or a combination of these end-member scenarios (e.g., Trop and Ridgway, 2007; Lowey, 2019; Waldien et al., 2021). The presence of oceanic crust is implied by the apparently disparate geologic histories between the eastern margin of the Wrangellia composite terrane and western margin of North America prior to collision in the mid-Cretaceous (Trop et al., 2020). Alternatively, it has been suggested that early Cretaceous collision of the Wrangellia composite terrane with western North America was followed by transtensional rifting that re-opened the marine basin (McClelland et al., 1992), yet it is not clear if the rift basins evolved to full seafloor spreading. An argument against the presence of a wide marginal seaway along

between the Wrangellia terrane and North America draws on the presence of an early-mid Cretaceous magmatic belt in Yukon (Whitehorse, Dawson Range, Tombstone suites) and lack of mid-Cretaceous arc rocks south of the Maclaren schist in southern Alaska. Because deposition and accretion of the McHugh Creek Assemblage record paleo-east-dipping subduction along the western margin of the Wrangellia composite terrane from ca. 100-90 Ma (Amato and Pavlis, 2010; Amato et al., 2013), the singular magmatic belt in Yukon could be explained by that subduction zone alone, and eastward migration of the arc magmatism across Yukon (Figure 11) could be attributed changes in the geometry of that slab leading up to underplating of the Maclaren-Kluane schist and cessation of arc magmatism between ca. 83-78 Ma (e.g. Gehrels et al., 2009; Figure 8). If a second subduction zone were present between the Wrangellia composite terrane and the North American margin, then two sub-parallel mid-Cretaceous igneous belts should be present. Acknowledging the aforementioned uncertainties regarding the nature of the crust beneath the mid-to-late Cretaceous marginal seaway between the Wrangellia composite terrane and western North America, we drafted figure 11 to include queried oceanic crust along the eastern margin of the Wrangellia composite terrane.

Ca. 82-65 Ma (Figure 11A): Tectonic underplating of the Maclaren-Kluane schist beneath the western margin of North America resulted in Barrovian series metamorphism that began shortly after deposition. During underplating, the schist experienced kyanite grade conditions (e.g., Davidson et al., 1992; Mezger et al., 2001) and growth of ca. 82 Ma metamorphic zircon rims.
In Yukon, the structure responsible for burial and metamorphism of the Kluane schist is largely overprinted by the Ruby Ranges batholith (e.g., Israel et al., 2011). Along strike to the south of Kluane Lake, the Kluhini River shear zone has been described as an east-dipping shear zone that

thrusts the Yukon-Tanana terrane and related igneous belts over pelitic gneiss with an early Cretaceous protolith age (Vice, 2017). In Alaska, a structure beneath the Susitna Glacier (SGTF-Figure 2) places pre-Jurassic continental margin rocks hosting ca. 98 Ma plutons in the north against the Maclaren schist and East Susitna batholith in the south (Figure 2). We infer that historic and Neogene slip on the Susitna Glacier thrust fault reactivated a Mesozoic collisional structure correlative with the Kluhini River shear zone.

Following underplating, shortening continued by formation of the Valdez Creek shear zone along the former plate boundary between the Maclaren-Kluane schist to the northeast and the Clearwater-Nutzotin-Dezadeash strata to the southwest (Waldien et al., 2021). Our date of ca. 76 Ma on the garnet-biotite leucocratic body within the Maclaren schist suggests that initiation of slip on the Valdez Creek shear zone may have facilitated decompression partial melting in the schist or served as a conduit for melt migration (e.g. Hollister, 1993). Shortening along the Valdez Creek-Tatshenshini shear zone developed an inverted metamorphic field gradient preserved in the footwall Clearwater-Dezadeash metasediments, which reached peak upper greenschist-lower amphibolite facies conditions at ca. 65 Ma (Lowey, 2000; Waldien et al., 2021).

Ca. 60-50 Ma (Figure 11B): Cessation of slip on the Valdez Creek-Tatshenshini shear zone was followed by isothermal decompression throughout much of the Maclaren-Kluane schist (Mezger et al., 2001a), local cooling near the Valdez Creek shear zone in the Clearwater Mountains (AK) (Ridgway et al., 2002), and reheating associated with voluminous magmatism in the Ruby Range batholith in Yukon (Mezger et al., 2001a; Israel et al., 2011). The magmatism was accompanied by regional extension, which preserved volcanic strata within grabens throughout eastern Alaska, southwestern Yukon, and northern British Columbia (Bacon et al., 1990; Morris and Creaser,

2003; Miskovic and Francis, 2004). South of the Denali fault in Alaska, syn-extensional volcanic strata and intrusions near the Gulkana Glacier record formation of the McCallum Creek fault as part of the Paleogene extensional system (Terhune et al., 2015; Gillis et al., 2019; Figure 12A). Despite the regional importance of Paleogene extension, eastern Alaska and southwestern Yukon appear not to have experienced the high magnitude of extension that occurred in coeval extensional systems farther south in the Cordillera (e.g., Parrish et al., 1988). The ca. 60-50 Ma syn-extensional volcanism may record initiation of dextral motion along the modern Denali fault in concert with dextral-slip on the Tintina and Border Ranges fault systems during oblique subduction of a spreading center along the outboard margin of the Wrangellia composite terrane (Roeske et al., 2003; Gabrielse et al., 2006; Davidson and Garver, 2017). However, our correlation of the Shakwak and Ann Creek plutons asserts that localization of the modern Denali fault and subsequent dissection of the Maclaren-Kluane schist and the associated batholith is restricted to post-52 Ma (Figure 12A).

Ca. 33 Ma (Figure 12B): The ca. 42-33 Ma phase of the East Susitna batholith (AK) and absence of age-equivalent plutons in the Ruby Range batholith (YT) support our hypothesis of localized dextral slip on the Denali fault by ca. 42 Ma (see also Figure 8). The 42-33 Ma plutons within the Maclaren schist constitute the eastern-most extent of a suite of plutons emplaced along the Denali fault as far west as Mt. Foraker in the Central Alaska Range (Regan et al., 2020, 2021). Rapid post-emplacement cooling and thermal resetting of the Ar isotopic system in biotite and muscovite only within ~3 km of the plutons (e.g., Benowitz et al., 2011, 2014, 2019; Waldien et al., 2021) indicate that this phase of the batholith was emplaced at a relatively shallow crustal level.

Ca. 30-20 Ma (Figure 12C): The Oligocene and early Miocene marks a major change in the geology of southern Alaska and southwestern Yukon, which involves the onset of exhumation in the Alaska Range and the Kluane Ranges (Benowitz et al., 2011, 2012, 2014; Lease et al., 2016; McDermott et al., 2019), drainage reorganization (Finzel et al., 2011, 2015; Brennan and Ridgway, 2015; Benowitz et al., 2019), onset of Wrangell volcanism (Berkelhammer et al., 2019; Breuseke et al., 2019), and development of the St. Elias fold-and-thrust belt (Bruhn et al., 2004; Pavlis et al., 2012). Contemporaneous events in our study area include the post-32 Ma reactivation of the Valdez Creek shear zone indicated by cooling ages and brittle deformation features, development of an imbricate thrust system along the southern flank of the eastern Alaska Range (Valdez Creek, Broxson Gulch, Airstrip, and Rainy Creek faults), and retrograde metamorphism of the Maclaren schist (Waldien et al., 2021). The onset of transpressional deformation in the Denali fault system may have nucleated a short-lived structural complexity (e.g., a restraining bend), which resulted in abandonment of the Cottonwood terrane, a fragment of the Maclaren schist and ca. 33 Ma orthogneiss, on the north side of the active Denali fault strand near the present-day Yukon-Alaska border (Nokleberg and Richter, 2007; Regan et al., 2021; see also Figure 12B). The widespread ca. 30-25 Ma tectonic modification of southern Alaska is generally regarded as an upper plate response to increased plate coupling and progressive flat slab subduction of the Yakutat oceanic plateau beneath southern Alaska (Enkelmann et al., 2008, 2010; Jadamec et al., 2013; Haynie and Jadamec, 2017).

Late Miocene to Present (Figure 12D): Southern Alaska experienced pulses in bedrock cooling and basin development beginning in the late Miocene. Regional events at this time include uplift and exhumation of the Denali massif (Fitzgerald et al., 1993, 1995; Burkett et al., 2016), pulses of

low-temperature cooling in the western Alaska Range (Haeussler et al., 2008; Benowitz et al., 2012; Lease, 2018), a transition from lacustrine to alluvial facies in basins north and south of the Denali fault (Ridgway et al., 2002, 2007; Allen et al., 2016), development of the Northern Foothills fold and thrust belt (Bemis and Wallace, 2007; Ridgway et al. 2007), reactivation of shortening structures along the southern flank of the Alaska Range (Waldien et al., 2018), expansion of the Wrangell volcanic field (Preece and Hart, 2004), and a regional shift in precipitation related to topographic development (Bill et al., 2018; Otiniano et al., 2020).

One aspect of the late Miocene tectonic event that is integral to the development of the Denali fault system is post-18 Ma dextral slip on the Totschunda fault (Milde, 2014; Berkelhammer et al., 2019). Although it is plausible that the Totschunda fault was part of the proto-Denali fault system prior to 114 Ma (Trop et al., 2020), the present data only imply linkage with the modern Denali fault since the late Miocene. Contemporaneous dextral slip on the Totschunda and Denali faults feeds slip from the Totschunda fault onto the Denali fault west of their intersection (Haeussler et al., 2017), which produces transpression west of the junction (Bemis et al., 2015). Due to these observations and the similarity in magnitudes (~80-90 km) of post-7 Ma separation on the Denali fault west of the Denali-Totschunda juncture and post-18 Ma separation on the Totschunda fault, it is likely that both separations accumulated entirely since ca. 7 Ma. Restoring ~85 km of late Miocene to Present separation on the Totschunda and Denali faults places the Clearwater metasediments adjacent to the Nutzotin Mountains Sequence and would also match the Talkeetna fault to the Totschunda fault (see also Figures 11, 12A, B, and C). Such a restoration is supported both by the rock types near these structures and by crustal tomography revealing nearly identical contrasts in crustal seismic properties across those faults (Allam et al., 2017). Incorporating the ~85 km of dextral separation on the Totschunda fault is a key component of our

palinspastic reconstruction of the Denali fault system because it allows both the ~370 km of separation recorded by correlation of the Dezadeash and Nutzotin strata and the <505 km of separation recorded by the correlation of the Clearwater metasediments and Dezadeash formation to be correct.

Transpressional deformation in the Denali fault system during the Neogene was highly partitioned between dextral strike-slip on the Denali fault master strand and Totschunda fault and shortening on thrust systems at the northern and southern flanks of the Alaska Range. The record of long-term cooperation between strike-slip and shortening structures is also reflected in historic seismicity, including the 2002 $M_w$ 7.9 Denali earthquake, which indicates that both strike-slip and shortening structures remain active components of the Denali fault system (Eberhart-Phillips et al., 2003; Doser, 2004; Ratchkovski et al., 2004; Vallage et al., 2014).

## Implications for strike-slip faulting in the North American Cordillera

### *Separation versus slip on the Denali fault*

Cenozoic shortening on structures in the Alaska Range causes the measurements of strike-slip separation to underestimate the magnitude of slip on the Denali fault between the offset markers. Our favored correlation of the ca. 52 Ma Shakwak and Ann Creek plutons yields 465 km of dextral separation. Post-32 Ma reactivation of the Valdez Creek shear zone nucleated the southeast-vergent thrust system that carried the Maclaren schist, Clearwater metasediments, and associated intrusive rocks in the hanging wall (Waldien et al., 2021). Synchronous slip between the thrust system and Denali fault resulted in slip transfer from the Denali fault to the thrusts. As a result of the slip transfer, translation of the Ann Creek pluton relative to the Shakwak pluton took place at a rate lower than the slip rate on the Denali fault. Over time, the accumulated shortening

led to a discrepancy in the separation of the offset features relative to the amount of slip on the section of the Denali fault between the correlative plutons. It is not entirely clear how much slip has taken place on the Valdez Creek or Broxson Gulch faults, yet detailed mapping paired with thermochronological and geophysical datasets suggest that these structures accommodated at least 15 km of shortening during the Oligocene and Miocene (Allam et al., 2017; Waldien et al., 2021). Incorporating the Cenozoic shortening into our model of Denali fault evolution reveals that the 465 km of strike-slip separation corresponds to a total slip estimate of ~480 km.

*Timing of strike-slip displacement*

In agreement with other recent studies (e.g., Murphy, 2018), our review of the ages and separation of features displaced by the Denali fault requires that the ~480 km of displacement on the fault system took place entirely during the Cenozoic. There are two major implications of this outcome.

First, formation and localization of slip on the modern Denali fault appears to have begun as slip on other major strike-slip faults in the Cordillera was decreasing. Both the Border Ranges and Tintina fault systems were active dextral fault systems during the Paleogene, but appear to have experienced minor dextral slip since the late Eocene (Little, 1990; Roeske et al., 2003; Gabrielse et al., 2006; Till et al., 2007; Ryan et al., 2017). In contrast, we have documented that localization and major slip on the modern Denali fault took place after ca. 52 Ma. This time period corresponds to major changes in the tectonic configuration along the entire margin of western North America, which may be related to changes in the obliquity, rates, and physical properties of incoming oceanic plates (e.g., Atwater, 1989; Doubrovine and Tarduno, 2008; McCrory and Wilson, 2015). The prevalence of Paleogene extensional complexes from British Columbia,

Canada into the northern contiguous United States may partially correspond to the coexistence of multiple dextral fault systems that were active at that time (e.g., Andronicos et al., 2003; Gabrielse et al., 2006; Foster et al., 2007). Likewise, the apparent decline of widespread extension in the late Eocene may record an increase in localized slip on the Denali fault and a decrease in major slip on neighboring strike-slip fault systems in concert with changing plate boundary conditions.

Second, the recognition of Cenozoic slip on the modern Denali fault allows for larger cumulative margin-parallel displacement of the Wrangellia composite terrane relative to inboard terranes since the early Cretaceous. Recently published geology-based datasets bear on long-standing hypotheses that the Cordilleran terranes experienced large magnitude (>1500 km) northward transport along dextral fault systems in the mid and late Cretaceous (Rusmore et al., 2013; Garver and Davidson, 2015; Matthews et al., 2017; Sauer et al., 2019; Coutts et al., 2020). Our review of slip in the Denali fault system reveals that the oft-cited ≥370-400 km of slip that was inferred to have taken place since the early Cretaceous is not an accurate assessment of Denali fault slip. We have shown herein that ~480 km of slip on the modern Denali fault took place entirely since ca. 52 Ma. Thus, the modern Denali fault should not be grouped with other fault systems contributing to large-scale margin-parallel displacement in the Cretaceous. Rather, thermochronological data and regional geologic correlations suggest the existence of a proto-Denali strike-slip fault system that was likely active during the early-mid Cretaceous (Wahrhaftig et al., 1975; Miller et al., 2002; McDermott et al., 2019). The amount of displacement and the sense of motion on the proto-Denali fault system are presently not well understood. Finding and interrogating the rock packages that record the slip history of the proto-Denali fault will undoubtedly help reconcile disputes regarding margin-parallel transport of Cordilleran terranes during the Cretaceous. If the proto-Denali fault experienced a phase of dextral slip, northward

displacement of the Wrangellia composite terrane along the Denali fault system relative to the North American margin would exceed the ~480 km of Cenozoic displacement established herein.

*Lithospheric strength heterogeneity following terrane accretion*

The key feature that allows offset on the modern Denali fault to be determined is the presence of correlative syn-collisional rock packages on both sides of the fault. Thermochronological and thermobarometric data indicate that the Maclaren-Kluane schist and associated batholithic rocks were in the upper ~15 km of the crust when the modern Denali fault formed. Because these rock packages, and fabrics within them, were cut obliquely by the fault, it is implied that their mechanical properties did not influence localization of the fault. Instead, we propose that the mechanical properties of the lower crust and/or lithospheric mantle were more important for controlling formation and localization of the modern Denali fault. Elements of the post-collisional lower crust and lithospheric mantle in the Cordillera that may have guided localization of the modern Denali fault include: a thick mafic root within the Wrangellia composite terrane, differences in mantle hydration as a result of subduction-related magmatism, and/or differences in the thickness of the mantle lithosphere. Such inferences are supported by a variety of geophysical datasets, all of which indicate a fundamental change in the properties of the lower crust and upper mantle across the eastern Denali fault (Saltus and Hudson, 2007; Rasendra et al., 2014; O'Driscoll and Miller, 2015; Audet et al., 2016; Allam et al., 2017; Miller et al., 2018; Berg et al., 2020). The sum of geophysical and geological data from the Denali fault, together with thermochronological and geophysical datasets from other regions of the Cordillera (Enkelmann et al., 2019; Estève et al., 2020), challenge the hypothesis of an active Cordillera-wide weak lower crustal décollement (e.g., Hyndman et al., 2005).

Instead, the contrasting mechanical properties of individual terranes may cause terrane-bounding structures to penetrate the lithosphere. Such a scenario is highly likely for southern Alaska, where the thermal structure of the lithosphere is strongly controlled by the shape of the subducting plate, and lithospheric-scale weaknesses along terrane boundaries (i.e., the Denali fault) are required to accurately model active deformation (Jadamec et al., 2013; Haynie and Jadamec, 2017).

## CONCLUSIONS

Integration of new geologic mapping and geochronology data from the eastern Alaska Range with existing datasets from southwestern Yukon reveals five distinct rock packages that record total displacement on the Denali fault: (1) ca. 94-86 Ma Maclaren schist and Kluane schist; (2) the 74-57 Ma phase of the East Susitna batholith and the Ruby Range batholith; (3) ca. 52 Ma granodiorite bodies in a low structural position of the Maclaren schist and the Hayden Lake intrusive suite; (4) the ca. 160-144 Ma Clearwater metasediments, Nutzotin Mountains Sequence, and Dezadeash formation strata and ca. 102 Ma zoned pyroxenite-granodiorite bodies that intrude the strata; and (5) Eocene extension-related volcanic rocks and associated shallow intrusions. Restoring these offset features results in ~465 km of dextral separation, and accounting for Neogene shortening in the eastern Alaska Range results in ~480 km of dextral slip in the Denali fault system. All of this slip accumulated since ca. 52 Ma, following the main phase of slip on other major Cordilleran strike-slip faults.

Prior to offset by the Denali fault system, protolith deposition and prograde metamorphism of the Maclaren-Kluane schist records the closure of a marine basin between the Wrangellia composite terrane and the Cordilleran margin at ca. 95-86 Ma. Underplating and regional

metamorphism of the schist took place along east-dipping ductile thrusts (Kluhini River and Valdez Creek shear zones) between ca. 82 and 65 Ma. The data presented and summarized herein provide additional evidence for diachronous accretion of the Wrangellia composite terrane along east-dipping structures.

## FIGURES:

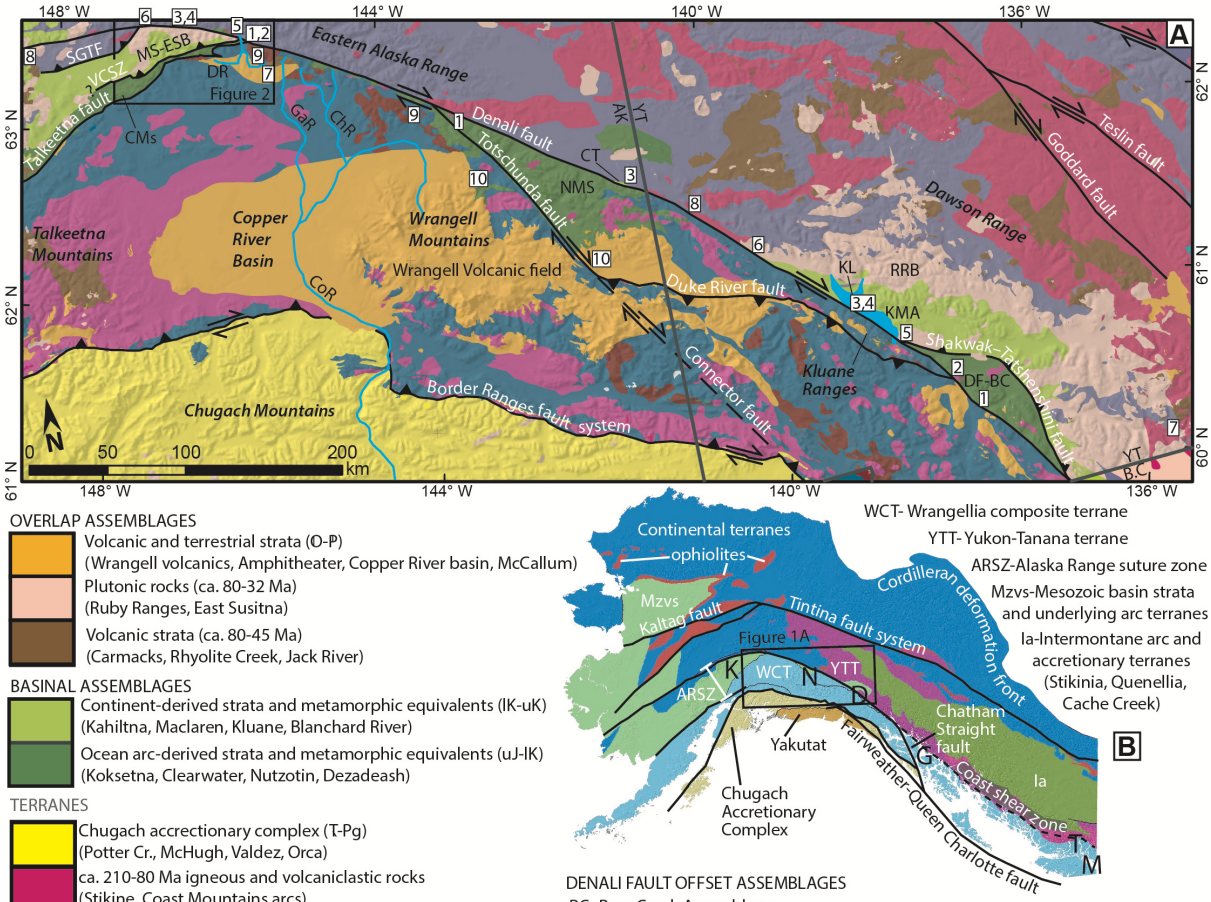


OVERLAP ASSEMBLAGES
- Volcanic and terrestrial strata (O-P) (Wrangell volcanics, Amphitheater, Copper River basin, McCallum)
- Plutonic rocks (ca. 80-32 Ma) (Ruby Ranges, East Susitna)
- Volcanic strata (ca. 80-45 Ma) (Carmacks, Rhyolite Creek, Jack River)

BASINAL ASSEMBLAGES
- Continent-derived strata and metamorphic equivalents (lK-uK) (Kahiltna, Maclaren, Kluane, Blanchard River)
- Ocean arc-derived strata and metamorphic equivalents (uJ-lK) (Koksetna, Clearwater, Nutzotin, Dezadeash)

TERRANES
- Chugach accretionary complex (T-Pg) (Potter Cr., McHugh, Valdez, Orca)
- ca. 210-80 Ma igneous and volcaniclastic rocks (Stikine, Coast Mountains arcs)
- ca. 205-110 Ma igneous and volcaniclastic rocks (Talkeetna, Chitina, Chisana arcs)
- Carboniferous plutonic rocks (Skolai arc plutons)
- Island arc and oceanic strata (D-T) (Wrangellia-Peninsular-Alexander terranes)
- Continental margin metamorphic rocks (pC-T) (parautochthonous North America and Yukon-Tanana terrane)

WCT- Wrangellia composite terrane
YTT- Yukon-Tanana terrane
ARSZ-Alaska Range suture zone
Mzvs-Mesozoic basin strata and underlying arc terranes
Ia-Intermontane arc and accretionary terranes (Stikinia, Quenellia, Cache Creek)

DENALI FAULT OFFSET ASSEMBLAGES
- BC- Bear Creek Assemblage
- CMs- Clearwater Metasediments
- CT- Cottonwood Terrane
- DF- Dezadeash Formation
- ESB- East Susitna Batholith
- KMA- Kluane Metamorphic Assemblage
- MS- Maclaren Schist
- NMS- Nutzotin Mountains Sequence
- RRB- Ruby Range Batholith

INLAND WATERWAYS
- ChR- Chistochina River
- CoR- Copper River
- DR- Delta River
- GaR- Gakona River
- KL- Kluane Lake

MARGINAL MARINE BASINS
- K-Kahiltna
- N-Nutzotin
- D-Dezadeash
- G-Gravina
- T-Tyaughton
- M-Methow

**Figure 1 (Previous page): (A)** Simplified geologic map of the southwestern Yukon and eastern Alaska region around the Denali fault (modified from Wilson et al., 2015 and Colpron et al., 2016). Basement geology is combined into the Wrangellia and Yukon composite terranes south and north of the Denali fault, respectively. Mesozoic-Cenozoic igneous belts and basinal assemblages are delineated as either pre-Wrangellia-collisional terranes and marginal marine strata (≥80 Ma) or overlap (≤80 Ma). The legend contains regional formation, metamorphic belt, or plutonic suite names that are contained within the map area and are pertinent to the study. The location of figure 2 is contained within the black box. Boxed numbers denote the locations of correlative geologic features that are listed in Table 1. SGTF–Susitna Glacier thrust fault; VCSZ–Valdez Creek shear zone; AK–Alaska; YT–Yukon Territory; B.C. British Columbia. **(B)** Regional terrane map of the Canadian-Alaska Cordillera showing the location of figure 1A and major strike-slip fault systems. Modified from Colpron et al. (2011). Abbreviations denoting the Methow, Tyaughton, Gravina, Dezadeash, Nutzotin, and Kahiltna basins are shown in the general locations.

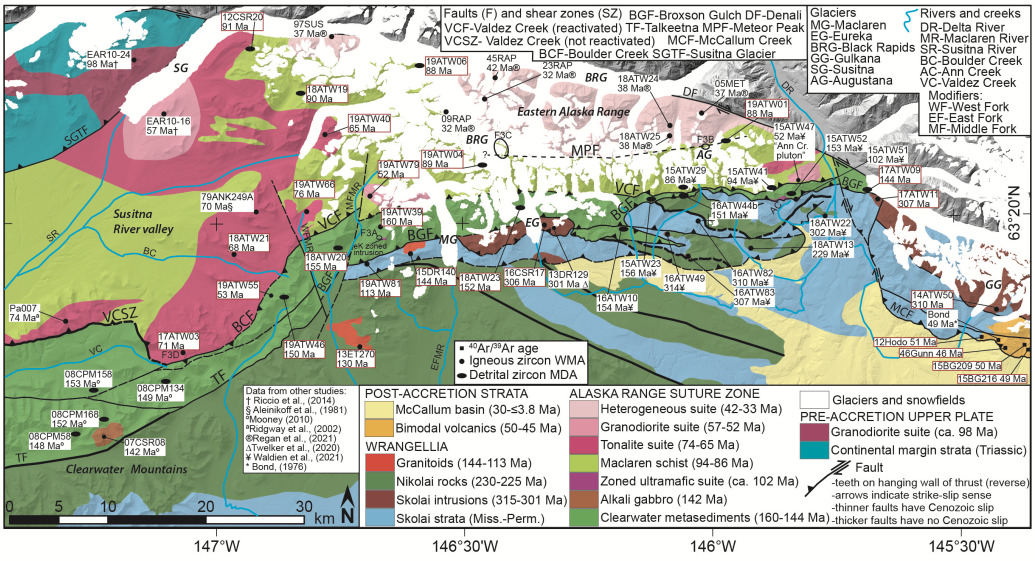


**Figure 2:** Regional geologic and age compilation map of the study area in the eastern Alaska Range. The map is compiled from Smith and Turner (1974), Mooney (2010), Waldien et al. (2018), Twelker et al. (2020), Waldien et al. (2021) and our new mapping near the headwaters of the Maclaren River. Previously published ages are annotated with a symbol, whereas new ages are outlined by a red box. The locations of field photographs in figure 3 are shown as "F3A-D". WMA–Weighted mean age; MDA–Maximum Depositional age.

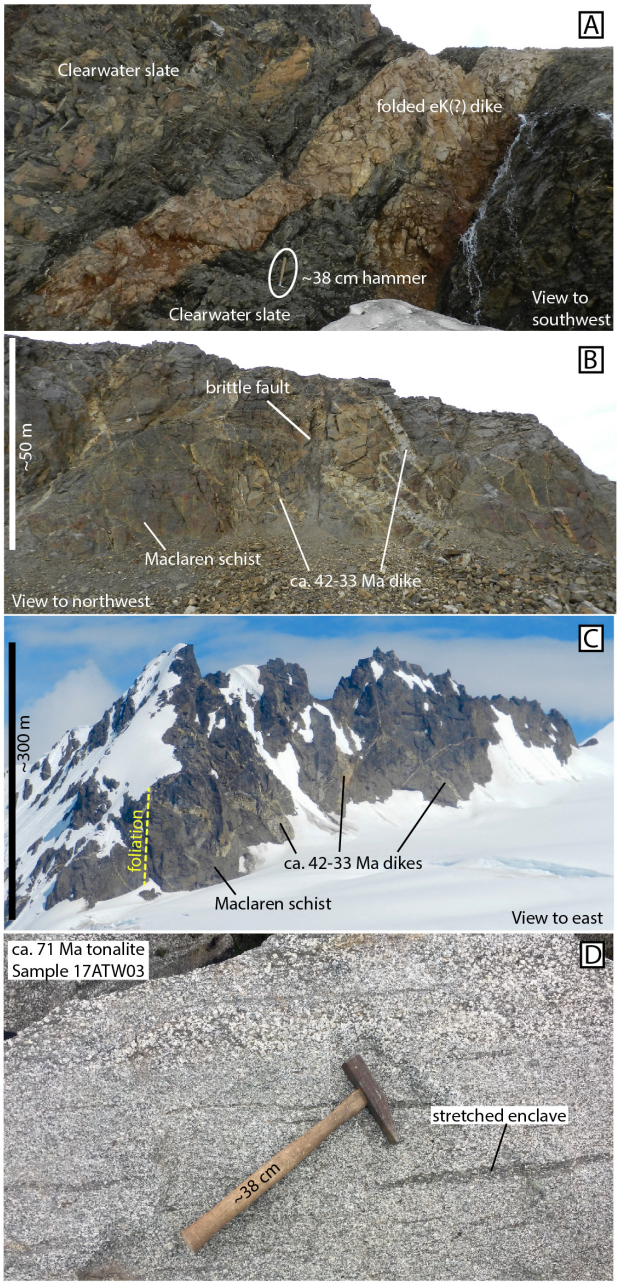


**Figure 3:** Field photos show key relationships in the map area. **(A)** An intermediate dike associated with a zoned mafic-intermediate intrusion is folded with the foliation in the Clearwater slate. Photo is from an outcrop east of the middle fork of the Maclaren River. **(B)** Distributed brittle deformation is associated with the southern margin of the ca. 42-33 Ma plutonic suite. Nokleberg et al. (1992a) mapped this outcrop as an exposure of the Meteor Peak fault. Dikes commonly cross cut the metamorphic foliation in the Maclaren schist and are cut by small brittle faults. Photo is from an outcrop north of the Augustana Glacier. **(C)** Dikes associated with the ca. 42-33 Ma plutonic suite intersect the Maclaren schist foliation (yellow broken line) at multiple angles both south and north of the Meteor Peak fault. Photo is of an arête east of the Black Rapids Glacier. **(D)** Mafic enclaves in the ca. 74-65 Ma tonalite suite are highly stretched and commonly elongate in the down-dip direction. Photo is from sample location 17ATW03.

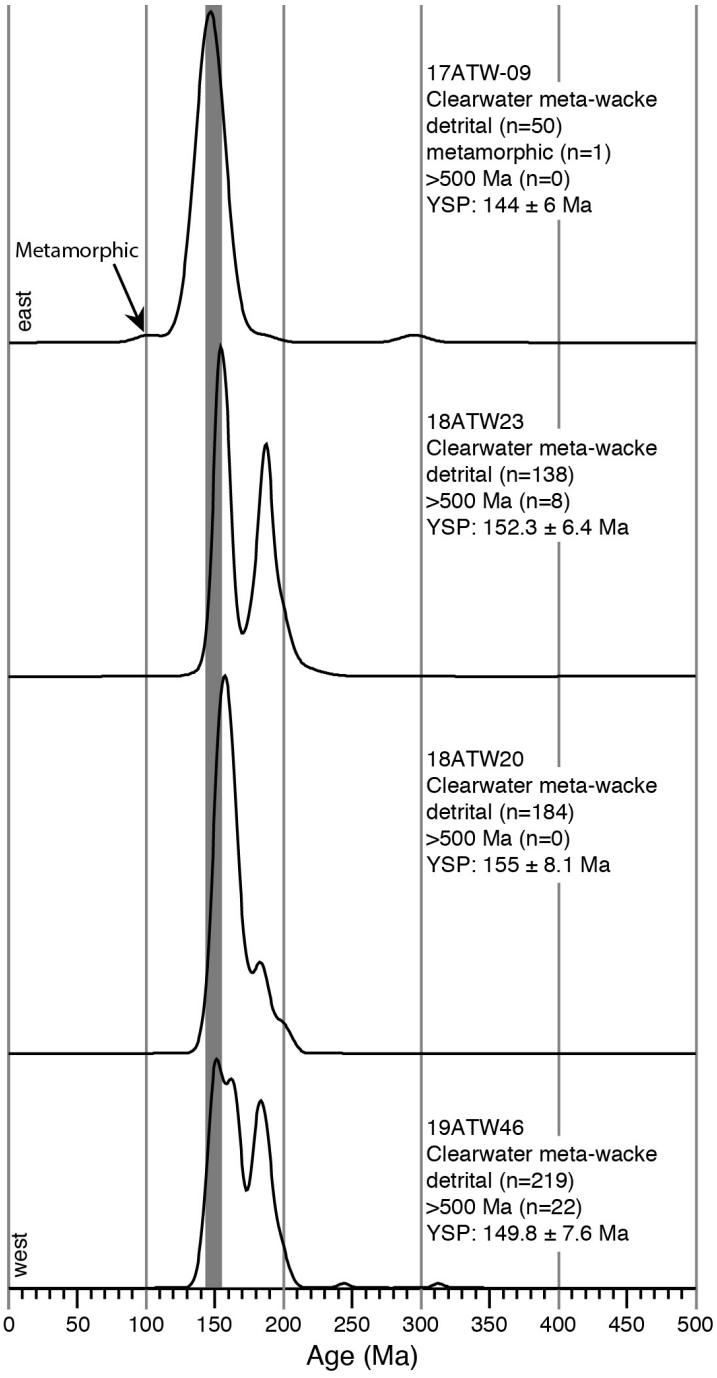


**Figure 4:** Kernel density estimate (KDE) plots of detrital zircon U-Pb age spectra (<500 Ma) for individual samples of Clearwater metagreywacke ordered from east (top) to west (bottom). Post-depositional metamorphic dates are indicated for sample 17ATW-09. The dark gray bar at 155-144 Ma highlights the range of maximum depositional ages for individual samples. KDE plots were made using the DensityPlotter program (Vermeesch, 2012). YSP–weighted mean and 2s uncertainty of the youngest statistical detrital population, taken to be the maximum depositional age; n–number of analyses composing the plot.

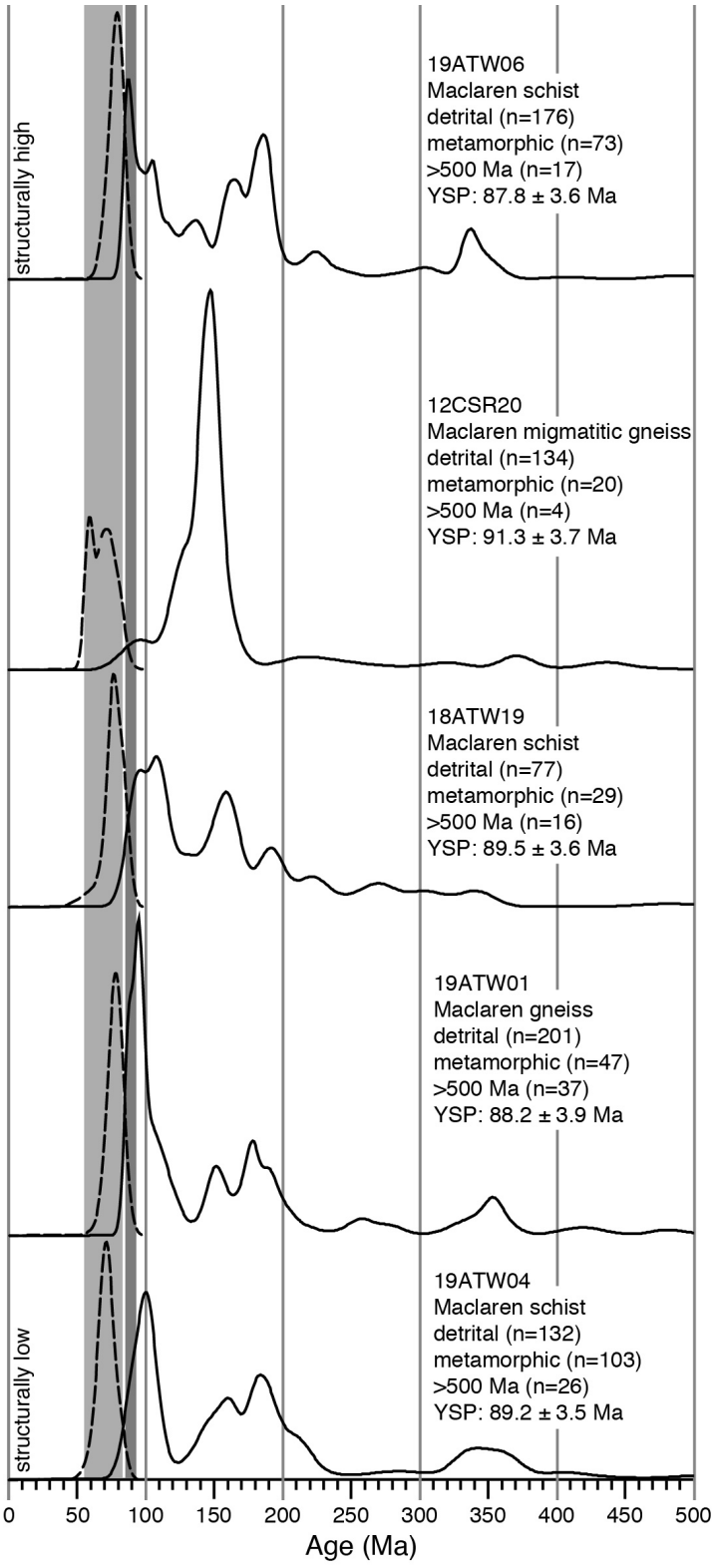


**Figure 5:** Kernel density estimate (KDE) plots of detrital zircon U-Pb age spectra (<500 Ma) for individual samples of Maclaren schist ordered from structurally highest (top) to structurally lowest (bottom). Post-depositional metamorphic dates are shown as a dashed line KDE curve and are outlined by a light grey bar at ca. 84-55 Ma. The dark gray bar at 91-87 Ma highlights the range of maximum depositional ages for individual samples in this study. KDE plots were made using the DensityPlotter program (Vermeesch, 2012). YSP– weighted mean and 2s uncertainty of the youngest statistical detrital population, taken to be the maximum depositional age; n– number of analyses in the plot.

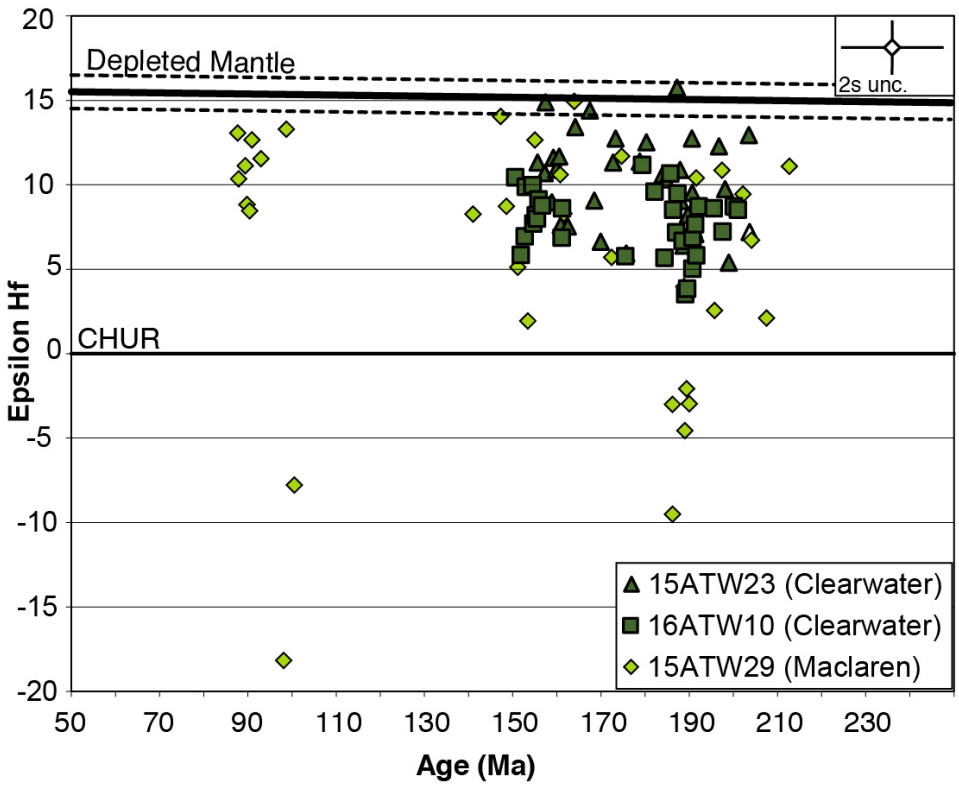


**Figure 6:** Epsilon (ε) Hf-versus-age plot of single grain analyses from the Maclaren schist and Clearwater metasediments (colored as in figure 1). The maximum 2s uncertainties (unc.) associated with the data points are represented by the data symbol in the upper right. CHUR–Chondritic uniform reservoir.

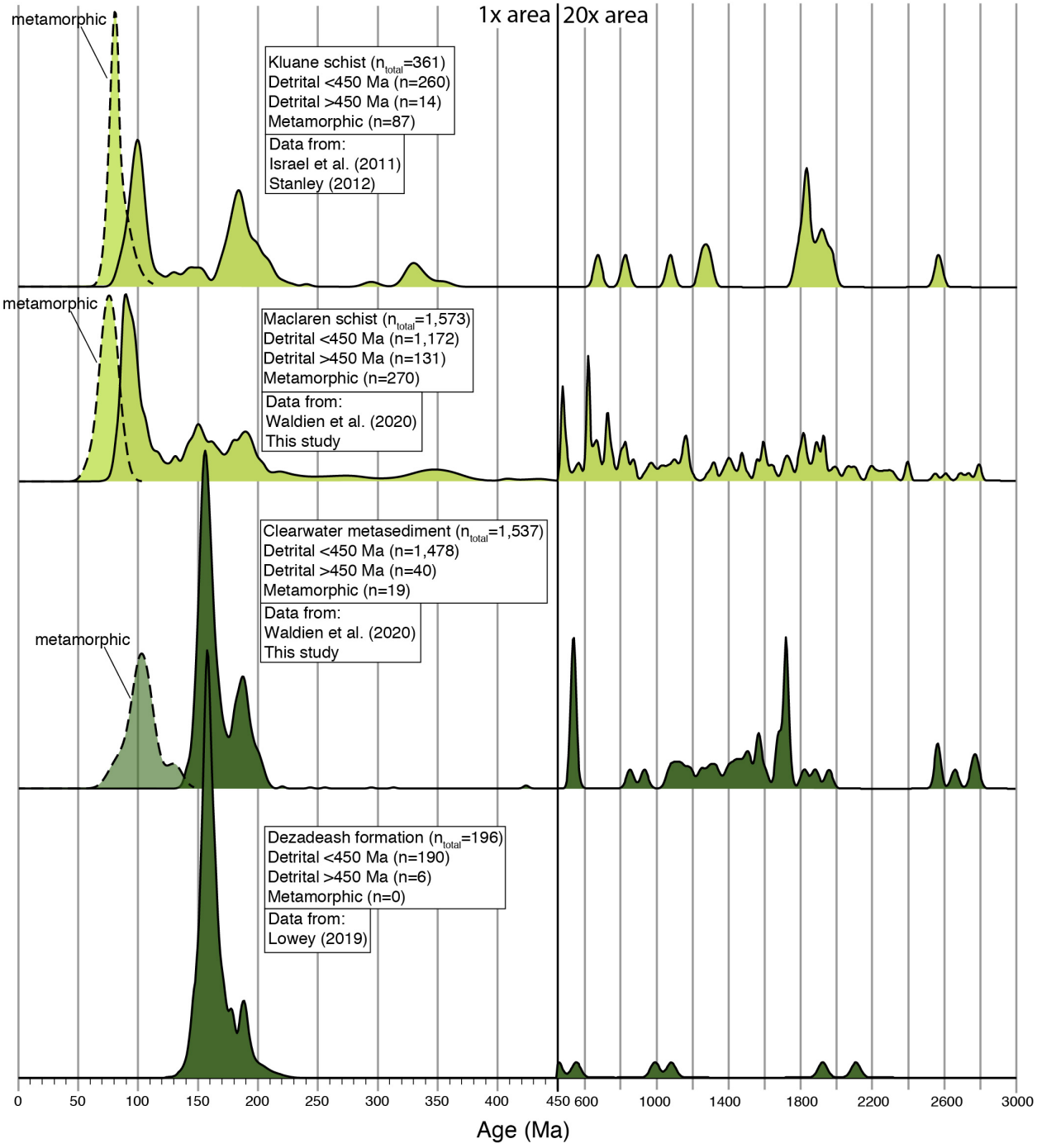
1x area
20x area
metamorphic
Kluane schist (n_total=361)
Detrital <450 Ma (n=260)
Detrital >450 Ma (n=14)
Metamorphic (n=87)
Data from:
Israel et al. (2011)
Stanley (2012)
metamorphic
Maclaren schist (n_total=1,573)
Detrital <450 Ma (n=1,172)
Detrital >450 Ma (n=131)
Metamorphic (n=270)
Data from:
Waldien et al. (2020)
This study
Clearwater metasediment (n_total=1,537)
Detrital <450 Ma (n=1,478)
Detrital >450 Ma (n=40)
Metamorphic (n=19)
Data from:
Waldien et al. (2020)
This study
metamorphic
Dezadeash formation (n_total=196)
Detrital <450 Ma (n=190)
Detrital >450 Ma (n=6)
Metamorphic (n=0)
Data from:
Lowey (2019)
0 50 100 150 200 250 300 350 400 450 600 1000 1400 1800 2200 2600 3000
Age (Ma)

**Figure 7 (Previous page):** Kernel density estimate (KDE) plots of compiled detrital zircon U-Pb age spectra for the Maclaren schist, Kluane schist, Clearwater metasediments, and Dezadeash formation, colored as in figure 1. Note the change in horizontal scale and the 20x increase in area under the curves at 450 Ma. The dashed line KDE curves represent post-depositional metamorphic grains, which are plotted at half the vertical scale of the <450 Ma detrital age spectra. KDE plots were made using the DZStats and Density Plotter programs.

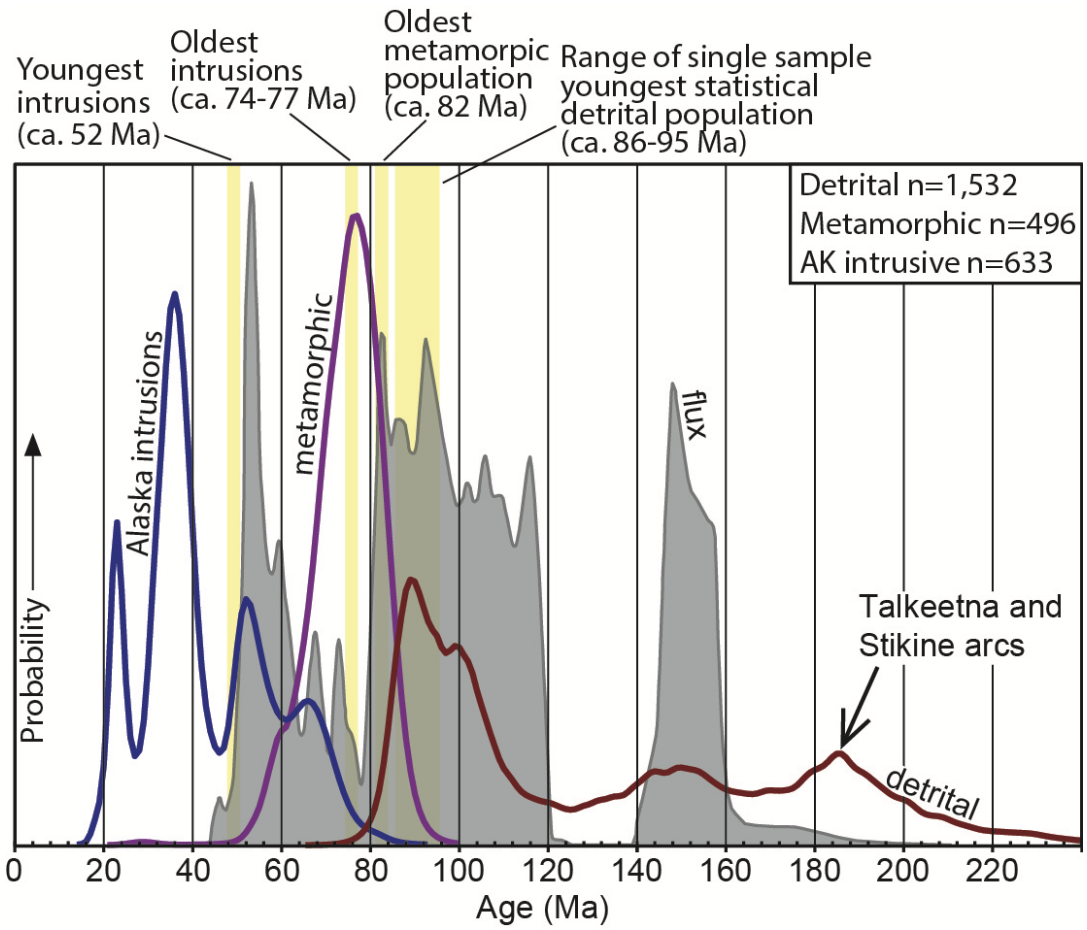


**Figure 8:** Probability density plot comparing ≤240 Ma detrital (dark red curve) and metamorphic (purple curve) U-Pb dates from the Maclaren-Kluane schist (this study; Israel et al., 2011; Stanley, 2012; Waldien et al., 2021) with the 240-40 Ma magmatic flux curve of the central Coast Mountains arc (filled gray curve; from Gehrels et al., 2009). LA-ICPMS dates from plutonic rocks within the Maclaren and Cottonwood schists constitute the blue curve (this study; Regan et al., 2021). The vertical yellow bars highlight important time periods that are shared in the evolution of the Maclaren-Kluane schist and associated batholithic rocks. Note how magmatism within the Maclaren and Cottonwood schists (Alaska intrusions) outlasts the shared magmatism. n–number of grains used in each curve.

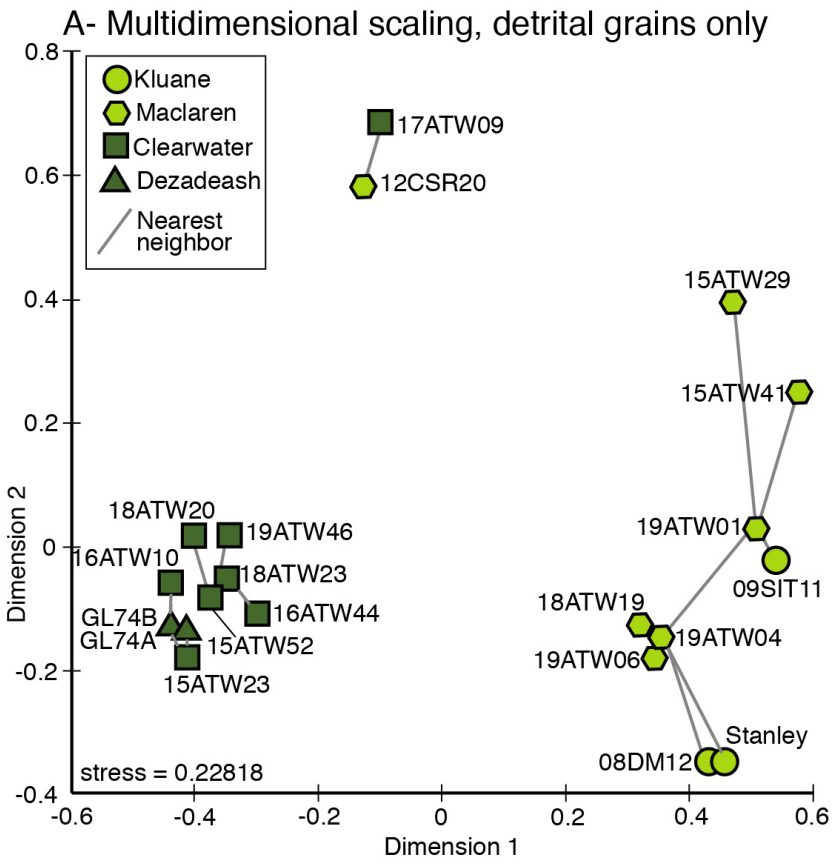
A- Multidimensional scaling, detrital grains only
Kluane
Maclaren
Clearwater
Dezadeash
Nearest neighbor
17ATW09
12CSR20
15ATW29
15ATW41
18ATW20
19ATW46
16ATW10
18ATW23
16ATW44
GL74B
GL74A
15ATW52
15ATW23
19ATW01
09SIT11
18ATW19
19ATW04
19ATW06
Stanley
08DM12
stress = 0.22818
Dimension 1
Dimension 2
0.8
0.6
0.4
0.2
0
-0.2
-0.4
-0.6
-0.4
-0.2
0.2
0.4
0.6

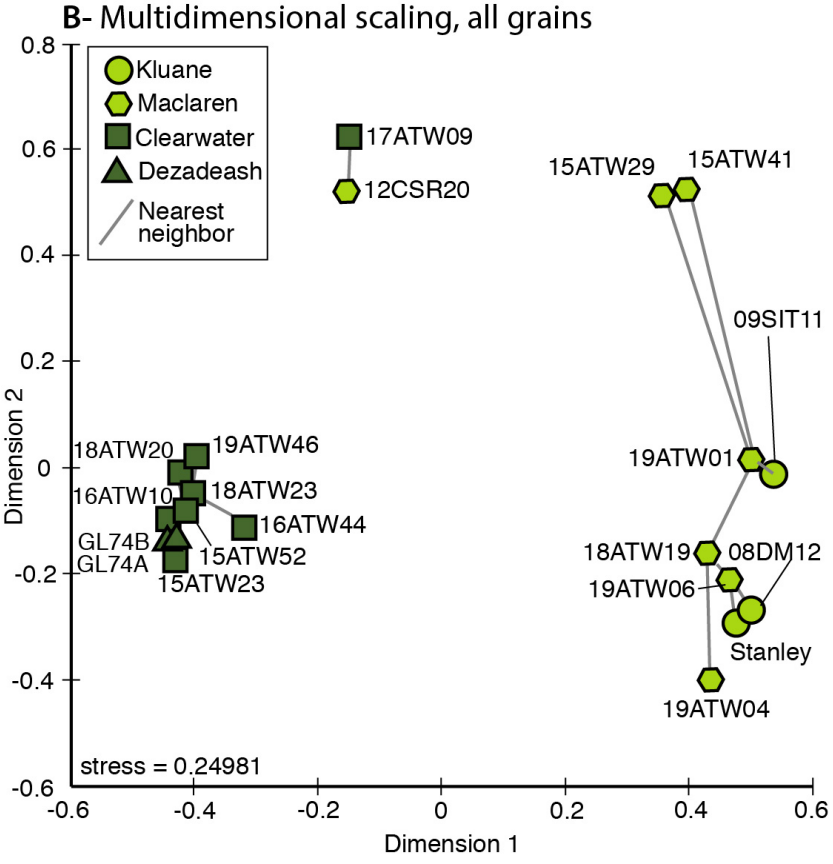
B- Multidimensional scaling, all grains
Kluane
Maclaren
Clearwater
Dezadeash
Nearest neighbor
17ATW09
12CSR20
15ATW29
15ATW41
09SIT11
18ATW20
19ATW46
19ATW01
16ATW10
18ATW23
16ATW44
GL74B
GL74A
15ATW52
15ATW23
18ATW19
08DM12
19ATW06
Stanley
19ATW04
stress = 0.24981
Dimension 1
Dimension 2
0.8
0.6
0.4
0.2
0
-0.2
-0.4
-0.6
-0.6
-0.4
-0.2
0.2
0.4
0.6

**Figure 9 (Previous page):** Multidimensional scaling (MDS) plots of U-Pb age spectra from individual samples of Maclaren schist (hexagons), Kluane schist (circles), Clearwater metasediments (squares), and Dezadeash formation (triangles). All symbols are colored to match map units on figure 1. **(A)** Multidimensional scaling of U-Pb age spectra excluding post-depositional metamorphic grains. **(B)** Multidimensional scaling of U-Pb age spectra including post-depositional metamorphic grains. MDS plots were made using the DZmds program of (Saylor et al., 2017). Maclaren and Clearwater data are from this study and Waldien et al. (2021); Kluane data are from Israel et al. (2011) and Stanley (2012); Dezadeash data are from Lowey (2019).

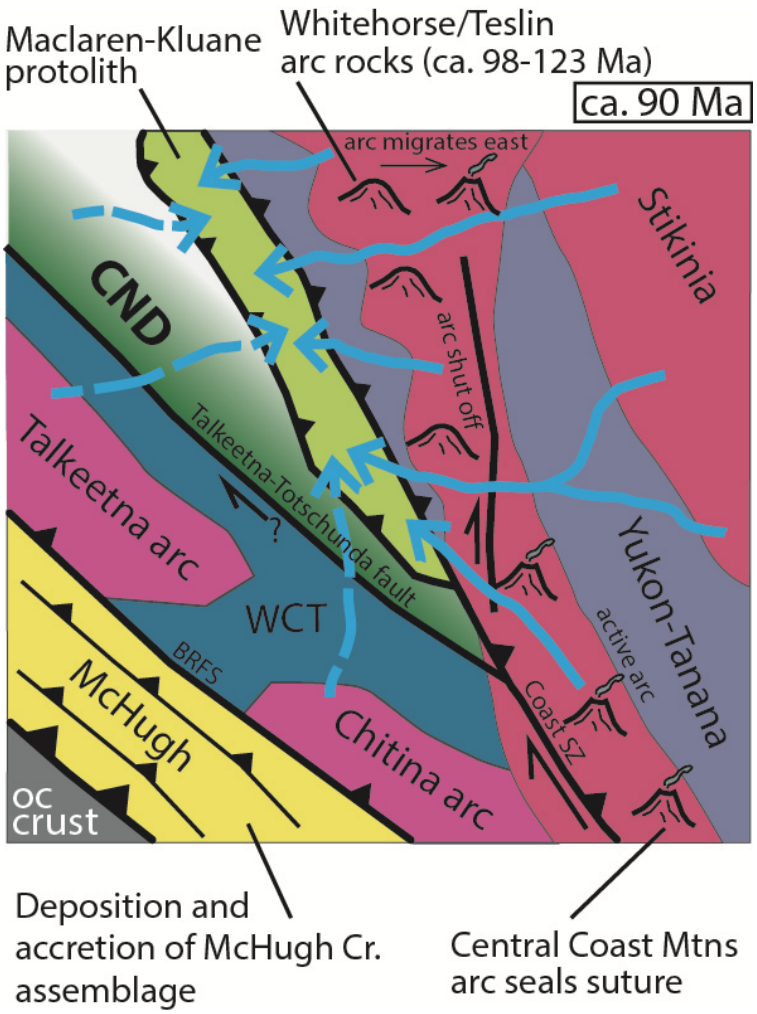


**Figure 10:** Schematic map view diagram showing the tectonic setting of the Maclaren-Kluane protolith basin. Sediment was delivered to the basin by drainage systems (blue lines/arrows; dashed lines where uncertain) that sourced uplifted terranes to the east, south, and possibly the west. Strike-slip fault systems in the Coast shear zone (Coast SZ) and on both sides of the Maclaren-Kluane basin have been documented to be active at this time. Deposition and accretion of the McHugh Creek assemblage records ongoing subduction along the outboard margin of the Wrangellia composite terrane. Map unit colors are the same as figure 1. WCT–Wrangellia composite terrane; CND– Clearwater, Nutzotin, and Dezadeash assemblages; oc–oceanic; BRFS–Border Ranges fault system.

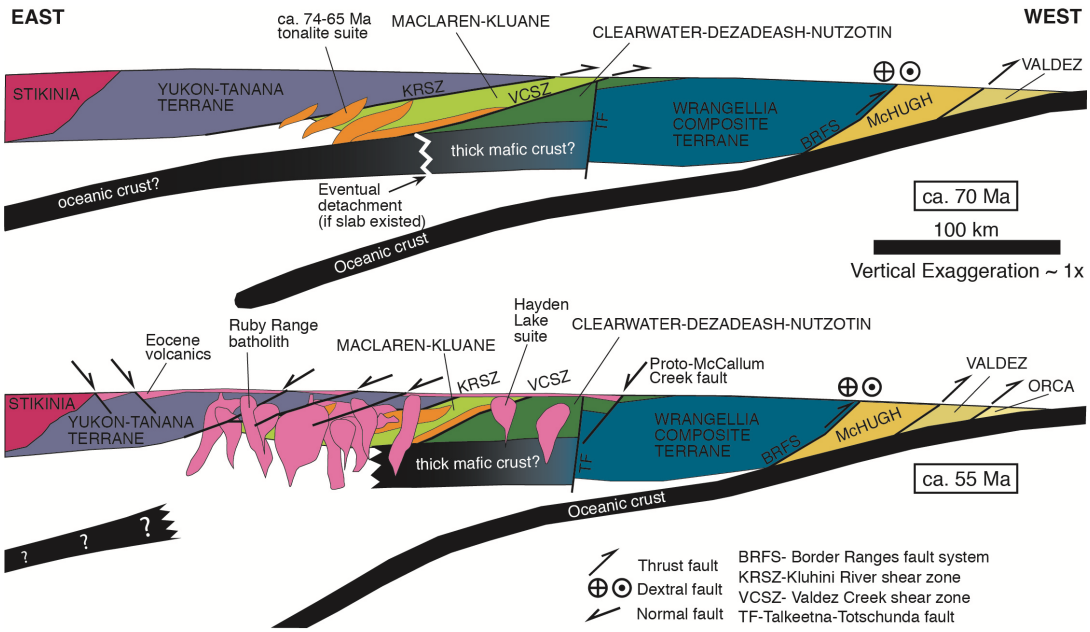


**Figure 11:** Schematic cross sections showing generalized crustal structure during accretion of the Wrangellia composite terrane and metamorphism of the Maclaren-Kluane schist. Colors are the same as figure 1. **(A)** From ca. 74-65 Ma the Maclaren-Kluane schist was undergoing regional amphibolite facies metamorphism contemporaneous with slip on the Valdez Creek shear zone and intrusion of tonalite bodies. Oceanic lithosphere may have been attached to the inboard margin of the Wrangellia composite terrane, but subduction in the marginal seaway is not necessary to explain regional magmatism. Deposition and accretion of the Valdez Group records ongoing subduction along the outboard margin of the Wrangellia composite terrane. **(B)** From ca. 60-50 Ma the Maclaren-Kluane schist were undergoing regional high temperature-low pressure metamorphic conditions contemporaneous with intrusion of the main voluminous phase of the Ruby Range batholith. If oceanic lithosphere were attached to the inboard margin of the Wrangellia composite terrane, it likely would have detached by this time. Deposition and accretion of the Orca Group records ongoing subduction along the outboard margin of the Wrangellia composite terrane.

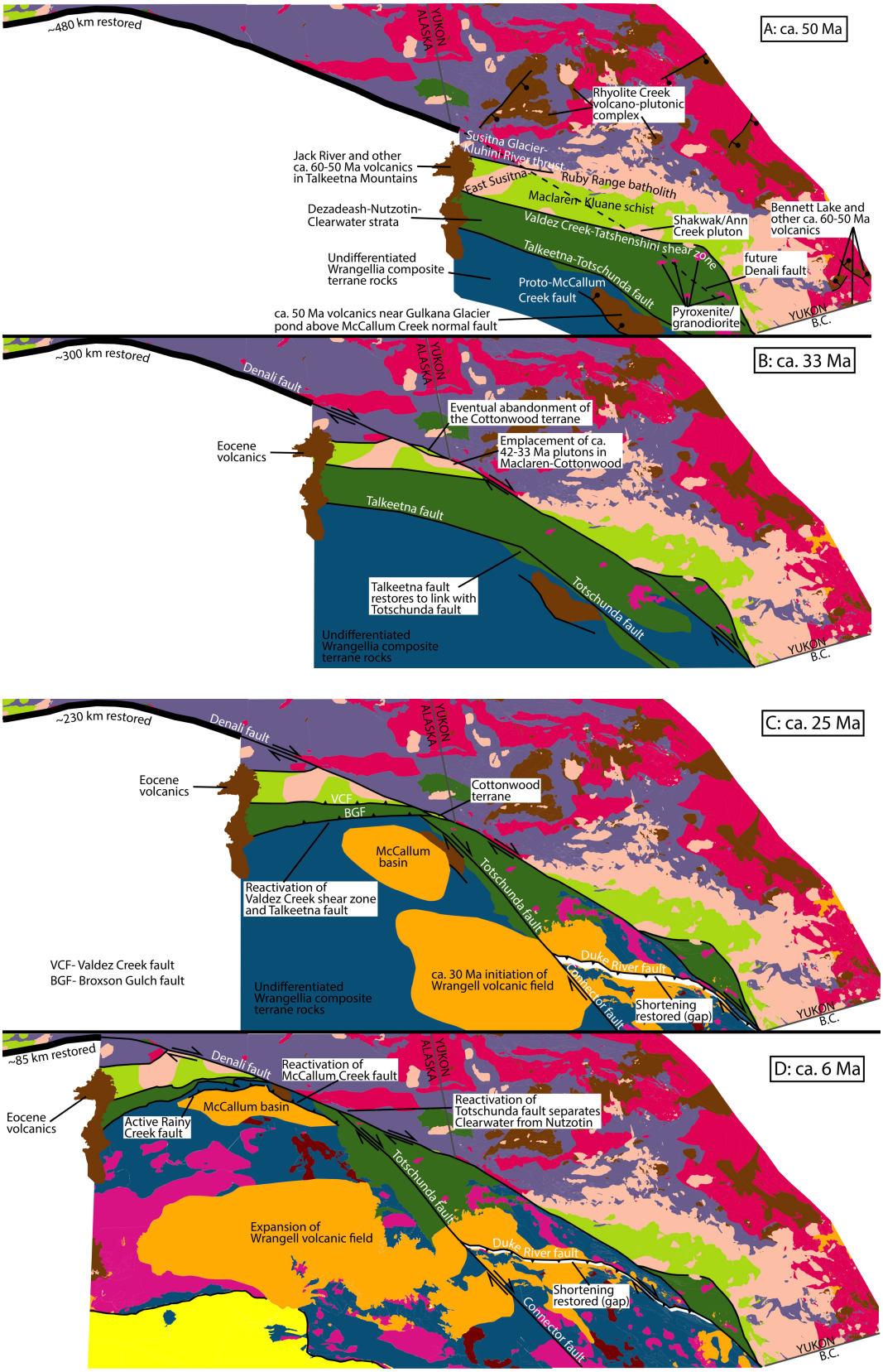
A: ca. 50 Ma
~480 km restored
YUKON
ALASKA
Rhyolite Creek volcano-plutonic complex
Susitna Glacier-Kluhini River thrust
Jack River and other ca. 60-50 Ma volcanics in Talkeetna Mountains
East Susitna
Ruby Range batholith
Maclaren-Kluane schist
Dezadeash-Nutzotin-Clearwater strata
Shakwak/Ann Creek pluton
Bennett Lake and other ca. 60-50 Ma volcanics
Valdez Creek-Tatshenshini shear zone
Undifferentiated Wrangellia composite terrane rocks
Talkeetna-Totschunda fault
future Denali fault
Proto-McCallum Creek fault
ca. 50 Ma volcanics near Gulkana Glacier pond above McCallum Creek normal fault
Pyroxenite/granodiorite
YUKON
B.C.
B: ca. 33 Ma
~300 km restored
Denali fault
Eventual abandonment of the Cottonwood terrane
Eocene volcanics
Emplacement of ca. 42-33 Ma plutons in Maclaren-Cottonwood
Talkeetna fault
Talkeetna fault restores to link with Totschunda fault
Totschunda fault
Undifferentiated Wrangellia composite terrane rocks
C: ca. 25 Ma
~230 km restored
Eocene volcanics
VCF
BGF
Cottonwood terrane
McCallum basin
Reactivation of Valdez Creek shear zone and Talkeetna fault
Totschunda fault
Duke River fault
Connector fault
VCF- Valdez Creek fault
BGF- Broxson Gulch fault
ca. 30 Ma initiation of Wrangell volcanic field
Undifferentiated Wrangellia composite terrane rocks
Shortening restored (gap)
D: ca. 6 Ma
~85 km restored
Denali fault
Reactivation of McCallum Creek fault
Eocene volcanics
McCallum basin
Active Rainy Creek fault
Reactivation of Totschunda fault separates Clearwater from Nutzotin
Totschunda fault
Expansion of Wrangell volcanic field
Duke River fault
Shortening restored (gap)
Connector fault

**Figure 12 (previous page):** Schematic map-view diagrams illustrating the ca. 50 Ma-Present evolution of the Denali fault system. The diagrams focus on correlative rock units and thus do not account for eroded material. The geology north and east of the Denali fault is not modified from figure 1 and modern political borders are retained as reference markers. The geology south and west of the Denali fault becomes increasingly schematic further back in time. Eocene volcanic rocks presently in the Talkeetna Mountains may be used to track restoration of the Denali fault. Kinematics are shown on faults that are active during the time frame. Colors are the same as figure 1. See text and map annotations for key events in each time frame and figure 1 for a Present-day time frame. **(A)** By ca. 50 Ma, all correlative rock packages between the Delta River region and Kluane Lake region had formed. Upon localization, the Denali fault will cut obliquely through the geology. **(B)** By ca. 33 Ma the Denali fault had localized as a dextral fault. The ca. 42-33 Ma intrusions that are shared among the Maclaren and Cottonwood schists are not present in the Kluane schist (see also figure 8). A structural complexity in the Denali fault abandons the Cottonwood schist near Alaska-Yukon border between 33 and 25 Ma. **(C)** By ca. 25 Ma, slip on the Valdez Creek fault had nucleated the imbricate thrust system along the south flank of the eastern Alaska Range. Deposition into the McCallum basin records sediment input from uplifted regions of the surrounding Alaska Range (Allen et al., 2016). The Totschunda fault was likely active at this time (Milde, 2014). **(D)** By ca. 6 Ma dextral slip transfer from the Totschunda fault to the Denali fault was ongoing, which resulted in transpression in the eastern Alaska Range and separation of the Clearwater metasediments from the Nutzotin Mountains sequence. Shortening on the Duke River fault absorbs a portion of the plate boundary convergence (Cobbett et al., 2017). The McCallum basin inverts as thrust systems expand the region of elevated Alaska Range topography (Waldien et al., 2018).

TABLE 1: OFFSET MARKERS FOR THE MODERN DENALI FAULT SYSTEM

| Reference | Fault section | Offset markers | Separation and Timing | Number on Figure 1 |
|---|---|---|---|---|
| Lowey (1998) | Eastern Denali | Megaboulder channel in Dezadeash (YT)-Nutzotin (AK) strata | 370 km since 52 Ma** | 1 |
| Waldien et al. (2021) | Eastern Denali | Clearwater metasediments (AK)-Dezadeash formation (YT) | 465 km since 52 Ma** | 1 |
| Waldien et al. (2021) | Eastern Denali | Granodiorite and pyroxenite near Ann Creek (AK)-Shorty Creek granodiorite and Pyroxenite Cr. Pyroxenite (YT)* | ≤505 km since 52 Ma** | 2 |
| Regan et al. (2021), This study | Eastern Denali | Cottonwoodschist (AK)-Maclaren schist (AK) | 305 km since 33 Ma | 3 |
| | | Cottonwood schist (AK)-Kluane schist (YT) | 100-125 km, 52-33 Ma | |
| Nokleberg et al. (1985), Riccio et al. (2014) | Eastern Denali | Maclaren schist and East Susitna batholith (AK)-Kluane schist and Ruby Range batholith (YT) | 445 km since 52 Ma** | 4 |
| This Study | Eastern Denali | Shakwak pluton (YT)-Ann Creek pluton (AK) | 465km since 52 Ma | 5 |
| | | 74-65Ma intrusions within Kluane schist and Maclaren schist* | ≥425 km since 52 Ma | 6 |
| | | Eocene bimodal volcanic strata near Gakona Gl. (AK)-Bennett Lake igneous complex (YT)* | ~580km since 52 Ma* | 7 |
| | | Jack River Igneous field (AK)- Rhyolite Creek volcanics (YT)* | 480 km since 52 Ma** | 8 |
| This Study; D. Murphy personal communication | Eastern Denali | Kluhini River Shear zone (YT)-Susitna Glacier thrust (AK) | ≥425 km post 52 Ma** | 7 |
| Waldien et al. (2018) | Totschunda-Eastern Denali | Strain compatibility with fault linkage | ≤91 km since 7 Ma | 9 |
| Berkelhammer et al. (2019) | Totschunda | Wrangell volcanics and intrusions (AK) | ≤85 km since 7 Ma** | 10 |
| Fasulo et al. (2020); This study | Totschunda-Eastern Denali | Nutzotin basin strata and associated ca. 120 Ma intrusions (AK) | >75 km since 7 Ma** | Similar to 9 |
| Allen et al. (2016) | Totschunda-Eastern Denali | Transtensional lower McCallum basin (AK) to transtension zone at Denali-Totschunda intersection (AK) | <95 km since 7 Ma** | Similar to 9 |
| Regan et al. (2021) | Central Denali | Schist Creek pluton-Foraker pluton (AK) | 155 km since 37 Ma | Not Shown |
| Trop et al. (2019) | Central Denali | Colorado Cr. Basin detritus-eastern Alaska Range sources (AK) | 150 km since 29 Ma | Not Shown |
| Miller et al. (2002) | Western Denali | Algal Reef in Farewell terrane strata (AK) | 134 km, post mid-K | Not Shown |

*Matched features may be different bodies

**Separation remeasured and/or new timing inferred from our data

TABLE 2: IGNEOUS ZIRCON U-Pb ANALYTICAL RESULTS

| Host rocks | Sample name | Latitude (ºN) | Longitude (ºW) | Rock type | Weighted mean $^{206}Pb/^{238}U$ Age (Ma)* | MSWD | Number of acceptable grains in age calculation[a] | Total number of zircons anlyzed[b] |
|---|---|---|---|---|---|---|---|---|
| Wrangellia terrane | 19ATW81 | 63.2986 | 146.6962 | Tonalite | 112.9 ± 1.3 | 1.7 | 31 | 31 |
| Wrangellia terrane | 13ET270 | 63.2216 | 146.7085 | Diorite | 129.8 ± 2.4 | 1.5 | 31 | 31 |
| Wrangellia terrane | 15DR140 | 63.3054 | 146.6025 | Quartz syenite | 144.1 ± 2.3 | 1.9 | 15 | 17 |
| Wrangellia terrane | 16CSR17 | 63.3330 | 146.3319 | Granite | 306.3 ± 4.0 | 0.48 | 14 | 16 |
| Wrangellia terrane | 17ATW11 | 63.3498 | 145.6523 | Granodiorite | 307.2 ± 6.1 | 0.9 | 12 | 14 |
| Wrangellia terrane | 14ATW50 | 63.2483 | 145.4092 | Granodiorite | 309.8 ± 3.9 | 3.2 | 30 | 32 |
| Clearwater metasediments | 19ATW55 | 63.2699 | 146.8861 | Diorite | 53.1 ± 0.6 | 0.71 | 16 | 21 |
| Clearwater metasediments | 19ATW39 | 63.3318 | 146.6695 | Felsic Tuff | 160.4 ± 1.5 | 0.74 | 22 | 22 |
| Maclaren schist | 19ATW79 | 63.3548 | 146.6812 | Quartz Monzonite | 51.9 ± 0.6 | 3.2 | 45 | 53 |
| Maclaren schist | 19ATW40 | 63.4155 | 146.7800 | Tonalite | 64.6 ± 0.7 | 1.9 | 46 | 49 |
| Maclaren schist | 18ATW21 | 63.3070 | 146.9629 | Tonalite | 68.3 ± 1.3 | 3.7 | 33 | 40 |
| Maclaren schist | 17ATW03 | 63.2163 | 147.0698 | Tonalite | 70.5 ± 1.0 | 2.6 | 28 | 35 |
| Maclaren schist | 19ATW66 | 63.3473 | 146.8130 | Biotite-garnet leucogranite | 75.8 ± 1.9 | 1.14 | 9[c] | 29 |

*Weighted mean uncertainties represent quadratic addition of internal and external uncertainties at 2s.

MSWD: Mean Square Weighted Deviation

a- The number of analyses that passed the filtering criteria

b- The total number of analyzed grains

c- Rim analyses: Filtering criteria relaxed to allow more analyses in age calculation

TABLE 3: $^{40}Ar/^{39}Ar$ ANALYTICAL RESULTS FOR VOLCANIC ROCKS

| Sample name | Latitude (ºN) | Longitude (ºW) | Rock type | Phase analyzed | Grain size analyzed (um) | Integrated age (Ma)** | Plateau age (Ma)** | Plateau information |
|---|---|---|---|---|---|---|---|---|
| 12HODO | 63.2233 | 145.4485 | Rhyodacite tuff | Biotite | 500-1000 | 50.9 ± 0.3 | **50.9 ± 0.5** | 6 of 12 steps 91.8% $^{39}Ar$ release MSWD = 1.91 |
| 46GUNN | 63.2108 | 145.4025 | Dacite flow | Whole rock | 212-500 | 45.1 ± 0.1 | **45.5 ± 0.2** | 3 of 8 fractions 49.7% $^{39}Ar$ release MSWD = 1.55 |
| 15BG216 | 63.2098 | 145.3516 | Dacite flow | Whole rock | 212-501 | 48.8 ± 0.4 | **49.3 ± 0.7*** | 7 of 8 fractions 94% $^{39}Ar$ release MSWD = 3.34 |
| 15BG209 | 63.2123 | 145.3635 | Rhyodacite tuff | Whole rock | 212-502 | 49.6 ± 0.4 | **49.8 ± 0.3*** | 2 of 8 fractions 50.8% $^{39}Ar$ release MSWD = 3.18 |

** Uncertainties are 1s.

*Did not meet all the criteria of a plateau age, hence a weighted average age is presented.

MSWD- Mean Square Weighted Deviation

## REFERENCES CITED


Aleinikoff, J. N., Nokleberg, W. J., and Herzon, P. L. (1981). Age of intrusion and metamorphism of the East Susitna batholith. Mount Hayes B-6 quadrangle, eastern Alaska Range, Alaska. *U.S. Geological Survey Circular 844*, 100-102.

Allam, A. A., Schulte-Pelkum, V., Ben-Zion, Y., Tape, C., Ruppert, N., & Ross, Z. E. (2017). Ten kilometer vertical Moho offset and shallow velocity contrast along the Denali fault zone from double-difference tomography, receiver functions, and fault zone head waves. *Tectonophysics*, *721*, 56–69. https://doi.org/10.1016/j.tecto.2017.09.003

Allan, M. M., Mortensen, J. K., Hart, C. J. R., Bailey, L. A., Sanchez, M. G., Ciolkiewicz, W., McKenzie, G.G., & Creaser, R.A. (2013). Magmatic and metallogenic framework of west-central Yukon and eastern Alaska. In M. Colpron, T. Bissig, B.G. Rusk, J.F.H. Thomposon (Ed.). *Tectonics, Metallogeny, and Discovery: The North American Cordillera and Similar Accretionary Settings:* (Society of Economic Geologists Special Publication 17, pp.111-168). Littleton, Colorado: Society of Economic Geologists https://doi.org/10.5382/SP.17

Allen, W.K., Ridgway, K.D., Benowitz, J.A., Waldien, T.S., & Roeske, S.M. (2016). Sedimentary and volcanic record of Neogene transpressional foreland basin development along the central Denali Fault system, Eastern Alaska Range. *Geological Society of America Abstracts with Programs, 48*. doi: 10.1130/abs/2016AM-284817

Amato, J. M., & Pavlis, T. L. (2010). Detrital zircon ages from the Chugach terrane, southern Alaska, reveal multiple episodes of accretion and erosion in a subduction complex. *Geology*, *38*(5), 459–462. https://doi.org/10.1130/G30719.1

Amato, J. M., Pavlis, T. L., Clift, P. D., Kochelek, E. J., Hecker, J. P., Worthman, C. M., & Day, E. M. (2013). Architecture of the Chugach accretionary complex as revealed by detrital zircon ages and lithologic variations: Evidence for Mesozoic subduction erosion in south-central Alaska. *GSA Bulletin*, *125*(11-12), 1891-1911.

Amato, J. M., Rioux, M. E., Kelemen, P. B., Gehrels, G. E., Clift, P. D., Pavlis, T. L., & Draut, A. E. (2007). U-Pb geochronology of volcanic rocks from the Jurassic Talkeetna Formation and detrital zircons from prearc and postarc sequences: Implications for the age of magmatism and inheritance in the Talkeetna arc. . In Ridgway, K.D., Trop, J.M., Glen, J.M.G., O'Neill, J.M. (Eds.). *Special Paper 431: Tectonic Growth of a Collisional Continental Margin: Crustal Evolution of Southern Alaska* (Vol. 431, pp. 253–271). Boulder, Colorado: Geological Society of America.

Andronicos, C. L., Chardon, D. H., Hollister, L. S., Gehrels, G. E., & Woodsworth, G. J. (2003). Strain partitioning in an obliquely convergent orogen, plutonism, and synorogenic collapse: Coast Mountains Batholith, British Columbia, Canada. *Tectonics*, *22*(2).

Atwater, T. (1989). Plate tectonic history of the northeast Pacific and western North America. In E. L. Winterer, D. M. Hussong, & R. W. Decker (Eds.). *Geology of North America: Volume N, The Eastern Pacific Ocean and Hawaii.* (pp. 21–72). Boulder, Colorado: Geological Society of America. https://doi.org/10.1130/DNAG-GNA-N.21

Audet, P., Sole, C., & Schaeffer, A. J. (2016). Control of lithospheric inheritance on neotectonic activity in northwestern Canada? *Geology*, *44*(10), 807–810. https://doi.org/10.1130/G38118.1

Avé Lallemant, H. G. (1997). Transpression, displacement partitioning, and exhumation in the eastern Caribbean/South American plate boundary zone. *Tectonics*, *16*(2), 272-289.

Avé Lallemant, H. G., & Oldow, J. S. (1988). Early Mesozoic southward migration of Cordilleran transpressional terranes. *Tectonics*, *7*(5), 1057-1075.

Bacon, C. R., Foster, H. L., & Smith, J. G. (1990). Rhyolitic calderas of the Yukon-Tanana Terrane, east central Alaska: Volcanic remnants of a Mid-Cretaceous magmatic arc. *Journal of Geophysical Research: Solid Earth*, *95*(B13), 21451-21461.

Beck Jr, M. E. (1986). Model for late Mesozoic-early Tertiary tectonics of coastal California and western Mexico and speculations on the origin of the San Andreas fault. *Tectonics*, *5*(1), 49-64.

Bemis, S. P., & Wallace, W. K. (2007). Neotectonic framework of the north-central Alaska Range foothills. In Ridgway, K.D., Trop, J.M., Glen, J.M.G., O'Neill, J.M. (Eds.). *Special Paper 431: Tectonic Growth of a Collisional Continental Margin: Crustal Evolution of Southern Alaska* (Vol. 431, pp. 549–572). Boulder, Colorado: Geological Society of America. https://doi.org/10.1130/2007.2431(21)

Benowitz, J. A., Davis, K., & Roeske, S. (2019). A river runs through it both ways across time: 40Ar/39Ar detrital and bedrock muscovite geochronology constraints on the Neogene paleodrainage history of the Nenana River system, Alaska Range. *Geosphere*, *15*(3), 682–701. https://doi.org/10.1130/GES01673.1

Benowitz, J. A., Haeussler, P. J., Layer, P. W., O'Sullivan, P. B., Wallace, W. K., & Gillis, R. J. (2012). Cenozoic tectono-thermal history of the Tordrillo Mountains, Alaska: Paleocene-Eocene ridge subduction, decreasing relief, and late Neogene faulting. *Geochemistry, Geophysics, Geosystems*, *13*(4), n/a-n/a. https://doi.org/10.1029/2011GC003951

Benowitz, J. A., Roeske, S.M., Layer, P. W. (2011). Deep exhumation, neotectonics, and constraints on the Denali fault system long-term off-set history: The Totschunda strand and the south-eastern Alaska Range. *Geological Society of America abstracts with programs, 43*(5), p. 438.

Benowitz, J. A., Layer, P. W., & Vanlaningham, S. (2014). Persistent long-term (*c.* 24 Ma) exhumation in the Eastern Alaska Range constrained by stacked thermochronology. *Geological Society, London, Special Publications*, *378*(1), 225–243. https://doi.org/10.1144/SP378.12

Benowitz, J. A., Layer, P. W., Armstrong, P., Perry, S. E., Haeussler, P. J., Fitzgerald, P. G., & VanLaningham, S. (2011). Spatial variations in focused exhumation along a continental-scale strike-slip fault: The Denali fault of the eastern Alaska Range. *Geosphere*, *7*(2), 455–467. https://doi.org/10.1130/GES00589.1

Beranek, L. P., McClelland, W. C., van Staal, C. R., Israel, S., & Gordee, S. M. (2017). Late Jurassic flare-up of the Coast Mountains arc system, NW Canada, and dynamic linkages across the northern Cordilleran orogen: Flare-Up of the Coast Mountains Arc. *Tectonics*, *36*(5), 877–901. https://doi.org/10.1002/2016TC004254

Beranek, L. P., van Staal, C. R., McClelland, W. C., Joyce, N., & Israel, S. (2014). Late Paleozoic assembly of the Alexander-Wrangellia-Peninsular composite terrane, Canadian and Alaskan Cordillera. *Geological Society of America Bulletin*, 20.

Berg, E. M., Lin, F., Allam, A., Schulte-Pelkum, V., Ward, K. M., & Shen, W. (2020). Shear Velocity Model of Alaska Via Joint Inversion of Rayleigh Wave Ellipticity, Phase Velocities, and Receiver Functions Across the Alaska Transportable Array. *Journal of Geophysical Research: Solid Earth*, *125*(2). https://doi.org/10.1029/2019JB018582

Berg, H. C., D. L. Jones, and D. H. Richter (1972), Gravina-Nutzotin belt: Tectonic significance of an upper Mesozoic sedimentary and volcanic sequence in southern and southeastern Alaska, U.S. Geol. Surv. Prof. Pap., 800D, D1–D24.

Berkelhammer, S. E., Brueseke, M. E., Benowitz, J. A., Trop, J. M., Davis, K., Layer, P. W., & Weber, M. (2019). Geochemical and geochronological records of tectonic changes along a flat-slab arc-transform junction: Circa 30 Ma to ca. 19 Ma Sonya Creek volcanic field, Wrangell Arc, Alaska. *Geosphere*, *15*(5), 1508–1538. https://doi.org/10.1130/GES02114.1

Bill, N. S., Mix, H. T., Clark, P. U., Reilly, S. P., Jensen, B. J. L., & Benowitz, J. A. (2018). A stable isotope record of late Cenozoic surface uplift of southern Alaska. *Earth and Planetary Science Letters*, *482*, 300–311. https://doi.org/10.1016/j.epsl.2017.11.029

Bittenbender, P.E., Bean, K.W., Kurtak, J.M., & Deininger, J. (2007). Mineral assessment of the Delta River mining district area, east-central Alaska. U*.S. Bureau of Land Management Alaska Technical Report 57*, 697 p.

Bond, G. C. (1973). A Late Paleozoic Volcanic Arc in the Eastern Alaska Range, Alaska. *The Journal of Geology*, *81*(5), 557–575.

Bond, G.C. (1976). Geology of the Rainbow Mountain-Gulkana Glacier Area, Eastern Alaska Range, with Emphasis on Upper Paleozoic Strata. *State of Alaska Geologic Division of Geological & Geophysical Surveys Geologic Report 45*, 47 p., scale 1:40:000, 3 sheets.

Box, S. E., Karl, S. M., Jones III, J. V., Bradley, D. C., Haeussler, P. J., & O'Sullivan, P. B. (2019). Detrital zircon geochronology along a structural transect across the Kahiltna assemblage in the western Alaska Range: Implications for emplacement of the Alexander-Wrangellia-Peninsular terrane against North America. *Geosphere*, *15*(6), 1774-1808. https://doi.org/10.1130/GES02060.1

Brennan, P. R. K., Gilbert, H., & Ridgway, K. D. (2011). Crustal structure across the central Alaska Range: Anatomy of a Mesozoic collisional zone. *Geochemistry, Geophysics, Geosystems*, *12*(4). https://doi.org/10.1029/2011GC003519

Brennan, P. R., & Ridgway, K. D. (2015). Detrital zircon record of Neogene exhumation of the central Alaska Range: A far-field upper plate response to flat-slab subduction. *GSA Bulletin*, *127*(7-8), 945-961.

Brothers, D. S., Elliott, J. L., Conrad, J. E., Haeussler, P. J., & Kluesner, J. W. (2018). Strain partitioning in Southeastern Alaska: Is the Chatham Strait Fault active?. *Earth and Planetary Science Letters*, *481*, 362-371.

Brueseke, M. E., Benowitz, J. A., Trop, J. M., Davis, K. N., Berkelhammer, S. E., Layer, P. W., & Morter, B. K. (2019). The Alaska Wrangell Arc:~ 30 Ma of subduction-related magmatism along a still active arc-transform junction. *Terra Nova*, *31*(1), 59-66.

Bruhn, R. L., Pavlis, T. L., Plafker, G., & Serpa, L. (2004). Deformation during terrane accretion in the Saint Elias orogen, Alaska. *Geological Society of America Bulletin*, *116*(7-8), 771-787.

Burkett, C. A., Bemis, S. P., & Benowitz, J. A. (2016). Along-fault migration of the Mount McKinley restraining bend of the Denali fault defined by late Quaternary fault patterns and seismicity, Denali National Park & Preserve, Alaska. *Tectonophysics*, *693*, 489–506. https://doi.org/10.1016/j.tecto.2016.05.009

Busby-Spera, C. J., & Saleeby, J. B. (1990). Intra-arc strike-slip fault exposed at batholithic levels in the southern Sierra Nevada, California. *Geology*, *18*(3), 255-259.

Canil, D., Johnston, S. T., D'Souza, R. J., & Heaman, L. M. (2015). Protolith of ultramafic rocks in the Kluane Schist, Yukon, and implications for arc collisions in the northern Cordillera. *Canadian Journal of Earth Sciences*, *52*(7), 431–443. https://doi.org/10.1139/cjes-2014-0138

Cecil, M. R., Gehrels, G., Ducea, M. N., & Patchett, P. J. (2011). U-Pb-Hf characterization of the central Coast Mountains batholith: Implications for petrogenesis and crustal architecture. *Lithosphere*, *3*(4), 247–260. https://doi.org/10.1130/L134.1

Chardon, D., Andronicos, C. L., & Hollister, L. S. (1999). Large-scale transpressive shear zone patterns and displacements within magmatic arcs: The Coast Plutonic Complex, British Columbia. *Tectonics*, *18*(2), 278–292. https://doi.org/10.1029/1998TC900035

Cobbett, R., Israel, S., Mortensen, J., Joyce, N., & Crowley, J. (2017). Structure and kinematic evolution of the Duke River fault, southwestern Yukon. *Canadian Journal of Earth Sciences*, *54*(3), 322–344. https://doi.org/10.1139/cjes-2016-0074

Cole, R. B., Layer, P. W., Hooks, B., Cyr, A., & Turner, J. (2007). Magmatism and deformation in a terrane suture zone south of the Denali Fault, northern Talkeetna Mountains, Alaska. In Ridgway, K.D., Trop, J.M., Glen, J.M.G., O'Neill, J.M. (Eds.). *Special Paper 431: Tectonic Growth of a Collisional Continental Margin: Crustal Evolution of Southern Alaska* (Vol. 431, pp. 477–506). Boulder, Colorado: Geological Society of America.

Cole, R. B., Ridgway, K. D., Layer, P. W., & Drake, J. (1999). Kinematics of basin development during the transition from terrane accretion to strike-slip tectonics. Late Cretaceous-early Tertiary Cantwell Formation, south central Alaska. *Tectonics*, *18*(6), 1224-1244.

Colpron, M. and Nelson, J.L., 2011, A Digital Atlas of Terranes for the Northern Cordillera. *British Columbia Ministry of Energy and Mines, BCGS GeoFile 2011-11*.

Colpron, M., Crowley, J. L., Gehrels, G., Long, D. G. F., Murphy, D. C., Beranek, L., & Bickerton, L. (2015). Birth of the northern Cordilleran orogen, as recorded by detrital zircons in Jurassic synorogenic strata and regional exhumation in Yukon. *Lithosphere*, *7*(5), 541–562. https://doi.org/10.1130/L451.1

Colpron, M., Israel, S., Murphy, D., Pigage, L. and Moynihan, D. (2016). Yukon Bedrock Geology Map. *Yukon Geological Survey*, *Open File 2016-1,* 1:1,000,000 scale map and legend.

Coney, P. J., Jones, D. L., & Monger, J. W. (1980). Cordilleran suspect terranes. *Nature*, *288*(5789), 329-333.

Coutts, D. S., Matthews, W. A., Englert, R. G., Brooks, M. D., Boivin, M. P., & Hubbard, S. M. (2020). Along-strike variations in sediment provenance within the Nanaimo basin reveal mechanisms of forearc basin sediment influx events. *Lithosphere*, *12*(1), 180-197.

Csejtey, B., Cox, D. P., Evarts, R. C., Stricker, G. D., & Foster, H. L. (1982). The Cenozoic Denali Fault System and the Cretaceous accretionary development of southern Alaska. *Journal of Geophysical Research*, *87*(B5), 3741. https://doi.org/10.1029/JB087iB05p03741

Csejtey, B., Mullen, M.W., Cox, D.P., and Stricker, G.D. (1992). Geology and geochronology of the Healy Quadrangle, south-central Alaska, *U.S. Geological Survey Miscellaneous Investigations Series Map 1961*, 63 p., 2 sheets, scale 1:250,000.

Csejtey, B., Nelson, W.H., Jones, D.L., Silberling, N.J., Dean, R.M., Morris, M.S., Lanphere, M.A., Smith, J.G., & Silberman, M.L. (1978). Reconnaissance geologic map and geochronology, Talkeetna Mountains Quadrangle, northern part of Anchorage Quadrangle, and southwest corner of Healy Quadrangle, Alaska. *U.S. Geological Survey Open-File Report 78-558-A, 60* p., 1 sheet, scale 1:250,000.

Davidson, C., & Garver, J. I. (2017). Age and origin of the resurrection ophiolite and associated turbidites of the Chugach–Prince William Terrane, Kenai Peninsula, Alaska. *The Journal of Geology*, *125*(6), 681-700.

Davidson, C., & McPhillips, D. (2007). Along strike variations in metamorphism and deformation of the strata of the Kahiltna basin, south-central Alaska. In Ridgway, K.D., Trop, J.M., Glen, J.M.G., O'Neill, J.M. (Eds.). *Special Paper 431: Tectonic Growth of a Collisional Continental Margin: Crustal Evolution of Southern Alaska* (Vol. 431, pp. 439–453). Boulder, Colorado: Geological Society of America. https://doi.org/10.1130/2007.2431(17)

Davidson, C., Hollister, L. S., & Schmid, S. M. (1992). Role of melt in the formation of a deep-crustal compressive shear zone: The Maclaren Glacier Metamorphic Belt, south central Alaska. *Tectonics*, *11*(2), 348–359. https://doi.org/10.1029/91TC02907

Day, E. M., Pavlis, T. L., & Amato, J. M. (2016). Detrital zircon ages indicate an Early Cretaceous episode of blueschist-facies metamorphism in southern Alaska: Implications for the Mesozoic paleogeography of the northern Cordillera. *Lithosphere*, *8*(5), 451–462. https://doi.org/10.1130/L525.1

Dominguez, S., S. E. Lallemand, J. Malavieille, & von Huene. R. (1998). Upper plate deformation associated with seamount subduction. *Tectonophysics 293*,(3-4), 207-224.

Doser, D. I. (2004). Seismicity of the Denali-Totschunda Fault Zone in Central Alaska (1912-1988) and Its Relation to the 2002 Denali Fault Earthquake Sequence. *Bulletin of the Seismological Society of America*, *94*(6B), S132–S144. https://doi.org/10.1785/0120040611

Doser, D. I. (2014). Seismicity of Southwestern Yukon, Canada, and its relation to slip transfer between the Fairweather and Denali fault systems. *Tectonophysics*, *611*, 121-129.

Doubrovine, P. V., & Tarduno, J. A. (2008). A revised kinematic model for the relative motion between Pacific oceanic plates and North America since the Late Cretaceous. *Journal of Geophysical Research*, *113*(B12), B12101. https://doi.org/10.1029/2008JB005585

Dusel-Bacon, C., & Williams, I. S. (2009). Evidence for prolonged mid-Paleozoic plutonism and ages of crustal sources in east-central Alaska from SHRIMP U–Pb dating of syn-magmatic, inherited, and detrital zircon. *Canadian Journal of Earth Sciences*, *46*(1), 21-39.

Dusel-Bacon, C., Holm-Denoma, C. S., Jones, J. V., Aleinikoff, J. N., & Mortensen, J. K. (2017). Detrital zircon geochronology of quartzose metasedimentary rocks from parautochthonous North America, east-central Alaska. *Lithosphere*, *9*(6), 927-952.

Eberhart-Phillips, D., Haeussler, P. J., Freymueller, J. T., Frankel, A. D., Rubin, C. M., Craw, P., ... & Dawson, T. E. (2003). The 2002 Denali fault earthquake, Alaska: A large magnitude, slip-partitioned event. *Science*, *300*(5622), 1113-1118.

Eisbacher, G. H. (1976). Sedimentology of the Dezadeash flysch and its implications for strike-slip faulting along the Denali Fault, Yukon Territory and Alaska. *Canadian Journal of Earth Sciences*, *13*(11), 1495–1513. https://doi.org/10.1139/e76-157

Elliott, J., & Freymueller, J. T. (2020). A Block Model of Present-Day Kinematics of Alaska and Western Canada. *Journal of Geophysical Research: Solid Earth*, *125*(7), e2019JB018378.

Enkelmann, E., Garver, J. I., & Pavlis, T. L. (2008). Rapid exhumation of ice-covered rocks of the Chugach–St. Elias orogen, Southeast Alaska. *Geology*, *36*(12), 915-918.

Enkelmann, E., Zeitler, P. K., Garver, J. I., Pavlis, T. L., & Hooks, B. P. (2010). The thermochronological record of tectonic and surface process interaction at the Yakutat-North American collision zone in southeast Alaska. *American Journal of Science*, *310*(4), 231–260. https://doi.org/10.2475/04.2010.01

Enkelmann, Eva, Finzel, E., & Arkle, J. (2019). Deformation at the eastern margin of the Northern Canadian Cordillera: Potentially related to opening of the North Atlantic. *Terra Nova*, *31*(3), 151–158. https://doi.org/10.1111/ter.12374

Enkin, R. J. (2006). Paleomagnetism and the case for Baja British Columbia. In J.W. Haggart, R.J. Enkin, J.W.H. Monger (Eds.). *Paleogeography of the North American Cordillera: Evidence for and against large-scale displacements*. (Geological Association of Canada Special Paper 46 pp. 233-254). St. Johns, Newfoundland: Geological Association of Canada.

Estève, C., Audet, P., Schaeffer, A. J., Schutt, D. L., Aster, R. C., & Cubley, J. F. (2020). Seismic evidence for craton chiseling and displacement of lithospheric mantle by the Tintina fault in the northern Canadian Cordillera. *Geology, 48.*

Evenchick, C. A. (1991). Geometry, evolution, and tectonic framework of the Skeena Fold Belt, north central British Columbia. *Tectonics*, *10*(3), 527–546. https://doi.org/10.1029/90TC02680

Fasulo, C. R., Ridgway, K. D., & Trop, J. M. (2020). Detrital zircon geochronology and Hf isotope geochemistry of Mesozoic sedimentary basins in south-central Alaska: Insights into regional sediment transport, basin development, and tectonics along the NW Cordilleran margin. *Geosphere*.

Finzel, E. S., Ridgway, K. D., & Trop, J. M. (2015). Provenance signature of changing plate boundary conditions along a convergent margin: Detrital record of spreading-ridge and flat-slab subduction processes, Cenozoic forearc basins, Alaska. *Geosphere*, *11*(3), 823-849.

Finzel, E. S., Trop, J. M., Ridgway, K. D., & Enkelmann, E. (2011). Upper plate proxies for flat-slab subduction processes in southern Alaska. *Earth and Planetary Science Letters*, *303*(3-4), 348-360.

Fitzgerald, P. G., Roeske, S. M., Benowitz, J. A., Riccio, S. J., Perry, S. E., & Armstrong, P. A. (2014). Alternating asymmetric topography of the Alaska range along the strike-slip Denali fault: Strain partitioning and lithospheric control across a terrane suture zone. *Tectonics*, *33*(8), 1519–1533. https://doi.org/10.1002/2013TC003432

Fitzgerald, P. G., Sorkhabi, R. B., Redfield, T. F., & Stump, E. (1995). Uplift and denudation of the central Alaska Range: A case study in the use of apatite fission track thermochronology to determine absolute uplift parameters. *Journal of Geophysical Research: Solid Earth*, *100*(B10), 20175–20191. https://doi.org/10.1029/95JB02150

Fitzgerald, P. G., Stump, E., & Redfield, T. F. (1993). Late Cenozoic uplift of Denali and its relation to relative plate motion and fault morphology. *Science*, *259*(5094), 497-499.

Forbes, R. B., Smith, T. E., & Turner, D. L. (1974). Comparative petrology and structure of the Maclaren, Ruby Range, and Coast Range belts: Implications for offset along the Denali fault system, *Geological Society of America Abstracts with Programs*, v. 6, p. 177.

Foster, D. A., Doughty, P. T., Kalakay, T. J., Fanning, C. M., Coyner, S., Grice, W. C., & Vogl, J. (2007). Kinematics and timing of exhumation of metamorphic core complexes along the Lewis and Clark fault zone, northern Rocky Mountains, USA. In A.B. Till, S.M. Roeske, J.C. Sample, D.A. Foster (Eds.). *Special Paper 434: Exhumation Associated with Continental Strike-Slip Fault Systems* (pp. 207-232). Boulder, Colorado: Geological Society of America.

Gabrielse, H., Murphy, D. C., & Mortensen, J. K. (2006). Cretaceous and Cenozoic dextral orogen-parallel displacements, magmatism, and paleogeography, north-central Canadian Cordillera. In J.W. Haggart, R.J. Enkin, J.W.H. Monger (Eds.). *Paleogeography of the North American Cordillera: Evidence for and against large-scale displacements*. (Geological Association of Canada Special Paper 46 pp. 255-276). St. Johns, Newfoundland: Geological Association of Canada

Gardner, M. C., Bergman, S. C., Cushing, G. W., MacKevett Jr, E. M., Plafker, GR. B. Campbell, C. J. Dodds, W. C. McClelland, & Mueller, P. A. (1988). Pennsylvanian pluton stitching of Wrangellia and the Alexander terrane, Wrangell Mountains, Alaska. *Geology*, *16*(11), 967-971.

Garver, J. I., & Davidson, C. M. (2015). Southwestern Laurentian zircons in upper Cretaceous flysch of the Chugach-Prince William terrane in Alaska. *American Journal of Science*, *315*(6), 537-556.

Gehrels, G., & Pecha, M. (2014). Detrital zircon U-Pb geochronology and Hf isotope geochemistry of Paleozoic and Triassic passive margin strata of western North America. *Geosphere*, *10*(1), 49-65.

Gehrels, G., Rusmore, M., Woodsworth, G., Crawford, M., Andronicos, C., Hollister, L., Patchett, J., Ducea, M., Butler, R., Klepeis, K., Davidson, C., Friedman, R., Haggart, J., Mahoney, B., Crawford, W., Pearson, D., & Girardi, J. (2009). U-Th-Pb geochronology of the Coast Mountains batholith in north-coastal British Columbia: Constraints on age and tectonic evolution. *Geological Society of America Bulletin*, *121*(9–10), 1341–1361. https://doi.org/10.1130/B26404.1

Gillis, R.J., Fitzgerald, P.G., Ridgway, K.D., Keough, B.M., Benowitz, J.A., and Allen, W.K. (2019). Overview of the new 1:25,000-scale geologic mapping of the McCallum-Slate Creek fault system, eastern Alaska Range, Alaska, *Alaska Division of Geological & Geophysical Surveys Preliminary Interpretive Report 2018-3*, 10 p. http://doi.org/10.14509/30136

Greene, A. R., Scoates, J. S., & Weis, D. (2008). Wrangellia flood basalts in Alaska: A record of plume-lithosphere interaction in a Late Triassic accreted oceanic plateau. *Geochemistry, Geophysics, Geosystems*, *9*(12).

Greene, A. R., Scoates, J. S., Weis, D., Katvala, E. C., Israel, S., & Nixon, G. T. (2010). The architecture of oceanic plateaus revealed by the volcanic stratigraphy of the accreted Wrangellia oceanic plateau. *Geosphere*, *6*(1), 47-73.

Haeussler, P. J., Matmon, A., Schwartz, D. P., & Seitz, G. G. (2017). Neotectonics of interior Alaska and the late Quaternary slip rate along the Denali fault system. *Geosphere*, *13*(5), 1445-1463.

Haeussler, P. J., O'sullivan, P., Berger, A. L., & Spotila, J. A. (2008). Neogene Exhumation of the Tordrillo Mountains, Alaska, and Correlations With Denali (Mount Mckinley). In J. T. Freymueller, P. J. Haeussler, R. L. Wesson, & G. Ekström (Eds.), *Geophysical Monograph Series* (pp. 269–285). Washington D.C.: American Geophysical Union. https://doi.org/10.1029/179GM15

Hampton, B. A., Ridgway, K. D., & Gehrels, G. E. (2010). A detrital record of Mesozoic island arc accretion and exhumation in the North American Cordillera: U-Pb geochronology of the Kahiltna basin, southern Alaska: A DETRITAL RECORD OF ARC ACCRETION. *Tectonics*, *29*(4), n/a-n/a. https://doi.org/10.1029/2009TC002544

Hampton, B. A., Ridgway, K. D., O'Neill, J. M., Gehrels, G. E., Schmidt, J., & Blodgett, R. B. (2007). Pre-, syn-, and postcollisional stratigraphic framework and provenance of Upper Triassic–Upper Cretaceous strata in the northwestern Talkeetna Mountains, Alaska. In In Ridgway, K.D., Trop, J.M., Glen, J.M.G., O'Neill, J.M. (Eds.). *Special Paper 431: Tectonic Growth of a Collisional*

*Continental Margin: Crustal Evolution of Southern Alaska* (Vol. 431, pp. 401–438). Boulder, Colorado: Geological Society of America. https://doi.org/10.1130/2007.2431(16)

Hart, C. J., Mair, J. L., Goldfarb, R. J., & Groves, D. I. (2004). Source and redox controls on metallogenic variations in intrusion-related ore systems, Tombstone-Tungsten Belt, Yukon Territory, Canada. *Earth and Environmental Science Transactions of The Royal Society of Edinburgh*, *95*(1-2), 339-356.

Haynie, K. L., & Jadamec, M. A. (2017). Tectonic drivers of the Wrangell block: Insights on fore-arc sliver processes from 3-D geodynamic models of Alaska. *Tectonics*, *36*(7), 1180-1206.

Herriott, T. M., Crowley, J. L., Schmitz, M. D., Wartes, M. A., & Gillis, R. J. (2019). Exploring the law of detrital zircon: LA-ICP-MS and CA-TIMS geochronology of Jurassic forearc strata, Cook Inlet, Alaska, USA. *Geology*, *47*(11), 1044–1048. https://doi.org/10.1130/G46312.1

Hildebrand, R. S. (2015). Dismemberment and northward migration of the Cordilleran orogen: Baja-BC resolved. *GSA Today*, 4–11. https://doi.org/10.1130/GSATG255A.1

Hillhouse, J. W., Coe, R. S. (1994). Paleomagnetic data from Alaska. In G. Plafker, & H.C. Berg, (eds.). *The geology of Alaska: Geology of North America*, *1*, (Vol. G-1, pp. 797-812). *Boulder, Colorado: Geological Society of America.*

Hollister, L. S. (1993). The role of melt in the uplift and exhumation of orogenic belts. *Chemical Geology*, *108*(1–4), 31–48. https://doi.org/10.1016/0009-2541(93)90316-B

Horstwood, M. S. A., Košler, J., Gehrels, G., Jackson, S. E., McLean, N. M., Paton, C., Pearson, N. J., Sircombe, K., Sylvester, P., Vermeesch, P., Bowring, J. F., Condon, D. J., & Schoene, B. (2016). Community-Derived Standards for LA-ICP-MS U-(Th-)Pb Geochronology—Uncertainty Propagation, Age Interpretation and Data Reporting. *Geostandards and Geoanalytical Research*, *40*(3), 311–332. https://doi.org/10.1111/j.1751-908X.2016.00379.x

Hoskin, P. W., & Schaltegger, U. (2003). The composition of zircon and igneous and metamorphic petrogenesis. In J.M Hanchar and P.W.O Hoskin (Eds.). *Reviews in mineralogy and geochemistry: Zircon* , *53*(1), 27-62. Chantilly, Virginia: Mineralogical Society of America

Hults, C. P., Wilson, F. H., Donelick, R. A., & O'Sullivan, P. B. (2013). Two flysch belts having distinctly different provenance suggest no stratigraphic link between the Wrangellia composite terrane and the paleo-Alaskan margin. *Lithosphere*, *5*(6), 575-594.

Hults, C.P. & Athey, J.E. (2011). Similarities between early Tertiary conglomerates along the Slate Creek and Duke River faults, Alaska and Yukon. *2011 Cordilleran Tectonics Workshop; Yukon Geological Survey Miscellaneous Report 3*, 11-12.

Hyndman, R. D., Currie, C. A., & Mazzotti, S. P. (2005). Subduction zone backarcs, mobile belts, and orogenic heat. *GSA Today*, *15*(2), 4-10.

Israel, S., Beranek, L., Friedman, R. M., & Crowley, J. L. (2014). New ties between the Alexander terrane and Wrangellia and implications for North America Cordilleran evolution. *Lithosphere*, *6*(4), 270–276. https://doi.org/10.1130/L364.1

Israel, S., Colpron, M., Cubley, J., Moynihan, D., Murphy, D.C. and Relf, C. (2015). The Bear Creek assemblage: A latest Triassic volcano-sedimentary succession in southwest Yukon. In: K.E. MacFarlane, M.G. Nordling and P.J. Sack (eds.), Yukon Exploration and Geology 2014, Yukon Geological Survey, p. 99-112.

Israel, S., Murphy, D., Bennett, V., Mortensen, J., & Crowley, J. (2011). New insights into the geology and mineral potential of the Coast Belt in southwestern Yukon. *Yukon exploration and geology*, 101-123.

Israel, S., Schiarizza, P., Kennedy, L. A., Friedman, R. M., & Villeneuve, M. (2006). Evidence for Early to Late Cretaceous sinistral deformation in the Tchaikazan River area, southwestern British Columbia: Implications for the tectonic evolution of the southern Coast belt. In J.W. Haggart, R.J. Enkin, J.W.H. Monger (Eds.). *Paleogeography of the North American Cordillera: Evidence for and against large-scale displacements*. (Geological Association of Canada Special Paper 46 pp. 331-350). St. Johns, Newfoundland: Geological Association of Canada.

Jadamec, M. A., Billen, M. I., & Roeske, S. M. (2013). Three-dimensional numerical models of flat slab subduction and the Denali fault driving deformation in south-central Alaska. *Earth and Planetary Science Letters*, *376*, 29–42. https://doi.org/10.1016/j.epsl.2013.06.009

Jarrard, R. D. (1986). Terrane motion by strike-slip faulting of forearc slivers. *Geology*, *14*(9), 780-783.

Johnston, S. T. (1999). Large-scale coast-parallel displacements in the Cordillera: a granitic resolution to a paleomagnetic dilemma. *Journal of Structural Geology*, *21*(8-9), 1103-1108.

Johnston, S. T. (2008). The Cordilleran Ribbon Continent of North America. *Annual Review of Earth and Planetary Sciences*, *36*(1), 495–530. https://doi.org/10.1146/annurev.earth.36.031207.124331

Johnston, S. T., & Canil, D. (2007). Crustal architecture of SW Yukon, northern Cordillera: Implications for crustal growth in a convergent margin orogen. *Tectonics*, *26*(1).

Johnston, S. T., Jane Wynne, P., Francis, D., Hart, C. J., Enkin, R. J., & Engebretson, D. C. (1996a). Yellowstone in Yukon: the late Cretaceous Carmacks group. *Geology*, *24*(11), 997-1000.

Johnston, S. T., Mortensens, J. K., & Erdmer, P. (1996b). Igneous and metaigneous age constraints for the Aishihik metamorphic suite, southwest Yukon. *Canadian Journal of Earth Sciences*, *33*(11), 1543-1555.

Kalbas, J. L., Ridgway, K. D., & Gehrels, G. E. (2007). Stratigraphy, depositional systems, and provenance of the Lower Cretaceous Kahiltna assemblage, western Alaska Range: Basin development in response to oblique collision. In In Ridgway, K.D., Trop, J.M., Glen, J.M.G., O'Neill, J.M. (Eds.). *Special Paper 431: Tectonic Growth of a Collisional Continental Margin: Crustal Evolution of Southern Alaska* (Vol. 431, pp. 307–343). Boulder, Colorado: Geological Society of America. https://doi.org/10.1130/2007.2431(13)

Kapp, P. A., & Gehrels, G. E. (1998). Detrital zircon constraints on the tectonic evolution of the Gravina belt, southeastern Alaska. *Canadian Journal of Earth Sciences*, *35*(3), 253-268.

Lange, D., Cembrano, J., Rietbrock, A., Haberland, C., Dahm, T., & Bataille, K. (2008). First seismic record for intra-arc strike-slip tectonics along the Liquiñe-Ofqui fault zone at the obliquely convergent plate margin of the southern Andes. *Tectonophysics*, *455*(1-4), 14-24.

Layer, P. W., Hall, C. M., & York, D. (1987). The derivation of $^{40}Ar/^{39}Ar$ age spectra of single grains of hornblende and biotite by laser step-heating. *Geophysical Research Letters*, *14*(7), 757-760.

Lease, R. O., Haeussler, P. J., & O'Sullivan, P. (2016). Changing exhumation patterns during Cenozoic growth and glaciation of the Alaska Range: Insights from detrital thermochronology and geochronology. *Tectonics*, *35*(4), 934–955. https://doi.org/10.1002/2015TC004067

Lease, R.O. (2018). Pliocene erosional pulse and glacier-landscape feedbacks in the western Alaska Range. *Earth and Planetary Science Letters, 497*, 62-68, https://doi.org/10.1016/j.epsl.2018.06.009.

Light, T. D., Tripp, R. B., & King, H. D. (1990). Interpretation of reconnaissance geochemical data from the Healy quadrangle, Alaska. *US Geological Survey Bulletin 1894*.

Link, B.J. (2017). From Deposition to Deformation Within an Accretionary Suture Zone: An Example from the Clearwater and Talkeetna Mountains, Alaska Range Suture Zone (unpublished master's thesis), Purdue University, West Lafayette, Indiana.

Little, T. A. (1990). Kinematics of wrench and divergent-wrench deformation along a central part of the Border Ranges Fault System, Northern Chugach Mountains, Alaska. *Tectonics*, *9*(4), 585-611.

Lowey, G. W. (1998). A new estimate of the amount of displacement on the Denali fault system based on the occurrence of carbonate megaboulders in the Dezadeash Formation (Jura-Cretaceous), Yukon, and the Nutzotin Mountains sequence (Jura-Cretaceous), Alaska. *Bulletin of Canadian Petroleum Geology*, *46*(3), 379-386.

Lowey, G. W. (2000). The Tatshenshini shear zone (new) in southwestern Yukon, Canada: Comparison with the Coast shear zone in British Columbia and southeastern Alaska and implications regarding the Shakwak suture. *Tectonics*, *19*(3), 512–528. https://doi.org/10.1029/1999TC001119

Lowey, G. W. (2011). Volcaniclastic gravity flow deposits in the Dezadeash Formation (Jura-Cretaceous), Yukon, Canada: Implications regarding the tectonomagmatic evolution of the

Chitina arc in the northern Cordillera of North America. *Lithos*, *125*(1–2), 86–100. https://doi.org/10.1016/j.lithos.2011.01.014

Lowey, G. W. (2019). Provenance analysis of the Dezadeash Formation (Jurassic–Cretaceous), Yukon, Canada: Implications regarding a linkage between the Wrangellia composite terrane and the western margin of Laurasia. *Canadian Journal of Earth Sciences*, *56*(1), 77–100. https://doi.org/10.1139/cjes-2017-0244

Ludwig, K. R. (2008). User's manual for Isoplot 3.70. *Berkeley Geochronology Center Special Publication*, *4*, 76.

Mahoney, J. B., Gordee, S. M., Haggart, J. W., Friedman, R. M., Diakow, L. J., & Woodsworth, G. J. (2009). Magmatic evolution of the eastern Coast Plutonic Complex, Bella Coola region, west-central British Columbia. *Geological Society of America Bulletin*, *121*(9–10), 1362–1380. https://doi.org/10.1130/B26325.1

Mair, J. L., Hart, C. J., & Stephens, J. R. (2006). Deformation history of the northwestern Selwyn Basin, Yukon, Canada: Implications for orogen evolution and mid-Cretaceous magmatism. *Geological Society of America Bulletin*, *118*(3-4), 304-323.

Manselle, P., Brueseke, M. E., Trop, J. M., Benowitz, J. A., Snyder, D. C., & Hart, W. K. (2020). Geochemical and stratigraphic analysis of the Chisana Formation, Wrangellia terrane, eastern Alaska: Insights into Early Cretaceous magmatism and tectonics along the northern Cordilleran margin. *Tectonics*, e2020TC006131.

Manuszak, J. D., Ridgway, K. D., Trop, J. M., & Gehrels, G. E. (2007). Sedimentary record of the tectonic growth of a collisional continental margin: Upper Jurassic-Lower Cretaceous Nutzotin Mountains sequence, eastern Alaska Range, Alaska. In Ridgway, K.D., Trop, J.M., Glen, J.M.G., O'Neill, J.M. (Eds.). *Special Paper 431: Tectonic Growth of a Collisional Continental Margin: Crustal Evolution of Southern Alaska* (Vol. 431, pp. 345–377). Boulder, Colorado: Geological Society of America.

Matthews, W. A., Guest, B., Coutts, D., Bain, H., & Hubbard, S. (2017). Detrital zircons from the Nanaimo basin, Vancouver Island, British Columbia: An independent test of Late Cretaceous to Cenozoic northward translation. *Tectonics*, *36*(5), 854-876.

McClelland, W. C., Gehrels, G. E., & Saleeby, J. B. (1992). Upper Jurassic-Lower Cretaceous basinal strata along the Cordilleran Margin: Implications for the accretionary history of the Alexander-Wrangellia-Peninsular Terrane. *Tectonics*, *11*(4), 823–835. https://doi.org/10.1029/92TC00241

McCrory, P. A., & Wilson, D. S. (2013). A kinematic model for the formation of the Siletz-Crescent forearc terrane by capture of coherent fragments of the Farallon and Resurrection plates: *Tectonics*, *32*(3), 718–736. https://doi.org/10.1002/tect.20045

McDermott, R. G., Ault, A. K., Caine, J. S., & Thomson, S. N. (2019). Thermotectonic History of the Kluane Ranges and Evolution of the Eastern Denali Fault Zone in Southwestern Yukon, Canada. *Tectonics*, *38*(8), 2983–3010. https://doi.org/10.1029/2019TC005545

Mezger, J. E. (1999). Alpine-type'ultramafic rocks of the Kluane metamorphic assemblage, southwest Yukon: Oceanic crust fragments of a late Mesozoic back-arc basin along the northern Coast Belt. *Yukon exploration and geology*, 127-138.

Mezger, J. E. (2002). Geology of the Dezadeash Range and adjacent northern Coast Mountains (115A), southwestern Yukon: Re-examination of a terrane boundary. Yukon Exploration and Geology, 149-163.

Mezger, J. E., Chacko, T., & Erdmer, P. (2001a). Metamorphism at a late Mesozoic accretionary margin: A study from the Coast Belt of the North American Cordillera: *Journal of Metamorphic Geology*, *19*(2), 121–137. https://doi.org/10.1046/j.0263-4929.2000.00300.x

Mezger, J. E., Creaser, R. A., Erdmer, P., & Johnston, S. T. (2001b). A Cretaceous back-arc basin in the Coast Belt of the northern Canadian Cordillera: evidence from geochemical and neodymium isotope characteristics of the Kluane metamorphic assemblage, southwest Yukon. *Canadian Journal of Earth Sciences*, *38*(1), 91-103.

Milde, E. R. (2014). Using Low-Temperature Thermochronology to Constrain the Role of the Totschunda Fault in Southeastern Alaskan Tectonics. (unpublished master's thesis). Syracuse University, Syracuse, New York.

Miller, M. L., Bradley, D. C., Bundtzen, T. K., & McClelland, W. (2002). Late Cretaceous through Cenozoic Strike-Slip Tectonics of Southwestern Alaska. *The Journal of Geology*, *110*(3), 247–270. https://doi.org/10.1086/339531

Miller, M. S., O'Driscoll, L. J., Porritt, R. W., & Roeske, S. M. (2018). Multiscale crustal architecture of Alaska inferred from P receiver functions. *Lithosphere*, *10*(2), 267–278. https://doi.org/10.1130/L701.1

Miskovic, A., & Francis, D. (2003). The Early Tertiary Sifton Range volcanic complex, southwestern Yukon. *Yukon exploration and geology*, 143-155.

Monger, J. W. H., Van Der Heyden, P., Journeay, J. M., Evenchick, C. A., & Mahoney, J. B. (1994). Jurassic-Cretaceous basins along the Canadian Coast Belt: Their bearing on pre-mid-Cretaceous sinistral displacements. *Geology*, *22*(2), 175-178.

Monger, J.W.H., & Gibson, H. D. (2019). Mesozoic-Cenozoic deformation in the Canadian Cordillera: The record of a "Continental Bulldozer"? *Tectonophysics*, *757*, 153–169. https://doi.org/10.1016/j.tecto.2018.12.023

Mooney P.R. (2010). Geology of the Clearwater Mountains and Southern Boundary of the Alaska Range Suture Zone (unpublished master's thesis). University of California, Davis, California.

Moores, E. (1970). Ultramafics and orogeny, with models of the US Cordillera and the Tethys. *Nature, 228*(5274), 837-842.

Morris, G. A., & Creaser, R. A. (2003). Crustal recycling during subduction at the Eocene Cordilleran margin of North America: a petrogenetic study from the southwestern Yukon. *Canadian Journal of Earth Sciences*, *40*(12), 1805-1821.

Morrison, G. W., Godwin, C. I., & Armstrong, R. L. (1979). Interpretation of isotopic ages and 87Sr/86Sr initial ratios for plutonic rocks in the Whitehorse map area, Yukon. *Canadian Journal of Earth Sciences*, *16*(10), 1988-1997.

Murphy, D. C. (2018). Latest Cretaceous–early Eocene Pacific-Arctic?-Atlantic connection: Co-evolution of strike-slip fault systems, oroclines, and transverse fold-and-thrust belts in the northwestern North American Cordillera. In K. Piepjohn, J. V. Strauss, L. Reinhardt, & W. C. McClelland (Eds.). *Special Paper 541 Circum-Arctic Structural Events: Tectonic Evolution of the Arctic Margins and Trans-Arctic Links with Adjacent Orogens*. Boulder, Colorado: Geological Society of America. https://doi.org/10.1130/2018.2541(28)

Nelson, J., & Colpron, M. (2007). Tectonics and metallogeny of the British Columbia, Yukon and Alaskan Cordillera, 1.8 Ga to the present. Mineral deposits of Canada: a synthesis of major deposit-types, district metallogeny, the evolution of geological provinces, and exploration methods: *Geological Association of Canada, Mineral Deposits Division, Special Publication, 5*, pp. 755-791.

Nokleberg, W. J., Jones, D. L., & Silberling, N. J. (1985). Origin and tectonic evolution of the Maclaren and Wrangellia terranes, eastern Alaska Range, Alaska. *Geological Society of America Bulletin*, *96*(10), 1251-1270.

Nokleberg, W.J. Aleinikoff, J.N., Dutro, J.T., Jr. Lanphere, M.A. Silberling, N.J., Silva, S.R., Smith, T.E., & Turner, D.L. (1992b). Map, tables, and summary of fossil and isotopic age data, Mount Hayes quadrangle, eastern Alaska Range, Alaska. *U.S. Geological Survey Miscellaneous Field Studies map 1996-D*, 43 p., 1 sheet, scale 1:250,000.

Nokleberg, W.J. and Richter, D.H. (2007). Origin of narrow terranes and adjacent major terranes occurring along the Denali fault in the Eastern and Central Alaska Range, Alaska. In Ridgway, K.D., Trop, J.M., Glen, J.M.G., O'Neill, J.M. (Eds.). *Special Paper 431: Tectonic Growth of a Collisional Continental Margin: Crustal Evolution of Southern Alaska: (*Vol. 431, pp. 129-154.). Boulder, Colorado, Geological Society of America.

Nokleberg, W.J., Aleinikoff, J.N., Lange, I.M., Silva, S.R., Miyaoka, R.T., Schwab, C.E., & Zehner, R.E. (1992a). Preliminary geologic map of the Mount Hayes quadrangle, eastern Alaska Range, Alaska. *U.S. Geological Survey Open File Report 92-594*, 39p., 1 sheet, scale 1:250,000.

O'Driscoll, L. J., & Miller, M. S. (2015). Lithospheric discontinuity structure in Alaska, thickness variations determined by *Sp* receiver functions. *Tectonics*, *34*(4), 694–714. https://doi.org/10.1002/2014TC003669

O'Neill, J. M., Ridgway, K. D., & Eastham, K. R. (2001). Mesozoic Sedimentation and Deformation Along the Talkeetna Thrust Fault, South-Central Alaska—New Insights and Their Regional Tectonic Significance. 10. *U.S. Geological Survey Professional Paper 1678*.

Otiniano, G. A., Porter, T. J., Benowitz, J. A., Bindeman, I. N., Froese, D. G., Jensen, B. J., ... & Phillips, M. A. A late Miocene to late Pleistocene reconstruction of precipitation isotopes and climate from hydrated volcanic glass shards and biomarkers in central Alaska and Yukon. *Paleoceanography and Paleoclimatology*, e2019PA003791.

Parrish, R. R., Carr, S. D., & Parkinson, D. L. (1988). Eocene extensional tectonics and geochronology of the southern Omineca Belt, British Columbia and Washington. *Tectonics*, *7*(2), 181-212.

Pavlis, T. L., Amato, J. M., Trop, J. M., Ridgway, K. D., Roeske, S. M., & Gehrels, G. E. (2019). Subduction polarity in ancient arcs: A call to integrate geology and geophysics to decipher the Mesozoic tectonic history of the Northern Cordillera of North America. *GSA Today*, *29*(11).

Pavlis, T. L., Chapman, J. B., Bruhn, R. L., Ridgway, K., Worthington, L. L., Gulick, S. P., & Spotila, J. (2012). Structure of the actively deforming fold-thrust belt of the St. Elias orogen with implications for glacial exhumation and three-dimensional tectonic processes. *Geosphere*, *8*(5), 991-1019.

Pecha, M. E., Gehrels, G. E., McClelland, W. C., Giesler, D., White, C., & Yokelson, I. (2016). Detrital zircon U-Pb geochronology and Hf isotope geochemistry of the Yukon-Tanana terrane, Coast Mountains, southeast Alaska. *Geosphere*, *12*(5), 1556-1574.

Piercey, S. J., & Colpron, M. (2009). Composition and provenance of the Snowcap assemblage, basement to the Yukon-Tanana terrane, northern Cordillera: Implications for Cordilleran crustal growth. *Geosphere*, *5*(5), 439-464.

Piercey, S. J., Mortensen, J. K., & Creaser, R. A. (2003). Neodymium isotope geochemistry of felsic volcanic and intrusive rocks from the Yukon–Tanana Terrane in the Finlayson Lake Region, Yukon, Canada. *Canadian Journal of Earth Sciences*, *40*(1), 77-97.

Preece, S. J., & Hart, W. K. (2004). Geochemical variations in the< 5 Ma Wrangell Volcanic Field, Alaska: implications for the magmatic and tectonic development of a complex continental arc system. *Tectonophysics*, *392*(1-4), 165-191.

Rasendra, N., Bonnin, M., Mazzotti, S., & Tiberi, C. (2014). Crustal and Upper-Mantle Anisotropy Related to Fossilized Transpression Fabric along the Denali Fault, Northern Canadian Cordillera. *Bulletin of the Seismological Society of America*, *104*(4), 1964–1975. https://doi.org/10.1785/0120130233

Ratchkovski, N. A., Wiemer, S., & Hansen, R. A. (2004). Seismotectonics of the central Denali fault, Alaska, and the 2002 Denali fault earthquake sequence. *Bulletin of the Seismological Society of America*, *94*(6B), S156-S174.

Regan, S. P., Benowitz, J. A., & Holland, M. E. (2020). A plutonic brother from another magma mother: Disproving the Eocene Foraker-McGonagall pluton piercing point and implications for long-term slip on the Denali Fault. *Terra Nova*, *32*(1), 66–74. https://doi.org/10.1111/ter.12437

Regan, S., Benowitz, J.B., Waldien, T.S., Holland, M., Roeske, S.M., O'Sullivan. P.B., and Layer, P. Tectonic social distancing: strained long distance plutonic relationships along the Denali fault: *Submitted to Geology*

Renne, P. R., Deino, A. L., Walter, R. C., Turrin, B. D., Swisher III, C. C., Becker, T. A., ... & Jaouni, A. R. (1994). Intercalibration of astronomical and radioisotopic time. *Geology*, *22*(9), 783-786.

Renne, P. R., Mundil, R., Balco, G., Min, K., & Ludwig, K. R. (2010). Joint determination of $^{40}K$ decay constants and $^{40}Ar^*/^{40}K$ for the Fish Canyon sanidine standard, and improved accuracy for $^{40}Ar/^{39}Ar$ geochronology. *Geochimica et Cosmochimica Acta*, *74*(18), 5349-5367.

Riccio, S. J., Fitzgerald, P. G., Benowitz, J. A., & Roeske, S. M. (2014). The role of thrust faulting in the formation of the eastern Alaska Range: Thermochronological constraints from the Susitna Glacier Thrust Fault region of the intracontinental strike-slip Denali Fault system: Susitna Glacier thrust fault. *Tectonics*, *33*(11), 2195–2217. https://doi.org/10.1002/2014TC003646

Richter, D.H. & Dutro, J.T., Jr. (1975). Revision of the type Mankommen Formation (Pennsylvanian and Permian), Eagle Creek area, eastern Alaska Range, Alaska. *U.S. Geological Survey Bulletin 1395–B*, p. B1–B25.

Ridgway, K. D., Thoms, E. E., Layer, P. W., Lesh, M. E., White, J. M., & Smith, S. V. (2007). Neogene transpressional foreland basin development on the north side of the central Alaska Range, Usibelli Group and Nenana Gravel, Tanana basin. In Ridgway, K.D., Trop, J.M., Glen, J.M.G., O'Neill, J.M. (Eds.). *Special Paper 431: Tectonic Growth of a Collisional Continental Margin: Crustal Evolution of Southern Alaska* (Vol. 431, pp. 507–547). Boulder, Colorado: Geological Society of America. https://doi.org/10.1130/2007.2431(20)

Ridgway, K. D., Trop, J. M., Nokleberg, W. J., Davidson, C. M., & Eastham, K. R. (2002). Mesozoic and Cenozoic tectonics of the eastern and central Alaska Range: Progressive basin development and deformation in a suture zone. *Geological Society of America Bulletin, 114*(12), 1480-1504.

Rioux, M., Hacker, B., Mattinson, J., Kelemen, P., Blusztajn, J., & Gehrels, G. (2007). Magmatic development of an intra-oceanic arc: High-precision U-Pb zircon and whole-rock isotopic analyses from the accreted Talkeetna arc, south-central Alaska. *Geological Society of America Bulletin*, *119*(9-10), 1168-1184.

Roeske, S. M., Mattinson, J. M., & Armstrong, R. L. (1989). Isotopic ages of glaucophane schists on the Kodiak Islands, southern Alaska, and their implications for the Mesozoic tectonic history of the Border Ranges fault system. *Geological Society of America Bulletin*, *101*(8), 1021-1037.

Roeske, S. M., Snee, L. W., Pavlis, T. L., & Sisson, V. B. (2003). Dextral-slip reactivation of an arc-forearc boundary during Late Cretaceous-early Eocene oblique convergence in the northern Cordillera. In Sisson, V.B., Roeske, S.M., Pavlis, T.L. (Eds.). *Special Paper 371: Geology of a Transpressional Orogen Developed during Ridge-Trench interaction along the North Pacific Margin* (Vol. 371, pp. 141–169). Boulder, Colorado: Geological Society of America.

Romero, M. C., Ridgway, K. D., & Gehrels, G. E. (2020). Geology, U-Pb Geochronology, and Hf Isotope Geochemistry Across the Mesozoic Alaska Range Suture Zone (South-Central Alaska): Implications for Cordilleran Collisional Processes and Tectonic Growth of North America. *Tectonics*, *39*(3). https://doi.org/10.1029/2019TC005946.

Rusmore, M. E., Bogue, S. W., & Woodsworth, G. J. (2013). Paleogeography of the insular and intermontane terranes reconsidered: Evidence from the southern Coast Mountains Batholith, British Columbia. *Lithosphere*, *5*(5), 521-536.

Ryan, J.J., Hayward, N., & Jackson, L. E. (2017). Landscape antiquity and Cenozoic drainage development of southern Yukon, through restoration modeling of the Tintina Fault. *Canadian Journal of Earth Sciences*, *54*(10), 1085–1100. https://doi.org/10.1139/cjes-2017-0053

Sack, P. J., Colpron, M., Crowley, J. L., Ryan, J. J., Allan, M. M., Beranek, L. P., & Joyce, N. L. (2020) *Atlas of Late Triassic to Jurassic plutons in the Intermontane terranes of Yukon*. 378.

Saltus, R. W., & Hudson, T. L. (2007). Regional magnetic anomalies, crustal strength, and the location of the northern Cordilleran fold-and-thrust belt. *Geology*, *35*(6), 567-570.

Saltus, R. W., Hudson, T. L., & Wilson, F. H. (2007). The geophysical character of southern Alaska—Implications for crustal evolution. In Ridgway, K.D., Trop, J.M., Glen, J.M.G., O'Neill, J.M. (Eds.). *Special Paper 431: Tectonic Growth of a Collisional Continental Margin: Crustal Evolution of Southern Alaska* (Vol. 431, pp. 1–20). Boulder, Colorado: Geological Society of America. https://doi.org/10.1130/2007.2431(01)

Samson, S. D., & Alexander Jr, E. C. (1987). Calibration of the interlaboratory $^{40}Ar/^{39}Ar$ dating standard, MMhb-1. *Chemical Geology: Isotope Geoscience section*, *66*(1-2), 27-34.
Sauer, K. B., Gordon, S. M., Miller, R. B., Jacobson, C. E., Grove, M., Vervoort, J. D., & Fisher, C. M. (2019). Deep-crustal metasedimentary rocks support Late Cretaceous "Mojave-BC" translation. *Geology*, *47*(2), 99-102.
Saylor, J. E., & Sundell, K. E. (2016). Quantifying comparison of large detrital geochronology data sets. *Geosphere*, *12*(1), 203-220.
Saylor, J. E., Jordan, J. C., Sundell, K. E., Wang, X., Wang, S., & Deng, T. (2018). Topographic growth of the Jishi Shan and its impact on basin and hydrology evolution, NE Tibetan Plateau. *Basin Research*, *30*(3), 544-563.
Sigloch, K., & Mihalynuk, M. G. (2017). Mantle and geological evidence for a Late Jurassic–Cretaceous suture spanning North America. *GSA Bulletin*, *129*(11-12), 1489-1520.
Smith, T.E. (1981). Geology of the Clearwater Mountains, south-central Alaska. *Alaska Division of Geological & Geophysical Surveys Geologic Report 60*, 72 p., 3 sheets, scale 1:63,360. doi:10.14509/406
St. Amand, P. (1957). Geological and geophysical synthesis of the tectonics of portions of British Columbia, the Yukon Territory, and Alaska. *Geological Society of America Bulletin, 68*(10), 1343-1370.
Stamatakos, J. A., Trop, J. M., & Ridgway, K. D. (2001). Late Cretaceous paleogeography of Wrangellia: paleomagnetism of the MacColl Ridge Formation, southern Alaska, revisited. *Geology*, *29*(10), 947-950.
Stanley, B. (2012). Structural geology and geochronology of the Kluane schist, southwestern Yukon Territory. (unpublished master's thesis). University of Waterloo, Waterloo, Ontario.
Stout, J.H. (1965). Bedrock geology between Rainy Creek and the Denali fault, Eastern Alaska Range, Alaska (unpublished master's thesis). University of Alaska, Fairbanks, Alaska.
Tempelman-Kluit, D. J., & Wanless, R. K. (1975). Potassium–argon age determinations of metamorphic and plutonic rocks in the Yukon Crystalline Terrane. *Canadian Journal of Earth Sciences*, *12*(11), 1895-1909.
Terhune, P.J., Benowitz, J.A., Waldien, T.S., Allen, W.K., Davis, K.N., Ridgway, K.D., Roeske, S.M., Fitzgerald, P.G., Brueseke, M.E., O'sullivan, P.B. (2015). Geochronological framework for the Cenozoic history of the southern Alaska Range fold and thrust belt: *Geological Society of America Abstracts with Programs, 47*(4), p. 60.
Till, A.B, Roeske, S.M., Bradley, D.C., Friedman, R., Layer, P.W. (2007). Early Tertiary transtension-related deformation and magmatism along the Tintina fault system, Alaska, In Till, A.B., Roeske, S.M., Sample, J.C., and Foster, D.A. (Eds.). *Special Paper 434 Exhumation Associated with Continental Strike-Slip Fault Systems: Geological Society of America.* (Vol. 434, pp. 233–264). doi: 10.1130/2007.2434(11).
Trop, J. M., & Ridgway, K. D. (2007). Mesozoic and Cenozoic tectonic growth of southern Alaska: A sedimentary basin perspective. In Ridgway, K.D., Trop, J.M., Glen, J.M.G., O'Neill, J.M. (Eds.). *Special Paper 431: Tectonic Growth of a Collisional Continental Margin: Crustal Evolution of Southern Alaska* (Vol. 431, pp. 55–94). Boulder, Colorado: Geological Society of America. https://doi.org/10.1130/2007.2431(04)
Trop, J. M., Benowitz, J. A., Koepp, D. Q., Sunderlin, D., Brueseke, M. E., Layer, P. W., & Fitzgerald, P. G. (2020). Stitch in the ditch: Nutzotin Mountains (Alaska) fluvial strata and a dike record ca. 117–114 Ma accretion of Wrangellia with western North America and initiation of the Totschunda fault. *Geosphere*, *16*(1), 82–110. https://doi.org/10.1130/GES02127.1
Trop, J. M., Benowitz, J., Cole, R. B., & O'Sullivan, P. (2019). Cretaceous to Miocene magmatism, sedimentation, and exhumation within the Alaska Range suture zone: A polyphase reactivated terrane boundary. *Geosphere*, *15*(4), 1066–1101. https://doi.org/10.1130/GES02014.1
Turner, D.L., and Smith, T.E. (1974). Geochronology and generalized geology of the central Alaska Range, Clearwater Mountains, and northern Talkeetna Mountains. *Alaska Division of Geological*

*& Geophysical Surveys Alaska Open-File Report 72*, 13 p., 1 sheet, scale 1:250,000. http://doi.org/10.14509/167

Twelker, E., Waldien, T.S., Newberry, R.J., Freeman, L.K., Sicard, K.R., Lande, L.L., Wypych, A., Reioux, D.A., and Bachmann, E.N. (2020). Bedrock geologic map of the eastern Denali Highway area, Mount Hayes, Healy, and Talkeetna Mountains quadrangles, Alaska. *Alaska Division of Geological & Geophysical Surveys Report of Investigation 2020-7*: 1 sheet, 1:100,000 scale. http://doi.org/10.14509/30469

Vallage, A., Devès, M. H., Klinger, Y., King, G. C. P., & Ruppert, N. A. (2014). Localized slip and distributed deformation in oblique settings: The example of the Denali fault system, Alaska. *Geophysical Journal International*, *197*(3), 1284–1298. https://doi.org/10.1093/gji/ggu100

Vermeesch, P. (2004). How many grains are needed for a provenance study?. *Earth and Planetary Science Letters*, *224*(3-4), 441-451.

Vermeesch, P. (2012). On the visualisation of detrital age distributions. *Chemical Geology*, *312*, 190-194.

Vice, L. (2017) Late Cretaceous to Paleocene evolution of the Blanchard River assemblage, southwest Yukon; implications for Mesozoic accretionary processes in the northwestern Cordillera (unpublished master's thesis). Simon Fraser University, Burnaby, British Columbia.

Wahrhaftig, C., Turner, D. L., Weber, F. R., & Smith, T. E. (1975). Nature and timing of movement on Hines Creek strand of Denali fault system, Alaska. *Geology*, *3*(8), 463-466.

Waldien, T. S., Roeske, S. M., Benowitz, J. A., Allen, W. K., Ridgway, K. D., & O'Sullivan, P. B. (2018). Late Miocene to Quaternary evolution of the McCallum Creek thrust system, Alaska: Insights for range-boundary thrusts in transpressional orogens. *Geosphere*, *14*(6), 2379–2406. https://doi.org/10.1130/GES01676.1

Waldien, T.S., Roeske, S.M., Benowitz, J.A., Twelker, E., & Miller, M.S. (2021). Oligocene-Neogene reactivation of Mesozoic lithospheric-scale terrane accretionary structures in the Alaska Range suture zone, southern Alaska, USA: Geological Society of America Bulletin, v. 133 (3-4), p. 691-716.

Wallace, W. K., Hanks, C. L., & Rogers, J. F. (1989). The southern Kahiltna terrane: Implications for the tectonic evolution of southwestern Alaska. *Geological Society of America Bulletin, 101*(11), 1389-1407.

Wilson, F.H., Dover, J.H., Bradley, D.C., Weber, F.R., Bundtzen, T.K., and Haeussler, P.J. (1998). Geologic map of Central (interior) Alaska. *U.S. Geological Survey Open-File Report 98-133-A*, 62 p., 3 sheets.

Wilson, F.H., Hults, C.P., Mull, C.G., and Karl, S.M. (2015). Geologic map of Alaska. *U.S. Geological Survey Scientific Investigations Map 3340*, 196 p., 2 sheets, scale 1:1,584,000, https://alaska.usgs.gov/science/geology/state_map/interactive_map/AKgeologic_map.html.

Wyld, S. J., Umhoefer, P. J., & Wright, J. E. (2006). Reconstructing northern Cordilleran terranes along known Cretaceous and Cenozoic strike-slip faults: Implications for the Baja British Columbia hypothesis and other models. In J.W. Haggart, R.J. Enkin, J.W.H. Monger (Eds.). *Paleogeography of the North American Cordillera: Evidence for and against large-scale displacements*. (Geological Association of Canada Special Paper 46 pp. 277-298). St. Johns, Newfoundland: Geological Association of Canada.

Yokelson, I., Gehrels, G. E., Pecha, M., Giesler, D., White, C., & McClelland, W. C. (2015). U-Pb and Hf isotope analysis of detrital zircons from Mesozoic strata of the Gravina belt, southeast Alaska: *Tectonics*, *34*(10), 2052–2066. https://doi.org/10.1002/2015TC003955

York, D., Hall, C. M., Yanase, Y., Hanes, J. A., & Kenyon, W. J. (1981). $^{40}Ar/^{39}Ar$ dating of terrestrial minerals with a continuous laser. *Geophysical Research Letters*, *8*(11), 1136-1138.

Yukon Geological Survey. (2020, May 15). Yukon Geochronology – A database of Yukon isotopic age determinations. Retrieved from http://data.geology.gov.yk.ca/Compilation/22.

## SUPPLEMENTS

### Supplemental information SI 1: Zircon U-Pb and Lu-Hf methods

### Sample preparation and zircon extraction at UC Davis:

Sample preparation for zircon extraction at UC Davis involves: 1) washing the sample with soap and warm water, 2) crushing the rock with a combination of a hydraulic press (if needed), mortar/pestle, and Bico Pulverizer, 3) sieving to the preferred size fraction (generally <250 um for detrital zircon samples, 63-125 um for igneous zircon samples), 4) heavy mineral concentration by decanting and panning, 5) magnetic separation using a Frantz isodynamic separater, 6) density separation with Lithium Polytungstate. These steps usually result in a sufficiently pure zircon separate. However, additional steps are sometimes required to further concentrate zircon. These steps include: 7) additional panning, 8) density separation with Methylene Iodide, 9) acid wash to dissolve pyrite. Once the mineral separate is sufficiently pure, zircon grains are mounted by pouring the detrital the zircon concentrate onto sticky tape or by picking for igneous zircon analysis.

### Mounting:

Once the desired zircon separate is obtained, we mount the zircons in epoxy. This involves pressing double-sided sticky tape on a flat glass plate and placing (or pouring) the zircon grains and reference materials on the tape. Once grains are mounted, we submerge them en epoxy, which is contained by a 1” diameter plastic cylinder. After curing, the epoxy cylinder is removed from the sticky tape and ground/polished until the zircon grains are exposed. In contrast to a typical grain mount wherein the crystal interiors are exposed, we grind the mount until the crystals are barely exposed. This approach allows us to, in some cases, analyze the age

of the exterior of the crystal in addition to the core via depth profiling (described in more detail in the data reduction section) and retain imaging capabilities.

**Imaging:**

We image all zircon grains and standards prior to analysis by LA-ICP-MS. Our imaging protocol makes use of the Cameca SX-100 electron microprobe housed in the Earth and Planetary Sciences department at UC Davis. We image the zircon grains using the 'high-gain' electron beam setting on the Cameca SX-100. By adjusting the brightness and contrast of the backscattered electron (BSE) image, the high gain beam reveals internal zoning structure of the zircon grains. Increasing the scan rate on these BSE images yields a high-resolution greyscale image of the zircon crystal and its internal zoning structure. For igneous or metamorphic zircon analyses, we image each individual crystal and use the high-resolution BSE images to choose our laser spots prior to analysis. We also use the Cameca SX-100 to measure the width of metamorphic growth rims, which helps us determine whether or not it will yield a reliable U-Pb date. For detrital analyses, we use the high-gain beam with a moderate scan rate. This approach still displays zoning features of the zircon grain interior, but at a decreased resolution, which allows imaging of an entire detrital mount in a reasonable timeframe (generally less than 1.5 hr). We image the detrital grain mounts using the 'Video map' feature of the Cameca SX-100. This feature images user-designated domains of the mount in series and then stiches the images together into a rasterized image of the entire grain mount. The end result is a moderate resolution, high contrast image of all grains on the 1" epoxy round. We print all zircon images for igneous, metamorphic, and detrital analyses prior to LA-ICP-MS analysis and mark the printed images during the laser session.

**U-Pb zircon data collection with the LA-Q-ICP-MS at UC Davis:**

U-Pb geochronology of zircon is conducted by laser ablation quadrupole inductively coupled plasma mass spectrometry (LA-Q-ICP-MS) at UC Davis. The analyses involve ablation of zircon with a Photon Machines Analyte G2 excimer laser equipped with HelEx ablation cell using a spot diameter of 25 microns. The ablated material is carried in helium into the plasma source of an Agilent 7700 Series Q-ICP-MS, which sequences rapidly through masses corresponding to U, Th, Pb, and Hg isotopes. Dwell times for each of these masses are listed in Table S1.2.

Instrument settings on the LA-Q-ICP-MS system at UC Davis are based on a published calibration using nearly identical equipment (Matthews and Guest, 2017). Matthews and Guest (2017) used optical profilometry to measure a pit depth of ~12 um using the laser settings listed in Table S1.2. Since we used the instrument settings published by Matthews and Guest (2017), we infer that the analyses performed at UC Davis result in a laser pit depth of ~12 um. Uranium sensitivity with these settings is approximately ~230 cps/ppm, which we approximate using the NIST 610 glass. Each analysis consists of 10 sec on peaks with the laser off (for backgrounds) and 10 sec with the laser firing (for peak intensities),

Table SI1.1: Instrument settings and data processing at UC Davis

| **Laboratory & Sample Preparation** | |
|---|---|
| Laboratory name | Dept. of Earth and Planetary Sciences, UC Davis |
| Sample type/mineral | Zircon U-Pb detrital and igneous |
| Sample preparation | Conventional mineral separation, 1 inch resin mount, 1μm polish to finish |
| Imaging | BSE images Cameca SX-100 electron microprobe |

| **Laser ablation system** | |
|---|---|
| Make, Model & type | Photon Machines Analyte G2 Excimer Laser |
| Ablation cell & volume | HelEx ablation cell |
| Laser wavelength (nm) | 193 nm |
| Pulse width (ns) | ~8 ns |
| Fluence ($J.cm^{-2}$) | 1.88 $J.cm^{-2}$ |
| Repetition rate (Hz) | 10 Hz |
| Ablation duration (secs) | 10 s |
| Ablation pit depth / ablation rate | ~10μm pit depth, inferred from Mathews and Guest (2017). |
| Spot diameter (μm) nominal/actual | 25 μm / ~30 μm, square aperture |
| Sampling mode / pattern | Static spot ablation |
| Carrier gas | Helium |
| Cell carrier gas flow (l/min) | 0.75 |
| **ICP-MS Instrument** | |
| Make, Model & type | Agilent 7700 series Q-ICP-MS |
| Sample introduction | Ablation aerosol |
| RF power (W) | 1350W |
| Make-up gas flow (l/min) | 1.1 |
| Detection system | Electron Multiplier |
| Masses measured | 91, 201, 202, 204, 206 207, 235, 238 |
| Integration time per peak/dwell times (s); quadrupole settling time between mass jumps | 0.01, 0.01, 0.01, 0.03, 0.04, 0.07,<br>0.015, 0.015, 0.02 s. In order of masses listed above. |
| Total integration | 0.239 s |
| 'Sensitivity' as useful yield | ~230 cps/ppm U<br>Estimated on NIST 610 glass |
| IC Dead time (ns) | |
| **Data Processing** | |
| Gas blank | 15 second on-peak zero subtracted |
| Calibration strategy | FC-1 used as primary reference material, R-33 used as secondary/validation |

| | |
|---|---|
| Reference Material info | FC-1 (Paces and Miller, 1993; Schmitz et al., 2003)<br>R-33 (Black et al. 2004) |
| Data processing package used / Correction for LIEF | Iolite-Igor data reduction scheme based on methods of Patton et al, (2010) and Petrus and Kamber (2012). Laser-Induced Elemental Fractionation correction assumes reference material and samples behave identically. |
| Mass discrimination | $^{206}Pb/^{238}U$ additionally normalized to reference material |
| Common-Pb correction, composition and uncertainty | No common-Pb correction applied to the data. |
| Uncertainty level & propagation | Ages are quoted at 2*s* absolute, propagation is by quadratic addition. Reproducibility and age uncertainty of reference material are propagated where appropriate. |
| Quality control / Validation | FC-1 and R-33 natural zircon reference materials |
| **Other information** | |

**U-Pb data reduction methods at UC Davis:**

Data from the Q-ICP-MS are imported into Igor Pro-Iolite and displayed as a time series. Integration periods for gas blanks (backgrounds), standards, and unknowns are selected manually. FC-1 (Paces and Miller, 1993; Schmitz et al., 2003) is used as the primary reference material and R-33 (Black et al., 2004) is used as a secondary reference. Estimates of elemental concentrations, and thus U/Th, are also determined using FC-1. Isotope ratios, dates, and associated uncertainties are calculated from the integrations using the *U_Pb_geochronology3* data reduction scheme (Paton et al., 2010). After initial dates are calculated, we use the *Live Concordia* feature of the *VizualAge* data reduction scheme (Petrus and Kamber, 2012) to screen each integration period for discordance related to inclusions and/or mixed age domains (e.g., a spurious date resulting from ablating through a younger rim into an older core). If an analysis is found to be discordant apparently related to the aforementioned causes, we conservatively adjust the integration interval to obtain the most reliable date at reasonable uncertainty. Additionally,

screening the analyses in this way allows us to determine if the zircon crystal has zones of different ages (e.g. a growth rim). If the zircon is zoned, we select integration periods for each age domain. This allows us to salvage what would otherwise be a discordant analysis resulting from mixed age domains and yields instead separate ages for the core and rim of the crystal. Once integration periods are adjusted, we export the data, 2s internal and external uncertainties, and elemental concentrations. We report our data using the data table template suggested by Horstwood et al. (2016), which may be found at www.Plasmage.org.

It is important to convey that the Agilent 7700 Q-ICP-MS at UC Davis is not currently equipped with a Hg trap in the carrier gas line. This results in generally high background $^{204}$Hg. Although we monitor mass 204 (Hg + Pb) during analysis sessions, the elevated background 204 signal precludes determination of meaningful $^{204}$Pb/$^{206}$Pb ratios. Thus, we do not apply any common Pb correction to the data. However, we do consider the 204 signal during integration periods. If the 204 signal is elevated above background levels during ablation of a zircon, it is likely indicating the presence of $^{204}$Pb. Due to the assumptions and high level of uncertainty that would be introduced by attempting to do a common Pb correction on such analyses, we reject analyses on grains that display elevated 204 relative to the background gas blank. Such rejections are uncommon.

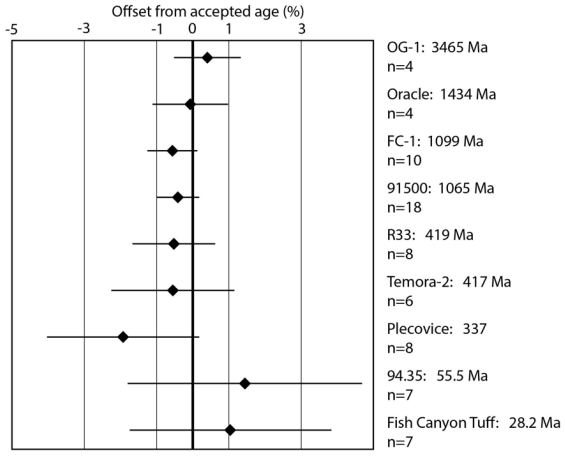

**Figure S1.1 (Previous page):** Calibration of zircon reference materials ranging from 28.2 to 3465 Ma using the LA-Q-ICP-MS at UC Davis. All analyses were performed using the ablation settings described above. Each diamond represents multiple analyses on multiple grains (n=number of analyses) during a single session.

**Data filtering methods:**

We parsed the single grain dates from both labs using Tera-Wasserburg concordia diagrams, U/Th ratios, and zoning patterns.

≤900 Ma detrital grain dates are used in KDE plots if the $^{206}Pb/^{238}U$ date has an uncertainty (2s internal) of <10% and <u>either</u> of the following criteria are met:

1. The 2s internal uncertainty ellipse intersects the concordia curve on a Tera-Wasserburg diagram, allowing the concordia curve to account for decay constant uncertainties.
2. The date is discordant, but the $^{207}Pb/^{206}Pb$ date is <3 times the $^{206}Pb/^{238}U$ date.

≥900 Ma detrital grain dates are used in KDE plots if <u>both</u> of the following criteria are met:

1. The date is <5% reverse discordant
2. The date is <20% normally discordant

Dates are interpreted to record post-depositional metamorphic recrystallization if the grain was recovered from a metamorphic rock that experienced appropriate temperatures to recrystallize zircon (estimated petrographically using mineral assemblages) and <u>one or more</u> of the following criteria are met:

1. The date overlaps with the known age of cross cutting intrusive rocks within the map unit.
2. The dated grain, or region of the grain, lacks internal zoning, which is suggestive of metamorphic recrystallization (Hoskin and Schaltegger, 2003).
3. The analysis targeted an overgrowth rim identified in BSE images, or was interpreted as an overgrowth rim based on laser depth profiling.
4. The U/Th ratio of the analysis is elevated (>10) and/or high dispersion is present within the population of dates.

Dates (as part of a population) are used to calculate metamorphic or igneous ages if all of the following criteria are met:

1. The 2s internal uncertainty ellipse intersects the concordia curve on a Tera-Wasserburg diagram, allowing the concordia curve to account for decay constant uncertainties.
2. The $^{206}Pb/^{238}U$ date has <10% uncertainty (2s internal) (For igneous analyses only).
3. Isoplot does not reject the date during the weighted mean calculation.

For populations of igneous or metamorphic grain dates, ages are calculated using the weighted mean function in Isoplot (Ludwig, 2008). Following the protocol of Horstwood et al. (2016), only 2s internal uncertainties are used in the weighted mean calculation and systematic uncertainties are added quadratically to the internal uncertainty after the weighted mean is calculated. Uncertainties on igneous or metamorphic ages reported in the main text include both internal (included in weighted mean calculation) and systematic (added on after weighted mean calculation) unless otherwise indicated.

Maximum depositional ages are estimated to be the mean age of the youngest statistical population of detrital dates (Herriott et al., 2019).

**U-Pb data parsing for Maclaren schist samples:**

Zircon age spectra from samples of the Maclaren schist display a mix of detrital grains and detrital grains with post-depositional metamorphic grains. This supplement contains plots that we used to parse the detrital grains from the post-depositional metamorphic grains and representative images of zircon grains that we interpret as containing a metamorphic overgrowth on a detrital core.

Plots for each sample-

A- Probability density plots (PDP) of the young age populations. The bold black curve is the PDP of all the data in the young age range. We used the "unmixing" function in the Density Plotter program (Vermeesch, 2012) to deconvolve the bulk dataset into age component populations (vertical lines centered on bell curves). Bell curves representing each constituent age population are plotted at 5% uncertainty and scaled vertically to the area equal to their proportion of the bulk PDP. Ages, uncertainties, and proportions for each constituent age population are given atop the vertical lines. Pink bell curves are interpreted as metamorphic populations and hollow black bell curves are interpreted as detrital.

B- U/Th vs. age graph

C- [U] (concentration in ppm) vs. age graph

B/C- Red squares are rim analyses and black dots are analyses either from cores or uniform age grains. The cutoff between metamorphic and detrital grains (red vertical line) is interpreted on the basis of dispersion in U/Th and [U], the ages of rim analyses, and component population clustering.

**Criteria for choosing cutoffs between detrital and post-depositional metamorphism-**

The cutoff between detrital and post-depositional metamorphic zircon grains is determined by considering together the U/Th, [U], and deconvolved age populations. Although high U/Th and elevated [U] are generally considered hallmarks of zircon recrystallized in the solid state, zircon recrystallized in the presence of anatectic or igneous melts may not display such geochemical characteristics (Hoskin and Schaltegger, 2003). Moreover, because the Maclaren schist displays evidence for both partial melting of the sediment and protracted igneous intrusion ranging from ca. 80-50 Ma (Link, 2017 and this study), we view it as unlikely that all neo-formed metamorphic zircon in the Maclaren schist will display elevated U/Th or anomalously high [U]. Instead, we argue that *dispersion* in these geochemical parameters, the rim ages, and data clustering used together are the best metrics for identifying the cutoff between detrital and post-depositional metamorphic zircon. Accordingly, in the plots that follow we interpretted the cutoff (vertical red line) at locations- 1) between dispersed and undispersed U/Th and/or [U], 2) older than the oldest rim analyses determined from laser depth profiling, and 3) between component age populations.

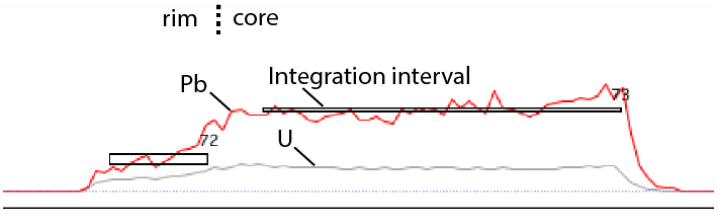


**Figure S1.2:** Example of a time-series recording ablation through a zircon crystal with age zoning. The red curve represents Pb counts measured by the mass spectrometer and the grey curve represents U counts. The Pb and U curves are not plotted on the same vertical scale. Integration intervals (black boxes) #72 and #73 correspond to ages of 87.3 Ma

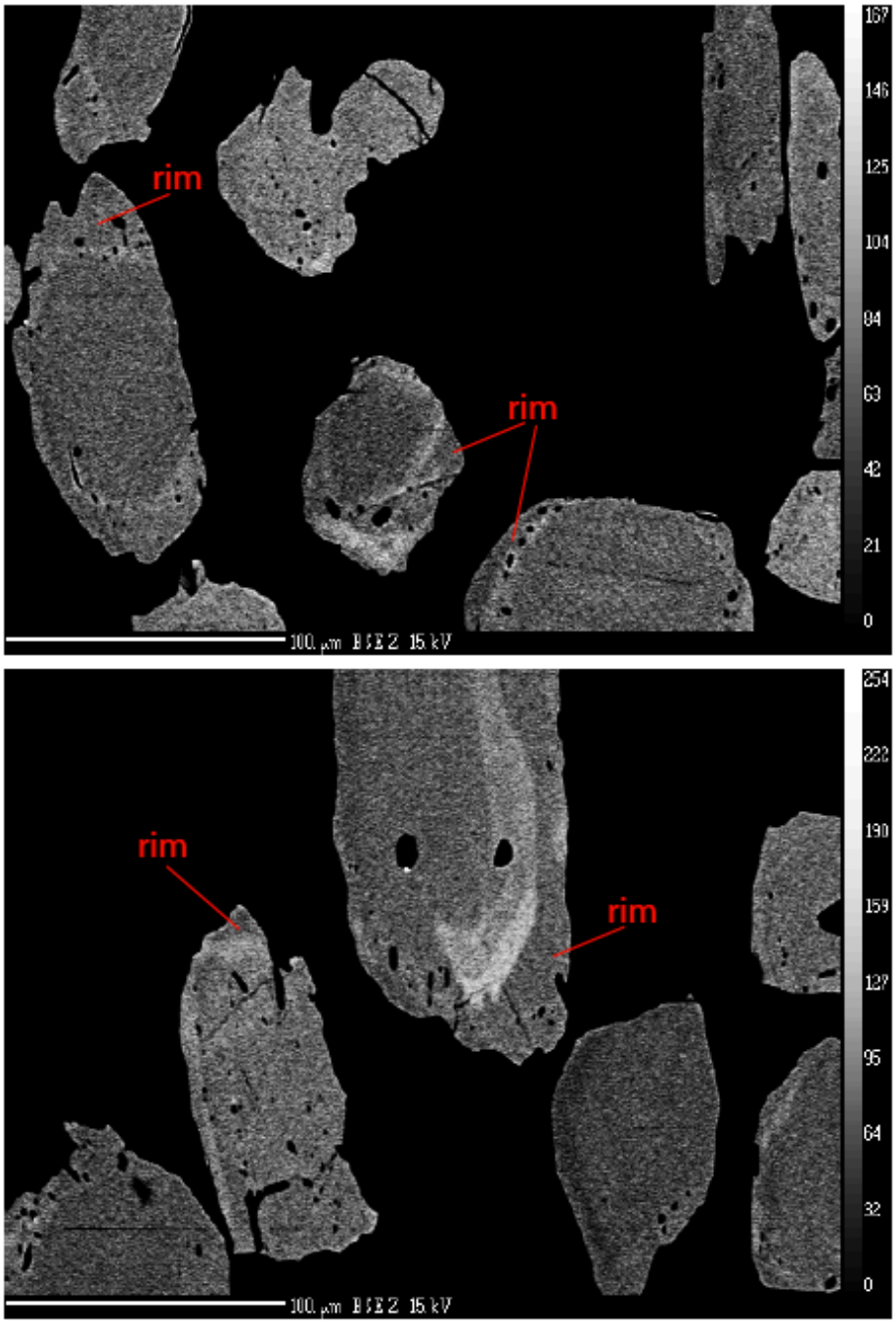


**Figure S1.3:** Backscatter electron (BSE) image of representative zircon grains extracted from samples of the Maclaren schist. Note how several grains contain dark rims that are commonly associated with a sieve texture in the crystal.

**Hf analytical methods at the Arizona LaserChron Center**

Hf isotope analyses are conducted with a Nu HR ICPMS connected to a Photon Machines Analyte G2 excimer laser. Instrument settings are established first by analysis of 10 ppb solutions of JMC475 and a Spex Hf solution, and then by analysis of 10 ppb solutions containing Spex Hf, Yb, and Lu. The mixtures range in concentration of Yb and Lu, with $^{176}$(Yb+Lu) up to 70% of the $^{176}$Hf. When all solutions yield $^{176}$Hf/$^{177}$Hf of ~0.28216, instrument settings are optimized for laser ablation analyses and seven different standard zircons (Mud Tank, 91500, Temora, R33, FC52, Plesovice, and Sri Lanka) are analyzed. These standards are included with unknowns on the same epoxy mounts. When precision and accuracy are acceptable, unknowns are analyzed using exactly the same acquisition parameters.

Laser ablation analyses are conducted with a laser beam diameter of 40 microns, with the ablation pits located on top of the U-Pb analysis pits. CL images are used to ensure that the ablation pits do not overlap multiple age domains or inclusions. Each acquisition consists of one 40-second integration on backgrounds (on peaks with no laser firing) followed by 60 one-second integrations with the laser firing. Using a typical laser fluence of ~5 J/cm2 and pulse rate of 7 hz, the ablation rate is ~0.8 microns per second. Each standard is analyzed once for every ~20 unknowns.

Isotope fractionation is accounted for using the method of Woodhead et al. (2004): βHf is determined from the measured $^{179}$Hf/$^{177}$Hf; βYb is determined from the measured $^{173}$Yb/$^{171}$Yb (except for very low Yb signals); βLu is assumed to be the same as βYb; and an exponential formula is used for fractionation correction. Yb and Lu interferences are corrected by measurement of $^{176}$Yb/$^{171}$Yb and $^{176}$Lu/$^{175}$Lu (respectively), as advocated by Woodhead et al. (2004). Critical isotope ratios are $^{179}$Hf/$^{177}$Hf =0.73250 (Patchett & Tatsumoto, 1980);

$^{173}Yb/^{171}Yb$ = 1.132338 (Vervoort et al. 2004); $^{176}Yb/^{171}Yb$ =0.901691 (Vervoort et al., 2004; Amelin and Davis, 2005); $^{176}Lu/^{175}Lu$ = 0.02653 (Patchett, 1983). All corrections are done line-by-line. For very low Yb signals, βHf is used for fractionation of Yb isotopes. The corrected $^{176}Hf/^{177}Hf$ values are filtered for outliers (2-sigma filter), and the average and standard error are calculated from the resulting ~58 integrations. There is no capability to use only a portion of the acquired data.

All solutions, standards, and unknowns analyzed during a session are reduced together. The cutoff for using βHf versus βYb is determined by monitoring the average offset of the standards from their known values, and the cutoff is set at the minimum offset. For most data sets, this is achieved at ~6 mv of $^{171}Yb$. For sessions in which the standards yield $^{176}Hf/^{177}Hf$ values that are shifted consistently from the know values, a correction factor is applied to the $^{176}Hf/^{177}Hf$ of all standards and unknowns. This correction factor, which is not necessary for most sessions, averages 1 epsilon unit.

The $^{176}Hf/^{177}Hf$ at time of crystallization is calculated from measurement of present-day $^{176}Hf/^{177}Hf$ and $^{176}Lu/^{177}Hf$, using the decay constant of $^{176}Lu$ ($\lambda = 1.867e^{-11}$) from Scherer et al. (2001) and Söderlund et al. (2004). No capability is provided for calculating Hf Depleted Mantle model ages because the $^{176}Hf/^{177}Hf$ and $^{176}Lu/^{177}Hf$ of the source material(s) from which the zircon crystallized is not known.

# Supplemental Information S2: U-Pb and Hf isotopic data

| | | | | Isotope ratios | | | | | | | Dates | | | | | | Dates used in plots | |
|---|---|---|---|---|---|---|---|---|---|---|---|---|---|---|---|---|---|---|
| Identifier | 206Pb (CPS) | U (ug/g) | U/Th | 206Pb / 238U | 1s (%) | 207Pb / 206Pb | 1s (%) | 207Pb / 235U | 1s (%) | Error Corr. | 207Pb / 206Pb | 2s abs | 206Pb / 238U | 2s abs | 207Pb / 235U | 2s abs | Preferred age | 2s sys abs |
| **Sample 15ATW-07** | | | | | | | | | | | | | | | | | | |
| Output_1_14 | 67700 | 5390 | 561.0 | 0.01 | 1.12 | 0.05 | 1.03 | 0.09 | 1.24 | 0.81 | 122.0 | 46.0 | 85.6 | 1.9 | 86.4 | 2.0 | 85.6 | 2.4 |
| Output_1_32 | 63700 | 6360 | 273.0 | 0.01 | 1.32 | 0.05 | 1.23 | 0.10 | 1.37 | 0.58 | 133.0 | 55.0 | 89.7 | 2.3 | 92.2 | 2.4 | 89.7 | 2.8 |
| Output_1_57 | 2120 | 186 | 2.4 | 0.02 | 2.22 | 0.06 | 5.60 | 0.11 | 6.19 | 0.36 | 310.0 | 230.0 | 97.8 | 4.3 | 103.0 | 12.0 | 97.8 | 4.6 |
| Output_1_50 | 3650 | 316 | 1.5 | 0.02 | 2.14 | 0.05 | 4.58 | 0.11 | 4.20 | 0.29 | 100.0 | 170.0 | 101.7 | 4.3 | 105.0 | 8.5 | 101.7 | 4.6 |
| Output_1_12 | 13720 | 840 | 24.3 | 0.02 | 1.66 | 0.05 | 2.99 | 0.12 | 2.96 | 0.37 | 180.0 | 130.0 | 113.8 | 3.7 | 114.9 | 6.5 | 113.8 | 4.2 |
| Output_1_25 | 7350 | 369 | 1.5 | 0.02 | 1.77 | 0.06 | 4.00 | 0.18 | 5.40 | 0.47 | 320.0 | 160.0 | 144.3 | 5.0 | 163.0 | 15.0 | 144.3 | 5.6 |
| Output_1_16 | 2360 | 109 | 2.0 | 0.02 | 1.73 | 0.05 | 5.43 | 0.16 | 5.35 | 0.20 | 180.0 | 210.0 | 145.3 | 5.0 | 150.0 | 14.0 | 145.3 | 5.6 |
| Output_1_36 | 5290 | 367 | 1.0 | 0.02 | 1.30 | 0.05 | 3.54 | 0.16 | 3.37 | 0.07 | 230.0 | 150.0 | 146.9 | 3.8 | 154.3 | 8.8 | 146.9 | 4.5 |
| Output_1_34 | 3450 | 223 | 1.1 | 0.02 | 1.60 | 0.05 | 5.19 | 0.17 | 5.09 | 0.14 | 240.0 | 210.0 | 147.5 | 4.7 | 158.0 | 15.0 | 147.5 | 5.3 |
| Output_1_51 | 4130 | 248 | 1.2 | 0.02 | 1.59 | 0.05 | 4.90 | 0.17 | 4.46 | 0.17 | 320.0 | 210.0 | 148.0 | 4.6 | 157.0 | 13.0 | 148.0 | 5.3 |
| Output_1_28 | 1512 | 76 | 2.1 | 0.02 | 2.31 | 0.05 | 5.71 | 0.17 | 5.15 | 0.11 | 240.0 | 230.0 | 151.4 | 6.6 | 155.0 | 14.0 | 151.4 | 7.1 |
| Output_1_27 | 4910 | 241 | 1.7 | 0.02 | 1.28 | 0.05 | 3.31 | 0.16 | 3.37 | 0.32 | 120.0 | 140.0 | 151.9 | 3.8 | 153.5 | 9.7 | 151.9 | 4.6 |
| Output_1_31 | 1295 | 74 | 1.0 | 0.02 | 3.36 | 0.06 | 11.21 | 0.19 | 9.41 | 0.26 | 380.0 | 450.0 | 152.0 | 10.0 | 177.0 | 32.0 | 152.0 | 11.0 |
| Output_1_4 | 10390 | 568 | 1.2 | 0.02 | 0.96 | 0.05 | 2.59 | 0.17 | 2.73 | 0.05 | 270.0 | 120.0 | 152.1 | 2.9 | 157.6 | 8.0 | 152.1 | 3.8 |
| Output_1_45 | 1172 | 76 | 2.1 | 0.02 | 2.72 | 0.05 | 9.26 | 0.17 | 9.36 | 0.02 | 150.0 | 360.0 | 152.4 | 7.9 | 156.0 | 27.0 | 152.4 | 8.3 |
| Output_1_54 | 619 | 34 | 2.7 | 0.02 | 3.33 | 0.05 | 11.46 | 0.16 | 11.66 | 0.12 | 50.0 | 410.0 | 152.7 | 9.8 | 151.0 | 34.0 | 152.7 | 10.0 |
| Output_1_47 | 1911 | 120 | 1.5 | 0.02 | 2.07 | 0.05 | 5.92 | 0.18 | 5.83 | 0.10 | 280.0 | 240.0 | 153.2 | 6.4 | 166.0 | 18.0 | 153.2 | 6.9 |
| Output_1_7 | 3000 | 145 | 1.5 | 0.02 | 2.04 | 0.05 | 4.73 | 0.17 | 4.62 | 0.19 | 270.0 | 200.0 | 156.1 | 6.5 | 161.0 | 14.0 | 156.1 | 7.0 |
| Output_1_6 | 2454 | 124 | 2.2 | 0.02 | 1.91 | 0.06 | 4.73 | 0.19 | 5.08 | 0.31 | 390.0 | 190.0 | 156.4 | 5.9 | 177.0 | 15.0 | 156.4 | 6.4 |
| Output_1_24 | 938 | 42 | 2.9 | 0.02 | 2.64 | 0.05 | 9.06 | 0.17 | 9.12 | 0.19 | 80.0 | 340.0 | 156.5 | 7.9 | 155.0 | 27.0 | 156.5 | 8.3 |
| Output_1_13 | 526 | 23 | 1.9 | 0.02 | 3.28 | 0.07 | 10.77 | 0.21 | 10.14 | 0.11 | 480.0 | 430.0 | 157.0 | 11.0 | 187.0 | 36.0 | 157.0 | 11.0 |
| Output_1_18 | 1169 | 48 | 3.0 | 0.02 | 3.04 | 0.05 | 7.51 | 0.18 | 8.33 | 0.26 | 210.0 | 290.0 | 157.3 | 9.4 | 164.0 | 25.0 | 157.3 | 9.7 |
| Output_1_60 | 1627 | 94 | 2.3 | 0.02 | 2.02 | 0.05 | 5.71 | 0.18 | 5.56 | 0.04 | 350.0 | 230.0 | 157.3 | 6.4 | 169.0 | 17.0 | 157.3 | 6.9 |
| Output_1_49 | 3350 | 195 | 1.4 | 0.02 | 1.60 | 0.06 | 4.71 | 0.19 | 4.52 | 0.19 | 360.0 | 190.0 | 157.6 | 5.0 | 175.0 | 14.0 | 157.6 | 5.6 |
| Output_1_21 | 4240 | 180 | 1.2 | 0.02 | 1.13 | 0.05 | 4.82 | 0.16 | 4.66 | 0.10 | 30.0 | 190.0 | 157.9 | 3.5 | 153.0 | 13.0 | 157.9 | 4.4 |
| Output_1_11 | 4390 | 194 | 1.6 | 0.02 | 1.83 | 0.05 | 3.95 | 0.18 | 3.95 | 0.28 | 290.0 | 160.0 | 157.9 | 5.7 | 164.0 | 12.0 | 157.9 | 6.3 |
| Output_1_22 | 1198 | 52 | 3.1 | 0.02 | 2.64 | 0.06 | 6.73 | 0.19 | 6.38 | 0.25 | 370.0 | 260.0 | 158.0 | 8.5 | 178.0 | 21.0 | 158.0 | 8.9 |
| Output_1_58 | 1850 | 105 | 2.7 | 0.02 | 2.01 | 0.05 | 6.24 | 0.17 | 5.88 | 0.04 | 100.0 | 250.0 | 158.2 | 6.3 | 157.0 | 17.0 | 158.2 | 6.9 |
| Output_1_8 | 2203 | 104 | 1.7 | 0.02 | 2.01 | 0.05 | 5.67 | 0.19 | 5.61 | 0.12 | 360.0 | 230.0 | 158.3 | 6.6 | 172.0 | 18.0 | 158.3 | 7.1 |
| Output_1_39 | 765 | 54 | 1.9 | 0.03 | 3.00 | 0.06 | 10.17 | 0.19 | 10.05 | 0.00 | 230.0 | 400.0 | 158.8 | 9.4 | 173.0 | 33.0 | 158.8 | 9.8 |
| Output_1_41 | 2750 | 189 | 1.8 | 0.03 | 1.75 | 0.05 | 4.87 | 0.18 | 4.52 | 0.00 | 140.0 | 190.0 | 159.8 | 5.5 | 164.0 | 14.0 | 159.8 | 6.2 |
| Output_1_20 | 2670 | 113 | 2.0 | 0.03 | 1.72 | 0.05 | 5.42 | 0.17 | 4.97 | 0.06 | 200.0 | 210.0 | 161.0 | 5.5 | 163.0 | 15.0 | 161.0 | 6.1 |
| Output_1_10 | 2447 | 109 | 1.9 | 0.03 | 1.85 | 0.05 | 5.32 | 0.17 | 5.59 | 0.21 | 150.0 | 200.0 | 161.8 | 5.9 | 157.0 | 17.0 | 161.8 | 6.5 |
| Output_1_44 | 3300 | 209 | 2.0 | 0.03 | 1.78 | 0.05 | 4.30 | 0.17 | 4.44 | 0.10 | 120.0 | 180.0 | 161.9 | 5.5 | 157.0 | 13.0 | 161.9 | 6.1 |

| | | | | | | | | | | | | | | | | | | |
|---|---|---|---|---|---|---|---|---|---|---|---|---|---|---|---|---|---|---|
| Output_1_48 | 1048 | 62 | 1.7 | 0.03 | 1.95 | 0.06 | 8.11 | 0.19 | 7.51 | 0.01 | 350.0 | 300.0 | 163.7 | 6.4 | 183.0 | 25.0 | 163.7 | 7.0 |
| Output_1_55 | 2294 | 119 | 1.5 | 0.03 | 2.13 | 0.06 | 4.84 | 0.21 | 4.59 | 0.17 | 410.0 | 200.0 | 163.8 | 7.1 | 189.0 | 16.0 | 163.8 | 7.6 |
| Output_1_59 | 3739 | 202 | 1.8 | 0.03 | 1.50 | 0.05 | 4.29 | 0.17 | 4.39 | 0.11 | 150.0 | 180.0 | 165.2 | 4.9 | 163.0 | 13.0 | 165.2 | 5.6 |
| Output_1_37 | 985 | 64 | 1.6 | 0.03 | 2.66 | 0.06 | 8.47 | 0.21 | 8.29 | 0.05 | 370.0 | 340.0 | 167.3 | 8.7 | 183.0 | 28.0 | 167.3 | 9.1 |
| Output_1_1 | 8250 | 426 | 1.3 | 0.03 | 0.90 | 0.05 | 3.49 | 0.19 | 3.37 | 0.09 | 270.0 | 150.0 | 173.1 | 3.1 | 180.0 | 11.0 | 173.1 | 4.2 |
| Output_1_19 | 24200 | 905 | 0.5 | 0.03 | 0.73 | 0.05 | 1.66 | 0.19 | 1.74 | 0.31 | 279.0 | 76.0 | 175.1 | 2.5 | 179.0 | 5.7 | 175.1 | 3.8 |
| Output_1_15 | 6980 | 266 | 2.5 | 0.03 | 0.77 | 0.05 | 2.98 | 0.20 | 2.94 | 0.01 | 340.0 | 130.0 | 176.8 | 2.7 | 188.1 | 9.9 | 176.8 | 4.0 |
| Output_1_2 | 4511 | 217 | 0.1 | 0.03 | 0.96 | 0.05 | 4.31 | 0.19 | 3.99 | 0.20 | 100.0 | 170.0 | 178.8 | 3.4 | 174.0 | 13.0 | 178.8 | 4.5 |
| Output_1_23 | 8570 | 332 | 2.1 | 0.03 | 1.07 | 0.05 | 2.11 | 0.20 | 2.41 | 0.33 | 315.0 | 97.0 | 178.8 | 3.8 | 184.1 | 8.1 | 178.8 | 4.8 |
| Output_1_26 | 15390 | 622 | 0.2 | 0.03 | 1.07 | 0.06 | 3.08 | 0.22 | 2.75 | 0.16 | 390.0 | 120.0 | 181.9 | 3.8 | 199.3 | 9.9 | 181.9 | 4.9 |
| Output_1_9 | 6470 | 246 | 2.5 | 0.03 | 1.53 | 0.05 | 3.75 | 0.21 | 3.40 | 0.00 | 190.0 | 150.0 | 186.4 | 5.6 | 189.0 | 12.0 | 186.4 | 6.4 |
| Output_1_46 | 19300 | 1022 | 0.1 | 0.03 | 1.18 | 0.05 | 1.93 | 0.21 | 2.04 | 0.38 | 263.0 | 84.0 | 188.4 | 4.4 | 191.7 | 7.1 | 188.4 | 5.4 |
| Output_1_35 | 5490 | 274 | 2.2 | 0.03 | 1.98 | 0.05 | 3.33 | 0.23 | 3.42 | 0.29 | 380.0 | 140.0 | 192.3 | 7.4 | 214.0 | 13.0 | 192.3 | 8.0 |
| Output_1_33 | 9120 | 421 | 1.4 | 0.03 | 1.40 | 0.05 | 3.10 | 0.22 | 3.15 | 0.19 | 230.0 | 130.0 | 194.8 | 5.4 | 202.0 | 12.0 | 194.8 | 6.3 |
| Output_1_43 | 5290 | 290 | 1.8 | 0.03 | 1.25 | 0.05 | 3.26 | 0.22 | 2.93 | 0.07 | 260.0 | 140.0 | 195.1 | 4.8 | 203.0 | 11.0 | 195.1 | 5.8 |
| Output_1_53 | 4690 | 205 | 2.2 | 0.03 | 1.50 | 0.05 | 3.31 | 0.22 | 3.14 | 0.20 | 290.0 | 140.0 | 196.4 | 5.8 | 205.0 | 12.0 | 196.4 | 6.7 |
| Output_1_30 | 71200 | 443 | 4.3 | 0.20 | 0.78 | 0.10 | 0.78 | 2.93 | 1.01 | 0.65 | 1680.0 | 29.0 | 1201.0 | 17.0 | ##### | 15.0 | 1680.0 | 38.0 |
| Output_1_38 | 17020 | 998 | 0.4 | 0.03 | 1.09 | 0.06 | 2.62 | 0.24 | 2.55 | 0.32 | 570.0 | 110.0 | 183.3 | 4.0 | 213.7 | 9.9 | 183.3 | 5.0 |
| Output_1_52 | 3360 | 171 | 1.5 | 0.03 | 3.36 | 0.06 | 7.74 | 0.23 | 7.36 | 0.01 | 540.0 | 350.0 | 171.0 | 11.0 | 210.0 | 28.0 | 171.0 | 11.0 |
| Output_1_42 | 2630 | 162 | 1.2 | 0.03 | 1.43 | 0.06 | 5.23 | 0.24 | 4.87 | 0.04 | 620.0 | 220.0 | 175.1 | 5.0 | 216.0 | 18.0 | 175.1 | 5.8 |
| Output_1_29 | 1869 | 99 | 1.6 | 0.02 | 1.95 | 0.06 | 5.83 | 0.19 | 5.93 | 0.23 | 600.0 | 250.0 | 146.9 | 5.7 | 178.0 | 20.0 | 146.9 | 6.2 |
| Output_1_17 | 1349 | 57 | 2.4 | 0.03 | 2.17 | 0.07 | 6.86 | 0.21 | 5.84 | 0.09 | 670.0 | 270.0 | 160.8 | 7.2 | 194.0 | 21.0 | 160.8 | 7.7 |
| Output_1_3 | 1700 | 99 | 1.4 | 0.02 | 2.16 | 0.06 | 4.98 | 0.20 | 5.08 | 0.15 | 680.0 | 210.0 | 147.3 | 6.5 | 186.0 | 17.0 | 147.3 | 6.9 |
| Output_1_40 | 1202 | 90 | 1.4 | 0.02 | 2.53 | 0.07 | 9.03 | 0.23 | 8.55 | 0.10 | 770.0 | 410.0 | 151.1 | 7.5 | 211.0 | 31.0 | 151.1 | 7.9 |
| Output_1_5 | 1090 | 56 | 1.8 | 0.03 | 2.60 | 0.09 | 6.99 | 0.31 | 6.75 | 0.11 | 1510.0 | 270.0 | 159.3 | 8.3 | 293.0 | 30.0 | 159.3 | 8.7 |
| Output_1_56 | 1357 | 70 | 3.3 | 0.03 | 2.87 | 0.04 | 8.14 | 0.15 | 7.48 | 0.02 | -200.0 | 270.0 | 165.9 | 9.2 | 136.0 | 20.0 | 165.9 | 9.6 |
| | | | | | | | | | | | | | | | | | | |
| **Sample 15ATW52** | | | | | | | | | | | | | | | | | | |
| Output_1_161 | 799 | 20 | 4.6 | 0.02 | 6.17 | 0.05 | 22.92 | 0.14 | 23.24 | 0.12 | -20.0 | 360.0 | 144.9 | 8.7 | 129.0 | 29.0 | 144.9 | 10.0 |
| Output_1_263 | 1826 | 73 | 2.2 | 0.02 | 3.87 | 0.05 | 12.32 | 0.15 | 12.34 | 0.04 | 180.0 | 220.0 | 145.8 | 5.4 | 146.0 | 16.0 | 145.8 | 7.4 |
| Output_1_136 | 2660 | 139 | 1.8 | 0.02 | 3.56 | 0.05 | 11.63 | 0.16 | 9.76 | 0.23 | 260.0 | 220.0 | 146.8 | 5.2 | 153.0 | 14.0 | 146.8 | 7.4 |
| Output_1_53 | 1107 | 70 | 1.4 | 0.02 | 4.72 | 0.05 | 15.83 | 0.16 | 16.35 | 0.01 | 70.0 | 260.0 | 148.4 | 6.9 | 146.0 | 22.0 | 148.4 | 8.8 |
| Output_1_275 | 1863 | 62 | 3.1 | 0.02 | 4.12 | 0.05 | 11.46 | 0.16 | 10.63 | 0.04 | 220.0 | 220.0 | 148.5 | 6.0 | 149.0 | 15.0 | 148.5 | 8.1 |
| Output_1_42 | 4990 | 215 | 2.0 | 0.02 | 2.47 | 0.05 | 7.07 | 0.17 | 6.98 | 0.07 | 260.0 | 140.0 | 149.3 | 3.7 | 160.0 | 11.0 | 149.3 | 6.5 |
| Output_1_113 | 6810 | 161 | 1.7 | 0.02 | 2.26 | 0.05 | 7.32 | 0.16 | 7.93 | 0.25 | 240.0 | 140.0 | 149.5 | 3.4 | 154.0 | 11.0 | 149.5 | 6.3 |
| Output_1_172 | 4460 | 120 | 3.6 | 0.02 | 2.98 | 0.05 | 5.65 | 0.17 | 6.36 | 0.43 | 300.0 | 110.0 | 149.7 | 4.4 | 161.2 | 9.3 | 149.7 | 6.9 |
| Output_1_75 | 4500 | 102 | 2.5 | 0.02 | 2.34 | 0.05 | 7.62 | 0.17 | 6.67 | 0.01 | 230.0 | 150.0 | 149.9 | 3.5 | 154.2 | 9.9 | 149.9 | 6.4 |
| Output_1_220 | 3840 | 188 | 4.0 | 0.02 | 3.10 | 0.05 | 8.49 | 0.15 | 7.79 | 0.05 | 60.0 | 160.0 | 150.0 | 4.6 | 145.0 | 10.0 | 150.0 | 7.1 |
| Output_1_194 | 618 | 10 | 3.1 | 0.02 | 6.36 | 0.06 | 25.45 | 0.18 | 23.89 | 0.05 | 340.0 | 420.0 | 150.0 | 9.7 | 159.0 | 36.0 | 150.0 | 11.0 |
| Output_1_152 | 1718 | 52 | 1.3 | 0.02 | 3.99 | 0.05 | 13.38 | 0.15 | 14.29 | 0.34 | 70.0 | 240.0 | 150.1 | 5.9 | 145.0 | 20.0 | 150.1 | 8.0 |

| | | | | | | | | | | | | | | | | | | |
|---|---|---|---|---|---|---|---|---|---|---|---|---|---|---|---|---|---|---|
| Output_1_137 | 4550 | 233 | 3.4 | 0.02 | 2.76 | 0.05 | 7.00 | 0.16 | 6.96 | 0.29 | 160.0 | 130.0 | 150.2 | 4.1 | 148.2 | 9.6 | 150.2 | 6.8 |
| Output_1_207 | 1307 | 24 | 1.6 | 0.02 | 4.66 | 0.05 | 13.83 | 0.17 | 12.94 | 0.03 | 270.0 | 250.0 | 150.4 | 6.9 | 157.0 | 19.0 | 150.4 | 8.8 |
| Output_1_154 | 2315 | 65 | 2.6 | 0.02 | 3.52 | 0.05 | 11.07 | 0.17 | 10.92 | 0.05 | 310.0 | 220.0 | 150.4 | 5.2 | 161.0 | 16.0 | 150.4 | 7.5 |
| Output_1_184 | 4030 | 95 | 3.9 | 0.02 | 2.58 | 0.05 | 8.21 | 0.18 | 8.00 | 0.06 | 350.0 | 160.0 | 150.6 | 3.8 | 164.0 | 12.0 | 150.6 | 6.6 |
| Output_1_281 | 2813 | 114 | 4.9 | 0.02 | 3.34 | 0.05 | 9.72 | 0.16 | 9.94 | 0.30 | 160.0 | 180.0 | 150.8 | 5.0 | 150.0 | 14.0 | 150.8 | 7.4 |
| Output_1_130 | 7710 | 377 | 2.6 | 0.02 | 2.07 | 0.05 | 7.62 | 0.17 | 7.60 | 0.12 | 260.0 | 150.0 | 150.8 | 3.1 | 159.0 | 11.0 | 150.8 | 6.2 |
| Output_1_121 | 1723 | 56 | 2.1 | 0.02 | 4.01 | 0.05 | 14.99 | 0.17 | 14.94 | 0.13 | 290.0 | 280.0 | 150.8 | 6.0 | 163.0 | 23.0 | 150.8 | 8.1 |
| Output_1_14 | 1262 | 94 | 1.7 | 0.02 | 4.64 | 0.04 | 19.72 | 0.14 | 19.42 | 0.12 | -70.0 | 310.0 | 151.1 | 6.7 | 128.0 | 24.0 | 151.1 | 8.7 |
| Output_1_173 | 1238 | 33 | 2.0 | 0.02 | 5.06 | 0.05 | 14.73 | 0.16 | 14.47 | 0.09 | 220.0 | 270.0 | 151.1 | 7.7 | 150.0 | 19.0 | 151.1 | 9.5 |
| Output_1_87 | 4100 | 61 | 2.9 | 0.02 | 3.37 | 0.05 | 9.33 | 0.17 | 8.82 | 0.20 | 290.0 | 180.0 | 151.1 | 5.0 | 159.0 | 13.0 | 151.1 | 7.4 |
| Output_1_132 | 3110 | 155 | 1.9 | 0.02 | 4.22 | 0.05 | 11.37 | 0.16 | 10.43 | 0.10 | 220.0 | 220.0 | 151.2 | 6.6 | 152.0 | 15.0 | 151.2 | 8.5 |
| Output_1_144 | 940 | 38 | 1.7 | 0.02 | 5.88 | 0.04 | 19.22 | 0.16 | 19.25 | 0.17 | 110.0 | 320.0 | 151.3 | 8.5 | 154.0 | 28.0 | 151.3 | 10.0 |
| Output_1_216 | 5500 | 184 | 1.7 | 0.02 | 2.56 | 0.05 | 6.61 | 0.16 | 5.66 | 0.11 | 190.0 | 130.0 | 151.6 | 3.8 | 154.1 | 8.1 | 151.6 | 6.7 |
| Output_1_94 | 6140 | 88 | 3.6 | 0.02 | 2.73 | 0.05 | 7.03 | 0.16 | 6.25 | 0.04 | 200.0 | 140.0 | 151.6 | 4.1 | 150.2 | 9.0 | 151.6 | 6.8 |
| Output_1_191 | 9800 | 185 | 2.4 | 0.02 | 2.18 | 0.05 | 4.74 | 0.16 | 4.09 | 0.06 | 138.0 | 97.0 | 151.7 | 3.3 | 149.5 | 5.7 | 151.7 | 6.4 |
| Output_1_297 | 2163 | 39 | 2.4 | 0.02 | 3.64 | 0.05 | 8.44 | 0.17 | 9.94 | 0.23 | 290.0 | 170.0 | 152.0 | 5.5 | 164.0 | 14.0 | 152.0 | 7.7 |
| Output_1_160 | 5100 | 126 | 3.3 | 0.02 | 2.59 | 0.05 | 6.87 | 0.16 | 7.01 | 0.24 | 60.0 | 130.0 | 152.2 | 3.9 | 148.0 | 10.0 | 152.2 | 6.7 |
| Output_1_225 | 1721 | 153 | 4.3 | 0.02 | 3.26 | 0.05 | 16.09 | 0.15 | 14.67 | 0.22 | -50.0 | 260.0 | 152.3 | 4.9 | 142.0 | 19.0 | 152.3 | 7.4 |
| Output_1_142 | 6580 | 285 | 2.6 | 0.02 | 2.46 | 0.05 | 6.52 | 0.16 | 6.01 | 0.09 | 200.0 | 130.0 | 152.8 | 3.7 | 154.4 | 8.6 | 152.8 | 6.6 |
| Output_1_90 | 2926 | 42 | 2.3 | 0.02 | 2.96 | 0.05 | 11.66 | 0.17 | 11.83 | 0.19 | 270.0 | 220.0 | 152.8 | 4.5 | 156.0 | 18.0 | 152.8 | 7.1 |
| Output_1_40 | 1876 | 72 | 2.8 | 0.02 | 4.58 | 0.06 | 12.76 | 0.19 | 11.70 | 0.11 | 410.0 | 240.0 | 152.8 | 7.0 | 175.0 | 19.0 | 152.8 | 8.9 |
| Output_1_259 | 3051 | 127 | 3.1 | 0.02 | 3.25 | 0.05 | 9.86 | 0.17 | 9.52 | 0.05 | 210.0 | 190.0 | 152.9 | 4.9 | 156.0 | 14.0 | 152.9 | 7.4 |
| Output_1_232 | 1774 | 126 | 2.2 | 0.02 | 5.00 | 0.05 | 14.76 | 0.15 | 14.29 | 0.10 | 50.0 | 250.0 | 153.0 | 7.3 | 143.0 | 19.0 | 153.0 | 9.1 |
| Output_1_26 | 1142 | 45 | 1.8 | 0.02 | 4.58 | 0.05 | 18.50 | 0.18 | 17.49 | 0.04 | 330.0 | 300.0 | 153.1 | 6.7 | 165.0 | 27.0 | 153.1 | 8.7 |
| Output_1_28 | 3180 | 122 | 2.3 | 0.02 | 3.20 | 0.05 | 8.69 | 0.17 | 8.93 | 0.09 | 150.0 | 160.0 | 153.2 | 4.9 | 158.0 | 13.0 | 153.2 | 7.4 |
| Output_1_186 | 8060 | 173 | 1.2 | 0.02 | 2.45 | 0.05 | 6.14 | 0.17 | 5.59 | 0.17 | 220.0 | 120.0 | 153.2 | 3.7 | 155.7 | 8.0 | 153.2 | 6.7 |
| Output_1_5 | 4720 | 567 | 3.6 | 0.02 | 2.82 | 0.05 | 8.91 | 0.17 | 8.38 | 0.07 | 260.0 | 170.0 | 153.4 | 4.3 | 159.0 | 12.0 | 153.4 | 7.0 |
| Output_1_63 | 5220 | 304 | 1.1 | 0.02 | 2.65 | 0.05 | 7.23 | 0.17 | 6.63 | 0.24 | 220.0 | 140.0 | 153.6 | 4.0 | 155.2 | 9.9 | 153.6 | 6.8 |
| Output_1_18 | 2178 | 125 | 2.1 | 0.02 | 3.36 | 0.05 | 12.86 | 0.17 | 12.73 | 0.06 | 90.0 | 230.0 | 153.8 | 5.1 | 156.0 | 19.0 | 153.8 | 7.5 |
| Output_1_51 | 2730 | 145 | 2.9 | 0.02 | 3.11 | 0.05 | 12.43 | 0.17 | 12.07 | 0.03 | 280.0 | 230.0 | 153.8 | 4.7 | 166.0 | 19.0 | 153.8 | 7.3 |
| Output_1_143 | 13060 | 540 | 2.3 | 0.02 | 2.32 | 0.05 | 4.77 | 0.17 | 4.90 | 0.35 | 209.0 | 99.0 | 153.9 | 3.5 | 155.0 | 7.1 | 153.9 | 6.6 |
| Output_1_278 | 2042 | 68 | 2.4 | 0.02 | 4.55 | 0.06 | 13.71 | 0.18 | 13.26 | 0.05 | 360.0 | 250.0 | 154.0 | 6.8 | 169.0 | 20.0 | 154.0 | 8.8 |
| Output_1_174 | 828 | 22 | 2.9 | 0.02 | 4.96 | 0.04 | 25.58 | 0.13 | 24.63 | 0.12 | -110.0 | 380.0 | 154.2 | 7.7 | 122.0 | 30.0 | 154.2 | 9.5 |
| Output_1_46 | 4510 | 209 | 3.0 | 0.02 | 2.73 | 0.05 | 7.93 | 0.17 | 7.06 | 0.18 | 250.0 | 160.0 | 154.2 | 4.2 | 159.0 | 11.0 | 154.2 | 7.0 |
| Output_1_205 | 1977 | 33 | 2.7 | 0.02 | 3.63 | 0.05 | 11.86 | 0.18 | 10.99 | 0.03 | 390.0 | 230.0 | 154.2 | 5.6 | 168.0 | 18.0 | 154.2 | 7.9 |
| Output_1_264 | 1546 | 56 | 1.7 | 0.02 | 4.55 | 0.05 | 16.95 | 0.16 | 14.74 | 0.02 | 40.0 | 270.0 | 154.3 | 6.7 | 147.0 | 21.0 | 154.3 | 8.7 |
| Output_1_29 | 3910 | 144 | 2.1 | 0.02 | 2.97 | 0.05 | 9.80 | 0.17 | 8.88 | 0.06 | 210.0 | 190.0 | 154.4 | 4.5 | 160.0 | 14.0 | 154.4 | 7.2 |
| Output_1_196 | 2479 | 40 | 1.7 | 0.02 | 3.46 | 0.05 | 8.75 | 0.17 | 9.41 | 0.20 | 190.0 | 180.0 | 154.5 | 5.3 | 159.0 | 13.0 | 154.5 | 7.7 |
| Output_1_119 | 3007 | 87 | 4.8 | 0.02 | 2.76 | 0.05 | 10.44 | 0.17 | 10.18 | 0.08 | 140.0 | 190.0 | 154.6 | 4.2 | 155.0 | 15.0 | 154.6 | 7.0 |
| Output_1_6 | 3210 | 374 | 3.1 | 0.02 | 3.95 | 0.05 | 10.68 | 0.18 | 8.99 | 0.12 | 290.0 | 200.0 | 154.7 | 6.0 | 165.0 | 14.0 | 154.7 | 8.2 |

| | | | | | | | | | | | | | | | | | | |
|---|---|---|---|---|---|---|---|---|---|---|---|---|---|---|---|---|---|---|
| Output_1_293 | 2331 | 79 | 3.1 | 0.02 | 4.12 | 0.05 | 11.09 | 0.18 | 11.67 | 0.38 | 330.0 | 220.0 | 154.8 | 6.3 | 166.0 | 18.0 | 154.8 | 8.4 |
| Output_1_271 | 3690 | 117 | 1.6 | 0.02 | 2.92 | 0.05 | 10.54 | 0.16 | 10.37 | 0.18 | 210.0 | 190.0 | 154.9 | 4.5 | 155.0 | 15.0 | 154.9 | 7.1 |
| Output_1_151 | 1853 | 57 | 3.1 | 0.02 | 3.74 | 0.05 | 13.66 | 0.18 | 12.22 | 0.07 | 310.0 | 250.0 | 154.9 | 5.8 | 168.0 | 19.0 | 154.9 | 8.0 |
| Output_1_98 | 4890 | 71 | 2.0 | 0.02 | 2.92 | 0.05 | 9.38 | 0.15 | 8.50 | 0.23 | 50.0 | 170.0 | 155.0 | 4.5 | 144.0 | 11.0 | 155.0 | 7.2 |
| Output_1_180 | 891 | 23 | 3.0 | 0.02 | 6.17 | 0.06 | 21.31 | 0.20 | 20.00 | 0.24 | 350.0 | 390.0 | 155.0 | 9.4 | 178.0 | 34.0 | 155.0 | 11.0 |
| Output_1_125 | 6530 | 261 | 4.5 | 0.02 | 2.51 | 0.05 | 7.27 | 0.17 | 6.32 | 0.09 | 280.0 | 150.0 | 155.1 | 3.8 | 162.6 | 9.5 | 155.1 | 6.8 |
| Output_1_228 | 4280 | 460 | 1.9 | 0.02 | 2.67 | 0.05 | 7.94 | 0.18 | 7.82 | 0.15 | 300.0 | 160.0 | 155.2 | 4.1 | 168.0 | 12.0 | 155.2 | 6.9 |
| Output_1_286 | 4180 | 666 | 6.9 | 0.02 | 3.97 | 0.05 | 8.68 | 0.17 | 8.14 | 0.15 | 240.0 | 170.0 | 155.4 | 6.1 | 160.0 | 12.0 | 155.4 | 8.3 |
| Output_1_183 | 3462 | 80 | 1.7 | 0.02 | 3.77 | 0.05 | 8.91 | 0.18 | 9.14 | 0.34 | 220.0 | 170.0 | 155.5 | 5.8 | 162.0 | 14.0 | 155.5 | 8.1 |
| Output_1_209 | 3460 | 69 | 1.8 | 0.02 | 4.10 | 0.05 | 9.07 | 0.17 | 9.77 | 0.30 | 260.0 | 180.0 | 155.6 | 6.5 | 164.0 | 14.0 | 155.6 | 8.6 |
| Output_1_57 | 726 | 50 | 1.9 | 0.02 | 5.74 | 0.06 | 19.35 | 0.19 | 17.02 | 0.07 | 520.0 | 340.0 | 155.6 | 8.6 | 183.0 | 30.0 | 155.6 | 10.0 |
| Output_1_124 | 4200 | 158 | 4.1 | 0.02 | 3.92 | 0.05 | 8.80 | 0.18 | 8.52 | 0.26 | 300.0 | 180.0 | 155.8 | 6.1 | 163.0 | 13.0 | 155.8 | 8.3 |
| Output_1_245 | 6390 | 273 | 3.1 | 0.02 | 3.92 | 0.05 | 6.24 | 0.16 | 6.83 | 0.37 | 100.0 | 120.0 | 155.9 | 6.0 | 151.0 | 9.3 | 155.9 | 8.2 |
| Output_1_49 | 2706 | 133 | 2.0 | 0.02 | 3.43 | 0.05 | 9.57 | 0.17 | 9.41 | 0.05 | 150.0 | 180.0 | 155.9 | 5.3 | 158.0 | 14.0 | 155.9 | 7.7 |
| Output_1_284 | 4750 | 403 | 2.4 | 0.02 | 2.90 | 0.05 | 6.24 | 0.17 | 6.55 | 0.23 | 190.0 | 130.0 | 155.9 | 4.4 | 158.6 | 9.4 | 155.9 | 7.2 |
| Output_1_41 | 4640 | 184 | 2.3 | 0.02 | 2.69 | 0.05 | 7.26 | 0.17 | 8.43 | 0.43 | 200.0 | 140.0 | 155.9 | 4.2 | 157.0 | 12.0 | 155.9 | 7.0 |
| Output_1_127 | 1000 | 42 | 4.1 | 0.02 | 4.90 | 0.05 | 18.87 | 0.18 | 18.58 | 0.11 | 210.0 | 340.0 | 155.9 | 7.6 | 164.0 | 29.0 | 155.9 | 9.4 |
| Output_1_123 | 2603 | 95 | 2.2 | 0.02 | 3.10 | 0.05 | 13.38 | 0.17 | 12.35 | 0.10 | 220.0 | 240.0 | 155.9 | 4.8 | 160.0 | 19.0 | 155.9 | 7.4 |
| Output_1_208 | 1424 | 27 | 1.5 | 0.02 | 4.90 | 0.05 | 13.18 | 0.18 | 12.15 | 0.07 | 270.0 | 250.0 | 156.1 | 7.5 | 166.0 | 19.0 | 156.1 | 9.4 |
| Output_1_3 | 13860 | 1755 | 2.7 | 0.02 | 1.55 | 0.05 | 4.60 | 0.18 | 4.13 | 0.10 | 274.0 | 96.0 | 156.1 | 2.4 | 165.9 | 6.5 | 156.1 | 6.1 |
| Output_1_299 | 2921 | 48 | 2.3 | 0.02 | 3.14 | 0.06 | 8.30 | 0.19 | 8.47 | 0.15 | 370.0 | 170.0 | 156.2 | 4.8 | 174.0 | 13.0 | 156.2 | 7.4 |
| Output_1_197 | 2909 | 44 | 1.2 | 0.02 | 3.91 | 0.05 | 10.38 | 0.18 | 10.56 | 0.23 | 250.0 | 200.0 | 156.3 | 6.0 | 166.0 | 16.0 | 156.3 | 8.2 |
| Output_1_221 | 2965 | 158 | 2.9 | 0.02 | 4.49 | 0.05 | 9.16 | 0.18 | 9.60 | 0.14 | 270.0 | 170.0 | 156.3 | 6.6 | 164.0 | 14.0 | 156.3 | 8.7 |
| Output_1_25 | 1983 | 80 | 2.4 | 0.02 | 3.95 | 0.05 | 14.08 | 0.17 | 14.12 | 0.14 | 190.0 | 260.0 | 156.4 | 6.1 | 157.0 | 21.0 | 156.4 | 8.3 |
| Output_1_116 | 6080 | 153 | 1.4 | 0.02 | 2.73 | 0.05 | 6.79 | 0.17 | 7.14 | 0.15 | 200.0 | 130.0 | 156.4 | 4.2 | 157.0 | 10.0 | 156.4 | 7.0 |
| Output_1_266 | 12060 | 411 | 1.0 | 0.02 | 1.99 | 0.05 | 6.48 | 0.16 | 6.75 | 0.36 | 40.0 | 120.0 | 156.6 | 3.1 | 152.6 | 9.7 | 156.6 | 6.4 |
| Output_1_282 | 9090 | 508 | 0.9 | 0.02 | 2.60 | 0.05 | 5.62 | 0.17 | 5.62 | 0.17 | 180.0 | 110.0 | 156.7 | 4.0 | 160.9 | 8.5 | 156.7 | 6.9 |
| Output_1_89 | 7110 | 98 | 1.3 | 0.02 | 2.52 | 0.05 | 7.47 | 0.17 | 6.40 | 0.03 | 250.0 | 140.0 | 156.8 | 3.9 | 160.8 | 9.9 | 156.8 | 6.9 |
| Output_1_217 | 3070 | 107 | 1.4 | 0.02 | 3.04 | 0.05 | 10.80 | 0.16 | 10.43 | 0.08 | 20.0 | 190.0 | 157.0 | 4.7 | 154.0 | 14.0 | 157.0 | 7.4 |
| Output_1_72 | 8500 | 223 | 2.1 | 0.02 | 3.28 | 0.05 | 5.92 | 0.16 | 5.77 | 0.31 | 180.0 | 120.0 | 157.0 | 5.1 | 154.2 | 8.3 | 157.0 | 7.6 |
| Output_1_101 | 2517 | 37 | 2.2 | 0.02 | 4.45 | 0.05 | 11.61 | 0.17 | 12.64 | 0.07 | 200.0 | 220.0 | 157.0 | 7.0 | 160.0 | 19.0 | 157.0 | 9.0 |
| Output_1_238 | 4090 | 209 | 1.7 | 0.02 | 3.57 | 0.05 | 10.06 | 0.17 | 9.58 | 0.04 | 100.0 | 180.0 | 157.1 | 5.5 | 160.0 | 14.0 | 157.1 | 7.9 |
| Output_1_255 | 1612 | 67 | 1.9 | 0.02 | 3.40 | 0.05 | 12.99 | 0.19 | 12.11 | 0.16 | 430.0 | 240.0 | 157.1 | 5.3 | 180.0 | 19.0 | 157.1 | 7.8 |
| Output_1_230 | 1135 | 132 | 1.8 | 0.02 | 3.60 | 0.05 | 19.21 | 0.16 | 18.01 | 0.04 | 30.0 | 310.0 | 157.2 | 5.6 | 147.0 | 25.0 | 157.2 | 8.0 |
| Output_1_35 | 2369 | 83 | 2.3 | 0.02 | 3.97 | 0.05 | 12.60 | 0.16 | 12.20 | 0.04 | 180.0 | 230.0 | 157.2 | 6.2 | 153.0 | 17.0 | 157.2 | 8.4 |
| Output_1_22 | 2640 | 119 | 2.3 | 0.02 | 3.84 | 0.05 | 10.40 | 0.18 | 8.99 | 0.14 | 240.0 | 190.0 | 157.3 | 6.0 | 165.0 | 13.0 | 157.3 | 8.2 |
| Output_1_56 | 8750 | 587 | 2.5 | 0.02 | 2.95 | 0.05 | 5.35 | 0.18 | 5.41 | 0.23 | 280.0 | 110.0 | 157.4 | 4.6 | 169.9 | 8.7 | 157.4 | 7.3 |
| Output_1_223 | 5710 | 406 | 3.8 | 0.02 | 3.55 | 0.05 | 6.54 | 0.17 | 7.14 | 0.29 | 120.0 | 130.0 | 157.7 | 5.5 | 157.0 | 10.0 | 157.7 | 7.9 |
| Output_1_159 | 2605 | 64 | 8.2 | 0.02 | 3.63 | 0.05 | 9.27 | 0.17 | 8.88 | 0.08 | 190.0 | 180.0 | 157.7 | 5.7 | 157.0 | 13.0 | 157.7 | 8.0 |
| Output_1_234 | 5430 | 330 | 3.3 | 0.02 | 3.47 | 0.06 | 7.30 | 0.19 | 7.73 | 0.33 | 430.0 | 160.0 | 157.9 | 5.4 | 179.0 | 12.0 | 157.9 | 7.8 |

| | | | | | | | | | | | | | | | | | | |
|---|---|---|---|---|---|---|---|---|---|---|---|---|---|---|---|---|---|---|
| Output_1_15 | 4080 | 277 | 2.4 | 0.02 | 3.06 | 0.05 | 9.45 | 0.18 | 8.84 | 0.18 | 270.0 | 180.0 | 158.0 | 4.8 | 168.0 | 14.0 | 158.0 | 7.4 |
| Output_1_103 | 3670 | 58 | 1.6 | 0.02 | 3.10 | 0.05 | 7.63 | 0.16 | 7.50 | 0.07 | 110.0 | 150.0 | 158.1 | 4.8 | 150.0 | 11.0 | 158.1 | 7.5 |
| Output_1_179 | 12670 | 322 | 1.6 | 0.02 | 2.74 | 0.05 | 4.41 | 0.17 | 4.02 | 0.29 | 182.0 | 89.0 | 158.2 | 4.3 | 160.5 | 6.0 | 158.2 | 7.1 |
| Output_1_201 | 3540 | 54 | 1.2 | 0.02 | 3.46 | 0.05 | 7.74 | 0.18 | 8.24 | 0.36 | 320.0 | 150.0 | 158.2 | 5.4 | 173.0 | 13.0 | 158.2 | 7.9 |
| Output_1_7 | 3122 | 345 | 1.9 | 0.02 | 3.30 | 0.05 | 10.36 | 0.17 | 9.83 | 0.04 | 180.0 | 200.0 | 158.4 | 5.1 | 160.0 | 15.0 | 158.4 | 7.7 |
| Output_1_114 | 1639 | 37 | 1.2 | 0.03 | 4.80 | 0.05 | 13.39 | 0.17 | 14.97 | 0.28 | 110.0 | 240.0 | 158.9 | 7.3 | 157.0 | 21.0 | 158.9 | 9.3 |
| Output_1_34 | 5320 | 184 | 2.2 | 0.02 | 2.36 | 0.05 | 7.33 | 0.17 | 7.51 | 0.37 | 160.0 | 140.0 | 158.9 | 3.7 | 163.0 | 12.0 | 158.9 | 6.8 |
| Output_1_147 | 10370 | 357 | 8.8 | 0.02 | 3.45 | 0.05 | 5.77 | 0.17 | 5.44 | 0.41 | 210.0 | 120.0 | 158.9 | 5.4 | 161.3 | 8.2 | 158.9 | 7.9 |
| Output_1_120 | 2510 | 76 | 3.2 | 0.02 | 3.93 | 0.05 | 10.43 | 0.19 | 10.81 | 0.27 | 310.0 | 200.0 | 158.9 | 6.2 | 173.0 | 17.0 | 158.9 | 8.4 |
| Output_1_298 | 5100 | 86 | 2.3 | 0.03 | 4.40 | 0.05 | 7.33 | 0.17 | 8.24 | 0.44 | 140.0 | 140.0 | 159.0 | 6.7 | 158.0 | 12.0 | 159.0 | 8.8 |
| Output_1_31 | 14800 | 517 | 1.3 | 0.02 | 1.76 | 0.05 | 4.39 | 0.17 | 3.89 | 0.15 | 185.0 | 91.0 | 159.0 | 2.8 | 161.3 | 5.8 | 159.0 | 6.4 |
| Output_1_251 | 1483 | 63 | 4.6 | 0.03 | 5.20 | 0.06 | 14.79 | 0.18 | 14.84 | 0.23 | 370.0 | 280.0 | 159.1 | 8.1 | 170.0 | 23.0 | 159.1 | 9.9 |
| Output_1_177 | 3520 | 89 | 6.0 | 0.03 | 3.84 | 0.05 | 8.70 | 0.17 | 8.05 | 0.09 | 230.0 | 170.0 | 159.2 | 6.1 | 164.0 | 12.0 | 159.2 | 8.3 |
| Output_1_272 | 2072 | 63 | 2.8 | 0.03 | 3.36 | 0.05 | 11.11 | 0.16 | 10.83 | 0.19 | -40.0 | 180.0 | 159.3 | 5.3 | 146.0 | 15.0 | 159.3 | 7.8 |
| Output_1_235 | 2924 | 170 | 2.7 | 0.03 | 3.04 | 0.05 | 10.78 | 0.17 | 11.05 | 0.10 | 200.0 | 190.0 | 159.3 | 4.8 | 162.0 | 17.0 | 159.3 | 7.5 |
| Output_1_274 | 7790 | 241 | 1.7 | 0.03 | 2.20 | 0.05 | 6.46 | 0.17 | 5.64 | 0.17 | 150.0 | 130.0 | 159.4 | 3.4 | 160.1 | 8.3 | 159.4 | 6.7 |
| Output_1_95 | 6480 | 90 | 1.1 | 0.03 | 2.71 | 0.05 | 5.71 | 0.17 | 5.52 | 0.05 | 230.0 | 120.0 | 159.5 | 4.3 | 160.7 | 8.2 | 159.5 | 7.2 |
| Output_1_168 | 3350 | 81 | 5.2 | 0.03 | 3.19 | 0.05 | 9.02 | 0.18 | 8.52 | 0.10 | 270.0 | 170.0 | 159.5 | 5.0 | 163.0 | 13.0 | 159.5 | 7.6 |
| Output_1_150 | 4600 | 142 | 2.8 | 0.03 | 3.23 | 0.05 | 8.54 | 0.18 | 9.04 | 0.40 | 160.0 | 160.0 | 159.8 | 5.1 | 166.0 | 13.0 | 159.8 | 7.7 |
| Output_1_182 | 7140 | 165 | 1.5 | 0.03 | 2.55 | 0.05 | 6.47 | 0.18 | 6.74 | 0.21 | 230.0 | 130.0 | 159.9 | 4.0 | 166.0 | 10.0 | 159.9 | 7.0 |
| Output_1_73 | 4820 | 114 | 2.7 | 0.03 | 2.39 | 0.05 | 7.28 | 0.18 | 7.10 | 0.11 | 330.0 | 140.0 | 159.9 | 3.8 | 169.0 | 12.0 | 159.9 | 6.9 |
| Output_1_60 | 2156 | 147 | 1.7 | 0.03 | 2.99 | 0.06 | 10.99 | 0.18 | 11.05 | 0.02 | 390.0 | 210.0 | 159.9 | 4.7 | 174.0 | 17.0 | 159.9 | 7.4 |
| Output_1_247 | 6210 | 261 | 1.2 | 0.03 | 3.06 | 0.05 | 7.38 | 0.16 | 6.88 | 0.04 | 90.0 | 140.0 | 160.0 | 4.9 | 150.0 | 9.4 | 160.0 | 7.5 |
| Output_1_157 | 2786 | 69 | 2.5 | 0.03 | 3.18 | 0.05 | 9.26 | 0.17 | 9.77 | 0.23 | 170.0 | 170.0 | 160.0 | 5.0 | 164.0 | 14.0 | 160.0 | 7.7 |
| Output_1_62 | 2599 | 153 | 1.9 | 0.03 | 3.30 | 0.05 | 8.17 | 0.19 | 7.49 | 0.19 | 240.0 | 160.0 | 160.0 | 5.2 | 173.0 | 12.0 | 160.0 | 7.8 |
| Output_1_139 | 3950 | 182 | 1.2 | 0.03 | 2.35 | 0.05 | 10.50 | 0.17 | 10.24 | 0.10 | 100.0 | 190.0 | 160.1 | 3.7 | 154.0 | 15.0 | 160.1 | 6.9 |
| Output_1_24 | 16600 | 678 | 1.1 | 0.03 | 2.18 | 0.05 | 3.51 | 0.17 | 3.40 | 0.30 | 123.0 | 70.0 | 160.4 | 3.4 | 162.4 | 5.1 | 160.4 | 6.7 |
| Output_1_68 | 2596 | 97 | 1.2 | 0.03 | 3.69 | 0.05 | 11.67 | 0.17 | 10.84 | 0.10 | 200.0 | 220.0 | 160.4 | 5.9 | 157.0 | 15.0 | 160.4 | 8.2 |
| Output_1_43 | 5700 | 231 | 1.4 | 0.03 | 2.10 | 0.05 | 6.19 | 0.18 | 6.08 | 0.08 | 250.0 | 130.0 | 160.4 | 3.4 | 168.3 | 9.4 | 160.4 | 6.7 |
| Output_1_226 | 2332 | 209 | 1.8 | 0.03 | 4.35 | 0.04 | 12.35 | 0.16 | 12.74 | 0.11 | -90.0 | 210.0 | 161.1 | 6.9 | 146.0 | 17.0 | 161.1 | 9.0 |
| Output_1_134 | 3010 | 144 | 1.9 | 0.03 | 3.75 | 0.04 | 10.32 | 0.16 | 10.76 | 0.27 | -30.0 | 180.0 | 161.1 | 5.9 | 148.0 | 15.0 | 161.1 | 8.3 |
| Output_1_148 | 9080 | 297 | 1.5 | 0.03 | 2.41 | 0.05 | 6.12 | 0.17 | 6.32 | 0.30 | 140.0 | 120.0 | 161.1 | 3.8 | 162.4 | 9.5 | 161.1 | 6.9 |
| Output_1_30 | 16890 | 604 | 1.9 | 0.03 | 2.25 | 0.05 | 3.73 | 0.18 | 4.16 | 0.18 | 223.0 | 81.0 | 161.4 | 3.6 | 167.8 | 6.4 | 161.4 | 6.8 |
| Output_1_129 | 2448 | 108 | 2.9 | 0.03 | 3.23 | 0.05 | 8.67 | 0.19 | 8.47 | 0.00 | 290.0 | 170.0 | 161.4 | 5.1 | 174.0 | 13.0 | 161.4 | 7.7 |
| Output_1_61 | 3147 | 206 | 2.0 | 0.03 | 2.84 | 0.05 | 9.25 | 0.18 | 8.38 | 0.08 | 250.0 | 180.0 | 161.5 | 4.5 | 168.0 | 14.0 | 161.5 | 7.4 |
| Output_1_240 | 2135 | 97 | 1.5 | 0.03 | 4.72 | 0.05 | 15.52 | 0.17 | 15.57 | 0.03 | 120.0 | 270.0 | 161.7 | 7.7 | 157.0 | 23.0 | 161.7 | 9.6 |
| Output_1_229 | 1243 | 137 | 2.0 | 0.03 | 5.12 | 0.04 | 18.69 | 0.14 | 18.88 | 0.23 | -120.0 | 290.0 | 161.8 | 8.0 | 135.0 | 25.0 | 161.8 | 9.9 |
| Output_1_285 | 2398 | 264 | 6.0 | 0.03 | 4.33 | 0.05 | 12.12 | 0.17 | 12.64 | 0.27 | 210.0 | 230.0 | 161.8 | 6.8 | 160.0 | 19.0 | 161.8 | 8.9 |
| Output_1_96 | 3390 | 47 | 1.0 | 0.03 | 3.46 | 0.05 | 8.74 | 0.19 | 8.11 | 0.08 | 360.0 | 180.0 | 162.0 | 5.5 | 171.0 | 13.0 | 162.0 | 8.0 |
| Output_1_210 | 3930 | 77 | 1.5 | 0.03 | 3.42 | 0.05 | 8.51 | 0.17 | 8.09 | 0.06 | 190.0 | 170.0 | 162.1 | 5.5 | 161.0 | 12.0 | 162.1 | 8.0 |

| | | | | | | | | | | | | | | | | | | |
|---|---|---|---|---|---|---|---|---|---|---|---|---|---|---|---|---|---|---|
| Output_1_254 | 6780 | 269 | 1.5 | 0.03 | 3.85 | 0.05 | 6.79 | 0.17 | 8.38 | 0.56 | 80.0 | 130.0 | 162.2 | 6.1 | 160.0 | 12.0 | 162.2 | 8.5 |
| Output_1_13 | 1752 | 130 | 3.3 | 0.03 | 3.77 | 0.05 | 12.17 | 0.18 | 11.93 | 0.03 | 150.0 | 230.0 | 162.2 | 6.0 | 165.0 | 19.0 | 162.2 | 8.4 |
| Output_1_214 | 3454 | 91 | 1.7 | 0.03 | 2.55 | 0.05 | 7.98 | 0.19 | 7.81 | 0.18 | 350.0 | 170.0 | 162.2 | 4.1 | 179.0 | 14.0 | 162.2 | 7.1 |
| Output_1_48 | 7990 | 367 | 1.6 | 0.03 | 2.27 | 0.05 | 6.86 | 0.18 | 6.63 | 0.31 | 230.0 | 140.0 | 162.3 | 3.6 | 168.0 | 11.0 | 162.3 | 6.9 |
| Output_1_133 | 1482 | 71 | 2.3 | 0.03 | 3.92 | 0.06 | 15.09 | 0.19 | 15.26 | 0.27 | 290.0 | 280.0 | 162.3 | 6.6 | 179.0 | 26.0 | 162.3 | 8.8 |
| Output_1_33 | 4710 | 160 | 2.3 | 0.03 | 2.55 | 0.05 | 6.74 | 0.19 | 6.70 | 0.06 | 380.0 | 140.0 | 162.3 | 4.1 | 179.0 | 11.0 | 162.3 | 7.1 |
| Output_1_162 | 2840 | 67 | 2.1 | 0.03 | 3.92 | 0.06 | 10.25 | 0.19 | 9.95 | 0.01 | 400.0 | 200.0 | 162.3 | 6.3 | 180.0 | 16.0 | 162.3 | 8.6 |
| Output_1_181 | 2810 | 67 | 2.3 | 0.03 | 3.25 | 0.05 | 10.34 | 0.19 | 9.52 | 0.05 | 350.0 | 200.0 | 162.4 | 5.2 | 176.0 | 16.0 | 162.4 | 7.8 |
| Output_1_97 | 3950 | 53 | 1.3 | 0.03 | 3.56 | 0.05 | 9.24 | 0.17 | 9.30 | 0.15 | 160.0 | 180.0 | 162.5 | 5.8 | 160.0 | 14.0 | 162.5 | 8.2 |
| Output_1_77 | 2051 | 39 | 2.0 | 0.03 | 3.91 | 0.05 | 12.11 | 0.17 | 11.70 | 0.09 | 150.0 | 220.0 | 163.0 | 6.6 | 160.0 | 18.0 | 163.0 | 8.8 |
| Output_1_111 | 2965 | 56 | 1.7 | 0.03 | 3.20 | 0.05 | 12.55 | 0.18 | 11.17 | 0.04 | 260.0 | 230.0 | 163.3 | 5.2 | 165.0 | 17.0 | 163.3 | 7.8 |
| Output_1_188 | 3270 | 62 | 2.2 | 0.03 | 3.66 | 0.05 | 10.40 | 0.17 | 10.47 | 0.07 | 130.0 | 190.0 | 163.5 | 5.9 | 159.0 | 16.0 | 163.5 | 8.4 |
| Output_1_118 | 1226 | 33 | 2.0 | 0.03 | 5.06 | 0.05 | 18.27 | 0.17 | 16.57 | 0.23 | 200.0 | 320.0 | 163.6 | 8.4 | 158.0 | 24.0 | 163.6 | 10.0 |
| Output_1_27 | 2200 | 80 | 2.8 | 0.03 | 2.68 | 0.05 | 11.65 | 0.18 | 10.86 | 0.14 | 140.0 | 210.0 | 163.8 | 4.4 | 162.0 | 17.0 | 163.8 | 7.3 |
| Output_1_193 | 4320 | 69 | 4.3 | 0.03 | 2.72 | 0.05 | 9.69 | 0.17 | 9.20 | 0.02 | 120.0 | 180.0 | 163.9 | 4.4 | 162.0 | 14.0 | 163.9 | 7.4 |
| Output_1_170 | 2755 | 65 | 3.3 | 0.03 | 3.88 | 0.05 | 9.25 | 0.19 | 9.04 | 0.12 | 290.0 | 180.0 | 163.9 | 6.4 | 178.0 | 15.0 | 163.9 | 8.7 |
| Output_1_218 | 2883 | 105 | 5.1 | 0.03 | 3.35 | 0.05 | 8.66 | 0.18 | 9.66 | 0.28 | 140.0 | 170.0 | 165.1 | 5.5 | 164.0 | 15.0 | 165.1 | 8.1 |
| Output_1_166 | 18810 | 431 | 1.2 | 0.03 | 1.66 | 0.05 | 3.91 | 0.18 | 3.83 | 0.21 | 233.0 | 83.0 | 165.2 | 2.7 | 170.1 | 6.0 | 165.2 | 6.5 |
| Output_1_280 | 1567 | 55 | 1.8 | 0.03 | 5.00 | 0.05 | 15.46 | 0.17 | 15.79 | 0.25 | 50.0 | 270.0 | 165.4 | 7.9 | 160.0 | 24.0 | 165.4 | 9.9 |
| Output_1_276 | 5201 | 156 | 2.6 | 0.03 | 2.81 | 0.05 | 7.39 | 0.19 | 7.94 | 0.28 | 210.0 | 140.0 | 165.4 | 4.6 | 174.0 | 13.0 | 165.4 | 7.5 |
| Output_1_126 | 1212 | 45 | 3.8 | 0.03 | 5.00 | 0.05 | 16.14 | 0.21 | 17.62 | 0.40 | 230.0 | 290.0 | 165.6 | 8.5 | 187.0 | 30.0 | 165.6 | 10.0 |
| Output_1_212 | 3460 | 79 | 1.5 | 0.03 | 3.03 | 0.05 | 10.72 | 0.16 | 10.49 | 0.01 | -10.0 | 180.0 | 165.7 | 4.9 | 151.0 | 14.0 | 165.7 | 7.7 |
| Output_1_138 | 2710 | 120 | 1.1 | 0.03 | 3.85 | 0.05 | 9.74 | 0.19 | 10.58 | 0.14 | 240.0 | 190.0 | 165.7 | 6.6 | 174.0 | 17.0 | 165.7 | 8.9 |
| Output_1_8 | 2096 | 207 | 2.2 | 0.03 | 3.65 | 0.05 | 12.07 | 0.19 | 11.86 | 0.11 | 330.0 | 220.0 | 165.7 | 6.0 | 178.0 | 20.0 | 165.7 | 8.4 |
| Output_1_211 | 3800 | 79 | 2.2 | 0.03 | 3.30 | 0.05 | 9.61 | 0.17 | 8.67 | 0.17 | 160.0 | 170.0 | 165.8 | 5.4 | 161.0 | 13.0 | 165.8 | 8.1 |
| Output_1_106 | 834 | 13 | 1.9 | 0.03 | 5.36 | 0.06 | 21.82 | 0.19 | 21.39 | 0.24 | 220.0 | 380.0 | 165.8 | 8.9 | 171.0 | 35.0 | 165.8 | 11.0 |
| Output_1_241 | 4760 | 211 | 1.9 | 0.03 | 2.95 | 0.05 | 7.36 | 0.18 | 7.10 | 0.09 | 260.0 | 150.0 | 166.0 | 4.8 | 169.0 | 11.0 | 166.0 | 7.7 |
| Output_1_153 | 3570 | 94 | 3.2 | 0.03 | 2.84 | 0.06 | 7.09 | 0.20 | 6.15 | 0.03 | 420.0 | 140.0 | 166.5 | 4.5 | 183.0 | 11.0 | 166.5 | 7.3 |
| Output_1_99 | 4130 | 57 | 2.1 | 0.03 | 4.20 | 0.05 | 9.81 | 0.18 | 8.84 | 0.06 | 240.0 | 190.0 | 166.6 | 6.9 | 170.0 | 14.0 | 166.6 | 9.2 |
| Output_1_69 | 2479 | 80 | 1.6 | 0.03 | 3.82 | 0.05 | 9.63 | 0.18 | 8.89 | 0.01 | 130.0 | 180.0 | 166.7 | 6.3 | 171.0 | 13.0 | 166.7 | 8.7 |
| Output_1_265 | 2479 | 79 | 2.1 | 0.03 | 4.20 | 0.05 | 11.29 | 0.18 | 10.73 | 0.05 | 150.0 | 200.0 | 166.7 | 6.6 | 164.0 | 16.0 | 166.7 | 8.9 |
| Output_1_175 | 3820 | 93 | 3.9 | 0.03 | 3.43 | 0.05 | 9.84 | 0.20 | 9.50 | 0.04 | 340.0 | 190.0 | 166.8 | 5.6 | 184.0 | 16.0 | 166.8 | 8.2 |
| Output_1_32 | 9710 | 318 | 2.7 | 0.03 | 2.67 | 0.05 | 4.67 | 0.18 | 4.95 | 0.37 | 169.0 | 98.0 | 167.1 | 4.4 | 169.1 | 7.7 | 167.1 | 7.4 |
| Output_1_36 | 5190 | 174 | 2.3 | 0.03 | 3.50 | 0.05 | 8.80 | 0.18 | 8.15 | 0.12 | 190.0 | 170.0 | 167.1 | 5.8 | 170.0 | 13.0 | 167.1 | 8.3 |
| Output_1_192 | 8340 | 134 | 2.2 | 0.03 | 2.13 | 0.05 | 5.64 | 0.17 | 5.75 | 0.30 | 90.0 | 110.0 | 167.3 | 3.5 | 162.4 | 8.7 | 167.3 | 7.0 |
| Output_1_82 | 3036 | 45 | 1.4 | 0.03 | 3.42 | 0.05 | 9.75 | 0.17 | 9.36 | 0.03 | 140.0 | 180.0 | 167.5 | 5.6 | 161.0 | 14.0 | 167.5 | 8.2 |
| Output_1_246 | 2324 | 91 | 1.9 | 0.03 | 3.79 | 0.05 | 11.90 | 0.18 | 11.67 | 0.03 | 200.0 | 210.0 | 167.7 | 6.5 | 166.0 | 18.0 | 167.7 | 8.9 |
| Output_1_262 | 5980 | 211 | 1.8 | 0.03 | 2.88 | 0.05 | 7.25 | 0.19 | 7.53 | 0.27 | 250.0 | 140.0 | 167.9 | 4.8 | 172.0 | 12.0 | 167.9 | 7.7 |
| Output_1_291 | 4690 | 644 | 1.9 | 0.03 | 3.14 | 0.05 | 8.76 | 0.17 | 8.82 | 0.07 | 40.0 | 160.0 | 168.0 | 5.2 | 160.0 | 12.0 | 168.0 | 8.0 |
| Output_1_244 | 841 | 34 | 2.6 | 0.03 | 7.20 | 0.05 | 20.41 | 0.18 | 20.99 | 0.14 | 120.0 | 350.0 | 168.0 | 12.0 | 166.0 | 33.0 | 168.0 | 13.0 |

| | | | | | | | | | | | | | | | | | | |
|---|---|---|---|---|---|---|---|---|---|---|---|---|---|---|---|---|---|---|
| Output_1_249 | 2530 | 101 | 3.4 | 0.03 | 4.55 | 0.05 | 9.25 | 0.18 | 10.73 | 0.30 | 130.0 | 190.0 | 168.0 | 7.6 | 164.0 | 16.0 | 168.0 | 9.7 |
| Output_1_2 | 3430 | 401 | 1.8 | 0.03 | 3.21 | 0.05 | 8.59 | 0.18 | 8.15 | 0.19 | 150.0 | 150.0 | 168.4 | 5.3 | 171.0 | 13.0 | 168.4 | 8.1 |
| Output_1_279 | 12620 | 410 | 4.5 | 0.03 | 3.36 | 0.05 | 4.48 | 0.19 | 5.03 | 0.48 | 236.0 | 95.0 | 168.4 | 5.6 | 173.5 | 8.0 | 168.4 | 8.2 |
| Output_1_122 | 4123 | 131 | 1.6 | 0.03 | 3.77 | 0.05 | 8.54 | 0.20 | 8.63 | 0.36 | 290.0 | 160.0 | 168.4 | 6.6 | 183.0 | 14.0 | 168.4 | 8.9 |
| Output_1_222 | 4950 | 299 | 3.1 | 0.03 | 3.77 | 0.05 | 7.68 | 0.18 | 8.20 | 0.34 | 150.0 | 150.0 | 168.7 | 6.4 | 169.0 | 12.0 | 168.7 | 8.8 |
| Output_1_250 | 2044 | 80 | 2.9 | 0.03 | 4.49 | 0.05 | 11.18 | 0.18 | 11.60 | 0.27 | 250.0 | 210.0 | 169.8 | 7.8 | 172.0 | 18.0 | 169.8 | 9.9 |
| Output_1_169 | 1339 | 31 | 3.2 | 0.03 | 5.24 | 0.05 | 16.48 | 0.20 | 15.15 | 0.04 | 260.0 | 300.0 | 170.0 | 8.5 | 179.0 | 26.0 | 170.0 | 10.0 |
| Output_1_21 | 6580 | 291 | 1.9 | 0.03 | 2.84 | 0.05 | 6.57 | 0.19 | 6.38 | 0.08 | 200.0 | 130.0 | 170.2 | 4.8 | 175.0 | 10.0 | 170.2 | 7.8 |
| Output_1_55 | 28820 | 1723 | 0.4 | 0.03 | 1.46 | 0.05 | 2.99 | 0.19 | 2.95 | 0.29 | 205.0 | 67.0 | 170.5 | 2.4 | 173.2 | 4.7 | 170.5 | 6.6 |
| Output_1_294 | 2686 | 66 | 2.4 | 0.03 | 3.54 | 0.05 | 12.83 | 0.18 | 11.36 | 0.02 | -10.0 | 200.0 | 170.8 | 6.0 | 162.0 | 17.0 | 170.8 | 8.6 |
| Output_1_20 | 2027 | 96 | 3.3 | 0.03 | 3.72 | 0.04 | 14.57 | 0.17 | 14.12 | 0.04 | 40.0 | 250.0 | 171.3 | 6.3 | 163.0 | 21.0 | 171.3 | 8.8 |
| Output_1_233 | 10430 | 622 | 1.6 | 0.03 | 1.67 | 0.05 | 6.04 | 0.19 | 6.35 | 0.31 | 290.0 | 120.0 | 171.5 | 2.8 | 176.0 | 10.0 | 171.5 | 6.8 |
| Output_1_167 | 17050 | 379 | 2.3 | 0.03 | 1.52 | 0.05 | 5.14 | 0.18 | 5.04 | 0.14 | 150.0 | 110.0 | 171.7 | 2.5 | 171.5 | 8.0 | 171.7 | 6.7 |
| Output_1_239 | 10220 | 463 | 2.2 | 0.03 | 3.37 | 0.05 | 4.99 | 0.18 | 6.52 | 0.48 | 200.0 | 100.0 | 171.8 | 5.7 | 171.0 | 10.0 | 171.8 | 8.4 |
| Output_1_243 | 3870 | 157 | 2.8 | 0.03 | 3.28 | 0.05 | 8.70 | 0.19 | 8.56 | 0.20 | 260.0 | 170.0 | 172.5 | 5.6 | 173.0 | 14.0 | 172.5 | 8.4 |
| Output_1_236 | 25900 | 1308 | 2.8 | 0.03 | 1.88 | 0.05 | 3.39 | 0.19 | 3.90 | 0.45 | 196.0 | 70.0 | 172.6 | 3.2 | 174.8 | 6.4 | 172.6 | 7.0 |
| Output_1_273 | 6350 | 181 | 1.7 | 0.03 | 3.05 | 0.05 | 7.14 | 0.19 | 6.91 | 0.02 | 170.0 | 140.0 | 172.8 | 5.2 | 174.0 | 11.0 | 172.8 | 8.1 |
| Output_1_252 | 5160 | 194 | 1.6 | 0.03 | 2.61 | 0.05 | 7.56 | 0.19 | 7.22 | 0.04 | 270.0 | 150.0 | 172.8 | 4.4 | 179.0 | 12.0 | 172.8 | 7.6 |
| Output_1_10 | 3630 | 320 | 2.4 | 0.03 | 3.01 | 0.05 | 10.80 | 0.20 | 10.26 | 0.00 | 260.0 | 200.0 | 173.3 | 5.1 | 179.0 | 17.0 | 173.3 | 8.1 |
| Output_1_260 | 10930 | 392 | 0.7 | 0.03 | 3.63 | 0.05 | 5.79 | 0.20 | 6.37 | 0.39 | 350.0 | 120.0 | 173.6 | 6.2 | 187.0 | 11.0 | 173.6 | 8.8 |
| Output_1_88 | 4530 | 59 | 2.8 | 0.03 | 3.58 | 0.05 | 8.02 | 0.20 | 7.11 | 0.08 | 280.0 | 160.0 | 173.8 | 6.1 | 183.0 | 12.0 | 173.8 | 8.8 |
| Output_1_165 | 5550 | 118 | 2.7 | 0.03 | 2.62 | 0.05 | 7.23 | 0.19 | 5.41 | 0.15 | 130.0 | 140.0 | 174.7 | 4.5 | 172.0 | 8.9 | 174.7 | 7.7 |
| Output_1_9 | 3410 | 311 | 2.1 | 0.03 | 2.33 | 0.05 | 10.39 | 0.20 | 9.23 | 0.06 | 190.0 | 190.0 | 174.9 | 4.0 | 181.0 | 15.0 | 174.9 | 7.5 |
| Output_1_202 | 2976 | 41 | 1.3 | 0.03 | 3.52 | 0.05 | 12.02 | 0.19 | 12.37 | 0.24 | 140.0 | 220.0 | 175.3 | 6.1 | 177.0 | 20.0 | 175.3 | 8.8 |
| Output_1_52 | 7580 | 395 | 0.9 | 0.03 | 2.13 | 0.05 | 6.12 | 0.19 | 5.88 | 0.12 | 140.0 | 120.0 | 176.1 | 3.7 | 173.3 | 9.3 | 176.1 | 7.3 |
| Output_1_16 | 7500 | 421 | 1.7 | 0.03 | 2.13 | 0.05 | 6.36 | 0.19 | 5.70 | 0.02 | 210.0 | 130.0 | 176.3 | 3.7 | 180.1 | 9.5 | 176.3 | 7.3 |
| Output_1_83 | 11940 | 164 | 2.0 | 0.03 | 2.81 | 0.05 | 5.24 | 0.19 | 5.16 | 0.15 | 160.0 | 110.0 | 176.4 | 4.9 | 172.7 | 8.2 | 176.4 | 8.0 |
| Output_1_215 | 8140 | 213 | 1.2 | 0.03 | 2.77 | 0.05 | 5.75 | 0.19 | 5.67 | 0.41 | 200.0 | 120.0 | 176.4 | 4.8 | 179.7 | 9.6 | 176.4 | 8.0 |
| Output_1_187 | 8970 | 163 | 1.2 | 0.03 | 1.94 | 0.05 | 5.73 | 0.21 | 5.29 | 0.08 | 290.0 | 120.0 | 176.9 | 3.4 | 191.1 | 8.9 | 176.9 | 7.2 |
| Output_1_195 | 5250 | 74 | 1.9 | 0.03 | 2.77 | 0.05 | 8.57 | 0.21 | 8.78 | 0.11 | 300.0 | 170.0 | 177.0 | 4.8 | 188.0 | 15.0 | 177.0 | 8.0 |
| Output_1_227 | 4180 | 380 | 2.3 | 0.03 | 2.90 | 0.05 | 9.18 | 0.20 | 9.41 | 0.16 | 220.0 | 180.0 | 177.5 | 5.1 | 189.0 | 16.0 | 177.5 | 8.1 |
| Output_1_79 | 2208 | 36 | 2.0 | 0.03 | 3.93 | 0.05 | 9.67 | 0.19 | 9.38 | 0.21 | 240.0 | 180.0 | 177.7 | 7.0 | 177.0 | 15.0 | 177.7 | 9.4 |
| Output_1_270 | 6510 | 181 | 1.7 | 0.03 | 2.68 | 0.05 | 6.17 | 0.18 | 6.18 | 0.09 | 20.0 | 120.0 | 177.8 | 4.7 | 165.5 | 9.1 | 177.8 | 7.9 |
| Output_1_190 | 3510 | 57 | 1.9 | 0.03 | 3.47 | 0.05 | 9.09 | 0.20 | 8.96 | 0.05 | 250.0 | 180.0 | 177.9 | 6.1 | 187.0 | 15.0 | 177.9 | 8.8 |
| Output_1_19 | 2866 | 135 | 2.3 | 0.03 | 3.20 | 0.05 | 11.06 | 0.19 | 10.88 | 0.05 | 100.0 | 200.0 | 178.6 | 5.6 | 177.0 | 18.0 | 178.6 | 8.5 |
| Output_1_37 | 7010 | 223 | 2.4 | 0.03 | 2.49 | 0.05 | 6.83 | 0.20 | 6.63 | 0.21 | 190.0 | 140.0 | 178.6 | 4.4 | 181.0 | 11.0 | 178.6 | 7.8 |
| Output_1_17 | 4130 | 216 | 2.0 | 0.03 | 3.39 | 0.05 | 10.04 | 0.19 | 9.14 | 0.13 | 80.0 | 180.0 | 179.9 | 6.0 | 172.0 | 14.0 | 179.9 | 8.8 |
| Output_1_156 | 4567 | 102 | 1.6 | 0.03 | 3.07 | 0.05 | 8.96 | 0.20 | 9.60 | 0.21 | 140.0 | 170.0 | 180.3 | 5.5 | 182.0 | 16.0 | 180.3 | 8.5 |
| Output_1_203 | 5380 | 74 | 1.7 | 0.03 | 2.96 | 0.05 | 8.41 | 0.20 | 8.08 | 0.18 | 240.0 | 160.0 | 180.5 | 5.3 | 183.0 | 14.0 | 180.5 | 8.4 |
| Output_1_163 | 3930 | 81 | 2.0 | 0.03 | 2.71 | 0.05 | 9.32 | 0.21 | 7.08 | 0.26 | 320.0 | 170.0 | 180.5 | 4.8 | 196.0 | 12.0 | 180.5 | 8.1 |

| | | | | | | | | | | | | | | | | | | |
|---|---|---|---|---|---|---|---|---|---|---|---|---|---|---|---|---|---|---|
| Output_1_86 | 14560 | 185 | 1.9 | 0.03 | 1.94 | 0.05 | 5.33 | 0.20 | 5.47 | 0.05 | 240.0 | 110.0 | 181.2 | 3.4 | 185.5 | 9.3 | 181.2 | 7.1 |
| Output_1_23 | 2951 | 110 | 2.6 | 0.03 | 3.51 | 0.05 | 10.35 | 0.21 | 10.58 | 0.15 | 270.0 | 200.0 | 181.2 | 6.5 | 190.0 | 19.0 | 181.2 | 9.2 |
| Output_1_237 | 6170 | 287 | 0.9 | 0.03 | 1.89 | 0.05 | 4.92 | 0.21 | 4.81 | 0.24 | 320.0 | 110.0 | 181.4 | 3.4 | 192.4 | 8.8 | 181.4 | 7.3 |
| Output_1_91 | 7680 | 91 | 1.6 | 0.03 | 1.99 | 0.05 | 6.42 | 0.20 | 6.40 | 0.01 | 290.0 | 130.0 | 181.7 | 3.5 | 189.0 | 10.0 | 181.7 | 7.4 |
| Output_1_206 | 5430 | 81 | 2.3 | 0.03 | 2.59 | 0.05 | 6.68 | 0.22 | 6.88 | 0.15 | 360.0 | 140.0 | 181.7 | 4.7 | 199.0 | 13.0 | 181.7 | 8.0 |
| Output_1_65 | 6610 | 276 | 1.9 | 0.03 | 2.83 | 0.05 | 6.57 | 0.19 | 6.22 | 0.01 | 150.0 | 130.0 | 181.8 | 5.1 | 178.0 | 11.0 | 181.8 | 8.3 |
| Output_1_146 | 1805 | 57 | 2.4 | 0.03 | 4.88 | 0.05 | 14.17 | 0.21 | 14.01 | 0.02 | 210.0 | 260.0 | 182.2 | 8.6 | 187.0 | 24.0 | 182.2 | 11.0 |
| Output_1_300 | 1386 | 20 | 2.9 | 0.03 | 4.88 | 0.05 | 15.33 | 0.21 | 15.17 | 0.08 | 300.0 | 280.0 | 182.2 | 8.6 | 197.0 | 27.0 | 182.2 | 11.0 |
| Output_1_74 | 9650 | 190 | 1.8 | 0.03 | 2.58 | 0.05 | 5.95 | 0.21 | 5.29 | 0.07 | 300.0 | 130.0 | 182.4 | 4.6 | 190.9 | 9.3 | 182.4 | 8.0 |
| Output_1_295 | 14510 | 281 | 2.2 | 0.03 | 1.81 | 0.05 | 3.88 | 0.21 | 4.51 | 0.34 | 249.0 | 83.0 | 182.9 | 3.2 | 192.2 | 7.8 | 182.9 | 7.3 |
| Output_1_287 | 4530 | 894 | 1.9 | 0.03 | 4.17 | 0.05 | 13.54 | 0.21 | 13.81 | 0.24 | 290.0 | 280.0 | 183.0 | 7.5 | 192.0 | 25.0 | 183.0 | 10.0 |
| Output_1_44 | 9590 | 351 | 1.3 | 0.03 | 2.99 | 0.06 | 8.70 | 0.22 | 8.22 | 0.24 | 410.0 | 180.0 | 183.0 | 5.4 | 203.0 | 16.0 | 183.0 | 8.5 |
| Output_1_84 | 2800 | 36 | 1.6 | 0.03 | 3.03 | 0.05 | 10.25 | 0.20 | 10.05 | 0.15 | 210.0 | 190.0 | 183.2 | 5.6 | 182.0 | 17.0 | 183.2 | 8.8 |
| Output_1_105 | 10260 | 147 | 1.3 | 0.03 | 2.46 | 0.05 | 4.05 | 0.21 | 4.54 | 0.39 | 358.0 | 90.0 | 183.2 | 4.5 | 190.5 | 7.9 | 183.2 | 7.9 |
| Output_1_92 | 3190 | 37 | 1.7 | 0.03 | 3.15 | 0.05 | 9.12 | 0.22 | 9.63 | 0.29 | 350.0 | 170.0 | 183.5 | 5.7 | 198.0 | 18.0 | 183.5 | 8.7 |
| Output_1_242 | 3007 | 115 | 2.3 | 0.03 | 4.50 | 0.05 | 10.69 | 0.19 | 10.11 | 0.16 | 120.0 | 200.0 | 183.9 | 8.0 | 173.0 | 16.0 | 183.9 | 10.0 |
| Output_1_290 | 7800 | 1563 | 1.1 | 0.03 | 2.32 | 0.05 | 5.53 | 0.20 | 5.47 | 0.14 | 230.0 | 120.0 | 183.9 | 4.2 | 185.4 | 9.3 | 183.9 | 7.8 |
| Output_1_178 | 1610 | 36 | 2.4 | 0.03 | 3.42 | 0.05 | 14.10 | 0.22 | 13.43 | 0.09 | 440.0 | 260.0 | 184.0 | 6.2 | 194.0 | 24.0 | 184.0 | 9.1 |
| Output_1_301 | 11070 | 180 | 1.6 | 0.03 | 1.79 | 0.05 | 4.85 | 0.21 | 4.88 | 0.06 | 250.0 | 100.0 | 184.1 | 3.3 | 191.7 | 7.8 | 184.1 | 7.4 |
| Output_1_277 | 3420 | 95 | 2.9 | 0.03 | 2.75 | 0.05 | 8.70 | 0.21 | 8.13 | 0.01 | 290.0 | 180.0 | 184.8 | 5.0 | 194.0 | 14.0 | 184.8 | 8.3 |
| Output_1_253 | 3600 | 126 | 2.2 | 0.03 | 3.12 | 0.05 | 8.15 | 0.20 | 8.37 | 0.24 | 220.0 | 160.0 | 185.1 | 5.7 | 190.0 | 14.0 | 185.1 | 8.8 |
| Output_1_158 | 4860 | 102 | 1.6 | 0.03 | 3.40 | 0.05 | 7.00 | 0.20 | 7.46 | 0.33 | 240.0 | 130.0 | 185.1 | 6.2 | 185.0 | 13.0 | 185.1 | 9.1 |
| Output_1_59 | 5800 | 348 | 1.0 | 0.03 | 3.33 | 0.05 | 6.84 | 0.22 | 6.45 | 0.11 | 350.0 | 140.0 | 185.1 | 6.1 | 200.0 | 12.0 | 185.1 | 9.0 |
| Output_1_198 | 22160 | 288 | 1.1 | 0.03 | 1.61 | 0.05 | 4.35 | 0.22 | 4.59 | 0.22 | 321.0 | 91.0 | 185.4 | 2.9 | 197.9 | 8.3 | 185.4 | 7.3 |
| Output_1_204 | 3509 | 48 | 2.1 | 0.03 | 2.53 | 0.05 | 10.22 | 0.21 | 10.10 | 0.06 | 230.0 | 190.0 | 185.6 | 4.7 | 192.0 | 17.0 | 185.6 | 8.1 |
| Output_1_70 | 4330 | 117 | 0.9 | 0.03 | 1.95 | 0.06 | 8.63 | 0.23 | 8.15 | 0.00 | 490.0 | 170.0 | 185.6 | 3.6 | 213.0 | 16.0 | 185.6 | 7.6 |
| Output_1_149 | 9920 | 273 | 2.0 | 0.03 | 1.95 | 0.05 | 5.95 | 0.21 | 5.77 | 0.07 | 300.0 | 130.0 | 185.8 | 3.5 | 191.0 | 10.0 | 185.8 | 7.6 |
| Output_1_109 | 3760 | 59 | 1.8 | 0.03 | 3.11 | 0.05 | 7.94 | 0.20 | 7.58 | 0.20 | 200.0 | 160.0 | 186.0 | 5.7 | 182.0 | 13.0 | 186.0 | 8.8 |
| Output_1_289 | 9170 | 2452 | 0.9 | 0.03 | 2.39 | 0.05 | 5.37 | 0.21 | 5.69 | 0.25 | 290.0 | 120.0 | 186.4 | 4.4 | 194.0 | 10.0 | 186.4 | 8.0 |
| Output_1_64 | 5590 | 246 | 1.5 | 0.03 | 3.20 | 0.05 | 7.09 | 0.21 | 6.64 | 0.17 | 330.0 | 150.0 | 186.5 | 5.9 | 193.0 | 12.0 | 186.5 | 8.9 |
| Output_1_199 | 1761 | 23 | 1.2 | 0.03 | 4.76 | 0.05 | 15.78 | 0.19 | 15.71 | 0.26 | 20.0 | 260.0 | 186.9 | 8.8 | 173.0 | 25.0 | 186.9 | 11.0 |
| Output_1_102 | 28600 | 365 | 1.1 | 0.03 | 2.45 | 0.05 | 3.84 | 0.21 | 3.67 | 0.41 | 270.0 | 80.0 | 186.9 | 4.5 | 191.0 | 6.3 | 186.9 | 8.1 |
| Output_1_231 | 2302 | 227 | 1.8 | 0.03 | 4.07 | 0.06 | 11.42 | 0.23 | 12.23 | 0.27 | 370.0 | 230.0 | 187.2 | 7.3 | 206.0 | 23.0 | 187.2 | 9.9 |
| Output_1_171 | 12660 | 270 | 1.3 | 0.03 | 2.60 | 0.05 | 6.38 | 0.22 | 6.02 | 0.18 | 370.0 | 130.0 | 187.8 | 4.8 | 198.0 | 11.0 | 187.8 | 8.3 |
| Output_1_39 | 4740 | 145 | 1.8 | 0.03 | 3.23 | 0.06 | 8.24 | 0.22 | 8.11 | 0.20 | 440.0 | 160.0 | 187.8 | 5.9 | 204.0 | 14.0 | 187.8 | 8.8 |
| Output_1_283 | 5240 | 295 | 2.1 | 0.03 | 2.84 | 0.05 | 8.20 | 0.20 | 7.96 | 0.20 | 190.0 | 160.0 | 187.9 | 5.3 | 184.0 | 13.0 | 187.9 | 8.6 |
| Output_1_85 | 4400 | 54 | 2.0 | 0.03 | 3.70 | 0.05 | 7.90 | 0.21 | 7.21 | 0.06 | 290.0 | 150.0 | 188.6 | 7.0 | 193.0 | 12.0 | 188.6 | 9.8 |
| Output_1_110 | 5280 | 84 | 1.2 | 0.03 | 3.26 | 0.05 | 7.20 | 0.21 | 6.83 | 0.19 | 240.0 | 140.0 | 188.8 | 6.1 | 188.0 | 12.0 | 188.8 | 9.1 |
| Output_1_115 | 5080 | 103 | 2.3 | 0.03 | 3.31 | 0.05 | 8.08 | 0.20 | 8.04 | 0.18 | 170.0 | 150.0 | 190.0 | 6.2 | 185.0 | 13.0 | 190.0 | 9.2 |
| Output_1_58 | 7000 | 412 | 1.2 | 0.03 | 2.23 | 0.05 | 7.95 | 0.22 | 7.41 | 0.04 | 330.0 | 160.0 | 190.4 | 4.2 | 199.0 | 14.0 | 190.4 | 8.0 |

| | | | | | | | | | | | | | | | | | | |
|---|---|---|---|---|---|---|---|---|---|---|---|---|---|---|---|---|---|---|
| Output_1_257 | 2870 | 99 | 0.9 | 0.03 | 3.33 | 0.05 | 11.48 | 0.20 | 10.71 | 0.06 | 120.0 | 210.0 | 190.5 | 6.4 | 182.0 | 18.0 | 190.5 | 9.3 |
| Output_1_78 | 2920 | 45 | 1.6 | 0.03 | 3.67 | 0.05 | 9.47 | 0.21 | 9.52 | 0.24 | 210.0 | 180.0 | 190.6 | 6.7 | 191.0 | 17.0 | 190.6 | 9.6 |
| Output_1_4 | 3650 | 360 | 2.4 | 0.03 | 2.50 | 0.05 | 10.27 | 0.21 | 9.71 | 0.13 | 160.0 | 180.0 | 190.8 | 4.7 | 188.0 | 17.0 | 190.8 | 8.3 |
| Output_1_128 | 8220 | 296 | 1.3 | 0.03 | 1.83 | 0.05 | 5.77 | 0.20 | 5.88 | 0.13 | 150.0 | 120.0 | 191.2 | 3.4 | 187.0 | 10.0 | 191.2 | 7.7 |
| Output_1_135 | 4840 | 196 | 2.1 | 0.03 | 3.32 | 0.05 | 7.69 | 0.20 | 6.93 | 0.00 | 140.0 | 150.0 | 191.4 | 6.6 | 187.0 | 11.0 | 191.4 | 9.5 |
| Output_1_292 | 3240 | 117 | 2.0 | 0.03 | 3.97 | 0.06 | 8.33 | 0.22 | 8.07 | 0.31 | 370.0 | 170.0 | 191.8 | 7.5 | 205.0 | 16.0 | 191.8 | 10.0 |
| Output_1_104 | 5580 | 74 | 1.5 | 0.03 | 2.51 | 0.05 | 6.77 | 0.21 | 6.60 | 0.23 | 250.0 | 140.0 | 191.9 | 4.8 | 196.0 | 12.0 | 191.9 | 8.4 |
| Output_1_50 | 7130 | 297 | 0.9 | 0.03 | 2.84 | 0.05 | 5.37 | 0.22 | 5.53 | 0.34 | 280.0 | 110.0 | 192.4 | 5.4 | 200.2 | 9.7 | 192.4 | 8.7 |
| Output_1_93 | 5850 | 66 | 3.3 | 0.03 | 2.37 | 0.05 | 7.74 | 0.21 | 6.76 | 0.06 | 230.0 | 160.0 | 192.7 | 4.5 | 190.0 | 12.0 | 192.7 | 8.2 |
| Output_1_140 | 7630 | 286 | 1.7 | 0.03 | 3.23 | 0.05 | 7.10 | 0.20 | 6.37 | 0.08 | 140.0 | 140.0 | 192.9 | 6.1 | 188.0 | 11.0 | 192.9 | 9.2 |
| Output_1_54 | 3990 | 202 | 1.3 | 0.03 | 3.29 | 0.06 | 7.34 | 0.25 | 7.54 | 0.40 | 560.0 | 150.0 | 193.0 | 6.3 | 226.0 | 16.0 | 193.0 | 9.3 |
| Output_1_145 | 5787 | 178 | 1.9 | 0.03 | 2.20 | 0.05 | 6.69 | 0.21 | 6.13 | 0.32 | 280.0 | 130.0 | 193.3 | 4.2 | 197.0 | 12.0 | 193.3 | 8.1 |
| Output_1_67 | 15270 | 513 | 1.1 | 0.03 | 1.71 | 0.05 | 4.59 | 0.21 | 4.33 | 0.31 | 210.0 | 97.0 | 193.5 | 3.2 | 193.4 | 7.6 | 193.5 | 7.7 |
| Output_1_112 | 5140 | 89 | 1.1 | 0.03 | 2.91 | 0.05 | 6.39 | 0.22 | 6.39 | 0.15 | 290.0 | 130.0 | 194.0 | 5.5 | 203.0 | 11.0 | 194.0 | 8.9 |
| Output_1_80 | 5720 | 80 | 1.8 | 0.03 | 2.65 | 0.05 | 7.03 | 0.22 | 7.41 | 0.21 | 160.0 | 130.0 | 194.1 | 5.1 | 199.0 | 13.0 | 194.1 | 8.6 |
| Output_1_164 | 4770 | 93 | 2.9 | 0.03 | 2.94 | 0.05 | 8.07 | 0.21 | 7.80 | 0.08 | 150.0 | 150.0 | 194.6 | 5.6 | 190.0 | 13.0 | 194.6 | 9.0 |
| Output_1_141 | 6090 | 216 | 2.0 | 0.03 | 3.91 | 0.05 | 7.22 | 0.22 | 6.31 | 0.11 | 310.0 | 150.0 | 194.6 | 7.4 | 204.0 | 12.0 | 194.6 | 10.0 |
| Output_1_108 | 3720 | 53 | 1.6 | 0.03 | 3.16 | 0.06 | 10.20 | 0.22 | 9.63 | 0.18 | 400.0 | 200.0 | 194.7 | 6.1 | 201.0 | 17.0 | 194.7 | 9.2 |
| Output_1_268 | 5090 | 135 | 1.8 | 0.03 | 3.19 | 0.05 | 8.66 | 0.20 | 8.91 | 0.14 | 180.0 | 170.0 | 195.2 | 6.2 | 189.0 | 15.0 | 195.2 | 9.3 |
| Output_1_200 | 1343 | 16 | 2.2 | 0.03 | 4.87 | 0.06 | 15.69 | 0.23 | 14.54 | 0.20 | 320.0 | 270.0 | 195.3 | 9.6 | 207.0 | 26.0 | 195.3 | 12.0 |
| Output_1_1 | 6230 | 649 | 0.9 | 0.03 | 2.24 | 0.05 | 5.87 | 0.23 | 5.73 | 0.08 | 360.0 | 130.0 | 195.3 | 4.3 | 210.0 | 11.0 | 195.3 | 8.2 |
| Output_1_261 | 11970 | 379 | 1.1 | 0.03 | 2.50 | 0.05 | 4.26 | 0.21 | 4.65 | 0.37 | 171.0 | 88.0 | 195.8 | 4.8 | 193.7 | 8.2 | 195.8 | 8.5 |
| Output_1_296 | 5640 | 88 | 2.2 | 0.03 | 3.15 | 0.05 | 7.30 | 0.23 | 6.47 | 0.19 | 390.0 | 150.0 | 195.8 | 6.1 | 215.0 | 12.0 | 195.8 | 9.3 |
| Output_1_256 | 9250 | 308 | 2.3 | 0.03 | 3.24 | 0.05 | 6.65 | 0.21 | 6.25 | 0.20 | 160.0 | 130.0 | 196.3 | 6.3 | 191.0 | 11.0 | 196.3 | 9.5 |
| Output_1_11 | 6860 | 470 | 2.8 | 0.03 | 2.26 | 0.05 | 6.15 | 0.22 | 6.39 | 0.18 | 190.0 | 120.0 | 196.6 | 4.4 | 200.0 | 11.0 | 196.6 | 8.3 |
| Output_1_100 | 5860 | 69 | 1.3 | 0.03 | 3.06 | 0.05 | 5.42 | 0.22 | 6.05 | 0.22 | 210.0 | 110.0 | 196.9 | 5.9 | 197.0 | 10.0 | 196.9 | 9.2 |
| Output_1_258 | 12220 | 397 | 1.9 | 0.03 | 1.80 | 0.05 | 5.31 | 0.23 | 5.31 | 0.20 | 290.0 | 110.0 | 196.9 | 3.3 | 206.0 | 9.8 | 196.9 | 7.5 |
| Output_1_47 | 3715 | 132 | 1.7 | 0.03 | 2.90 | 0.05 | 9.48 | 0.24 | 8.86 | 0.04 | 360.0 | 190.0 | 198.8 | 5.7 | 218.0 | 17.0 | 198.8 | 9.1 |
| Output_1_76 | 5500 | 91 | 2.2 | 0.03 | 3.50 | 0.05 | 7.20 | 0.22 | 7.31 | 0.17 | 240.0 | 140.0 | 199.3 | 6.6 | 202.0 | 14.0 | 199.3 | 9.7 |
| Output_1_267 | 8150 | 214 | 2.3 | 0.03 | 3.12 | 0.05 | 5.71 | 0.22 | 6.33 | 0.45 | 210.0 | 110.0 | 201.6 | 6.2 | 204.0 | 12.0 | 201.6 | 9.5 |
| Output_1_117 | 9060 | 185 | 1.2 | 0.03 | 2.88 | 0.05 | 5.91 | 0.22 | 5.83 | 0.18 | 210.0 | 120.0 | 205.0 | 5.8 | 204.0 | 11.0 | 205.0 | 9.4 |
| Output_1_71 | 13950 | 325 | 1.6 | 0.03 | 3.08 | 0.05 | 3.93 | 0.22 | 4.41 | 0.50 | 222.0 | 85.0 | 205.8 | 6.2 | 205.3 | 8.2 | 205.8 | 9.6 |
| Output_1_176 | 4810 | 76 | 2.9 | 0.04 | 3.20 | 0.05 | 7.55 | 0.31 | 7.74 | 0.16 | 440.0 | 150.0 | 256.6 | 7.8 | 271.0 | 19.0 | 256.6 | 12.0 |
| Output_1_288 | 47580 | 5156 | 3.7 | 0.07 | 1.62 | 0.06 | 2.36 | 0.52 | 2.68 | 0.46 | 409.0 | 54.0 | 422.9 | 6.6 | 426.9 | 9.1 | 422.9 | 16.0 |
| Output_1_12 | 5390 | 159 | 2.6 | 0.07 | 3.24 | 0.06 | 7.21 | 0.54 | 7.25 | 0.22 | 460.0 | 150.0 | 423.0 | 13.0 | 432.0 | 26.0 | 423.0 | 20.0 |
| Output_1_81 | 233000 | 389 | 1.9 | 0.25 | 1.49 | 0.09 | 1.28 | 3.17 | 1.71 | 0.69 | 1507.0 | 25.0 | 1431.0 | 19.0 | ##### | 13.0 | 1507.0 | 28.0 |
| Output_1_224 | 39310 | 307 | 1.7 | 0.25 | 2.84 | 0.09 | 2.43 | 3.33 | 3.00 | 0.60 | 1522.0 | 46.0 | 1453.0 | 37.0 | ##### | 24.0 | 1522.0 | 47.0 |
| Output_1_38 | 84500 | 145 | 1.3 | 0.52 | 1.93 | 0.20 | 1.54 | 14.14 | 1.98 | 0.71 | 2785.0 | 25.0 | 2689.0 | 43.0 | ##### | 18.0 | 2785.0 | 27.0 |
| Output_1_189 | 11410 | 225 | 1.3 | 0.02 | 2.10 | 0.06 | 4.83 | 0.19 | 4.33 | 0.18 | 500.0 | 110.0 | 154.4 | 3.2 | 177.9 | 7.1 | 154.4 | 6.4 |
| Output_1_185 | 2186 | 48 | 4.7 | 0.02 | 3.18 | 0.06 | 10.72 | 0.21 | 9.62 | 0.07 | 600.0 | 210.0 | 157.9 | 5.0 | 190.0 | 17.0 | 157.9 | 7.6 |

| | | | | | | | | | | | | | | | | | | |
|---|---|---|---|---|---|---|---|---|---|---|---|---|---|---|---|---|---|---|
| Output_1_66 | 1216 | 53 | 1.1 | 0.02 | 5.35 | 0.07 | 16.67 | 0.21 | 15.71 | 0.06 | 610.0 | 310.0 | 154.8 | 8.2 | 193.0 | 29.0 | 154.8 | 9.9 |
| Output_1_219 | 8230 | 314 | 1.6 | 0.03 | 2.97 | 0.06 | 4.93 | 0.25 | 4.78 | 0.33 | 750.0 | 110.0 | 175.7 | 5.1 | 226.7 | 9.9 | 175.7 | 8.1 |
| Output_1_213 | 4690 | 96 | 0.7 | 0.03 | 2.49 | 0.09 | 7.46 | 0.41 | 8.31 | 0.25 | 1440.0 | 160.0 | 199.1 | 4.9 | 344.0 | 24.0 | 199.1 | 8.6 |
| Output_1_107 | 2710 | 37 | 1.9 | 0.03 | 4.40 | 0.13 | 10.40 | 0.53 | 12.57 | 0.55 | 1880.0 | 220.0 | 201.6 | 8.4 | 427.0 | 43.0 | 201.6 | 11.0 |
| Output_1_45 | 12900 | 405 | 1.0 | 0.03 | 6.19 | 0.16 | 11.11 | 0.78 | 15.38 | 0.70 | 2400.0 | 200.0 | 215.0 | 13.0 | 573.0 | 69.0 | 215.0 | 15.0 |
| Output_1_131 | 651 | 32 | 2.7 | 0.02 | 6.67 | 0.03 | 29.41 | 0.10 | 28.16 | 0.05 | -430.0 | 380.0 | 154.0 | 9.5 | 95.0 | 27.0 | 154.0 | 11.0 |
| Output_1_155 | 4130 | 93 | 2.4 | 0.03 | 3.03 | 0.04 | 10.02 | 0.17 | 9.83 | 0.12 | -120.0 | 170.0 | 186.3 | 5.6 | 163.0 | 15.0 | 186.3 | 8.7 |
| Output_1_269 | 5290 | 170 | 1.5 | 0.02 | 3.05 | 0.04 | 7.87 | 0.15 | 6.67 | 0.08 | -20.0 | 140.0 | 156.8 | 4.7 | 141.5 | 8.9 | 156.8 | 7.4 |
| Output_1_248 | 13550 | 484 | 1.4 | 0.03 | 2.60 | 0.05 | 4.65 | 0.19 | 4.37 | 0.30 | 88.0 | 92.0 | 185.7 | 4.7 | 173.4 | 6.8 | 185.7 | 8.2 |
| **Sample 18ATW-13** | | | | | | | | | | | | | | | | | | |
| 18ATW-13-15 | 8340 | 2609 | 9.5 | 0.03 | 4.06 | 0.05 | 5.80 | 0.24 | 6.17 | 0.31 | 160.0 | 120.0 | 218.7 | 8.5 | 220.0 | 12.0 | 218.7 | 8.6 |
| 18ATW-13-37 | 3790 | 398 | 1.5 | 0.03 | 4.05 | 0.05 | 7.68 | 0.26 | 8.88 | 0.37 | 280.0 | 160.0 | 219.4 | 8.8 | 232.0 | 18.0 | 219.4 | 8.9 |
| 18ATW-13-22 | 11060 | 1659 | 0.9 | 0.03 | 2.47 | 0.05 | 4.12 | 0.24 | 4.92 | 0.45 | 217.0 | 91.0 | 220.3 | 5.4 | 221.0 | 9.5 | 220.3 | 5.6 |
| 18ATW-13-6 | 11950 | 1312 | 0.6 | 0.04 | 3.11 | 0.05 | 5.44 | 0.26 | 5.02 | 0.27 | 340.0 | 120.0 | 224.4 | 7.1 | 233.0 | 11.0 | 224.4 | 7.4 |
| 18ATW-13-16 | 14580 | 3725 | 3.2 | 0.04 | 3.37 | 0.05 | 4.76 | 0.25 | 4.72 | 0.42 | 280.0 | 100.0 | 225.3 | 7.2 | 232.0 | 11.0 | 225.3 | 7.4 |
| 18ATW-13-27 | 5960 | 1642 | 0.5 | 0.04 | 2.58 | 0.05 | 6.99 | 0.26 | 6.67 | 0.19 | 290.0 | 150.0 | 225.6 | 5.7 | 229.0 | 13.0 | 225.6 | 6.0 |
| 18ATW-13-36 | 5560 | 532 | 1.0 | 0.04 | 5.32 | 0.05 | 11.33 | 0.25 | 11.79 | 0.11 | 210.0 | 250.0 | 226.0 | 12.0 | 221.0 | 23.0 | 226.0 | 12.0 |
| 18ATW-13-17 | 10980 | 2276 | 0.9 | 0.04 | 3.35 | 0.05 | 4.60 | 0.26 | 4.67 | 0.25 | 320.0 | 110.0 | 226.6 | 7.5 | 232.0 | 10.0 | 226.6 | 7.7 |
| 18ATW-13-19 | 9690 | 1406 | 4.6 | 0.04 | 3.37 | 0.05 | 4.35 | 0.26 | 4.69 | 0.48 | 315.0 | 93.0 | 226.6 | 7.6 | 231.3 | 9.7 | 226.6 | 7.8 |
| 18ATW-13-4 | 11840 | 1440 | 0.6 | 0.04 | 2.11 | 0.05 | 4.60 | 0.26 | 3.91 | 0.15 | 277.0 | 97.0 | 227.8 | 4.8 | 231.3 | 8.3 | 227.8 | 5.1 |
| 18ATW-13-8 | 8520 | 923 | 1.1 | 0.04 | 3.33 | 0.05 | 5.96 | 0.26 | 5.45 | 0.21 | 250.0 | 130.0 | 228.0 | 7.7 | 232.0 | 11.0 | 228.0 | 7.9 |
| 18ATW-13-13 | 11930 | 2597 | 1.8 | 0.04 | 4.97 | 0.06 | 5.06 | 0.27 | 5.19 | 0.57 | 390.0 | 110.0 | 229.0 | 11.0 | 242.0 | 12.0 | 229.0 | 11.0 |
| 18ATW-13-14 | 19040 | 5016 | 0.6 | 0.04 | 3.04 | 0.05 | 5.02 | 0.27 | 4.87 | 0.26 | 350.0 | 100.0 | 229.1 | 6.7 | 240.0 | 11.0 | 229.1 | 6.9 |
| 18ATW-13-7 | 13370 | 1408 | 0.7 | 0.04 | 3.58 | 0.05 | 5.17 | 0.26 | 5.38 | 0.48 | 280.0 | 120.0 | 229.7 | 8.3 | 234.0 | 11.0 | 229.7 | 8.5 |
| 18ATW-13-12 | 6540 | 1160 | 0.9 | 0.04 | 4.67 | 0.05 | 6.71 | 0.26 | 6.64 | 0.37 | 190.0 | 140.0 | 230.0 | 10.0 | 233.0 | 14.0 | 230.0 | 10.0 |
| 18ATW-13-23 | 7950 | 1514 | 1.5 | 0.04 | 4.68 | 0.06 | 7.07 | 0.27 | 5.66 | 0.21 | 410.0 | 150.0 | 230.0 | 10.0 | 238.0 | 12.0 | 230.0 | 11.0 |
| 18ATW-13-21 | 8690 | 1088 | 1.5 | 0.04 | 3.57 | 0.05 | 6.33 | 0.26 | 6.61 | 0.32 | 260.0 | 140.0 | 230.2 | 7.9 | 231.0 | 14.0 | 230.2 | 8.1 |
| 18ATW-13-26 | 9750 | 3328 | 1.3 | 0.04 | 3.57 | 0.05 | 4.73 | 0.26 | 5.79 | 0.58 | 290.0 | 100.0 | 230.3 | 8.2 | 234.0 | 13.0 | 230.3 | 8.4 |
| 18ATW-13-42 | 16760 | 2831 | 0.7 | 0.04 | 3.56 | 0.05 | 4.94 | 0.26 | 5.86 | 0.57 | 310.0 | 100.0 | 230.9 | 8.0 | 234.0 | 11.0 | 230.9 | 8.2 |
| 18ATW-13-28 | 11670 | 2396 | 1.1 | 0.04 | 4.68 | 0.05 | 4.36 | 0.26 | 5.38 | 0.58 | 306.0 | 93.0 | 231.0 | 11.0 | 236.0 | 12.0 | 231.0 | 11.0 |
| 18ATW-13-35 | 12590 | 1067 | 0.9 | 0.04 | 2.60 | 0.05 | 5.12 | 0.25 | 5.51 | 0.25 | 220.0 | 110.0 | 231.6 | 5.9 | 229.0 | 11.0 | 231.6 | 6.2 |
| 18ATW-13-43 | 18940 | 3101 | 1.1 | 0.04 | 5.72 | 0.05 | 6.32 | 0.25 | 5.14 | 0.37 | 260.0 | 130.0 | 232.0 | 13.0 | 228.0 | 11.0 | 232.0 | 13.0 |
| 18ATW-13-25 | 15920 | 5092 | 0.8 | 0.04 | 7.90 | 0.06 | 5.05 | 0.26 | 6.90 | 0.72 | 410.0 | 110.0 | 232.0 | 18.0 | 235.0 | 14.0 | 232.0 | 18.0 |
| 18ATW-13-39 | 8880 | 1049 | 1.6 | 0.04 | 3.54 | 0.06 | 6.68 | 0.27 | 6.34 | 0.11 | 380.0 | 140.0 | 232.1 | 8.2 | 240.0 | 14.0 | 232.1 | 8.4 |
| 18ATW-13-41 | 13340 | 2149 | 1.0 | 0.04 | 3.00 | 0.05 | 4.33 | 0.25 | 4.35 | 0.19 | 227.0 | 98.0 | 232.1 | 6.7 | 228.9 | 8.8 | 232.1 | 6.9 |
| 18ATW-13-34 | 13430 | 1082 | 0.9 | 0.04 | 4.36 | 0.05 | 6.62 | 0.26 | 7.34 | 0.35 | 290.0 | 140.0 | 232.4 | 9.8 | 236.0 | 16.0 | 232.4 | 9.9 |
| 18ATW-13-10 | 18000 | 2029 | 0.8 | 0.04 | 3.25 | 0.05 | 3.75 | 0.26 | 4.18 | 0.52 | 326.0 | 83.0 | 233.5 | 7.3 | 236.3 | 8.9 | 233.5 | 7.5 |
| 18ATW-13-20 | 11060 | 1409 | 0.7 | 0.04 | 3.78 | 0.05 | 5.58 | 0.25 | 5.14 | 0.36 | 250.0 | 120.0 | 234.0 | 8.6 | 228.0 | 11.0 | 234.0 | 8.8 |
| 18ATW-13-31 | 14330 | 1201 | 0.9 | 0.04 | 3.23 | 0.05 | 4.77 | 0.26 | 4.63 | 0.49 | 270.0 | 110.0 | 234.5 | 7.7 | 234.8 | 9.5 | 234.5 | 7.9 |

| | | | | | | | | | | | | | | | | | | |
|---|---|---|---|---|---|---|---|---|---|---|---|---|---|---|---|---|---|---|
| 18ATW-13-9 | 6830 | 711 | 1.2 | 0.04 | 4.85 | 0.05 | 7.81 | 0.27 | 5.86 | 0.02 | 320.0 | 180.0 | 235.0 | 11.0 | 245.0 | 13.0 | 235.0 | 11.0 |
| 18ATW-13-30 | 6400 | 760 | 1.0 | 0.04 | 4.58 | 0.05 | 6.78 | 0.26 | 6.13 | 0.21 | 250.0 | 150.0 | 235.0 | 11.0 | 234.0 | 13.0 | 235.0 | 11.0 |
| 18ATW-13-24 | 4220 | 1036 | 1.7 | 0.04 | 4.80 | 0.05 | 7.74 | 0.26 | 6.15 | 0.26 | 170.0 | 170.0 | 237.0 | 11.0 | 233.0 | 13.0 | 237.0 | 11.0 |
| 18ATW-13-11 | 16000 | 2359 | 0.8 | 0.04 | 3.73 | 0.05 | 4.53 | 0.26 | 4.62 | 0.39 | 240.0 | 100.0 | 237.2 | 8.6 | 235.7 | 9.1 | 237.2 | 8.8 |
| 18ATW-13-29 | 14590 | 2112 | 1.0 | 0.04 | 4.24 | 0.05 | 4.76 | 0.26 | 6.13 | 0.53 | 200.0 | 100.0 | 238.7 | 9.7 | 235.0 | 13.0 | 238.7 | 9.9 |
| 18ATW-13-18 | 23910 | 3876 | 0.6 | 0.04 | 3.95 | 0.05 | 4.99 | 0.26 | 4.96 | 0.32 | 180.0 | 110.0 | 240.3 | 9.1 | 237.6 | 9.6 | 240.3 | 9.3 |
| 18ATW-13-33 | 14460 | 1139 | 1.5 | 0.04 | 2.60 | 0.05 | 4.33 | 0.28 | 4.00 | 0.28 | 316.0 | 97.0 | 243.7 | 6.6 | 246.5 | 8.9 | 243.7 | 6.8 |
| 18ATW-13-32 | 15450 | 1234 | 0.8 | 0.04 | 3.36 | 0.05 | 5.11 | 0.26 | 5.32 | 0.38 | 280.0 | 110.0 | 244.6 | 7.8 | 237.0 | 11.0 | 244.6 | 8.0 |
| 18ATW-13-38 | 4760 | 541 | 1.6 | 0.03 | 3.20 | 0.06 | 5.89 | 0.28 | 6.05 | 0.22 | 570.0 | 130.0 | 218.2 | 7.1 | 250.0 | 13.0 | 218.2 | 7.4 |
| 18ATW-13-40 | 7870 | 1047 | 1.1 | 0.04 | 4.41 | 0.06 | 8.55 | 0.29 | 7.69 | 0.06 | 510.0 | 180.0 | 230.0 | 9.6 | 257.0 | 18.0 | 230.0 | 9.8 |
| 18ATW-13-5 | 27500 | 2837 | 0.6 | 0.04 | 2.10 | 0.05 | 3.29 | 0.29 | 3.00 | 0.29 | 295.0 | 73.0 | 252.6 | 5.2 | 257.6 | 6.8 | 252.6 | 5.6 |
| **Sample 18ATW-22** | | | | | | | | | | | | | | | | | | |
| 18ATW-22 Spot 57 | 9720 | 534 | 3.2 | 0.05 | 1.98 | 0.05 | 5.11 | 0.36 | 5.31 | 0.05 | 370.0 | 110.0 | 293.2 | 5.7 | 309.0 | 14.0 | 293.2 | 12.0 |
| 18ATW-22 Spot 63 | 4540 | 311 | 3.0 | 0.05 | 2.33 | 0.05 | 5.71 | 0.35 | 5.80 | 0.02 | 320.0 | 120.0 | 297.1 | 6.5 | 301.0 | 15.0 | 297.1 | 13.0 |
| 18ATW-22 Spot 59 | 2660 | 149 | 2.8 | 0.05 | 2.75 | 0.05 | 8.32 | 0.33 | 8.51 | 0.21 | 190.0 | 160.0 | 299.0 | 7.8 | 288.0 | 20.0 | 299.0 | 13.0 |
| 18ATW-22 Spot 60 | 21280 | 1271 | 2.4 | 0.05 | 2.32 | 0.05 | 4.82 | 0.35 | 5.48 | 0.20 | 290.0 | 110.0 | 299.1 | 7.0 | 302.0 | 15.0 | 299.1 | 13.0 |
| 18ATW-22 Spot 41 | 2370 | 169 | 3.8 | 0.05 | 2.74 | 0.05 | 9.67 | 0.36 | 9.55 | 0.09 | 320.0 | 190.0 | 299.2 | 8.2 | 308.0 | 25.0 | 299.2 | 14.0 |
| 18ATW-22 Spot 46 | 2220 | 136 | 4.6 | 0.05 | 2.74 | 0.05 | 8.42 | 0.36 | 8.52 | 0.11 | 420.0 | 160.0 | 299.2 | 8.0 | 317.0 | 22.0 | 299.2 | 13.0 |
| 18ATW-22 Spot 53 | 5220 | 283 | 4.1 | 0.05 | 2.06 | 0.05 | 6.02 | 0.36 | 6.09 | 0.01 | 360.0 | 130.0 | 299.7 | 6.0 | 311.0 | 16.0 | 299.7 | 12.0 |
| 18ATW-22 Spot 65 | 16950 | 1261 | 1.7 | 0.05 | 3.14 | 0.05 | 3.85 | 0.35 | 4.84 | 0.22 | 268.0 | 86.0 | 301.0 | 9.1 | 305.0 | 12.0 | 301.0 | 14.0 |
| 18ATW-22 Spot 48 | 15160 | 893 | 3.0 | 0.05 | 1.31 | 0.05 | 3.23 | 0.35 | 2.87 | 0.03 | 298.0 | 71.0 | 302.0 | 3.9 | 303.2 | 7.8 | 302.0 | 12.0 |
| 18ATW-22 Spot 61 | 13180 | 809 | 2.7 | 0.05 | 2.30 | 0.05 | 5.51 | 0.36 | 5.82 | 0.10 | 350.0 | 110.0 | 302.4 | 7.0 | 311.0 | 16.0 | 302.4 | 13.0 |
| 18ATW-22 Spot 47 | 7070 | 418 | 3.3 | 0.05 | 1.94 | 0.05 | 4.80 | 0.35 | 4.57 | 0.00 | 280.0 | 100.0 | 304.3 | 5.8 | 303.0 | 12.0 | 304.3 | 12.0 |
| 18ATW-22 Spot 42 | 8810 | 616 | 2.7 | 0.05 | 1.92 | 0.05 | 4.01 | 0.36 | 4.16 | 0.16 | 381.0 | 87.0 | 304.9 | 5.7 | 312.0 | 11.0 | 304.9 | 12.0 |
| 18ATW-22 Spot 43 | 15790 | 1052 | 1.7 | 0.05 | 1.47 | 0.05 | 2.82 | 0.36 | 3.09 | 0.30 | 326.0 | 64.0 | 305.0 | 4.3 | 310.1 | 8.2 | 305.0 | 12.0 |
| 18ATW-22 Spot 66 | 27100 | 2170 | 3.2 | 0.05 | 2.88 | 0.05 | 4.18 | 0.35 | 5.17 | 0.39 | 306.0 | 95.0 | 305.9 | 8.5 | 303.0 | 14.0 | 305.9 | 14.0 |
| 18ATW-22 Spot 49 | 5330 | 306 | 2.4 | 0.05 | 3.07 | 0.05 | 6.10 | 0.35 | 5.65 | 0.11 | 330.0 | 130.0 | 307.1 | 9.1 | 311.0 | 15.0 | 307.1 | 14.0 |
| 18ATW-22 Spot 58 | 9590 | 503 | 2.2 | 0.05 | 2.45 | 0.05 | 4.42 | 0.35 | 5.40 | 0.40 | 268.0 | 96.0 | 308.2 | 7.1 | 305.0 | 14.0 | 308.2 | 13.0 |
| 18ATW-22 Spot 62 | 66700 | 4289 | 3.5 | 0.05 | 1.11 | 0.05 | 1.76 | 0.35 | 1.81 | 0.46 | 354.0 | 38.0 | 299.5 | 3.3 | 307.9 | 4.7 | 299.5 | 11.0 |
| 18ATW-22 Spot 64 | 3010 | 212 | 3.7 | 0.05 | 2.95 | 0.06 | 6.89 | 0.43 | 6.51 | 0.12 | 690.0 | 150.0 | 298.3 | 8.4 | 361.0 | 20.0 | 298.3 | 14.0 |
| 18ATW-22 Spot 67 | 12140 | 909 | 3.9 | 0.05 | 1.24 | 0.06 | 3.55 | 0.41 | 3.46 | 0.13 | 439.0 | 77.0 | 318.6 | 3.9 | 344.0 | 10.0 | 318.6 | 12.0 |
| 18ATW-22 Spot 54 | 15220 | 775 | 2.5 | 0.05 | 5.75 | 0.05 | 9.98 | 0.35 | 13.29 | 0.75 | 230.0 | 210.0 | 317.0 | 18.0 | 300.0 | 33.0 | 317.0 | 21.0 |
| 18ATW-22 Spot 45 | 9390 | 552 | 2.5 | 0.05 | 2.13 | 0.05 | 4.82 | 0.37 | 4.89 | 0.03 | 270.0 | 100.0 | 324.2 | 6.9 | 320.0 | 14.0 | 324.2 | 14.0 |
| 18ATW-22 Spot 52 | 31310 | 1588 | 2.1 | 0.05 | 1.64 | 0.05 | 2.66 | 0.37 | 2.53 | 0.31 | 313.0 | 60.0 | 321.2 | 5.1 | 320.6 | 7.0 | 321.2 | 13.0 |
| 18ATW-22 Spot 50 | 2960 | 170 | 3.4 | 0.05 | 3.18 | 0.05 | 7.95 | 0.34 | 8.19 | 0.52 | 340.0 | 160.0 | 297.4 | 9.4 | 295.0 | 21.0 | 297.4 | 14.0 |
| 18ATW-22 Spot 51 | 9460 | 528 | 2.3 | 0.05 | 1.95 | 0.05 | 5.63 | 0.34 | 4.94 | 0.09 | 310.0 | 120.0 | 297.8 | 5.7 | 299.0 | 13.0 | 297.8 | 12.0 |
| 18ATW-22 Spot 55 | 4420 | 257 | 7.2 | 0.04 | 3.02 | 0.05 | 5.77 | 0.32 | 6.21 | 0.32 | 330.0 | 120.0 | 271.6 | 7.9 | 283.0 | 15.0 | 271.6 | 13.0 |
| 18ATW-22 Spot 56 | 2190 | 125 | 3.3 | 0.04 | 3.83 | 0.05 | 11.70 | 0.32 | 12.96 | 0.28 | 380.0 | 230.0 | 280.0 | 10.0 | 289.0 | 34.0 | 280.0 | 14.0 |

| **Sample 13ET270** | | | | | | | | | | | | | | | | | | |
|---|---|---|---|---|---|---|---|---|---|---|---|---|---|---|---|---|---|---|
| 13ET270-Spot 47 | 3140 | 592 | 1.7 | 0.02 | 4.41 | 0.05 | 12.14 | 0.13 | 12.03 | 0.10 | 190.0 | 230.0 | 125.8 | 5.5 | 125.0 | 14.0 | 125.8 | 7.1 |
| 13ET270-Spot 52 | 7320 | 1096 | 1.2 | 0.02 | 2.28 | 0.05 | 5.79 | 0.14 | 5.50 | 0.23 | 250.0 | 120.0 | 125.9 | 2.8 | 131.2 | 6.7 | 125.9 | 5.4 |
| 13ET270-Spot 53 | 7900 | 1077 | 1.3 | 0.02 | 3.04 | 0.05 | 6.15 | 0.13 | 5.67 | 0.26 | 130.0 | 120.0 | 125.9 | 3.8 | 125.9 | 6.7 | 125.9 | 5.9 |
| 13ET270-Spot 48 | 4880 | 1045 | 1.8 | 0.02 | 2.77 | 0.05 | 6.91 | 0.13 | 6.59 | 0.16 | 160.0 | 140.0 | 126.8 | 3.5 | 126.8 | 8.1 | 126.8 | 5.7 |
| 13ET270-Spot 45 | 8590 | 990 | 1.1 | 0.02 | 2.74 | 0.05 | 6.34 | 0.13 | 6.10 | 0.31 | 150.0 | 120.0 | 127.9 | 3.4 | 128.8 | 7.5 | 127.9 | 5.8 |
| 13ET270-Spot 61 | 6540 | 453 | 1.1 | 0.02 | 2.94 | 0.05 | 6.45 | 0.13 | 5.83 | 0.19 | 190.0 | 130.0 | 128.0 | 3.7 | 127.1 | 7.0 | 128.0 | 5.9 |
| 13ET270-Spot 66 | 5750 | 368 | 1.7 | 0.02 | 3.24 | 0.05 | 7.76 | 0.13 | 6.77 | 0.11 | 140.0 | 150.0 | 128.1 | 4.1 | 125.0 | 8.0 | 128.1 | 6.2 |
| 13ET270-Spot 41 | 6800 | 510 | 1.2 | 0.02 | 3.08 | 0.05 | 7.36 | 0.13 | 7.14 | 0.24 | 120.0 | 140.0 | 128.3 | 3.9 | 127.6 | 8.6 | 128.3 | 6.1 |
| 13ET270-Spot 70 | 5580 | 504 | 1.5 | 0.02 | 3.52 | 0.05 | 7.75 | 0.14 | 8.09 | 0.19 | 190.0 | 150.0 | 128.6 | 4.5 | 128.5 | 9.7 | 128.6 | 6.5 |
| 13ET270-Spot 46 | 6450 | 861 | 1.2 | 0.02 | 2.58 | 0.05 | 6.14 | 0.13 | 5.61 | 0.27 | 90.0 | 120.0 | 128.7 | 3.3 | 125.1 | 6.8 | 128.7 | 5.7 |
| 13ET270-Spot 57 | 3400 | 528 | 1.5 | 0.02 | 3.12 | 0.05 | 10.19 | 0.14 | 9.42 | 0.05 | 240.0 | 190.0 | 128.8 | 4.0 | 130.0 | 12.0 | 128.8 | 6.1 |
| 13ET270-Spot 63 | 3150 | 185 | 1.6 | 0.02 | 3.32 | 0.05 | 10.64 | 0.14 | 10.37 | 0.01 | 160.0 | 200.0 | 128.8 | 4.3 | 128.0 | 12.0 | 128.8 | 6.3 |
| 13ET270-Spot 50 | 3540 | 707 | 1.8 | 0.02 | 3.91 | 0.05 | 7.97 | 0.15 | 8.22 | 0.34 | 280.0 | 150.0 | 128.9 | 5.0 | 139.0 | 11.0 | 128.9 | 6.8 |
| 13ET270-Spot 49 | 6200 | 1434 | 1.8 | 0.02 | 2.56 | 0.05 | 6.14 | 0.14 | 6.50 | 0.27 | 270.0 | 130.0 | 129.6 | 3.3 | 135.2 | 8.3 | 129.6 | 5.7 |
| 13ET270-Spot 64 | 7970 | 456 | 1.4 | 0.02 | 2.51 | 0.05 | 6.04 | 0.14 | 6.44 | 0.31 | 230.0 | 120.0 | 129.8 | 3.2 | 136.4 | 8.2 | 129.8 | 5.7 |
| 13ET270-Spot 58 | 8420 | 1067 | 1.0 | 0.02 | 2.36 | 0.05 | 5.93 | 0.14 | 5.51 | 0.22 | 200.0 | 120.0 | 129.9 | 3.0 | 135.2 | 6.7 | 129.9 | 5.6 |
| 13ET270-Spot 44 | 4610 | 467 | 1.3 | 0.02 | 3.04 | 0.05 | 7.33 | 0.14 | 6.87 | 0.09 | 200.0 | 140.0 | 130.2 | 3.9 | 132.3 | 8.5 | 130.2 | 6.1 |
| 13ET270-Spot 65 | 2930 | 175 | 1.9 | 0.02 | 2.89 | 0.05 | 9.19 | 0.14 | 8.82 | 0.09 | 130.0 | 180.0 | 130.2 | 3.7 | 128.0 | 10.0 | 130.2 | 6.0 |
| 13ET270-Spot 67 | 6160 | 429 | 1.5 | 0.02 | 2.73 | 0.05 | 6.95 | 0.14 | 6.81 | 0.15 | 170.0 | 140.0 | 130.8 | 3.5 | 128.1 | 8.2 | 130.8 | 5.9 |
| 13ET270-Spot 51 | 5420 | 891 | 1.3 | 0.02 | 2.96 | 0.05 | 7.39 | 0.14 | 8.45 | 0.33 | 190.0 | 150.0 | 131.6 | 3.8 | 137.0 | 10.0 | 131.6 | 6.1 |
| 13ET270-Spot 42 | 4870 | 365 | 1.4 | 0.02 | 3.44 | 0.05 | 7.51 | 0.14 | 8.39 | 0.38 | 180.0 | 140.0 | 131.7 | 4.5 | 135.0 | 10.0 | 131.7 | 6.5 |
| 13ET270-Spot 43 | 2570 | 230 | 1.7 | 0.02 | 4.07 | 0.05 | 10.59 | 0.14 | 10.79 | 0.07 | 140.0 | 200.0 | 131.8 | 5.3 | 133.0 | 13.0 | 131.8 | 7.1 |
| 13ET270-Spot 60 | 3980 | 360 | 1.9 | 0.02 | 2.66 | 0.05 | 7.92 | 0.14 | 7.86 | 0.19 | 180.0 | 150.0 | 131.9 | 3.5 | 132.5 | 9.9 | 131.9 | 5.9 |
| 13ET270-Spot 68 | 12060 | 906 | 1.1 | 0.02 | 3.09 | 0.05 | 4.72 | 0.14 | 5.04 | 0.34 | 231.0 | 99.0 | 132.0 | 4.0 | 136.9 | 6.5 | 132.0 | 6.2 |
| 13ET270-Spot 69 | 7640 | 666 | 2.0 | 0.02 | 2.60 | 0.05 | 5.45 | 0.15 | 5.43 | 0.09 | 250.0 | 110.0 | 132.3 | 3.4 | 137.5 | 7.0 | 132.3 | 5.9 |
| 13ET270-Spot 62 | 5500 | 332 | 1.3 | 0.02 | 3.03 | 0.05 | 6.54 | 0.13 | 6.87 | 0.29 | 80.0 | 120.0 | 132.4 | 4.0 | 127.1 | 8.0 | 132.4 | 6.2 |
| 13ET270-Spot 54 | 6820 | 1007 | 1.6 | 0.02 | 3.32 | 0.05 | 5.75 | 0.14 | 5.77 | 0.29 | 130.0 | 110.0 | 132.6 | 4.4 | 134.7 | 7.3 | 132.6 | 6.5 |
| 13ET270-Spot 40 | 7590 | 552 | 1.2 | 0.02 | 2.55 | 0.05 | 5.63 | 0.14 | 5.28 | 0.03 | 100.0 | 110.0 | 132.7 | 3.3 | 129.6 | 6.4 | 132.7 | 5.8 |
| 13ET270-Spot 55 | 3940 | 656 | 1.4 | 0.02 | 3.68 | 0.05 | 9.80 | 0.14 | 8.51 | 0.02 | 170.0 | 180.0 | 133.7 | 4.9 | 133.0 | 11.0 | 133.7 | 6.9 |
| 13ET270-Spot 56 | 6000 | 994 | 1.6 | 0.02 | 3.35 | 0.05 | 8.37 | 0.15 | 7.59 | 0.00 | 170.0 | 160.0 | 135.1 | 4.5 | 139.6 | 9.3 | 135.1 | 6.6 |
| 13ET270-Spot 59 | 3068 | 303 | 1.5 | 0.02 | 3.36 | 0.05 | 11.53 | 0.14 | 10.64 | 0.08 | 150.0 | 210.0 | 138.6 | 4.6 | 132.0 | 13.0 | 138.6 | 6.8 |

| **Sample 16CSR17** | | | | | | | | | | | | | | | | | | |
|---|---|---|---|---|---|---|---|---|---|---|---|---|---|---|---|---|---|---|
| -16CSR-17A Spot 8 | 16720 | 2672 | 2671.7 | 0.05 | 2.27 | 19.04 | 0.89 | 0.34 | 2.44 | 0.93 | 307.7 | 20.3 | 298.5 | 6.6 | 299.4 | 6.3 | 298.5 | 12.6 |
| -16CSR-17A Spot 14 | 19110 | 1772 | 1772.2 | 0.05 | 2.40 | 18.79 | 0.87 | 0.35 | 2.55 | 0.94 | 337.8 | 19.6 | 301.1 | 7.1 | 305.2 | 6.7 | 301.1 | 13.4 |
| -16CSR-17A Spot 17 | 15330 | 2496 | 2495.8 | 0.05 | 2.61 | 18.95 | 1.13 | 0.35 | 2.84 | 0.92 | 318.6 | 25.7 | 302.5 | 7.7 | 304.3 | 7.5 | 302.5 | 14.7 |
| -16CSR-17A Spot 7 | 14830 | 2325 | 2325.0 | 0.05 | 1.51 | 18.82 | 0.81 | 0.35 | 1.72 | 0.88 | 334.0 | 18.4 | 303.8 | 4.5 | 307.2 | 4.6 | 303.8 | 8.5 |
| -16CSR-17A Spot 23 | 20350 | 1764 | 1763.7 | 0.05 | 4.33 | 18.89 | 1.19 | 0.35 | 4.49 | 0.96 | 326.5 | 27.1 | 304.0 | 12.9 | 306.5 | 11.9 | 304.0 | 24.4 |
| -16CSR-17A Spot 12 | 8540 | 3000 | 3000.2 | 0.05 | 2.58 | 19.20 | 0.91 | 0.35 | 2.73 | 0.94 | 288.9 | 20.9 | 304.3 | 7.7 | 302.4 | 7.1 | 304.3 | 14.5 |

| | | | | | | | | | | | | | | | | | | |
|---|---|---|---|---|---|---|---|---|---|---|---|---|---|---|---|---|---|---|
| -16CSR-17A Spot 28 | 17760 | 2247 | 2247.0 | 0.05 | 2.26 | 19.08 | 1.09 | 0.35 | 2.51 | 0.90 | 303.3 | 24.9 | 304.9 | 6.7 | 304.6 | 6.6 | 304.9 | 12.8 |
| -16CSR-17A Spot 35 | 25160 | 2362 | 2362.2 | 0.05 | 1.90 | 19.07 | 0.89 | 0.35 | 2.10 | 0.91 | 304.9 | 20.3 | 305.0 | 5.7 | 304.9 | 5.5 | 305.0 | 10.8 |
| -16CSR-17A Spot 27 | 20170 | 1743 | 1743.4 | 0.05 | 2.13 | 19.21 | 0.83 | 0.35 | 2.29 | 0.93 | 287.4 | 19.1 | 305.5 | 6.3 | 303.3 | 6.0 | 305.5 | 12.1 |
| -16CSR-17A Spot 13 | 15520 | 2769 | 2769.4 | 0.05 | 2.01 | 18.97 | 0.86 | 0.35 | 2.18 | 0.92 | 316.4 | 19.5 | 305.7 | 6.0 | 306.9 | 5.8 | 305.7 | 11.4 |
| -16CSR-17A Spot 10 | 25190 | 1920 | 1919.9 | 0.05 | 2.29 | 18.84 | 1.06 | 0.36 | 2.52 | 0.91 | 332.4 | 24.0 | 306.1 | 6.8 | 309.0 | 6.7 | 306.1 | 13.0 |
| -16CSR-17A Spot 29 | 17140 | 951 | 950.8 | 0.05 | 2.50 | 19.13 | 1.01 | 0.35 | 2.69 | 0.93 | 297.8 | 23.0 | 306.9 | 7.5 | 305.7 | 7.1 | 306.9 | 14.2 |
| -16CSR-17A Spot 15 | 20600 | 2215 | 2215.2 | 0.05 | 1.94 | 19.11 | 1.02 | 0.35 | 2.19 | 0.88 | 300.0 | 23.3 | 309.7 | 5.9 | 308.5 | 5.8 | 309.7 | 11.2 |
| -16CSR-17A Spot 26 | 16760 | 2031 | 2030.9 | 0.05 | 2.55 | 18.93 | 0.96 | 0.36 | 2.72 | 0.94 | 321.4 | 21.9 | 310.2 | 7.7 | 311.4 | 7.3 | 310.2 | 14.7 |
| -16CSR-17A Spot 22 | 14900 | 3788 | 3787.6 | 0.05 | 2.21 | 18.82 | 0.76 | 0.36 | 2.34 | 0.95 | 334.5 | 17.2 | 311.4 | 6.7 | 314.0 | 6.3 | 311.4 | 12.8 |
| -16CSR-17A Spot 16 | 20680 | 1562 | 1561.7 | 0.05 | 2.57 | 19.13 | 0.85 | 0.36 | 2.71 | 0.95 | 297.6 | 19.5 | 313.9 | 7.9 | 311.9 | 7.3 | 313.9 | 15.0 |
| -16CSR-17A Spot 1 | 15870 | 1031 | 1031.0 | 0.05 | 2.37 | 19.20 | 0.92 | 0.36 | 2.54 | 0.93 | 289.3 | 21.0 | 318.7 | 7.4 | 315.1 | 6.9 | 318.7 | 14.0 |
| -16CSR-17A Spot 20 | 29510 | 1010 | 1010.2 | 0.05 | 2.28 | 17.76 | 1.64 | 0.39 | 2.81 | 0.81 | 464.6 | 36.4 | 312.2 | 7.0 | 330.8 | 7.9 | 312.2 | 13.2 |
| -16CSR-17A Spot 11 | 65700 | 4375 | 4375.1 | 0.03 | 3.37 | 18.56 | 0.84 | 0.24 | 3.47 | 0.97 | 366.1 | 19.0 | 207.9 | 6.9 | 221.2 | 6.9 | 207.9 | 13.1 |

**14ATW50**

| | | | | | | | | | | | | | | | | | | |
|---|---|---|---|---|---|---|---|---|---|---|---|---|---|---|---|---|---|---|
| 14ATW-50 Spot24 | 20040 | 20000 | 1.6 | 0.05 | 2.97 | 0.05 | 4.31 | 0.35 | 4.34 | 0.48 | 319.0 | 93.0 | 296.6 | 8.3 | 302.0 | 12.0 | 296.6 | 11.0 |
| 14ATW-50 Spot48 | 21380 | 413 | 2.4 | 0.05 | 2.32 | 0.05 | 4.02 | 0.35 | 3.97 | 0.24 | 403.0 | 93.0 | 299.3 | 6.8 | 306.0 | 11.0 | 299.3 | 10.0 |
| 14ATW-50 Spot49 | 14750 | 229 | 2.3 | 0.05 | 2.72 | 0.05 | 5.51 | 0.34 | 5.04 | 0.13 | 300.0 | 120.0 | 300.7 | 8.0 | 296.0 | 13.0 | 300.7 | 11.0 |
| 14ATW-50 Spot51 | 19430 | 181 | 2.0 | 0.05 | 2.92 | 0.05 | 4.47 | 0.36 | 5.07 | 0.36 | 332.0 | 95.0 | 301.6 | 8.4 | 307.0 | 14.0 | 301.6 | 11.0 |
| 14ATW-50 Spot40 | 8740 | 785 | 3.1 | 0.05 | 2.92 | 0.05 | 5.87 | 0.35 | 5.65 | 0.26 | 370.0 | 120.0 | 301.7 | 8.6 | 308.0 | 16.0 | 301.7 | 11.0 |
| 14ATW-50 Spot47 | 20910 | 437 | 1.8 | 0.05 | 2.49 | 0.05 | 3.52 | 0.35 | 4.00 | 0.42 | 352.0 | 76.0 | 303.4 | 7.4 | 304.0 | 10.0 | 303.4 | 10.0 |
| 14ATW-50 Spot43 | 16700 | 142 | 2.8 | 0.05 | 2.90 | 0.05 | 4.10 | 0.35 | 4.84 | 0.50 | 353.0 | 87.0 | 303.7 | 8.5 | 306.0 | 12.0 | 303.7 | 11.0 |
| 14ATW-50 Spot35 | 19280 | 480 | 1.6 | 0.05 | 2.69 | 0.05 | 4.07 | 0.37 | 3.54 | 0.19 | 353.0 | 89.0 | 304.0 | 7.9 | 317.3 | 9.8 | 304.0 | 11.0 |
| 14ATW-50 Spot34 | 24290 | 896 | 1.4 | 0.05 | 2.26 | 0.05 | 3.93 | 0.37 | 3.54 | 0.08 | 362.0 | 90.0 | 305.6 | 7.0 | 316.9 | 9.6 | 305.6 | 10.0 |
| 14ATW-50 Spot38 | 21680 | 745 | 1.8 | 0.05 | 2.67 | 0.05 | 4.01 | 0.37 | 4.61 | 0.47 | 390.0 | 90.0 | 306.5 | 7.8 | 318.0 | 13.0 | 306.5 | 11.0 |
| 14ATW-50 Spot50 | 16720 | 202 | 2.1 | 0.05 | 2.05 | 0.05 | 3.72 | 0.36 | 4.21 | 0.43 | 353.0 | 83.0 | 306.7 | 6.4 | 313.0 | 11.0 | 306.7 | 10.0 |
| 14ATW-50 Spot37 | 19110 | 431 | 1.8 | 0.05 | 2.25 | 0.05 | 3.93 | 0.36 | 3.88 | 0.36 | 323.0 | 83.0 | 307.1 | 6.9 | 313.0 | 10.0 | 307.1 | 9.9 |
| 14ATW-50 Spot45 | 15330 | 148 | 2.1 | 0.05 | 2.85 | 0.05 | 5.36 | 0.36 | 5.25 | 0.13 | 370.0 | 120.0 | 308.9 | 8.5 | 314.0 | 14.0 | 308.9 | 11.0 |
| 14ATW-50 Spot31 | 14830 | 2530 | 1.8 | 0.05 | 2.84 | 0.05 | 4.11 | 0.36 | 4.46 | 0.52 | 341.0 | 92.0 | 309.8 | 8.4 | 313.0 | 12.0 | 309.8 | 11.0 |
| 14ATW-50 Spot46 | 20350 | 261 | 1.8 | 0.05 | 2.84 | 0.05 | 3.08 | 0.35 | 4.03 | 0.64 | 287.0 | 73.0 | 310.2 | 8.3 | 302.0 | 11.0 | 310.2 | 11.0 |
| 14ATW-50 Spot27 | 8540 | 335 | 2.1 | 0.05 | 2.63 | 0.05 | 6.11 | 0.38 | 5.84 | 0.17 | 360.0 | 140.0 | 310.9 | 7.7 | 324.0 | 16.0 | 310.9 | 11.0 |
| 14ATW-50 Spot26 | 17760 | 688 | 1.4 | 0.05 | 3.44 | 0.05 | 5.86 | 0.38 | 4.75 | 0.13 | 390.0 | 130.0 | 311.0 | 10.0 | 326.0 | 13.0 | 311.0 | 13.0 |
| 14ATW-50 Spot28 | 25160 | 1505 | 1.4 | 0.05 | 3.44 | 0.05 | 6.59 | 0.38 | 4.72 | 0.23 | 380.0 | 140.0 | 311.0 | 10.0 | 327.0 | 13.0 | 311.0 | 12.0 |
| 14ATW-50 Spot36 | 20170 | 406 | 2.7 | 0.05 | 3.03 | 0.05 | 4.09 | 0.37 | 4.07 | 0.38 | 360.0 | 86.0 | 311.2 | 9.0 | 321.0 | 11.0 | 311.2 | 12.0 |
| 14ATW-50 Spot39 | 15520 | 940 | 2.0 | 0.05 | 2.61 | 0.05 | 4.57 | 0.37 | 4.37 | 0.21 | 384.0 | 93.0 | 313.6 | 7.8 | 316.0 | 12.0 | 313.6 | 11.0 |
| 14ATW-50 Spot32 | 25190 | 4150 | 1.4 | 0.05 | 2.79 | 0.05 | 3.04 | 0.36 | 3.89 | 0.57 | 321.0 | 70.0 | 315.1 | 8.8 | 312.0 | 10.0 | 315.1 | 12.0 |
| 14ATW-50 Spot33 | 17140 | 1830 | 1.8 | 0.05 | 2.39 | 0.05 | 3.45 | 0.37 | 4.02 | 0.38 | 280.0 | 73.0 | 315.4 | 7.2 | 321.0 | 11.0 | 315.4 | 10.0 |
| 14ATW-50 Spot23 | 20600 | -1615 | 1.8 | 0.05 | 2.58 | 0.05 | 4.28 | 0.38 | 3.67 | 0.26 | 362.0 | 90.0 | 316.5 | 8.3 | 327.0 | 10.0 | 316.5 | 11.0 |
| 14ATW-50 Spot30 | 16760 | 2187 | 1.9 | 0.05 | 1.97 | 0.05 | 3.95 | 0.36 | 3.61 | 0.14 | 313.0 | 87.0 | 316.8 | 6.1 | 311.2 | 9.8 | 316.8 | 9.3 |
| 14ATW-50 Spot42 | 14900 | 178 | 3.0 | 0.05 | 2.78 | 0.06 | 4.70 | 0.38 | 4.47 | 0.22 | 400.0 | 96.0 | 316.8 | 8.3 | 328.0 | 12.0 | 316.8 | 11.0 |

| | | | | | | | | | | | | | | | | | | |
|---|---|---|---|---|---|---|---|---|---|---|---|---|---|---|---|---|---|---|
| 14ATW-50 Spot54 | 20680 | 180 | 1.9 | 0.05 | 2.38 | 0.05 | 3.17 | 0.38 | 3.93 | 0.50 | 369.0 | 73.0 | 317.1 | 7.6 | 329.0 | 11.0 | 317.1 | 11.0 |
| 14ATW-50 Spot53 | 15870 | 137 | 2.4 | 0.05 | 2.94 | 0.05 | 3.56 | 0.38 | 4.22 | 0.22 | 372.0 | 81.0 | 320.4 | 9.2 | 325.0 | 12.0 | 320.4 | 12.0 |
| 14ATW-50 Spot41 | 19200 | 367 | 1.9 | 0.05 | 2.73 | 0.05 | 4.28 | 0.37 | 4.62 | 0.12 | 335.0 | 91.0 | 322.1 | 8.7 | 317.0 | 13.0 | 322.1 | 11.0 |
| 14ATW-50 Spot44 | 29510 | 222 | 2.2 | 0.05 | 2.51 | 0.05 | 3.71 | 0.39 | 3.88 | 0.46 | 344.0 | 79.0 | 324.7 | 7.7 | 332.0 | 11.0 | 324.7 | 11.0 |
| 14ATW-50 Spot29 | 65700 | 4200 | 1.6 | 0.05 | 2.30 | 0.05 | 2.38 | 0.39 | 2.81 | 0.54 | 385.0 | 54.0 | 327.6 | 7.2 | 335.3 | 7.7 | 327.6 | 10.0 |
| 14ATW-50 Spot25 | 18200 | 756 | 1.4 | 0.05 | 2.36 | 0.06 | 3.80 | 0.39 | 4.07 | 0.43 | 413.0 | 80.0 | 319.1 | 7.6 | 336.0 | 12.0 | 319.1 | 11.0 |
| 14ATW-50 Spot52 | 48200 | 393 | 1.7 | 0.05 | 2.97 | 0.05 | 3.07 | 0.39 | 2.84 | 0.51 | 273.0 | 65.0 | 337.6 | 9.5 | 331.8 | 8.2 | 337.6 | 12.0 |
| **Sample 15DR140** | | | | | | | | | | | | | | | | | | |
| 15DR-140 Spot 1 | 3775 | 89 | 8.0 | 0.02 | 2.89 | 0.05 | 11.64 | 0.15 | 11.26 | 0.00 | 190.0 | 220.0 | 139.1 | 4.0 | 141.0 | 15.0 | 139.1 | 5.5 |
| 15DR-140 Spot 13 | 10660 | 993 | 2.4 | 0.02 | 3.77 | 0.05 | 5.94 | 0.15 | 6.62 | 0.43 | 220.0 | 120.0 | 140.5 | 5.3 | 143.9 | 8.6 | 140.5 | 6.5 |
| 15DR-140 Spot 2 | 2072 | 53 | 10.2 | 0.02 | 3.61 | 0.05 | 10.18 | 0.15 | 10.39 | 0.18 | 220.0 | 200.0 | 141.4 | 5.1 | 144.0 | 14.0 | 141.4 | 6.3 |
| 15DR-140 Spot 18 | 4050 | 181 | 7.6 | 0.02 | 3.38 | 0.05 | 7.76 | 0.15 | 8.28 | 0.34 | 110.0 | 150.0 | 141.5 | 4.7 | 137.0 | 10.0 | 141.5 | 6.1 |
| 15DR-140 Spot 7 | 2340 | 100 | 14.3 | 0.02 | 3.00 | 0.05 | 12.06 | 0.16 | 10.83 | 0.18 | 210.0 | 220.0 | 142.2 | 4.2 | 146.0 | 15.0 | 142.2 | 5.7 |
| 15DR-140 Spot 5 | 2710 | 91 | 18.2 | 0.02 | 3.36 | 0.05 | 11.24 | 0.16 | 10.13 | 0.17 | 300.0 | 210.0 | 142.4 | 4.7 | 152.0 | 14.0 | 142.4 | 6.1 |
| 15DR-140 Spot 9 | 3010 | 242 | 6.9 | 0.02 | 3.66 | 0.05 | 14.50 | 0.17 | 13.94 | 0.11 | 410.0 | 280.0 | 142.9 | 5.1 | 157.0 | 19.0 | 142.9 | 6.4 |
| 15DR-140 Spot 4 | 2460 | 75 | 8.6 | 0.02 | 3.92 | 0.05 | 21.57 | 0.16 | 19.62 | 0.14 | 160.0 | 380.0 | 143.2 | 5.5 | 148.0 | 27.0 | 143.2 | 6.8 |
| 15DR-140 Spot 14 | 5720 | 388 | 5.0 | 0.02 | 2.77 | 0.05 | 7.79 | 0.15 | 7.79 | 0.19 | 140.0 | 150.0 | 145.2 | 4.0 | 145.0 | 10.0 | 145.2 | 5.6 |
| 15DR-140 Spot 12 | 7060 | 1123 | 2.1 | 0.02 | 2.48 | 0.05 | 6.82 | 0.15 | 7.28 | 0.28 | 110.0 | 130.0 | 146.8 | 3.6 | 141.8 | 9.3 | 146.8 | 5.4 |
| 15DR-140 Spot 16 | 5060 | 217 | 7.3 | 0.02 | 2.99 | 0.05 | 8.03 | 0.16 | 7.69 | 0.14 | 220.0 | 150.0 | 147.1 | 4.3 | 150.0 | 10.0 | 147.1 | 5.9 |
| 15DR-140 Spot 8 | 3650 | 217 | 4.7 | 0.02 | 3.03 | 0.05 | 11.51 | 0.16 | 10.32 | 0.05 | 110.0 | 200.0 | 147.3 | 4.4 | 145.0 | 14.0 | 147.3 | 6.0 |
| 15DR-140 Spot 6 | 2600 | 94 | 14.4 | 0.02 | 3.52 | 0.05 | 9.48 | 0.16 | 9.76 | 0.22 | 260.0 | 200.0 | 148.3 | 5.2 | 153.0 | 14.0 | 148.3 | 6.6 |
| 15DR-140 Spot 17 | 4350 | 181 | 8.3 | 0.02 | 4.27 | 0.05 | 9.28 | 0.16 | 10.00 | 0.41 | 160.0 | 180.0 | 149.3 | 6.3 | 149.0 | 14.0 | 149.3 | 7.5 |
| 15DR-140 Spot 15 | 3368 | 175 | 7.9 | 0.02 | 2.38 | 0.05 | 7.78 | 0.17 | 7.51 | 0.15 | 300.0 | 160.0 | 152.7 | 3.6 | 162.0 | 11.0 | 152.7 | 5.5 |
| 15DR-140 Spot 3 | 2800 | 71 | 5.6 | 0.02 | 4.64 | 0.08 | 15.58 | 0.26 | 13.18 | 0.06 | 1060.0 | 300.0 | 151.3 | 6.9 | 236.0 | 28.0 | 151.3 | 8.0 |
| 15DR-140 Spot 10 | 3340 | 366 | 5.8 | 0.02 | 3.55 | 0.05 | 9.79 | 0.14 | 9.35 | 0.19 | 140.0 | 190.0 | 132.8 | 4.6 | 131.0 | 12.0 | 132.8 | 5.9 |
| **Sample 17ATW03** | | | | | | | | | | | | | | | | | | |
| 17ATW03 Spot 38 | 5540 | 839 | 3.4 | 0.01 | 2.85 | 0.05 | 6.54 | 0.07 | 6.03 | 0.06 | 130.0 | 130.0 | 67.6 | 1.9 | 68.3 | 4.0 | 67.6 | 2.6 |
| 17ATW03 Spot 47 | 2640 | 2657 | 4.1 | 0.01 | 3.70 | 0.05 | 10.04 | 0.07 | 10.24 | 0.16 | 120.0 | 190.0 | 67.7 | 2.5 | 65.9 | 6.6 | 67.7 | 3.1 |
| 17ATW03 Spot 37 | 1841 | 237 | 5.6 | 0.01 | 4.05 | 0.05 | 12.78 | 0.07 | 12.43 | 0.03 | 140.0 | 240.0 | 68.0 | 2.7 | 70.9 | 8.6 | 68.0 | 3.3 |
| 17ATW-03 Spot 11 | 4791 | 1856 | 2.1 | 0.01 | 2.24 | 0.05 | 6.65 | 0.07 | 5.97 | 0.01 | 80.0 | 130.0 | 68.8 | 1.5 | 68.9 | 4.0 | 68.8 | 2.4 |
| 17ATW03 Spot 31 | 2995 | 410 | 2.4 | 0.01 | 2.70 | 0.05 | 7.49 | 0.07 | 6.91 | 0.04 | 140.0 | 140.0 | 69.0 | 1.8 | 70.8 | 4.7 | 69.0 | 2.6 |
| 17ATW03 Spot 21 | 3820 | 500 | 6.0 | 0.01 | 2.88 | 0.04 | 10.09 | 0.07 | 10.30 | 0.02 | -60.0 | 170.0 | 69.1 | 2.0 | 65.5 | 6.3 | 69.1 | 2.8 |
| 17ATW03 Spot 34 | 5860 | 597 | 3.5 | 0.01 | 2.59 | 0.05 | 7.33 | 0.07 | 6.90 | 0.11 | 30.0 | 130.0 | 69.3 | 1.8 | 66.8 | 4.5 | 69.3 | 2.6 |
| 17ATW03 Spot 25 | 4230 | 972 | 3.2 | 0.01 | 2.68 | 0.05 | 8.00 | 0.07 | 8.25 | 0.30 | 100.0 | 150.0 | 69.4 | 1.8 | 69.9 | 5.6 | 69.4 | 2.6 |
| 17ATW03 Spot 28 | 4680 | 822 | 3.1 | 0.01 | 3.51 | 0.05 | 11.24 | 0.07 | 11.05 | 0.17 | 220.0 | 220.0 | 69.4 | 2.4 | 72.4 | 7.7 | 69.4 | 3.1 |
| 17ATW03 Spot 44 | 4810 | 4900 | 3.0 | 0.01 | 3.12 | 0.05 | 7.29 | 0.07 | 7.17 | 0.12 | 100.0 | 140.0 | 69.9 | 2.2 | 71.6 | 4.8 | 69.9 | 2.9 |
| 17ATW03 Spot 41 | 3240 | 1145 | 3.6 | 0.01 | 2.74 | 0.05 | 9.67 | 0.07 | 9.04 | 0.06 | 130.0 | 180.0 | 70.1 | 1.9 | 69.2 | 6.0 | 70.1 | 2.7 |
| 17ATW03 Spot 48 | 3493 | 2091 | 5.0 | 0.01 | 2.91 | 0.05 | 7.49 | 0.07 | 7.62 | 0.30 | 170.0 | 140.0 | 70.5 | 2.0 | 73.1 | 5.3 | 70.5 | 2.8 |

| | | | | | | | | | | | | | | | | | | |
|---|---|---|---|---|---|---|---|---|---|---|---|---|---|---|---|---|---|---|
| 17ATW03 Spot 50 | 2830 | 911 | 3.3 | 0.01 | 2.90 | 0.05 | 9.41 | 0.08 | 8.92 | 0.02 | 150.0 | 180.0 | 70.7 | 2.0 | 73.2 | 6.3 | 70.7 | 2.8 |
| 17ATW03 Spot 27 | 3430 | 634 | 3.8 | 0.01 | 2.71 | 0.05 | 8.45 | 0.08 | 8.30 | 0.15 | 280.0 | 170.0 | 71.1 | 1.9 | 77.4 | 6.2 | 71.1 | 2.7 |
| 17ATW03 Spot 32 | 4840 | 577 | 4.0 | 0.01 | 2.98 | 0.05 | 7.82 | 0.08 | 7.55 | 0.03 | 140.0 | 150.0 | 71.1 | 2.1 | 73.7 | 5.4 | 71.1 | 2.8 |
| 17ATW03 Spot 53 | 6000 | 1230 | 5.9 | 0.01 | 2.88 | 0.05 | 6.37 | 0.07 | 6.77 | 0.17 | 0.0 | 120.0 | 71.3 | 2.0 | 69.4 | 4.5 | 71.3 | 2.8 |
| 17ATW03 Spot 45 | 8350 | 9490 | 2.7 | 0.01 | 2.33 | 0.05 | 6.51 | 0.07 | 5.82 | 0.01 | 30.0 | 120.0 | 71.4 | 1.7 | 69.0 | 3.9 | 71.4 | 2.6 |
| 17ATW03 Spot 49 | 4460 | 2140 | 6.7 | 0.01 | 3.40 | 0.05 | 7.04 | 0.07 | 7.85 | 0.33 | 60.0 | 130.0 | 71.6 | 2.4 | 69.8 | 5.3 | 71.6 | 3.1 |
| 17ATW03 Spot 22 | 7700 | 1200 | 2.7 | 0.01 | 3.49 | 0.05 | 9.51 | 0.08 | 8.96 | 0.19 | 160.0 | 190.0 | 71.8 | 2.5 | 74.1 | 6.4 | 71.8 | 3.2 |
| 17ATW03 Spot 52 | 5780 | 1346 | 4.8 | 0.01 | 4.81 | 0.05 | 11.09 | 0.08 | 9.34 | 0.08 | 220.0 | 220.0 | 72.0 | 3.5 | 76.2 | 6.9 | 72.0 | 4.0 |
| 17ATW03 Spot 51 | 4150 | 1124 | 3.9 | 0.01 | 2.93 | 0.05 | 7.71 | 0.07 | 7.07 | 0.09 | 140.0 | 150.0 | 72.1 | 2.1 | 71.9 | 4.9 | 72.1 | 2.9 |
| 17ATW03 Spot 39 | 7130 | 1214 | 4.0 | 0.01 | 3.73 | 0.05 | 6.90 | 0.07 | 6.64 | 0.09 | 90.0 | 130.0 | 72.2 | 2.7 | 72.1 | 4.6 | 72.2 | 3.3 |
| 17ATW03 Spot 30 | 4670 | 719 | 3.6 | 0.01 | 3.44 | 0.05 | 9.13 | 0.07 | 8.84 | 0.19 | 50.0 | 160.0 | 72.8 | 2.5 | 70.7 | 6.1 | 72.8 | 3.2 |
| 17ATW03 Spot 42 | 540 | 315 | 4.2 | 0.01 | 6.16 | 0.05 | 30.19 | 0.08 | 27.27 | 0.08 | -20.0 | 470.0 | 72.8 | 4.5 | 78.0 | 21.0 | 72.8 | 4.9 |
| 17ATW03 Spot 24 | 4330 | 943 | 3.8 | 0.01 | 4.57 | 0.05 | 8.61 | 0.08 | 9.33 | 0.00 | 200.0 | 160.0 | 73.0 | 3.3 | 78.2 | 7.0 | 73.0 | 3.8 |
| 17ATW03 Spot 40 | 9910 | 2632 | 3.1 | 0.01 | 2.53 | 0.05 | 5.64 | 0.07 | 5.75 | 0.25 | 120.0 | 110.0 | 73.3 | 1.9 | 73.1 | 4.0 | 73.3 | 2.7 |
| 17ATW03 Spot 26 | 4760 | 883 | 3.4 | 0.01 | 2.77 | 0.05 | 6.55 | 0.08 | 7.10 | 0.05 | 190.0 | 130.0 | 74.1 | 2.1 | 76.9 | 5.2 | 74.1 | 2.9 |
| 17ATW03 Spot 23 | 12320 | 2513 | 1.9 | 0.01 | 3.57 | 0.05 | 4.77 | 0.07 | 5.21 | 0.47 | 13.0 | 93.0 | 75.5 | 2.7 | 73.2 | 3.7 | 75.5 | 3.4 |
| 17ATW03 Spot 36 | 4120 | 432 | 5.3 | 0.01 | 2.92 | 0.05 | 7.51 | 0.09 | 7.73 | 0.19 | 380.0 | 160.0 | 72.4 | 2.1 | 82.9 | 6.1 | 72.4 | 2.9 |
| 17ATW03 Spot 29 | 5550 | 882 | 3.6 | 0.01 | 4.74 | 0.06 | 8.01 | 0.09 | 7.84 | 0.13 | 420.0 | 170.0 | 73.1 | 3.5 | 84.3 | 6.3 | 73.1 | 4.0 |
| 17ATW03 Spot 20 | 4202 | 477 | 3.0 | 0.01 | 2.57 | 0.06 | 7.22 | 0.09 | 7.39 | 0.36 | 500.0 | 150.0 | 69.8 | 1.8 | 85.4 | 6.0 | 69.8 | 2.6 |
| 17ATW03 Spot 35 | 3740 | 382 | 5.8 | 0.01 | 2.91 | 0.06 | 8.93 | 0.08 | 8.87 | 0.22 | 360.0 | 180.0 | 70.5 | 2.0 | 78.9 | 6.8 | 70.5 | 2.8 |
| 17ATW03 Spot 43 | 2999 | 841 | 1.9 | 0.03 | 3.53 | 0.06 | 9.32 | 0.23 | 9.40 | 0.19 | 420.0 | 190.0 | 197.9 | 7.2 | 212.0 | 18.0 | 197.9 | 8.9 |
| 17ATW03 Spot 46 | 31000 | 1680 | 0.9 | 0.22 | 3.59 | 0.11 | 2.27 | 3.31 | 4.53 | 0.81 | 1807.0 | 44.0 | 1286.0 | 43.0 | ##### | 35.0 | 1286.0 | 54.0 |
| 17ATW03 Spot 33 | 3790 | 377 | 4.9 | 0.01 | 3.37 | 0.04 | 9.63 | 0.07 | 8.85 | 0.02 | -80.0 | 160.0 | 74.2 | 2.5 | 66.4 | 5.7 | 74.2 | 3.2 |
| **Sample 17ATW11** | | | | | | | | | | | | | | | | | | |
| 17ATW11-Spot 33 | 11830 | 447 | 2.5 | 0.05 | 2.27 | 0.05 | 4.45 | 0.35 | 5.38 | 0.38 | 383.0 | 98.0 | 304.4 | 7.0 | 307.0 | 14.0 | 304.4 | 13.0 |
| 17ATW11-Spot 30 | 21500 | 1490 | 1.6 | 0.05 | 1.22 | 0.05 | 2.82 | 0.35 | 3.12 | 0.26 | 323.0 | 64.0 | 304.5 | 3.6 | 306.6 | 8.0 | 304.5 | 11.0 |
| 17ATW11-Spot 28 | 11970 | 1149 | 2.1 | 0.05 | 1.78 | 0.05 | 5.46 | 0.35 | 5.44 | 0.33 | 310.0 | 120.0 | 305.0 | 5.3 | 306.0 | 15.0 | 305.0 | 12.0 |
| 17ATW11-Spot 37 | 5040 | 151 | 3.9 | 0.05 | 3.30 | 0.06 | 6.36 | 0.37 | 6.99 | 0.41 | 370.0 | 130.0 | 305.4 | 9.8 | 319.0 | 19.0 | 305.4 | 15.0 |
| 17ATW11-Spot 34 | 6620 | 227 | 4.5 | 0.05 | 3.29 | 0.05 | 6.01 | 0.34 | 6.69 | 0.44 | 280.0 | 120.0 | 306.3 | 9.7 | 298.0 | 17.0 | 306.3 | 15.0 |
| 17ATW11-Spot 39 | 18100 | 540 | 2.5 | 0.05 | 2.45 | 0.06 | 4.90 | 0.36 | 5.34 | 0.48 | 390.0 | 100.0 | 308.1 | 7.4 | 308.0 | 14.0 | 308.1 | 13.0 |
| 17ATW11-Spot 31 | 33900 | 1674 | 4.9 | 0.05 | 2.24 | 0.06 | 3.07 | 0.37 | 2.52 | 0.25 | 436.0 | 63.0 | 308.7 | 6.9 | 316.2 | 6.8 | 308.7 | 13.0 |
| 17ATW11-Spot 27 | 9300 | 910 | 5.3 | 0.05 | 2.65 | 0.05 | 6.75 | 0.36 | 5.77 | 0.09 | 370.0 | 140.0 | 309.7 | 7.8 | 316.0 | 15.0 | 309.7 | 13.0 |
| 17ATW11-Spot 38 | 6300 | 182 | 4.6 | 0.05 | 3.25 | 0.05 | 5.66 | 0.36 | 5.54 | 0.21 | 390.0 | 120.0 | 310.0 | 10.0 | 315.0 | 14.0 | 310.0 | 15.0 |
| 17ATW11-Spot 35 | 29700 | 874 | 2.2 | 0.05 | 2.23 | 0.05 | 3.05 | 0.35 | 3.70 | 0.53 | 293.0 | 68.0 | 310.2 | 7.0 | 304.8 | 9.5 | 310.2 | 13.0 |
| 17ATW11-Spot 32 | 26900 | 1152 | 1.5 | 0.05 | 2.43 | 0.05 | 4.21 | 0.36 | 3.91 | 0.00 | 308.0 | 86.0 | 310.4 | 7.3 | 310.0 | 11.0 | 310.4 | 13.0 |
| 17ATW11-Spot 26 | 15290 | 1401 | 2.5 | 0.05 | 2.21 | 0.05 | 4.12 | 0.36 | 4.18 | 0.24 | 318.0 | 90.0 | 313.4 | 6.5 | 310.0 | 11.0 | 313.4 | 13.0 |
| 17ATW11-Spot 29 | 11100 | 960 | 3.2 | 0.05 | 3.09 | 0.06 | 7.38 | 0.39 | 8.38 | 0.39 | 610.0 | 160.0 | 305.5 | 9.1 | 343.0 | 22.0 | 305.5 | 14.0 |
| 17ATW11-Spot 36 | 13800 | 399 | 2.4 | 0.05 | 2.86 | 0.06 | 4.65 | 0.38 | 4.50 | 0.29 | 457.0 | 99.0 | 307.6 | 8.5 | 326.0 | 12.0 | 307.6 | 14.0 |

| Sample 18ATW21 | | | | | | | | | | | | | | | | | | |
|---|---|---|---|---|---|---|---|---|---|---|---|---|---|---|---|---|---|---|
| 18ATW-21 Spot 7 | 1664 | 374 | 3.8 | 0.01 | 5.77 | 0.05 | 9.63 | 0.07 | 9.29 | 0.21 | 260.0 | 180.0 | 64.4 | 3.7 | 68.5 | 6.2 | 64.4 | 4.4 |
| 18ATW-21 Spot 4 | 3040 | 677 | 4.1 | 0.01 | 2.98 | 0.05 | 7.37 | 0.07 | 7.45 | 0.16 | 190.0 | 140.0 | 64.9 | 1.9 | 66.4 | 4.7 | 64.9 | 3.0 |
| 18ATW-21 Spot 2 | 2565 | 612 | 4.3 | 0.01 | 3.46 | 0.05 | 10.39 | 0.07 | 10.24 | 0.10 | 80.0 | 190.0 | 64.9 | 2.2 | 64.1 | 6.4 | 64.9 | 3.3 |
| 18ATW-21 Spot 9 | 5190 | 1200 | 3.7 | 0.01 | 3.03 | 0.05 | 6.85 | 0.07 | 6.79 | 0.25 | 170.0 | 130.0 | 65.5 | 1.9 | 65.0 | 4.3 | 65.5 | 3.1 |
| 18ATW-21 Spot 3 | 4810 | 1086 | 3.1 | 0.01 | 2.25 | 0.05 | 6.79 | 0.07 | 6.92 | 0.24 | 70.0 | 130.0 | 65.6 | 1.5 | 65.3 | 4.4 | 65.6 | 2.8 |
| 18ATW-21 Spot 1 | 2277 | 567 | 5.1 | 0.01 | 2.92 | 0.05 | 10.31 | 0.07 | 9.56 | 0.03 | 150.0 | 180.0 | 65.8 | 1.9 | 69.4 | 6.4 | 65.8 | 3.1 |
| 18ATW-21 Spot 6 | 930 | 196 | 2.8 | 0.01 | 4.99 | 0.04 | 20.60 | 0.06 | 21.67 | 0.02 | -210.0 | 310.0 | 66.8 | 3.3 | 58.0 | 12.0 | 66.8 | 4.1 |
| 18ATW-21 Spot 10 | 3070 | 733 | 3.8 | 0.01 | 2.78 | 0.05 | 7.26 | 0.07 | 7.29 | 0.16 | 130.0 | 140.0 | 66.9 | 1.9 | 67.2 | 4.7 | 66.9 | 3.1 |
| 18ATW-21 Spot 17 | 3327 | 1273 | 2.6 | 0.01 | 2.59 | 0.05 | 8.58 | 0.07 | 8.50 | 0.11 | 220.0 | 160.0 | 67.0 | 1.8 | 70.2 | 5.7 | 67.0 | 3.0 |
| 18ATW-21 Spot 26 | 1931 | 666 | 3.6 | 0.01 | 2.77 | 0.05 | 10.32 | 0.07 | 10.03 | 0.10 | 120.0 | 190.0 | 67.2 | 1.9 | 69.1 | 6.8 | 67.2 | 3.1 |
| 18ATW-21 Spot 8 | 4290 | 924 | 3.7 | 0.01 | 2.66 | 0.05 | 7.39 | 0.07 | 7.53 | 0.09 | 120.0 | 140.0 | 67.4 | 1.8 | 68.9 | 5.0 | 67.4 | 3.0 |
| 18ATW-21 Spot 38 | 2886 | 1025 | 3.6 | 0.01 | 2.16 | 0.05 | 10.06 | 0.07 | 10.62 | 0.22 | 200.0 | 200.0 | 68.2 | 1.5 | 72.6 | 7.4 | 68.2 | 2.9 |
| 18ATW-21 Spot 22 | 1802 | 669 | 4.3 | 0.01 | 4.21 | 0.05 | 11.97 | 0.07 | 10.92 | 0.08 | 160.0 | 220.0 | 68.5 | 2.9 | 69.6 | 7.4 | 68.5 | 3.8 |
| 18ATW-21 Spot 34 | 2292 | 842 | 4.2 | 0.01 | 3.27 | 0.05 | 8.95 | 0.07 | 7.25 | 0.24 | 220.0 | 170.0 | 68.6 | 2.2 | 71.4 | 5.0 | 68.6 | 3.4 |
| 18ATW-21 Spot 14 | 1886 | 562 | 5.1 | 0.01 | 4.11 | 0.05 | 13.53 | 0.07 | 12.10 | 0.28 | 240.0 | 250.0 | 68.7 | 2.8 | 72.5 | 8.4 | 68.7 | 3.8 |
| 18ATW-21 Spot 11 | 1801 | 456 | 4.2 | 0.01 | 4.38 | 0.05 | 16.10 | 0.08 | 15.58 | 0.20 | 180.0 | 300.0 | 68.8 | 3.0 | 75.0 | 12.0 | 68.8 | 3.9 |
| 18ATW-21 Spot 12 | 2070 | 572 | 6.4 | 0.01 | 2.89 | 0.05 | 10.02 | 0.07 | 9.52 | 0.08 | 240.0 | 180.0 | 68.8 | 2.0 | 68.8 | 6.3 | 68.8 | 3.2 |
| 18ATW-21 Spot 24 | 2560 | 918 | 3.4 | 0.01 | 3.34 | 0.05 | 12.50 | 0.07 | 11.66 | 0.16 | 10.0 | 220.0 | 69.2 | 2.3 | 65.4 | 7.4 | 69.2 | 3.4 |
| 18ATW-21 Spot 32 | 2600 | 990 | 3.0 | 0.01 | 4.15 | 0.05 | 12.01 | 0.08 | 11.57 | 0.11 | 170.0 | 220.0 | 69.5 | 2.8 | 74.5 | 8.4 | 69.5 | 3.8 |
| 18ATW-21 Spot 29 | 1400 | 475 | 4.3 | 0.01 | 4.69 | 0.04 | 16.21 | 0.07 | 14.67 | 0.22 | -110.0 | 250.0 | 69.7 | 3.3 | 65.2 | 9.3 | 69.7 | 4.2 |
| 18ATW-21 Spot 15 | 2740 | 859 | 4.3 | 0.01 | 2.84 | 0.05 | 8.25 | 0.07 | 7.98 | 0.14 | 170.0 | 160.0 | 69.9 | 2.0 | 71.0 | 5.5 | 69.9 | 3.2 |
| 18ATW-21 Spot 18 | 1649 | 632 | 4.4 | 0.01 | 4.67 | 0.05 | 15.07 | 0.08 | 13.92 | 0.01 | 300.0 | 280.0 | 70.0 | 3.2 | 78.7 | 9.6 | 70.0 | 4.1 |
| 18ATW-21 Spot 30 | 2193 | 782 | 3.0 | 0.01 | 2.47 | 0.05 | 9.90 | 0.07 | 9.92 | 0.06 | 120.0 | 170.0 | 70.1 | 1.7 | 72.6 | 7.0 | 70.1 | 3.1 |
| 18ATW-21 Spot 27 | 5130 | 1730 | 4.3 | 0.01 | 2.74 | 0.05 | 7.68 | 0.07 | 7.21 | 0.15 | 110.0 | 140.0 | 70.2 | 1.9 | 70.5 | 4.9 | 70.2 | 3.2 |
| 18ATW-21 Spot 33 | 2390 | 862 | 4.1 | 0.01 | 3.11 | 0.05 | 8.48 | 0.07 | 8.44 | 0.12 | 190.0 | 170.0 | 70.2 | 2.1 | 71.7 | 5.9 | 70.2 | 3.4 |
| 18ATW-21 Spot 19 | 3120 | 1223 | 4.1 | 0.01 | 2.83 | 0.05 | 10.00 | 0.07 | 9.70 | 0.01 | 220.0 | 200.0 | 70.3 | 2.0 | 72.4 | 6.8 | 70.3 | 3.3 |
| 18ATW-21 Spot 31 | 2343 | 829 | 3.5 | 0.01 | 3.56 | 0.05 | 8.90 | 0.07 | 8.87 | 0.15 | 60.0 | 160.0 | 70.3 | 2.5 | 68.3 | 5.9 | 70.3 | 3.6 |
| 18ATW-21 Spot 23 | 4230 | 1511 | 2.2 | 0.01 | 4.90 | 0.05 | 10.20 | 0.07 | 10.35 | 0.28 | 20.0 | 180.0 | 70.6 | 3.5 | 68.9 | 6.9 | 70.6 | 4.3 |
| 18ATW-21 Spot 28 | 1599 | 536 | 4.2 | 0.01 | 3.72 | 0.05 | 12.55 | 0.07 | 12.15 | 0.10 | 50.0 | 220.0 | 70.6 | 2.6 | 66.7 | 7.9 | 70.6 | 3.7 |
| 18ATW-21 Spot 21 | 2351 | 873 | 4.6 | 0.01 | 3.80 | 0.05 | 10.73 | 0.08 | 9.71 | 0.02 | 210.0 | 200.0 | 70.8 | 2.7 | 74.3 | 7.0 | 70.8 | 3.7 |
| 18ATW-21 Spot 37 | 1747 | 591 | 3.7 | 0.01 | 3.51 | 0.05 | 10.27 | 0.07 | 9.03 | 0.12 | 170.0 | 200.0 | 71.3 | 2.5 | 72.3 | 6.3 | 71.3 | 3.6 |
| 18ATW-21 Spot 20 | 2070 | 783 | 4.1 | 0.01 | 3.23 | 0.04 | 11.19 | 0.07 | 11.05 | 0.11 | -30.0 | 190.0 | 71.6 | 2.3 | 67.1 | 7.2 | 71.6 | 3.5 |
| 18ATW-21 Spot 36 | 2120 | 728 | 4.4 | 0.01 | 3.39 | 0.05 | 9.59 | 0.07 | 9.92 | 0.13 | 70.0 | 180.0 | 71.8 | 2.4 | 69.9 | 6.7 | 71.8 | 3.6 |
| 18ATW-21 Spot 5 | 5920 | 931 | 4.0 | 0.01 | 2.70 | 0.06 | 5.88 | 0.11 | 5.44 | 0.16 | 530.0 | 120.0 | 90.0 | 2.4 | 109.2 | 5.6 | 90.0 | 4.1 |
| 18ATW-21 Spot 13 | 6020 | 606 | 5.8 | 0.03 | 8.75 | 0.09 | 6.03 | 0.36 | 11.60 | 0.47 | 1350.0 | 130.0 | 188.0 | 16.0 | 305.0 | 31.0 | 188.0 | 18.0 |
| 18ATW-21 Spot 40 | 1924 | 229 | 1.5 | 0.03 | 3.79 | 0.05 | 7.98 | 0.19 | 7.77 | 0.17 | 140.0 | 150.0 | 184.2 | 6.9 | 179.0 | 13.0 | 184.2 | 9.6 |
| 18ATW-21 Spot 35 | 3470 | 1225 | 3.8 | 0.01 | 3.40 | 0.05 | 8.04 | 0.08 | 7.72 | 0.02 | 120.0 | 150.0 | 73.4 | 2.5 | 74.0 | 5.4 | 73.4 | 3.7 |
| 18ATW-21 Spot 39 | 3910 | 1281 | 3.3 | 0.01 | 2.87 | 0.05 | 7.13 | 0.08 | 6.77 | 0.18 | 150.0 | 130.0 | 71.5 | 2.0 | 73.5 | 4.9 | 71.5 | 3.3 |
| 18ATW-21 Spot 25 | 3560 | 1151 | 3.2 | 0.01 | 2.58 | 0.10 | 59.38 | 0.15 | 58.50 | 0.39 | 900.0 | ##### | 74.5 | 1.9 | 134.0 | 73.0 | 74.5 | 3.3 |

| | | | | | | | | | | | | | | | | | | |
|---|---|---|---|---|---|---|---|---|---|---|---|---|---|---|---|---|---|---|
| 18ATW-21 Spot 16 | 3568 | 1195 | 2.5 | 0.01 | 2.88 | 0.05 | 7.42 | 0.07 | 6.59 | 0.08 | 60.0 | 130.0 | 73.4 | 2.1 | 69.8 | 4.5 | 73.4 | 3.4 |
| **Sample 12CSR20** | | | | | | | | | | | | | | | | | | |
| Output_1_13 | 56450 | 1673 | 14.0 | 0.01 | 1.92 | 0.05 | 4.88 | 0.06 | 4.54 | 0.07 | 70.0 | 100.0 | 56.9 | 1.1 | 56.5 | 2.5 | 56.9 | 1.1 |
| Output_1_67 | 28990 | 902 | 9.5 | 0.01 | 2.21 | 0.05 | 7.55 | 0.06 | 7.07 | 0.28 | 180.0 | 170.0 | 58.0 | 1.3 | 61.2 | 4.2 | 58.0 | 1.2 |
| Output_1_42 | 37900 | 4420 | 23.4 | 0.01 | 6.16 | 0.05 | 11.20 | 0.06 | 14.48 | 0.82 | 110.0 | 240.0 | 58.3 | 3.6 | 59.2 | 8.3 | 58.3 | 4.3 |
| Output_1_65 | 13600 | 365 | 18.0 | 0.01 | 1.74 | 0.05 | 4.69 | 0.06 | 4.58 | 0.03 | 147.0 | 94.0 | 59.2 | 1.0 | 60.3 | 2.7 | 59.2 | 1.0 |
| Output_1_18 | 20800 | 561 | 41.3 | 0.01 | 4.00 | 0.05 | 8.30 | 0.06 | 4.15 | 0.15 | 70.0 | 160.0 | 59.3 | 2.4 | 61.7 | 2.5 | 59.3 | 5.3 |
| Output_1_156 | 38690 | 1836 | 13.4 | 0.01 | 1.72 | 0.05 | 3.13 | 0.06 | 3.13 | 0.32 | 97.0 | 65.0 | 59.8 | 1.0 | 60.1 | 1.9 | 59.8 | 1.0 |
| Output_1_58 | 7740 | 196 | 49.2 | 0.01 | 2.33 | 0.05 | 6.30 | 0.07 | 7.14 | 0.18 | 150.0 | 130.0 | 63.3 | 1.5 | 66.0 | 4.6 | 63.3 | 2.2 |
| Output_1_28 | 7870 | 400 | 19.1 | 0.01 | 2.80 | 0.05 | 8.32 | 0.07 | 8.93 | 0.06 | 230.0 | 180.0 | 66.4 | 1.9 | 70.2 | 6.0 | 66.4 | 2.0 |
| Output_1_103 | 1063 | 28 | 14.8 | 0.01 | 5.33 | 0.06 | 20.00 | 0.08 | 17.50 | 0.08 | 350.0 | 360.0 | 67.3 | 3.5 | 77.0 | 13.0 | 67.3 | 3.5 |
| Output_1_57 | 7170 | 173 | 39.2 | 0.01 | 3.12 | 0.05 | 13.26 | 0.07 | 13.51 | 0.08 | 230.0 | 260.0 | 67.8 | 2.1 | 72.6 | 9.7 | 67.8 | 2.1 |
| Output_1_88 | 5400 | 159 | 4.6 | 0.01 | 3.84 | 0.05 | 8.62 | 0.07 | 9.58 | 0.19 | 140.0 | 180.0 | 68.6 | 2.6 | 71.5 | 6.6 | 68.6 | 2.7 |
| Output_1_17 | 14590 | 352 | 10.5 | 0.01 | 5.07 | 0.05 | 11.90 | 0.08 | 12.99 | 0.58 | 200.0 | 250.0 | 70.9 | 3.6 | 75.1 | 9.8 | 70.9 | 3.8 |
| Output_1_166 | 4400 | 171 | 14.0 | 0.01 | 4.13 | 0.05 | 14.12 | 0.08 | 14.46 | 0.10 | 260.0 | 300.0 | 72.9 | 3.0 | 84.0 | 10.0 | 72.9 | 3.0 |
| Output_1_89 | 4130 | 114 | 4.3 | 0.01 | 5.55 | 0.05 | 16.60 | 0.08 | 16.67 | 0.29 | 210.0 | 330.0 | 74.0 | 4.1 | 76.0 | 12.0 | 74.0 | 4.1 |
| Output_1_60 | 14820 | 280 | 8.1 | 0.01 | 2.49 | 0.05 | 10.70 | 0.08 | 9.11 | 0.13 | 120.0 | 210.0 | 74.5 | 1.8 | 75.0 | 6.5 | 74.5 | 2.8 |
| Output_1_167 | 4680 | 180 | 16.1 | 0.01 | 3.23 | 0.05 | 12.62 | 0.08 | 13.25 | 0.42 | 210.0 | 260.0 | 75.4 | 2.4 | 81.0 | 10.0 | 75.4 | 2.6 |
| Output_1_22 | 7880 | 185 | 4.7 | 0.01 | 4.21 | 0.05 | 11.86 | 0.09 | 13.04 | 0.34 | 300.0 | 250.0 | 79.1 | 3.3 | 89.0 | 11.0 | 79.1 | 3.4 |
| Output_1_41 | 14970 | 1392 | 10.1 | 0.01 | 6.06 | 0.05 | 9.92 | 0.09 | 11.49 | 0.65 | 200.0 | 210.0 | 80.4 | 4.8 | 85.0 | 9.5 | 80.4 | 5.1 |
| Output_1_91 | 3430 | 82 | 8.0 | 0.01 | 2.37 | 0.07 | 7.50 | 0.12 | 7.28 | 0.16 | 940.0 | 150.0 | 81.0 | 1.9 | 115.6 | 7.9 | 81.0 | 1.9 |
| Output_1_10 | 10530 | 223 | 19.9 | 0.01 | 2.83 | 0.05 | 6.39 | 0.09 | 6.10 | 0.01 | 210.0 | 130.0 | 83.7 | 2.4 | 85.9 | 5.0 | 83.7 | 2.6 |
| Output_1_5 | 7680 | 160 | 8.0 | 0.01 | 3.07 | 0.05 | 11.95 | 0.09 | 11.70 | 0.19 | 320.0 | 210.0 | 85.6 | 2.6 | 91.0 | 10.0 | 85.6 | 2.5 |
| Output_1_138 | 5900 | 269 | 4.8 | 0.01 | 5.58 | 0.05 | 15.06 | 0.10 | 13.68 | 0.03 | 170.0 | 290.0 | 87.2 | 4.9 | 92.0 | 12.0 | 87.2 | 4.9 |
| Output_1_72 | 3170 | 84 | 12.7 | 0.01 | 9.56 | 0.05 | 21.57 | 0.10 | 26.53 | 0.76 | 190.0 | 430.0 | 87.3 | 8.4 | 94.0 | 24.0 | 87.3 | 8.5 |
| Output_1_66 | 14870 | 278 | 3.1 | 0.01 | 2.58 | 0.05 | 9.96 | 0.10 | 9.84 | 0.41 | 150.0 | 190.0 | 91.8 | 2.3 | 93.3 | 8.7 | 91.8 | 2.1 |
| Output_1_115 | 3390 | 83 | 5.7 | 0.01 | 4.57 | 0.05 | 14.97 | 0.10 | 15.00 | 0.18 | 240.0 | 290.0 | 93.9 | 4.2 | 97.0 | 14.0 | 93.9 | 4.2 |
| Output_1_43 | 7580 | 469 | 3.2 | 0.02 | 2.59 | 0.05 | 7.80 | 0.11 | 7.47 | 0.20 | 200.0 | 140.0 | 98.9 | 2.6 | 104.4 | 7.4 | 98.9 | 3.0 |
| Output_1_122 | 4300 | 130 | 5.3 | 0.02 | 6.37 | 0.06 | 18.97 | 0.13 | 21.09 | 0.51 | 460.0 | 410.0 | 100.3 | 6.4 | 121.0 | 25.0 | 100.3 | 5.2 |
| Output_1_34 | 16420 | 915 | 2.9 | 0.02 | 1.74 | 0.05 | 4.63 | 0.11 | 4.37 | 0.08 | 171.0 | 96.0 | 103.0 | 1.8 | 105.7 | 4.4 | 103.0 | 2.0 |
| Output_1_75 | 21080 | 785 | 2.8 | 0.02 | 2.64 | 0.05 | 6.01 | 0.11 | 6.12 | 0.40 | 180.0 | 120.0 | 104.0 | 2.7 | 103.9 | 6.0 | 104.0 | 2.4 |
| Output_1_51 | 22510 | 620 | 4.1 | 0.02 | 1.87 | 0.05 | 5.11 | 0.11 | 5.31 | 0.14 | 220.0 | 110.0 | 105.8 | 2.0 | 110.2 | 5.5 | 105.8 | 1.9 |
| Output_1_83 | 9800 | 214 | 2.2 | 0.02 | 2.92 | 0.05 | 7.28 | 0.13 | 6.77 | 0.10 | 210.0 | 150.0 | 118.3 | 3.4 | 121.2 | 7.8 | 118.3 | 3.6 |
| Output_1_157 | 19300 | 468 | 5.3 | 0.02 | 1.83 | 0.05 | 5.61 | 0.13 | 5.21 | 0.23 | 180.0 | 120.0 | 118.6 | 2.2 | 121.1 | 5.9 | 118.6 | 2.2 |
| Output_1_87 | 6690 | 115 | 1.8 | 0.02 | 3.76 | 0.06 | 17.86 | 0.14 | 18.44 | 0.03 | 370.0 | 370.0 | 118.8 | 4.4 | 133.0 | 23.0 | 118.8 | 4.4 |
| Output_1_8 | 9550 | 142 | 1.4 | 0.02 | 2.15 | 0.05 | 5.51 | 0.13 | 5.50 | 0.11 | 150.0 | 110.0 | 119.0 | 2.6 | 119.8 | 6.2 | 119.0 | 2.7 |
| Output_1_139 | 6040 | 204 | 1.9 | 0.02 | 3.91 | 0.05 | 8.37 | 0.13 | 8.80 | 0.21 | 120.0 | 170.0 | 120.8 | 4.7 | 119.5 | 9.5 | 120.8 | 4.7 |
| Output_1_107 | 8860 | 131 | 2.8 | 0.02 | 2.11 | 0.05 | 5.47 | 0.13 | 5.72 | 0.14 | 270.0 | 110.0 | 121.3 | 2.5 | 126.4 | 6.8 | 121.3 | 2.7 |
| Output_1_76 | 21140 | 641 | 1.6 | 0.02 | 2.75 | 0.05 | 8.56 | 0.13 | 6.98 | 0.08 | 290.0 | 180.0 | 123.0 | 3.4 | 128.2 | 8.5 | 123.0 | 2.6 |

| | | | | | | | | | | | | | | | | | | |
|---|---|---|---|---|---|---|---|---|---|---|---|---|---|---|---|---|---|---|
| Output_1_163 | 14130 | 334 | 1.5 | 0.02 | 1.92 | 0.05 | 4.50 | 0.14 | 4.45 | 0.10 | 229.0 | 96.0 | 123.3 | 2.3 | 130.2 | 5.4 | 123.3 | 2.2 |
| Output_1_82 | 25510 | 567 | 1.1 | 0.02 | 3.10 | 0.05 | 3.19 | 0.13 | 4.51 | 0.72 | 198.0 | 68.0 | 123.5 | 3.8 | 124.7 | 5.3 | 123.5 | 4.4 |
| Output_1_20 | 45900 | 650 | 5.5 | 0.02 | 4.72 | 0.05 | 4.44 | 0.13 | 7.11 | 0.80 | 170.0 | 100.0 | 124.6 | 5.8 | 126.1 | 8.5 | 124.6 | 5.8 |
| Output_1_97 | 11090 | 151 | 2.2 | 0.02 | 2.71 | 0.05 | 5.61 | 0.14 | 5.11 | 0.13 | 320.0 | 120.0 | 124.7 | 3.3 | 137.1 | 6.6 | 124.7 | 3.0 |
| Output_1_71 | 11780 | 196 | 1.7 | 0.02 | 2.51 | 0.05 | 5.27 | 0.15 | 5.34 | 0.25 | 330.0 | 110.0 | 127.0 | 3.2 | 139.8 | 7.0 | 127.0 | 3.5 |
| Output_1_98 | 10070 | 129 | 2.2 | 0.02 | 3.08 | 0.05 | 9.53 | 0.14 | 9.72 | 0.59 | 330.0 | 210.0 | 128.3 | 3.9 | 136.0 | 13.0 | 128.3 | 3.5 |
| Output_1_73 | 7290 | 130 | 4.0 | 0.02 | 3.32 | 0.05 | 8.10 | 0.15 | 8.97 | 0.33 | 170.0 | 170.0 | 128.7 | 4.2 | 137.0 | 11.0 | 128.7 | 6.4 |
| Output_1_61 | 9360 | 107 | 1.7 | 0.02 | 2.52 | 0.05 | 6.34 | 0.13 | 6.18 | 0.09 | 130.0 | 120.0 | 128.9 | 3.2 | 127.6 | 7.4 | 128.9 | 3.3 |
| Output_1_173 | 9990 | 201 | 1.5 | 0.02 | 1.86 | 0.05 | 5.64 | 0.15 | 5.37 | 0.07 | 240.0 | 120.0 | 130.6 | 2.4 | 139.0 | 7.0 | 130.6 | 2.6 |
| Output_1_16 | 6040 | 75 | 2.9 | 0.02 | 2.78 | 0.06 | 12.52 | 0.15 | 11.92 | 0.02 | 330.0 | 250.0 | 130.7 | 3.6 | 142.0 | 16.0 | 130.7 | 5.7 |
| Output_1_7 | 22810 | 308 | 3.2 | 0.02 | 1.46 | 0.05 | 3.45 | 0.14 | 3.65 | 0.30 | 153.0 | 73.0 | 130.8 | 1.9 | 130.3 | 4.5 | 130.8 | 1.8 |
| Output_1_39 | 6340 | 369 | 1.2 | 0.02 | 4.18 | 0.06 | 12.73 | 0.15 | 10.74 | 0.18 | 350.0 | 260.0 | 131.1 | 5.4 | 141.0 | 14.0 | 131.1 | 5.4 |
| Output_1_2 | 32740 | 533 | 3.0 | 0.02 | 3.15 | 0.05 | 6.47 | 0.14 | 5.58 | 0.22 | 230.0 | 140.0 | 131.7 | 4.1 | 132.9 | 7.0 | 131.7 | 4.0 |
| Output_1_74 | 15900 | 294 | 2.4 | 0.02 | 1.40 | 0.05 | 4.31 | 0.14 | 4.04 | 0.13 | 222.0 | 91.0 | 132.3 | 1.8 | 136.1 | 5.1 | 132.3 | 1.7 |
| Output_1_9 | 3950 | 52 | 1.9 | 0.02 | 3.52 | 0.05 | 10.00 | 0.15 | 10.27 | 0.14 | 200.0 | 190.0 | 134.0 | 4.7 | 137.0 | 13.0 | 134.0 | 4.8 |
| Output_1_6 | 13200 | 178 | 1.6 | 0.02 | 2.73 | 0.05 | 5.31 | 0.16 | 5.02 | 0.26 | 360.0 | 110.0 | 135.5 | 3.7 | 146.4 | 6.9 | 135.5 | 3.5 |
| Output_1_132 | 4680 | 150 | 3.3 | 0.02 | 3.45 | 0.05 | 7.41 | 0.15 | 8.78 | 0.28 | 290.0 | 150.0 | 136.6 | 4.7 | 141.0 | 12.0 | 136.6 | 4.4 |
| Output_1_33 | 14860 | 479 | 2.0 | 0.02 | 2.14 | 0.05 | 7.09 | 0.15 | 7.38 | 0.36 | 170.0 | 140.0 | 136.8 | 2.9 | 141.0 | 10.0 | 136.8 | 4.6 |
| Output_1_1 | 13620 | 230 | 1.6 | 0.02 | 2.52 | 0.05 | 6.15 | 0.15 | 6.68 | 0.35 | 200.0 | 130.0 | 136.8 | 3.4 | 141.2 | 8.5 | 136.8 | 3.6 |
| Output_1_3 | 3680 | 53 | 1.4 | 0.02 | 3.39 | 0.05 | 10.17 | 0.15 | 9.15 | 0.01 | 300.0 | 200.0 | 137.5 | 4.6 | 144.0 | 13.0 | 137.5 | 4.6 |
| Output_1_63 | 5540 | 60 | 1.5 | 0.02 | 2.73 | 0.05 | 8.13 | 0.15 | 6.76 | 0.13 | 140.0 | 150.0 | 138.0 | 3.7 | 139.7 | 9.1 | 138.0 | 3.6 |
| Output_1_130 | 5280 | 159 | 2.4 | 0.02 | 2.43 | 0.05 | 8.58 | 0.16 | 8.64 | 0.09 | 320.0 | 180.0 | 139.3 | 3.4 | 152.0 | 12.0 | 139.3 | 3.3 |
| Output_1_123 | 3740 | 84 | 2.7 | 0.02 | 5.94 | 0.05 | 15.92 | 0.15 | 13.73 | 0.08 | 270.0 | 300.0 | 139.7 | 8.2 | 144.0 | 19.0 | 139.7 | 8.1 |
| Output_1_45 | 5350 | 187 | 1.0 | 0.02 | 5.02 | 0.05 | 13.43 | 0.16 | 16.77 | 0.44 | 240.0 | 280.0 | 139.9 | 7.2 | 146.0 | 23.0 | 139.9 | 7.0 |
| Output_1_137 | 48500 | 1421 | 1.2 | 0.02 | 1.73 | 0.05 | 2.57 | 0.16 | 2.44 | 0.19 | 213.0 | 56.0 | 140.4 | 2.4 | 146.9 | 3.3 | 140.4 | 2.6 |
| Output_1_56 | 11600 | 137 | 1.2 | 0.02 | 1.41 | 0.05 | 8.35 | 0.16 | 7.45 | 0.02 | 350.0 | 180.0 | 140.4 | 2.0 | 153.0 | 12.0 | 140.4 | 2.2 |
| Output_1_55 | 6240 | 75 | 1.6 | 0.02 | 2.40 | 0.05 | 8.83 | 0.16 | 8.75 | 0.04 | 310.0 | 180.0 | 140.5 | 3.4 | 150.0 | 12.0 | 140.5 | 3.5 |
| Output_1_172 | 7990 | 156 | 2.6 | 0.02 | 2.86 | 0.05 | 8.60 | 0.15 | 8.61 | 0.26 | 170.0 | 170.0 | 140.7 | 4.0 | 142.0 | 11.0 | 140.7 | 4.7 |
| Output_1_153 | 5350 | 107 | 2.3 | 0.02 | 2.34 | 0.05 | 6.65 | 0.17 | 6.02 | 0.16 | 330.0 | 140.0 | 141.4 | 3.3 | 155.8 | 9.1 | 141.4 | 3.5 |
| Output_1_21 | 27430 | 350 | 2.0 | 0.02 | 1.98 | 0.05 | 3.77 | 0.15 | 3.92 | 0.07 | 212.0 | 82.0 | 141.5 | 2.8 | 144.5 | 5.3 | 141.5 | 3.4 |
| Output_1_92 | 28450 | 381 | 2.3 | 0.02 | 3.10 | 0.05 | 3.56 | 0.16 | 4.68 | 0.59 | 331.0 | 80.0 | 142.0 | 4.3 | 154.6 | 6.7 | 142.0 | 3.8 |
| Output_1_12 | 10440 | 124 | 1.2 | 0.02 | 1.66 | 0.05 | 4.25 | 0.16 | 4.73 | 0.21 | 259.0 | 92.0 | 142.3 | 2.3 | 149.0 | 6.6 | 142.3 | 2.4 |
| Output_1_54 | 13230 | 209 | 1.7 | 0.02 | 1.92 | 0.05 | 4.66 | 0.15 | 4.79 | 0.32 | 161.0 | 95.0 | 142.5 | 2.7 | 145.5 | 6.5 | 142.5 | 2.6 |
| Output_1_52 | 16600 | 314 | 2.0 | 0.02 | 1.88 | 0.05 | 5.10 | 0.16 | 5.27 | 0.22 | 220.0 | 110.0 | 142.6 | 2.6 | 149.4 | 7.6 | 142.6 | 2.4 |
| Output_1_32 | 9990 | 283 | 1.0 | 0.02 | 2.98 | 0.05 | 8.92 | 0.17 | 8.88 | 0.18 | 370.0 | 190.0 | 143.1 | 4.3 | 158.0 | 13.0 | 143.1 | 5.5 |
| Output_1_100 | 8040 | 95 | 2.4 | 0.02 | 2.27 | 0.05 | 5.41 | 0.15 | 5.09 | 0.12 | 190.0 | 110.0 | 143.3 | 3.2 | 144.3 | 6.9 | 143.3 | 3.4 |
| Output_1_148 | 30520 | 665 | 1.4 | 0.02 | 1.78 | 0.05 | 3.46 | 0.15 | 3.33 | 0.33 | 168.0 | 74.0 | 143.4 | 2.5 | 144.6 | 4.5 | 143.4 | 2.6 |
| Output_1_160 | 3750 | 76 | 1.5 | 0.02 | 2.49 | 0.05 | 8.38 | 0.17 | 8.67 | 0.01 | 370.0 | 170.0 | 143.4 | 3.5 | 161.0 | 13.0 | 143.4 | 3.7 |
| Output_1_23 | 8400 | 118 | 2.6 | 0.02 | 5.31 | 0.05 | 7.60 | 0.15 | 7.79 | 0.53 | 210.0 | 160.0 | 143.7 | 7.6 | 145.0 | 11.0 | 143.7 | 7.3 |
| Output_1_14 | 27340 | 317 | 1.9 | 0.02 | 1.55 | 0.05 | 3.62 | 0.16 | 3.73 | 0.02 | 183.0 | 79.0 | 143.8 | 2.2 | 146.5 | 5.0 | 143.8 | 2.3 |

| | | | | | | | | | | | | | | | | | | |
|---|---|---|---|---|---|---|---|---|---|---|---|---|---|---|---|---|---|---|
| Output_1_19 | 8710 | 102 | 1.3 | 0.02 | 3.44 | 0.05 | 11.93 | 0.15 | 11.11 | 0.22 | 180.0 | 230.0 | 144.4 | 4.9 | 144.0 | 15.0 | 144.4 | 5.6 |
| Output_1_104 | 11850 | 144 | 3.7 | 0.02 | 2.16 | 0.05 | 4.68 | 0.16 | 5.47 | 0.42 | 242.0 | 98.0 | 144.6 | 3.1 | 149.2 | 7.4 | 144.6 | 2.9 |
| Output_1_116 | 8370 | 133 | 1.9 | 0.02 | 2.73 | 0.05 | 5.32 | 0.16 | 5.19 | 0.16 | 140.0 | 100.0 | 144.7 | 3.9 | 148.0 | 7.3 | 144.7 | 3.8 |
| Output_1_145 | 15760 | 357 | 2.7 | 0.02 | 2.11 | 0.05 | 4.15 | 0.16 | 5.07 | 0.58 | 213.0 | 90.0 | 144.8 | 3.0 | 149.8 | 6.7 | 144.8 | 3.0 |
| Output_1_151 | 13490 | 281 | 1.0 | 0.02 | 2.37 | 0.05 | 6.20 | 0.17 | 6.51 | 0.06 | 240.0 | 130.0 | 145.4 | 3.4 | 158.2 | 9.1 | 145.4 | 3.2 |
| Output_1_105 | 46600 | 570 | 1.7 | 0.02 | 3.28 | 0.05 | 3.29 | 0.16 | 3.57 | 0.53 | 274.0 | 74.0 | 145.7 | 4.7 | 149.1 | 4.6 | 145.7 | 4.7 |
| Output_1_95 | 2930 | 35 | 1.4 | 0.02 | 3.44 | 0.05 | 10.85 | 0.16 | 10.32 | 0.19 | 260.0 | 200.0 | 146.3 | 5.0 | 147.0 | 13.0 | 146.3 | 5.5 |
| Output_1_69 | 3550 | 46 | 1.5 | 0.02 | 2.91 | 0.05 | 11.18 | 0.16 | 11.18 | 0.11 | 180.0 | 210.0 | 146.5 | 4.2 | 150.0 | 16.0 | 146.5 | 4.4 |
| Output_1_70 | 19530 | 262 | 1.9 | 0.02 | 1.47 | 0.05 | 4.61 | 0.15 | 4.46 | 0.01 | 87.0 | 92.0 | 147.0 | 2.1 | 144.0 | 6.0 | 147.0 | 2.1 |
| Output_1_141 | 5590 | 146 | 2.4 | 0.02 | 2.25 | 0.05 | 9.07 | 0.16 | 8.59 | 0.12 | 220.0 | 180.0 | 147.2 | 3.3 | 152.0 | 12.0 | 147.2 | 3.5 |
| Output_1_140 | 5380 | 145 | 2.1 | 0.02 | 3.24 | 0.05 | 8.64 | 0.16 | 8.18 | 0.19 | 270.0 | 160.0 | 147.3 | 4.7 | 149.0 | 12.0 | 147.3 | 4.8 |
| Output_1_128 | 3690 | 94 | 1.3 | 0.02 | 3.26 | 0.05 | 9.42 | 0.17 | 9.41 | 0.14 | 270.0 | 180.0 | 147.5 | 4.6 | 160.0 | 13.0 | 147.5 | 4.5 |
| Output_1_114 | 15960 | 237 | 1.6 | 0.02 | 2.36 | 0.05 | 5.03 | 0.18 | 5.08 | 0.40 | 330.0 | 110.0 | 148.3 | 3.4 | 164.9 | 8.0 | 148.3 | 3.3 |
| Output_1_112 | 60300 | 832 | 1.5 | 0.02 | 1.98 | 0.05 | 3.39 | 0.16 | 3.20 | 0.32 | 199.0 | 75.0 | 148.4 | 2.9 | 150.3 | 4.5 | 148.4 | 3.1 |
| Output_1_99 | 2860 | 32 | 2.2 | 0.02 | 4.29 | 0.06 | 13.25 | 0.18 | 11.24 | 0.31 | 380.0 | 280.0 | 148.4 | 6.3 | 165.0 | 18.0 | 148.4 | 7.0 |
| Output_1_154 | 9550 | 184 | 1.6 | 0.02 | 2.27 | 0.05 | 5.15 | 0.16 | 5.52 | 0.19 | 140.0 | 100.0 | 148.6 | 3.3 | 148.3 | 7.6 | 148.6 | 3.6 |
| Output_1_111 | 3620 | 49 | 2.8 | 0.02 | 3.58 | 0.05 | 8.98 | 0.16 | 9.32 | 0.30 | 180.0 | 170.0 | 148.7 | 5.0 | 153.0 | 13.0 | 148.7 | 5.2 |
| Output_1_142 | 6080 | 154 | 2.3 | 0.02 | 2.96 | 0.05 | 6.41 | 0.17 | 7.02 | 0.19 | 270.0 | 130.0 | 148.7 | 4.4 | 160.0 | 10.0 | 148.7 | 4.2 |
| Output_1_77 | 5230 | 125 | 1.8 | 0.02 | 2.44 | 0.05 | 7.26 | 0.16 | 6.83 | 0.16 | 180.0 | 140.0 | 148.8 | 3.6 | 151.2 | 9.8 | 148.8 | 3.5 |
| Output_1_35 | 3630 | 143 | 1.5 | 0.02 | 3.41 | 0.05 | 11.16 | 0.16 | 11.54 | 0.19 | 150.0 | 210.0 | 149.5 | 5.0 | 148.0 | 15.0 | 149.5 | 5.0 |
| Output_1_36 | 85300 | 4040 | 5.3 | 0.02 | 1.83 | 0.05 | 2.20 | 0.16 | 2.50 | 0.66 | 186.0 | 47.0 | 150.1 | 2.7 | 154.1 | 3.6 | 150.1 | 2.8 |
| Output_1_131 | 11410 | 325 | 1.3 | 0.02 | 2.72 | 0.05 | 7.36 | 0.17 | 6.51 | 0.08 | 240.0 | 150.0 | 150.1 | 4.1 | 158.2 | 9.9 | 150.1 | 4.1 |
| Output_1_164 | 3660 | 70 | 3.0 | 0.02 | 2.71 | 0.05 | 8.78 | 0.15 | 8.44 | 0.14 | 90.0 | 170.0 | 150.6 | 4.0 | 146.0 | 12.0 | 150.6 | 4.3 |
| Output_1_134 | 13990 | 402 | 1.4 | 0.02 | 1.86 | 0.05 | 4.74 | 0.16 | 5.06 | 0.40 | 124.0 | 94.0 | 150.7 | 2.7 | 148.6 | 7.1 | 150.7 | 2.7 |
| Output_1_102 | 3290 | 36 | 2.6 | 0.02 | 3.68 | 0.05 | 10.40 | 0.17 | 10.47 | 0.04 | 240.0 | 210.0 | 150.7 | 5.4 | 163.0 | 16.0 | 150.7 | 5.4 |
| Output_1_171 | 11570 | 214 | 1.3 | 0.02 | 1.82 | 0.05 | 6.07 | 0.16 | 6.03 | 0.23 | 150.0 | 120.0 | 150.8 | 2.7 | 149.4 | 8.4 | 150.8 | 2.5 |
| Output_1_135 | 28750 | 815 | 3.1 | 0.02 | 2.32 | 0.05 | 3.77 | 0.17 | 4.23 | 0.30 | 208.0 | 82.0 | 150.9 | 3.5 | 155.3 | 6.1 | 150.9 | 3.3 |
| Output_1_125 | 6310 | 142 | 1.5 | 0.02 | 2.62 | 0.05 | 7.44 | 0.16 | 6.75 | 0.08 | 170.0 | 140.0 | 151.0 | 3.9 | 153.2 | 9.7 | 151.0 | 3.9 |
| Output_1_49 | 3540 | 86 | 4.2 | 0.02 | 2.74 | 0.05 | 10.18 | 0.17 | 9.52 | 0.18 | 240.0 | 200.0 | 151.2 | 4.1 | 157.0 | 14.0 | 151.2 | 4.6 |
| Output_1_158 | 20880 | 388 | 2.4 | 0.02 | 1.64 | 0.05 | 3.92 | 0.17 | 3.77 | 0.13 | 226.0 | 84.0 | 151.6 | 2.5 | 161.4 | 5.6 | 151.6 | 2.7 |
| Output_1_118 | 11280 | 193 | 2.3 | 0.02 | 2.22 | 0.05 | 5.40 | 0.17 | 5.62 | 0.17 | 220.0 | 110.0 | 151.8 | 3.3 | 156.8 | 8.1 | 151.8 | 3.4 |
| Output_1_168 | 3400 | 63 | 2.4 | 0.02 | 2.59 | 0.05 | 11.72 | 0.17 | 10.30 | 0.19 | 260.0 | 220.0 | 152.6 | 3.9 | 154.0 | 14.0 | 152.6 | 3.9 |
| Output_1_68 | 49200 | 561 | 2.4 | 0.02 | 2.95 | 0.05 | 2.85 | 0.17 | 3.82 | 0.63 | 166.0 | 64.0 | 153.1 | 4.5 | 155.0 | 5.5 | 153.1 | 4.0 |
| Output_1_86 | 34560 | 511 | 1.9 | 0.02 | 2.74 | 0.05 | 4.01 | 0.17 | 4.76 | 0.39 | 182.0 | 88.0 | 153.3 | 4.2 | 155.7 | 6.9 | 153.3 | 4.0 |
| Output_1_62 | 16200 | 154 | 1.7 | 0.02 | 1.70 | 0.05 | 4.33 | 0.17 | 3.71 | 0.01 | 219.0 | 90.0 | 153.3 | 2.5 | 156.9 | 5.3 | 153.3 | 2.7 |
| Output_1_127 | 5290 | 125 | 2.4 | 0.02 | 2.91 | 0.05 | 10.87 | 0.17 | 9.70 | 0.02 | 140.0 | 190.0 | 153.5 | 4.4 | 153.0 | 14.0 | 153.5 | 4.7 |
| Output_1_155 | 49400 | 912 | 1.8 | 0.02 | 2.74 | 0.05 | 2.39 | 0.17 | 3.95 | 0.74 | 205.0 | 56.0 | 153.6 | 4.1 | 156.6 | 5.7 | 153.6 | 4.2 |
| Output_1_59 | 28570 | 271 | 1.8 | 0.02 | 1.24 | 0.05 | 4.09 | 0.16 | 4.19 | 0.02 | 139.0 | 87.0 | 154.4 | 1.9 | 154.7 | 6.0 | 154.4 | 1.8 |
| Output_1_15 | 11410 | 121 | 2.0 | 0.02 | 1.64 | 0.05 | 6.16 | 0.17 | 5.71 | 0.11 | 220.0 | 130.0 | 155.6 | 2.5 | 158.6 | 8.1 | 155.6 | 2.9 |
| Output_1_44 | 6280 | 221 | 2.1 | 0.02 | 4.49 | 0.06 | 15.30 | 0.19 | 15.87 | 0.23 | 510.0 | 360.0 | 156.0 | 6.9 | 175.0 | 26.0 | 156.0 | 6.5 |

| | | | | | | | | | | | | | | | | | | |
|---|---|---|---|---|---|---|---|---|---|---|---|---|---|---|---|---|---|---|
| Output_1_146 | 32830 | 686 | 4.0 | 0.02 | 1.59 | 0.05 | 3.50 | 0.17 | 3.36 | 0.30 | 129.0 | 71.0 | 156.1 | 2.5 | 156.3 | 4.9 | 156.1 | 2.6 |
| Output_1_37 | 6250 | 296 | 1.9 | 0.02 | 2.90 | 0.05 | 7.28 | 0.17 | 7.10 | 0.08 | 230.0 | 140.0 | 156.1 | 4.5 | 158.0 | 10.0 | 156.1 | 4.7 |
| Output_1_101 | 10490 | 111 | 2.7 | 0.02 | 2.15 | 0.05 | 5.36 | 0.17 | 5.21 | 0.12 | 270.0 | 110.0 | 156.9 | 3.3 | 161.4 | 7.8 | 156.9 | 3.3 |
| Output_1_4 | 18520 | 228 | 2.4 | 0.02 | 1.86 | 0.05 | 5.58 | 0.17 | 5.75 | 0.22 | 260.0 | 120.0 | 157.1 | 2.9 | 162.4 | 8.6 | 157.1 | 2.9 |
| Output_1_120 | 9180 | 173 | 6.5 | 0.02 | 3.15 | 0.05 | 10.69 | 0.18 | 10.80 | 0.24 | 200.0 | 220.0 | 157.5 | 4.9 | 164.0 | 16.0 | 157.5 | 4.1 |
| Output_1_79 | 2981 | 60 | 1.4 | 0.02 | 3.25 | 0.05 | 10.51 | 0.17 | 10.47 | 0.01 | 310.0 | 200.0 | 158.8 | 5.1 | 163.0 | 16.0 | 158.8 | 5.2 |
| Output_1_144 | 12120 | 258 | 1.1 | 0.03 | 2.95 | 0.05 | 4.96 | 0.18 | 5.42 | 0.31 | 300.0 | 110.0 | 159.8 | 4.7 | 171.0 | 8.3 | 159.8 | 4.6 |
| Output_1_27 | 4410 | 78 | 1.9 | 0.03 | 2.67 | 0.05 | 9.05 | 0.17 | 8.93 | 0.18 | 80.0 | 170.0 | 161.9 | 4.3 | 157.0 | 13.0 | 161.9 | 4.2 |
| Output_1_129 | 20800 | 532 | 2.4 | 0.03 | 2.71 | 0.05 | 5.36 | 0.17 | 4.56 | 0.13 | 140.0 | 110.0 | 162.0 | 4.3 | 158.2 | 6.7 | 162.0 | 4.0 |
| Output_1_93 | 22690 | 257 | 2.1 | 0.03 | 1.76 | 0.05 | 5.13 | 0.19 | 4.48 | 0.01 | 300.0 | 110.0 | 163.0 | 2.8 | 172.5 | 7.1 | 163.0 | 2.5 |
| Output_1_25 | 9230 | 144 | 1.7 | 0.03 | 1.75 | 0.05 | 6.13 | 0.19 | 5.67 | 0.18 | 320.0 | 120.0 | 163.8 | 2.9 | 179.0 | 9.5 | 163.8 | 3.7 |
| Output_1_109 | 63910 | 726 | 2.0 | 0.03 | 1.99 | 0.05 | 2.38 | 0.18 | 2.34 | 0.45 | 214.0 | 53.0 | 166.0 | 3.3 | 170.9 | 3.7 | 166.0 | 3.3 |
| Output_1_106 | 4680 | 51 | 4.5 | 0.03 | 2.71 | 0.06 | 10.68 | 0.20 | 10.20 | 0.31 | 390.0 | 210.0 | 166.8 | 4.5 | 183.0 | 18.0 | 166.8 | 4.4 |
| Output_1_117 | 3980 | 58 | 2.8 | 0.03 | 3.46 | 0.05 | 7.78 | 0.18 | 8.29 | 0.18 | 200.0 | 150.0 | 169.2 | 5.8 | 168.0 | 13.0 | 169.2 | 5.7 |
| Output_1_152 | 12570 | 214 | 2.3 | 0.03 | 2.17 | 0.05 | 4.48 | 0.19 | 4.21 | 0.06 | 162.0 | 93.0 | 172.5 | 3.7 | 172.2 | 6.7 | 172.5 | 3.6 |
| Output_1_46 | 20730 | 485 | 1.9 | 0.03 | 3.14 | 0.06 | 4.30 | 0.26 | 3.88 | 0.27 | 531.0 | 91.0 | 199.9 | 6.2 | 232.7 | 8.3 | 199.9 | 5.4 |
| Output_1_50 | 11000 | 168 | 4.5 | 0.03 | 2.13 | 0.06 | 5.40 | 0.25 | 5.91 | 0.40 | 470.0 | 120.0 | 205.7 | 4.3 | 231.0 | 12.0 | 205.7 | 4.8 |
| Output_1_121 | 9000 | 124 | 3.8 | 0.03 | 4.50 | 0.05 | 15.93 | 0.25 | 16.40 | 0.05 | 360.0 | 340.0 | 210.9 | 9.1 | 226.0 | 33.0 | 210.9 | 7.5 |
| Output_1_170 | 8080 | 103 | 2.3 | 0.03 | 3.17 | 0.05 | 6.01 | 0.24 | 7.02 | 0.47 | 180.0 | 120.0 | 220.1 | 6.6 | 219.0 | 14.0 | 220.1 | 6.9 |
| Output_1_126 | 10730 | 169 | 1.9 | 0.03 | 2.54 | 0.06 | 5.94 | 0.28 | 5.38 | 0.14 | 530.0 | 130.0 | 220.4 | 5.3 | 249.0 | 12.0 | 220.4 | 5.6 |
| Output_1_29 | 21400 | 318 | 2.4 | 0.04 | 3.20 | 0.05 | 6.85 | 0.28 | 6.81 | 0.43 | 340.0 | 150.0 | 237.3 | 7.2 | 250.0 | 15.0 | 237.3 | 6.7 |
| Output_1_136 | 20050 | 348 | 1.2 | 0.04 | 2.64 | 0.05 | 4.80 | 0.27 | 4.91 | 0.21 | 200.0 | 100.0 | 239.9 | 6.3 | 238.0 | 10.0 | 239.9 | 6.5 |
| Output_1_119 | 19010 | 211 | 3.8 | 0.04 | 4.24 | 0.06 | 7.90 | 0.32 | 7.76 | 0.29 | 550.0 | 180.0 | 253.0 | 10.0 | 283.0 | 19.0 | 253.0 | 13.0 |
| Output_1_84 | 13520 | 124 | 2.5 | 0.04 | 3.82 | 0.06 | 5.70 | 0.37 | 4.07 | 0.30 | 650.0 | 120.0 | 264.4 | 9.9 | 319.0 | 11.0 | 264.4 | 10.0 |
| Output_1_90 | 95000 | 648 | 1.3 | 0.05 | 1.50 | 0.05 | 2.77 | 0.33 | 2.68 | 0.12 | 369.0 | 63.0 | 285.1 | 4.2 | 290.8 | 6.8 | 285.1 | 4.4 |
| Output_1_150 | 12930 | 123 | 1.0 | 0.05 | 3.78 | 0.06 | 4.24 | 0.41 | 5.10 | 0.47 | 577.0 | 90.0 | 316.0 | 12.0 | 349.0 | 15.0 | 316.0 | 12.0 |
| Output_1_81 | 9100 | 84 | 1.8 | 0.05 | 2.34 | 0.06 | 5.51 | 0.42 | 5.26 | 0.49 | 600.0 | 130.0 | 322.5 | 7.4 | 354.0 | 16.0 | 322.5 | 7.5 |
| Output_1_169 | 67780 | 577 | 2.1 | 0.05 | 1.79 | 0.06 | 2.78 | 0.42 | 2.38 | 0.27 | 508.0 | 61.0 | 326.5 | 5.7 | 356.3 | 7.4 | 326.5 | 5.0 |
| Output_1_143 | 39550 | 370 | 4.2 | 0.06 | 1.86 | 0.06 | 2.60 | 0.50 | 2.21 | 0.13 | 651.0 | 59.0 | 369.7 | 6.8 | 410.8 | 7.5 | 369.7 | 6.1 |
| Output_1_24 | 23620 | 136 | 3.3 | 0.06 | 3.21 | 0.07 | 3.21 | 0.55 | 4.77 | 0.67 | 791.0 | 71.0 | 370.0 | 12.0 | 440.0 | 17.0 | 370.0 | 11.0 |
| Output_1_11 | 14570 | 67 | 1.9 | 0.06 | 1.85 | 0.06 | 5.10 | 0.47 | 5.36 | 0.17 | 480.0 | 110.0 | 371.9 | 6.6 | 387.0 | 17.0 | 371.9 | 7.0 |
| Output_1_80 | 11520 | 93 | 1.6 | 0.06 | 6.21 | 0.06 | 10.86 | 0.51 | 12.57 | 0.38 | 810.0 | 210.0 | 373.0 | 23.0 | 431.0 | 50.0 | 373.0 | 23.0 |
| Output_1_162 | 25250 | 184 | 2.0 | 0.06 | 1.76 | 0.06 | 3.32 | 0.52 | 3.63 | 0.14 | 618.0 | 65.0 | 389.9 | 6.8 | 427.0 | 12.0 | 389.9 | 6.2 |
| Output_1_161 | 92100 | 601 | 1.1 | 0.07 | 1.45 | 0.06 | 2.04 | 0.57 | 2.30 | 0.56 | 550.0 | 44.0 | 430.1 | 6.1 | 456.1 | 8.5 | 430.1 | 6.6 |
| Output_1_124 | 55000 | 409 | 2.9 | 0.07 | 1.99 | 0.06 | 2.04 | 0.62 | 2.27 | 0.54 | 724.0 | 43.0 | 438.2 | 8.5 | 488.3 | 8.7 | 438.2 | 7.6 |
| Output_1_94 | 45300 | 179 | 1.7 | 0.07 | 1.70 | 0.06 | 3.48 | 0.56 | 3.06 | 0.03 | 484.0 | 79.0 | 439.1 | 7.4 | 450.0 | 10.0 | 439.1 | 9.8 |
| Output_1_113 | 73500 | 326 | 1.6 | 0.08 | 1.70 | 0.06 | 2.18 | 0.62 | 2.25 | 0.41 | 575.0 | 49.0 | 474.2 | 7.5 | 489.9 | 8.9 | 474.2 | 8.8 |
| Output_1_149 | 47180 | 226 | 0.4 | 0.10 | 1.70 | 0.07 | 2.20 | 0.93 | 2.57 | 0.51 | 870.0 | 46.0 | 614.3 | 9.9 | 668.0 | 13.0 | 614.3 | 10.0 |
| Output_1_48 | 19110 | 118 | 1.1 | 0.10 | 2.60 | 0.07 | 3.67 | 0.98 | 3.68 | 0.55 | 855.0 | 78.0 | 637.0 | 16.0 | 694.0 | 18.0 | 637.0 | 15.0 |
| Output_1_108 | 34850 | 86 | 1.0 | 0.12 | 1.50 | 0.07 | 2.56 | 1.10 | 2.64 | 0.44 | 812.0 | 54.0 | 729.0 | 10.0 | 750.0 | 14.0 | 729.0 | 11.0 |

| | | | | | | | | | | | | | | | | | | |
|---|---|---|---|---|---|---|---|---|---|---|---|---|---|---|---|---|---|---|
| Output_1_38 | 60500 | 537 | 6.8 | 0.15 | 6.11 | 0.11 | 1.71 | 2.10 | 5.71 | 0.95 | 1710.0 | 32.0 | 874.0 | 50.0 | ##### | 41.0 | 874.0 | 53.0 |
| **Sample 18ATW19** | | | | | | | | | | | | | | | | | | |
| Output_1_59 | 7340 | 1251 | 136.0 | 0.01 | 3.39 | 0.05 | 10.41 | 0.06 | 10.14 | 0.13 | 230.0 | 220.0 | 58.6 | 2.0 | 62.0 | 6.1 | 58.6 | 2.3 |
| Output_1_7 | 9860 | 361 | 109.0 | 0.01 | 2.39 | 0.05 | 9.48 | 0.06 | 9.03 | 0.07 | 90.0 | 190.0 | 59.0 | 1.4 | 59.9 | 5.3 | 59.0 | 1.8 |
| Output_1_124 | 8800 | 405 | 80.4 | 0.01 | 3.85 | 0.05 | 9.52 | 0.07 | 7.40 | 0.30 | 230.0 | 220.0 | 66.7 | 2.5 | 69.0 | 4.9 | 66.7 | 2.8 |
| Output_1_66 | 10090 | 1071 | 13.4 | 0.01 | 3.50 | 0.05 | 9.49 | 0.07 | 10.01 | 0.17 | 180.0 | 200.0 | 69.6 | 2.4 | 73.2 | 7.1 | 69.6 | 2.8 |
| Output_1_11 | 8900 | 223 | 11.3 | 0.01 | 3.58 | 0.05 | 8.86 | 0.07 | 8.97 | 0.31 | 50.0 | 170.0 | 71.5 | 2.6 | 72.0 | 6.2 | 71.5 | 2.9 |
| Output_1_135 | 10440 | 474 | 5.6 | 0.01 | 2.58 | 0.05 | 6.33 | 0.08 | 5.30 | 0.17 | 130.0 | 140.0 | 72.1 | 1.8 | 73.9 | 3.8 | 72.1 | 2.3 |
| Output_1_71 | 10290 | 423 | 37.2 | 0.01 | 3.59 | 0.05 | 7.57 | 0.08 | 8.35 | 0.41 | 180.0 | 160.0 | 73.2 | 2.6 | 77.1 | 6.2 | 73.2 | 2.9 |
| Output_1_139 | 14890 | 517 | 31.4 | 0.01 | 2.24 | 0.05 | 5.67 | 0.08 | 6.11 | 0.25 | 150.0 | 120.0 | 74.3 | 1.6 | 76.7 | 4.5 | 74.3 | 2.2 |
| Output_1_67 | 6920 | 459 | 5.7 | 0.01 | 3.43 | 0.05 | 10.51 | 0.08 | 10.47 | 0.01 | 210.0 | 220.0 | 74.8 | 2.5 | 79.1 | 8.0 | 74.8 | 2.9 |
| Output_1_43 | 23500 | 2009 | 109.1 | 0.01 | 4.78 | 0.05 | 6.84 | 0.08 | 6.57 | 0.31 | 240.0 | 160.0 | 75.0 | 3.6 | 80.2 | 5.1 | 75.0 | 3.8 |
| Output_1_127 | 3550 | 156 | 4.2 | 0.01 | 3.22 | 0.05 | 8.86 | 0.08 | 8.44 | 0.29 | 170.0 | 180.0 | 75.6 | 2.4 | 80.5 | 6.4 | 75.6 | 2.8 |
| Output_1_128 | 12510 | 583 | 2.6 | 0.01 | 2.95 | 0.05 | 6.18 | 0.08 | 5.30 | 0.03 | 190.0 | 140.0 | 76.0 | 2.2 | 79.1 | 4.0 | 76.0 | 2.7 |
| Output_1_136 | 3480 | 140 | 2.0 | 0.01 | 3.71 | 0.05 | 7.65 | 0.08 | 7.60 | 0.07 | 260.0 | 170.0 | 76.1 | 2.8 | 81.6 | 5.7 | 76.1 | 3.2 |
| Output_1_106 | 4500 | 303 | 1.5 | 0.01 | 2.27 | 0.05 | 8.51 | 0.08 | 7.91 | 0.09 | 200.0 | 170.0 | 76.2 | 1.7 | 80.0 | 6.1 | 76.2 | 2.3 |
| Output_1_20 | 8530 | 875 | 7.2 | 0.01 | 4.62 | 0.05 | 8.62 | 0.08 | 7.50 | 0.24 | 150.0 | 180.0 | 76.3 | 3.5 | 78.1 | 5.7 | 76.3 | 3.8 |
| Output_1_107 | 7600 | 505 | 3.3 | 0.01 | 3.24 | 0.05 | 12.18 | 0.09 | 11.36 | 0.07 | 360.0 | 250.0 | 77.0 | 2.5 | 85.3 | 9.3 | 77.0 | 2.9 |
| Output_1_30 | 3160 | 232 | 5.8 | 0.01 | 4.56 | 0.05 | 13.67 | 0.09 | 11.50 | 0.37 | 260.0 | 280.0 | 77.3 | 3.5 | 83.5 | 9.3 | 77.3 | 3.8 |
| Output_1_5 | 10130 | 357 | 71.3 | 0.01 | 3.43 | 0.05 | 10.78 | 0.09 | 11.76 | 0.27 | 290.0 | 190.0 | 78.4 | 2.6 | 83.0 | 9.3 | 78.4 | 3.1 |
| Output_1_81 | 9420 | 1384 | 1.4 | 0.01 | 2.53 | 0.05 | 8.33 | 0.08 | 8.14 | 0.05 | 160.0 | 170.0 | 78.4 | 2.0 | 82.0 | 6.3 | 78.4 | 2.5 |
| Output_1_144 | 11240 | 390 | 2.0 | 0.01 | 3.00 | 0.05 | 8.63 | 0.09 | 9.42 | 0.31 | 190.0 | 190.0 | 81.1 | 2.4 | 86.5 | 7.8 | 81.1 | 2.9 |
| Output_1_98 | 8290 | 296 | 28.6 | 0.01 | 3.22 | 0.05 | 5.04 | 0.08 | 5.56 | 0.45 | 90.0 | 110.0 | 81.5 | 2.6 | 82.3 | 4.4 | 81.5 | 3.1 |
| Output_1_138 | 11250 | 346 | 0.5 | 0.01 | 1.87 | 0.05 | 7.30 | 0.09 | 7.10 | 0.05 | 240.0 | 150.0 | 82.1 | 1.6 | 86.1 | 5.8 | 82.1 | 2.2 |
| Output_1_120 | 1217 | 43 | 1.4 | 0.01 | 8.40 | 0.07 | 27.27 | 0.12 | 28.21 | 0.02 | 440.0 | 510.0 | 84.1 | 7.0 | 109.0 | 29.0 | 84.1 | 7.1 |
| Output_1_88 | 1960 | 224 | 2.3 | 0.01 | 5.79 | 0.06 | 23.21 | 0.10 | 20.59 | 0.21 | 370.0 | 450.0 | 84.1 | 4.8 | 98.0 | 19.0 | 84.1 | 5.1 |
| Output_1_16 | 10240 | 324 | 16.7 | 0.01 | 6.07 | 0.05 | 10.04 | 0.09 | 9.37 | 0.18 | 220.0 | 220.0 | 84.3 | 5.1 | 88.0 | 7.9 | 84.3 | 5.3 |
| Output_1_125 | 20500 | 730 | 22.1 | 0.01 | 5.69 | 0.05 | 6.02 | 0.09 | 4.93 | 0.56 | 170.0 | 130.0 | 84.4 | 4.8 | 86.7 | 4.1 | 84.4 | 5.0 |
| Output_1_12 | 4450 | 103 | 2.1 | 0.01 | 4.14 | 0.05 | 8.25 | 0.09 | 7.97 | 0.20 | 170.0 | 170.0 | 84.9 | 3.5 | 85.1 | 6.5 | 84.9 | 3.9 |
| Output_1_31 | 18880 | 1299 | 3.8 | 0.01 | 2.11 | 0.05 | 6.34 | 0.09 | 6.95 | 0.27 | 130.0 | 140.0 | 84.9 | 1.8 | 88.0 | 5.8 | 84.9 | 2.4 |
| Output_1_61 | 2250 | 285 | 2.6 | 0.01 | 3.84 | 0.05 | 13.86 | 0.09 | 13.19 | 0.04 | 190.0 | 280.0 | 85.0 | 3.2 | 88.0 | 11.0 | 85.0 | 3.6 |
| Output_1_13 | 13240 | 300 | 4.8 | 0.01 | 4.50 | 0.05 | 6.02 | 0.09 | 6.93 | 0.42 | 130.0 | 130.0 | 86.9 | 3.9 | 89.1 | 6.0 | 86.9 | 4.2 |
| Output_1_10 | 22700 | 497 | 3.4 | 0.01 | 4.72 | 0.05 | 8.12 | 0.10 | 8.42 | 0.28 | 230.0 | 180.0 | 88.1 | 4.1 | 94.2 | 7.6 | 88.1 | 4.5 |
| Output_1_102 | 15770 | 745 | 2.1 | 0.01 | 5.29 | 0.05 | 10.31 | 0.10 | 9.62 | 0.23 | 370.0 | 270.0 | 89.6 | 4.7 | 96.5 | 8.9 | 89.6 | 5.0 |
| Output_1_8 | 9190 | 204 | 2.5 | 0.01 | 2.84 | 0.05 | 6.68 | 0.10 | 6.86 | 0.23 | 160.0 | 140.0 | 90.1 | 2.6 | 93.1 | 6.1 | 90.1 | 3.1 |
| Output_1_37 | 9290 | 590 | 3.8 | 0.01 | 4.25 | 0.05 | 7.33 | 0.10 | 7.77 | 0.49 | 190.0 | 160.0 | 91.9 | 3.9 | 96.3 | 7.5 | 91.9 | 4.2 |
| Output_1_62 | 9090 | 1027 | 1.2 | 0.01 | 2.00 | 0.05 | 9.13 | 0.09 | 8.40 | 0.11 | 60.0 | 180.0 | 92.9 | 1.8 | 91.0 | 7.3 | 92.9 | 2.6 |
| Output_1_32 | 17530 | 1098 | 3.0 | 0.01 | 6.16 | 0.05 | 10.47 | 0.10 | 8.76 | 0.16 | 230.0 | 230.0 | 93.6 | 5.7 | 99.1 | 8.3 | 93.6 | 6.0 |
| Output_1_27 | 13450 | 784 | 2.2 | 0.01 | 2.46 | 0.05 | 4.62 | 0.10 | 5.35 | 0.38 | 90.0 | 100.0 | 93.7 | 2.3 | 92.3 | 4.7 | 93.7 | 2.9 |

| | | | | | | | | | | | | | | | | | | |
|---|---|---|---|---|---|---|---|---|---|---|---|---|---|---|---|---|---|---|
| Output_1_126 | 13640 | 461 | 1.1 | 0.01 | 2.72 | 0.05 | 6.53 | 0.10 | 6.94 | 0.35 | 80.0 | 140.0 | 94.0 | 2.6 | 93.4 | 6.1 | 94.0 | 3.1 |
| Output_1_103 | 17460 | 757 | 2.1 | 0.01 | 2.38 | 0.05 | 4.79 | 0.10 | 5.23 | 0.46 | 180.0 | 110.0 | 94.3 | 2.3 | 97.2 | 5.0 | 94.3 | 2.9 |
| Output_1_3 | 15530 | 648 | 2.8 | 0.02 | 4.57 | 0.05 | 6.10 | 0.11 | 6.48 | 0.44 | 270.0 | 130.0 | 96.7 | 4.4 | 101.3 | 6.2 | 96.7 | 4.8 |
| Output_1_141 | 10270 | 259 | 4.8 | 0.02 | 3.75 | 0.05 | 11.36 | 0.10 | 10.78 | 0.05 | 90.0 | 240.0 | 99.0 | 3.7 | 99.0 | 10.0 | 99.0 | 4.2 |
| Output_1_95 | 16920 | 444 | 1.4 | 0.02 | 2.69 | 0.05 | 6.67 | 0.11 | 5.26 | 0.31 | 220.0 | 150.0 | 99.9 | 2.6 | 104.4 | 5.2 | 99.9 | 3.3 |
| Output_1_33 | 34400 | 1987 | 0.6 | 0.02 | 3.44 | 0.05 | 5.53 | 0.11 | 7.21 | 0.52 | 150.0 | 130.0 | 102.2 | 3.5 | 101.6 | 7.0 | 102.2 | 4.0 |
| Output_1_140 | 13200 | 322 | 4.5 | 0.02 | 3.23 | 0.05 | 7.00 | 0.11 | 8.10 | 0.53 | 190.0 | 150.0 | 105.0 | 3.4 | 109.0 | 8.3 | 105.0 | 3.9 |
| Output_1_76 | 10630 | 320 | 1.7 | 0.02 | 2.92 | 0.05 | 7.03 | 0.11 | 7.44 | 0.40 | 210.0 | 150.0 | 105.1 | 3.0 | 108.2 | 7.7 | 105.1 | 3.6 |
| Output_1_110 | 13430 | 630 | 2.2 | 0.02 | 2.94 | 0.05 | 5.72 | 0.12 | 6.08 | 0.30 | 230.0 | 130.0 | 106.5 | 3.1 | 112.0 | 6.4 | 106.5 | 3.7 |
| Output_1_35 | 25990 | 1416 | 1.3 | 0.02 | 5.13 | 0.05 | 6.80 | 0.12 | 6.71 | 0.37 | 200.0 | 150.0 | 107.2 | 5.5 | 111.5 | 7.1 | 107.2 | 5.9 |
| Output_1_46 | 13180 | 815 | 2.8 | 0.02 | 2.35 | 0.05 | 4.90 | 0.12 | 5.39 | 0.39 | 130.0 | 100.0 | 108.9 | 2.5 | 110.4 | 5.7 | 108.9 | 3.3 |
| Output_1_51 | 7960 | 546 | 6.0 | 0.02 | 6.47 | 0.05 | 12.14 | 0.12 | 13.82 | 0.52 | 260.0 | 260.0 | 108.9 | 6.8 | 117.0 | 16.0 | 108.9 | 7.1 |
| Output_1_83 | 13290 | 2310 | 10.5 | 0.02 | 3.13 | 0.05 | 5.78 | 0.12 | 5.60 | 0.26 | 240.0 | 130.0 | 110.1 | 3.4 | 112.9 | 6.0 | 110.1 | 4.0 |
| Output_1_34 | 39800 | 2139 | 0.6 | 0.02 | 3.06 | 0.05 | 6.49 | 0.12 | 5.84 | 0.26 | 170.0 | 140.0 | 110.6 | 3.3 | 113.3 | 6.3 | 110.6 | 4.0 |
| Output_1_109 | 9960 | 462 | 3.0 | 0.02 | 3.68 | 0.05 | 7.14 | 0.12 | 7.25 | 0.26 | 190.0 | 160.0 | 111.2 | 4.0 | 114.9 | 7.8 | 111.2 | 4.6 |
| Output_1_70 | 14750 | 410 | 3.6 | 0.02 | 4.76 | 0.05 | 6.37 | 0.13 | 7.87 | 0.31 | 330.0 | 150.0 | 112.6 | 5.3 | 120.2 | 9.0 | 112.6 | 5.7 |
| Output_1_92 | 10340 | 301 | 15.1 | 0.02 | 3.42 | 0.05 | 13.83 | 0.12 | 13.71 | 0.15 | 190.0 | 300.0 | 113.9 | 3.9 | 119.0 | 15.0 | 113.9 | 4.4 |
| Output_1_49 | 20500 | 1313 | 2.1 | 0.02 | 7.14 | 0.05 | 7.49 | 0.13 | 7.69 | 0.55 | 270.0 | 170.0 | 116.3 | 8.1 | 123.6 | 9.0 | 116.3 | 8.4 |
| Output_1_90 | 11530 | 461 | 23.2 | 0.02 | 7.69 | 0.06 | 7.26 | 0.13 | 6.73 | 0.53 | 360.0 | 160.0 | 116.4 | 8.8 | 125.8 | 8.0 | 116.4 | 9.0 |
| Output_1_91 | 27400 | 877 | 1.7 | 0.02 | 2.83 | 0.05 | 4.06 | 0.12 | 3.89 | 0.26 | 160.0 | 88.0 | 117.5 | 3.3 | 118.0 | 4.4 | 117.5 | 4.0 |
| Output_1_64 | 11280 | 830 | 2.0 | 0.02 | 6.97 | 0.05 | 15.15 | 0.14 | 14.18 | 0.02 | 220.0 | 330.0 | 128.1 | 8.9 | 133.0 | 17.0 | 128.1 | 9.2 |
| Output_1_26 | 20730 | 854 | 3.9 | 0.02 | 2.29 | 0.05 | 3.61 | 0.14 | 3.80 | 0.39 | 185.0 | 84.0 | 128.4 | 2.9 | 130.1 | 4.6 | 128.4 | 3.9 |
| Output_1_50 | 23850 | 1304 | 1.3 | 0.02 | 4.93 | 0.05 | 5.53 | 0.14 | 5.69 | 0.25 | 130.0 | 120.0 | 129.7 | 6.4 | 131.8 | 7.0 | 129.7 | 6.8 |
| Output_1_117 | 2001 | 52 | 2.1 | 0.02 | 5.83 | 0.05 | 16.42 | 0.14 | 14.69 | 0.09 | 170.0 | 320.0 | 131.7 | 7.8 | 134.0 | 19.0 | 131.7 | 8.2 |
| Output_1_24 | 12100 | 451 | 1.3 | 0.02 | 2.90 | 0.05 | 6.81 | 0.15 | 7.33 | 0.43 | 290.0 | 150.0 | 131.9 | 3.8 | 141.4 | 9.7 | 131.9 | 4.6 |
| Output_1_74 | 11600 | 244 | 1.9 | 0.02 | 2.56 | 0.05 | 9.49 | 0.16 | 8.97 | 0.20 | 340.0 | 220.0 | 139.5 | 3.5 | 147.0 | 12.0 | 139.5 | 4.5 |
| Output_1_73 | 35780 | 672 | 3.6 | 0.02 | 1.95 | 0.05 | 5.60 | 0.16 | 5.30 | 0.03 | 280.0 | 130.0 | 144.1 | 2.8 | 150.9 | 7.4 | 144.1 | 4.0 |
| Output_1_45 | 1013 | 43 | 2.8 | 0.02 | 5.60 | 0.04 | 21.34 | 0.14 | 20.57 | 0.08 | -190.0 | 370.0 | 147.6 | 8.5 | 130.0 | 26.0 | 147.6 | 8.9 |
| Output_1_36 | 13440 | 525 | 3.1 | 0.02 | 3.99 | 0.05 | 5.23 | 0.16 | 6.96 | 0.49 | 220.0 | 110.0 | 148.6 | 5.9 | 150.8 | 8.9 | 148.6 | 6.5 |
| Output_1_53 | 7990 | 420 | 1.5 | 0.02 | 5.13 | 0.05 | 8.35 | 0.16 | 9.62 | 0.42 | 130.0 | 180.0 | 149.3 | 7.4 | 146.0 | 13.0 | 149.3 | 7.9 |
| Output_1_72 | 39810 | 764 | 3.5 | 0.02 | 2.93 | 0.05 | 6.30 | 0.16 | 6.79 | 0.43 | 220.0 | 140.0 | 150.0 | 4.3 | 153.0 | 10.0 | 150.0 | 5.2 |
| Output_1_54 | 9460 | 514 | 1.4 | 0.02 | 3.83 | 0.05 | 8.24 | 0.17 | 7.23 | 0.13 | 210.0 | 170.0 | 154.5 | 5.8 | 156.0 | 11.0 | 154.5 | 6.6 |
| Output_1_99 | 2130 | 44 | 4.8 | 0.02 | 5.74 | 0.05 | 13.08 | 0.18 | 13.14 | 0.28 | 330.0 | 270.0 | 155.1 | 9.1 | 168.0 | 20.0 | 155.1 | 9.6 |
| Output_1_116 | 36440 | 854 | 2.4 | 0.02 | 3.77 | 0.05 | 3.73 | 0.17 | 3.99 | 0.47 | 240.0 | 86.0 | 157.1 | 5.9 | 162.9 | 6.2 | 157.1 | 6.6 |
| Output_1_38 | 2127 | 79 | 1.4 | 0.03 | 3.98 | 0.05 | 11.36 | 0.18 | 11.36 | 0.18 | 100.0 | 230.0 | 159.5 | 6.4 | 163.0 | 17.0 | 159.5 | 7.1 |
| Output_1_9 | 11600 | 141 | 2.7 | 0.03 | 3.31 | 0.05 | 5.70 | 0.17 | 6.40 | 0.36 | 220.0 | 120.0 | 159.8 | 5.2 | 160.7 | 9.4 | 159.8 | 6.1 |
| Output_1_41 | 8320 | 321 | 2.8 | 0.03 | 3.05 | 0.05 | 6.30 | 0.17 | 5.75 | 0.26 | 230.0 | 140.0 | 160.8 | 4.9 | 162.1 | 8.9 | 160.8 | 5.8 |
| Output_1_14 | 10280 | 134 | 3.3 | 0.03 | 2.82 | 0.05 | 6.67 | 0.18 | 6.15 | 0.08 | 270.0 | 140.0 | 160.8 | 4.4 | 166.3 | 9.3 | 160.8 | 5.3 |
| Output_1_97 | 5940 | 103 | 3.2 | 0.03 | 3.94 | 0.05 | 6.52 | 0.17 | 7.56 | 0.32 | 150.0 | 130.0 | 161.8 | 6.3 | 161.0 | 11.0 | 161.8 | 7.0 |
| Output_1_108 | 11270 | 355 | 1.8 | 0.03 | 2.35 | 0.05 | 6.13 | 0.18 | 6.01 | 0.21 | 270.0 | 120.0 | 165.5 | 3.8 | 170.1 | 9.6 | 165.5 | 5.2 |

| | | | | | | | | | | | | | | | | | | |
|---|---|---|---|---|---|---|---|---|---|---|---|---|---|---|---|---|---|---|
| Output_1_63 | 32520 | 1981 | 0.7 | 0.03 | 2.17 | 0.05 | 3.28 | 0.18 | 3.62 | 0.34 | 277.0 | 77.0 | 167.1 | 3.6 | 169.8 | 5.7 | 167.1 | 4.9 |
| Output_1_146 | 15090 | 280 | 2.2 | 0.03 | 3.18 | 0.05 | 5.92 | 0.18 | 6.15 | 0.24 | 130.0 | 120.0 | 168.0 | 5.3 | 166.6 | 9.4 | 168.0 | 6.2 |
| Output_1_75 | 12340 | 208 | 1.2 | 0.03 | 4.58 | 0.05 | 4.52 | 0.18 | 5.56 | 0.58 | 250.0 | 110.0 | 168.2 | 7.2 | 169.9 | 9.4 | 168.2 | 7.8 |
| Output_1_2 | 17640 | 476 | 4.2 | 0.03 | 3.56 | 0.06 | 6.54 | 0.22 | 6.02 | 0.10 | 440.0 | 140.0 | 175.2 | 6.2 | 198.0 | 11.0 | 175.2 | 7.0 |
| Output_1_142 | 19780 | 281 | 2.6 | 0.03 | 2.05 | 0.05 | 4.73 | 0.21 | 4.82 | 0.34 | 320.0 | 100.0 | 186.1 | 3.8 | 190.5 | 8.0 | 186.1 | 5.2 |
| Output_1_79 | 14800 | 399 | 3.8 | 0.03 | 3.69 | 0.05 | 4.65 | 0.21 | 5.16 | 0.49 | 260.0 | 100.0 | 189.3 | 6.9 | 195.3 | 8.9 | 189.3 | 7.8 |
| Output_1_19 | 18400 | 559 | 2.3 | 0.03 | 5.02 | 0.05 | 5.74 | 0.21 | 5.80 | 0.42 | 250.0 | 120.0 | 189.6 | 9.2 | 192.0 | 11.0 | 189.6 | 9.9 |
| Output_1_132 | 10950 | 217 | 2.5 | 0.03 | 3.03 | 0.05 | 5.14 | 0.21 | 5.24 | 0.38 | 210.0 | 110.0 | 190.5 | 5.7 | 193.4 | 9.1 | 190.5 | 6.8 |
| Output_1_133 | 72300 | 1390 | 5.5 | 0.03 | 9.21 | 0.05 | 6.59 | 0.22 | 11.57 | 0.86 | 260.0 | 150.0 | 193.0 | 18.0 | 198.0 | 21.0 | 193.0 | 18.0 |
| Output_1_18 | 13530 | 335 | 3.1 | 0.03 | 4.95 | 0.05 | 5.98 | 0.22 | 7.37 | 0.47 | 300.0 | 130.0 | 193.5 | 9.1 | 198.0 | 13.0 | 193.5 | 9.8 |
| Output_1_80 | 11840 | 540 | 3.3 | 0.03 | 2.06 | 0.05 | 5.26 | 0.22 | 5.50 | 0.26 | 180.0 | 110.0 | 197.0 | 4.0 | 199.0 | 10.0 | 197.0 | 5.5 |
| Output_1_119 | 13110 | 202 | 2.2 | 0.03 | 2.97 | 0.06 | 4.92 | 0.25 | 5.16 | 0.39 | 580.0 | 100.0 | 200.7 | 5.9 | 227.0 | 11.0 | 200.7 | 7.0 |
| Output_1_28 | 21570 | 546 | 2.1 | 0.03 | 2.88 | 0.06 | 3.83 | 0.26 | 3.80 | 0.39 | 503.0 | 91.0 | 218.6 | 6.3 | 236.8 | 8.3 | 218.6 | 7.5 |
| Output_1_1 | 25640 | 593 | 2.9 | 0.03 | 2.71 | 0.06 | 6.96 | 0.28 | 6.03 | 0.07 | 520.0 | 150.0 | 219.8 | 5.9 | 252.0 | 14.0 | 219.8 | 7.2 |
| Output_1_148 | 19240 | 318 | 1.6 | 0.03 | 2.44 | 0.06 | 3.56 | 0.28 | 3.94 | 0.44 | 565.0 | 74.0 | 220.3 | 5.3 | 249.0 | 8.7 | 220.3 | 6.8 |
| Output_1_56 | 18610 | 787 | 3.2 | 0.04 | 2.80 | 0.05 | 5.95 | 0.25 | 6.37 | 0.41 | 340.0 | 130.0 | 225.9 | 6.5 | 230.0 | 14.0 | 225.9 | 7.8 |
| Output_1_96 | 3190 | 38 | 9.1 | 0.04 | 3.86 | 0.05 | 12.21 | 0.26 | 12.31 | 0.15 | 180.0 | 240.0 | 230.0 | 8.9 | 231.0 | 26.0 | 230.0 | 9.9 |
| Output_1_52 | 23570 | 724 | 2.4 | 0.04 | 4.95 | 0.06 | 3.99 | 0.34 | 5.52 | 0.74 | 622.0 | 92.0 | 255.0 | 12.0 | 298.0 | 15.0 | 255.0 | 13.0 |
| Output_1_101 | 20470 | 300 | 2.1 | 0.04 | 1.97 | 0.05 | 4.49 | 0.30 | 4.64 | 0.29 | 347.0 | 97.0 | 260.4 | 4.8 | 269.0 | 10.0 | 260.4 | 7.0 |
| Output_1_57 | 14310 | 488 | 2.2 | 0.04 | 2.56 | 0.06 | 7.18 | 0.32 | 7.19 | 0.24 | 400.0 | 160.0 | 270.6 | 7.0 | 286.0 | 19.0 | 270.6 | 8.8 |
| Output_1_55 | 5800 | 200 | 2.5 | 0.04 | 4.63 | 0.06 | 7.03 | 0.32 | 7.79 | 0.45 | 410.0 | 160.0 | 273.0 | 12.0 | 281.0 | 19.0 | 273.0 | 13.0 |
| Output_1_134 | 96700 | 1210 | 2.1 | 0.04 | 4.36 | 0.06 | 3.45 | 0.33 | 4.28 | 0.71 | 420.0 | 73.0 | 275.0 | 12.0 | 287.0 | 11.0 | 275.0 | 13.0 |
| Output_1_84 | 19890 | 1437 | 3.1 | 0.05 | 2.92 | 0.06 | 3.95 | 0.39 | 4.39 | 0.45 | 557.0 | 79.0 | 301.8 | 8.4 | 332.0 | 12.0 | 301.8 | 10.0 |
| Output_1_89 | 17300 | 432 | 4.3 | 0.05 | 1.84 | 0.06 | 3.93 | 0.37 | 4.11 | 0.44 | 433.0 | 90.0 | 304.8 | 5.5 | 317.0 | 12.0 | 304.8 | 8.1 |
| Output_1_40 | 51200 | 976 | 5.2 | 0.05 | 3.27 | 0.07 | 3.36 | 0.46 | 4.12 | 0.36 | 876.0 | 70.0 | 307.8 | 9.6 | 384.0 | 13.0 | 307.8 | 11.0 |
| Output_1_82 | 31890 | 1328 | 2.2 | 0.05 | 2.21 | 0.05 | 3.10 | 0.41 | 3.21 | 0.34 | 391.0 | 71.0 | 340.2 | 7.1 | 345.1 | 9.0 | 340.2 | 9.7 |
| Output_1_25 | 23190 | 350 | 2.0 | 0.05 | 4.24 | 0.07 | 4.02 | 0.50 | 5.80 | 0.71 | 849.0 | 89.0 | 341.0 | 14.0 | 415.0 | 21.0 | 341.0 | 15.0 |
| Output_1_42 | 26130 | 461 | 1.7 | 0.05 | 2.20 | 0.05 | 3.49 | 0.41 | 3.69 | 0.41 | 380.0 | 79.0 | 342.3 | 7.1 | 346.0 | 11.0 | 342.3 | 9.7 |
| Output_1_22 | 79400 | 679 | 16.0 | 0.08 | 1.80 | 0.07 | 2.06 | 0.72 | 2.21 | 0.54 | 867.0 | 42.0 | 481.9 | 8.3 | 555.3 | 9.2 | 481.9 | 12.0 |
| Output_1_115 | 16240 | 109 | 1.4 | 0.09 | 5.56 | 0.08 | 4.44 | 1.06 | 8.14 | 0.76 | 1271.0 | 93.0 | 571.0 | 29.0 | 739.0 | 40.0 | 571.0 | 31.0 |
| Output_1_112 | 37180 | 265 | 1.9 | 0.10 | 5.71 | 0.11 | 3.46 | 1.53 | 6.20 | 0.81 | 1835.0 | 64.0 | 623.0 | 34.0 | 940.0 | 38.0 | 623.0 | 36.0 |
| Output_1_47 | 20180 | 197 | 1.6 | 0.11 | 2.82 | 0.06 | 4.44 | 0.95 | 4.96 | 0.49 | 715.0 | 93.0 | 673.0 | 18.0 | 677.0 | 26.0 | 673.0 | 22.0 |
| Output_1_78 | 31970 | 188 | 5.8 | 0.11 | 2.68 | 0.09 | 3.31 | 1.35 | 3.34 | 0.45 | 1370.0 | 62.0 | 683.0 | 18.0 | 867.0 | 20.0 | 683.0 | 22.0 |
| Output_1_131 | 61090 | 317 | 4.0 | 0.12 | 6.10 | 0.11 | 3.42 | 1.73 | 6.94 | 0.85 | 1722.0 | 60.0 | 727.0 | 42.0 | ##### | 45.0 | 727.0 | 44.0 |
| Output_1_114 | 16360 | 85 | 1.0 | 0.12 | 6.09 | 0.09 | 7.73 | 1.48 | 8.11 | 0.51 | 1360.0 | 150.0 | 748.0 | 43.0 | 920.0 | 50.0 | 748.0 | 45.0 |
| Output_1_100 | 32200 | 144 | 8.0 | 0.13 | 5.91 | 0.11 | 4.46 | 2.03 | 6.40 | 0.48 | 1843.0 | 94.0 | 769.0 | 43.0 | ##### | 47.0 | 769.0 | 45.0 |
| Output_1_4 | 156800 | 602 | 3.1 | 0.13 | 2.09 | 0.10 | 2.18 | 1.79 | 1.96 | 0.53 | 1557.0 | 40.0 | 812.0 | 16.0 | ##### | 13.0 | 812.0 | 22.0 |
| Output_1_113 | 71100 | 311 | 1.7 | 0.15 | 3.47 | 0.07 | 2.82 | 1.44 | 3.05 | 0.65 | 941.0 | 59.0 | 888.0 | 30.0 | 911.0 | 18.0 | 941.0 | 80.0 |
| Output_1_122 | 80200 | 228 | 3.4 | 0.16 | 3.06 | 0.07 | 3.50 | 1.61 | 2.99 | 0.58 | 967.0 | 71.0 | 976.0 | 28.0 | 973.0 | 19.0 | 967.0 | 89.0 |
| Output_1_6 | 48780 | 136 | 1.2 | 0.14 | 2.31 | 0.07 | 2.09 | 1.38 | 2.91 | 0.66 | 976.0 | 43.0 | 838.0 | 18.0 | 883.0 | 16.0 | 976.0 | 69.0 |

| | | | | | | | | | | | | | | | | | |
|---|---|---|---|---|---|---|---|---|---|---|---|---|---|---|---|---|---|
| Output_1_150 | 82900 | 290 | 1.5 | 0.19 | 3.34 | 0.08 | 2.99 | 1.99 | 3.17 | 0.57 | 1101.0 | 60.0 | 1130.0 | 35.0 | ##### | 21.0 | 1101.0 | 80.0 |
| Output_1_123 | 72100 | 204 | 2.8 | 0.16 | 2.47 | 0.08 | 2.71 | 1.70 | 3.06 | 0.63 | 1127.0 | 55.0 | 946.0 | 22.0 | ##### | 20.0 | 1127.0 | 77.0 |
| Output_1_143 | 75500 | 192 | 2.5 | 0.17 | 3.03 | 0.08 | 2.93 | 1.80 | 2.95 | 0.65 | 1166.0 | 56.0 | 985.0 | 27.0 | ##### | 19.0 | 1166.0 | 76.0 |
| Output_1_118 | 36220 | 115 | 2.4 | 0.16 | 3.02 | 0.08 | 2.89 | 1.76 | 3.86 | 0.70 | 1174.0 | 58.0 | 968.0 | 27.0 | ##### | 25.0 | 1174.0 | 79.0 |
| Output_1_149 | 78400 | 325 | 2.1 | 0.19 | 3.00 | 0.08 | 1.99 | 2.02 | 3.42 | 0.76 | 1198.0 | 39.0 | 1103.0 | 30.0 | ##### | 24.0 | 1198.0 | 66.0 |
| **Sample 17ATW09** | | | | | | | | | | | | | | | | | | |
| Output_1_019 | 2190 | 122 | 1.7 | 0.02 | 5.23 | 0.06 | 13.88 | 0.13 | 13.60 | 0.17 | 440.0 | 280.0 | 102.6 | 5.3 | 121.0 | 16.0 | 102.6 | 6.2 |
| Output_1_012 | 1990 | 129 | 2.1 | 0.02 | 5.14 | 0.05 | 24.53 | 0.16 | 20.50 | 0.21 | 350.0 | 350.0 | 136.2 | 6.7 | 145.0 | 31.0 | 136.2 | 8.6 |
| Output_1_006 | 4440 | 170 | 1.6 | 0.02 | 5.07 | 0.05 | 10.85 | 0.15 | 9.52 | 0.02 | 180.0 | 220.0 | 138.5 | 6.7 | 138.0 | 12.0 | 138.5 | 8.0 |
| Output_1_034 | 2220 | 56 | 2.1 | 0.02 | 4.19 | 0.05 | 15.58 | 0.16 | 13.29 | 0.26 | 260.0 | 300.0 | 140.2 | 5.8 | 151.0 | 19.0 | 140.2 | 7.2 |
| Output_1_046 | 2490 | 70 | 1.4 | 0.02 | 4.00 | 0.05 | 16.94 | 0.15 | 15.86 | 0.20 | 140.0 | 310.0 | 140.4 | 5.6 | 136.0 | 20.0 | 140.4 | 7.1 |
| Output_1_010 | 2220 | 138 | 1.8 | 0.02 | 3.54 | 0.05 | 14.89 | 0.16 | 14.47 | 0.10 | 120.0 | 280.0 | 140.7 | 4.9 | 147.0 | 20.0 | 140.7 | 6.6 |
| Output_1_044 | 5890 | 208 | 1.9 | 0.02 | 3.40 | 0.06 | 9.62 | 0.16 | 10.43 | 0.13 | 320.0 | 210.0 | 140.7 | 4.7 | 154.0 | 14.0 | 140.7 | 6.4 |
| Output_1_045 | 4220 | 143 | 1.8 | 0.02 | 3.43 | 0.05 | 9.26 | 0.16 | 9.38 | 0.19 | 290.0 | 190.0 | 141.1 | 4.8 | 149.0 | 13.0 | 141.1 | 6.5 |
| Output_1_037 | 6570 | 231 | 1.9 | 0.02 | 5.43 | 0.05 | 7.86 | 0.15 | 8.44 | 0.50 | 220.0 | 170.0 | 141.2 | 7.7 | 145.0 | 12.0 | 141.2 | 8.9 |
| Output_1_009 | 3800 | 214 | 2.5 | 0.02 | 4.44 | 0.05 | 10.87 | 0.15 | 10.53 | 0.15 | 150.0 | 220.0 | 142.0 | 6.2 | 142.0 | 14.0 | 142.0 | 8.0 |
| Output_1_028 | 2570 | 55 | 1.8 | 0.02 | 3.67 | 0.05 | 11.54 | 0.15 | 11.72 | 0.04 | 50.0 | 210.0 | 142.4 | 5.2 | 141.0 | 15.0 | 142.4 | 6.8 |
| Output_1_041 | 2700 | 109 | 2.5 | 0.02 | 5.31 | 0.05 | 13.11 | 0.16 | 12.82 | 0.23 | 230.0 | 250.0 | 144.1 | 7.4 | 148.0 | 17.0 | 144.1 | 8.6 |
| Output_1_029 | 19450 | 416 | 1.5 | 0.02 | 1.68 | 0.05 | 3.52 | 0.15 | 3.42 | 0.27 | 131.0 | 77.0 | 144.2 | 2.4 | 143.5 | 4.6 | 144.2 | 5.1 |
| Output_1_033 | 4370 | 104 | 1.6 | 0.02 | 3.13 | 0.05 | 8.59 | 0.17 | 8.48 | 0.11 | 260.0 | 190.0 | 144.5 | 4.5 | 154.0 | 13.0 | 144.5 | 6.4 |
| Output_1_031 | 1580 | 34 | 2.8 | 0.02 | 6.61 | 0.06 | 27.59 | 0.17 | 30.77 | 0.89 | 100.0 | 560.0 | 144.7 | 9.7 | 169.0 | 30.0 | 144.7 | 11.0 |
| Output_1_048 | 2368 | 57 | 2.3 | 0.02 | 3.89 | 0.05 | 13.24 | 0.16 | 12.90 | 0.27 | 90.0 | 250.0 | 145.6 | 5.6 | 144.0 | 17.0 | 145.6 | 7.3 |
| Output_1_027 | 2420 | 53 | 2.1 | 0.02 | 4.80 | 0.05 | 9.90 | 0.16 | 10.56 | 0.34 | 270.0 | 200.0 | 146.0 | 6.7 | 152.0 | 15.0 | 146.0 | 7.8 |
| Output_1_032 | 2045 | 46 | 2.0 | 0.02 | 5.24 | 0.06 | 15.91 | 0.17 | 15.20 | 0.15 | 410.0 | 350.0 | 146.0 | 7.7 | 159.0 | 22.0 | 146.0 | 8.9 |
| Output_1_017 | 1837 | 78 | 2.5 | 0.02 | 6.52 | 0.05 | 12.28 | 0.16 | 14.01 | 0.39 | 170.0 | 260.0 | 146.2 | 9.7 | 148.0 | 19.0 | 146.2 | 11.0 |
| Output_1_043 | 3200 | 116 | 2.7 | 0.02 | 6.17 | 0.05 | 11.40 | 0.17 | 11.18 | 0.08 | 330.0 | 220.0 | 146.2 | 8.8 | 161.0 | 16.0 | 146.2 | 9.9 |
| Output_1_015 | 1586 | 78 | 2.2 | 0.02 | 5.22 | 0.05 | 17.78 | 0.16 | 16.56 | 0.04 | 140.0 | 320.0 | 146.3 | 7.4 | 144.0 | 22.0 | 146.3 | 8.7 |
| Output_1_039 | 4850 | 188 | 1.8 | 0.02 | 4.26 | 0.05 | 8.79 | 0.15 | 8.50 | 0.25 | 80.0 | 180.0 | 146.5 | 6.2 | 144.0 | 12.0 | 146.5 | 7.7 |
| Output_1_016 | 8120 | 353 | 1.4 | 0.02 | 4.26 | 0.05 | 8.07 | 0.16 | 6.92 | 0.26 | 200.0 | 170.0 | 146.7 | 6.2 | 149.0 | 10.0 | 146.7 | 7.7 |
| Output_1_035 | 1591 | 42 | 2.4 | 0.02 | 4.78 | 0.06 | 15.44 | 0.18 | 14.61 | 0.08 | 320.0 | 320.0 | 146.7 | 6.7 | 164.0 | 23.0 | 146.7 | 8.2 |
| Output_1_011 | 2150 | 136 | 1.8 | 0.02 | 6.06 | 0.06 | 20.00 | 0.18 | 20.56 | 0.03 | 430.0 | 410.0 | 147.0 | 8.9 | 166.0 | 31.0 | 147.0 | 10.0 |
| Output_1_020 | 16520 | 612 | 1.2 | 0.02 | 2.99 | 0.05 | 6.83 | 0.17 | 5.57 | 0.04 | 310.0 | 160.0 | 147.0 | 4.3 | 155.1 | 8.0 | 147.0 | 6.3 |
| Output_1_004 | 1910 | 39 | 2.5 | 0.02 | 5.19 | 0.05 | 22.64 | 0.16 | 21.74 | 0.16 | 280.0 | 390.0 | 147.3 | 7.8 | 161.0 | 27.0 | 147.3 | 9.1 |
| Output_1_023 | 2320 | 66 | 2.4 | 0.02 | 5.17 | 0.05 | 12.77 | 0.17 | 11.76 | 0.16 | 230.0 | 250.0 | 147.5 | 7.6 | 157.0 | 17.0 | 147.5 | 8.7 |
| Output_1_042 | 2251 | 86 | 2.6 | 0.02 | 5.60 | 0.05 | 12.97 | 0.16 | 13.66 | 0.27 | 210.0 | 260.0 | 147.5 | 8.0 | 149.0 | 19.0 | 147.5 | 9.2 |
| Output_1_030 | 2200 | 45 | 3.5 | 0.02 | 6.90 | 0.06 | 11.66 | 0.18 | 12.09 | 0.32 | 430.0 | 250.0 | 147.7 | 9.8 | 171.0 | 19.0 | 147.7 | 11.0 |
| Output_1_001 | 2245 | 35 | 3.3 | 0.02 | 6.09 | 0.05 | 9.65 | 0.16 | 10.00 | 0.22 | 290.0 | 190.0 | 147.9 | 8.4 | 152.0 | 14.0 | 147.9 | 9.4 |
| Output_1_026 | 2940 | 64 | 1.6 | 0.02 | 3.66 | 0.05 | 11.07 | 0.15 | 9.80 | 0.09 | 120.0 | 220.0 | 148.0 | 5.4 | 144.0 | 14.0 | 148.0 | 7.1 |
| Output_1_018 | 2427 | 96 | 1.8 | 0.02 | 4.33 | 0.06 | 11.67 | 0.17 | 11.24 | 0.12 | 430.0 | 230.0 | 148.1 | 6.8 | 160.0 | 17.0 | 148.1 | 8.0 |

| | | | | | | | | | | | | | | | | | | |
|---|---|---|---|---|---|---|---|---|---|---|---|---|---|---|---|---|---|---|
| Output_1_003 | 3070 | 56 | 2.0 | 0.02 | 4.72 | 0.06 | 10.69 | 0.19 | 11.76 | 0.08 | 430.0 | 230.0 | 148.3 | 6.7 | 173.0 | 19.0 | 148.3 | 8.1 |
| Output_1_050 | 2080 | 46 | 3.0 | 0.02 | 6.01 | 0.04 | 22.28 | 0.13 | 27.69 | 0.16 | -320.0 | 360.0 | 148.3 | 8.6 | 122.0 | 23.0 | 148.3 | 10.0 |
| Output_1_021 | 1824 | 59 | 2.0 | 0.02 | 5.15 | 0.04 | 14.51 | 0.15 | 14.67 | 0.33 | -100.0 | 250.0 | 148.4 | 7.6 | 139.0 | 19.0 | 148.4 | 8.9 |
| Output_1_049 | 3350 | 73 | 2.7 | 0.02 | 5.15 | 0.05 | 11.57 | 0.15 | 10.67 | 0.21 | 80.0 | 230.0 | 148.5 | 7.5 | 141.0 | 14.0 | 148.5 | 8.8 |
| Output_1_036 | 3070 | 95 | 1.7 | 0.02 | 3.76 | 0.05 | 11.85 | 0.17 | 10.92 | 0.09 | 320.0 | 240.0 | 148.6 | 5.7 | 161.0 | 16.0 | 148.6 | 7.4 |
| Output_1_007 | 3230 | 128 | 2.5 | 0.02 | 4.70 | 0.05 | 15.42 | 0.14 | 13.29 | 0.09 | -80.0 | 240.0 | 149.0 | 7.0 | 134.0 | 17.0 | 149.0 | 8.4 |
| Output_1_013 | 2790 | 152 | 2.2 | 0.02 | 5.93 | 0.05 | 10.88 | 0.17 | 9.47 | 0.23 | 320.0 | 220.0 | 150.0 | 8.9 | 159.0 | 15.0 | 150.0 | 9.7 |
| Output_1_024 | 2950 | 75 | 1.9 | 0.02 | 5.08 | 0.05 | 12.24 | 0.15 | 12.34 | 0.30 | 70.0 | 230.0 | 150.3 | 7.3 | 144.0 | 17.0 | 150.3 | 8.7 |
| Output_1_008 | 2050 | 95 | 2.1 | 0.02 | 5.49 | 0.06 | 15.52 | 0.17 | 14.45 | 0.07 | 280.0 | 310.0 | 150.7 | 8.1 | 159.0 | 21.0 | 150.7 | 9.4 |
| Output_1_014 | 6350 | 312 | 1.7 | 0.02 | 5.49 | 0.05 | 12.20 | 0.17 | 13.37 | 0.46 | 330.0 | 240.0 | 151.0 | 8.4 | 169.0 | 19.0 | 151.0 | 9.7 |
| Output_1_025 | 14110 | 345 | 1.9 | 0.02 | 2.44 | 0.05 | 7.62 | 0.16 | 6.17 | 0.13 | 210.0 | 160.0 | 151.4 | 3.6 | 152.2 | 9.0 | 151.4 | 6.0 |
| Output_1_047 | 1632 | 41 | 3.2 | 0.02 | 4.18 | 0.05 | 16.39 | 0.16 | 16.88 | 0.04 | 10.0 | 290.0 | 152.0 | 6.5 | 147.0 | 23.0 | 152.0 | 8.1 |
| Output_1_005 | 2950 | 66 | 1.9 | 0.02 | 5.00 | 0.06 | 14.34 | 0.20 | 16.50 | 0.38 | 500.0 | 330.0 | 152.7 | 7.7 | 183.0 | 28.0 | 152.7 | 9.0 |
| Output_1_038 | 3490 | 118 | 2.9 | 0.02 | 4.12 | 0.05 | 10.59 | 0.17 | 10.06 | 0.01 | 240.0 | 220.0 | 155.0 | 6.4 | 157.0 | 15.0 | 155.0 | 8.0 |
| Output_1_051 | 1461 | 27 | 3.9 | 0.02 | 6.48 | 0.05 | 16.57 | 0.17 | 17.06 | 0.05 | 110.0 | 300.0 | 157.0 | 10.0 | 169.0 | 31.0 | 157.0 | 11.0 |
| Output_1_002 | 9770 | 131 | 1.9 | 0.03 | 2.35 | 0.05 | 6.47 | 0.20 | 6.86 | 0.24 | 270.0 | 140.0 | 183.9 | 4.3 | 189.0 | 11.0 | 183.9 | 7.2 |
| Output_1_040 | 19900 | 396 | 2.2 | 0.05 | 2.12 | 0.05 | 4.14 | 0.34 | 4.15 | 0.26 | 339.0 | 90.0 | 294.8 | 6.1 | 297.0 | 11.0 | 294.8 | 11.0 |

**Sample 18ATW20**

| | | | | | | | | | | | | | | | | | | |
|---|---|---|---|---|---|---|---|---|---|---|---|---|---|---|---|---|---|---|
| Output_1_019 | 2190 | 122 | 1.7 | 0.02 | 5.23 | 0.06 | 13.88 | 0.13 | 13.60 | 0.17 | 440.0 | 280.0 | 102.6 | 5.3 | 121.0 | 16.0 | 102.6 | 6.2 |
| Output_1_012 | 1990 | 129 | 2.1 | 0.02 | 5.14 | 0.05 | 24.53 | 0.16 | 20.50 | 0.21 | 350.0 | 350.0 | 136.2 | 6.7 | 145.0 | 31.0 | 136.2 | 8.6 |
| Output_1_006 | 4440 | 170 | 1.6 | 0.02 | 5.07 | 0.05 | 10.85 | 0.15 | 9.52 | 0.02 | 180.0 | 220.0 | 138.5 | 6.7 | 138.0 | 12.0 | 138.5 | 8.0 |
| Output_1_034 | 2220 | 56 | 2.1 | 0.02 | 4.19 | 0.05 | 15.58 | 0.16 | 13.29 | 0.26 | 260.0 | 300.0 | 140.2 | 5.8 | 151.0 | 19.0 | 140.2 | 7.2 |
| Output_1_046 | 2490 | 70 | 1.4 | 0.02 | 4.00 | 0.05 | 16.94 | 0.15 | 15.86 | 0.20 | 140.0 | 310.0 | 140.4 | 5.6 | 136.0 | 20.0 | 140.4 | 7.1 |
| Output_1_010 | 2220 | 138 | 1.8 | 0.02 | 3.54 | 0.05 | 14.89 | 0.16 | 14.47 | 0.10 | 120.0 | 280.0 | 140.7 | 4.9 | 147.0 | 20.0 | 140.7 | 6.6 |
| Output_1_044 | 5890 | 208 | 1.9 | 0.02 | 3.40 | 0.06 | 9.62 | 0.16 | 10.43 | 0.13 | 320.0 | 210.0 | 140.7 | 4.7 | 154.0 | 14.0 | 140.7 | 6.4 |
| Output_1_045 | 4220 | 143 | 1.8 | 0.02 | 3.43 | 0.05 | 9.26 | 0.16 | 9.38 | 0.19 | 290.0 | 190.0 | 141.1 | 4.8 | 149.0 | 13.0 | 141.1 | 6.5 |
| Output_1_037 | 6570 | 231 | 1.9 | 0.02 | 5.43 | 0.05 | 7.86 | 0.15 | 8.44 | 0.50 | 220.0 | 170.0 | 141.2 | 7.7 | 145.0 | 12.0 | 141.2 | 8.9 |
| Output_1_009 | 3800 | 214 | 2.5 | 0.02 | 4.44 | 0.05 | 10.87 | 0.15 | 10.53 | 0.15 | 150.0 | 220.0 | 142.0 | 6.2 | 142.0 | 14.0 | 142.0 | 8.0 |
| Output_1_028 | 2570 | 55 | 1.8 | 0.02 | 3.67 | 0.05 | 11.54 | 0.15 | 11.72 | 0.04 | 50.0 | 210.0 | 142.4 | 5.2 | 141.0 | 15.0 | 142.4 | 6.8 |
| Output_1_041 | 2700 | 109 | 2.5 | 0.02 | 5.31 | 0.05 | 13.11 | 0.16 | 12.82 | 0.23 | 230.0 | 250.0 | 144.1 | 7.4 | 148.0 | 17.0 | 144.1 | 8.6 |
| Output_1_029 | 19450 | 416 | 1.5 | 0.02 | 1.68 | 0.05 | 3.52 | 0.15 | 3.42 | 0.27 | 131.0 | 77.0 | 144.2 | 2.4 | 143.5 | 4.6 | 144.2 | 5.1 |
| Output_1_033 | 4370 | 104 | 1.6 | 0.02 | 3.13 | 0.05 | 8.59 | 0.17 | 8.48 | 0.11 | 260.0 | 190.0 | 144.5 | 4.5 | 154.0 | 13.0 | 144.5 | 6.4 |
| Output_1_031 | 1580 | 34 | 2.8 | 0.02 | 6.61 | 0.06 | 27.59 | 0.17 | 30.77 | 0.89 | 100.0 | 560.0 | 144.7 | 9.7 | 169.0 | 30.0 | 144.7 | 11.0 |
| Output_1_048 | 2368 | 57 | 2.3 | 0.02 | 3.89 | 0.05 | 13.24 | 0.16 | 12.90 | 0.27 | 90.0 | 250.0 | 145.6 | 5.6 | 144.0 | 17.0 | 145.6 | 7.3 |
| Output_1_027 | 2420 | 53 | 2.1 | 0.02 | 4.80 | 0.05 | 9.90 | 0.16 | 10.56 | 0.34 | 270.0 | 200.0 | 146.0 | 6.7 | 152.0 | 15.0 | 146.0 | 7.8 |
| Output_1_032 | 2045 | 46 | 2.0 | 0.02 | 5.24 | 0.06 | 15.91 | 0.17 | 15.20 | 0.15 | 410.0 | 350.0 | 146.0 | 7.7 | 159.0 | 22.0 | 146.0 | 8.9 |
| Output_1_017 | 1837 | 78 | 2.5 | 0.02 | 6.52 | 0.05 | 12.28 | 0.16 | 14.01 | 0.39 | 170.0 | 260.0 | 146.2 | 9.7 | 148.0 | 19.0 | 146.2 | 11.0 |
| Output_1_043 | 3200 | 116 | 2.7 | 0.02 | 6.17 | 0.05 | 11.40 | 0.17 | 11.18 | 0.08 | 330.0 | 220.0 | 146.2 | 8.8 | 161.0 | 16.0 | 146.2 | 9.9 |
| Output_1_015 | 1586 | 78 | 2.2 | 0.02 | 5.22 | 0.05 | 17.78 | 0.16 | 16.56 | 0.04 | 140.0 | 320.0 | 146.3 | 7.4 | 144.0 | 22.0 | 146.3 | 8.7 |

| | | | | | | | | | | | | | | | | | | |
|---|---|---|---|---|---|---|---|---|---|---|---|---|---|---|---|---|---|---|
| Output_1_039 | 4850 | 188 | 1.8 | 0.02 | 4.26 | 0.05 | 8.79 | 0.15 | 8.50 | 0.25 | 80.0 | 180.0 | 146.5 | 6.2 | 144.0 | 12.0 | 146.5 | 7.7 |
| Output_1_016 | 8120 | 353 | 1.4 | 0.02 | 4.26 | 0.05 | 8.07 | 0.16 | 6.92 | 0.26 | 200.0 | 170.0 | 146.7 | 6.2 | 149.0 | 10.0 | 146.7 | 7.7 |
| Output_1_035 | 1591 | 42 | 2.4 | 0.02 | 4.78 | 0.06 | 15.44 | 0.18 | 14.61 | 0.08 | 320.0 | 320.0 | 146.7 | 6.7 | 164.0 | 23.0 | 146.7 | 8.2 |
| Output_1_011 | 2150 | 136 | 1.8 | 0.02 | 6.06 | 0.06 | 20.00 | 0.18 | 20.56 | 0.03 | 430.0 | 410.0 | 147.0 | 8.9 | 166.0 | 31.0 | 147.0 | 10.0 |
| Output_1_020 | 16520 | 612 | 1.2 | 0.02 | 2.99 | 0.05 | 6.83 | 0.17 | 5.57 | 0.04 | 310.0 | 160.0 | 147.0 | 4.3 | 155.1 | 8.0 | 147.0 | 6.3 |
| Output_1_004 | 1910 | 39 | 2.5 | 0.02 | 5.19 | 0.05 | 22.64 | 0.16 | 21.74 | 0.16 | 280.0 | 390.0 | 147.3 | 7.8 | 161.0 | 27.0 | 147.3 | 9.1 |
| Output_1_023 | 2320 | 66 | 2.4 | 0.02 | 5.17 | 0.05 | 12.77 | 0.17 | 11.76 | 0.16 | 230.0 | 250.0 | 147.5 | 7.6 | 157.0 | 17.0 | 147.5 | 8.7 |
| Output_1_042 | 2251 | 86 | 2.6 | 0.02 | 5.60 | 0.05 | 12.97 | 0.16 | 13.66 | 0.27 | 210.0 | 260.0 | 147.5 | 8.0 | 149.0 | 19.0 | 147.5 | 9.2 |
| Output_1_030 | 2200 | 45 | 3.5 | 0.02 | 6.90 | 0.06 | 11.66 | 0.18 | 12.09 | 0.32 | 430.0 | 250.0 | 147.7 | 9.8 | 171.0 | 19.0 | 147.7 | 11.0 |
| Output_1_001 | 2245 | 35 | 3.3 | 0.02 | 6.09 | 0.05 | 9.65 | 0.16 | 10.00 | 0.22 | 290.0 | 190.0 | 147.9 | 8.4 | 152.0 | 14.0 | 147.9 | 9.4 |
| Output_1_026 | 2940 | 64 | 1.6 | 0.02 | 3.66 | 0.05 | 11.07 | 0.15 | 9.80 | 0.09 | 120.0 | 220.0 | 148.0 | 5.4 | 144.0 | 14.0 | 148.0 | 7.1 |
| Output_1_018 | 2427 | 96 | 1.8 | 0.02 | 4.33 | 0.06 | 11.67 | 0.17 | 11.24 | 0.12 | 430.0 | 230.0 | 148.1 | 6.8 | 160.0 | 17.0 | 148.1 | 8.0 |
| Output_1_003 | 3070 | 56 | 2.0 | 0.02 | 4.72 | 0.06 | 10.69 | 0.19 | 11.76 | 0.08 | 430.0 | 230.0 | 148.3 | 6.7 | 173.0 | 19.0 | 148.3 | 8.1 |
| Output_1_050 | 2080 | 46 | 3.0 | 0.02 | 6.01 | 0.04 | 22.28 | 0.13 | 27.69 | 0.16 | -320.0 | 360.0 | 148.3 | 8.6 | 122.0 | 23.0 | 148.3 | 10.0 |
| Output_1_021 | 1824 | 59 | 2.0 | 0.02 | 5.15 | 0.04 | 14.51 | 0.15 | 14.67 | 0.33 | -100.0 | 250.0 | 148.4 | 7.6 | 139.0 | 19.0 | 148.4 | 8.9 |
| Output_1_049 | 3350 | 73 | 2.7 | 0.02 | 5.15 | 0.05 | 11.57 | 0.15 | 10.67 | 0.21 | 80.0 | 230.0 | 148.5 | 7.5 | 141.0 | 14.0 | 148.5 | 8.8 |
| Output_1_036 | 3070 | 95 | 1.7 | 0.02 | 3.76 | 0.05 | 11.85 | 0.17 | 10.92 | 0.09 | 320.0 | 240.0 | 148.6 | 5.7 | 161.0 | 16.0 | 148.6 | 7.4 |
| Output_1_007 | 3230 | 128 | 2.5 | 0.02 | 4.70 | 0.05 | 15.42 | 0.14 | 13.29 | 0.09 | -80.0 | 240.0 | 149.0 | 7.0 | 134.0 | 17.0 | 149.0 | 8.4 |
| Output_1_013 | 2790 | 152 | 2.2 | 0.02 | 5.93 | 0.05 | 10.88 | 0.17 | 9.47 | 0.23 | 320.0 | 220.0 | 150.0 | 8.9 | 159.0 | 15.0 | 150.0 | 9.7 |
| Output_1_024 | 2950 | 75 | 1.9 | 0.02 | 5.08 | 0.05 | 12.24 | 0.15 | 12.34 | 0.30 | 70.0 | 230.0 | 150.3 | 7.3 | 144.0 | 17.0 | 150.3 | 8.7 |
| Output_1_008 | 2050 | 95 | 2.1 | 0.02 | 5.49 | 0.06 | 15.52 | 0.17 | 14.45 | 0.07 | 280.0 | 310.0 | 150.7 | 8.1 | 159.0 | 21.0 | 150.7 | 9.4 |
| Output_1_014 | 6350 | 312 | 1.7 | 0.02 | 5.49 | 0.05 | 12.20 | 0.17 | 13.37 | 0.46 | 330.0 | 240.0 | 151.0 | 8.4 | 169.0 | 19.0 | 151.0 | 9.7 |
| Output_1_025 | 14110 | 345 | 1.9 | 0.02 | 2.44 | 0.05 | 7.62 | 0.16 | 6.17 | 0.13 | 210.0 | 160.0 | 151.4 | 3.6 | 152.2 | 9.0 | 151.4 | 6.0 |
| Output_1_047 | 1632 | 41 | 3.2 | 0.02 | 4.18 | 0.05 | 16.39 | 0.16 | 16.88 | 0.04 | 10.0 | 290.0 | 152.0 | 6.5 | 147.0 | 23.0 | 152.0 | 8.1 |
| Output_1_005 | 2950 | 66 | 1.9 | 0.02 | 5.00 | 0.06 | 14.34 | 0.20 | 16.50 | 0.38 | 500.0 | 330.0 | 152.7 | 7.7 | 183.0 | 28.0 | 152.7 | 9.0 |
| Output_1_038 | 3490 | 118 | 2.9 | 0.02 | 4.12 | 0.05 | 10.59 | 0.17 | 10.06 | 0.01 | 240.0 | 220.0 | 155.0 | 6.4 | 157.0 | 15.0 | 155.0 | 8.0 |
| Output_1_051 | 1461 | 27 | 3.9 | 0.02 | 6.48 | 0.05 | 16.57 | 0.17 | 17.06 | 0.05 | 110.0 | 300.0 | 157.0 | 10.0 | 169.0 | 31.0 | 157.0 | 11.0 |
| Output_1_002 | 9770 | 131 | 1.9 | 0.03 | 2.35 | 0.05 | 6.47 | 0.20 | 6.86 | 0.24 | 270.0 | 140.0 | 183.9 | 4.3 | 189.0 | 11.0 | 183.9 | 7.2 |
| Output_1_040 | 19900 | 396 | 2.2 | 0.05 | 2.12 | 0.05 | 4.14 | 0.34 | 4.15 | 0.26 | 339.0 | 90.0 | 294.8 | 6.1 | 297.0 | 11.0 | 294.8 | 11.0 |
| Output_1_233 | 687 | 23 | 3.2 | 0.02 | 8.07 | 0.06 | 22.58 | 0.18 | 19.67 | 0.09 | 390.0 | 430.0 | 142.0 | 11.0 | 165.0 | 31.0 | 142.0 | 12.0 |
| Output_1_83 | 1310 | 36 | 3.6 | 0.02 | 8.89 | 0.05 | 33.96 | 0.16 | 33.75 | 0.08 | 40.0 | 610.0 | 143.0 | 13.0 | 153.0 | 48.0 | 143.0 | 14.0 |
| Output_1_195 | 1097 | 25 | 3.2 | 0.02 | 5.75 | 0.05 | 20.75 | 0.17 | 22.54 | 0.21 | 120.0 | 400.0 | 144.0 | 8.3 | 156.0 | 33.0 | 144.0 | 9.5 |
| Output_1_96 | 2030 | 63 | 3.3 | 0.02 | 5.68 | 0.06 | 16.20 | 0.17 | 14.71 | 0.10 | 270.0 | 290.0 | 146.0 | 8.2 | 162.0 | 23.0 | 146.0 | 9.4 |
| Output_1_057 | 909 | 20 | 2.4 | 0.02 | 6.90 | 0.05 | 20.37 | 0.16 | 20.37 | 0.16 | 220.0 | 400.0 | 148.0 | 9.8 | 147.0 | 29.0 | 148.0 | 11.0 |
| Output_1_134 | 3310 | 193 | 1.7 | 0.02 | 7.73 | 0.05 | 12.48 | 0.17 | 12.72 | 0.44 | 310.0 | 260.0 | 148.0 | 12.0 | 160.0 | 19.0 | 148.0 | 12.0 |
| Output_1_62 | 2100 | 58 | 4.4 | 0.02 | 7.73 | 0.06 | 15.26 | 0.18 | 14.12 | 0.19 | 300.0 | 310.0 | 148.0 | 11.0 | 162.0 | 21.0 | 148.0 | 12.0 |
| Output_1_176 | 2310 | 31 | 3.3 | 0.02 | 8.09 | 0.05 | 13.17 | 0.16 | 14.11 | 0.35 | 90.0 | 250.0 | 149.0 | 12.0 | 154.0 | 21.0 | 149.0 | 13.0 |
| Output_1_162 | 1216 | 30 | 3.6 | 0.02 | 5.56 | 0.06 | 21.05 | 0.18 | 23.20 | 0.07 | 210.0 | 380.0 | 149.2 | 8.0 | 168.0 | 33.0 | 149.2 | 9.2 |
| Output_1_72 | 1685 | 37 | 3.2 | 0.02 | 6.03 | 0.05 | 20.00 | 0.15 | 20.00 | 0.29 | -20.0 | 360.0 | 149.3 | 8.9 | 139.0 | 27.0 | 149.3 | 9.7 |
| Output_1_198 | 1295 | 23 | 4.4 | 0.02 | 5.58 | 0.06 | 19.64 | 0.17 | 18.82 | 0.08 | 220.0 | 360.0 | 149.4 | 8.4 | 159.0 | 28.0 | 149.4 | 9.6 |

| | | | | | | | | | | | | | | | | | | |
|---|---|---|---|---|---|---|---|---|---|---|---|---|---|---|---|---|---|---|
| Output_1_120 | 3340 | 350 | 2.4 | 0.02 | 5.51 | 0.06 | 13.67 | 0.18 | 13.89 | 0.28 | 390.0 | 280.0 | 150.1 | 8.2 | 166.0 | 22.0 | 150.1 | 9.5 |
| Output_1_243 | 6340 | 483 | 1.1 | 0.02 | 4.66 | 0.05 | 10.44 | 0.16 | 11.59 | 0.13 | 160.0 | 180.0 | 150.4 | 6.7 | 157.0 | 15.0 | 150.4 | 8.4 |
| Output_1_202 | 6060 | 131 | 1.6 | 0.02 | 4.64 | 0.05 | 6.02 | 0.16 | 6.29 | 0.29 | 90.0 | 130.0 | 150.8 | 6.8 | 149.1 | 8.8 | 150.8 | 8.3 |
| Output_1_201 | 4690 | 92 | 2.8 | 0.02 | 4.64 | 0.05 | 10.06 | 0.16 | 9.94 | 0.39 | 190.0 | 210.0 | 151.0 | 6.9 | 151.0 | 14.0 | 151.0 | 8.4 |
| Output_1_89 | 1245 | 54 | 3.1 | 0.02 | 6.84 | 0.05 | 25.53 | 0.16 | 25.95 | 0.23 | 30.0 | 450.0 | 151.0 | 10.0 | 149.0 | 37.0 | 151.0 | 11.0 |
| Output_1_059 | 5150 | 127 | 2.5 | 0.02 | 4.05 | 0.05 | 9.27 | 0.17 | 9.77 | 0.13 | 240.0 | 190.0 | 151.2 | 6.1 | 162.0 | 15.0 | 151.2 | 7.7 |
| Output_1_128 | 3040 | 312 | 2.1 | 0.02 | 4.64 | 0.05 | 10.63 | 0.18 | 11.43 | 0.30 | 450.0 | 190.0 | 151.3 | 6.7 | 162.0 | 18.0 | 151.3 | 8.9 |
| Output_1_121 | 2490 | 278 | 1.4 | 0.02 | 5.04 | 0.06 | 12.50 | 0.18 | 12.29 | 0.17 | 310.0 | 250.0 | 151.5 | 7.8 | 171.0 | 19.0 | 151.5 | 9.2 |
| Output_1_160 | 3950 | 122 | 1.9 | 0.02 | 3.49 | 0.05 | 10.65 | 0.17 | 9.70 | 0.10 | 130.0 | 210.0 | 151.7 | 5.2 | 158.0 | 14.0 | 151.7 | 7.1 |
| Output_1_053 | 3660 | 67 | 9.3 | 0.02 | 6.30 | 0.05 | 10.42 | 0.16 | 10.49 | 0.38 | 120.0 | 220.0 | 151.8 | 9.7 | 151.0 | 15.0 | 151.8 | 11.0 |
| Output_1_111 | 2310 | 79 | 1.5 | 0.02 | 5.46 | 0.05 | 13.18 | 0.17 | 12.35 | 0.07 | 230.0 | 270.0 | 151.8 | 8.2 | 157.0 | 18.0 | 151.8 | 9.5 |
| Output_1_179 | 6680 | 115 | 4.4 | 0.02 | 4.62 | 0.05 | 7.85 | 0.17 | 8.33 | 0.39 | 200.0 | 160.0 | 151.8 | 6.9 | 157.0 | 12.0 | 151.8 | 8.4 |
| Output_1_116 | 2960 | 170 | 2.0 | 0.02 | 5.46 | 0.05 | 14.59 | 0.18 | 12.71 | 0.04 | 290.0 | 280.0 | 151.9 | 8.0 | 167.0 | 19.0 | 151.9 | 9.4 |
| Output_1_169 | 2710 | 37 | 2.9 | 0.02 | 7.56 | 0.06 | 20.69 | 0.19 | 17.02 | 0.16 | 320.0 | 320.0 | 152.0 | 12.0 | 172.0 | 27.0 | 152.0 | 12.0 |
| Output_1_227 | 2420 | 52 | 2.9 | 0.02 | 7.53 | 0.05 | 12.42 | 0.17 | 12.50 | 0.25 | 110.0 | 240.0 | 152.0 | 11.0 | 155.0 | 18.0 | 152.0 | 12.0 |
| Output_1_71 | 3450 | 75 | 3.9 | 0.02 | 5.02 | 0.04 | 17.59 | 0.15 | 12.75 | 0.21 | -200.0 | 300.0 | 152.2 | 7.7 | 144.0 | 19.0 | 152.2 | 8.9 |
| Output_1_109 | 1920 | 55 | 2.5 | 0.02 | 5.44 | 0.05 | 14.03 | 0.17 | 14.71 | 0.36 | 170.0 | 280.0 | 152.4 | 8.2 | 160.0 | 22.0 | 152.4 | 9.5 |
| Output_1_95 | 2370 | 77 | 3.4 | 0.02 | 6.28 | 0.06 | 15.15 | 0.18 | 13.74 | 0.10 | 320.0 | 300.0 | 152.4 | 9.7 | 167.0 | 22.0 | 152.4 | 11.0 |
| Output_1_230 | 5530 | 139 | 2.1 | 0.02 | 5.86 | 0.05 | 7.92 | 0.16 | 8.23 | 0.32 | 90.0 | 160.0 | 152.5 | 8.6 | 148.0 | 12.0 | 152.5 | 9.9 |
| Output_1_85 | 1047 | 36 | 3.5 | 0.02 | 5.49 | 0.05 | 19.22 | 0.17 | 18.50 | 0.37 | 120.0 | 370.0 | 152.5 | 7.9 | 157.0 | 28.0 | 152.5 | 9.6 |
| Output_1_166 | 1014 | 17 | 2.7 | 0.02 | 5.42 | 0.05 | 25.49 | 0.18 | 25.14 | 0.37 | 30.0 | 390.0 | 152.6 | 7.9 | 154.0 | 38.0 | 152.6 | 9.4 |
| Output_1_183 | 3480 | 97 | 2.6 | 0.02 | 3.92 | 0.05 | 10.96 | 0.17 | 11.90 | 0.21 | 200.0 | 220.0 | 152.8 | 5.9 | 156.0 | 17.0 | 152.8 | 7.6 |
| Output_1_164 | 2380 | 46 | 3.1 | 0.02 | 5.42 | 0.05 | 13.56 | 0.17 | 12.12 | 0.08 | 200.0 | 240.0 | 153.0 | 8.4 | 162.0 | 18.0 | 153.0 | 9.7 |
| Output_1_211 | 3350 | 280 | 3.5 | 0.02 | 4.58 | 0.05 | 10.74 | 0.16 | 11.73 | 0.39 | 160.0 | 220.0 | 153.1 | 7.0 | 151.0 | 17.0 | 153.1 | 8.4 |
| Output_1_22 | 2040 | 59 | 2.5 | 0.02 | 4.58 | 0.05 | 14.57 | 0.16 | 14.02 | 0.34 | 90.0 | 270.0 | 153.1 | 7.1 | 152.0 | 20.0 | 153.1 | 8.6 |
| Output_1_132 | 2430 | 156 | 2.8 | 0.02 | 4.56 | 0.05 | 14.43 | 0.17 | 13.77 | 0.07 | 140.0 | 270.0 | 153.4 | 6.6 | 154.0 | 20.0 | 153.4 | 8.2 |
| Output_1_196 | 2337 | 47 | 5.0 | 0.02 | 5.81 | 0.05 | 12.65 | 0.16 | 12.96 | 0.40 | 70.0 | 230.0 | 153.6 | 9.1 | 151.0 | 18.0 | 153.6 | 10.0 |
| Output_1_118 | 4260 | 300 | 1.7 | 0.02 | 6.20 | 0.06 | 9.69 | 0.18 | 10.56 | 0.20 | 350.0 | 200.0 | 153.7 | 9.7 | 167.0 | 16.0 | 153.7 | 11.0 |
| Output_1_223 | 1692 | 40 | 2.9 | 0.02 | 4.15 | 0.05 | 15.66 | 0.17 | 14.20 | 0.19 | 260.0 | 290.0 | 153.7 | 6.5 | 165.0 | 21.0 | 153.7 | 8.0 |
| Output_1_112 | 3160 | 119 | 1.1 | 0.02 | 3.56 | 0.05 | 11.67 | 0.17 | 11.18 | 0.01 | 120.0 | 230.0 | 153.8 | 5.4 | 157.0 | 16.0 | 153.8 | 7.3 |
| Output_1_69 | 4570 | 102 | 4.5 | 0.02 | 5.79 | 0.05 | 9.81 | 0.17 | 10.98 | 0.22 | 230.0 | 210.0 | 153.9 | 8.7 | 164.0 | 16.0 | 153.9 | 10.0 |
| Output_1_222 | 4820 | 118 | 2.3 | 0.02 | 3.88 | 0.05 | 8.13 | 0.17 | 7.74 | 0.20 | 220.0 | 160.0 | 154.1 | 5.9 | 160.0 | 11.0 | 154.1 | 7.6 |
| Output_1_99 | 2410 | 61 | 1.6 | 0.02 | 5.37 | 0.05 | 14.29 | 0.18 | 13.97 | 0.12 | 320.0 | 270.0 | 154.1 | 8.2 | 168.0 | 22.0 | 154.1 | 9.5 |
| Output_1_130 | 80000 | 5880 | 3.2 | 0.02 | 3.51 | 0.05 | 3.14 | 0.17 | 3.91 | 0.66 | 220.0 | 73.0 | 154.2 | 5.3 | 158.1 | 5.7 | 154.2 | 7.2 |
| Output_1_177 | 1610 | 20 | 3.5 | 0.02 | 6.20 | 0.05 | 15.33 | 0.18 | 14.77 | 0.07 | 240.0 | 310.0 | 154.2 | 9.4 | 165.0 | 23.0 | 154.2 | 11.0 |
| Output_1_184 | 5150 | 169 | 2.3 | 0.02 | 5.37 | 0.05 | 10.43 | 0.17 | 10.06 | 0.37 | 210.0 | 220.0 | 154.3 | 8.1 | 157.0 | 15.0 | 154.3 | 9.5 |
| Output_1_167 | 3330 | 51 | 2.9 | 0.02 | 4.53 | 0.05 | 10.74 | 0.16 | 10.37 | 0.02 | 120.0 | 220.0 | 154.4 | 6.8 | 153.0 | 15.0 | 154.4 | 8.4 |
| Output_1_73 | 15110 | 306 | 12.6 | 0.02 | 4.55 | 0.05 | 6.60 | 0.17 | 6.32 | 0.43 | 260.0 | 140.0 | 154.4 | 6.9 | 162.2 | 9.6 | 154.4 | 8.5 |
| Output_1_203 | 3180 | 74 | 2.4 | 0.02 | 5.44 | 0.05 | 10.28 | 0.16 | 10.43 | 0.39 | 170.0 | 220.0 | 154.8 | 7.9 | 152.0 | 15.0 | 154.8 | 9.3 |
| Output_1_144 | 4940 | 203 | 1.7 | 0.02 | 4.12 | 0.05 | 9.41 | 0.16 | 9.88 | 0.14 | 80.0 | 190.0 | 154.9 | 6.3 | 151.0 | 14.0 | 154.9 | 8.0 |

| | | | | | | | | | | | | | | | | | | |
|---|---|---|---|---|---|---|---|---|---|---|---|---|---|---|---|---|---|---|
| Output_1_214 | 7510 | 427 | 2.5 | 0.02 | 4.53 | 0.05 | 7.19 | 0.17 | 6.51 | 0.14 | 180.0 | 140.0 | 154.9 | 6.8 | 158.5 | 9.3 | 154.9 | 8.4 |
| Output_1_133 | 2860 | 175 | 1.2 | 0.02 | 7.41 | 0.06 | 13.44 | 0.19 | 12.95 | 0.02 | 470.0 | 260.0 | 155.0 | 11.0 | 176.0 | 21.0 | 155.0 | 12.0 |
| Output_1_143 | 2004 | 86 | 3.8 | 0.02 | 6.58 | 0.05 | 16.56 | 0.15 | 14.94 | 0.16 | 90.0 | 300.0 | 155.0 | 10.0 | 143.0 | 20.0 | 155.0 | 11.0 |
| Output_1_68 | 1820 | 42 | 3.9 | 0.02 | 7.47 | 0.04 | 13.48 | 0.14 | 12.68 | 0.26 | -70.0 | 260.0 | 155.0 | 11.0 | 134.0 | 16.0 | 155.0 | 12.0 |
| Output_1_67 | 14760 | 346 | 3.9 | 0.02 | 5.74 | 0.05 | 6.40 | 0.17 | 6.63 | 0.39 | 250.0 | 130.0 | 155.3 | 8.5 | 157.4 | 9.8 | 155.3 | 9.8 |
| Output_1_156 | 7930 | 354 | 2.0 | 0.02 | 5.33 | 0.05 | 8.87 | 0.16 | 9.20 | 0.23 | 170.0 | 180.0 | 155.4 | 7.9 | 152.0 | 13.0 | 155.4 | 9.4 |
| Output_1_63 | 2770 | 71 | 3.5 | 0.02 | 5.33 | 0.05 | 10.04 | 0.17 | 10.40 | 0.24 | 210.0 | 200.0 | 155.6 | 7.9 | 160.0 | 15.0 | 155.6 | 9.3 |
| Output_1_052 | 4490 | 82 | 7.5 | 0.02 | 4.51 | 0.05 | 11.16 | 0.17 | 10.71 | 0.16 | 170.0 | 220.0 | 155.7 | 6.9 | 156.0 | 16.0 | 155.7 | 8.5 |
| Output_1_142 | 4260 | 175 | 2.2 | 0.02 | 5.31 | 0.05 | 9.36 | 0.17 | 9.58 | 0.32 | 260.0 | 180.0 | 155.7 | 8.1 | 156.0 | 13.0 | 155.7 | 9.5 |
| Output_1_208 | 3400 | 183 | 2.5 | 0.02 | 7.35 | 0.05 | 10.18 | 0.17 | 10.06 | 0.23 | 210.0 | 220.0 | 156.0 | 11.0 | 158.0 | 15.0 | 156.0 | 12.0 |
| Output_1_234 | 2420 | 80 | 2.7 | 0.02 | 6.56 | 0.05 | 15.25 | 0.18 | 16.00 | 0.39 | 150.0 | 300.0 | 156.0 | 10.0 | 166.0 | 25.0 | 156.0 | 11.0 |
| Output_1_79 | 7340 | 144 | 2.4 | 0.02 | 3.67 | 0.05 | 7.33 | 0.17 | 7.56 | 0.24 | 250.0 | 150.0 | 156.2 | 5.6 | 162.0 | 12.0 | 156.2 | 7.5 |
| Output_1_151 | 3220 | 144 | 2.4 | 0.02 | 6.10 | 0.05 | 12.22 | 0.17 | 12.07 | 0.16 | 140.0 | 230.0 | 156.3 | 9.6 | 161.0 | 18.0 | 156.3 | 11.0 |
| Output_1_106 | 14900 | 374 | 1.3 | 0.02 | 4.07 | 0.05 | 3.56 | 0.18 | 4.28 | 0.57 | 227.0 | 83.0 | 156.9 | 6.4 | 164.5 | 6.3 | 156.9 | 8.1 |
| Output_1_192 | 2460 | 103 | 4.5 | 0.02 | 6.07 | 0.05 | 13.78 | 0.17 | 14.53 | 0.53 | 70.0 | 240.0 | 157.3 | 9.5 | 158.0 | 21.0 | 157.3 | 10.0 |
| Output_1_170 | 2912 | 35 | 3.2 | 0.02 | 6.07 | 0.05 | 13.10 | 0.16 | 13.41 | 0.20 | 90.0 | 260.0 | 157.4 | 9.5 | 155.0 | 19.0 | 157.4 | 11.0 |
| Output_1_81 | 7510 | 174 | 4.1 | 0.02 | 4.05 | 0.05 | 6.50 | 0.17 | 7.47 | 0.51 | 220.0 | 140.0 | 157.4 | 6.3 | 164.0 | 11.0 | 157.4 | 8.0 |
| Output_1_194 | 2790 | 68 | 5.3 | 0.02 | 5.65 | 0.05 | 13.43 | 0.17 | 15.61 | 0.10 | 50.0 | 260.0 | 157.7 | 9.1 | 158.0 | 23.0 | 157.7 | 10.0 |
| Output_1_060 | 4070 | 119 | 9.0 | 0.02 | 5.65 | 0.05 | 9.36 | 0.17 | 10.00 | 0.19 | 130.0 | 190.0 | 157.8 | 9.0 | 158.0 | 14.0 | 157.8 | 10.0 |
| Output_1_058 | 7140 | 157 | 1.7 | 0.02 | 6.85 | 0.05 | 6.23 | 0.18 | 7.91 | 0.74 | 340.0 | 130.0 | 158.0 | 11.0 | 165.0 | 12.0 | 158.0 | 12.0 |
| Output_1_117 | 1492 | 92 | 1.4 | 0.02 | 8.03 | 0.05 | 17.58 | 0.18 | 17.32 | 0.29 | 280.0 | 350.0 | 158.0 | 13.0 | 164.0 | 27.0 | 158.0 | 15.0 |
| Output_1_225 | 4260 | 89 | 3.2 | 0.02 | 6.85 | 0.05 | 10.65 | 0.16 | 10.37 | 0.18 | 50.0 | 210.0 | 158.0 | 11.0 | 153.0 | 15.0 | 158.0 | 12.0 |
| Output_1_61 18ATW-20 | 747 | 19 | 4.9 | 0.02 | 8.84 | 0.06 | 22.58 | 0.20 | 21.11 | 0.17 | 410.0 | 380.0 | 158.0 | 14.0 | 177.0 | 35.0 | 158.0 | 15.0 |
| Output_1_140 | 6520 | 271 | 3.1 | 0.02 | 5.22 | 0.05 | 8.50 | 0.17 | 7.60 | 0.02 | 180.0 | 170.0 | 158.2 | 7.9 | 159.0 | 12.0 | 158.2 | 9.5 |
| Output_1_66 | 2021 | 47 | 2.9 | 0.02 | 5.22 | 0.05 | 12.90 | 0.18 | 11.93 | 0.18 | 260.0 | 240.0 | 158.3 | 8.1 | 163.0 | 18.0 | 158.3 | 9.5 |
| Output_1_224 | 3780 | 82 | 1.9 | 0.02 | 4.82 | 0.05 | 10.59 | 0.18 | 10.00 | 0.17 | 260.0 | 210.0 | 158.5 | 7.6 | 169.0 | 16.0 | 158.5 | 9.1 |
| Output_1_113 | 9880 | 396 | 1.7 | 0.02 | 3.61 | 0.05 | 7.10 | 0.18 | 7.39 | 0.38 | 180.0 | 140.0 | 158.6 | 5.6 | 163.0 | 11.0 | 158.6 | 7.5 |
| Output_1_199 | 1341 | 23 | 4.3 | 0.02 | 6.02 | 0.05 | 16.85 | 0.17 | 18.18 | 0.27 | 70.0 | 290.0 | 158.7 | 9.7 | 151.0 | 26.0 | 158.7 | 11.0 |
| Output_1_240 | 2820 | 149 | 3.6 | 0.02 | 5.22 | 0.05 | 10.61 | 0.17 | 8.33 | 0.16 | 70.0 | 200.0 | 158.7 | 8.1 | 159.0 | 12.0 | 158.7 | 9.5 |
| Output_1_215 | 1261 | 61 | 3.8 | 0.03 | 5.60 | 0.05 | 18.14 | 0.16 | 17.61 | 0.03 | 100.0 | 340.0 | 158.8 | 9.0 | 151.0 | 25.0 | 158.8 | 10.0 |
| Output_1_77 | 5970 | 117 | 1.2 | 0.03 | 4.00 | 0.05 | 8.58 | 0.16 | 9.32 | 0.09 | 80.0 | 170.0 | 158.8 | 6.3 | 151.0 | 13.0 | 158.8 | 7.7 |
| Output_1_148 | 1070 | 45 | 4.2 | 0.02 | 7.23 | 0.05 | 19.79 | 0.16 | 20.13 | 0.10 | -60.0 | 360.0 | 159.0 | 11.0 | 144.0 | 28.0 | 159.0 | 12.0 |
| Output_1_80 | 5290 | 113 | 3.4 | 0.02 | 7.63 | 0.05 | 13.32 | 0.19 | 13.51 | 0.31 | 220.0 | 260.0 | 159.0 | 12.0 | 174.0 | 20.0 | 159.0 | 13.0 |
| Output_1_217 | 7110 | 263 | 1.4 | 0.03 | 4.00 | 0.05 | 7.50 | 0.17 | 6.94 | 0.32 | 240.0 | 160.0 | 159.3 | 6.3 | 162.0 | 11.0 | 159.3 | 8.1 |
| Output_1_241 | 3020 | 178 | 1.9 | 0.03 | 5.98 | 0.05 | 11.76 | 0.16 | 11.04 | 0.22 | 140.0 | 230.0 | 159.7 | 9.7 | 154.0 | 15.0 | 159.7 | 11.0 |
| Output_1_124 | 5130 | 612 | 1.4 | 0.03 | 3.98 | 0.05 | 8.15 | 0.17 | 8.09 | 0.21 | 140.0 | 160.0 | 160.0 | 6.4 | 162.0 | 12.0 | 160.0 | 8.2 |
| Output_1_216 | 1532 | 67 | 4.9 | 0.03 | 6.75 | 0.05 | 15.67 | 0.17 | 15.20 | 0.52 | 30.0 | 270.0 | 160.0 | 10.0 | 157.0 | 22.0 | 160.0 | 12.0 |
| Output_1_056 | 1098 | 20 | 2.2 | 0.03 | 5.60 | 0.05 | 17.98 | 0.17 | 17.96 | 0.04 | -20.0 | 300.0 | 160.1 | 8.3 | 152.0 | 25.0 | 160.1 | 9.7 |
| Output_1_146 | 1423 | 59 | 2.9 | 0.03 | 5.95 | 0.05 | 16.97 | 0.19 | 17.20 | 0.11 | 180.0 | 340.0 | 160.2 | 9.4 | 169.0 | 27.0 | 160.2 | 11.0 |
| Output_1_155 | 52300 | 2310 | 0.9 | 0.03 | 3.61 | 0.05 | 3.04 | 0.17 | 3.88 | 0.66 | 156.0 | 67.0 | 160.3 | 5.7 | 162.5 | 5.9 | 160.3 | 7.6 |

| | | | | | | | | | | | | | | | | | | |
|---|---|---|---|---|---|---|---|---|---|---|---|---|---|---|---|---|---|---|
| Output_1_186 | 1400 | 70 | 5.5 | 0.03 | 5.95 | 0.05 | 17.56 | 0.18 | 18.58 | 0.32 | 250.0 | 330.0 | 160.3 | 9.5 | 170.0 | 30.0 | 160.3 | 11.0 |
| Output_1_182 | 4220 | 95 | 3.1 | 0.03 | 5.56 | 0.05 | 11.45 | 0.17 | 10.53 | 0.00 | 170.0 | 240.0 | 160.4 | 9.1 | 159.0 | 15.0 | 160.4 | 10.0 |
| Output_1_220 | 3930 | 106 | 2.2 | 0.03 | 5.56 | 0.05 | 11.75 | 0.19 | 11.29 | 0.25 | 340.0 | 240.0 | 160.4 | 9.0 | 175.0 | 17.0 | 160.4 | 10.0 |
| Output_1_171 | 748 | 9 | 4.0 | 0.03 | 8.70 | 0.05 | 22.64 | 0.20 | 21.11 | 0.22 | 400.0 | 380.0 | 161.0 | 14.0 | 183.0 | 34.0 | 161.0 | 14.0 |
| Output_1_185 | 2350 | 94 | 3.3 | 0.03 | 6.75 | 0.05 | 14.86 | 0.19 | 15.14 | 0.24 | 290.0 | 290.0 | 161.0 | 11.0 | 170.0 | 23.0 | 161.0 | 12.0 |
| Output_1_210 | 6250 | 548 | 2.3 | 0.03 | 6.30 | 0.05 | 9.20 | 0.18 | 9.55 | 0.38 | 150.0 | 190.0 | 161.0 | 10.0 | 166.0 | 14.0 | 161.0 | 11.0 |
| Output_1_153 | 11700 | 533 | 2.5 | 0.03 | 3.94 | 0.05 | 5.74 | 0.18 | 6.78 | 0.47 | 280.0 | 120.0 | 161.4 | 6.5 | 165.0 | 10.0 | 161.4 | 8.2 |
| Output_1_231 | 4060 | 99 | 2.2 | 0.03 | 4.72 | 0.05 | 8.84 | 0.18 | 8.84 | 0.27 | 230.0 | 180.0 | 161.5 | 7.6 | 167.0 | 14.0 | 161.5 | 9.4 |
| Output_1_101 | 2480 | 55 | 2.4 | 0.03 | 5.91 | 0.05 | 12.30 | 0.17 | 11.98 | 0.24 | 140.0 | 230.0 | 161.6 | 9.2 | 155.0 | 17.0 | 161.6 | 10.0 |
| Output_1_206 | 5910 | 205 | 2.1 | 0.03 | 5.51 | 0.05 | 11.09 | 0.18 | 12.09 | 0.22 | 200.0 | 210.0 | 161.6 | 9.0 | 168.0 | 19.0 | 161.6 | 10.0 |
| Output_1_65 | 4770 | 113 | 3.3 | 0.03 | 5.91 | 0.05 | 8.47 | 0.18 | 8.89 | 0.26 | 190.0 | 190.0 | 161.6 | 9.2 | 169.0 | 13.0 | 161.6 | 10.0 |
| Output_1_105 | 4650 | 107 | 3.1 | 0.03 | 5.51 | 0.05 | 11.31 | 0.17 | 11.70 | 0.55 | 80.0 | 220.0 | 161.9 | 8.8 | 158.0 | 17.0 | 161.9 | 11.0 |
| Output_1_138 | 5910 | 255 | 4.5 | 0.03 | 4.71 | 0.05 | 10.02 | 0.18 | 8.89 | 0.08 | 310.0 | 210.0 | 162.0 | 7.5 | 167.0 | 14.0 | 162.0 | 9.1 |
| Output_1_213 | 2162 | 140 | 5.9 | 0.03 | 6.27 | 0.05 | 11.94 | 0.18 | 11.60 | 0.28 | 220.0 | 240.0 | 162.0 | 10.0 | 167.0 | 18.0 | 162.0 | 11.0 |
| Output_1_92 | 2290 | 88 | 2.6 | 0.03 | 4.71 | 0.05 | 15.40 | 0.19 | 15.87 | 0.14 | 180.0 | 310.0 | 162.3 | 7.6 | 171.0 | 25.0 | 162.3 | 9.2 |
| Output_1_135 | 2430 | 117 | 2.0 | 0.03 | 4.71 | 0.05 | 11.11 | 0.18 | 9.78 | 0.02 | 230.0 | 230.0 | 162.4 | 7.3 | 170.0 | 15.0 | 162.4 | 8.9 |
| Output_1_226 | 3820 | 81 | 5.3 | 0.03 | 5.10 | 0.05 | 12.71 | 0.18 | 11.80 | 0.06 | 330.0 | 240.0 | 162.4 | 8.4 | 167.0 | 17.0 | 162.4 | 9.9 |
| Output_1_102 | 1880 | 42 | 3.2 | 0.03 | 5.86 | 0.05 | 16.86 | 0.18 | 17.88 | 0.41 | 120.0 | 320.0 | 162.7 | 9.1 | 163.0 | 27.0 | 162.7 | 10.0 |
| Output_1_204 | 3250 | 82 | 3.7 | 0.03 | 5.08 | 0.05 | 12.17 | 0.18 | 12.99 | 0.36 | 190.0 | 230.0 | 162.7 | 8.2 | 163.0 | 19.0 | 162.7 | 9.8 |
| Output_1_104 | 2850 | 64 | 1.5 | 0.03 | 4.69 | 0.05 | 12.43 | 0.18 | 12.57 | 0.26 | 270.0 | 240.0 | 162.9 | 7.6 | 171.0 | 19.0 | 162.9 | 9.1 |
| Output_1_178 | 3370 | 42 | 2.5 | 0.03 | 7.42 | 0.05 | 15.35 | 0.17 | 14.45 | 0.25 | 180.0 | 300.0 | 163.0 | 12.0 | 160.0 | 21.0 | 163.0 | 13.0 |
| Output_1_238 | 3530 | 166 | 2.6 | 0.03 | 7.78 | 0.05 | 10.35 | 0.19 | 10.58 | 0.34 | 210.0 | 210.0 | 163.0 | 12.0 | 174.0 | 17.0 | 163.0 | 13.0 |
| Output_1_90 | 4350 | 183 | 2.2 | 0.03 | 8.20 | 0.05 | 12.02 | 0.18 | 12.92 | 0.36 | 250.0 | 210.0 | 163.0 | 13.0 | 166.0 | 19.0 | 163.0 | 14.0 |
| Output_1_157 | 3830 | 156 | 2.9 | 0.03 | 5.86 | 0.05 | 10.19 | 0.20 | 12.56 | 0.06 | 410.0 | 160.0 | 163.1 | 9.3 | 182.0 | 21.0 | 163.1 | 12.0 |
| Output_1_209 | 5280 | 478 | 2.9 | 0.03 | 4.67 | 0.05 | 9.86 | 0.18 | 10.06 | 0.23 | 210.0 | 200.0 | 163.3 | 7.7 | 169.0 | 16.0 | 163.3 | 9.3 |
| Output_1_110 | 7070 | 210 | 2.3 | 0.03 | 3.89 | 0.05 | 6.90 | 0.19 | 8.51 | 0.53 | 330.0 | 150.0 | 163.4 | 6.5 | 174.0 | 13.0 | 163.4 | 8.3 |
| Output_1_158 | 5260 | 196 | 2.4 | 0.03 | 4.67 | 0.05 | 9.90 | 0.18 | 10.99 | 0.58 | 80.0 | 190.0 | 163.4 | 7.4 | 167.0 | 17.0 | 163.4 | 9.3 |
| Output_1_189 | 9580 | 677 | 3.1 | 0.03 | 4.31 | 0.05 | 6.48 | 0.17 | 7.51 | 0.46 | 150.0 | 140.0 | 163.5 | 7.3 | 162.0 | 11.0 | 163.5 | 8.8 |
| Output_1_193 | 3050 | 99 | 4.7 | 0.03 | 6.23 | 0.05 | 10.36 | 0.18 | 9.94 | 0.41 | 270.0 | 210.0 | 163.5 | 9.9 | 167.0 | 15.0 | 163.5 | 11.0 |
| Output_1_212 | 3010 | 216 | 2.2 | 0.03 | 5.06 | 0.05 | 9.25 | 0.19 | 9.14 | 0.10 | 250.0 | 190.0 | 163.5 | 8.1 | 172.0 | 14.0 | 163.5 | 9.6 |
| Output_1_191 | 6250 | 309 | 2.6 | 0.03 | 5.84 | 0.05 | 6.49 | 0.18 | 6.78 | 0.17 | 130.0 | 130.0 | 163.7 | 9.3 | 165.0 | 10.0 | 163.7 | 11.0 |
| Output_1_126 | 4090 | 445 | 1.9 | 0.03 | 4.67 | 0.05 | 12.18 | 0.17 | 12.43 | 0.60 | 40.0 | 220.0 | 163.8 | 7.6 | 156.0 | 18.0 | 163.8 | 9.2 |
| Output_1_245 | 2051 | 136 | 2.5 | 0.03 | 6.59 | 0.05 | 10.44 | 0.19 | 11.89 | 0.36 | 400.0 | 230.0 | 164.0 | 10.0 | 174.0 | 18.0 | 164.0 | 12.0 |
| Output_1_200 | 21510 | 360 | 3.2 | 0.03 | 4.25 | 0.05 | 5.41 | 0.18 | 4.75 | 0.34 | 290.0 | 110.0 | 164.6 | 6.7 | 168.8 | 7.4 | 164.6 | 8.5 |
| Output_1_107 | 1965 | 48 | 2.6 | 0.03 | 5.79 | 0.06 | 12.43 | 0.19 | 12.77 | 0.20 | 340.0 | 250.0 | 164.9 | 9.7 | 175.0 | 21.0 | 164.9 | 11.0 |
| Output_1_168 | 6560 | 86 | 3.1 | 0.03 | 8.08 | 0.06 | 13.58 | 0.21 | 17.37 | 0.31 | 540.0 | 310.0 | 165.0 | 13.0 | 195.0 | 31.0 | 165.0 | 14.0 |
| Output_1_235 | 6880 | 239 | 2.5 | 0.03 | 5.00 | 0.05 | 8.43 | 0.18 | 8.38 | 0.41 | 130.0 | 170.0 | 165.5 | 8.4 | 166.0 | 13.0 | 165.5 | 10.0 |
| Output_1_152 | 5590 | 246 | 2.3 | 0.03 | 5.36 | 0.05 | 7.97 | 0.18 | 8.89 | 0.43 | 150.0 | 160.0 | 165.8 | 9.0 | 167.0 | 14.0 | 165.8 | 10.0 |
| Output_1_232 | 28500 | 722 | 1.0 | 0.03 | 7.66 | 0.05 | 6.46 | 0.19 | 8.95 | 0.61 | 350.0 | 150.0 | 166.0 | 12.0 | 180.0 | 14.0 | 166.0 | 13.0 |
| Output_1_154 | 3470 | 153 | 2.4 | 0.03 | 5.36 | 0.05 | 10.95 | 0.17 | 11.76 | 0.35 | 120.0 | 210.0 | 166.3 | 8.9 | 158.0 | 17.0 | 166.3 | 10.0 |

| | | | | | | | | | | | | | | | | | | |
|---|---|---|---|---|---|---|---|---|---|---|---|---|---|---|---|---|---|---|
| Output_1_88 | 11680 | 456 | 2.7 | 0.03 | 3.58 | 0.05 | 6.22 | 0.18 | 5.98 | 0.15 | 200.0 | 140.0 | 166.9 | 5.9 | 172.4 | 9.0 | 166.9 | 7.9 |
| Output_1_207 | 1730 | 73 | 3.1 | 0.03 | 6.87 | 0.05 | 26.09 | 0.16 | 26.54 | 0.54 | -150.0 | 450.0 | 167.0 | 11.0 | 145.0 | 38.0 | 167.0 | 12.0 |
| Output_1_86 | 10460 | 351 | 3.3 | 0.03 | 4.56 | 0.05 | 6.22 | 0.18 | 7.91 | 0.64 | 150.0 | 130.0 | 167.0 | 7.5 | 165.0 | 12.0 | 167.0 | 9.1 |
| Output_1_221 | 8250 | 201 | 4.5 | 0.03 | 4.18 | 0.05 | 6.28 | 0.18 | 6.08 | 0.28 | 170.0 | 140.0 | 167.6 | 7.0 | 168.3 | 9.8 | 167.6 | 8.8 |
| Output_1_244 | 6780 | 443 | 2.1 | 0.03 | 4.58 | 0.05 | 9.72 | 0.18 | 10.50 | 0.46 | 120.0 | 200.0 | 167.7 | 7.0 | 167.0 | 16.0 | 167.7 | 8.9 |
| Output_1_70 | 6800 | 135 | 2.5 | 0.03 | 4.92 | 0.05 | 8.38 | 0.18 | 9.24 | 0.46 | 150.0 | 170.0 | 167.7 | 7.8 | 172.0 | 15.0 | 167.7 | 9.5 |
| Output_1_139 | 3140 | 122 | 2.8 | 0.03 | 6.06 | 0.05 | 13.45 | 0.18 | 13.07 | 0.02 | 80.0 | 260.0 | 168.0 | 10.0 | 162.0 | 19.0 | 168.0 | 11.0 |
| Output_1_175 | 6930 | 75 | 1.7 | 0.03 | 5.30 | 0.05 | 8.72 | 0.19 | 8.11 | 0.13 | 220.0 | 180.0 | 168.1 | 8.8 | 172.0 | 13.0 | 168.1 | 10.0 |
| Output_1_74 | 4160 | 76 | 3.9 | 0.03 | 7.12 | 0.05 | 11.73 | 0.20 | 14.29 | 0.42 | 270.0 | 250.0 | 170.0 | 12.0 | 179.0 | 24.0 | 170.0 | 13.0 |
| Output_1_149 | 10590 | 419 | 1.7 | 0.03 | 3.73 | 0.05 | 5.80 | 0.19 | 6.84 | 0.39 | 230.0 | 120.0 | 170.2 | 6.3 | 175.0 | 11.0 | 170.2 | 8.3 |
| Output_1_242 | 6930 | 439 | 1.7 | 0.03 | 5.22 | 0.05 | 10.82 | 0.19 | 12.37 | 0.47 | 240.0 | 220.0 | 170.5 | 8.7 | 178.0 | 20.0 | 170.5 | 10.0 |
| Output_1_150 | 12300 | 503 | 2.5 | 0.03 | 5.19 | 0.05 | 6.15 | 0.19 | 6.28 | 0.59 | 180.0 | 130.0 | 171.5 | 8.7 | 177.0 | 10.0 | 171.5 | 10.0 |
| Output_1_163 | 4140 | 80 | 2.2 | 0.03 | 5.19 | 0.05 | 11.21 | 0.21 | 9.71 | 0.06 | 330.0 | 210.0 | 171.9 | 8.8 | 188.0 | 17.0 | 171.9 | 11.0 |
| Output_1_114 | 1256 | 55 | 1.2 | 0.03 | 7.38 | 0.06 | 16.75 | 0.21 | 16.43 | 0.16 | 490.0 | 380.0 | 172.0 | 13.0 | 193.0 | 30.0 | 172.0 | 14.0 |
| Output_1_174 | 6170 | 66 | 1.8 | 0.03 | 6.67 | 0.05 | 8.79 | 0.18 | 9.24 | 0.34 | 150.0 | 170.0 | 172.0 | 11.0 | 175.0 | 14.0 | 172.0 | 12.0 |
| Output_1_78 | 42200 | 751 | 3.9 | 0.03 | 4.76 | 0.05 | 4.12 | 0.19 | 4.11 | 0.52 | 217.0 | 90.0 | 173.3 | 8.3 | 174.2 | 6.6 | 173.3 | 9.9 |
| Output_1_228 | 6910 | 143 | 3.0 | 0.03 | 5.86 | 0.05 | 8.78 | 0.18 | 8.15 | 0.45 | 100.0 | 170.0 | 173.4 | 9.9 | 171.0 | 13.0 | 173.4 | 11.0 |
| Output_1_75 | 9990 | 178 | 4.3 | 0.03 | 5.47 | 0.05 | 6.86 | 0.19 | 6.49 | 0.34 | 200.0 | 140.0 | 174.4 | 9.6 | 172.0 | 10.0 | 174.4 | 11.0 |
| Output_1_173 | 5260 | 53 | 2.5 | 0.03 | 5.43 | 0.05 | 8.15 | 0.19 | 9.52 | 0.45 | 180.0 | 170.0 | 175.3 | 9.2 | 177.0 | 15.0 | 175.3 | 11.0 |
| Output_1_229 | 2170 | 48 | 4.3 | 0.03 | 7.97 | 0.05 | 12.84 | 0.18 | 12.09 | 0.29 | 220.0 | 270.0 | 176.0 | 14.0 | 172.0 | 20.0 | 176.0 | 15.0 |
| Output_1_147 | 4650 | 175 | 2.7 | 0.03 | 5.40 | 0.05 | 10.23 | 0.19 | 9.28 | 0.19 | 240.0 | 210.0 | 176.6 | 9.1 | 178.0 | 15.0 | 176.6 | 11.0 |
| Output_1_165 | 5640 | 92 | 3.3 | 0.03 | 7.14 | 0.06 | 14.95 | 0.21 | 15.96 | 0.49 | 330.0 | 320.0 | 178.0 | 13.0 | 194.0 | 29.0 | 178.0 | 14.0 |
| Output_1_141 | 96200 | 3440 | 1.2 | 0.03 | 4.24 | 0.05 | 6.43 | 0.21 | 5.34 | 0.12 | 204.0 | 72.0 | 180.1 | 7.3 | 189.4 | 8.9 | 180.1 | 10.0 |
| Output_1_161 | 6540 | 152 | 2.8 | 0.03 | 4.23 | 0.05 | 6.33 | 0.20 | 7.88 | 0.56 | 250.0 | 140.0 | 180.4 | 7.5 | 187.0 | 13.0 | 180.4 | 9.4 |
| Output_1_93 | 4510 | 155 | 2.5 | 0.03 | 6.32 | 0.05 | 13.06 | 0.21 | 12.68 | 0.23 | 40.0 | 250.0 | 181.0 | 11.0 | 186.0 | 22.0 | 181.0 | 13.0 |
| Output_1_119 | 6840 | 457 | 2.4 | 0.03 | 5.26 | 0.05 | 8.18 | 0.20 | 8.37 | 0.38 | 130.0 | 160.0 | 181.2 | 9.5 | 186.0 | 14.0 | 181.2 | 12.0 |
| Output_1_205 | 2050 | 54 | 2.6 | 0.03 | 8.74 | 0.06 | 20.63 | 0.24 | 19.58 | 0.04 | 690.0 | 380.0 | 182.0 | 15.0 | 215.0 | 39.0 | 182.0 | 16.0 |
| Output_1_103 | 10340 | 205 | 1.4 | 0.03 | 3.23 | 0.05 | 6.63 | 0.21 | 6.80 | 0.38 | 260.0 | 140.0 | 182.7 | 5.8 | 190.0 | 12.0 | 182.7 | 8.2 |
| Output_1_64 | 4520 | 93 | 2.4 | 0.03 | 6.25 | 0.05 | 10.98 | 0.20 | 9.69 | 0.16 | 80.0 | 210.0 | 183.0 | 11.0 | 180.0 | 16.0 | 183.0 | 13.0 |
| Output_1_84 | 5890 | 135 | 2.2 | 0.03 | 6.94 | 0.06 | 18.18 | 0.22 | 18.81 | 0.26 | 330.0 | 340.0 | 183.0 | 13.0 | 197.0 | 34.0 | 183.0 | 15.0 |
| Output_1_91 | 3920 | 142 | 2.3 | 0.03 | 5.90 | 0.05 | 11.66 | 0.21 | 10.10 | 0.49 | 200.0 | 190.0 | 183.0 | 11.0 | 194.0 | 19.0 | 183.0 | 12.0 |
| Output_1_108 | 5340 | 123 | 1.9 | 0.03 | 4.84 | 0.05 | 7.39 | 0.20 | 7.14 | 0.24 | 150.0 | 150.0 | 183.5 | 8.7 | 181.0 | 12.0 | 183.5 | 10.0 |
| Output_1_187 | 3400 | 191 | 7.8 | 0.03 | 5.86 | 0.05 | 14.47 | 0.18 | 13.04 | 0.29 | -20.0 | 240.0 | 184.0 | 11.0 | 168.0 | 20.0 | 184.0 | 13.0 |
| Output_1_237 | 6700 | 258 | 1.9 | 0.03 | 6.21 | 0.05 | 13.70 | 0.22 | 14.93 | 0.44 | 390.0 | 260.0 | 184.0 | 11.0 | 209.0 | 24.0 | 184.0 | 13.0 |
| Output_1_94 | 5860 | 169 | 2.0 | 0.03 | 3.78 | 0.05 | 9.00 | 0.21 | 8.21 | 0.08 | 300.0 | 180.0 | 184.9 | 7.1 | 192.0 | 15.0 | 184.9 | 9.2 |
| Output_1_181 | 13840 | 246 | 2.7 | 0.03 | 5.84 | 0.05 | 6.07 | 0.20 | 7.00 | 0.50 | 250.0 | 130.0 | 185.0 | 10.0 | 185.0 | 11.0 | 185.0 | 12.0 |
| Output_1_131 | 3830 | 217 | 2.4 | 0.03 | 6.83 | 0.05 | 11.70 | 0.22 | 11.98 | 0.29 | 330.0 | 250.0 | 186.0 | 13.0 | 197.0 | 21.0 | 186.0 | 14.0 |
| Output_1_172 | 4400 | 43 | 3.1 | 0.03 | 5.80 | 0.05 | 9.70 | 0.19 | 10.82 | 0.23 | 130.0 | 200.0 | 186.0 | 10.0 | 184.0 | 18.0 | 186.0 | 12.0 |
| Output_1_055 | 6230 | 93 | 4.2 | 0.03 | 4.42 | 0.05 | 7.50 | 0.22 | 8.29 | 0.53 | 380.0 | 160.0 | 187.0 | 8.1 | 201.0 | 16.0 | 187.0 | 10.0 |
| Output_1_82 | 13120 | 259 | 4.0 | 0.03 | 4.07 | 0.05 | 6.37 | 0.20 | 6.50 | 0.39 | 140.0 | 130.0 | 187.3 | 7.8 | 184.0 | 11.0 | 187.3 | 9.7 |

| | | | | | | | | | | | | | | | | | | |
|---|---|---|---|---|---|---|---|---|---|---|---|---|---|---|---|---|---|---|
| Output_1_054 | 4780 | 69 | 3.8 | 0.03 | 8.78 | 0.05 | 11.17 | 0.23 | 9.91 | 0.34 | 400.0 | 250.0 | 188.0 | 16.0 | 211.0 | 19.0 | 188.0 | 17.0 |
| Output_1_100 | 10740 | 212 | 2.0 | 0.03 | 5.05 | 0.05 | 5.55 | 0.21 | 6.70 | 0.60 | 330.0 | 120.0 | 188.6 | 9.4 | 192.0 | 12.0 | 188.6 | 11.0 |
| Output_1_125 | 12240 | 1188 | 2.0 | 0.03 | 4.67 | 0.05 | 6.15 | 0.21 | 6.83 | 0.43 | 110.0 | 130.0 | 190.2 | 8.8 | 191.0 | 11.0 | 190.2 | 11.0 |
| Output_1_190 | 2350 | 121 | 2.6 | 0.03 | 4.33 | 0.05 | 14.47 | 0.22 | 12.95 | 0.43 | 190.0 | 280.0 | 190.6 | 8.4 | 201.0 | 24.0 | 190.6 | 10.0 |
| Output_1_123 | 5220 | 525 | 2.3 | 0.03 | 4.93 | 0.05 | 8.16 | 0.21 | 9.39 | 0.35 | 250.0 | 180.0 | 193.0 | 9.4 | 197.0 | 17.0 | 193.0 | 11.0 |
| Output_1_137 | 9190 | 334 | 2.4 | 0.03 | 4.89 | 0.05 | 7.51 | 0.21 | 7.66 | 0.44 | 130.0 | 160.0 | 195.1 | 9.2 | 191.0 | 13.0 | 195.1 | 11.0 |
| Output_1_188 | 17710 | 1098 | 2.0 | 0.03 | 3.56 | 0.05 | 6.11 | 0.21 | 5.21 | 0.31 | 290.0 | 130.0 | 196.2 | 6.6 | 194.2 | 9.0 | 196.2 | 9.0 |
| Output_1_136 | 24500 | 900 | 2.0 | 0.03 | 3.81 | 0.05 | 4.17 | 0.23 | 5.31 | 0.56 | 297.0 | 93.0 | 199.6 | 7.4 | 207.0 | 10.0 | 199.6 | 9.7 |
| Output_1_239 | 26180 | 1050 | 3.3 | 0.03 | 4.44 | 0.05 | 4.77 | 0.22 | 5.41 | 0.63 | 270.0 | 110.0 | 199.9 | 8.6 | 205.0 | 11.0 | 199.9 | 11.0 |
| Output_1_98 | 44700 | 911 | 2.2 | 0.03 | 1.49 | 0.05 | 2.59 | 0.22 | 2.51 | 0.25 | 194.0 | 59.0 | 200.1 | 2.9 | 201.4 | 4.6 | 200.1 | 7.0 |
| Output_1_218 | 15580 | 392 | 2.2 | 0.03 | 5.99 | 0.06 | 5.09 | 0.23 | 8.62 | 0.63 | 390.0 | 110.0 | 201.0 | 12.0 | 211.0 | 16.0 | 201.0 | 13.0 |
| Output_1_127 | 35200 | 2830 | 0.9 | 0.03 | 2.62 | 0.05 | 3.56 | 0.22 | 3.52 | 0.32 | 236.0 | 79.0 | 205.4 | 5.3 | 205.5 | 6.5 | 205.4 | 8.4 |
| Output_1_159 | 7010 | 200 | 4.8 | 0.03 | 5.86 | 0.05 | 7.63 | 0.22 | 8.07 | 0.39 | 180.0 | 160.0 | 206.0 | 12.0 | 203.0 | 15.0 | 206.0 | 13.0 |

**Sample 18ATW23**

| | | | | | | | | | | | | | | | | | | |
|---|---|---|---|---|---|---|---|---|---|---|---|---|---|---|---|---|---|---|
| Output_1_127 | 642 | 35 | 3.3 | 0.02 | 8.11 | 0.05 | 29.17 | 0.15 | 25.85 | 0.14 | 170.0 | 470.0 | 141.0 | 11.0 | 134.0 | 34.0 | 141.0 | 11.0 |
| Output_1_65 | 2700 | 61 | 1.8 | 0.02 | 4.07 | 0.05 | 11.65 | 0.16 | 10.63 | 0.05 | 200.0 | 230.0 | 144.0 | 5.8 | 150.0 | 15.0 | 144.0 | 6.0 |
| Output_1_2 | 2750 | 142 | 2.8 | 0.02 | 5.24 | 0.04 | 17.10 | 0.14 | 16.90 | 0.07 | -50.0 | 300.0 | 146.2 | 7.5 | 133.0 | 22.0 | 146.2 | 7.6 |
| Output_1_17 | 1580 | 59 | 2.0 | 0.02 | 4.31 | 0.06 | 18.18 | 0.18 | 17.42 | 0.04 | 370.0 | 350.0 | 147.7 | 6.6 | 163.0 | 27.0 | 147.7 | 6.7 |
| Output_1_92 | 3050 | 100 | 2.4 | 0.02 | 3.66 | 0.06 | 10.61 | 0.17 | 9.25 | 0.04 | 400.0 | 220.0 | 148.1 | 5.4 | 161.0 | 14.0 | 148.1 | 5.5 |
| Output_1_80 | 6250 | 216 | 1.3 | 0.02 | 3.44 | 0.05 | 9.25 | 0.16 | 9.26 | 0.13 | 190.0 | 180.0 | 148.2 | 5.1 | 151.0 | 13.0 | 148.2 | 5.3 |
| Output_1_72 | 1334 | 30 | 1.5 | 0.02 | 6.01 | 0.06 | 21.05 | 0.17 | 20.00 | 0.11 | 350.0 | 390.0 | 148.5 | 8.9 | 161.0 | 31.0 | 148.5 | 9.0 |
| Output_1_25 | 1118 | 17 | 2.4 | 0.02 | 6.41 | 0.06 | 22.03 | 0.18 | 20.00 | 0.06 | 380.0 | 400.0 | 148.8 | 9.6 | 164.0 | 31.0 | 148.8 | 9.7 |
| Output_1_77 | 1940 | 55 | 2.5 | 0.02 | 5.98 | 0.06 | 17.82 | 0.18 | 15.22 | 0.36 | 430.0 | 340.0 | 148.8 | 8.6 | 169.0 | 24.0 | 148.8 | 8.8 |
| Output_1_7 | 1205 | 97 | 3.2 | 0.02 | 5.53 | 0.06 | 20.00 | 0.19 | 18.28 | 0.20 | 570.0 | 330.0 | 149.7 | 8.4 | 177.0 | 31.0 | 149.7 | 8.5 |
| Output_1_90 | 2620 | 96 | 2.8 | 0.02 | 6.78 | 0.05 | 18.82 | 0.17 | 16.17 | 0.16 | 300.0 | 360.0 | 150.0 | 10.0 | 155.0 | 23.0 | 150.0 | 10.0 |
| Output_1_132 | 2201 | 89 | 2.0 | 0.02 | 4.66 | 0.05 | 13.64 | 0.17 | 15.20 | 0.39 | 180.0 | 260.0 | 150.1 | 7.1 | 158.0 | 22.0 | 150.1 | 7.2 |
| Output_1_5 | 5260 | 389 | 2.7 | 0.02 | 3.65 | 0.05 | 11.20 | 0.17 | 10.78 | 0.10 | 250.0 | 230.0 | 150.1 | 5.4 | 159.0 | 15.0 | 150.1 | 5.6 |
| Output_1_43 | 3410 | 146 | 2.0 | 0.02 | 3.14 | 0.05 | 11.07 | 0.17 | 10.30 | 0.15 | 240.0 | 210.0 | 150.4 | 4.6 | 154.0 | 15.0 | 150.4 | 4.9 |
| Output_1_53 | 1350 | 53 | 2.1 | 0.02 | 5.93 | 0.05 | 17.80 | 0.18 | 16.85 | 0.05 | 450.0 | 320.0 | 150.6 | 9.0 | 164.0 | 26.0 | 150.6 | 9.1 |
| Output_1_45 | 2092 | 113 | 2.1 | 0.02 | 5.06 | 0.04 | 16.33 | 0.15 | 14.94 | 0.10 | -20.0 | 270.0 | 151.2 | 7.3 | 143.0 | 20.0 | 151.2 | 7.5 |
| Output_1_136 | 4540 | 115 | 3.9 | 0.02 | 3.40 | 0.05 | 9.62 | 0.17 | 8.82 | 0.02 | 250.0 | 190.0 | 151.9 | 5.1 | 159.0 | 13.0 | 151.9 | 5.3 |
| Output_1_10 | 3730 | 269 | 2.1 | 0.02 | 3.47 | 0.05 | 13.38 | 0.18 | 13.48 | 0.21 | 310.0 | 260.0 | 152.2 | 5.2 | 171.0 | 22.0 | 152.2 | 5.4 |
| Output_1_58 | 1598 | 47 | 1.8 | 0.02 | 6.25 | 0.06 | 16.95 | 0.19 | 17.46 | 0.07 | 390.0 | 330.0 | 152.5 | 9.6 | 173.0 | 28.0 | 152.5 | 9.7 |
| Output_1_139 | 4080 | 97 | 2.3 | 0.02 | 3.88 | 0.05 | 10.25 | 0.16 | 10.06 | 0.36 | 120.0 | 190.0 | 152.6 | 5.8 | 149.0 | 14.0 | 152.6 | 6.0 |
| Output_1_98 | 5370 | 167 | 2.8 | 0.02 | 3.67 | 0.05 | 9.39 | 0.16 | 9.20 | 0.11 | 140.0 | 180.0 | 152.6 | 5.5 | 152.0 | 13.0 | 152.6 | 5.7 |
| Output_1_41 | 1674 | 47 | 4.2 | 0.02 | 5.42 | 0.05 | 17.94 | 0.16 | 17.07 | 0.36 | 130.0 | 310.0 | 152.8 | 8.4 | 151.0 | 24.0 | 152.8 | 8.5 |
| Output_1_40 | 3850 | 93 | 2.0 | 0.02 | 3.79 | 0.05 | 11.63 | 0.16 | 11.73 | 0.04 | 100.0 | 220.0 | 153.1 | 5.7 | 151.0 | 17.0 | 153.1 | 5.9 |
| Output_1_138 | 17090 | 404 | 2.4 | 0.02 | 3.12 | 0.05 | 5.11 | 0.16 | 6.71 | 0.44 | 170.0 | 110.0 | 153.1 | 4.7 | 153.4 | 9.6 | 153.1 | 4.9 |
| Output_1_15 | 1794 | 78 | 3.9 | 0.02 | 6.67 | 0.05 | 17.01 | 0.18 | 16.02 | 0.09 | 350.0 | 310.0 | 153.1 | 9.9 | 171.0 | 24.0 | 153.1 | 10.0 |

| | | | | | | | | | | | | | | | | | | |
|---|---|---|---|---|---|---|---|---|---|---|---|---|---|---|---|---|---|---|
| Output_1_141 | 1065 | 23 | 1.8 | 0.02 | 5.81 | 0.06 | 23.64 | 0.16 | 21.74 | 0.21 | 170.0 | 380.0 | 153.5 | 8.8 | 154.0 | 32.0 | 153.5 | 8.9 |
| Output_1_126 | 1242 | 70 | 2.4 | 0.02 | 6.22 | 0.06 | 21.05 | 0.18 | 18.99 | 0.15 | 450.0 | 400.0 | 153.5 | 9.4 | 169.0 | 31.0 | 153.5 | 9.5 |
| Output_1_83 | 2056 | 82 | 2.8 | 0.02 | 4.15 | 0.05 | 12.52 | 0.18 | 13.64 | 0.24 | 200.0 | 250.0 | 153.6 | 6.5 | 163.0 | 21.0 | 153.6 | 6.7 |
| Output_1_140 | 2242 | 51 | 2.1 | 0.02 | 4.15 | 0.06 | 17.24 | 0.18 | 16.02 | 0.10 | 350.0 | 320.0 | 153.6 | 6.6 | 166.0 | 25.0 | 153.6 | 6.7 |
| Output_1_9 | 2697 | 205 | 1.7 | 0.02 | 4.15 | 0.06 | 15.73 | 0.18 | 16.20 | 0.21 | 310.0 | 300.0 | 153.7 | 6.4 | 165.0 | 24.0 | 153.7 | 6.6 |
| Output_1_99 | 5330 | 168 | 1.4 | 0.02 | 3.52 | 0.05 | 10.68 | 0.17 | 10.59 | 0.19 | 220.0 | 210.0 | 153.9 | 5.3 | 158.0 | 16.0 | 153.9 | 5.5 |
| Output_1_13 | 3400 | 175 | 2.9 | 0.02 | 3.64 | 0.05 | 10.90 | 0.16 | 10.19 | 0.09 | 110.0 | 190.0 | 154.0 | 5.5 | 147.0 | 14.0 | 154.0 | 5.7 |
| Output_1_30 | 3720 | 45 | 1.9 | 0.02 | 5.37 | 0.05 | 12.57 | 0.18 | 11.43 | 0.25 | 290.0 | 240.0 | 154.0 | 8.1 | 163.0 | 17.0 | 154.0 | 8.2 |
| Output_1_116 | 4980 | 372 | 2.9 | 0.02 | 2.94 | 0.05 | 10.93 | 0.18 | 9.50 | 0.15 | 300.0 | 210.0 | 154.0 | 4.5 | 166.0 | 15.0 | 154.0 | 4.7 |
| Output_1_81 | 2970 | 105 | 3.0 | 0.02 | 3.68 | 0.05 | 13.25 | 0.18 | 11.43 | 0.16 | 220.0 | 240.0 | 154.2 | 5.6 | 162.0 | 18.0 | 154.2 | 5.8 |
| Output_1_145 | 7130 | 164 | 2.5 | 0.02 | 3.70 | 0.05 | 6.97 | 0.17 | 6.94 | 0.21 | 220.0 | 150.0 | 155.0 | 5.6 | 163.9 | 9.6 | 155.0 | 5.8 |
| Output_1_109 | 10710 | 746 | 1.5 | 0.02 | 9.47 | 0.05 | 6.82 | 0.18 | 12.85 | 0.80 | 290.0 | 160.0 | 155.0 | 14.0 | 167.0 | 19.0 | 155.0 | 15.0 |
| Output_1_20 | 4000 | 114 | 1.4 | 0.02 | 3.67 | 0.05 | 10.18 | 0.17 | 8.38 | 0.22 | 140.0 | 190.0 | 156.3 | 5.7 | 157.0 | 12.0 | 156.3 | 5.9 |
| Output_1_148 | 4180 | 102 | 1.6 | 0.02 | 4.49 | 0.06 | 10.45 | 0.18 | 9.34 | 0.22 | 390.0 | 220.0 | 156.3 | 6.6 | 169.0 | 14.0 | 156.3 | 6.8 |
| Output_1_59 | 2790 | 75 | 2.2 | 0.02 | 4.47 | 0.05 | 14.49 | 0.18 | 13.14 | 0.13 | 210.0 | 250.0 | 156.4 | 6.9 | 162.0 | 20.0 | 156.4 | 7.1 |
| Output_1_21 | 5430 | 138 | 1.5 | 0.02 | 2.93 | 0.05 | 8.03 | 0.17 | 7.51 | 0.07 | 290.0 | 170.0 | 156.4 | 4.5 | 161.0 | 11.0 | 156.4 | 4.8 |
| Output_1_78 | 3230 | 93 | 2.4 | 0.02 | 3.98 | 0.05 | 10.50 | 0.19 | 11.89 | 0.14 | 210.0 | 180.0 | 156.9 | 6.2 | 170.0 | 19.0 | 156.9 | 6.4 |
| Output_1_101 | 1108 | 57 | 2.9 | 0.02 | 6.88 | 0.05 | 19.23 | 0.18 | 18.75 | 0.08 | 210.0 | 340.0 | 157.0 | 11.0 | 167.0 | 29.0 | 157.0 | 11.0 |
| Output_1_124 | 1652 | 100 | 1.9 | 0.02 | 6.05 | 0.05 | 17.84 | 0.18 | 18.13 | 0.04 | 190.0 | 320.0 | 157.6 | 9.1 | 166.0 | 28.0 | 157.6 | 9.2 |
| Output_1_46 | 3690 | 203 | 1.6 | 0.02 | 3.92 | 0.05 | 11.95 | 0.18 | 11.11 | 0.05 | 310.0 | 230.0 | 157.7 | 6.1 | 166.0 | 17.0 | 157.7 | 6.3 |
| Output_1_115 | 4400 | 326 | 2.0 | 0.02 | 4.84 | 0.05 | 10.58 | 0.18 | 10.33 | 0.30 | 340.0 | 210.0 | 157.7 | 7.6 | 170.0 | 16.0 | 157.7 | 7.8 |
| Output_1_93 | 1494 | 46 | 3.4 | 0.02 | 6.05 | 0.05 | 17.03 | 0.18 | 15.08 | 0.06 | 340.0 | 320.0 | 157.8 | 9.5 | 169.0 | 22.0 | 157.8 | 9.6 |
| Output_1_143 | 3700 | 81 | 3.5 | 0.02 | 3.38 | 0.06 | 11.55 | 0.19 | 10.53 | 0.13 | 380.0 | 230.0 | 158.4 | 5.3 | 175.0 | 17.0 | 158.4 | 5.5 |
| Output_1_137 | 4170 | 100 | 2.6 | 0.02 | 4.82 | 0.05 | 11.07 | 0.17 | 10.34 | 0.14 | 250.0 | 220.0 | 158.6 | 7.7 | 164.0 | 15.0 | 158.6 | 7.8 |
| Output_1_28 | 8250 | 101 | 1.5 | 0.02 | 2.65 | 0.05 | 8.46 | 0.17 | 8.62 | 0.02 | 210.0 | 170.0 | 158.7 | 4.2 | 162.0 | 13.0 | 158.7 | 4.5 |
| Output_1_1 | 3980 | 157 | 2.8 | 0.02 | 4.02 | 0.04 | 9.80 | 0.17 | 11.52 | 0.20 | 20.0 | 190.0 | 158.8 | 6.3 | 154.0 | 17.0 | 158.8 | 6.5 |
| Output_1_39 | 2860 | 61 | 2.9 | 0.03 | 4.40 | 0.05 | 11.66 | 0.18 | 12.09 | 0.27 | 320.0 | 220.0 | 158.9 | 6.9 | 175.0 | 19.0 | 158.9 | 7.1 |
| Output_1_142 | 2120 | 45 | 1.9 | 0.03 | 4.80 | 0.05 | 17.13 | 0.18 | 16.48 | 0.13 | 290.0 | 320.0 | 159.1 | 7.2 | 162.0 | 25.0 | 159.1 | 7.4 |
| Output_1_95 | 14940 | 437 | 1.8 | 0.03 | 3.07 | 0.05 | 9.27 | 0.18 | 10.06 | 0.38 | 220.0 | 200.0 | 159.7 | 4.8 | 167.0 | 16.0 | 159.7 | 5.1 |
| Output_1_100 | 849 | 42 | 3.2 | 0.02 | 7.29 | 0.06 | 25.42 | 0.21 | 25.48 | 0.12 | 400.0 | 470.0 | 160.0 | 12.0 | 191.0 | 46.0 | 160.0 | 12.0 |
| Output_1_85 | 1648 | 65 | 2.1 | 0.03 | 6.35 | 0.06 | 14.90 | 0.20 | 14.14 | 0.14 | 440.0 | 300.0 | 160.0 | 10.0 | 181.0 | 24.0 | 160.0 | 10.0 |
| Output_1_89 | 1440 | 51 | 2.7 | 0.03 | 9.52 | 0.06 | 20.00 | 0.20 | 19.40 | 0.07 | 490.0 | 400.0 | 160.0 | 15.0 | 183.0 | 33.0 | 160.0 | 15.0 |
| Output_1_42 | 1810 | 65 | 1.8 | 0.03 | 5.56 | 0.05 | 15.89 | 0.19 | 14.97 | 0.04 | 270.0 | 300.0 | 160.2 | 8.7 | 176.0 | 23.0 | 160.2 | 8.8 |
| Output_1_113 | 100800 | 7200 | 3.5 | 0.03 | 2.30 | 0.05 | 2.56 | 0.18 | 2.88 | 0.79 | 223.0 | 55.0 | 160.4 | 3.7 | 165.4 | 4.4 | 160.4 | 4.0 |
| Output_1_75 | 3010 | 70 | 2.5 | 0.03 | 5.53 | 0.05 | 13.71 | 0.19 | 14.44 | 0.41 | 340.0 | 280.0 | 160.8 | 9.1 | 173.0 | 24.0 | 160.8 | 9.2 |
| Output_1_69 | 2048 | 39 | 1.5 | 0.03 | 5.53 | 0.05 | 20.00 | 0.19 | 20.00 | 0.06 | 250.0 | 400.0 | 160.9 | 8.7 | 169.0 | 32.0 | 160.9 | 8.8 |
| Output_1_94 | 2070 | 62 | 3.3 | 0.03 | 4.74 | 0.04 | 17.50 | 0.16 | 17.61 | 0.19 | 10.0 | 300.0 | 161.3 | 7.8 | 151.0 | 25.0 | 161.3 | 7.9 |
| Output_1_47 | 866 | 44 | 2.5 | 0.03 | 5.91 | 0.05 | 28.26 | 0.16 | 28.57 | 0.04 | -50.0 | 430.0 | 161.4 | 9.4 | 144.0 | 39.0 | 161.4 | 9.6 |
| Output_1_104 | 3120 | 172 | 2.2 | 0.03 | 3.27 | 0.05 | 9.88 | 0.17 | 9.83 | 0.49 | 230.0 | 190.0 | 161.7 | 5.2 | 161.0 | 15.0 | 161.7 | 5.4 |
| Output_1_66 | 848 | 17 | 2.8 | 0.03 | 5.49 | 0.06 | 24.59 | 0.20 | 25.00 | 0.10 | 470.0 | 450.0 | 162.5 | 9.0 | 178.0 | 41.0 | 162.5 | 9.1 |

| | | | | | | | | | | | | | | | | | | |
|---|---|---|---|---|---|---|---|---|---|---|---|---|---|---|---|---|---|---|
| Output_1_55 | 951 | 29 | 2.7 | 0.03 | 5.47 | 0.05 | 24.44 | 0.16 | 22.98 | 0.08 | -30.0 | 400.0 | 163.0 | 9.0 | 146.0 | 33.0 | 163.0 | 9.1 |
| Output_1_102 | 3990 | 202 | 3.3 | 0.03 | 3.91 | 0.05 | 11.21 | 0.19 | 10.27 | 0.05 | 350.0 | 210.0 | 163.1 | 6.3 | 174.0 | 17.0 | 163.1 | 6.5 |
| Output_1_67 | 4080 | 76 | 2.0 | 0.03 | 3.57 | 0.05 | 11.32 | 0.16 | 10.98 | 0.10 | 40.0 | 200.0 | 163.8 | 5.8 | 153.0 | 16.0 | 163.8 | 6.0 |
| Output_1_26 | 2603 | 34 | 2.7 | 0.03 | 3.88 | 0.05 | 14.34 | 0.18 | 14.29 | 0.04 | 160.0 | 260.0 | 164.0 | 6.5 | 168.0 | 22.0 | 164.0 | 6.7 |
| Output_1_131 | 3178 | 120 | 4.3 | 0.03 | 3.82 | 0.05 | 12.92 | 0.18 | 12.64 | 0.10 | 230.0 | 250.0 | 166.4 | 6.5 | 171.0 | 20.0 | 166.4 | 6.7 |
| Output_1_135 | 3650 | 86 | 1.4 | 0.03 | 3.77 | 0.05 | 13.09 | 0.18 | 13.56 | 0.34 | 60.0 | 230.0 | 168.6 | 6.4 | 163.0 | 21.0 | 168.6 | 6.6 |
| Output_1_79 | 4060 | 116 | 3.1 | 0.03 | 3.53 | 0.05 | 12.63 | 0.18 | 13.11 | 0.14 | 100.0 | 230.0 | 169.6 | 5.9 | 168.0 | 20.0 | 169.6 | 6.1 |
| Output_1_123 | 5600 | 323 | 2.4 | 0.03 | 4.49 | 0.05 | 11.33 | 0.19 | 10.70 | 0.06 | 170.0 | 220.0 | 170.0 | 7.7 | 173.0 | 17.0 | 170.0 | 7.8 |
| Output_1_111 | 3480 | 221 | 2.7 | 0.03 | 3.48 | 0.05 | 13.72 | 0.19 | 11.92 | 0.26 | 210.0 | 250.0 | 173.4 | 5.9 | 177.0 | 20.0 | 173.4 | 6.2 |
| Output_1_125 | 6220 | 318 | 3.8 | 0.03 | 4.03 | 0.05 | 9.03 | 0.18 | 7.73 | 0.02 | 150.0 | 180.0 | 173.5 | 7.0 | 168.0 | 12.0 | 173.5 | 7.2 |
| Output_1_91 | 4630 | 133 | 3.1 | 0.03 | 3.20 | 0.05 | 7.29 | 0.21 | 7.80 | 0.42 | 360.0 | 150.0 | 174.9 | 5.5 | 191.0 | 13.0 | 174.9 | 5.8 |
| Output_1_38 | 5760 | 91 | 2.0 | 0.03 | 3.58 | 0.05 | 7.88 | 0.20 | 9.23 | 0.44 | 260.0 | 160.0 | 177.4 | 6.4 | 182.0 | 15.0 | 177.4 | 6.6 |
| Output_1_27 | 14580 | 168 | 2.7 | 0.03 | 2.03 | 0.05 | 4.86 | 0.19 | 4.84 | 0.11 | 180.0 | 110.0 | 178.7 | 3.6 | 180.0 | 8.0 | 178.7 | 4.0 |
| Output_1_112 | 16870 | 1054 | 1.8 | 0.03 | 2.48 | 0.05 | 6.33 | 0.20 | 6.50 | 0.39 | 270.0 | 130.0 | 179.4 | 4.4 | 185.0 | 11.0 | 179.4 | 4.7 |
| Output_1_108 | 2310 | 135 | 2.9 | 0.03 | 4.61 | 0.05 | 13.13 | 0.21 | 13.68 | 0.11 | 380.0 | 250.0 | 179.4 | 8.0 | 192.0 | 24.0 | 179.4 | 8.2 |
| Output_1_144 | 10990 | 211 | 2.5 | 0.03 | 3.15 | 0.05 | 8.96 | 0.19 | 8.56 | 0.09 | 100.0 | 170.0 | 179.8 | 5.6 | 174.0 | 13.0 | 179.8 | 5.8 |
| Output_1_16 | 26310 | 876 | 1.5 | 0.03 | 3.39 | 0.05 | 7.00 | 0.20 | 6.97 | 0.29 | 240.0 | 150.0 | 179.9 | 6.0 | 186.0 | 12.0 | 179.9 | 6.2 |
| Output_1_149 | 7380 | 165 | 1.4 | 0.03 | 3.53 | 0.05 | 7.06 | 0.21 | 7.28 | 0.18 | 220.0 | 140.0 | 180.0 | 6.5 | 190.0 | 13.0 | 180.0 | 6.8 |
| Output_1_147 | 10250 | 212 | 3.2 | 0.03 | 3.31 | 0.05 | 7.62 | 0.19 | 6.19 | 0.13 | 220.0 | 150.0 | 180.4 | 5.9 | 179.9 | 9.9 | 180.4 | 6.2 |
| Output_1_34 | 4720 | 54 | 3.6 | 0.03 | 3.42 | 0.06 | 12.24 | 0.22 | 11.47 | 0.29 | 400.0 | 240.0 | 180.4 | 6.1 | 198.0 | 21.0 | 180.4 | 6.3 |
| Output_1_97 | 10750 | 277 | 1.5 | 0.03 | 3.04 | 0.06 | 4.49 | 0.22 | 4.23 | 0.18 | 416.0 | 94.0 | 181.9 | 5.4 | 201.4 | 7.7 | 181.9 | 5.7 |
| Output_1_36 | 6840 | 86 | 1.6 | 0.03 | 4.17 | 0.05 | 10.97 | 0.20 | 10.40 | 0.23 | 40.0 | 200.0 | 183.2 | 7.5 | 186.0 | 18.0 | 183.2 | 7.7 |
| Output_1_12 | 6570 | 303 | 6.0 | 0.03 | 3.81 | 0.06 | 9.87 | 0.23 | 8.37 | 0.04 | 420.0 | 200.0 | 183.5 | 6.6 | 207.0 | 16.0 | 183.5 | 6.8 |
| Output_1_118 | 17440 | 1076 | 1.4 | 0.03 | 2.01 | 0.05 | 4.99 | 0.20 | 5.05 | 0.46 | 190.0 | 100.0 | 183.7 | 3.6 | 183.0 | 8.6 | 183.7 | 4.1 |
| Output_1_103 | 11280 | 539 | 2.1 | 0.03 | 2.77 | 0.05 | 6.73 | 0.20 | 5.97 | 0.21 | 260.0 | 140.0 | 183.8 | 5.0 | 188.0 | 11.0 | 183.8 | 5.3 |
| Output_1_130 | 6400 | 252 | 2.8 | 0.03 | 2.72 | 0.05 | 8.00 | 0.21 | 7.51 | 0.01 | 320.0 | 180.0 | 184.7 | 5.0 | 196.0 | 14.0 | 184.7 | 5.3 |
| Output_1_31 | 14200 | 141 | 2.9 | 0.03 | 2.57 | 0.05 | 4.13 | 0.21 | 3.92 | 0.42 | 224.0 | 89.0 | 185.2 | 4.7 | 192.6 | 6.9 | 185.2 | 5.0 |
| Output_1_84 | 22820 | 777 | 1.5 | 0.03 | 2.64 | 0.05 | 4.41 | 0.21 | 5.29 | 0.37 | 290.0 | 100.0 | 185.2 | 4.8 | 192.0 | 8.8 | 185.2 | 5.1 |
| Output_1_23 | 7880 | 119 | 2.1 | 0.03 | 4.11 | 0.05 | 13.75 | 0.22 | 14.29 | 0.14 | 300.0 | 280.0 | 185.4 | 7.5 | 198.0 | 26.0 | 185.4 | 7.7 |
| Output_1_14 | 9010 | 350 | 2.5 | 0.03 | 3.42 | 0.05 | 6.98 | 0.19 | 7.77 | 0.37 | 110.0 | 140.0 | 185.6 | 6.5 | 179.0 | 13.0 | 185.6 | 6.7 |
| Output_1_76 | 2620 | 55 | 1.9 | 0.03 | 5.14 | 0.05 | 15.75 | 0.22 | 14.48 | 0.25 | 300.0 | 290.0 | 185.7 | 9.2 | 200.0 | 27.0 | 185.7 | 9.4 |
| Output_1_119 | 8580 | 518 | 2.4 | 0.03 | 2.80 | 0.05 | 8.64 | 0.21 | 7.51 | 0.03 | 250.0 | 170.0 | 185.9 | 5.2 | 195.0 | 13.0 | 185.9 | 5.5 |
| Output_1_122 | 9790 | 535 | 2.2 | 0.03 | 3.04 | 0.05 | 7.04 | 0.20 | 7.61 | 0.31 | 140.0 | 140.0 | 186.2 | 5.5 | 182.0 | 12.0 | 186.2 | 5.8 |
| Output_1_129 | 14560 | 591 | 1.9 | 0.03 | 3.20 | 0.06 | 5.17 | 0.22 | 6.31 | 0.43 | 430.0 | 120.0 | 186.4 | 5.9 | 203.0 | 12.0 | 186.4 | 6.1 |
| Output_1_73 | 6870 | 123 | 2.0 | 0.03 | 2.79 | 0.05 | 8.05 | 0.20 | 7.92 | 0.09 | 190.0 | 160.0 | 187.0 | 5.2 | 186.0 | 13.0 | 187.0 | 5.5 |
| Output_1_44 | 6010 | 245 | 2.1 | 0.03 | 3.29 | 0.05 | 8.61 | 0.21 | 8.49 | 0.12 | 250.0 | 180.0 | 187.0 | 6.1 | 196.0 | 15.0 | 187.0 | 6.4 |
| Output_1_6 | 3380 | 210 | 2.7 | 0.03 | 5.08 | 0.05 | 9.70 | 0.21 | 9.35 | 0.03 | 260.0 | 200.0 | 187.4 | 9.1 | 195.0 | 17.0 | 187.4 | 9.3 |
| Output_1_32 | 29310 | 293 | 2.3 | 0.03 | 2.23 | 0.05 | 4.08 | 0.22 | 4.31 | 0.64 | 345.0 | 90.0 | 187.8 | 4.1 | 201.8 | 7.9 | 187.8 | 4.5 |
| Output_1_134 | 8590 | 251 | 2.6 | 0.03 | 2.87 | 0.05 | 8.55 | 0.20 | 7.92 | 0.05 | 190.0 | 170.0 | 188.3 | 5.3 | 186.0 | 14.0 | 188.3 | 5.6 |
| Output_1_11 | 6010 | 291 | 1.8 | 0.03 | 3.37 | 0.05 | 11.15 | 0.22 | 10.00 | 0.12 | 310.0 | 220.0 | 188.5 | 6.4 | 201.0 | 18.0 | 188.5 | 6.7 |

| | | | | | | | | | | | | | | | | | | |
|---|---|---|---|---|---|---|---|---|---|---|---|---|---|---|---|---|---|---|
| Output_1_71 | 8460 | 138 | 2.3 | 0.03 | 2.29 | 0.05 | 7.74 | 0.22 | 7.37 | 0.04 | 330.0 | 170.0 | 188.7 | 4.2 | 199.0 | 14.0 | 188.7 | 4.6 |
| Output_1_63 | 22540 | 422 | 1.5 | 0.03 | 2.45 | 0.05 | 6.05 | 0.21 | 6.64 | 0.03 | 280.0 | 150.0 | 189.2 | 4.6 | 195.0 | 12.0 | 189.2 | 4.9 |
| Output_1_52 | 8840 | 287 | 1.6 | 0.03 | 2.78 | 0.05 | 6.31 | 0.21 | 6.67 | 0.38 | 340.0 | 130.0 | 189.4 | 5.2 | 193.0 | 12.0 | 189.4 | 5.5 |
| Output_1_8 | 32520 | 2082 | 2.1 | 0.03 | 2.75 | 0.05 | 3.45 | 0.21 | 3.70 | 0.42 | 174.0 | 74.0 | 189.7 | 5.1 | 191.0 | 6.8 | 189.7 | 5.4 |
| Output_1_96 | 13980 | 345 | 2.1 | 0.03 | 2.64 | 0.05 | 5.04 | 0.22 | 5.56 | 0.37 | 270.0 | 110.0 | 189.7 | 5.0 | 198.0 | 10.0 | 189.7 | 5.3 |
| Output_1_35 | 116800 | 1368 | 2.3 | 0.03 | 2.14 | 0.05 | 1.96 | 0.21 | 2.47 | 0.57 | 212.0 | 45.0 | 189.9 | 4.0 | 193.8 | 4.4 | 189.9 | 4.4 |
| Output_1_82 | 18250 | 585 | 2.3 | 0.03 | 1.97 | 0.05 | 4.68 | 0.21 | 4.14 | 0.26 | 240.0 | 100.0 | 189.9 | 3.7 | 197.1 | 7.9 | 189.9 | 4.1 |
| Output_1_74 | 9380 | 172 | 1.9 | 0.03 | 2.44 | 0.06 | 4.21 | 0.24 | 4.60 | 0.28 | 485.0 | 97.0 | 190.1 | 4.6 | 218.5 | 8.4 | 190.1 | 4.9 |
| Output_1_54 | 13220 | 376 | 2.5 | 0.03 | 2.20 | 0.05 | 6.32 | 0.21 | 6.10 | 0.21 | 260.0 | 130.0 | 190.2 | 4.1 | 196.0 | 11.0 | 190.2 | 4.5 |
| Output_1_107 | 3860 | 206 | 3.1 | 0.03 | 3.33 | 0.05 | 10.20 | 0.21 | 12.21 | 0.44 | 190.0 | 200.0 | 190.4 | 6.5 | 198.0 | 22.0 | 190.4 | 6.7 |
| Output_1_114 | 15360 | 934 | 1.8 | 0.03 | 3.12 | 0.05 | 6.75 | 0.20 | 6.86 | 0.14 | 190.0 | 140.0 | 191.5 | 5.9 | 188.0 | 12.0 | 191.5 | 6.2 |
| Output_1_110 | 12350 | 699 | 1.5 | 0.03 | 4.30 | 0.06 | 6.53 | 0.23 | 5.65 | 0.47 | 460.0 | 150.0 | 191.5 | 8.0 | 210.0 | 11.0 | 191.5 | 8.2 |
| Output_1_61 | 48400 | 903 | 2.0 | 0.03 | 2.11 | 0.05 | 3.20 | 0.21 | 3.32 | 0.38 | 188.0 | 71.0 | 192.6 | 4.0 | 195.5 | 6.2 | 192.6 | 4.4 |
| Output_1_70 | 8340 | 132 | 1.9 | 0.03 | 2.47 | 0.05 | 10.40 | 0.23 | 10.22 | 0.13 | 290.0 | 220.0 | 192.6 | 4.7 | 205.0 | 19.0 | 192.6 | 5.1 |
| Output_1_4 | 43370 | 2256 | 1.8 | 0.03 | 2.26 | 0.05 | 2.99 | 0.21 | 2.91 | 0.34 | 206.0 | 69.0 | 194.1 | 4.3 | 196.1 | 5.2 | 194.1 | 4.7 |
| Output_1_19 | 6010 | 146 | 1.3 | 0.03 | 4.23 | 0.06 | 10.26 | 0.23 | 10.30 | 0.27 | 510.0 | 200.0 | 194.8 | 7.9 | 217.0 | 22.0 | 194.8 | 8.2 |
| Output_1_128 | 7540 | 306 | 3.3 | 0.03 | 1.79 | 0.05 | 8.51 | 0.21 | 7.25 | 0.27 | 200.0 | 170.0 | 195.2 | 3.4 | 191.0 | 13.0 | 195.2 | 3.9 |
| Output_1_51 | 4300 | 143 | 1.7 | 0.03 | 2.99 | 0.05 | 11.11 | 0.23 | 11.06 | 0.14 | 330.0 | 240.0 | 195.6 | 5.7 | 209.0 | 22.0 | 195.6 | 6.1 |
| Output_1_86 | 9840 | 312 | 1.6 | 0.03 | 3.04 | 0.05 | 7.78 | 0.21 | 7.94 | 0.27 | 180.0 | 150.0 | 196.1 | 5.9 | 196.0 | 15.0 | 196.1 | 6.2 |
| Output_1_3 | 4860 | 222 | 2.6 | 0.03 | 3.03 | 0.05 | 10.40 | 0.21 | 10.58 | 0.09 | 130.0 | 190.0 | 196.8 | 5.9 | 194.0 | 18.0 | 196.8 | 6.2 |
| Output_1_22 | 10620 | 173 | 2.2 | 0.03 | 2.77 | 0.05 | 5.18 | 0.23 | 5.75 | 0.17 | 270.0 | 110.0 | 199.1 | 5.4 | 206.0 | 10.0 | 199.1 | 5.8 |
| Output_1_60 | 7560 | 148 | 2.9 | 0.03 | 3.02 | 0.05 | 7.92 | 0.21 | 7.28 | 0.03 | 70.0 | 150.0 | 199.9 | 6.0 | 189.0 | 12.0 | 199.9 | 6.3 |
| Output_1_146 | 8170 | 152 | 2.1 | 0.03 | 4.75 | 0.05 | 9.07 | 0.22 | 9.42 | 0.30 | 300.0 | 190.0 | 200.4 | 9.6 | 203.0 | 17.0 | 200.4 | 9.8 |
| Output_1_56 | 2660 | 65 | 2.6 | 0.03 | 4.11 | 0.06 | 11.41 | 0.24 | 11.34 | 0.12 | 380.0 | 230.0 | 200.4 | 7.9 | 215.0 | 22.0 | 200.4 | 8.2 |
| Output_1_62 | 30300 | 536 | 1.5 | 0.03 | 1.96 | 0.05 | 5.49 | 0.23 | 4.74 | 0.02 | 310.0 | 120.0 | 200.7 | 3.9 | 211.7 | 9.4 | 200.7 | 4.3 |
| Output_1_33 | 59300 | 568 | 2.2 | 0.03 | 2.40 | 0.05 | 2.61 | 0.22 | 3.31 | 0.64 | 167.0 | 61.0 | 201.1 | 4.8 | 199.4 | 6.0 | 201.1 | 5.1 |
| Output_1_48 | 4330 | 166 | 2.3 | 0.03 | 3.46 | 0.05 | 10.98 | 0.24 | 9.62 | 0.01 | 300.0 | 220.0 | 201.9 | 6.7 | 216.0 | 19.0 | 201.9 | 7.0 |
| Output_1_120 | 14860 | 784 | 3.3 | 0.03 | 2.09 | 0.05 | 4.75 | 0.23 | 4.89 | 0.21 | 210.0 | 100.0 | 203.0 | 4.2 | 205.3 | 9.3 | 203.0 | 4.6 |
| Output_1_133 | 20150 | 569 | 2.4 | 0.03 | 2.70 | 0.05 | 5.77 | 0.24 | 5.49 | 0.01 | 320.0 | 120.0 | 206.5 | 5.5 | 215.0 | 11.0 | 206.5 | 5.8 |
| Output_1_68 | 5900 | 86 | 2.3 | 0.03 | 4.24 | 0.05 | 9.33 | 0.24 | 8.75 | 0.00 | 320.0 | 180.0 | 209.1 | 8.5 | 221.0 | 16.0 | 209.1 | 8.7 |
| Output_1_64 | 4100 | 67 | 3.1 | 0.03 | 3.92 | 0.05 | 11.52 | 0.22 | 11.42 | 0.18 | 100.0 | 210.0 | 210.4 | 8.3 | 203.0 | 21.0 | 210.4 | 8.5 |
| Output_1_18 | 7930 | 166 | 1.7 | 0.03 | 4.32 | 0.05 | 6.68 | 0.25 | 9.88 | 0.50 | 160.0 | 150.0 | 219.9 | 9.6 | 229.0 | 20.0 | 219.9 | 9.8 |
| Output_1_106 | 23900 | 1050 | 1.6 | 0.03 | 2.60 | 0.05 | 3.77 | 0.24 | 4.17 | 0.52 | 216.0 | 82.0 | 221.4 | 5.7 | 218.2 | 8.4 | 221.4 | 6.1 |
| Output_1_49 | 29440 | 404 | 1.6 | 0.09 | 1.70 | 0.06 | 3.59 | 0.73 | 3.97 | 0.25 | 577.0 | 81.0 | 544.2 | 9.1 | 555.0 | 17.0 | 544.2 | 10.0 |
| Output_1_88 | 9460 | 48 | 1.3 | 0.18 | 3.18 | 0.08 | 5.61 | 1.90 | 4.94 | 0.20 | 1150.0 | 110.0 | 1046.0 | 31.0 | ##### | 35.0 | 1150.0 | 110.0 |
| Output_1_105 | 46380 | 291 | 2.3 | 0.23 | 2.14 | 0.09 | 2.70 | 2.90 | 3.79 | 0.70 | 1401.0 | 52.0 | 1351.0 | 26.0 | ##### | 28.0 | 1401.0 | 52.0 |
| Output_1_24 | 86200 | 122 | 1.6 | 0.28 | 2.45 | 0.10 | 2.16 | 3.86 | 3.63 | 0.65 | 1573.0 | 40.0 | 1601.0 | 35.0 | ##### | 28.0 | 1573.0 | 40.0 |
| Output_1_121 | 84000 | 476 | 3.4 | 0.28 | 1.94 | 0.10 | 2.63 | 3.97 | 3.02 | 0.52 | 1681.0 | 52.0 | 1606.0 | 28.0 | ##### | 25.0 | 1681.0 | 52.0 |
| Output_1_117 | 51270 | 317 | 1.2 | 0.29 | 2.44 | 0.11 | 2.26 | 4.24 | 2.59 | 0.56 | 1727.0 | 42.0 | 1647.0 | 35.0 | ##### | 21.0 | 1727.0 | 42.0 |
| Output_1_57 | 107200 | 258 | 1.1 | 0.30 | 1.52 | 0.11 | 1.60 | 4.39 | 2.10 | 0.72 | 1738.0 | 29.0 | 1669.0 | 22.0 | ##### | 17.0 | 1738.0 | 29.0 |

| | | | | | | | | | | | | | | | | | | |
|---|---|---|---|---|---|---|---|---|---|---|---|---|---|---|---|---|---|---|
| Output_1_37 | 109900 | 153 | 3.0 | 0.29 | 2.64 | 0.11 | 2.77 | 4.52 | 2.21 | 0.66 | 1827.0 | 50.0 | 1647.0 | 39.0 | ##### | 21.0 | 1827.0 | 50.0 |
| **Sample 19ATW40** | | | | | | | | | | | | | | | | | | |
| Output_1_7 | 24700 | 4810 | 7.2 | 0.01 | 6.19 | 0.05 | 6.99 | 0.06 | 7.60 | 0.50 | 70.0 | 140.0 | 57.0 | 3.5 | 58.4 | 4.3 | 57.0 | 3.7 |
| Output_1_4 | 13070 | 2259 | 7.7 | 0.01 | 4.73 | 0.05 | 9.04 | 0.06 | 11.15 | 0.46 | 180.0 | 180.0 | 58.4 | 2.7 | 62.6 | 6.8 | 58.4 | 3.0 |
| Output_1_11 | 4980 | 963 | 4.7 | 0.01 | 4.88 | 0.05 | 9.80 | 0.06 | 9.72 | 0.32 | 10.0 | 180.0 | 60.5 | 2.9 | 58.8 | 5.6 | 60.5 | 3.2 |
| Output_1_44 | 13190 | 2442 | 22.0 | 0.01 | 4.53 | 0.05 | 7.71 | 0.06 | 6.18 | 0.26 | 100.0 | 150.0 | 60.9 | 2.8 | 59.0 | 3.6 | 60.9 | 3.0 |
| Output_1_37 | 13110 | 2060 | 0.6 | 0.01 | 4.81 | 0.05 | 7.14 | 0.06 | 7.96 | 0.39 | 200.0 | 140.0 | 61.4 | 3.0 | 63.0 | 4.9 | 61.4 | 3.2 |
| Output_1_34 | 3760 | 461 | 12.2 | 0.01 | 5.19 | 0.05 | 14.51 | 0.07 | 14.20 | 0.09 | 280.0 | 290.0 | 61.8 | 3.2 | 67.4 | 9.3 | 61.8 | 3.4 |
| Output_1_10 | 1360 | 245 | 2.3 | 0.01 | 6.83 | 0.05 | 24.53 | 0.08 | 22.37 | 0.03 | 300.0 | 400.0 | 62.0 | 4.2 | 77.0 | 16.0 | 62.0 | 4.4 |
| Output_1_24 | 7480 | 870 | 3.6 | 0.01 | 5.05 | 0.05 | 10.24 | 0.07 | 9.86 | 0.37 | 150.0 | 190.0 | 62.2 | 3.2 | 64.6 | 6.2 | 62.2 | 3.4 |
| Output_1_49 | 7690 | 1058 | 4.5 | 0.01 | 4.13 | 0.05 | 8.26 | 0.06 | 8.03 | 0.05 | 100.0 | 170.0 | 62.2 | 2.6 | 62.5 | 4.8 | 62.2 | 2.9 |
| Output_1_47 | 1430 | 217 | 2.3 | 0.01 | 9.32 | 0.05 | 23.53 | 0.07 | 20.90 | 0.02 | 250.0 | 380.0 | 62.6 | 5.8 | 68.0 | 14.0 | 62.6 | 5.9 |
| Output_1_6 | 9820 | 1689 | 3.9 | 0.01 | 4.07 | 0.05 | 7.80 | 0.07 | 7.75 | 0.40 | 160.0 | 160.0 | 63.0 | 2.6 | 65.9 | 5.0 | 63.0 | 2.9 |
| Output_1_22 | 11860 | 1405 | 2.9 | 0.01 | 4.18 | 0.05 | 7.19 | 0.06 | 7.57 | 0.21 | 130.0 | 140.0 | 63.0 | 2.6 | 63.6 | 4.7 | 63.0 | 2.9 |
| Output_1_20 | 9850 | 1283 | 7.7 | 0.01 | 4.47 | 0.05 | 6.55 | 0.07 | 7.20 | 0.59 | 70.0 | 130.0 | 63.1 | 2.8 | 64.2 | 4.5 | 63.1 | 3.1 |
| Output_1_42 | 8430 | 1632 | 2.6 | 0.01 | 4.17 | 0.05 | 8.14 | 0.06 | 9.11 | 0.34 | 50.0 | 150.0 | 63.1 | 2.6 | 61.5 | 5.4 | 63.1 | 2.9 |
| Output_1_36 | 8570 | 1223 | 6.7 | 0.01 | 4.26 | 0.05 | 8.88 | 0.07 | 7.84 | 0.35 | 240.0 | 180.0 | 63.3 | 2.7 | 66.3 | 5.0 | 63.3 | 3.0 |
| Output_1_15 | 8630 | 1370 | 5.7 | 0.01 | 3.73 | 0.05 | 8.67 | 0.07 | 9.24 | 0.33 | 90.0 | 170.0 | 63.6 | 2.4 | 65.8 | 5.9 | 63.6 | 2.7 |
| Output_1_28 | 8500 | 873 | 4.8 | 0.01 | 4.94 | 0.05 | 8.98 | 0.07 | 9.27 | 0.26 | 120.0 | 180.0 | 63.6 | 3.2 | 65.8 | 6.1 | 63.6 | 3.4 |
| Output_1_30 | 7550 | 780 | 9.0 | 0.01 | 5.44 | 0.05 | 9.20 | 0.07 | 9.45 | 0.36 | 160.0 | 180.0 | 63.7 | 3.4 | 64.4 | 5.9 | 63.7 | 3.7 |
| Output_1_1 | 11200 | 1744 | 3.8 | 0.01 | 5.51 | 0.05 | 8.76 | 0.07 | 9.04 | 0.33 | 90.0 | 170.0 | 64.1 | 3.5 | 65.1 | 5.7 | 64.1 | 3.8 |
| Output_1_27 | 9460 | 940 | 3.7 | 0.01 | 5.91 | 0.05 | 8.73 | 0.07 | 9.31 | 0.54 | 100.0 | 170.0 | 64.1 | 3.8 | 65.4 | 5.9 | 64.1 | 4.0 |
| Output_1_3 | 7830 | 1278 | 6.7 | 0.01 | 5.48 | 0.05 | 14.54 | 0.07 | 11.03 | 0.46 | 80.0 | 180.0 | 64.4 | 3.5 | 64.8 | 6.8 | 64.4 | 3.8 |
| Output_1_12 | 11320 | 1940 | 4.0 | 0.01 | 4.59 | 0.05 | 11.88 | 0.07 | 11.97 | 0.00 | 250.0 | 230.0 | 64.4 | 2.9 | 67.2 | 7.8 | 64.4 | 3.2 |
| Output_1_33 | 10010 | 1141 | 3.3 | 0.01 | 5.65 | 0.05 | 12.04 | 0.07 | 11.34 | 0.44 | 320.0 | 250.0 | 64.7 | 3.6 | 70.8 | 7.7 | 64.7 | 3.9 |
| Output_1_23 | 1930 | 205 | 5.1 | 0.01 | 4.75 | 0.05 | 19.03 | 0.07 | 20.29 | 0.14 | 10.0 | 330.0 | 64.8 | 3.1 | 67.0 | 13.0 | 64.8 | 3.4 |
| Output_1_5 | 13500 | 2154 | 3.8 | 0.01 | 4.85 | 0.05 | 6.06 | 0.07 | 7.70 | 0.59 | 190.0 | 130.0 | 64.9 | 3.2 | 68.7 | 5.1 | 64.9 | 3.4 |
| Output_1_17 | 5550 | 795 | 2.5 | 0.01 | 6.22 | 0.05 | 16.36 | 0.07 | 13.30 | 0.09 | 130.0 | 290.0 | 65.0 | 4.0 | 64.2 | 8.3 | 65.0 | 4.2 |
| Output_1_32 | 14490 | 1630 | 3.3 | 0.01 | 6.09 | 0.05 | 5.30 | 0.07 | 7.61 | 0.68 | 200.0 | 120.0 | 65.3 | 4.0 | 68.2 | 5.0 | 65.3 | 4.2 |
| Output_1_41 | 13540 | 2557 | 7.2 | 0.01 | 4.72 | 0.05 | 9.13 | 0.07 | 8.23 | 0.13 | 150.0 | 170.0 | 65.3 | 3.0 | 65.6 | 5.2 | 65.3 | 3.3 |
| Output_1_31 | 4510 | 497 | 16.1 | 0.01 | 7.15 | 0.05 | 10.75 | 0.07 | 10.78 | 0.21 | 70.0 | 200.0 | 65.5 | 4.6 | 65.4 | 6.8 | 65.5 | 4.8 |
| Output_1_13 | 1307 | 204 | 2.9 | 0.01 | 5.84 | 0.04 | 28.21 | 0.06 | 31.03 | 0.28 | -260.0 | 410.0 | 65.8 | 3.8 | 57.0 | 17.0 | 65.8 | 4.1 |
| Output_1_26 | 10830 | 1090 | 4.1 | 0.01 | 4.19 | 0.05 | 8.55 | 0.07 | 7.32 | 0.04 | 190.0 | 160.0 | 65.9 | 2.8 | 69.5 | 5.0 | 65.9 | 3.1 |
| Output_1_43 | 8610 | 1525 | 5.6 | 0.01 | 6.10 | 0.05 | 9.15 | 0.06 | 9.22 | 0.06 | 20.0 | 170.0 | 66.2 | 4.0 | 62.9 | 5.7 | 66.2 | 4.3 |
| Output_1_2 | 6980 | 1079 | 0.4 | 0.01 | 4.93 | 0.05 | 9.49 | 0.07 | 9.61 | 0.40 | 190.0 | 180.0 | 66.4 | 3.3 | 68.2 | 6.3 | 66.4 | 3.5 |
| Output_1_39 | 4510 | 782 | 2.3 | 0.01 | 6.08 | 0.06 | 13.31 | 0.07 | 10.67 | 0.06 | 340.0 | 260.0 | 66.4 | 4.0 | 71.2 | 6.8 | 66.4 | 4.2 |
| Output_1_38 | 10190 | 1668 | 3.8 | 0.01 | 5.96 | 0.05 | 6.75 | 0.07 | 7.16 | 0.24 | 200.0 | 140.0 | 66.7 | 4.0 | 67.1 | 4.7 | 66.7 | 4.2 |
| Output_1_29 | 21090 | 2102 | 1.4 | 0.01 | 5.00 | 0.05 | 6.57 | 0.07 | 6.53 | 0.43 | 70.0 | 130.0 | 66.8 | 3.3 | 66.2 | 4.2 | 66.8 | 3.6 |
| Output_1_14 | 16070 | 2472 | 4.6 | 0.01 | 4.60 | 0.05 | 6.37 | 0.07 | 6.66 | 0.55 | 0.0 | 120.0 | 66.9 | 3.0 | 67.8 | 4.4 | 66.9 | 3.3 |

| | | | | | | | | | | | | | | | | | | |
|---|---|---|---|---|---|---|---|---|---|---|---|---|---|---|---|---|---|---|
| Output_1_8 | 11620 | 1938 | 5.9 | 0.01 | 3.73 | 0.05 | 7.31 | 0.07 | 7.30 | 0.35 | 40.0 | 140.0 | 67.0 | 2.5 | 65.9 | 4.7 | 67.0 | 2.9 |
| Output_1_48 | 10080 | 1343 | 7.7 | 0.01 | 4.98 | 0.05 | 7.99 | 0.07 | 7.83 | 0.27 | 190.0 | 170.0 | 67.0 | 3.3 | 68.8 | 5.2 | 67.0 | 3.6 |
| Output_1_25 | 16400 | 1626 | 4.9 | 0.01 | 7.07 | 0.05 | 8.00 | 0.07 | 8.42 | 0.51 | 110.0 | 160.0 | 67.1 | 4.7 | 68.6 | 5.3 | 67.1 | 4.9 |
| Output_1_45 | 15270 | 2490 | 2.3 | 0.01 | 5.06 | 0.05 | 8.04 | 0.07 | 8.28 | 0.39 | 120.0 | 150.0 | 67.1 | 3.4 | 66.3 | 5.4 | 67.1 | 3.7 |
| Output_1_21 | 17940 | 2010 | 3.6 | 0.01 | 5.16 | 0.05 | 10.95 | 0.07 | 10.29 | 0.20 | 150.0 | 220.0 | 67.2 | 3.4 | 70.4 | 7.0 | 67.2 | 3.7 |
| Output_1_16 | 3920 | 552 | 5.2 | 0.01 | 5.08 | 0.05 | 12.32 | 0.07 | 12.13 | 0.16 | 140.0 | 230.0 | 68.1 | 3.4 | 71.6 | 8.4 | 68.1 | 3.7 |
| Output_1_35 | 12750 | 1484 | 3.2 | 0.01 | 4.21 | 0.05 | 7.39 | 0.07 | 7.02 | 0.34 | 180.0 | 150.0 | 68.6 | 2.9 | 69.3 | 4.4 | 68.6 | 3.2 |
| Output_1_19 | 3980 | 511 | 2.0 | 0.01 | 6.78 | 0.05 | 12.13 | 0.07 | 11.64 | 0.32 | 80.0 | 220.0 | 69.0 | 4.6 | 67.2 | 7.6 | 69.0 | 4.8 |
| Output_1_18 | 5340 | 676 | 3.0 | 0.01 | 5.79 | 0.04 | 12.87 | 0.07 | 12.52 | 0.02 | -80.0 | 220.0 | 69.8 | 4.0 | 64.9 | 7.9 | 69.8 | 4.3 |
| **Sample 19ATW55** | | | | | | | | | | | | | | | | | | |
| Output_1_101 | 4150 | 746 | 1.1 | 0.01 | 5.73 | 0.05 | 11.72 | 0.06 | 12.67 | 0.40 | 320.0 | 230.0 | 53.7 | 3.1 | 56.6 | 7.0 | 53.7 | 3.3 |
| Output_1_93 | 36210 | 5560 | 0.5 | 0.01 | 3.44 | 0.05 | 4.49 | 0.05 | 5.28 | 0.55 | 146.0 | 93.0 | 52.2 | 1.8 | 54.2 | 2.8 | 52.2 | 2.1 |
| Output_1_90 | 14500 | 2485 | 0.8 | 0.01 | 3.06 | 0.05 | 6.26 | 0.06 | 6.52 | 0.32 | 100.0 | 120.0 | 52.4 | 1.6 | 54.5 | 3.5 | 52.4 | 1.9 |
| Output_1_95 | 5900 | 846 | 0.9 | 0.01 | 3.91 | 0.05 | 10.08 | 0.06 | 10.16 | 0.11 | 150.0 | 200.0 | 52.5 | 2.0 | 54.4 | 5.4 | 52.5 | 2.3 |
| Output_1_96 | 3780 | 515 | 1.4 | 0.01 | 4.65 | 0.05 | 11.65 | 0.06 | 12.03 | 0.16 | 160.0 | 210.0 | 52.5 | 2.4 | 57.2 | 6.7 | 52.5 | 2.6 |
| Output_1_89 | 7870 | 1374 | 0.9 | 0.01 | 5.73 | 0.05 | 9.07 | 0.06 | 8.74 | 0.29 | 160.0 | 180.0 | 52.6 | 3.0 | 56.4 | 4.8 | 52.6 | 3.2 |
| Output_1_91 | 14940 | 2408 | 0.7 | 0.01 | 3.41 | 0.05 | 6.45 | 0.06 | 7.16 | 0.51 | 160.0 | 130.0 | 52.6 | 1.8 | 55.2 | 3.8 | 52.6 | 2.1 |
| Output_1_98 | 10700 | 1520 | 0.9 | 0.01 | 4.03 | 0.05 | 7.33 | 0.06 | 6.90 | 0.21 | 180.0 | 160.0 | 52.6 | 2.1 | 54.4 | 3.7 | 52.6 | 2.4 |
| Output_1_94 | 16050 | 2279 | 0.6 | 0.01 | 3.77 | 0.05 | 11.49 | 0.06 | 12.16 | 0.33 | 180.0 | 240.0 | 52.8 | 2.0 | 57.6 | 6.9 | 52.8 | 2.2 |
| Output_1_97 | 13190 | 1815 | 0.8 | 0.01 | 4.13 | 0.05 | 5.14 | 0.05 | 6.68 | 0.58 | 130.0 | 110.0 | 52.9 | 2.2 | 53.2 | 3.5 | 52.9 | 2.4 |
| Output_1_81 | 5040 | 750 | 1.1 | 0.01 | 6.24 | 0.05 | 13.63 | 0.06 | 13.49 | 0.34 | 100.0 | 260.0 | 53.5 | 3.4 | 56.3 | 7.3 | 53.5 | 3.5 |
| Output_1_88 | 8740 | 1539 | 1.2 | 0.01 | 5.76 | 0.05 | 11.13 | 0.06 | 12.74 | 0.23 | 180.0 | 220.0 | 53.6 | 3.1 | 56.4 | 7.0 | 53.6 | 3.3 |
| Output_1_99 | 7750 | 1112 | 1.0 | 0.01 | 3.22 | 0.05 | 8.92 | 0.06 | 8.83 | 0.15 | 170.0 | 170.0 | 53.8 | 1.7 | 55.6 | 4.5 | 53.8 | 2.0 |
| Output_1_82 | 11840 | 1747 | 0.8 | 0.01 | 5.21 | 0.05 | 10.46 | 0.06 | 10.52 | 0.32 | 180.0 | 220.0 | 54.2 | 2.8 | 57.2 | 5.8 | 54.2 | 3.0 |
| Output_1_84 | 12290 | 1912 | 0.9 | 0.01 | 4.01 | 0.05 | 8.18 | 0.06 | 6.75 | 0.19 | 140.0 | 160.0 | 54.3 | 2.2 | 57.0 | 3.8 | 54.3 | 2.4 |
| Output_1_83 | 7420 | 1119 | 1.0 | 0.01 | 4.27 | 0.05 | 9.42 | 0.06 | 7.72 | 0.12 | 200.0 | 170.0 | 55.7 | 2.4 | 60.0 | 4.5 | 55.7 | 2.6 |
| **Sample 19ATW66** | | | | | | | | | | | | | | | | | | |
| Output_1_61 | 417 | 43 | 0.3 | 0.01 | 12.96 | 0.07 | 28.99 | 0.10 | 35.35 | 0.29 | 350.0 | 570.0 | 69.0 | 8.8 | 91.0 | 31.0 | 69.0 | 9.2 |
| Output_1_64 | 987 | 110 | 13.3 | 0.01 | 6.34 | 0.04 | 20.36 | 0.07 | 20.00 | 0.02 | 30.0 | 350.0 | 72.8 | 4.6 | 68.0 | 13.0 | 72.8 | 5.4 |
| Output_1_59 | 492 | 41 | 0.1 | 0.01 | 16.67 | 0.06 | 35.94 | 0.10 | 31.25 | 0.03 | 630.0 | 680.0 | 73.0 | 12.0 | 92.0 | 28.0 | 73.0 | 13.0 |
| Output_1_71 | 649 | 110 | 12.2 | 0.01 | 7.36 | 0.06 | 26.32 | 0.09 | 22.73 | 0.10 | 330.0 | 450.0 | 73.2 | 5.3 | 88.0 | 20.0 | 73.2 | 6.0 |
| Output_1_70 | 370 | 61 | 8.0 | 0.01 | 13.04 | 0.07 | 35.14 | 0.10 | 31.68 | 0.11 | 470.0 | 630.0 | 73.9 | 9.3 | 94.0 | 28.0 | 73.9 | 9.8 |
| Output_1_49 | 1180 | 79 | 8.0 | 0.01 | 6.49 | 0.05 | 23.40 | 0.08 | 21.25 | 0.17 | 20.0 | 350.0 | 76.0 | 4.9 | 77.0 | 16.0 | 76.0 | 5.7 |
| Output_1_63 | 250 | 25 | 32.0 | 0.01 | 14.05 | 0.05 | 71.11 | 0.10 | 68.93 | 0.29 | -100.0 | ####### | 77.0 | 11.0 | 91.0 | 62.0 | 77.0 | 11.0 |
| Output_1_72 | 4270 | 692 | 38.2 | 0.01 | 4.36 | 0.05 | 11.38 | 0.08 | 11.44 | 0.13 | 160.0 | 210.0 | 77.8 | 3.4 | 82.3 | 9.0 | 77.8 | 4.5 |
| Output_1_62 | 1876 | 175 | 10.4 | 0.01 | 5.04 | 0.05 | 14.07 | 0.09 | 14.29 | 0.21 | 370.0 | 270.0 | 78.8 | 4.0 | 88.0 | 12.0 | 78.8 | 5.0 |
| **Sample 19ATW81** | | | | | | | | | | | | | | | | | | |

| | | | | | | | | | | | | | | | | | | |
|---|---|---|---|---|---|---|---|---|---|---|---|---|---|---|---|---|---|---|
| Output_1_75 | 2750 | 249 | 2.1 | 0.02 | 6.43 | 0.06 | 16.52 | 0.13 | 15.91 | 0.04 | 370.0 | 330.0 | 109.2 | 6.9 | 124.0 | 19.0 | 109.2 | 7.3 |
| Output_1_70 | 2930 | 296 | 3.1 | 0.02 | 5.57 | 0.05 | 15.99 | 0.14 | 14.71 | 0.03 | 330.0 | 280.0 | 113.5 | 6.3 | 129.0 | 18.0 | 113.5 | 6.7 |
| Output_1_77 | 3920 | 281 | 1.3 | 0.02 | 5.26 | 0.05 | 11.33 | 0.13 | 9.92 | 0.20 | 330.0 | 230.0 | 115.3 | 6.0 | 125.0 | 12.0 | 115.3 | 6.5 |
| Output_1_78 | 3280 | 235 | 2.9 | 0.02 | 5.01 | 0.05 | 13.43 | 0.13 | 14.39 | 0.13 | 270.0 | 260.0 | 113.6 | 5.6 | 124.0 | 17.0 | 113.6 | 6.1 |
| Output_1_61 | 2330 | 203 | 2.7 | 0.02 | 5.31 | 0.05 | 16.18 | 0.12 | 16.26 | 0.18 | 260.0 | 310.0 | 110.7 | 5.8 | 123.0 | 20.0 | 110.7 | 6.2 |
| Output_1_56 | 2620 | 190 | 2.5 | 0.02 | 7.73 | 0.05 | 14.39 | 0.13 | 12.12 | 0.14 | 260.0 | 280.0 | 115.3 | 8.7 | 125.0 | 15.0 | 115.3 | 9.0 |
| Output_1_69 | 7280 | 692 | 1.9 | 0.02 | 4.49 | 0.05 | 9.48 | 0.13 | 9.02 | 0.27 | 240.0 | 180.0 | 119.6 | 5.3 | 126.0 | 10.0 | 119.6 | 5.8 |
| Output_1_57 | 6640 | 494 | 2.1 | 0.02 | 4.06 | 0.05 | 9.88 | 0.13 | 10.85 | 0.26 | 230.0 | 200.0 | 114.9 | 4.7 | 123.0 | 12.0 | 114.9 | 5.2 |
| Output_1_60 | 3350 | 273 | 3.7 | 0.02 | 5.10 | 0.05 | 15.19 | 0.13 | 14.29 | 0.05 | 210.0 | 290.0 | 111.4 | 5.6 | 120.0 | 16.0 | 111.4 | 6.0 |
| Output_1_53 | 7980 | 562 | 1.7 | 0.02 | 2.88 | 0.05 | 9.88 | 0.12 | 8.70 | 0.12 | 200.0 | 190.0 | 108.6 | 3.1 | 112.3 | 9.9 | 108.6 | 3.8 |
| Output_1_80 | 4660 | 334 | 1.3 | 0.02 | 3.38 | 0.05 | 11.99 | 0.12 | 11.48 | 0.07 | 190.0 | 240.0 | 109.7 | 3.7 | 117.0 | 13.0 | 109.7 | 4.3 |
| Output_1_55 | 14060 | 969 | 1.4 | 0.02 | 4.35 | 0.05 | 6.83 | 0.12 | 6.34 | 0.40 | 200.0 | 150.0 | 116.0 | 5.0 | 116.3 | 7.0 | 116.0 | 5.5 |
| Output_1_50 | 3720 | 257 | 2.3 | 0.02 | 6.52 | 0.05 | 16.96 | 0.13 | 17.19 | 0.36 | 200.0 | 320.0 | 117.8 | 7.8 | 122.0 | 20.0 | 117.8 | 8.2 |
| Output_1_67 | 3550 | 363 | 2.1 | 0.02 | 6.74 | 0.05 | 11.62 | 0.12 | 10.83 | 0.10 | 190.0 | 220.0 | 113.9 | 7.9 | 114.0 | 11.0 | 113.9 | 8.2 |
| Output_1_59 | 3320 | 279 | 1.9 | 0.02 | 3.38 | 0.05 | 16.67 | 0.12 | 16.67 | 0.22 | 180.0 | 290.0 | 109.6 | 3.7 | 114.0 | 18.0 | 109.6 | 4.3 |
| Output_1_54 | 3640 | 257 | 1.7 | 0.02 | 5.21 | 0.05 | 14.12 | 0.12 | 13.45 | 0.24 | 170.0 | 260.0 | 110.5 | 5.7 | 113.0 | 14.0 | 110.5 | 6.1 |
| Output_1_64 | 8230 | 767 | 1.5 | 0.02 | 4.68 | 0.05 | 8.67 | 0.13 | 10.08 | 0.56 | 160.0 | 170.0 | 116.0 | 5.4 | 123.0 | 12.0 | 116.0 | 5.9 |
| Output_1_65 | 2150 | 215 | 3.2 | 0.02 | 6.40 | 0.05 | 16.36 | 0.12 | 15.70 | 0.01 | 150.0 | 300.0 | 110.2 | 6.9 | 115.0 | 17.0 | 110.2 | 7.3 |
| Output_1_51 | 3390 | 219 | 3.0 | 0.02 | 4.88 | 0.05 | 11.38 | 0.13 | 10.40 | 0.06 | 160.0 | 210.0 | 117.8 | 5.7 | 121.0 | 11.0 | 117.8 | 6.2 |
| Output_1_73 | 5490 | 492 | 1.3 | 0.02 | 3.74 | 0.05 | 12.12 | 0.12 | 10.66 | 0.08 | 150.0 | 230.0 | 111.2 | 4.1 | 117.0 | 11.0 | 111.2 | 4.7 |
| Output_1_72 | 5950 | 538 | 1.6 | 0.02 | 3.05 | 0.05 | 9.55 | 0.13 | 8.80 | 0.13 | 140.0 | 180.0 | 117.1 | 3.5 | 119.0 | 10.0 | 117.1 | 4.3 |
| Output_1_58 | 2990 | 225 | 2.9 | 0.02 | 5.19 | 0.05 | 14.40 | 0.13 | 16.80 | 0.36 | 130.0 | 270.0 | 116.8 | 6.0 | 122.0 | 18.0 | 116.8 | 6.4 |
| Output_1_79 | 5100 | 379 | 1.5 | 0.02 | 4.47 | 0.05 | 10.02 | 0.12 | 10.26 | 0.21 | 120.0 | 190.0 | 110.2 | 4.9 | 112.0 | 11.0 | 110.2 | 5.4 |
| Output_1_66 | 5270 | 543 | 2.0 | 0.02 | 3.17 | 0.05 | 9.50 | 0.12 | 8.34 | 0.06 | 110.0 | 180.0 | 110.9 | 3.5 | 112.4 | 8.8 | 110.9 | 4.1 |
| Output_1_63 | 6880 | 640 | 1.4 | 0.02 | 4.22 | 0.05 | 10.74 | 0.12 | 9.32 | 0.04 | 110.0 | 200.0 | 112.1 | 4.7 | 112.0 | 10.0 | 112.1 | 5.2 |
| Output_1_76 | 4950 | 380 | 1.5 | 0.02 | 5.01 | 0.05 | 10.60 | 0.13 | 10.94 | 0.06 | 110.0 | 210.0 | 117.2 | 5.8 | 122.0 | 12.0 | 117.2 | 6.3 |
| Output_1_68 | 4080 | 402 | 2.8 | 0.02 | 5.32 | 0.05 | 13.21 | 0.12 | 12.10 | 0.04 | 100.0 | 240.0 | 117.7 | 6.2 | 120.0 | 14.0 | 117.7 | 6.7 |
| Output_1_71 | 3420 | 331 | 2.0 | 0.02 | 5.38 | 0.05 | 15.21 | 0.12 | 15.97 | 0.14 | 50.0 | 260.0 | 111.6 | 6.0 | 113.0 | 17.0 | 111.6 | 6.4 |
| Output_1_74 | 7130 | 622 | 6.6 | 0.02 | 4.27 | 0.05 | 7.48 | 0.12 | 7.93 | 0.22 | 50.0 | 140.0 | 113.6 | 4.8 | 117.0 | 9.5 | 113.6 | 5.4 |
| Output_1_52 | 3630 | 241 | 2.0 | 0.02 | 6.01 | 0.05 | 13.53 | 0.12 | 11.30 | 0.06 | 50.0 | 240.0 | 116.7 | 7.0 | 110.0 | 12.0 | 116.7 | 7.4 |
| Output_1_62 | 1900 | 177 | 3.3 | 0.02 | 6.98 | 0.05 | 17.08 | 0.12 | 18.18 | 0.25 | 40.0 | 290.0 | 110.1 | 7.4 | 114.0 | 19.0 | 110.1 | 7.7 |

**Sample 19ATW01**

| | | | | | | | | | | | | | | | | | | |
|---|---|---|---|---|---|---|---|---|---|---|---|---|---|---|---|---|---|---|
| Output_1_120 | 8430 | 1010 | 4.5 | 0.01 | 3.70 | 0.05 | 7.46 | 0.08 | 7.70 | 0.34 | 20.0 | 140.0 | 76.2 | 2.8 | 73.6 | 5.4 | 76.2 | 2.8 |
| Output_1_135 | 1410 | 97 | 3.2 | 0.01 | 7.00 | 0.05 | 16.46 | 0.07 | 15.94 | 0.20 | 70.0 | 270.0 | 72.3 | 5.1 | 67.0 | 11.0 | 72.3 | 5.1 |
| Output_1_147 | 1431 | 88 | 2.0 | 0.01 | 5.65 | 0.05 | 20.43 | 0.07 | 21.62 | 0.29 | -20.0 | 330.0 | 73.7 | 4.1 | 71.0 | 15.0 | 73.7 | 4.1 |
| Output_1_149 | 1310 | 81 | 1.9 | 0.01 | 5.79 | 0.05 | 19.23 | 0.08 | 19.05 | 0.12 | 190.0 | 350.0 | 77.5 | 4.5 | 81.0 | 15.0 | 77.5 | 4.5 |
| Output_1_15 | 4630 | 473 | 1.9 | 0.01 | 4.11 | 0.05 | 10.63 | 0.08 | 10.33 | 0.09 | 120.0 | 200.0 | 81.1 | 3.3 | 81.8 | 8.1 | 81.1 | 3.3 |
| Output_1_154 | 7800 | 604 | 5.9 | 0.01 | 3.92 | 0.05 | 7.47 | 0.09 | 7.69 | 0.39 | 190.0 | 140.0 | 83.3 | 3.2 | 84.6 | 6.3 | 83.3 | 3.2 |
| Output_1_157 | 2130 | 192 | 2.0 | 0.01 | 5.92 | 0.05 | 17.57 | 0.09 | 14.29 | 0.11 | 270.0 | 310.0 | 81.1 | 4.8 | 87.0 | 12.0 | 81.1 | 4.8 |

| | | | | | | | | | | | | | | | | | | |
|---|---|---|---|---|---|---|---|---|---|---|---|---|---|---|---|---|---|---|
| Output_1_163 | 634 | 93 | 2.6 | 0.01 | 8.06 | 0.05 | 23.53 | 0.08 | 21.25 | 0.01 | 120.0 | 390.0 | 79.6 | 6.4 | 77.0 | 16.0 | 79.6 | 6.4 |
| Output_1_164 | 43000 | 5900 | 1.2 | 0.01 | 5.40 | 0.05 | 5.49 | 0.09 | 5.80 | 0.53 | 100.0 | 120.0 | 84.3 | 4.5 | 85.6 | 4.8 | 84.3 | 4.5 |
| Output_1_166 | 9990 | 1487 | 1.8 | 0.01 | 3.93 | 0.05 | 5.77 | 0.09 | 5.64 | 0.28 | 120.0 | 120.0 | 83.1 | 3.3 | 82.8 | 4.5 | 83.1 | 3.3 |
| Output_1_169 | 2090 | 349 | 1.8 | 0.01 | 6.97 | 0.05 | 15.26 | 0.09 | 14.61 | 0.12 | 330.0 | 300.0 | 80.8 | 5.6 | 88.0 | 13.0 | 80.8 | 5.6 |
| Output_1_192 | 7370 | 384 | 1.2 | 0.01 | 3.42 | 0.05 | 7.20 | 0.09 | 7.61 | 0.24 | 350.0 | 160.0 | 82.4 | 2.8 | 86.7 | 6.3 | 82.4 | 2.8 |
| Output_1_193 | 9080 | 484 | 2.7 | 0.01 | 4.42 | 0.05 | 7.53 | 0.08 | 7.93 | 0.38 | 40.0 | 140.0 | 78.2 | 3.4 | 78.7 | 6.0 | 78.2 | 3.4 |
| Output_1_195 | 9670 | 472 | 3.8 | 0.01 | 3.28 | 0.05 | 7.24 | 0.08 | 8.00 | 0.37 | 170.0 | 140.0 | 80.1 | 2.6 | 82.7 | 6.0 | 80.1 | 2.6 |
| Output_1_200 | 2520 | 108 | 1.8 | 0.01 | 7.69 | 0.05 | 14.22 | 0.08 | 12.60 | 0.07 | -30.0 | 240.0 | 83.2 | 6.4 | 75.7 | 9.2 | 83.2 | 6.4 |
| Output_1_201 | 6850 | 323 | 1.6 | 0.01 | 3.10 | 0.05 | 5.87 | 0.08 | 7.25 | 0.22 | 190.0 | 130.0 | 74.4 | 2.3 | 76.7 | 5.3 | 74.4 | 2.3 |
| Output_1_22 | 13460 | 2101 | 1.0 | 0.01 | 3.16 | 0.05 | 6.02 | 0.09 | 6.89 | 0.27 | 170.0 | 120.0 | 83.2 | 2.6 | 86.0 | 5.7 | 83.2 | 2.6 |
| Output_1_221 | 781 | 92 | 2.2 | 0.01 | 8.44 | 0.06 | 31.03 | 0.08 | 29.11 | 0.25 | 200.0 | 530.0 | 67.6 | 5.7 | 75.0 | 22.0 | 67.6 | 5.7 |
| Output_1_225 | 10280 | 1260 | 2.3 | 0.01 | 5.06 | 0.05 | 8.40 | 0.09 | 7.86 | 0.35 | 340.0 | 170.0 | 81.0 | 4.1 | 85.3 | 6.4 | 81.0 | 4.1 |
| Output_1_226 | 2400 | 302 | 1.9 | 0.01 | 4.54 | 0.05 | 15.53 | 0.07 | 13.51 | 0.11 | 20.0 | 260.0 | 73.4 | 3.3 | 72.4 | 9.7 | 73.4 | 3.3 |
| Output_1_228 | 3730 | 445 | 2.4 | 0.01 | 5.57 | 0.05 | 14.32 | 0.08 | 12.66 | 0.11 | 110.0 | 270.0 | 78.2 | 4.4 | 76.4 | 9.6 | 78.2 | 4.4 |
| Output_1_230 | 12900 | 1567 | 1.6 | 0.01 | 2.74 | 0.05 | 5.59 | 0.08 | 6.05 | 0.35 | 190.0 | 110.0 | 72.6 | 2.0 | 75.9 | 4.4 | 72.6 | 2.0 |
| Output_1_233 | 39900 | 4620 | 3.3 | 0.01 | 2.94 | 0.05 | 8.13 | 0.08 | 9.41 | 0.38 | 200.0 | 170.0 | 76.2 | 2.3 | 78.8 | 7.1 | 76.2 | 2.3 |
| Output_1_234 | 9160 | 1021 | 2.5 | 0.01 | 3.56 | 0.05 | 7.25 | 0.08 | 6.93 | 0.24 | 140.0 | 150.0 | 77.5 | 2.7 | 81.2 | 5.1 | 77.5 | 2.7 |
| Output_1_239 | 6230 | 775 | 2.1 | 0.01 | 5.58 | 0.05 | 7.54 | 0.08 | 7.50 | 0.35 | 190.0 | 150.0 | 78.0 | 4.3 | 80.5 | 5.8 | 78.0 | 4.3 |
| Output_1_240 | 29830 | 4030 | 2.6 | 0.01 | 4.42 | 0.05 | 5.29 | 0.07 | 6.98 | 0.64 | 70.0 | 100.0 | 72.4 | 3.2 | 72.8 | 4.9 | 72.4 | 3.2 |
| Output_1_241 | 20310 | 2689 | 1.5 | 0.01 | 3.50 | 0.05 | 6.16 | 0.08 | 5.34 | 0.27 | 70.0 | 120.0 | 78.8 | 2.7 | 76.8 | 4.0 | 78.8 | 2.7 |
| Output_1_245 | 62400 | 11250 | 2.9 | 0.01 | 4.63 | 0.05 | 4.85 | 0.08 | 4.79 | 0.57 | 72.0 | 95.0 | 76.0 | 3.5 | 75.6 | 3.5 | 76.0 | 3.5 |
| Output_1_248 | 4080 | 845 | 2.3 | 0.01 | 5.32 | 0.05 | 11.84 | 0.08 | 10.20 | 0.08 | 270.0 | 230.0 | 73.4 | 3.9 | 79.2 | 7.8 | 73.4 | 3.9 |
| Output_1_25 | 4430 | 531 | 2.0 | 0.01 | 4.07 | 0.05 | 7.00 | 0.08 | 8.22 | 0.34 | 130.0 | 140.0 | 75.5 | 3.1 | 78.3 | 6.2 | 75.5 | 3.1 |
| Output_1_250 | 15190 | 3255 | 2.1 | 0.01 | 3.35 | 0.05 | 5.30 | 0.08 | 5.40 | 0.40 | 150.0 | 110.0 | 78.4 | 2.6 | 81.1 | 4.2 | 78.4 | 2.6 |
| Output_1_254 | 5800 | 1186 | 0.8 | 0.01 | 7.44 | 0.05 | 14.17 | 0.09 | 13.19 | 0.21 | 300.0 | 320.0 | 83.5 | 6.2 | 88.0 | 11.0 | 83.5 | 6.2 |
| Output_1_258 | 1394 | 304 | 2.0 | 0.01 | 6.52 | 0.05 | 18.04 | 0.08 | 16.88 | 0.06 | 230.0 | 310.0 | 70.8 | 4.6 | 76.0 | 12.0 | 70.8 | 4.6 |
| Output_1_259 | 3510 | 658 | 4.9 | 0.01 | 7.12 | 0.05 | 12.97 | 0.08 | 11.90 | 0.01 | 230.0 | 260.0 | 75.5 | 5.3 | 82.1 | 9.6 | 75.5 | 5.3 |
| Output_1_26 | 5630 | 569 | 9.9 | 0.01 | 4.80 | 0.05 | 10.06 | 0.08 | 10.96 | 0.37 | 120.0 | 190.0 | 78.7 | 3.8 | 79.8 | 8.4 | 78.7 | 3.8 |
| Output_1_265 | 2290 | 286 | 1.4 | 0.01 | 8.16 | 0.05 | 23.53 | 0.09 | 21.84 | 0.13 | 180.0 | 440.0 | 76.1 | 6.2 | 84.0 | 18.0 | 76.1 | 6.2 |
| Output_1_27 | 15300 | 1520 | 67.0 | 0.01 | 9.10 | 0.06 | 21.05 | 0.07 | 15.28 | 0.58 | 430.0 | 420.0 | 67.7 | 6.1 | 71.0 | 10.0 | 67.7 | 6.1 |
| Output_1_282 | 1850 | 111 | 8.5 | 0.01 | 6.98 | 0.04 | 17.55 | 0.07 | 17.81 | 0.27 | -110.0 | 280.0 | 78.0 | 5.4 | 71.0 | 13.0 | 78.0 | 5.4 |
| Output_1_285 | 1153 | 69 | 2.5 | 0.01 | 6.42 | 0.06 | 21.67 | 0.10 | 20.20 | 0.15 | 360.0 | 410.0 | 82.7 | 5.3 | 95.0 | 18.0 | 82.7 | 5.3 |
| Output_1_286 | 3280 | 224 | 2.7 | 0.01 | 4.94 | 0.06 | 25.40 | 0.10 | 27.55 | 0.53 | 280.0 | 310.0 | 74.6 | 3.5 | 92.0 | 23.0 | 74.6 | 3.5 |
| Output_1_301 | 2070 | 332 | 2.7 | 0.01 | 8.33 | 0.05 | 18.42 | 0.09 | 19.54 | 0.44 | 220.0 | 320.0 | 73.1 | 6.0 | 84.0 | 16.0 | 73.1 | 6.0 |
| Output_1_4 | 2323 | 212 | 1.9 | 0.01 | 5.50 | 0.04 | 13.09 | 0.08 | 15.79 | 0.22 | -190.0 | 210.0 | 80.4 | 4.4 | 74.0 | 11.0 | 80.4 | 4.4 |
| Output_1_52 | 11380 | 910 | 2.8 | 0.01 | 2.71 | 0.05 | 6.29 | 0.09 | 7.07 | 0.55 | 210.0 | 130.0 | 80.4 | 2.2 | 83.9 | 5.7 | 80.4 | 2.2 |
| Output_1_53 | 13680 | 1311 | 1.7 | 0.01 | 3.29 | 0.05 | 6.37 | 0.08 | 5.97 | 0.01 | 90.0 | 130.0 | 72.1 | 2.3 | 73.7 | 4.2 | 72.1 | 2.3 |
| Output_1_65 | 3590 | 856 | 1.6 | 0.01 | 6.48 | 0.06 | 20.00 | 0.09 | 24.14 | 0.33 | 300.0 | 370.0 | 83.1 | 5.3 | 90.0 | 18.0 | 83.1 | 5.3 |
| Output_1_80 | 633 | 91 | 2.7 | 0.01 | 9.01 | 0.05 | 32.65 | 0.08 | 30.77 | 0.18 | -90.0 | 480.0 | 70.8 | 6.7 | 74.0 | 22.0 | 70.8 | 6.7 |
| Output_1_98 | 4240 | 297 | 1.6 | 0.01 | 4.02 | 0.05 | 12.33 | 0.07 | 12.47 | 0.10 | -10.0 | 210.0 | 71.7 | 2.9 | 71.2 | 8.5 | 71.7 | 2.9 |

| | | | | | | | | | | | | | | | | | | |
|---|---|---|---|---|---|---|---|---|---|---|---|---|---|---|---|---|---|---|
| Output_1_76 | 3340 | 509 | 1.6 | 0.01 | 4.47 | 0.05 | 11.94 | 0.09 | 11.36 | 0.18 | 130.0 | 230.0 | 84.5 | 3.7 | 85.0 | 9.3 | 84.5 | 3.7 |
| Output_1_293 | 2600 | 213 | 1.8 | 0.01 | 7.32 | 0.05 | 20.75 | 0.10 | 19.61 | 0.29 | 230.0 | 370.0 | 84.9 | 6.2 | 98.0 | 19.0 | 84.9 | 6.2 |
| Output_1_202 | 5260 | 220 | 1.5 | 0.01 | 5.42 | 0.05 | 9.78 | 0.09 | 10.11 | 0.25 | 130.0 | 180.0 | 85.0 | 4.6 | 89.0 | 8.6 | 85.0 | 4.6 |
| Output_1_102 | 4090 | 302 | 1.5 | 0.01 | 5.80 | 0.06 | 13.95 | 0.10 | 14.14 | 0.36 | 380.0 | 280.0 | 85.0 | 4.9 | 95.0 | 13.0 | 85.0 | 4.9 |
| Output_1_66 | 3870 | 880 | 1.6 | 0.01 | 4.51 | 0.05 | 14.20 | 0.09 | 12.50 | 0.19 | 160.0 | 260.0 | 85.2 | 3.8 | 85.0 | 10.0 | 85.2 | 3.8 |
| Output_1_144 | 1750 | 92 | 2.3 | 0.01 | 9.02 | 0.06 | 22.95 | 0.11 | 21.50 | 0.08 | 450.0 | 430.0 | 85.4 | 7.7 | 103.0 | 21.0 | 85.4 | 7.7 |
| Output_1_204 | 18980 | 782 | 2.3 | 0.01 | 3.55 | 0.05 | 4.85 | 0.09 | 5.08 | 0.44 | 100.0 | 100.0 | 86.5 | 3.0 | 86.1 | 4.2 | 86.5 | 3.0 |
| Output_1_44 | 20660 | 1052 | 1.0 | 0.01 | 5.45 | 0.05 | 7.49 | 0.09 | 6.19 | 0.39 | 50.0 | 140.0 | 86.9 | 4.7 | 84.9 | 5.0 | 86.9 | 4.7 |
| Output_1_93 | 5700 | 314 | 1.2 | 0.01 | 4.19 | 0.05 | 6.17 | 0.09 | 6.31 | 0.40 | 120.0 | 120.0 | 87.0 | 3.6 | 85.9 | 5.5 | 87.0 | 3.6 |
| Output_1_72 | 3900 | 730 | 2.9 | 0.01 | 4.26 | 0.05 | 12.06 | 0.09 | 13.04 | 0.06 | 140.0 | 230.0 | 87.1 | 3.7 | 89.0 | 11.0 | 87.1 | 3.7 |
| Output_1_171 | 11130 | 1680 | 1.7 | 0.01 | 4.63 | 0.05 | 6.99 | 0.09 | 7.61 | 0.31 | 180.0 | 140.0 | 87.1 | 4.0 | 91.5 | 6.8 | 87.1 | 4.0 |
| Output_1_168 | 3800 | 561 | 2.4 | 0.01 | 4.91 | 0.05 | 14.57 | 0.09 | 14.12 | 0.00 | 20.0 | 260.0 | 87.3 | 4.3 | 82.0 | 11.0 | 87.3 | 4.3 |
| Output_1_302 | 5560 | 723 | 2.0 | 0.01 | 3.37 | 0.05 | 9.70 | 0.09 | 9.89 | 0.11 | 70.0 | 180.0 | 87.5 | 2.9 | 86.3 | 8.2 | 87.5 | 2.9 |
| Output_1_294 | 3320 | 284 | 2.6 | 0.01 | 6.79 | 0.06 | 17.86 | 0.11 | 17.76 | 0.07 | 470.0 | 320.0 | 87.7 | 5.9 | 103.0 | 17.0 | 87.7 | 5.9 |
| Output_1_28 | 9600 | 760 | 46.0 | 0.01 | 8.76 | 0.05 | 19.61 | 0.09 | 18.48 | 0.18 | 190.0 | 380.0 | 87.8 | 7.9 | 94.0 | 18.0 | 87.8 | 7.9 |
| Output_1_264 | 1880 | 224 | 2.7 | 0.01 | 5.95 | 0.05 | 16.94 | 0.09 | 17.20 | 0.40 | 180.0 | 290.0 | 88.3 | 5.2 | 89.0 | 15.0 | 88.3 | 5.2 |
| Output_1_243 | 15270 | 2076 | 0.6 | 0.01 | 3.83 | 0.05 | 5.59 | 0.09 | 7.22 | 0.57 | 120.0 | 110.0 | 88.5 | 3.3 | 91.2 | 6.3 | 88.5 | 3.3 |
| Output_1_260 | 4080 | 671 | 4.6 | 0.01 | 5.84 | 0.04 | 11.53 | 0.09 | 14.12 | 0.11 | -120.0 | 200.0 | 88.7 | 5.1 | 83.0 | 12.0 | 88.7 | 5.1 |
| Output_1_90 | 21590 | 1283 | 4.5 | 0.01 | 2.09 | 0.05 | 5.16 | 0.09 | 4.88 | 0.13 | 40.0 | 100.0 | 88.8 | 1.8 | 87.7 | 4.1 | 88.8 | 1.8 |
| Output_1_2 | 5650 | 484 | 1.9 | 0.01 | 3.96 | 0.05 | 9.98 | 0.10 | 10.20 | 0.07 | 240.0 | 210.0 | 88.9 | 3.5 | 94.7 | 9.5 | 88.9 | 3.5 |
| Output_1_113 | 21670 | 2118 | 2.4 | 0.01 | 3.52 | 0.05 | 7.71 | 0.10 | 7.92 | 0.44 | 250.0 | 160.0 | 89.1 | 3.1 | 93.0 | 7.0 | 89.1 | 3.1 |
| Output_1_213 | 1005 | 49 | 2.6 | 0.01 | 6.60 | 0.04 | 22.73 | 0.10 | 21.88 | 0.02 | 140.0 | 400.0 | 89.2 | 5.8 | 91.0 | 19.0 | 89.2 | 5.8 |
| Output_1_14 | 21160 | 1755 | 1.7 | 0.01 | 3.57 | 0.05 | 4.88 | 0.09 | 5.64 | 0.60 | 150.0 | 100.0 | 89.7 | 3.2 | 91.2 | 5.0 | 89.7 | 3.2 |
| Output_1_17 | 3200 | 404 | 1.4 | 0.01 | 4.77 | 0.05 | 11.84 | 0.09 | 11.70 | 0.14 | 120.0 | 220.0 | 89.9 | 4.2 | 90.7 | 9.7 | 89.9 | 4.2 |
| Output_1_115 | 8810 | 890 | 1.2 | 0.01 | 3.93 | 0.05 | 6.67 | 0.09 | 6.04 | 0.30 | 160.0 | 130.0 | 91.3 | 3.6 | 91.4 | 5.3 | 91.3 | 3.6 |
| Output_1_175 | 3550 | 459 | 1.4 | 0.01 | 4.48 | 0.05 | 10.52 | 0.10 | 10.42 | 0.15 | 120.0 | 200.0 | 91.3 | 4.0 | 93.0 | 9.6 | 91.3 | 4.0 |
| Output_1_83 | 4190 | 346 | 1.5 | 0.01 | 4.48 | 0.05 | 10.91 | 0.10 | 9.71 | 0.01 | 310.0 | 220.0 | 91.5 | 4.1 | 98.2 | 9.1 | 91.5 | 4.1 |
| Output_1_183 | 2710 | 196 | 2.4 | 0.01 | 4.62 | 0.05 | 15.18 | 0.10 | 13.54 | 0.03 | 220.0 | 280.0 | 91.5 | 4.2 | 93.0 | 12.0 | 91.5 | 4.2 |
| Output_1_224 | 2500 | 256 | 2.4 | 0.01 | 5.35 | 0.05 | 17.19 | 0.10 | 18.00 | 0.22 | 140.0 | 310.0 | 92.0 | 4.9 | 98.0 | 17.0 | 92.0 | 4.9 |
| Output_1_13 | 18320 | 1376 | 2.8 | 0.01 | 3.45 | 0.05 | 5.29 | 0.10 | 5.79 | 0.25 | 210.0 | 120.0 | 92.7 | 3.2 | 95.2 | 5.3 | 92.7 | 3.2 |
| Output_1_30 | 1198 | 75 | 3.3 | 0.01 | 6.34 | 0.04 | 21.13 | 0.09 | 20.93 | 0.29 | -170.0 | 320.0 | 92.8 | 5.8 | 82.0 | 17.0 | 92.8 | 5.8 |
| Output_1_218 | 19440 | 1216 | 2.1 | 0.01 | 4.10 | 0.05 | 4.95 | 0.10 | 6.69 | 0.61 | 120.0 | 100.0 | 92.9 | 3.9 | 92.6 | 5.9 | 92.9 | 3.9 |
| Output_1_185 | 4740 | 300 | 2.3 | 0.01 | 5.44 | 0.05 | 8.83 | 0.09 | 9.88 | 0.26 | 130.0 | 170.0 | 92.9 | 5.0 | 91.0 | 8.6 | 92.9 | 5.0 |
| Output_1_134 | 4320 | 228 | 1.7 | 0.01 | 5.92 | 0.05 | 14.76 | 0.10 | 12.87 | 0.12 | 190.0 | 270.0 | 92.9 | 5.5 | 97.0 | 12.0 | 92.9 | 5.5 |
| Output_1_1 | 11990 | 996 | 3.5 | 0.01 | 3.02 | 0.05 | 8.70 | 0.09 | 8.22 | 0.24 | 110.0 | 170.0 | 93.3 | 2.8 | 89.6 | 7.1 | 93.3 | 2.8 |
| Output_1_206 | 7360 | 286 | 3.7 | 0.01 | 4.86 | 0.05 | 9.06 | 0.10 | 9.73 | 0.42 | 210.0 | 180.0 | 93.5 | 4.5 | 97.1 | 9.0 | 93.5 | 4.5 |
| Output_1_96 | 38730 | 2085 | 3.8 | 0.01 | 3.49 | 0.05 | 4.99 | 0.10 | 4.91 | 0.36 | 190.0 | 110.0 | 93.6 | 3.3 | 94.7 | 4.4 | 93.6 | 3.3 |
| Output_1_73 | 7230 | 1180 | 2.5 | 0.01 | 5.12 | 0.05 | 7.22 | 0.10 | 7.92 | 0.46 | 70.0 | 140.0 | 93.8 | 4.8 | 92.9 | 7.0 | 93.8 | 4.8 |
| Output_1_174 | 9760 | 1262 | 1.1 | 0.01 | 3.95 | 0.05 | 7.69 | 0.10 | 7.76 | 0.32 | 150.0 | 150.0 | 94.0 | 3.7 | 94.7 | 7.0 | 94.0 | 3.7 |
| Output_1_162 | 1667 | 191 | 2.2 | 0.01 | 6.76 | 0.05 | 20.47 | 0.09 | 19.15 | 0.12 | 70.0 | 350.0 | 94.4 | 6.5 | 90.0 | 16.0 | 94.4 | 6.5 |

| | | | | | | | | | | | | | | | | | | |
|---|---|---|---|---|---|---|---|---|---|---|---|---|---|---|---|---|---|---|
| Output_1_141 | 7380 | 340 | 1.5 | 0.01 | 2.37 | 0.05 | 7.69 | 0.10 | 7.98 | 0.18 | 110.0 | 150.0 | 94.6 | 2.2 | 94.4 | 7.2 | 94.6 | 2.2 |
| Output_1_87 | 45700 | 2870 | 2.8 | 0.01 | 3.78 | 0.05 | 4.42 | 0.10 | 4.64 | 0.54 | 174.0 | 94.0 | 94.8 | 3.6 | 96.0 | 4.2 | 94.8 | 3.6 |
| Output_1_114 | 22700 | 2200 | 1.8 | 0.01 | 7.43 | 0.05 | 13.86 | 0.10 | 10.20 | 0.12 | 170.0 | 270.0 | 94.8 | 7.3 | 94.6 | 9.5 | 94.8 | 7.3 |
| Output_1_136 | 1460 | 73 | 2.4 | 0.01 | 6.76 | 0.05 | 20.83 | 0.09 | 18.48 | 0.01 | -10.0 | 340.0 | 94.9 | 6.3 | 88.0 | 16.0 | 94.9 | 6.3 |
| Output_1_160 | 11270 | 1059 | 1.4 | 0.01 | 5.04 | 0.05 | 8.62 | 0.10 | 8.55 | 0.12 | 210.0 | 160.0 | 95.2 | 4.8 | 98.1 | 8.0 | 95.2 | 4.8 |
| Output_1_3 | 33140 | 2609 | 3.0 | 0.01 | 5.04 | 0.05 | 3.29 | 0.10 | 5.25 | 0.77 | 133.0 | 68.0 | 95.3 | 4.8 | 94.0 | 4.8 | 95.3 | 4.8 |
| Output_1_253 | 3030 | 541 | 2.2 | 0.01 | 7.38 | 0.06 | 14.05 | 0.11 | 13.64 | 0.29 | 470.0 | 250.0 | 95.3 | 6.8 | 110.0 | 14.0 | 95.3 | 6.8 |
| Output_1_161 | 21800 | 2276 | 2.4 | 0.01 | 4.14 | 0.05 | 5.93 | 0.10 | 6.18 | 0.29 | 90.0 | 120.0 | 95.7 | 4.0 | 92.4 | 5.4 | 95.7 | 4.0 |
| Output_1_300 | 33600 | 4190 | 8.4 | 0.01 | 5.61 | 0.05 | 4.72 | 0.11 | 8.29 | 0.77 | 220.0 | 100.0 | 95.8 | 5.4 | 102.1 | 8.1 | 95.8 | 5.4 |
| Output_1_31 | 2400 | 132 | 1.0 | 0.02 | 6.19 | 0.05 | 13.33 | 0.10 | 13.40 | 0.28 | 130.0 | 240.0 | 96.2 | 5.9 | 93.0 | 12.0 | 96.2 | 5.9 |
| Output_1_32 | 5000 | 242 | 3.6 | 0.02 | 4.52 | 0.05 | 12.34 | 0.09 | 10.75 | 0.05 | 120.0 | 230.0 | 96.3 | 4.3 | 89.8 | 9.5 | 96.3 | 4.3 |
| Output_1_107 | 27720 | 2059 | 1.9 | 0.02 | 3.83 | 0.05 | 4.24 | 0.11 | 4.48 | 0.42 | 167.0 | 91.0 | 96.8 | 3.7 | 103.3 | 4.4 | 96.8 | 3.7 |
| Output_1_36 | 9220 | 390 | 1.6 | 0.02 | 2.84 | 0.05 | 7.07 | 0.11 | 6.88 | 0.13 | 210.0 | 140.0 | 96.9 | 2.7 | 103.4 | 6.8 | 96.9 | 2.7 |
| Output_1_235 | 18700 | 1640 | 0.9 | 0.02 | 6.58 | 0.05 | 9.77 | 0.11 | 8.01 | 0.15 | 300.0 | 230.0 | 97.0 | 6.6 | 105.7 | 8.0 | 97.0 | 6.6 |
| Output_1_291 | 3340 | 216 | 1.3 | 0.02 | 5.80 | 0.05 | 12.27 | 0.11 | 13.21 | 0.37 | 160.0 | 230.0 | 97.1 | 5.6 | 102.0 | 13.0 | 97.1 | 5.6 |
| Output_1_275 | 7610 | 408 | 1.7 | 0.02 | 3.61 | 0.05 | 7.28 | 0.11 | 8.80 | 0.34 | 260.0 | 150.0 | 97.5 | 3.5 | 103.8 | 8.7 | 97.5 | 3.5 |
| Output_1_280 | 1069 | 52 | 2.2 | 0.02 | 6.62 | 0.05 | 19.68 | 0.10 | 18.45 | 0.15 | 110.0 | 340.0 | 97.6 | 6.8 | 98.0 | 18.0 | 97.6 | 6.8 |
| Output_1_71 | 17580 | 3180 | 0.8 | 0.02 | 4.64 | 0.05 | 8.22 | 0.10 | 8.18 | 0.05 | 280.0 | 180.0 | 98.0 | 4.5 | 100.3 | 7.8 | 98.0 | 4.5 |
| Output_1_292 | 5880 | 385 | 2.8 | 0.02 | 5.48 | 0.05 | 11.42 | 0.11 | 13.64 | 0.57 | 260.0 | 240.0 | 98.1 | 5.3 | 106.0 | 13.0 | 98.1 | 5.3 |
| Output_1_85 | 7160 | 485 | 4.7 | 0.02 | 3.90 | 0.05 | 8.46 | 0.11 | 9.17 | 0.11 | 280.0 | 180.0 | 98.4 | 3.8 | 106.3 | 8.8 | 98.4 | 3.8 |
| Output_1_214 | 4640 | 223 | 1.9 | 0.02 | 8.44 | 0.05 | 11.42 | 0.11 | 13.33 | 0.39 | 140.0 | 240.0 | 98.5 | 8.3 | 101.0 | 13.0 | 98.5 | 8.3 |
| Output_1_126 | 19370 | 1412 | 6.5 | 0.02 | 3.23 | 0.05 | 5.38 | 0.10 | 4.69 | 0.26 | 110.0 | 110.0 | 98.9 | 3.2 | 95.0 | 4.2 | 98.9 | 3.2 |
| Output_1_57 | 2270 | 209 | 1.7 | 0.02 | 5.94 | 0.04 | 17.12 | 0.09 | 18.09 | 0.33 | -50.0 | 280.0 | 99.1 | 5.9 | 91.0 | 15.0 | 99.1 | 5.9 |
| Output_1_276 | 1604 | 84 | 1.3 | 0.02 | 5.80 | 0.06 | 16.46 | 0.12 | 14.53 | 0.08 | 350.0 | 300.0 | 99.3 | 5.7 | 112.0 | 16.0 | 99.3 | 5.7 |
| Output_1_78 | 7690 | 815 | 1.7 | 0.02 | 5.77 | 0.05 | 8.95 | 0.11 | 10.62 | 0.52 | 310.0 | 220.0 | 99.8 | 5.7 | 109.0 | 11.0 | 99.8 | 5.7 |
| Output_1_297 | 17620 | 1822 | 2.9 | 0.02 | 5.70 | 0.05 | 7.47 | 0.11 | 7.94 | 0.31 | 110.0 | 150.0 | 99.9 | 5.6 | 102.0 | 7.7 | 99.9 | 5.6 |
| Output_1_197 | 37260 | 1393 | 1.1 | 0.02 | 2.93 | 0.05 | 4.88 | 0.10 | 5.02 | 0.36 | 150.0 | 100.0 | 100.3 | 2.9 | 99.9 | 4.8 | 100.3 | 2.9 |
| Output_1_156 | 6050 | 461 | 6.1 | 0.02 | 6.33 | 0.06 | 14.67 | 0.11 | 10.09 | 0.04 | 380.0 | 300.0 | 100.9 | 6.5 | 105.0 | 10.0 | 100.9 | 6.5 |
| Output_1_189 | 3150 | 151 | 1.8 | 0.02 | 4.02 | 0.05 | 13.81 | 0.12 | 14.17 | 0.12 | 260.0 | 280.0 | 101.9 | 4.0 | 114.0 | 15.0 | 101.9 | 4.0 |
| Output_1_138 | 5360 | 239 | 2.3 | 0.02 | 4.57 | 0.05 | 10.10 | 0.11 | 9.21 | 0.07 | 170.0 | 200.0 | 102.2 | 4.7 | 102.3 | 8.9 | 102.2 | 4.7 |
| Output_1_94 | 14110 | 660 | 1.5 | 0.02 | 3.55 | 0.05 | 6.03 | 0.10 | 5.67 | 0.22 | 40.0 | 120.0 | 102.8 | 3.6 | 100.3 | 5.4 | 102.8 | 3.6 |
| Output_1_111 | 11340 | 904 | 1.3 | 0.02 | 4.04 | 0.05 | 6.55 | 0.11 | 6.36 | 0.12 | 260.0 | 140.0 | 102.9 | 4.1 | 108.8 | 6.6 | 102.9 | 4.1 |
| Output_1_287 | 6560 | 331 | 1.3 | 0.02 | 3.93 | 0.05 | 7.69 | 0.12 | 8.15 | 0.14 | 240.0 | 160.0 | 104.2 | 4.0 | 112.7 | 8.7 | 104.2 | 4.0 |
| Output_1_37 | 12620 | 497 | 2.4 | 0.02 | 3.23 | 0.05 | 7.32 | 0.12 | 8.01 | 0.42 | 280.0 | 150.0 | 104.9 | 3.4 | 112.4 | 8.5 | 104.9 | 3.4 |
| Output_1_205 | 5090 | 160 | 2.2 | 0.02 | 7.88 | 0.06 | 20.69 | 0.13 | 19.55 | 0.03 | 440.0 | 440.0 | 105.5 | 8.1 | 126.0 | 24.0 | 105.5 | 8.1 |
| Output_1_268 | 5190 | 394 | 1.1 | 0.02 | 4.59 | 0.05 | 6.33 | 0.11 | 8.19 | 0.45 | 60.0 | 130.0 | 105.9 | 4.8 | 103.3 | 8.0 | 105.9 | 4.8 |
| Output_1_68 | 26200 | 4730 | 3.3 | 0.02 | 4.98 | 0.05 | 8.02 | 0.11 | 8.64 | 0.35 | 70.0 | 160.0 | 106.6 | 5.3 | 108.9 | 9.0 | 106.6 | 5.3 |
| Output_1_215 | 4670 | 211 | 1.7 | 0.02 | 7.78 | 0.05 | 11.33 | 0.12 | 12.10 | 0.26 | 360.0 | 240.0 | 106.6 | 8.3 | 118.0 | 13.0 | 106.6 | 8.3 |
| Output_1_263 | 6310 | 733 | 3.2 | 0.02 | 4.00 | 0.05 | 9.63 | 0.12 | 9.68 | 0.19 | 260.0 | 200.0 | 107.0 | 4.2 | 118.0 | 11.0 | 107.0 | 4.2 |
| Output_1_142 | 21180 | 841 | 3.1 | 0.02 | 3.82 | 0.05 | 6.69 | 0.11 | 6.31 | 0.37 | 180.0 | 140.0 | 107.2 | 4.1 | 108.1 | 6.5 | 107.2 | 4.1 |

| | | | | | | | | | | | | | | | | | | |
|---|---|---|---|---|---|---|---|---|---|---|---|---|---|---|---|---|---|---|
| Output_1_133 | 1865 | 90 | 2.9 | 0.02 | 5.24 | 0.05 | 18.87 | 0.13 | 16.80 | 0.24 | 280.0 | 350.0 | 108.6 | 5.6 | 118.0 | 19.0 | 108.6 | 5.6 |
| Output_1_21 | 28800 | 3730 | 0.8 | 0.02 | 2.51 | 0.05 | 4.24 | 0.12 | 4.65 | 0.36 | 169.0 | 87.0 | 109.3 | 2.7 | 111.5 | 4.9 | 109.3 | 2.7 |
| Output_1_203 | 60000 | 1946 | 1.2 | 0.02 | 4.53 | 0.05 | 2.82 | 0.12 | 3.78 | 0.63 | 186.0 | 67.0 | 110.0 | 4.9 | 114.1 | 4.1 | 110.0 | 4.9 |
| Output_1_273 | 21330 | 1103 | 2.1 | 0.02 | 4.08 | 0.05 | 5.57 | 0.12 | 5.39 | 0.41 | 150.0 | 120.0 | 111.3 | 4.5 | 115.4 | 5.9 | 111.3 | 4.5 |
| Output_1_79 | 5590 | 560 | 1.6 | 0.02 | 6.90 | 0.05 | 17.67 | 0.12 | 17.65 | 0.40 | 230.0 | 340.0 | 111.5 | 7.5 | 113.0 | 20.0 | 111.5 | 7.5 |
| Output_1_101 | 14830 | 752 | 0.8 | 0.02 | 3.30 | 0.05 | 5.94 | 0.12 | 6.87 | 0.57 | 300.0 | 130.0 | 112.2 | 3.7 | 118.3 | 7.7 | 112.2 | 3.7 |
| Output_1_165 | 20900 | 2270 | 2.5 | 0.02 | 6.21 | 0.05 | 9.94 | 0.13 | 11.20 | 0.48 | 320.0 | 210.0 | 113.0 | 7.2 | 120.0 | 12.0 | 113.0 | 7.2 |
| Output_1_103 | 19470 | 1082 | 2.1 | 0.02 | 5.17 | 0.05 | 5.91 | 0.12 | 5.47 | 0.37 | 150.0 | 120.0 | 113.8 | 5.8 | 112.3 | 5.8 | 113.8 | 5.8 |
| Output_1_295 | 2789 | 211 | 0.7 | 0.02 | 6.70 | 0.05 | 14.07 | 0.12 | 11.97 | 0.07 | 100.0 | 250.0 | 114.4 | 7.3 | 112.0 | 13.0 | 114.4 | 7.3 |
| Output_1_34 | 15140 | 570 | 1.4 | 0.02 | 3.89 | 0.05 | 10.69 | 0.13 | 13.49 | 0.21 | 240.0 | 270.0 | 114.9 | 4.4 | 120.0 | 15.0 | 114.9 | 4.4 |
| Output_1_196 | 21170 | 698 | 1.7 | 0.02 | 4.11 | 0.05 | 5.25 | 0.12 | 5.85 | 0.53 | 80.0 | 100.0 | 115.0 | 4.7 | 114.6 | 6.4 | 115.0 | 4.7 |
| Output_1_91 | 2530 | 111 | 3.2 | 0.02 | 7.61 | 0.06 | 16.43 | 0.15 | 16.55 | 0.14 | 470.0 | 330.0 | 117.7 | 9.0 | 137.0 | 21.0 | 117.7 | 9.0 |
| Output_1_51 | 4570 | 222 | 1.2 | 0.02 | 6.91 | 0.05 | 10.19 | 0.12 | 10.92 | 0.49 | 170.0 | 200.0 | 119.8 | 8.2 | 117.0 | 12.0 | 119.8 | 8.2 |
| Output_1_74 | 5440 | 657 | 6.5 | 0.02 | 6.88 | 0.05 | 16.48 | 0.13 | 13.18 | 0.01 | 350.0 | 330.0 | 120.9 | 8.5 | 123.0 | 15.0 | 120.9 | 8.5 |
| Output_1_45 | 3680 | 137 | 7.4 | 0.02 | 5.17 | 0.05 | 17.49 | 0.13 | 16.42 | 0.09 | 240.0 | 330.0 | 121.1 | 6.2 | 127.0 | 19.0 | 121.1 | 6.2 |
| Output_1_55 | 2270 | 149 | 1.8 | 0.02 | 5.79 | 0.05 | 15.42 | 0.13 | 16.54 | 0.27 | 70.0 | 270.0 | 121.3 | 6.7 | 120.0 | 19.0 | 121.3 | 6.7 |
| Output_1_20 | 6090 | 722 | 2.2 | 0.02 | 6.22 | 0.05 | 10.25 | 0.13 | 11.19 | 0.43 | 340.0 | 230.0 | 122.9 | 7.9 | 127.0 | 13.0 | 122.9 | 7.9 |
| Output_1_67 | 5160 | 832 | 1.5 | 0.02 | 2.84 | 0.05 | 9.24 | 0.13 | 9.70 | 0.14 | 160.0 | 180.0 | 123.7 | 3.5 | 127.0 | 12.0 | 123.7 | 3.5 |
| Output_1_70 | 6830 | 961 | 2.5 | 0.02 | 3.49 | 0.05 | 8.76 | 0.14 | 7.75 | 0.15 | 180.0 | 170.0 | 131.8 | 4.5 | 134.4 | 9.6 | 131.8 | 4.5 |
| Output_1_270 | 4230 | 223 | 1.9 | 0.02 | 6.76 | 0.05 | 12.34 | 0.14 | 13.14 | 0.37 | 10.0 | 210.0 | 132.1 | 9.0 | 129.0 | 16.0 | 132.1 | 9.0 |
| Output_1_146 | 9090 | 291 | 1.0 | 0.02 | 4.42 | 0.05 | 5.64 | 0.15 | 6.34 | 0.49 | 260.0 | 120.0 | 138.3 | 6.1 | 145.5 | 8.6 | 138.3 | 6.1 |
| Output_1_172 | 6780 | 614 | 2.1 | 0.02 | 5.86 | 0.05 | 10.81 | 0.16 | 10.06 | 0.29 | 210.0 | 240.0 | 141.8 | 8.4 | 150.0 | 14.0 | 141.8 | 8.4 |
| Output_1_222 | 3570 | 215 | 2.5 | 0.02 | 4.85 | 0.05 | 12.52 | 0.16 | 11.59 | 0.19 | 290.0 | 250.0 | 144.6 | 6.7 | 153.0 | 17.0 | 144.6 | 6.7 |
| Output_1_9 | 13090 | 551 | 0.9 | 0.02 | 4.23 | 0.05 | 6.87 | 0.16 | 6.37 | 0.17 | 280.0 | 140.0 | 145.8 | 6.5 | 148.9 | 8.6 | 145.8 | 6.5 |
| Output_1_97 | 2330 | 79 | 2.9 | 0.02 | 5.65 | 0.04 | 14.22 | 0.15 | 14.86 | 0.05 | -60.0 | 240.0 | 146.5 | 8.3 | 142.0 | 18.0 | 146.5 | 8.3 |
| Output_1_274 | 13140 | 487 | 2.0 | 0.02 | 2.87 | 0.05 | 9.41 | 0.17 | 9.09 | 0.08 | 300.0 | 210.0 | 146.8 | 4.1 | 155.0 | 13.0 | 146.8 | 4.1 |
| Output_1_10 | 5750 | 236 | 1.0 | 0.02 | 3.46 | 0.05 | 9.16 | 0.16 | 9.88 | 0.36 | 250.0 | 180.0 | 149.2 | 5.1 | 154.0 | 14.0 | 149.2 | 5.1 |
| Output_1_219 | 15000 | 626 | 1.3 | 0.02 | 3.88 | 0.05 | 5.27 | 0.16 | 6.71 | 0.50 | 160.0 | 110.0 | 149.5 | 5.7 | 157.3 | 9.6 | 149.5 | 5.7 |
| Output_1_277 | 3590 | 115 | 1.7 | 0.02 | 4.68 | 0.05 | 13.60 | 0.18 | 13.26 | 0.06 | 390.0 | 250.0 | 149.7 | 6.8 | 167.0 | 20.0 | 149.7 | 6.8 |
| Output_1_232 | 5170 | 289 | 1.2 | 0.02 | 3.87 | 0.05 | 10.69 | 0.17 | 10.18 | 0.20 | 180.0 | 210.0 | 149.8 | 5.7 | 156.0 | 15.0 | 149.8 | 5.7 |
| Output_1_238 | 10210 | 614 | 2.6 | 0.02 | 5.04 | 0.05 | 7.74 | 0.16 | 9.15 | 0.47 | 90.0 | 150.0 | 151.5 | 7.6 | 153.0 | 13.0 | 151.5 | 7.6 |
| Output_1_60 | 4030 | 317 | 6.1 | 0.02 | 4.98 | 0.05 | 10.16 | 0.15 | 9.74 | 0.35 | 130.0 | 190.0 | 153.2 | 7.4 | 145.0 | 13.0 | 153.2 | 7.4 |
| Output_1_12 | 14610 | 618 | 3.6 | 0.02 | 2.81 | 0.05 | 6.03 | 0.17 | 6.47 | 0.28 | 260.0 | 130.0 | 154.2 | 4.3 | 159.3 | 9.9 | 154.2 | 4.3 |
| Output_1_198 | 5970 | 143 | 3.2 | 0.02 | 5.35 | 0.05 | 9.51 | 0.17 | 8.19 | 0.11 | 320.0 | 200.0 | 154.9 | 8.4 | 160.0 | 12.0 | 154.9 | 8.4 |
| Output_1_279 | 3320 | 102 | 2.8 | 0.02 | 7.41 | 0.05 | 12.34 | 0.18 | 13.81 | 0.00 | 320.0 | 250.0 | 155.0 | 11.0 | 169.0 | 21.0 | 155.0 | 11.0 |
| Output_1_199 | 2605 | 58 | 2.5 | 0.02 | 5.71 | 0.05 | 12.72 | 0.17 | 12.94 | 0.34 | 240.0 | 250.0 | 156.3 | 8.5 | 158.0 | 19.0 | 156.3 | 8.5 |
| Output_1_145 | 6000 | 170 | 2.4 | 0.02 | 3.98 | 0.05 | 7.38 | 0.17 | 8.43 | 0.49 | 140.0 | 140.0 | 156.8 | 6.2 | 156.0 | 13.0 | 156.8 | 6.2 |
| Output_1_62 | 1370 | 127 | 2.6 | 0.03 | 6.37 | 0.05 | 18.40 | 0.19 | 17.71 | 0.02 | 290.0 | 350.0 | 159.5 | 9.9 | 174.0 | 29.0 | 159.5 | 9.9 |
| Output_1_104 | 7740 | 322 | 1.9 | 0.03 | 8.37 | 0.05 | 10.32 | 0.19 | 12.44 | 0.47 | 400.0 | 230.0 | 160.0 | 13.0 | 178.0 | 20.0 | 160.0 | 13.0 |
| Output_1_6 | 2820 | 122 | 3.7 | 0.03 | 5.12 | 0.05 | 13.75 | 0.17 | 13.79 | 0.03 | 140.0 | 250.0 | 161.9 | 7.9 | 165.0 | 21.0 | 161.9 | 7.9 |

| | | | | | | | | | | | | | | | | | | |
|---|---|---|---|---|---|---|---|---|---|---|---|---|---|---|---|---|---|---|
| Output_1_112 | 8790 | 447 | 1.3 | 0.03 | 5.38 | 0.05 | 10.97 | 0.17 | 8.98 | 0.08 | 150.0 | 220.0 | 165.4 | 9.0 | 160.0 | 14.0 | 165.4 | 9.0 |
| Output_1_123 | 18320 | 893 | 1.7 | 0.03 | 3.33 | 0.05 | 5.95 | 0.18 | 4.97 | 0.20 | 150.0 | 120.0 | 166.3 | 5.4 | 165.3 | 7.6 | 166.3 | 5.4 |
| Output_1_16 | 1805 | 99 | 5.7 | 0.03 | 7.22 | 0.06 | 15.79 | 0.22 | 16.67 | 0.08 | 530.0 | 320.0 | 167.0 | 12.0 | 200.0 | 30.0 | 167.0 | 12.0 |
| Output_1_95 | 3340 | 99 | 3.6 | 0.03 | 4.55 | 0.05 | 11.38 | 0.19 | 9.33 | 0.11 | 320.0 | 210.0 | 167.8 | 7.7 | 178.0 | 15.0 | 167.8 | 7.7 |
| Output_1_69 | 46500 | 5450 | 1.8 | 0.03 | 7.89 | 0.05 | 7.35 | 0.19 | 7.22 | 0.76 | 370.0 | 160.0 | 169.0 | 13.0 | 180.0 | 12.0 | 169.0 | 13.0 |
| Output_1_49 | 25040 | 776 | 1.1 | 0.03 | 2.14 | 0.05 | 5.14 | 0.19 | 4.27 | 0.25 | 290.0 | 110.0 | 172.3 | 3.7 | 176.2 | 6.9 | 172.3 | 3.7 |
| Output_1_216 | 7140 | 208 | 0.8 | 0.03 | 5.17 | 0.05 | 9.33 | 0.19 | 9.38 | 0.34 | 260.0 | 180.0 | 172.4 | 8.8 | 178.0 | 15.0 | 172.4 | 8.8 |
| Output_1_303 | 2810 | 178 | 3.5 | 0.03 | 6.23 | 0.04 | 12.71 | 0.16 | 12.88 | 0.26 | -80.0 | 220.0 | 174.0 | 11.0 | 151.0 | 18.0 | 174.0 | 11.0 |
| Output_1_75 | 3400 | 285 | 2.9 | 0.03 | 7.87 | 0.05 | 15.52 | 0.18 | 15.64 | 0.52 | 150.0 | 290.0 | 174.0 | 12.0 | 166.0 | 24.0 | 174.0 | 12.0 |
| Output_1_179 | 3400 | 175 | 1.3 | 0.03 | 5.09 | 0.06 | 14.26 | 0.21 | 11.21 | 0.29 | 480.0 | 290.0 | 175.0 | 8.8 | 197.0 | 20.0 | 175.0 | 8.8 |
| Output_1_153 | 8640 | 291 | 1.2 | 0.03 | 4.33 | 0.05 | 6.74 | 0.20 | 6.09 | 0.39 | 280.0 | 140.0 | 175.8 | 7.7 | 182.0 | 11.0 | 175.8 | 7.7 |
| Output_1_99 | 2950 | 87 | 2.1 | 0.03 | 6.50 | 0.05 | 16.24 | 0.18 | 14.75 | 0.06 | 160.0 | 300.0 | 176.0 | 11.0 | 173.0 | 23.0 | 176.0 | 11.0 |
| Output_1_211 | 2460 | 58 | 3.1 | 0.03 | 6.09 | 0.06 | 13.71 | 0.21 | 12.80 | 0.12 | 440.0 | 280.0 | 177.0 | 10.0 | 193.0 | 23.0 | 177.0 | 10.0 |
| Output_1_121 | 2250 | 111 | 3.6 | 0.03 | 5.71 | 0.05 | 15.08 | 0.20 | 14.71 | 0.13 | 270.0 | 300.0 | 178.1 | 9.8 | 186.0 | 25.0 | 178.1 | 9.8 |
| Output_1_11 | 19220 | 662 | 1.5 | 0.03 | 2.35 | 0.05 | 5.06 | 0.19 | 5.17 | 0.31 | 160.0 | 110.0 | 178.7 | 4.1 | 176.1 | 8.4 | 178.7 | 4.1 |
| Output_1_109 | 6900 | 296 | 2.3 | 0.03 | 3.27 | 0.05 | 8.59 | 0.19 | 8.06 | 0.12 | 160.0 | 170.0 | 179.1 | 5.7 | 173.0 | 13.0 | 179.1 | 5.7 |
| Output_1_63 | 43600 | 4310 | 1.0 | 0.03 | 4.26 | 0.05 | 4.37 | 0.19 | 4.83 | 0.68 | 220.0 | 100.0 | 179.3 | 7.3 | 181.0 | 8.8 | 179.3 | 7.3 |
| Output_1_257 | 12850 | 1162 | 1.8 | 0.03 | 4.59 | 0.05 | 6.29 | 0.20 | 8.46 | 0.36 | 280.0 | 150.0 | 179.7 | 8.4 | 185.0 | 14.0 | 179.7 | 8.4 |
| Output_1_305 | 3230 | 162 | 4.0 | 0.03 | 6.01 | 0.05 | 15.87 | 0.18 | 15.73 | 0.32 | 110.0 | 290.0 | 180.0 | 11.0 | 165.0 | 24.0 | 180.0 | 11.0 |
| Output_1_24 | 7230 | 406 | 2.1 | 0.03 | 3.87 | 0.05 | 6.94 | 0.20 | 6.53 | 0.32 | 220.0 | 140.0 | 180.3 | 7.1 | 184.0 | 11.0 | 180.3 | 7.1 |
| Output_1_41 | 10000 | 227 | 1.6 | 0.03 | 3.22 | 0.05 | 6.80 | 0.20 | 6.57 | 0.30 | 180.0 | 140.0 | 181.6 | 5.8 | 185.0 | 11.0 | 181.6 | 5.8 |
| Output_1_59 | 16500 | 977 | 1.5 | 0.03 | 3.83 | 0.05 | 6.13 | 0.21 | 5.74 | 0.27 | 330.0 | 130.0 | 182.3 | 6.7 | 192.3 | 9.8 | 182.3 | 6.7 |
| Output_1_46 | 9700 | 242 | 1.6 | 0.03 | 4.10 | 0.05 | 8.41 | 0.22 | 6.98 | 0.01 | 350.0 | 170.0 | 185.9 | 7.7 | 201.0 | 12.0 | 185.9 | 7.7 |
| Output_1_54 | 8990 | 364 | 1.9 | 0.03 | 4.78 | 0.06 | 7.04 | 0.23 | 8.00 | 0.53 | 430.0 | 150.0 | 185.9 | 8.5 | 205.0 | 15.0 | 185.9 | 8.5 |
| Output_1_131 | 27970 | 861 | 1.4 | 0.03 | 3.75 | 0.05 | 3.93 | 0.21 | 5.31 | 0.67 | 243.0 | 88.0 | 186.4 | 6.9 | 190.7 | 9.6 | 186.4 | 6.9 |
| Output_1_122 | 6030 | 266 | 2.3 | 0.03 | 3.73 | 0.05 | 9.90 | 0.21 | 9.95 | 0.05 | 260.0 | 200.0 | 187.2 | 7.0 | 193.0 | 17.0 | 187.2 | 7.0 |
| Output_1_236 | 19960 | 935 | 1.3 | 0.03 | 3.37 | 0.05 | 5.26 | 0.22 | 5.99 | 0.46 | 310.0 | 110.0 | 188.6 | 6.2 | 199.0 | 11.0 | 188.6 | 6.2 |
| Output_1_266 | 5860 | 282 | 4.6 | 0.03 | 5.72 | 0.05 | 9.70 | 0.21 | 11.54 | 0.38 | 280.0 | 200.0 | 189.0 | 11.0 | 196.0 | 18.0 | 189.0 | 11.0 |
| Output_1_190 | 8930 | 225 | 2.1 | 0.03 | 9.36 | 0.05 | 9.32 | 0.21 | 7.98 | 0.44 | 430.0 | 220.0 | 190.0 | 17.0 | 196.0 | 15.0 | 190.0 | 17.0 |
| Output_1_124 | 21610 | 872 | 1.5 | 0.03 | 3.64 | 0.05 | 5.81 | 0.22 | 6.02 | 0.30 | 320.0 | 120.0 | 191.6 | 6.6 | 198.0 | 11.0 | 191.6 | 6.6 |
| Output_1_129 | 6280 | 205 | 2.7 | 0.03 | 4.29 | 0.05 | 9.34 | 0.22 | 8.80 | 0.21 | 260.0 | 190.0 | 192.1 | 8.0 | 198.0 | 16.0 | 192.1 | 8.0 |
| Output_1_130 | 4250 | 131 | 1.8 | 0.03 | 4.95 | 0.05 | 11.04 | 0.20 | 12.81 | 0.45 | 100.0 | 210.0 | 192.5 | 9.2 | 191.0 | 23.0 | 192.5 | 9.2 |
| Output_1_289 | 3120 | 91 | 3.6 | 0.03 | 5.56 | 0.05 | 11.42 | 0.21 | 12.68 | 0.44 | 60.0 | 200.0 | 194.0 | 10.0 | 187.0 | 22.0 | 194.0 | 10.0 |
| Output_1_267 | 2570 | 112 | 3.2 | 0.03 | 8.82 | 0.06 | 17.46 | 0.25 | 15.87 | 0.27 | 550.0 | 340.0 | 194.0 | 17.0 | 226.0 | 32.0 | 194.0 | 17.0 |
| Output_1_262 | 14970 | 1011 | 1.8 | 0.03 | 3.15 | 0.05 | 4.87 | 0.23 | 5.73 | 0.32 | 340.0 | 100.0 | 195.6 | 6.0 | 208.0 | 10.0 | 195.6 | 6.0 |
| Output_1_110 | 3800 | 145 | 3.1 | 0.03 | 4.49 | 0.05 | 11.56 | 0.22 | 11.93 | 0.19 | 230.0 | 210.0 | 197.7 | 8.7 | 203.0 | 21.0 | 197.7 | 8.7 |
| Output_1_82 | 3300 | 143 | 1.9 | 0.03 | 5.36 | 0.05 | 11.42 | 0.23 | 10.22 | 0.05 | 190.0 | 220.0 | 201.0 | 11.0 | 204.0 | 20.0 | 201.0 | 11.0 |
| Output_1_249 | 12100 | 965 | 3.1 | 0.03 | 3.79 | 0.05 | 6.55 | 0.23 | 6.96 | 0.29 | 260.0 | 140.0 | 201.1 | 7.4 | 210.0 | 13.0 | 201.1 | 7.4 |
| Output_1_237 | 8400 | 372 | 3.1 | 0.03 | 5.00 | 0.05 | 8.22 | 0.22 | 9.17 | 0.30 | 170.0 | 160.0 | 203.0 | 10.0 | 199.0 | 16.0 | 203.0 | 10.0 |
| Output_1_132 | 3900 | 102 | 3.0 | 0.03 | 6.79 | 0.06 | 19.05 | 0.28 | 22.02 | 0.67 | 830.0 | 370.0 | 205.0 | 14.0 | 245.0 | 48.0 | 205.0 | 14.0 |

| | | | | | | | | | | | | | | | | | | |
|---|---|---|---|---|---|---|---|---|---|---|---|---|---|---|---|---|---|---|
| Output_1_252 | 27500 | 2330 | 1.8 | 0.03 | 5.54 | 0.05 | 4.68 | 0.23 | 5.63 | 0.58 | 240.0 | 100.0 | 206.0 | 11.0 | 210.0 | 10.0 | 206.0 | 11.0 |
| Output_1_42 | 2350 | 46 | 2.1 | 0.03 | 5.04 | 0.05 | 16.84 | 0.22 | 15.38 | 0.17 | 80.0 | 290.0 | 213.0 | 11.0 | 199.0 | 29.0 | 213.0 | 11.0 |
| Output_1_244 | 2530 | 151 | 3.8 | 0.03 | 4.96 | 0.05 | 13.74 | 0.27 | 13.65 | 0.08 | 510.0 | 250.0 | 217.0 | 11.0 | 251.0 | 27.0 | 217.0 | 11.0 |
| Output_1_178 | 14030 | 623 | 3.3 | 0.03 | 4.62 | 0.05 | 6.31 | 0.24 | 7.05 | 0.48 | 150.0 | 130.0 | 219.0 | 9.7 | 219.0 | 14.0 | 219.0 | 9.7 |
| Output_1_105 | 8810 | 234 | 2.5 | 0.04 | 6.81 | 0.05 | 11.00 | 0.27 | 7.78 | 0.09 | 210.0 | 230.0 | 242.0 | 16.0 | 242.0 | 17.0 | 242.0 | 16.0 |
| Output_1_38 | 18600 | 299 | 1.9 | 0.04 | 3.06 | 0.05 | 6.36 | 0.28 | 6.41 | 0.06 | 250.0 | 130.0 | 247.9 | 7.4 | 251.0 | 14.0 | 247.9 | 7.4 |
| Output_1_158 | 4110 | 125 | 3.3 | 0.04 | 5.45 | 0.05 | 10.02 | 0.28 | 11.43 | 0.52 | 100.0 | 170.0 | 255.0 | 14.0 | 254.0 | 27.0 | 255.0 | 14.0 |
| Output_1_278 | 26060 | 479 | 4.2 | 0.04 | 3.92 | 0.05 | 4.62 | 0.30 | 6.02 | 0.48 | 269.0 | 98.0 | 257.0 | 10.0 | 265.0 | 14.0 | 257.0 | 10.0 |
| Output_1_18 | 8870 | 426 | 1.7 | 0.04 | 3.92 | 0.05 | 7.00 | 0.29 | 7.32 | 0.28 | 240.0 | 140.0 | 258.0 | 10.0 | 255.0 | 16.0 | 258.0 | 10.0 |
| Output_1_217 | 21320 | 437 | 3.8 | 0.04 | 3.13 | 0.05 | 5.60 | 0.30 | 5.32 | 0.19 | 330.0 | 120.0 | 262.2 | 8.1 | 267.0 | 12.0 | 262.2 | 8.1 |
| Output_1_106 | 1950 | 49 | 0.5 | 0.04 | 6.34 | 0.05 | 14.89 | 0.32 | 13.66 | 0.07 | 280.0 | 270.0 | 269.0 | 16.0 | 279.0 | 34.0 | 269.0 | 16.0 |
| Output_1_23 | 6490 | 266 | 1.0 | 0.04 | 3.63 | 0.05 | 8.59 | 0.32 | 9.35 | 0.28 | 290.0 | 180.0 | 277.9 | 9.8 | 280.0 | 23.0 | 277.9 | 9.8 |
| Output_1_19 | 81900 | 3830 | 4.7 | 0.04 | 2.95 | 0.06 | 3.59 | 0.34 | 4.17 | 0.61 | 425.0 | 81.0 | 278.4 | 7.9 | 294.0 | 10.0 | 278.4 | 7.9 |
| Output_1_64 | 10090 | 641 | 1.6 | 0.04 | 3.56 | 0.05 | 6.38 | 0.34 | 6.76 | 0.40 | 400.0 | 130.0 | 283.0 | 10.0 | 296.0 | 17.0 | 283.0 | 10.0 |
| Output_1_186 | 21400 | 360 | 1.4 | 0.05 | 3.57 | 0.06 | 5.99 | 0.38 | 6.32 | 0.52 | 390.0 | 130.0 | 317.0 | 11.0 | 326.0 | 18.0 | 317.0 | 11.0 |
| Output_1_151 | 9650 | 160 | 2.5 | 0.05 | 2.70 | 0.06 | 5.76 | 0.43 | 6.00 | 0.27 | 590.0 | 130.0 | 325.8 | 8.3 | 364.0 | 19.0 | 325.8 | 8.3 |
| Output_1_182 | 14200 | 294 | 1.4 | 0.05 | 3.63 | 0.05 | 7.82 | 0.37 | 7.95 | 0.34 | 190.0 | 160.0 | 328.0 | 12.0 | 314.0 | 21.0 | 328.0 | 12.0 |
| Output_1_261 | 41200 | 1670 | 0.7 | 0.05 | 5.67 | 0.06 | 5.15 | 0.45 | 8.43 | 0.79 | 590.0 | 110.0 | 332.0 | 18.0 | 374.0 | 27.0 | 332.0 | 18.0 |
| Output_1_180 | 26700 | 657 | 1.6 | 0.05 | 4.07 | 0.06 | 4.50 | 0.41 | 5.37 | 0.60 | 413.0 | 97.0 | 339.0 | 13.0 | 348.0 | 16.0 | 339.0 | 13.0 |
| Output_1_187 | 7280 | 114 | 2.2 | 0.05 | 5.18 | 0.06 | 6.89 | 0.46 | 6.49 | 0.06 | 680.0 | 150.0 | 339.0 | 17.0 | 384.0 | 21.0 | 339.0 | 17.0 |
| Output_1_299 | 19470 | 664 | 2.4 | 0.05 | 3.67 | 0.06 | 4.33 | 0.45 | 4.91 | 0.57 | 599.0 | 99.0 | 342.0 | 12.0 | 375.0 | 15.0 | 342.0 | 12.0 |
| Output_1_298 | 48100 | 1541 | 1.9 | 0.06 | 5.23 | 0.06 | 7.12 | 0.42 | 5.25 | 0.33 | 440.0 | 160.0 | 347.0 | 18.0 | 355.0 | 16.0 | 347.0 | 18.0 |
| Output_1_223 | 19210 | 508 | 0.9 | 0.06 | 4.85 | 0.05 | 5.39 | 0.42 | 5.06 | 0.47 | 350.0 | 120.0 | 349.0 | 17.0 | 352.0 | 16.0 | 349.0 | 17.0 |
| Output_1_207 | 11450 | 117 | 1.7 | 0.06 | 5.20 | 0.05 | 6.39 | 0.42 | 7.57 | 0.45 | 400.0 | 140.0 | 350.0 | 18.0 | 357.0 | 23.0 | 350.0 | 18.0 |
| Output_1_271 | 28880 | 516 | 1.4 | 0.06 | 4.63 | 0.06 | 6.18 | 0.43 | 5.76 | 0.40 | 400.0 | 140.0 | 352.0 | 16.0 | 368.0 | 18.0 | 352.0 | 16.0 |
| Output_1_181 | 36400 | 733 | 2.6 | 0.06 | 4.42 | 0.05 | 4.29 | 0.41 | 4.62 | 0.65 | 352.0 | 98.0 | 354.0 | 15.0 | 348.0 | 14.0 | 354.0 | 15.0 |
| Output_1_281 | 53800 | 686 | 1.6 | 0.06 | 3.00 | 0.06 | 4.00 | 0.46 | 4.17 | 0.39 | 491.0 | 91.0 | 355.0 | 10.0 | 381.0 | 14.0 | 355.0 | 10.0 |
| Output_1_170 | 38260 | 1379 | 2.0 | 0.06 | 3.35 | 0.06 | 2.75 | 0.46 | 3.91 | 0.74 | 533.0 | 64.0 | 356.0 | 12.0 | 383.0 | 12.0 | 356.0 | 12.0 |
| Output_1_148 | 27320 | 343 | 2.1 | 0.06 | 4.04 | 0.05 | 2.97 | 0.43 | 3.98 | 0.71 | 350.0 | 67.0 | 357.0 | 14.0 | 360.0 | 12.0 | 357.0 | 14.0 |
| Output_1_177 | 49300 | 1438 | 1.3 | 0.06 | 5.37 | 0.06 | 4.86 | 0.43 | 4.44 | 0.54 | 430.0 | 110.0 | 361.0 | 19.0 | 361.0 | 14.0 | 361.0 | 19.0 |
| Output_1_304 | 9370 | 257 | 2.3 | 0.06 | 3.46 | 0.05 | 7.12 | 0.43 | 6.81 | 0.15 | 330.0 | 150.0 | 362.0 | 12.0 | 362.0 | 20.0 | 362.0 | 12.0 |
| Output_1_118 | 22830 | 595 | 2.3 | 0.06 | 7.68 | 0.06 | 6.34 | 0.48 | 5.42 | 0.54 | 730.0 | 140.0 | 367.0 | 27.0 | 397.0 | 18.0 | 367.0 | 27.0 |
| Output_1_212 | 31640 | 371 | 4.7 | 0.06 | 4.27 | 0.06 | 4.16 | 0.46 | 5.05 | 0.56 | 443.0 | 92.0 | 369.0 | 16.0 | 380.0 | 16.0 | 369.0 | 16.0 |
| Output_1_208 | 14870 | 134 | 2.2 | 0.06 | 4.17 | 0.05 | 6.22 | 0.49 | 7.13 | 0.56 | 410.0 | 140.0 | 405.0 | 16.0 | 403.0 | 24.0 | 405.0 | 16.0 |
| Output_1_290 | 58800 | 846 | 1.7 | 0.07 | 3.05 | 0.06 | 3.65 | 0.53 | 3.99 | 0.46 | 495.0 | 81.0 | 410.0 | 12.0 | 428.0 | 14.0 | 410.0 | 12.0 |
| Output_1_43 | 28230 | 276 | 1.2 | 0.07 | 3.25 | 0.06 | 3.79 | 0.54 | 4.06 | 0.45 | 530.0 | 88.0 | 422.0 | 13.0 | 439.0 | 15.0 | 422.0 | 13.0 |
| Output_1_256 | 27860 | 1075 | 1.7 | 0.07 | 4.41 | 0.06 | 4.60 | 0.54 | 5.55 | 0.59 | 530.0 | 110.0 | 425.0 | 18.0 | 438.0 | 20.0 | 425.0 | 18.0 |
| Output_1_176 | 56200 | 1367 | 2.6 | 0.07 | 3.13 | 0.06 | 3.89 | 0.56 | 3.60 | 0.36 | 558.0 | 89.0 | 437.0 | 14.0 | 448.0 | 13.0 | 437.0 | 14.0 |
| Output_1_47 | 9270 | 93 | 1.2 | 0.08 | 2.74 | 0.06 | 7.16 | 0.61 | 7.00 | 0.11 | 530.0 | 150.0 | 477.0 | 12.0 | 483.0 | 27.0 | 477.0 | 12.0 |
| Output_1_269 | 15460 | 224 | 2.5 | 0.08 | 4.13 | 0.06 | 7.15 | 0.63 | 7.28 | 0.29 | 550.0 | 150.0 | 481.0 | 19.0 | 494.0 | 28.0 | 481.0 | 19.0 |

| | | | | | | | | | | | | | | | | | | |
|---|---|---|---|---|---|---|---|---|---|---|---|---|---|---|---|---|---|---|
| Output_1_61 | 3040 | 77 | 3.9 | 0.08 | 4.89 | 0.06 | 11.41 | 0.62 | 13.33 | 0.30 | 460.0 | 240.0 | 494.0 | 23.0 | 485.0 | 49.0 | 494.0 | 23.0 |
| Output_1_58 | 27490 | 433 | 5.2 | 0.10 | 3.99 | 0.06 | 5.12 | 0.80 | 5.23 | 0.35 | 610.0 | 110.0 | 616.0 | 23.0 | 605.0 | 23.0 | 616.0 | 23.0 |
| Output_1_251 | 13440 | 353 | 2.7 | 0.10 | 7.54 | 0.08 | 6.99 | 1.09 | 10.09 | 0.72 | 1100.0 | 140.0 | 618.0 | 45.0 | 745.0 | 56.0 | 618.0 | 45.0 |
| Output_1_246 | 7520 | 167 | 1.4 | 0.10 | 5.90 | 0.06 | 9.06 | 0.84 | 8.89 | 0.41 | 510.0 | 190.0 | 623.0 | 35.0 | 621.0 | 44.0 | 623.0 | 35.0 |
| Output_1_159 | 18960 | 253 | 1.3 | 0.10 | 6.11 | 0.08 | 5.53 | 1.09 | 10.09 | 0.87 | 1121.0 | 93.0 | 623.0 | 36.0 | 746.0 | 56.0 | 623.0 | 36.0 |
| Output_1_247 | 10800 | 237 | 3.1 | 0.10 | 6.65 | 0.06 | 7.42 | 0.92 | 9.11 | 0.55 | 680.0 | 160.0 | 627.0 | 40.0 | 659.0 | 44.0 | 627.0 | 40.0 |
| Output_1_288 | 7540 | 63 | 0.7 | 0.10 | 4.57 | 0.06 | 7.50 | 0.92 | 7.96 | 0.24 | 730.0 | 170.0 | 631.0 | 28.0 | 661.0 | 38.0 | 631.0 | 28.0 |
| Output_1_33 | 18400 | 121 | 0.7 | 0.11 | 3.20 | 0.06 | 4.44 | 0.92 | 4.90 | 0.43 | 719.0 | 99.0 | 649.0 | 20.0 | 673.0 | 23.0 | 649.0 | 20.0 |
| Output_1_152 | 47800 | 364 | 9.9 | 0.12 | 3.21 | 0.07 | 4.14 | 1.10 | 4.18 | 0.39 | 852.0 | 82.0 | 721.0 | 22.0 | 751.0 | 23.0 | 721.0 | 22.0 |
| Output_1_77 | 17390 | 268 | 6.8 | 0.12 | 3.91 | 0.10 | 3.56 | 1.63 | 3.94 | 0.58 | 1581.0 | 68.0 | 746.0 | 28.0 | 983.0 | 26.0 | 746.0 | 28.0 |
| Output_1_128 | 89800 | 669 | 4.0 | 0.14 | 4.80 | 0.11 | 4.84 | 2.05 | 6.34 | 0.64 | 1818.0 | 89.0 | 831.0 | 38.0 | ##### | 50.0 | 831.0 | 38.0 |
| Output_1_137 | 21750 | 109 | 1.4 | 0.15 | 4.24 | 0.07 | 5.12 | 1.47 | 5.43 | 0.46 | 980.0 | 100.0 | 878.0 | 35.0 | 915.0 | 33.0 | 878.0 | 35.0 |
| Output_1_155 | 80500 | 526 | 1.7 | 0.16 | 2.85 | 0.07 | 2.60 | 1.60 | 3.37 | 0.62 | 1027.0 | 48.0 | 944.0 | 25.0 | 969.0 | 21.0 | 1027.0 | 48.0 |
| Output_1_127 | 26630 | 176 | 2.9 | 0.16 | 3.23 | 0.07 | 3.88 | 1.63 | 4.42 | 0.59 | 1065.0 | 74.0 | 962.0 | 29.0 | 979.0 | 28.0 | 1065.0 | 74.0 |
| Output_1_7 | 12160 | 76 | 0.7 | 0.16 | 4.37 | 0.08 | 4.93 | 1.71 | 5.37 | 0.46 | 1080.0 | 100.0 | 983.0 | 40.0 | ##### | 36.0 | 1080.0 | 100.0 |
| Output_1_50 | 12950 | 58 | 2.2 | 0.19 | 3.85 | 0.08 | 4.52 | 2.05 | 4.88 | 0.48 | 1108.0 | 92.0 | 1118.0 | 40.0 | ##### | 33.0 | 1108.0 | 92.0 |
| Output_1_284 | 93500 | 351 | 1.6 | 0.20 | 5.13 | 0.08 | 2.68 | 2.10 | 5.24 | 0.83 | 1147.0 | 54.0 | 1166.0 | 50.0 | ##### | 38.0 | 1147.0 | 54.0 |
| Output_1_191 | 68200 | 231 | 1.0 | 0.20 | 4.30 | 0.08 | 5.26 | 2.21 | 2.94 | 0.08 | 1152.0 | 99.0 | 1187.0 | 46.0 | ##### | 21.0 | 1152.0 | 99.0 |
| Output_1_150 | 24300 | 103 | 18.3 | 0.19 | 4.04 | 0.08 | 4.31 | 2.14 | 5.14 | 0.47 | 1291.0 | 89.0 | 1109.0 | 41.0 | ##### | 35.0 | 1291.0 | 89.0 |
| Output_1_184 | 46100 | 216 | 1.7 | 0.21 | 3.55 | 0.09 | 3.60 | 2.40 | 3.71 | 0.55 | 1325.0 | 70.0 | 1203.0 | 39.0 | ##### | 27.0 | 1325.0 | 70.0 |
| Output_1_194 | 42920 | 118 | 2.3 | 0.23 | 2.19 | 0.09 | 2.70 | 2.82 | 3.02 | 0.39 | 1406.0 | 54.0 | 1322.0 | 26.0 | ##### | 23.0 | 1406.0 | 54.0 |
| Output_1_39 | 41900 | 117 | 1.1 | 0.23 | 3.64 | 0.09 | 2.67 | 2.85 | 3.86 | 0.76 | 1414.0 | 52.0 | 1336.0 | 44.0 | ##### | 29.0 | 1414.0 | 52.0 |
| Output_1_255 | 31810 | 355 | 2.8 | 0.24 | 3.46 | 0.09 | 3.39 | 2.95 | 3.15 | 0.53 | 1467.0 | 69.0 | 1392.0 | 45.0 | ##### | 24.0 | 1467.0 | 69.0 |
| Output_1_5 | 72400 | 316 | 2.9 | 0.25 | 3.30 | 0.09 | 3.02 | 3.26 | 3.68 | 0.72 | 1479.0 | 56.0 | 1446.0 | 43.0 | ##### | 29.0 | 1479.0 | 56.0 |
| Output_1_29 | 38660 | 134 | 1.2 | 0.28 | 3.43 | 0.10 | 3.40 | 3.85 | 4.16 | 0.56 | 1644.0 | 61.0 | 1602.0 | 49.0 | ##### | 31.0 | 1644.0 | 61.0 |
| Output_1_296 | 70600 | 467 | 2.1 | 0.24 | 5.88 | 0.10 | 2.88 | 3.46 | 5.20 | 0.86 | 1710.0 | 57.0 | 1372.0 | 72.0 | ##### | 41.0 | 1710.0 | 57.0 |
| Output_1_100 | 33840 | 92 | 1.5 | 0.31 | 4.23 | 0.11 | 4.34 | 4.68 | 4.06 | 0.45 | 1752.0 | 79.0 | 1721.0 | 66.0 | ##### | 34.0 | 1752.0 | 79.0 |
| Output_1_48 | 48300 | 120 | 2.8 | 0.32 | 4.02 | 0.11 | 4.90 | 4.88 | 4.10 | 0.48 | 1798.0 | 92.0 | 1800.0 | 63.0 | ##### | 34.0 | 1798.0 | 92.0 |
| Output_1_117 | 164600 | 766 | 62.1 | 0.30 | 2.15 | 0.12 | 1.70 | 4.95 | 2.63 | 0.79 | 1920.0 | 31.0 | 1700.0 | 32.0 | ##### | 23.0 | 1920.0 | 31.0 |
| Output_1_86 | 127000 | 361 | 3.9 | 0.35 | 4.00 | 0.12 | 3.14 | 5.79 | 3.63 | 0.65 | 1965.0 | 56.0 | 1930.0 | 68.0 | ##### | 32.0 | 1965.0 | 56.0 |
| Output_1_89 | 280100 | 680 | 1.2 | 0.36 | 2.31 | 0.13 | 2.27 | 6.10 | 2.62 | 0.70 | 2073.0 | 39.0 | 1960.0 | 39.0 | ##### | 22.0 | 2073.0 | 39.0 |
| Output_1_272 | 68200 | 189 | 1.9 | 0.34 | 3.22 | 0.13 | 3.11 | 6.29 | 4.45 | 0.73 | 2115.0 | 55.0 | 1896.0 | 54.0 | ##### | 40.0 | 2115.0 | 55.0 |
| Output_1_229 | 108900 | 452 | 1.7 | 0.34 | 3.85 | 0.14 | 3.70 | 6.37 | 3.77 | 0.78 | 2191.0 | 66.0 | 1874.0 | 64.0 | ##### | 37.0 | 2191.0 | 66.0 |
| Output_1_92 | 96700 | 225 | 1.1 | 0.33 | 2.79 | 0.14 | 2.35 | 6.38 | 2.35 | 0.57 | 2231.0 | 40.0 | 1851.0 | 45.0 | ##### | 22.0 | 2231.0 | 40.0 |
| Output_1_88 | 327000 | 679 | 30.8 | 0.42 | 3.79 | 0.15 | 2.72 | 9.19 | 3.70 | 0.68 | 2398.0 | 50.0 | 2267.0 | 72.0 | ##### | 33.0 | 2398.0 | 50.0 |
| Output_1_283 | 55800 | 81 | 3.4 | 0.51 | 4.33 | 0.19 | 3.07 | 13.59 | 3.53 | 0.76 | 2695.0 | 51.0 | 2642.0 | 92.0 | ##### | 35.0 | 2695.0 | 51.0 |
| Output_1_139 | 48310 | 69 | 0.6 | 0.49 | 2.25 | 0.19 | 2.06 | 12.56 | 2.47 | 0.56 | 2740.0 | 33.0 | 2559.0 | 46.0 | ##### | 23.0 | 2740.0 | 33.0 |
| Output_1_167 | 91100 | 362 | 0.9 | 0.50 | 4.41 | 0.19 | 2.93 | 13.86 | 3.75 | 0.72 | 2793.0 | 53.0 | 2603.0 | 95.0 | ##### | 36.0 | 2793.0 | 53.0 |

**Sample 19ATW04**

| | | | | | | | | | | | | | | | | | | |
|---|---|---|---|---|---|---|---|---|---|---|---|---|---|---|---|---|---|---|
| Output_1_115 | 5650 | 485 | 7.3 | 0.01 | 2.84 | 0.05 | 7.95 | 0.05 | 7.10 | 0.05 | 52.9 | 150.0 | 54.3 | 1.5 | 20.0 | 3.6 | 54.3 | 1.9 |
| Output_1_20 | 5660 | 1141 | 36.0 | 0.01 | 4.16 | 0.05 | 16.77 | 0.06 | 16.23 | 0.18 | 60.0 | 320.0 | 55.5 | 2.3 | 200.0 | 9.5 | 55.5 | 2.5 |
| Output_1_76 | 4050 | 225 | 7.3 | 0.01 | 6.95 | 0.06 | 17.54 | 0.07 | 16.67 | 0.06 | 71.0 | 410.0 | 61.0 | 4.2 | 510.0 | 12.0 | 61.0 | 4.4 |
| Output_1_211 | 3400 | 497 | 3.2 | 0.01 | 4.52 | 0.06 | 15.26 | 0.07 | 18.57 | 0.33 | 68.0 | 310.0 | 61.1 | 2.8 | 380.0 | 12.0 | 61.1 | 3.0 |
| Output_1_77 | 5780 | 304 | 1.7 | 0.01 | 4.30 | 0.05 | 10.45 | 0.06 | 10.33 | 0.16 | 61.7 | 200.0 | 61.2 | 2.6 | 120.0 | 6.2 | 61.2 | 2.9 |
| Output_1_183 | 1592 | 367 | 3.5 | 0.01 | 5.64 | 0.05 | 12.27 | 0.07 | 12.75 | 0.14 | 63.8 | 220.0 | 62.5 | 3.5 | 80.0 | 7.8 | 62.5 | 3.8 |
| Output_1_232 | 4930 | 372 | 9.3 | 0.01 | 7.68 | 0.05 | 11.57 | 0.07 | 12.28 | 0.41 | 67.8 | 220.0 | 62.6 | 4.8 | 190.0 | 8.0 | 62.6 | 4.9 |
| Output_1_184 | 17740 | 4860 | 66.5 | 0.01 | 2.74 | 0.05 | 7.05 | 0.07 | 7.45 | 0.49 | 64.7 | 140.0 | 63.3 | 1.7 | 110.0 | 4.7 | 63.3 | 2.2 |
| Output_1_29 | 6820 | 848 | 5.2 | 0.01 | 3.13 | 0.05 | 7.96 | 0.07 | 7.82 | 0.37 | 65.3 | 160.0 | 63.4 | 2.0 | 170.0 | 4.9 | 63.4 | 2.3 |
| Output_1_119 | 5740 | 494 | 1.2 | 0.01 | 3.54 | 0.05 | 10.34 | 0.07 | 8.62 | 0.14 | 64.8 | 190.0 | 63.5 | 2.3 | 100.0 | 5.4 | 63.5 | 2.6 |
| Output_1_185 | 6520 | 1993 | 7.2 | 0.01 | 3.68 | 0.05 | 11.30 | 0.07 | 11.48 | 0.13 | 68.5 | 220.0 | 64.4 | 2.4 | 150.0 | 7.7 | 64.4 | 2.7 |
| Output_1_133 | 6820 | 564 | 4.0 | 0.01 | 4.27 | 0.05 | 10.34 | 0.07 | 10.33 | 0.09 | 67.3 | 190.0 | 64.5 | 2.8 | 140.0 | 6.8 | 64.5 | 3.1 |
| Output_1_156 | 3110 | 281 | 0.8 | 0.01 | 3.44 | 0.05 | 16.70 | 0.07 | 14.24 | 0.28 | 65.9 | 300.0 | 65.2 | 2.2 | 150.0 | 9.1 | 65.2 | 2.6 |
| Output_1_90 | 33200 | 2016 | 94.6 | 0.01 | 3.81 | 0.05 | 7.23 | 0.07 | 7.57 | 0.30 | 66.1 | 140.0 | 65.6 | 2.5 | 60.0 | 4.9 | 65.6 | 2.8 |
| Output_1_46 | 5500 | 545 | 6.5 | 0.01 | 5.36 | 0.06 | 16.64 | 0.08 | 16.00 | 0.44 | 74.0 | 340.0 | 65.9 | 3.5 | 340.0 | 11.0 | 65.9 | 3.8 |
| Output_1_18 | 4170 | 754 | 7.5 | 0.01 | 3.46 | 0.05 | 10.93 | 0.08 | 12.34 | 0.13 | 76.6 | 230.0 | 66.7 | 2.3 | 420.0 | 8.6 | 66.7 | 2.7 |
| Output_1_61 | 3860 | 321 | 2.0 | 0.01 | 6.15 | 0.05 | 10.76 | 0.07 | 11.04 | 0.37 | 71.7 | 210.0 | 66.7 | 4.1 | 300.0 | 7.6 | 66.7 | 4.3 |
| Output_1_84 | 3660 | 184 | 1.8 | 0.01 | 3.93 | 0.05 | 12.63 | 0.07 | 12.48 | 0.01 | 72.7 | 260.0 | 66.9 | 2.6 | 220.0 | 8.8 | 66.9 | 2.9 |
| Output_1_88 | 4770 | 258 | 3.4 | 0.01 | 7.52 | 0.05 | 11.32 | 0.07 | 11.82 | 0.43 | 66.4 | 220.0 | 67.3 | 5.0 | 60.0 | 7.6 | 67.3 | 5.2 |
| Output_1_12 | 6900 | 1030 | 13.2 | 0.01 | 7.39 | 0.06 | 18.97 | 0.08 | 15.00 | 0.33 | 78.0 | 400.0 | 67.7 | 4.9 | 450.0 | 11.0 | 67.7 | 5.1 |
| Output_1_245 | 7170 | 353 | 6.5 | 0.01 | 3.58 | 0.05 | 11.58 | 0.07 | 11.48 | 0.28 | 69.8 | 220.0 | 68.1 | 2.5 | 170.0 | 7.8 | 68.1 | 2.8 |
| Output_1_92 | 2850 | 176 | 1.7 | 0.01 | 4.80 | 0.05 | 16.15 | 0.08 | 15.19 | 0.19 | 76.0 | 290.0 | 68.2 | 3.3 | 190.0 | 12.0 | 68.2 | 3.6 |
| Output_1_196 | 5120 | 389 | 4.2 | 0.01 | 3.93 | 0.05 | 10.39 | 0.07 | 9.48 | 0.11 | 71.2 | 200.0 | 68.4 | 2.7 | 210.0 | 6.6 | 68.4 | 3.0 |
| Output_1_5 | 4120 | 302 | 1.9 | 0.01 | 4.57 | 0.05 | 13.18 | 0.07 | 13.00 | 0.19 | 70.6 | 240.0 | 68.8 | 3.1 | 120.0 | 8.9 | 68.8 | 3.4 |
| Output_1_95 | 2238 | 143 | 1.5 | 0.01 | 5.84 | 0.05 | 14.61 | 0.08 | 14.10 | 0.08 | 76.0 | 270.0 | 69.1 | 4.0 | 300.0 | 10.0 | 69.1 | 4.3 |
| Output_1_207 | 6700 | 747 | 9.7 | 0.01 | 2.97 | 0.05 | 9.77 | 0.07 | 9.30 | 0.09 | 68.4 | 190.0 | 69.2 | 2.0 | 120.0 | 6.2 | 69.2 | 2.5 |
| Output_1_147 | 3200 | 178 | 1.3 | 0.01 | 4.81 | 0.05 | 14.06 | 0.08 | 12.87 | 0.04 | 74.8 | 240.0 | 69.3 | 3.3 | 260.0 | 9.3 | 69.3 | 3.6 |
| Output_1_190 | 5180 | 7470 | 1.0 | 0.01 | 4.16 | 0.05 | 9.50 | 0.07 | 9.67 | 0.29 | 70.8 | 190.0 | 69.3 | 2.9 | 220.0 | 6.7 | 69.3 | 3.2 |
| Output_1_158 | 2940 | 341 | 1.5 | 0.01 | 5.27 | 0.05 | 18.60 | 0.07 | 18.31 | 0.13 | 69.0 | 330.0 | 69.4 | 3.6 | 50.0 | 13.0 | 69.4 | 3.9 |
| Output_1_78 | 5610 | 261 | 1.5 | 0.01 | 4.99 | 0.05 | 9.56 | 0.07 | 8.17 | 0.19 | 71.8 | 180.0 | 69.4 | 3.4 | 170.0 | 5.7 | 69.4 | 3.7 |
| Output_1_142 | 2490 | 208 | 1.6 | 0.01 | 5.81 | 0.06 | 22.81 | 0.08 | 23.81 | 0.04 | 81.0 | 450.0 | 69.5 | 4.0 | 360.0 | 19.0 | 69.5 | 4.2 |
| Output_1_204 | 3970 | 392 | 2.0 | 0.01 | 3.96 | 0.05 | 11.75 | 0.08 | 11.05 | 0.09 | 74.1 | 220.0 | 69.7 | 2.7 | 270.0 | 7.9 | 69.7 | 3.0 |
| Output_1_240 | 14090 | 652 | 2.2 | 0.01 | 3.22 | 0.05 | 7.02 | 0.07 | 6.11 | 0.02 | 70.5 | 140.0 | 69.8 | 2.2 | 120.0 | 4.2 | 69.8 | 2.6 |
| Output_1_174 | 4880 | 462 | 1.2 | 0.01 | 4.95 | 0.05 | 9.90 | 0.08 | 10.37 | 0.37 | 77.1 | 210.0 | 69.9 | 3.5 | 320.0 | 7.8 | 69.9 | 3.7 |
| Output_1_243 | 3570 | 164 | 2.6 | 0.01 | 4.95 | 0.05 | 11.81 | 0.07 | 12.61 | 0.37 | 69.0 | 230.0 | 69.9 | 3.4 | 140.0 | 8.4 | 69.9 | 3.7 |
| Output_1_1 | 4890 | 396 | 2.0 | 0.01 | 4.12 | 0.05 | 10.60 | 0.07 | 11.52 | 0.27 | 68.7 | 190.0 | 70.0 | 2.8 | -10.0 | 7.7 | 70.0 | 3.2 |
| Output_1_161 | 8260 | 1665 | 2.5 | 0.01 | 3.21 | 0.05 | 6.63 | 0.07 | 5.91 | 0.18 | 72.8 | 130.0 | 70.0 | 2.2 | 120.0 | 4.2 | 70.0 | 2.6 |
| Output_1_80 | 5090 | 234 | 5.5 | 0.01 | 3.57 | 0.05 | 12.55 | 0.08 | 10.86 | 0.15 | 74.6 | 250.0 | 70.1 | 2.5 | 150.0 | 7.8 | 70.1 | 2.9 |
| Output_1_260 | 2280 | 160 | 2.0 | 0.01 | 5.39 | 0.05 | 12.17 | 0.07 | 12.68 | 0.06 | 66.3 | 220.0 | 70.2 | 3.8 | 70.0 | 8.2 | 70.2 | 4.0 |
| Output_1_72 | 5760 | 274 | 1.3 | 0.01 | 3.38 | 0.05 | 9.55 | 0.07 | 8.91 | 0.09 | 70.2 | 180.0 | 70.2 | 2.3 | 60.0 | 6.1 | 70.2 | 2.7 |

| | | | | | | | | | | | | | | | | | | |
|---|---|---|---|---|---|---|---|---|---|---|---|---|---|---|---|---|---|---|
| Output_1_106 | 5380 | 322 | 1.0 | 0.01 | 6.47 | 0.05 | 13.53 | 0.08 | 12.66 | 0.31 | 77.3 | 270.0 | 70.3 | 4.5 | 310.0 | 9.4 | 70.3 | 4.8 |
| Output_1_24 | 23530 | 3074 | 10.6 | 0.01 | 2.64 | 0.05 | 5.44 | 0.07 | 4.31 | 0.06 | 70.6 | 110.0 | 70.4 | 1.9 | 100.0 | 3.0 | 70.4 | 2.3 |
| Output_1_113 | 5850 | 358 | 1.7 | 0.01 | 3.73 | 0.05 | 7.93 | 0.07 | 7.53 | 0.21 | 72.8 | 150.0 | 70.5 | 2.6 | 170.0 | 5.3 | 70.5 | 2.9 |
| Output_1_159 | 1175 | 153 | 2.3 | 0.01 | 6.73 | 0.04 | 22.73 | 0.07 | 20.00 | 0.14 | 71.0 | 370.0 | 70.5 | 4.7 | 50.0 | 14.0 | 70.5 | 4.9 |
| Output_1_180 | 2340 | 298 | 1.7 | 0.01 | 5.45 | 0.06 | 18.97 | 0.08 | 17.86 | 0.07 | 82.0 | 330.0 | 70.5 | 3.8 | 460.0 | 14.0 | 70.5 | 4.1 |
| Output_1_214 | 13220 | 1741 | 1.0 | 0.01 | 3.55 | 0.05 | 6.67 | 0.07 | 7.74 | 0.44 | 70.5 | 130.0 | 70.5 | 2.5 | 40.0 | 5.0 | 70.5 | 2.8 |
| Output_1_128 | 5280 | 391 | 0.6 | 0.01 | 5.27 | 0.05 | 12.13 | 0.08 | 11.64 | 0.06 | 76.1 | 220.0 | 70.6 | 3.7 | 240.0 | 8.6 | 70.6 | 4.0 |
| Output_1_14 | 3450 | 548 | 1.5 | 0.01 | 4.90 | 0.05 | 12.74 | 0.08 | 12.09 | 0.08 | 77.9 | 250.0 | 70.7 | 3.4 | 280.0 | 9.1 | 70.7 | 3.7 |
| Output_1_197 | 2640 | 202 | 1.8 | 0.01 | 5.17 | 0.05 | 13.31 | 0.08 | 11.74 | 0.05 | 75.4 | 250.0 | 70.7 | 3.7 | 270.0 | 8.6 | 70.7 | 3.9 |
| Output_1_137 | 11710 | 1027 | 3.7 | 0.01 | 4.07 | 0.05 | 6.60 | 0.07 | 7.67 | 0.44 | 72.6 | 130.0 | 70.9 | 2.9 | 60.0 | 5.4 | 70.9 | 3.2 |
| Output_1_157 | 8770 | 849 | 2.1 | 0.01 | 3.62 | 0.05 | 8.47 | 0.07 | 9.24 | 0.40 | 73.0 | 170.0 | 70.9 | 2.5 | 120.0 | 6.5 | 70.9 | 2.9 |
| Output_1_218 | 6720 | 876 | 34.9 | 0.01 | 5.61 | 0.05 | 9.76 | 0.07 | 8.83 | 0.20 | 68.7 | 190.0 | 70.9 | 4.0 | 130.0 | 5.9 | 70.9 | 4.2 |
| Output_1_222 | 3840 | 436 | 2.4 | 0.01 | 4.96 | 0.05 | 12.27 | 0.07 | 9.94 | 0.18 | 69.8 | 240.0 | 71.1 | 3.5 | 170.0 | 6.8 | 71.1 | 3.8 |
| Output_1_251 | 6760 | 384 | 2.7 | 0.01 | 4.33 | 0.05 | 7.91 | 0.07 | 6.08 | 0.35 | 70.9 | 160.0 | 71.1 | 3.1 | 160.0 | 4.2 | 71.1 | 3.4 |
| Output_1_107 | 3990 | 245 | 1.6 | 0.01 | 4.50 | 0.05 | 11.27 | 0.08 | 11.24 | 0.30 | 73.7 | 210.0 | 71.2 | 3.2 | 160.0 | 8.0 | 71.2 | 3.5 |
| Output_1_189 | 4860 | 3520 | 1.2 | 0.01 | 5.49 | 0.05 | 13.15 | 0.07 | 10.24 | 0.08 | 68.8 | 230.0 | 71.3 | 3.9 | 60.0 | 6.9 | 71.3 | 4.2 |
| Output_1_27 | 3100 | 362 | 1.7 | 0.01 | 5.85 | 0.05 | 12.95 | 0.08 | 13.41 | 0.27 | 79.6 | 250.0 | 71.3 | 4.1 | 260.0 | 9.9 | 71.3 | 4.4 |
| Output_1_172 | 3136 | 278 | 1.4 | 0.01 | 4.40 | 0.05 | 12.97 | 0.07 | 12.83 | 0.16 | 70.7 | 240.0 | 71.4 | 3.1 | 110.0 | 8.7 | 71.4 | 3.4 |
| Output_1_134 | 5530 | 437 | 0.9 | 0.01 | 5.11 | 0.05 | 9.86 | 0.08 | 9.51 | 0.23 | 73.9 | 190.0 | 71.5 | 3.6 | 190.0 | 6.8 | 71.5 | 3.9 |
| Output_1_164 | 1561 | 268 | 1.5 | 0.01 | 4.93 | 0.05 | 20.75 | 0.08 | 18.75 | 0.20 | 80.0 | 360.0 | 71.5 | 3.5 | 240.0 | 15.0 | 71.5 | 3.8 |
| Output_1_163 | 3110 | 601 | 1.4 | 0.01 | 4.61 | 0.05 | 14.26 | 0.08 | 13.41 | 0.05 | 80.0 | 270.0 | 72.2 | 3.3 | 220.0 | 11.0 | 72.2 | 3.6 |
| Output_1_104 | 3750 | 236 | 1.7 | 0.01 | 4.32 | 0.05 | 13.73 | 0.08 | 12.99 | 0.26 | 75.3 | 260.0 | 72.7 | 3.1 | 160.0 | 9.4 | 72.7 | 3.5 |
| Output_1_200 | 2076 | 173 | 1.8 | 0.01 | 5.64 | 0.05 | 15.15 | 0.08 | 14.46 | 0.03 | 81.0 | 270.0 | 72.7 | 4.1 | 400.0 | 12.0 | 72.7 | 4.3 |
| Output_1_265 | 2358 | 186 | 2.6 | 0.01 | 5.62 | 0.05 | 18.48 | 0.07 | 16.90 | 0.22 | 70.0 | 340.0 | 72.9 | 4.1 | 150.0 | 12.0 | 72.9 | 4.3 |
| Output_1_4 | 5290 | 358 | 2.0 | 0.01 | 3.86 | 0.05 | 7.55 | 0.08 | 8.08 | 0.29 | 74.9 | 150.0 | 73.1 | 2.8 | 140.0 | 5.9 | 73.1 | 3.2 |
| Output_1_89 | 3200 | 168 | 1.9 | 0.01 | 3.33 | 0.05 | 13.40 | 0.08 | 11.17 | 0.34 | 75.1 | 240.0 | 73.1 | 2.5 | 80.0 | 8.1 | 73.1 | 2.9 |
| Output_1_94 | 1870 | 115 | 0.9 | 0.01 | 6.57 | 0.06 | 22.58 | 0.09 | 22.47 | 0.22 | 86.0 | 440.0 | 73.2 | 4.8 | 440.0 | 19.0 | 73.2 | 5.0 |
| Output_1_247 | 1460 | 66 | 1.3 | 0.01 | 6.11 | 0.05 | 17.32 | 0.08 | 17.11 | 0.41 | 74.0 | 290.0 | 73.4 | 4.5 | 280.0 | 12.0 | 73.4 | 4.7 |
| Output_1_15 | 5150 | 813 | 2.7 | 0.01 | 3.49 | 0.05 | 9.28 | 0.08 | 8.67 | 0.12 | 74.3 | 180.0 | 73.5 | 2.5 | 120.0 | 6.2 | 73.5 | 2.9 |
| Output_1_237 | 2760 | 134 | 1.5 | 0.01 | 6.63 | 0.06 | 21.82 | 0.08 | 20.00 | 0.18 | 78.0 | 400.0 | 73.5 | 4.8 | 280.0 | 15.0 | 73.5 | 5.1 |
| Output_1_257 | 3530 | 215 | 3.5 | 0.01 | 7.14 | 0.05 | 13.15 | 0.07 | 11.07 | 0.20 | 71.6 | 240.0 | 73.6 | 5.2 | 30.0 | 7.7 | 73.6 | 5.4 |
| Output_1_116 | 57800 | 3770 | 0.6 | 0.01 | 3.48 | 0.05 | 3.60 | 0.08 | 4.47 | 0.53 | 74.3 | 73.0 | 73.7 | 2.6 | 70.0 | 3.2 | 73.7 | 3.0 |
| Output_1_216 | 3470 | 441 | 1.7 | 0.01 | 4.52 | 0.05 | 8.84 | 0.08 | 10.63 | 0.34 | 80.2 | 190.0 | 73.7 | 3.3 | 230.0 | 8.3 | 73.7 | 3.6 |
| Output_1_231 | 18210 | 1258 | 19.8 | 0.01 | 3.55 | 0.05 | 5.14 | 0.07 | 6.54 | 0.43 | 72.7 | 100.0 | 74.1 | 2.6 | 50.0 | 4.3 | 74.1 | 3.0 |
| Output_1_169 | 4040 | 403 | 1.7 | 0.01 | 4.40 | 0.05 | 10.82 | 0.08 | 11.15 | 0.13 | 78.6 | 210.0 | 74.4 | 3.2 | 180.0 | 8.4 | 74.4 | 3.6 |
| Output_1_233 | 2092 | 124 | 2.0 | 0.01 | 5.00 | 0.04 | 17.17 | 0.07 | 17.39 | 0.03 | 68.0 | 280.0 | 74.4 | 3.7 | -110.0 | 11.0 | 74.4 | 4.0 |
| Output_1_215 | 4250 | 526 | 1.0 | 0.01 | 4.20 | 0.05 | 13.69 | 0.08 | 12.35 | 0.21 | 78.2 | 250.0 | 74.7 | 3.1 | 150.0 | 9.4 | 74.7 | 3.5 |
| Output_1_7 | 6440 | 493 | 2.0 | 0.01 | 5.05 | 0.05 | 7.35 | 0.08 | 8.47 | 0.26 | 74.8 | 150.0 | 74.8 | 3.7 | 150.0 | 6.1 | 74.8 | 4.0 |
| Output_1_221 | 4360 | 505 | 3.8 | 0.01 | 4.62 | 0.05 | 11.66 | 0.08 | 11.48 | 0.25 | 77.1 | 220.0 | 74.9 | 3.5 | 150.0 | 8.6 | 74.9 | 3.8 |
| Output_1_230 | 3570 | 266 | 5.3 | 0.01 | 4.94 | 0.05 | 13.19 | 0.08 | 12.16 | 0.19 | 79.0 | 250.0 | 75.1 | 3.7 | 210.0 | 9.3 | 75.1 | 4.0 |

| | | | | | | | | | | | | | | | | | | |
|---|---|---|---|---|---|---|---|---|---|---|---|---|---|---|---|---|---|---|
| Output_1_28 | 4460 | 491 | 2.1 | 0.01 | 5.28 | 0.05 | 8.14 | 0.08 | 8.41 | 0.32 | 82.1 | 170.0 | 75.2 | 4.0 | 280.0 | 6.6 | 75.2 | 4.2 |
| Output_1_69 | 12990 | 642 | 7.6 | 0.01 | 4.06 | 0.05 | 10.47 | 0.08 | 8.45 | 0.17 | 78.6 | 220.0 | 75.7 | 3.0 | 250.0 | 6.4 | 75.7 | 3.4 |
| Output_1_149 | 141900 | 6610 | 6.2 | 0.01 | 5.40 | 0.05 | 4.99 | 0.08 | 4.96 | 0.59 | 76.8 | 110.0 | 75.9 | 4.1 | 190.0 | 3.7 | 75.9 | 4.3 |
| Output_1_210 | 4090 | 452 | 5.2 | 0.01 | 6.05 | 0.05 | 18.86 | 0.09 | 17.58 | 0.10 | 88.0 | 370.0 | 76.3 | 4.6 | 310.0 | 15.0 | 76.3 | 4.9 |
| Output_1_108 | 8280 | 443 | 3.7 | 0.01 | 3.68 | 0.05 | 9.13 | 0.08 | 9.00 | 0.01 | 79.0 | 180.0 | 76.7 | 2.8 | 140.0 | 6.8 | 76.7 | 3.2 |
| Output_1_228 | 1820 | 146 | 2.8 | 0.01 | 6.85 | 0.05 | 12.78 | 0.09 | 15.29 | 0.41 | 82.0 | 280.0 | 76.7 | 5.2 | 400.0 | 12.0 | 76.7 | 5.4 |
| Output_1_239 | 3140 | 132 | 1.7 | 0.01 | 4.65 | 0.05 | 9.69 | 0.08 | 9.56 | 0.13 | 80.3 | 180.0 | 77.1 | 3.6 | 120.0 | 7.4 | 77.1 | 3.9 |
| Output_1_235 | 828 | 39 | 2.3 | 0.01 | 5.51 | 0.05 | 22.64 | 0.09 | 21.11 | 0.02 | 86.0 | 400.0 | 77.9 | 4.2 | 220.0 | 17.0 | 77.9 | 4.5 |
| Output_1_39 | 3350 | 296 | 2.4 | 0.01 | 3.61 | 0.05 | 12.04 | 0.08 | 10.73 | 0.18 | 78.9 | 230.0 | 78.1 | 2.8 | 280.0 | 8.2 | 78.1 | 3.2 |
| Output_1_176 | 16270 | 1417 | 4.1 | 0.01 | 3.32 | 0.05 | 4.16 | 0.08 | 4.49 | 0.46 | 80.4 | 86.0 | 79.1 | 2.6 | 107.0 | 3.5 | 79.1 | 3.0 |
| Output_1_97 | 10300 | 608 | 3.3 | 0.01 | 3.61 | 0.05 | 5.60 | 0.08 | 6.13 | 0.18 | 79.5 | 110.0 | 80.0 | 2.9 | 40.0 | 4.7 | 80.0 | 3.3 |
| Output_1_34 | 5010 | 464 | 9.0 | 0.01 | 4.56 | 0.05 | 9.15 | 0.09 | 8.90 | 0.28 | 84.0 | 180.0 | 81.5 | 3.7 | 180.0 | 7.2 | 81.5 | 4.0 |
| Output_1_70 | 20610 | 924 | 1.1 | 0.01 | 3.46 | 0.05 | 4.71 | 0.08 | 5.52 | 0.40 | 81.2 | 91.0 | 81.5 | 2.8 | 48.0 | 4.3 | 81.5 | 3.3 |
| Output_1_126 | 8340 | 577 | 1.7 | 0.01 | 2.65 | 0.05 | 7.27 | 0.09 | 7.04 | 0.21 | 84.3 | 140.0 | 82.0 | 2.1 | 160.0 | 5.7 | 82.0 | 2.7 |
| Output_1_208 | 6010 | 581 | 5.2 | 0.01 | 3.90 | 0.05 | 7.55 | 0.09 | 6.60 | 0.06 | 83.9 | 150.0 | 82.2 | 3.2 | 110.0 | 5.4 | 82.2 | 3.6 |
| Output_1_32 | 17840 | 1555 | 1.1 | 0.01 | 3.35 | 0.05 | 4.31 | 0.09 | 4.57 | 0.34 | 85.1 | 88.0 | 82.3 | 2.7 | 131.0 | 3.7 | 82.3 | 3.2 |
| Output_1_50 | 23900 | 1900 | 1.8 | 0.01 | 6.53 | 0.05 | 9.79 | 0.09 | 10.82 | 0.65 | 88.8 | 210.0 | 82.4 | 5.3 | 320.0 | 9.2 | 82.4 | 5.6 |
| Output_1_114 | 2950 | 153 | 2.0 | 0.01 | 4.49 | 0.05 | 16.11 | 0.09 | 13.95 | 0.08 | 83.0 | 270.0 | 82.7 | 3.7 | 70.0 | 11.0 | 82.7 | 4.1 |
| Output_1_52 | 7980 | 626 | 1.1 | 0.01 | 3.48 | 0.05 | 8.71 | 0.08 | 9.93 | 0.48 | 79.4 | 160.0 | 82.8 | 2.8 | 10.0 | 7.6 | 82.8 | 3.3 |
| Output_1_144 | 6630 | 396 | 1.4 | 0.01 | 5.79 | 0.07 | 7.81 | 0.12 | 8.20 | 0.38 | 116.2 | 170.0 | 82.9 | 4.8 | 920.0 | 9.2 | 82.9 | 5.0 |
| Output_1_217 | 16320 | 1809 | 1.9 | 0.01 | 2.01 | 0.05 | 5.50 | 0.09 | 5.34 | 0.15 | 83.9 | 110.0 | 82.9 | 1.7 | 150.0 | 4.3 | 82.9 | 2.3 |
| Output_1_132 | 8070 | 524 | 2.7 | 0.01 | 4.06 | 0.05 | 9.62 | 0.09 | 10.71 | 0.22 | 84.3 | 180.0 | 83.7 | 3.4 | 90.0 | 8.7 | 83.7 | 3.8 |
| Output_1_170 | 13930 | 1158 | 2.8 | 0.01 | 3.41 | 0.05 | 7.68 | 0.08 | 7.47 | 0.26 | 82.1 | 140.0 | 84.6 | 2.9 | 60.0 | 5.9 | 84.6 | 3.3 |
| Output_1_229 | 18640 | 1284 | 5.1 | 0.01 | 3.98 | 0.05 | 5.05 | 0.09 | 5.15 | 0.56 | 86.7 | 100.0 | 86.8 | 3.4 | 90.0 | 4.3 | 86.8 | 3.9 |
| Output_1_112 | 2140 | 109 | 2.0 | 0.01 | 6.57 | 0.05 | 31.48 | 0.11 | 37.14 | 0.25 | 113.0 | 650.0 | 86.8 | 5.7 | 430.0 | 41.0 | 86.8 | 5.9 |
| Output_1_67 | 18530 | 835 | 4.2 | 0.01 | 3.30 | 0.05 | 5.58 | 0.09 | 5.82 | 0.24 | 88.4 | 110.0 | 87.2 | 2.9 | 120.0 | 4.9 | 87.2 | 3.3 |
| Output_1_150 | 13430 | 522 | 1.2 | 0.01 | 4.05 | 0.05 | 8.35 | 0.09 | 9.06 | 0.43 | 89.9 | 170.0 | 88.6 | 3.6 | 150.0 | 7.8 | 88.6 | 4.0 |
| Output_1_11 | 3510 | 379 | 1.9 | 0.01 | 4.02 | 0.05 | 11.03 | 0.10 | 11.22 | 0.02 | 94.8 | 220.0 | 89.1 | 3.5 | 260.0 | 9.8 | 89.1 | 4.0 |
| Output_1_148 | 17730 | 725 | 1.3 | 0.01 | 4.92 | 0.05 | 6.67 | 0.10 | 5.73 | 0.22 | 94.5 | 140.0 | 89.8 | 4.4 | 220.0 | 5.2 | 89.8 | 4.7 |
| Output_1_173 | 11550 | 811 | 1.3 | 0.01 | 3.12 | 0.05 | 7.48 | 0.10 | 7.86 | 0.08 | 99.8 | 180.0 | 90.4 | 2.8 | 280.0 | 8.5 | 90.4 | 3.3 |
| Output_1_127 | 2500 | 152 | 1.7 | 0.01 | 5.50 | 0.05 | 13.03 | 0.10 | 13.27 | 0.33 | 94.0 | 240.0 | 90.8 | 5.0 | 220.0 | 12.0 | 90.8 | 5.3 |
| Output_1_58 | 17430 | 1116 | 3.1 | 0.01 | 3.14 | 0.05 | 8.29 | 0.10 | 7.01 | 0.14 | 96.6 | 170.0 | 91.8 | 2.9 | 340.0 | 6.5 | 91.8 | 3.4 |
| Output_1_131 | 1960 | 112 | 3.6 | 0.01 | 6.99 | 0.05 | 21.57 | 0.10 | 19.80 | 0.23 | 97.0 | 360.0 | 92.5 | 6.7 | 150.0 | 18.0 | 92.5 | 7.0 |
| Output_1_146 | 8180 | 354 | 1.5 | 0.01 | 3.99 | 0.05 | 7.77 | 0.10 | 8.34 | 0.24 | 97.1 | 150.0 | 93.1 | 3.7 | 190.0 | 7.7 | 93.1 | 4.1 |
| Output_1_266 | 4120 | 262 | 1.3 | 0.01 | 3.72 | 0.05 | 9.15 | 0.09 | 8.65 | 0.13 | 89.6 | 170.0 | 94.7 | 3.5 | 10.0 | 7.5 | 94.7 | 4.0 |
| Output_1_68 | 1700 | 73 | 2.0 | 0.01 | 8.72 | 0.06 | 20.69 | 0.11 | 17.86 | 0.02 | 106.0 | 410.0 | 95.2 | 8.0 | 410.0 | 18.0 | 95.2 | 8.3 |
| Output_1_65 | 6680 | 327 | 4.3 | 0.01 | 5.56 | 0.05 | 9.66 | 0.10 | 9.84 | 0.10 | 96.1 | 180.0 | 95.6 | 5.2 | 150.0 | 9.0 | 95.6 | 5.6 |
| Output_1_49 | 22690 | 1518 | 0.8 | 0.02 | 4.30 | 0.05 | 8.69 | 0.11 | 7.65 | 0.03 | 103.2 | 180.0 | 96.7 | 4.1 | 250.0 | 7.5 | 96.7 | 4.6 |
| Output_1_248 | 4010 | 145 | 1.1 | 0.02 | 4.52 | 0.05 | 11.15 | 0.11 | 10.91 | 0.15 | 106.0 | 230.0 | 97.6 | 4.4 | 350.0 | 11.0 | 97.6 | 4.8 |
| Output_1_21 | 7800 | 830 | 2.1 | 0.02 | 3.99 | 0.05 | 11.28 | 0.11 | 10.91 | 0.23 | 106.0 | 230.0 | 97.7 | 3.9 | 320.0 | 11.0 | 97.7 | 4.3 |

| | | | | | | | | | | | | | | | | | | |
|---|---|---|---|---|---|---|---|---|---|---|---|---|---|---|---|---|---|---|
| Output_1_223 | 6660 | 536 | 4.9 | 0.02 | 3.40 | 0.05 | 8.23 | 0.10 | 8.82 | 0.39 | 98.3 | 160.0 | 97.8 | 3.3 | 200.0 | 8.2 | 97.8 | 3.8 |
| Output_1_179 | 2160 | 181 | 2.8 | 0.02 | 6.22 | 0.05 | 17.50 | 0.12 | 16.52 | 0.05 | 109.0 | 330.0 | 98.7 | 6.1 | 290.0 | 17.0 | 98.7 | 6.4 |
| Output_1_59 | 17140 | 1001 | 3.6 | 0.02 | 4.72 | 0.05 | 5.06 | 0.10 | 5.43 | 0.30 | 101.2 | 110.0 | 99.0 | 4.6 | 170.0 | 5.3 | 99.0 | 5.0 |
| Output_1_62 | 8600 | 442 | 2.2 | 0.02 | 4.10 | 0.05 | 8.23 | 0.10 | 8.37 | 0.24 | 99.1 | 170.0 | 99.8 | 4.1 | 160.0 | 7.9 | 99.8 | 4.5 |
| Output_1_136 | 7320 | 445 | 1.6 | 0.02 | 3.83 | 0.05 | 11.20 | 0.11 | 10.62 | 0.14 | 108.0 | 230.0 | 100.1 | 3.8 | 280.0 | 11.0 | 100.1 | 4.3 |
| Output_1_102 | 9490 | 450 | 2.4 | 0.02 | 5.48 | 0.05 | 10.12 | 0.11 | 11.32 | 0.44 | 104.0 | 200.0 | 100.4 | 5.5 | 110.0 | 12.0 | 100.4 | 5.8 |
| Output_1_155 | 60400 | 3024 | 1.1 | 0.02 | 3.56 | 0.05 | 4.62 | 0.11 | 5.41 | 0.50 | 101.7 | 99.0 | 100.5 | 3.6 | 177.0 | 5.2 | 100.5 | 4.1 |
| Output_1_56 | 4430 | 270 | 2.4 | 0.02 | 4.61 | 0.05 | 11.62 | 0.11 | 12.84 | 0.50 | 108.0 | 230.0 | 101.2 | 4.7 | 220.0 | 14.0 | 101.2 | 5.1 |
| Output_1_206 | 8420 | 621 | 2.5 | 0.02 | 4.18 | 0.05 | 8.48 | 0.11 | 8.01 | 0.21 | 108.0 | 170.0 | 102.4 | 4.3 | 330.0 | 8.2 | 102.4 | 4.7 |
| Output_1_263 | 7350 | 395 | 7.9 | 0.02 | 5.49 | 0.05 | 9.28 | 0.11 | 9.65 | 0.39 | 109.3 | 180.0 | 102.5 | 5.6 | 270.0 | 9.6 | 102.5 | 6.0 |
| Output_1_13 | 2190 | 234 | 5.5 | 0.02 | 7.45 | 0.05 | 16.54 | 0.13 | 18.40 | 0.45 | 118.0 | 330.0 | 102.6 | 7.8 | 420.0 | 20.0 | 102.6 | 8.0 |
| Output_1_138 | 18690 | 1218 | 1.5 | 0.02 | 3.80 | 0.05 | 6.67 | 0.11 | 6.19 | 0.13 | 105.6 | 140.0 | 102.8 | 3.8 | 160.0 | 6.2 | 102.8 | 4.3 |
| Output_1_178 | 43300 | 3240 | 1.2 | 0.02 | 3.47 | 0.05 | 6.58 | 0.11 | 7.15 | 0.28 | 107.6 | 140.0 | 103.2 | 3.5 | 130.0 | 7.3 | 103.2 | 4.1 |
| Output_1_209 | 13620 | 1049 | 2.4 | 0.02 | 3.44 | 0.05 | 8.11 | 0.11 | 6.68 | 0.12 | 105.1 | 160.0 | 104.0 | 3.6 | 140.0 | 6.7 | 104.0 | 4.1 |
| Output_1_19 | 13920 | 1513 | 1.2 | 0.02 | 2.32 | 0.05 | 6.32 | 0.11 | 6.65 | 0.14 | 104.2 | 120.0 | 104.6 | 2.4 | 80.0 | 6.6 | 104.6 | 3.2 |
| Output_1_199 | 9510 | 531 | 2.9 | 0.02 | 4.03 | 0.05 | 9.66 | 0.11 | 9.91 | 0.08 | 106.0 | 180.0 | 104.7 | 4.2 | 40.0 | 11.0 | 104.7 | 4.7 |
| Output_1_205 | 2661 | 182 | 1.4 | 0.02 | 4.80 | 0.05 | 18.36 | 0.10 | 16.33 | 0.10 | 96.0 | 310.0 | 106.5 | 5.0 | -10.0 | 16.0 | 106.5 | 5.5 |
| Output_1_195 | 28760 | 1351 | 1.9 | 0.02 | 3.27 | 0.05 | 6.37 | 0.12 | 5.69 | 0.18 | 111.3 | 130.0 | 107.5 | 3.5 | 130.0 | 6.0 | 107.5 | 4.1 |
| Output_1_220 | 7610 | 624 | 2.5 | 0.02 | 5.19 | 0.05 | 14.65 | 0.12 | 14.52 | 0.00 | 118.0 | 290.0 | 108.4 | 5.6 | 240.0 | 16.0 | 108.4 | 6.0 |
| Output_1_177 | 4250 | 287 | 1.1 | 0.02 | 5.83 | 0.05 | 11.56 | 0.12 | 13.71 | 0.57 | 118.0 | 220.0 | 108.5 | 6.3 | 220.0 | 15.0 | 108.5 | 6.7 |
| Output_1_130 | 18410 | 846 | 2.7 | 0.02 | 3.99 | 0.05 | 5.59 | 0.12 | 6.04 | 0.35 | 111.1 | 110.0 | 108.9 | 4.3 | 120.0 | 6.4 | 108.9 | 4.8 |
| Output_1_166 | 5860 | 560 | 6.1 | 0.02 | 6.43 | 0.06 | 9.34 | 0.15 | 10.20 | 0.42 | 141.0 | 190.0 | 109.1 | 7.1 | 660.0 | 13.0 | 109.1 | 7.5 |
| Output_1_33 | 3760 | 248 | 3.7 | 0.02 | 4.88 | 0.05 | 11.04 | 0.11 | 10.09 | 0.10 | 104.0 | 210.0 | 111.3 | 5.4 | 90.0 | 10.0 | 111.3 | 5.8 |
| Output_1_252 | 9760 | 360 | 0.9 | 0.02 | 3.38 | 0.05 | 7.28 | 0.12 | 6.78 | 0.03 | 110.4 | 140.0 | 111.6 | 3.8 | 110.0 | 7.1 | 111.6 | 4.4 |
| Output_1_60 | 5010 | 250 | 3.0 | 0.02 | 3.55 | 0.05 | 8.71 | 0.13 | 8.66 | 0.11 | 121.0 | 180.0 | 117.0 | 4.1 | 280.0 | 10.0 | 117.0 | 4.7 |
| Output_1_234 | 8310 | 264 | 2.8 | 0.02 | 4.63 | 0.05 | 8.51 | 0.15 | 9.59 | 0.36 | 138.0 | 180.0 | 129.5 | 5.9 | 390.0 | 12.0 | 129.5 | 6.5 |
| Output_1_124 | 3960 | 178 | 1.8 | 0.02 | 5.37 | 0.05 | 10.92 | 0.15 | 9.59 | 0.24 | 138.0 | 210.0 | 131.0 | 6.7 | 210.0 | 13.0 | 131.0 | 7.2 |
| Output_1_47 | 7790 | 399 | 0.8 | 0.02 | 3.40 | 0.05 | 7.83 | 0.14 | 9.15 | 0.30 | 134.0 | 160.0 | 131.3 | 4.4 | 220.0 | 11.0 | 131.3 | 5.1 |
| Output_1_43 | 22830 | 1102 | 2.0 | 0.02 | 3.27 | 0.05 | 4.93 | 0.15 | 5.21 | 0.39 | 138.0 | 100.0 | 136.6 | 4.4 | 220.0 | 6.7 | 136.6 | 5.2 |
| Output_1_101 | 18530 | 655 | 4.1 | 0.02 | 3.24 | 0.05 | 6.29 | 0.15 | 7.14 | 0.43 | 145.4 | 140.0 | 139.6 | 4.5 | 270.0 | 9.3 | 139.6 | 5.3 |
| Output_1_83 | 9340 | 220 | 1.8 | 0.02 | 3.48 | 0.05 | 7.48 | 0.16 | 7.69 | 0.23 | 147.0 | 150.0 | 142.9 | 4.9 | 240.0 | 10.0 | 142.9 | 5.7 |
| Output_1_201 | 12460 | 542 | 2.5 | 0.02 | 3.38 | 0.05 | 6.88 | 0.16 | 8.13 | 0.45 | 150.0 | 160.0 | 143.4 | 4.8 | 320.0 | 11.0 | 143.4 | 5.6 |
| Output_1_110 | 2810 | 79 | 2.6 | 0.02 | 8.41 | 0.05 | 9.46 | 0.15 | 15.54 | 0.81 | 140.0 | 180.0 | 144.0 | 12.0 | 40.0 | 20.0 | 144.0 | 12.0 |
| Output_1_105 | 2350 | 72 | 1.8 | 0.02 | 6.17 | 0.05 | 10.28 | 0.18 | 11.86 | 0.38 | 167.0 | 210.0 | 144.5 | 8.6 | 370.0 | 18.0 | 144.5 | 9.1 |
| Output_1_256 | 6240 | 187 | 2.2 | 0.02 | 4.72 | 0.05 | 9.56 | 0.16 | 8.86 | 0.11 | 148.0 | 190.0 | 148.3 | 7.2 | 130.0 | 12.0 | 148.3 | 7.8 |
| Output_1_191 | 21710 | 77100 | 3.2 | 0.02 | 5.98 | 0.05 | 12.60 | 0.16 | 12.96 | 0.21 | 152.0 | 250.0 | 148.8 | 8.5 | 150.0 | 19.0 | 148.8 | 9.0 |
| Output_1_91 | 5240 | 139 | 2.8 | 0.02 | 4.70 | 0.05 | 9.51 | 0.16 | 10.56 | 0.45 | 151.0 | 180.0 | 148.9 | 6.9 | 180.0 | 14.0 | 148.9 | 7.5 |
| Output_1_16 | 5140 | 400 | 2.6 | 0.02 | 5.86 | 0.05 | 8.81 | 0.17 | 8.28 | 0.38 | 157.0 | 170.0 | 152.3 | 9.0 | 250.0 | 12.0 | 152.3 | 9.5 |
| Output_1_86 | 4600 | 106 | 3.1 | 0.02 | 5.00 | 0.06 | 19.30 | 0.19 | 16.76 | 0.18 | 171.0 | 380.0 | 152.9 | 7.9 | 490.0 | 27.0 | 152.9 | 8.4 |
| Output_1_244 | 7290 | 150 | 3.0 | 0.02 | 3.82 | 0.05 | 8.22 | 0.16 | 8.59 | 0.38 | 153.0 | 160.0 | 155.1 | 5.8 | 220.0 | 12.0 | 155.1 | 6.6 |

| | | | | | | | | | | | | | | | | | | |
|---|---|---|---|---|---|---|---|---|---|---|---|---|---|---|---|---|---|---|
| Output_1_167 | 37420 | 2205 | 2.3 | 0.02 | 3.57 | 0.05 | 5.05 | 0.17 | 5.59 | 0.28 | 160.7 | 110.0 | 157.0 | 5.6 | 250.0 | 8.3 | 157.0 | 6.4 |
| Output_1_3 | 3090 | 97 | 2.4 | 0.02 | 4.44 | 0.05 | 11.37 | 0.17 | 11.49 | 0.31 | 161.0 | 220.0 | 158.0 | 6.7 | 260.0 | 17.0 | 158.0 | 7.4 |
| Output_1_238 | 12880 | 266 | 0.8 | 0.03 | 3.58 | 0.05 | 8.62 | 0.18 | 8.84 | 0.16 | 171.0 | 180.0 | 160.2 | 5.7 | 290.0 | 13.0 | 160.2 | 6.5 |
| Output_1_117 | 7230 | 227 | 1.9 | 0.03 | 3.81 | 0.05 | 9.09 | 0.18 | 7.26 | 0.13 | 166.0 | 180.0 | 160.3 | 6.0 | 180.0 | 11.0 | 160.3 | 6.8 |
| Output_1_53 | 4810 | 176 | 2.2 | 0.03 | 7.11 | 0.05 | 7.14 | 0.17 | 13.29 | 0.40 | 162.0 | 150.0 | 161.0 | 11.0 | 90.0 | 20.0 | 161.0 | 12.0 |
| Output_1_145 | 12310 | 322 | 3.3 | 0.03 | 6.30 | 0.05 | 10.85 | 0.16 | 10.98 | 0.01 | 153.0 | 210.0 | 161.5 | 9.9 | 70.0 | 16.0 | 161.5 | 10.0 |
| Output_1_85 | 35000 | 765 | 12.2 | 0.03 | 5.51 | 0.06 | 3.66 | 0.22 | 6.70 | 0.80 | 204.0 | 74.0 | 161.8 | 8.9 | 719.0 | 13.0 | 161.8 | 9.5 |
| Output_1_187 | 9030 | 1613 | 1.3 | 0.03 | 4.28 | 0.05 | 7.77 | 0.18 | 7.07 | 0.22 | 174.0 | 160.0 | 163.6 | 6.9 | 290.0 | 12.0 | 163.6 | 7.6 |
| Output_1_203 | 11080 | 448 | 1.8 | 0.03 | 3.34 | 0.05 | 6.50 | 0.18 | 8.00 | 0.45 | 163.0 | 120.0 | 163.7 | 5.4 | 90.0 | 12.0 | 163.7 | 6.3 |
| Output_1_259 | 12330 | 358 | 4.9 | 0.03 | 3.42 | 0.05 | 5.87 | 0.17 | 6.36 | 0.40 | 163.0 | 120.0 | 165.5 | 5.6 | 160.0 | 9.8 | 165.5 | 6.5 |
| Output_1_241 | 3800 | 70 | 1.4 | 0.03 | 4.55 | 0.05 | 11.74 | 0.17 | 11.63 | 0.21 | 159.0 | 220.0 | 168.1 | 7.7 | 100.0 | 17.0 | 168.1 | 8.4 |
| Output_1_213 | 15000 | 807 | 1.3 | 0.03 | 3.14 | 0.05 | 5.35 | 0.18 | 6.52 | 0.46 | 171.4 | 110.0 | 168.3 | 5.2 | 200.0 | 9.9 | 168.3 | 6.2 |
| Output_1_250 | 7120 | 155 | 2.7 | 0.03 | 4.43 | 0.05 | 8.16 | 0.19 | 9.28 | 0.28 | 182.0 | 180.0 | 172.5 | 7.2 | 360.0 | 14.0 | 172.5 | 8.0 |
| Output_1_154 | 7670 | 197 | 2.6 | 0.03 | 4.00 | 0.05 | 7.07 | 0.18 | 7.26 | 0.26 | 167.0 | 130.0 | 174.6 | 7.0 | 50.0 | 11.0 | 174.6 | 7.8 |
| Output_1_64 | 8870 | 242 | 4.1 | 0.03 | 4.33 | 0.05 | 7.27 | 0.20 | 7.14 | 0.11 | 181.0 | 160.0 | 175.8 | 7.8 | 320.0 | 12.0 | 175.8 | 8.5 |
| Output_1_168 | 8770 | 406 | 1.8 | 0.03 | 3.51 | 0.05 | 7.74 | 0.20 | 8.54 | 0.35 | 184.0 | 160.0 | 177.3 | 6.1 | 240.0 | 14.0 | 177.3 | 7.1 |
| Output_1_261 | 9520 | 268 | 2.0 | 0.03 | 3.91 | 0.05 | 8.71 | 0.18 | 8.20 | 0.03 | 170.0 | 160.0 | 178.5 | 6.6 | 110.0 | 13.0 | 178.5 | 7.5 |
| Output_1_212 | 12550 | 621 | 1.7 | 0.03 | 3.45 | 0.05 | 6.09 | 0.20 | 6.57 | 0.44 | 182.0 | 130.0 | 178.7 | 6.1 | 180.0 | 11.0 | 178.7 | 7.0 |
| Output_1_123 | 14740 | 476 | 2.0 | 0.03 | 4.26 | 0.05 | 7.04 | 0.19 | 6.25 | 0.07 | 179.0 | 140.0 | 179.2 | 7.5 | 140.0 | 10.0 | 179.2 | 8.3 |
| Output_1_30 | 13370 | 559 | 2.2 | 0.03 | 3.55 | 0.05 | 6.18 | 0.20 | 5.61 | 0.08 | 181.2 | 140.0 | 179.5 | 6.6 | 240.0 | 9.6 | 179.5 | 7.5 |
| Output_1_81 | 15090 | 265 | 2.4 | 0.03 | 3.35 | 0.05 | 4.93 | 0.20 | 5.47 | 0.36 | 185.4 | 110.0 | 181.5 | 5.7 | 230.0 | 9.3 | 181.5 | 6.7 |
| Output_1_23 | 24700 | 1250 | 6.8 | 0.03 | 3.50 | 0.05 | 5.82 | 0.21 | 5.29 | 0.30 | 193.0 | 120.0 | 181.8 | 6.5 | 310.0 | 10.0 | 181.8 | 7.4 |
| Output_1_42 | 32200 | 1110 | 5.0 | 0.03 | 4.88 | 0.05 | 5.35 | 0.22 | 8.18 | 0.66 | 201.0 | 120.0 | 182.1 | 8.6 | 350.0 | 15.0 | 182.1 | 9.3 |
| Output_1_226 | 3770 | 141 | 2.5 | 0.03 | 3.83 | 0.05 | 13.10 | 0.18 | 11.05 | 0.11 | 171.0 | 220.0 | 182.6 | 6.9 | 50.0 | 18.0 | 182.6 | 7.8 |
| Output_1_103 | 10390 | 257 | 2.0 | 0.03 | 4.14 | 0.05 | 5.63 | 0.22 | 5.50 | 0.33 | 199.5 | 130.0 | 184.4 | 7.8 | 330.0 | 9.9 | 184.4 | 8.6 |
| Output_1_188 | 7450 | 1500 | 2.1 | 0.03 | 3.40 | 0.05 | 8.59 | 0.20 | 7.58 | 0.16 | 183.0 | 170.0 | 186.7 | 6.4 | 160.0 | 12.0 | 186.7 | 7.4 |
| Output_1_96 | 6880 | 171 | 2.2 | 0.03 | 3.72 | 0.05 | 7.39 | 0.22 | 6.76 | 0.02 | 203.0 | 160.0 | 187.7 | 6.6 | 360.0 | 12.0 | 187.7 | 7.6 |
| Output_1_111 | 11590 | 249 | 2.9 | 0.03 | 4.05 | 0.05 | 5.12 | 0.21 | 5.66 | 0.27 | 194.8 | 110.0 | 187.9 | 7.2 | 250.0 | 9.9 | 187.9 | 8.1 |
| Output_1_122 | 7680 | 236 | 1.4 | 0.03 | 4.05 | 0.05 | 7.68 | 0.21 | 7.98 | 0.30 | 195.0 | 160.0 | 188.0 | 7.6 | 290.0 | 14.0 | 188.0 | 8.4 |
| Output_1_192 | 5210 | 127 | 1.8 | 0.03 | 3.72 | 0.05 | 9.50 | 0.21 | 8.21 | 0.11 | 190.0 | 190.0 | 188.1 | 7.0 | 310.0 | 15.0 | 188.1 | 7.9 |
| Output_1_31 | 23620 | 909 | 1.7 | 0.03 | 3.67 | 0.05 | 5.47 | 0.21 | 5.14 | 0.40 | 196.5 | 120.0 | 190.7 | 6.9 | 250.0 | 9.4 | 190.7 | 7.9 |
| Output_1_118 | 13040 | 356 | 1.1 | 0.03 | 2.53 | 0.05 | 6.50 | 0.21 | 5.63 | 0.02 | 197.0 | 130.0 | 191.1 | 4.7 | 210.0 | 11.0 | 191.1 | 6.1 |
| Output_1_54 | 12150 | 410 | 1.4 | 0.03 | 4.97 | 0.05 | 6.60 | 0.20 | 5.03 | 0.28 | 183.7 | 130.0 | 191.7 | 9.2 | 130.0 | 8.9 | 191.7 | 10.0 |
| Output_1_160 | 1989 | 113 | 4.1 | 0.03 | 4.92 | 0.05 | 17.25 | 0.22 | 17.57 | 0.26 | 204.0 | 290.0 | 193.8 | 9.2 | 180.0 | 31.0 | 193.8 | 10.0 |
| Output_1_109 | 13030 | 266 | 2.6 | 0.03 | 4.58 | 0.05 | 6.22 | 0.21 | 7.25 | 0.57 | 190.0 | 130.0 | 194.5 | 8.6 | 110.0 | 13.0 | 194.5 | 9.4 |
| Output_1_219 | 14170 | 649 | 1.2 | 0.03 | 3.24 | 0.05 | 5.65 | 0.21 | 6.25 | 0.19 | 191.0 | 120.0 | 196.5 | 6.4 | 170.0 | 11.0 | 196.5 | 7.5 |
| Output_1_198 | 8890 | 252 | 2.3 | 0.03 | 4.19 | 0.05 | 6.65 | 0.22 | 7.76 | 0.53 | 200.0 | 140.0 | 196.9 | 7.9 | 240.0 | 14.0 | 196.9 | 8.8 |
| Output_1_25 | 6990 | 301 | 2.5 | 0.03 | 4.76 | 0.05 | 8.33 | 0.24 | 8.47 | 0.20 | 214.0 | 170.0 | 200.0 | 9.5 | 330.0 | 16.0 | 200.0 | 10.0 |
| Output_1_139 | 32920 | 1102 | 2.0 | 0.03 | 2.61 | 0.05 | 4.41 | 0.22 | 4.33 | 0.40 | 205.1 | 95.0 | 201.4 | 5.2 | 202.0 | 8.0 | 201.4 | 6.5 |
| Output_1_55 | 8530 | 262 | 2.3 | 0.03 | 3.73 | 0.05 | 6.83 | 0.23 | 6.93 | 0.29 | 211.0 | 140.0 | 204.5 | 7.8 | 310.0 | 13.0 | 204.5 | 8.8 |

| | | | | | | | | | | | | | | | | | | |
|---|---|---|---|---|---|---|---|---|---|---|---|---|---|---|---|---|---|---|
| Output_1_57 | 19420 | 625 | 1.0 | 0.03 | 7.72 | 0.05 | 4.66 | 0.24 | 8.82 | 0.12 | 215.0 | 100.0 | 205.0 | 16.0 | 350.0 | 17.0 | 205.0 | 16.0 |
| Output_1_17 | 17670 | 1002 | 1.5 | 0.03 | 4.26 | 0.06 | 6.07 | 0.25 | 7.29 | 0.58 | 224.0 | 130.0 | 208.9 | 8.9 | 420.0 | 15.0 | 208.9 | 9.8 |
| Output_1_151 | 46980 | 770 | 1.2 | 0.03 | 3.31 | 0.05 | 2.78 | 0.23 | 3.52 | 0.48 | 212.2 | 66.0 | 210.5 | 6.7 | 220.0 | 6.8 | 210.5 | 7.9 |
| Output_1_253 | 19950 | 390 | 2.1 | 0.03 | 4.73 | 0.05 | 6.10 | 0.24 | 5.06 | 0.40 | 220.0 | 130.0 | 214.0 | 10.0 | 280.0 | 11.0 | 214.0 | 11.0 |
| Output_1_153 | 8620 | 157 | 2.9 | 0.03 | 3.54 | 0.05 | 6.93 | 0.25 | 7.35 | 0.21 | 224.0 | 140.0 | 215.1 | 7.5 | 200.0 | 14.0 | 215.1 | 8.6 |
| Output_1_22 | 9190 | 421 | 3.5 | 0.03 | 3.82 | 0.05 | 6.05 | 0.25 | 5.98 | 0.18 | 227.0 | 140.0 | 215.5 | 8.0 | 350.0 | 12.0 | 215.5 | 9.1 |
| Output_1_121 | 2990 | 81 | 3.0 | 0.03 | 4.99 | 0.05 | 11.86 | 0.26 | 12.64 | 0.30 | 237.0 | 240.0 | 216.0 | 10.0 | 330.0 | 28.0 | 216.0 | 11.0 |
| Output_1_236 | 12710 | 206 | 1.9 | 0.04 | 3.99 | 0.06 | 5.25 | 0.29 | 5.15 | 0.29 | 261.0 | 110.0 | 222.3 | 8.4 | 620.0 | 11.0 | 222.3 | 9.5 |
| Output_1_225 | 5690 | 181 | 2.1 | 0.04 | 5.54 | 0.05 | 6.64 | 0.25 | 7.17 | 0.67 | 227.0 | 140.0 | 228.0 | 13.0 | 250.0 | 15.0 | 228.0 | 13.0 |
| Output_1_75 | 50700 | 676 | 4.2 | 0.04 | 3.09 | 0.05 | 3.75 | 0.28 | 3.56 | 0.13 | 251.6 | 85.0 | 245.4 | 7.6 | 333.0 | 8.0 | 245.4 | 9.0 |
| Output_1_246 | 5200 | 62 | 1.0 | 0.04 | 5.14 | 0.05 | 8.86 | 0.30 | 8.55 | 0.29 | 271.0 | 180.0 | 270.0 | 14.0 | 280.0 | 21.0 | 270.0 | 15.0 |
| Output_1_255 | 15560 | 247 | 3.4 | 0.04 | 3.17 | 0.06 | 5.75 | 0.34 | 6.45 | 0.50 | 297.0 | 140.0 | 278.5 | 8.4 | 460.0 | 17.0 | 278.5 | 10.0 |
| Output_1_63 | 15230 | 256 | 1.9 | 0.05 | 2.59 | 0.05 | 5.40 | 0.34 | 5.28 | 0.33 | 297.0 | 110.0 | 292.0 | 7.6 | 360.0 | 13.0 | 292.0 | 9.5 |
| Output_1_38 | 37610 | 844 | 1.7 | 0.05 | 2.75 | 0.05 | 3.16 | 0.34 | 4.39 | 0.62 | 298.0 | 72.0 | 297.4 | 8.1 | 349.0 | 12.0 | 297.4 | 9.9 |
| Output_1_26 | 39600 | 1058 | 2.4 | 0.05 | 6.42 | 0.05 | 8.33 | 0.38 | 6.53 | 0.27 | 329.0 | 180.0 | 323.0 | 20.0 | 340.0 | 19.0 | 323.0 | 21.0 |
| Output_1_186 | 8460 | 589 | 2.0 | 0.05 | 3.99 | 0.05 | 6.18 | 0.39 | 7.99 | 0.48 | 339.0 | 130.0 | 330.0 | 13.0 | 320.0 | 20.0 | 330.0 | 14.0 |
| Output_1_93 | 12810 | 171 | 2.6 | 0.05 | 5.52 | 0.06 | 8.81 | 0.40 | 8.02 | 0.34 | 340.0 | 170.0 | 330.0 | 18.0 | 520.0 | 23.0 | 330.0 | 19.0 |
| Output_1_182 | 6450 | 249 | 1.5 | 0.05 | 4.34 | 0.06 | 10.66 | 0.40 | 10.64 | 0.26 | 347.0 | 210.0 | 333.0 | 14.0 | 380.0 | 32.0 | 333.0 | 16.0 |
| Output_1_175 | 22100 | 418 | 1.5 | 0.05 | 3.75 | 0.05 | 5.11 | 0.39 | 6.65 | 0.50 | 342.0 | 110.0 | 335.0 | 12.0 | 310.0 | 19.0 | 335.0 | 14.0 |
| Output_1_82 | 78800 | 759 | 1.0 | 0.05 | 3.72 | 0.05 | 3.55 | 0.41 | 4.15 | 0.49 | 348.0 | 87.0 | 337.0 | 12.0 | 364.0 | 12.0 | 337.0 | 14.0 |
| Output_1_264 | 14780 | 229 | 1.3 | 0.06 | 3.82 | 0.05 | 7.06 | 0.42 | 6.18 | 0.12 | 356.0 | 170.0 | 345.0 | 13.0 | 380.0 | 19.0 | 345.0 | 15.0 |
| Output_1_79 | 21900 | 196 | 1.9 | 0.06 | 2.71 | 0.05 | 4.37 | 0.42 | 5.23 | 0.28 | 355.0 | 100.0 | 346.9 | 9.3 | 400.0 | 16.0 | 346.9 | 12.0 |
| Output_1_152 | 40200 | 433 | 1.5 | 0.06 | 3.62 | 0.06 | 4.17 | 0.42 | 4.96 | 0.56 | 358.0 | 93.0 | 347.0 | 12.0 | 400.0 | 15.0 | 347.0 | 14.0 |
| Output_1_45 | 12350 | 235 | 2.8 | 0.06 | 5.38 | 0.06 | 9.87 | 0.45 | 8.48 | 0.09 | 380.0 | 220.0 | 350.0 | 18.0 | 570.0 | 25.0 | 350.0 | 19.0 |
| Output_1_194 | 5940 | 80 | 1.4 | 0.06 | 4.23 | 0.06 | 7.50 | 0.44 | 7.47 | 0.16 | 369.0 | 170.0 | 356.0 | 14.0 | 550.0 | 23.0 | 356.0 | 16.0 |
| Output_1_140 | 26440 | 483 | 10.5 | 0.06 | 3.29 | 0.06 | 4.02 | 0.46 | 4.18 | 0.36 | 380.0 | 90.0 | 362.0 | 12.0 | 490.0 | 13.0 | 362.0 | 14.0 |
| Output_1_74 | 26160 | 240 | 1.7 | 0.06 | 6.56 | 0.06 | 8.87 | 0.47 | 11.21 | 0.77 | 392.0 | 200.0 | 363.0 | 23.0 | 530.0 | 36.0 | 363.0 | 24.0 |
| Output_1_37 | 32160 | 601 | 3.3 | 0.06 | 3.61 | 0.06 | 6.14 | 0.45 | 6.29 | 0.50 | 373.0 | 140.0 | 365.0 | 13.0 | 460.0 | 20.0 | 365.0 | 15.0 |
| Output_1_9 | 22380 | 414 | 2.0 | 0.06 | 4.09 | 0.05 | 5.85 | 0.45 | 5.38 | 0.42 | 373.0 | 130.0 | 367.0 | 14.0 | 370.0 | 17.0 | 367.0 | 16.0 |
| Output_1_6 | 31080 | 439 | 2.0 | 0.06 | 3.88 | 0.06 | 4.00 | 0.44 | 3.65 | 0.20 | 368.0 | 89.0 | 371.0 | 14.0 | 392.0 | 12.0 | 371.0 | 16.0 |
| Output_1_262 | 25870 | 344 | 0.6 | 0.06 | 2.91 | 0.06 | 4.29 | 0.47 | 5.15 | 0.51 | 387.0 | 90.0 | 387.0 | 11.0 | 439.0 | 17.0 | 387.0 | 13.0 |
| Output_1_258 | 32600 | 364 | 2.9 | 0.07 | 3.84 | 0.06 | 4.96 | 0.52 | 4.80 | 0.45 | 425.0 | 110.0 | 406.0 | 15.0 | 560.0 | 16.0 | 406.0 | 17.0 |
| Output_1_181 | 71700 | 1970 | 1.0 | 0.07 | 3.52 | 0.06 | 3.04 | 0.52 | 4.23 | 0.66 | 429.0 | 68.0 | 408.0 | 14.0 | 438.0 | 14.0 | 408.0 | 16.0 |
| Output_1_242 | 54300 | 392 | 0.9 | 0.07 | 2.86 | 0.06 | 4.09 | 0.54 | 5.34 | 0.63 | 444.0 | 91.0 | 436.0 | 12.0 | 543.0 | 20.0 | 436.0 | 15.0 |
| Output_1_120 | 39850 | 429 | 1.7 | 0.08 | 3.72 | 0.06 | 4.08 | 0.68 | 5.60 | 0.51 | 531.0 | 92.0 | 500.0 | 18.0 | 555.0 | 22.0 | 500.0 | 20.0 |
| Output_1_193 | 72400 | 648 | 1.6 | 0.08 | 3.02 | 0.07 | 4.59 | 0.73 | 5.31 | 0.49 | 557.0 | 99.0 | 514.0 | 15.0 | 828.0 | 23.0 | 514.0 | 18.0 |
| Output_1_35 | 25570 | 309 | 6.4 | 0.09 | 5.72 | 0.10 | 5.24 | 1.18 | 6.72 | 0.60 | 787.0 | 95.0 | 551.0 | 30.0 | ##### | 36.0 | 551.0 | 32.0 |
| Output_1_162 | 19310 | 478 | 3.8 | 0.09 | 8.17 | 0.16 | 3.51 | 2.17 | 9.22 | 0.40 | 1153.0 | 56.0 | 579.0 | 45.0 | ##### | 63.0 | 579.0 | 46.0 |
| Output_1_99 | 12560 | 90 | 1.0 | 0.11 | 4.25 | 0.14 | 3.61 | 2.05 | 4.88 | 0.71 | 1139.0 | 61.0 | 662.0 | 27.0 | ##### | 34.0 | 662.0 | 30.0 |
| Output_1_48 | 18790 | 164 | 1.6 | 0.12 | 3.08 | 0.11 | 3.16 | 1.85 | 4.34 | 0.53 | 1063.0 | 62.0 | 732.0 | 21.0 | ##### | 28.0 | 732.0 | 25.0 |

| | | | | | | | | | | | | | | | | | | |
|---|---|---|---|---|---|---|---|---|---|---|---|---|---|---|---|---|---|---|
| Output_1_141 | 87100 | 679 | 8.5 | 0.12 | 6.90 | 0.10 | 3.15 | 1.82 | 6.04 | 0.84 | 1048.0 | 60.0 | 757.0 | 49.0 | ##### | 40.0 | 757.0 | 51.0 |
| Output_1_165 | 12320 | 170 | 1.2 | 0.13 | 6.24 | 0.07 | 5.38 | 1.31 | 8.40 | 0.25 | 841.0 | 110.0 | 803.0 | 47.0 | 910.0 | 45.0 | 803.0 | 49.0 |
| Output_1_44 | 38910 | 284 | 3.3 | 0.14 | 3.95 | 0.09 | 3.08 | 1.82 | 4.95 | 0.82 | 1058.0 | 58.0 | 854.0 | 31.0 | ##### | 35.0 | 854.0 | 35.0 |
| Output_1_227 | 38560 | 241 | 5.7 | 0.17 | 3.82 | 0.08 | 3.81 | 1.79 | 3.74 | 0.43 | 1040.0 | 81.0 | 997.0 | 36.0 | ##### | 24.0 | 997.0 | 40.0 |
| Output_1_125 | 112200 | 513 | 3.4 | 0.20 | 4.70 | 0.09 | 4.43 | 2.67 | 3.40 | 0.52 | 1320.0 | 91.0 | 1162.0 | 50.0 | ##### | 25.0 | 1040.0 | 92.0 |
| Output_1_10 | 67100 | 380 | 2.1 | 0.21 | 3.67 | 0.10 | 3.18 | 2.86 | 3.22 | 0.51 | 1374.0 | 58.0 | 1226.0 | 41.0 | ##### | 25.0 | 1320.0 | 100.0 |
| Output_1_143 | 91200 | 327 | 1.7 | 0.23 | 2.66 | 0.14 | 2.43 | 4.51 | 3.99 | 0.67 | 1728.0 | 42.0 | 1332.0 | 32.0 | ##### | 34.0 | 1374.0 | 70.0 |
| Output_1_8 | 55200 | 227 | 1.7 | 0.24 | 4.06 | 0.12 | 2.60 | 3.95 | 4.05 | 0.64 | 1622.0 | 47.0 | 1381.0 | 50.0 | ##### | 33.0 | 1433.0 | 66.0 |
| Output_1_36 | 50800 | 205 | 2.2 | 0.27 | 3.41 | 0.12 | 2.93 | 4.44 | 4.95 | 0.73 | 1719.0 | 54.0 | 1523.0 | 46.0 | ##### | 44.0 | 1562.0 | 76.0 |
| Output_1_98 | 60700 | 173 | 1.6 | 0.27 | 4.14 | 0.10 | 3.44 | 3.62 | 4.14 | 0.60 | 1562.0 | 66.0 | 1516.0 | 54.0 | ##### | 33.0 | 1563.0 | 66.0 |
| Output_1_202 | 52600 | 187 | 1.0 | 0.29 | 3.86 | 0.11 | 3.05 | 4.46 | 4.04 | 0.59 | 1730.0 | 51.0 | 1622.0 | 54.0 | ##### | 34.0 | 1591.0 | 62.0 |
| Output_1_129 | 122500 | 367 | 1.7 | 0.27 | 3.43 | 0.14 | 2.77 | 5.46 | 3.30 | 0.53 | 1891.0 | 48.0 | 1558.0 | 47.0 | ##### | 29.0 | 1602.0 | 58.0 |
| Output_1_2 | 47200 | 140 | 0.8 | 0.28 | 2.50 | 0.10 | 2.99 | 3.81 | 3.41 | 0.31 | 1591.0 | 51.0 | 1569.0 | 35.0 | ##### | 28.0 | 1604.0 | 55.0 |
| Output_1_87 | 76500 | 165 | 0.9 | 0.26 | 3.45 | 0.10 | 2.43 | 3.67 | 4.36 | 0.73 | 1563.0 | 50.0 | 1465.0 | 45.0 | ##### | 36.0 | 1622.0 | 60.0 |
| Output_1_40 | 41120 | 155 | 3.1 | 0.27 | 3.24 | 0.10 | 2.33 | 3.86 | 3.37 | 0.72 | 1602.0 | 43.0 | 1548.0 | 45.0 | ##### | 26.0 | 1719.0 | 67.0 |
| Output_1_71 | 42200 | 73 | 1.3 | 0.32 | 5.70 | 0.13 | 3.71 | 5.47 | 6.58 | 0.77 | 1904.0 | 66.0 | 1766.0 | 91.0 | ##### | 52.0 | 1730.0 | 62.0 |
| Output_1_224 | 356000 | 1321 | 15.0 | 0.33 | 4.82 | 0.12 | 4.45 | 5.29 | 4.73 | 0.50 | 1862.0 | 75.0 | 1866.0 | 69.0 | ##### | 40.0 | 1844.0 | 72.0 |
| Output_1_249 | 435000 | 716 | 39.4 | 0.34 | 3.51 | 0.12 | 2.68 | 5.72 | 2.62 | 0.55 | 1936.0 | 45.0 | 1892.0 | 58.0 | ##### | 23.0 | 1862.0 | 83.0 |
| Output_1_66 | 90000 | 215 | 1.0 | 0.27 | 3.13 | 0.10 | 2.21 | 3.85 | 3.12 | 0.64 | 1604.0 | 40.0 | 1562.0 | 43.0 | ##### | 25.0 | 1891.0 | 60.0 |
| Output_1_135 | 51900 | 151 | 2.0 | 0.32 | 3.48 | 0.12 | 3.59 | 5.17 | 3.48 | 0.66 | 1844.0 | 62.0 | 1770.0 | 54.0 | ##### | 30.0 | 1904.0 | 75.0 |
| Output_1_41 | 60600 | 134 | 4.1 | 0.48 | 4.20 | 0.20 | 3.48 | 13.07 | 3.67 | 0.65 | 2680.0 | 57.0 | 2503.0 | 86.0 | ##### | 35.0 | 1936.0 | 57.0 |

**Sample 19ATW06**

| | | | | | | | | | | | | | | | | | | |
|---|---|---|---|---|---|---|---|---|---|---|---|---|---|---|---|---|---|---|
| Output_1_292 | 10800 | 759 | 45.8 | 0.01 | 4.51 | 0.05 | 7.79 | 0.07 | 7.78 | 0.37 | 160.0 | 150.0 | 66.8 | 3.0 | 69.2 | 5.2 | 66.8 | 3.0 |
| Output_1_100 | 2920 | 203 | 5.6 | 0.01 | 7.58 | 0.05 | 16.76 | 0.08 | 19.51 | 0.23 | 300.0 | 330.0 | 68.6 | 5.2 | 80.0 | 15.0 | 68.6 | 5.2 |
| Output_1_63 | 18330 | 1620 | 173.0 | 0.01 | 2.49 | 0.05 | 10.33 | 0.07 | 9.75 | 0.07 | 130.0 | 210.0 | 69.6 | 1.7 | 73.3 | 6.9 | 69.6 | 1.8 |
| Output_1_130 | 13790 | 4800 | 49.0 | 0.01 | 3.02 | 0.05 | 7.48 | 0.07 | 6.69 | 0.08 | 90.0 | 160.0 | 70.0 | 2.1 | 70.2 | 4.5 | 70.0 | 2.1 |
| Output_1_178 | 11430 | 950 | 59.9 | 0.01 | 2.81 | 0.05 | 14.80 | 0.07 | 15.07 | 0.24 | 70.0 | 280.0 | 70.7 | 2.0 | 71.0 | 11.0 | 70.7 | 2.0 |
| Output_1_303 | 8310 | 630 | 38.6 | 0.01 | 2.89 | 0.05 | 6.48 | 0.08 | 7.28 | 0.51 | 190.0 | 140.0 | 71.1 | 2.0 | 73.9 | 5.2 | 71.1 | 2.1 |
| Output_1_201 | 4510 | 436 | 2.4 | 0.01 | 4.02 | 0.05 | 7.85 | 0.07 | 10.36 | 0.06 | 280.0 | 170.0 | 71.8 | 2.9 | 70.9 | 7.2 | 71.8 | 2.9 |
| Output_1_183 | 1586 | 148 | 3.0 | 0.01 | 6.41 | 0.05 | 16.70 | 0.08 | 19.05 | 0.36 | 270.0 | 340.0 | 72.0 | 4.6 | 82.0 | 15.0 | 72.0 | 4.6 |
| Output_1_277 | 8680 | 628 | 31.1 | 0.01 | 4.48 | 0.05 | 12.60 | 0.08 | 11.53 | 0.34 | 250.0 | 250.0 | 73.0 | 3.2 | 74.6 | 8.3 | 73.0 | 3.3 |
| Output_1_1 | 6630 | 703 | 14.9 | 0.01 | 4.56 | 0.05 | 13.10 | 0.08 | 11.41 | 0.37 | 330.0 | 270.0 | 73.1 | 3.3 | 80.3 | 8.8 | 73.1 | 3.3 |
| Output_1_72 | 25830 | 2095 | 7.0 | 0.01 | 2.80 | 0.05 | 4.25 | 0.08 | 4.93 | 0.51 | 54.0 | 88.0 | 73.3 | 2.0 | 73.4 | 3.5 | 73.3 | 2.1 |
| Output_1_172 | 3730 | 270 | 3.2 | 0.01 | 7.64 | 0.05 | 27.45 | 0.09 | 24.42 | 0.21 | 170.0 | 510.0 | 73.9 | 5.6 | 84.0 | 20.0 | 73.9 | 5.7 |
| Output_1_117 | 4710 | 943 | 1.2 | 0.01 | 5.88 | 0.05 | 16.53 | 0.09 | 17.05 | 0.01 | 300.0 | 350.0 | 75.2 | 4.4 | 85.0 | 14.0 | 75.2 | 4.5 |
| Output_1_132 | 3800 | 1152 | 1.2 | 0.01 | 3.81 | 0.05 | 12.21 | 0.08 | 12.36 | 0.26 | 110.0 | 230.0 | 75.7 | 2.9 | 76.3 | 9.1 | 75.7 | 2.9 |
| Output_1_146 | 4200 | 443 | 3.4 | 0.01 | 4.49 | 0.05 | 10.25 | 0.08 | 10.04 | 0.20 | 270.0 | 190.0 | 75.7 | 3.4 | 80.4 | 7.8 | 75.7 | 3.4 |
| Output_1_8 | 6290 | 1008 | 2.7 | 0.01 | 2.78 | 0.05 | 9.38 | 0.08 | 9.25 | 0.02 | 90.0 | 170.0 | 76.0 | 2.1 | 76.9 | 6.8 | 76.0 | 2.2 |
| Output_1_239 | 3080 | 1070 | 5.8 | 0.01 | 5.39 | 0.05 | 12.78 | 0.08 | 10.77 | 0.01 | 180.0 | 230.0 | 76.1 | 4.1 | 78.6 | 8.2 | 76.1 | 4.1 |

| | | | | | | | | | | | | | | | | | | |
|---|---|---|---|---|---|---|---|---|---|---|---|---|---|---|---|---|---|---|
| Output_1_52 | 1810 | 129 | 4.5 | 0.01 | 5.47 | 0.06 | 14.86 | 0.09 | 13.48 | 0.00 | 350.0 | 280.0 | 76.2 | 4.1 | 86.0 | 11.0 | 76.2 | 4.2 |
| Output_1_112 | 10730 | 1252 | 8.8 | 0.01 | 4.69 | 0.05 | 7.59 | 0.08 | 9.21 | 0.41 | 290.0 | 160.0 | 76.4 | 3.5 | 81.4 | 7.2 | 76.4 | 3.6 |
| Output_1_99 | 6600 | 419 | 4.7 | 0.01 | 3.18 | 0.05 | 8.17 | 0.08 | 7.60 | 0.10 | 190.0 | 160.0 | 76.5 | 2.4 | 79.4 | 5.8 | 76.5 | 2.4 |
| Output_1_166 | 4990 | 392 | 2.0 | 0.01 | 6.77 | 0.05 | 16.76 | 0.09 | 16.28 | 0.05 | 310.0 | 330.0 | 76.6 | 5.2 | 83.0 | 13.0 | 76.6 | 5.2 |
| Output_1_202 | 2160 | 188 | 1.7 | 0.01 | 5.77 | 0.05 | 14.15 | 0.09 | 12.64 | 0.04 | 320.0 | 260.0 | 76.6 | 4.4 | 86.0 | 11.0 | 76.6 | 4.4 |
| Output_1_103 | 12690 | 853 | 18.7 | 0.01 | 3.76 | 0.05 | 6.81 | 0.08 | 7.02 | 0.34 | 180.0 | 140.0 | 76.8 | 2.8 | 80.5 | 5.4 | 76.8 | 2.9 |
| Output_1_21 | 11800 | 1830 | 1.5 | 0.01 | 2.59 | 0.05 | 7.30 | 0.08 | 7.46 | 0.09 | 180.0 | 150.0 | 76.8 | 2.0 | 78.4 | 5.6 | 76.8 | 2.0 |
| Output_1_218 | 6290 | 537 | 3.6 | 0.01 | 3.66 | 0.05 | 10.33 | 0.09 | 9.27 | 0.33 | 320.0 | 180.0 | 77.0 | 2.8 | 82.9 | 7.4 | 77.0 | 2.9 |
| Output_1_87 | 13490 | 828 | 0.8 | 0.01 | 3.90 | 0.05 | 6.59 | 0.08 | 6.47 | 0.34 | 210.0 | 140.0 | 77.2 | 3.0 | 79.8 | 5.0 | 77.2 | 3.0 |
| Output_1_114 | 4880 | 674 | 4.3 | 0.01 | 6.35 | 0.05 | 13.12 | 0.09 | 11.24 | 0.04 | 310.0 | 270.0 | 77.6 | 4.9 | 86.3 | 9.3 | 77.6 | 4.9 |
| Output_1_219 | 7960 | 745 | 2.5 | 0.01 | 3.47 | 0.05 | 7.27 | 0.08 | 6.87 | 0.17 | 160.0 | 140.0 | 77.6 | 2.7 | 79.4 | 5.2 | 77.6 | 2.7 |
| Output_1_265 | 4930 | 908 | 27.4 | 0.01 | 6.03 | 0.04 | 11.29 | 0.08 | 11.38 | 0.19 | -50.0 | 200.0 | 77.6 | 4.7 | 77.2 | 8.5 | 77.6 | 4.7 |
| Output_1_248 | 2740 | 1010 | 7.1 | 0.01 | 5.69 | 0.05 | 18.67 | 0.08 | 18.18 | 0.01 | 60.0 | 330.0 | 77.7 | 4.4 | 75.0 | 13.0 | 77.7 | 4.4 |
| Output_1_111 | 1219 | 134 | 2.0 | 0.01 | 7.81 | 0.05 | 16.27 | 0.09 | 16.13 | 0.08 | 340.0 | 270.0 | 77.9 | 6.1 | 92.0 | 13.0 | 77.9 | 6.1 |
| Output_1_91 | 8670 | 491 | 0.9 | 0.01 | 5.59 | 0.05 | 17.31 | 0.09 | 17.24 | 0.10 | 240.0 | 340.0 | 78.0 | 4.3 | 85.0 | 14.0 | 78.0 | 4.4 |
| Output_1_148 | 6110 | 611 | 1.5 | 0.01 | 3.77 | 0.05 | 8.43 | 0.09 | 7.06 | 0.05 | 240.0 | 170.0 | 78.1 | 2.9 | 83.8 | 5.3 | 78.1 | 3.0 |
| Output_1_81 | 1572 | 107 | 1.9 | 0.01 | 6.48 | 0.05 | 18.74 | 0.09 | 17.24 | 0.04 | 200.0 | 300.0 | 78.1 | 5.0 | 84.0 | 14.0 | 78.1 | 5.1 |
| Output_1_167 | 4620 | 336 | 1.0 | 0.01 | 4.58 | 0.05 | 10.34 | 0.09 | 10.22 | 0.23 | 140.0 | 200.0 | 78.3 | 3.5 | 83.6 | 8.2 | 78.3 | 3.6 |
| Output_1_247 | 2600 | 944 | 1.1 | 0.01 | 5.55 | 0.05 | 14.23 | 0.09 | 12.64 | 0.14 | 250.0 | 270.0 | 78.5 | 4.3 | 84.0 | 10.0 | 78.5 | 4.4 |
| Output_1_104 | 2990 | 197 | 1.4 | 0.01 | 4.15 | 0.05 | 12.91 | 0.08 | 12.35 | 0.15 | 120.0 | 240.0 | 78.7 | 3.3 | 78.3 | 9.8 | 78.7 | 3.3 |
| Output_1_131 | 23000 | 7080 | 9.0 | 0.01 | 3.91 | 0.05 | 11.94 | 0.09 | 10.98 | 0.11 | 230.0 | 250.0 | 78.7 | 3.0 | 84.2 | 8.8 | 78.7 | 3.1 |
| Output_1_160 | 2020 | 175 | 1.6 | 0.01 | 5.13 | 0.06 | 17.54 | 0.10 | 18.75 | 0.42 | 470.0 | 290.0 | 78.7 | 4.0 | 95.0 | 16.0 | 78.7 | 4.0 |
| Output_1_173 | 3980 | 262 | 1.9 | 0.01 | 6.18 | 0.05 | 11.72 | 0.09 | 11.38 | 0.51 | 220.0 | 240.0 | 78.8 | 4.8 | 84.5 | 9.3 | 78.8 | 4.9 |
| Output_1_144 | 8360 | 866 | 28.0 | 0.01 | 2.68 | 0.05 | 7.28 | 0.08 | 7.34 | 0.23 | 210.0 | 150.0 | 78.9 | 2.1 | 78.4 | 5.6 | 78.9 | 2.1 |
| Output_1_200 | 2122 | 194 | 2.4 | 0.01 | 4.78 | 0.06 | 16.64 | 0.09 | 16.13 | 0.23 | 330.0 | 320.0 | 79.1 | 3.8 | 90.0 | 14.0 | 79.1 | 3.8 |
| Output_1_27 | 4260 | 462 | 2.3 | 0.01 | 3.88 | 0.05 | 11.26 | 0.09 | 10.58 | 0.13 | 250.0 | 230.0 | 79.2 | 3.1 | 83.9 | 8.7 | 79.2 | 3.1 |
| Output_1_66 | 945 | 75 | 2.1 | 0.01 | 6.99 | 0.05 | 22.64 | 0.09 | 21.51 | 0.08 | 270.0 | 410.0 | 79.7 | 5.6 | 89.0 | 18.0 | 79.7 | 5.6 |
| Output_1_177 | 1970 | 140 | 1.8 | 0.01 | 7.69 | 0.04 | 18.31 | 0.08 | 18.75 | 0.36 | -90.0 | 300.0 | 80.0 | 6.1 | 77.0 | 14.0 | 80.0 | 6.1 |
| Output_1_82 | 12660 | 808 | 7.2 | 0.01 | 4.64 | 0.05 | 7.94 | 0.09 | 7.03 | 0.15 | 200.0 | 160.0 | 80.2 | 3.7 | 84.4 | 5.7 | 80.2 | 3.8 |
| Output_1_17 | 55700 | 9680 | 48.1 | 0.01 | 5.90 | 0.06 | 8.11 | 0.09 | 6.11 | 0.63 | 410.0 | 170.0 | 80.3 | 4.7 | 82.9 | 4.9 | 80.3 | 4.8 |
| Output_1_168 | 20670 | 1474 | 0.8 | 0.01 | 2.93 | 0.05 | 4.01 | 0.09 | 4.04 | 0.31 | 94.0 | 86.0 | 80.8 | 2.3 | 84.4 | 3.2 | 80.8 | 2.4 |
| Output_1_135 | 4540 | 536 | 2.8 | 0.01 | 3.40 | 0.05 | 10.61 | 0.09 | 10.75 | 0.15 | 330.0 | 220.0 | 81.1 | 2.7 | 90.3 | 9.5 | 81.1 | 2.8 |
| Output_1_236 | 1337 | 382 | 2.8 | 0.01 | 6.24 | 0.04 | 20.27 | 0.08 | 21.25 | 0.37 | 0.0 | 340.0 | 81.1 | 5.0 | 77.0 | 16.0 | 81.1 | 5.0 |
| Output_1_282 | 1870 | 114 | 1.4 | 0.01 | 7.56 | 0.05 | 23.40 | 0.09 | 28.09 | 0.39 | 160.0 | 470.0 | 81.4 | 6.1 | 86.0 | 23.0 | 81.4 | 6.1 |
| Output_1_296 | 2670 | 153 | 2.9 | 0.01 | 3.70 | 0.06 | 14.73 | 0.09 | 13.98 | 0.04 | 300.0 | 280.0 | 81.4 | 3.0 | 90.0 | 12.0 | 81.4 | 3.1 |
| Output_1_4 | 9470 | 1078 | 1.6 | 0.01 | 4.01 | 0.05 | 8.96 | 0.09 | 9.38 | 0.50 | 250.0 | 160.0 | 81.5 | 3.3 | 83.0 | 7.5 | 81.5 | 3.3 |
| Output_1_118 | 5350 | 1274 | 14.1 | 0.01 | 2.74 | 0.05 | 10.30 | 0.09 | 9.80 | 0.03 | 220.0 | 210.0 | 81.7 | 2.3 | 88.0 | 8.2 | 81.7 | 2.3 |
| Output_1_122 | 4170 | 1267 | 1.6 | 0.01 | 5.33 | 0.05 | 11.69 | 0.09 | 10.86 | 0.05 | 250.0 | 230.0 | 81.7 | 4.3 | 88.3 | 9.2 | 81.7 | 4.3 |
| Output_1_305 | 2000 | 139 | 2.0 | 0.01 | 5.41 | 0.05 | 13.46 | 0.08 | 13.41 | 0.06 | 80.0 | 230.0 | 81.7 | 4.4 | 80.0 | 10.0 | 81.7 | 4.4 |
| Output_1_254 | 4000 | 1108 | 2.7 | 0.01 | 4.38 | 0.05 | 13.12 | 0.09 | 10.32 | 0.37 | 200.0 | 230.0 | 81.9 | 3.6 | 87.2 | 8.7 | 81.9 | 3.6 |

| | | | | | | | | | | | | | | | | | | |
|---|---|---|---|---|---|---|---|---|---|---|---|---|---|---|---|---|---|---|
| Output_1_279 | 6010 | 360 | 2.9 | 0.01 | 4.98 | 0.05 | 9.35 | 0.09 | 9.01 | 0.23 | 140.0 | 180.0 | 82.3 | 4.1 | 83.1 | 7.2 | 82.3 | 4.1 |
| Output_1_234 | 3760 | 934 | 1.3 | 0.01 | 3.11 | 0.05 | 9.03 | 0.09 | 9.09 | 0.11 | 120.0 | 170.0 | 82.4 | 2.5 | 83.4 | 7.3 | 82.4 | 2.6 |
| Output_1_41 | 25100 | 1710 | 9.3 | 0.01 | 3.03 | 0.05 | 4.18 | 0.08 | 4.97 | 0.41 | 100.0 | 87.0 | 82.4 | 2.5 | 82.3 | 3.9 | 82.4 | 2.5 |
| Output_1_241 | 10810 | 3780 | 14.4 | 0.01 | 5.28 | 0.05 | 11.28 | 0.09 | 9.39 | 0.17 | 310.0 | 230.0 | 82.5 | 4.3 | 87.8 | 7.9 | 82.5 | 4.4 |
| Output_1_126 | 3780 | 1245 | 1.1 | 0.01 | 5.97 | 0.05 | 11.83 | 0.09 | 11.96 | 0.15 | 300.0 | 240.0 | 82.6 | 4.9 | 93.0 | 11.0 | 82.6 | 4.9 |
| Output_1_16 | 3360 | 578 | 3.9 | 0.01 | 3.95 | 0.05 | 11.13 | 0.08 | 10.94 | 0.17 | 110.0 | 200.0 | 82.7 | 3.3 | 83.4 | 9.2 | 82.7 | 3.3 |
| Output_1_15 | 2760 | 493 | 2.4 | 0.01 | 5.77 | 0.06 | 11.82 | 0.09 | 10.75 | 0.02 | 410.0 | 260.0 | 83.2 | 4.8 | 89.7 | 9.2 | 83.2 | 4.8 |
| Output_1_61 | 5240 | 387 | 1.1 | 0.01 | 4.45 | 0.05 | 9.78 | 0.09 | 12.09 | 0.49 | 140.0 | 190.0 | 83.4 | 3.7 | 88.1 | 9.9 | 83.4 | 3.7 |
| Output_1_101 | 3050 | 177 | 2.2 | 0.01 | 4.45 | 0.05 | 12.86 | 0.08 | 11.69 | 0.14 | 140.0 | 240.0 | 83.5 | 3.7 | 81.3 | 9.2 | 83.5 | 3.7 |
| Output_1_266 | 3260 | 265 | 1.5 | 0.01 | 4.68 | 0.05 | 13.69 | 0.09 | 13.04 | 0.04 | 240.0 | 270.0 | 83.5 | 3.9 | 91.0 | 12.0 | 83.5 | 3.9 |
| Output_1_285 | 7770 | 429 | 2.5 | 0.01 | 6.58 | 0.05 | 12.50 | 0.09 | 13.33 | 0.28 | 200.0 | 250.0 | 83.6 | 5.5 | 90.0 | 12.0 | 83.6 | 5.5 |
| Output_1_306 | 7920 | 558 | 2.9 | 0.01 | 3.67 | 0.05 | 9.11 | 0.09 | 9.07 | 0.43 | 150.0 | 180.0 | 83.7 | 3.1 | 86.6 | 7.5 | 83.7 | 3.1 |
| Output_1_139 | 1670 | 173 | 3.0 | 0.01 | 5.65 | 0.06 | 16.99 | 0.10 | 17.00 | 0.14 | 420.0 | 320.0 | 83.8 | 4.7 | 96.0 | 16.0 | 83.8 | 4.7 |
| Output_1_46 | 2708 | 166 | 2.1 | 0.01 | 4.51 | 0.05 | 9.54 | 0.09 | 10.06 | 0.18 | 180.0 | 190.0 | 83.8 | 3.7 | 90.3 | 8.7 | 83.8 | 3.8 |
| Output_1_143 | 9020 | 876 | 1.6 | 0.01 | 2.80 | 0.05 | 7.35 | 0.08 | 5.90 | 0.14 | 90.0 | 140.0 | 84.5 | 2.4 | 82.6 | 4.7 | 84.5 | 2.4 |
| Output_1_252 | 6760 | 1970 | 35.0 | 0.01 | 5.37 | 0.05 | 8.15 | 0.09 | 10.01 | 0.18 | 150.0 | 160.0 | 84.6 | 4.5 | 86.2 | 8.3 | 84.6 | 4.6 |
| Output_1_212 | 2380 | 143 | 2.1 | 0.01 | 6.41 | 0.05 | 12.36 | 0.10 | 12.63 | 0.25 | 390.0 | 240.0 | 85.0 | 5.4 | 92.0 | 11.0 | 85.0 | 5.5 |
| Output_1_137 | 2890 | 308 | 1.7 | 0.01 | 5.27 | 0.05 | 13.72 | 0.09 | 13.04 | 0.21 | 270.0 | 260.0 | 85.1 | 4.5 | 88.0 | 11.0 | 85.1 | 4.5 |
| Output_1_301 | 2130 | 129 | 2.4 | 0.01 | 5.55 | 0.05 | 13.84 | 0.08 | 11.90 | 0.05 | 110.0 | 250.0 | 85.3 | 4.7 | 81.2 | 9.5 | 85.3 | 4.7 |
| Output_1_2 | 8290 | 787 | 8.1 | 0.01 | 5.37 | 0.05 | 12.15 | 0.09 | 10.71 | 0.12 | 160.0 | 250.0 | 85.8 | 4.6 | 87.0 | 9.0 | 85.8 | 4.6 |
| Output_1_86 | 7360 | 405 | 1.6 | 0.01 | 4.02 | 0.05 | 8.25 | 0.09 | 8.43 | 0.22 | 250.0 | 170.0 | 86.0 | 3.4 | 90.7 | 7.4 | 86.0 | 3.5 |
| Output_1_29 | 3860 | 355 | 1.8 | 0.01 | 6.09 | 0.05 | 16.35 | 0.10 | 14.74 | 0.09 | 140.0 | 250.0 | 86.2 | 5.2 | 92.0 | 13.0 | 86.2 | 5.3 |
| Output_1_238 | 2130 | 642 | 2.3 | 0.01 | 6.09 | 0.05 | 17.87 | 0.10 | 17.35 | 0.19 | 320.0 | 340.0 | 86.2 | 5.2 | 94.0 | 16.0 | 86.2 | 5.2 |
| Output_1_79 | 26830 | 1674 | 3.6 | 0.01 | 3.04 | 0.05 | 4.39 | 0.09 | 4.29 | 0.34 | 191.0 | 90.0 | 86.3 | 2.6 | 90.5 | 3.7 | 86.3 | 2.7 |
| Output_1_300 | 4660 | 271 | 4.8 | 0.01 | 3.55 | 0.05 | 9.52 | 0.10 | 9.42 | 0.06 | 190.0 | 190.0 | 86.5 | 3.1 | 92.3 | 8.3 | 86.5 | 3.1 |
| Output_1_85 | 677 | 40 | 2.4 | 0.01 | 8.15 | 0.06 | 28.07 | 0.10 | 27.45 | 0.11 | 250.0 | 480.0 | 86.6 | 7.2 | 95.0 | 25.0 | 86.6 | 7.2 |
| Output_1_260 | 13360 | 2760 | 3.0 | 0.01 | 3.39 | 0.05 | 6.67 | 0.09 | 6.98 | 0.10 | 210.0 | 130.0 | 86.8 | 2.9 | 91.7 | 6.1 | 86.8 | 3.0 |
| Output_1_153 | 12260 | 1050 | 1.6 | 0.01 | 2.95 | 0.05 | 10.47 | 0.10 | 9.70 | 0.25 | 290.0 | 220.0 | 86.9 | 2.5 | 94.6 | 8.9 | 86.9 | 2.6 |
| Output_1_199 | 9030 | 794 | 2.0 | 0.01 | 4.27 | 0.05 | 8.30 | 0.09 | 8.99 | 0.12 | 240.0 | 160.0 | 86.9 | 3.7 | 91.5 | 8.0 | 86.9 | 3.7 |
| Output_1_13 | 6800 | 1158 | 1.1 | 0.01 | 6.17 | 0.05 | 10.29 | 0.09 | 7.64 | 0.26 | 230.0 | 210.0 | 87.2 | 5.3 | 86.5 | 6.4 | 87.2 | 5.4 |
| Output_1_113 | 8030 | 908 | 1.1 | 0.01 | 3.29 | 0.05 | 7.87 | 0.09 | 7.08 | 0.26 | 120.0 | 150.0 | 87.4 | 2.9 | 87.7 | 5.9 | 87.4 | 2.9 |
| Output_1_253 | 16030 | 4280 | 2.1 | 0.01 | 2.75 | 0.05 | 6.07 | 0.09 | 5.30 | 0.18 | 110.0 | 120.0 | 88.3 | 2.4 | 87.9 | 4.4 | 88.3 | 2.5 |
| Output_1_293 | 1291 | 65 | 2.6 | 0.01 | 6.44 | 0.05 | 19.23 | 0.10 | 17.82 | 0.17 | 310.0 | 380.0 | 88.4 | 5.7 | 97.0 | 17.0 | 88.4 | 5.7 |
| Output_1_262 | 3590 | 669 | 1.2 | 0.01 | 4.41 | 0.05 | 14.07 | 0.10 | 14.42 | 0.08 | 310.0 | 280.0 | 88.5 | 3.9 | 100.0 | 13.0 | 88.5 | 3.9 |
| Output_1_302 | 5200 | 293 | 8.8 | 0.01 | 3.72 | 0.05 | 8.28 | 0.09 | 8.70 | 0.23 | 150.0 | 170.0 | 89.6 | 3.3 | 93.0 | 8.0 | 89.6 | 3.3 |
| Output_1_33 | 8520 | 665 | 5.8 | 0.01 | 4.00 | 0.05 | 6.84 | 0.09 | 7.62 | 0.22 | 220.0 | 150.0 | 89.7 | 3.6 | 91.6 | 6.7 | 89.7 | 3.6 |
| Output_1_203 | 12610 | 880 | 1.9 | 0.01 | 2.56 | 0.05 | 7.75 | 0.10 | 7.72 | 0.09 | 240.0 | 180.0 | 90.1 | 2.3 | 95.3 | 7.0 | 90.1 | 2.4 |
| Output_1_278 | 3820 | 222 | 1.3 | 0.01 | 4.90 | 0.05 | 12.62 | 0.10 | 11.34 | 0.15 | 170.0 | 240.0 | 90.2 | 4.4 | 93.4 | 9.9 | 90.2 | 4.4 |
| Output_1_59 | 16400 | 1081 | 1.2 | 0.01 | 3.56 | 0.05 | 5.76 | 0.10 | 5.00 | 0.06 | 130.0 | 120.0 | 91.6 | 3.3 | 96.8 | 4.6 | 91.6 | 3.3 |
| Output_1_233 | 5430 | 1157 | 1.1 | 0.01 | 4.94 | 0.05 | 11.32 | 0.10 | 12.24 | 0.23 | 170.0 | 220.0 | 93.3 | 4.6 | 95.0 | 11.0 | 93.3 | 4.6 |

| | | | | | | | | | | | | | | | | | | |
|---|---|---|---|---|---|---|---|---|---|---|---|---|---|---|---|---|---|---|
| Output_1_229 | 8250 | 1430 | 1.6 | 0.01 | 4.45 | 0.05 | 7.57 | 0.10 | 6.71 | 0.18 | 170.0 | 150.0 | 93.5 | 4.2 | 93.8 | 6.0 | 93.5 | 4.2 |
| Output_1_154 | 6360 | 495 | 1.6 | 0.01 | 4.02 | 0.05 | 7.03 | 0.10 | 7.61 | 0.39 | 200.0 | 150.0 | 93.8 | 3.7 | 97.7 | 7.0 | 93.8 | 3.8 |
| Output_1_31 | 4200 | 333 | 1.5 | 0.01 | 5.51 | 0.05 | 9.16 | 0.10 | 10.10 | 0.36 | 180.0 | 180.0 | 94.0 | 5.1 | 97.7 | 9.7 | 94.0 | 5.2 |
| Output_1_45 | 9110 | 498 | 1.4 | 0.01 | 3.42 | 0.05 | 7.61 | 0.10 | 6.19 | 0.16 | 70.0 | 150.0 | 95.5 | 3.2 | 95.3 | 5.6 | 95.5 | 3.3 |
| Output_1_209 | 12820 | 689 | 10.2 | 0.02 | 4.71 | 0.05 | 5.47 | 0.11 | 5.23 | 0.41 | 200.0 | 120.0 | 96.4 | 4.5 | 101.5 | 5.1 | 96.4 | 4.5 |
| Output_1_165 | 4550 | 283 | 1.9 | 0.02 | 7.95 | 0.05 | 15.93 | 0.12 | 20.17 | 0.41 | 330.0 | 320.0 | 96.4 | 7.3 | 113.0 | 21.0 | 96.4 | 7.3 |
| Output_1_54 | 4410 | 256 | 1.3 | 0.02 | 4.93 | 0.05 | 13.46 | 0.11 | 12.50 | 0.08 | 290.0 | 270.0 | 97.2 | 4.8 | 107.0 | 12.0 | 97.2 | 4.8 |
| Output_1_214 | 48500 | 2530 | 1.1 | 0.02 | 2.15 | 0.05 | 3.64 | 0.10 | 4.39 | 0.32 | 160.0 | 77.0 | 98.0 | 2.1 | 101.2 | 4.3 | 98.0 | 2.2 |
| Output_1_55 | 12140 | 722 | 0.5 | 0.02 | 3.07 | 0.05 | 6.53 | 0.11 | 6.03 | 0.08 | 130.0 | 140.0 | 98.0 | 3.0 | 102.3 | 5.8 | 98.0 | 3.0 |
| Output_1_97 | 3013 | 140 | 1.2 | 0.02 | 3.36 | 0.05 | 9.94 | 0.11 | 11.71 | 0.44 | 290.0 | 200.0 | 98.9 | 3.3 | 106.0 | 12.0 | 98.9 | 3.4 |
| Output_1_23 | 13400 | 1371 | 2.6 | 0.02 | 2.96 | 0.05 | 5.93 | 0.11 | 6.04 | 0.28 | 270.0 | 120.0 | 99.3 | 2.9 | 106.1 | 6.2 | 99.3 | 3.0 |
| Output_1_264 | 3090 | 480 | 2.2 | 0.02 | 3.84 | 0.05 | 11.13 | 0.11 | 12.73 | 0.43 | 300.0 | 220.0 | 99.9 | 3.8 | 105.0 | 13.0 | 99.9 | 3.9 |
| Output_1_5 | 8260 | 890 | 12.5 | 0.02 | 8.23 | 0.05 | 9.94 | 0.11 | 10.09 | 0.53 | 270.0 | 200.0 | 101.0 | 8.0 | 105.0 | 10.0 | 101.0 | 8.0 |
| Output_1_192 | 36970 | 3154 | 3.6 | 0.02 | 2.05 | 0.05 | 3.75 | 0.11 | 3.79 | 0.30 | 230.0 | 83.0 | 103.0 | 2.1 | 109.1 | 3.9 | 103.0 | 2.2 |
| Output_1_92 | 4290 | 185 | 1.9 | 0.02 | 3.63 | 0.05 | 12.45 | 0.12 | 13.04 | 0.19 | 290.0 | 260.0 | 103.8 | 3.7 | 110.0 | 14.0 | 103.8 | 3.8 |
| Output_1_56 | 5620 | 309 | 1.8 | 0.02 | 4.66 | 0.05 | 8.28 | 0.12 | 9.57 | 0.37 | 110.0 | 160.0 | 104.3 | 4.8 | 110.0 | 10.0 | 104.3 | 4.8 |
| Output_1_210 | 1380 | 69 | 2.5 | 0.02 | 5.62 | 0.05 | 17.28 | 0.11 | 16.04 | 0.14 | 40.0 | 300.0 | 104.6 | 5.8 | 101.0 | 16.0 | 104.6 | 5.8 |
| Output_1_213 | 1980 | 94 | 2.2 | 0.02 | 6.67 | 0.06 | 14.31 | 0.13 | 13.60 | 0.14 | 410.0 | 290.0 | 105.3 | 6.9 | 119.0 | 15.0 | 105.3 | 7.0 |
| Output_1_259 | 42100 | 7350 | 1.4 | 0.02 | 3.92 | 0.05 | 4.82 | 0.11 | 4.60 | 0.45 | 94.0 | 97.0 | 106.0 | 4.1 | 104.6 | 4.6 | 106.0 | 4.2 |
| Output_1_40 | 10230 | 538 | 1.3 | 0.02 | 3.00 | 0.05 | 7.98 | 0.11 | 6.85 | 0.04 | 130.0 | 150.0 | 106.4 | 3.2 | 106.6 | 7.0 | 106.4 | 3.3 |
| Output_1_304 | 2750 | 143 | 7.4 | 0.02 | 4.98 | 0.05 | 10.32 | 0.12 | 10.83 | 0.26 | 220.0 | 210.0 | 106.4 | 5.3 | 114.0 | 12.0 | 106.4 | 5.3 |
| Output_1_298 | 5030 | 234 | 11.6 | 0.02 | 8.43 | 0.05 | 15.28 | 0.11 | 11.11 | 0.27 | 360.0 | 320.0 | 106.4 | 9.0 | 104.0 | 11.0 | 106.4 | 9.1 |
| Output_1_228 | 13840 | 1881 | 1.6 | 0.02 | 4.20 | 0.05 | 5.00 | 0.11 | 5.96 | 0.50 | 110.0 | 100.0 | 106.6 | 4.5 | 108.0 | 6.1 | 106.6 | 4.5 |
| Output_1_272 | 7380 | 409 | 5.1 | 0.02 | 6.59 | 0.05 | 11.54 | 0.11 | 9.73 | 0.49 | 250.0 | 240.0 | 106.6 | 6.8 | 108.0 | 11.0 | 106.6 | 6.8 |
| Output_1_64 | 12580 | 695 | 6.7 | 0.02 | 5.36 | 0.05 | 8.25 | 0.13 | 9.77 | 0.26 | 270.0 | 180.0 | 107.3 | 5.7 | 127.0 | 11.0 | 107.3 | 5.7 |
| Output_1_120 | 12400 | 2530 | 2.1 | 0.02 | 4.62 | 0.05 | 9.73 | 0.12 | 9.40 | 0.52 | 110.0 | 190.0 | 107.8 | 4.9 | 112.1 | 9.7 | 107.8 | 5.0 |
| Output_1_246 | 1696 | 489 | 3.0 | 0.02 | 6.25 | 0.05 | 20.75 | 0.13 | 20.45 | 0.31 | 230.0 | 370.0 | 112.2 | 6.8 | 123.0 | 24.0 | 112.2 | 6.9 |
| Output_1_60 | 1489 | 77 | 3.4 | 0.02 | 7.34 | 0.05 | 20.00 | 0.12 | 21.67 | 0.24 | 30.0 | 330.0 | 113.3 | 8.3 | 112.0 | 23.0 | 113.3 | 8.4 |
| Output_1_251 | 3250 | 734 | 5.8 | 0.02 | 4.09 | 0.05 | 12.16 | 0.12 | 12.30 | 0.18 | 130.0 | 230.0 | 114.1 | 4.6 | 116.0 | 14.0 | 114.1 | 4.7 |
| Output_1_280 | 15470 | 672 | 1.6 | 0.02 | 2.09 | 0.05 | 6.27 | 0.13 | 6.47 | 0.04 | 220.0 | 130.0 | 116.0 | 2.4 | 120.9 | 7.4 | 116.0 | 2.6 |
| Output_1_128 | 6420 | 1400 | 7.1 | 0.02 | 6.01 | 0.05 | 8.16 | 0.14 | 10.14 | 0.92 | 340.0 | 170.0 | 116.8 | 6.8 | 131.0 | 12.0 | 116.8 | 6.8 |
| Output_1_161 | 11350 | 625 | 1.2 | 0.02 | 3.88 | 0.05 | 6.19 | 0.13 | 6.25 | 0.43 | 270.0 | 120.0 | 116.9 | 4.5 | 124.8 | 7.3 | 116.9 | 4.5 |
| Output_1_65 | 6820 | 362 | 4.1 | 0.02 | 5.11 | 0.05 | 12.36 | 0.13 | 10.45 | 0.41 | 340.0 | 270.0 | 117.4 | 6.0 | 127.0 | 13.0 | 117.4 | 6.0 |
| Output_1_189 | 2900 | 209 | 4.2 | 0.02 | 7.07 | 0.05 | 19.61 | 0.14 | 20.86 | 0.35 | 220.0 | 390.0 | 117.6 | 8.0 | 131.0 | 26.0 | 117.6 | 8.1 |
| Output_1_25 | 21200 | 1663 | 2.8 | 0.02 | 3.30 | 0.05 | 6.05 | 0.13 | 6.13 | 0.33 | 230.0 | 120.0 | 121.8 | 4.0 | 124.4 | 7.2 | 121.8 | 4.0 |
| Output_1_187 | 16860 | 1108 | 1.0 | 0.02 | 4.60 | 0.05 | 8.41 | 0.14 | 8.09 | 0.27 | 230.0 | 170.0 | 124.8 | 5.7 | 128.9 | 9.7 | 124.8 | 5.7 |
| Output_1_185 | 7600 | 452 | 4.3 | 0.02 | 6.63 | 0.05 | 9.02 | 0.13 | 9.02 | 0.39 | 260.0 | 190.0 | 125.3 | 8.5 | 127.0 | 11.0 | 125.3 | 8.6 |
| Output_1_107 | 12810 | 642 | 1.8 | 0.02 | 3.96 | 0.05 | 5.60 | 0.13 | 5.83 | 0.35 | 190.0 | 120.0 | 127.3 | 5.0 | 127.2 | 7.0 | 127.3 | 5.1 |
| Output_1_89 | 1640 | 58 | 4.1 | 0.02 | 8.46 | 0.06 | 17.82 | 0.15 | 19.18 | 0.36 | 300.0 | 330.0 | 128.0 | 11.0 | 141.0 | 24.0 | 128.0 | 11.0 |
| Output_1_18 | 3410 | 352 | 2.4 | 0.02 | 3.60 | 0.06 | 12.96 | 0.15 | 12.08 | 0.07 | 370.0 | 250.0 | 131.0 | 4.7 | 140.0 | 16.0 | 131.0 | 4.8 |

| | | | | | | | | | | | | | | | | | | |
|---|---|---|---|---|---|---|---|---|---|---|---|---|---|---|---|---|---|---|
| Output_1_181 | 7960 | 387 | 2.0 | 0.02 | 3.41 | 0.05 | 8.56 | 0.15 | 8.55 | 0.26 | 270.0 | 170.0 | 131.1 | 4.4 | 143.0 | 12.0 | 131.1 | 4.5 |
| Output_1_51 | 4140 | 168 | 2.6 | 0.02 | 3.86 | 0.06 | 12.79 | 0.17 | 9.58 | 0.00 | 380.0 | 240.0 | 132.1 | 5.1 | 156.0 | 14.0 | 132.1 | 5.1 |
| Output_1_98 | 1071 | 36 | 2.3 | 0.02 | 7.14 | 0.05 | 28.00 | 0.14 | 26.76 | 0.08 | 100.0 | 460.0 | 134.1 | 9.5 | 136.0 | 34.0 | 134.1 | 9.5 |
| Output_1_136 | 8430 | 581 | 2.4 | 0.02 | 4.34 | 0.05 | 9.29 | 0.15 | 7.89 | 0.16 | 340.0 | 190.0 | 135.1 | 5.8 | 143.0 | 11.0 | 135.1 | 5.9 |
| Output_1_11 | 9420 | 982 | 0.8 | 0.02 | 2.99 | 0.05 | 6.15 | 0.14 | 6.29 | 0.14 | 200.0 | 120.0 | 136.6 | 4.0 | 135.4 | 8.0 | 136.6 | 4.1 |
| Output_1_133 | 20880 | 3270 | 9.6 | 0.02 | 3.61 | 0.05 | 8.65 | 0.16 | 6.45 | 0.07 | 310.0 | 190.0 | 137.8 | 4.9 | 146.3 | 8.9 | 137.8 | 5.0 |
| Output_1_119 | 20020 | 2984 | 1.3 | 0.02 | 2.28 | 0.05 | 4.10 | 0.15 | 5.00 | 0.69 | 138.0 | 83.0 | 139.9 | 3.1 | 144.6 | 6.4 | 139.9 | 3.3 |
| Output_1_156 | 57400 | 2797 | 1.0 | 0.02 | 3.57 | 0.05 | 5.15 | 0.16 | 4.51 | 0.67 | 290.0 | 110.0 | 141.1 | 5.0 | 152.3 | 6.4 | 141.1 | 5.1 |
| Output_1_273 | 4460 | 183 | 2.7 | 0.02 | 5.88 | 0.06 | 14.69 | 0.17 | 12.79 | 0.11 | 430.0 | 310.0 | 141.1 | 8.3 | 161.0 | 19.0 | 141.1 | 8.3 |
| Output_1_240 | 17390 | 3408 | 1.8 | 0.02 | 3.02 | 0.05 | 5.22 | 0.16 | 5.30 | 0.32 | 270.0 | 110.0 | 141.3 | 4.2 | 149.2 | 7.3 | 141.3 | 4.3 |
| Output_1_190 | 2100 | 131 | 2.2 | 0.02 | 5.78 | 0.06 | 18.18 | 0.16 | 15.92 | 0.05 | 420.0 | 290.0 | 143.6 | 7.9 | 147.0 | 22.0 | 143.6 | 8.0 |
| Output_1_216 | 9980 | 384 | 2.2 | 0.02 | 4.85 | 0.05 | 8.37 | 0.16 | 7.10 | 0.16 | 260.0 | 170.0 | 144.7 | 7.1 | 145.7 | 9.7 | 144.7 | 7.2 |
| Output_1_196 | 16200 | 886 | 3.8 | 0.02 | 4.70 | 0.05 | 7.75 | 0.17 | 7.14 | 0.57 | 340.0 | 170.0 | 148.9 | 7.0 | 157.0 | 11.0 | 148.9 | 7.0 |
| Output_1_134 | 15700 | 2010 | 23.9 | 0.02 | 5.83 | 0.05 | 7.28 | 0.16 | 10.43 | 0.09 | 250.0 | 220.0 | 153.1 | 8.8 | 158.0 | 11.0 | 153.1 | 8.8 |
| Output_1_90 | 4380 | 127 | 2.7 | 0.02 | 4.53 | 0.05 | 20.37 | 0.18 | 20.77 | 0.32 | 310.0 | 390.0 | 154.5 | 7.2 | 169.0 | 33.0 | 154.5 | 7.3 |
| Output_1_6 | 3650 | 239 | 3.4 | 0.02 | 5.31 | 0.05 | 25.93 | 0.21 | 33.01 | 0.64 | 420.0 | 550.0 | 156.2 | 8.4 | 189.0 | 57.0 | 156.2 | 8.4 |
| Output_1_176 | 2040 | 78 | 1.8 | 0.02 | 7.02 | 0.05 | 17.95 | 0.18 | 17.98 | 0.10 | 280.0 | 350.0 | 157.0 | 12.0 | 165.0 | 27.0 | 157.0 | 12.0 |
| Output_1_129 | 7120 | 1197 | 4.1 | 0.02 | 6.05 | 0.06 | 8.26 | 0.19 | 9.52 | 0.57 | 450.0 | 170.0 | 157.7 | 9.7 | 179.0 | 15.0 | 157.7 | 9.8 |
| Output_1_62 | 6670 | 265 | 2.1 | 0.02 | 3.43 | 0.05 | 9.34 | 0.18 | 10.73 | 0.45 | 210.0 | 190.0 | 157.8 | 5.3 | 167.0 | 17.0 | 157.8 | 5.4 |
| Output_1_57 | 11750 | 440 | 5.7 | 0.02 | 5.24 | 0.05 | 11.45 | 0.18 | 8.70 | 0.13 | 270.0 | 240.0 | 157.8 | 8.4 | 171.0 | 14.0 | 157.8 | 8.4 |
| Output_1_287 | 9350 | 276 | 12.0 | 0.02 | 5.62 | 0.05 | 9.44 | 0.17 | 11.56 | 0.39 | 180.0 | 190.0 | 158.6 | 8.8 | 161.0 | 17.0 | 158.6 | 8.8 |
| Output_1_73 | 33300 | 1206 | 1.9 | 0.03 | 3.70 | 0.05 | 4.79 | 0.18 | 5.12 | 0.35 | 300.0 | 110.0 | 160.0 | 5.9 | 170.5 | 7.7 | 160.0 | 6.0 |
| Output_1_74 | 13080 | 471 | 4.4 | 0.03 | 3.17 | 0.05 | 5.17 | 0.18 | 6.56 | 0.45 | 290.0 | 110.0 | 160.6 | 5.0 | 171.0 | 10.0 | 160.6 | 5.1 |
| Output_1_58 | 15920 | 573 | 6.0 | 0.03 | 3.92 | 0.05 | 5.75 | 0.18 | 6.21 | 0.42 | 130.0 | 120.0 | 162.5 | 6.4 | 165.3 | 9.5 | 162.5 | 6.4 |
| Output_1_295 | 30570 | 885 | 1.3 | 0.03 | 2.98 | 0.05 | 3.69 | 0.18 | 3.88 | 0.35 | 253.0 | 80.0 | 162.6 | 4.8 | 168.3 | 6.0 | 162.6 | 4.9 |
| Output_1_109 | 5810 | 266 | 1.6 | 0.03 | 3.91 | 0.05 | 8.30 | 0.18 | 9.29 | 0.22 | 290.0 | 170.0 | 163.1 | 6.5 | 172.0 | 14.0 | 163.1 | 6.6 |
| Output_1_244 | 1450 | 268 | 3.1 | 0.03 | 6.61 | 0.06 | 21.67 | 0.22 | 20.37 | 0.20 | 390.0 | 390.0 | 164.0 | 11.0 | 193.0 | 36.0 | 164.0 | 11.0 |
| Output_1_294 | 2319 | 65 | 1.7 | 0.03 | 5.02 | 0.05 | 16.95 | 0.16 | 15.53 | 0.30 | 0.0 | 280.0 | 165.0 | 8.0 | 149.0 | 22.0 | 165.0 | 8.1 |
| Output_1_70 | 11790 | 425 | 1.6 | 0.03 | 2.96 | 0.05 | 8.00 | 0.18 | 7.87 | 0.36 | 170.0 | 160.0 | 165.7 | 4.8 | 168.0 | 13.0 | 165.7 | 5.0 |
| Output_1_7 | 50920 | 3207 | 2.0 | 0.03 | 2.33 | 0.05 | 3.81 | 0.19 | 3.96 | 0.38 | 290.0 | 85.0 | 166.7 | 3.8 | 178.2 | 6.5 | 166.7 | 4.0 |
| Output_1_48 | 8390 | 262 | 1.4 | 0.03 | 3.51 | 0.05 | 7.74 | 0.19 | 7.49 | 0.38 | 250.0 | 160.0 | 166.8 | 5.8 | 173.0 | 12.0 | 166.8 | 5.9 |
| Output_1_235 | 6780 | 895 | 2.5 | 0.03 | 4.58 | 0.05 | 11.90 | 0.19 | 11.64 | 0.27 | 330.0 | 240.0 | 166.9 | 7.5 | 175.0 | 19.0 | 166.9 | 7.6 |
| Output_1_67 | 4770 | 172 | 2.1 | 0.03 | 4.15 | 0.06 | 15.46 | 0.20 | 15.84 | 0.13 | 480.0 | 310.0 | 168.5 | 6.9 | 183.0 | 27.0 | 168.5 | 7.0 |
| Output_1_14 | 8910 | 784 | 2.9 | 0.03 | 4.87 | 0.05 | 7.81 | 0.19 | 10.00 | 0.51 | 360.0 | 170.0 | 169.7 | 8.1 | 176.0 | 16.0 | 169.7 | 8.2 |
| Output_1_299 | 5360 | 150 | 2.9 | 0.03 | 5.62 | 0.05 | 12.45 | 0.18 | 10.56 | 0.52 | 210.0 | 260.0 | 169.9 | 9.7 | 168.0 | 16.0 | 169.9 | 9.8 |
| Output_1_69 | 6400 | 232 | 2.9 | 0.03 | 3.01 | 0.05 | 9.02 | 0.20 | 9.69 | 0.39 | 300.0 | 190.0 | 170.9 | 5.1 | 184.0 | 17.0 | 170.9 | 5.2 |
| Output_1_102 | 3680 | 108 | 2.8 | 0.03 | 4.46 | 0.06 | 12.78 | 0.20 | 11.06 | 0.08 | 450.0 | 240.0 | 171.3 | 7.3 | 190.0 | 17.0 | 171.3 | 7.4 |
| Output_1_22 | 9790 | 645 | 3.8 | 0.03 | 5.19 | 0.05 | 7.62 | 0.18 | 8.15 | 0.29 | 200.0 | 150.0 | 171.8 | 9.0 | 173.0 | 12.0 | 171.8 | 9.1 |
| Output_1_84 | 1443 | 41 | 2.9 | 0.03 | 5.13 | 0.05 | 17.95 | 0.18 | 17.49 | 0.20 | 90.0 | 310.0 | 173.4 | 8.5 | 167.0 | 28.0 | 173.4 | 8.6 |
| Output_1_276 | 6060 | 187 | 1.6 | 0.03 | 5.45 | 0.05 | 11.70 | 0.19 | 9.33 | 0.13 | 280.0 | 240.0 | 174.7 | 9.5 | 178.0 | 15.0 | 174.7 | 9.6 |

| | | | | | | | | | | | | | | | | | | |
|---|---|---|---|---|---|---|---|---|---|---|---|---|---|---|---|---|---|---|
| Output_1_223 | 1923 | 104 | 2.5 | 0.03 | 7.25 | 0.05 | 13.04 | 0.21 | 14.22 | 0.26 | 480.0 | 270.0 | 175.0 | 12.0 | 198.0 | 27.0 | 175.0 | 12.0 |
| Output_1_138 | 30000 | 1487 | 1.1 | 0.03 | 3.58 | 0.05 | 4.37 | 0.19 | 4.64 | 0.55 | 200.0 | 94.0 | 177.2 | 6.3 | 177.8 | 6.9 | 177.2 | 6.5 |
| Output_1_124 | 17000 | 2610 | 1.8 | 0.03 | 3.10 | 0.05 | 4.31 | 0.19 | 4.84 | 0.72 | 118.0 | 90.0 | 178.6 | 5.4 | 178.0 | 7.9 | 178.6 | 5.6 |
| Output_1_256 | 22760 | 2730 | 1.8 | 0.03 | 4.27 | 0.05 | 4.56 | 0.20 | 5.64 | 0.40 | 199.0 | 96.0 | 178.7 | 7.4 | 180.1 | 9.2 | 178.7 | 7.5 |
| Output_1_83 | 5230 | 143 | 2.3 | 0.03 | 3.34 | 0.05 | 8.78 | 0.18 | 8.33 | 0.04 | 40.0 | 160.0 | 178.9 | 5.9 | 170.0 | 14.0 | 178.9 | 6.0 |
| Output_1_195 | 12390 | 594 | 2.1 | 0.03 | 5.69 | 0.05 | 7.01 | 0.20 | 7.58 | 0.35 | 190.0 | 160.0 | 179.0 | 10.0 | 183.0 | 13.0 | 179.0 | 10.0 |
| Output_1_140 | 10080 | 467 | 2.0 | 0.03 | 2.80 | 0.05 | 7.06 | 0.20 | 6.97 | 0.34 | 270.0 | 140.0 | 179.4 | 5.0 | 186.0 | 12.0 | 179.4 | 5.1 |
| Output_1_175 | 15070 | 456 | 2.5 | 0.03 | 3.87 | 0.05 | 6.94 | 0.21 | 6.70 | 0.21 | 180.0 | 150.0 | 180.2 | 7.1 | 192.0 | 11.0 | 180.2 | 7.2 |
| Output_1_207 | 15790 | 457 | 1.1 | 0.03 | 2.93 | 0.05 | 4.93 | 0.20 | 6.47 | 0.52 | 300.0 | 110.0 | 180.3 | 5.2 | 188.0 | 11.0 | 180.3 | 5.3 |
| Output_1_96 | 8070 | 203 | 1.8 | 0.03 | 2.92 | 0.05 | 7.98 | 0.21 | 8.29 | 0.18 | 300.0 | 170.0 | 180.7 | 5.2 | 188.0 | 14.0 | 180.7 | 5.4 |
| Output_1_281 | 8540 | 232 | 5.4 | 0.03 | 5.26 | 0.05 | 8.97 | 0.21 | 8.61 | 0.22 | 360.0 | 190.0 | 181.3 | 9.2 | 192.0 | 15.0 | 181.3 | 9.3 |
| Output_1_157 | 63400 | 2380 | 1.0 | 0.03 | 7.29 | 0.05 | 5.79 | 0.21 | 8.29 | 0.48 | 260.0 | 120.0 | 183.0 | 13.0 | 189.0 | 14.0 | 183.0 | 13.0 |
| Output_1_150 | 16000 | 642 | 1.8 | 0.03 | 4.84 | 0.05 | 10.37 | 0.21 | 9.05 | 0.02 | 330.0 | 220.0 | 183.6 | 8.9 | 193.0 | 16.0 | 183.6 | 9.0 |
| Output_1_78 | 5300 | 152 | 3.5 | 0.03 | 4.48 | 0.05 | 7.07 | 0.21 | 7.14 | 0.42 | 270.0 | 140.0 | 184.0 | 8.4 | 193.0 | 13.0 | 184.0 | 8.5 |
| Output_1_145 | 9100 | 385 | 1.5 | 0.03 | 2.10 | 0.05 | 7.10 | 0.20 | 8.54 | 0.39 | 210.0 | 150.0 | 184.2 | 3.8 | 185.0 | 14.0 | 184.2 | 4.0 |
| Output_1_211 | 5840 | 156 | 1.3 | 0.03 | 5.52 | 0.05 | 12.10 | 0.21 | 11.48 | 0.10 | 350.0 | 260.0 | 184.5 | 9.9 | 192.0 | 20.0 | 184.5 | 10.0 |
| Output_1_208 | 9280 | 255 | 1.2 | 0.03 | 3.28 | 0.05 | 8.32 | 0.21 | 7.69 | 0.01 | 280.0 | 170.0 | 185.7 | 6.0 | 195.0 | 13.0 | 185.7 | 6.1 |
| Output_1_286 | 7410 | 186 | 26.3 | 0.03 | 4.11 | 0.05 | 8.30 | 0.20 | 9.41 | 0.35 | 190.0 | 170.0 | 185.7 | 7.6 | 186.0 | 16.0 | 185.7 | 7.7 |
| Output_1_77 | 7190 | 209 | 4.8 | 0.03 | 5.46 | 0.06 | 11.99 | 0.21 | 10.28 | 0.00 | 380.0 | 240.0 | 185.9 | 9.8 | 196.0 | 18.0 | 185.9 | 9.9 |
| Output_1_194 | 14990 | 700 | 1.7 | 0.03 | 3.41 | 0.05 | 6.48 | 0.20 | 6.90 | 0.33 | 180.0 | 130.0 | 186.1 | 6.4 | 187.0 | 12.0 | 186.1 | 6.5 |
| Output_1_125 | 10990 | 1619 | 2.3 | 0.03 | 3.73 | 0.05 | 8.67 | 0.21 | 9.52 | 0.33 | 190.0 | 170.0 | 187.5 | 6.7 | 193.0 | 17.0 | 187.5 | 6.8 |
| Output_1_206 | 4100 | 114 | 2.4 | 0.03 | 3.70 | 0.05 | 11.61 | 0.22 | 12.11 | 0.12 | 330.0 | 240.0 | 188.3 | 7.1 | 202.0 | 22.0 | 188.3 | 7.3 |
| Output_1_307 | 14090 | 456 | 1.6 | 0.03 | 4.71 | 0.05 | 8.09 | 0.20 | 7.84 | 0.36 | 200.0 | 160.0 | 188.5 | 8.5 | 190.0 | 13.0 | 188.5 | 8.6 |
| Output_1_204 | 23120 | 728 | 2.1 | 0.03 | 3.69 | 0.05 | 4.90 | 0.22 | 5.53 | 0.43 | 300.0 | 110.0 | 189.2 | 7.0 | 199.1 | 9.9 | 189.2 | 7.2 |
| Output_1_50 | 9040 | 249 | 2.6 | 0.03 | 4.35 | 0.05 | 8.43 | 0.22 | 7.37 | 0.17 | 210.0 | 170.0 | 189.8 | 8.1 | 201.0 | 14.0 | 189.8 | 8.2 |
| Output_1_297 | 19070 | 476 | 2.5 | 0.03 | 3.21 | 0.05 | 4.89 | 0.20 | 4.65 | 0.39 | 142.0 | 99.0 | 190.0 | 6.0 | 184.9 | 7.8 | 190.0 | 6.2 |
| Output_1_71 | 21330 | 669 | 1.4 | 0.03 | 5.67 | 0.05 | 5.63 | 0.21 | 7.01 | 0.66 | 250.0 | 120.0 | 190.0 | 11.0 | 196.0 | 13.0 | 190.0 | 11.0 |
| Output_1_152 | 15120 | 578 | 1.3 | 0.03 | 4.67 | 0.05 | 6.86 | 0.22 | 6.48 | 0.39 | 220.0 | 140.0 | 190.4 | 9.0 | 198.0 | 12.0 | 190.4 | 9.1 |
| Output_1_217 | 7530 | 235 | 4.3 | 0.03 | 7.97 | 0.06 | 12.61 | 0.22 | 11.26 | 0.21 | 450.0 | 270.0 | 191.0 | 15.0 | 202.0 | 21.0 | 191.0 | 15.0 |
| Output_1_68 | 12800 | 399 | 2.2 | 0.03 | 3.97 | 0.05 | 5.84 | 0.21 | 5.19 | 0.43 | 180.0 | 120.0 | 191.6 | 7.7 | 194.6 | 9.6 | 191.6 | 7.8 |
| Output_1_170 | 11500 | 318 | 2.4 | 0.03 | 3.62 | 0.05 | 7.80 | 0.22 | 8.18 | 0.18 | 210.0 | 150.0 | 192.9 | 7.0 | 201.0 | 15.0 | 192.9 | 7.1 |
| Output_1_47 | 15840 | 414 | 1.0 | 0.03 | 3.61 | 0.05 | 5.99 | 0.21 | 6.07 | 0.51 | 190.0 | 120.0 | 193.5 | 6.9 | 196.0 | 11.0 | 193.5 | 7.0 |
| Output_1_93 | 18200 | 422 | 3.0 | 0.03 | 3.91 | 0.05 | 7.16 | 0.23 | 7.05 | 0.13 | 390.0 | 160.0 | 195.0 | 7.2 | 207.0 | 13.0 | 195.0 | 7.4 |
| Output_1_205 | 5590 | 168 | 1.6 | 0.03 | 3.25 | 0.05 | 7.55 | 0.23 | 7.39 | 0.19 | 360.0 | 160.0 | 195.3 | 6.4 | 210.0 | 14.0 | 195.3 | 6.5 |
| Output_1_226 | 32100 | 2050 | 1.9 | 0.03 | 2.96 | 0.05 | 4.80 | 0.22 | 4.45 | 0.35 | 180.0 | 100.0 | 197.4 | 5.7 | 198.2 | 8.0 | 197.4 | 5.9 |
| Output_1_32 | 13640 | 490 | 2.7 | 0.03 | 3.45 | 0.05 | 4.42 | 0.23 | 5.33 | 0.56 | 310.0 | 100.0 | 202.6 | 6.7 | 205.5 | 9.8 | 202.6 | 6.8 |
| Output_1_19 | 9650 | 594 | 1.6 | 0.03 | 3.02 | 0.05 | 6.86 | 0.22 | 6.28 | 0.10 | 280.0 | 140.0 | 203.6 | 6.1 | 206.0 | 10.0 | 203.6 | 6.2 |
| Output_1_30 | 14370 | 541 | 2.8 | 0.03 | 4.28 | 0.05 | 5.75 | 0.23 | 6.64 | 0.42 | 200.0 | 120.0 | 207.6 | 8.8 | 209.0 | 13.0 | 207.6 | 9.0 |
| Output_1_271 | 4830 | 134 | 2.9 | 0.03 | 3.24 | 0.05 | 10.34 | 0.23 | 10.43 | 0.26 | 210.0 | 200.0 | 214.9 | 6.9 | 209.0 | 20.0 | 214.9 | 7.0 |
| Output_1_163 | 4860 | 137 | 1.3 | 0.03 | 5.44 | 0.05 | 19.05 | 0.24 | 18.18 | 0.25 | 270.0 | 300.0 | 221.0 | 12.0 | 216.0 | 37.0 | 221.0 | 12.0 |

| | | | | | | | | | | | | | | | | | | |
|---|---|---|---|---|---|---|---|---|---|---|---|---|---|---|---|---|---|---|
| Output_1_290 | 30800 | 665 | 10.6 | 0.03 | 5.44 | 0.06 | 5.09 | 0.26 | 5.75 | 0.70 | 470.0 | 110.0 | 221.0 | 12.0 | 235.0 | 12.0 | 221.0 | 12.0 |
| Output_1_9 | 6010 | 345 | 1.8 | 0.04 | 3.13 | 0.05 | 7.09 | 0.25 | 8.50 | 0.32 | 370.0 | 160.0 | 222.8 | 7.1 | 223.0 | 18.0 | 222.8 | 7.3 |
| Output_1_44 | 13480 | 316 | 1.4 | 0.04 | 5.34 | 0.06 | 9.67 | 0.27 | 8.24 | 0.16 | 420.0 | 200.0 | 226.0 | 12.0 | 240.0 | 17.0 | 226.0 | 12.0 |
| Output_1_115 | 47900 | 2670 | 1.0 | 0.04 | 3.90 | 0.05 | 4.59 | 0.26 | 5.36 | 0.32 | 301.0 | 93.0 | 227.3 | 8.9 | 235.0 | 11.0 | 227.3 | 9.1 |
| Output_1_53 | 21630 | 508 | 2.8 | 0.04 | 6.28 | 0.05 | 8.91 | 0.27 | 9.89 | 0.44 | 370.0 | 180.0 | 231.0 | 15.0 | 243.0 | 21.0 | 231.0 | 15.0 |
| Output_1_188 | 3820 | 132 | 0.8 | 0.04 | 4.56 | 0.05 | 12.16 | 0.28 | 12.64 | 0.29 | 260.0 | 240.0 | 236.0 | 11.0 | 246.0 | 28.0 | 236.0 | 11.0 |
| Output_1_149 | 213500 | 6700 | 2.0 | 0.04 | 3.62 | 0.05 | 2.25 | 0.27 | 3.61 | 0.60 | 338.0 | 53.0 | 244.8 | 8.6 | 245.7 | 7.9 | 244.8 | 8.8 |
| Output_1_193 | 72600 | 2540 | 3.1 | 0.04 | 4.34 | 0.06 | 3.43 | 0.31 | 4.22 | 0.64 | 440.0 | 78.0 | 248.0 | 10.0 | 272.0 | 10.0 | 248.0 | 11.0 |
| Output_1_198 | 13260 | 366 | 1.4 | 0.04 | 4.49 | 0.05 | 7.40 | 0.32 | 6.25 | 0.12 | 310.0 | 160.0 | 280.0 | 12.0 | 281.0 | 15.0 | 280.0 | 12.0 |
| Output_1_180 | 48920 | 1036 | 1.6 | 0.05 | 2.03 | 0.06 | 3.19 | 0.37 | 3.80 | 0.36 | 454.0 | 74.0 | 286.4 | 5.7 | 318.0 | 10.0 | 286.4 | 6.0 |
| Output_1_243 | 29740 | 3016 | 1.6 | 0.05 | 3.57 | 0.06 | 5.18 | 0.37 | 5.91 | 0.43 | 430.0 | 120.0 | 300.0 | 11.0 | 320.0 | 16.0 | 300.0 | 11.0 |
| Output_1_197 | 10900 | 262 | 1.5 | 0.05 | 9.90 | 0.06 | 14.01 | 0.37 | 13.21 | 0.41 | 420.0 | 300.0 | 305.0 | 30.0 | 319.0 | 36.0 | 305.0 | 30.0 |
| Output_1_179 | 3250 | 64 | 1.1 | 0.05 | 4.10 | 0.06 | 11.85 | 0.41 | 9.95 | 0.22 | 580.0 | 250.0 | 307.0 | 12.0 | 347.0 | 29.0 | 307.0 | 12.0 |
| Output_1_20 | 59500 | 2333 | 5.7 | 0.05 | 4.37 | 0.07 | 4.46 | 0.44 | 6.82 | 0.67 | 833.0 | 97.0 | 317.0 | 13.0 | 370.0 | 21.0 | 317.0 | 14.0 |
| Output_1_28 | 76800 | 1875 | 1.0 | 0.05 | 3.79 | 0.05 | 4.45 | 0.39 | 3.11 | 0.55 | 350.0 | 100.0 | 332.0 | 12.0 | 334.0 | 10.0 | 332.0 | 12.0 |
| Output_1_142 | 10510 | 257 | 1.4 | 0.05 | 2.64 | 0.06 | 6.09 | 0.40 | 6.68 | 0.46 | 490.0 | 140.0 | 332.7 | 8.7 | 350.0 | 20.0 | 332.7 | 9.0 |
| Output_1_249 | 104200 | 8460 | 9.7 | 0.05 | 3.00 | 0.05 | 3.00 | 0.40 | 3.79 | 0.68 | 328.0 | 69.0 | 335.0 | 10.0 | 338.0 | 11.0 | 335.0 | 10.0 |
| Output_1_267 | 17830 | 344 | 1.0 | 0.05 | 3.18 | 0.05 | 6.23 | 0.38 | 6.51 | 0.25 | 300.0 | 130.0 | 335.0 | 11.0 | 329.0 | 18.0 | 335.0 | 11.0 |
| Output_1_88 | 26790 | 364 | 1.7 | 0.05 | 2.99 | 0.06 | 3.81 | 0.42 | 3.10 | 0.22 | 498.0 | 83.0 | 335.6 | 9.6 | 355.2 | 9.2 | 335.6 | 9.9 |
| Output_1_258 | 14490 | 828 | 5.0 | 0.05 | 3.35 | 0.06 | 7.64 | 0.41 | 7.06 | 0.09 | 370.0 | 160.0 | 337.0 | 11.0 | 348.0 | 20.0 | 337.0 | 11.0 |
| Output_1_289 | 29660 | 401 | 1.5 | 0.05 | 4.44 | 0.05 | 5.35 | 0.39 | 4.85 | 0.24 | 340.0 | 130.0 | 339.0 | 15.0 | 335.0 | 14.0 | 339.0 | 15.0 |
| Output_1_155 | 30900 | 644 | 3.0 | 0.05 | 6.65 | 0.06 | 8.59 | 0.40 | 8.93 | 0.42 | 420.0 | 190.0 | 339.0 | 22.0 | 343.0 | 25.0 | 339.0 | 22.0 |
| Output_1_158 | 14710 | 287 | 1.8 | 0.05 | 4.06 | 0.06 | 7.07 | 0.49 | 6.53 | 0.18 | 680.0 | 140.0 | 340.0 | 14.0 | 404.0 | 22.0 | 340.0 | 14.0 |
| Output_1_24 | 22740 | 645 | 2.3 | 0.06 | 3.26 | 0.06 | 4.09 | 0.43 | 4.21 | 0.34 | 538.0 | 90.0 | 346.0 | 11.0 | 361.0 | 12.0 | 346.0 | 11.0 |
| Output_1_257 | 27010 | 1565 | 1.5 | 0.06 | 3.07 | 0.05 | 4.75 | 0.41 | 5.13 | 0.36 | 310.0 | 110.0 | 347.0 | 10.0 | 350.0 | 14.0 | 347.0 | 11.0 |
| Output_1_288 | 9180 | 121 | 1.6 | 0.06 | 4.13 | 0.06 | 5.03 | 0.44 | 5.63 | 0.58 | 560.0 | 110.0 | 349.0 | 14.0 | 372.0 | 18.0 | 349.0 | 14.0 |
| Output_1_110 | 81200 | 1847 | 0.5 | 0.06 | 3.74 | 0.06 | 3.83 | 0.43 | 3.03 | 0.27 | 496.0 | 86.0 | 352.0 | 13.0 | 362.1 | 9.5 | 352.0 | 13.0 |
| Output_1_95 | 20800 | 257 | 2.1 | 0.06 | 3.51 | 0.06 | 6.26 | 0.46 | 6.93 | 0.42 | 500.0 | 140.0 | 357.0 | 12.0 | 388.0 | 23.0 | 357.0 | 13.0 |
| Output_1_164 | 22060 | 370 | 1.5 | 0.06 | 3.67 | 0.06 | 3.80 | 0.46 | 4.15 | 0.37 | 521.0 | 88.0 | 358.0 | 13.0 | 382.0 | 13.0 | 358.0 | 13.0 |
| Output_1_275 | 6830 | 89 | 1.2 | 0.07 | 4.43 | 0.06 | 5.38 | 0.50 | 5.81 | 0.44 | 410.0 | 110.0 | 408.0 | 17.0 | 409.0 | 20.0 | 408.0 | 17.0 |
| Output_1_49 | 44800 | 471 | 15.3 | 0.08 | 5.17 | 0.07 | 4.66 | 0.76 | 7.62 | 0.78 | 879.0 | 91.0 | 480.0 | 24.0 | 570.0 | 33.0 | 480.0 | 24.0 |
| Output_1_116 | 17940 | 488 | 1.4 | 0.08 | 3.86 | 0.06 | 5.22 | 0.64 | 5.92 | 0.46 | 500.0 | 110.0 | 498.0 | 19.0 | 501.0 | 23.0 | 498.0 | 19.0 |
| Output_1_10 | 45000 | 908 | 0.9 | 0.10 | 2.06 | 0.06 | 3.18 | 0.86 | 3.62 | 0.47 | 702.0 | 66.0 | 626.0 | 13.0 | 627.0 | 17.0 | 626.0 | 13.0 |
| Output_1_184 | 71100 | 750 | 0.9 | 0.11 | 3.75 | 0.11 | 3.58 | 1.57 | 4.91 | 0.57 | 1777.0 | 68.0 | 654.0 | 23.0 | 957.0 | 31.0 | 654.0 | 24.0 |
| Output_1_106 | 156200 | 1310 | 3.0 | 0.11 | 3.09 | 0.06 | 3.30 | 0.96 | 2.92 | 0.32 | 730.0 | 75.0 | 674.0 | 20.0 | 682.0 | 15.0 | 674.0 | 20.0 |
| Output_1_245 | 25570 | 1038 | 1.5 | 0.12 | 4.90 | 0.07 | 4.15 | 1.21 | 6.11 | 0.61 | 978.0 | 82.0 | 732.0 | 34.0 | 807.0 | 33.0 | 732.0 | 34.0 |
| Output_1_108 | 40610 | 335 | 3.0 | 0.13 | 3.37 | 0.08 | 3.55 | 1.43 | 3.44 | 0.57 | 1091.0 | 68.0 | 807.0 | 26.0 | 898.0 | 21.0 | 807.0 | 26.0 |
| Output_1_105 | 64300 | 420 | 2.9 | 0.14 | 3.80 | 0.09 | 3.25 | 1.73 | 3.40 | 0.43 | 1474.0 | 59.0 | 830.0 | 28.0 | ##### | 22.0 | 830.0 | 29.0 |
| Output_1_227 | 36400 | 558 | 2.2 | 0.14 | 4.40 | 0.08 | 3.60 | 1.61 | 4.79 | 0.64 | 1302.0 | 72.0 | 836.0 | 34.0 | 968.0 | 31.0 | 836.0 | 35.0 |
| Output_1_221 | 79300 | 629 | 0.8 | 0.16 | 4.41 | 0.08 | 3.29 | 1.71 | 4.20 | 0.63 | 1162.0 | 63.0 | 961.0 | 40.0 | ##### | 27.0 | 1162.0 | 71.0 |

| | | | | | | | | | | | | | | | | | |
|---|---|---|---|---|---|---|---|---|---|---|---|---|---|---|---|---|---|
| Output_1_263 | 51540 | 507 | 1.0 | 0.25 | 2.79 | 0.09 | 2.86 | 3.25 | 4.00 | 0.70 | 1506.0 | 55.0 | 1422.0 | 35.0 | ##### | 31.0 | 1506.0 | 63.0 |
| Output_1_123 | 35720 | 513 | 0.9 | 0.28 | 3.42 | 0.10 | 3.59 | 3.95 | 4.05 | 0.42 | 1593.0 | 75.0 | 1609.0 | 49.0 | ##### | 33.0 | 1593.0 | 82.0 |
| Output_1_220 | 274200 | 1243 | 236.0 | 0.26 | 3.06 | 0.10 | 1.96 | 3.66 | 2.73 | 0.82 | 1656.0 | 37.0 | 1495.0 | 41.0 | ##### | 23.0 | 1656.0 | 48.0 |
| Output_1_225 | 19580 | 112 | 2.3 | 0.30 | 4.35 | 0.11 | 4.10 | 4.64 | 6.03 | 0.71 | 1817.0 | 74.0 | 1683.0 | 65.0 | ##### | 46.0 | 1817.0 | 80.0 |
| Output_1_269 | 69000 | 208 | 2.3 | 0.32 | 2.64 | 0.11 | 2.42 | 4.80 | 2.71 | 0.57 | 1824.0 | 43.0 | 1782.0 | 41.0 | ##### | 23.0 | 1824.0 | 52.0 |
| Output_1_75 | 154500 | 504 | 1.9 | 0.27 | 3.35 | 0.11 | 2.09 | 4.24 | 3.54 | 0.74 | 1882.0 | 40.0 | 1532.0 | 46.0 | ##### | 27.0 | 1882.0 | 50.0 |
| Output_1_274 | 115500 | 380 | 2.1 | 0.27 | 4.06 | 0.12 | 2.39 | 4.34 | 4.15 | 0.70 | 1912.0 | 44.0 | 1544.0 | 58.0 | ##### | 34.0 | 1912.0 | 52.0 |
| Output_1_270 | 65100 | 188 | 0.4 | 0.33 | 3.66 | 0.12 | 2.36 | 5.22 | 3.45 | 0.71 | 1936.0 | 39.0 | 1828.0 | 56.0 | ##### | 27.0 | 1936.0 | 47.0 |
| Output_1_34 | 48910 | 144 | 2.0 | 0.36 | 2.64 | 0.13 | 2.28 | 6.23 | 3.05 | 0.62 | 2059.0 | 41.0 | 1961.0 | 45.0 | ##### | 27.0 | 2059.0 | 51.0 |
| Output_1_141 | 137400 | 508 | 2.8 | 0.36 | 3.31 | 0.14 | 2.67 | 6.66 | 2.55 | 0.64 | 2202.0 | 46.0 | 1991.0 | 57.0 | ##### | 22.0 | 2202.0 | 54.0 |

**Sample 19ATW39**

| | | | | | | | | | | | | | | | | | |
|---|---|---|---|---|---|---|---|---|---|---|---|---|---|---|---|---|---|
| Output_1_122 | 2100 | 91 | 1.9 | 0.03 | 5.00 | 0.05 | 13.26 | 0.17 | 14.12 | 0.20 | 50.0 | 240.0 | 165.3 | 8.1 | 158.0 | 21.0 | 165.3 | 8.7 |
| Output_1_125 | 3030 | 169 | 1.3 | 0.02 | 3.73 | 0.05 | 11.91 | 0.16 | 12.42 | 0.13 | 50.0 | 210.0 | 158.7 | 5.9 | 150.0 | 18.0 | 158.7 | 6.6 |
| Output_1_121 | 1310 | 55 | 2.2 | 0.03 | 8.00 | 0.04 | 20.57 | 0.16 | 22.64 | 0.24 | 60.0 | 400.0 | 159.0 | 12.0 | 155.0 | 33.0 | 159.0 | 13.0 |
| Output_1_113 | 29710 | 1061 | 1.6 | 0.02 | 2.00 | 0.05 | 3.71 | 0.17 | 3.56 | 0.47 | 127.0 | 78.0 | 159.1 | 3.1 | 158.2 | 5.3 | 159.1 | 4.4 |
| Output_1_104 | 5430 | 338 | 2.5 | 0.03 | 4.28 | 0.05 | 10.53 | 0.18 | 10.86 | 0.34 | 140.0 | 210.0 | 163.7 | 6.9 | 162.0 | 17.0 | 163.7 | 7.6 |
| Output_1_112 | 3400 | 124 | 1.9 | 0.02 | 4.84 | 0.05 | 12.72 | 0.17 | 10.98 | 0.11 | 150.0 | 240.0 | 158.0 | 7.5 | 161.0 | 17.0 | 158.0 | 8.1 |
| Output_1_117 | 8250 | 303 | 1.7 | 0.03 | 3.88 | 0.05 | 7.09 | 0.18 | 7.18 | 0.36 | 160.0 | 140.0 | 162.2 | 6.2 | 168.0 | 11.0 | 162.2 | 7.0 |
| Output_1_118 | 12560 | 477 | 2.0 | 0.03 | 3.17 | 0.05 | 6.95 | 0.17 | 6.43 | 0.51 | 160.0 | 140.0 | 160.8 | 5.1 | 161.6 | 8.8 | 160.8 | 6.0 |
| Output_1_110 | 9920 | 387 | 1.5 | 0.03 | 3.55 | 0.05 | 5.98 | 0.17 | 6.36 | 0.11 | 170.0 | 140.0 | 161.4 | 5.6 | 165.0 | 11.0 | 161.4 | 6.5 |
| Output_1_108 | 7500 | 331 | 2.3 | 0.03 | 3.33 | 0.05 | 7.30 | 0.17 | 7.51 | 0.32 | 180.0 | 150.0 | 160.6 | 5.3 | 162.0 | 11.0 | 160.6 | 6.1 |
| Output_1_115 | 2444 | 84 | 1.6 | 0.03 | 4.30 | 0.05 | 18.91 | 0.18 | 18.58 | 0.11 | 200.0 | 340.0 | 162.7 | 7.1 | 167.0 | 30.0 | 162.7 | 7.8 |
| Output_1_107 | 5620 | 270 | 1.3 | 0.02 | 4.44 | 0.05 | 11.00 | 0.17 | 10.00 | 0.03 | 200.0 | 210.0 | 157.6 | 7.1 | 159.0 | 15.0 | 157.6 | 7.8 |
| Output_1_126 | 3180 | 189 | 1.4 | 0.02 | 5.44 | 0.05 | 16.63 | 0.16 | 14.02 | 0.61 | 210.0 | 330.0 | 152.2 | 7.9 | 153.0 | 21.0 | 152.2 | 8.5 |
| Output_1_105 | 2830 | 164 | 1.2 | 0.03 | 6.72 | 0.05 | 16.24 | 0.18 | 15.73 | 0.14 | 230.0 | 310.0 | 161.0 | 11.0 | 175.0 | 24.0 | 161.0 | 11.0 |
| Output_1_120 | 8850 | 363 | 1.8 | 0.03 | 3.19 | 0.05 | 5.10 | 0.18 | 5.31 | 0.30 | 240.0 | 110.0 | 163.5 | 5.2 | 168.4 | 8.2 | 163.5 | 6.1 |
| Output_1_106 | 4520 | 231 | 1.7 | 0.03 | 4.71 | 0.05 | 12.45 | 0.18 | 11.41 | 0.00 | 240.0 | 240.0 | 162.1 | 7.3 | 174.0 | 19.0 | 162.1 | 8.0 |
| Output_1_116 | 12680 | 448 | 1.4 | 0.03 | 3.61 | 0.05 | 7.24 | 0.17 | 7.56 | 0.41 | 290.0 | 150.0 | 162.0 | 5.8 | 161.0 | 11.0 | 162.0 | 6.6 |
| Output_1_114 | 2890 | 101 | 1.9 | 0.02 | 5.62 | 0.05 | 13.64 | 0.18 | 12.29 | 0.09 | 350.0 | 250.0 | 158.8 | 8.7 | 170.0 | 18.0 | 158.8 | 9.2 |
| Output_1_119 | 10910 | 417 | 2.3 | 0.03 | 3.88 | 0.05 | 6.15 | 0.18 | 6.70 | 0.38 | 370.0 | 120.0 | 163.9 | 6.4 | 167.0 | 10.0 | 163.9 | 7.2 |
| Output_1_109 | 4060 | 174 | 2.6 | 0.03 | 4.72 | 0.05 | 14.13 | 0.18 | 12.78 | 0.39 | 370.0 | 280.0 | 161.8 | 7.5 | 167.0 | 19.0 | 161.8 | 8.1 |
| Output_1_111 | 1760 | 70 | 1.7 | 0.02 | 4.10 | 0.05 | 13.22 | 0.18 | 13.11 | 0.02 | 370.0 | 270.0 | 155.5 | 6.5 | 169.0 | 20.0 | 155.5 | 7.2 |
| Output_1_124 | 1926 | 93 | 1.9 | 0.03 | 3.98 | 0.06 | 14.29 | 0.19 | 13.83 | 0.12 | 430.0 | 290.0 | 159.6 | 6.6 | 173.0 | 22.0 | 159.6 | 7.3 |

**Sample 19ATW46**

| | | | | | | | | | | | | | | | | | |
|---|---|---|---|---|---|---|---|---|---|---|---|---|---|---|---|---|---|
| Output_1_32 | 3220 | 156 | 2.1 | 0.02 | 4.25 | 0.05 | 11.72 | 0.15 | 10.60 | 0.03 | 140.0 | 240.0 | 139.5 | 5.8 | 142.0 | 14.0 | 139.5 | 7.9 |
| Output_1_68 | 2320 | 86 | 1.8 | 0.02 | 6.36 | 0.05 | 19.52 | 0.16 | 20.51 | 0.30 | 70.0 | 350.0 | 139.9 | 8.7 | 145.0 | 28.0 | 139.9 | 10.0 |
| Output_1_70 | 11840 | 434 | 1.0 | 0.02 | 4.48 | 0.05 | 7.16 | 0.15 | 7.38 | 0.34 | 170.0 | 150.0 | 142.4 | 6.6 | 140.6 | 9.9 | 142.4 | 8.5 |
| Output_1_61 | 6890 | 239 | 0.8 | 0.02 | 5.38 | 0.05 | 9.46 | 0.15 | 7.79 | 0.12 | 140.0 | 200.0 | 142.4 | 7.3 | 145.0 | 10.0 | 142.4 | 9.0 |

| | | | | | | | | | | | | | | | | | | |
|---|---|---|---|---|---|---|---|---|---|---|---|---|---|---|---|---|---|---|
| Output_1_197 | 1172 | 62 | 2.3 | 0.02 | 7.59 | 0.05 | 18.90 | 0.15 | 17.76 | 0.09 | 50.0 | 350.0 | 143.0 | 11.0 | 141.0 | 23.0 | 143.0 | 12.0 |
| Output_1_93 | 1323 | 85 | 2.1 | 0.02 | 7.59 | 0.05 | 20.37 | 0.17 | 20.36 | 0.22 | 320.0 | 390.0 | 143.0 | 10.0 | 166.0 | 29.0 | 143.0 | 12.0 |
| Output_1_3 | 2640 | 184 | 2.3 | 0.02 | 5.33 | 0.05 | 14.40 | 0.16 | 14.74 | 0.19 | 240.0 | 300.0 | 143.2 | 7.3 | 145.0 | 20.0 | 143.2 | 9.1 |
| Output_1_227 | 1343 | 66 | 2.0 | 0.02 | 7.08 | 0.05 | 20.37 | 0.17 | 21.21 | 0.30 | 350.0 | 400.0 | 144.0 | 10.0 | 152.0 | 31.0 | 144.0 | 12.0 |
| Output_1_263 | 3850 | 276 | 2.6 | 0.02 | 4.82 | 0.05 | 12.79 | 0.16 | 12.35 | 0.15 | 250.0 | 250.0 | 145.5 | 6.8 | 151.0 | 17.0 | 145.5 | 8.7 |
| Output_1_241 | 1990 | 139 | 2.7 | 0.02 | 4.80 | 0.06 | 14.54 | 0.17 | 13.45 | 0.12 | 370.0 | 270.0 | 145.7 | 6.7 | 167.0 | 20.0 | 145.7 | 8.7 |
| Output_1_204 | 1560 | 58 | 2.4 | 0.02 | 6.55 | 0.06 | 21.43 | 0.17 | 21.97 | 0.37 | 240.0 | 410.0 | 145.9 | 9.8 | 158.0 | 32.0 | 145.9 | 11.0 |
| Output_1_259 | 6530 | 435 | 2.5 | 0.02 | 5.22 | 0.05 | 9.46 | 0.16 | 11.59 | 0.81 | 200.0 | 190.0 | 146.4 | 7.7 | 147.0 | 15.0 | 146.4 | 9.5 |
| Output_1_206 | 1103 | 40 | 2.4 | 0.02 | 6.52 | 0.05 | 15.99 | 0.17 | 17.44 | 0.39 | 470.0 | 310.0 | 146.5 | 9.7 | 158.0 | 26.0 | 146.5 | 11.0 |
| Output_1_47 | 1330 | 51 | 2.7 | 0.02 | 8.66 | 0.05 | 17.65 | 0.16 | 17.18 | 0.22 | 200.0 | 310.0 | 147.0 | 12.0 | 161.0 | 22.0 | 147.0 | 14.0 |
| Output_1_161 | 3360 | 132 | 1.9 | 0.02 | 4.07 | 0.05 | 14.81 | 0.17 | 14.97 | 0.21 | 250.0 | 310.0 | 147.2 | 6.0 | 155.0 | 22.0 | 147.2 | 8.1 |
| Output_1_98 | 3130 | 230 | 2.4 | 0.02 | 4.33 | 0.05 | 16.10 | 0.16 | 16.88 | 0.13 | 20.0 | 300.0 | 147.4 | 6.4 | 148.0 | 23.0 | 147.4 | 8.5 |
| Output_1_231 | 1707 | 97 | 4.3 | 0.02 | 6.90 | 0.05 | 14.92 | 0.16 | 14.38 | 0.10 | 290.0 | 310.0 | 147.7 | 9.8 | 149.0 | 20.0 | 147.7 | 11.0 |
| Output_1_95 | 2010 | 134 | 2.4 | 0.02 | 4.74 | 0.06 | 14.08 | 0.17 | 12.07 | 0.12 | 480.0 | 300.0 | 147.8 | 6.6 | 162.0 | 19.0 | 147.8 | 8.7 |
| Output_1_15 | 4890 | 213 | 4.0 | 0.02 | 5.17 | 0.05 | 9.53 | 0.16 | 9.62 | 0.24 | 110.0 | 190.0 | 147.9 | 7.3 | 149.0 | 14.0 | 147.9 | 9.2 |
| Output_1_189 | 3790 | 408 | 2.0 | 0.02 | 4.31 | 0.05 | 11.31 | 0.16 | 11.66 | 0.02 | 220.0 | 230.0 | 148.1 | 6.4 | 152.0 | 17.0 | 148.1 | 8.5 |
| Output_1_87 | 3020 | 148 | 1.9 | 0.02 | 4.72 | 0.05 | 14.06 | 0.16 | 12.58 | 0.19 | 200.0 | 290.0 | 148.2 | 6.6 | 149.0 | 17.0 | 148.2 | 8.7 |
| Output_1_235 | 1643 | 107 | 2.1 | 0.02 | 6.01 | 0.06 | 20.69 | 0.18 | 20.34 | 0.25 | 330.0 | 410.0 | 148.3 | 8.9 | 162.0 | 30.0 | 148.3 | 11.0 |
| Output_1_19 | 3910 | 167 | 1.8 | 0.02 | 3.95 | 0.05 | 9.68 | 0.16 | 9.55 | 0.23 | 150.0 | 200.0 | 148.5 | 5.8 | 147.0 | 13.0 | 148.5 | 8.1 |
| Output_1_60 | 3330 | 115 | 2.1 | 0.02 | 4.72 | 0.05 | 12.88 | 0.16 | 12.96 | 0.11 | 100.0 | 250.0 | 148.7 | 6.9 | 154.0 | 19.0 | 148.7 | 8.9 |
| Output_1_45 | 1800 | 66 | 1.8 | 0.02 | 5.15 | 0.07 | 18.46 | 0.19 | 15.98 | 0.14 | 620.0 | 400.0 | 148.7 | 7.3 | 188.0 | 30.0 | 148.7 | 9.2 |
| Output_1_240 | 7100 | 497 | 2.4 | 0.02 | 3.77 | 0.05 | 12.20 | 0.16 | 12.35 | 0.01 | 230.0 | 240.0 | 148.9 | 5.5 | 151.0 | 17.0 | 148.9 | 7.9 |
| Output_1_130 | 652 | 38 | 3.8 | 0.02 | 8.94 | 0.06 | 21.05 | 0.17 | 21.76 | 0.06 | 360.0 | 410.0 | 149.0 | 13.0 | 166.0 | 32.0 | 149.0 | 15.0 |
| Output_1_63 | 2980 | 100 | 1.0 | 0.02 | 3.88 | 0.05 | 12.23 | 0.17 | 12.05 | 0.04 | 230.0 | 260.0 | 149.4 | 5.7 | 155.0 | 18.0 | 149.4 | 8.0 |
| Output_1_36 | 1258 | 53 | 1.9 | 0.02 | 6.38 | 0.04 | 21.92 | 0.16 | 21.25 | 0.16 | 0.0 | 400.0 | 149.5 | 9.4 | 147.0 | 30.0 | 149.5 | 11.0 |
| Output_1_222 | 2310 | 96 | 2.7 | 0.02 | 6.38 | 0.06 | 20.69 | 0.18 | 18.33 | 0.09 | 350.0 | 400.0 | 149.5 | 9.3 | 165.0 | 28.0 | 149.5 | 11.0 |
| Output_1_50 | 2540 | 94 | 2.2 | 0.02 | 5.53 | 0.05 | 10.98 | 0.16 | 9.88 | 0.06 | 240.0 | 230.0 | 149.6 | 8.4 | 152.0 | 14.0 | 149.6 | 10.0 |
| Output_1_35 | 13230 | 587 | 1.2 | 0.02 | 2.89 | 0.05 | 6.90 | 0.16 | 6.75 | 0.22 | 250.0 | 150.0 | 149.7 | 4.3 | 152.7 | 9.3 | 149.7 | 7.1 |
| Output_1_125 | 2020 | 143 | 5.3 | 0.02 | 7.23 | 0.05 | 13.30 | 0.17 | 12.21 | 0.23 | 350.0 | 280.0 | 150.0 | 11.0 | 164.0 | 20.0 | 150.0 | 12.0 |
| Output_1_219 | 1850 | 74 | 4.0 | 0.02 | 5.93 | 0.05 | 16.11 | 0.18 | 13.89 | 0.28 | 310.0 | 310.0 | 150.1 | 9.1 | 166.0 | 21.0 | 150.1 | 11.0 |
| Output_1_131 | 1192 | 62 | 2.6 | 0.02 | 6.36 | 0.06 | 23.64 | 0.17 | 23.84 | 0.10 | 90.0 | 450.0 | 150.2 | 9.6 | 156.0 | 35.0 | 150.2 | 11.0 |
| Output_1_85 | 4450 | 207 | 15.2 | 0.02 | 4.66 | 0.05 | 10.50 | 0.16 | 11.61 | 0.28 | 0.0 | 220.0 | 150.3 | 6.9 | 145.0 | 16.0 | 150.3 | 8.9 |
| Output_1_218 | 1740 | 68 | 2.5 | 0.02 | 5.51 | 0.06 | 11.60 | 0.19 | 13.30 | 0.14 | 450.0 | 260.0 | 150.5 | 8.3 | 174.0 | 21.0 | 150.5 | 10.0 |
| Output_1_20 | 6830 | 292 | 1.8 | 0.02 | 3.38 | 0.05 | 9.71 | 0.17 | 10.47 | 0.37 | 280.0 | 210.0 | 150.7 | 5.1 | 163.0 | 16.0 | 150.7 | 7.6 |
| Output_1_24 | 3510 | 158 | 3.2 | 0.02 | 5.49 | 0.06 | 13.53 | 0.19 | 13.09 | 0.24 | 550.0 | 280.0 | 150.7 | 8.2 | 176.0 | 21.0 | 150.7 | 10.0 |
| Output_1_132 | 3420 | 175 | 3.2 | 0.02 | 6.33 | 0.06 | 13.13 | 0.17 | 14.62 | 0.15 | 310.0 | 280.0 | 150.8 | 9.4 | 158.0 | 22.0 | 150.8 | 11.0 |
| Output_1_243 | 1781 | 116 | 2.6 | 0.02 | 5.06 | 0.05 | 18.35 | 0.15 | 18.30 | 0.35 | 120.0 | 360.0 | 150.9 | 7.4 | 148.0 | 27.0 | 150.9 | 9.3 |
| Output_1_59 | 1650 | 54 | 2.2 | 0.02 | 8.02 | 0.05 | 19.43 | 0.17 | 18.07 | 0.02 | 260.0 | 370.0 | 151.0 | 12.0 | 160.0 | 25.0 | 151.0 | 13.0 |
| Output_1_250 | 2202 | 131 | 2.9 | 0.02 | 4.22 | 0.04 | 15.44 | 0.15 | 16.22 | 0.38 | -20.0 | 300.0 | 151.1 | 6.4 | 138.0 | 21.0 | 151.1 | 8.5 |
| Output_1_11 | 4490 | 217 | 1.2 | 0.02 | 2.90 | 0.05 | 16.28 | 0.17 | 16.07 | 0.35 | 280.0 | 290.0 | 151.5 | 4.4 | 156.0 | 23.0 | 151.5 | 7.2 |

| | | | | | | | | | | | | | | | | | | |
|---|---|---|---|---|---|---|---|---|---|---|---|---|---|---|---|---|---|---|
| Output_1_136 | 3650 | 155 | 1.9 | 0.02 | 3.99 | 0.05 | 15.33 | 0.15 | 14.67 | 0.00 | -10.0 | 290.0 | 151.5 | 6.0 | 140.0 | 19.0 | 151.5 | 8.3 |
| Output_1_78 | 2861 | 115 | 1.8 | 0.02 | 4.62 | 0.05 | 10.55 | 0.16 | 9.68 | 0.12 | 160.0 | 220.0 | 151.7 | 6.9 | 145.0 | 13.0 | 151.7 | 8.9 |
| Output_1_246 | 1400 | 91 | 4.1 | 0.02 | 7.14 | 0.06 | 15.37 | 0.18 | 16.57 | 0.35 | 410.0 | 310.0 | 152.0 | 11.0 | 166.0 | 25.0 | 152.0 | 12.0 |
| Output_1_258 | 1160 | 77 | 3.0 | 0.02 | 8.37 | 0.05 | 16.12 | 0.18 | 17.68 | 0.24 | 220.0 | 310.0 | 152.0 | 13.0 | 165.0 | 27.0 | 152.0 | 14.0 |
| Output_1_251 | 1284 | 78 | 2.9 | 0.02 | 9.21 | 0.07 | 30.30 | 0.21 | 26.57 | 0.08 | 410.0 | 630.0 | 152.0 | 14.0 | 186.0 | 47.0 | 152.0 | 15.0 |
| Output_1_166 | 2026 | 84 | 2.0 | 0.02 | 6.28 | 0.05 | 14.26 | 0.18 | 15.17 | 0.12 | 360.0 | 270.0 | 152.1 | 9.2 | 164.0 | 22.0 | 152.1 | 11.0 |
| Output_1_100 | 3170 | 238 | 1.6 | 0.02 | 4.60 | 0.05 | 11.92 | 0.16 | 12.80 | 0.27 | 190.0 | 240.0 | 152.5 | 7.2 | 158.0 | 19.0 | 152.5 | 9.2 |
| Output_1_168 | 1400 | 64 | 2.2 | 0.02 | 6.67 | 0.06 | 20.34 | 0.20 | 20.30 | 0.09 | 370.0 | 400.0 | 153.0 | 10.0 | 185.0 | 32.0 | 153.0 | 12.0 |
| Output_1_139 | 2066 | 80 | 1.9 | 0.02 | 4.15 | 0.05 | 13.75 | 0.19 | 13.51 | 0.30 | 360.0 | 300.0 | 153.4 | 6.4 | 170.0 | 21.0 | 153.4 | 8.6 |
| Output_1_186 | 2930 | 355 | 1.4 | 0.02 | 6.64 | 0.04 | 13.48 | 0.15 | 14.09 | 0.38 | -90.0 | 260.0 | 153.6 | 9.9 | 140.0 | 19.0 | 153.6 | 11.0 |
| Output_1_55 | 3780 | 123 | 2.1 | 0.02 | 3.40 | 0.05 | 10.77 | 0.17 | 10.24 | 0.09 | 170.0 | 230.0 | 153.7 | 5.2 | 158.0 | 15.0 | 153.7 | 7.8 |
| Output_1_56 | 3350 | 111 | 1.4 | 0.02 | 4.55 | 0.06 | 9.68 | 0.18 | 9.66 | 0.16 | 400.0 | 190.0 | 153.9 | 7.1 | 166.0 | 13.0 | 153.9 | 9.2 |
| Output_1_57 | 1860 | 59 | 1.6 | 0.02 | 6.20 | 0.05 | 13.49 | 0.16 | 14.11 | 0.11 | 270.0 | 270.0 | 154.0 | 9.6 | 156.0 | 22.0 | 154.0 | 11.0 |
| Output_1_262 | 3730 | 238 | 1.9 | 0.02 | 7.47 | 0.05 | 20.37 | 0.18 | 21.71 | 0.72 | 290.0 | 410.0 | 154.0 | 11.0 | 162.0 | 33.0 | 154.0 | 12.0 |
| Output_1_179 | 3330 | 281 | 1.6 | 0.02 | 4.13 | 0.06 | 11.49 | 0.19 | 10.75 | 0.05 | 410.0 | 240.0 | 154.2 | 6.5 | 175.0 | 18.0 | 154.2 | 8.7 |
| Output_1_65 | 2660 | 88 | 0.9 | 0.02 | 6.20 | 0.05 | 14.37 | 0.17 | 14.04 | 0.27 | 250.0 | 270.0 | 154.2 | 9.2 | 166.0 | 19.0 | 154.2 | 11.0 |
| Output_1_214 | 2090 | 72 | 3.0 | 0.02 | 5.79 | 0.05 | 16.29 | 0.17 | 16.76 | 0.08 | 330.0 | 310.0 | 154.3 | 8.9 | 163.0 | 27.0 | 154.3 | 11.0 |
| Output_1_221 | 2070 | 80 | 2.7 | 0.02 | 6.20 | 0.05 | 17.75 | 0.16 | 17.39 | 0.08 | 240.0 | 310.0 | 154.4 | 9.2 | 149.0 | 25.0 | 154.4 | 11.0 |
| Output_1_49 | 6350 | 219 | 2.4 | 0.02 | 3.83 | 0.06 | 8.45 | 0.18 | 11.24 | 0.14 | 390.0 | 190.0 | 154.5 | 5.8 | 169.0 | 16.0 | 154.5 | 8.2 |
| Output_1_133 | 1487 | 69 | 1.8 | 0.02 | 6.17 | 0.05 | 23.08 | 0.16 | 20.13 | 0.24 | 40.0 | 400.0 | 154.9 | 9.2 | 153.0 | 29.0 | 154.9 | 11.0 |
| Output_1_143 | 1110 | 42 | 2.4 | 0.02 | 7.00 | 0.06 | 22.58 | 0.20 | 20.40 | 0.30 | 480.0 | 430.0 | 155.0 | 11.0 | 182.0 | 35.0 | 155.0 | 12.0 |
| Output_1_196 | 1183 | 63 | 2.3 | 0.02 | 7.79 | 0.05 | 21.74 | 0.15 | 20.53 | 0.19 | -20.0 | 410.0 | 155.0 | 12.0 | 140.0 | 27.0 | 155.0 | 13.0 |
| Output_1_58 | 8900 | 286 | 2.1 | 0.02 | 2.83 | 0.05 | 7.96 | 0.17 | 8.28 | 0.08 | 120.0 | 160.0 | 155.2 | 4.3 | 158.0 | 12.0 | 155.2 | 7.3 |
| Output_1_111 | 7760 | 682 | 2.1 | 0.02 | 4.51 | 0.05 | 10.10 | 0.18 | 11.43 | 0.24 | 250.0 | 240.0 | 155.6 | 7.0 | 163.0 | 17.0 | 155.6 | 9.1 |
| Output_1_126 | 2460 | 158 | 3.7 | 0.02 | 5.26 | 0.05 | 14.74 | 0.17 | 12.79 | 0.04 | 190.0 | 290.0 | 157.2 | 7.9 | 163.0 | 19.0 | 157.2 | 9.9 |
| Output_1_104 | 16460 | 1301 | 3.5 | 0.02 | 4.44 | 0.05 | 5.15 | 0.17 | 5.53 | 0.57 | 200.0 | 110.0 | 157.9 | 6.8 | 162.3 | 8.3 | 157.9 | 9.0 |
| Output_1_245 | 1860 | 121 | 4.1 | 0.02 | 7.66 | 0.05 | 18.82 | 0.17 | 17.44 | 0.33 | 40.0 | 350.0 | 158.0 | 12.0 | 157.0 | 26.0 | 158.0 | 13.0 |
| Output_1_110 | 11360 | 970 | 2.7 | 0.02 | 2.78 | 0.05 | 5.61 | 0.18 | 6.25 | 0.44 | 240.0 | 120.0 | 158.1 | 4.4 | 164.6 | 9.7 | 158.1 | 7.4 |
| Output_1_190 | 7260 | 641 | 2.0 | 0.02 | 4.03 | 0.05 | 8.70 | 0.18 | 7.91 | 0.27 | 290.0 | 180.0 | 158.1 | 6.4 | 165.0 | 12.0 | 158.1 | 8.7 |
| Output_1_265 | 3540 | 241 | 3.7 | 0.02 | 4.84 | 0.05 | 10.20 | 0.18 | 10.61 | 0.39 | 280.0 | 210.0 | 158.1 | 7.3 | 166.0 | 17.0 | 158.1 | 9.4 |
| Output_1_194 | 2978 | 186 | 1.6 | 0.02 | 5.22 | 0.05 | 12.66 | 0.18 | 13.41 | 0.39 | 290.0 | 260.0 | 158.4 | 8.1 | 166.0 | 21.0 | 158.4 | 10.0 |
| Output_1_107 | 1758 | 143 | 1.6 | 0.02 | 5.62 | 0.06 | 20.00 | 0.20 | 19.70 | 0.09 | 320.0 | 410.0 | 158.7 | 8.5 | 184.0 | 34.0 | 158.7 | 10.0 |
| Output_1_119 | 27800 | 2870 | 1.1 | 0.02 | 2.92 | 0.05 | 4.36 | 0.17 | 4.81 | 0.27 | 130.0 | 100.0 | 158.9 | 4.6 | 158.0 | 7.0 | 158.9 | 7.5 |
| Output_1_17 | 9770 | 395 | 6.4 | 0.02 | 3.44 | 0.05 | 7.68 | 0.17 | 7.60 | 0.27 | 190.0 | 160.0 | 159.0 | 5.4 | 159.0 | 12.0 | 159.0 | 8.1 |
| Output_1_207 | 5890 | 199 | 4.8 | 0.03 | 4.80 | 0.05 | 8.65 | 0.17 | 7.74 | 0.12 | 80.0 | 180.0 | 159.0 | 7.3 | 157.0 | 12.0 | 159.0 | 9.4 |
| Output_1_256 | 1710 | 101 | 1.6 | 0.02 | 6.83 | 0.06 | 20.34 | 0.20 | 20.20 | 0.07 | 420.0 | 420.0 | 159.0 | 10.0 | 179.0 | 34.0 | 159.0 | 12.0 |
| Output_1_71 | 2052 | 67 | 1.8 | 0.03 | 4.78 | 0.05 | 18.69 | 0.17 | 17.06 | 0.21 | 170.0 | 370.0 | 159.5 | 7.5 | 157.0 | 25.0 | 159.5 | 9.6 |
| Output_1_266 | 3620 | 251 | 6.6 | 0.03 | 5.18 | 0.05 | 14.02 | 0.19 | 13.23 | 0.06 | 340.0 | 290.0 | 159.6 | 7.9 | 174.0 | 21.0 | 159.6 | 9.9 |
| Output_1_232 | 2650 | 141 | 2.2 | 0.03 | 4.38 | 0.05 | 12.30 | 0.18 | 10.67 | 0.12 | 220.0 | 240.0 | 159.7 | 6.8 | 165.0 | 16.0 | 159.7 | 9.1 |
| Output_1_4 | 29900 | 1710 | 2.9 | 0.03 | 5.18 | 0.06 | 9.26 | 0.18 | 7.14 | 0.57 | 390.0 | 220.0 | 159.7 | 7.9 | 170.0 | 12.0 | 159.7 | 10.0 |

| | | | | | | | | | | | | | | | | | | | |
|---|---|---|---|---|---|---|---|---|---|---|---|---|---|---|---|---|---|---|---|
| Output_1_217 | 1227 | 43 | 2.2 | 0.03 | 8.37 | 0.05 | 19.23 | 0.18 | 19.77 | 0.31 | 160.0 | 400.0 | 160.0 | 13.0 | 167.0 | 32.0 | 160.0 | 14.0 |
| Output_1_228 | 1220 | 60 | 3.9 | 0.03 | 9.16 | 0.07 | 25.76 | 0.24 | 24.68 | 0.26 | 770.0 | 510.0 | 160.0 | 14.0 | 207.0 | 48.0 | 160.0 | 16.0 |
| Output_1_180 | 3330 | 321 | 1.4 | 0.03 | 5.56 | 0.05 | 14.55 | 0.16 | 13.84 | 0.15 | 60.0 | 280.0 | 160.1 | 8.8 | 151.0 | 20.0 | 160.1 | 11.0 |
| Output_1_102 | 1600 | 119 | 2.2 | 0.03 | 7.87 | 0.06 | 17.24 | 0.20 | 15.90 | 0.19 | 450.0 | 370.0 | 161.0 | 13.0 | 178.0 | 26.0 | 161.0 | 14.0 |
| Output_1_43 | 13130 | 474 | 3.6 | 0.03 | 3.48 | 0.05 | 6.75 | 0.17 | 7.06 | 0.55 | 180.0 | 140.0 | 161.1 | 5.5 | 159.0 | 10.0 | 161.1 | 8.2 |
| Output_1_257 | 1661 | 97 | 3.3 | 0.03 | 5.51 | 0.06 | 21.05 | 0.20 | 18.50 | 0.03 | 420.0 | 430.0 | 161.4 | 9.1 | 183.0 | 31.0 | 161.4 | 11.0 |
| Output_1_99 | 4400 | 295 | 1.9 | 0.03 | 4.33 | 0.05 | 9.19 | 0.17 | 9.94 | 0.34 | 10.0 | 180.0 | 161.9 | 6.9 | 159.0 | 14.0 | 161.9 | 9.2 |
| Output_1_67 | 2020 | 61 | 1.4 | 0.03 | 7.87 | 0.06 | 17.05 | 0.19 | 19.90 | 0.53 | 410.0 | 350.0 | 162.0 | 12.0 | 184.0 | 28.0 | 162.0 | 14.0 |
| Output_1_80 | 1354 | 51 | 2.4 | 0.03 | 8.63 | 0.05 | 20.00 | 0.19 | 21.39 | 0.14 | 20.0 | 360.0 | 162.0 | 14.0 | 174.0 | 34.0 | 162.0 | 15.0 |
| Output_1_209 | 4910 | 156 | 3.3 | 0.03 | 4.71 | 0.05 | 8.51 | 0.19 | 9.57 | 0.26 | 360.0 | 190.0 | 162.2 | 7.4 | 174.0 | 15.0 | 162.2 | 9.6 |
| Output_1_121 | 5340 | 588 | 2.9 | 0.03 | 3.92 | 0.05 | 10.72 | 0.18 | 7.65 | 0.21 | 220.0 | 210.0 | 162.4 | 6.5 | 170.0 | 12.0 | 162.4 | 8.9 |
| Output_1_113 | 4010 | 351 | 2.6 | 0.03 | 3.76 | 0.05 | 13.22 | 0.19 | 11.46 | 0.05 | 410.0 | 270.0 | 162.6 | 6.0 | 178.0 | 19.0 | 162.6 | 8.6 |
| Output_1_103 | 10910 | 801 | 3.3 | 0.03 | 4.30 | 0.05 | 5.86 | 0.18 | 6.67 | 0.45 | 220.0 | 130.0 | 162.7 | 6.7 | 167.0 | 11.0 | 162.7 | 9.0 |
| Output_1_188 | 2230 | 230 | 2.2 | 0.03 | 6.64 | 0.05 | 22.00 | 0.17 | 20.47 | 0.42 | 320.0 | 400.0 | 163.0 | 11.0 | 168.0 | 27.0 | 163.0 | 12.0 |
| Output_1_144 | 5790 | 205 | 2.3 | 0.03 | 3.28 | 0.05 | 9.11 | 0.18 | 10.17 | 0.34 | 160.0 | 200.0 | 163.2 | 5.3 | 168.0 | 16.0 | 163.2 | 8.1 |
| Output_1_94 | 3530 | 197 | 2.5 | 0.03 | 4.67 | 0.05 | 10.08 | 0.18 | 9.89 | 0.06 | 160.0 | 200.0 | 163.4 | 7.8 | 172.0 | 17.0 | 163.4 | 9.9 |
| Output_1_13 | 1840 | 79 | 4.6 | 0.03 | 6.23 | 0.05 | 19.25 | 0.17 | 16.76 | 0.19 | 130.0 | 360.0 | 163.5 | 9.8 | 159.0 | 25.0 | 163.5 | 12.0 |
| Output_1_14 | 2910 | 120 | 3.0 | 0.03 | 3.04 | 0.06 | 12.45 | 0.19 | 12.50 | 0.02 | 360.0 | 270.0 | 163.6 | 4.9 | 176.0 | 20.0 | 163.6 | 7.9 |
| Output_1_178 | 3330 | 247 | 2.2 | 0.03 | 5.04 | 0.06 | 12.32 | 0.19 | 11.34 | 0.22 | 410.0 | 250.0 | 164.2 | 8.1 | 178.0 | 19.0 | 164.2 | 10.0 |
| Output_1_21 | 3520 | 140 | 3.1 | 0.03 | 4.63 | 0.05 | 10.00 | 0.18 | 8.33 | 0.08 | 290.0 | 190.0 | 164.6 | 7.7 | 167.0 | 13.0 | 164.6 | 9.9 |
| Output_1_134 | 10230 | 436 | 2.6 | 0.03 | 3.07 | 0.05 | 7.30 | 0.18 | 6.59 | 0.07 | 380.0 | 160.0 | 164.7 | 5.2 | 170.0 | 10.0 | 164.7 | 8.3 |
| Output_1_160 | 2440 | 89 | 2.1 | 0.03 | 5.41 | 0.06 | 15.64 | 0.20 | 11.56 | 0.33 | 530.0 | 310.0 | 164.9 | 8.9 | 183.0 | 20.0 | 164.9 | 11.0 |
| Output_1_225 | 1382 | 57 | 3.1 | 0.03 | 6.18 | 0.06 | 22.41 | 0.19 | 20.83 | 0.03 | 260.0 | 420.0 | 165.0 | 10.0 | 183.0 | 36.0 | 165.0 | 12.0 |
| Output_1_116 | 1433 | 130 | 2.1 | 0.03 | 7.31 | 0.05 | 22.00 | 0.18 | 22.53 | 0.19 | 60.0 | 400.0 | 165.0 | 12.0 | 165.0 | 35.0 | 165.0 | 13.0 |
| Output_1_150 | 2680 | 94 | 2.5 | 0.03 | 4.63 | 0.06 | 13.11 | 0.19 | 12.95 | 0.16 | 340.0 | 260.0 | 165.1 | 7.4 | 181.0 | 22.0 | 165.1 | 9.7 |
| Output_1_210 | 3050 | 98 | 3.5 | 0.03 | 5.38 | 0.05 | 13.37 | 0.19 | 13.92 | 0.19 | 340.0 | 260.0 | 165.2 | 8.7 | 178.0 | 23.0 | 165.2 | 11.0 |
| Output_1_10 | 6600 | 289 | 2.1 | 0.03 | 4.23 | 0.05 | 11.20 | 0.19 | 11.83 | 0.21 | 280.0 | 250.0 | 165.4 | 6.9 | 173.0 | 18.0 | 165.4 | 9.3 |
| Output_1_1 | 1700 | 105 | 1.9 | 0.03 | 5.00 | 0.06 | 16.53 | 0.19 | 16.23 | 0.06 | 510.0 | 340.0 | 165.5 | 8.0 | 186.0 | 27.0 | 165.5 | 10.0 |
| Output_1_157 | 4730 | 165 | 2.4 | 0.03 | 4.60 | 0.05 | 13.14 | 0.18 | 13.07 | 0.15 | 140.0 | 260.0 | 165.9 | 7.2 | 166.0 | 20.0 | 165.9 | 9.6 |
| Output_1_120 | 9940 | 990 | 2.0 | 0.03 | 6.51 | 0.05 | 9.05 | 0.17 | 6.90 | 0.54 | 60.0 | 190.0 | 166.0 | 11.0 | 163.0 | 10.0 | 166.0 | 13.0 |
| Output_1_12 | 992 | 43 | 3.4 | 0.03 | 8.46 | 0.07 | 25.71 | 0.22 | 21.46 | 0.36 | 550.0 | 500.0 | 166.0 | 14.0 | 197.0 | 39.0 | 166.0 | 15.0 |
| Output_1_192 | 5310 | 367 | 2.4 | 0.03 | 3.29 | 0.06 | 7.03 | 0.20 | 8.04 | 0.41 | 410.0 | 160.0 | 166.2 | 5.4 | 183.0 | 14.0 | 166.2 | 8.3 |
| Output_1_145 | 2480 | 83 | 3.9 | 0.03 | 6.13 | 0.06 | 14.64 | 0.21 | 17.48 | 0.52 | 620.0 | 320.0 | 166.2 | 9.8 | 188.0 | 30.0 | 166.2 | 12.0 |
| Output_1_198 | 1716 | 73 | 2.3 | 0.03 | 3.75 | 0.06 | 16.32 | 0.20 | 15.58 | 0.18 | 500.0 | 320.0 | 166.3 | 6.2 | 196.0 | 25.0 | 166.3 | 8.8 |
| Output_1_89 | 7300 | 353 | 2.6 | 0.03 | 4.20 | 0.05 | 8.69 | 0.17 | 8.77 | 0.23 | 40.0 | 170.0 | 166.5 | 6.6 | 159.0 | 13.0 | 166.5 | 9.1 |
| Output_1_41 | 2093 | 75 | 1.5 | 0.03 | 4.58 | 0.06 | 19.64 | 0.21 | 20.57 | 0.16 | 450.0 | 420.0 | 166.5 | 7.6 | 190.0 | 35.0 | 166.5 | 9.8 |
| Output_1_106 | 4710 | 363 | 2.1 | 0.03 | 4.96 | 0.05 | 10.32 | 0.17 | 12.07 | 0.40 | 30.0 | 210.0 | 166.8 | 7.8 | 164.0 | 18.0 | 166.8 | 10.0 |
| Output_1_153 | 3450 | 120 | 2.1 | 0.03 | 4.20 | 0.05 | 11.58 | 0.20 | 11.22 | 0.13 | 350.0 | 230.0 | 166.9 | 7.0 | 184.0 | 17.0 | 166.9 | 9.4 |
| Output_1_129 | 2060 | 107 | 2.8 | 0.03 | 6.84 | 0.05 | 20.43 | 0.17 | 19.30 | 0.05 | 40.0 | 380.0 | 167.0 | 11.0 | 157.0 | 28.0 | 167.0 | 13.0 |
| Output_1_141 | 6440 | 225 | 2.3 | 0.03 | 3.01 | 0.05 | 9.30 | 0.19 | 9.63 | 0.31 | 240.0 | 200.0 | 167.1 | 5.0 | 173.0 | 15.0 | 167.1 | 8.0 |

| | | | | | | | | | | | | | | | | | | |
|---|---|---|---|---|---|---|---|---|---|---|---|---|---|---|---|---|---|---|
| Output_1_77 | 2550 | 87 | 2.2 | 0.03 | 5.70 | 0.05 | 12.30 | 0.18 | 12.22 | 0.18 | 260.0 | 250.0 | 167.3 | 9.1 | 166.0 | 19.0 | 167.3 | 11.0 |
| Output_1_75 | 1980 | 67 | 2.9 | 0.03 | 5.70 | 0.05 | 16.67 | 0.20 | 17.35 | 0.31 | 180.0 | 330.0 | 167.4 | 9.4 | 178.0 | 29.0 | 167.4 | 11.0 |
| Output_1_64 | 2720 | 82 | 2.0 | 0.03 | 3.79 | 0.05 | 15.74 | 0.20 | 14.80 | 0.02 | 190.0 | 310.0 | 168.0 | 6.3 | 179.0 | 25.0 | 168.0 | 8.9 |
| Output_1_90 | 2180 | 106 | 2.7 | 0.03 | 6.82 | 0.04 | 14.64 | 0.18 | 13.56 | 0.11 | 100.0 | 290.0 | 168.0 | 11.0 | 167.0 | 22.0 | 168.0 | 13.0 |
| Output_1_23 | 2130 | 87 | 3.3 | 0.03 | 5.64 | 0.05 | 15.10 | 0.19 | 15.87 | 0.18 | 300.0 | 310.0 | 169.3 | 9.6 | 173.0 | 26.0 | 169.3 | 12.0 |
| Output_1_28 | 16160 | 663 | 1.1 | 0.03 | 3.60 | 0.05 | 8.38 | 0.19 | 8.33 | 0.13 | 270.0 | 180.0 | 169.7 | 6.0 | 178.0 | 13.0 | 169.7 | 8.8 |
| Output_1_48 | 2870 | 93 | 2.0 | 0.03 | 6.37 | 0.05 | 13.08 | 0.19 | 12.37 | 0.27 | 220.0 | 260.0 | 170.0 | 11.0 | 171.0 | 19.0 | 170.0 | 13.0 |
| Output_1_83 | 3330 | 129 | 1.3 | 0.03 | 4.09 | 0.05 | 10.84 | 0.18 | 10.56 | 0.19 | 130.0 | 230.0 | 171.1 | 6.6 | 170.0 | 17.0 | 171.1 | 9.2 |
| Output_1_9 | 8120 | 355 | 1.2 | 0.03 | 3.70 | 0.05 | 13.12 | 0.19 | 13.02 | 0.19 | 290.0 | 280.0 | 172.0 | 6.4 | 177.0 | 21.0 | 172.0 | 9.1 |
| Output_1_159 | 3580 | 123 | 1.2 | 0.03 | 4.43 | 0.05 | 10.02 | 0.20 | 9.90 | 0.02 | 460.0 | 230.0 | 172.2 | 7.7 | 186.0 | 17.0 | 172.2 | 10.0 |
| Output_1_195 | 2200 | 113 | 3.0 | 0.03 | 5.54 | 0.05 | 21.28 | 0.18 | 21.23 | 0.03 | 0.0 | 400.0 | 172.4 | 9.2 | 162.0 | 33.0 | 172.4 | 11.0 |
| Output_1_88 | 4360 | 193 | 1.5 | 0.03 | 4.41 | 0.05 | 9.16 | 0.19 | 8.42 | 0.03 | 150.0 | 190.0 | 172.8 | 7.8 | 176.0 | 14.0 | 172.8 | 10.0 |
| Output_1_128 | 3360 | 178 | 2.7 | 0.03 | 6.57 | 0.06 | 14.94 | 0.21 | 12.38 | 0.09 | 460.0 | 310.0 | 174.0 | 11.0 | 192.0 | 22.0 | 174.0 | 13.0 |
| Output_1_16 | 37420 | 1366 | 3.7 | 0.03 | 1.85 | 0.05 | 4.20 | 0.19 | 4.00 | 0.02 | 179.0 | 93.0 | 175.4 | 3.2 | 176.3 | 6.5 | 175.4 | 7.3 |
| Output_1_92 | 4520 | 220 | 3.0 | 0.03 | 3.99 | 0.05 | 12.63 | 0.19 | 13.23 | 0.27 | 80.0 | 250.0 | 175.7 | 7.1 | 174.0 | 21.0 | 175.7 | 9.7 |
| Output_1_185 | 2600 | 276 | 2.1 | 0.03 | 7.58 | 0.05 | 16.56 | 0.17 | 14.71 | 0.18 | 40.0 | 320.0 | 176.0 | 13.0 | 158.0 | 22.0 | 176.0 | 15.0 |
| Output_1_261 | 6990 | 407 | 3.9 | 0.03 | 4.32 | 0.06 | 8.87 | 0.21 | 8.49 | 0.23 | 400.0 | 190.0 | 176.4 | 7.5 | 194.0 | 15.0 | 176.4 | 10.0 |
| Output_1_193 | 5780 | 342 | 2.3 | 0.03 | 4.69 | 0.05 | 8.50 | 0.19 | 8.95 | 0.35 | 130.0 | 170.0 | 177.4 | 8.6 | 176.0 | 14.0 | 177.4 | 11.0 |
| Output_1_154 | 27900 | 900 | 3.8 | 0.03 | 1.99 | 0.05 | 5.16 | 0.19 | 4.70 | 0.03 | 290.0 | 110.0 | 178.6 | 3.5 | 179.4 | 7.7 | 178.6 | 7.6 |
| Output_1_220 | 5830 | 188 | 2.1 | 0.03 | 3.90 | 0.06 | 8.84 | 0.22 | 9.46 | 0.36 | 400.0 | 180.0 | 179.2 | 7.1 | 202.0 | 18.0 | 179.2 | 9.8 |
| Output_1_33 | 6490 | 243 | 0.9 | 0.03 | 4.26 | 0.05 | 8.05 | 0.19 | 8.76 | 0.26 | 260.0 | 170.0 | 179.5 | 7.2 | 183.0 | 13.0 | 179.5 | 9.9 |
| Output_1_148 | 4640 | 147 | 2.6 | 0.03 | 5.30 | 0.06 | 11.11 | 0.21 | 12.86 | 0.32 | 480.0 | 240.0 | 179.9 | 9.2 | 192.0 | 23.0 | 179.9 | 11.0 |
| Output_1_264 | 16470 | 989 | 4.1 | 0.03 | 3.53 | 0.05 | 5.49 | 0.20 | 6.44 | 0.50 | 210.0 | 120.0 | 180.0 | 6.4 | 186.0 | 11.0 | 180.0 | 9.3 |
| Output_1_177 | 1460 | 93 | 1.9 | 0.03 | 6.71 | 0.06 | 27.27 | 0.22 | 25.23 | 0.04 | 350.0 | 490.0 | 180.0 | 12.0 | 198.0 | 45.0 | 180.0 | 14.0 |
| Output_1_167 | 18900 | 710 | 1.4 | 0.03 | 3.89 | 0.05 | 6.26 | 0.20 | 5.53 | 0.46 | 300.0 | 140.0 | 180.1 | 7.1 | 183.9 | 9.5 | 180.1 | 9.8 |
| Output_1_174 | 4190 | 233 | 2.0 | 0.03 | 5.30 | 0.06 | 11.95 | 0.22 | 10.00 | 0.07 | 480.0 | 240.0 | 180.1 | 9.5 | 201.0 | 18.0 | 180.1 | 12.0 |
| Output_1_165 | 11930 | 422 | 1.7 | 0.03 | 4.95 | 0.06 | 8.00 | 0.20 | 8.33 | 0.10 | 350.0 | 180.0 | 180.2 | 8.6 | 191.0 | 14.0 | 180.2 | 11.0 |
| Output_1_200 | 3120 | 108 | 2.5 | 0.03 | 4.93 | 0.05 | 13.05 | 0.19 | 11.64 | 0.09 | 220.0 | 260.0 | 180.4 | 8.9 | 174.0 | 19.0 | 180.4 | 11.0 |
| Output_1_72 | 36920 | 1074 | 1.9 | 0.03 | 5.28 | 0.05 | 4.73 | 0.19 | 4.53 | 0.36 | 210.0 | 110.0 | 180.5 | 9.1 | 180.1 | 7.4 | 180.5 | 11.0 |
| Output_1_109 | 12300 | 901 | 1.8 | 0.03 | 3.24 | 0.05 | 5.37 | 0.20 | 5.94 | 0.45 | 290.0 | 110.0 | 180.7 | 5.8 | 189.0 | 11.0 | 180.7 | 8.9 |
| Output_1_226 | 3550 | 134 | 3.0 | 0.03 | 4.58 | 0.06 | 14.63 | 0.22 | 13.43 | 0.02 | 480.0 | 300.0 | 180.7 | 7.9 | 196.0 | 25.0 | 180.7 | 10.0 |
| Output_1_155 | 7920 | 258 | 1.9 | 0.03 | 4.91 | 0.05 | 7.99 | 0.20 | 7.54 | 0.18 | 300.0 | 170.0 | 180.8 | 8.5 | 183.0 | 13.0 | 180.8 | 11.0 |
| Output_1_223 | 5020 | 181 | 1.9 | 0.03 | 5.94 | 0.05 | 12.31 | 0.21 | 10.05 | 0.06 | 280.0 | 230.0 | 181.0 | 11.0 | 191.0 | 17.0 | 181.0 | 13.0 |
| Output_1_138 | 36930 | 1236 | 1.0 | 0.03 | 2.63 | 0.05 | 3.20 | 0.20 | 3.17 | 0.30 | 323.0 | 73.0 | 181.2 | 4.7 | 186.7 | 5.4 | 181.2 | 8.3 |
| Output_1_137 | 23900 | 839 | 0.8 | 0.03 | 2.98 | 0.05 | 5.14 | 0.21 | 4.66 | 0.39 | 290.0 | 110.0 | 181.2 | 5.3 | 193.6 | 8.3 | 181.2 | 8.7 |
| Output_1_238 | 13920 | 797 | 1.7 | 0.03 | 2.63 | 0.05 | 6.43 | 0.19 | 6.19 | 0.22 | 210.0 | 140.0 | 181.4 | 4.7 | 180.0 | 11.0 | 181.4 | 8.3 |
| Output_1_26 | 13450 | 512 | 4.8 | 0.03 | 3.29 | 0.05 | 9.49 | 0.20 | 9.36 | 0.04 | 200.0 | 200.0 | 181.4 | 5.9 | 187.0 | 16.0 | 181.4 | 9.0 |
| Output_1_213 | 28130 | 833 | 2.6 | 0.03 | 3.51 | 0.05 | 6.43 | 0.21 | 7.48 | 0.54 | 430.0 | 140.0 | 181.4 | 6.5 | 196.0 | 14.0 | 181.4 | 9.5 |
| Output_1_101 | 4960 | 313 | 2.3 | 0.03 | 4.55 | 0.05 | 11.11 | 0.21 | 9.95 | 0.06 | 270.0 | 230.0 | 181.7 | 8.2 | 193.0 | 18.0 | 181.7 | 11.0 |
| Output_1_249 | 28200 | 1392 | 4.8 | 0.03 | 2.66 | 0.05 | 3.78 | 0.20 | 4.80 | 0.92 | 211.0 | 91.0 | 181.9 | 4.8 | 186.3 | 7.0 | 181.9 | 8.3 |

| | | | | | | | | | | | | | | | | | | |
|---|---|---|---|---|---|---|---|---|---|---|---|---|---|---|---|---|---|---|
| Output_1_152 | 3110 | 99 | 1.8 | 0.03 | 5.57 | 0.06 | 16.17 | 0.22 | 13.84 | 0.25 | 370.0 | 320.0 | 182.0 | 10.0 | 204.0 | 25.0 | 182.0 | 12.0 |
| Output_1_247 | 2760 | 151 | 4.6 | 0.03 | 6.27 | 0.05 | 24.53 | 0.20 | 24.63 | 0.28 | 230.0 | 490.0 | 182.0 | 11.0 | 186.0 | 42.0 | 182.0 | 13.0 |
| Output_1_253 | 5150 | 255 | 2.8 | 0.03 | 3.41 | 0.06 | 10.97 | 0.21 | 9.35 | 0.15 | 340.0 | 230.0 | 182.6 | 6.2 | 199.0 | 18.0 | 182.6 | 9.2 |
| Output_1_37 | 7420 | 261 | 1.5 | 0.03 | 3.10 | 0.05 | 8.75 | 0.20 | 8.72 | 0.23 | 230.0 | 190.0 | 182.7 | 5.6 | 183.0 | 14.0 | 182.7 | 8.8 |
| Output_1_51 | 3860 | 110 | 2.1 | 0.03 | 4.84 | 0.05 | 13.76 | 0.19 | 12.89 | 0.19 | 170.0 | 270.0 | 183.5 | 8.8 | 178.0 | 21.0 | 183.5 | 11.0 |
| Output_1_25 | 10770 | 388 | 2.1 | 0.03 | 3.35 | 0.05 | 7.07 | 0.19 | 7.29 | 0.26 | 110.0 | 150.0 | 184.0 | 6.1 | 178.0 | 12.0 | 184.0 | 9.2 |
| Output_1_2 | 8090 | 431 | 2.6 | 0.03 | 4.14 | 0.05 | 7.19 | 0.20 | 7.50 | 0.28 | 200.0 | 140.0 | 184.0 | 7.8 | 184.0 | 13.0 | 184.0 | 10.0 |
| Output_1_182 | 5020 | 461 | 1.4 | 0.03 | 5.86 | 0.05 | 8.29 | 0.20 | 8.00 | 0.57 | 270.0 | 170.0 | 184.0 | 11.0 | 185.0 | 14.0 | 184.0 | 13.0 |
| Output_1_248 | 2500 | 125 | 3.3 | 0.03 | 6.23 | 0.06 | 12.17 | 0.22 | 11.47 | 0.01 | 430.0 | 270.0 | 184.0 | 12.0 | 198.0 | 21.0 | 184.0 | 13.0 |
| Output_1_229 | 4420 | 190 | 2.4 | 0.03 | 4.83 | 0.05 | 11.50 | 0.21 | 11.59 | 0.15 | 290.0 | 240.0 | 184.2 | 8.5 | 190.0 | 20.0 | 184.2 | 11.0 |
| Output_1_81 | 5210 | 180 | 1.3 | 0.03 | 3.79 | 0.05 | 9.40 | 0.20 | 9.74 | 0.18 | 40.0 | 190.0 | 184.6 | 6.8 | 180.0 | 16.0 | 184.6 | 9.7 |
| Output_1_172 | 245800 | 11070 | 0.9 | 0.03 | 2.84 | 0.05 | 2.37 | 0.21 | 2.78 | 0.76 | 239.0 | 54.0 | 185.5 | 5.2 | 189.6 | 4.8 | 185.5 | 8.7 |
| Output_1_147 | 9150 | 277 | 2.0 | 0.03 | 3.42 | 0.05 | 7.51 | 0.20 | 7.11 | 0.10 | 190.0 | 160.0 | 185.6 | 6.4 | 182.0 | 12.0 | 185.6 | 9.5 |
| Output_1_76 | 10850 | 328 | 1.8 | 0.03 | 3.75 | 0.05 | 6.20 | 0.20 | 6.47 | 0.03 | 200.0 | 120.0 | 186.1 | 7.0 | 185.0 | 11.0 | 186.1 | 9.9 |
| Output_1_208 | 11670 | 324 | 2.0 | 0.03 | 4.10 | 0.05 | 6.08 | 0.21 | 6.19 | 0.43 | 320.0 | 130.0 | 186.1 | 7.3 | 193.0 | 11.0 | 186.1 | 10.0 |
| Output_1_5 | 11800 | 586 | 2.7 | 0.03 | 3.74 | 0.05 | 7.07 | 0.21 | 7.62 | 0.31 | 340.0 | 160.0 | 186.8 | 6.8 | 195.0 | 13.0 | 186.8 | 9.8 |
| Output_1_216 | 14300 | 433 | 2.7 | 0.03 | 3.74 | 0.05 | 6.22 | 0.20 | 7.84 | 0.46 | 170.0 | 130.0 | 186.8 | 6.9 | 188.0 | 13.0 | 186.8 | 9.9 |
| Output_1_96 | 11840 | 641 | 2.1 | 0.03 | 3.40 | 0.05 | 8.37 | 0.22 | 7.44 | 0.02 | 300.0 | 170.0 | 186.9 | 6.5 | 197.0 | 14.0 | 186.9 | 9.6 |
| Output_1_158 | 5340 | 166 | 1.9 | 0.03 | 6.12 | 0.05 | 8.70 | 0.22 | 8.84 | 0.20 | 280.0 | 180.0 | 187.0 | 11.0 | 197.0 | 16.0 | 187.0 | 13.0 |
| Output_1_149 | 2770 | 85 | 2.5 | 0.03 | 6.44 | 0.06 | 13.11 | 0.22 | 14.48 | 0.48 | 320.0 | 280.0 | 187.0 | 12.0 | 205.0 | 27.0 | 187.0 | 14.0 |
| Output_1_84 | 1366 | 50 | 2.5 | 0.03 | 7.48 | 0.05 | 19.18 | 0.19 | 18.56 | 0.12 | 40.0 | 330.0 | 187.0 | 13.0 | 176.0 | 30.0 | 187.0 | 15.0 |
| Output_1_162 | 15000 | 481 | 2.7 | 0.03 | 3.08 | 0.05 | 5.03 | 0.22 | 5.58 | 0.43 | 330.0 | 110.0 | 187.4 | 5.7 | 197.0 | 10.0 | 187.4 | 9.1 |
| Output_1_123 | 12390 | 1295 | 2.4 | 0.03 | 3.28 | 0.05 | 7.18 | 0.21 | 8.10 | 0.39 | 260.0 | 150.0 | 187.7 | 6.1 | 196.0 | 13.0 | 187.7 | 9.3 |
| Output_1_38 | 38300 | 1317 | 1.0 | 0.03 | 2.94 | 0.05 | 4.44 | 0.20 | 4.83 | 0.41 | 155.0 | 95.0 | 187.8 | 5.4 | 185.5 | 8.2 | 187.8 | 8.9 |
| Output_1_156 | 3430 | 107 | 2.0 | 0.03 | 5.41 | 0.06 | 13.54 | 0.22 | 13.36 | 0.20 | 420.0 | 270.0 | 188.0 | 10.0 | 211.0 | 25.0 | 188.0 | 12.0 |
| Output_1_74 | 15400 | 453 | 1.0 | 0.03 | 2.70 | 0.05 | 7.39 | 0.22 | 7.41 | 0.37 | 340.0 | 160.0 | 188.4 | 5.0 | 198.0 | 13.0 | 188.4 | 8.7 |
| Output_1_242 | 5860 | 314 | 2.5 | 0.03 | 4.04 | 0.05 | 10.33 | 0.20 | 10.20 | 0.19 | 60.0 | 200.0 | 188.7 | 7.5 | 181.0 | 17.0 | 188.7 | 10.0 |
| Output_1_151 | 8500 | 264 | 1.1 | 0.03 | 2.52 | 0.06 | 11.03 | 0.22 | 8.29 | 0.02 | 510.0 | 280.0 | 188.8 | 4.7 | 199.0 | 16.0 | 188.8 | 8.5 |
| Output_1_18 | 16560 | 570 | 1.7 | 0.03 | 2.96 | 0.05 | 6.05 | 0.22 | 5.58 | 0.12 | 320.0 | 140.0 | 188.8 | 5.5 | 197.0 | 10.0 | 188.8 | 9.0 |
| Output_1_82 | 20590 | 711 | 3.1 | 0.03 | 3.69 | 0.05 | 5.72 | 0.21 | 4.88 | 0.32 | 220.0 | 120.0 | 189.0 | 6.6 | 189.4 | 8.7 | 189.0 | 9.7 |
| Output_1_254 | 3160 | 154 | 2.6 | 0.03 | 7.07 | 0.06 | 19.67 | 0.24 | 19.67 | 0.18 | 450.0 | 430.0 | 189.0 | 13.0 | 215.0 | 39.0 | 189.0 | 15.0 |
| Output_1_108 | 5230 | 353 | 3.3 | 0.03 | 7.38 | 0.05 | 18.30 | 0.23 | 18.70 | 0.09 | 450.0 | 300.0 | 189.0 | 14.0 | 209.0 | 35.0 | 189.0 | 16.0 |
| Output_1_127 | 91100 | 4550 | 1.6 | 0.03 | 3.26 | 0.05 | 2.61 | 0.20 | 3.37 | 0.63 | 178.0 | 59.0 | 189.1 | 6.1 | 190.2 | 5.6 | 189.1 | 9.4 |
| Output_1_42 | 7280 | 219 | 1.1 | 0.03 | 4.03 | 0.05 | 8.25 | 0.21 | 8.70 | 0.13 | 220.0 | 180.0 | 189.4 | 7.7 | 190.0 | 15.0 | 189.4 | 10.0 |
| Output_1_122 | 17740 | 1733 | 1.6 | 0.03 | 4.03 | 0.05 | 5.65 | 0.21 | 5.14 | 0.25 | 310.0 | 130.0 | 189.4 | 7.8 | 196.9 | 9.5 | 189.4 | 11.0 |
| Output_1_69 | 5310 | 142 | 1.5 | 0.03 | 3.26 | 0.05 | 11.31 | 0.22 | 11.01 | 0.22 | 350.0 | 240.0 | 191.0 | 6.2 | 204.0 | 21.0 | 191.0 | 9.5 |
| Output_1_146 | 3320 | 101 | 2.5 | 0.03 | 5.98 | 0.06 | 13.29 | 0.22 | 11.82 | 0.07 | 390.0 | 290.0 | 191.0 | 11.0 | 200.0 | 22.0 | 191.0 | 13.0 |
| Output_1_203 | 4660 | 137 | 1.9 | 0.03 | 4.32 | 0.05 | 10.54 | 0.22 | 9.17 | 0.01 | 330.0 | 220.0 | 191.2 | 8.1 | 203.0 | 18.0 | 191.2 | 11.0 |
| Output_1_187 | 35500 | 3250 | 2.7 | 0.03 | 2.62 | 0.06 | 3.39 | 0.24 | 2.71 | 0.17 | 456.0 | 79.0 | 191.6 | 4.9 | 215.0 | 5.2 | 191.6 | 8.7 |
| Output_1_237 | 7280 | 378 | 1.4 | 0.03 | 3.29 | 0.05 | 8.95 | 0.22 | 8.76 | 0.08 | 280.0 | 200.0 | 193.2 | 6.3 | 198.0 | 16.0 | 193.2 | 9.6 |

| | | | | | | | | | | | | | | | | | | |
|---|---|---|---|---|---|---|---|---|---|---|---|---|---|---|---|---|---|---|
| Output_1_53 | 20670 | 553 | 3.1 | 0.03 | 4.59 | 0.05 | 5.98 | 0.20 | 5.88 | 0.43 | 180.0 | 130.0 | 193.5 | 8.5 | 188.0 | 11.0 | 193.5 | 11.0 |
| Output_1_40 | 7900 | 254 | 1.7 | 0.03 | 4.58 | 0.05 | 6.36 | 0.21 | 7.04 | 0.29 | 220.0 | 150.0 | 194.1 | 8.9 | 196.0 | 12.0 | 194.1 | 11.0 |
| Output_1_22 | 6900 | 230 | 2.5 | 0.03 | 4.55 | 0.05 | 10.88 | 0.23 | 10.22 | 0.18 | 350.0 | 250.0 | 195.2 | 8.7 | 205.0 | 20.0 | 195.2 | 11.0 |
| Output_1_205 | 13940 | 381 | 4.2 | 0.03 | 2.98 | 0.05 | 6.71 | 0.22 | 6.48 | 0.29 | 190.0 | 140.0 | 196.1 | 5.8 | 198.0 | 11.0 | 196.1 | 9.4 |
| Output_1_252 | 15620 | 728 | 9.5 | 0.03 | 1.97 | 0.06 | 5.44 | 0.25 | 5.65 | 0.06 | 520.0 | 120.0 | 196.6 | 3.8 | 225.0 | 12.0 | 196.6 | 8.3 |
| Output_1_169 | 10440 | 381 | 1.3 | 0.03 | 3.54 | 0.06 | 5.81 | 0.25 | 6.30 | 0.23 | 450.0 | 130.0 | 197.2 | 7.0 | 229.0 | 13.0 | 197.2 | 10.0 |
| Output_1_201 | 6120 | 184 | 2.6 | 0.03 | 5.13 | 0.05 | 8.41 | 0.22 | 9.05 | 0.28 | 330.0 | 160.0 | 198.0 | 10.0 | 202.0 | 17.0 | 198.0 | 13.0 |
| Output_1_239 | 13670 | 730 | 3.9 | 0.03 | 2.14 | 0.05 | 8.58 | 0.23 | 8.37 | 0.08 | 310.0 | 180.0 | 198.8 | 4.2 | 207.0 | 16.0 | 198.8 | 8.6 |
| Output_1_54 | 4820 | 121 | 1.6 | 0.03 | 4.13 | 0.06 | 15.10 | 0.24 | 13.93 | 0.00 | 420.0 | 320.0 | 199.7 | 7.9 | 220.0 | 28.0 | 199.7 | 11.0 |
| Output_1_86 | 7170 | 267 | 1.7 | 0.03 | 4.13 | 0.05 | 7.93 | 0.22 | 8.33 | 0.38 | 130.0 | 170.0 | 200.1 | 8.3 | 200.0 | 16.0 | 200.1 | 11.0 |
| Output_1_199 | 4080 | 133 | 2.1 | 0.03 | 5.06 | 0.06 | 11.45 | 0.25 | 10.84 | 0.27 | 550.0 | 220.0 | 201.0 | 10.0 | 225.0 | 22.0 | 201.0 | 13.0 |
| Output_1_34 | 4890 | 162 | 2.4 | 0.03 | 3.43 | 0.05 | 9.21 | 0.23 | 9.05 | 0.09 | 260.0 | 200.0 | 203.4 | 6.9 | 211.0 | 17.0 | 203.4 | 10.0 |
| Output_1_29 | 4440 | 149 | 1.2 | 0.03 | 3.70 | 0.06 | 9.71 | 0.24 | 9.09 | 0.28 | 380.0 | 210.0 | 205.7 | 7.3 | 219.0 | 18.0 | 205.7 | 11.0 |
| Output_1_142 | 93900 | 2280 | 31.5 | 0.04 | 4.39 | 0.06 | 2.91 | 0.32 | 3.79 | 0.79 | 536.0 | 63.0 | 244.0 | 10.0 | 279.4 | 9.6 | 244.0 | 14.0 |
| Output_1_202 | 13600 | 248 | 1.4 | 0.05 | 4.43 | 0.06 | 8.71 | 0.38 | 8.78 | 0.29 | 370.0 | 190.0 | 313.0 | 13.0 | 323.0 | 25.0 | 313.0 | 18.0 |
| Output_1_97 | 10900 | 207 | 2.7 | 0.09 | 2.89 | 0.06 | 5.56 | 0.73 | 6.19 | 0.46 | 640.0 | 110.0 | 534.0 | 15.0 | 552.0 | 27.0 | 534.0 | 24.0 |
| Output_1_31 | 23100 | 287 | 1.6 | 0.09 | 2.77 | 0.06 | 3.87 | 0.73 | 5.23 | 0.64 | 578.0 | 83.0 | 536.0 | 14.0 | 552.0 | 22.0 | 536.0 | 24.0 |
| Output_1_191 | 17500 | 402 | 11.2 | 0.09 | 3.51 | 0.07 | 4.37 | 0.88 | 3.98 | 0.52 | 1014.0 | 85.0 | 545.0 | 18.0 | 640.0 | 19.0 | 545.0 | 27.0 |
| Output_1_118 | 4520 | 126 | 2.7 | 0.09 | 4.95 | 0.06 | 10.92 | 0.75 | 10.72 | 0.04 | 560.0 | 230.0 | 548.0 | 26.0 | 556.0 | 47.0 | 548.0 | 33.0 |
| Output_1_105 | 5010 | 106 | 2.4 | 0.09 | 4.77 | 0.06 | 13.22 | 0.74 | 11.82 | 0.04 | 430.0 | 270.0 | 556.0 | 26.0 | 551.0 | 51.0 | 556.0 | 33.0 |
| Output_1_260 | 42300 | 493 | 4.5 | 0.14 | 9.09 | 0.13 | 3.04 | 2.56 | 10.16 | 0.92 | 2067.0 | 53.0 | 858.0 | 75.0 | ##### | 73.0 | 858.0 | 81.0 |
| Output_1_73 | 23100 | 126 | 0.6 | 0.15 | 2.92 | 0.07 | 2.84 | 1.48 | 3.50 | 0.67 | 938.0 | 60.0 | 924.0 | 25.0 | 922.0 | 21.0 | 938.0 | 60.0 |
| Output_1_164 | 43300 | 284 | 3.1 | 0.15 | 4.17 | 0.08 | 4.26 | 1.56 | 4.55 | 0.61 | 1078.0 | 87.0 | 907.0 | 35.0 | 956.0 | 28.0 | 1078.0 | 87.0 |
| Output_1_91 | 38800 | 267 | 1.2 | 0.19 | 3.99 | 0.08 | 4.00 | 2.12 | 4.25 | 0.52 | 1193.0 | 82.0 | 1123.0 | 41.0 | ##### | 28.0 | 1193.0 | 82.0 |
| Output_1_52 | 43400 | 177 | 0.9 | 0.20 | 3.30 | 0.08 | 2.90 | 2.30 | 3.04 | 0.64 | 1255.0 | 57.0 | 1192.0 | 36.0 | ##### | 20.0 | 1255.0 | 58.0 |
| Output_1_255 | 72200 | 498 | 2.0 | 0.21 | 2.89 | 0.08 | 3.19 | 2.50 | 3.44 | 0.74 | 1302.0 | 62.0 | 1252.0 | 33.0 | ##### | 25.0 | 1302.0 | 62.0 |
| Output_1_6 | 45100 | 297 | 2.3 | 0.22 | 4.15 | 0.09 | 2.68 | 2.56 | 3.60 | 0.67 | 1340.0 | 47.0 | 1265.0 | 48.0 | ##### | 26.0 | 1340.0 | 47.0 |
| Output_1_212 | 11830 | 40 | 1.5 | 0.26 | 4.69 | 0.09 | 6.17 | 3.29 | 9.42 | 0.74 | 1470.0 | 120.0 | 1468.0 | 61.0 | ##### | 74.0 | 1470.0 | 120.0 |
| Output_1_175 | 52300 | 352 | 1.7 | 0.23 | 5.60 | 0.10 | 3.10 | 3.14 | 5.73 | 0.83 | 1570.0 | 62.0 | 1344.0 | 69.0 | ##### | 43.0 | 1570.0 | 62.0 |
| Output_1_66 | 91300 | 276 | 2.3 | 0.27 | 3.77 | 0.10 | 2.41 | 3.58 | 2.79 | 0.79 | 1607.0 | 45.0 | 1514.0 | 51.0 | ##### | 24.0 | 1607.0 | 45.0 |
| Output_1_114 | 40400 | 281 | 1.6 | 0.31 | 2.61 | 0.10 | 3.18 | 4.46 | 3.36 | 0.58 | 1685.0 | 58.0 | 1724.0 | 39.0 | ##### | 27.0 | 1685.0 | 58.0 |
| Output_1_170 | 74000 | 329 | 1.8 | 0.26 | 2.36 | 0.10 | 2.40 | 3.75 | 2.26 | 0.42 | 1711.0 | 44.0 | 1481.0 | 31.0 | ##### | 18.0 | 1711.0 | 44.0 |
| Output_1_176 | 43200 | 283 | 1.3 | 0.26 | 7.39 | 0.11 | 3.78 | 3.58 | 7.26 | 0.67 | 1723.0 | 71.0 | 1474.0 | 95.0 | ##### | 57.0 | 1723.0 | 71.0 |
| Output_1_224 | 32200 | 106 | 5.7 | 0.31 | 3.86 | 0.11 | 4.21 | 4.54 | 3.96 | 0.52 | 1724.0 | 77.0 | 1743.0 | 58.0 | ##### | 31.0 | 1724.0 | 77.0 |
| Output_1_46 | 28400 | 84 | 0.9 | 0.30 | 2.92 | 0.11 | 3.37 | 4.23 | 4.26 | 0.57 | 1732.0 | 63.0 | 1679.0 | 43.0 | ##### | 35.0 | 1732.0 | 63.0 |
| Output_1_112 | 24400 | 164 | 1.4 | 0.33 | 3.89 | 0.11 | 5.00 | 5.27 | 4.74 | 0.55 | 1888.0 | 86.0 | 1855.0 | 64.0 | ##### | 40.0 | 1888.0 | 86.0 |
| Output_1_44 | 21970 | 65 | 0.4 | 0.31 | 3.07 | 0.12 | 3.32 | 5.05 | 3.96 | 0.60 | 1964.0 | 57.0 | 1723.0 | 46.0 | ##### | 32.0 | 1964.0 | 57.0 |
| Output_1_173 | 21500 | 65 | 0.9 | 0.48 | 5.04 | 0.17 | 3.75 | 11.31 | 6.01 | 0.72 | 2567.0 | 67.0 | 2500.0 | ### | ##### | 58.0 | 2567.0 | 67.0 |
| Output_1_171 | 94700 | 286 | 1.0 | 0.42 | 3.12 | 0.17 | 2.86 | 9.95 | 4.22 | 0.76 | 2572.0 | 46.0 | 2245.0 | 61.0 | ##### | 38.0 | 2572.0 | 47.0 |
| Output_1_30 | 4730 | 12 | 0.6 | 0.43 | 4.19 | 0.18 | 5.46 | 11.00 | 6.18 | 0.46 | 2665.0 | 99.0 | 2300.0 | 79.0 | ##### | 54.0 | 2665.0 | 99.0 |

| | | | | | | | | | | | | | | | | | | |
|---|---|---|---|---|---|---|---|---|---|---|---|---|---|---|---|---|---|---|
| Output_1_181 | 195000 | 986 | 0.8 | 0.49 | 3.70 | 0.19 | 2.17 | 13.07 | 2.68 | 0.74 | 2768.0 | 36.0 | 2549.0 | 80.0 | ##### | 25.0 | 2768.0 | 36.0 |
| **Sample 19ATW79** | | | | | | | | | | | | | | | | | | |
| Output_1_55 | 4290 | 540 | 11.6 | 0.01 | 3.88 | 0.04 | 12.53 | 0.05 | 12.52 | 0.06 | -60.0 | 220.0 | 54.7 | 2.1 | 51.2 | 6.3 | 54.7 | 2.4 |
| Output_1_98 | 17230 | 2033 | 4.6 | 0.01 | 5.73 | 0.04 | 10.34 | 0.05 | 5.93 | 0.15 | -40.0 | 190.0 | 50.5 | 2.8 | 51.7 | 3.0 | 50.5 | 3.0 |
| Output_1_101 | 3420 | 457 | 8.8 | 0.01 | 4.25 | 0.04 | 11.62 | 0.05 | 11.29 | 0.05 | -40.0 | 200.0 | 51.4 | 2.2 | 49.9 | 5.5 | 51.4 | 2.4 |
| Output_1_76 | 8330 | 878 | 7.4 | 0.01 | 3.10 | 0.05 | 7.33 | 0.05 | 7.66 | 0.34 | 10.0 | 140.0 | 51.8 | 1.6 | 51.6 | 3.9 | 51.8 | 1.9 |
| Output_1_65 | 2980 | 361 | 7.7 | 0.01 | 3.72 | 0.05 | 13.86 | 0.05 | 13.90 | 0.07 | 40.0 | 250.0 | 50.1 | 1.8 | 51.1 | 6.9 | 50.1 | 2.1 |
| Output_1_93 | 6850 | 637 | 9.5 | 0.01 | 3.49 | 0.05 | 9.55 | 0.05 | 9.18 | 0.06 | 60.0 | 180.0 | 51.6 | 1.8 | 52.7 | 4.8 | 51.6 | 2.1 |
| Output_1_103 | 15060 | 2455 | 11.7 | 0.01 | 2.78 | 0.05 | 7.01 | 0.05 | 6.19 | 0.17 | 60.0 | 130.0 | 50.9 | 1.4 | 52.6 | 3.2 | 50.9 | 1.7 |
| Output_1_54 | 23800 | 3240 | 7.9 | 0.01 | 2.97 | 0.05 | 5.08 | 0.06 | 4.80 | 0.34 | 69.0 | 99.0 | 54.1 | 1.6 | 55.5 | 2.6 | 54.1 | 1.9 |
| Output_1_95 | 7700 | 690 | 7.1 | 0.01 | 3.76 | 0.05 | 10.92 | 0.06 | 10.19 | 0.05 | 70.0 | 200.0 | 54.6 | 2.0 | 57.0 | 5.6 | 54.6 | 2.3 |
| Output_1_77 | 4450 | 443 | 9.8 | 0.01 | 4.48 | 0.05 | 12.53 | 0.05 | 13.11 | 0.13 | 70.0 | 230.0 | 50.2 | 2.2 | 52.7 | 6.7 | 50.2 | 2.4 |
| Output_1_87 | 4000 | 306 | 7.2 | 0.01 | 4.49 | 0.05 | 14.47 | 0.06 | 14.08 | 0.10 | 80.0 | 260.0 | 54.3 | 2.4 | 55.2 | 7.6 | 54.3 | 2.6 |
| Output_1_85 | 9980 | 806 | 8.7 | 0.01 | 3.37 | 0.05 | 8.39 | 0.05 | 7.85 | 0.17 | 80.0 | 160.0 | 51.5 | 1.7 | 52.9 | 4.0 | 51.5 | 2.0 |
| Output_1_78 | 4940 | 474 | 7.7 | 0.01 | 3.23 | 0.05 | 13.89 | 0.05 | 14.18 | 0.24 | 80.0 | 250.0 | 49.7 | 1.6 | 52.1 | 7.2 | 49.7 | 1.9 |
| Output_1_63 | 17960 | 1959 | 12.1 | 0.01 | 2.70 | 0.05 | 5.72 | 0.06 | 6.18 | 0.44 | 90.0 | 110.0 | 54.7 | 1.5 | 55.8 | 3.4 | 54.7 | 1.8 |
| Output_1_57 | 13040 | 1615 | 9.4 | 0.01 | 2.99 | 0.05 | 6.51 | 0.05 | 6.94 | 0.25 | 90.0 | 130.0 | 51.5 | 1.5 | 52.7 | 3.6 | 51.5 | 1.8 |
| Output_1_83 | 2850 | 226 | 7.4 | 0.01 | 5.26 | 0.05 | 13.31 | 0.06 | 13.93 | 0.11 | 90.0 | 250.0 | 51.3 | 2.7 | 55.1 | 7.5 | 51.3 | 2.8 |
| Output_1_82 | 13900 | 1161 | 7.9 | 0.01 | 3.03 | 0.05 | 6.51 | 0.05 | 7.12 | 0.20 | 90.0 | 130.0 | 50.9 | 1.5 | 52.1 | 3.3 | 50.9 | 1.8 |
| Output_1_71 | 6540 | 847 | 11.6 | 0.01 | 3.75 | 0.05 | 10.78 | 0.05 | 8.98 | 0.16 | 90.0 | 200.0 | 49.7 | 1.8 | 50.7 | 4.5 | 49.7 | 2.1 |
| Output_1_90 | 9770 | 830 | 8.4 | 0.01 | 3.06 | 0.05 | 5.64 | 0.06 | 6.17 | 0.42 | 100.0 | 110.0 | 52.5 | 1.6 | 54.4 | 3.3 | 52.5 | 1.9 |
| Output_1_70 | 3570 | 422 | 6.6 | 0.01 | 5.25 | 0.05 | 17.23 | 0.06 | 15.51 | 0.40 | 110.0 | 320.0 | 56.3 | 2.9 | 55.2 | 8.4 | 56.3 | 3.1 |
| Output_1_72 | 12500 | 1505 | 6.0 | 0.01 | 2.12 | 0.05 | 5.82 | 0.05 | 6.31 | 0.15 | 110.0 | 110.0 | 51.5 | 1.1 | 53.2 | 3.3 | 51.5 | 1.5 |
| Output_1_102 | 5700 | 815 | 8.0 | 0.01 | 2.94 | 0.05 | 11.55 | 0.05 | 12.31 | 0.17 | 110.0 | 220.0 | 50.2 | 1.5 | 52.9 | 6.3 | 50.2 | 1.8 |
| Output_1_84 | 5910 | 494 | 5.8 | 0.01 | 3.73 | 0.05 | 10.32 | 0.05 | 10.85 | 0.33 | 110.0 | 210.0 | 49.9 | 1.8 | 51.0 | 5.4 | 49.9 | 2.1 |
| Output_1_60 | 3540 | 400 | 8.1 | 0.01 | 3.77 | 0.05 | 12.71 | 0.05 | 13.04 | 0.39 | 120.0 | 240.0 | 52.8 | 2.0 | 52.9 | 6.8 | 52.8 | 2.3 |
| Output_1_94 | 11520 | 1125 | 8.0 | 0.01 | 2.85 | 0.05 | 8.21 | 0.05 | 8.26 | 0.23 | 130.0 | 160.0 | 51.8 | 1.5 | 53.8 | 4.4 | 51.8 | 1.8 |
| Output_1_81 | 19000 | 1660 | 9.6 | 0.01 | 3.71 | 0.05 | 8.23 | 0.05 | 6.53 | 0.04 | 130.0 | 160.0 | 50.2 | 1.8 | 52.9 | 3.4 | 50.2 | 2.1 |
| Output_1_80 | 21900 | 1880 | 14.6 | 0.01 | 3.41 | 0.05 | 6.35 | 0.06 | 6.72 | 0.59 | 140.0 | 130.0 | 52.8 | 1.8 | 54.4 | 3.6 | 52.8 | 2.1 |
| Output_1_66 | 2210 | 286 | 7.4 | 0.01 | 6.46 | 0.05 | 21.57 | 0.05 | 22.22 | 0.36 | 130.0 | 370.0 | 48.7 | 3.1 | 53.0 | 11.0 | 48.7 | 3.3 |
| Output_1_99 | 2315 | 296 | 4.0 | 0.01 | 4.76 | 0.05 | 15.22 | 0.05 | 15.38 | 0.12 | 130.0 | 280.0 | 48.6 | 2.3 | 51.2 | 7.7 | 48.6 | 2.5 |
| Output_1_53 | 7750 | 1099 | 10.8 | 0.01 | 3.14 | 0.05 | 7.69 | 0.05 | 7.32 | 0.19 | 140.0 | 160.0 | 51.1 | 1.6 | 52.7 | 3.8 | 51.1 | 1.9 |
| Output_1_89 | 4230 | 338 | 8.1 | 0.01 | 4.18 | 0.05 | 10.64 | 0.06 | 11.47 | 0.46 | 150.0 | 200.0 | 53.7 | 2.3 | 58.8 | 6.7 | 53.7 | 2.5 |
| Output_1_88 | 10520 | 867 | 13.0 | 0.01 | 4.17 | 0.05 | 8.23 | 0.06 | 9.14 | 0.42 | 160.0 | 160.0 | 53.9 | 2.3 | 55.0 | 4.9 | 53.9 | 2.5 |
| Output_1_91 | 25100 | 2181 | 7.7 | 0.01 | 2.85 | 0.05 | 6.06 | 0.05 | 6.77 | 0.45 | 160.0 | 130.0 | 51.8 | 1.5 | 52.6 | 3.5 | 51.8 | 1.8 |
| Output_1_100 | 5820 | 658 | 5.9 | 0.01 | 4.37 | 0.05 | 8.35 | 0.06 | 11.56 | 0.35 | 190.0 | 160.0 | 55.8 | 2.5 | 57.9 | 6.5 | 55.8 | 2.7 |
| Output_1_86 | 29160 | 2306 | 13.8 | 0.01 | 2.93 | 0.05 | 6.22 | 0.06 | 5.40 | 0.13 | 180.0 | 130.0 | 52.6 | 1.5 | 54.9 | 2.9 | 52.6 | 1.9 |
| Output_1_64 | 6140 | 681 | 10.1 | 0.01 | 4.18 | 0.05 | 9.37 | 0.06 | 9.29 | 0.15 | 200.0 | 200.0 | 55.4 | 2.3 | 58.4 | 5.2 | 55.4 | 2.6 |
| Output_1_58 | 2270 | 272 | 12.9 | 0.01 | 4.60 | 0.05 | 14.29 | 0.06 | 14.53 | 0.15 | 200.0 | 260.0 | 51.6 | 2.4 | 56.7 | 8.1 | 51.6 | 2.6 |

| | | | | | | | | | | | | | | | | | | | |
|---|---|---|---|---|---|---|---|---|---|---|---|---|---|---|---|---|---|---|---|
| Output_1_69 | 4140 | 502 | 9.0 | 0.01 | 5.15 | 0.05 | 13.62 | 0.06 | 12.84 | 0.07 | 220.0 | 250.0 | 52.4 | 2.7 | 55.9 | 6.5 | 52.4 | 2.9 |
| Output_1_73 | 2550 | 302 | 9.1 | 0.01 | 4.02 | 0.05 | 14.11 | 0.06 | 13.51 | 0.01 | 220.0 | 280.0 | 51.2 | 2.0 | 54.6 | 7.3 | 51.2 | 2.3 |
| Output_1_52 | 4740 | 724 | 6.3 | 0.01 | 4.28 | 0.05 | 12.82 | 0.05 | 13.36 | 0.14 | 220.0 | 250.0 | 49.5 | 2.1 | 50.3 | 6.6 | 49.5 | 2.4 |
| Output_1_56 | 6260 | 812 | 5.9 | 0.01 | 5.13 | 0.05 | 11.29 | 0.06 | 11.03 | 0.15 | 240.0 | 230.0 | 53.8 | 2.8 | 55.4 | 6.0 | 53.8 | 3.0 |
| Output_1_59 | 3630 | 416 | 6.5 | 0.01 | 3.99 | 0.05 | 12.95 | 0.06 | 11.25 | 0.01 | 270.0 | 240.0 | 53.2 | 2.1 | 57.7 | 6.8 | 53.2 | 2.4 |
| Output_1_68 | 4090 | 524 | 8.2 | 0.01 | 4.36 | 0.05 | 18.87 | 0.06 | 20.69 | 0.02 | 320.0 | 380.0 | 51.6 | 2.2 | 60.0 | 12.0 | 51.6 | 2.5 |
| Output_1_79 | 3800 | 305 | 10.7 | 0.01 | 5.38 | 0.05 | 16.54 | 0.06 | 14.24 | 0.04 | 380.0 | 340.0 | 56.0 | 3.0 | 62.0 | 8.6 | 56.0 | 3.2 |
| Output_1_75 | 2460 | 262 | 7.0 | 0.01 | 5.75 | 0.06 | 15.63 | 0.06 | 14.00 | 0.01 | 410.0 | 320.0 | 52.5 | 3.0 | 59.0 | 8.1 | 52.5 | 3.2 |

# Supplemental Information S3: $^{40}Ar/^{39}Ar$ data

**12JB12HODO Biotite**

Weighted average of J from standards = 1.151e-04 +/- 5.842e-07

| Laser Power | Cumulative | 40Ar/ 39Ar | +/- | 37Ar/ 39Ar | +/- | 36Ar/ 39Ar | +/- | % Atm. | +/- | Ca/K | +/- | Cl/K | +/- | 40*/ 39K | +/- | Age | +/- |
|---|---|---|---|---|---|---|---|---|---|---|---|---|---|---|---|---|---|
| (mW) | 39Ar | meas. | | meas. | | meas. | | 40Ar | | | | | | | | (Ma) | (Ma) |
| 500 | 0.0018 | 549.57 | 38.18 | 0.425 | 0.178 | 1.302 | 0.130 | 70.023 | 5.099 | 0.781 | 0.326 | 0.030 | 0.014 | 164.784 | 30.463 | 33.85 | 6.2 |
| 1000 | 0.0087 | 440.52 | 13.45 | 0.339 | 0.084 | 0.748 | 0.041 | 50.172 | 2.330 | 0.622 | 0.154 | 0.016 | 0.004 | 219.542 | 12.436 | 44.96 | 2.52 |
| 1500 | 0.017 | 332.24 | 6.08 | 0.160 | 0.044 | 0.276 | 0.022 | 24.528 | 1.952 | 0.294 | 0.080 | 0.016 | 0.004 | 250.755 | 8.015 | 51.26 | 1.62 |
| 2000 | 0.0285 | 320.07 | 4.54 | 0.095 | 0.025 | 0.220 | 0.019 | 20.356 | 1.786 | 0.175 | 0.045 | 0.018 | 0.002 | 254.908 | 6.861 | 52.1 | 1.38 |
| 2500 | 0.0487 | 320.54 | 4.49 | 0.132 | 0.017 | 0.211 | 0.013 | 19.458 | 1.226 | 0.242 | 0.032 | 0.021 | 0.001 | 258.165 | 5.550 | 52.76 | 1.12 |
| 3000 | 0.0822 | 289.46 | 3.78 | 0.076 | 0.008 | 0.076 | 0.007 | 7.769 | 0.718 | 0.140 | 0.015 | 0.020 | 0.001 | 266.954 | 4.183 | 54.52 | 0.84 |
| 3500 | 0.1449 | 272.89 | 3.57 | 0.061 | 0.007 | 0.032 | 0.003 | 3.472 | 0.283 | 0.111 | 0.013 | 0.021 | 0.001 | 263.394 | 3.621 | 53.81 | 0.73 |
| 4000 | 0.2366 | 265.26 | 2.64 | 0.069 | 0.008 | 0.020 | 0.002 | 2.202 | 0.260 | 0.127 | 0.014 | 0.020 | 0.000 | 259.398 | 2.678 | 53 | 0.54 |
| 4500 | 0.3557 | 259.37 | 2.16 | 0.068 | 0.004 | 0.018 | 0.002 | 1.992 | 0.247 | 0.125 | 0.008 | 0.020 | 0.000 | 254.184 | 2.218 | 51.95 | 0.45 |
| 5000 | 0.6084 | 258.53 | 2.15 | 0.066 | 0.003 | 0.010 | 0.001 | 1.087 | 0.097 | 0.122 | 0.006 | 0.020 | 0.000 | 255.704 | 2.148 | 52.26 | 0.43 |
| 6000 | 0.9274 | 257.35 | 2.46 | 0.078 | 0.003 | 0.009 | 0.001 | 1.072 | 0.109 | 0.142 | 0.005 | 0.020 | 0.000 | 254.571 | 2.448 | 52.03 | 0.49 |
| 9000 | 1 | 256.30 | 2.97 | 0.113 | 0.006 | 0.018 | 0.003 | 2.085 | 0.290 | 0.208 | 0.011 | 0.020 | 0.000 | 250.947 | 3.047 | 51.3 | 0.61 |
| Integrated | | 264.99 | 1.10 | 0.079 | 0.002 | 0.032 | 0.001 | 3.538 | 0.087 | 0.144 | 0.003 | 0.020 | 0.000 | 255.601 | 1.092 | 52.24 | 0.34 |

**46GUNN Whole rock**

Weighted average of J from standards = 4.044e-03 +/- 1.101e-05

| Laser Power | Cumulative | 40Ar/39Ar | +/- | 37Ar/39Ar | +/- | 36Ar/39Ar | +/- | % Atm. | +/- | Ca/K | +/- | Cl/K | +/- | 40*/39K | +/- | Age | +/- |
|---|---|---|---|---|---|---|---|---|---|---|---|---|---|---|---|---|---|
| (mW) | 39Ar | meas. | | meas. | | meas. | | 40Ar | | | | | | | | (Ma) | (Ma) |
| 500 | 0.0088 | 7.71 | 0.04 | 0.117 | 0.002 | 0.016 | 0.001 | 59.963 | 3.474 | 0.216 | 0.003 | 0.002 | 0.000 | 3.077 | 0.268 | 22.28 | 1.93 |
| 1000 | 0.0422 | 7.24 | 0.02 | 0.051 | 0.001 | 0.006 | 0.000 | 24.201 | 0.719 | 0.094 | 0.001 | 0.001 | 0.000 | 5.466 | 0.054 | 39.4 | 0.39 |
| 1500 | 0.1089 | 6.80 | 0.02 | 0.026 | 0.000 | 0.002 | 0.000 | 10.210 | 0.361 | 0.048 | 0.001 | 0.000 | 0.000 | 6.083 | 0.030 | 43.79 | 0.22 |
| 2000 | 0.1962 | 6.78 | 0.02 | 0.060 | 0.000 | 0.002 | 0.000 | 7.705 | 0.287 | 0.109 | 0.001 | 0.000 | 0.000 | 6.234 | 0.028 | 44.87 | 0.2 |
| 2500 | 0.2805 | 6.64 | 0.02 | 0.166 | 0.001 | 0.001 | 0.000 | 5.120 | 0.377 | 0.305 | 0.002 | 0.000 | 0.000 | 6.271 | 0.033 | 45.13 | 0.24 |
| 3000 | 0.4158 | 6.56 | 0.01 | 0.148 | 0.001 | 0.001 | 0.000 | 3.156 | 0.227 | 0.272 | 0.001 | 0.000 | 0.000 | 6.322 | 0.021 | 45.49 | 0.15 |
| 4000 | 0.6934 | 6.45 | 0.01 | 0.013 | 0.000 | 0.000 | 0.000 | 1.297 | 0.102 | 0.024 | 0.000 | 0.000 | 0.000 | 6.334 | 0.014 | 45.57 | 0.1 |
| 9000 | 1 | 6.51 | 0.01 | 0.013 | 0.000 | 0.000 | 0.000 | 1.102 | 0.097 | 0.025 | 0.000 | 0.000 | 0.000 | 6.409 | 0.015 | 46.11 | 0.1 |
| Integrated | | 6.59 | 0.01 | 0.052 | 0.000 | 0.001 | 0.000 | 4.451 | 0.083 | 0.095 | 0.000 | 0.000 | 0.000 | 6.267 | 0.008 | 45.1 | 0.13 |

**15BG209 Whole rock**

Weighted average of J from standards = 4.044e-03 +/- 1.101e-05

| Laser Power | Cumulative | 40Ar/39Ar | +/- | 37Ar/39Ar | +/- | 36Ar/39Ar | +/- | % Atm. | +/- | Ca/K | +/- | Cl/K | +/- | 40*/39K | +/- | Age | +/- |
|---|---|---|---|---|---|---|---|---|---|---|---|---|---|---|---|---|---|
| (mW) | 39Ar | meas. | | meas. | | meas. | | 40Ar | | | | | | | | (Ma) | (Ma) |
| 500 | 0.0098 | 9.43 | 0.05 | 0.040 | 0.002 | 0.026 | 0.001 | 80.305 | 3.436 | 0.073 | 0.004 | 0.004 | 0.000 | 1.852 | 0.323 | 13.45 | 2.34 |
| 1000 | 0.0422 | 8.34 | 0.03 | 0.040 | 0.001 | 0.008 | 0.000 | 28.529 | 1.073 | 0.073 | 0.001 | 0.002 | 0.000 | 5.941 | 0.093 | 42.78 | 0.67 |
| 1500 | 0.0982 | 8.58 | 0.02 | 0.035 | 0.000 | 0.004 | 0.000 | 13.974 | 0.818 | 0.065 | 0.001 | 0.002 | 0.000 | 7.353 | 0.073 | 52.8 | 0.52 |
| 2000 | 0.1679 | 8.28 | 0.03 | 0.039 | 0.001 | 0.003 | 0.000 | 11.043 | 0.513 | 0.072 | 0.001 | 0.001 | 0.000 | 7.339 | 0.049 | 52.7 | 0.35 |
| 2500 | 0.2839 | 7.67 | 0.02 | 0.065 | 0.000 | 0.002 | 0.000 | 7.313 | 0.346 | 0.119 | 0.001 | 0.001 | 0.000 | 7.083 | 0.034 | 50.89 | 0.24 |
| 3000 | 0.4007 | 7.37 | 0.02 | 0.091 | 0.000 | 0.001 | 0.000 | 4.790 | 0.421 | 0.166 | 0.001 | 0.001 | 0.000 | 6.988 | 0.038 | 50.22 | 0.27 |
| 4000 | 0.7923 | 7.13 | 0.01 | 0.075 | 0.000 | 0.001 | 0.000 | 2.589 | 0.147 | 0.138 | 0.000 | 0.000 | 0.000 | 6.915 | 0.017 | 49.7 | 0.12 |
| 9000 | 1 | 7.09 | 0.01 | 0.054 | 0.000 | 0.001 | 0.000 | 3.509 | 0.242 | 0.100 | 0.001 | 0.001 | 0.000 | 6.811 | 0.021 | 48.96 | 0.15 |
| Integrated | | 7.43 | 0.01 | 0.065 | 0.000 | 0.002 | 0.000 | 6.896 | 0.131 | 0.120 | 0.000 | 0.001 | 0.000 | 6.894 | 0.012 | 49.55 | 0.16 |

**15BG216 Whole rock**

Weighted average of J from standards = 4.044e-03 +/- 1.101e-05

| Laser Power | Cumulative | 40Ar/39Ar | +/- | 37Ar/39Ar | +/- | 36Ar/39Ar | +/- | % Atm. | +/- | Ca/K | +/- | Cl/K | +/- | 40*/39K | +/- | Age | +/- |
|---|---|---|---|---|---|---|---|---|---|---|---|---|---|---|---|---|---|
| (mW) | 39Ar | meas. | | meas. | | meas. | | 40Ar | | | | | | | | (Ma) | (Ma) |
| 500 | 0.0603 | 33.55 | 0.19 | 0.260 | 0.003 | 0.094 | 0.002 | 83.136 | 1.546 | 0.476 | 0.006 | 0.009 | 0.000 | 5.654 | 0.521 | 40.74 | 3.71 |
| 1000 | 0.1711 | 11.36 | 0.04 | 0.232 | 0.002 | 0.016 | 0.001 | 41.710 | 1.751 | 0.426 | 0.003 | 0.001 | 0.000 | 6.605 | 0.201 | 47.5 | 1.42 |
| 1500 | 0.276 | 11.42 | 0.05 | 0.311 | 0.002 | 0.015 | 0.001 | 37.934 | 1.536 | 0.570 | 0.004 | 0.000 | 0.000 | 7.071 | 0.179 | 50.8 | 1.27 |
| 2000 | 0.4507 | 9.93 | 0.04 | 0.335 | 0.002 | 0.009 | 0.000 | 27.811 | 1.273 | 0.615 | 0.004 | 0.000 | 0.000 | 7.148 | 0.130 | 51.35 | 0.92 |
| 2500 | 0.5161 | 8.90 | 0.04 | 0.362 | 0.002 | 0.006 | 0.001 | 20.018 | 2.022 | 0.664 | 0.004 | 0.001 | 0.000 | 7.100 | 0.183 | 51.01 | 1.29 |
| 3000 | 0.6069 | 7.75 | 0.03 | 0.387 | 0.002 | 0.003 | 0.001 | 11.801 | 2.085 | 0.709 | 0.004 | 0.000 | 0.000 | 6.814 | 0.164 | 48.98 | 1.16 |
| 4000 | 0.9577 | 7.47 | 0.03 | 0.574 | 0.003 | 0.003 | 0.000 | 9.610 | 0.477 | 1.054 | 0.005 | 0.000 | 0.000 | 6.727 | 0.043 | 48.36 | 0.3 |
| 9000 | 1 | 6.78 | 0.05 | 0.923 | 0.009 | 0.000 | 0.001 | 0.493 | 4.600 | 1.695 | 0.016 | 0.001 | 0.000 | 6.726 | 0.314 | 48.36 | 2.23 |
| Integrated | | 10.41 | 0.02 | 0.432 | 0.001 | 0.012 | 0.000 | 34.587 | 0.524 | 0.792 | 0.002 | 0.001 | 0.000 | 6.790 | 0.056 | 48.82 | 0.42 |

# Supplemental Information S4: U-Pb age plots

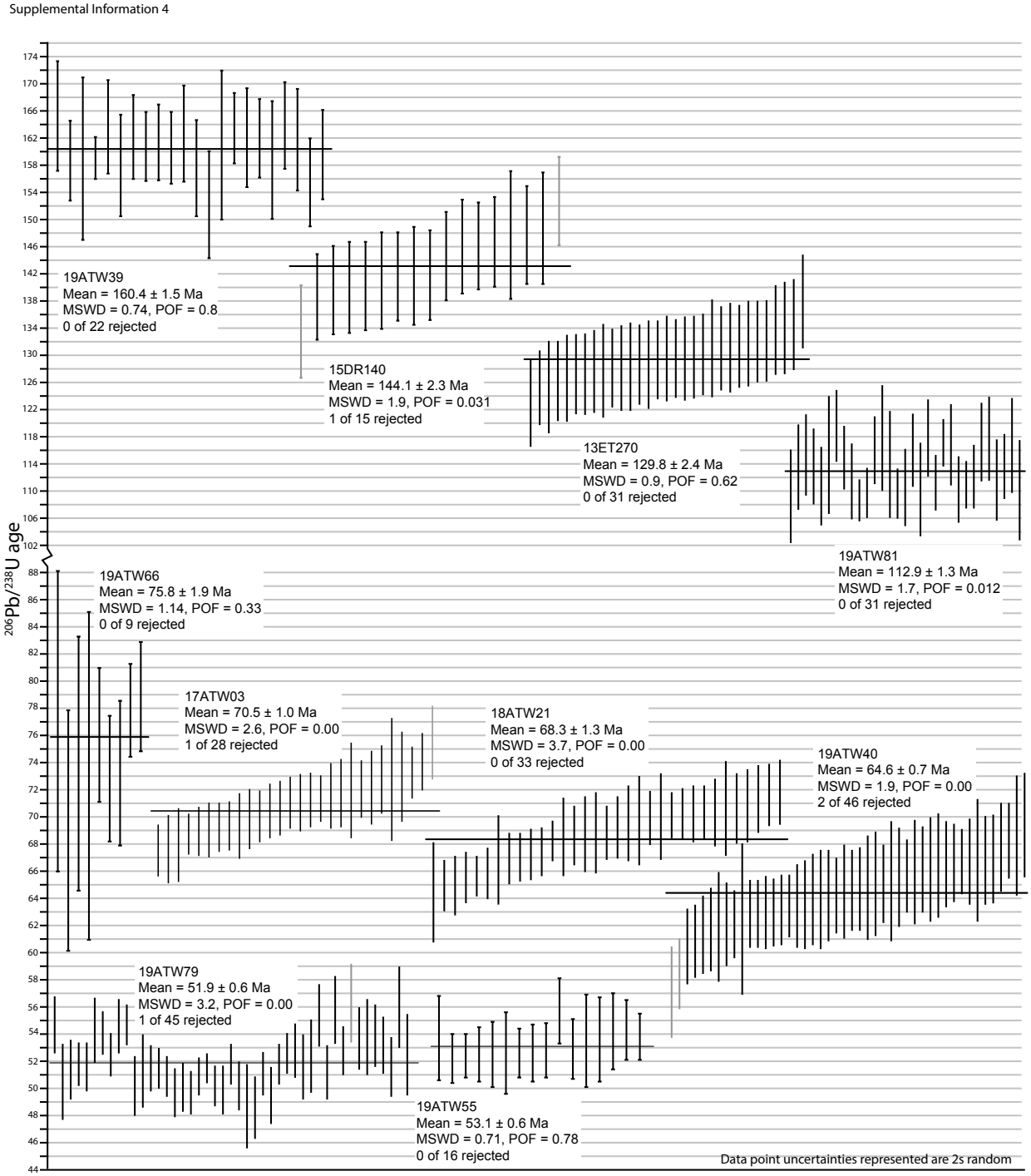


Supplemental Figure 4.1: Weighted mean U-Pb plots of Cenozoic and Mesozoic igneous zircon samples. Weighted mean ages are interpreted as crystalization ages. The horizontal line represented the weighted mean age. Black bars are used in age claculation and grey bars were rejected by Isoplot. MSWD: Mean Square Weighted Deviation; POF: Probability of Fit. Rejected analyses met our filtering criteria, but were rejected by Isoplot.

Supplemental Information 4

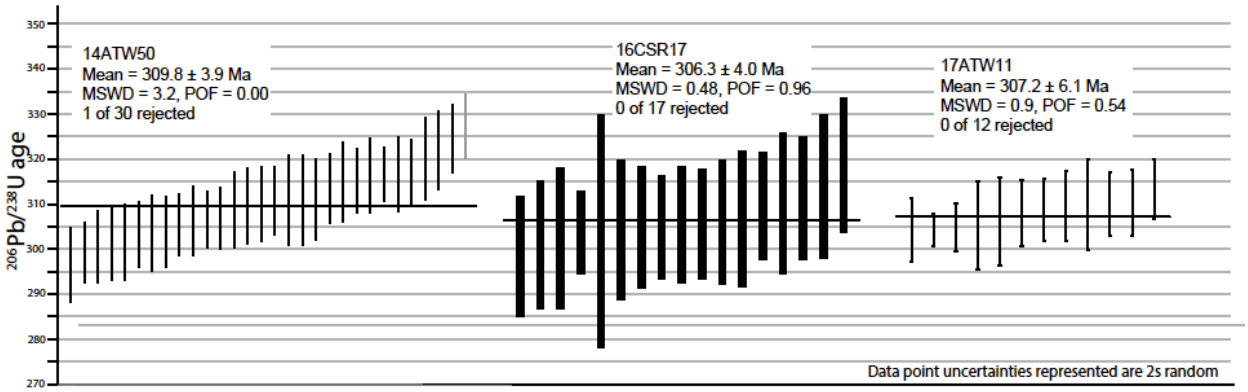


Supplemental Figure 4.2: Weighted mean U-Pb plots of Paleozoic igneous zircon samples. Weighted mean ages are interpreted as crystalization ages. The horizontal line represented the weighted mean age. Black bars are used in age claculation and grey bars were rejected by Isoplot. MSWD: Mean Square Weighted Deviation; POF: Probability of Fit. Rejected analyses met our filtering criteria, but were rejected by Isoplot.

Supplemental Information 4

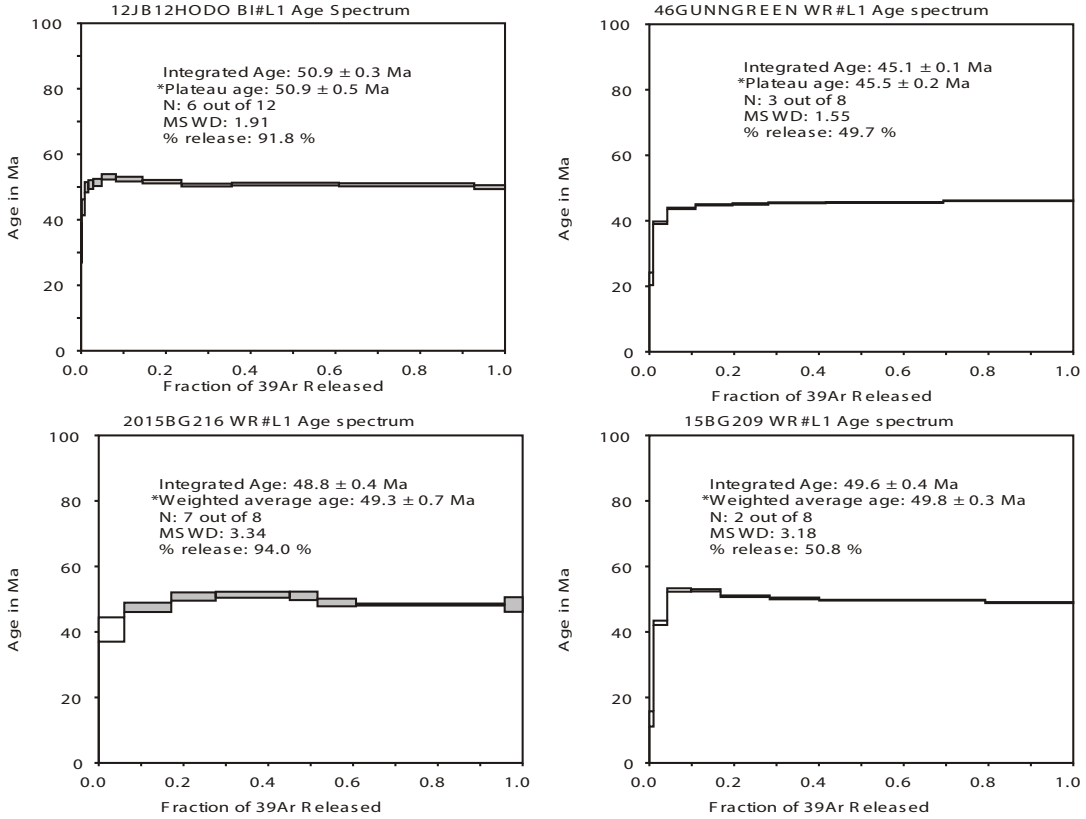


Supplemental Figure 4.3: $^{40}Ar/^{39}Ar$ age spectra. Prefered ages aare indicated with an asterisk*. Only filled steps are used to calculate plateau or weighted mean ages. MSWD: Mean Square Weighted Deviation. N= number of steps used in age calculation.

# Ch. 3: The role of upper plate strike-slip faults during long-lived oblique flat slab subduction, southern Alaska

**T. S. Waldien[1], R. O. Lease[2], S. M. Roeske[1], J. A. Benowitz[3], P.B. O'Sullivan[4]**

*[1]Department of Earth and Planetary Sciences, University of California, Davis, 1 Shields Ave. Davis, California 95616, USA*

*[2] U.S. Geological Survey, Alaska Science Center, 4210 University Drive, Anchorage, AK 99508*

*[3]Geophysical Institute, University of Alaska, Fairbanks, 900 Yukon Drive Fairbanks, Alaska 99775, USA*

*[4]GeoSep Services, 1521 Pine Cone Road, Moscow, ID 83843*

**ABSTRACT**

Upper plates of subduction zones commonly respond to flat slab subduction by structural reactivation, magmatic arc disruption, and foreland basin inversion. However, the role of pre-existing strike-slip faults in focusing deformation and magmatism in response to oblique flat slab subduction remains less clear. Here we present new detrital apatite fission-track (dAFT) ages from twelve modern catchments in the eastern Alaska Range, Alaska, USA, to reveal how the dextral Denali fault system has facilitated bedrock exhumation and topographic growth during ca. 30 Ma-to-Present oblique flat slab subduction of the Yakutat oceanic plateau. Additionally, a 940 ka ($^{40}Ar/^{39}Ar$ whole rock) basalt flow is spatially associated with Cenozoic structures and provides the first evidence for Quaternary volcanism along the southern flank of the eastern Alaska Range. We integrate our new data with other thermochronologic, geochronologic, and regional geologic datasets to show that: 1) most high topography regions in southern Alaska have undergone rapid bedrock cooling and exhumation since ca. 30 Ma, 2) elevated topography and young cooling are spatially associated with long-lived active strike-slip fault systems, 3) topographic growth associated with strike-slip fault systems led to local inversion and compartmentalization of a previously interconnected foreland basin system, 4) the onset of oblique flat slab subduction is coeval with a southward shift in arc magmatism from one region of active strike-slip faulting to another above the edge of the flat slab, and 5) Quaternary volcanism marks the revival of magmatism in the eastern Alaska Range above the geophysically-imaged northeastern edge of the flat slab. Our analysis of the post-30 Ma geologic evolution of southern Alaska demonstrates that strike-slip fault systems that were active at the time of slab flattening evolved into transpression zones that focused bedrock cooling, rock exhumation, and topographic growth.

## INTRODUCTION

Active deformation at plate boundaries involving continental lithosphere commonly deviates from plate-like behavior (e.g. Freymueller, 2010; Kreemer et al., 2014). Spatially distributed deformation is clearly evident in flat slab subduction environments where increased coupling along the plate boundary interface associated with slab flattening can drive widespread upper plate deformation hundreds of kilometers inboard of the trench (e.g. Ramos and Folguera, 2009). Distributed fault reactivation, basin inversion, and inboard migration of the magmatic arc are considered hallmarks of upper plate tectonic evolution in both modern flat slab regions of South America (Ramos et al., 2002) and inferred ancient flat slab regions of North America (Saleeby, 2003). The down-dip extent of increased plate boundary coupling (Espurt et al., 2008) and locations of inherited major crustal structures (Marshak et al., 2000) are thought to primarily control the degree to which upper plate shortening is localized or distributed. Minor strike-slip structures have been shown to form perpendicular to the plate boundary as part of the upper plate shortening regime in response to the subduction of buoyant crust (e.g. Gardner et al. 2013). However, the role of pervasive, large-magnitude strike-slip faulting in oblique flat slab environments has received relatively little attention to date. Here we investigate how pre-existing continental strike-slip fault systems influence the distribution of upper plate deformation and magmatism in the long-lived oblique flat slab subduction setting of southern Alaska.

### Crustal deformation during oblique flat slab subduction in southern Alaska

Subduction of the Yakutat oceanic plateau (Plafker, 1987; Christeson et al., 2010) beneath southern Alaska is a long-lived, and still active, example of a flat slab environment wherein the upper plate is dissected by numerous crustal scale pre-existing strike-slip faults (Finzel et al.,

2011a; Allam et al., 2017; Ziwu et al., 2020). Flat slab subduction is inferred to have begun by ca. 30 Ma based on modification of the upper plate thermal structure, migration of arc magmatism, and topographic growth at that time (Enkelmann et al., 2008; 2010; Benowitz et al., 2014; Trop et al., 2019; Brueseke et al., 2019). Long lived and still active upper plate dextral strike-slip faults in southern Alaska include the Denali, Castle Mountain-Lake Clark, eastern Contact, Totschunda, and Fairweather fault systems (Figure 1) (e.g. Wyld et al., 2006).

Geophysical models of southern Alaska deformation yield variable importance of strike-slip fault systems in regional deformation above the flat slab. Despite generally sparse coverage of GPS stations in southern Alaska (e.g. Freymueller et al., 2008), the geodetic velocity field and distribution of crustal seismicity together highlight the strike-slip fault systems as zones of focused deformation (Ruppert, 2008). Inverse numerical simulations of the geodetic velocity field suggest a somewhat different view wherein the strike-slip fault systems occupy high strain rate zones embedded into regionally diffuse deformation above the flat slab (Finzel et al., 2011b). Alternatively, forward geodynamic modeling favors high coupling between the subducted flat slab and base of the upper plate, which would act to increase the strength of the upper plate by refrigeration and mechanical thickening (Jadamec et al., 2013). In the forward simulations, lateral rheological contrasts in the upper plate (e.g. lithospheric scale strike-slip faults) are crucial for focusing upper plate deformation (e.g. Haynie and Jadamec, 2017). More recent block-modeling of geodetic data suggests an intermediate scenario wherein the size of the blocks, and thus the localization of regional deformation, increases with distance from the plate boundary (Elliott and Freymueller, 2020). A potential implication of the block modeling is that the importance of pre-existing strike-slip fault systems increases with distance from the plate boundary fault system.

In this contribution, we assess the role of pre-existing upper plate strike-slip faults in the oblique flat slab environment of southern Alaska by evaluating regional exhumation patterns through the lens of detrital thermochronology. Studies using detrital mineral chronometers from modern sediment and Neogene-Quaternary stratigraphic sections have proven foundational for understanding long-term patterns of bedrock cooling, erosion, and magmatism in largely inaccessible regions of southern Alaska (e.g. Enkelmann et al., 2009; 2019). Detrital thermochronology data are particularly well suited to capture regional exhumation responses to changes in plate boundary forcing due to the spatial-temporal sensitivity of the technique to tectonic events affecting broad regions (e.g. Carrapa et al., 2019). We present modern river detrital apatite fission-track (dAFT) data from twelve catchments in the eastern Alaska Range (yellow circles in figure 1). We compare the new dAFT data to published dAFT and detrital zircon fission-track (dZFT) datasets sampled from modern catchments in other mountainous regions across southern Alaska (red, blue, and white circles in figure 1) to evaluate if deformation is diffuse across the upper plate of the flat slab region or primarily focused along pre-existing strike-slip fault systems. Additionally, we present the first field observations and $^{40}Ar/^{39}Ar$ date documenting a newly recognized Quaternary volcanic field in the eastern Alaska Range. Our integration of new and published data reveal loci of Oligocene to Neogene upper plate deformation and topographic growth, which inform a comprehensive model describing the tectono-magmatic response to oblique flat slab subduction of the Yakutat oceanic plateau beneath southern Alaska.

## REGIONAL GEOLOGY OF SOUTHERN ALASKA:

Much of the geology of the northern North American Cordillera formed by accretion of allochthonous terranes during the Mesozoic (Nelson and Colpron, 2007). From north to south,

important tectonostratigraphic terranes in southern Alaska include peri-continental North American metamorphic rocks north of the Denali fault, the Wrangellia composite island arc terrane south of the Denali fault, and the Chugach accretionary complex south of the Border Ranges fault system (Figure 1B). The boundaries between these terranes are in most places occupied by dextral strike-slip faults that are interpreted to penetrate the lithosphere based on receiver function seismology (e.g. O'Driscoll and Miller, 2015; Miller et al., 2018) and seismic anisotropy studies (e.g. Rasendra et al., 2014; Audet et al., 2016; Estéve et al., 2020). The Denali fault system juxtaposes the accreted Wrangellia arc terrane in the south against continental North American-affinity terranes to the north. A region underlain by imbricated Mesozoic marginal marine basin strata, plutonic rocks, oceanic fragments, and disparate continental terranes known as the Alaska Range suture zone (Ridgway et al., 2002) is intersected by the Denali fault and appears to focus post-suturing deformation (Fitzgerald et al., 2014), which has facilitated rapid Neogene exhumation of the Alaska Range (Benowitz et al., 2011, 2019; Lease et al., 2016). South of the Wrangellia terrane, the Chugach accretionary complex represents the forearc to Mesozoic arcs that were built upon the Wrangellia composite terrane, although the accretionary complex has been translated hundreds of kilometers from the associated arc rocks by dextral slip along the Border Ranges fault system (e.g. Roeske et al., 2003; Garver and Davidson, 2015). Oligocene to present exhumation of the accretionary complex is largely associated with underplating of the Yakutat slab and is mainly focused along the Contact fault system in the western Chugach Range and the Bagley Fault in the eastern Chugach Range (Bruhn et al., 2012; Arkle et al., 2013).

## METHODS

### Apatite fission-track thermochronology

New dAFT data reveal the ≤110ºC (Green et al., 1986) cooling history of twelve catchments spanning 330 km of the eastern Alaska Range (Figure 2). Samples comprise several sub-samples of medium-coarse sand collected from gravel bars along a 10-100 m river length to ensure a representative, well-mixed sample. In 2019, sample collection involved heavy mineral concentration in the field using a miner's gold pan and further concentration at UC Davis using standard magnetic and density techniques. Apatite concentration from samples collected prior to 2019 took place at GeoSeps Services using standard magnetic and density separation techniques. Fission-track dating at GeoSeps Services involved counting spontaneous fission tracks on 70-110 grains per sample and parent isotope ratio measurement using the laser ablation inductively coupled plasma mass spectrometer (LA-ICP-MS) method (Donelick et al., 2005) at Washington State University (detailed methods in DR1 and data in DR2). We filtered the dAFT data and rejected analyzed grains if they exhibited a Uranium concentration less than 0.5 ppm and an AFT age that is not within uncertainty of the oldest known bedrock crystallization age in the catchment (<2% of the total dataset). We deconvolved the dAFT datasets into constituent age populations for each catchment (Figure 2; Table 1) using the mixture modeling methods of Galbraith and Green (1990) and Galbraith (2005) as implemented in DensityPlotter v. 8.4 (Vermeesch, 2012).

We compared the new and existing modern river dAFT and dZFT datasets from across southern Alaska based on the abundance and proportions of constituent age populations in different regions (Figure 3). We compiled the resolved age components for each detrital fission-track sample analyzed within a region and generated probability density plots of the age population data for each region. Because the age population plots do not account for the proportion of dated grains

that constitute each age population, we augment the probability density plots with pie charts that show the data binned into regionally important time intervals (<4, 4-30, and >30 Ma) and weighted by the proportion of dated grains in those time bins.

### $^{40}Ar/^{39}Ar$ geochronology

$^{40}Ar/^{39}Ar$ analysis performed on one basalt sample at the Geochronology laboratory at the University of Alaska, Fairbanks involved crushing the sample, sieving for the 500-1000 um fraction, washing dust from the fraction, and hand-picking for a pure phase of phenocryst-free groundmass. Monitoring of the neutron flux and calculation of the irradiation parameter (J) were based on the monitor mineral TCR-2 with an age of 28.619 Ma (Renne et al, 2010). See DR3 for detailed $^{40}Ar/^{39}Ar$ methods and data.

## RESULTS: NEW AND COMPILED DATA

### New Detrital fission-track data

Individual catchments in the eastern Alaska Range predominantly yield AFT age populations of ca. 8-15 Ma, 20-30 Ma, and 50-65 Ma (Figure 2; Table 1). The middle and west forks of the Maclaren River contain small (~5%) populations centered at ca. 1.6-1.9 Ma, and several catchments also yield older (>90 Ma) age populations.

The combined dAFT dataset (n=1210 single-grain dates) for catchments in the eastern Alaska Range presented herein records widespread Cenozoic cooling (Figure 3A). Of the dated grains, ~69% document cooling between 4-30 Ma and resolved age populations are present at ca. 8-12 Ma and 22-28 Ma. Approximately 30% of the grains record cooling between 30-197 Ma, and the remaining ~1% record cooling since 4 Ma.

**Compiled Detrital fission-track data**

Modern river detrital fission-track data from the western and central Alaska Range compiled here from Lease et al. (2016) and Enkelmann et al. (2019) display multiple phases of Cenozoic cooling (Figure 3B). The combined dAFT dataset predominantly records cooling from 4-30 Ma, wherein ~46% of the dated grains fall into age populations at ca. 20-25 Ma and 6-10 Ma. Approximately 17% of the dated apatite grains record cooling younger than 4 Ma, which is linked to enhanced glacial erosion in the mid-late Pliocene (Benowitz et al, 2011; Lease, 2018). Detrital zircon fission-track data from the same catchments do not contain age populations younger than 4 Ma, yet ~37% of the dZFT cooling ages form an age population at ca. 15-30 Ma. Both the combined dAFT and dZFT datasets record significant (dAFT~37% and dZFT~63%) bedrock cooling older than 30 Ma, which can be correlated with regional magmatic/thermal events (Lease et al., 2016; Terhune et al., 2019; Regan et al., 2020).

Modern river and pro-glacial dZFT data from the northern Chugach Mountains (Arkle et al., 2013) and southern Talkeetna Mountains (Enkelmann et al., 2019) display a spectrum of mid-Cenozoic cooling ages (Figure 3C). The majority (~82%) of the dated grains record cooling at ca. 45 Ma and 65 Ma, which can be correlated to magmatic/thermal events at those times (Terhune et al., 2019). Post-30 Ma cooling is recorded in the remaining ~37% of the dated grains, which primarily compose a ca. 22-29 Ma age population.

Modern river detrital fission-track data from catchments draining the northern flank of the St. Elias Mountains published by Enkelmann et al. (2008, 2015) and Falkowski and Enkelmann (2016) record cooling that spans the Cretaceous and Cenozoic (Figure 3D). The majority (~53% dAFT and ~80% dZFT) of the dated grains record bedrock cooling older than 30 Ma, which is interpreted to reflect cooling during terrane accretion and multiple pulses of regional magmatism

(Falkowski and Enkelmann 2016). Cooling from 4-30 Ma is recorded by ~39% of the compiled dAFT data and ~20% of the dZFT data and likely records development of the St. Elias orogen in response to flat slab subduction of the Yakutat slab. Cooling younger than 4 Ma is mainly recorded in the dAFT data (8% of the dated grains) and likely records enhanced glacial erosion in the region of Mt. Logan (Enkelmann et al., 2009).

Modern river and proglacial detrital fission-track data from catchments draining the southern flank of the St. Elias Range compiled by Enkelmann et al. (2015) record profound late Cenozoic cooling in the upper plate proximal to the Yakutat collision zone (Figure 3E). The comparable proportions of <4 Ma (46%) and 4-30 Ma (45%) grains in the compiled dAFT data indicate that enhanced glacial erosion and tectonically driven exhumation work in tandem to generate the high relief of the St. Elias Mountains (e.g. Enkelmann et al., 2008, 2009, 2010; Berger and Spotila, 2008; Gulick et al., 2015). The remaining ~9% of dAFT grains fall into a distributed age range as old as ca. 128 Ma. Detrital ZFT data from the same catchments predominantly record cooling older than 30 Ma (65% of the dated grains), yet those grains largely do not cluster into discrete age populations. Younger, discrete dZFT age populations are present at ca. 25 Ma, 18 Ma, and younger than 10 Ma, which together comprise ~23% of the analyzed grains. Cooling younger than 4 Ma is recorded by ~12% of the dated zircon grains, which suggests that the combined tectonic forcing and glacial erosion was locally significant enough to exhume rocks from below the ZFT closure temperature (~240ºC- Bernet, [2009]) since 4 Ma.

**Quaternary volcanism in the eastern Alaska Range**

We present the first description of Quaternary volcanic rocks along the south flank of the eastern Alaska Range. Stout (1976) mapped isolated exposures of “Tertiary basalt flows” that

unconformably overlie older structures in the area. Based on the recent recognition that many of the structures beneath the basalt flows have post-Oligocene slip (Waldien et al., 2021; Twelker et al., 2020), the field relationships alone suggest that the basalt flows are Neogene or younger. We dated one outcrop of olivine basalt near the southern flank of the Alaska Range (red star on figure 1), which yielded an $^{40}Ar/^{39}Ar$ whole rock plateau age of 940.4 ± 27.1 ka (Figure 4A). In addition to the dated locale, our reconnaissance fieldwork has revealed additional outcrops of similar, potentially younger lavas wherein delicate flow features and rock types including brecciated flow tops and scoria are locally preserved. Owing to their low preservation potential, the presence of scoria, cinder, and volcanic landforms implies that portions of the newly documented volcanic field along the southern flank of the Alaska Range may be younger than the regional Pleistocene glaciations (e.g. Kaufman et al., 2011). Table 2 and figure 4 contain locations and photos of features in the Quaternary volcanic field.

## DISCUSSION

### Regional integration of thermochronology datasets

The new dAFT data from the eastern Alaska Range augment existing bedrock and detrital thermochronology datasets from southern Alaska indicating a major shift in the regional tectonic framework at ca. 30 Ma (Benowitz et al., 2011, 2014, 2019; Riccio et al., 2014; Lease et al., 2016; Waldien et al., 2021). Assessing the dAFT data from the entire Alaska Range reveals that >60% of detrital apatite grains record cooling since 30 Ma and tectonic-related cooling in that timeframe may be further split into populations at ca. 28, 20-22, and 8-12 Ma (Figure 3A-B). Quaternary cooling ages in the eastern Alaska Range dataset are ca. 1.5 Myr younger than cooling attributed to enhanced glacial erosion in the central-western Alaska Range (Figures 2 and 3A-B) and are

limited to two catchments that contain relatively unweathered basalt clasts near our newly identified Quaternary volcanic province (Figure 1). On the basis of the above observations, we attribute the Quaternary AFT dates in the eastern Alaska Range to reflect volcanic provenance, annealing of apatite fission tracks from interaction with volcanic fluids, and/or the thermal effects associated with the newly identified Quaternary volcanism in the region.

Detrital ZFT data from the western and central Alaska Range mimic the cooling pattern shown by the dAFT data from that region with the addition of relatively persistent cooling throughout the Miocene (Figure 3B). Post-30 Ma events in the Alaska Range that may have facilitated cooling include: exhumation related to thrust reactivation of terrane accretionary structures (Waldien et al., 2021), waning magmatism along the Denali fault (Trop et al., 2019; Regan et al., 2019), and rock uplift focused within restraining bends along the Denali fault (Fitzgerald et al., 1995; Benowitz et al., 2011, 2014: Burkett et al., 2016; Lease et al., 2016). Heterogeneity in the major cooling age populations among catchments (Figures 2 and 3; Table 1) suggests that cooling, exhumation, and related topographic growth in the Alaska Range was likely not uniform across the entire range. Instead, variation in the location, rate, and episodicity of rock uplift/exhumation are more probable (e.g. Bill et al., 2018; Otiniano et al., 2020), and may be related to a spatially variable structural and kinematic evolution of the Denali fault system (cf. Fitzgerald et al., 1995; Benowitz et al., 2014; Riccio et al., 2014; Waldien et al., 2018).

Both bedrock and detrital thermochronology datasets display abundant post-30 Ma cooling and exhumation in mountainous regions across southern Alaska (Figures 3 and 5). The dZFT data compiled herein indicate that most high-elevation regions of southern Alaska have, at least locally, experienced bedrock exhumation from depths of ≥8 km depth (assuming a geothermal gradient of ~30 ºC/km and ZFT closure temperature of 240ºC [Bernet, 2009]). Additionally, bedrock cooling

ages suggest Oligocene-to-present exhumation depths of ≥11 km north of the Denali fault in the eastern Alaska Range (Benowitz et al., 2011), ≤10 km south of the Denali fault in the eastern Alaska Range (Waldien et al., 2018, 2021), <6 km south of the Denali fault in the Kluane Ranges (McDermott et al., 2019), >8.5 km in the Denali massif (Fitzgerald et al., 1995), >5 km in the central Chugach mountains (Arkle et al., 2013), ≤4 km in the Talkeetna Mountains (Terhune et al., 2019), and ≤10 km depth in the St. Elias Mountains (Enkelmann et al., 2010). The bedrock and detrital cooling age data together suggest that, aside from elements of paleo-topography in the Talkeetna Mountains (Terhune et al., 2019; Figure 5) and in the western Alaska Range (Benowitz et al., 2012), the topographic signature of southern Alaska has largely taken form since ca. 30 Ma.

**Oligocene-to-Present arc magmatism in southern Alaska**

The Oligocene marks a fundamental shift in the loci of arc magmatism in southern Alaska. U-Pb zircon dating from exhumed batholithic rocks and modern river sands indicate that prior to ca. 32 Ma, the Alaska Range was the locus of Cenozoic subduction-related magmatism (Lease et al. 2016; Regan et al., 2019; Jones et al., 2020). From ca. 32-25 Ma, arc magmatism waned in the Alaska Range (Trop et al., 2019) and re-focused in the region of the present-day Wrangell Mountains, which contain calc-alkaline igneous rocks as old as ca. 30 Ma (Berkelhammer et al., 2019; Brueseke et al., 2019). The migration of arc magmatism developed a magmatic gap throughout the eastern and central Alaska Range between the eastern Aleutian and Wrangell Mountains arcs, which broadly aligns with the present-day subducted extent of the Yakutat slab (Figure 1).

Although ca. 2-to-25 Ma igneous rocks are absent from the eastern and central Alaska Range, the presence of Quaternary volcanic fields along the southern (940.4 ± 27.1 ka lava flow;

Figure 4) and northern (Jumbo Dome–1.026 ± 0.057 Ma; Athey et al., 2006, and Buzzard Maar–ca.10 ka; Andronikov, and Mukasa, 2010) flanks of the Alaska Range demonstrate that active magmatism has recently resumed in the region. Preliminary geochemical data from Jumbo Dome lavas suggest adakite-like characteristics (Cameron et al., 2015). Similarly, adakite-like geochemical signatures are relatively common in Wrangell Arc lavas of all ages and have been attributed to melting along the edge of the Yakutat slab (Brueseke et al., 2019). Considering the northeastern extent of subducted Yakutat slab from recent geophysical studies (Bauer et al., 2014; Wech, 2016; Ward and Lin, 2018), it is clear that the Quaternary lava flows along the southern flank of the eastern Alaska Range are located above the edge of the slab (Figure 1) and thus their petrogenesis is likely also influenced by the slab edge. Due to the observation that the yet un-subducted portion of the Yakutat slab is thicker than the imaged subducted section (~30 km vs. ~17 km; Worthington et al., 2012), Gulick et al. (2013) postulated that an enhanced stage of collision between the Yakutat microplate and southern Alaska began at ca. 1 Ma, which may lead to accretion of a Pacific plate sliver. We further hypothesize that the increased plate coupling in the Quaternary may have facilitated tearing of the Yakutat slab (Fuis et al., 2008), a lull in Wrangell arc magmatism after 200,000 ka (Richter et al., 1990), and the revival of Alaska Range magmatism. Albeit cursory, our preliminary documentation provides a foundation for ongoing detailed petrologic and geochemical studies to address the origin of the Quaternary lavas in the eastern Alaska Range.

**Upper plate response to oblique flat slab subduction of the Yakutat oceanic plateau in southern Alaska**

The compiled regional thermochronology dataset from southern Alaska summarized herein reflects widespread, yet heterogeneously distributed, ca. 30 Ma-to-Present cooling and associated bedrock exhumation and topographic growth focused along pre-existing active strike-slip fault systems (Figure 6). In the proximal hanging wall of the flat slab collision zone, deep and rapid exhumation in the St. Elias Mountains is mainly focused in the syntaxis region (Figure 1A), where localized motion on the dextral transpressional Fairweather fault transitions to convergence across the thrust belt, and residual motion is bifurcated northward on the Connector fault and westward on the Chugach-St. Elias fault and eastern end of the Contact fault, which was renamed as the Bagley fault (McAleer et al., 2009; Bruhn et al., 2012; Enkelmann et al., 2015, 2017). These structures accommodated margin-parallel translation of the Yakutat terrane throughout the Cenozoic (Pavlis et al., 2019; Lease et al., 2021) and were thus active throughout the onset of Yakutat flat slab subduction. Rock uplift and exhumation in the Alaska Range has been focused along the dextral transpressional Denali fault system since ca. 30 Ma (Lease et al., 2016). Prior to ca. 30 Ma, the Denali fault accommodated mainly lateral motion of outboard terranes, which transitioned to transpression upon introduction of the Yakutat flat slab at ca. 30 Ma (e.g. Finzel et al., 2015). Localized recent exhumation in the high peak regions of the northern Chugach Mountains (Mt. Marcus Baker) and southern Talkeetna Mountains (Hatcher Pass) has been attributed to Oligocene-Neogene slip on the Castle Mountain fault, Contact fault, and subsidiary structures in the Matanuska Valley, which likely were active during initial subduction of the Yakutat oceanic plateau (Little and Naeser, 1989; Parry et al., 2001; Arkle et al., 2013; Terhune et al., 2019).

One peculiar aspect of the upper plate structural configuration is that major inactive structures, despite their importance as significant geologic-geophysical boundaries, appear to have experienced limited reactivation upon the transition to the flat slab setting. For example, the Talkeetna and Border Ranges faults are the two most profound geophysical features in southern Alaska and likely penetrate the crust (Saltus et al., 2007; Miller et al., 2018), yet the only sections of these faults with demonstrable Cenozoic slip are the sections near the aforementioned active strike-slip fault systems (Pavlis and Roeske, 2007; Waldien et al., 2021). Cooling age profiles that span the inherited active and inactive structures clearly show that bedrock cooling ages increase with distance away from the currently active transpressional fault systems toward unreactivated inherited structures and sedimentary basins (Figure 5).

Four long-lived and still active sedimentary basin systems (Copper River, Tanana, Susitna, Cook Inlet–Figure 1A) were active prior to, and during, flat slab subduction of the Yakutat oceanic plateau (Trop and Ridgway, 2007). Flexural subsidence in response to tectonic drivers likely controls depocenter locations and stability (Ridgway et al., 2007, 2011). Additionally, subsidence in the Cook Inlet area has been correlated with dynamic subsidence related to the geometry of the subducted slab (Jadamec et al., 2013). In the the Copper River basin, sparse geodetic data (Freymueller et al., 2008) suggest that a small amount of regional shortening may accompany flexural subsidence between the St. Elias Mountains and Alaska Range where active shortening structures have not been identified. Whereas protracted subsidence has created accommodation space near relatively stable basin axes throughout the Cenozoic, evidence for basin inversion is abundant along the boundaries of the high topography regions (e.g. Finzel et al., 2011a; Ridgway et al., 2011). Inversion of Oligocene-Neogene strata at the basin margins is linked to outward growth of the topography in response to slip on range-front shortening structures (e.g. Bemis and

Wallace, 2007; Haeussler et al., 2017; Allen, 2016; Waldien et al., 2018; Bender et al., 2019). The shortening and associated topographic growth led to widespread drainage reorganization throughout southern Alaska (Brennan and Ridgway, 2015; Finzel et al., 2015; Benowitz et al. 2019), which eventually compartmentalized the formerly connected basin system, resulting in isolated basins separated by high relief regions centered on the active transpression zones (Figures 1A and 6).

Oblique flat slab subduction of the Yakutat oceanic plateau resulted in a wholesale refocusing of arc magmatism in southern Alaska (Figure 6). Yakutat flat slab subduction synchronously resulted in the birth of the Wrangell Arc at ca. 30 Ma (Brueseke et al., 2019) and a decline in Alaska Range arc magmatism from ca. 30 Ma to 25 Ma (Trop et al., 2019; Jones et al., 2020). The compiled regional data indicate that arc magmatism prior to Yakutat subduction was focused along the Denali fault ~200-500 km inboard (north) of the plate boundary (inferred to be the Chugach-St. Elias fault–Figure 1). Upon introduction of the Yakutat oceanic plateau, arc magmatism was refocused laterally to a region of precursor strike-slip faulting (the Totschunda fault) above the slab edge and has persisted in that location for ca. 30 Myr (Brueseke et al., 2019; Trop et al., 2020). The newly recognized Quaternary volcanic field in the eastern Alaska Range (Figures 1A and 4) also coincides with the imaged edge of the subducted Yakutat slab and magma ascent may have been facilitated by deep-seated structures associated with the Denali fault system. These observations together suggest that the geometry of the Yakutat slab has remained relatively stable with respect to the upper plate south of the Denali fault from ca. 30-to-1 Ma.

The salient features of upper plate geologic evolution in response to oblique subduction of the Yakutat oceanic plateau in southern Alaska are portrayed in figure 6 and include: 1) bedrock exhumation and topographic development are focused along strike-slip fault systems that were

active at the time of slab flattening; 2) foreland basin inversion is restricted to the periphery of regions of growing topographic relief; and 3) arc magmatism refocuses into the region above the slab edge and loci of volcanism is generally spatially associated with active strike-slip fault systems.

**The role of pre-existing upper plate strike-slip faults in the tectono-magmatic response to oblique subduction of oceanic plateaus**

The geophysical and geological datasets summarized herein indicate that the post-30 Ma geologic evolution of southern Alaska provides an archive of oblique subduction of an oceanic plateau. Yet, owing to the oblique nature of the subduction system and pre-existing upper plate strike-slip fault systems, the Oligocene-to-present tectono-magmatic evolution of southern Alaska displays a noteworthy departure from the upper plate evolution in orthogonal flat slab regions (e.g. Mexico–Arce et al., 2020; Costa Rica–Gardner et al. 2013; Peru–Bishop et al, 2017) and in oblique flat slab environments without active pre-existing continental scale strike-slip faults (e.g. Ontong Java–Mann and Taira, 2004, central Argentina–Siame et al., 2005; Allmendinger and Judge, 2014).

In light of the observations discussed herein, we propose that oblique convergent margins with pre-existing upper plate strike-slip structures experiencing oblique flat slab subduction will undergo focused bedrock exhumation and associated topographic growth along major strike-slip structures that were active prior to, and during, the slab flattening process. Increased upper plate convergence would likely have the effect of transitioning the active fault systems from transcurrent to transpressional kinematics rather than wholesale reactivation of inactive structures. Magmatism will not necessarily migrate inboard as has been documented along other oblique flat slab

convergent margins (e.g. central Chile-Argentina–Capaldi et al., 2020), but instead melting may be focused along the edge of the down-going slab and magma ascent through the upper plate may be facilitated by lithospheric-scale strike-slip fault systems. A key finding from our analysis is that upper plate strike-slip faults systems are loci of bedrock cooling, magmatism, and topographic growth, which does not support diffuse deformation models for oblique flat slab subduction regions (e.g. Finzel et al., 2011b).

Modern and ancient examples of oblique subduction of oceanic plateaus share similarities with our documentation of the Oligocene-to-Present setting of southern Alaska. Active oblique subduction of the Samoan and Louisville Ridges into the Tonga trench has led to loci of upper plate convergence, strike-slip faulting, and focusing of magmatism into upper plate structures, which sets these sections of the margin apart from the otherwise extensional upper plate (Pelletier et al., 1998). In the northern Andes of Ecuador and Columbia, protracted slip histories alternating between transpressional and transtensional deformation within upper plate strike-slip fault systems appear to record changes in the obliquity, thickness and dip (inferred from upper plate convergence) of subducting slabs throughout the Cenozoic (Flinch, 2003; Mora et al., 2017). Multiple angular unconformities and changes in sediment provenance areas in sedimentary basins adjacent to the strike-slip fault systems suggest that basin compartmentalization and magma focusing along pre-existing lithospheric-scale structures were coeval with the changes in upper plate deformation regime (Litherland and Aspden 1992; Mora et al., 2017). Lastly, the late Cretaceous upper plate tectonic setting of western North America at the latitude of the contiguous United States involved a regional intra-arc strike-slip fault system that accommodated oblique convergence (Tikoff and de Saint Blanquat, 1997) and aided in magma ascent (e.g. Tikoff and Teyssier, 1992, among several others). The kinematics of the intra-arc shear system evolved with

changes in the convergence angle and rate (Nadin et al., 2016) until inferred slab flattening related to oblique subduction of a hypothesized oceanic plateau exhumed the batholith as deformation and magmatism migrated inboard (e.g. Gilmer et al., 2003; Saleeby, 2003; Liu et al., 2010; Fan and Carrapa, 2014). Shortening and focused cooling of the upper plate took place along pre-existing structures, some of which were strike-slip faults that were active at the onset of plateau oblique subduction (e.g. Bartley et al., 2007; Nadin et al., 2016; Fan and Carrapa, 2014).

Given the abundance of oceanic plateaus on the modern seafloor (e.g. Mann and Taira, 2004), the correlation between oceanic plateau subduction and shallow slab dip (e.g. Gutscher et al., 2000), and the observation that nearly all plate boundaries have some amount of obliquity (e.g. Philippon and Corti, 2016), it follows that oblique flat slab subduction of oceanic plateaus is a fundamental, yet often overlooked, geologic process. In addition to our synthesis of oblique flat slab subduction in southern Alaska, the active and ancient examples discussed above demonstrate the importance of upper plate strike-slip fault systems in focusing deformation and magmatism during oblique flat slab subduction. Although common themes regarding fault system kinematic evolution, topographic-basin evolution, and magma routing have become apparent from our analysis, it is also clear that the details of upper plate geologic evolution are in part controlled by the geologic history endemic to each margin.

## CONCLUSIONS

We have demonstrated herein that the post-30 Ma tectono-magmatic evolution of southern Alaska should be viewed as an archetypical example of oblique flat slab subduction of an oceanic plateau. Key conclusions from our study include:

1) Post-30 Ma bedrock cooling and exhumation are widespread in the eastern Alaska Range. Most of the post-30 Ma bedrock cooling and interpreted topographic growth are associated with transpression in the Denali fault system. Quaternary cooling in the eastern Alaska Range is best explained by thermal effects related to ca. 1 Ma volcanism.
2) The youngest cooling ages across southern Alaska are spatially associated with regions of high topographic relief adjacent to major strike-slip fault systems. Increased upper plate convergence related to the Yakutat slab is focused on strike-slip fault systems that were active at the time of slab flattening. The shift to oblique flat slab subduction had the effect of changing the bulk deformation regime within the strike-slip fault systems from transcurrent to transpressional. There is no evidence for wholesale reactivation of inherited structures with distance away from the active transpressional fault systems.
3) A regionally integrated basin system across southern Alaska became compartmentalized upon subduction of the Yakutat flat slab. The basins were isolated by inversion along their margins where topography developed in response to transpressional deformation, but the basin axes remain active depocenters.
4) Introduction of the Yakutat oceanic plateau led to the demise of subduction-related magmatism along the Denali fault at ca. 32-25 Ma and the refocusing of arc magmatism above the northeastern edge of the slab after ca. 30 Ma. Arc magmatism was spatially associated with active strike-slip fault systems during both time intervals.

5) Quaternary volcanism in the eastern Alaska Range records the resumption of magmatism in central Alaska after a ca. 24 Myr hiatus and is focused above the Yakutat slab edge. We infer the revival of Alaska Range magmatism is related to a recent (ca. 1 Ma) increase in subduction resistance of the Yakutat oceanic plateau.
6) The angle of convergence and precursor structural configuration of the upper plate play first-order roles in how deformation is manifest and magmatism is focused during flat slab subduction.

## FIGURES

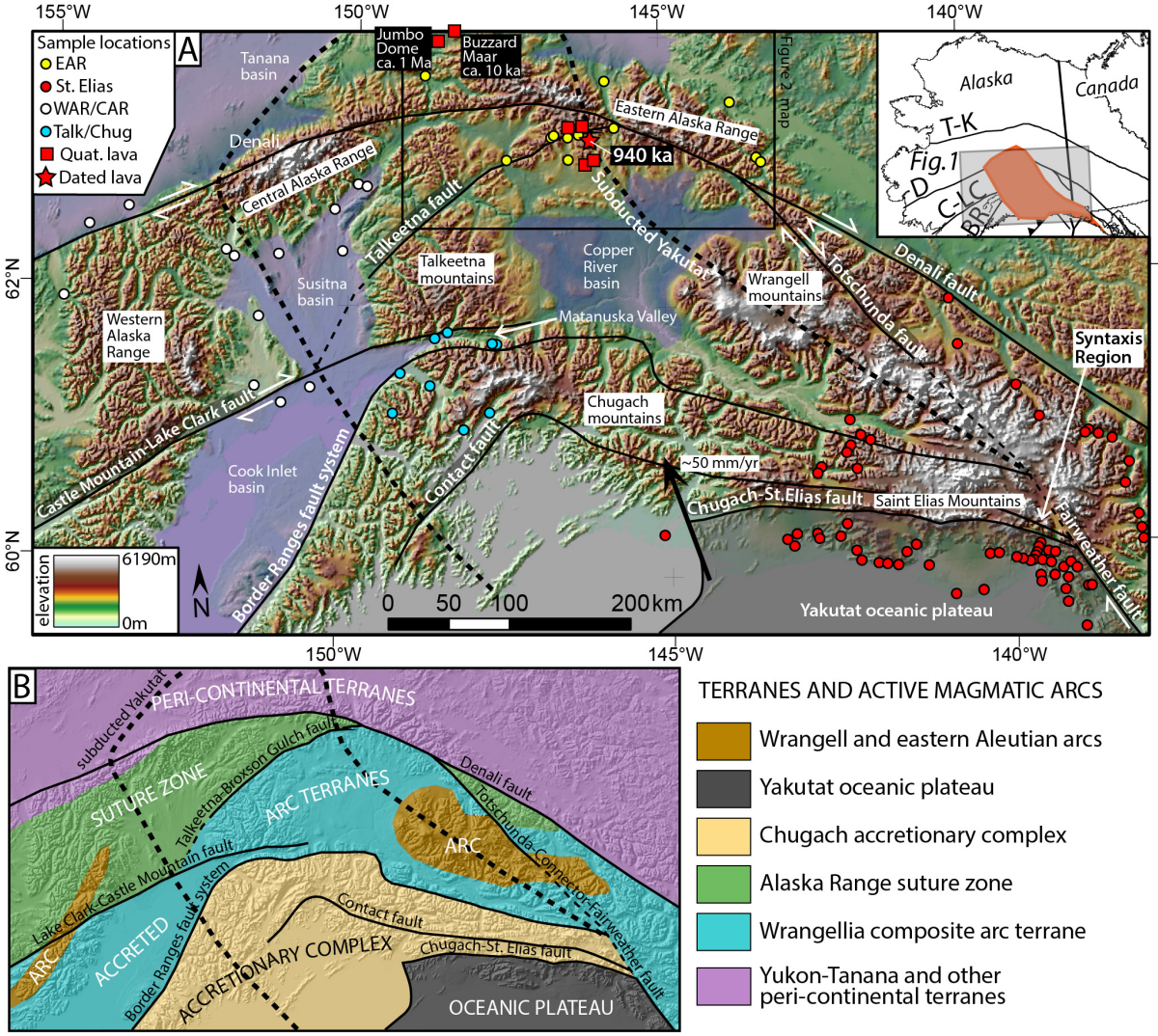
155°W
150°W
145°W
140°W
62°N
60°N
A
Sample locations
EAR
St. Elias
WAR/CAR
Talk/Chug
Quat. lava
Dated lava
Tanana basin
Jumbo Dome ca. 1 Ma
Buzzard Maar ca. 10 ka
Figure 2 map
Eastern Alaska Range
940 ka
Denali
Central Alaska Range
Talkeetna fault
Subducted Yakutat
Alaska
Canada
T-K
Fig. 1
D
C-I-C
BP
Talkeetna mountains
Copper River basin
Susitna basin
Wrangell mountains
Denali fault
Totschunda fault
Western Alaska Range
Matanuska Valley
Syntaxis Region
Chugach mountains
Castle Mountain-Lake Clark fault
Cook Inlet basin
Border Ranges fault system
Contact fault
~50 mm/yr
Chugach-St.Elias fault
Saint Elias Mountains
Fairweather fault
elevation
6190m
0m
N
0 50 100 200 km
Yakutat oceanic plateau
B
subducted Yakutat
PERI-CONTINENTAL TERRANES
Denali fault
Talkeetna-Broxson Gulch fault
SUTURE ZONE
ARC TERRANES
Totschunda-Connector-Fairweather fault
Talkeetna Mountain fault
ARC
Lake Clark-Castle Mountain fault
Contact fault
ACCRETED ARC
Border Ranges fault system
ACCRETIONARY COMPLEX
Chugach-St. Elias fault
OCEANIC PLATEAU
TERRANES AND ACTIVE MAGMATIC ARCS
Wrangell and eastern Aleutian arcs
Yakutat oceanic plateau
Chugach accretionary complex
Alaska Range suture zone
Wrangellia composite arc terrane
Yukon-Tanana and other peri-continental terranes

**Figure 1 (Previous page): A)** Shaded relief map of southern Alaska showing new and compiled modern river detrital fission-track sample locations (colored circles) and locations of Alaska Range Quaternary (Quat.) volcanic fields relative to major structures (black lines) and basins (blue shaded regions). The exposed Yakutat terrane (transparent-black shaded region) and flat-slab subducted extent (broken bold black line compiled from Bauer et al., [2014], Wech [2016], and Ward and Lin [2018]) is inferred to drive upper plate deformation in southern Alaska. EAR–Eastern Alaska Range; WAR–Western Alaska Range; CAR–Central Alaska Range; Talk–Talkeetna Mountains; Chug–Chugach Mountains. Faults in inset: T-K–Tintina-Kaltag; D–Denali; C-LC–Castle Mountain-Lake Clark; BR–Border Ranges. **B)** Hillshade map of the same extent as Figure 1A overlain by terrane geology (see text for details). Colored domains are labelled generically on the map and represent generalized southern Alaska terranes in the legend.

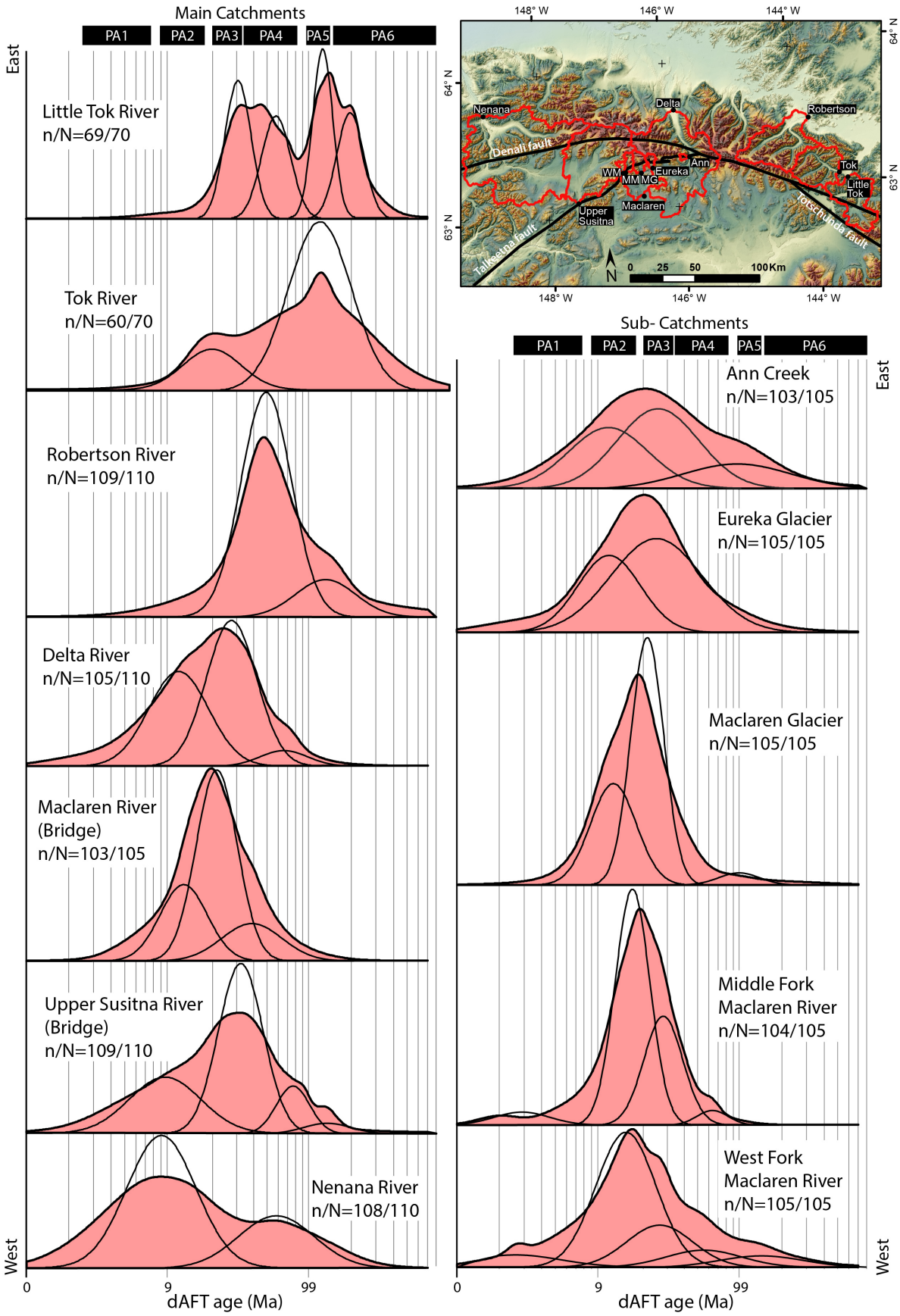
Main Catchments
PA1
PA2
PA3
PA4
PA5
PA6
East
Little Tok River
n/N=69/70
Tok River
n/N=60/70
Robertson River
n/N=109/110
Delta River
n/N=105/110
Maclaren River
(Bridge)
n/N=103/105
Upper Susitna River
(Bridge)
n/N=109/110
Nenana River
n/N=108/110
West
0
9
99
dAFT age (Ma)
148° W
146° W
144° W
64° N
63° N
Nenana
Delta
Robertson
Denali fault
WM
MM
MG
Eureka
Ann
Tok
Little Tok
Maclaren
Upper Susitna
Talkeetna fault
Totschunda fault
N
0 25 50 100Km
Sub- Catchments
PA1
PA2
PA3
PA4
PA5
PA6
East
Ann Creek
n/N=103/105
Eureka Glacier
n/N=105/105
Maclaren Glacier
n/N=105/105
Middle Fork
Maclaren River
n/N=104/105
West Fork
Maclaren River
n/N=105/105
West
0
9
99
dAFT age (Ma)

**Figure 2 (Previous page):** Equal-area probability density plots (PDPs) of detrital apatite fission-track data from individual catchments in the eastern Alaska Range. Filled PDPs represent the entire unmixed dataset, whereas unfilled black PDPs represent unmixed age populations. The inset map in the upper right shows the locations of the catchments. N–total number of analyzed grains; n–number of grains used in the unmixing analysis; PA1-5–Apatite fission track age populations defined in table 1. Abbreviated catchment names: WM– West fork Maclaren river; MM–Middle fork Maclaren River; MG–Maclaren glacier.

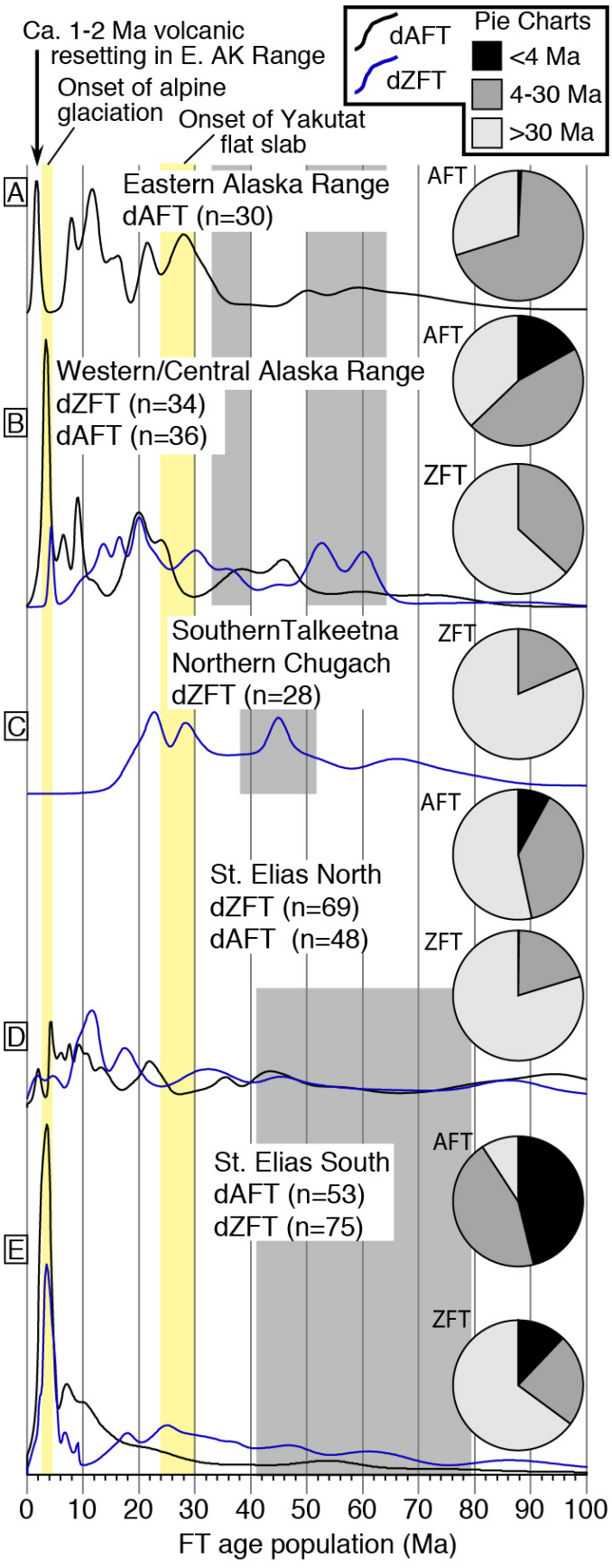
Ca. 1-2 Ma volcanic resetting in E. AK Range
Onset of alpine glaciation
Onset of Yakutat flat slab
dAFT
dZFT
Pie Charts
<4 Ma
4-30 Ma
>30 Ma
A
Eastern Alaska Range
dAFT (n=30)
AFT
B
Western/Central Alaska Range
dZFT (n=34)
dAFT (n=36)
AFT
ZFT
C
SouthernTalkeetna
Northern Chugach
dZFT (n=28)
ZFT
D
St. Elias North
dZFT (n=69)
dAFT (n=48)
AFT
ZFT
E
St. Elias South
dAFT (n=53)
dZFT (n=75)
AFT
ZFT
0 10 20 30 40 50 60 70 80 90 100
FT age population (Ma)

**Figure 3 (Previous page):** Equal-area probability density plots of compiled modern river detrital apatite and zircon fission-track age populations from (A) the eastern Alaska Range (this study), (B) central-western Alaska Range, (C) Chugach and Talkeetna Mountains, and (D and E) St. Elias Mountains (see text for references). Pie charts summarize the age populations normalized by their proportions of the entire single grain dataset and binned into <4 Ma, 4-30 Ma, and <30 Ma time intervals. Grey shaded time intervals represent times of known magmatism in each region and yellow shaded time intervals represent known times of regional cooling events. dAFT–detrital apatite fission-track; dZFT-detrital zircon fission-track.

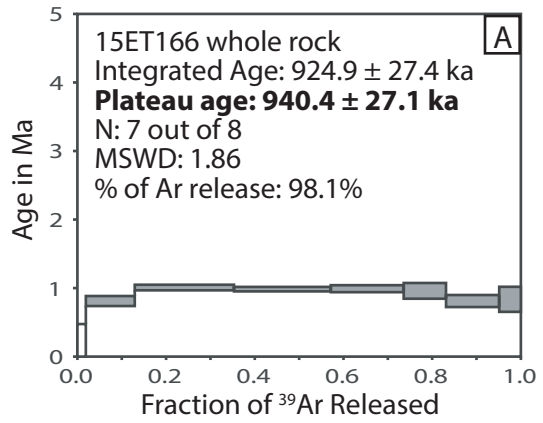
A
15ET166 whole rock
Integrated Age: 924.9 ± 27.4 ka
**Plateau age: 940.4 ± 27.1 ka**
N: 7 out of 8
MSWD: 1.86
% of Ar release: 98.1%
Age in Ma
Fraction of $^{39}$Ar Released

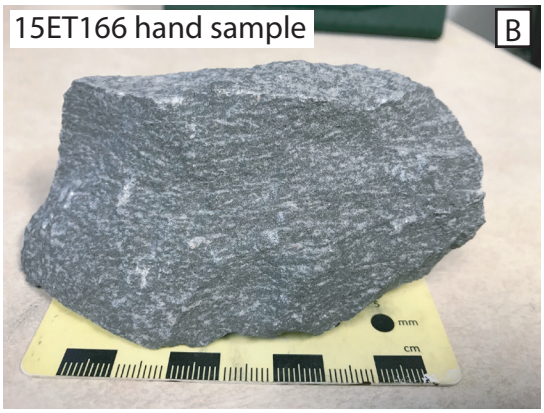
15ET166 hand sample
B


C
15ET166 outcrop

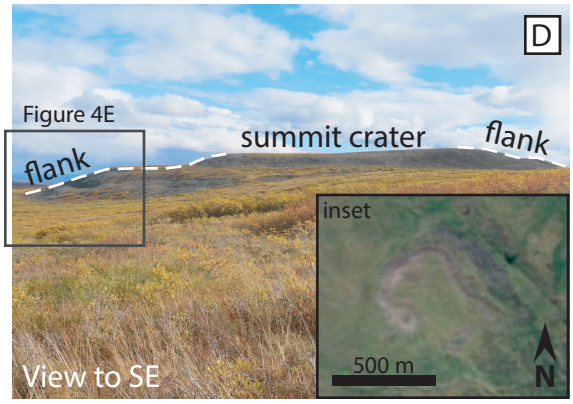
D
Figure 4E
flank
summit crater
flank
inset
500 m
N
View to SE

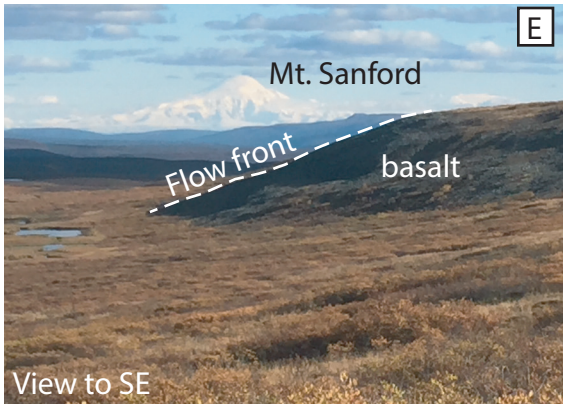
E
Mt. Sanford
Flow front
basalt
View to SE

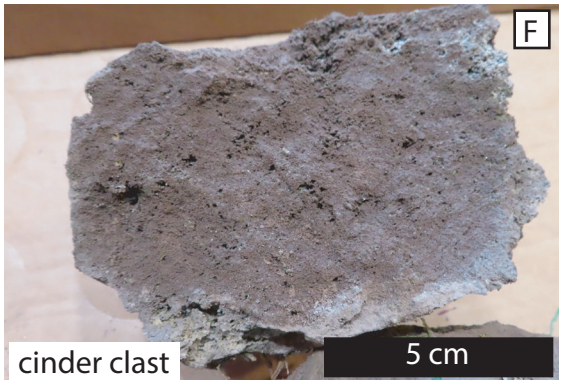
F
cinder clast
5 cm

**Figure 4 (Previous page):** Features of Quaternary volcanic rocks in the eastern Alaska Range. **A)** $^{40}Ar/^{39}Ar$ age spectrum for sample 15ET166. Grey-filled gas release steps are used to calculate the age of the sample. N–number of gas release steps used to calculate the age; MSWD– Mean Square Weighted Deviation. **B)** 15ET166 hand sample. **C)** Outcrop photo of 15ET166. The platy outcrop pattern pictured here is common among outcrops of young volcanic rocks in the eastern Alaska Range. The hammer for scale is ~40 cm long. **D)** Geomorphic features indicative of young volcanism are preserved in the landscape. Here, a semi-conic feature composed of oxidized basalt is preserved. ***Inset***: Google Earth image showing that the cone appears to have breached out of the southeast flank. **E)** Zoomed-in image of the cone flank illustrating the along-strike relationship with the Wrangell arc (Mt. Sanford). **F)** A late Pleistocene, potentially post-glacial Holocene, age for some volcanic features is suggested by the presence of unaltered cinder ejecta (pictured here) among oxidized basalt, scoria and the preserved landforms.

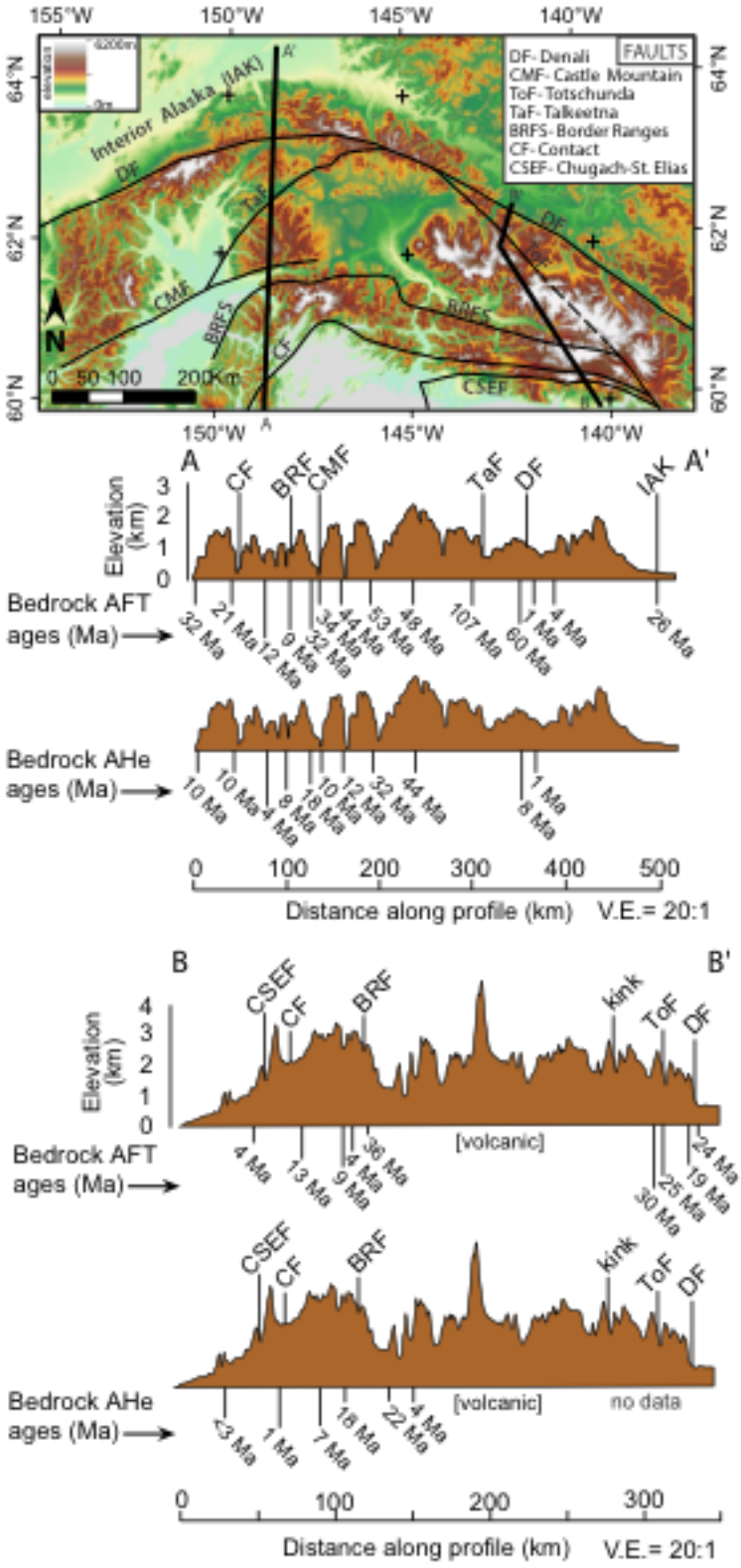
155°W
150°W
145°W
140°W
64°N
62°N
60°N
Interior Alaska (IAK)
A
A'
B
B'
DF- Denali
CMF- Castle Mountain
ToF- Totschunda
TaF- Talkeetna
BRFS- Border Ranges
CF- Contact
CSEF- Chugach-St. Elias
FAULTS
DF
TaF
CMF
BRFS
CF
CSEF
N
0 50 100 200Km
Elevation (km)
Bedrock AFT ages (Ma)
Bedrock AHe ages (Ma)
32 Ma
21 Ma
12 Ma
9 Ma
32 Ma
34 Ma
44 Ma
53 Ma
48 Ma
107 Ma
60 Ma
7 Ma
4 Ma
26 Ma
10 Ma
10 Ma
4 Ma
9 Ma
18 Ma
10 Ma
12 Ma
32 Ma
44 Ma
1 Ma
8 Ma
0 100 200 300 400 500
Distance along profile (km) V.E.= 20:1
CSEF
CF
BRF
kink
ToF
DF
[volcanic]
4 Ma
13 Ma
9 Ma
4 Ma
36 Ma
30 Ma
25 Ma
19 Ma
24 Ma
<3 Ma
1 Ma
7 Ma
18 Ma
22 Ma
4 Ma
no data
0 100 200 300
Distance along profile (km) V.E.= 20:1

**Figure 5 (Previous page):** Topographic profiles showing that the youngest bedrock apatite fission-track (AFT) and apatite (U-Th)/He cooling ages are spatially associated with major Cenozoic strike-slip fault systems in southern Alaska. Profile A-A' is modified from Terhune et al. (2019). Data are compiled from Terhune et al. (2019), Arkle et al. (2013), Berger and Spotila (2008), Berger et al., (2008), Enkelmann et al. (2010), O'Sullivan and Currie (1995), Meigs et al. (2008), Spotila et al. (2004).

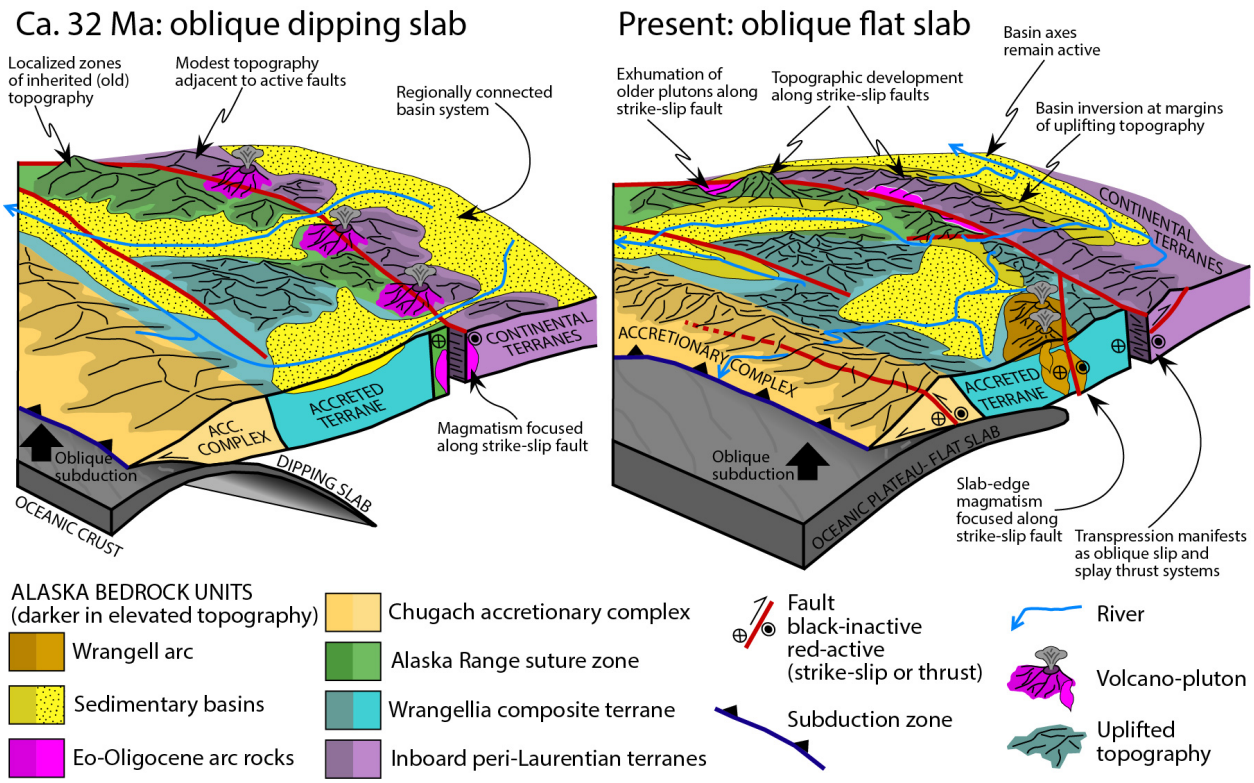


**Figure 6:** Schematic diagrams showing the ca. 32-0 Ma southern Alaska tectonic evolution as it displays salient features of "normal" (left) and flat slab (right) subduction in obliquely convergent environments. Key features of the tectonic evolution upon the onset of oblique flat slab subduction include: 1) active strike-slip fault systems transition into transpressional deformation zones with bedrock cooling/exhumation/uplift focused along the fault systems; 2) topographic growth associated with transpression zones causes the through-going basin system to become compartmentalized into isolated depocenters; and 3) magmatism is focused above the slab edge and active strike-slip fault systems play a role in facilitating magma ascent. Paleo-drainage directions are inferred from Finzel et al. (2015) and Trop and Ridgway (2007).

TABLE 1: Eastern Alaska Range detrital apatite fission-track age populations

| Sample | Sample collection year | PA1 (1.6-7 Ma) | PA2 (8-17 Ma) | PA3 (20-33 Ma) | PA4 (38-77 Ma) | PA5 (96-134 Ma) | PA6 (≥145 Ma) | n[1](N)[2] |
|---|---|---|---|---|---|---|---|---|
| Ann Creek | 2019 | | 10.9±2.7 (35%) | 25.7±4.8 (47%) | | 96±19 (18%) | | 103(105) |
| Eureka Glacier | 2019 | | 11.1±1.7 (36%) | 25.2±2.5 (64%) | | | | 105(105) |
| Maclaren Glacier | 2019 | | 11.9±1 (35%) | 21.4±1.1 (62%) | | 99±31 (3%) | | 105(105) |
| M. Fork Maclaren River | 2019 | 1.9±0.6 (5%) | 16.6±0.8 (61%) | 28.1±1.6 (31%) | 63.9±7.7 (3%) | | | 104(105) |
| W. Fork Maclaren River | 2019 | 1.6±0.4 (4%) | 14.9±0.9 (60%) | 26.6±2.6 (21%) | 55.9±8.5 (9%) | | 145±28 (6%) | 105(105) |
| Maclaren Bridge | 2019 | | 12±1.2 (26%) | 21.3±1.4 (57) | 38.5±4.8 (17%) | | | 103(105) |
| Little Tok River | 2016 | | | 30.6±2.1 (29%) | 57.9±3.4 (23%) | 125.3±5.2 (26%) | 197±12 (21%) | 69(70) |
| Robertson River | 2012 | | | | 49.8±2.3 (84%) | 133±14 (16%) | | 109(110) |
| Delta River | 2014 | | 11.1±1.3 (41%) | 27.6±1.9 (54%) | 66.1±7.7 (5%) | | | 105(110) |
| Upper Susitna River | 2014 | | 8.6±1.3 (30%) | 32±2 (56%) | 76.3±7.5 (11%) | 134±15 (3%) | | 109(110) |
| Tok River | 2016 | | | 20±4.5 (18%) | | 119±14 (82%) | | 60(70) |
| Nenana River | 2014 | | 7.8±0.6 (73%) | | 65.5±6.9 (27%) | | | 108(110) |

1- n– number of analyzed grains used in unmixing

2- N–total number of analyzed grains

TABLE 2: Quaternary volcanic features in the eastern Alaska Range

| Feature | LAT. (N) | LONG. (W) |
|---|---|---|
| Scoria | 63.1358 | 146.3252 |
| Blocky lava flow | 63.1371 | 146.3217 |
| Possible tuff interbedded with lava | 63.0553 | 146.3132 |
| Platey lava | 63.0547 | 146.3110 |
| Oxidized lavas- possible vent | 63.0569 | 146.3125 |
| 15ET166- Platey lava | 63.2357 | 146.1944 |
| Cinder | 63.1364 | 146.3199 |

**REFERENCES CITED**


Allen, W.K., 2016, Miocene-Pliocene strike-slip basin development along the Denali fault system in the eastern Alaska Range: Chronostratigraphy and provenance of the McCallum formation and implications for displacement [M.S. Thesis]: Purdue University, 160 p.

Allmendinger, R. W., & Judge, P. A. (2014). The Argentine Precordillera: A foreland thrust belt proximal to the subducted plate. *Geosphere*, *10*(6), 1203-1218.

Andronikov, A.V. and Mukasa, S.B., 2010. 40Ar/39Ar eruption ages and geochemical characteristics of Late Tertiary to Quaternary intraplate and arc-related lavas in interior Alaska. *Lithos*, *115*(1-4), pp.1-14.

Arce, J.L., Ferrari, L., Morales-Casique, E., Vasquez-Serrano, A., Arroyo, S.M., Layer, P.W., Benowitz, J. and López-Martínez, M., 2020. Early Miocene arc volcanism in the Mexico City Basin: Inception of the Trans-Mexican Volcanic Belt. *Journal of Volcanology and Geothermal Research*, *408*, p.107104.

Arkle, J. C., Armstrong, P. A., Haeussler, P. J., Prior, M. G., Hartman, S., Sendziak, K. L., & Brush, J. A. (2013). Focused exhumation in the syntaxis of the western Chugach Mountains and Prince William Sound, Alaska. *Bulletin*, *125*(5-6), 776-793.

Athey, J.E., Newberry, R.J., Werdon, M.B., Freeman, L.K., Smith, R.L., and Szumigala, D.J., 2006, Bedrock geologic map of the Liberty Bell area, Fairbanks A-4 Quadrangle, Bonnifield mining district, Alaska: Alaska Division of Geological & Geophysical Surveys Report of Investigation 2006-2 v. 1.0.1, 98 p., 1 sheet, scale 1:50,000. https://doi.org/10.14509/15026

Audet, P., Sole, C., & Schaeffer, A. J. (2016). Control of lithospheric inheritance on neotectonic activity in northwestern Canada?. *Geology*, *44*(10), 807-810.

Bartley, J. M., Glazner, A. F., Coleman, D. S., Kylander-Clark, A., Mapes, R., Friedrich, A. M., ... & Foster, D. A. (2007). Large Laramide dextral offset across Owens Valley, California, and its possible relation to tectonic unroofing of the southern Sierra Nevada. *SPECIAL PAPERS-GEOLOGICAL SOCIETY OF AMERICA*, *434*, 129.

Bauer, M. A., Pavlis, G. L., & Landes, M. (2014). Subduction geometry of the Yakutat terrane, southeastern Alaska. *Geosphere*, *10*(6), 1161-1176.

Bemis, S. P., & Wallace, W. K. (2007). Neotectonic framework of the north-central Alaska Range foothills. In Ridgway, K.D., Trop, J.M., Glen, J.M.G., O'Neill, J.M. (Eds.). *Special Paper 431: Tectonic Growth of a Collisional Continental Margin: Crustal Evolution of Southern Alaska* (Vol. 431, pp. 549–572). Boulder, Colorado: Geological Society of America. https://doi.org/10.1130/2007.2431(21)

Bender, A. M., Lease, R. O., Haeussler, P. J., Rittenour, T., Corbett, L. B., Bierman, P. R., & Caffee, M. W. (2019). Pace and process of active folding and fluvial incision across the Kantishna Hills anticline, central Alaska. *Geophysical Research Letters*, *46*(6), 3235-3244.

Benowitz, J. A., Davis, K., & Roeske, S. (2019). A river runs through it both ways across time: 40Ar/39Ar detrital and bedrock muscovite geochronology constraints on the Neogene paleodrainage history of the Nenana River system, Alaska Range. *Geosphere*, *15*(3), 682-701.

Benowitz, J. A., Haeussler, P. J., Layer, P. W., O'Sullivan, P. B., Wallace, W. K., & Gillis, R. J. (2012). Cenozoic tectono-thermal history of the Tordrillo Mountains, Alaska: Paleocene-

Eocene ridge subduction, decreasing relief, and late Neogene faulting. *Geochemistry, Geophysics, Geosystems*, *13*(4).
Benowitz, J. A., Layer, P. W., & Vanlaningham, S. (2014). Persistent long-term (c. 24 Ma) exhumation in the Eastern Alaska Range constrained by stacked thermochronology. *Geological Society, London, Special Publications*, *378*(1), 225-243.
Benowitz, J. A., Layer, P. W., Armstrong, P., Perry, S. E., Haeussler, P. J., Fitzgerald, P. G., & VanLaningham, S. (2011). Spatial variations in focused exhumation along a continental-scale strike-slip fault: The Denali fault of the eastern Alaska Range. *Geosphere*, *7*(2), 455-467.
Berger, A. L., & Spotila, J. A. (2008). Denudation and deformation in a glaciated orogenic wedge: The St. Elias orogen, Alaska. *Geology*, *36*(7), 523-526.
Berger, A. L., Spotila, J. A., Chapman, J. B., Pavlis, T. L., Enkelmann, E., Ruppert, N. A., & Buscher, J. T. (2008). Architecture, kinematics, and exhumation of a convergent orogenic wedge: A thermochronological investigation of tectonic–climatic interactions within the central St. Elias orogen, Alaska. *Earth and Planetary Science Letters*, *270*(1-2), 13-24.
Berkelhammer, S. E., Brueseke, M. E., Benowitz, J. A., Trop, J. M., Davis, K., Layer, P. W., & Weber, M. (2019). Geochemical and geochronological records of tectonic changes along a flat-slab arc-transform junction: Circa 30 Ma to ca. 19 Ma Sonya Creek volcanic field, Wrangell Arc, Alaska. *Geosphere*, *15*(5), 1508-1538.
Bernet, M. (2009). A field-based estimate of the zircon fission-track closure temperature. *Chemical Geology*, *259*(3-4), 181-189.
Bill, N. S., Mix, H. T., Clark, P. U., Reilly, S. P., Jensen, B. J., & Benowitz, J. A. (2018). A stable isotope record of late Cenozoic surface uplift of southern Alaska. *Earth and Planetary Science Letters*, *482*, 300-311.
Bishop, B.T., Beck, S.L., Zandt, G., Wagner, L., Long, M., Antonijevic, S.K., Kumar, A. and Tavera, H., 2017. Causes and consequences of flat-slab subduction in southern Peru. *Geosphere*, *13*(5), pp.1392-1407.
Brennan, P. R., & Ridgway, K. D. (2015). Detrital zircon record of Neogene exhumation of the central Alaska Range: A far-field upper plate response to flat-slab subduction. *Bulletin*, *127*(7-8), 945-961.
Brueseke, M. E., Benowitz, J. A., Trop, J. M., Davis, K. N., Berkelhammer, S. E., Layer, P. W., & Morter, B. K. (2019). The Alaska Wrangell Arc:~ 30 Ma of subduction-related magmatism along a still active arc-transform junction. *Terra Nova*, *31*(1), 59-66.
Burkett, C. A., Bemis, S. P., & Benowitz, J. A. (2016). Along-fault migration of the Mount McKinley restraining bend of the Denali fault defined by late Quaternary fault patterns and seismicity, Denali National Park & Preserve, Alaska. *Tectonophysics*, *693*, 489-506.
Cameron, C.E., Nye, C.J., Bull, K.F., and Woods, Rebecca-Ellen, 2015, Jumbo Dome, interior Alaska: Whole-rock, major- and trace-element analyses: Alaska Division of Geological & Geophysical Surveys Raw Data File 2015-14, 3 p. https://doi.org/10.14509/29520
Capaldi, T.N., Horton, B.K., McKenzie, N.R., Mackaman-Lofland, C., Stockli, D.F., Ortiz, G. and Alvarado, P., 2020. Neogene retroarc foreland basin evolution, sediment provenance, and magmatism in response to flat slab subduction, western Argentina. *Tectonics*, *39*(7), p.e2019TC005958.
Carrapa, B., DeCelles, P.G. and Romero, M., 2019. Early inception of the Laramide orogeny in southwestern Montana and northern Wyoming: Implications for models of flat-slab subduction. *Journal of Geophysical Research: Solid Earth*, *124*(2), pp.2102-2123.

Donelick, R. A., O'Sullivan, P. B., & Ketcham, R. A. (2005). Apatite fission-track analysis. *Reviews in Mineralogy and Geochemistry*, *58*(1), 49-94.
Elliott, J., & Freymueller, J. T. (2020). A block model of present-day kinematics of Alaska and western Canada. *Journal of Geophysical Research: Solid Earth*, *125*(7), e2019JB018378.
Enkelmann, E., Garver, J. I., & Pavlis, T. L. (2008). Rapid exhumation of ice-covered rocks of the Chugach–St. Elias orogen, Southeast Alaska. *Geology*, *36*(12), 915-918.
Enkelmann, E., Koons, P. O., Pavlis, T. L., Hallet, B., Barker, A., Elliott, J., ... & Van Avendonk, H. J. (2015). Cooperation among tectonic and surface processes in the St. Elias Range, Earth's highest coastal mountains. *Geophysical Research Letters*, *42*(14), 5838-5846.
Enkelmann, E., Piestrzeniewicz, A., Falkowski, S., Stübner, K., & Ehlers, T. A. (2017). Thermochronology in southeast Alaska and southwest Yukon: Implications for North American Plate response to terrane accretion. *Earth and Planetary Science Letters*, *457*, 348-358.
Enkelmann, E., Sanchez Lohff, S. K., & Finzel, E. S. (2019). Detrital zircon double-dating of forearc basin strata reveals magmatic, exhumational, and thermal history of sediment source areas. *Bulletin*, *131*(7-8), 1364-1384.
Enkelmann, E., Zeitler, P. K., Garver, J. I., Pavlis, T. L., & Hooks, B. P. (2010). The thermochronological record of tectonic and surface process interaction at the Yakutat–North American collision zone in southeast Alaska. *American Journal of Science*, *310*(4), 231-260.
Enkelmann, E., Zeitler, P. K., Pavlis, T. L., Garver, J. I., & Ridgway, K. D. (2009). Intense localized rock uplift and erosion in the St Elias orogen of Alaska. *Nature Geoscience*, *2*(5), 360-363.
Espurt, N., Funiciello, F., Martinod, J., Guillaume, B., Regard, V., Faccenna, C., & Brusset, S. (2008). Flat subduction dynamics and deformation of the South American plate: Insights from analog modeling. *Tectonics*, *27*(3).
Estève, C., Audet, P., Schaeffer, A. J., Schutt, D., Aster, R. C., & Cubley, J. (2020). The upper mantle structure of northwestern Canada from teleseismic body wave tomography. *Journal of Geophysical Research: Solid Earth*, *125*(2), e2019JB018837.
Falkowski, S., Enkelmann, E., Drost, K., Pfänder, J. A., Stübner, K., & Ehlers, T. A. (2016). Cooling history of the St. Elias syntaxis, southeast Alaska, revealed by geochronology and thermochronology of cobble-sized glacial detritus. *Tectonics*, *35*(2), 447-468.
Fan, M., & Carrapa, B. (2014). Late Cretaceous–early Eocene Laramide uplift, exhumation, and basin subsidence in Wyoming: Crustal responses to flat slab subduction. *Tectonics*, *33*(4), 509-529.
Finzel, E. S., Flesch, L. M., Ridgway, K. D., Holt, W. E., & Ghosh, A. (2015). Surface motions and intraplate continental deformation in Alaska driven by mantle flow. *Geophysical Research Letters*, *42*(11), 4350-4358.
Finzel, E. S., Trop, J. M., Ridgway, K. D., & Enkelmann, E. (2011). Upper plate proxies for flat-slab subduction processes in southern Alaska. *Earth and Planetary Science Letters*, *303*(3-4), 348-360.
Fitzgerald, P. G., Roeske, S. M., Benowitz, J. A., Riccio, S. J., Perry, S. E., & Armstrong, P. A. (2014). Alternating asymmetric topography of the Alaska range along the strike-slip Denali fault: Strain partitioning and lithospheric control across a terrane suture zone. *Tectonics*, *33*(8), 1519-1533.

Fitzgerald, P. G., Sorkhabi, R. B., Redfield, T. F., & Stump, E. (1995). Uplift and denudation of the central Alaska Range: A case study in the use of apatite fission track thermochronology to determine absolute uplift parameters. *Journal of Geophysical Research: Solid Earth*, *100*(B10), 20175-20191.

Flinch, J. F. (2003). Structural evolution of the Sinu-Lower Magdalena area (northern Colombia).

Freymueller, J. T. (2010). Active tectonics of plate boundary zones and the continuity of plate boundary deformation from Asia to North America. *Current Science*, 1719-1732.

Freymueller, J. T., Woodard, H., Cohen, S. C., Cross, R., Elliott, J., Larsen, C. F., ... & Ekström, G. (2008). Active deformation processes in Alaska, based on 15 years of GPS measurements. *Active tectonics and seismic potential of Alaska*, *179*, 1-42.

Fuis, G. S., Moore, T. E., Plafker, G., Brocher, T. M., Fisher, M. A., Mooney, W. D., ... & Ruppert, N. A. (2008). Trans-Alaska Crustal Transect and continental evolution involving subduction underplating and synchronous foreland thrusting. *Geology*, *36*(3), 267-270.

Galbraith, R. (2005), *Statistics for Fission Track Analysis*, Chapman & Hall / CRC, Boca Raton, FL.

Galbraith, R. F., and P.F. Green (1990), Estimating the component ages in a finite mixture, *Nuclear Tracks and Radiation Measurements*, 17, 197-206.

Gardner, T. W., Fisher, D. M., Morell, K. D., & Cupper, M. L. (2013). Upper-plate deformation in response to flat slab subduction inboard of the aseismic Cocos Ridge, Osa Peninsula, Costa Rica. *Lithosphere*, *5*(3), 247-264.

Garver, J. I., & Davidson, C. M. (2015). Southwestern Laurentian zircons in upper Cretaceous flysch of the Chugach-Prince William terrane in Alaska. *American Journal of Science*, *315*(6), 537-556.

Gilmer, A. K., Kyle, J. R., Connelly, J. N., Mathur, R. D., & Henry, C. D. (2003). Extension of Laramide magmatism in southwestern North America into Trans-Pecos Texas. *Geology*, *31*(5), 447-450.

GREEN, P.F., DUDDY, I.R., GLEADOW, A.J.W., TINGATE, P.R. & LASLETT, G.M. (1986): Thermal annealing of fission tracks in apatite.1. A qualitative description. Chem. Geol. 59, 237-253

Gulick, S.P., Jaeger, J.M., Mix, A.C., Asahi, H., Bahlburg, H., Belanger, C.L., Berbel, G.B., Childress, L., Cowan, E., Drab, L. and Forwick, M., 2015. Mid-Pleistocene climate transition drives net mass loss from rapidly uplifting St. Elias Mountains, Alaska. *Proceedings of the National Academy of Sciences*, *112*(49), pp.15042-15047.

Gutscher, M. A., Spakman, W., Bijwaard, H., & Engdahl, E. R. (2000). Geodynamics of flat subduction: Seismicity and tomographic constraints from the Andean margin. *Tectonics*, *19*(5), 814-833.

Haeussler, P. J., Saltus, R. W., Stanley, R. G., Ruppert, N., Lewis, K., Karl, S. M., & Bender, A. (2017). The Peters Hills basin, a Neogene wedge-top basin on the Broad Pass thrust fault, south-central Alaska. *Geosphere*, *13*(5), 1464-1488.

Haynie, K. L., & Jadamec, M. A. (2017). Tectonic drivers of the Wrangell block: Insights on fore-arc sliver processes from 3-D geodynamic models of Alaska. *Tectonics*, *36*(7), 1180-1206.

Jadamec, M. A., Billen, M. I., & Roeske, S. M. (2013). Three-dimensional numerical models of flat slab subduction and the Denali fault driving deformation in south-central Alaska. *Earth and Planetary Science Letters*, *376*, 29-42.

Jones III, J. V., Todd, E., Box, S. E., Haeussler, P. J., Holm-Denoma, C. S., Karl, S. M., ... & Layer, P. W. (2021). Cretaceous to Oligocene magmatic and tectonic evolution of the western Alaska Range: Insights from U-Pb and 40Ar/39Ar geochronology. *Geosphere*, *17*(1), 118-153.

Kaufman, D.S., Young, N.E., Briner, J.P. and Manley, W.F., 2011. Alaska palaeo-glacier atlas (version 2). In *Developments in Quaternary Sciences* (Vol. 15, pp. 427-445). Elsevier.

Kreemer, C., Blewitt, G., & Klein, E. C. (2014). A geodetic plate motion and Global Strain Rate Model. *Geochemistry, Geophysics, Geosystems*, *15*(10), 3849-3889.

Lease, R. O., Haeussler, P. J., & O'Sullivan, P. (2016). Changing exhumation patterns during Cenozoic growth and glaciation of the Alaska Range: Insights from detrital thermochronology and geochronology. *Tectonics*, *35*(4), 934-955.

Lease, R. O. (2018). Pliocene erosional pulse and glacier-landscape feedbacks in the western Alaska Range. *Earth and Planetary Science Letters*, **497**, 62– 68. https://doi.org/10.1016/j.epsl.2018.06.009

Lease, R.O., et al., 2021, Extreme Quaternary plate boundary exhumation and strike slip localized along the southern Fairweather fault, Alaska, USA: Geology, v. 49, p. XXX–XXX, https://doi.org/10.1130/G48464.1

Litherland, M., & Aspden, J. A. (1992). Terrane-boundary reactivation: a control on the evolution of the Northern Andes. *Journal of South American Earth Sciences*, *5*(1), 71-76.

Little, T. A., & Naeser, C. W. (1989). Tertiary tectonics of the Border Ranges fault system, Chugach Mountains, Alaska: Deformation and uplift in a forearc setting. *Journal of Geophysical Research: Solid Earth*, *94*(B4), 4333-4359.

Liu, L., Gurnis, M., Seton, M., Saleeby, J., Müller, R. D., & Jackson, J. M. (2010). The role of oceanic plateau subduction in the Laramide orogeny. *Nature Geoscience*, *3*(5), 353-357.

Mann, P. and Taira, A., 2004. Global tectonic significance of the Solomon Islands and Ontong Java Plateau convergent zone. *Tectonophysics*, *389*(3-4), pp.137-190.

Marshak, S., Karlstrom, K., & Timmons, J. M. (2000). Inversion of Proterozoic extensional faults: An explanation for the pattern of Laramide and Ancestral Rockies intracratonic deformation, United States. *Geology*, *28*(8), 735-738.

McAleer, R. J., Spotila, J. A., Enkelmann, E., & Berger, A. L. (2009). Exhumation along the Fairweather fault, southeastern Alaska, based on low-temperature thermochronometry. *Tectonics*, *28*(1).

McDermott, R. G., Ault, A. K., Caine, J. S., & Thomson, S. N. (2019). Thermotectonic history of the Kluane Ranges and evolution of the eastern Denali fault zone in southwestern Yukon, Canada. *Tectonics*, *38*(8), 2983-3010.

Miller, M. S., O'Driscoll, L. J., Porritt, R. W., & Roeske, S. M. (2018). Multiscale crustal architecture of Alaska inferred from P receiver functions. *Lithosphere*, *10*(2), 267-278.

Mora, J. A., Oncken, O., Le Breton, E., Ibánez-Mejia, M., Faccenna, C., Veloza, G., ... & Mesa, A. (2017). Linking Late Cretaceous to Eocene tectonostratigraphy of the San Jacinto fold belt of NW Colombia with Caribbean Plateau collision and flat subduction. *Tectonics*, *36*(11), 2599-2629.

Nadin, E. S., Saleeby, J., & Wong, M. (2016). Thermal evolution of the Sierra Nevada batholith, California, and implications for strain localization. *Geosphere*, *12*(2), 377-399.

Nelson, J. & Colpron, M. (2007). Tectonics and metallogeny of the British Columbia, Yukon and Alaskan Cordillera, 1.8 Ga to the present. *Mineral deposits of Canada: a synthesis of major deposit-types, district metallogeny, the evolution of geological provinces, and exploration methods: Geological Association of Canada, Mineral Deposits Division, Special Publication*, *5*, 755-791.

O'Driscoll, L. J., & Miller, M. S. (2015). Lithospheric discontinuity structure in Alaska, thickness variations determined by Sp receiver functions. *Tectonics*, *34*(4), 694-714.

Otiniano, G. A., Porter, T. J., Benowitz, J. A., Bindeman, I. N., Froese, D. G., Jensen, B. J., ... & Phillips, M. A. (2020). A late Miocene to late Pleistocene reconstruction of precipitation isotopes and climate from hydrated volcanic glass shards and biomarkers in central Alaska and Yukon. *Paleoceanography and Paleoclimatology*, *35*(7), e2019PA003791.

Parry, W. T., Bunds, M. P., Bruhn, R. L., Hall, C. M., & Murphy, J. M. (2001). Mineralogy, 40Ar/39Ar dating and apatite fission track dating of rocks along the Castle Mountain fault, Alaska. *Tectonophysics*, *337*(3-4), 149-172.

Pavlis, G. L., Bauer, M. A., Elliott, J. L., Koons, P., Pavlis, T. L., Ruppert, N., ... & Worthington, L. L. (2019). A unified three-dimensional model of the lithospheric structure at the subduction corner in southeast Alaska: Summary results from STEEP. *Geosphere*, *15*(2), 382-406.

Pavlis, T. L., Roeske, S. M., Ridgway, K. D., Trop, J. M., Glen, J. M. G., & O'Neill, J. M. (2007). The Border Ranges fault system, southern Alaska. *SPECIAL PAPERS-GEOLOGICAL SOCIETY OF AMERICA*, *431*, 95.

Pelletier, B., Calmant, S. and Pillet, R., 1998. Current tectonics of the Tonga–New Hebrides region. *Earth and Planetary Science Letters*, *164*(1-2), pp.263-276.

Philippon, M., & Corti, G. (2016). Obliquity along plate boundaries. *Tectonophysics*, *693*, 171-182.

Plafker, G. (1987). Regional geology and petroleum potential of the northern Gulf of Alaska continental margin.

Ramos, V. A., & Folguera, A. (2009). Andean flat-slab subduction through time. *Geological Society, London, Special Publications*, *327*(1), 31-54.

Ramos, V. A., Cristallini, E. O., & Pérez, D. J. (2002). The Pampean flat-slab of the Central Andes. *Journal of South American earth sciences*, *15*(1), 59-78.

Rasendra, N., Bonnin, M., Mazzotti, S., & Tiberi, C. (2014). Crustal and upper-mantle anisotropy related to fossilized transpression fabric along the Denali fault, northern Canadian Cordillera. *Bulletin of the Seismological Society of America*, *104*(4), 1964-1975.

Regan, S. P., Benowitz, J. A., & Holland, M. E. (2020). A plutonic brother from another magma mother: Disproving the Eocene Foraker-McGonagall pluton piercing point and implications for long-term slip on the Denali Fault. *Terra Nova*, *32*(1), 66-74.

Renne, P.R., Mundil, R., Balco, G., Min, K., and Ludwig, K.R., 2010, Joint determination of $^{40}K$ decay constants and $^{40}Ar/^{40}K$ for the Fish Canyon sanidine standard, and improved accuracy for $^{40}Ar/^{39}Ar$ geochronology: Geochimica et Cosmochimica Acta, v. 74, p. 5349.

Riccio, S.J., Fitzgerald, P.G., Benowitz, J.A. and Roeske, S.M., 2014. The role of thrust faulting in the formation of the eastern Alaska Range: Thermochronological constraints from the Susitna Glacier thrust fault region of the intracontinental strike-slip Denali fault system. *Tectonics*, *33*(11), pp.2195-2217.

Richter, D. H., Smith, J. G., Lanphere, M. A., Dalrymple, G. B., Reed, B. L., & Shew, N. (1990). Age and progression of volcanism, Wrangell volcanic field, Alaska. *Bulletin of Volcanology*, *53*(1), 29-44.

Ridgway, K. D., Thoms, E. E., Layer, P. W., Lesh, M. E., White, J. M., & Smith, S. V. (2007). Neogene transpressional foreland basin development on the north side of the central Alaska Range, Usibelli Group and Nenana Gravel, Tanana basin. *Special Paper of the Geological Society of America*, (431), 507-547.

Ridgway, K. D., Trop, J. M., & Finzel, E. S. (2011). Modification of continental forearc basins by flat-slab subduction processes: A case study from southern Alaska. *Tectonics of Sedimentary Basins: Recent Advances*, 327-346.

Ridgway, K. D., Trop, J. M., Nokleberg, W. J., Davidson, C. M., & Eastham, K. R. (2002). Mesozoic and Cenozoic tectonics of the eastern and central Alaska Range: Progressive basin development and deformation in a suture zone. *Geological Society of America Bulletin*, *114*(12), 1480-1504.

Roeske, S. M., Snee, L. W., Pavlis, T. L., & Sisson, V. B. (2003). Dextral-slip reactivation of an arc-forearc boundary during Late Cretaceous-early Eocene oblique convergence in the northern Cordillera. *SPECIAL PAPERS-GEOLOGICAL SOCIETY OF AMERICA*, 141-170.

Ruppert, N. A., Ridgway, K. D., Freymueller, J. T., Cross, R. S., & Hansen, R. A. (2008). Active tectonics of interior Alaska: Seismicity, GPS geodesy, and local geomorphology. *Washington DC American Geophysical Union Geophysical Monograph Series*, *179*, 109-133.

Saleeby, J. (2003). Segmentation of the Laramide slab—Evidence from the southern Sierra Nevada region. *Geological Society of America Bulletin*, *115*(6), 655-668.

Saltus, R. W., Hudson, T. L., Wilson, F. H., Ridgway, K. D., Trop, J. M., Glen, J. M. G., & O'Neill, J. M. (2007). The geophysical character of southern Alaska-Implications for crustal evolution. *SPECIAL PAPERS-GEOLOGICAL SOCIETY OF AMERICA*, *431*, 1.

Siame, L. L., Bellier, O., Sébrier, M., & Araujo, M. (2005). Deformation partitioning in flat subduction setting: Case of the Andean foreland of western Argentina (28 S–33 S). *Tectonics*, *24*(5).

Stout, J.H., 1976, Geology of the Eureka Creek area, east-central Alaska Range, State of Alaska, Department of Natural Resources, Division of Geological & Geophysical Surveys Geologic Report 46, 32 p., 1 sheet, scale 1:63,360.

Terhune, P.J., Benowitz, J.A., Trop, J.M., O'Sullivan, P.B., Gillis, R.J. and Freymueller, J.T., 2019. Cenozoic tectono-thermal history of the southern Talkeetna Mountains, Alaska: Insights into a potentially alternating convergent and transform plate margin. *Geosphere*, *15*(5), pp.1539-1576.

Tikoff, B., & de Saint Blanquat, M. (1997). Transpressional shearing and strike-slip partitioning in the Late Cretaceous Sierra Nevada magmatic arc, California. *Tectonics*, *16*(3), 442-459.

Tikoff, B., & Teyssier, C. (1992). Crustal-scale, en echelon" P-shear" tensional bridges: A possible solution to the batholithic room problem. *Geology*, *20*(10), 927-930.

Trop, J.M., Benowitz, J.A., Koepp, D.Q., Sunderlin, D., Brueseke, M.E., Layer, P.W. and Fitzgerald, P.G. (2020). Stitch in the ditch: Nutzotin Mountains (Alaska) fluvial strata and a dike record ca. 117–114 Ma accretion of Wrangellia with western North America and initiation of the Totschunda fault. *Geosphere*, *16*(1), pp.82-110.

Trop, J. M., Benowitz, J., Cole, R. B., & O'Sullivan, P. (2019). Cretaceous to Miocene magmatism, sedimentation, and exhumation within the Alaska Range suture zone: A polyphase reactivated terrane boundary. *Geosphere*, *15*(4), 1066-1101.

Trop, J. M., Ridgway, K. D., Glen, J. M. G., & O'Neill, J. M. (2007). Mesozoic and Cenozoic tectonic growth of southern Alaska: A sedimentary basin perspective. *Special Papers-Geological Society of America*, *431*, 55.

Twelker, E., Waldien, T.S., Newberry, R.J., Freeman, L.K., Sicard, K.R., Lande, L.L., Wypych, A., Reioux, D.A., and Bachmann, E.N. (2020). Bedrock geologic map of the eastern Denali Highway area, Mount Hayes, Healy, and Talkeetna Mountains quadrangles, Alaska. *Alaska Division of Geological & Geophysical Surveys Report of Investigation 2020-7*: 1 sheet, 1:100,000 scale. http://doi.org/10.14509/30469

Vermeesch, P. (2012). On the visualisation of detrital age distributions. *Chemical Geology*, *312*, 190-194.

Waldien, T. S., Roeske, S. M., Benowitz, J. A., Twelker, E., & Miller, M. S. (2020). Oligocene-Neogene lithospheric-scale reactivation of Mesozoic terrane accretionary structures in the Alaska Range suture zone, southern Alaska, USA. *GSA Bulletin*.

Waldien, T.S., Roeske, S.M., Benowitz, J.A., Allen, W.K., Ridgway, K.D. and O'Sullivan, P.B., 2018. Late Miocene to Quaternary evolution of the McCallum Creek thrust system, Alaska: Insights for range-boundary thrusts in transpressional orogens. *Geosphere*, *14*(6), pp.2379-2406.

Ward, K. M., & Lin, F. C. (2018). Lithospheric structure across the Alaskan cordillera from the joint inversion of surface waves and receiver functions. *Journal of Geophysical Research: Solid Earth*, *123*(10), 8780-8797.

Wech, A. G. (2016). Extending Alaska's plate boundary: Tectonic tremor generated by Yakutat subduction. *Geology*, *44*(7), 587-590.

Worthington, L.L., Van Avendonk, H.J.A., Gu- lick, S.P.S., Christeson, G.L., and Pavlis, T.L., 2012, Crustal structure of the Yakutat terrane and the evolution of subduction and collision in southern Alaska: Journal of Geophysical Research, v. 117, B01102, https://doi. org/10.1029/2011JB008493.

Wyld, S. J., Umhoefer, P. J., Wright, J. E., Haggart, J. W., Enkin, R. J., & Monger, J. W. H. (2006). Reconstructing northern Cordilleran terranes along known Cretaceous and Cenozoic strike-slip faults: Implications for the Baja British Columbia hypothesis and other models. *Paleogeography of the North American cordillera: Evidence for and against large-scale displacements: Geological Association of Canada Special Paper*, *46*, 277-298.

Ziwu, F.D., Doser, D.I. and Schinagel, S.M. (2020). A geophysical study of the Castle Mountain Fault, southcentral Alaska. *Tectonophysics*, *789*, p.228567.

## SUPPLEMENTS

### SUPPLEMENT S1: AFT laboratory procedures at Geosep Services

Apatite separates for all samples were obtained from crushed and separated material using standard gravimetric and magnetic mineral separation techniques. Apatite grain mounts were prepared by Paul O'Sullivan at the GeoSep Services (GSS) facilities in Moscow, Idaho. Spontaneous track counts and confined track length measurements were performed by Paul O'Sullivan using nonpolarized light at 2000x magnification. Laser ablation–inductively coupled plasma–mass spectrometer (LA-ICP-MS) analyses of samples used in age determinations were performed using the Element2 mass spectrometer located at the Washington State University School of Earth and Environmental Sciences GeoAnalytical Laboratory in Pullman, Washington.

A general discussion of the methods undertaken to process and analyze samples by GSS is presented below; see Donelick et al. (2005) for a complete and detailed discussion of these methods and their justification. For each sample subjected to apatite fission-track analysis (AFT), at least one 1cm$^2$ grain mount, consisting of apatite grains immersed in epoxy resin, was prepared, cured at 90°C for 1 hour, and polished to expose internal surfaces of the apatite grains. After polishing, mounts were immersed in 5.5N $HNO_3$ for 20.0 seconds (± 0.5 seconds) at 21°C (± 1°C) to reveal all natural fission tracks that intersected the polished grain surfaces.

The feasibility of measurement of apatite fission-track grain ages was assessed by scanning the polished and etched grain mount to determine if any dateable apatite grains were present. Measurement of fission-track parameters was considered feasible if more than one dateable grain was observed.

Representative kinetic parameters (*D*par—the maximum diameter of fission track etch pits at their intersection with the polished and etched, c-axis-parallel apatite surface, which is used as a

proxy for the solubility of fission tracks in their host apatite grains) were measured and spontaneous (natural) fission-track densities were counted for each grain considered suitable for dating. Between one and four etch pit diameters were measured and an arithmetic mean *D*par value was calculated for each datable grain.

**LA-ICP-MS Analysis**

Grains were then revisited using the LA-ICP-MS to make spot analyses to determine U, Th, and Sm concentrations of each grain for which natural fission-track densities had been previously determined. A single stationary spot of 16 μm diameter was used for each grain, centered in the approximate center of the area where tracks had been counted. Note that if optical examination suggested that natural track densities were even moderately inconsistent within a grain, which is evidence of U zoning, that grain was not dated.

For apatite, the fundamental assumption is made that Ca occurs in stoichiometric amounts in all grains analyzed. The isotope $^{43}$Ca is used as the indicator of the volume of apatite ablated. Samples were ablated in a helium atmosphere to reduce condensation and elemental fractionation. A total of 30 scans for $^{238}$U, $^{232}$Th, $^{147}$Sm, and $^{43}$Ca were performed for each spot analyzed. Of these scans, approximately 10 were performed while the laser was warming up and blocked from contacting the grain surface, during which time background counts were collected. Once the laser was permitted to hit the grain surface, a cylindrical pit was excavated to a depth beyond which uranium did not contribute fission tracks to the etched grain surface. Between 15 and 20 scans performed during pit excavation were required to reach this depth. The depths of a representative number of laser pits were measured and the $^{238}$U/$^{43}$Ca value for each pit as a whole was determined based on the weighted mean of the $^{238}$U/$^{43}$Ca value for individual scans relative

to the depths from which the ablated material was derived (see Hasebe et al. 2004; Donelick et al. 2005).

**Fission-Track Age Measurement**

Fission-track ages and errors were calculated using: (a) the ratio of the density of natural fission tracks present in the grain to the amount of $^{238}U$ present and (b) a modified version of the radioactive decay equation that includes a LA-ICP-MS zeta calibration factor (see equations 1b for age equation and 2b for error calculation in Donelick et al. 2005). The zeta calibration factor is determined for each sample analyzed during each LA-ICP-MS session by analyzing the U:Ca ratio of apatite calibration standards with known ages at the beginning and end of each LA-ICP-MS session. The standard used are Durango apatite, 30.6 ± 0.3 Ma.

Calculation of a single pooled AFT age for each sample takes into account the distribution of all of the individual grain ages and their uncertainties, which are a function of the number of spontaneous tracks counted over a known area, the U content determined by LA-ICP-MS, and thermal history. Only pooled ages are reported as these incorporate original track counts and isotopic values for each grain, and therefore are most representative of the original data generated for each sample, even when multiple grain-age populations might be present as suggested by the $Chi^2$ value.

## SUPPLEMENT 2: Apatite fission track data

### Table S2-1 dAFT sample locations

| Catchment | Lat [ºN] | Long [ºE] |
|---|---|---|
| Robertson River | 63.4964 | -143.8366 |
| Upper Susitna River | 63.1045 | -147.5173 |
| Delta River | 63.6727 | -145.9079 |
| Nenana River | 63.7510 | -148.9080 |
| Little Tok River | 63.0447 | -143.3675 |
| Tok River | 63.0787 | -143.4033 |
| Ann Creek | 63.3357 | -145.7671 |
| Eureka Glacier | 63.2986 | -146.3554 |
| Maclaren Glacier | 63.2732 | -146.5182 |
| Mid Maclaren River | 63.2958 | -146.7487 |
| East Maclaren River | 63.2703 | -146.7781 |
| Maclaren Bridge | 63.1176 | -146.5326 |

### Table S2-2: Detrital Apatite fission-track data

**Ann Creek**

| Spot Name | FT Age (Ma) | 1sig (Ma) | UPb Age (Ma) | 2 sig (Ma) | Ns | Area cm^2 | U/Ca | 1sig | Etch Figs. | Dpar (um) | Dper (um) | [U] (ppm) | [Th] (ppm) | [Sm] (ppm) |
|---|---|---|---|---|---|---|---|---|---|---|---|---|---|---|
| 4391A_26 | 0.0 | 18725.5 | 0.0 | 0 | 0 | 0.0000 1 | 0.00 | 0.0 0 | 1 | 1.64 | 0.30 | 0.0 | 0.0 | 0.1 |
| 4391A_79 | 0.0 | 9.6 | 0.0 | 0 | 0 | 0.0000 3 | 0.02 | 0.0 0 | 1 | 1.93 | 0.30 | 0.0 | 0.0 | 0.1 |
| 4391A_42 | 0.0 | 18.1 | 0.0 | 0 | 0 | 0.0000 2 | 0.02 | 0.0 0 | 1 | 1.81 | 0.37 | 0.0 | 0.0 | 0.0 |
| 4391A_37 | 0.0 | 44.4 | 0.0 | 0 | 0 | 0.0000 2 | 0.01 | 0.0 0 | 1 | 1.40 | 0.41 | 0.0 | 0.3 | 0.2 |
| 4391A_22 | 0.0 | 61.8 | 0.0 | 0 | 0 | 0.0000 2 | 0.00 | 0.0 0 | 1 | 1.64 | 0.23 | 0.0 | 4.3 | 28.8 |
| 4391A_11 | 0.0 | 4.2 | 0.0 | 0 | 0 | 0.0000 3 | 0.04 | 0.0 0 | 2 | 1.56 | 0.35 | 0.1 | 0.1 | 8.9 |
| 4391A_89 | 0.0 | 530.6 | 0.0 | 0 | 0 | 0.0000 3 | 0.00 | 0.0 0 | 1 | 1.84 | 0.43 | 0.1 | 0.5 | 7.9 |
| 4391A_17 | 0.0 | 49.9 | 0.0 | 0 | 0 | 0.0000 3 | 0.00 | 0.0 0 | 1 | 1.81 | 0.35 | 0.1 | 0.0 | 3.7 |
| 4391A_43 | 0.0 | 175.0 | 0.0 | 0 | 0 | 0.0000 3 | 0.00 | 0.0 0 | 1 | 1.85 | 0.29 | 0.1 | 0.1 | 6.3 |
| 4391A_65 | 0.0 | 192.6 | 0.0 | 0 | 0 | 0.0000 3 | 0.00 | 0.0 0 | 1 | 1.36 | 0.36 | 0.2 | 13.9 | 10.4 |
| 4391A_2 | 0.0 | 128.7 | 0.0 | 0 | 0 | 0.0000 5 | 0.00 | 0.0 0 | 1 | 1.65 | 0.28 | 0.2 | 0.1 | 7.8 |
| 4391A_66 | 0.0 | 116.6 | 0.0 | 0 | 0 | 0.0000 2 | 0.00 | 0.0 0 | 2 | 1.68 | 0.28 | 0.4 | 1.2 | 37.2 |
| 4391A_68 | 0.0 | 43.5 | 0.0 | 0 | 0 | 0.0000 4 | 0.00 | 0.0 0 | 1 | 1.55 | 0.23 | 0.4 | 0.2 | 39.0 |
| 4391A_1 | 0.0 | 84.3 | 356.4 | 501 | 0 | 0.0000 3 | 0.00 | 0.0 0 | 1 | 1.26 | 0.30 | 0.5 | 3.3 | 32.9 |
| 4391A_15 | 0.0 | 12.1 | 0.0 | 0 | 0 | 0.0000 2 | 0.03 | 0.0 0 | 1 | 1.76 | 0.30 | 0.6 | 1.2 | 2.7 |
| 4391A_87 | 0.0 | 14.2 | 0.0 | 0 | 0 | 0.0000 2 | 0.02 | 0.0 0 | 1 | 1.72 | 0.35 | 0.7 | 18.6 | 8.6 |
| 4391A_82 | 0.0 | 71.6 | 0.0 | 0 | 0 | 0.0000 2 | 0.00 | 0.0 0 | 1 | 1.70 | 0.59 | 0.7 | 6.3 | 9.3 |
| 4391A_86 | 0.0 | 53.2 | 146.4 | 451 | 0 | 0.0000 2 | 0.01 | 0.0 0 | 1 | 1.68 | 0.25 | 1.0 | 5.8 | 61.2 |

| | | | | | | | | | | | | | | |
|---|---|---|---|---|---|---|---|---|---|---|---|---|---|---|
| 4391A_13 | 0.0 | 29.6 | 286.9 | 570 | 0 | 0.0000 3 | 0.01 | 0.0 0 | 3 | 1.67 | 0.32 | 1.4 | 4.5 | 36.8 |
| 4391A_64 | 0.0 | 70.5 | 0.0 | 0 | 0 | 0.0000 3 | 0.00 | 0.0 0 | 1 | 1.80 | 0.22 | 1.7 | 5.6 | 10.5 |
| 4391A_90 | 0.0 | 31.6 | 217.7 | 262 | 0 | 0.0000 2 | 0.01 | 0.0 0 | 1 | 1.83 | 0.32 | 1.8 | 1.6 | 27.3 |
| 4391A_39 | 0.0 | 18.1 | 0.0 | 0 | 0 | 0.0000 2 | 0.01 | 0.0 0 | 1 | 1.69 | 0.27 | 2.1 | 61.9 | 19.4 |
| 4391A_67 | 0.0 | 15.4 | 498.9 | 284 | 0 | 0.0000 3 | 0.01 | 0.0 0 | 1 | 1.64 | 0.39 | 2.7 | 10.4 | 194.0 |
| 4391A_28 | 0.0 | 11.6 | 0.0 | 0 | 0 | 0.0000 3 | 0.01 | 0.0 0 | 1 | 2.06 | 0.31 | 2.9 | 12.0 | 59.5 |
| 4391A_35 | 0.0 | 0.7 | 0.0 | 0 | 0 | 0.0000 2 | 0.38 | 0.0 8 | 1 | 1.71 | 0.36 | 3.0 | 43.9 | 8.4 |
| 4391A_62 | 0.0 | 21.4 | 245.4 | 245 | 0 | 0.0000 2 | 0.02 | 0.0 0 | 1 | 2.01 | 0.36 | 3.2 | 9.5 | 71.6 |
| 4391A_33 | 0.0 | 9.8 | 0.0 | 0 | 0 | 0.0000 2 | 0.03 | 0.0 0 | 1 | 1.52 | 0.26 | 3.6 | 14.1 | 6.1 |
| 4391A_24 | 0.0 | 3.9 | 0.0 | 0 | 0 | 0.0000 2 | 0.06 | 0.0 1 | 1 | 1.58 | 0.20 | 4.1 | 10.5 | 196.2 |
| 4391A_21 | 0.0 | 23.4 | 168.4 | 166 | 0 | 0.0000 1 | 0.03 | 0.0 0 | 2 | 1.77 | 0.32 | 5.4 | 6.2 | 34.8 |
| 4391A_72 | 0.0 | 2.4 | 0.0 | 0 | 0 | 0.0000 2 | 0.12 | 0.0 1 | 1 | 1.83 | 0.30 | 16.2 | 27.7 | 26.3 |
| 4391A_36 | 0.0 | 3.1 | 0.0 | 0 | 0 | 0.0000 2 | 0.10 | 0.0 1 | 1 | 1.74 | 0.35 | 20.7 | 144.1 | 9.1 |
| 4391A_97 | 4.0 | 4.0 | 100.5 | 114 | 1 | 0.0000 4 | 0.05 | 0.0 0 | 2 | 1.85 | 0.30 | 9.7 | 30.1 | 82.4 |
| 4391A_7 | 4.1 | 4.1 | 0.0 | 0 | 1 | 0.0000 5 | 0.04 | 0.0 0 | 1 | 1.89 | 0.23 | 0.2 | 0.8 | 3.8 |
| 4391A_104 | 4.4 | 2.2 | 0.0 | 0 | 4 | 0.0000 3 | 0.22 | 0.0 1 | 2 | 1.71 | 0.32 | 40.5 | 412.2 | 159.5 |
| 4391A_85 | 5.4 | 5.4 | 107.6 | 345 | 1 | 0.0000 3 | 0.05 | 0.0 0 | 1 | 1.72 | 0.46 | 8.4 | 28.0 | 53.5 |
| 4391A_103 | 6.0 | 4.2 | 61.1 | 61 | 2 | 0.0000 1 | 0.23 | 0.0 0 | 1 | 1.74 | 0.23 | 45.4 | 4.3 | 52.2 |
| 4391A_105 | 6.3 | 6.3 | 109.7 | 64 | 1 | 0.0000 2 | 0.06 | 0.0 0 | 2 | 1.81 | 0.53 | 13.3 | 36.0 | 97.4 |
| 4391A_54 | 6.6 | 4.6 | 179.1 | 161 | 2 | 0.0000 2 | 0.14 | 0.0 0 | 2 | 1.98 | 0.42 | 30.2 | 25.1 | 71.1 |
| 4391A_92 | 6.7 | 6.7 | 194.0 | 404 | 1 | 0.0000 3 | 0.04 | 0.0 0 | 1 | 1.91 | 0.33 | 8.2 | 36.6 | 87.1 |
| 4391A_32 | 7.8 | 7.8 | 0.0 | 0 | 1 | 0.0000 2 | 0.06 | 0.0 0 | 2 | 1.47 | 0.23 | 8.4 | 38.3 | 17.9 |
| 4391A_30 | 8.3 | 8.3 | 122.0 | 100 | 1 | 0.0000 2 | 0.04 | 0.0 0 | 2 | 1.88 | 0.25 | 8.2 | 20.7 | 37.3 |
| 4391A_96 | 9.2 | 4.1 | 0.0 | 0 | 5 | 0.0000 2 | 0.22 | 0.0 1 | 2 | 1.60 | 0.22 | 142.6 | 4.8 | 65.1 |
| 4391A_73 | 9.2 | 6.5 | 0.0 | 0 | 2 | 0.0000 2 | 0.09 | 0.0 1 | 1 | 1.70 | 0.30 | 3.5 | 6.0 | 25.6 |
| 4391A_58 | 10.4 | 10.4 | 0.0 | 0 | 1 | 0.0000 5 | 0.02 | 0.0 0 | 2 | 1.44 | 0.30 | 0.0 | 0.0 | 0.2 |
| 4391A_76 | 10.6 | 5.3 | 116.3 | 44 | 4 | 0.0000 2 | 0.13 | 0.0 0 | 3 | 1.53 | 0.29 | 27.1 | 54.8 | 40.8 |
| 4391A_29 | 10.8 | 7.6 | 131.7 | 89 | 2 | 0.0000 1 | 0.11 | 0.0 0 | 1 | 1.65 | 0.30 | 20.9 | 27.9 | 72.0 |
| 4391A_48 | 11.0 | 5.5 | 195.2 | 550 | 4 | 0.0000 2 | 0.15 | 0.0 0 | 3 | 1.56 | 0.31 | 30.5 | 123.0 | 100.5 |
| 4391A_57 | 11.5 | 8.1 | 354.5 | 281 | 2 | 0.0000 4 | 0.04 | 0.0 0 | 2 | 1.80 | 0.59 | 7.2 | 15.5 | 22.6 |
| 4391A_8 | 11.5 | 11.5 | 249.1 | 304 | 1 | 0.0000 2 | 0.04 | 0.0 0 | 2 | 1.98 | 0.34 | 8.4 | 19.7 | 121.2 |
| 4391A_83 | 12.4 | 3.5 | 0.0 | 0 | 13 | 0.0000 4 | 0.22 | 0.0 1 | 4 | 1.90 | 0.41 | 276.6 | 850.6 | 496.8 |
| 4391A_47 | 13.3 | 13.3 | 77.4 | 918 | 1 | 0.0000 2 | 0.03 | 0.0 0 | 2 | 1.71 | 0.34 | 6.7 | 19.8 | 59.5 |
| 4391A_46 | 13.4 | 13.4 | 490.2 | 380 | 1 | 0.0000 2 | 0.03 | 0.0 0 | 1 | 1.24 | 0.35 | 4.7 | 53.7 | 118.6 |
| 4391A_84 | 14.7 | 14.7 | 181.3 | 219 | 1 | 0.0000 1 | 0.05 | 0.0 0 | 1 | 1.48 | 0.25 | 9.6 | 40.5 | 98.3 |
| 4391A_102 | 14.7 | 8.5 | 0.0 | 0 | 3 | 0.0000 2 | 0.09 | 0.0 1 | 2 | 1.76 | 0.37 | 11.8 | 168.7 | 371.2 |
| 4391A_19 | 15.3 | 10.8 | 376.0 | 152 | 2 | 0.0000 3 | 0.04 | 0.0 0 | 2 | 1.85 | 0.37 | 6.7 | 10.9 | 87.1 |

| | | | | | | | | | | | | | | |
|---|---|---|---|---|---|---|---|---|---|---|---|---|---|---|
| | | | | | | 0.0000 | | 0.0 | | | | | | |
| 4391A_69 | 15.5 | 11.0 | 426.7 | 595 | 2 | 5 | 0.02 | 0 | 1 | 1.70 | 0.29 | 4.5 | 10.3 | 63.0 |
| | | | | | | 0.0000 | | 0.0 | | | | | | |
| 4391A_44 | 15.7 | 11.1 | 124.5 | 71 | 2 | 2 | 0.05 | 0 | 2 | 1.68 | 0.46 | 10.8 | 25.2 | 60.8 |
| | | | | | | 0.0000 | | 0.0 | | | | | | |
| 4391A_49 | 16.8 | 11.9 | 334.2 | 188 | 2 | 2 | 0.04 | 0 | 2 | 1.44 | 0.40 | 8.6 | 28.2 | 49.2 |
| | | | | | | 0.0000 | | 0.0 | | | | | | |
| 4391A_12 | 16.9 | 9.8 | 164.4 | 186 | 3 | 3 | 0.04 | 0 | 2 | 2.20 | 0.46 | 8.3 | 26.8 | 73.3 |
| | | | | | | 0.0000 | | 0.0 | | | | | | |
| 4391A_60 | 17.3 | 17.3 | 0.0 | 0 | 1 | 3 | 0.02 | 0 | 1 | 1.52 | 0.21 | 0.0 | 0.2 | 3.0 |
| | | | | | | 0.0000 | | 0.0 | | | | | | |
| 4391A_45 | 17.4 | 12.3 | 134.0 | 95 | 2 | 2 | 0.04 | 0 | 1 | 1.47 | 0.38 | 8.2 | 29.4 | 69.4 |
| | | | | | | 0.0000 | | 0.0 | | | | | | |
| 4391A_88 | 17.8 | 12.6 | 99.1 | 103 | 2 | 2 | 0.04 | 0 | 2 | 1.72 | 0.30 | 8.4 | 31.7 | 42.5 |
| | | | | | | 0.0000 | | 0.0 | | | | | | |
| 4391A_9 | 18.7 | 8.5 | 0.0 | 0 | 5 | 2 | 0.11 | 1 | 3 | 1.84 | 0.34 | 15.1 | 67.5 | 108.7 |
| | | | | | | 0.0000 | | 0.0 | | | | | | |
| 4391A_59 | 18.8 | 10.9 | 0.0 | 0 | 3 | 1 | 0.09 | 0 | 2 | 1.21 | 0.29 | 18.4 | 27.9 | 38.9 |
| | | | | | | 0.0000 | | 0.0 | | | | | | |
| 4391A_53 | 20.5 | 11.8 | 131.2 | 184 | 3 | 4 | 0.03 | 0 | 2 | 1.82 | 0.39 | 6.2 | 11.7 | 63.4 |
| | | | | | | 0.0000 | | 0.0 | | | | | | |
| 4391A_93 | 23.0 | 13.6 | 0.0 | 0 | 3 | 2 | 0.05 | 1 | 2 | 2.25 | 0.41 | 11.3 | 206.5 | 223.8 |
| | | | | | | 0.0000 | | 0.0 | | | | | ##### | |
| 4391A_14 | 23.2 | 16.5 | 140.1 | 548 | 2 | 1 | 0.06 | 0 | 3 | 1.32 | 0.28 | 500.3 | # | 105.6 |
| | | | | | | 0.0000 | | 0.0 | | | | | | |
| 4391A_78 | 23.5 | 6.9 | 241.0 | 274 | 12 | 3 | 0.12 | 1 | 3 | 1.94 | 0.35 | 6.3 | 31.4 | 53.3 |
| | | | | | | 0.0000 | | 0.0 | | | | | | |
| 4391A_10 | 23.7 | 13.7 | 409.2 | 496 | 3 | 3 | 0.03 | 0 | 2 | 1.68 | 0.46 | 6.1 | 20.6 | 37.2 |
| | | | | | | 0.0000 | | 0.0 | | | | | | |
| 4391A_71 | 23.9 | 16.9 | 0.0 | 0 | 2 | 3 | 0.02 | 0 | 2 | 1.58 | 0.24 | 4.5 | 14.8 | 73.3 |
| | | | | | | 0.0000 | | 0.0 | | | | | | |
| 4391A_94 | 24.3 | 9.9 | 296.4 | 80 | 6 | 2 | 0.12 | 0 | 4 | 2.21 | 0.55 | 25.4 | 110.7 | 157.4 |
| | | | | | | 0.0000 | | 0.0 | | | | | | |
| 4391A_51 | 24.5 | 24.5 | 681.6 | 978 | 1 | 2 | 0.02 | 0 | 1 | 1.94 | 0.28 | 3.3 | 19.7 | 60.8 |
| | | | | | | 0.0000 | | 0.0 | | | | | | |
| 4391A_77 | 25.4 | 14.7 | 274.4 | 325 | 3 | 3 | 0.03 | 0 | 3 | 1.99 | 0.32 | 5.9 | 19.4 | 27.9 |
| | | | | | | 0.0000 | | 0.0 | | | | | | |
| 4391A_18 | 25.8 | 18.2 | 233.5 | 247 | 2 | 2 | 0.03 | 0 | 1 | 1.66 | 0.24 | 6.5 | 18.6 | 48.3 |
| | | | | | | 0.0000 | | 0.0 | | | | | | |
| 4391A_61 | 26.7 | 12.0 | 377.8 | 229 | 5 | 2 | 0.06 | 0 | 4 | 2.01 | 0.52 | 12.9 | 63.3 | 217.3 |
| | | | | | | 0.0000 | | 0.0 | | | | | | |
| 4391A_55 | 31.0 | 21.9 | 0.0 | 0 | 2 | 2 | 0.03 | 0 | 3 | 1.21 | 0.32 | 1.7 | 32.0 | 21.9 |
| | | | | | | 0.0000 | | 0.0 | | | | | | |
| 4391A_56 | 31.8 | 15.9 | 175.5 | 155 | 4 | 2 | 0.04 | 0 | 3 | 1.59 | 0.41 | 8.8 | 11.5 | 94.4 |
| | | | | | | 0.0000 | | 0.0 | | | | | | |
| 4391A_100 | 31.9 | 18.4 | 163.6 | 188 | 3 | 4 | 0.02 | 0 | 4 | 2.01 | 0.60 | 3.7 | 12.4 | 37.7 |
| | | | | | | 0.0000 | | 0.0 | | | | | | |
| 4391A_38 | 32.5 | 23.0 | 272.4 | 135 | 2 | 2 | 0.03 | 0 | 1 | 1.76 | 0.29 | 5.7 | 23.6 | 218.2 |
| | | | | | | 0.0000 | | 0.0 | | | | | | |
| 4391A_31 | 33.1 | 23.4 | 189.1 | 144 | 2 | 3 | 0.01 | 0 | 1 | 1.72 | 0.22 | 2.5 | 14.1 | 251.4 |
| | | | | | | 0.0000 | | 0.0 | | | | | | |
| 4391A_75 | 34.9 | 24.7 | 202.8 | 335 | 2 | 3 | 0.02 | 0 | 1 | 1.80 | 0.53 | 3.3 | 0.5 | 11.9 |
| | | | | | | 0.0000 | | 0.0 | | | | | | |
| 4391A_95 | 34.9 | 24.9 | 0.0 | 0 | 2 | 2 | 0.02 | 0 | 2 | 1.71 | 0.40 | 0.1 | 0.2 | 0.6 |
| | | | | | | 0.0000 | | 0.0 | | | | | | |
| 4391A_52 | 38.3 | 27.1 | 400.7 | 189 | 2 | 1 | 0.04 | 0 | 1 | 2.12 | 0.38 | 7.3 | 49.3 | 269.5 |
| | | | | | | 0.0000 | | 0.0 | | | | | | |
| 4391A_74 | 40.4 | 28.7 | 0.0 | 0 | 2 | 2 | 0.02 | 0 | 1 | 1.99 | 0.25 | 1.5 | 6.8 | 40.9 |
| | | | | | | 0.0000 | | 0.0 | | | | | | |
| 4391A_3 | 41.1 | 10.8 | 0.0 | 0 | 15 | 2 | 0.13 | 1 | 4 | 2.18 | 0.41 | 17.4 | 117.8 | 114.7 |
| | | | | | | 0.0000 | | 0.0 | | | | | | |
| 4391A_16 | 42.3 | 42.3 | 0.0 | 0 | 1 | 5 | 0.00 | 0 | 1 | 2.33 | 0.43 | 0.0 | 0.1 | 9.3 |
| | | | | | | 0.0000 | | 0.0 | | | | | | |
| 4391A_25 | 48.0 | 48.1 | 0.0 | 0 | 1 | 1 | 0.01 | 0 | 1 | 1.72 | 0.34 | 1.9 | 14.0 | 93.6 |
| | | | | | | 0.0000 | | 0.0 | | | | | | |
| 4391A_98 | 52.0 | 36.8 | 144.4 | 314 | 2 | 2 | 0.02 | 0 | 2 | 2.20 | 0.31 | 4.3 | 12.1 | 63.0 |
| | | | | | | 0.0000 | | 0.0 | | | | | | |
| 4391A_63 | 57.0 | 40.4 | 297.9 | 414 | 2 | 4 | 0.01 | 0 | 2 | 1.94 | 0.37 | 1.5 | 6.4 | 38.0 |
| | | | | | | 0.0000 | | 0.0 | | | | | | |
| 4391A_40 | 58.8 | 58.8 | 47.8 | 535 | 1 | 3 | 0.00 | 0 | 1 | 1.31 | 0.30 | 0.9 | 5.8 | 41.3 |
| | | | | | | 0.0000 | | 0.0 | | | | | | |
| 4391A_5 | 78.0 | 39.1 | 426.9 | 290 | 4 | 2 | 0.02 | 0 | 3 | 2.08 | 0.41 | 4.2 | 26.7 | 200.9 |
| | | | | | | 0.0000 | | 0.0 | | | | | | |
| 4391A_20 | 79.8 | 56.4 | 242.5 | 234 | 2 | 1 | 0.03 | 0 | 2 | 1.81 | 0.25 | 4.7 | 7.5 | 75.0 |

| | | | | | | | | | | | | | | |
|---|---|---|---|---|---|---|---|---|---|---|---|---|---|---|
| 4391A_4 | 83.8 | 83.9 | 417.4 | 828 | 1 | 0.0000 2 | 0.00 | 0.0 0 | 1 | 1.81 | 0.55 | 0.8 | 8.0 | 106.1 |
| 4391A_81 | 92.0 | 53.2 | 0.0 | 0 | 3 | 0.0000 4 | 0.01 | 0.0 0 | 3 | 1.97 | 0.35 | 1.5 | 6.0 | 40.8 |
| 4391A_70 | 96.5 | 68.3 | 0.0 | 0 | 2 | 0.0000 2 | 0.01 | 0.0 0 | 1 | 2.01 | 0.49 | 1.5 | 3.4 | 37.0 |
| 4391A_101 | 97.0 | 68.8 | 0.0 | 0 | 2 | 0.0000 2 | 0.01 | 0.0 0 | 2 | 1.82 | 0.29 | 1.7 | 6.6 | 52.6 |
| 4391A_50 | 98.5 | 37.3 | 371.2 | 598 | 7 | 0.0000 2 | 0.02 | 0.0 0 | 3 | 2.58 | 0.57 | 4.9 | 19.9 | 247.5 |
| 4391A_23 | 101.3 | 50.7 | 893.3 | #### | 4 | 0.0000 2 | 0.01 | 0.0 0 | 2 | 1.47 | 0.30 | 2.7 | 11.1 | 34.1 |
| 4391A_6 | 104.7 | 60.5 | 542.0 | 550 | 3 | 0.0000 2 | 0.01 | 0.0 0 | 2 | 1.65 | 0.44 | 2.9 | 14.7 | 90.1 |
| 4391A_34 | 123.9 | 62.1 | 120.2 | 229 | 4 | 0.0000 3 | 0.01 | 0.0 0 | 2 | 2.21 | 0.79 | 1.6 | 6.5 | 41.1 |
| 4391A_41 | 131.3 | 93.0 | 0.0 | 0 | 2 | 0.0000 2 | 0.01 | 0.0 0 | 2 | 1.71 | 0.38 | 0.9 | 5.2 | 3.6 |
| 4391A_91 | 162.1 | 79.9 | 0.0 | 0 | 5 | 0.0000 2 | 0.01 | 0.0 0 | 3 | 2.12 | 0.46 | 1.9 | 166.2 | 164.7 |
| 4391A_80 | 214.9 | 215.2 | 0.0 | 0 | 1 | 0.0000 1 | 0.00 | 0.0 0 | 1 | 1.82 | 0.24 | 0.5 | 0.6 | 135.0 |
| 4391A_99 | 344.0 | 345.5 | 0.0 | 0 | 1 | 0.0000 2 | 0.00 | 0.0 0 | 2 | 1.48 | 0.28 | 0.1 | 0.2 | 1.8 |
| 4391A_27 | 1179.9 | 1183.2 | 0.0 | 0 | 1 | 0.0000 1 | 0.00 | 0.0 0 | 1 | 1.50 | 0.31 | 0.1 | 5.0 | 7.5 |

**Delta River**

| Spot Name | FT Age (Ma) | 1s Symm (Ma) | UPb Age (Ma) | 2 sigma (Ma) | Ns | Area cm^2 | U/Catio n | +/- 1sig | Etch Figs. | Dpar (um) | Dper (um) | [U] (ppm ) | [Th] (ppm) | [Sm] (ppm) |
|---|---|---|---|---|---|---|---|---|---|---|---|---|---|---|
| 03917A_2 | 0.0 | 488.0 | 0.0 | 0 | 0 | 0.0000 3 | 0.00 | 0.0 0 | 1 | 2.13 | 0.29 | 0.0 | 0.0 | 7.0 |
| 03917A_5 | 0.0 | 281.0 | 0.0 | 0 | 1 | 0.0000 5 | 0.00 | 0.0 0 | 1 | 2.31 | 0.58 | 0.0 | 0.0 | 4.0 |
| 03917A_7 | 0.0 | 3.6 | 29.5 | 53 | 0 | 0.0000 3 | 0.08 | 0.0 0 | 1 | 1.99 | 0.48 | 20.0 | 83.0 | 182.0 |
| 03917A_18 | 0.0 | 2.4 | 0.0 | 0 | 0 | 0.0000 1 | 0.26 | 0.0 8 | 1 | 1.78 | 0.33 | 1.0 | 46.0 | 36.0 |
| 03917A_22 | 0.0 | 23.0 | 0.0 | 0 | 3 | 0.0000 1 | 0.07 | 0.0 1 | 2 | 2.28 | 0.46 | 19.0 | 54.0 | 26.0 |
| 03917A_23 | 0.0 | 14.6 | 0.0 | 0 | 0 | 0.0000 1 | 0.04 | 0.0 2 | 1 | 2.12 | 0.38 | 2.0 | 248.0 | 194.0 |
| 03917A_27 | 0.0 | 351.1 | 0.0 | 0 | 0 | 0.0000 2 | 0.00 | 0.0 0 | 1 | 2.46 | 0.50 | 0.0 | 8.0 | 8.0 |
| 03917A_51 | 0.0 | 2267.1 | 0.0 | 0 | 0 | 0.0000 2 | 0.00 | 0.0 0 | 1 | 2.40 | 0.51 | 0.0 | 1.0 | 86.0 |
| 03917A_56 | 0.0 | 886.2 | 0.0 | 0 | 0 | 0.0000 2 | 0.00 | 0.0 0 | 1 | 1.67 | 0.26 | 0.0 | 0.0 | 3.0 |
| 03917A_60 | 0.0 | 746.2 | 0.0 | 0 | 0 | 0.0000 2 | 0.00 | 0.0 0 | 1 | 1.72 | 0.41 | 0.0 | 0.0 | 5.0 |
| 03917A_61 | 0.0 | 133.3 | 0.0 | 0 | 0 | 0.0000 2 | 0.00 | 0.0 0 | 1 | 1.63 | 0.41 | 1.0 | 49.0 | 103.0 |
| 03917A_63 | 0.0 | 751.6 | 0.0 | 0 | 0 | 0.0000 1 | 0.00 | 0.0 0 | 1 | 1.70 | 0.30 | 0.0 | 0.0 | 5.0 |
| 03917A_73 | 0.0 | 199.7 | 696.0 | #### | 0 | 0.0000 1 | 0.01 | 0.0 0 | 1 | 1.57 | 0.28 | 1.0 | 6.0 | 163.0 |
| 03917A_74 | 0.0 | 29.0 | 0.0 | 0 | 0 | 0.0000 2 | 0.01 | 0.0 0 | 1 | 2.46 | 0.57 | 3.0 | 161.0 | 126.0 |
| 03917A_75 | 0.0 | 249.4 | 0.0 | 0 | 0 | 0.0000 3 | 0.00 | 0.0 0 | 1 | 2.15 | 0.31 | 0.0 | 1.0 | 6.0 |
| 03917A_78 | 0.0 | 676.7 | 0.0 | 0 | 0 | 0.0000 2 | 0.00 | 0.0 0 | 1 | 1.85 | 0.57 | 0.0 | 0.0 | 6.0 |
| 03917A_80 | 0.0 | 1846.6 | 0.0 | 0 | 0 | 0.0000 2 | 0.00 | 0.0 0 | 1 | 1.92 | 0.45 | 0.0 | 0.0 | 1.0 |
| 03917A_84 | 0.0 | 6.7 | 75.2 | 98 | 0 | 0.0000 1 | 0.09 | 0.0 0 | 1 | 2.13 | 0.41 | 19.0 | 4.0 | 82.0 |
| 03917A_86 | 0.0 | 7.1 | 85.4 | 167 | 0 | 0.0000 3 | 0.04 | 0.0 0 | 1 | 2.18 | 0.53 | 7.0 | 27.0 | 166.0 |
| 03917A_87 | 0.0 | 588.8 | 0.0 | 0 | 0 | 0.0000 3 | 0.00 | 0.0 0 | 1 | 2.31 | 0.50 | 0.0 | 1.0 | 4.0 |

| | | | | | | | | | | | | | | |
|---|---|---|---|---|---|---|---|---|---|---|---|---|---|---|
| | | | | | | 0.0000 | | 0.0 | | | | | | |
| 03917A_88 | 0.0 | 605.4 | 0.0 | 0 | 0 | 5 | 0.00 | 0 | 1 | 2.07 | 0.51 | 0.0 | 0.0 | 50.0 |
| | | | | | | 0.0000 | | 0.0 | | | | | | |
| 03917A_91 | 0.0 | 18.0 | 72.4 | 112 | 0 | 1 | 0.05 | 0 | 1 | 1.39 | 0.41 | 11.0 | 42.0 | 194.0 |
| | | | | | | 0.0000 | | 0.0 | | | | | | |
| 03917A_96 | 0.0 | 11.8 | 56.0 | 112 | 0 | 2 | 0.03 | 0 | 1 | 2.07 | 0.27 | 7.0 | 25.0 | 121.0 |
| 03917A_10 | | | | | | 0.0000 | | 0.0 | | | | | | |
| 1 | 0.0 | 308.4 | 0.0 | 0 | 0 | 2 | 0.00 | 0 | 1 | 2.04 | 0.32 | 0.0 | 0.0 | 5.0 |
| 03917A_10 | | | | | | 0.0000 | | 0.0 | | | | | | |
| 4 | 0.0 | 751.2 | 0.0 | 0 | 0 | 3 | 0.00 | 0 | 1 | 1.89 | 0.33 | 0.0 | 0.0 | 1.0 |
| 03917A_10 | | | | | | 0.0000 | | 0.0 | | | | | | |
| 5 | 0.0 | 110.0 | 0.0 | 0 | 0 | 2 | 0.00 | 0 | 1 | 2.04 | 0.50 | 1.0 | 0.0 | 39.0 |
| | | | | | | 0.0000 | | 0.0 | | | | | | |
| 03917A_85 | 0.8 | 0.8 | 26.7 | 21 | 1 | 3 | 0.53 | 1 | 2 | 2.46 | 0.52 | 111.0 | 25.0 | 228.0 |
| | | | | | | 0.0000 | | 0.0 | | | | | | |
| 03917A_34 | 2.9 | 2.9 | 46.4 | 73 | 1 | 2 | 0.22 | 0 | 1 | 2.06 | 0.68 | 41.0 | 12.0 | 267.0 |
| | | | | | | 0.0000 | | 0.0 | | | | | | |
| 03917A_53 | 4.8 | 3.4 | 194.7 | 59 | 2 | 3 | 0.18 | 0 | 2 | 1.97 | 0.40 | 35.0 | 30.0 | 110.0 |
| | | | | | | 0.0000 | | 0.0 | | | | | | |
| 03917A_32 | 5.5 | 5.5 | 48.6 | 88 | 1 | 3 | 0.07 | 0 | 2 | 2.23 | 0.49 | 11.0 | 40.0 | 117.0 |
| | | | | | | 0.0000 | | 0.0 | | | | | | |
| 03917A_29 | 6.5 | 4.6 | 82.0 | 131 | 2 | 3 | 0.11 | 0 | 2 | 2.04 | 0.53 | 23.0 | 0.0 | 103.0 |
| | | | | | | 0.0000 | | 0.0 | | | | | | |
| 03917A_55 | 6.5 | 6.5 | 65.6 | 58 | 1 | 1 | 0.20 | 1 | 1 | 1.86 | 0.30 | 44.0 | 2.0 | 150.0 |
| | | | | | | 0.0000 | | 0.0 | | | | | | |
| 03917A_59 | 6.8 | 3.0 | 55.3 | 40 | 5 | 3 | 0.27 | 0 | 2 | 2.05 | 0.52 | 57.0 | 37.0 | 60.0 |
| | | | | | | 0.0000 | | 0.0 | | | | | | |
| 03917A_15 | 6.9 | 6.9 | 79.1 | 97 | 1 | 4 | 0.05 | 0 | 1 | 2.02 | 0.38 | 8.0 | 31.0 | 171.0 |
| | | | | | | 0.0000 | | 0.0 | | | | | | |
| 03917A_26 | 7.0 | 7.0 | 132.4 | 96 | 1 | 2 | 0.07 | 0 | 1 | 1.76 | 0.42 | 14.0 | 57.0 | 74.0 |
| | | | | | | 0.0000 | | 0.0 | | | | | | |
| 03917A_40 | 7.3 | 5.1 | 70.7 | 84 | 2 | 3 | 0.11 | 0 | 2 | 1.70 | 0.46 | 21.0 | 0.0 | 252.0 |
| | | | | | | 0.0000 | | 0.0 | | | | | | |
| 03917A_48 | 7.8 | 7.8 | 0.0 | 0 | 1 | 2 | 0.07 | 0 | 1 | 2.32 | 0.30 | 0.0 | 0.0 | 2.0 |
| | | | | | | 0.0000 | | 0.0 | | | | | | |
| 03917A_62 | 8.0 | 3.0 | 115.1 | 46 | 7 | 3 | 0.40 | 1 | 3 | 2.12 | 0.46 | 85.0 | 113.0 | 271.0 |
| | | | | | | 0.0000 | | 0.0 | | | | | | |
| 03917A_20 | 8.0 | 5.7 | 63.8 | 89 | 2 | 4 | 0.08 | 0 | 2 | 1.93 | 0.38 | 16.0 | 3.0 | 216.0 |
| 03917A_10 | | | | | | 0.0000 | | 0.0 | | | | | | |
| 0 | 8.3 | 5.9 | 73.2 | 89 | 2 | 3 | 0.10 | 0 | 3 | 2.55 | 0.49 | 20.0 | 33.0 | 93.0 |
| | | | | | | 0.0000 | | 0.0 | | | | | | |
| 03917A_93 | 8.4 | 6.0 | 38.4 | 49 | 2 | 2 | 0.15 | 0 | 2 | 2.37 | 0.48 | 33.0 | 138.0 | 125.0 |
| | | | | | | 0.0000 | | 0.0 | | | | | | |
| 03917A_81 | 8.8 | 5.1 | 52.4 | 74 | 3 | 3 | 0.12 | 0 | 2 | 2.25 | 0.45 | 26.0 | 78.0 | 119.0 |
| | | | | | | 0.0000 | | 0.0 | | | | | | |
| 03917A_82 | 9.5 | 9.5 | 90.7 | 137 | 1 | 2 | 0.05 | 0 | 1 | 1.74 | 0.41 | 13.0 | 2.0 | 182.0 |
| | | | | | | 0.0000 | | 0.0 | | | | | | |
| 03917A_14 | 9.9 | 9.9 | 54.3 | 65 | 1 | 3 | 0.04 | 0 | 1 | 1.85 | 0.73 | 13.0 | 43.0 | 204.0 |
| 03917A_10 | | | | | | 0.0000 | | 0.0 | | | | | | |
| 2 | 10.0 | 5.0 | 131.6 | 162 | 4 | 5 | 0.10 | 0 | 2 | 1.90 | 0.62 | 20.0 | 1.0 | 123.0 |
| | | | | | | 0.0000 | | 0.0 | | | | | | |
| 03917A_38 | 10.1 | 5.1 | 42.0 | 23 | 4 | 2 | 0.21 | 1 | 3 | 1.97 | 0.41 | 147.0 | 12.0 | 67.0 |
| | | | | | | 0.0000 | | 0.0 | | | | | | |
| 03917A_77 | 10.2 | 10.2 | 0.0 | 0 | 1 | 2 | 0.05 | 0 | 1 | 2.17 | 0.46 | 11.0 | 46.0 | 217.0 |
| | | | | | | 0.0000 | | 0.0 | | | | | | |
| 03917A_8 | 11.0 | 4.2 | 32.5 | 37 | 7 | 3 | 0.27 | 1 | 3 | 2.17 | 0.39 | 55.0 | 7.0 | 285.0 |
| 03917A_10 | | | | | | 0.0000 | | 0.0 | | | | | | |
| 6 | 11.0 | 5.5 | 47.2 | 51 | 4 | 2 | 0.23 | 0 | 2 | 2.02 | 0.48 | 47.0 | 3.0 | 197.0 |
| | | | | | | 0.0000 | | 0.0 | | | | | | |
| 03917A_83 | 11.2 | 11.2 | 85.2 | 112 | 1 | 2 | 0.05 | 0 | 1 | 1.94 | 0.46 | 8.0 | 31.0 | 203.0 |
| | | | | | | 0.0000 | | 0.0 | | | | | | |
| 03917A_52 | 12.0 | 12.0 | 103.3 | 130 | 1 | 4 | 0.03 | 0 | 1 | 2.13 | 0.51 | 6.0 | 23.0 | 140.0 |
| | | | | | | 0.0000 | | 0.0 | | | | | | |
| 03917A_99 | 12.5 | 3.5 | 46.0 | 52 | 13 | 5 | 0.26 | 1 | 4 | 2.10 | 0.47 | 58.0 | 35.0 | 329.0 |
| | | | | | | 0.0000 | | 0.0 | | | | | | |
| 03917A_72 | 12.5 | 5.6 | 46.2 | 48 | 5 | 1 | 0.34 | 1 | 2 | 1.96 | 0.37 | 75.0 | 3.0 | 81.0 |
| | | | | | | 0.0000 | | 0.0 | | | | | | |
| 03917A_25 | 12.6 | 8.9 | 45.4 | 98 | 2 | 4 | 0.05 | 0 | 2 | 2.23 | 0.41 | 10.0 | 1.0 | 228.0 |
| | | | | | | 0.0000 | | 0.0 | | | | | | |
| 03917A_9 | 12.9 | 3.1 | 42.0 | 31 | 18 | 3 | 0.59 | 2 | 3 | 1.97 | 0.33 | 128.0 | 21.0 | 253.0 |
| | | | | | | 0.0000 | | 0.0 | | | | | | |
| 03917A_31 | 13.9 | 5.7 | 41.3 | 54 | 6 | 4 | 0.14 | 0 | 3 | 2.23 | 0.45 | 34.0 | 1.0 | 117.0 |
| | | | | | | 0.0000 | | 0.0 | | | | | | |
| 03917A_36 | 14.2 | 5.0 | 62.5 | 40 | 8 | 2 | 0.29 | 1 | 2 | 1.66 | 0.35 | 59.0 | 1.0 | 161.0 |

| | | | | | | | | | | | | | | |
|---|---|---|---|---|---|---|---|---|---|---|---|---|---|---|
| | | | | | | 0.0000 | | 0.0 | | | | | | |
| 03917A_33 | 15.3 | 4.8 | 50.3 | 56 | 10 | 3 | 0.24 | 1 | 4 | 2.06 | 0.39 | 49.0 | 6.0 | 195.0 |
| | | | | | | 0.0000 | | 0.0 | | | | | | |
| 03917A_1 | 16.0 | 8.0 | 146.2 | 55 | 4 | 1 | 0.21 | 1 | 2 | 1.97 | 0.34 | 41.0 | 88.0 | 39.0 |
| | | | | | | 0.0000 | | 0.0 | | | | | | |
| 03917A_47 | 16.4 | 7.3 | 35.4 | 39 | 5 | 1 | 0.32 | 1 | 4 | 2.04 | 0.39 | 62.0 | 26.0 | 143.0 |
| | | | | | | 0.0000 | | 0.0 | | | | | | |
| 03917A_4 | 16.7 | 5.1 | 56.7 | 132 | 11 | 5 | 0.17 | 1 | 2 | 2.23 | 0.63 | 31.0 | 0.0 | 155.0 |
| | | | | | | 0.0000 | | 0.0 | | | | | | |
| 03917A_30 | 16.8 | 11.9 | 27.8 | 77 | 2 | 3 | 0.05 | 0 | 2 | 2.32 | 0.45 | 11.0 | 49.0 | 209.0 |
| | | | | | | 0.0000 | | 0.0 | | | | | | |
| 03917A_39 | 17.6 | 12.4 | 58.7 | 120 | 2 | 1 | 0.12 | 0 | 3 | 2.04 | 0.41 | 24.0 | 1.0 | 120.0 |
| | | | | | | 0.0000 | | 0.0 | | | | | | |
| 03917A_41 | 18.3 | 10.5 | 62.7 | 80 | 3 | 4 | 0.05 | 0 | 2 | 1.96 | 0.49 | 11.0 | 44.0 | 90.0 |
| | | | | | | 0.0000 | | 0.0 | | | | | | |
| 03917A_28 | 18.9 | 13.3 | 104.2 | 151 | 2 | 4 | 0.03 | 0 | 2 | 2.34 | 0.39 | 7.0 | 21.0 | 148.0 |
| 03917A_10 | | | | | | 0.0000 | | 0.0 | | | | | | |
| 7 | 19.3 | 9.7 | 114.8 | 191 | 4 | 3 | 0.09 | 0 | 3 | 1.98 | 0.47 | 18.0 | 0.0 | 113.0 |
| | | | | | | 0.0000 | | 0.0 | | | | | | |
| 03917A_69 | 19.4 | 11.2 | 50.1 | 48 | 3 | 1 | 0.16 | 0 | 3 | 2.56 | 0.51 | 37.0 | 120.0 | 81.0 |
| | | | | | | 0.0000 | | 0.0 | | | | | | |
| 03917A_90 | 19.6 | 19.6 | 61.0 | 190 | 1 | 1 | 0.06 | 0 | 1 | 2.25 | 0.63 | 14.0 | 0.0 | 128.0 |
| | | | | | | 0.0000 | | 0.0 | | | | | | |
| 03917A_46 | 19.7 | 13.9 | 151.7 | 124 | 2 | 2 | 0.07 | 0 | 2 | 2.28 | 0.62 | 15.0 | 0.0 | 191.0 |
| | | | | | | 0.0000 | | 0.0 | | | | | | |
| 03917A_70 | 20.7 | 12.0 | 100.0 | 126 | 3 | 2 | 0.10 | 0 | 2 | 1.69 | 0.46 | 23.0 | 0.0 | 132.0 |
| | | | | | | 0.0000 | | 0.0 | | | | | | |
| 03917A_3 | 21.3 | 3.9 | 51.3 | 50 | 31 | 5 | 0.37 | 1 | 3 | 2.32 | 0.47 | 68.0 | 1.0 | 183.0 |
| | | | | | | 0.0000 | | 0.0 | | | | | | |
| 03917A_37 | 21.4 | 4.9 | 55.6 | 35 | 19 | 3 | 0.38 | 1 | 2 | 1.82 | 0.37 | 77.0 | 38.0 | 225.0 |
| | | | | | | 0.0000 | | 0.0 | | | | | | |
| 03917A_19 | 21.6 | 6.0 | 63.6 | 91 | 13 | 4 | 0.19 | 1 | 2 | 2.04 | 0.48 | 48.0 | 1.0 | 171.0 |
| | | | | | | 0.0000 | | 0.0 | | | | | | |
| 03917A_44 | 21.8 | 12.6 | 53.1 | 88 | 3 | 2 | 0.09 | 0 | 2 | 2.23 | 0.50 | 19.0 | 12.0 | 162.0 |
| | | | | | | 0.0000 | | 0.0 | | | | | | |
| 03917A_17 | 22.7 | 6.6 | 113.7 | 125 | 12 | 5 | 0.13 | 0 | 4 | 1.84 | 0.64 | 27.0 | 0.0 | 114.0 |
| | | | | | | 0.0000 | | 0.0 | | | | | | |
| 03917A_57 | 24.4 | 6.6 | 61.1 | 37 | 14 | 3 | 0.21 | 0 | 3 | 2.04 | 0.45 | 43.0 | 1.0 | 199.0 |
| | | | | | | 0.0000 | | 0.0 | | | | | | |
| 03917A_6 | 25.2 | 11.3 | 128.5 | 165 | 5 | 3 | 0.08 | 0 | 2 | 1.46 | 0.33 | 18.0 | 0.0 | 145.0 |
| | | | | | | 0.0000 | | 0.0 | | | | | | |
| 03917A_66 | 25.7 | 14.9 | 0.0 | 0 | 3 | 4 | 0.03 | 0 | 2 | 2.18 | 0.53 | 7.0 | 20.0 | 140.0 |
| | | | | | | 0.0000 | | 0.0 | | | | | | |
| 03917A_68 | 27.2 | 11.1 | 89.0 | 159 | 6 | 3 | 0.09 | 0 | 2 | 2.27 | 0.60 | 19.0 | 1.0 | 160.0 |
| 03917A_10 | | | | | | 0.0000 | | 0.0 | | | | | | |
| 3 | 27.3 | 9.7 | 39.6 | 55 | 8 | 2 | 0.19 | 0 | 3 | 2.01 | 0.41 | 38.0 | 7.0 | 241.0 |
| 03917A_10 | | | | | | 0.0000 | | 0.0 | | | | | | |
| 8 | 27.6 | 9.8 | 34.8 | 53 | 8 | 3 | 0.11 | 0 | 2 | 2.04 | 0.42 | 20.0 | 13.0 | 58.0 |
| | | | | | | 0.0000 | | 0.0 | | | | | | |
| 03917A_64 | 28.1 | 8.9 | 50.1 | 62 | 10 | 3 | 0.15 | 1 | 2 | 2.22 | 0.32 | 26.0 | 4.0 | 164.0 |
| | | | | | | 0.0000 | | 0.0 | | | | | | |
| 03917A_58 | 28.1 | 10.7 | 59.4 | 84 | 7 | 4 | 0.08 | 0 | 2 | 2.37 | 0.55 | 16.0 | 23.0 | 76.0 |
| | | | | | | 0.0000 | | 0.0 | | | | | | |
| 03917A_42 | 28.5 | 28.6 | 131.9 | 165 | 1 | 1 | 0.04 | 0 | 1 | 2.68 | 0.49 | 9.0 | 56.0 | 107.0 |
| | | | | | | 0.0000 | | 0.0 | | | | | | |
| 03917A_71 | 29.3 | 29.3 | 192.7 | 358 | 1 | 2 | 0.02 | 0 | 1 | 1.80 | 0.34 | 5.0 | 21.0 | 141.0 |
| | | | | | | 0.0000 | | 0.0 | | | | | | |
| 03917A_67 | 29.8 | 8.6 | 0.0 | 0 | 12 | 5 | 0.10 | 0 | 2 | 2.05 | 0.41 | 21.0 | 4.0 | 116.0 |
| | | | | | | 0.0000 | | 0.0 | | | | | | |
| 03917A_54 | 29.9 | 7.1 | 40.1 | 26 | 18 | 1 | 0.64 | 2 | 3 | 1.66 | 0.41 | 128.0 | 2.0 | 329.0 |
| | | | | | | 0.0000 | | 0.0 | | | | | | |
| 03917A_11 | 30.6 | 10.2 | 104.9 | 170 | 9 | 5 | 0.07 | 0 | 2 | 1.62 | 0.42 | 15.0 | 2.0 | 51.0 |
| 03917A_10 | | | | | | 0.0000 | | 0.0 | | | | | | |
| 9 | 31.3 | 7.1 | 85.9 | 80 | 20 | 4 | 0.20 | 0 | 4 | 2.05 | 0.40 | 43.0 | 1.0 | 194.0 |
| | | | | | | 0.0000 | | 0.0 | | | | | | |
| 03917A_94 | 31.5 | 7.3 | 50.6 | 45 | 19 | 2 | 0.37 | 1 | 3 | 2.16 | 0.44 | 76.0 | 2.0 | 234.0 |
| | | | | | | 0.0000 | | 0.0 | | | | | | |
| 03917A_92 | 31.7 | 18.3 | 64.0 | 90 | 3 | 1 | 0.12 | 0 | 2 | 1.77 | 0.44 | 21.0 | 3.0 | 251.0 |
| | | | | | | 0.0000 | | 0.0 | | | | | | |
| 03917A_16 | 32.2 | 18.6 | 257.6 | 419 | 3 | 3 | 0.04 | 0 | 3 | 1.78 | 0.34 | 8.0 | 0.0 | 100.0 |
| | | | | | | 0.0000 | | 0.0 | | | | | | |
| 03917A_97 | 35.6 | 9.6 | 136.5 | 54 | 14 | 3 | 0.17 | 0 | 3 | 2.83 | 0.53 | 33.0 | 75.0 | 44.0 |
| | | | | | | 0.0000 | | 0.0 | | | | | | |
| 03917A_10 | 36.6 | 16.4 | 195.7 | 255 | 5 | 3 | 0.06 | 0 | 4 | 2.14 | 0.57 | 11.0 | 1.0 | 48.0 |

| | | | | | | | | | | | | | | |
|---|---|---|---|---|---|---|---|---|---|---|---|---|---|---|
| | | | | | | 0.0000 | | 0.0 | | | | | | |
| 03917A_89 | 37.8 | 11.4 | 54.9 | 113 | 11 | 4 | 0.09 | 0 | 3 | 2.20 | 0.31 | 19.0 | 2.0 | 94.0 |
| | | | | | | 0.0000 | | 0.0 | | | | | | |
| 03917A_95 | 39.2 | 16.1 | 141.2 | 161 | 6 | 2 | 0.09 | 0 | 3 | 1.97 | 0.44 | 20.0 | 0.0 | 127.0 |
| | | | | | | 0.0000 | | 0.0 | | | | | | |
| 03917A_21 | 39.6 | 22.9 | 27.1 | 168 | 3 | 3 | 0.03 | 0 | 2 | 1.90 | 0.42 | 8.0 | 1.0 | 101.0 |
| | | | | | | 0.0000 | | 0.0 | | | | | | |
| 03917A_12 | 39.8 | 6.0 | 42.0 | 17 | 47 | 4 | 0.38 | 1 | 4 | 2.03 | 0.46 | 217.0 | 2.0 | 253.0 |
| | | | | | | 0.0000 | | 0.0 | | | | | | |
| 03917A_79 | 41.6 | 10.2 | 80.2 | 97 | 17 | 5 | 0.10 | 0 | 4 | 2.38 | 0.60 | 23.0 | 23.0 | 86.0 |
| | | | | | | 0.0000 | | 0.0 | | | | | | |
| 03917A_50 | 45.1 | 31.9 | 129.0 | 96 | 2 | 1 | 0.07 | 0 | 2 | 1.82 | 0.44 | 15.0 | 71.0 | 53.0 |
| 03917A_11 | | | | | | 0.0000 | | 0.0 | | | | | | |
| 0 | 58.7 | 10.4 | 18.5 | 56 | 34 | 3 | 0.27 | 1 | 4 | 2.02 | 0.40 | 51.0 | 13.0 | 299.0 |
| | | | | | | 0.0000 | | 0.0 | | | | | | |
| 03917A_98 | 69.7 | 31.3 | 41.5 | 125 | 5 | 1 | 0.06 | 0 | 3 | 2.36 | 0.46 | 13.0 | 0.0 | 129.0 |
| | | | | | | 0.0000 | | 0.0 | | | | | | |
| 03917A_24 | 74.0 | 26.2 | 153.8 | 102 | 8 | 2 | 0.08 | 0 | 3 | 2.30 | 0.56 | 16.0 | 67.0 | 92.0 |
| | | | | | | 0.0000 | | 0.0 | | | | | | |
| 03917A_13 | 74.4 | 11.0 | 50.3 | 31 | 49 | 5 | 0.17 | 1 | 4 | 1.95 | 0.35 | 164.0 | 1.0 | 238.0 |
| | | | | | | 0.0000 | | 0.0 | | | | | | |
| 03917A_35 | 85.9 | 60.8 | 80.9 | 135 | 2 | 1 | 0.03 | 0 | 1 | 2.07 | 0.43 | 6.0 | 2.0 | 111.0 |
| | | | | | | 0.0000 | | 0.0 | | | | | | |
| 03917A_65 | 330.0 | 125.6 | 29.4 | 182 | 7 | 1 | 0.02 | 0 | 2 | 2.26 | 0.41 | 7.0 | 4.0 | 173.0 |
| | | | | | | 0.0000 | | 0.0 | | | | | | |
| 03917A_49 | 464.7 | 468.1 | 0.0 | 0 | 1 | 3 | 0.00 | 0 | 1 | 1.89 | 0.47 | 0.0 | 0.0 | 5.0 |
| | | | | | | 0.0000 | | 0.0 | | | | | | |
| 03917A_45 | 466.8 | 468.5 | 0.0 | 0 | 1 | 2 | 0.00 | 0 | 1 | 2.68 | 0.52 | 0.0 | 1.0 | 9.0 |
| | | | | | | 0.0000 | | 0.0 | | | | | | |
| 03917A_43 | 552.2 | 556.6 | 0.0 | 0 | 1 | 4 | 0.00 | 0 | 1 | 2.17 | 0.49 | 0.0 | 0.0 | 6.0 |
| | | | | | | 0.0000 | | 0.0 | | | | | | |
| 03917A_76 | 616.9 | 444.4 | 0.0 | 0 | 2 | 5 | 0.00 | 0 | 2 | 1.81 | 0.35 | 0.0 | 3.0 | 15.0 |

**Eureka Glacier**

| Spot Name | FT Age (Ma) | sigma sym (Ma) | UPb Age (Ma) | 2 sigma (Ma) | Ns | Area cm^2 | U/Catio n | +/- 1sig | Etch Figs. | Dpar (um) | Dper (um) | [U] (ppm ) | [Th] (ppm) | [Sm] (ppm) |
|---|---|---|---|---|---|---|---|---|---|---|---|---|---|---|
| | | | | | | 0.0000 | | 0.0 | | | | | | |
| 4393A_5 | 0.0 | 727.8 | 0.0 | 0 | 0 | 4 | 0.00 | 0 | 1 | 1.48 | 0.41 | 0.0 | 0.0 | 6.3 |
| | | | | | | 0.0000 | | 0.0 | | | | | | |
| 4393A_4 | 0.0 | 633.9 | 0.0 | 0 | 0 | 5 | 0.00 | 0 | 1 | 1.82 | 0.28 | 0.0 | 0.0 | 3.2 |
| | | | | | | 0.0000 | | 0.0 | | | | | | |
| 4393A_49 | 0.0 | 700.6 | 0.0 | 0 | 0 | 2 | 0.00 | 0 | 1 | 1.60 | 0.38 | 0.1 | 0.1 | 6.8 |
| | | | | | | 0.0000 | | 0.0 | | | | | | |
| 4393A_68 | 0.0 | 3.8 | 0.0 | 0 | 0 | 5 | 0.03 | 0 | 1 | 1.57 | 0.27 | 0.1 | 0.0 | 17.0 |
| | | | | | | 0.0000 | | 0.0 | | | | | | |
| 4393A_45 | 0.0 | 298.7 | 0.0 | 0 | 0 | 2 | 0.00 | 0 | 1 | 1.61 | 0.21 | 0.2 | 0.0 | 7.2 |
| | | | | | | 0.0000 | | 0.0 | | | | | | |
| 4393A_95 | 0.0 | 1.7 | 0.0 | 0 | 0 | 4 | 0.09 | 0 | 1 | 1.34 | 0.25 | 0.4 | 0.5 | 4.4 |
| | | | | | | 0.0000 | | 0.0 | | | | | | |
| 4393A_61 | 0.0 | 48.9 | 0.0 | 0 | 0 | 4 | 0.00 | 0 | 1 | 1.64 | 0.35 | 0.6 | 0.1 | 27.9 |
| | | | | | | 0.0000 | | 0.0 | | | | | | |
| 4393A_56 | 0.0 | 17.2 | 0.0 | 0 | 0 | 5 | 0.01 | 0 | 1 | 1.46 | 0.33 | 1.1 | 2.6 | 33.5 |
| | | | | | | 0.0000 | | 0.0 | | | | | | |
| 4393A_83 | 0.0 | 14.4 | 0.0 | 0 | 0 | 3 | 0.01 | 0 | 1 | 1.83 | 0.27 | 1.4 | 9.1 | 6.2 |
| | | | | | | 0.0000 | | 0.0 | | | | | | |
| 4393A_71 | 0.0 | 16.4 | 0.0 | 0 | 0 | 2 | 0.02 | 1 | 1 | 1.72 | 0.44 | 1.4 | 2.5 | 105.2 |
| | | | | | | 0.0000 | | 0.0 | | | | | | |
| 4393A_33 | 0.0 | 41.3 | 0.0 | 0 | 0 | 1 | 0.01 | 0 | 1 | 1.74 | 0.22 | 1.7 | 22.4 | 82.8 |
| | | | | | | 0.0000 | | 0.0 | | | | | | |
| 4393A_50 | 0.0 | 4.9 | 0.0 | 0 | 0 | 4 | 0.03 | 0 | 1 | 1.72 | 0.28 | 2.7 | 13.4 | 10.8 |
| | | | | | | 0.0000 | | 0.0 | | | | | | |
| 4393A_79 | 0.0 | 1.8 | 0.0 | 0 | 0 | 2 | 0.21 | 2 | 1 | 2.03 | 0.30 | 4.4 | 9.1 | 1.8 |
| | | | | | | 0.0000 | | 0.0 | | | | | | |
| 4393A_103 | 0.0 | 4.0 | 0.0 | 0 | 0 | 2 | 0.06 | 0 | 1 | 1.60 | 0.30 | 4.6 | 13.1 | 16.4 |
| | | | | | | 0.0000 | | 0.0 | | | | | | |
| 4393A_9 | 0.0 | 17.6 | 0.0 | 0 | 0 | 3 | 0.01 | 0 | 1 | 1.50 | 0.27 | 4.8 | 5.7 | 27.3 |
| | | | | | | 0.0000 | | 0.0 | | | | | | |
| 4393A_6 | 0.0 | 2.2 | 0.0 | 0 | 0 | 4 | 0.06 | 0 | 1 | 1.57 | 0.35 | 4.9 | 3.2 | 19.9 |
| | | | | | | 0.0000 | | 0.0 | | | | | | |
| 4393A_2 | 0.0 | 11.9 | 207.8 | 179 | 0 | 2 | 0.02 | 0 | 1 | 1.33 | 0.27 | 5.2 | 13.4 | 68.1 |
| | | | | | | 0.0000 | | 0.0 | | | | | | |
| 4393A_28 | 0.0 | 2.1 | 0.0 | 0 | 0 | 2 | 0.12 | 1 | 1 | 1.38 | 0.30 | 6.2 | 16.1 | 20.5 |

| | | | | | | | | | | | | | | |
|---|---|---|---|---|---|---|---|---|---|---|---|---|---|---|
| | | | | | | 0.0000 | | 0.0 | | | | | | |
| 4393A_44 | 0.0 | 5.7 | 0.0 | 0 | 0 | 2 | 0.04 | 0 | 1 | 1.77 | 0.39 | 7.0 | 1.5 | 83.8 |
| | | | | | | 0.0000 | | 0.0 | | | | | | |
| 4393A_12 | 0.0 | 5.1 | 0.0 | 0 | 0 | 3 | 0.04 | 0 | 1 | 1.51 | 0.31 | 8.7 | 7.3 | 20.4 |
| | | | | | | 0.0000 | | 0.0 | | | | | | |
| 4393A_69 | 0.0 | 59.4 | 276.1 | 182 | 0 | 1 | 0.01 | 0 | 1 | 2.14 | 0.30 | 11.2 | 0.5 | 77.2 |
| | | | | | | 0.0000 | | 0.0 | | | | | | |
| 4393A_55 | 0.9 | 0.9 | 0.0 | 0 | 1 | 4 | 0.23 | 5 | 1 | 1.62 | 0.27 | 7.8 | 11.8 | 20.8 |
| | | | | | | 0.0000 | | 0.0 | | | | | | |
| 4393A_90 | 2.4 | 2.4 | 793.3 | 849 | 1 | 3 | 0.10 | 0 | 1 | 1.61 | 0.36 | 0.8 | 0.9 | 53.5 |
| | | | | | | 0.0000 | | 0.0 | | | | | | |
| 4393A_53 | 2.9 | 2.9 | 0.0 | 0 | 1 | 3 | 0.10 | 2 | 1 | 1.72 | 0.36 | 9.0 | 46.1 | 122.9 |
| | | | | | | 0.0000 | | 0.0 | | | | | | |
| 4393A_89 | 3.8 | 3.8 | 0.0 | 0 | 1 | 2 | 0.13 | 3 | 2 | 1.57 | 0.32 | 12.9 | 8.1 | 31.5 |
| | | | | | | 0.0000 | | 0.0 | | | | | | |
| 4393A_20 | 3.8 | 3.8 | 0.0 | 0 | 1 | 5 | 0.04 | 0 | 1 | 1.53 | 0.25 | 0.1 | 0.1 | 25.5 |
| | | | | | | 0.0000 | | 0.0 | | | | | | |
| 4393A_13 | 4.5 | 4.5 | 0.0 | 0 | 1 | 1 | 0.13 | 1 | 1 | 1.92 | 0.29 | 21.9 | 14.3 | 63.8 |
| | | | | | | 0.0000 | | 0.0 | | | | | | |
| 4393A_60 | 4.8 | 4.8 | 0.0 | 0 | 1 | 2 | 0.07 | 0 | 1 | 1.72 | 0.33 | 7.3 | 4.7 | 44.8 |
| | | | | | | 0.0000 | | 0.0 | | | | | | |
| 4393A_59 | 6.9 | 2.3 | ###### | #### | 10 | 4 | 0.31 | 2 | 4 | 1.66 | 0.30 | 26.5 | 10.2 | 115.6 |
| | | | | | | 0.0000 | | 0.0 | | | | | | |
| 4393A_73 | 7.9 | 5.6 | 0.0 | 0 | 2 | 1 | 0.17 | 2 | 1 | 1.72 | 0.25 | 25.0 | 19.2 | 86.2 |
| | | | | | | 0.0000 | | 0.0 | | | | | | |
| 4393A_58 | 8.1 | 2.2 | 815.2 | #### | 15 | 3 | 0.53 | 5 | 2 | 1.59 | 0.41 | 39.7 | 18.1 | 114.7 |
| | | | | | | 0.0000 | | 0.0 | | | | | | |
| 4393A_81 | 8.7 | 6.2 | 136.6 | 124 | 2 | 3 | 0.06 | 0 | 1 | 1.59 | 0.33 | 13.2 | 0.4 | 80.6 |
| | | | | | | 0.0000 | | 0.0 | | | | | | |
| 4393A_32 | 8.8 | 6.3 | 0.0 | 0 | 2 | 1 | 0.16 | 2 | 2 | 1.62 | 0.24 | 44.7 | 11.9 | 79.3 |
| | | | | | | 0.0000 | | 0.0 | | | | | | |
| 4393A_47 | 8.9 | 3.6 | 66.3 | 151 | 6 | 2 | 0.23 | 1 | 2 | 1.39 | 0.30 | 20.6 | 0.5 | 145.8 |
| | | | | | | 0.0000 | | 0.0 | | | | | | |
| 4393A_18 | 9.9 | 5.0 | 97.7 | 133 | 4 | 5 | 0.07 | 0 | 3 | 1.60 | 0.35 | 14.9 | 0.5 | 105.6 |
| | | | | | | 0.0000 | | 0.0 | | | | | | |
| 4393A_26 | 9.9 | 5.7 | 72.7 | 98 | 3 | 3 | 0.09 | 0 | 2 | 1.33 | 0.31 | 18.0 | 0.4 | 119.4 |
| | | | | | | 0.0000 | | 0.0 | | | | | | |
| 4393A_39 | 10.4 | 4.6 | 78.3 | 115 | 5 | 5 | 0.08 | 0 | 2 | 1.52 | 0.34 | 15.0 | 0.6 | 72.4 |
| | | | | | | 0.0000 | | 0.0 | | | | | | |
| 4393A_10 | 10.4 | 4.2 | 126.8 | 70 | 6 | 5 | 0.10 | 0 | 3 | 1.78 | 0.38 | 20.3 | 0.4 | 104.3 |
| | | | | | | 0.0000 | | 0.0 | | | | | | |
| 4393A_65 | 10.4 | 4.3 | 86.0 | 82 | 6 | 5 | 0.10 | 0 | 4 | 1.89 | 0.26 | 20.7 | 0.7 | 94.0 |
| | | | | | | 0.0000 | | 0.0 | | | | | | |
| 4393A_91 | 10.6 | 5.1 | 0.0 | 0 | 5 | 5 | 0.08 | 1 | 2 | 2.03 | 0.34 | 16.4 | 6.5 | 82.4 |
| | | | | | | 0.0000 | | 0.0 | | | | | | |
| 4393A_74 | 11.8 | 11.8 | 751.0 | #### | 1 | 5 | 0.01 | 0 | 2 | 1.44 | 0.41 | 3.0 | 0.3 | 26.7 |
| | | | | | | 0.0000 | | 0.0 | | | | | | |
| 4393A_72 | 11.8 | 5.9 | 120.0 | 101 | 4 | 3 | 0.10 | 0 | 2 | 1.58 | 0.41 | 19.7 | 0.7 | 106.9 |
| | | | | | | 0.0000 | | 0.0 | | | | | | |
| 4393A_7 | 12.5 | 6.3 | 90.7 | 123 | 4 | 4 | 0.07 | 0 | 3 | 1.78 | 0.36 | 14.4 | 0.3 | 104.8 |
| | | | | | | 0.0000 | | 0.0 | | | | | | |
| 4393A_22 | 12.8 | 6.4 | 175.6 | 170 | 4 | 4 | 0.07 | 0 | 3 | 1.50 | 0.27 | 13.7 | 0.2 | 97.4 |
| | | | | | | 0.0000 | | 0.0 | | | | | | |
| 4393A_30 | 13.3 | 9.4 | 118.8 | 126 | 2 | 2 | 0.05 | 0 | 2 | 1.64 | 0.32 | 10.7 | 0.3 | 98.7 |
| | | | | | | 0.0000 | | 0.0 | | | | | | |
| 4393A_27 | 13.9 | 13.9 | 752.5 | 839 | 1 | 4 | 0.01 | 0 | 1 | 1.38 | 0.24 | 2.8 | 0.3 | 41.5 |
| | | | | | | 0.0000 | | 0.0 | | | | | | |
| 4393A_93 | 14.0 | 2.6 | 94.2 | 64 | 29 | 5 | 0.35 | 1 | 4 | 1.85 | 0.42 | 77.2 | 40.5 | 35.9 |
| | | | | | | 0.0000 | | 0.0 | | | | | | |
| 4393A_23 | 14.5 | 14.6 | 0.0 | 0 | 1 | 5 | 0.01 | 0 | 2 | 1.44 | 0.32 | 1.7 | 4.3 | 17.0 |
| | | | | | | 0.0000 | | 0.0 | | | | | | |
| 4393A_16 | 14.5 | 6.5 | 0.0 | 0 | 5 | 5 | 0.06 | 0 | 3 | 1.83 | 0.30 | 6.0 | 1.3 | 29.1 |
| | | | | | | 0.0000 | | 0.0 | | | | | | |
| 4393A_67 | 14.7 | 8.5 | 112.7 | 133 | 3 | 3 | 0.06 | 0 | 1 | 1.59 | 0.27 | 12.2 | 0.5 | 83.6 |
| | | | | | | 0.0000 | | 0.0 | | | | | | |
| 4393A_31 | 14.8 | 14.8 | 195.3 | 203 | 1 | 1 | 0.05 | 0 | 1 | 1.90 | 0.47 | 9.8 | 0.4 | 80.8 |
| | | | | | | 0.0000 | | 0.0 | | | | | | |
| 4393A_94 | 15.0 | 8.7 | 134.6 | 153 | 3 | 3 | 0.06 | 0 | 2 | 1.62 | 0.32 | 11.9 | 16.3 | 11.8 |
| | | | | | | 0.0000 | | 0.0 | | | | | | |
| 4393A_85 | 16.3 | 5.2 | 78.5 | 71 | 10 | 4 | 0.13 | 0 | 3 | 1.38 | 0.30 | 27.0 | 0.3 | 115.1 |
| | | | | | | 0.0000 | | 0.0 | | | | | | |
| 4393A_76 | 16.4 | 8.2 | 146.9 | 148 | 4 | 4 | 0.05 | 0 | 3 | 1.55 | 0.41 | 10.9 | 0.4 | 92.7 |
| | | | | | | 0.0000 | | 0.0 | | | | | | |
| 4393A_14 | 16.5 | 6.7 | 92.5 | 98 | 6 | 3 | 0.10 | 0 | 3 | 1.49 | 0.34 | 21.4 | 0.3 | 117.3 |

| | | | | | | | | | | | | | | |
|---|---|---|---|---|---|---|---|---|---|---|---|---|---|---|
| | | | | | | 0.0000 | | 0.0 | | | | | | |
| 4393A_84 | 17.2 | 5.5 | 106.0 | 71 | 10 | 3 | 0.14 | 0 | 3 | 1.72 | 0.46 | 29.7 | 0.9 | 108.7 |
| | | | | | | 0.0000 | | 0.0 | | | | | | |
| 4393A_41 | 18.6 | 6.6 | 90.2 | 73 | 8 | 4 | 0.09 | 0 | 4 | 1.66 | 0.35 | 18.4 | 0.2 | 90.6 |
| | | | | | | 0.0000 | | 0.0 | | | | | | |
| 4393A_25 | 19.2 | 6.8 | 109.7 | 153 | 8 | 5 | 0.07 | 0 | 4 | 1.56 | 0.29 | 15.1 | 0.8 | 40.3 |
| | | | | | | 0.0000 | | 0.0 | | | | | | |
| 4393A_11 | 19.5 | 8.0 | 138.1 | 132 | 6 | 3 | 0.09 | 0 | 4 | 1.42 | 0.39 | 18.3 | 0.5 | 84.9 |
| | | | | | | 0.0000 | | 0.0 | | | | | | |
| 4393A_105 | 20.2 | 8.3 | 0.0 | 0 | 6 | 3 | 0.08 | 0 | 3 | 1.58 | 0.34 | 18.2 | 3.8 | 97.4 |
| | | | | | | 0.0000 | | 0.0 | | | | | | |
| 4393A_21 | 20.9 | 20.9 | 0.0 | 0 | 1 | 5 | 0.01 | 0 | 1 | 1.31 | 0.35 | 10.2 | 10.5 | 6.2 |
| | | | | | | 0.0000 | | 0.0 | | | | | | |
| 4393A_35 | 21.1 | 10.5 | 176.8 | 158 | 4 | 3 | 0.05 | 0 | 3 | 1.59 | 0.25 | 9.9 | 0.3 | 86.7 |
| | | | | | | 0.0000 | | 0.0 | | | | | | |
| 4393A_17 | 21.5 | 15.2 | 163.1 | 189 | 2 | 1 | 0.05 | 0 | 2 | 1.55 | 0.30 | 11.1 | 1.3 | 95.3 |
| | | | | | | 0.0000 | | 0.0 | | | | | | |
| 4393A_62 | 21.7 | 8.2 | 67.1 | 145 | 7 | 3 | 0.09 | 0 | 3 | 1.50 | 0.33 | 19.6 | 1.1 | 128.5 |
| | | | | | | 0.0000 | | 0.0 | | | | | | |
| 4393A_46 | 22.3 | 11.2 | 109.0 | 67 | 4 | 1 | 0.10 | 0 | 2 | 1.51 | 0.37 | 22.6 | 0.5 | 125.1 |
| | | | | | | 0.0000 | | 0.0 | | | | | | |
| 4393A_40 | 22.4 | 15.8 | 218.0 | 210 | 2 | 4 | 0.02 | 0 | 2 | 1.55 | 0.47 | 4.3 | 0.3 | 80.2 |
| | | | | | | 0.0000 | | 0.0 | | | | | | |
| 4393A_43 | 22.4 | 13.0 | 304.3 | 382 | 3 | 5 | 0.02 | 0 | 2 | 1.63 | 0.36 | 4.6 | 0.8 | 75.5 |
| | | | | | | 0.0000 | | 0.0 | | | | | | |
| 4393A_34 | 22.5 | 22.5 | 137.8 | 263 | 1 | 2 | 0.02 | 0 | 1 | 1.80 | 0.31 | 3.9 | 0.2 | 59.9 |
| | | | | | | 0.0000 | | 0.0 | | | | | | |
| 4393A_24 | 22.6 | 7.5 | 66.5 | 76 | 9 | 5 | 0.07 | 0 | 3 | 1.48 | 0.37 | 13.8 | 5.0 | 22.2 |
| | | | | | | 0.0000 | | 0.0 | | | | | | |
| 4393A_80 | 22.6 | 13.1 | 109.8 | 154 | 3 | 1 | 0.09 | 0 | 2 | 1.59 | 0.35 | 15.8 | 2.2 | 99.6 |
| | | | | | | 0.0000 | | 0.0 | | | | | | |
| 4393A_102 | 23.2 | 8.8 | 141.1 | 422 | 7 | 3 | 0.07 | 0 | 4 | 1.62 | 0.30 | 15.6 | 1.1 | 121.6 |
| | | | | | | 0.0000 | | 0.0 | | | | | | |
| 4393A_52 | 23.4 | 7.0 | 0.0 | 0 | 14 | 4 | 0.11 | 1 | 3 | 1.51 | 0.41 | 30.8 | 22.8 | 86.2 |
| | | | | | | 0.0000 | | 0.0 | | | | | | |
| 4393A_100 | 23.8 | 9.7 | 90.1 | 101 | 6 | 4 | 0.05 | 0 | 3 | 1.52 | 0.22 | 11.1 | 0.7 | 93.6 |
| | | | | | | 0.0000 | | 0.0 | | | | | | |
| 4393A_63 | 24.2 | 9.2 | 81.7 | 98 | 7 | 3 | 0.08 | 0 | 3 | 1.78 | 0.30 | 17.1 | 0.4 | 98.3 |
| | | | | | | 0.0000 | | 0.0 | | | | | | |
| 4393A_88 | 24.6 | 9.3 | 146.8 | 183 | 7 | 4 | 0.06 | 0 | 3 | 1.76 | 0.41 | 12.0 | 3.1 | 50.4 |
| | | | | | | 0.0000 | | 0.0 | | | | | | |
| 4393A_97 | 25.0 | 25.0 | 0.0 | 0 | 1 | 5 | 0.01 | 0 | 1 | 1.67 | 0.49 | 1.4 | 0.7 | 22.1 |
| | | | | | | 0.0000 | | 0.0 | | | | | | |
| 4393A_104 | 25.1 | 12.6 | 191.1 | 232 | 4 | 4 | 0.03 | 0 | 3 | 1.61 | 0.39 | 7.2 | 0.5 | 88.4 |
| | | | | | | 0.0000 | | 0.0 | | | | | | |
| 4393A_48 | 25.1 | 12.6 | 76.2 | 108 | 4 | 2 | 0.06 | 0 | 2 | 1.53 | 0.41 | 13.6 | 0.2 | 100.0 |
| | | | | | | 0.0000 | | 0.0 | | | | | | |
| 4393A_57 | 25.5 | 8.1 | 56.8 | 107 | 10 | 5 | 0.07 | 0 | 4 | 1.45 | 0.38 | 14.6 | 0.7 | 96.2 |
| | | | | | | 0.0000 | | 0.0 | | | | | | |
| 4393A_86 | 26.3 | 11.8 | 173.0 | 218 | 5 | 3 | 0.05 | 0 | 3 | 1.55 | 0.32 | 10.0 | 1.4 | 104.3 |
| | | | | | | 0.0000 | | 0.0 | | | | | | |
| 4393A_82 | 26.6 | 13.3 | 233.4 | 153 | 4 | 2 | 0.05 | 0 | 3 | 1.83 | 0.29 | 10.4 | 0.3 | 97.4 |
| | | | | | | 0.0000 | | 0.0 | | | | | | |
| 4393A_78 | 26.9 | 13.5 | 81.0 | 112 | 4 | 1 | 0.10 | 0 | 3 | 1.78 | 0.30 | 20.7 | 0.6 | 118.6 |
| | | | | | | 0.0000 | | 0.0 | | | | | | |
| 4393A_66 | 26.9 | 12.0 | 119.6 | 137 | 5 | 3 | 0.06 | 0 | 4 | 1.62 | 0.40 | 12.2 | 0.2 | 99.0 |
| | | | | | | 0.0000 | | 0.0 | | | | | | |
| 4393A_42 | 27.6 | 19.5 | 427.8 | 338 | 2 | 3 | 0.02 | 0 | 1 | 2.02 | 0.49 | 3.6 | 0.7 | 87.5 |
| | | | | | | 0.0000 | | 0.0 | | | | | | |
| 4393A_54 | 28.1 | 8.5 | 123.2 | 134 | 11 | 5 | 0.07 | 0 | 3 | 1.48 | 0.30 | 14.3 | 0.3 | 96.6 |
| | | | | | | 0.0000 | | 0.0 | | | | | | |
| 4393A_3 | 28.7 | 28.7 | 338.2 | 487 | 1 | 5 | 0.01 | 0 | 1 | 1.70 | 0.31 | 1.2 | 0.0 | 7.7 |
| | | | | | | 0.0000 | | 0.0 | | | | | | |
| 4393A_19 | 29.0 | 29.0 | 0.0 | 0 | 1 | 5 | 0.01 | 0 | 1 | 1.33 | 0.30 | 0.1 | 0.2 | 2.6 |
| | | | | | | 0.0000 | | 0.0 | | | | | | |
| 4393A_99 | 29.5 | 20.8 | 232.6 | 284 | 2 | 2 | 0.02 | 0 | 1 | 1.77 | 0.25 | 5.0 | 23.7 | 170.7 |
| | | | | | | 0.0000 | | 0.0 | | | | | | |
| 4393A_37 | 32.0 | 22.7 | 152.6 | 176 | 2 | 1 | 0.04 | 0 | 2 | 1.59 | 0.41 | 9.0 | 2.7 | 31.7 |
| | | | | | | 0.0000 | | 0.0 | | | | | | |
| 4393A_70 | 32.3 | 12.2 | 67.1 | 76 | 7 | 2 | 0.07 | 0 | 3 | 1.68 | 0.36 | 16.5 | 0.3 | 91.8 |
| | | | | | | 0.0000 | | 0.0 | | | | | | |
| 4393A_101 | 33.6 | 8.0 | 63.3 | 63 | 18 | 3 | 0.14 | 0 | 2 | 1.48 | 0.41 | 30.2 | 3.5 | 120.3 |
| | | | | | | 0.0000 | | 0.0 | | | | | | |
| 4393A_29 | 35.1 | 35.1 | 0.0 | 0 | 1 | 2 | 0.01 | 0 | 1 | 1.82 | 0.26 | 2.3 | 2.5 | 61.6 |

| | | | | | | | | | | | | | | |
|---|---|---|---|---|---|---|---|---|---|---|---|---|---|---|
| 4393A_38 | 37.0 | 26.2 | 128.4 | 217 | 2 | 0.0000 2 | 0.02 | 0.0 0 | 1 | 1.64 | 0.42 | 4.6 | 0.2 | 72.5 |
| 4393A_64 | 45.6 | 26.3 | 233.9 | 251 | 3 | 0.0000 2 | 0.03 | 0.0 0 | 2 | 1.57 | 0.33 | 6.0 | 0.8 | 67.1 |
| 4393A_77 | 47.2 | 11.9 | 562.8 | 462 | 16 | 0.0000 5 | 0.06 | 0.0 0 | 4 | 2.00 | 0.48 | 10.9 | 1.1 | 55.2 |
| 4393A_75 | 50.4 | 29.2 | 0.0 | 0 | 3 | 0.0000 2 | 0.03 | 0.0 0 | 2 | 2.28 | 0.34 | 1.4 | 0.7 | 48.3 |
| 4393A_1 | 51.6 | 36.5 | 0.0 | 0 | 2 | 0.0000 4 | 0.01 | 0.0 0 | 2 | 1.66 | 0.35 | 1.5 | 0.4 | 29.3 |
| 4393A_92 | 52.8 | 37.6 | 0.0 | 0 | 2 | 0.0000 2 | 0.02 | 0.0 0 | 1 | 1.51 | 0.28 | 4.0 | 15.6 | 18.4 |
| 4393A_87 | 60.3 | 34.9 | 253.4 | 495 | 3 | 0.0000 3 | 0.01 | 0.0 0 | 2 | 1.63 | 0.40 | 3.0 | 0.6 | 74.6 |
| 4393A_36 | 61.5 | 43.5 | 846.4 | #### | 2 | 0.0000 1 | 0.02 | 0.0 0 | 1 | 1.31 | 0.23 | 1.9 | 3.6 | 56.1 |
| 4393A_15 | 77.1 | 54.5 | 241.2 | 269 | 2 | 0.0000 2 | 0.01 | 0.0 0 | 1 | 1.57 | 0.38 | 2.1 | 9.0 | 114.3 |
| 4393A_51 | 77.3 | 34.7 | 308.9 | 403 | 5 | 0.0000 2 | 0.02 | 0.0 0 | 2 | 1.51 | 0.31 | 4.8 | 0.4 | 75.0 |
| 4393A_96 | 81.9 | 47.3 | 315.6 | 404 | 3 | 0.0000 3 | 0.01 | 0.0 0 | 2 | 1.96 | 0.55 | 1.9 | 7.4 | 82.8 |
| 4393A_98 | 99.9 | 100.0 | 851.4 | #### | 1 | 0.0000 2 | 0.00 | 0.0 0 | 1 | 1.32 | 0.25 | 0.9 | 0.2 | 28.8 |
| 4393A_8 | 133.4 | 133.6 | 0.0 | 0 | 1 | 2 | 0.00 | 0 | 1 | 1.50 | 0.25 | 0.7 | 0.5 | 34.7 |

**Little Tok**

| Spot Name | FT Age (Ma) | symm err (Ma) | UPb Age (Ma) | 2 sigma (Ma) | Ns | Area cm^2 | U/Catio n | +/- 1sig | Etch Figs. | Dpar (um) | Dper (um) | [U] (ppm ) | [Th] (ppm) | [Sm] (ppm) |
|---|---|---|---|---|---|---|---|---|---|---|---|---|---|---|
| 1422A_15 | 0.0 | 5.6 | 0.0 | 0 | 0 | 0.0000 5 | 0.03 | 0.0 0 | 1 | 1.77 | 0.37 | 7.0 | 40.0 | 142.0 |
| 1422A_16 | 0.0 | 15.3 | 93.1 | 245 | 0 | 0.0000 5 | 0.01 | 0.0 0 | 1 | 1.73 | 0.23 | 3.0 | 11.0 | 59.0 |
| 1422A_34 | 0.0 | 12.6 | 17.2 | 121 | 0 | 0.0000 4 | 0.02 | 0.0 0 | 1 | 1.36 | 0.34 | 3.0 | 14.0 | 64.0 |
| 1422A_63 | 0.0 | 25.5 | 94.0 | 190 | 0 | 0.0000 3 | 0.01 | 0.0 0 | 1 | 2.14 | 0.35 | 3.0 | 11.0 | 57.0 |
| 1422A_58 | 8.9 | 7.3 | 201.7 | 110 | 1 | 0.0000 3 | 0.05 | 0.0 0 | 1 | 2.25 | 0.25 | 10.0 | 46.0 | 118.0 |
| 1422A_7 | 11.1 | 5.2 | 177.0 | 107 | 4 | 0.0000 5 | 0.09 | 0.0 0 | 4 | 1.91 | 0.36 | 20.0 | 112.0 | 238.0 |
| 1422A_37 | 18.2 | 4.3 | 135.2 | 38 | 18 | 0.0000 5 | 0.25 | 0.0 1 | 4 | 1.59 | 0.29 | 52.0 | 186.0 | 274.0 |
| 1422A_54 | 23.7 | 5.6 | 120.6 | 38 | 18 | 0.0000 5 | 0.19 | 0.0 1 | 3 | 1.75 | 0.27 | 40.0 | 208.0 | 301.0 |
| 1422A_11 | 25.0 | 6.6 | 127.4 | 65 | 14 | 0.0000 5 | 0.14 | 0.0 0 | 4 | 2.07 | 0.46 | 31.0 | 87.0 | 379.0 |
| 1422A_49 | 26.0 | 4.4 | 98.1 | 25 | 35 | 0.0000 4 | 0.43 | 0.0 1 | 4 | 1.92 | 0.25 | 102.0 | 239.0 | 183.0 |
| 1422A_55 | 27.3 | 4.9 | 111.3 | 23 | 31 | 0.0000 3 | 0.41 | 0.0 1 | 4 | 1.87 | 0.33 | 90.0 | 144.0 | 144.0 |
| 1422A_43 | 27.6 | 6.6 | 107.4 | 24 | 17 | 0.0000 2 | 0.43 | 0.0 1 | 4 | 1.47 | 0.30 | 93.0 | 279.0 | 284.0 |
| 1422A_4 | 28.6 | 5.7 | 91.0 | 49 | 26 | 0.0000 4 | 0.26 | 0.0 1 | 3 | 1.49 | 0.37 | 52.0 | 158.0 | 139.0 |
| 1422A_44 | 29.1 | 6.9 | 136.2 | 84 | 18 | 0.0000 5 | 0.16 | 0.0 1 | 4 | 1.73 | 0.33 | 33.0 | 165.0 | 113.0 |
| 1422A_17 | 32.0 | 4.7 | 109.4 | 43 | 49 | 0.0000 5 | 0.39 | 0.0 1 | 4 | 1.92 | 0.27 | 83.0 | 131.0 | 246.0 |
| 1422A_3 | 32.1 | 4.3 | 115.3 | 25 | 61 | 0.0000 5 | 0.48 | 0.0 2 | 4 | 2.02 | 0.38 | 96.0 | 162.0 | 217.0 |
| 1422A_65 | 33.4 | 6.7 | 117.0 | 26 | 25 | 0.0000 3 | 0.32 | 0.0 1 | 3 | 1.76 | 0.33 | 68.0 | 148.0 | 128.0 |
| 1422A_36 | 33.9 | 7.7 | 119.2 | 43 | 19 | 0.0000 3 | 0.20 | 0.0 0 | 3 | 1.75 | 0.37 | 44.0 | 226.0 | 302.0 |
| 1422A_1 | 34.0 | 13.4 | 120.2 | 144 | 6 | 0.0000 5 | 0.04 | 0.0 0 | 2 | 1.74 | 0.27 | 10.0 | 19.0 | 300.0 |
| 1422A_41 | 35.6 | 8.3 | 137.7 | 42 | 18 | 3 | 0.18 | 0 | 4 | 2.06 | 0.41 | 39.0 | 175.0 | 200.0 |

| | | | | | | | | | | | | | | |
|---|---|---|---|---|---|---|---|---|---|---|---|---|---|---|
| | | | | | | 0.0000 | | 0.0 | | | | | | |
| 1422A_51 | 39.9 | 6.4 | 117.8 | 26 | 40 | 3 | 0.42 | 1 | 4 | 1.87 | 0.46 | 83.0 | 59.0 | 195.0 |
| | | | | | | 0.0000 | | 0.0 | | | | | | |
| 1422A_30 | 40.8 | 13.3 | 160.9 | 60 | 9 | 3 | 0.09 | 0 | 4 | 1.84 | 0.35 | 19.0 | 122.0 | 151.0 |
| | | | | | | 0.0000 | | 0.0 | | | | | | |
| 1422A_64 | 42.0 | 8.9 | 113.1 | 29 | 22 | 3 | 0.22 | 0 | 4 | 1.56 | 0.34 | 48.0 | 160.0 | 212.0 |
| | | | | | | 0.0000 | | 0.0 | | | | | | |
| 1422A_69 | 45.3 | 7.5 | 105.1 | 28 | 37 | 4 | 0.26 | 1 | 3 | 1.83 | 0.31 | 54.0 | 279.0 | 324.0 |
| | | | | | | 0.0000 | | 0.0 | | | | | | |
| 1422A_14 | 45.5 | 10.4 | 138.8 | 52 | 19 | 3 | 0.17 | 0 | 3 | 1.73 | 0.37 | 36.0 | 163.0 | 143.0 |
| | | | | | | 0.0000 | | 0.0 | | | | | | |
| 1422A_52 | 46.4 | 6.6 | 81.4 | 28 | 51 | 4 | 0.35 | 1 | 4 | 1.96 | 0.40 | 74.0 | 36.0 | 194.0 |
| | | | | | | 0.0000 | | 0.0 | | | | | | |
| 1422A_29 | 48.1 | 9.4 | 118.0 | 33 | 26 | 2 | 0.29 | 1 | 4 | 1.80 | 0.32 | 60.0 | 130.0 | 124.0 |
| | | | | | | 0.0000 | | 0.0 | | | | | | |
| 1422A_24 | 49.6 | 8.0 | 104.3 | 39 | 39 | 4 | 0.25 | 1 | 4 | 1.59 | 0.34 | 55.0 | 254.0 | 435.0 |
| | | | | | | 0.0000 | | 0.0 | | | | | | |
| 1422A_12 | 51.4 | 14.1 | 134.5 | 92 | 13 | 3 | 0.10 | 0 | 4 | 2.02 | 0.31 | 20.0 | 63.0 | 190.0 |
| | | | | | | 0.0000 | | 0.0 | | | | | | |
| 1422A_53 | 53.4 | 13.2 | 119.1 | 38 | 16 | 3 | 0.11 | 0 | 3 | 1.75 | 0.29 | 22.0 | 61.0 | 59.0 |
| | | | | | | 0.0000 | | 0.0 | | | | | | |
| 1422A_47 | 56.1 | 13.1 | 141.0 | 64 | 18 | 5 | 0.08 | 0 | 4 | 1.73 | 0.30 | 18.0 | 86.0 | 414.0 |
| | | | | | | 0.0000 | | 0.0 | | | | | | |
| 1422A_60 | 59.1 | 9.3 | 111.5 | 45 | 41 | 3 | 0.25 | 1 | 4 | 1.72 | 0.29 | 55.0 | 112.0 | 146.0 |
| | | | | | | 0.0000 | | 0.0 | | | | | | |
| 1422A_2 | 61.7 | 16.3 | 361.5 | 106 | 14 | 2 | 0.14 | 0 | 3 | 1.88 | 0.38 | 31.0 | 329.0 | 531.0 |
| | | | | | | 0.0000 | | 0.0 | | | | | | |
| 1422A_28 | 62.1 | 15.4 | 99.0 | 94 | 16 | 3 | 0.11 | 0 | 4 | 1.55 | 0.44 | 23.0 | 77.0 | 175.0 |
| | | | | | | 0.0000 | | 0.0 | | | | | | |
| 1422A_42 | 63.5 | 8.1 | 122.0 | 36 | 64 | 4 | 0.28 | 1 | 4 | 1.98 | 0.32 | 60.0 | 100.0 | 120.0 |
| | | | | | | 0.0000 | | 0.0 | | | | | | |
| 1422A_22 | 67.5 | 55.2 | 143.1 | 543 | 1 | 4 | 0.00 | 0 | 1 | 2.02 | 0.31 | 1.0 | 5.0 | 189.0 |
| | | | | | 11 | 0.0000 | | 0.0 | | | | | | |
| 1422A_38 | 72.8 | 7.0 | 118.6 | 27 | 4 | 5 | 0.40 | 1 | 4 | 1.99 | 0.33 | 84.0 | 106.0 | 137.0 |
| | | | | | | 0.0000 | | 0.0 | | | | | | |
| 1422A_35 | 77.8 | 13.5 | 523.0 | 693 | 48 | 3 | 0.26 | 3 | 4 | 1.91 | 0.36 | 53.0 | 115.0 | 742.0 |
| | | | | | | 0.0000 | | 0.0 | | | | | | |
| 1422A_70 | 88.7 | 24.2 | 188.6 | 125 | 13 | 5 | 0.04 | 0 | 4 | 2.97 | 0.50 | 8.0 | 56.0 | 113.0 |
| | | | | | 10 | 0.0000 | | 0.0 | | | | | | |
| 1422A_19 | 91.7 | 9.2 | 120.6 | 35 | 7 | 4 | 0.37 | 1 | 4 | 2.14 | 0.36 | 78.0 | 146.0 | 238.0 |
| | | | | | | 0.0000 | | 0.0 | | | | | | |
| 1422A_40 | 109.3 | 15.0 | 147.7 | 48 | 55 | 4 | 0.16 | 0 | 4 | 2.91 | 0.38 | 33.0 | 221.0 | 351.0 |
| | | | | | | 0.0000 | | 0.0 | | | | | | |
| 1422A_20 | 109.4 | 16.8 | 109.0 | 67 | 43 | 3 | 0.14 | 0 | 4 | 1.81 | 0.33 | 26.0 | 131.0 | 493.0 |
| | | | | | | 0.0000 | | 0.0 | | | | | | |
| 1422A_31 | 113.4 | 14.5 | 230.4 | 49 | 64 | 5 | 0.14 | 0 | 4 | 2.41 | 0.69 | 31.0 | 91.0 | 53.0 |
| | | | | | 14 | 0.0000 | | 0.0 | | | | | | |
| 1422A_59 | 113.6 | 9.9 | 105.7 | 26 | 3 | 4 | 0.40 | 1 | 4 | 2.16 | 0.70 | 184.0 | 196.0 | 157.0 |
| | | | | | | 0.0000 | | 0.0 | | | | | | |
| 1422A_39 | 120.1 | 34.1 | 161.7 | 135 | 12 | 2 | 0.05 | 0 | 4 | 1.68 | 0.32 | 11.0 | 30.0 | 259.0 |
| | | | | | | 0.0000 | | 0.0 | | | | | | |
| 1422A_13 | 123.1 | 18.2 | 218.2 | 59 | 49 | 3 | 0.17 | 1 | 4 | 1.88 | 0.41 | 37.0 | 4.0 | 316.0 |
| | | | | | | 0.0000 | | 0.0 | | | | | | |
| 1422A_8 | 126.0 | 15.7 | 110.2 | 19 | 69 | 5 | 0.14 | 0 | 4 | 2.01 | 0.35 | 117.0 | 180.0 | 281.0 |
| | | | | | 10 | 0.0000 | | 0.0 | | | | | | |
| 1422A_23 | 132.8 | 13.6 | 328.8 | 38 | 1 | 2 | 0.38 | 1 | 4 | 1.75 | 0.35 | 83.0 | 225.0 | 466.0 |
| | | | | | | 0.0000 | | 0.0 | | | | | | |
| 1422A_56 | 135.2 | 16.3 | 215.5 | 40 | 72 | 5 | 0.13 | 0 | 4 | 1.93 | 0.35 | 29.0 | 8.0 | 56.0 |
| | | | | | | 0.0000 | | 0.0 | | | | | | |
| 1422A_6 | 139.9 | 48.2 | 154.8 | 251 | 8 | 5 | 0.01 | 0 | 4 | 2.61 | 0.63 | 3.0 | 11.0 | 67.0 |
| | | | | | | 0.0000 | | 0.0 | | | | | | |
| 1422A_21 | 141.1 | 22.8 | 265.4 | 120 | 39 | 5 | 0.07 | 0 | 4 | 1.78 | 0.33 | 14.0 | 0.0 | 135.0 |
| | | | | | 16 | 0.0000 | | 0.0 | | | | | | |
| 1422A_50 | 145.1 | 11.9 | 140.6 | 21 | 7 | 3 | 0.48 | 1 | 4 | 2.02 | 0.39 | 103.0 | 153.0 | 101.0 |
| | | | | | | 0.0000 | | 0.0 | | | | | | |
| 1422A_18 | 148.2 | 21.2 | 226.1 | 44 | 50 | 3 | 0.14 | 0 | 4 | 1.88 | 0.43 | 30.0 | 7.0 | 233.0 |
| | | | | | | 0.0000 | | 0.0 | | | | | | |
| 1422A_62 | 151.8 | 33.1 | 363.2 | 236 | 21 | 3 | 0.06 | 0 | 3 | 1.55 | 0.30 | 13.0 | 1.0 | 132.0 |
| | | | | | | 0.0000 | | 0.0 | | | | | | |
| 1422A_68 | 156.0 | 17.0 | 155.4 | 69 | 96 | 5 | 0.15 | 1 | 4 | 2.43 | 0.62 | 33.0 | 284.0 | 645.0 |
| | | | | | | 0.0000 | | 0.0 | | | | | | |
| 1422A_25 | 163.7 | 18.9 | 106.7 | 81 | 81 | 4 | 0.14 | 0 | 4 | 1.57 | 0.27 | 31.0 | 145.0 | 108.0 |
| | | | | | | 0.0000 | | 0.0 | | | | | | |
| 1422A_57 | 178.8 | 23.3 | 0.0 | 0 | 61 | 3 | 0.14 | 0 | 4 | 1.97 | 0.40 | 0.0 | 0.0 | 0.0 |

| | | | | | | | | | | | | | | |
|---|---|---|---|---|---|---|---|---|---|---|---|---|---|---|
| 1422A_9 | 190.1 | 52.1 | 191.9 | 264 | 13 | 0.0000 5 | 0.02 | 0.0 0 | 3 | 2.61 | 0.42 | 4.0 | 12.0 | 68.0 |
| 1422A_67 | 192.4 | 59.7 | 149.7 | 255 | 10 | 0.0000 5 | 0.01 | 0.0 0 | 4 | 3.47 | 0.78 | 3.0 | 12.0 | 67.0 |
| 1422A_45 | 193.8 | 28.9 | 204.1 | 129 | 47 | 0.0000 5 | 0.06 | 0.0 0 | 4 | 1.73 | 0.30 | 13.0 | 76.0 | 203.0 |
| 1422A_61 | 198.2 | 21.6 | 226.1 | 43 | 90 | 0.0000 4 | 0.14 | 0.0 0 | 4 | 2.08 | 0.30 | 29.0 | 140.0 | 216.0 |
| 1422A_48 | 212.2 | 22.0 | 148.2 | 42 | 99 | 0.0000 3 | 0.19 | 0.0 0 | 4 | 2.25 | 0.56 | 42.0 | 155.0 | 116.0 |
| 1422A_66 | 214.1 | 24.5 | 63.2 | 13 | 83 | 0.0000 3 | 0.14 | 0.0 0 | 4 | 2.02 | 0.51 | 166.0 | 37.0 | 206.0 |
| 1422A_5 | 219.0 | 80.6 | 144.6 | 325 | 7 | 0.0000 4 | 0.01 | 0.0 0 | 3 | 2.28 | 0.69 | 2.0 | 5.0 | 43.0 |
| 1422A_46 | 224.6 | 38.3 | 259.8 | 104 | 35 | 0.0000 4 | 0.04 | 0.0 0 | 4 | 1.91 | 0.39 | 10.0 | 9.0 | 258.0 |
| 1422A_33 | 235.8 | 62.3 | 173.9 | 184 | 14 | 0.0000 4 | 0.02 | 0.0 0 | 4 | 2.57 | 0.41 | 4.0 | 38.0 | 86.0 |
| 1422A_10 | 247.8 | 61.6 | 318.4 | 199 | 16 | 0.0000 2 | 0.03 | 0.0 0 | 2 | 1.51 | 0.29 | 7.0 | 4.0 | 110.0 |
| 1422A_32 | 319.9 | 77.1 | 248.9 | 265 | 17 | 0.0000 3 | 0.02 | 0.0 0 | 4 | 2.81 | 0.66 | 4.0 | 19.0 | 42.0 |
| 1422A_26 | 375.2 | 307.4 | 0.0 | 0 | 1 | 0.0000 3 | 0.00 | 0.0 0 | 1 | 2.59 | 0.47 | 0.0 | 2.0 | 54.0 |
| 1422A_27 | 524.1 | 737.2 | 0.0 | 0 | 7 | 0.0000 2 | 0.01 | 0.0 1 | 4 | 1.75 | 0.30 | 7.0 | 13.0 | 215.0 |

**Maclaren Bridge**

| Spot Name | FT Age (Ma) | sigma sym (Ma) | UPb Age (Ma) | 2 sigma (Ma) | Ns | Area cm^2 | U/Cation | +/- 1sig | Etch Figs. | Dpar (um) | Dper (um) | [U] (ppm) | [Th] (ppm) | [Sm] (ppm) |
|---|---|---|---|---|---|---|---|---|---|---|---|---|---|---|
| 4396A_4 | 0.0 | 38.0 | 0.0 | 0 | 0 | 0.0000 5 | 0.00 | 0.0 0 | 1 | 1.58 | 0.26 | 0.1 | 0.0 | 1.4 |
| 4396A_55 | 0.0 | 141.2 | 0.0 | 0 | 0 | 0.0000 2 | 0.00 | 0.0 0 | 1 | 1.28 | 0.24 | 0.3 | 0.1 | 5.0 |
| 4396A_80 | 0.0 | 3.9 | 0.0 | 0 | 0 | 0.0000 4 | 0.04 | 0.0 0 | 1 | 1.79 | 0.28 | 2.6 | 17.8 | 12.3 |
| 4396A_82 | 0.0 | 115.0 | 0.0 | 0 | 0 | 0.0000 2 | 0.00 | 0.0 0 | 1 | 1.34 | 0.25 | 0.3 | 0.7 | 22.5 |
| 4396A_102 | 0.0 | 2.0 | 0.0 | 0 | 0 | 0.0000 5 | 0.06 | 0.0 1 | 1 | 1.83 | 0.29 | 1.5 | 2.0 | 24.1 |
| 4396A_54 | 3.7 | 1.5 | 0.0 | 0 | 7 | 0.0000 2 | 0.76 | 0.0 9 | 2 | 1.68 | 0.36 | 45.9 | 205.6 | 56.5 |
| 4396A_35 | 5.0 | 1.8 | 0.0 | 0 | 8 | 0.0000 2 | 0.57 | 0.0 6 | 4 | 1.60 | 0.37 | 42.7 | 40.6 | 203.5 |
| 4396A_73 | 5.4 | 3.1 | 0.0 | 0 | 3 | 0.0000 2 | 0.27 | 0.0 2 | 2 | 1.61 | 0.30 | 48.6 | 76.7 | 49.6 |
| 4396A_6 | 6.5 | 2.5 | 81.4 | 76 | 7 | 0.0000 5 | 0.18 | 0.0 1 | 3 | 1.93 | 0.30 | 36.2 | 2.9 | 115.6 |
| 4396A_76 | 6.9 | 6.9 | 0.0 | 0 | 1 | 0.0000 2 | 0.06 | 0.0 1 | 1 | 1.58 | 0.49 | 7.0 | 16.6 | 80.6 |
| 4396A_42 | 7.6 | 3.5 | 0.0 | 0 | 5 | 0.0000 1 | 0.37 | 0.0 4 | 4 | 1.70 | 0.40 | 38.1 | 105.5 | 67.7 |
| 4396A_28 | 7.9 | 5.8 | 0.0 | 0 | 2 | 0.0000 1 | 0.17 | 0.0 3 | 2 | 1.84 | 0.40 | 17.6 | 70.8 | 85.4 |
| 4396A_44 | 8.2 | 4.7 | 180.1 | 144 | 3 | 0.0000 3 | 0.09 | 0.1 0 | 2 | 1.95 | 0.43 | 16.4 | 34.6 | 120.3 |
| 4396A_18 | 8.4 | 3.2 | 0.0 | 0 | 10 | 0.0000 2 | 0.48 | 0.1 0 | 3 | 1.71 | 0.30 | 26.3 | 375.3 | 48.8 |
| 4396A_68 | 8.7 | 3.2 | 0.0 | 0 | 15 | 0.0000 3 | 0.46 | 0.0 2 | 4 | 1.86 | 0.29 | 13.0 | 66.5 | 34.8 |
| 4396A_50 | 9.2 | 3.5 | 54.5 | 73 | 7 | 0.0000 3 | 0.22 | 0.0 1 | 4 | 1.94 | 0.47 | 37.5 | 116.9 | 75.5 |
| 4396A_101 | 9.3 | 4.7 | 0.0 | 0 | 4 | 0.0000 4 | 0.09 | 0.0 1 | 1 | 1.76 | 0.39 | 8.9 | 21.3 | 8.1 |
| 4396A_77 | 9.8 | 2.9 | 0.0 | 0 | 13 | 0.0000 3 | 0.40 | 0.0 4 | 3 | 1.66 | 0.51 | 39.2 | 11.5 | 110.0 |
| 4396A_30 | 10.1 | 3.5 | 0.0 | 0 | 9 | 0.0000 2 | 0.30 | 0.0 2 | 3 | 1.43 | 0.36 | 46.1 | 19.7 | 77.2 |
| 4396A_40 | 10.4 | 7.4 | 0.0 | 0 | 2 | 2 | 0.09 | 1 | 2 | 1.62 | 0.46 | 18.8 | 6.4 | 21.4 |

| | | | | | | | | | | | | | | |
|---|---|---|---|---|---|---|---|---|---|---|---|---|---|---|
| | | | | | | 0.0000 | | 0.0 | | | | | | |
| 4396A_90 | 12.4 | 1.9 | 57.1 | 13 | 47 | 2 | 1.80 | 5 | 4 | 1.77 | 0.39 | 249.8 | 6.0 | 199.6 |
| | | | | | | 0.0000 | | 0.0 | | | | | | |
| 4396A_104 | 13.0 | 4.6 | 101.8 | 83 | 8 | 3 | 0.17 | 1 | 4 | 1.80 | 0.31 | 19.2 | 18.7 | 90.5 |
| | | | | | | 0.0000 | | 0.0 | | | | | | |
| 4396A_105 | 13.0 | 3.2 | 0.0 | 0 | 17 | 2 | 0.45 | 2 | 4 | 1.73 | 0.36 | 0.1 | 4.8 | 5.9 |
| | | | | | | 0.0000 | | 0.0 | | | | | | |
| 4396A_86 | 13.5 | 3.6 | 272.3 | 424 | 14 | 3 | 0.32 | 1 | 4 | 1.94 | 0.46 | 39.9 | 134.5 | 68.6 |
| | | | | | | 0.0000 | | 0.2 | | | | | | |
| 4396A_27 | 13.6 | 4.0 | ###### | #### | 41 | 2 | 1.03 | 6 | 4 | 1.94 | 0.49 | 55.4 | 30.2 | 97.0 |
| | | | | | | 0.0000 | | 0.0 | | | | | | |
| 4396A_67 | 13.7 | 5.6 | 143.2 | 119 | 6 | 3 | 0.12 | 1 | 3 | 1.56 | 0.38 | 16.8 | 35.2 | 132.4 |
| | | | | | | 0.0000 | | 0.0 | | | | | | |
| 4396A_11 | 13.8 | 3.4 | ###### | #### | 17 | 2 | 0.42 | 1 | 4 | 1.87 | 0.30 | 80.4 | 9.8 | 125.1 |
| | | | | | | 0.0000 | | 0.0 | | | | | | |
| 4396A_7 | 14.1 | 2.0 | 60.3 | 20 | 51 | 4 | 0.70 | 3 | 4 | 1.90 | 0.41 | 131.7 | 3.2 | 220.8 |
| | | | | | | 0.0000 | | 0.0 | | | | | | |
| 4396A_41 | 15.1 | 4.6 | 85.2 | 60 | 11 | 2 | 0.26 | 1 | 3 | 1.66 | 0.37 | 44.7 | 18.1 | 53.0 |
| | | | | | | 0.0000 | | 0.0 | | | | | | |
| 4396A_46 | 15.1 | 6.8 | 0.0 | 0 | 5 | 1 | 0.22 | 1 | 4 | 1.71 | 0.33 | 31.4 | 49.9 | 143.6 |
| | | | | | | 0.0000 | | 0.0 | | | | | | |
| 4396A_3 | 15.2 | 4.6 | 0.0 | 0 | 11 | 2 | 0.25 | 1 | 4 | 2.18 | 0.48 | 43.1 | 200.4 | 104.3 |
| | | | | | | 0.0000 | | 0.0 | | | | | | |
| 4396A_43 | 15.2 | 4.1 | 72.4 | 30 | 14 | 2 | 0.39 | 1 | 3 | 1.67 | 0.29 | 79.0 | 21.5 | 172.5 |
| | | | | | | 0.0000 | | 0.0 | | | | | | |
| 4396A_16 | 15.2 | 6.2 | 74.7 | 62 | 6 | 2 | 0.16 | 0 | 2 | 1.61 | 0.28 | 34.6 | 57.6 | 88.0 |
| | | | | | | 0.0000 | | 0.0 | | | | | | |
| 4396A_92 | 15.6 | 4.5 | 46.3 | 59 | 12 | 3 | 0.21 | 1 | 4 | 1.91 | 0.45 | 35.3 | 27.2 | 236.3 |
| | | | | | | 0.0000 | | 0.0 | | | | | | |
| 4396A_57 | 15.8 | 9.1 | 112.3 | 160 | 3 | 2 | 0.08 | 0 | 2 | 1.53 | 0.28 | 14.2 | 10.9 | 18.0 |
| | | | | | | 0.0000 | | 0.0 | | | | | | |
| 4396A_15 | 16.4 | 5.8 | 79.2 | 61 | 8 | 2 | 0.21 | 1 | 4 | 1.64 | 0.34 | 37.7 | 0.3 | 70.7 |
| | | | | | | 0.0000 | | 0.0 | | | | | | |
| 4396A_74 | 16.5 | 3.8 | 57.1 | 33 | 20 | 4 | 0.26 | 1 | 3 | 2.08 | 0.33 | 49.1 | 203.0 | 81.9 |
| | | | | | | 0.0000 | | 0.0 | | | | | | |
| 4396A_17 | 16.9 | 17.0 | 0.0 | 0 | 1 | 2 | 0.03 | 0 | 1 | 1.68 | 0.31 | 6.1 | 12.5 | 31.6 |
| | | | | | | 0.0000 | | 0.0 | | | | | | |
| 4396A_2 | 17.0 | 7.6 | 0.0 | 0 | 5 | 1 | 0.20 | 1 | 3 | 1.80 | 0.40 | 38.6 | 103.7 | 156.6 |
| | | | | | | 0.0000 | | 0.0 | | | | | | |
| 4396A_81 | 17.1 | 6.1 | 95.6 | 62 | 8 | 2 | 0.20 | 1 | 2 | 1.46 | 0.40 | 34.3 | 63.0 | 119.0 |
| | | | | | | 0.0000 | | 0.0 | | | | | | |
| 4396A_89 | 17.3 | 6.6 | 135.8 | 180 | 7 | 3 | 0.11 | 1 | 4 | 1.63 | 0.31 | 17.8 | 1.4 | 103.5 |
| | | | | | | 0.0000 | | 0.0 | | | | | | |
| 4396A_45 | 17.8 | 9.1 | 0.0 | 0 | 4 | 2 | 0.08 | 1 | 4 | 1.77 | 0.32 | 8.9 | 24.3 | 51.3 |
| | | | | | | 0.0000 | | 0.0 | | | | | | |
| 4396A_29 | 17.9 | 6.8 | 0.0 | 0 | 7 | 2 | 0.16 | 0 | 4 | 1.61 | 0.41 | 169.4 | 44.5 | 102.6 |
| | | | | | | 0.0000 | | 0.0 | | | | | | |
| 4396A_49 | 18.3 | 3.6 | 66.5 | 32 | 27 | 2 | 0.70 | 3 | 4 | 1.90 | 0.31 | 116.3 | 25.7 | 272.5 |
| | | | | | | 0.0000 | | 0.0 | | | | | | |
| 4396A_1 | 18.5 | 18.5 | 471.7 | 472 | 1 | 2 | 0.02 | 0 | 1 | 1.78 | 0.19 | 3.8 | 0.3 | 60.8 |
| | | | | | | 0.0000 | | 0.0 | | | | | | |
| 4396A_84 | 18.5 | 4.4 | 62.7 | 31 | 18 | 2 | 0.46 | 2 | 4 | 1.62 | 0.38 | 92.7 | 4.9 | 194.0 |
| | | | | | | 0.0000 | | 0.0 | | | | | | |
| 4396A_22 | 19.0 | 4.2 | 56.8 | 21 | 21 | 2 | 0.39 | 1 | 2 | 1.67 | 0.36 | 77.2 | 283.0 | 127.6 |
| | | | | | | 0.0000 | | 0.0 | | | | | | |
| 4396A_103 | 19.1 | 6.1 | 85.8 | 59 | 10 | 2 | 0.19 | 1 | 4 | 1.82 | 0.41 | 32.8 | 35.0 | 81.9 |
| | | | | | | 0.0000 | | 0.0 | | | | | | |
| 4396A_100 | 19.1 | 3.4 | 60.3 | 13 | 33 | 2 | 0.61 | 2 | 4 | 1.61 | 0.31 | 123.1 | 100.2 | 301.3 |
| | | | | | | 0.0000 | | 0.0 | | | | | | |
| 4396A_31 | 19.4 | 4.5 | 58.8 | 41 | 19 | 2 | 0.42 | 1 | 2 | 1.48 | 0.31 | 74.9 | 26.3 | 218.2 |
| | | | | | | 0.0000 | | 0.0 | | | | | | |
| 4396A_34 | 20.0 | 4.0 | 60.7 | 23 | 26 | 2 | 0.46 | 2 | 4 | 1.93 | 0.37 | 78.1 | 203.9 | 143.2 |
| | | | | | | 0.0000 | | 0.0 | | | | | | |
| 4396A_88 | 20.0 | 3.5 | 56.5 | 23 | 35 | 2 | 0.62 | 2 | 4 | 1.83 | 0.32 | 117.2 | 89.6 | 72.9 |
| | | | | | | 0.0000 | | 0.0 | | | | | | |
| 4396A_10 | 20.1 | 5.3 | 66.3 | 71 | 15 | 5 | 0.13 | 1 | 4 | 1.85 | 0.58 | 24.5 | 43.1 | 83.2 |
| | | | | | | 0.0000 | | 0.0 | | | | | | |
| 4396A_75 | 20.1 | 8.9 | 0.0 | 0 | 6 | 3 | 0.08 | 1 | 3 | 1.71 | 0.33 | 15.6 | 578.3 | 74.0 |
| | | | | | | 0.0000 | | 0.0 | | | | | | |
| 4396A_87 | 20.3 | 20.3 | 0.0 | 0 | 1 | 2 | 0.02 | 0 | 1 | 1.86 | 0.30 | 0.3 | 2.0 | 5.1 |
| | | | | | | 0.0000 | | 0.0 | | | | | | |
| 4396A_21 | 20.7 | 5.2 | 62.3 | 35 | 16 | 3 | 0.19 | 0 | 4 | 2.05 | 0.39 | 38.3 | 38.7 | 113.0 |
| | | | | | | 0.0000 | | 0.0 | | | | | | |
| 4396A_98 | 20.9 | 8.6 | 92.0 | 95 | 6 | 2 | 0.10 | 0 | 4 | 1.78 | 0.38 | 16.9 | 0.1 | 99.2 |

| | | | | | | | | | | | | | | |
|---|---|---|---|---|---|---|---|---|---|---|---|---|---|---|
| | | | | | | 0.0000 | | 0.0 | | | | | | |
| 4396A_23 | 21.1 | 5.5 | 70.6 | 59 | 15 | 3 | 0.19 | 1 | 4 | 1.69 | 0.31 | 43.8 | 131.8 | 92.7 |
| | | | | | | 0.0000 | | 0.0 | | | | | | |
| 4396A_93 | 21.2 | 8.8 | 0.0 | 0 | 6 | 2 | 0.10 | 1 | 2 | 1.98 | 0.30 | 8.2 | 16.2 | 53.5 |
| | | | | | | 0.0000 | | 0.0 | | | | | | |
| 4396A_39 | 21.2 | 7.2 | 0.0 | 0 | 11 | 2 | 0.18 | 3 | 4 | 2.01 | 0.38 | 41.6 | 35.0 | 56.9 |
| | | | | | | 0.0000 | | 0.0 | | | | | | |
| 4396A_95 | 21.4 | 6.2 | 0.0 | 0 | 12 | 2 | 0.24 | 1 | 3 | 1.68 | 0.35 | 41.1 | 19.3 | 140.6 |
| | | | | | | 0.0000 | | 0.1 | | | | | | |
| 4396A_38 | 22.0 | 7.9 | 0.0 | 0 | 17 | 1 | 0.47 | 2 | 4 | 1.98 | 0.38 | 80.4 | 129.2 | 50.4 |
| | | | | | | 0.0000 | | 0.0 | | | | | | |
| 4396A_33 | 22.2 | 4.0 | 66.7 | 40 | 31 | 3 | 0.34 | 1 | 4 | 2.03 | 0.41 | 67.2 | 135.3 | 102.6 |
| | | | | | | 0.0000 | | 0.1 | | | | | | |
| 4396A_99 | 22.2 | 10.4 | 0.0 | 0 | 20 | 3 | 0.24 | 0 | 4 | 2.10 | 0.40 | 7.8 | 13.2 | 7.7 |
| | | | | | | 0.0000 | | 0.0 | | | | | | |
| 4396A_26 | 22.2 | 6.5 | 97.7 | 82 | 12 | 3 | 0.14 | 0 | 4 | 1.96 | 0.44 | 27.2 | 6.1 | 23.5 |
| | | | | | | 0.0000 | | 0.0 | | | | | | |
| 4396A_13 | 22.3 | 9.5 | 0.0 | 0 | 6 | 1 | 0.20 | 2 | 3 | 1.99 | 0.40 | 39.9 | 37.9 | 50.5 |
| | | | | | | 0.0000 | | 0.0 | | | | | | |
| 4396A_36 | 22.4 | 6.3 | 0.0 | 0 | 17 | 2 | 0.26 | 4 | 4 | 2.01 | 0.61 | 30.6 | 262.8 | 87.7 |
| | | | | | | 0.0000 | | 0.0 | | | | | | |
| 4396A_19 | 22.8 | 6.7 | 125.6 | 144 | 12 | 4 | 0.11 | 0 | 4 | 1.89 | 0.35 | 18.8 | 18.5 | 241.5 |
| | | | | | | 0.0000 | | 0.0 | | | | | | |
| 4396A_9 | 23.6 | 7.1 | 0.0 | 0 | 11 | 2 | 0.19 | 0 | 4 | 1.74 | 0.32 | 39.9 | 93.2 | 73.3 |
| | | | | | | 0.0000 | | 0.0 | | | | | | |
| 4396A_48 | 24.0 | 11.0 | 0.0 | 0 | 7 | 2 | 0.14 | 4 | 3 | 1.74 | 0.35 | 22.2 | 412.2 | 109.5 |
| | | | | | | 0.0000 | | 0.0 | | | | | | |
| 4396A_32 | 24.8 | 8.3 | 78.9 | 93 | 9 | 3 | 0.10 | 0 | 4 | 1.63 | 0.29 | 16.4 | 17.7 | 137.5 |
| | | | | | | 0.0000 | | 0.0 | | | | | | |
| 4396A_62 | 24.8 | 6.3 | 44.8 | 50 | 16 | 2 | 0.24 | 1 | 4 | 1.84 | 0.29 | 41.5 | 71.7 | 135.0 |
| | | | | | | 0.0000 | | 0.0 | | | | | | |
| 4396A_66 | 25.2 | 5.1 | 69.6 | 58 | 25 | 4 | 0.21 | 1 | 4 | 2.10 | 0.61 | 36.3 | 32.5 | 235.0 |
| | | | | | | 0.0000 | | 0.1 | | | | | | |
| 4396A_79 | 25.6 | 11.8 | 0.0 | 0 | 26 | 3 | 0.25 | 0 | 4 | 1.70 | 0.37 | 17.0 | 67.6 | 75.8 |
| | | | | | | 0.0000 | | 0.0 | | | | | | |
| 4396A_71 | 25.7 | 10.5 | 80.8 | 90 | 6 | 2 | 0.08 | 0 | 4 | 1.95 | 0.41 | 15.9 | 28.7 | 94.4 |
| | | | | | | 0.0000 | | 0.0 | | | | | | |
| 4396A_59 | 27.2 | 10.5 | 0.0 | 0 | 7 | 3 | 0.07 | 1 | 4 | 1.77 | 0.51 | 8.2 | 27.0 | 45.3 |
| | | | | | | 0.0000 | | 0.0 | | | | | | |
| 4396A_94 | 27.8 | 3.0 | 54.4 | 11 | 92 | 2 | 1.17 | 3 | 4 | 1.68 | 0.35 | 220.8 | 265.7 | 86.7 |
| | | | | | | 0.0000 | | 0.0 | | | | | | |
| 4396A_72 | 28.5 | 28.5 | 0.0 | 0 | 1 | 2 | 0.02 | 0 | 1 | 1.65 | 0.33 | 2.8 | 17.7 | 25.4 |
| | | | | | | 0.0000 | | 0.0 | | | | | ##### | |
| 4396A_60 | 29.0 | 16.2 | 50.6 | 13 | 8 | 2 | 0.12 | 5 | 4 | 2.12 | 0.51 | 434.3 | # | 732.7 |
| | | | | | | 0.0000 | | 0.0 | | | | | | |
| 4396A_64 | 29.5 | 29.5 | 314.9 | 499 | 1 | 2 | 0.01 | 0 | 1 | 1.51 | 0.37 | 4.1 | 9.3 | 63.3 |
| | | | | | | 0.0000 | | 0.0 | | | | | | |
| 4396A_96 | 29.7 | 6.7 | 91.2 | 79 | 20 | 3 | 0.19 | 1 | 3 | 1.64 | 0.30 | 25.6 | 52.5 | 78.0 |
| | | | | | | 0.0000 | | 0.0 | | | | | | |
| 4396A_69 | 30.1 | 17.5 | 297.8 | 780 | 3 | 4 | 0.02 | 0 | 3 | 2.40 | 0.56 | 2.9 | 10.6 | 94.4 |
| | | | | | | 0.0000 | | 0.0 | | | | | | |
| 4396A_14 | 30.4 | 31.1 | 0.0 | 0 | 6 | 2 | 0.09 | 9 | 4 | 1.75 | 0.34 | 7.3 | 75.8 | 34.9 |
| | | | | | | 0.0000 | | 0.0 | | | | | | |
| 4396A_56 | 31.8 | 13.0 | 0.0 | 0 | 6 | 2 | 0.09 | 0 | 3 | 1.80 | 0.38 | 0.2 | 0.4 | 8.0 |
| | | | | | | 0.0000 | | 0.0 | | | | | | |
| 4396A_52 | 34.5 | 9.0 | 84.8 | 88 | 15 | 3 | 0.12 | 0 | 4 | 2.02 | 0.59 | 17.8 | 29.1 | 87.1 |
| | | | | | | 0.0000 | | 0.0 | | | | | | |
| 4396A_78 | 34.7 | 17.2 | 0.0 | 0 | 9 | 2 | 0.09 | 3 | 4 | 2.29 | 0.41 | 18.6 | 252.2 | 26.0 |
| | | | | | | 0.0000 | | 0.0 | | | | | | |
| 4396A_47 | 36.5 | 24.6 | 0.0 | 0 | 5 | 2 | 0.07 | 3 | 3 | 1.69 | 0.31 | 16.1 | 103.7 | 114.3 |
| | | | | | | 0.0000 | | 0.0 | | | | | | |
| 4396A_37 | 36.5 | 7.7 | 0.0 | 0 | 23 | 2 | 0.21 | 1 | 4 | 1.61 | 0.30 | 28.6 | 7.4 | 75.9 |
| | | | | | | 0.0000 | | 0.0 | | | | | | |
| 4396A_97 | 38.4 | 5.3 | 69.5 | 48 | 55 | 4 | 0.30 | 1 | 4 | 1.76 | 0.45 | 53.3 | 18.4 | 235.0 |
| | | | | | | 0.0000 | | 0.0 | | | | | | |
| 4396A_70 | 38.4 | 14.6 | 101.9 | 116 | 7 | 3 | 0.05 | 0 | 2 | 2.09 | 0.57 | 8.0 | 24.9 | 84.5 |
| | | | | | | 0.0000 | | 0.0 | | | | | | |
| 4396A_8 | 39.4 | 15.7 | 0.0 | 0 | 7 | 3 | 0.05 | 1 | 3 | 1.78 | 0.35 | 6.3 | 239.9 | 69.9 |
| | | | | | | 0.0000 | | 0.0 | | | | | | |
| 4396A_20 | 40.4 | 9.3 | 62.2 | 49 | 19 | 3 | 0.11 | 0 | 4 | 1.81 | 0.38 | 22.6 | 82.1 | 90.1 |
| | | | | | | 0.0000 | | 0.0 | | | | | | |
| 4396A_51 | 41.2 | 10.3 | 0.0 | 0 | 21 | 4 | 0.10 | 1 | 4 | 1.73 | 0.31 | 9.3 | 53.5 | 45.3 |
| | | | | | | 0.0000 | | 0.0 | | | | | | |
| 4396A_65 | 41.3 | 25.4 | 0.0 | 0 | 3 | 2 | 0.03 | 1 | 4 | 1.59 | 0.48 | 3.5 | 15.6 | 83.2 |

| | | | | | | | | | | | | | | |
|---|---|---|---|---|---|---|---|---|---|---|---|---|---|---|
| | | | | | | 0.0000 | | 0.0 | | | | | | |
| 4396A_58 | 41.6 | 15.8 | 0.0 | 0 | 7 | 2 | 0.07 | 0 | 4 | 1.74 | 0.27 | 10.0 | 54.8 | 19.2 |
| | | | | | | 0.0000 | | 0.0 | | | | | | |
| 4396A_63 | 46.3 | 25.1 | 0.0 | 0 | 5 | 2 | 0.06 | 2 | 3 | 1.77 | 0.23 | 5.2 | 17.6 | 35.0 |
| | | | | | | 0.0000 | | 0.0 | | | | | | |
| 4396A_85 | 47.2 | 16.9 | 388.7 | 506 | 8 | 4 | 0.04 | 0 | 4 | 1.92 | 0.40 | 10.4 | 1.5 | 65.5 |
| | | | | | | 0.0000 | | 0.0 | | | | | | |
| 4396A_12 | 48.0 | 21.8 | 0.0 | 0 | 5 | 2 | 0.04 | 0 | 2 | 1.78 | 0.39 | 8.8 | 15.6 | 41.0 |
| | | | | | | 0.0000 | | 0.0 | | | | | | |
| 4396A_61 | 48.1 | 17.6 | 93.4 | 127 | 8 | 1 | 0.09 | 1 | 3 | 1.81 | 0.29 | 14.7 | 25.0 | 100.5 |
| | | | | | | 0.0000 | | 0.0 | | | | | | |
| 4396A_25 | 49.7 | 13.9 | 110.4 | 90 | 13 | 3 | 0.07 | 0 | 4 | 2.19 | 0.40 | 10.3 | 6.1 | 50.0 |
| | | | | | | 0.0000 | | 0.0 | | | | | | |
| 4396A_5 | 66.5 | 47.2 | 359.0 | 464 | 2 | 2 | 0.01 | 0 | 2 | 1.71 | 0.25 | 2.1 | 8.3 | 79.4 |
| | | | | | | 0.0000 | | 0.0 | | | | | | |
| 4396A_83 | 73.2 | 34.8 | 0.0 | 0 | 25 | 2 | 0.12 | 5 | 4 | 1.76 | 0.33 | 26.8 | 384.0 | 72.4 |
| | | | | | | 0.0000 | | 0.0 | | | | | | |
| 4396A_53 | 90.0 | 36.9 | 121.9 | 349 | 6 | 2 | 0.02 | 0 | 3 | 2.00 | 0.44 | 4.5 | 19.9 | 188.9 |
| | | | | | | 0.0000 | | 0.0 | | | | | | |
| 4396A_91 | 152.7 | 46.6 | 0.0 | 0 | 17 | 2 | 0.04 | 1 | 4 | 1.66 | 0.24 | 7.8 | 34.7 | 39.6 |
| | | | | | | 0.0000 | | 0.0 | | | | | | |
| 4396A_24 | 375.0 | 72.9 | 102.5 | 172 | 90 | 4 | 0.05 | 1 | 4 | 1.60 | 0.32 | 18.0 | 2.5 | 76.7 |

**Maclaren Glacier**

| Spot Name | FT Age (Ma) | sigma sym (Ma) | UPb Age (Ma) | 2 sigma (Ma) | Ns | Area cm^2 | U/Cation | +/- 1sig | Etch Figs. | Dpar (um) | Dper (um) | [U] (ppm) | [Th] (ppm) | [Sm] (ppm) |
|---|---|---|---|---|---|---|---|---|---|---|---|---|---|---|
| | | | | | | 0.0000 | | 0.0 | | | | | | |
| 4392A_35 | 0.0 | 348.0 | 0.0 | 0 | 0 | 3 | 0.00 | 0 | 1 | 1.34 | 0.26 | 0.1 | 0.0 | 2.2 |
| | | | | | | 0.0000 | | 0.0 | | | | | | |
| 4392A_13 | 0.0 | 228.9 | 0.0 | 0 | 0 | 2 | 0.00 | 0 | 1 | 1.61 | 0.43 | 0.2 | 0.0 | 3.7 |
| | | | | | | 0.0000 | | 0.0 | | | | | | |
| 4392A_47 | 0.0 | 79.0 | 0.0 | 0 | 0 | 4 | 0.00 | 0 | 1 | 1.30 | 0.19 | 0.3 | 0.1 | 26.3 |
| | | | | | | 0.0000 | | 0.0 | | | | | | |
| 4392A_70 | 0.0 | 64.3 | 0.0 | 0 | 0 | 1 | 0.01 | 0 | 1 | 1.52 | 0.24 | 0.4 | 0.0 | 18.0 |
| | | | | | | 0.0000 | | 0.0 | | | | | | |
| 4392A_40 | 0.0 | 5.4 | 0.0 | 0 | 0 | 2 | 0.04 | 0 | 1 | 2.10 | 0.38 | 0.6 | 4.2 | 9.1 |
| | | | | | | 0.0000 | | 0.0 | | | | | | |
| 4392A_95 | 0.0 | 20.4 | 0.0 | 0 | 0 | 5 | 0.01 | 0 | 1 | 1.40 | 0.31 | 0.6 | 1.7 | 62.0 |
| | | | | | | 0.0000 | | 0.0 | | | | | | |
| 4392A_83 | 0.0 | 30.1 | 0.0 | 0 | 0 | 5 | 0.00 | 0 | 1 | 1.46 | 0.33 | 0.9 | 11.7 | 7.5 |
| | | | | | | 0.0000 | | 0.0 | | | | | | |
| 4392A_24 | 0.0 | 43.1 | 0.0 | 0 | 0 | 2 | 0.01 | 0 | 1 | 1.66 | 0.39 | 0.9 | 5.2 | 67.7 |
| | | | | | | 0.0000 | | 0.0 | | | | | | |
| 4392A_71 | 0.0 | 42.6 | 0.0 | 0 | 0 | 3 | 0.00 | 0 | 1 | 1.27 | 0.26 | 0.9 | 0.5 | 54.3 |
| | | | | | | 0.0000 | | 0.0 | | | | | | |
| 4392A_22 | 0.0 | 34.8 | 0.0 | 0 | 0 | 3 | 0.01 | 0 | 1 | 1.90 | 0.35 | 1.0 | 0.2 | 17.2 |
| | | | | | | 0.0000 | | 0.0 | | | | | | |
| 4392A_16 | 0.0 | 36.1 | 563.4 | 948 | 0 | 3 | 0.01 | 0 | 1 | 2.02 | 0.27 | 1.1 | 1.6 | 36.9 |
| | | | | | | 0.0000 | | 0.0 | | | | | | |
| 4392A_73 | 0.0 | 32.1 | 0.0 | 0 | 0 | 3 | 0.01 | 0 | 1 | 1.96 | 0.34 | 1.1 | 0.2 | 44.4 |
| | | | | | | 0.0000 | | 0.0 | | | | | | |
| 4392A_75 | 0.0 | 46.0 | 867.2 | #### | 0 | 2 | 0.01 | 0 | 1 | 1.94 | 0.38 | 1.4 | 0.5 | 36.4 |
| | | | | | | 0.0000 | | 0.0 | | | | | | |
| 4392A_17 | 0.0 | 21.0 | 0.0 | 0 | 0 | 3 | 0.01 | 0 | 1 | 1.36 | 0.25 | 1.5 | 1.9 | 78.0 |
| | | | | | | 0.0000 | | 0.0 | | | | | | |
| 4392A_38 | 0.0 | 22.8 | 429.8 | 589 | 0 | 3 | 0.01 | 0 | 1 | 1.79 | 0.31 | 1.7 | 2.0 | 35.2 |
| | | | | | | 0.0000 | | 0.0 | | | | | | |
| 4392A_42 | 0.0 | 5.9 | 0.0 | 0 | 0 | 2 | 0.05 | 1 | 1 | 1.65 | 0.21 | 4.3 | 66.6 | 75.9 |
| | | | | | | 0.0000 | | 0.0 | | | | | | |
| 4392A_77 | 6.0 | 2.3 | 455.7 | #### | 7 | 2 | 0.55 | 4 | 4 | 1.90 | 0.35 | 114.5 | 155.6 | 200.5 |
| | | | | | | 0.0000 | | 0.0 | | | | | | |
| 4392A_50 | 7.6 | 7.6 | 0.0 | 0 | 1 | 2 | 0.04 | 0 | 1 | 1.97 | 0.69 | 7.4 | 28.6 | 211.7 |
| | | | | | | 0.0000 | | 0.0 | | | | | | |
| 4392A_78 | 7.7 | 2.8 | 0.0 | 0 | 8 | 3 | 0.28 | 2 | 4 | 1.91 | 0.33 | 47.9 | 48.1 | 127.2 |
| | | | | | | 0.0000 | | 0.0 | | | | | | |
| 4392A_29 | 8.1 | 8.1 | 52.6 | 8 | 1 | 3 | 0.04 | 0 | 1 | 1.71 | 0.45 | 166.8 | 214.9 | 174.2 |
| | | | | | | 0.0000 | | 0.1 | | | | | | |
| 4392A_74 | 8.8 | 4.6 | 0.0 | 0 | 13 | 3 | 0.39 | 8 | 4 | 1.62 | 0.33 | 23.3 | 10.8 | 42.4 |
| | | | | | | 0.0000 | | 0.0 | | | | | | |
| 4392A_102 | 8.8 | 3.1 | 0.0 | 0 | 9 | 2 | 0.35 | 3 | 4 | 1.80 | 0.38 | 95.4 | 9.0 | 207.4 |
| | | | | | | 0.0000 | | 0.0 | | | | | | |
| 4392A_11 | 8.8 | 2.7 | 59.3 | 43 | 11 | 4 | 0.27 | 1 | 4 | 1.88 | 0.53 | 52.7 | 127.2 | 103.1 |

| | | | | | | | | | | | | | | |
|---|---|---|---|---|---|---|---|---|---|---|---|---|---|---|
| | | | | | | 0.0000 | | 0.0 | | | | | | |
| 4392A_41 | 8.9 | 2.8 | 56.8 | 50 | 10 | 3 | 0.27 | 1 | 4 | 1.97 | 0.31 | 49.1 | 59.5 | 113.4 |
| | | | | | | 0.0000 | | 0.0 | | | | | | |
| 4392A_4 | 9.0 | 2.8 | 0.0 | 0 | 11 | 3 | 0.35 | 2 | 4 | 1.81 | 0.39 | 54.5 | 23.6 | 79.1 |
| | | | | | | 0.0000 | | 0.0 | | | | | | |
| 4392A_1 | 9.1 | 2.1 | 81.7 | 52 | 19 | 4 | 0.44 | 1 | 4 | 2.06 | 0.40 | 82.7 | 23.6 | 300.1 |
| | | | | | | 0.0000 | | 0.0 | | | | | | |
| 4392A_33 | 9.7 | 4.9 | 53.7 | 47 | 4 | 2 | 0.19 | 0 | 3 | 1.72 | 0.35 | 36.3 | 48.7 | 125.5 |
| | | | | | | 0.0000 | | 0.0 | | | | | | |
| 4392A_87 | 9.8 | 9.8 | 636.5 | #### | 1 | 2 | 0.04 | 0 | 2 | 1.91 | 0.30 | 5.6 | 11.6 | 31.2 |
| | | | | | | 0.0000 | | 0.0 | | | | | | |
| 4392A_12 | 9.9 | 2.4 | 50.4 | 39 | 17 | 4 | 0.33 | 1 | 4 | 2.14 | 0.35 | 55.9 | 77.7 | 186.7 |
| | | | | | | 0.0000 | | 0.0 | | | | | | |
| 4392A_52 | 9.9 | 4.9 | 27.9 | 52 | 4 | 2 | 0.14 | 0 | 2 | 1.84 | 0.35 | 26.4 | 10.5 | 216.5 |
| | | | | | | 0.0000 | | 0.0 | | | | | | |
| 4392A_31 | 10.0 | 7.1 | 70.9 | 63 | 2 | 1 | 0.11 | 0 | 2 | 1.76 | 0.32 | 20.7 | 15.5 | 147.9 |
| | | | | | | 0.0000 | | 0.0 | | | | | | |
| 4392A_86 | 10.4 | 1.8 | 45.7 | 16 | 33 | 4 | 0.60 | 1 | 3 | 1.65 | 0.41 | 125.4 | 10.7 | 289.5 |
| | | | | | | 0.0000 | | 0.0 | | | | | | |
| 4392A_5 | 10.5 | 7.4 | 191.8 | 175 | 2 | 3 | 0.05 | 0 | 2 | 1.63 | 0.23 | 7.9 | 17.8 | 216.0 |
| | | | | | | 0.0000 | | 0.0 | | | | | | |
| 4392A_44 | 10.6 | 10.6 | 0.0 | 0 | 1 | 3 | 0.03 | 0 | 1 | 1.90 | 0.39 | 4.2 | 37.1 | 47.0 |
| | | | | | | 0.0000 | | 0.0 | | | | | | |
| 4392A_84 | 11.2 | 3.7 | 0.0 | 0 | 10 | 1 | 0.61 | 6 | 4 | 1.77 | 0.35 | 189.9 | 399.0 | 64.7 |
| | | | | | | 0.0000 | | 0.0 | | | | | | |
| 4392A_93 | 11.3 | 2.5 | 48.1 | 30 | 20 | 3 | 0.50 | 1 | 4 | 1.95 | 0.32 | 84.5 | 123.0 | 121.2 |
| | | | | | | 0.0000 | | 0.0 | | | | | | |
| 4392A_89 | 11.7 | 3.9 | 56.5 | 31 | 9 | 4 | 0.16 | 0 | 3 | 1.77 | 0.37 | 58.1 | 109.0 | 52.6 |
| | | | | | | 0.0000 | | 0.0 | | | | | | |
| 4392A_67 | 12.1 | 6.0 | 79.5 | 66 | 4 | 2 | 0.13 | 0 | 3 | 1.64 | 0.31 | 27.6 | 22.1 | 134.9 |
| | | | | | | 0.0000 | | 0.0 | | | | | | |
| 4392A_37 | 12.2 | 5.0 | 72.6 | 74 | 6 | 2 | 0.17 | 1 | 3 | 1.79 | 0.34 | 29.3 | 14.1 | 250.1 |
| | | | | | | 0.0000 | | 0.0 | | | | | | |
| 4392A_66 | 12.3 | 3.1 | 41.0 | 15 | 16 | 2 | 0.44 | 1 | 4 | 1.82 | 0.46 | 85.4 | 82.4 | 112.5 |
| | | | | | | 0.0000 | | 0.0 | | | | | | |
| 4392A_46 | 12.6 | 4.5 | 545.3 | #### | 8 | 2 | 0.26 | 1 | 3 | 1.68 | 0.41 | 38.3 | 162.6 | 77.6 |
| | | | | | | 0.0000 | | 0.0 | | | | | | |
| 4392A_20 | 12.6 | 4.5 | 71.8 | 43 | 8 | 2 | 0.26 | 0 | 4 | 1.52 | 0.26 | 51.3 | 28.4 | 274.2 |
| | | | | | | 0.0000 | | 0.0 | | | | | | |
| 4392A_98 | 12.7 | 7.3 | 206.6 | 231 | 3 | 3 | 0.07 | 0 | 2 | 1.70 | 0.24 | 12.0 | 23.2 | 426.9 |
| | | | | | | 0.0000 | | 0.0 | | | | | | |
| 4392A_28 | 13.3 | 6.0 | 0.0 | 0 | 5 | 2 | 0.15 | 0 | 2 | 1.71 | 0.43 | 12.5 | 8.1 | 100.4 |
| | | | | | | 0.0000 | | 0.0 | | | | | | |
| 4392A_18 | 13.4 | 3.6 | 64.9 | 44 | 14 | 4 | 0.22 | 0 | 3 | 1.96 | 0.32 | 49.1 | 55.8 | 370.8 |
| | | | | | | 0.0000 | | 0.0 | | | | | | |
| 4392A_25 | 13.5 | 13.5 | 265.7 | 313 | 1 | 2 | 0.04 | 0 | 1 | 2.03 | 0.47 | 5.5 | 12.7 | 181.5 |
| | | | | | | 0.0000 | | 0.0 | | | | | | |
| 4392A_91 | 13.5 | 3.9 | 74.3 | 73 | 12 | 3 | 0.25 | 1 | 4 | 1.58 | 0.30 | 39.0 | 78.6 | 154.4 |
| | | | | | | 0.0000 | | 0.0 | | | | | | |
| 4392A_34 | 13.7 | 4.0 | 59.8 | 30 | 12 | 2 | 0.31 | 1 | 4 | 1.82 | 0.37 | 60.0 | 56.7 | 135.4 |
| | | | | | | 0.0000 | | 0.0 | | | | | | |
| 4392A_36 | 14.1 | 3.4 | 60.3 | 27 | 18 | 3 | 0.36 | 2 | 4 | 1.90 | 0.42 | 71.8 | 81.7 | 125.9 |
| | | | | | | 0.0000 | | 0.0 | | | | | | |
| 4392A_62 | 14.6 | 5.6 | 81.0 | 87 | 7 | 2 | 0.26 | 1 | 4 | 1.43 | 0.38 | 38.0 | 57.4 | 213.0 |
| | | | | | | 0.0000 | | 0.0 | | | | | | |
| 4392A_69 | 14.6 | 4.0 | 76.1 | 79 | 14 | 3 | 0.27 | 1 | 4 | 1.81 | 0.33 | 34.2 | 23.2 | 344.1 |
| | | | | | | 0.0000 | | 0.0 | | | | | | |
| 4392A_51 | 14.7 | 2.8 | 38.2 | 22 | 29 | 3 | 0.53 | 1 | 4 | 1.81 | 0.39 | 100.6 | 8.9 | 200.1 |
| | | | | | | 0.0000 | | 0.0 | | | | | | |
| 4392A_81 | 14.7 | 4.5 | 873.6 | #### | 11 | 3 | 0.21 | 1 | 4 | 1.71 | 0.42 | 2.6 | 2.1 | 74.2 |
| | | | | | | 0.0000 | | 0.0 | | | | | | |
| 4392A_39 | 14.9 | 4.5 | 75.1 | 79 | 11 | 3 | 0.18 | 0 | 2 | 1.52 | 0.33 | 32.8 | 46.8 | 113.0 |
| | | | | | | 0.0000 | | 0.0 | | | | | | |
| 4392A_30 | 14.9 | 5.3 | 63.7 | 36 | 8 | 2 | 0.25 | 0 | 4 | 1.59 | 0.36 | 49.5 | 42.4 | 250.5 |
| | | | | | | 0.0000 | | 0.0 | | | | | | |
| 4392A_58 | 15.0 | 2.8 | 47.9 | 16 | 30 | 3 | 0.52 | 1 | 4 | 1.65 | 0.46 | 151.3 | 53.9 | 414.4 |
| | | | | | | 0.0000 | | 0.0 | | | | | | |
| 4392A_53 | 15.4 | 4.9 | 66.3 | 52 | 10 | 2 | 0.22 | 0 | 3 | 1.35 | 0.41 | 37.2 | 66.3 | 185.0 |
| | | | | | | 0.0000 | | 0.0 | | | | | | |
| 4392A_49 | 15.9 | 5.5 | 0.0 | 0 | 11 | 3 | 0.22 | 4 | 3 | 1.89 | 0.41 | 47.2 | 100.4 | 71.6 |
| | | | | | | 0.0000 | | 0.0 | | | | | | |
| 4392A_15 | 16.1 | 3.8 | 56.9 | 40 | 18 | 3 | 0.27 | 1 | 4 | 2.09 | 0.32 | 59.5 | 1.3 | 169.9 |
| | | | | | | 0.0000 | | 0.0 | | | | | | |
| 4392A_48 | 16.4 | 5.0 | 55.6 | 61 | 11 | 4 | 0.15 | 0 | 3 | 1.44 | 0.34 | 29.3 | 0.1 | 143.2 |

| | | | | | | | | | | | | | | |
|---|---|---|---|---|---|---|---|---|---|---|---|---|---|---|
| | | | | | | 0.0000 | | 0.0 | | | | | | |
| 4392A_8 | 16.5 | 4.6 | 61.6 | 35 | 13 | 2 | 0.32 | 1 | 4 | 1.60 | 0.33 | 60.0 | 16.6 | 231.5 |
| | | | | | | 0.0000 | | 0.0 | | | | | | |
| 4392A_2 | 17.6 | 2.6 | 54.1 | 15 | 50 | 2 | 1.34 | 4 | 4 | 1.96 | 0.46 | 309.3 | 22.4 | 285.4 |
| | | | | | | 0.0000 | | 0.0 | | | | | | |
| 4392A_97 | 17.9 | 3.9 | 54.6 | 14 | 22 | 2 | 0.58 | 1 | 4 | 1.93 | 0.41 | 125.4 | 148.5 | 119.9 |
| | | | | | | 0.0000 | | 0.0 | | | | | | |
| 4392A_85 | 18.3 | 2.8 | 51.4 | 28 | 45 | 4 | 0.47 | 1 | 4 | 1.61 | 0.30 | 78.1 | 0.3 | 178.1 |
| | | | | | | 0.0000 | | 0.0 | | | | | | |
| 4392A_96 | 18.4 | 6.2 | 100.6 | 88 | 9 | 3 | 0.14 | 0 | 2 | 2.05 | 0.26 | 25.9 | 47.5 | 178.9 |
| | | | | | | 0.0000 | | 0.0 | | | | | | |
| 4392A_14 | 18.6 | 3.2 | 58.7 | 18 | 35 | 3 | 0.53 | 1 | 4 | 1.75 | 0.36 | 104.0 | 97.5 | 153.1 |
| | | | | | | 0.0000 | | 0.0 | | | | | | |
| 4392A_21 | 18.7 | 7.8 | 0.0 | 0 | 13 | 2 | 0.24 | 7 | 4 | 2.18 | 0.48 | 68.1 | 65.6 | 75.9 |
| | | | | | | 0.0000 | | 0.0 | | | | | | |
| 4392A_65 | 18.8 | 18.8 | 0.0 | 0 | 1 | 3 | 0.01 | 0 | 1 | 1.70 | 0.33 | 2.1 | 1.0 | 46.3 |
| | | | | | | 0.0000 | | 0.0 | | | | | | |
| 4392A_56 | 19.1 | 3.1 | 53.9 | 24 | 40 | 3 | 0.51 | 1 | 4 | 2.16 | 0.33 | 90.4 | 191.4 | 113.4 |
| | | | | | | 0.0000 | | 0.0 | | | | | | |
| 4392A_63 | 19.2 | 3.7 | 49.5 | 32 | 29 | 4 | 0.32 | 2 | 4 | 2.08 | 0.41 | 53.1 | 102.8 | 124.6 |
| | | | | | | 0.0000 | | 0.0 | | | | | | |
| 4392A_43 | 19.2 | 6.4 | 0.0 | 0 | 9 | 2 | 0.17 | 0 | 4 | 1.50 | 0.30 | 189.7 | 53.0 | 339.3 |
| | | | | | | 0.0000 | | 0.0 | | | | | | |
| 4392A_88 | 19.8 | 4.4 | 56.7 | 28 | 20 | 3 | 0.29 | 0 | 4 | 1.81 | 0.36 | 59.1 | 36.1 | 329.9 |
| | | | | | | 0.0000 | | 0.0 | | | | | | |
| 4392A_9 | 20.0 | 5.4 | 92.6 | 103 | 14 | 4 | 0.15 | 0 | 4 | 2.06 | 0.35 | 25.0 | 38.1 | 80.6 |
| | | | | | | 0.0000 | | 0.0 | | | | | | |
| 4392A_6 | 20.1 | 6.4 | 73.1 | 59 | 10 | 3 | 0.15 | 0 | 4 | 1.70 | 0.34 | 25.6 | 43.5 | 145.7 |
| | | | | | | 0.0000 | | 0.0 | | | | | | |
| 4392A_92 | 20.7 | 4.9 | 83.5 | 85 | 18 | 3 | 0.21 | 1 | 4 | 2.09 | 0.48 | 35.7 | 47.9 | 175.1 |
| | | | | | | 0.0000 | | 0.0 | | | | | | |
| 4392A_19 | 20.8 | 4.0 | 47.7 | 26 | 28 | 3 | 0.33 | 1 | 4 | 1.85 | 0.31 | 72.2 | 46.1 | 291.0 |
| | | | | | | 0.0000 | | 0.0 | | | | | | |
| 4392A_105 | 21.2 | 3.5 | 0.0 | 0 | 38 | 3 | 0.51 | 1 | 4 | 1.56 | 0.48 | 558.7 | 253.8 | 152.2 |
| | | | | | | 0.0000 | | 0.0 | | | | | | |
| 4392A_55 | 22.3 | 5.1 | 72.9 | 49 | 19 | 2 | 0.29 | 1 | 4 | 1.83 | 0.34 | 41.4 | 76.7 | 132.8 |
| | | | | | | 0.0000 | | 0.0 | | | | | | |
| 4392A_7 | 22.4 | 5.0 | 46.2 | 18 | 20 | 2 | 0.30 | 1 | 4 | 2.20 | 0.45 | 65.4 | 117.8 | 126.3 |
| | | | | | | 0.0000 | | 0.0 | | | | | | |
| 4392A_60 | 22.4 | 5.0 | 55.5 | 38 | 20 | 2 | 0.30 | 1 | 4 | 1.91 | 0.42 | 55.0 | 103.7 | 116.8 |
| | | | | | | 0.0000 | | 0.0 | | | | | | |
| 4392A_82 | 22.4 | 6.6 | 0.0 | 0 | 13 | 3 | 0.16 | 2 | 3 | 2.08 | 0.33 | 35.3 | 13.3 | 52.3 |
| | | | | | | 0.0000 | | 0.0 | | | | | | |
| 4392A_61 | 23.1 | 4.3 | 46.0 | 43 | 30 | 3 | 0.32 | 0 | 4 | 1.67 | 0.30 | 60.6 | 27.4 | 257.0 |
| | | | | | | 0.0000 | | 0.0 | | | | | | |
| 4392A_76 | 23.2 | 5.0 | 0.0 | 0 | 23 | 4 | 0.19 | 1 | 3 | 1.54 | 0.46 | 36.7 | 19.2 | 153.9 |
| | | | | | | 0.0000 | | 0.0 | | | | | | |
| 4392A_72 | 24.0 | 6.7 | 67.8 | 67 | 13 | 3 | 0.16 | 0 | 4 | 1.70 | 0.37 | 29.5 | 53.3 | 145.7 |
| | | | | | | 0.0000 | | 0.0 | | | | | | |
| 4392A_68 | 24.8 | 8.3 | 94.8 | 149 | 9 | 3 | 0.10 | 0 | 4 | 1.18 | 0.70 | 13.7 | 25.5 | 247.9 |
| | | | | | | 0.0000 | | 0.0 | | | | | | |
| 4392A_3 | 25.4 | 7.7 | 61.6 | 114 | 11 | 3 | 0.11 | 0 | 4 | 1.88 | 0.40 | 21.2 | 35.9 | 160.8 |
| | | | | | | 0.0000 | | 0.0 | | | | | | |
| 4392A_27 | 27.5 | 9.2 | 115.9 | 104 | 9 | 3 | 0.08 | 0 | 2 | 1.83 | 0.34 | 15.1 | 22.1 | 269.9 |
| | | | | | | 0.0000 | | 0.0 | | | | | | |
| 4392A_64 | 28.0 | 4.2 | 46.0 | 24 | 48 | 3 | 0.46 | 2 | 4 | 2.18 | 0.42 | 89.9 | 123.0 | 69.9 |
| | | | | | | 0.0000 | | 0.0 | | | | | | |
| 4392A_54 | 30.0 | 13.5 | 158.1 | 198 | 5 | 3 | 0.05 | 0 | 3 | 1.45 | 0.30 | 8.4 | 17.9 | 124.2 |
| | | | | | | 0.0000 | | 0.0 | | | | | | |
| 4392A_94 | 30.4 | 5.5 | 31.3 | 11 | 32 | 2 | 0.45 | 2 | 4 | 1.74 | 0.34 | 263.0 | 2.7 | 59.1 |
| | | | | | | 0.0000 | | 0.0 | | | | | | |
| 4392A_90 | 30.8 | 10.3 | 61.8 | 76 | 9 | 3 | 0.08 | 0 | 3 | 1.72 | 0.33 | 16.9 | 18.8 | 30.6 |
| | | | | | | 0.0000 | | 0.0 | | | | | | |
| 4392A_100 | 30.8 | 8.9 | 75.0 | 78 | 12 | 3 | 0.11 | 0 | 3 | 1.67 | 0.32 | 17.9 | 33.8 | 223.8 |
| | | | | | | 0.0000 | | 0.0 | | | | | | |
| 4392A_23 | 32.3 | 9.8 | 79.9 | 88 | 11 | 2 | 0.12 | 0 | 4 | 1.70 | 0.33 | 22.3 | 19.1 | 254.0 |
| | | | | | | 0.0000 | | 0.0 | | | | | | |
| 4392A_99 | 34.0 | 9.5 | 104.7 | 107 | 13 | 2 | 0.13 | 0 | 3 | 1.91 | 0.35 | 22.7 | 30.4 | 357.0 |
| | | | | | | 0.0000 | | 0.0 | | | | | | |
| 4392A_32 | 34.5 | 8.9 | 79.9 | 61 | 15 | 2 | 0.15 | 0 | 4 | 1.66 | 0.38 | 32.8 | 27.9 | 358.7 |
| | | | | | | 0.0000 | | 0.0 | | | | | | |
| 4392A_26 | 35.3 | 9.8 | 99.0 | 72 | 13 | 3 | 0.10 | 0 | 4 | 1.79 | 0.41 | 17.0 | 20.5 | 110.4 |
| | | | | | | 0.0000 | | 0.0 | | | | | | |
| 4392A_59 | 36.2 | 12.1 | 89.1 | 114 | 9 | 2 | 0.10 | 0 | 3 | 1.87 | 0.34 | 19.3 | 34.7 | 130.2 |

| | | | | | | | | | | | | | | |
|---|---|---|---|---|---|---|---|---|---|---|---|---|---|---|
| 4392A_80 | 37.8 | 14.3 | 56.2 | 181 | 7 | 0.0000 5 | 0.03 | 0.0 0 | 2 | 1.35 | 0.34 | 6.5 | 6.2 | 49.2 |
| 4392A_45 | 39.4 | 19.7 | 96.7 | 175 | 4 | 0.0000 2 | 0.04 | 0.0 0 | 2 | 1.79 | 0.42 | 7.2 | 15.5 | 123.3 |
| 4392A_79 | 40.3 | 11.7 | 95.1 | 93 | 12 | 0.0000 3 | 0.08 | 0.0 0 | 4 | 1.44 | 0.43 | 17.5 | 33.5 | 370.0 |
| 4392A_57 | 42.7 | 11.9 | 94.3 | 147 | 13 | 0.0000 4 | 0.07 | 0.0 0 | 3 | 1.65 | 0.35 | 14.4 | 30.0 | 221.2 |
| 4392A_101 | 64.9 | 37.5 | 254.4 | 334 | 3 | 0.0000 3 | 0.01 | 0.0 0 | 3 | 1.36 | 0.29 | 2.5 | 4.0 | 39.0 |
| 4392A_103 | 88.5 | 28.1 | 305.8 | 366 | 10 | 0.0000 3 | 0.03 | 0.0 0 | 4 | 1.75 | 0.44 | 6.3 | 2.2 | 59.9 |
| 4392A_10 | 142.1 | 100.7 | 0.0 | 0 | 2 | 0.0000 4 | 0.00 | 0.0 0 | 2 | 1.74 | 0.34 | 0.3 | 0.2 | 11.6 |
| 4392A_104 | 226.8 | 163.7 | 0.0 | 0 | 3 | 0.0000 2 | 0.00 | 0.0 0 | 3 | 1.35 | 0.35 | 0.8 | 7.4 | 10.7 |

**Middle fork Maclaren River**

| Spot Name | FT Age (Ma) | signma sym (Ma) | UPb Age (Ma) | 2 sigma (Ma) | Ns | Area cm^2 | U/Catio n | +/- 1sig | Etch Figs. | Dpar (um) | Dper (um) | [U] (ppm ) | [Th] (ppm) | [Sm] (ppm) |
|---|---|---|---|---|---|---|---|---|---|---|---|---|---|---|
| 4395A_4 | 0.0 | 25.7 | 0.0 | 0 | 0 | 0.0000 3 | 0.01 | 0.0 0 | 1 | 1.87 | 0.24 | 1.5 | 7.3 | 5.6 |
| 4395A_8 | 0.0 | 2.1 | 0.0 | 0 | 0 | 0.0000 4 | 0.07 | 0.0 1 | 1 | 1.78 | 0.41 | 6.0 | 8.2 | 24.1 |
| 4395A_13 | 0.0 | 5.8 | 0.0 | 0 | 0 | 0.0000 4 | 0.03 | 0.0 0 | 1 | 1.69 | 0.42 | 0.7 | 17.8 | 9.4 |
| 4395A_34 | 0.0 | 1.4 | 0.0 | 0 | 0 | 0.0000 3 | 0.12 | 0.0 1 | 1 | 1.70 | 0.31 | 24.6 | 51.1 | 29.8 |
| 4395A_57 | 0.0 | 220.9 | 0.0 | 0 | 0 | 0.0000 3 | 0.00 | 0.0 0 | 1 | 1.58 | 0.42 | 0.2 | 0.2 | 0.6 |
| 4395A_72 | 0.0 | 1.3 | 0.0 | 0 | 0 | 0.0000 3 | 0.15 | 0.0 1 | 1 | 1.50 | 0.33 | 12.4 | 3.0 | 20.4 |
| 4395A_75 | 0.7 | 0.5 | 0.0 | 0 | 2 | 0.0000 4 | 0.60 | 0.0 3 | 1 | 1.86 | 0.38 | 106.7 | 47.3 | 168.2 |
| 4395A_20 | 1.2 | 0.6 | 0.0 | 0 | 4 | 0.0000 3 | 0.82 | 0.0 5 | 2 | 1.63 | 0.26 | 141.3 | 981.0 | 221.6 |
| 4395A_86 | 2.0 | 2.0 | 46.9 | 96 | 1 | 0.0000 5 | 0.08 | 0.0 0 | 1 | 1.76 | 0.46 | 17.3 | 28.6 | 25.8 |
| 4395A_65 | 3.8 | 1.4 | 0.0 | 0 | 8 | 0.0000 4 | 0.40 | 0.0 3 | 4 | 1.93 | 0.37 | 31.6 | 37.4 | 111.7 |
| 4395A_41 | 5.3 | 2.0 | 0.0 | 0 | 8 | 0.0000 3 | 0.36 | 0.0 4 | 4 | 1.82 | 0.27 | 41.0 | 11.9 | 29.8 |
| 4395A_3 | 6.6 | 2.4 | 0.0 | 0 | 10 | 0.0000 4 | 0.32 | 0.0 6 | 4 | 1.81 | 0.46 | 49.1 | 11.9 | 99.2 |
| 4395A_21 | 7.8 | 3.7 | 0.0 | 0 | 5 | 0.0000 3 | 0.18 | 0.0 2 | 2 | 1.77 | 0.31 | 46.8 | 145.9 | 86.2 |
| 4395A_28 | 8.0 | 8.0 | 68.7 | 99 | 1 | 0.0000 3 | 0.03 | 0.0 0 | 1 | 1.35 | 0.30 | 5.7 | 8.5 | 37.1 |
| 4395A_6 | 8.2 | 8.2 | 89.3 | 119 | 1 | 0.0000 3 | 0.03 | 0.0 0 | 1 | 1.92 | 0.24 | 5.4 | 5.7 | 41.7 |
| 4395A_105 | 8.3 | 3.4 | 0.0 | 0 | 6 | 0.0000 3 | 0.18 | 0.0 0 | 4 | 1.94 | 0.28 | 15.0 | 44.1 | 27.4 |
| 4395A_17 | 9.2 | 2.9 | 58.6 | 29 | 10 | 0.0000 4 | 0.23 | 0.0 1 | 4 | 1.79 | 0.31 | 44.9 | 303.2 | 159.5 |
| 4395A_90 | 9.5 | 5.1 | 0.0 | 0 | 5 | 0.0000 5 | 0.09 | 0.0 3 | 3 | 1.47 | 0.38 | 18.6 | 34.0 | 83.6 |
| 4395A_69 | 9.6 | 6.8 | 80.2 | 132 | 2 | 0.0000 5 | 0.04 | 0.0 0 | 1 | 1.34 | 0.28 | 6.9 | 23.2 | 67.7 |
| 4395A_67 | 9.7 | 2.4 | 0.0 | 0 | 18 | 0.0000 3 | 0.45 | 0.0 4 | 4 | 1.91 | 0.31 | 84.5 | 5.1 | 85.8 |
| 4395A_15 | 11.5 | 4.8 | 0.0 | 0 | 6 | 0.0000 4 | 0.11 | 0.1 1 | 4 | 2.27 | 0.27 | 14.2 | 2.9 | 60.8 |
| 4395A_47 | 11.5 | 3.1 | ###### | #### | 29 | 0.0000 4 | 0.54 | 0.0 0 | 4 | 1.66 | 0.43 | 71.3 | 224.1 | 165.6 |
| 4395A_25 | 12.4 | 4.1 | 0.0 | 0 | 13 | 0.0000 3 | 0.32 | 0.0 6 | 4 | 2.14 | 0.44 | 2.1 | 8.5 | 1.7 |
| 4395A_31 | 12.6 | 2.1 | 57.9 | 42 | 36 | 0.0000 4 | 0.54 | 0.0 2 | 4 | 1.79 | 0.41 | 98.1 | 12.5 | 317.8 |
| 4395A_62 | 13.1 | 5.0 | 0.0 | 0 | 7 | 0.0000 3 | 0.15 | 0.0 1 | 4 | 1.71 | 0.38 | 24.6 | 38.3 | 128.1 |
| 4395A_74 | 13.3 | 2.0 | 61.4 | 18 | 48 | 0.0000 5 | 0.62 | 0.0 2 | 4 | 1.80 | 0.31 | 119.9 | 7.2 | 157.8 |

| | | | | | | | | | | | | | | |
|---|---|---|---|---|---|---|---|---|---|---|---|---|---|---|
| | | | | | | 0.0000 | | 0.0 | | | | | | |
| 4395A_87 | 13.3 | 6.7 | 168.0 | 145 | 4 | 5 | 0.05 | 0 | 4 | 1.52 | 0.41 | 10.0 | 19.2 | 141.4 |
| | | | | | | 0.0000 | | 0.0 | | | | | | |
| 4395A_27 | 13.4 | 7.7 | 119.1 | 145 | 3 | 5 | 0.04 | 0 | 2 | 1.95 | 0.28 | 6.8 | 32.3 | 148.3 |
| | | | | | | 0.0000 | | 0.0 | | | | | | |
| 4395A_10 | 13.5 | 9.5 | 57.4 | 38 | 2 | 2 | 0.06 | 0 | 2 | 1.66 | 0.38 | 12.1 | 43.0 | 82.8 |
| | | | | | | 0.0000 | | 0.0 | | | | | | |
| 4395A_52 | 13.6 | 3.7 | 57.4 | 41 | 14 | 5 | 0.18 | 0 | 4 | 2.07 | 0.35 | 34.4 | 18.6 | 223.4 |
| | | | | | | 0.0000 | | 0.0 | | | | | | |
| 4395A_96 | 14.0 | 4.1 | 66.4 | 27 | 12 | 3 | 0.21 | 1 | 4 | 2.04 | 0.36 | 49.5 | 47.6 | 66.0 |
| | | | | | | 0.0000 | | 0.0 | | | | | | |
| 4395A_9 | 14.2 | 6.4 | 93.9 | 108 | 5 | 3 | 0.09 | 0 | 4 | 1.42 | 0.25 | 16.1 | 13.4 | 39.3 |
| | | | | | | 0.0000 | | 0.0 | | | | | | |
| 4395A_33 | 14.3 | 6.5 | 0.0 | 0 | 5 | 3 | 0.08 | 1 | 3 | 1.46 | 0.25 | 11.8 | 56.9 | 25.2 |
| | | | | | | 0.0000 | | 0.0 | | | | | | |
| 4395A_85 | 14.4 | 3.0 | 0.0 | 0 | 28 | 3 | 0.47 | 4 | 4 | 1.76 | 0.39 | 78.6 | 64.8 | 50.9 |
| | | | | | | 0.0000 | | 0.0 | | | | | | |
| 4395A_104 | 14.4 | 2.7 | 81.7 | 32 | 29 | 5 | 0.34 | 1 | 4 | 1.77 | 0.42 | 65.4 | 0.9 | 172.5 |
| | | | | | | 0.0000 | | 0.0 | | | | | | |
| 4395A_93 | 14.5 | 8.4 | 110.7 | 81 | 3 | 3 | 0.05 | 0 | 2 | 1.96 | 0.24 | 11.0 | 32.3 | 86.9 |
| | | | | | | 0.0000 | | 0.0 | | | | | | |
| 4395A_30 | 15.0 | 6.2 | 69.5 | 75 | 6 | 4 | 0.08 | 0 | 3 | 1.62 | 0.24 | 15.0 | 9.9 | 51.3 |
| | | | | | | 0.0000 | | 0.0 | | | | | | |
| 4395A_12 | 15.0 | 7.5 | 101.1 | 92 | 4 | 3 | 0.06 | 0 | 3 | 1.94 | 0.34 | 12.4 | 36.6 | 260.9 |
| | | | | | | 0.0000 | | 0.0 | | | | | | |
| 4395A_102 | 15.3 | 4.3 | 0.0 | 0 | 13 | 5 | 0.14 | 0 | 4 | 1.64 | 0.33 | 0.0 | 0.0 | 1.7 |
| | | | | | | 0.0000 | | 0.0 | | | | | | |
| 4395A_46 | 15.4 | 4.9 | 59.2 | 30 | 10 | 3 | 0.17 | 0 | 4 | 1.74 | 0.28 | 33.1 | 38.0 | 102.2 |
| | | | | | | 0.0000 | | 0.0 | | | | | | |
| 4395A_14 | 15.4 | 3.7 | 53.0 | 25 | 18 | 3 | 0.28 | 1 | 4 | 1.76 | 0.28 | 55.0 | 10.2 | 104.3 |
| | | | | | | 0.0000 | | 0.0 | | | | | | |
| 4395A_101 | 15.5 | 4.0 | 62.1 | 43 | 15 | 5 | 0.16 | 0 | 4 | 1.79 | 0.47 | 33.0 | 13.8 | 188.9 |
| | | | | | | 0.0000 | | 0.0 | | | | | | |
| 4395A_84 | 15.6 | 5.9 | 88.2 | 96 | 7 | 4 | 0.08 | 0 | 4 | 1.91 | 0.30 | 16.6 | 25.7 | 80.2 |
| | | | | | | 0.0000 | | 0.0 | | | | | | |
| 4395A_42 | 15.8 | 3.9 | 0.0 | 0 | 17 | 4 | 0.23 | 1 | 4 | 1.91 | 0.44 | 82.7 | 6.7 | 10.4 |
| | | | | | | 0.0000 | | 0.0 | | | | | | |
| 4395A_63 | 15.8 | 6.0 | 88.1 | 76 | 7 | 4 | 0.09 | 0 | 4 | 1.66 | 0.28 | 19.2 | 0.0 | 192.3 |
| | | | | | | 0.0000 | | 0.0 | | | | | | |
| 4395A_55 | 15.8 | 5.7 | 0.0 | 0 | 8 | 3 | 0.16 | 1 | 3 | 1.88 | 0.31 | 31.7 | 29.4 | 32.8 |
| | | | | | | 0.0000 | | 0.0 | | | | | | |
| 4395A_61 | 16.2 | 6.6 | 0.0 | 0 | 6 | 4 | 0.08 | 0 | 4 | 2.05 | 0.44 | 9.8 | 13.4 | 69.4 |
| | | | | | | 0.0000 | | 0.0 | | | | | | |
| 4395A_37 | 16.3 | 3.4 | 64.3 | 24 | 23 | 4 | 0.27 | 1 | 4 | 2.00 | 0.35 | 51.8 | 210.9 | 215.2 |
| | | | | | | 0.0000 | | 0.0 | | | | | | |
| 4395A_71 | 16.4 | 6.7 | 91.1 | 102 | 6 | 4 | 0.07 | 0 | 3 | 2.06 | 0.35 | 14.1 | 20.0 | 37.3 |
| | | | | | | 0.0000 | | 0.0 | | | | | | |
| 4395A_88 | 16.5 | 4.8 | 91.4 | 136 | 12 | 4 | 0.15 | 1 | 4 | 1.55 | 0.27 | 9.0 | 29.0 | 148.3 |
| | | | | | | 0.0000 | | 0.0 | | | | | | |
| 4395A_43 | 16.8 | 4.2 | 0.0 | 0 | 16 | 3 | 0.27 | 1 | 4 | 2.13 | 0.35 | 50.4 | 49.1 | 202.7 |
| | | | | | | 0.0000 | | 0.0 | | | | | | |
| 4395A_92 | 16.9 | 7.6 | 78.7 | 60 | 5 | 4 | 0.06 | 0 | 4 | 1.65 | 0.34 | 12.2 | 30.1 | 78.7 |
| | | | | | | 0.0000 | | 0.0 | | | | | | |
| 4395A_40 | 17.3 | 2.3 | 53.5 | 11 | 61 | 4 | 0.75 | 2 | 4 | 2.23 | 0.46 | 149.0 | 209.2 | 59.5 |
| | | | | | | 0.0000 | | 0.0 | | | | | | |
| 4395A_99 | 17.7 | 2.5 | 55.3 | 16 | 52 | 2 | 1.00 | 3 | 4 | 1.85 | 0.30 | 218.0 | 18.3 | 235.4 |
| | | | | | | 0.0000 | | 0.0 | | | | | | |
| 4395A_18 | 17.9 | 6.3 | 75.6 | 60 | 8 | 4 | 0.10 | 0 | 4 | 2.15 | 0.41 | 15.8 | 40.9 | 159.5 |
| | | | | | | 0.0000 | | 0.0 | | | | | | |
| 4395A_49 | 17.9 | 5.0 | 0.0 | 0 | 21 | 3 | 0.33 | 6 | 4 | 2.10 | 0.47 | 39.8 | 106.3 | 71.6 |
| | | | | | | 0.0000 | | 0.0 | | | | | | |
| 4395A_94 | 18.5 | 4.7 | 114.2 | 84 | 16 | 5 | 0.15 | 0 | 4 | 1.44 | 0.38 | 27.1 | 13.9 | 125.0 |
| | | | | | | 0.0000 | | 0.0 | | | | | | |
| 4395A_22 | 18.5 | 2.0 | 59.7 | 11 | 91 | 4 | 1.05 | 3 | 4 | 1.71 | 0.31 | 194.9 | 1.9 | 217.3 |
| | | | | | | 0.0000 | | 0.0 | | | | | | |
| 4395A_83 | 18.6 | 4.7 | 127.5 | 78 | 16 | 5 | 0.15 | 0 | 4 | 1.84 | 0.32 | 28.8 | 0.7 | 186.3 |
| | | | | | | 0.0000 | | 0.0 | | | | | | |
| 4395A_23 | 18.7 | 3.0 | 66.9 | 16 | 40 | 3 | 0.52 | 1 | 4 | 2.07 | 0.34 | 101.8 | 1.2 | 191.3 |
| | | | | | | 0.0000 | | 0.0 | | | | | | |
| 4395A_32 | 18.8 | 7.6 | 0.0 | 0 | 7 | 2 | 0.15 | 2 | 3 | 1.67 | 0.29 | 27.4 | 56.1 | 113.8 |
| | | | | | | 0.0000 | | 0.0 | | | | | | |
| 4395A_98 | 19.6 | 6.5 | 80.5 | 62 | 9 | 2 | 0.16 | 0 | 4 | 1.78 | 0.44 | 30.0 | 49.0 | 111.7 |
| | | | | | | 0.0000 | | 0.0 | | | | | | |
| 4395A_35 | 20.1 | 2.7 | 78.1 | 20 | 57 | 3 | 0.69 | 2 | 4 | 1.83 | 0.35 | 128.6 | 48.4 | 291.9 |

| | | | | | | | | | | | | | | |
|---|---|---|---|---|---|---|---|---|---|---|---|---|---|---|
| | | | | | | 0.0000 | | 0.0 | | | | | | |
| 4395A_76 | 20.5 | 2.9 | 61.3 | 11 | 52 | 2 | 0.90 | 2 | 4 | 1.75 | 0.35 | 168.5 | 4.3 | 268.6 |
| | | | | | | 0.0000 | | 0.0 | | | | | | |
| 4395A_100 | 20.5 | 7.8 | 64.8 | 62 | 7 | 5 | 0.06 | 0 | 2 | 1.63 | 0.23 | 11.6 | 21.8 | 72.4 |
| | | | | | | 0.0000 | | 0.0 | | | | | | |
| 4395A_56 | 20.6 | 4.7 | 0.0 | 0 | 20 | 5 | 0.16 | 0 | 4 | 1.80 | 0.28 | 30.8 | 0.2 | 153.5 |
| | | | | | | 0.0000 | | 0.0 | | | | | | |
| 4395A_1 | 20.7 | 4.0 | 58.5 | 31 | 28 | 5 | 0.23 | 1 | 4 | 1.77 | 0.45 | 44.2 | 72.2 | 125.9 |
| | | | | | | 0.0000 | | 0.0 | | | | | | |
| 4395A_5 | 21.4 | 8.8 | 71.6 | 115 | 6 | 3 | 0.07 | 0 | 4 | 1.83 | 0.30 | 13.4 | 28.4 | 294.5 |
| | | | | | | 0.0000 | | 0.0 | | | | | | |
| 4395A_38 | 21.5 | 5.8 | 63.8 | 22 | 14 | 2 | 0.23 | 1 | 4 | 1.67 | 0.47 | 40.3 | 71.6 | 102.6 |
| | | | | | | 0.0000 | | 0.0 | | | | | | |
| 4395A_103 | 21.6 | 4.0 | 70.8 | 22 | 30 | 3 | 0.34 | 1 | 4 | 1.97 | 0.37 | 65.0 | 213.7 | 101.8 |
| | | | | | | 0.0000 | | 0.0 | | | | | | |
| 4395A_70 | 21.7 | 7.7 | 162.4 | 173 | 8 | 3 | 0.09 | 0 | 4 | 1.83 | 0.44 | 16.6 | 29.4 | 169.5 |
| | | | | | | 0.0000 | | 0.0 | | | | | | |
| 4395A_16 | 22.9 | 3.4 | 57.4 | 12 | 48 | 3 | 0.57 | 2 | 4 | 2.29 | 0.41 | 107.7 | 189.8 | 211.3 |
| | | | | | | 0.0000 | | 0.0 | | | | | | |
| 4395A_54 | 23.0 | 5.3 | 66.8 | 21 | 19 | 2 | 0.39 | 1 | 4 | 1.79 | 0.36 | 78.3 | 5.8 | 174.6 |
| | | | | | | 0.0000 | | 0.0 | | | | | | |
| 4395A_81 | 23.2 | 3.3 | 65.4 | 21 | 51 | 5 | 0.37 | 1 | 4 | 1.78 | 0.36 | 71.8 | 30.4 | 178.5 |
| | | | | | | 0.0000 | | 0.0 | | | | | | |
| 4395A_77 | 23.6 | 4.1 | 60.2 | 23 | 34 | 5 | 0.24 | 1 | 4 | 1.89 | 0.32 | 46.3 | 9.7 | 163.8 |
| | | | | | | 0.0000 | | 0.0 | | | | | | |
| 4395A_91 | 24.3 | 4.0 | 63.5 | 28 | 39 | 4 | 0.30 | 1 | 4 | 2.04 | 0.39 | 56.8 | 37.0 | 100.5 |
| | | | | | | 0.0000 | | 0.0 | | | | | | |
| 4395A_36 | 26.2 | 10.4 | 0.0 | 0 | 7 | 4 | 0.06 | 1 | 2 | 1.47 | 0.35 | 7.4 | 2.7 | 17.5 |
| | | | | | | 0.0000 | | 0.0 | | | | | | |
| 4395A_2 | 26.4 | 3.5 | 63.5 | 17 | 61 | 2 | 0.82 | 2 | 4 | 1.70 | 0.42 | 155.8 | 14.8 | 183.7 |
| | | | | | | 0.0000 | | 0.0 | | | | | | |
| 4395A_95 | 26.5 | 8.9 | 124.3 | 140 | 9 | 4 | 0.06 | 0 | 3 | 1.87 | 0.28 | 12.9 | 21.2 | 113.0 |
| | | | | | | 0.0000 | | 0.0 | | | | | | |
| 4395A_64 | 27.2 | 11.1 | 58.5 | 78 | 6 | 4 | 0.05 | 0 | 3 | 1.88 | 0.34 | 8.5 | 27.4 | 107.4 |
| | | | | | | 0.0000 | | 0.0 | | | | | | |
| 4395A_51 | 27.4 | 4.6 | 65.1 | 32 | 37 | 5 | 0.23 | 1 | 4 | 1.76 | 0.33 | 44.2 | 0.0 | 134.5 |
| | | | | | | 0.0000 | | 0.0 | | | | | | |
| 4395A_7 | 27.6 | 9.2 | 114.4 | 80 | 9 | 3 | 0.08 | 0 | 4 | 1.41 | 0.27 | 14.4 | 6.9 | 47.4 |
| | | | | | | 0.0000 | | 0.0 | | | | | | |
| 4395A_45 | 27.7 | 13.9 | 108.7 | 109 | 4 | 2 | 0.05 | 0 | 2 | 2.04 | 0.54 | 9.7 | 29.0 | 197.5 |
| | | | | | | 0.0000 | | 0.0 | | | | | | |
| 4395A_44 | 28.0 | 3.4 | 62.7 | 14 | 71 | 4 | 0.54 | 1 | 4 | 1.96 | 0.62 | 108.1 | 351.5 | 110.4 |
| | | | | | | 0.0000 | | 0.0 | | | | | | |
| 4395A_19 | 28.2 | 9.5 | 61.8 | 124 | 9 | 5 | 0.05 | 0 | 4 | 1.83 | 0.29 | 9.9 | 9.6 | 211.3 |
| | | | | | | 0.0000 | | 0.0 | | | | | | |
| 4395A_26 | 28.4 | 3.7 | 67.3 | 18 | 62 | 4 | 0.46 | 1 | 4 | 1.95 | 0.35 | 89.9 | 43.9 | 365.6 |
| | | | | | | 0.0000 | | 0.0 | | | | | | |
| 4395A_24 | 28.7 | 5.1 | 62.7 | 49 | 32 | 4 | 0.24 | 1 | 4 | 1.97 | 0.25 | 43.3 | 38.1 | 366.5 |
| | | | | | | 0.0000 | | 0.0 | | | | | | |
| 4395A_89 | 28.8 | 7.5 | 118.0 | 85 | 15 | 2 | 0.18 | 0 | 4 | 1.73 | 0.38 | 34.8 | 30.1 | 253.1 |
| | | | | | | 0.0000 | | 0.0 | | | | | | |
| 4395A_66 | 30.0 | 12.3 | 92.9 | 107 | 6 | 4 | 0.04 | 0 | 4 | 1.75 | 0.32 | 8.4 | 5.4 | 135.0 |
| | | | | | | 0.0000 | | 0.0 | | | | | | |
| 4395A_59 | 30.1 | 12.2 | 0.0 | 0 | 17 | 3 | 0.14 | 4 | 4 | 1.77 | 0.51 | 12.6 | 65.2 | 100.5 |
| | | | | | | 0.0000 | | 0.0 | | | | | | |
| 4395A_60 | 32.5 | 8.2 | 48.0 | 66 | 16 | 5 | 0.08 | 0 | 4 | 1.95 | 0.46 | 15.8 | 15.6 | 260.9 |
| | | | | | | 0.0000 | | 0.0 | | | | | | |
| 4395A_82 | 33.3 | 5.2 | 84.7 | 33 | 43 | 5 | 0.22 | 1 | 4 | 1.88 | 0.29 | 41.1 | 16.5 | 369.5 |
| | | | | | | 0.0000 | | 0.0 | | | | | | |
| 4395A_58 | 33.6 | 6.7 | 61.6 | 32 | 26 | 2 | 0.37 | 1 | 4 | 1.93 | 0.42 | 63.1 | 105.1 | 110.4 |
| | | | | | | 0.0000 | | 0.0 | | | | | | |
| 4395A_80 | 34.4 | 7.9 | 0.0 | 0 | 32 | 3 | 0.23 | 3 | 4 | 1.73 | 0.31 | 52.7 | 110.7 | 48.3 |
| | | | | | | 0.0000 | | 0.0 | | | | | | |
| 4395A_50 | 37.7 | 5.0 | 0.0 | 0 | 61 | 3 | 0.46 | 1 | 4 | 2.15 | 0.50 | 280.8 | 10.2 | 121.2 |
| | | | | | | 0.0000 | | 0.0 | | | | | | |
| 4395A_11 | 38.1 | 19.1 | 140.6 | 150 | 4 | 2 | 0.04 | 0 | 3 | 1.89 | 0.37 | 7.8 | 12.7 | 100.9 |
| | | | | | | 0.0000 | | 0.0 | | | | | | |
| 4395A_97 | 39.6 | 10.3 | 0.0 | 0 | 25 | 3 | 0.15 | 3 | 3 | 1.82 | 0.46 | 12.2 | 39.8 | 30.7 |
| | | | | | | 0.0000 | | 0.0 | | | | | | |
| 4395A_29 | 40.3 | 30.4 | 0.0 | 0 | 2 | 5 | 0.01 | 0 | 1 | 2.00 | 0.26 | 1.5 | 17.3 | 25.6 |
| | | | | | | 0.0000 | | 0.0 | | | | | | |
| 4395A_39 | 42.2 | 12.4 | 0.0 | 0 | 13 | 3 | 0.09 | 1 | 4 | 1.97 | 0.25 | 21.6 | 111.6 | 39.7 |
| | | | | | | 0.0000 | | 0.0 | | | | | | |
| 4395A_79 | 43.5 | 12.6 | 175.1 | 175 | 12 | 3 | 0.08 | 0 | 4 | 1.90 | 0.32 | 14.5 | 22.7 | 155.2 |

| | | | | | | | | | | | | | | |
|---|---|---|---|---|---|---|---|---|---|---|---|---|---|---|
| | | | | | | 0.0000 | | 0.0 | | | | | | |
| 4395A_78 | 45.2 | 13.7 | 101.9 | 59 | 11 | 2 | 0.13 | 0 | 4 | 2.06 | 0.44 | 23.5 | 65.8 | 78.5 |
| | | | | | | 0.0000 | | 0.0 | | | | | | |
| 4395A_68 | 52.3 | 15.3 | 0.0 | 0 | 27 | 4 | 0.10 | 2 | 4 | 1.97 | 0.34 | 17.9 | 24.5 | 29.1 |
| | | | | | | 0.0000 | | 0.0 | | | | | | |
| 4395A_48 | 64.1 | 7.9 | 80.7 | 74 | 72 | 3 | 0.27 | 1 | 4 | 1.85 | 0.49 | 55.0 | 54.3 | 83.6 |
| | | | | | | 0.0000 | | 0.0 | | | | | | |
| 4395A_53 | 85.9 | 27.2 | 0.0 | 0 | 14 | 5 | 0.03 | 0 | 4 | 2.30 | 0.32 | 8.8 | 25.7 | 18.0 |
| | | | | | | 0.0000 | | 0.0 | | | | | | |
| 4395A_73 | 798.8 | 802.3 | 0.0 | 0 | 1 | 5 | 0.00 | 0 | 1 | 1.81 | 0.36 | 0.1 | 0.0 | 1.9 |

**West fork Maclaren River**

| Spot Name | FT Age (Ma) | sigma Sym (Ma) | UPb Age (Ma) | 2 sigma (Ma) | Ns | Area cm^2 | U/Cation | +/- 1sig | Etch Figs. | Dpar (um) | Dper (um) | [U] (ppm) | [Th] (ppm) | [Sm] (ppm) |
|---|---|---|---|---|---|---|---|---|---|---|---|---|---|---|
| | | | | | | 0.0000 | | 0.0 | | | | | | |
| 4394A_12 | 0.0 | 471.1 | ###### | #### | 0 | 2 | 0.00 | 0 | 1 | 1.11 | 0.20 | 0.2 | 0.1 | 3.6 |
| | | | | | | 0.0000 | | 0.0 | | | | | | |
| 4394A_91 | 0.0 | 326.1 | 432.1 | #### | 0 | 2 | 0.00 | 0 | 1 | 1.83 | 0.33 | 0.2 | 1.0 | 1.7 |
| | | | | | | 0.0000 | | 0.0 | | | | | | |
| 4394A_42 | 0.0 | 31.3 | 751.6 | 949 | 0 | 3 | 0.01 | 0 | 1 | 1.99 | 0.45 | 1.1 | 5.1 | 24.0 |
| | | | | | | 0.0000 | | 0.0 | | | | | | |
| 4394A_81 | 0.0 | 38.7 | 271.3 | 310 | 0 | 2 | 0.01 | 0 | 1 | 1.93 | 0.21 | 1.1 | 5.9 | 6.3 |
| | | | | | | 0.0000 | | 0.0 | | | | | | |
| 4394A_95 | 0.0 | 3.8 | 0.0 | 0 | 0 | 5 | 0.03 | 1 | 1 | 1.61 | 0.31 | 1.2 | 5.1 | 6.8 |
| | | | | | | 0.0000 | | 0.0 | | | | | | |
| 4394A_93 | 0.0 | 6.4 | 0.0 | 0 | 0 | 3 | 0.03 | 0 | 1 | 1.97 | 0.25 | 2.0 | 6.0 | 11.0 |
| | | | | | | 0.0000 | | 0.0 | | | | | | |
| 4394A_39 | 0.0 | 18.0 | 0.0 | 0 | 0 | 3 | 0.01 | 0 | 1 | 1.84 | 0.30 | 2.0 | 12.9 | 17.5 |
| | | | | | | 0.0000 | | 0.0 | | | | | | |
| 4394A_52 | 0.0 | 24.2 | 297.1 | 390 | 0 | 2 | 0.01 | 0 | 1 | 1.81 | 0.35 | 2.7 | 0.7 | 9.0 |
| | | | | | | 0.0000 | | 0.0 | | | | | | |
| 4394A_28 | 0.0 | 24.9 | 514.6 | 689 | 0 | 2 | 0.02 | 0 | 1 | 1.33 | 0.28 | 2.8 | 17.7 | 65.1 |
| | | | | | | 0.0000 | | 0.0 | | | | | | |
| 4394A_51 | 0.0 | 12.2 | 176.2 | 237 | 0 | 2 | 0.02 | 0 | 1 | 1.41 | 0.24 | 3.9 | 21.2 | 12.8 |
| | | | | | | 0.0000 | | 0.0 | | | | | | |
| 4394A_31 | 0.0 | 8.6 | 256.2 | 334 | 0 | 3 | 0.02 | 0 | 1 | 2.29 | 0.46 | 4.4 | 31.5 | 10.3 |
| | | | | | | 0.0000 | | 0.0 | | | | | | |
| 4394A_16 | 0.0 | 9.5 | 256.7 | 277 | 0 | 2 | 0.03 | 0 | 1 | 1.51 | 0.29 | 4.8 | 6.4 | 12.0 |
| | | | | | | 0.0000 | | 0.0 | | | | | | |
| 4394A_34 | 0.0 | 10.2 | 365.8 | 336 | 0 | 2 | 0.03 | 0 | 1 | 1.81 | 0.36 | 5.7 | 20.8 | 94.0 |
| | | | | | | 0.0000 | | 0.0 | | | | | | |
| 4394A_50 | 0.0 | 1.4 | 0.0 | 0 | 0 | 2 | 0.20 | 2 | 1 | 1.47 | 0.28 | 6.0 | 11.3 | 22.0 |
| | | | | | | 0.0000 | | 0.0 | | | | | | |
| 4394A_56 | 0.0 | 1.7 | 0.0 | 0 | 0 | 3 | 0.10 | 1 | 1 | 1.61 | 0.26 | 7.0 | 12.1 | 7.4 |
| | | | | | | 0.0000 | | 0.0 | | | | | | |
| 4394A_82 | 0.0 | 2.6 | 0.0 | 0 | 0 | 3 | 0.08 | 0 | 1 | 1.62 | 0.34 | 7.8 | 22.8 | 44.8 |
| | | | | | | 0.0000 | | 0.0 | | | | | | |
| 4394A_66 | 0.0 | 2.4 | 0.0 | 0 | 0 | 4 | 0.06 | 2 | 1 | 1.63 | 0.40 | 9.7 | 24.2 | 86.2 |
| | | | | | | 0.0000 | | 0.0 | | | | | | |
| 4394A_58 | 0.7 | 0.7 | 0.0 | 0 | 1 | 3 | 0.39 | 1 | 1 | 1.92 | 0.49 | 267.6 | 615.2 | 114.3 |
| | | | | | | 0.0000 | | 0.4 | | | | | | |
| 4394A_45 | 1.7 | 0.4 | 337.1 | 900 | 20 | 2 | 5.74 | 6 | 4 | 1.74 | 0.40 | 80.9 | 45.2 | 123.3 |
| | | | | | | 0.0000 | | 0.0 | | | | | | |
| 4394A_59 | 2.8 | 2.8 | 0.0 | 0 | 1 | 2 | 0.12 | 2 | 1 | 2.10 | 0.54 | 9.0 | 14.0 | 16.7 |
| | | | | | | 0.0000 | | 0.0 | | | | | | |
| 4394A_13 | 4.0 | 4.0 | 0.0 | 0 | 1 | 1 | 0.14 | 1 | 2 | 1.90 | 0.35 | 5.0 | 34.4 | 27.3 |
| | | | | | | 0.0000 | | 0.0 | | | | | | |
| 4394A_5 | 4.1 | 2.9 | 0.0 | 0 | 2 | 2 | 0.17 | 2 | 2 | 1.68 | 0.56 | 7.8 | 1.7 | 9.6 |
| | | | | | | 0.0000 | | 0.0 | | | | | | |
| 4394A_46 | 4.3 | 3.0 | 0.0 | 0 | 2 | 2 | 0.19 | 2 | 2 | 1.94 | 0.28 | 10.6 | 3.5 | 23.0 |
| | | | | | | 0.0000 | | 0.0 | | | | | | |
| 4394A_69 | 4.5 | 4.5 | 0.0 | 0 | 1 | 2 | 0.08 | 1 | 1 | 1.48 | 0.37 | 2.1 | 10.1 | 11.2 |
| | | | | | | 0.0000 | | 0.0 | | | | | | |
| 4394A_54 | 4.8 | 4.8 | 99.1 | 137 | 1 | 3 | 0.06 | 0 | 1 | 1.57 | 0.36 | 11.8 | 97.5 | 57.3 |
| | | | | | | 0.0000 | | 0.0 | | | | | | |
| 4394A_47 | 5.2 | 5.2 | 216.9 | 542 | 1 | 3 | 0.05 | 0 | 2 | 1.74 | 0.25 | 6.5 | 26.8 | 27.0 |
| | | | | | | 0.0000 | | 0.0 | | | | | | |
| 4394A_22 | 6.5 | 6.5 | 94.5 | 112 | 1 | 4 | 0.03 | 0 | 1 | 2.18 | 0.32 | 7.4 | 11.5 | 20.4 |
| | | | | | | 0.0000 | | 0.0 | | | | | | |
| 4394A_63 | 6.6 | 6.7 | 0.0 | 0 | 1 | 3 | 0.04 | 1 | 1 | 1.57 | 0.49 | 0.9 | 3.4 | 8.3 |
| | | | | | | 0.0000 | | 0.0 | | | | | | |
| 4394A_19 | 6.7 | 4.3 | 0.0 | 0 | 3 | 2 | 0.15 | 4 | 2 | 1.99 | 0.46 | 6.1 | 16.5 | 148.8 |

| | | | | | | | | | | | | | | |
|---|---|---|---|---|---|---|---|---|---|---|---|---|---|---|
| | | | | | | 0.0000 | | 0.0 | | | | | | |
| 4394A_8 | 7.0 | 7.0 | 180.2 | 137 | 1 | 2 | 0.05 | 0 | 2 | 2.03 | 0.30 | 9.4 | 7.3 | 11.9 |
| | | | | | | 0.0000 | | 0.0 | | | | | | |
| 4394A_1 | 8.0 | 4.0 | 134.5 | 143 | 4 | 3 | 0.12 | 0 | 3 | 1.84 | 0.30 | 24.0 | 17.9 | 11.4 |
| | | | | | | 0.0000 | | 0.0 | | | | | | |
| 4394A_55 | 8.0 | 4.0 | 71.7 | 78 | 4 | 5 | 0.09 | 0 | 4 | 1.87 | 0.31 | 16.4 | 3.9 | 11.6 |
| | | | | | | 0.0000 | | 0.0 | | | | | | |
| 4394A_61 | 8.5 | 6.0 | 229.3 | 259 | 2 | 5 | 0.04 | 0 | 2 | 1.87 | 0.36 | 18.4 | 17.1 | 26.8 |
| | | | | | | 0.0000 | | 0.0 | | | | | | |
| 4394A_74 | 9.0 | 9.0 | 273.8 | 243 | 1 | 3 | 0.03 | 0 | 1 | 2.11 | 0.30 | 6.4 | 24.6 | 25.7 |
| | | | | | | 0.0000 | | 0.0 | | | | | | |
| 4394A_40 | 9.3 | 6.6 | 0.0 | 0 | 2 | 3 | 0.06 | 1 | 2 | 1.73 | 0.33 | 6.7 | 13.3 | 25.1 |
| | | | | | | 0.0000 | | 0.0 | | | | | | |
| 4394A_29 | 9.8 | 1.8 | 75.3 | 13 | 29 | 3 | 0.84 | 2 | 4 | 1.94 | 0.46 | 146.7 | 181.0 | 314.8 |
| | | | | | | 0.0000 | | 0.0 | | | | | | |
| 4394A_27 | 9.8 | 4.1 | 0.0 | 0 | 6 | 3 | 0.19 | 2 | 4 | 1.66 | 0.32 | 15.9 | 9.1 | 88.4 |
| | | | | | | 0.0000 | | 0.0 | | | | | | |
| 4394A_77 | 10.1 | 4.1 | 86.0 | 41 | 6 | 3 | 0.16 | 0 | 3 | 1.71 | 0.36 | 29.4 | 25.0 | 114.3 |
| | | | | | | 0.0000 | | 0.0 | | | | | | |
| 4394A_9 | 11.2 | 11.2 | 212.4 | 385 | 1 | 5 | 0.02 | 0 | 2 | 1.90 | 0.38 | 2.9 | 5.8 | 15.4 |
| | | | | | | 0.0000 | | 0.0 | | | | | | |
| 4394A_83 | 11.3 | 11.3 | 103.3 | 163 | 1 | 3 | 0.02 | 0 | 1 | 1.92 | 0.49 | 3.8 | 5.2 | 36.2 |
| | | | | | | 0.0000 | | 0.0 | | | | | | |
| 4394A_76 | 11.4 | 8.0 | 175.5 | 194 | 2 | 4 | 0.04 | 0 | 1 | 2.04 | 0.52 | 6.9 | 20.1 | 11.1 |
| | | | | | | 0.0000 | | 0.0 | | | | | | |
| 4394A_11 | 11.5 | 8.2 | 293.6 | 294 | 2 | 4 | 0.03 | 0 | 1 | 2.26 | 0.34 | 5.7 | 19.0 | 8.4 |
| | | | | | | 0.0000 | | 0.0 | | | | | | |
| 4394A_73 | 12.4 | 5.6 | 74.4 | 31 | 5 | 2 | 0.16 | 0 | 4 | 1.88 | 0.41 | 31.4 | 5.6 | 19.3 |
| | | | | | | 0.0000 | | 0.0 | | | | | | |
| 4394A_102 | 12.7 | 9.0 | ###### | #### | 2 | 3 | 0.04 | 0 | 1 | 1.98 | 0.35 | 4.1 | 145.9 | 99.7 |
| | | | | | | 0.0000 | | 0.0 | | | | | | |
| 4394A_72 | 13.1 | 2.4 | 73.2 | 21 | 31 | 3 | 0.57 | 2 | 4 | 1.77 | 0.56 | 98.6 | 106.3 | 152.6 |
| | | | | | | 0.0000 | | 0.0 | | | | | | |
| 4394A_105 | 13.6 | 2.7 | 65.3 | 21 | 27 | 3 | 0.53 | 2 | 4 | 1.72 | 0.40 | 103.6 | 187.2 | 219.5 |
| | | | | | | 0.0000 | | 0.0 | | | | | | |
| 4394A_25 | 14.1 | 6.3 | 0.0 | 0 | 5 | 2 | 0.12 | 0 | 4 | 2.22 | 0.51 | 12.5 | 26.4 | 43.0 |
| | | | | | | 0.0000 | | 0.0 | | | | | | |
| 4394A_98 | 14.3 | 3.2 | 73.2 | 27 | 20 | 4 | 0.26 | 1 | 4 | 1.69 | 0.29 | 48.1 | 13.1 | 26.7 |
| | | | | | | 0.0000 | | 0.0 | | | | | | |
| 4394A_14 | 15.0 | 15.8 | 0.0 | 0 | 1 | 1 | 0.05 | 2 | 1 | 1.70 | 0.34 | 2.1 | 55.9 | 11.9 |
| | | | | | | 0.0000 | | 0.0 | | | | | | |
| 4394A_101 | 15.0 | 3.9 | 71.4 | 14 | 15 | 2 | 0.47 | 1 | 4 | 1.78 | 0.37 | 97.7 | 14.9 | 102.2 |
| | | | | | | 0.0000 | | 0.0 | | | | | | |
| 4394A_44 | 15.1 | 4.6 | 70.4 | 49 | 11 | 3 | 0.21 | 1 | 4 | 1.63 | 0.37 | 42.4 | 14.6 | 53.9 |
| | | | | | | 0.0000 | | 0.0 | | | | | | |
| 4394A_35 | 15.4 | 5.8 | 135.6 | 119 | 7 | 5 | 0.08 | 0 | 3 | 1.83 | 0.35 | 14.3 | 15.3 | 46.6 |
| | | | | | | 0.0000 | | 0.0 | | | | | | |
| 4394A_49 | 15.5 | 10.9 | 121.7 | 177 | 2 | 3 | 0.03 | 0 | 2 | 1.61 | 0.32 | 5.8 | 21.0 | 40.2 |
| | | | | | | 0.0000 | | 0.0 | | | | | | |
| 4394A_53 | 15.6 | 9.0 | 134.9 | 122 | 3 | 3 | 0.05 | 0 | 2 | 1.50 | 0.38 | 8.9 | 18.0 | 15.0 |
| | | | | | | 0.0000 | | 0.0 | | | | | | |
| 4394A_4 | 15.8 | 15.8 | 192.0 | 164 | 1 | 2 | 0.03 | 0 | 1 | 2.25 | 0.37 | 5.6 | 11.9 | 21.0 |
| | | | | | | 0.0000 | | 0.0 | | | | | | |
| 4394A_80 | 16.0 | 2.6 | 73.8 | 20 | 39 | 3 | 0.69 | 2 | 4 | 1.94 | 0.57 | 116.7 | 136.2 | 164.7 |
| | | | | | | 0.0000 | | 0.0 | | | | | | |
| 4394A_36 | 16.0 | 3.2 | 73.9 | 15 | 26 | 4 | 0.35 | 1 | 4 | 1.83 | 0.49 | 65.6 | 72.5 | 131.5 |
| | | | | | | 0.0000 | | 0.0 | | | | | | |
| 4394A_48 | 16.1 | 5.7 | 88.3 | 81 | 8 | 5 | 0.08 | 0 | 4 | 1.88 | 0.31 | 15.2 | 6.5 | 55.2 |
| | | | | | | 0.0000 | | 0.0 | | | | | | |
| 4394A_67 | 17.8 | 5.6 | 82.9 | 66 | 10 | 5 | 0.10 | 0 | 4 | 2.05 | 0.52 | 18.1 | 27.5 | 106.1 |
| | | | | | | 0.0000 | | 0.0 | | | | | | |
| 4394A_7 | 18.0 | 12.7 | 164.9 | 193 | 2 | 3 | 0.03 | 0 | 2 | 2.01 | 0.37 | 6.1 | 13.1 | 20.1 |
| | | | | | | 0.0000 | | 0.0 | | | | | | |
| 4394A_3 | 18.0 | 2.8 | 73.3 | 17 | 42 | 3 | 0.57 | 2 | 4 | 2.15 | 0.35 | 104.0 | 130.9 | 237.2 |
| | | | | | | 0.0000 | | 0.0 | | | | | | |
| 4394A_96 | 18.1 | 5.8 | 67.4 | 67 | 10 | 2 | 0.26 | 1 | 4 | 1.80 | 0.42 | 46.8 | 14.3 | 222.5 |
| | | | | | | 0.0000 | | 0.0 | | | | | | |
| 4394A_97 | 18.1 | 12.9 | 0.0 | 0 | 2 | 2 | 0.04 | 0 | 2 | 1.90 | 0.51 | 0.4 | 1.1 | 3.5 |
| | | | | | | 0.0000 | | 0.0 | | | | | | |
| 4394A_100 | 18.5 | 3.1 | 0.0 | 0 | 37 | 3 | 0.57 | 2 | 4 | 1.81 | 0.40 | 0.7 | 4.1 | 58.2 |
| | | | | | | 0.0000 | | 0.0 | | | | | | |
| 4394A_88 | 20.2 | 14.3 | 167.0 | 150 | 2 | 2 | 0.04 | 0 | 2 | 2.05 | 0.44 | 7.6 | 4.4 | 35.5 |
| | | | | | | 0.0000 | | 0.0 | | | | | | |
| 4394A_23 | 20.5 | 5.2 | 91.6 | 56 | 16 | 4 | 0.17 | 0 | 4 | 2.02 | 0.53 | 32.1 | 42.3 | 101.3 |

| | | | | | | | | | | | | | | |
|---|---|---|---|---|---|---|---|---|---|---|---|---|---|---|
| | | | | | | 0.0000 | | 0.0 | | | | | | |
| 4394A_32 | 20.8 | 9.3 | 220.5 | 186 | 5 | 5 | 0.04 | 0 | 3 | 2.07 | 0.35 | 7.8 | 3.3 | 29.8 |
| | | | | | | 0.0000 | | 0.0 | | | | | | |
| 4394A_43 | 21.1 | 15.0 | 374.3 | 282 | 2 | 3 | 0.02 | 0 | 2 | 1.79 | 0.41 | 4.4 | 22.8 | 18.9 |
| | | | | | | 0.0000 | | 0.0 | | | | | | |
| 4394A_71 | 21.7 | 15.4 | 115.2 | 161 | 2 | 5 | 0.02 | 0 | 2 | 1.59 | 0.37 | 3.1 | 8.5 | 6.6 |
| | | | | | | 0.0000 | | 0.0 | | | | | | |
| 4394A_90 | 21.9 | 21.9 | 0.0 | 0 | 1 | 2 | 0.02 | 0 | 1 | 1.87 | 0.38 | 1.1 | 13.0 | 20.8 |
| | | | | | | 0.0000 | | 0.0 | | | | | | |
| 4394A_79 | 22.7 | 13.2 | 0.0 | 0 | 3 | 2 | 0.05 | 0 | 2 | 2.22 | 0.54 | 11.6 | 4.3 | 3.9 |
| | | | | | | 0.0000 | | 0.0 | | | | | | |
| 4394A_62 | 23.5 | 7.1 | 82.8 | 31 | 11 | 2 | 0.16 | 0 | 2 | 1.38 | 0.41 | 32.4 | 0.0 | 4.9 |
| | | | | | | 0.0000 | | 0.0 | | | | | | |
| 4394A_41 | 24.5 | 17.4 | 221.6 | 251 | 2 | 3 | 0.02 | 0 | 2 | 2.10 | 0.42 | 4.3 | 8.2 | 9.4 |
| | | | | | | 0.0000 | | 0.0 | | | | | | |
| 4394A_30 | 25.3 | 8.0 | 76.9 | 31 | 10 | 2 | 0.16 | 0 | 3 | 1.49 | 0.35 | 30.3 | 7.2 | 38.0 |
| | | | | | | 0.0000 | | 0.0 | | | | | | |
| 4394A_17 | 25.5 | 4.1 | 76.5 | 22 | 41 | 3 | 0.46 | 1 | 4 | 2.08 | 0.34 | 91.3 | 297.9 | 239.3 |
| | | | | | | 0.0000 | | 0.1 | | | | | | |
| 4394A_20 | 26.4 | 8.7 | 0.0 | 0 | 26 | 2 | 0.47 | 2 | 4 | 1.75 | 0.29 | 112.8 | 67.8 | 218.2 |
| | | | | | | 0.0000 | | 0.0 | | | | | | |
| 4394A_37 | 27.0 | 13.5 | 88.4 | 101 | 4 | 2 | 0.05 | 0 | 3 | 1.57 | 0.34 | 9.5 | 5.9 | 16.7 |
| | | | | | | 0.0000 | | 0.0 | | | | | | |
| 4394A_68 | 27.3 | 27.3 | 164.0 | 211 | 1 | 1 | 0.02 | 0 | 1 | 2.18 | 0.35 | 4.9 | 16.6 | 11.8 |
| | | | | | | 0.0000 | | 0.0 | | | | | | |
| 4394A_64 | 27.4 | 19.9 | 0.0 | 0 | 2 | 4 | 0.02 | 0 | 2 | 1.60 | 0.37 | 1.6 | 7.8 | 6.8 |
| | | | | | | 0.0000 | | 0.0 | | | | | | |
| 4394A_92 | 27.4 | 3.5 | 65.9 | 14 | 66 | 3 | 0.64 | 2 | 4 | 1.99 | 0.46 | 129.0 | 230.3 | 234.1 |
| | | | | | | 0.0000 | | 0.0 | | | | | | |
| 4394A_33 | 28.0 | 16.2 | 266.0 | 292 | 3 | 2 | 0.05 | 0 | 2 | 1.64 | 0.26 | 10.0 | 4.0 | 14.8 |
| | | | | | | 0.0000 | | 0.0 | | | | | | |
| 4394A_15 | 28.5 | 5.6 | 0.0 | 0 | 32 | 5 | 0.19 | 2 | 4 | 1.95 | 0.36 | 35.8 | 17.7 | 131.5 |
| | | | | | | 0.0000 | | 0.0 | | | | | | |
| 4394A_38 | 30.5 | 17.6 | 135.3 | 229 | 3 | 3 | 0.03 | 0 | 3 | 1.37 | 0.36 | 5.0 | 24.0 | 54.3 |
| | | | | | | 0.0000 | | 0.0 | | | | | | |
| 4394A_60 | 30.6 | 30.6 | 302.8 | 400 | 1 | 2 | 0.01 | 0 | 1 | 1.55 | 0.41 | 2.4 | 10.7 | 12.7 |
| | | | | | | 0.0000 | | 0.0 | | | | | | |
| 4394A_85 | 31.5 | 10.6 | 0.0 | 0 | 10 | 2 | 0.13 | 1 | 4 | 2.09 | 0.41 | 26.6 | 4.4 | 30.0 |
| | | | | | | 0.0000 | | 0.0 | | | | | | |
| 4394A_99 | 32.0 | 22.6 | 410.5 | 679 | 2 | 3 | 0.02 | 0 | 3 | 1.95 | 0.41 | 2.8 | 8.8 | 23.9 |
| | | | | | | 0.0000 | | 0.0 | | | | | | |
| 4394A_70 | 33.3 | 23.5 | 167.9 | 269 | 2 | 3 | 0.02 | 0 | 1 | 1.86 | 0.25 | 3.1 | 0.4 | 3.6 |
| | | | | | | 0.0000 | | 0.0 | | | | | | |
| 4394A_94 | 35.8 | 20.7 | 147.1 | 187 | 3 | 2 | 0.03 | 0 | 1 | 1.70 | 0.44 | 10.6 | 1.7 | 40.4 |
| | | | | | | 0.0000 | | 0.0 | | | | | | |
| 4394A_2 | 37.3 | 11.5 | 0.0 | 0 | 13 | 3 | 0.11 | 1 | 4 | 1.93 | 0.32 | 17.6 | 24.0 | 94.4 |
| | | | | | | 0.0000 | | 0.0 | | | | | | |
| 4394A_104 | 42.3 | 15.0 | 123.4 | 117 | 8 | 4 | 0.04 | 0 | 3 | 1.72 | 0.31 | 8.4 | 1.0 | 2.9 |
| | | | | | | 0.0000 | | 0.0 | | | | | | |
| 4394A_26 | 47.1 | 17.0 | 0.0 | 0 | 8 | 5 | 0.03 | 0 | 4 | 2.06 | 0.51 | 3.5 | 7.8 | 24.3 |
| | | | | | | 0.0000 | | 0.0 | | | | | | |
| 4394A_65 | 52.5 | 9.7 | 110.7 | 94 | 30 | 2 | 0.23 | 1 | 4 | 2.04 | 0.36 | 43.7 | 46.6 | 71.6 |
| | | | | | | 0.0000 | | 0.0 | | | | | | |
| 4394A_78 | 61.6 | 43.6 | 506.5 | 583 | 2 | 2 | 0.01 | 0 | 2 | 1.80 | 0.28 | 1.6 | 0.1 | 6.0 |
| | | | | | | 0.0000 | | 0.0 | | | | | | |
| 4394A_87 | 62.8 | 31.5 | 0.0 | 0 | 4 | 3 | 0.02 | 0 | 2 | 1.96 | 0.38 | 6.6 | 1.8 | 11.9 |
| | | | | | | 0.0000 | | 0.0 | | | | | | |
| 4394A_18 | 67.1 | 15.9 | 0.0 | 0 | 49 | 5 | 0.12 | 2 | 4 | 1.98 | 0.38 | 12.4 | 27.8 | 69.0 |
| | | | | | | 0.0000 | | 0.0 | | | | | | |
| 4394A_6 | 87.3 | 45.1 | 0.0 | 0 | 6 | 5 | 0.01 | 0 | 4 | 2.03 | 0.33 | 0.6 | 2.5 | 16.9 |
| | | | | | | 0.0000 | | 0.0 | | | | | | |
| 4394A_84 | 87.8 | 64.3 | 0.0 | 0 | 2 | 3 | 0.01 | 0 | 1 | 2.08 | 0.40 | 1.0 | 2.2 | 28.5 |
| | | | | | | 0.0000 | | 0.0 | | | | | | |
| 4394A_21 | 91.5 | 73.6 | 0.0 | 0 | 2 | 2 | 0.01 | 0 | 2 | 1.70 | 0.20 | 1.3 | 14.3 | 42.2 |
| | | | | | | 0.0000 | | 0.0 | | | | | | |
| 4394A_103 | 105.4 | 52.9 | 277.2 | 433 | 4 | 3 | 0.01 | 0 | 2 | 1.80 | 0.31 | 3.0 | 12.9 | 23.5 |
| | | | | | | 0.0000 | | 0.0 | | | | | | |
| 4394A_10 | 121.7 | 40.8 | 143.6 | 213 | 9 | 5 | 0.01 | 0 | 4 | 1.91 | 0.50 | 2.3 | 3.6 | 22.0 |
| | | | | | | 0.0000 | | 0.0 | | | | | | |
| 4394A_24 | 130.2 | 92.3 | 0.0 | 0 | 2 | 2 | 0.01 | 0 | 3 | 2.03 | 0.41 | 0.9 | 1.3 | 7.6 |
| | | | | | | 0.0000 | | 0.0 | | | | | | |
| 4394A_57 | 141.9 | 40.0 | 0.0 | 0 | 17 | 4 | 0.03 | 0 | 4 | 1.71 | 0.51 | 3.3 | 8.9 | 13.5 |
| | | | | | | 0.0000 | | 0.0 | | | | | | |
| 4394A_89 | 174.5 | 174.8 | 0.0 | 0 | 1 | 1 | 0.00 | 0 | 1 | 1.73 | 0.39 | 0.2 | 0.3 | 2.3 |

| | | | | | | | | | | | | | | |
|---|---|---|---|---|---|---|---|---|---|---|---|---|---|---|
| | | | | | | 0.0000 | | 0.0 | | | | | | |
| 4394A_75 | 219.5 | 220.4 | 0.0 | 0 | 1 | 2 | 0.00 | 0 | 1 | 1.41 | 0.30 | 0.1 | 0.5 | 1.2 |
| | | | | | | 0.0000 | | 0.0 | | | | | | |
| 4394A_86 | 256.2 | 95.3 | 0.0 | 0 | 8 | 3 | 0.01 | 0 | 4 | 1.84 | 0.41 | 0.4 | 0.8 | 4.4 |

**Nenana River**

| Spot Name | FT Age (Ma) | Sigma Symm (Ma) | UPb Age (Ma) | 2 sigma (Ma) | Ns | Area cm^2 | U/Cation | +/- 1sig | Etch Figs. | Dpar (um) | Dper (um) | [U] (ppm) | [Th] (ppm) | [Sm] (ppm) |
|---|---|---|---|---|---|---|---|---|---|---|---|---|---|---|
| | | | | | | 0.0000 | | 0.0 | | | | | | |
| 03918A_2 | 0.0 | 51105.0 | 0.0 | 0 | 1 | 2 | 0.00 | 0 | 1 | 2.34 | 0.30 | 0.0 | 272.0 | 721.0 |
| | | | | | | 0.0000 | | 0.0 | | | | | | |
| 03918A_11 | 0.0 | 1.3 | 95.2 | 66 | 0 | 2 | 0.29 | 1 | 1 | 2.33 | 0.51 | 56.0 | 104.0 | 224.0 |
| | | | | | | 0.0000 | | 0.0 | | | | | | |
| 03918A_41 | 0.0 | 2.3 | 136.4 | 116 | 0 | 3 | 0.13 | 0 | 1 | 2.40 | 0.42 | 25.0 | 76.0 | 309.0 |
| | | | | | | 0.0000 | | 0.0 | | | | | | |
| 03918A_65 | 0.0 | 9.0 | 156.8 | 153 | 0 | 1 | 0.11 | 0 | 1 | 1.66 | 0.39 | 23.0 | 60.0 | 220.0 |
| | | | | | | 0.0000 | | 0.0 | | | | | | |
| 03918A_87 | 0.0 | 62.8 | 302.5 | 638 | 0 | 1 | 0.01 | 0 | 1 | 2.34 | 0.42 | 2.0 | 9.0 | 372.0 |
| | | | | | | 0.0000 | | 0.0 | | | | | | |
| 03918A_90 | 0.0 | 16.1 | 0.0 | 0 | 0 | 1 | 0.06 | 0 | 1 | 2.45 | 0.41 | 11.0 | 30.0 | 131.0 |
| | | | | | | 0.0000 | | 0.0 | | | | | | |
| 03918A_92 | 0.0 | 21.6 | 102.2 | 168 | 0 | 1 | 0.06 | 0 | 1 | 2.43 | 0.50 | 10.0 | 25.0 | 323.0 |
| 03918A_10 | | | | | | 0.0000 | | 0.0 | | | | | | |
| 1 | 0.0 | 20.6 | 225.5 | 341 | 0 | 2 | 0.02 | 0 | 1 | 2.63 | 0.58 | 4.0 | 19.0 | 374.0 |
| | | | | | | 0.0000 | | 0.0 | | | | | | |
| 03918A_29 | 1.6 | 1.6 | 0.0 | 0 | 1 | 1 | 0.63 | 1 | 1 | 2.48 | 0.59 | 118.0 | 95.0 | 115.0 |
| | | | | | | 0.0000 | | 0.0 | | | | | | |
| 03918A_45 | 1.7 | 1.7 | 73.7 | 49 | 1 | 2 | 0.31 | 1 | 1 | 2.52 | 0.54 | 63.0 | 104.0 | 288.0 |
| | | | | | | 0.0000 | | 0.0 | | | | | | |
| 03918A_60 | 1.8 | 1.8 | 66.8 | 82 | 1 | 3 | 0.23 | 1 | 1 | 2.43 | 0.58 | 40.0 | 104.0 | 326.0 |
| | | | | | | 0.0000 | | 0.0 | | | | | | |
| 03918A_13 | 1.8 | 1.8 | 96.9 | 86 | 1 | 3 | 0.22 | 1 | 1 | 2.26 | 0.48 | 42.0 | 120.0 | 313.0 |
| | | | | | | 0.0000 | | 0.0 | | | | | | |
| 03918A_35 | 2.0 | 2.0 | 102.8 | 54 | 1 | 1 | 0.52 | 1 | 2 | 2.12 | 0.37 | 82.0 | 142.0 | 305.0 |
| 03918A_10 | | | | | | 0.0000 | | 0.0 | | | | | | |
| 2 | 2.3 | 2.3 | 111.5 | 54 | 1 | 1 | 0.37 | 1 | 1 | 1.91 | 0.35 | 73.0 | 190.0 | 277.0 |
| | | | | | | 0.0000 | | 0.0 | | | | | | |
| 03918A_44 | 2.4 | 2.4 | 123.1 | 95 | 1 | 2 | 0.21 | 1 | 1 | 2.32 | 0.37 | 43.0 | 122.0 | 355.0 |
| | | | | | | 0.0000 | | 0.0 | | | | | | |
| 03918A_53 | 2.8 | 2.8 | 0.0 | 0 | 1 | 1 | 0.31 | 1 | 1 | 2.09 | 0.40 | 2.0 | 14.0 | 174.0 |
| | | | | | | 0.0000 | | 0.0 | | | | | | |
| 03918A_55 | 3.0 | 3.0 | 84.2 | 88 | 1 | 2 | 0.21 | 1 | 2 | 2.30 | 0.59 | 43.0 | 65.0 | 101.0 |
| | | | | | | 0.0000 | | 0.0 | | | | | | |
| 03918A_12 | 3.3 | 2.3 | 31.9 | 41 | 2 | 2 | 0.43 | 1 | 2 | 1.92 | 0.36 | 84.0 | 184.0 | 148.0 |
| | | | | | | 0.0000 | | 0.0 | | | | | | |
| 03918A_64 | 3.3 | 1.9 | 108.3 | 80 | 3 | 4 | 0.29 | 1 | 2 | 1.96 | 0.64 | 50.0 | 129.0 | 370.0 |
| | | | | | | 0.0000 | | 0.0 | | | | | | |
| 03918A_26 | 3.4 | 5.1 | 0.0 | 0 | 1 | 4 | 0.08 | 9 | 1 | 2.55 | 0.39 | 16.0 | 136.0 | 419.0 |
| | | | | | | 0.0000 | | 0.0 | | | | | | |
| 03918A_79 | 3.5 | 3.5 | 64.3 | 48 | 1 | 1 | 0.30 | 1 | 1 | 2.35 | 0.46 | 59.0 | 141.0 | 209.0 |
| | | | | | | 0.0000 | | 0.0 | | | | | | |
| 03918A_71 | 3.5 | 2.5 | 97.0 | 44 | 2 | 2 | 0.37 | 1 | 2 | 2.27 | 0.49 | 76.0 | 136.0 | 240.0 |
| | | | | | | 0.0000 | | 0.0 | | | | | | |
| 03918A_96 | 3.5 | 2.5 | 95.0 | 48 | 2 | 3 | 0.21 | 0 | 2 | 2.02 | 0.46 | 44.0 | 134.0 | 215.0 |
| | | | | | | 0.0000 | | 0.0 | | | | | | |
| 03918A_70 | 3.5 | 2.5 | 79.9 | 54 | 2 | 2 | 0.36 | 1 | 2 | 1.60 | 0.33 | 74.0 | 194.0 | 63.0 |
| | | | | | | 0.0000 | | 0.0 | | | | | | |
| 03918A_67 | 3.7 | 3.7 | 104.7 | 76 | 1 | 1 | 0.28 | 1 | 3 | 2.31 | 0.52 | 53.0 | 112.0 | 212.0 |
| | | | | | | 0.0000 | | 0.0 | | | | | | |
| 03918A_14 | 3.7 | 3.7 | 92.7 | 91 | 1 | 2 | 0.17 | 0 | 1 | 2.32 | 0.51 | 37.0 | 80.0 | 269.0 |
| | | | | | | 0.0000 | | 0.0 | | | | | | |
| 03918A_25 | 3.9 | 3.9 | 0.0 | 0 | 1 | 2 | 0.21 | 1 | 2 | 1.99 | 0.46 | 35.0 | 103.0 | 307.0 |
| | | | | | | 0.0000 | | 0.0 | | | | | | |
| 03918A_69 | 4.3 | 2.5 | 52.4 | 62 | 3 | 2 | 0.36 | 1 | 2 | 2.06 | 0.39 | 76.0 | 4.0 | 103.0 |
| 03918A_10 | | | | | | 0.0000 | | 0.0 | | | | | | |
| 4 | 4.5 | 4.5 | 115.7 | 75 | 1 | 2 | 0.18 | 0 | 2 | 2.23 | 0.41 | 34.0 | 52.0 | 246.0 |
| | | | | | | 0.0000 | | 0.0 | | | | | | |
| 03918A_61 | 4.8 | 3.4 | 86.7 | 40 | 2 | 1 | 0.44 | 1 | 2 | 2.00 | 0.34 | 89.0 | 133.0 | 379.0 |
| | | | | | | 0.0000 | | 0.0 | | | | | | |
| 03918A_58 | 5.1 | 3.6 | 51.7 | 42 | 2 | 1 | 0.33 | 1 | 2 | 2.04 | 0.43 | 68.0 | 166.0 | 147.0 |
| 03918A_10 | | | | | | 0.0000 | | 0.0 | | | | | | |
| 9 | 5.2 | 2.1 | 45.6 | 31 | 6 | 3 | 0.49 | 1 | 2 | 2.65 | 0.56 | 111.0 | 249.0 | 115.0 |

| | | | | | | | | | | | | | | |
|---|---|---|---|---|---|---|---|---|---|---|---|---|---|---|
| | | | | | | 0.0000 | | 0.0 | | | | | | |
| 03918A_75 | 5.3 | 3.1 | 121.4 | 46 | 3 | 1 | 0.48 | 1 | 2 | 2.18 | 0.42 | 86.0 | 217.0 | 214.0 |
| | | | | | | 0.0000 | | 0.0 | | | | | | |
| 03918A_91 | 5.4 | 5.4 | 102.8 | 85 | 1 | 1 | 0.22 | 1 | 2 | 2.31 | 0.54 | 44.0 | 124.0 | 363.0 |
| | | | | | | 0.0000 | | 0.0 | | | | | | |
| 03918A_88 | 5.7 | 5.7 | 129.6 | 118 | 1 | 1 | 0.15 | 0 | 1 | 2.03 | 0.43 | 31.0 | 85.0 | 294.0 |
| | | | | | | 0.0000 | | 0.0 | | | | | | |
| 03918A_38 | 6.0 | 4.2 | 105.2 | 83 | 2 | 2 | 0.24 | 1 | 2 | 2.19 | 0.42 | 49.0 | 127.0 | 206.0 |
| | | | | | | 0.0000 | | 0.0 | | | | | | |
| 03918A_43 | 6.0 | 3.5 | 110.5 | 49 | 3 | 1 | 0.42 | 1 | 3 | 2.19 | 0.49 | 84.0 | 228.0 | 210.0 |
| | | | | | | 0.0000 | | 0.0 | | | | | | |
| 03918A_49 | 6.4 | 4.5 | 104.0 | 50 | 2 | 1 | 0.38 | 1 | 1 | 2.27 | 0.48 | 90.0 | 228.0 | 337.0 |
| | | | | | | 0.0000 | | 0.0 | | | | | | |
| 03918A_47 | 6.5 | 6.5 | 104.4 | 100 | 1 | 1 | 0.19 | 0 | 1 | 2.42 | 0.41 | 36.0 | 93.0 | 288.0 |
| | | | | | | 0.0000 | | 0.0 | | | | | | |
| 03918A_68 | 6.5 | 6.5 | 119.5 | 65 | 1 | 1 | 0.33 | 1 | 1 | 2.33 | 0.30 | 62.0 | 149.0 | 354.0 |
| 03918A_10 | | | | | | 0.0000 | | 0.0 | | | | | | |
| 6 | 6.5 | 4.6 | 111.7 | 64 | 2 | 2 | 0.24 | 0 | 2 | 2.63 | 0.44 | 49.0 | 86.0 | 126.0 |
| | | | | | | 0.0000 | | 0.0 | | | | | | |
| 03918A_19 | 6.6 | 2.5 | 0.0 | 0 | 7 | 3 | 0.39 | 1 | 2 | 2.09 | 0.38 | 73.0 | 178.0 | 180.0 |
| | | | | | | 0.0000 | | 0.0 | | | | | | |
| 03918A_23 | 6.9 | 4.0 | 0.0 | 0 | 3 | 2 | 0.23 | 2 | 2 | 2.28 | 0.57 | 43.0 | 128.0 | 243.0 |
| | | | | | | 0.0000 | | 0.0 | | | | | | |
| 03918A_17 | 7.1 | 7.1 | 0.0 | 0 | 1 | 1 | 0.15 | 0 | 1 | 2.53 | 0.54 | 32.0 | 126.0 | 176.0 |
| | | | | | | 0.0000 | | 0.0 | | | | | | |
| 03918A_31 | 7.1 | 7.1 | 0.0 | 0 | 1 | 2 | 0.09 | 0 | 1 | 2.62 | 0.61 | 21.0 | 25.0 | 78.0 |
| | | | | | | 0.0000 | | 0.0 | | | | | | |
| 03918A_89 | 7.3 | 7.3 | 104.4 | 137 | 1 | 1 | 0.12 | 0 | 1 | 2.32 | 0.54 | 24.0 | 49.0 | 165.0 |
| | | | | | | 0.0000 | | 0.0 | | | | | | |
| 03918A_7 | 7.8 | 5.5 | 0.0 | 0 | 2 | 2 | 0.16 | 0 | 2 | 2.29 | 0.51 | 40.0 | 105.0 | 344.0 |
| | | | | | | 0.0000 | | 0.0 | | | | | | |
| 03918A_27 | 7.8 | 4.5 | 0.0 | 0 | 3 | 3 | 0.14 | 0 | 2 | 2.10 | 0.56 | 28.0 | 66.0 | 337.0 |
| 03918A_10 | | | | | | 0.0000 | | 0.0 | | | | | | |
| 7 | 8.5 | 6.0 | 141.2 | 55 | 2 | 1 | 0.20 | 1 | 2 | 2.63 | 0.51 | 41.0 | 92.0 | 315.0 |
| 03918A_11 | | | | | | 0.0000 | | 0.0 | | | | | | |
| 0 | 8.8 | 3.9 | 117.4 | 55 | 5 | 2 | 0.30 | 1 | 3 | 2.23 | 0.51 | 64.0 | 157.0 | 241.0 |
| | | | | | | 0.0000 | | 0.0 | | | | | | |
| 03918A_50 | 9.0 | 6.4 | 0.0 | 0 | 2 | 2 | 0.16 | 1 | 1 | 2.26 | 0.48 | 31.0 | 84.0 | 279.0 |
| | | | | | | 0.0000 | | 0.0 | | | | | | |
| 03918A_18 | 9.0 | 9.0 | 0.0 | 0 | 1 | 2 | 0.08 | 0 | 1 | 2.18 | 0.33 | 12.0 | 28.0 | 150.0 |
| | | | | | | 0.0000 | | 0.0 | | | | | | |
| 03918A_34 | 9.1 | 6.5 | 123.0 | 83 | 2 | 1 | 0.22 | 1 | 2 | 1.96 | 0.44 | 44.0 | 103.0 | 240.0 |
| | | | | | | 0.0000 | | 0.0 | | | | | | |
| 03918A_77 | 9.4 | 9.4 | 139.5 | 99 | 1 | 1 | 0.14 | 0 | 1 | 2.13 | 0.31 | 29.0 | 70.0 | 270.0 |
| | | | | | | 0.0000 | | 0.0 | | | | | | |
| 03918A_99 | 9.5 | 6.7 | 147.8 | 136 | 2 | 2 | 0.13 | 0 | 2 | 2.18 | 0.41 | 28.0 | 73.0 | 215.0 |
| | | | | | | 0.0000 | | 0.0 | | | | | | |
| 03918A_93 | 9.9 | 9.9 | 0.0 | 0 | 1 | 1 | 0.09 | 0 | 1 | 1.78 | 0.22 | 20.0 | 73.0 | 503.0 |
| | | | | | | 0.0000 | | 0.0 | | | | | | |
| 03918A_24 | 10.0 | 5.9 | 0.0 | 0 | 3 | 2 | 0.15 | 2 | 2 | 2.31 | 0.38 | 33.0 | 83.0 | 315.0 |
| 03918A_10 | | | | | | 0.0000 | | 0.0 | | | | | | |
| 3 | 10.2 | 5.9 | 99.2 | 96 | 3 | 1 | 0.31 | 1 | 2 | 2.54 | 0.62 | 64.0 | 146.0 | 177.0 |
| | | | | | | 0.0000 | | 0.0 | | | | | | |
| 03918A_97 | 10.3 | 10.3 | 94.7 | 100 | 1 | 1 | 0.12 | 0 | 1 | 2.41 | 0.46 | 25.0 | 77.0 | 262.0 |
| | | | | | | 0.0000 | | 0.0 | | | | | | |
| 03918A_80 | 10.8 | 4.8 | 154.6 | 103 | 5 | 4 | 0.13 | 0 | 3 | 2.20 | 0.41 | 25.0 | 79.0 | 300.0 |
| | | | | | | 0.0000 | | 0.0 | | | | | | |
| 03918A_57 | 10.9 | 10.9 | 0.0 | 0 | 1 | 2 | 0.06 | 0 | 1 | 2.04 | 0.35 | 11.0 | 118.0 | 483.0 |
| | | | | | | 0.0000 | | 0.0 | | | | | | |
| 03918A_22 | 10.9 | 5.5 | 134.5 | 165 | 4 | 3 | 0.16 | 1 | 2 | 2.28 | 0.46 | 27.0 | 89.0 | 396.0 |
| | | | | | | 0.0000 | | 0.0 | | | | | | |
| 03918A_54 | 11.3 | 8.0 | 113.4 | 143 | 2 | 2 | 0.13 | 0 | 2 | 2.32 | 0.49 | 27.0 | 55.0 | 165.0 |
| | | | | | | 0.0000 | | 0.0 | | | | | | |
| 03918A_73 | 12.1 | 12.1 | 245.8 | 342 | 1 | 2 | 0.06 | 0 | 1 | 2.44 | 0.46 | 11.0 | 36.0 | 203.0 |
| | | | | | | 0.0000 | | 0.0 | | | | | | |
| 03918A_82 | 12.9 | 7.5 | 124.2 | 220 | 3 | 5 | 0.06 | 0 | 3 | 2.24 | 0.41 | 11.0 | 33.0 | 178.0 |
| | | | | | | 0.0000 | | 0.0 | | | | | | |
| 03918A_5 | 13.4 | 9.5 | 0.0 | 0 | 2 | 2 | 0.08 | 0 | 1 | 2.00 | 0.40 | 18.0 | 14.0 | 117.0 |
| | | | | | | 0.0000 | | 0.0 | | | | | | |
| 03918A_6 | 13.8 | 9.8 | 0.0 | 0 | 2 | 2 | 0.12 | 0 | 2 | 2.29 | 0.50 | 23.0 | 98.0 | 179.0 |
| | | | | | | 0.0000 | | 0.0 | | | | | | |
| 03918A_72 | 13.9 | 6.9 | 105.1 | 77 | 4 | 1 | 0.25 | 1 | 2 | 2.14 | 0.38 | 50.0 | 133.0 | 228.0 |
| | | | | | | 0.0000 | | 0.0 | | | | | | |
| 03918A_76 | 13.9 | 7.0 | 169.5 | 163 | 4 | 4 | 0.08 | 0 | 3 | 2.33 | 0.46 | 18.0 | 74.0 | 188.0 |

| | | | | | | | | | | | | | | |
|---|---|---|---|---|---|---|---|---|---|---|---|---|---|---|
| | | | | | | 0.0000 | | 0.0 | | | | | | |
| 03918A_84 | 14.1 | 9.9 | 138.7 | 123 | 2 | 2 | 0.09 | 0 | 4 | 2.51 | 0.56 | 18.0 | 33.0 | 81.0 |
| 03918A_10 | | | | | | 0.0000 | | 0.0 | | | | | | |
| 5 | 14.2 | 8.2 | 122.5 | 65 | 3 | 1 | 0.18 | 0 | 1 | 2.31 | 0.39 | 38.0 | 96.0 | 209.0 |
| | | | | | | 0.0000 | | 0.0 | | | | | | |
| 03918A_83 | 14.3 | 4.0 | 43.5 | 21 | 13 | 2 | 0.58 | 1 | 3 | 2.57 | 0.50 | 105.0 | 30.0 | 245.0 |
| | | | | | | 0.0000 | | 0.0 | | | | | | |
| 03918A_36 | 14.3 | 10.2 | 175.2 | 194 | 2 | 3 | 0.06 | 0 | 2 | 2.14 | 0.32 | 13.0 | 5.0 | 43.0 |
| | | | | | | 0.0000 | | 0.0 | | | | | | |
| 03918A_48 | 14.6 | 10.3 | 0.0 | 0 | 2 | 1 | 0.23 | 1 | 2 | 2.17 | 0.41 | 45.0 | 108.0 | 287.0 |
| 03918A_10 | | | | | | 0.0000 | | 0.0 | | | | | | |
| 8 | 15.5 | 8.9 | 104.0 | 121 | 3 | 2 | 0.12 | 0 | 2 | 2.17 | 0.41 | 22.0 | 62.0 | 301.0 |
| 03918A_10 | | | | | | 0.0000 | | 0.0 | | | | | | |
| 0 | 16.4 | 9.5 | 164.5 | 156 | 3 | 1 | 0.16 | 0 | 2 | 2.43 | 0.33 | 31.0 | 85.0 | 188.0 |
| | | | | | | 0.0000 | | 0.0 | | | | | | |
| 03918A_3 | 18.5 | 10.8 | 107.3 | 209 | 3 | 3 | 0.07 | 1 | 3 | 2.25 | 0.51 | 6.0 | 32.0 | 238.0 |
| | | | | | | 0.0000 | | 0.0 | | | | | | |
| 03918A_1 | 19.5 | 11.3 | 0.0 | 0 | 3 | 5 | 0.04 | 0 | 3 | 2.02 | 0.36 | 7.0 | 17.0 | 141.0 |
| | | | | | | 0.0000 | | 0.0 | | | | | | |
| 03918A_51 | 20.0 | 10.0 | 92.4 | 94 | 4 | 1 | 0.20 | 1 | 2 | 1.98 | 0.47 | 44.0 | 139.0 | 331.0 |
| | | | | | | 0.0000 | | 0.0 | | | | | | |
| 03918A_4 | 21.5 | 15.2 | 149.8 | 225 | 2 | 1 | 0.10 | 0 | 2 | 2.11 | 0.48 | 25.0 | 62.0 | 201.0 |
| | | | | | | 0.0000 | | 0.0 | | | | | | |
| 03918A_42 | 22.2 | 22.2 | 76.1 | 131 | 1 | 1 | 0.06 | 0 | 1 | 2.44 | 0.57 | 13.0 | 84.0 | 141.0 |
| | | | | | | 0.0000 | | 0.0 | | | | | | |
| 03918A_28 | 30.8 | 11.7 | 106.9 | 71 | 7 | 1 | 0.24 | 1 | 2 | 1.96 | 0.51 | 50.0 | 142.0 | 316.0 |
| | | | | | | 0.0000 | | 0.0 | | | | | | |
| 03918A_10 | 31.2 | 22.1 | 0.0 | 0 | 2 | 2 | 0.04 | 0 | 2 | 2.21 | 0.56 | 8.0 | 19.0 | 248.0 |
| | | | | | | 0.0000 | | 0.0 | | | | | | |
| 03918A_95 | 33.6 | 23.8 | 129.9 | 301 | 2 | 4 | 0.02 | 0 | 1 | 1.93 | 0.34 | 4.0 | 19.0 | 223.0 |
| | | | | | | 0.0000 | | 0.0 | | | | | | |
| 03918A_86 | 33.7 | 23.8 | 178.0 | 393 | 2 | 3 | 0.02 | 0 | 2 | 2.41 | 0.48 | 5.0 | 22.0 | 280.0 |
| | | | | | | 0.0000 | | 0.0 | | | | | | |
| 03918A_39 | 38.7 | 38.7 | 182.4 | 355 | 1 | 2 | 0.02 | 0 | 1 | 2.01 | 0.70 | 4.0 | 23.0 | 215.0 |
| | | | | | | 0.0000 | | 0.0 | | | | | | |
| 03918A_46 | 40.3 | 18.1 | 18.8 | 78 | 5 | 1 | 0.11 | 0 | 4 | 1.88 | 0.42 | 22.0 | 81.0 | 273.0 |
| | | | | | | 0.0000 | | 0.0 | | | | | | |
| 03918A_98 | 43.1 | 24.9 | 54.4 | 54 | 3 | 1 | 0.06 | 0 | 2 | 1.76 | 0.51 | 126.0 | 0.0 | 200.0 |
| | | | | | | 0.0000 | | 0.0 | | | | | | |
| 03918A_21 | 45.6 | 45.6 | 0.0 | 0 | 1 | 2 | 0.01 | 0 | 1 | 2.09 | 0.60 | 2.0 | 11.0 | 313.0 |
| | | | | | | 0.0000 | | 0.0 | | | | | | |
| 03918A_66 | 49.4 | 34.9 | 295.4 | 361 | 2 | 2 | 0.02 | 0 | 2 | 2.44 | 0.61 | 5.0 | 22.0 | 233.0 |
| | | | | | | 0.0000 | | 0.0 | | | | | | |
| 03918A_16 | 49.8 | 28.8 | 64.1 | 185 | 3 | 3 | 0.03 | 0 | 3 | 2.05 | 0.51 | 5.0 | 24.0 | 298.0 |
| | | | | | | 0.0000 | | 0.0 | | | | | | |
| 03918A_59 | 53.7 | 53.7 | 460.4 | 737 | 1 | 1 | 0.02 | 0 | 1 | 2.40 | 0.45 | 4.0 | 35.0 | 451.0 |
| | | | | | | 0.0000 | | 0.0 | | | | | | |
| 03918A_81 | 54.9 | 13.4 | 122.6 | 103 | 17 | 3 | 0.13 | 0 | 4 | 2.83 | 0.68 | 28.0 | 147.0 | 115.0 |
| | | | | | | 0.0000 | | 0.0 | | | | | | |
| 03918A_8 | 59.9 | 22.7 | 0.0 | 0 | 7 | 2 | 0.07 | 0 | 4 | 2.86 | 0.77 | 15.0 | 68.0 | 113.0 |
| | | | | | | 0.0000 | | 0.0 | | | | | | |
| 03918A_32 | 64.3 | 37.2 | 0.0 | 0 | 3 | 2 | 0.03 | 0 | 3 | 2.60 | 0.46 | 6.0 | 44.0 | 56.0 |
| | | | | | | 0.0000 | | 0.0 | | | | | | |
| 03918A_62 | 70.7 | 50.1 | 107.0 | 303 | 2 | 1 | 0.04 | 0 | 1 | 2.05 | 0.40 | 7.0 | 46.0 | 296.0 |
| | | | | | | 0.0000 | | 0.0 | | | | | | |
| 03918A_20 | 71.4 | 21.6 | 0.0 | 0 | 11 | 2 | 0.10 | 0 | 2 | 2.53 | 0.44 | 19.0 | 84.0 | 349.0 |
| | | | | | | 0.0000 | | 0.0 | | | | | | |
| 03918A_52 | 76.0 | 38.2 | 0.0 | 0 | 4 | 4 | 0.02 | 0 | 2 | 2.56 | 0.53 | 3.0 | 16.0 | 279.0 |
| | | | | | | 0.0000 | | 0.0 | | | | | | |
| 03918A_9 | 77.2 | 34.7 | 0.0 | 0 | 5 | 3 | 0.03 | 0 | 3 | 2.31 | 0.47 | 4.0 | 18.0 | 312.0 |
| | | | | | | 0.0000 | | 0.0 | | | | | | |
| 03918A_74 | 80.7 | 57.1 | 568.6 | 662 | 2 | 2 | 0.02 | 0 | 2 | 2.75 | 0.53 | 3.0 | 37.0 | 392.0 |
| | | | | | | 0.0000 | | 0.0 | | | | | | |
| 03918A_37 | 80.7 | 46.7 | 207.3 | 555 | 3 | 2 | 0.03 | 0 | 3 | 2.08 | 0.33 | 5.0 | 24.0 | 384.0 |
| | | | | | | 0.0000 | | 0.0 | | | | | | |
| 03918A_15 | 90.5 | 52.4 | 95.0 | 415 | 3 | 4 | 0.01 | 0 | 2 | 1.79 | 0.47 | 2.0 | 12.0 | 166.0 |
| | | | | | | 0.0000 | | 0.0 | | | | | | |
| 03918A_30 | 96.4 | 48.3 | 51.8 | 261 | 4 | 2 | 0.03 | 0 | 3 | 2.31 | 0.44 | 5.0 | 28.0 | 207.0 |
| | | | | | | 0.0000 | | 0.0 | | | | | | |
| 03918A_85 | 116.5 | 52.2 | 188.3 | 222 | 5 | 1 | 0.04 | 0 | 2 | 2.53 | 0.53 | 8.0 | 20.0 | 50.0 |
| | | | | | | 0.0000 | | 0.0 | | | | | | |
| 03918A_94 | 120.1 | 85.1 | 554.1 | 911 | 2 | 1 | 0.01 | 0 | 1 | 1.93 | 0.24 | 3.0 | 15.0 | 229.0 |
| | | | | | | 0.0000 | | 0.0 | | | | | | |
| 03918A_56 | 123.8 | 62.5 | 371.9 | 590 | 4 | 2 | 0.02 | 0 | 4 | 2.14 | 0.47 | 3.0 | 17.0 | 238.0 |

| | | | | | | | | | | | | | | |
|---|---|---|---|---|---|---|---|---|---|---|---|---|---|---|
| | | | | | | 0.0000 | | 0.0 | | | | | | |
| 03918A_63 | 130.4 | 75.5 | 176.3 | 359 | 3 | 1 | 0.02 | 0 | 2 | 2.02 | 0.37 | 4.0 | 25.0 | 355.0 |
| | | | | | | 0.0000 | | 0.0 | | | | | | |
| 03918A_78 | 143.7 | 64.4 | 352.2 | 423 | 5 | 1 | 0.03 | 0 | 3 | 2.32 | 0.68 | 6.0 | 32.0 | 382.0 |
| | | | | | | 0.0000 | | 0.0 | | | | | | |
| 03918A_40 | 169.7 | 98.2 | 75.2 | 231 | 3 | 1 | 0.02 | 0 | 2 | 2.60 | 0.51 | 4.0 | 21.0 | 213.0 |
| | | | | | | 0.0000 | | 0.0 | | | | | | |
| 03918A_33 | 7809.7 | 7813.2 | 0.0 | 0 | 1 | 1 | 0.00 | 0 | 1 | 2.12 | 0.73 | 0.0 | 0.0 | 2.0 |

**Robertson River**

| Spot Name | FT Age (Ma) | sigma Symm (Ma) | UPb Age (Ma) | 2 sigma (Ma) | Ns | Area cm^2 | U/Cation | +/- 1sig | Etch Figs. | Dpar (um) | Dper (um) | [U] (ppm) | [Th] (ppm) | [Sm] (ppm) |
|---|---|---|---|---|---|---|---|---|---|---|---|---|---|---|
| | | | | | | 0.0000 | | 0.0 | | | | | | |
| 03915A_5 | 0.0 | 591.9 | 0.0 | 0 | 0 | 2 | 0.00 | 0 | 1 | 2.43 | 0.55 | 0.0 | 0.0 | 8.0 |
| | | | | | | 0.0000 | | 0.0 | | | | | | |
| 03915A_11 | 0.0 | 1072.4 | 0.0 | 0 | 0 | 1 | 0.00 | 0 | 1 | 1.96 | 0.43 | 0.0 | 1.0 | 1.0 |
| | | | | | | 0.0000 | | 0.0 | | | | | | |
| 03915A_13 | 0.0 | 83.7 | 383.9 | 497 | 0 | 1 | 0.01 | 0 | 1 | 1.62 | 0.37 | 1.0 | 8.0 | 220.0 |
| | | | | | | 0.0000 | | 0.0 | | | | | | |
| 03915A_20 | 0.0 | 308.4 | 0.0 | 0 | 0 | 2 | 0.00 | 0 | 1 | 2.14 | 0.37 | 0.0 | 1.0 | 10.0 |
| | | | | | | 0.0000 | | 0.0 | | | | | | |
| 03915A_26 | 0.0 | 10.5 | 0.0 | 0 | 0 | 1 | 0.09 | 2 | 1 | 1.55 | 0.44 | 8.0 | 63.0 | 144.0 |
| | | | | | | 0.0000 | | 0.0 | | | | | | |
| 03915A_28 | 0.0 | 1002.7 | 0.0 | 0 | 0 | 1 | 0.00 | 0 | 1 | 2.42 | 0.50 | 0.0 | 21.0 | 5.0 |
| | | | | | | 0.0000 | | 0.0 | | | | | | |
| 03915A_33 | 0.0 | 23330.9 | 0.0 | 0 | 16 | 1 | 0.00 | 0 | 3 | 1.96 | 0.46 | 0.0 | 0.0 | 0.0 |
| | | | | | | 0.0000 | | 0.0 | | | | | | |
| 03915A_35 | 0.0 | 121.6 | 0.0 | 0 | 0 | 2 | 0.00 | 0 | 1 | 1.86 | 0.40 | 1.0 | 6.0 | 16.0 |
| | | | | | | 0.0000 | | 0.0 | | | | | | |
| 03915A_37 | 0.0 | 279.0 | 0.0 | 0 | 0 | 4 | 0.00 | 0 | 1 | 1.88 | 0.41 | 0.0 | 0.0 | 11.0 |
| | | | | | | 0.0000 | | 0.0 | | | | | | |
| 03915A_40 | 0.0 | 579.5 | 0.0 | 0 | 0 | 1 | 0.00 | 0 | 1 | 2.05 | 0.41 | 0.0 | 0.0 | 18.0 |
| | | | | | | 0.0000 | | 0.0 | | | | | | |
| 03915A_43 | 0.0 | 837.5 | 0.0 | 0 | 0 | 1 | 0.00 | 0 | 1 | 1.81 | 0.40 | 0.0 | 1.0 | 8.0 |
| | | | | | | 0.0000 | | 0.0 | | | | | | |
| 03915A_46 | 0.0 | 25.8 | 600.1 | 412 | 0 | 2 | 0.02 | 1 | 1 | 2.34 | 0.45 | 3.0 | 25.0 | 210.0 |
| | | | | | | 0.0000 | | 0.0 | | | | | | |
| 03915A_48 | 0.0 | 514.3 | 0.0 | 0 | 0 | 2 | 0.00 | 0 | 1 | 1.66 | 0.36 | 0.0 | 9.0 | 20.0 |
| | | | | | | 0.0000 | | 0.0 | | | | | | |
| 03915A_53 | 0.0 | 161.6 | 0.0 | 0 | 3 | 1 | 0.01 | 0 | 3 | 2.12 | 0.41 | 3.0 | 25.0 | 110.0 |
| | | | | | | 0.0000 | | 0.0 | | | | | | |
| 03915A_57 | 0.0 | 3315.2 | 0.0 | 0 | 0 | 1 | 0.00 | 0 | 1 | 1.94 | 0.25 | 0.0 | 0.0 | 5.0 |
| | | | | | | 0.0000 | | 0.0 | | | | | | |
| 03915A_63 | 0.0 | 2357.6 | 0.0 | 0 | 0 | 1 | 0.00 | 0 | 1 | 2.17 | 0.22 | 0.0 | 1.0 | 64.0 |
| | | | | | | 0.0000 | | 0.0 | | | | | | |
| 03915A_66 | 0.0 | 426.3 | 663.8 | #### | 0 | 2 | 0.00 | 0 | 1 | 1.50 | 0.31 | 0.0 | 0.0 | 3.0 |
| | | | | | | 0.0000 | | 1.1 | | | | | | |
| 03915A_67 | 0.0 | 11.8 | 62.6 | #### | 0 | 1 | 0.24 | 1 | 1 | 2.13 | 0.36 | 25.0 | 73.0 | 5.0 |
| | | | | | | 0.0000 | | 0.0 | | | | | | |
| 03915A_70 | 0.0 | 169.2 | 0.0 | 0 | 0 | 1 | 0.01 | 0 | 1 | 1.90 | 0.43 | 2.0 | 15.0 | 79.0 |
| | | | | | | 0.0000 | | 0.0 | | | | | | |
| 03915A_77 | 0.0 | 44.9 | 134.1 | 266 | 0 | 2 | 0.01 | 0 | 1 | 2.06 | 0.45 | 2.0 | 12.0 | 326.0 |
| | | | | | | 0.0000 | | 0.0 | | | | | | |
| 03915A_80 | 0.0 | 6749.8 | 0.0 | 0 | 0 | 1 | 0.00 | 0 | 1 | 2.56 | 0.81 | 0.0 | 0.0 | 0.0 |
| | | | | | | 0.0000 | | 0.0 | | | | | | |
| 03915A_87 | 0.0 | 173.5 | 0.0 | 0 | 0 | 1 | 0.01 | 0 | 1 | 1.66 | 0.53 | 1.0 | 2.0 | 31.0 |
| | | | | | | 0.0000 | | 0.0 | | | | | | |
| 03915A_90 | 0.0 | 188.2 | 0.0 | 0 | 0 | 2 | 0.00 | 0 | 1 | 1.78 | 0.41 | 1.0 | 2.0 | 2.0 |
| | | | | | | 0.0000 | | 0.0 | | | | | | |
| 03915A_93 | 0.0 | 59.5 | 0.0 | 0 | 0 | 1 | 0.01 | 0 | 1 | 2.12 | 0.34 | 2.0 | 42.0 | 36.0 |
| | | | | | | 0.0000 | | 0.0 | | | | | | |
| 03915A_95 | 0.0 | 1043.4 | 0.0 | 0 | 11 | 0 | 0.01 | 0 | 2 | 1.63 | 0.34 | 0.0 | 2.0 | 13.0 |
| 03915A_107 | 0.0 | 203.9 | 0.0 | 0 | 0 | 0.0000 1 | 0.00 | 0.0 0 | 1 | 1.48 | 0.24 | 1.0 | 104.0 | 106.0 |
| | | | | | | 0.0000 | | 0.0 | | | | | | |
| 03915A_19 | 8.7 | 8.7 | 147.2 | 404 | 1 | 1 | 0.12 | 1 | 1 | 1.73 | 0.41 | 3.0 | 17.0 | 159.0 |
| | | | | | | 0.0000 | | 0.0 | | | | | ##### | |
| 03915A_18 | 10.5 | 7.4 | 302.7 | #### | 2 | 1 | 0.20 | 1 | 1 | 2.13 | 0.32 | 40.0 | # | 141.0 |
| | | | | | | 0.0000 | | 0.0 | | | | | | |
| 03915A_86 | 14.3 | 10.9 | 0.0 | 0 | 2 | 1 | 0.18 | 5 | 2 | 2.21 | 0.47 | 0.0 | 0.0 | 1.0 |
| | | | | | | 0.0000 | | 0.0 | | | | | | |
| 03915A_25 | 14.5 | 8.4 | 144.5 | 68 | 3 | 1 | 0.26 | 1 | 4 | 2.07 | 0.50 | 54.0 | 210.0 | 239.0 |

| | | | | | | | | | | | | | | |
|---|---|---|---|---|---|---|---|---|---|---|---|---|---|---|
| | | | | | | 0.0000 | | 0.0 | | | | | | |
| 03915A_21 | 21.0 | 21.0 | 106.0 | 179 | 1 | 2 | 0.02 | 0 | 2 | 1.93 | 0.39 | 5.0 | 20.0 | 188.0 |
| | | | | | | 0.0000 | | 0.0 | | | | | | |
| 03915A_9 | 22.8 | 13.2 | 137.2 | 77 | 3 | 1 | 0.17 | 1 | 3 | 2.33 | 0.38 | 31.0 | 151.0 | 173.0 |
| | | | | | | 0.0000 | | 0.0 | | | | | | |
| 03915A_52 | 29.2 | 29.2 | 314.2 | 352 | 1 | 1 | 0.03 | 0 | 2 | 1.85 | 0.40 | 5.0 | 62.0 | 133.0 |
| | | | | | | 0.0000 | | 0.0 | | | | | | |
| 03915A_2 | 31.2 | 18.0 | 0.0 | 0 | 3 | 5 | 0.02 | 0 | 2 | 2.22 | 0.30 | 5.0 | 1.0 | 169.0 |
| | | | | | | 0.0000 | | 0.0 | | | | | | |
| 03915A_45 | 31.3 | 9.1 | 111.1 | 99 | 12 | 2 | 0.27 | 1 | 4 | 2.32 | 0.49 | 55.0 | 152.0 | 175.0 |
| 03915A_10 | | | | | | 0.0000 | | 0.0 | | | | | | |
| 8 | 31.5 | 18.2 | 0.0 | 0 | 3 | 1 | 0.10 | 0 | 2 | 2.22 | 0.43 | 20.0 | 176.0 | 526.0 |
| | | | | | | 0.0000 | | 0.0 | | | | | | |
| 03915A_36 | 31.6 | 31.7 | 486.8 | 634 | 1 | 5 | 0.01 | 0 | 2 | 1.78 | 0.52 | 2.0 | 16.0 | 160.0 |
| | | | | | | 0.0000 | | 0.0 | | | | | | |
| 03915A_24 | 31.7 | 13.0 | 148.4 | 81 | 6 | 1 | 0.17 | 0 | 3 | 1.86 | 0.44 | 35.0 | 114.0 | 211.0 |
| | | | | | | 0.0000 | | 0.0 | | | | | | |
| 03915A_58 | 33.2 | 19.2 | 114.3 | 63 | 3 | 0 | 0.26 | 1 | 2 | 2.01 | 0.53 | 53.0 | 169.0 | 246.0 |
| | | | | | | 0.0000 | | 0.0 | | | | | | |
| 03915A_8 | 33.4 | 12.7 | 108.0 | 51 | 7 | 1 | 0.27 | 1 | 4 | 2.06 | 0.38 | 55.0 | 32.0 | 52.0 |
| 03915A_10 | | | | | | 0.0000 | | 0.0 | | | | | | |
| 6 | 37.3 | 9.7 | 92.4 | 101 | 15 | 3 | 0.17 | 1 | 2 | 2.05 | 0.40 | 36.0 | 135.0 | 205.0 |
| | | | | | | 0.0000 | | 0.0 | | | | | | |
| 03915A_99 | 37.4 | 10.5 | 98.6 | 45 | 13 | 1 | 0.29 | 1 | 4 | 2.26 | 0.39 | 59.0 | 157.0 | 312.0 |
| | | | | | | 0.0000 | | 0.0 | | | | | | |
| 03915A_82 | 37.8 | 18.9 | 170.1 | 135 | 4 | 1 | 0.17 | 1 | 3 | 1.84 | 0.37 | 34.0 | 198.0 | 233.0 |
| | | | | | | 0.0000 | | 0.0 | | | | | | |
| 03915A_83 | 38.6 | 13.7 | 151.1 | 121 | 8 | 1 | 0.19 | 1 | 2 | 1.93 | 0.53 | 38.0 | 178.0 | 283.0 |
| | | | | | | 0.0000 | | 0.0 | | | | | | |
| 03915A_94 | 38.6 | 9.4 | 101.1 | 50 | 17 | 1 | 0.45 | 1 | 3 | 1.79 | 0.41 | 89.0 | 153.0 | 224.0 |
| | | | | | | 0.0000 | | 0.0 | | | | | | |
| 03915A_62 | 38.7 | 14.7 | 100.8 | 40 | 7 | 0 | 0.51 | 1 | 3 | 2.00 | 0.53 | 101.0 | 205.0 | 242.0 |
| | | | | | | 0.0000 | | 0.0 | | | | | | |
| 03915A_59 | 39.1 | 7.8 | 133.6 | 49 | 26 | 2 | 0.40 | 1 | 4 | 1.74 | 0.36 | 83.0 | 163.0 | 91.0 |
| | | | | | | 0.0000 | | 0.0 | | | | | | |
| 03915A_39 | 40.7 | 40.7 | 288.2 | 498 | 1 | 1 | 0.03 | 0 | 1 | 1.66 | 0.37 | 5.0 | 37.0 | 119.0 |
| | | | | | | 0.0000 | | 0.0 | | | | | | |
| 03915A_60 | 40.9 | 15.5 | 187.3 | 108 | 7 | 1 | 0.24 | 1 | 3 | 2.15 | 0.48 | 41.0 | 141.0 | 257.0 |
| | | | | | | 0.0000 | | 0.0 | | | | | | |
| 03915A_61 | 41.6 | 41.6 | 0.0 | 0 | 1 | 1 | 0.02 | 0 | 1 | 2.03 | 0.41 | 5.0 | 22.0 | 53.0 |
| | | | | | | 0.0000 | | 0.0 | | | | | | |
| 03915A_74 | 43.7 | 14.6 | 126.0 | 69 | 9 | 1 | 0.35 | 1 | 3 | 2.13 | 0.28 | 72.0 | 105.0 | 133.0 |
| | | | | | | 0.0000 | | 0.0 | | | | | | |
| 03915A_12 | 44.1 | 11.5 | 148.8 | 147 | 15 | 3 | 0.14 | 0 | 4 | 2.21 | 0.41 | 25.0 | 57.0 | 142.0 |
| | | | | | | 0.0000 | | 0.0 | | | | | | |
| 03915A_6 | 44.4 | 10.9 | 121.6 | 117 | 17 | 3 | 0.14 | 0 | 4 | 2.13 | 0.34 | 28.0 | 88.0 | 217.0 |
| | | | | | | 0.0000 | | 0.0 | | | | | | |
| 03915A_10 | 44.8 | 17.0 | 133.6 | 117 | 7 | 1 | 0.13 | 0 | 3 | 2.02 | 0.32 | 28.0 | 102.0 | 172.0 |
| | | | | | | 0.0000 | | 0.0 | | | | | | |
| 03915A_23 | 45.2 | 11.8 | 0.0 | 0 | 15 | 2 | 0.23 | 1 | 4 | 1.93 | 0.46 | 51.0 | 604.0 | 294.0 |
| | | | | | | 0.0000 | | 0.0 | | | | | | |
| 03915A_97 | 45.2 | 11.1 | 108.7 | 59 | 17 | 1 | 0.60 | 2 | 4 | 1.94 | 0.54 | 114.0 | 156.0 | 328.0 |
| 03915A_11 | | | | | | 0.0000 | | 0.0 | | | | | | |
| 0 | 46.4 | 8.0 | 0.0 | 0 | 36 | 1 | 0.66 | 3 | 4 | 2.14 | 0.57 | 122.0 | 69.0 | 255.0 |
| | | | | | | 0.0000 | | 0.0 | | | | | | |
| 03915A_76 | 46.5 | 13.5 | 0.0 | 0 | 12 | 1 | 0.33 | 1 | 3 | 1.94 | 0.49 | 79.0 | 707.0 | 447.0 |
| | | | | | | 0.0000 | | 0.0 | | | | | | |
| 03915A_55 | 46.9 | 17.8 | 159.5 | 88 | 7 | 1 | 0.27 | 1 | 3 | 2.34 | 0.47 | 52.0 | 198.0 | 279.0 |
| | | | | | | 0.0000 | | 0.0 | | | | | | |
| 03915A_7 | 47.3 | 47.3 | 2.6 | 404 | 1 | 1 | 0.02 | 0 | 1 | 2.01 | 0.41 | 4.0 | 21.0 | 173.0 |
| | | | | | | 0.0000 | | 0.0 | | | | | | |
| 03915A_73 | 47.3 | 36.2 | 0.0 | 0 | 2 | 0 | 0.18 | 5 | 2 | 2.21 | 0.39 | 38.0 | 112.0 | 442.0 |
| | | | | | | 0.0000 | | 0.0 | | | | | | |
| 03915A_79 | 48.1 | 8.2 | 121.6 | 34 | 35 | 2 | 0.39 | 1 | 4 | 2.72 | 0.57 | 79.0 | 317.0 | 173.0 |
| | | | | | | 0.0000 | | 0.0 | | | | | | |
| 03915A_1 | 49.3 | 49.4 | 188.7 | 348 | 1 | 3 | 0.01 | 0 | 2 | 1.89 | 0.37 | 2.0 | 20.0 | 176.0 |
| | | | | | | 0.0000 | | 0.0 | | | | | | |
| 03915A_89 | 49.6 | 17.6 | 132.9 | 148 | 8 | 1 | 0.14 | 0 | 4 | 2.34 | 0.48 | 26.0 | 83.0 | 189.0 |
| | | | | | | 0.0000 | | 0.0 | | | | | | |
| 03915A_54 | 49.7 | 16.6 | 140.1 | 78 | 9 | 1 | 0.19 | 0 | 2 | 2.00 | 0.31 | 40.0 | 120.0 | 189.0 |
| 03915A_10 | | | | | | 0.0000 | | 0.0 | | | | | | |
| 0 | 50.0 | 20.5 | 162.9 | 185 | 6 | 2 | 0.08 | 0 | 3 | 2.19 | 0.35 | 15.0 | 72.0 | 232.0 |
| | | | | | | 0.0000 | | 0.0 | | | | | | |
| 03915A_56 | 50.1 | 14.0 | 155.8 | 64 | 13 | 1 | 0.27 | 1 | 3 | 2.19 | 0.29 | 53.0 | 215.0 | 354.0 |

| | | | | | | | | | | | | | | |
|---|---|---|---|---|---|---|---|---|---|---|---|---|---|---|
| | | | | | | 0.0000 | | 0.0 | | | | | | |
| 03915A_41 | 50.4 | 25.2 | 144.9 | 206 | 4 | 2 | 0.06 | 0 | 3 | 1.74 | 0.38 | 12.0 | 95.0 | 336.0 |
| | | | | | | 0.0000 | | 0.0 | | | | | | |
| 03915A_75 | 50.5 | 13.2 | 133.3 | 87 | 15 | 1 | 0.25 | 1 | 4 | 2.25 | 0.44 | 50.0 | 176.0 | 289.0 |
| 03915A_10 | | | | | | 0.0000 | | 0.0 | | | | | | |
| 2 | 51.9 | 11.7 | 122.6 | 67 | 20 | 2 | 0.27 | 1 | 3 | 2.07 | 0.50 | 56.0 | 176.0 | 197.0 |
| | | | | | | 0.0000 | | 0.0 | | | | | | |
| 03915A_71 | 54.6 | 13.3 | 115.9 | 38 | 17 | 1 | 0.49 | 1 | 3 | 2.08 | 0.39 | 148.0 | 174.0 | 282.0 |
| | | | | | | 0.0000 | | 0.0 | | | | | | |
| 03915A_81 | 54.9 | 55.0 | 602.9 | 679 | 1 | 1 | 0.02 | 0 | 1 | 2.05 | 0.31 | 3.0 | 9.0 | 116.0 |
| 03915A_10 | | | | | | 0.0000 | | 0.0 | | | | | | |
| 5 | 54.9 | 13.1 | 98.8 | 110 | 18 | 2 | 0.17 | 1 | 4 | 2.03 | 0.53 | 33.0 | 116.0 | 191.0 |
| | | | | | | 0.0000 | | 0.0 | | | | | | |
| 03915A_85 | 55.0 | 55.0 | 0.0 | 0 | 1 | 1 | 0.03 | 0 | 2 | 2.15 | 0.35 | 0.0 | 1.0 | 16.0 |
| | | | | | | 0.0000 | | 0.0 | | | | | | |
| 03915A_17 | 55.7 | 55.8 | 207.5 | 488 | 1 | 4 | 0.01 | 0 | 1 | 2.20 | 0.40 | 1.0 | 7.0 | 196.0 |
| | | | | | | 0.0000 | | 0.0 | | | | | | |
| 03915A_88 | 59.5 | 26.7 | 169.1 | 149 | 5 | 1 | 0.09 | 0 | 3 | 2.34 | 0.57 | 18.0 | 86.0 | 123.0 |
| | | | | | | 0.0000 | | 0.0 | | | | | | |
| 03915A_92 | 64.2 | 22.8 | 128.5 | 52 | 8 | 0 | 0.35 | 1 | 4 | 2.09 | 0.45 | 68.0 | 170.0 | 218.0 |
| | | | | | | 0.0000 | | 0.0 | | | | | | |
| 03915A_50 | 65.4 | 20.8 | 204.2 | 130 | 10 | 1 | 0.26 | 0 | 4 | 2.30 | 0.35 | 42.0 | 22.0 | 177.0 |
| 03915A_10 | | | | | | 0.0000 | | 0.0 | | | | | | |
| 9 | 66.3 | 9.4 | 104.5 | 44 | 55 | 2 | 0.58 | 2 | 4 | 2.17 | 0.51 | 118.0 | 125.0 | 144.0 |
| | | | | | | 0.0000 | | 0.0 | | | | | | |
| 03915A_47 | 66.7 | 20.2 | 128.5 | 77 | 11 | 1 | 0.21 | 0 | 4 | 2.17 | 0.40 | 39.0 | 124.0 | 202.0 |
| | | | | | | 0.0000 | | 0.0 | | | | | | |
| 03915A_84 | 66.8 | 33.4 | 254.5 | 349 | 4 | 2 | 0.05 | 0 | 2 | 1.81 | 0.41 | 8.0 | 61.0 | 298.0 |
| 03915A_10 | | | | | | 0.0000 | | 0.0 | | | | | | |
| 4 | 66.9 | 22.4 | 110.5 | 106 | 9 | 1 | 0.17 | 0 | 2 | 2.55 | 0.63 | 35.0 | 169.0 | 113.0 |
| | | | | | | 0.0000 | | 0.0 | | | | | | |
| 03915A_91 | 69.8 | 26.5 | 97.3 | 102 | 7 | 0 | 0.25 | 0 | 2 | 2.04 | 0.39 | 52.0 | 153.0 | 256.0 |
| | | | | | | 0.0000 | | 0.0 | | | | | | |
| 03915A_98 | 70.0 | 18.9 | 210.8 | 204 | 14 | 2 | 0.10 | 0 | 4 | 2.04 | 0.46 | 22.0 | 61.0 | 190.0 |
| | | | | | | 0.0000 | | 0.0 | | | | | | |
| 03915A_15 | 70.0 | 70.0 | 202.0 | 296 | 1 | 1 | 0.01 | 0 | 1 | 1.85 | 0.49 | 2.0 | 14.0 | 322.0 |
| | | | | | | 0.0000 | | 0.0 | | | | | | |
| 03915A_27 | 72.4 | 72.5 | 0.0 | 0 | 1 | 1 | 0.03 | 0 | 1 | 2.40 | 0.56 | 0.0 | 0.0 | 3.0 |
| | | | | | | 0.0000 | | 0.0 | | | | | | |
| 03915A_32 | 80.0 | 80.1 | 379.0 | 407 | 1 | 1 | 0.01 | 0 | 1 | 1.50 | 0.50 | 3.0 | 30.0 | 207.0 |
| 03915A_10 | | | | | | 0.0000 | | 0.0 | | | | | | |
| 3 | 83.3 | 20.9 | 103.5 | 82 | 16 | 1 | 0.24 | 0 | 4 | 2.32 | 0.50 | 50.0 | 163.0 | 262.0 |
| | | | | | | 0.0000 | | 0.0 | | | | | | |
| 03915A_65 | 86.4 | 21.8 | 98.8 | 98 | 16 | 1 | 0.23 | 1 | 2 | 1.90 | 0.41 | 46.0 | 104.0 | 298.0 |
| | | | | | | 0.0000 | | 0.0 | | | | | | |
| 03915A_16 | 87.2 | 61.7 | 353.8 | 405 | 2 | 1 | 0.02 | 0 | 2 | 1.95 | 0.40 | 4.0 | 123.0 | 193.0 |
| | | | | | | 0.0000 | | 0.0 | | | | | | |
| 03915A_44 | 88.0 | 62.4 | ###### | #### | 2 | 2 | 0.01 | 0 | 4 | 2.14 | 0.33 | 2.0 | 328.0 | 435.0 |
| | | | | | | 0.0000 | | 0.0 | | | | | | |
| 03915A_69 | 90.0 | 90.2 | 340.6 | 475 | 1 | 1 | 0.01 | 0 | 2 | 2.39 | 0.47 | 2.0 | 21.0 | 196.0 |
| | | | | | | 0.0000 | | 0.0 | | | | | | |
| 03915A_4 | 90.9 | 90.9 | 506.3 | 397 | 1 | 1 | 0.01 | 0 | 1 | 1.95 | 0.42 | 2.0 | 18.0 | 157.0 |
| | | | | | | 0.0000 | | 0.0 | | | | | | |
| 03915A_29 | 97.7 | 26.3 | 115.0 | 40 | 14 | 1 | 0.18 | 1 | 4 | 2.28 | 0.57 | 120.0 | 295.0 | 214.0 |
| | | | | | | 0.0000 | | 0.0 | | | | | | |
| 03915A_3 | 105.4 | 43.2 | 152.4 | 286 | 6 | 1 | 0.05 | 0 | 3 | 2.33 | 0.51 | 9.0 | 86.0 | 222.0 |
| | | | | | | 0.0000 | | 0.0 | | | | | | |
| 03915A_42 | 112.4 | 25.4 | 245.4 | 607 | 20 | 1 | 0.28 | 1 | 3 | 2.26 | 0.51 | 6.0 | 67.0 | 135.0 |
| | | | | | | 0.0000 | | 0.0 | | | | | | |
| 03915A_96 | 112.6 | 112.7 | 0.0 | 0 | 1 | 2 | 0.01 | 0 | 1 | 2.17 | 0.44 | 0.0 | 0.0 | 0.0 |
| | | | | | | 0.0000 | | 0.0 | | | | | | |
| 03915A_14 | 124.4 | 34.7 | 123.1 | 81 | 13 | 0 | 0.29 | 1 | 4 | 1.94 | 0.41 | 60.0 | 28.0 | 389.0 |
| | | | | | | 0.0000 | | 0.0 | | | | | | |
| 03915A_30 | 129.1 | 91.4 | ###### | 999 | 2 | 1 | 0.03 | 0 | 2 | 2.09 | 0.39 | 7.0 | 266.0 | 57.0 |
| | | | | | | 0.0000 | | 0.0 | | | | | | |
| 03915A_68 | 131.8 | 131.9 | 827.1 | #### | 1 | 1 | 0.01 | 0 | 1 | 2.25 | 0.57 | 2.0 | 16.0 | 156.0 |
| | | | | | | 0.0000 | | 0.0 | | | | | | |
| 03915A_78 | 136.3 | 69.1 | 0.0 | 0 | 4 | 1 | 0.04 | 0 | 3 | 2.05 | 0.45 | 0.0 | 16.0 | 91.0 |
| | | | | | | 0.0000 | | 0.0 | | | | | | |
| 03915A_34 | 145.9 | 24.6 | 121.7 | 35 | 36 | 1 | 0.39 | 1 | 3 | 2.35 | 0.41 | 115.0 | 229.0 | 163.0 |
| 03915A_10 | | | | | | 0.0000 | | 0.0 | | | | | | |
| 1 | 147.6 | 38.6 | 94.4 | 22 | 15 | 1 | 0.17 | 1 | 3 | 1.99 | 0.55 | 199.0 | 296.0 | 85.0 |
| | | | | | | 0.0000 | | 0.0 | | | | | | |
| 03915A_64 | 176.0 | 34.8 | 114.9 | 54 | 26 | 1 | 0.23 | 0 | 4 | 2.04 | 0.55 | 144.0 | 131.0 | 206.0 |

| | | | | | | | | | | | | | | |
|---|---|---|---|---|---|---|---|---|---|---|---|---|---|---|
| | | | | | | 0.0000 | | 0.0 | | | | | | |
| 03915A_72 | 189.0 | 189.1 | 492.9 | 597 | 1 | 0 | 0.01 | 0 | 1 | 2.18 | 0.23 | 3.0 | 48.0 | 281.0 |
| | | | | | | 0.0000 | | 0.0 | | | | | | |
| 03915A_22 | 334.5 | 342.3 | 0.0 | 0 | 1 | 1 | 0.00 | 0 | 1 | 2.09 | 0.34 | 0.0 | 91.0 | 373.0 |
| | | | | | | 0.0000 | | 0.0 | | | | | | |
| 03915A_38 | 457.5 | 459.9 | 0.0 | 0 | 1 | 2 | 0.00 | 0 | 2 | 1.89 | 0.41 | 0.0 | 0.0 | 10.0 |
| | | | | | | 0.0000 | | 0.0 | | | | | | |
| 03915A_49 | 460.6 | 464.5 | 623.7 | 651 | 1 | 1 | 0.00 | 0 | 1 | 1.92 | 0.39 | 5.0 | 112.0 | 81.0 |
| | | | | | | 0.0000 | | 0.0 | | | | | | |
| 03915A_51 | 600.6 | 602.7 | 0.0 | 0 | 1 | 2 | 0.00 | 0 | 2 | 1.93 | 0.44 | 0.0 | 0.0 | 9.0 |
| | | | | | | 0.0000 | | 0.0 | | | | | | |
| 03915A_31 | 1035.5 | 1040.0 | 0.0 | 0 | 1 | 1 | 0.00 | 0 | 1 | 2.24 | 0.39 | 0.0 | 1.0 | 27.0 |

**Tok River**

| Spot Name | FT Age (Ma) | sigma sym | UPb Age (Ma) | 2 sigma (Ma) | Ns | Area cm^2 | U/Catio n | +/- 1sig | Etch Figs. | Dpar (um) | Dper (um) | [U] (ppm ) | [Th] (ppm) | [Sm] (ppm) |
|---|---|---|---|---|---|---|---|---|---|---|---|---|---|---|
| | | | | | | 0.0000 | | 0.0 | | | | | | ##### |
| 1421A_23 | 0.0 | #DIV/0! | 0.0 | 0 | 2 | 3 | 0.00 | 0 | 2 | 1.81 | 0.26 | 0.0 | 84.0 | # |
| | | | | | | 0.0000 | | 0.0 | | | | | | |
| 1421A_44 | 0.0 | 13773.7 | 0.0 | 0 | 0 | 3 | 0.00 | 0 | 1 | 1.44 | 0.23 | 0.0 | 0.0 | 0.0 |
| | | | | | | 0.0000 | | 0.0 | | | | | | |
| 1421A_64 | 0.0 | 8617.0 | 0.0 | 0 | 0 | 3 | 0.00 | 0 | 1 | 1.97 | 0.22 | 0.0 | 0.0 | 0.0 |
| | | | | | | 0.0000 | | 0.0 | | | | | | |
| 1421A_28 | 0.0 | 7425.8 | 0.0 | 0 | 0 | 5 | 0.00 | 0 | 1 | 1.63 | 0.31 | 0.0 | 0.0 | 1.0 |
| | | | | | | 0.0000 | | 0.0 | | | | | | |
| 1421A_17 | 0.0 | 5856.3 | 0.0 | 0 | 0 | 2 | 0.00 | 0 | 1 | 1.69 | 0.38 | 0.0 | 0.0 | 1.0 |
| | | | | | | 0.0000 | | 0.0 | | | | | | |
| 1421A_18 | 0.0 | 5705.0 | 0.0 | 0 | 1 | 3 | 0.00 | 0 | 1 | 1.71 | 0.25 | 0.0 | 0.0 | 1.0 |
| | | | | | | 0.0000 | | 0.0 | | | | | | |
| 1421A_14 | 0.0 | 4949.8 | 0.0 | 0 | 0 | 2 | 0.00 | 0 | 1 | 1.34 | 0.35 | 0.0 | 0.0 | 0.0 |
| | | | | | | 0.0000 | | 0.0 | | | | | | |
| 1421A_20 | 0.0 | 4767.8 | 0.0 | 0 | 0 | 2 | 0.00 | 0 | 1 | 1.89 | 0.31 | 0.0 | 3.0 | 233.0 |
| | | | | | | 0.0000 | | 0.0 | | | | | | |
| 1421A_27 | 0.0 | 1904.5 | 0.0 | 0 | 0 | 3 | 0.00 | 0 | 1 | 1.73 | 0.40 | 0.0 | 0.0 | 2.0 |
| | | | | | | 0.0000 | | 0.0 | | | | | | |
| 1421A_45 | 0.0 | 1878.8 | 0.0 | 0 | 0 | 4 | 0.00 | 0 | 1 | 1.82 | 0.39 | 0.0 | 0.0 | 3.0 |
| | | | | | | 0.0000 | | 0.0 | | | | | | |
| 1421A_5 | 0.0 | 1615.7 | 0.0 | 0 | 0 | 3 | 0.00 | 0 | 1 | 1.73 | 0.38 | 0.0 | 0.0 | 1.0 |
| | | | | | | 0.0000 | | 0.0 | | | | | | |
| 1421A_70 | 0.0 | 1538.5 | 0.0 | 0 | 0 | 3 | 0.00 | 0 | 1 | 1.56 | 0.30 | 0.0 | 0.0 | 2.0 |
| | | | | | | 0.0000 | | 0.0 | | | | | | |
| 1421A_2 | 0.0 | 1268.7 | 0.0 | 0 | 0 | 3 | 0.00 | 0 | 1 | 1.68 | 0.28 | 0.0 | 0.0 | 3.0 |
| | | | | | | 0.0000 | | 0.0 | | | | | | |
| 1421A_16 | 0.0 | 1100.0 | 0.0 | 0 | 0 | 2 | 0.00 | 0 | 1 | 1.62 | 0.35 | 0.0 | 0.0 | 9.0 |
| | | | | | | 0.0000 | | 0.0 | | | | | | |
| 1421A_24 | 0.0 | 897.1 | 0.0 | 0 | 0 | 2 | 0.00 | 0 | 1 | 1.07 | 0.43 | 0.0 | 0.0 | 52.0 |
| | | | | | | 0.0000 | | 0.0 | | | | | | |
| 1421A_43 | 0.0 | 886.0 | 0.0 | 0 | 0 | 2 | 0.00 | 0 | 1 | 1.30 | 0.33 | 0.0 | 0.0 | 6.0 |
| | | | | | | 0.0000 | | 0.0 | | | | | | |
| 1421A_13 | 0.0 | 857.1 | 0.0 | 0 | 0 | 4 | 0.00 | 0 | 1 | 1.56 | 0.35 | 0.0 | 0.0 | 4.0 |
| | | | | | | 0.0000 | | 0.0 | | | | | | |
| 1421A_59 | 0.0 | 776.3 | 0.0 | 0 | 0 | 2 | 0.00 | 0 | 1 | 1.68 | 0.21 | 0.0 | 0.0 | 11.0 |
| | | | | | | 0.0000 | | 0.0 | | | | | | |
| 1421A_62 | 0.0 | 757.0 | 0.0 | 0 | 1 | 2 | 0.00 | 0 | 1 | 2.04 | 0.21 | 0.0 | 1.0 | 14.0 |
| | | | | | | 0.0000 | | 0.0 | | | | | | |
| 1421A_47 | 0.0 | 693.3 | 0.0 | 0 | 0 | 2 | 0.00 | 0 | 1 | 1.55 | 0.32 | 0.0 | 3.0 | 63.0 |
| | | | | | | 0.0000 | | 0.0 | | | | | | |
| 1421A_42 | 0.0 | 581.4 | 0.0 | 0 | 0 | 1 | 0.00 | 0 | 1 | 1.42 | 0.25 | 0.0 | 0.0 | 41.0 |
| | | | | | | 0.0000 | | 0.0 | | | | | | |
| 1421A_51 | 0.0 | 501.6 | 0.0 | 0 | 0 | 2 | 0.00 | 0 | 1 | 1.59 | 0.27 | 0.0 | 5.0 | 107.0 |
| | | | | | | 0.0000 | | 0.0 | | | | | | |
| 1421A_7 | 0.0 | 496.2 | 0.0 | 0 | 0 | 4 | 0.00 | 0 | 1 | 1.60 | 0.28 | 0.0 | 1.0 | 7.0 |
| | | | | | | 0.0000 | | 0.0 | | | | | | |
| 1421A_53 | 0.0 | 320.6 | 0.0 | 0 | 0 | 2 | 0.00 | 0 | 1 | 1.54 | 0.26 | 0.0 | 0.0 | 8.0 |
| | | | | | | 0.0000 | | 0.0 | | | | | | |
| 1421A_35 | 0.0 | 306.8 | 0.0 | 0 | 0 | 4 | 0.00 | 0 | 1 | 1.64 | 0.46 | 0.0 | 0.0 | 7.0 |
| | | | | | | 0.0000 | | 0.0 | | | | | | |
| 1421A_8 | 0.0 | 272.6 | 0.0 | 0 | 0 | 3 | 0.00 | 0 | 1 | 1.79 | 0.46 | 0.0 | 0.0 | 6.0 |
| | | | | | | 0.0000 | | 0.0 | | | | | | |
| 1421A_66 | 0.0 | 246.3 | 0.0 | 0 | 0 | 3 | 0.00 | 0 | 1 | 1.75 | 0.36 | 0.0 | 0.0 | 140.0 |
| | | | | | | 0.0000 | | 0.0 | | | | | | |
| 1421A_26 | 0.0 | 181.9 | 0.0 | 0 | 0 | 4 | 0.00 | 0 | 1 | 1.65 | 0.25 | 0.0 | 1.0 | 34.0 |

| | | | | | | | | | | | | | | |
|---|---|---|---|---|---|---|---|---|---|---|---|---|---|---|
| | | | | | | 0.0000 | | 0.0 | | | | | | |
| 1421A_39 | 0.0 | 89.2 | ###### | #### | 0 | 3 | 0.00 | 0 | 1 | 1.86 | 0.52 | 1.0 | 123.0 | 91.0 |
| | | | | | | 0.0000 | | 0.0 | | | | | | |
| 1421A_22 | 0.0 | 88.6 | 0.0 | 0 | 0 | 4 | 0.00 | 0 | 1 | 1.91 | 0.65 | 0.0 | 36.0 | 244.0 |
| | | | | | | 0.0000 | | 0.0 | | | | | | |
| 1421A_48 | 0.0 | 44.2 | 426.3 | 460 | 0 | 3 | 0.01 | 0 | 1 | 1.45 | 0.27 | 1.0 | 7.0 | 376.0 |
| | | | | | | 0.0000 | | 0.0 | | | | | | |
| 1421A_41 | 0.0 | 42.9 | 364.3 | 337 | 0 | 3 | 0.01 | 0 | 1 | 1.58 | 0.47 | 1.0 | 12.0 | 131.0 |
| | | | | | | 0.0000 | | 0.0 | | | | | | |
| 1421A_68 | 0.0 | 27.0 | 331.2 | 313 | 0 | 4 | 0.01 | 0 | 1 | 1.43 | 0.22 | 2.0 | 9.0 | 248.0 |
| | | | | | | 0.0000 | | 0.0 | | | | | | |
| 1421A_9 | 0.0 | 21.2 | 243.3 | 285 | 0 | 4 | 0.01 | 0 | 1 | 1.40 | 0.42 | 2.0 | 10.0 | 285.0 |
| | | | | | | 0.0000 | | 0.0 | | | | | | |
| 1421A_49 | 0.0 | 11.7 | 361.2 | 218 | 0 | 4 | 0.02 | 0 | 1 | 1.57 | 0.53 | 5.0 | 63.0 | 78.0 |
| | | | | | | 0.0000 | | 0.0 | | | | | | |
| 1421A_54 | 16.3 | 4.9 | 48.3 | 26 | 11 | 3 | 0.29 | 0 | 4 | 1.69 | 0.38 | 50.0 | 181.0 | 243.0 |
| | | | | | | 0.0000 | | 0.0 | | | | | | |
| 1421A_1 | 19.5 | 6.2 | ###### | 853 | 11 | 4 | 0.18 | 2 | 2 | 1.57 | 0.26 | 38.0 | 18.0 | 810.0 |
| | | | | | | 0.0000 | | 0.0 | | | | | | |
| 1421A_57 | 27.5 | 27.5 | 562.9 | 314 | 1 | 2 | 0.02 | 0 | 1 | 1.46 | 0.32 | 5.0 | 60.0 | 263.0 |
| | | | | | | 0.0000 | | 0.0 | | | | | | |
| 1421A_60 | 29.6 | 29.6 | 373.6 | 341 | 1 | 4 | 0.01 | 0 | 2 | 1.79 | 0.36 | 2.0 | 11.0 | 254.0 |
| | | | | | | 0.0000 | | 0.0 | | | | | | |
| 1421A_46 | 29.7 | 21.1 | 517.0 | 490 | 2 | 3 | 0.02 | 0 | 2 | 2.01 | 0.24 | 6.0 | 44.0 | 227.0 |
| | | | | | | 0.0000 | | 0.0 | | | | | | |
| 1421A_4 | 35.2 | 35.2 | 285.3 | 313 | 1 | 4 | 0.01 | 0 | 1 | 1.66 | 0.35 | 2.0 | 10.0 | 338.0 |
| | | | | | | 0.0000 | | 0.0 | | | | | | |
| 1421A_56 | 41.6 | 24.1 | 436.8 | 224 | 3 | 4 | 0.02 | 0 | 3 | 2.01 | 0.29 | 5.0 | 39.0 | 165.0 |
| | | | | | | 0.0000 | | 0.0 | | | | | | |
| 1421A_58 | 59.7 | 42.2 | 436.4 | 203 | 2 | 3 | 0.01 | 0 | 1 | 2.35 | 0.30 | 3.0 | 20.0 | 196.0 |
| | | | | | | 0.0000 | | 0.0 | | | | | | |
| 1421A_32 | 69.9 | 69.9 | 435.7 | 546 | 1 | 2 | 0.01 | 0 | 1 | 1.74 | 0.30 | 2.0 | 16.0 | 140.0 |
| | | | | | | 0.0000 | | 0.0 | | | | | | |
| 1421A_55 | 73.0 | 73.0 | 631.5 | 377 | 1 | 2 | 0.01 | 0 | 1 | 1.77 | 0.39 | 2.0 | 14.0 | 177.0 |
| | | | | | | 0.0000 | | 0.0 | | | | | | |
| 1421A_31 | 82.5 | 58.4 | 271.7 | 349 | 2 | 3 | 0.01 | 0 | 2 | 1.32 | 0.34 | 2.0 | 9.0 | 266.0 |
| | | | | | | 0.0000 | | 0.0 | | | | | | |
| 1421A_63 | 92.7 | 65.6 | 528.7 | 323 | 2 | 3 | 0.01 | 0 | 2 | 1.96 | 0.36 | 2.0 | 14.0 | 158.0 |
| | | | | | | 0.0000 | | 0.0 | | | | | | |
| 1421A_33 | 96.8 | 56.4 | 436.9 | 408 | 3 | 4 | 0.01 | 0 | 2 | 1.74 | 0.28 | 2.0 | 15.0 | 164.0 |
| | | | | | | 0.0000 | | 0.0 | | | | | | |
| 1421A_50 | 112.7 | 79.8 | 444.2 | 407 | 2 | 4 | 0.01 | 0 | 2 | 1.23 | 0.30 | 1.0 | 6.0 | 185.0 |
| | | | | | | 0.0000 | | 0.0 | | | | | | |
| 1421A_10 | 114.9 | 81.3 | 357.3 | 351 | 2 | 2 | 0.01 | 0 | 1 | 1.72 | 0.34 | 2.0 | 8.0 | 277.0 |
| | | | | | | 0.0000 | | 0.0 | | | | | | |
| 1421A_67 | 115.4 | 115.5 | 0.0 | 0 | 1 | 4 | 0.00 | 0 | 1 | 1.60 | 0.42 | 1.0 | 0.0 | 72.0 |
| | | | | | | 0.0000 | | 0.0 | | | | | | |
| 1421A_3 | 122.1 | 18.3 | 217.3 | 338 | 48 | 3 | 0.17 | 1 | 3 | 1.68 | 0.35 | 166.0 | 96.0 | 521.0 |
| | | | | | | 0.0000 | | 0.0 | | | | | | |
| 1421A_6 | 131.6 | 140.6 | 0.0 | 0 | 1 | 2 | 0.00 | 0 | 1 | 1.38 | 0.27 | 1.0 | 12.0 | 101.0 |
| | | | | | | 0.0000 | | 0.0 | | | | | | |
| 1421A_25 | 134.0 | 67.5 | 343.0 | 407 | 4 | 5 | 0.01 | 0 | 4 | 1.45 | 0.41 | 2.0 | 8.0 | 213.0 |
| | | | | | | 0.0000 | | 0.0 | | | | | | |
| 1421A_61 | 137.2 | 97.1 | 579.1 | 299 | 2 | 2 | 0.01 | 0 | 2 | 2.03 | 0.37 | 2.0 | 13.0 | 163.0 |
| | | | | | | 0.0000 | | 0.0 | | | | | | |
| 1421A_19 | 175.6 | 175.6 | 392.3 | 336 | 1 | 1 | 0.01 | 0 | 1 | 1.73 | 0.25 | 2.0 | 12.0 | 144.0 |
| | | | | | | 0.0000 | | 0.0 | | | | | | |
| 1421A_30 | 196.1 | 98.2 | 389.5 | 359 | 4 | 3 | 0.01 | 0 | 2 | 1.36 | 0.33 | 2.0 | 15.0 | 182.0 |
| | | | | | | 0.0000 | | 0.0 | | | | | | |
| 1421A_34 | 204.4 | 119.4 | 101.3 | 398 | 3 | 3 | 0.01 | 0 | 2 | 1.65 | 0.35 | 1.0 | 4.0 | 269.0 |
| | | | | | | 0.0000 | | 0.0 | | | | | | |
| 1421A_15 | 207.9 | 148.2 | 268.1 | 548 | 2 | 3 | 0.00 | 0 | 1 | 1.55 | 0.28 | 1.0 | 4.0 | 145.0 |
| | | | | | | 0.0000 | | 0.0 | | | | | | |
| 1421A_37 | 347.1 | 205.1 | 113.2 | 834 | 3 | 3 | 0.00 | 0 | 2 | 1.74 | 0.38 | 1.0 | 4.0 | 204.0 |
| | | | | | | 0.0000 | | 0.0 | | | | | | |
| 1421A_12 | 466.2 | 466.8 | 0.0 | 0 | 1 | 4 | 0.00 | 0 | 1 | 1.74 | 0.35 | 0.0 | 0.0 | 8.0 |
| | | | | | | 0.0000 | | 0.0 | | | | | | |
| 1421A_40 | 795.1 | 565.3 | 0.0 | 0 | 2 | 3 | 0.00 | 0 | 1 | 1.67 | 0.39 | 1.0 | 46.0 | 121.0 |
| | | | | | | 0.0000 | | 0.0 | | | | | | |
| 1421A_69 | 1349.8 | 1356.2 | 0.0 | 0 | 1 | 2 | 0.00 | 0 | 2 | 1.67 | 0.22 | 0.0 | 0.0 | 8.0 |
| | | | | | | 0.0000 | | 0.0 | | | | | | |
| 1421A_21 | 1542.9 | 1094.4 | 0.0 | 0 | 2 | 2 | 0.00 | 0 | 2 | 1.48 | 0.46 | 0.0 | 0.0 | 66.0 |
| | | | | | | 0.0000 | | 0.0 | | | | | | |
| 1421A_11 | 1752.5 | 884.5 | 0.0 | 0 | 4 | 3 | 0.00 | 0 | 2 | 1.59 | 0.38 | 0.0 | 0.0 | 4.0 |

| | | | | | | | | | | | | | | |
|---|---|---|---|---|---|---|---|---|---|---|---|---|---|---|
| | | | | | | 0.0000 | | 0.0 | | | | | | |
| 1421A_38 | 1789.2 | 1792.7 | 0.0 | 0 | 1 | 2 | 0.00 | 0 | 2 | 1.76 | 0.25 | 0.0 | 1.0 | 65.0 |
| | | | | | | 0.0000 | | 0.0 | | | | | | |
| 1421A_36 | 1977.7 | 2028.1 | 0.0 | 0 | 1 | 4 | 0.00 | 0 | 1 | 1.65 | 0.30 | 0.0 | 0.0 | 5.0 |
| | | | | | | 0.0000 | | 0.0 | | | | | | |
| 1421A_65 | 3362.9 | 3442.7 | 0.0 | 0 | 1 | 4 | 0.00 | 0 | 1 | 1.90 | 0.26 | 0.0 | 0.0 | 1.0 |
| | | | | | | 0.0000 | | 0.0 | | | | | | |
| 1421A_29 | 3672.1 | 3771.1 | 0.0 | 0 | 1 | 4 | 0.00 | 0 | 1 | 1.46 | 0.20 | 0.0 | 0.0 | 1.0 |
| | | | | | | 0.0000 | | 0.0 | | | | | | |
| 1421A_52 | 4261.6 | 3036.1 | 0.0 | 0 | 2 | 2 | 0.00 | 0 | 2 | 1.49 | 0.34 | 0.0 | 0.0 | 39.0 |

**upper Susitna River**

| Spot Name | FT Age (Ma) | Sigma Symm (Ma) | UPb Age (Ma) | 2 sigma (Ma) | Ns | Area cm^2 | U/Cation | +/- 1sig | Etch Figs. | Dpar (um) | Dper (um) | [U] (ppm) | [Th] (ppm) | [Sm] (ppm) |
|---|---|---|---|---|---|---|---|---|---|---|---|---|---|---|
| | | | | | | 0.0000 | | 0.0 | | | | | | |
| 03916A_7 | 0.0 | 4.3 | 0.0 | 0 | 0 | 4 | 0.05 | 0 | 1 | 2.15 | 0.32 | 10.0 | 28.0 | 140.0 |
| | | | | | | 0.0000 | | 0.0 | | | | | | |
| 03916A_19 | 0.0 | 2.6 | 122.1 | 152 | 0 | 3 | 0.12 | 0 | 1 | 1.91 | 0.34 | 24.0 | 0.0 | 222.0 |
| | | | | | | 0.0000 | | 0.0 | | | | | | |
| 03916A_24 | 0.0 | 4.5 | 15.7 | 49 | 0 | 2 | 0.11 | 0 | 1 | 1.86 | 0.46 | 25.0 | 91.0 | 244.0 |
| | | | | | | 0.0000 | | 0.0 | | | | | | |
| 03916A_65 | 0.0 | 5.2 | 45.1 | 153 | 0 | 3 | 0.06 | 0 | 1 | 1.67 | 0.35 | 11.0 | 0.0 | 47.0 |
| | | | | | | 0.0000 | | 0.0 | | | | | | |
| 03916A_71 | 0.0 | 6.8 | 0.0 | 0 | 0 | 2 | 0.07 | 0 | 1 | 2.01 | 0.53 | 11.0 | 37.0 | 137.0 |
| | | | | | | 0.0000 | | 0.0 | | | | | | |
| 03916A_86 | 0.0 | 6.8 | 11.6 | 146 | 0 | 3 | 0.04 | 0 | 1 | 2.07 | 0.41 | 9.0 | 4.0 | 38.0 |
| | | | | | | 0.0000 | | 0.0 | | | | | | |
| 03916A_90 | 0.0 | 11.7 | 0.0 | 0 | 0 | 1 | 0.06 | 0 | 1 | 2.18 | 0.49 | 13.0 | 1.0 | 107.0 |
| | | | | | | 0.0000 | | 0.0 | | | | | | |
| 03916A_39 | 2.2 | 2.2 | 0.0 | 0 | 1 | 2 | 0.29 | 1 | 1 | 1.67 | 0.46 | 54.0 | 21.0 | 127.0 |
| | | | | | | 0.0000 | | 0.0 | | | | | | |
| 03916A_76 | 3.1 | 2.2 | 0.0 | 0 | 2 | 1 | 0.56 | 1 | 2 | 2.30 | 0.42 | 106.0 | 265.0 | 206.0 |
| | | | | | | 0.0000 | | 0.0 | | | | | | |
| 03916A_98 | 3.2 | 1.8 | 43.2 | 34 | 3 | 2 | 0.48 | 1 | 2 | 1.87 | 0.38 | 95.0 | 197.0 | 144.0 |
| | | | | | | 0.0000 | | 0.0 | | | | | | |
| 03916A_5 | 3.3 | 2.3 | 0.0 | 0 | 2 | 2 | 0.39 | 1 | 2 | 2.12 | 0.31 | 74.0 | 39.0 | 73.0 |
| | | | | | | 0.0000 | | 0.0 | | | | | | |
| 03916A_61 | 3.7 | 2.1 | 60.5 | 40 | 3 | 3 | 0.30 | 1 | 3 | 1.97 | 0.56 | 60.0 | 138.0 | 149.0 |
| | | | | | | 0.0000 | | 0.0 | | | | | | |
| 03916A_46 | 4.0 | 4.0 | 42.4 | 55 | 1 | 3 | 0.11 | 0 | 1 | 2.03 | 0.46 | 22.0 | 88.0 | 135.0 |
| | | | | | | 0.0000 | | 0.0 | | | | | | |
| 03916A_82 | 5.2 | 5.2 | 0.0 | 0 | 1 | 2 | 0.14 | 0 | 1 | 1.99 | 0.42 | 27.0 | 49.0 | 48.0 |
| | | | | | | 0.0000 | | 0.0 | | | | | | |
| 03916A_10 | 5.6 | 5.6 | 0.0 | 0 | 1 | 2 | 0.10 | 0 | 2 | 1.91 | 0.36 | 18.0 | 83.0 | 185.0 |
| | | | | | | 0.0000 | | 0.0 | | | | | | |
| 03916A_72 | 6.1 | 6.1 | 54.5 | 80 | 1 | 1 | 0.15 | 1 | 1 | 1.72 | 0.35 | 35.0 | 73.0 | 231.0 |
| | | | | | | 0.0000 | | 0.0 | | | | | | |
| 03916A_50 | 6.4 | 4.5 | 83.6 | 34 | 2 | 1 | 0.44 | 1 | 2 | 1.92 | 0.48 | 74.0 | 122.0 | 208.0 |
| | | | | | | 0.0000 | | 0.0 | | | | | | |
| 03916A_48 | 6.7 | 6.7 | 89.6 | 54 | 1 | 1 | 0.21 | 0 | 1 | 2.15 | 0.45 | 43.0 | 19.0 | 180.0 |
| | | | | | | 0.0000 | | 0.0 | | | | | | ##### |
| 03916A_17 | 6.7 | 6.7 | 0.0 | 0 | 1 | 2 | 0.11 | 0 | 2 | 2.15 | 0.53 | 224.0 | 778.0 | # |
| | | | | | | 0.0000 | | 0.0 | | | | | | |
| 03916A_41 | 6.9 | 4.9 | 0.0 | 0 | 2 | 1 | 0.25 | 1 | 2 | 2.46 | 0.55 | 40.0 | 127.0 | 270.0 |
| | | | | | | 0.0000 | | 0.0 | | | | | | |
| 03916A_28 | 6.9 | 6.9 | 0.0 | 0 | 1 | 2 | 0.09 | 0 | 1 | 1.88 | 0.22 | 24.0 | 49.0 | 84.0 |
| | | | | | | 0.0000 | | 0.0 | | | | | | |
| 03916A_79 | 6.9 | 3.5 | 0.0 | 0 | 4 | 3 | 0.25 | 1 | 2 | 2.01 | 0.37 | 50.0 | 121.0 | 226.0 |
| | | | | | | 0.0000 | | 0.0 | | | | | | |
| 03916A_73 | 7.2 | 5.1 | 0.0 | 0 | 2 | 1 | 0.44 | 1 | 1 | 2.07 | 0.40 | 151.0 | 286.0 | 229.0 |
| | | | | | | 0.0000 | | 0.0 | | | | | | |
| 03916A_88 | 7.3 | 4.2 | 0.0 | 0 | 3 | 2 | 0.21 | 1 | 3 | 2.04 | 0.46 | 43.0 | 11.0 | 183.0 |
| | | | | | | 0.0000 | | 0.0 | | | | | | |
| 03916A_77 | 7.4 | 4.3 | 0.0 | 0 | 3 | 2 | 0.29 | 1 | 2 | 2.07 | 0.46 | 56.0 | 121.0 | 166.0 |
| 03916A_109 | 7.7 | 5.5 | 30.8 | 22 | 2 | 0.0000 3 | 0.09 | 0.0 0 | 2 | 2.10 | 0.50 | 149.0 | 22.0 | 302.0 |
| 03916A_100 | 8.2 | 4.1 | 81.8 | 35 | 4 | 0.0000 2 | 0.39 | 0.0 1 | 2 | 1.94 | 0.37 | 77.0 | 158.0 | 373.0 |
| | | | | | | 0.0000 | | 0.0 | | | | | | |
| 03916A_59 | 8.3 | 8.3 | 27.8 | 32 | 1 | 1 | 0.15 | 1 | 2 | 2.14 | 0.35 | 28.0 | 143.0 | 178.0 |
| | | | | | | 0.0000 | | 0.0 | | | | | | |
| 03916A_52 | 8.9 | 6.3 | 6.9 | 55 | 2 | 3 | 0.10 | 0 | 1 | 2.09 | 0.24 | 19.0 | 48.0 | 162.0 |

| | | | | | | | | | | | | | | |
|---|---|---|---|---|---|---|---|---|---|---|---|---|---|---|
| | | | | | | 0.0000 | | 0.0 | | | | | | |
| 03916A_69 | 9.3 | 4.7 | 82.6 | 42 | 4 | 1 | 0.45 | 1 | 2 | 2.07 | 0.45 | 99.0 | 197.0 | 247.0 |
| | | | | | | 0.0000 | | 0.0 | | | | | | |
| 03916A_44 | 10.2 | 5.9 | 53.6 | 34 | 3 | 1 | 0.42 | 1 | 2 | 2.21 | 0.35 | 81.0 | 185.0 | 197.0 |
| | | | | | | 0.0000 | | 0.0 | | | | | | |
| 03916A_32 | 10.4 | 6.0 | 19.7 | 68 | 3 | 5 | 0.07 | 0 | 2 | 2.23 | 0.46 | 14.0 | 61.0 | 114.0 |
| | | | | | | 0.0000 | | 0.0 | | | | | | |
| 03916A_70 | 10.6 | 3.7 | 33.5 | 14 | 8 | 2 | 0.48 | 1 | 2 | 2.25 | 0.47 | 227.0 | 195.0 | 136.0 |
| | | | | | | 0.0000 | | 0.0 | | | | | | |
| 03916A_57 | 11.2 | 4.0 | 79.6 | 28 | 8 | 2 | 0.57 | 2 | 3 | 2.34 | 0.51 | 118.0 | 396.0 | 205.0 |
| 03916A_10 | | | | | | 0.0000 | | 0.0 | | | | | | |
| 6 | 11.8 | 4.2 | 88.6 | 53 | 8 | 2 | 0.48 | 1 | 2 | 2.23 | 0.41 | 92.0 | 110.0 | 270.0 |
| | | | | | | 0.0000 | | 0.0 | | | | | | |
| 03916A_18 | 12.2 | 7.1 | 29.3 | 42 | 3 | 2 | 0.16 | 0 | 3 | 2.13 | 0.51 | 30.0 | 6.0 | 49.0 |
| | | | | | | 0.0000 | | 0.0 | | | | | | |
| 03916A_92 | 12.9 | 7.5 | 0.0 | 0 | 3 | 1 | 0.20 | 0 | 2 | 2.38 | 0.46 | 40.0 | 29.0 | 156.0 |
| 03916A_10 | | | | | | 0.0000 | | 0.0 | | | | | | |
| 7 | 13.1 | 9.2 | 4.5 | 73 | 2 | 2 | 0.08 | 0 | 1 | 1.83 | 0.31 | 17.0 | 61.0 | 113.0 |
| | | | | | | 0.0000 | | 0.0 | | | | | | |
| 03916A_23 | 14.4 | 14.4 | 51.6 | 101 | 1 | 1 | 0.07 | 0 | 1 | 2.39 | 0.49 | 14.0 | 62.0 | 150.0 |
| | | | | | | 0.0000 | | 0.0 | | | | | | |
| 03916A_21 | 14.6 | 10.4 | 43.4 | 62 | 2 | 3 | 0.05 | 0 | 1 | 1.70 | 0.22 | 9.0 | 31.0 | 155.0 |
| | | | | | | 0.0000 | | 0.0 | | | | | | |
| 03916A_75 | 14.8 | 10.5 | 0.0 | 0 | 2 | 2 | 0.09 | 0 | 1 | 2.33 | 0.44 | 14.0 | 26.0 | 84.0 |
| | | | | | | 0.0000 | | 0.0 | | | | | | |
| 03916A_45 | 15.9 | 6.0 | 38.5 | 34 | 7 | 2 | 0.28 | 1 | 3 | 1.99 | 0.48 | 56.0 | 142.0 | 94.0 |
| 03916A_10 | | | | | | 0.0000 | | 0.0 | | | | | | |
| 2 | 17.2 | 10.0 | 60.6 | 96 | 3 | 3 | 0.06 | 0 | 2 | 2.15 | 0.46 | 14.0 | 1.0 | 76.0 |
| 03916A_10 | | | | | | 0.0000 | | 0.0 | | | | | | |
| 1 | 17.6 | 6.6 | 94.7 | 94 | 7 | 5 | 0.10 | 0 | 3 | 2.16 | 0.48 | 20.0 | 38.0 | 120.0 |
| 03916A_10 | | | | | | 0.0000 | | 0.0 | | | | | | |
| 5 | 18.3 | 4.9 | 65.7 | 38 | 14 | 2 | 0.49 | 1 | 4 | 2.21 | 0.50 | 78.0 | 152.0 | 173.0 |
| | | | | | | 0.0000 | | 0.0 | | | | | | |
| 03916A_30 | 18.6 | 10.8 | 0.0 | 0 | 3 | 3 | 0.06 | 0 | 2 | 2.26 | 0.46 | 12.0 | 72.0 | 199.0 |
| | | | | | | 0.0000 | | 0.0 | | | | | | |
| 03916A_64 | 18.8 | 7.1 | 32.3 | 26 | 7 | 3 | 0.14 | 0 | 2 | 2.17 | 0.35 | 98.0 | 126.0 | 219.0 |
| | | | | | | 0.0000 | | 0.0 | | | | | | |
| 03916A_53 | 19.3 | 11.2 | 56.3 | 80 | 3 | 2 | 0.10 | 0 | 2 | 1.99 | 0.42 | 21.0 | 38.0 | 163.0 |
| | | | | | | 0.0000 | | 0.0 | | | | | | |
| 03916A_67 | 19.9 | 4.1 | 65.2 | 33 | 24 | 3 | 0.51 | 1 | 4 | 2.39 | 0.56 | 104.0 | 86.0 | 179.0 |
| | | | | | | 0.0000 | | 0.0 | | | | | | |
| 03916A_4 | 20.0 | 5.4 | 0.0 | 0 | 14 | 5 | 0.18 | 1 | 3 | 1.98 | 0.34 | 33.0 | 19.0 | 92.0 |
| | | | | | | 0.0000 | | 0.0 | | | | | | |
| 03916A_63 | 20.2 | 9.1 | 104.4 | 84 | 5 | 2 | 0.13 | 0 | 3 | 2.10 | 0.51 | 21.0 | 5.0 | 170.0 |
| | | | | | | 0.0000 | | 0.0 | | | | | | |
| 03916A_14 | 21.3 | 7.6 | 56.7 | 21 | 8 | 3 | 0.16 | 1 | 3 | 2.27 | 0.42 | 130.0 | 237.0 | 200.0 |
| | | | | | | 0.0000 | | 0.0 | | | | | | |
| 03916A_36 | 22.3 | 10.0 | 0.0 | 0 | 5 | 3 | 0.09 | 0 | 2 | 1.92 | 0.43 | 18.0 | 1.0 | 177.0 |
| | | | | | | 0.0000 | | 0.0 | | | | | | |
| 03916A_97 | 22.7 | 10.2 | 66.0 | 79 | 5 | 1 | 0.23 | 1 | 3 | 1.96 | 0.35 | 51.0 | 151.0 | 233.0 |
| | | | | | | 0.0000 | | 0.0 | | | | | | |
| 03916A_1 | 22.9 | 4.9 | 0.0 | 0 | 22 | 4 | 0.27 | 1 | 3 | 1.86 | 0.35 | 0.0 | 20.0 | 130.0 |
| | | | | | | 0.0000 | | 0.0 | | | | | | |
| 03916A_13 | 23.1 | 5.2 | 41.6 | 42 | 20 | 4 | 0.28 | 1 | 3 | 2.09 | 0.45 | 59.0 | 61.0 | 187.0 |
| | | | | | | 0.0000 | | 0.0 | | | | | | |
| 03916A_60 | 24.4 | 24.5 | 0.0 | 0 | 1 | 2 | 0.03 | 0 | 1 | 2.56 | 0.31 | 6.0 | 24.0 | 134.0 |
| | | | | | | 0.0000 | | 0.0 | | | | | | |
| 03916A_56 | 24.7 | 12.4 | 21.0 | 19 | 4 | 1 | 0.17 | 0 | 2 | 2.08 | 0.41 | 174.0 | 406.0 | 168.0 |
| | | | | | | 0.0000 | | 0.0 | | | | | | |
| 03916A_96 | 24.9 | 5.9 | 83.2 | 41 | 18 | 4 | 0.20 | 0 | 4 | 2.58 | 0.66 | 137.0 | 282.0 | 141.0 |
| | | | | | | 0.0000 | | 0.0 | | | | | | |
| 03916A_55 | 25.4 | 7.1 | 33.2 | 39 | 13 | 3 | 0.22 | 1 | 3 | 2.09 | 0.46 | 43.0 | 57.0 | 132.0 |
| | | | | | | 0.0000 | | 0.0 | | | | | | |
| 03916A_31 | 27.3 | 5.3 | 0.0 | 0 | 29 | 4 | 0.34 | 2 | 4 | 1.91 | 0.41 | 68.0 | 273.0 | 101.0 |
| | | | | | | 0.0000 | | 0.0 | | | | | | |
| 03916A_99 | 27.4 | 15.8 | 50.1 | 135 | 3 | 3 | 0.05 | 0 | 2 | 2.03 | 0.43 | 10.0 | 49.0 | 81.0 |
| | | | | | | 0.0000 | | 0.0 | | | | | | |
| 03916A_2 | 27.7 | 16.1 | 0.0 | 0 | 3 | 3 | 0.05 | 0 | 2 | 2.11 | 0.36 | 9.0 | 17.0 | 48.0 |
| | | | | | | 0.0000 | | 0.0 | | | | | | |
| 03916A_49 | 28.0 | 10.9 | 0.0 | 0 | 7 | 2 | 0.16 | 1 | 3 | 2.25 | 0.46 | 19.0 | 38.0 | 70.0 |
| | | | | | | 0.0000 | | 0.0 | | | | | | |
| 03916A_12 | 28.2 | 5.7 | 0.0 | 0 | 25 | 3 | 0.38 | 1 | 4 | 1.98 | 0.49 | 81.0 | 134.0 | 390.0 |
| | | | | | | 0.0000 | | 0.0 | | | | | | |
| 03916A_81 | 28.7 | 12.9 | 0.0 | 0 | 5 | 2 | 0.09 | 0 | 2 | 2.19 | 0.46 | 123.0 | 456.0 | 145.0 |

| | | | | | | | | | | | | | | |
|---|---|---|---|---|---|---|---|---|---|---|---|---|---|---|
| | | | | | | 0.0000 | | 0.0 | | | | | | |
| 03916A_38 | 29.0 | 11.9 | 0.0 | 0 | 6 | 3 | 0.08 | 0 | 2 | 2.55 | 0.46 | 179.0 | 971.0 | 229.0 |
| 03916A_11 | | | | | | 0.0000 | | 0.0 | | | | | | |
| 0 | 29.6 | 17.1 | 86.8 | 194 | 3 | 3 | 0.04 | 0 | 2 | 2.05 | 0.33 | 7.0 | 30.0 | 324.0 |
| | | | | | | 0.0000 | | 0.0 | | | | | | |
| 03916A_26 | 30.0 | 5.8 | 59.7 | 62 | 27 | 5 | 0.23 | 0 | 4 | 2.07 | 0.46 | 42.0 | 12.0 | 92.0 |
| | | | | | | 0.0000 | | 0.0 | | | | | | |
| 03916A_93 | 30.6 | 30.6 | 101.3 | 211 | 1 | 1 | 0.03 | 0 | 1 | 2.12 | 0.46 | 8.0 | 35.0 | 246.0 |
| | | | | | | 0.0000 | | 0.0 | | | | | | |
| 03916A_94 | 31.4 | 10.0 | 65.3 | 83 | 10 | 2 | 0.16 | 1 | 3 | 2.17 | 0.46 | 33.0 | 96.0 | 97.0 |
| | | | | | | 0.0000 | | 0.0 | | | | | | |
| 03916A_35 | 32.0 | 11.4 | 0.0 | 0 | 8 | 2 | 0.16 | 1 | 2 | 1.92 | 0.34 | 22.0 | 58.0 | 81.0 |
| | | | | | | 0.0000 | | 0.0 | | | | | | |
| 03916A_47 | 32.1 | 10.2 | 68.5 | 66 | 10 | 1 | 0.33 | 1 | 2 | 2.31 | 0.55 | 71.0 | 1.0 | 168.0 |
| | | | | | | 0.0000 | | 0.0 | | | | | | |
| 03916A_95 | 32.2 | 9.0 | 78.7 | 37 | 13 | 1 | 0.34 | 1 | 4 | 2.18 | 0.38 | 87.0 | 152.0 | 223.0 |
| | | | | | | 0.0000 | | 0.0 | | | | | | |
| 03916A_66 | 32.8 | 8.1 | 65.9 | 28 | 17 | 1 | 0.53 | 2 | 4 | 2.12 | 0.53 | 109.0 | 206.0 | 426.0 |
| | | | | | | 0.0000 | | 0.0 | | | | | | |
| 03916A_87 | 32.9 | 32.9 | 0.0 | 0 | 1 | 2 | 0.02 | 0 | 1 | 2.22 | 0.81 | 4.0 | 14.0 | 183.0 |
| | | | | | | 0.0000 | | 0.0 | | | | | | |
| 03916A_3 | 34.4 | 20.0 | 0.0 | 0 | 3 | 1 | 0.07 | 0 | 3 | 1.84 | 0.33 | 147.0 | 321.0 | 132.0 |
| | | | | | | 0.0000 | | 0.0 | | | | | | |
| 03916A_68 | 34.5 | 9.7 | 63.0 | 40 | 13 | 1 | 0.32 | 1 | 2 | 2.04 | 0.52 | 63.0 | 111.0 | 272.0 |
| | | | | | | 0.0000 | | 0.0 | | | | | | |
| 03916A_6 | 34.5 | 5.5 | 0.0 | 0 | 41 | 4 | 0.38 | 1 | 4 | 2.37 | 0.53 | 73.0 | 30.0 | 204.0 |
| | | | | | | 0.0000 | | 0.0 | | | | | | |
| 03916A_78 | 35.2 | 17.7 | 0.0 | 0 | 4 | 2 | 0.07 | 0 | 2 | 2.26 | 0.57 | 13.0 | 53.0 | 126.0 |
| | | | | | | 0.0000 | | 0.0 | | | | | | |
| 03916A_51 | 35.7 | 8.7 | 46.2 | 17 | 17 | 1 | 0.48 | 1 | 4 | 2.34 | 0.52 | 95.0 | 324.0 | 115.0 |
| | | | | | | 0.0000 | | 0.0 | | | | | | |
| 03916A_84 | 36.3 | 4.9 | 59.4 | 40 | 62 | 4 | 0.54 | 2 | 4 | 2.49 | 0.67 | 107.0 | 19.0 | 135.0 |
| | | | | | | 0.0000 | | 0.0 | | | | | | |
| 03916A_85 | 43.1 | 9.0 | 0.0 | 0 | 24 | 3 | 0.24 | 1 | 2 | 2.09 | 0.46 | 54.0 | 5.0 | 94.0 |
| | | | | | | 0.0000 | | 0.0 | | | | | | |
| 03916A_83 | 43.7 | 6.3 | 0.0 | 0 | 52 | 4 | 0.38 | 1 | 3 | 2.21 | 0.56 | 79.0 | 1.0 | 241.0 |
| | | | | | | 0.0000 | | 0.0 | | | | | | |
| 03916A_22 | 44.3 | 18.9 | 0.0 | 0 | 6 | 2 | 0.09 | 1 | 2 | 1.91 | 0.36 | 11.0 | 31.0 | 73.0 |
| | | | | | | 0.0000 | | 0.0 | | | | | | |
| 03916A_91 | 44.8 | 7.9 | 0.0 | 0 | 33 | 2 | 0.37 | 1 | 4 | 2.46 | 0.51 | 145.0 | 54.0 | 213.0 |
| 03916A_10 | | | | | | 0.0000 | | 0.0 | | | | | | |
| 3 | 45.8 | 10.9 | 72.4 | 51 | 18 | 2 | 0.20 | 0 | 4 | 2.06 | 0.33 | 42.0 | 78.0 | 356.0 |
| 03916A_10 | | | | | | 0.0000 | | 0.0 | | | | | | |
| 4 | 46.5 | 10.2 | 83.2 | 68 | 21 | 2 | 0.29 | 1 | 4 | 2.29 | 0.46 | 56.0 | 37.0 | 166.0 |
| | | | | | | 0.0000 | | 0.0 | | | | | | |
| 03916A_43 | 47.0 | 14.2 | 0.0 | 0 | 11 | 1 | 0.21 | 0 | 3 | 2.21 | 0.34 | 35.0 | 18.0 | 217.0 |
| | | | | | | 0.0000 | | 0.0 | | | | | | |
| 03916A_74 | 50.9 | 10.9 | 60.6 | 24 | 22 | 1 | 0.55 | 1 | 3 | 2.44 | 0.51 | 159.0 | 178.0 | 351.0 |
| | | | | | | 0.0000 | | 0.0 | | | | | | |
| 03916A_27 | 52.6 | 8.5 | 0.0 | 0 | 40 | 3 | 0.32 | 1 | 4 | 2.08 | 0.73 | 63.0 | 7.0 | 159.0 |
| | | | | | | 0.0000 | | 0.0 | | | | | | |
| 03916A_33 | 53.7 | 31.1 | 133.7 | 163 | 3 | 1 | 0.06 | 0 | 2 | 2.15 | 0.50 | 11.0 | 31.0 | 71.0 |
| | | | | | | 0.0000 | | 0.0 | | | | | | |
| 03916A_9 | 55.5 | 12.2 | 81.3 | 108 | 21 | 5 | 0.10 | 0 | 2 | 1.61 | 0.51 | 18.0 | 1.0 | 117.0 |
| | | | | | | 0.0000 | | 0.0 | | | | | | |
| 03916A_15 | 59.9 | 30.0 | 49.6 | 23 | 4 | 2 | 0.05 | 0 | 2 | 2.12 | 0.48 | 142.0 | 76.0 | 197.0 |
| | | | | | | 0.0000 | | 0.0 | | | | | | |
| 03916A_80 | 61.6 | 31.0 | 0.0 | 0 | 4 | 2 | 0.04 | 0 | 2 | 2.15 | 0.39 | 9.0 | 40.0 | 47.0 |
| | | | | | | 0.0000 | | 0.0 | | | | | | |
| 03916A_42 | 61.8 | 43.8 | 0.0 | 0 | 2 | 1 | 0.03 | 0 | 2 | 2.16 | 0.45 | 5.0 | 17.0 | 185.0 |
| | | | | | | 0.0000 | | 0.0 | | | | | | |
| 03916A_25 | 61.8 | 21.9 | 76.5 | 108 | 8 | 1 | 0.14 | 0 | 3 | 2.40 | 0.42 | 16.0 | 4.0 | 63.0 |
| | | | | | | 0.0000 | | 0.0 | | | | | | |
| 03916A_16 | 69.7 | 12.9 | 57.1 | 40 | 30 | 1 | 0.36 | 1 | 4 | 1.91 | 0.42 | 76.0 | 105.0 | 318.0 |
| | | | | | | 0.0000 | | 0.0 | | | | | | |
| 03916A_58 | 73.0 | 12.2 | 45.8 | 47 | 37 | 3 | 0.21 | 1 | 4 | 2.36 | 0.51 | 40.0 | 37.0 | 272.0 |
| 03916A_10 | | | | | | 0.0000 | | 0.0 | | | | | | |
| 8 | 76.3 | 34.2 | 171.7 | 319 | 5 | 3 | 0.03 | 0 | 4 | 2.65 | 0.66 | 5.0 | 19.0 | 160.0 |
| | | | | | | 0.0000 | | 0.0 | | | | | | |
| 03916A_37 | 79.5 | 13.8 | 0.0 | 0 | 35 | 1 | 0.56 | 2 | 3 | 2.35 | 0.41 | 111.0 | 70.0 | 282.0 |
| | | | | | | 0.0000 | | 0.0 | | | | | | |
| 03916A_54 | 86.5 | 61.3 | 57.2 | 122 | 2 | 1 | 0.03 | 0 | 2 | 2.25 | 0.56 | 7.0 | 4.0 | 54.0 |
| | | | | | | 0.0000 | | 0.0 | | | | | | |
| 03916A_89 | 86.9 | 30.9 | 0.0 | 0 | 8 | 3 | 0.03 | 0 | 2 | 1.77 | 0.46 | 7.0 | 36.0 | 130.0 |

| | | | | | | | | | | | | | | | | | |
|---|---|---|---|---|---|---|---|---|---|---|---|---|---|---|---|---|---|
| | | | | | | 0.00005 | 0.06 | 0.0 0 | 3 | 2.32 | 0.61 | 38.0 | 9.0 | 91.0 |
| 03916A_29 | 87.1 | 20.8 | 0.0 | 0 | 19 | | | | | | | | | |
| | | | | | | 0.00004 | 0.02 | 0.0 0 | 3 | 1.63 | 0.30 | 3.0 | 14.0 | 158.0 |
| 03916A_11 | 89.7 | 40.3 | 0.0 | 0 | 5 | | | | | | | | | |
| | | | | | 11 | 0.00003 | 0.53 | 0.0 2 | 4 | 2.48 | 0.57 | 296.0 | 838.0 | 660.0 |
| 03916A_34 | 92.6 | 9.1 | 48.7 | 22 | 7 | | | | | | | | | |
| | | | | | | 0.00002 | 0.28 | 0.0 1 | 3 | 1.82 | 0.49 | 227.0 | 156.0 | 311.0 |
| 03916A_20 | 133.1 | 17.7 | 0.0 | 0 | 59 | | | | | | | | | |
| | | | | | | 0.00005 | 0.07 | 0.0 0 | 3 | 2.25 | 0.41 | 14.0 | 17.0 | 136.0 |
| 03916A_62 | 141.2 | 23.7 | 12.7 | 95 | 37 | | | | | | | | | |
| | | | | | | 0.00003 | 0.00 | 0.0 0 | 1 | 1.77 | 0.35 | 0.0 | 0.0 | 6.0 |
| 03916A_8 | 198.6 | 200.3 | 0.0 | 0 | 1 | | | | | | | | | |
| | | | | | | 0.00003 | 0.02 | 0.0 1 | 4 | 2.12 | 0.48 | 41.0 | 2.0 | 213.0 |
| 03916A_40 | 470.1 | 221.7 | 0.0 | 0 | 19 | | | | | | | | | |

# Supplement S3- $^{40}Ar/^{39}Ar$ data

**15ET166 WR#L1**

Weighted average of J from standards = 1.338e-04 ± 1.605e-06 (1-sigma error)

Days since irradiation = 73

| Laser Power (mW) | Cumulative 39Ar | 40Ar mV | ± mV | 39Ar mV | ± mV | 38Ar mV | ± mV | 37Ar mV | ± mV | 36Ar mV | ± mV | % Atm. 40Ar | ± | Ca/K | ± | Cl/K | ± | 40Ar*/39ArK | ± | Age (Ma) | ± (Ma) |
|---|---|---|---|---|---|---|---|---|---|---|---|---|---|---|---|---|---|---|---|---|---|
| 500 | 0.02 | 186.25 | 0.61 | 4.156 | 0.01 | 0.31 | ## # | 0.00 | 0.17 | 0.62 | 0.02 | 98.84 | 3.23 | 1.75 | 0.08 | 0.01 | 0.00 | 0.52 | 1.45 | 0.13 | 0.35 |
| 1000 | 0.13 | 245.22 | 0.90 | 24.06 | 0.10 | 0.73 | ## # | 0.04 | 0.41 | 0.50 | 0.02 | 66.92 | 2.92 | 2.74 | 0.03 | 0.00 | 0.00 | 3.37 | 0.30 | 0.81 | 0.07 |
| 1500 | 0.35 | 321.36 | 0.81 | 48.80 | 0.10 | 1.62 | ## # | 0.00 | 0.35 | 0.40 | 0.02 | 36.22 | 2.52 | 2.00 | 0.01 | 0.00 | 0.00 | 4.18 | 0.17 | 1.01 | 0.04 |
| 2000 | 0.57 | 275.56 | 0.75 | 47.59 | 0.20 | 1.45 | ## # | 0.00 | 0.24 | 0.23 | 0.02 | 29.13 | 2.34 | 1.50 | 0.01 | 0.00 | 0.00 | 4.08 | 0.14 | 0.98 | 0.03 |
| 2500 | 0.74 | 228.57 | 0.48 | 35.81 | 0.13 | 1.13 | ## # | 0.00 | 0.23 | 0.24 | 0.03 | 35.23 | 3.34 | 1.40 | 0.01 | 0.00 | 0.00 | 4.11 | 0.21 | 0.99 | 0.05 |
| 3000 | 0.83 | 150.15 | 0.49 | 20.81 | 0.06 | 0.78 | ## # | 0.00 | 0.29 | 0.23 | 0.03 | 44.63 | 6.63 | 1.46 | 0.02 | 0.00 | 0.00 | 3.98 | 0.48 | 0.96 | 0.12 |
| 5000 | 0.95 | 310.20 | 0.81 | 26.16 | 0.14 | 1.64 | ## # | 0.00 | 0.16 | 0.70 | 0.03 | 71.58 | 3.07 | 2.63 | 0.01 | 0.00 | 0.00 | 3.37 | 0.36 | 0.81 | 0.08 |
| 9000 | 1.00 | 215.43 | 0.66 | 10.68 | 0.09 | 0.94 | ## # | 0.00 | 0.25 | 0.62 | 0.03 | 82.84 | 3.76 | 7.81 | 0.01 | 0.00 | 0.00 | 3.47 | 0.76 | 0.84 | 0.18 |
| Integrated | | 1932.73 | 1.99 | ### # | 0.36 | 8.60 | ## # | 0.26 | 0.73 | 3.76 | 0.08 | 56.58 | 1.11 | 2.19 | 0.00 | 0.00 | 0.00 | 3.84 | 0.10 | 0.92 | 0.03 |

Irradiations done at McMaster Nuuclear Reactor: (39Ar/37Ar)Ca = 0.000706, (36Ar/37Ar)Ca = 0.000279, (40Ar/39Ar)K = 0.0297

Standard: TCR 28.619 with an age of (Renne et al., 2010)

All errors quoted at 1-sigma

Laser (mW): Laser power for each step of the step-heating experiment

40Ar, 39Ar, and 37Ar: Isotopic measurements corrected for system blank and decay of 37Ar and 39Ar

Ca/K: Calcium to potassium ratio as determined from 37Ar produced from 40Ca and 39Ar produced from 39K

Cl/K: chlorine to potassium ratio as determined from 38Ar produced from 37Cl and 39Ar produced from 39K

40Ar*/39ArK: ratio of radiogenic argon 40 to reactor-produced 39Ar from potassium, corrected for reactor interferences